

November 2007

Revision 38

NAC-LWT

Legal Weight Truck Cask System

SAFETY ANALYSIS REPORT

Docket No. 71-9225



Atlanta Corporate Headquarters: 3930 East Jones Bridge Road, Norcross, Georgia 30092 USA
Phone 770-447-1144, Fax 770-447-1797, www.nacintl.com

RECORD OF REVISIONS

<u>Issue Date</u>	<u>Revision Number</u>	<u>Change</u>	<u>Description of Change</u>
March 1988	0	N/A	Initial Release.
August 1988	1	2.10.8	Incorporate Drop Test Results.
July 1989	2	Throughout	General rewrite and reissue to incorporate NAC responses to NRC comments.
September 1989	3	Throughout	Provide revised stress tables. Clarify post-drop test revisions. Change from Fissile Class I to Fissile Class III. Vacuum drying required for PWR and BWR fuels.
November 1989	4	Throughout	Revise to Type B(U). Clarification of side and end drop analyses for the neutron shield and expansion tank. Correct containment calculations. Revise operating procedures.
June 1990	5		Deleted.
July 1990	6	2.10.14 and throughout	Incorporate failed metallic fuel as permissible contents of the packaging.
September 1990	6 (supplement)	7.1	Incorporate operational changes to 7/1990, Revision 6.

RECORD OF REVISIONS (continued)

<u>Issue Date</u>	<u>Revision Number</u>	<u>Change</u>	<u>Description of Change</u>
December 1990	7	2.10.13 and throughout	Renumber 2.10.14 as 2.10.13. Revise to include evaluation of three failed metallic fuel rods per canister.
August 1991	8	2.10.13	Revise to permit use of shipment of severely failed research reactor metallic fuel that has been accumulated in filters using failed fuel cans.
October 1991	9	1.0, 1.1, 1.2, 4.2, 4.4.3, 7.0, 7.1	Revise to incorporate response to NRC questions on Revision 8.
October 1994	10	1.4	Revise License Drawings to modify radiographic acceptance criteria.
November 1994	11	Throughout	Revise to permit shipment of MTR fuel.
January 1995	12	1.4	Revised License Drawings to incorporate new weld and inspection requirements.
March 1995	13	1.2, 2.2, 2.2.12.6, 5.1, 5.3.4, 6.4.4, 7.1.4	Submittal of consolidated SAR. Revised to incorporate responses to NRC questions on MTR fuel contents.
May 1995	14	1.4	Minor editorial corrections to consolidated SAR.

RECORD OF REVISIONS (continued)

<u>Issue Date</u>	<u>Revision Number</u>	<u>Change</u>	<u>Description of Change</u>
June 1995	15	Throughout	Revised to incorporate up to 25 individual PWR fuel rods as permissible contents.
August 1995	16	2.6.12.2	Revised to incorporate a description of the canister for individual intact PWR rods.
August 1995	17	2.6.12, 5.0, 5.1, 5.3, Table 6.2-1	Revised to incorporate shielding analysis for 25 PWR rods and editorial corrections.
October 1995	18	1,4,5 and 6	Revise to incorporate LEU MTR fuel elements as permissible contents.
December 1995	19	1.4	Submit revised MTR basket drawings incorporating additional fabrication details.
March 1996	20	1.2, 1.4, 7.1 and 7.2	Submit revised drawings for alternate drain configuration.
December 1997	21	1.2, 2.1.3, 2.4.3, 2.6, 2.7, 3.1, 3.4, 4.4, 5.0, 7.1.4, 7.1.5, 8.2, 9.0	Incorporates HEU MTR analysis for varying burnup and cool time. Incorporates note to clarify bolt thread chrome-plate requirements.
May 1998	22	1.0, 1.1, 1.2, 2.1, 2.6.12, 2.7.7, 2.9 (various), 3.1, 3.4, 3.5, 4.0 (all), 5.0, 5.1, 5.3, 6.0 (various), 7.0 (all), 8.1, 9.0	Incorporates 120 element TRIGA fuel analysis.
November 1998	23	1.0, 1.2.3, 2.7.1.6, 2.7.3, 2.7.5, 2.10.13.8, 3.2, 3.4, 3.5, 4.2, 4.3, 4.4, 5.1, 6 (all), 7.1, 8.1, 9.0	Incorporates changes for B(U)F-85 certification.

RECORD OF REVISIONS (continued)

<u>Issue Date</u>	<u>Revision Number</u>	<u>Change</u>	<u>Description of Change</u>
December 1998	24	1.2.3, 2.2.0, 2.3.0, 2.6.12, 2.7.7, 4.2, 4.3, 4.5.3, 5.1, 5.3.4, 6.4.3, 7.1, 7.2	Incorporates MTR-35 basket configuration, failed MTR fuel containment analysis, and various minor editorial changes.
February 1999	25	6.2.3 and 6.4.3	Added additional MTR configuration.
April 1999	26	1.0, 1.1, 1.2.2, 1.2.3, 2.6.12.7, 2.7.7.6, 2.7.7.9, 3.4.1.5, 3.4.1.6, 3.5.3.4, 4.2.1, 4.5.3, 5.0, 5.1, 5.3.6, 5.3.7, 6.0, 6.1, 6.2, 6.2.5, 6.2.6, 6.2.7, 6.3, 6.3.5, 6.4.5, 6.4.6, 6.6.5, 6.6.6, 7.0, 7.1.6, 8.1.7, 8.2	Incorporates TRIGA fuel cluster rod contents and TRIGA poisoned basket configuration.
June 1999	27	1.2.3.1.1.2 and 6.4.6.5	Incorporates increased fuel parameters for TRIGA fuel cluster rod contents.
December 1999	28	License drawings, 1.2, 2.3, 2.7, 2.10.8, 2.10.13, 3.2, 3.5, 5.4, 6.2, 6.4, 8.3, 9.0	Incorporates minor changes to numerous drawings to reflect changes facilitating fabrication and to increase the uranium loading of NISTR MTR fuel contents.
January 2000	29	Complete consolidation of SAR for CoC Renewal Application Chapter 7 License Drawings 315-40-01, 02, and 03	Consolidated SAR, removed all shading and revision bars and numbered all pages to Revision 29. Incorporated miscellaneous corrections and clarifications in the cask operating procedures based on cask operating experience. Incorporated changes in Name Plate attachment and information (for corporate name and B(U)F-85 designation). Revised slot dimension on shield tank (Section G-G, sheet 4).

RECORD OF REVISIONS (continued)

<u>Issue Date</u>	<u>Revision Number</u>	<u>Change</u>	<u>Description of Change</u>
January 2000 (continued)	29	License drawings 315-40-05 and 06	Corrected material callout to 6061-T651 AL ALY for Items 10, 17, and 19 on 315-04-05 and Item 5 on 315-40-06.
July 2000	30	Throughout	Revised to incorporate high burnup PWR and BWR fuel rods and McMaster MTR fuel as authorized contents; to incorporate a revised specification for the Ball-Lok impact limiter attachment pins; and to incorporate an alternate fabrication method for the impact limiter shells.
		License Drawing 315-40-03	Corrected slot dimension for neutron shield gusset.
		License Drawings 315-40-01, -048, -052, -079, -084, and - 094	Incorporated revised Ball-Lok pin specification.
		License Drawings 315-40-05 and -06	Incorporated alternate fabrication method for the impact limiter shells.
		License Drawings 315-40-098 through - 105	Added to define the components used for shipment of high burnup fuel rods.
November 2000	31	Throughout	Revised to incorporate drawing changes due to fabrication comments, as well as specific HEU-MTR fuel for Argentina research reactor.
		Licensing Drawings 315-40-03, -04, -08, - 099, -102, -105, and - 106	
January 2001	32	Throughout	Incorporated MEU-MTR fuel elements bounding MTR fuel element including tolerances for fabrication, enrichment, burnups and cool times. Incorporated revised dimensional tolerances for impact limiter shell dimensions and acceptance criteria for local scratches/gouges in the shells.
		Licensing Drawings 315-40-05 and -06	

RECORD OF REVISIONS (continued)

<u>Issue Date</u>	<u>Revision Number</u>	<u>Change</u>	<u>Description of Change</u>
September 2001	33	Throughout; Licensing Drawings 315-40-02, -03, -04, -08, -10, -074, -108, -109, -110, -111, -113	Incorporated Alternate Port Cover design, alternate PWR fuel basket configuration and DIDO/Petten fuel
November 2002	34	Throughout	Incorporated 02A (LEU MTR) and 02B (MTR)
May 2004	35	Throughout	Incorporated 03A, 03C, 03D, 03F & 03G (GA IFM) and 03B, 03E & 03H (EPRI/Framatome)
December 2004	36	Complete consolidation of SAR for CoC renewal application. License drawings: 315-40-02 315-40-03 315-40-08 315-40-10 315-40-087 315-40-127 315-40-128	General update incorporating LWT-03I (TPBAR), LWT-04B (updated drawings for obsolete part numbers), LWT-04C (TPBAR RAI), LWT-04D (-96 changes), and LWT-04F (updates to TPBAR RAI for tritium release limits). Additional changes to the SAR have been incorporated in accordance with NRC/NAC discussions: Section 1.1, Page 1.1-1, clarified that fuel rod insert may also be referred to as a rod holder and that encapsulated fuel rods are not rod holders; Section 1.2.3, clarified that fuel rod capsules may be placed in a rod holder and added sketch of typical fuel rod capsule in Figure 1.2-11 to replace Framatome drawings; Section 1.2.3.1.2, added "intact" before "TRIGA fuel elements" in five places to clarify the TRIGA contents; Section 1.2.3.6, added "stainless steel" before "consolidation canister" in last paragraph to identify the TPBAR consolidation canister material; Figure 1.2-10 revised to eliminate unnecessary

RECORD OF REVISIONS (continued)

<u>Issue Date</u>	<u>Revision Number</u>	<u>Change</u>	<u>Description of Change</u>
December 2004 (continued)	36	Complete consolidation of SAR for CoC renewal application. License drawings: 315-40-02 315-40-03 315-40-08 315-40-10 315-40-087 315-40-127 315-40-128	detail; added drawing 315-40-03, revision 6, to cover LWT units 1 through 5 per CoC specification; revised drawing 315-40-128, per revision 1, to delete the reference to the Westinghouse TPBAR consolidation canister drawing; Figures 2.10.2-4a through -4d and Figure 2.10.2-5 renumbered with consecutive numbers; Table 5.1-1 simplified to only specify the Transport Index that is based on shielding per IAEA -96 regulations; Tables 5.3-3a through -3d, Table 5.3-6a, Table 5.3-7a and Table 5.3-9a renumbered consecutively; Section 5.3.6, moved Figures 5.3-9 through 5.3-15 and Figures 5.3-19 through 5.3-23 to the end of the section; Section 5.3.7.1, added references to Tables 5.3-26 and 5.3-27; Section 5.3.9, added reference to Figure 5.3-24; Figure 5.3-46, corrected MCNP input for 300 TPBARS at 30 days cool times. Files were updated to take advantage of automatic TOC, LOF, & LOT numbering, correct preface page numbers to chp# + pg number, delete extra section breaks, and except for Chapter 2 change page numbering to two levels. Pagination corrected, "x" changed to "x" in formulas, format for continued figures and tables made consistent, some footnotes put into true format and made consistent, and some automatic cross references set up.

RECORD OF REVISIONS (continued)

<u>Issue Date</u>	<u>Revision Number</u>	<u>Change</u>	<u>Description of Change</u>
June 2005	37	Incorporation of LWT-04E, LWT-05A, LWT-05B, LWT-05C, LWT-05D & LWT-05E License drawings: 315-40-01, Rev. 5 315-40-086, Rev. 1 315-40-098, Rev. 3 315-40-100, Rev. 3 315-40-104, Rev. 1 315-40-129, Rev. 1 315-40-130, Rev. 1 315-40-133, Rev. 0 315-40-134, Rev. 1 315-40-135, Rev. 1	Added PULSTAR fuel, screened can option & TPBAR dunnage approved amendments to Revision 36.
November 2007	38	Incorporation of LWT-05F, LWT-06A, LWT-06B, LWT-06C, LWT-06E, LWT-06F, LWT-06G, LWT-07A, LWT-07B, LWT-07C, LWT-07D & LWT-07F License drawings: 315-40-01, Rev. 6; 315-40-02, Rev. 20; 315-40-03, Rev. 6; 315-40-03, Rev. 22; 315-40-08, Rev. 17; 315-40-048, Rev. 3; 315-40-052, Rev. 3; 315-40-079, Rev. 3; 315-40-084, Rev. 3; 315-40-085, Rev. 0; 315-40-094, Rev. 4; 315-40-104, Rev. 2; 315-40-111, Rev. 1; 315-40-124, Rev. 1; 315-40-125, Rev. 3; 315-40-127, Rev. 2; 315-40-128, Rev. 2; 315-40-133, Rev. 1; 315-40-139, Rev. 0; 315-40-140, Rev. 0; 315-40-141, Rev. 0; 315-40-142, Rev. 0; 315-40-145; Rev. 0 The following license drawings were deleted: 315-40-13, 315-40-14, 315-40-15, 315-40-17, 315-40-18 & 315-40-20	Added ANSTO, TPBAR, TRIGA & Petten approved amendments to Revision 37.

LIST OF EFFECTIVE PAGES

Chapter 1

1-i thru 1-iv.....	Revision 38
1-1 thru 1-5.....	Revision 38
1.1-1 thru 1.1-2.....	Revision 38
1.2-1 thru 1.2-49.....	Revision 38
1.3-1.....	Revision 38
1.4-1.....	Revision 38
1.5-1.....	Revision 38

76 drawings in the
Chapter 1 List of Drawings

Chapter 1 Appendices 1-A
through 1-G

Chapter 2

2-i thru 2-xxiv.....	Revision 38
2-1	Revision 38
2.1.1-1 thru 2.1.1-2.....	Revision 38
2.1.2-1 thru 2.1.2-3.....	Revision 38
2.1.3-1 thru 2.1.3-8.....	Revision 38
2.2.1-1 thru 2.2.1-3.....	Revision 38
2.3-1.....	Revision 38
2.3.1-1 thru 2.3.1-13.....	Revision 38
2.4-1	Revision 38
2.4.1-1	Revision 38
2.4.2-1	Revision 38
2.4.3-1	Revision 38
2.4.4-1	Revision 38
2.4.5-1	Revision 38
2.4.6-1	Revision 38
2.5.1-1 thru 2.5.1-11.....	Revision 38
2.5.2-1 thru 2.5.2-17.....	Revision 38
2.6.1-1 thru 2.6.1-7.....	Revision 38
2.6.2-1 thru 2.6.2-7.....	Revision 38

2.6.3-1	Revision 38
2.6.4-1	Revision 38
2.6.5-1 thru 2.6.5-2	Revision 38
2.6.6-1	Revision 38
2.6.7-1 thru 2.6.7-136	Revision 38
2.6.8-1	Revision 38
2.6.9-1	Revision 38
2.6.10-1 thru 2.6.10-15	Revision 38
2.6.11-1 thru 2.6.11-12	Revision 38
2.6.12-1 thru 2.6.12-91	Revision 38
2.7-1	Revision 38
2.7.1-1 thru 2.7.1-117	Revision 38
2.7.2-1 thru 2.7.2-23	Revision 38
2.7.3-1 thru 2.7.3-5	Revision 38
2.7.4-1	Revision 38
2.7.5-1 thru 2.7.5-5	Revision 38
2.7.6-1 thru 2.7.6-4	Revision 38
2.7.7-1 thru 2.7.7-70	Revision 38
2.8-1	Revision 38
2.9-1 thru 2.9-13	Revision 38
2.10.1-1 thru 2.10.1-3	Revision 38
2.10.2-1 thru 2.10.2-49	Revision 38
2.10.3-1 thru 2.10.3-18	Revision 38
2.10.4-1 thru 2.10.4-11	Revision 38
2.10.5-1	Revision 38
2.10.6-1 thru 2.10.6-19	Revision 38
2.10.7-1 thru 2.10.7-66	Revision 38
2.10.8-1 thru 2.10.8-67	Revision 38
2.10.9-1 thru 2.10.9-9	Revision 38
2.10.10-1 thru 2.10.10-97	Revision 38
2.10.11-1 thru 2.10.11-10	Revision 38
2.10.12-1 thru 2.10.12-31	Revision 38
2.10.13-1 thru 2.10.13-17	Revision 38
2.10.14-1 thru 2.10.14-38	Revision 38
2.10.15-1 thru 2.10.15-10	Revision 38

LIST OF EFFECTIVE PAGES (Continued)

Chapter 3

3-i thru 3-v..... Revision 38
3.1-1 thru 3.1-2..... Revision 38
3.2-1 thru 3.2-11..... Revision 38
3.3-1..... Revision 38
3.4-1 thru 3.4-82..... Revision 38
3.5-1 thru 3.5-34..... Revision 38
3.6-1 thru 3.6-12..... Revision 38

Chapter 4

4-i thru 4-iv..... Revision 38
4.1-1 thru 4.1-3..... Revision 38
4.2-1 thru 4.2-12..... Revision 38
4.3-1 thru 4.3-7..... Revision 38
4.4-1 thru 4.4-2..... Revision 38
4.5-1 thru 4.5-85..... Revision 38

Chapter 5

5-i thru 5-x..... Revision 38
5-1 thru 5-3..... Revision 38
5.1.1-1 thru 5.1.1-16..... Revision 38
5.2.1-1 thru 5.2.1-7..... Revision 38
5.3.1-1 thru 5.3.1-2..... Revision 38
5.3.2-1..... Revision 38
5.3.3-1 thru 5.3.3-8..... Revision 38
5.3.4-1 thru 5.3.4-19..... Revision 38
5.3.5-1 thru 5.3.5-4..... Revision 38
5.3.6-1 thru 5.3.6-18..... Revision 38
5.3.7-1 thru 5.3.7-11..... Revision 38
5.3.8-1 thru 5.3.8-25..... Revision 38
5.3.9-1 thru 5.3.9-26..... Revision 38
5.3.10-1 thru 5.3.10-14..... Revision 38
5.3.11-1 thru 5.3.11-48..... Revision 38
5.3.12-1 thru 5.3.12-26..... Revision 38

5.3.13-1 thru 5.3.13-17..... Revision 38
5.3.14-1 thru 5.3.14-21..... Revision 38
5.3.15-1 thru 5.3.15-9..... Revision 38
5.3.16-1 thru 5.3.16-5..... Revision 38
5.3.17-1 thru 5.3.17-9..... Revision 38
5.4.1-1 thru 5.4.1-6..... Revision 38

Chapter 6

6-i thru 6-xi..... Revision 38
6-1..... Revision 38
6.1-1 thru 6.1-4..... Revision 38
6.2-1..... Revision 38
6.2.1-1 thru 6.2.1-3..... Revision 38
6.2.2-1 thru 6.2.2-3..... Revision 38
6.2.3-1 thru 6.2.3-7..... Revision 38
6.2.4-1..... Revision 38
6.2.5-1 thru 6.2.5-5..... Revision 38
6.2.6-1 thru 6.2.6-3..... Revision 38
6.2.7-1 thru 6.2.7-2..... Revision 38
6.2.8-1 thru 6.2.8-3..... Revision 38
6.2.9-1 thru 6.2.9-4..... Revision 38
6.2.10-1 thru 6.2.10-3..... Revision 38
6.2.11-1 thru 6.2.11-3..... Revision 38
6.2.12-1 thru 6.2.12-4..... Revision 38
6.3.1-1 thru 6.3.1-6..... Revision 38
6.3.2-1 thru 6.3.2-4..... Revision 38
6.3.3-1 thru 6.3.3-9..... Revision 38
6.3.4-1 thru 6.3.4-9..... Revision 38
6.3.5-1 thru 6.3.5-12..... Revision 38
6.3.6-1 thru 6.3.6-9..... Revision 38
6.3.7-1 thru 6.3.7-4..... Revision 38
6.3.8-1 thru 6.3.8-7..... Revision 38
6.3.9-1 thru 6.3.9-7..... Revision 38

LIST OF EFFECTIVE PAGES (Continued)

6.4.1-1 thru 6.4.1-10..... Revision 38
6.4.2-1 thru 6.4.2-10..... Revision 38
6.4.3-1 thru 6.4.3-34..... Revision 38
6.4.4-1 thru 6.4.4-24..... Revision 38
6.4.5-1 thru 6.4.5-32..... Revision 38
6.4.6-1 thru 6.4.6-17..... Revision 38
6.4.7-1 thru 6.4.7-14..... Revision 38
6.4.8-1 thru 6.4.8-14..... Revision 38
6.4.9-1 thru 6.4.9-10..... Revision 38
6.4.10-1 thru 6.4.10-18..... Revision 38
6.5.1-1 thru 6.5.1-13..... Revision 38
6.5.2-1 thru 6.5.2-4..... Revision 38
6.5.3-1 thru 6.5.3-2..... Revision 38

Appendix 6.6

6.6-i thru 6.6-ii Revision 38
6.6-1..... Revision 38
6.6.1-1 thru 6.6.1-111..... Revision 38
6.6.2-1 thru 6.6.2-56..... Revision 38
6.6.3-1 thru 6.6.3-73..... Revision 38
6.6.4.-1 thru 6.6.4-77..... Revision 38
6.6.5-1 thru 6.6.5-101..... Revision 38
6.6.6-1 thru 6.6.6-76..... Revision 38
6.6.7-1 thru 6.6.7-84..... Revision 38
6.6.8-1 thru 6.6.8-183..... Revision 38
6.6.9-1 thru 6.6.9-52..... Revision 38
6.6.10-1 thru 6.6.10-33..... Revision 38
6.6.11-1 thru 6.6.11-47..... Revision 38
6.6.12-1 thru 6.6.12-20..... Revision 38
6.6.13-1 thru 6.6.13-22..... Revision 38
6.6.14-1 thru 6.6.14-7..... Revision 38

Chapter 7

7-i thru 7-ii Revision 38
7.1-1 thru 7.1-51 Revision 38
7.2-1 thru 7.2-12 Revision 38
7.3-1 thru 7.3-2 Revision 38

Chapter 8

8-i Revision 38
8.1-1 thru 8.1-11 Revision 38
8.2-1 thru 8.2-4 Revision 38
8.3-1 thru 8.3-4 Revision 38

Chapter 9

9-i Revision 38
9-1 thru 9-9 Revision 38

Table of Contents

4	CONTAINMENT	4.1-1
4.1	Containment Boundary	4.1-1
4.1.1	Containment Penetrations	4.1-1
4.1.2	Seals and Welds	4.1-1
4.1.3	Closure	4.1-3
4.2	Containment Requirements for Normal Conditions of Transport	4.2-1
4.2.1	Containment of Radioactive Material	4.2-1
4.2.2	Pressurization of Containment Vessel	4.2-8
4.2.3	Containment Criteria.....	4.2-9
4.3	Containment Requirements for Hypothetical Accident Conditions.....	4.3-1
4.3.1	Fission Gas Products.....	4.3-1
4.3.2	Containment of Radioactive Materials	4.3-1
4.3.3	Tritium Contamination Issues.....	4.3-5
4.4	Special Requirements.....	4.4-1
4.5	Appendices.....	4.5-1
4.5.1	Tetrafluoroethylene O-Rings.....	4.5-1
4.5.2	Metallic O-Rings.....	4.5-10
4.5.3	Viton® O-Rings	4.5-23
4.5.4	SAS2H Output and Group A ₂ Values for Design Basis PWR, BWR, TRIGA, MTR and DIDO Fuel	4.5-29
4.5.5	Containment Analysis of MTR Fuel Elements	4.5-51
4.5.6	Evaluation of Normal Conditions Allowable Leakage Rate for 25 BWR High Burnup Rods with up to 14 Damaged Rods.....	4.5-57
4.5.7	Containment Analysis of DIDO Fuel Assemblies	4.5-62
4.5.8	Containment Analysis for PULSTAR Fuel Elements.....	4.5-67
4.5.9	Metallic Face Seal.....	4.5-73
4.5.10	Containment Analysis of ANSTO Basket Payloads	4.5-85

List of Figures

Figure 4.5-1	SAE International Aerospace Standard AS8791	4.5-2
Figure 4.5-2	Metallic O-Rings Technical Bulletin	4.5-11
Figure 4.5-3	Parker Seals Material Report on the Viton® Material.....	4.5-25

List of Tables

Table 4.2-1	Release Fractions: Normal and Accident Conditions	4.2-10
Table 4.2-2	Allowable Release Rates for NAC-LWT Cask Contents: Normal Conditions	4.2-10
Table 4.2-3	Cask Free Volumes and Pressures	4.2-11
Table 4.2-4	Leak Rate and Leak Test Sensitivity - Normal Conditions	4.2-12
Table 4.3-1	A ₂ Calculation for PWR Spent Fuel	4.3-6
Table 4.3-2	Standard Leak Rates for Accident Conditions	4.3-6
Table 4.3-3	A ₂ Calculation for 25 High Burnup PWR Spent Fuel Rods.....	4.3-7
Table 4.3-4	A ₂ Calculation for 25 High Burnup BWR Spent Fuel Rods	4.3-7
Table 4.4-1	Transport Conditions for the TRIGA Sealed Failed Fuel Can	4.4-2
Table 4.4-2	A ₂ Calculation for Two Canned FLIP-LEU II Elements.....	4.4-2
Table 4.4-3	Normal and Accident Condition Leak Rates for the TRIGA Failed Fuel Can	4.4-2
Table 4.5-1	Westinghouse 15×15 SAS2H Output and Group A ₂ Value (Gas).....	4.5-30
Table 4.5-2	Westinghouse 15×15 SAS2H Output and Group A ₂ Value (Volatiles).....	4.5-30
Table 4.5-3	Westinghouse 15×15 SAS2H Output and Group A ₂ Value (Fuel Fines)	4.5-31
Table 4.5-4	General Electric 7×7 SAS2H Output and Group A ₂ Value (Gas).....	4.5-33
Table 4.5-5	General Electric 7×7 SAS2H Output and Group A ₂ Value (Volatiles)	4.5-33
Table 4.5-6	General Electric 7×7 SAS2H Output and Group A ₂ Value (Fuel Fines).....	4.5-34
Table 4.5-7	TRIGA (FLIP-LEU II) SAS2H Output and Group A ₂ Value (Gas)	4.5-36
Table 4.5-8	TRIGA (FLIP-LEU II) SAS2H Output and Group A ₂ Value (Volatiles)	4.5-36
Table 4.5-9	TRIGA (FLIP-LEU II) SAS2H Output and Group A ₂ Value (Fuel Fines).....	4.5-37
Table 4.5-10	MTR HEU SAS2H Output and Group A ₂ Value (Gas)	4.5-39
Table 4.5-11	MTR HEU SAS2H Output and Group A ₂ Value (Volatiles).....	4.5-39
Table 4.5-12	MTR HEU SAS2H Output and Group A ₂ Value (Fuel Fines)	4.5-40
Table 4.5-13	25 High Burnup BWR-Rod SAS2H Output and Group A ₂ Value (Gas).....	4.5-42
Table 4.5-14	25 High Burnup BWR-Rod SAS2H Output and Group A ₂ Value (Volatiles) ..	4.5-42
Table 4.5-15	25 High Burnup BWR-Rod SAS2H Output and Group A ₂ Value (Fuel Fines) ..	4.5-43
Table 4.5-16	25 High Burnup PWR-Rod SAS2H Output and Group A ₂ Value (Gas).....	4.5-45
Table 4.5-17	25 High Burnup PWR-Rod SAS2H Output and Group A ₂ Value (Volatiles)...	4.5-45
Table 4.5-18	25 High Burnup PWR-Rod SAS2H Output and Group A ₂ Value (Fuel Fines) ..	4.5-46
Table 4.5-19	DIDO LEU SAS2H Output and Group A ₂ Value (Gas)	4.5-48
Table 4.5-20	DIDO LEU SAS2H Output and Group A ₂ Value (Volatiles)	4.5-48
Table 4.5-21	DIDO LEU SAS2H Output and Group A ₂ Value (Fuel Fines).....	4.5-49
Table 4.5-22	Pressure Summary for PULSTAR Fuel	4.5-69
Table 4.5-23	PULSTAR Fuel SAS2H Output and Group A ₂ Value (Gas)	4.5-69
Table 4.5-24	PULSTAR Fuel SAS2H Output and Group A ₂ Value (Volatiles).....	4.5-69

List of Tables (continued)

Table 4.5-25	PULSTAR Fuel SAS2H Output and Group A ₂ Value (Fuel Fines)	4.5-70
Table 4.5-26	PULSTAR Fuel Containment Release Fractions.....	4.5-72
Table 4.5-27	Containment Analysis Results for PULSTAR Fuel Payloads.....	4.5-72
Table 4.5-28	PULSTAR Fuel Leakage Rate Calculation	4.5-72

4 CONTAINMENT

4.1 Containment Boundary

The containment boundary for the NAC-LWT cask consists of the 0.75-inch thick inner shell, the 4.0-inch thick bottom end plate, the 11.25-inch thick lid, and the upper ring forging. The inner shell is Type XM-19 stainless steel and the other components are Type 304 stainless steel. The valves used for filling and draining the cask cavity are not considered to be part of containment; this function is provided by the valve port covers. There are two port cover designs: alternate and Alternate B. The alternate port cover is fabricated from SA-705, Grade 630, condition H1150 precipitation-hardened stainless steel. The Alternate B port cover is fabricated from XM-19 stainless steel to withstand a higher MNOP and to provide a leaktight containment boundary. The metallic O-ring inner seal of the lid, the tetrafluoroethylene (TFE) O-ring, and the Viton® O-ring or metallic face seals of the valve port covers are also part of the containment boundary. The sealing surfaces for metallic O-rings and seals are machined in accordance with seal manufacturers' recommendations to a finish suitable to achieve sealing reliability. The metal face seal, located on the Alternate B port cover face, is in a 0.125-inch counterbore with a suitable surface finish, and provides a leaktight containment boundary seal when the Alternate B port cover design is used.

4.1.1 Containment Penetrations

The only containment penetrations in the NAC-LWT cask are the cask cavity vent and drain ports, and the cask lid.

4.1.2 Seals and Welds

4.1.2.1 Seals

The O-rings of the cask lid and valve port covers are the seals that affect containment for the radioactive contents of the NAC-LWT cask, as described in Section 4.1. Appendix 4.5.1 contains the military specification that prescribes the physical and chemical properties of the TFE O-rings. Appendix 4.5.2 is the manufacturer's technical bulletin for the metallic O-rings. Seal testing, prior to cask acceptance from the manufacturer, during routine maintenance, and upon assembly for transportation, includes the fabrication leakage rate test, the periodic maintenance leakage rate test, and the preshipment leakage rate test per the requirements of ANSI N14.5-1997. Appendix 4.5.3 contains a description of the leakage testing performed using the Viton® O-rings on the alternate port cover design at temperatures exceeding the manufacturer's elevated

temperature limit. Appendix 4.5.3 also contains the O-ring manufacturer's material report on the Viton® material. Appendix 4.5.9 contains the technical specification on the Alternate B port cover HELICOFLEX® metallic face seal.

4.1.2.1.1 Fabrication Leakage Rate Test

Upon completion of fabrication, the cask containment shall be tested as described in Section 8.1.3. This test verifies the sealing integrity of the package to a leakage rate of not more than 5.5×10^{-7} std cm³/ sec (helium) for the lid seal and alternate port cover seals. Per Section 8.1.3, the cask lid and Alternate B port cover are tested to leaktight conditions by verifying integrity of the seals to a leakage rate of no more than $\leq 2 \times 10^{-7}$ cm³/s for TPBAR contents.

4.1.2.1.2 Fabrication Pressure Test

During acceptance testing, the cask containment boundary shall be hydrostatically tested using the pressure test described in Section 8.1.2. This test verifies the sealing integrity of the package with a hydrostatic test pressure of 209 psig for fissile material shipments.

As an additional post-fabrication test, prior to performing the first TPBAR shipment in an NAC-LWT cask, the hydrostatic test described in Section 8.1.2 shall be performed with the Alternate B port covers installed. The test pressure for the hydrostatic test shall be 450 psig, which is 150% MNOP.

4.1.2.1.3 Preshipment Leakage Rate Test

Prior to shipment of a loaded NAC-LWT cask, the closure lid and vent and drain port cover containment seals shall be individually leakage tested. For the alternate port covers, a pressure drop test is performed by pressurizing the volume between the containment seal and the test seal. This preshipment leakage rate test assures that the port covers and seals are properly installed and that no leakage exists in excess of test sensitivity of 1×10^{-3} ref cm³/s.

If the Viton® containment O-ring is replaced, a maintenance leakage rate test is required to be performed per Section 8.1.3. The closure lid and Alternate B port cover both utilize metallic O-rings for the containment boundary seal. Metallic O-rings are designed for a single use and must be replaced prior to each loaded transport. Following installation of the closure lid and Alternate B port covers, maintenance leakage rate tests are performed on each component in accordance with the test procedures in Section 8.1.3.

4.1.2.2 Welds

All containment vessel welds are full penetration bevel or groove welds to ensure structural and containment integrity.

4.1.3 Closure

Closure of the containment vessel is provided by the twelve 1-8 UNC closure lid bolts, each tightened to 260 ft-lb of torque. The lid bolts are SA-453, Grade 660 high alloy steel bolting material. The lid bolts are preloaded so that the lid seals remain fully compressed for all load conditions. The structural adequacy of the lid bolts is documented in Sections 2.1.3.2.2, 2.6.7.6 and 2.10.9. The closure lid O-ring seals are specified on Drawing No 315-40-02 in Section 1.4. The O-ring seals and grooves are selected based on the manufacturer's specifications to satisfy the pressure and temperature conditions incurred by the NAC-LWT cask. The leakage test described in Section 8.1.3 verifies that the lid seal leakage rate does not exceed 5.5×10^{-7} std-cm³/sec (helium) for packages that do not require a leaktight containment boundary. Packages requiring a leaktight containment boundary are tested per Section 8.1.3 to a lid seal leakage rate not to exceed 1×10^{-7} ref cm³/sec. Per ANSI N14.5, the equivalent helium leakage rate for leaktight conditions is 2×10^{-7} cm³/sec.

Alternate port covers are retained by three 3/8 - 16 UNC bolts, each tightened to 100 in-lb of torque. The bolt material for these ports covers is SA-193, Grade B6 high alloy steel. The Alternate B port cover is retained by three 3/8 - 16 UNC bolts, made from SB-637 Grade N07718 nickel alloy steel, each tightened to 280 in-lb of torque. The Alternate B port covers are required for the transport of TPBAR contents, which require a leaktight containment configuration.

4.2 Containment Requirements for Normal Conditions of Transport

The NAC-LWT cask must maintain a radioactivity release rate less than 10^{-6} A₂/hr under normal conditions of transport, as required by 10 CFR 71.51 and IAEA Transportation Safety Standards (TS-R-1). For any of the evaluated fuels, this condition is satisfied by maintaining a maximum allowable leak rate of 6.39×10^{-7} ref. cm³/sec (air) at standard temperature and pressure conditions for normal conditions of transport as shown in Table 4.2-4. The equivalent maximum allowable helium leak rate is 1.06×10^{-6} std cm³/sec (helium). To ensure that the maximum allowable leak rate is not exceeded, the cask is conservatively leak tested to 5.5×10^{-7} std cm³/sec (helium). As shown in Table 4.3-2, the allowable leak rate for accident conditions is larger. For the transport of TPBAR contents, a leaktight containment boundary is required. Leaktight is defined per ANSI N14.5-1997 to be 1×10^{-7} ref cm³/sec (2×10^{-7} std cm³/sec helium).

The limiting transport contents for the containment analysis for non-TPBAR contents are 25 BWR high burnup fuel rods, assuming that 56%, or 14, of the fuel rods are classified as damaged. The analysis is based on the assumption that the fuel rods fail in transport, which is considered to bound the condition in which the fuel is already damaged. This is conservative since fuel classified as damaged is likely to have already lost initial charge and fission gases prior to loading in the transport cask. The calculated allowable leak rate for the 14 failed rod configuration is 1.06×10^{-6} std cm³/sec (helium). This value is greater than the helium leak test condition of 5.5×10^{-7} cm³/sec (helium). Therefore, transport of 25 high burnup PWR or BWR fuel rods, with up to 14 of the fuel rods classified as damaged, is acceptable.

The PULSTAR fuel element containment evaluations, compliant with a 10 CFR 71 B(U)F-96 designation as specified in the TS-R-1 compliance document, are presented in Section 4.5.8. Both intact and damaged fuel payloads are acceptable per the revised 10 CFR 71.63, as the plutonium produced in the PULSTAR fuel elements is in solid form.

The structural and thermal evaluations of the NAC-LWT are provided in Chapters 2 and 3, respectively. Results of these evaluations demonstrate that cask containment is maintained during normal conditions of transport and hypothetical accident conditions. Therefore, the package satisfies the containment requirements of 10 CFR 71.51

4.2.1 Containment of Radioactive Material

The 10 CFR 71 limit for the release of radioactive material under normal conditions of transport is 10^{-6} A₂/hr. The A₂ value for a mixture of isotopes is determined by using the method described in 10 CFR 71, Appendix A. The assumed release fractions for the cask contents, with

the exception of MTR and DIDO fuel assemblies, are obtained from NUREG/CR-6487 (Anderson) and are summarized in Table 4.2-1. The isotope curie contents for the cask design basis PWR and BWR fuel assemblies, 25 PWR or BWR high burnup rods, and TRIGA and MTR fuel elements and DIDO fuel assemblies are provided in Section 4.5.4. The isotopic curie content and displaced volume associated with TRIGA fuel cluster rods are bounded by that of the design basis TRIGA fuel element. As shown below, the allowable leak rate for TRIGA fuel characterized as failed bounds the allowable leak rate for the TRIGA spent fuel described in Table 1.2-1. The containment analyses for MTR and DIDO fuel are presented in Sections 4.1.1 and 4.5.7 and are performed in accordance with the methodology presented in "Bases for Containment Analysis for Transportation of Aluminum-Based Spent Nuclear Fuel," WSRC-TR-98-00317, October 1998. Spiral fuel and MOATA plate bundle ANSTO basket payloads are comprised of MTR/DIDO type fuel plates and rely on the bounding containment evaluations performed for the similar DIDO basket. Further discussions of the ANSTO basket payloads are included in Section 4.5.10.

The allowable leak rate for BWR fuel is primarily determined by the postulated concentration of ^{60}Co in crud that is assumed to coat the external surface of the fuel rods and channel of the BWR fuel assemblies. Crud is a mixture of impurities that are deposited on the exterior of the fuel assembly by reactor cooling water during power generation. NUREG/CR-6487 estimates the maximum ^{60}Co concentrations on spent fuel assemblies to be $140 \mu\text{Ci}/\text{cm}^2$ for PWR assemblies and $1,254 \mu\text{Ci}/\text{cm}^2$ for BWR assemblies at initial discharge. The calculated concentration, based on assembly surface area, is decayed 2 years based on the required cool time for design basis PWR and BWR fuel.

The combined payload isotopic content of the two General Atomics (GA) Irradiated Fuel Material (IFM) Fuel Handling Units (FHUs) is 3403 Ci, 86% of which is for the TRIGA elements in the RERTR/IFM FHU. Based on the FLIP-LEU II TRIGA element data in Table 4.5-7 through Table 4.5-9, the design basis activity inventory for a single TRIGA element is 2094 Ci. However, since up to 140 design basis elements can be loaded in the poisoned TRIGA basket, the cask inventory is 293,174 Ci. This bounds the 3403 Ci of the combined GA IFM payload (by a factor of more than 80). Thus, no containment evaluation is necessary for the NAC-LWT loaded with GA IFM.

4.2.1.1 Calculation of Permissible Leak Rates

The maximum permissible leak rate from the cask under normal conditions of transport is determined from the 10 CFR 71 limit of $10^{-6} \text{ A}_2/\text{hr}$:

$$R_N = L_N C_N \leq A_2 \times 10^{-6} \text{ hr}^{-1} \text{ or } 2.78 \times 10^{-10} \text{ sec}^{-1}$$

where:

L_N = allowable volumetric gas leakage rate [cm^3/s]

C_N = curies per unit volume (termed “activity density”) of the radioactive material that passes through the leak path [Ci/cm^3]

R_N = Release rate for normal transport conditions [Ci/sec]

Activity Density of Radioactive Material (C_N)

The total inventory of fission product gases, volatiles, fines and crud for the design basis PWR and BWR spent fuel are shown in Table 4.5-1 through Table 4.5-6. The inventories are calculated using the source terms produced by the SAS2H sequence (Hermann) and applying the release fractions (Table 4.2-1) and the postulated ^{60}Co content of the crud. The ^{60}Co content is decayed 2 years from discharge to the design basis fuel cool time. The PWR crud analysis is based on a single design basis fuel assembly, while the BWR crud analysis is based on 2 design basis fuel assemblies. The total inventories for metallic fuels are calculated in the same way, conservatively applying the release fractions for PWR and BWR spent fuel. Crud does not contribute to the source term for metallic fuels, as crud formation is not considered to be a significant contaminant for MTR, research reactor, and other metallic fuels. The radionuclide inventory of the bounding TRIGA fuel element, the FLIP LEU with type II end fittings, is shown in Table 4.5-7 through Table 4.5-9, for gases, volatiles and fines, respectively. The radionuclide inventory of the TRIGA fuel cluster rods is bounded by that of the design basis TRIGA fuel element. The radionuclide inventory of the bounding MTR fuel element is similarly shown in Table 4.5-10 through Table 4.5-12. The radionuclide inventory of the bounding DIDO fuel assembly is shown in Table 4.5-19 through Table 4.5-21. As indicated by the bounding source described in Chapter 5 and further discussed in Section 4.5.10, the spiral fuel assemblies and MOATA plate bundles in the ANSTO basket are bounded by DIDO evaluations.

As shown in Table 4.2-2, the allowable leak rate for TRIGA fuel characterized as failed bounds the allowable leak rate of the design basis PWR and BWR fuel, the intact high burnup 25 PWR or BWR rod configuration, and other MTR, research reactor, and the other metallic fuels considered. However, the 56% failed, high burnup 25 PWR or BWR fuel rod configuration allowable release rates are the most restrictive, as shown in Section 4.5.6.

The total activity density for the contents of the cask, C_N , is:

$$C_N = C_{\text{Crud}} + C_{\text{Volatiles}} + C_{\text{Fission Gas}} + C_{\text{Fines}}$$

The activity density for crud is:

$$C_{\text{crud}} = \frac{f_C M_T}{V} = \frac{f_C S_C N_A (N_R S_{AR} + S_{Ch})}{V}$$

where:

C_{crud} = activity density inside containment vessel resulting from crud spallation [Ci/cm³]

M_T = total crud activity inventory [Ci]

f_C = crud spallation factor

V = free volume inside containment vessel [cm³]

S_C = crud surface activity [Ci/cm²]

N_R = number of fuel rods per assembly

N_A = number of assemblies

S_{AR} = surface area per rod [cm²]

S_{Ch} = channel surface area [cm²] (BWR fuel only).

The activity density for fuel fines (particulates) is:

$$C_{\text{fines}} = \frac{f_F W_R A_R N_R N_A f_B}{V}$$

where:

C_{fines} = activity concentration inside containment vessel resulting from fines released from cladding breaches [Ci/cm³]

f_F = fraction of fuel rod's mass released as fines resulting from cladding breach

f_B = fraction of fuel rods that develop cladding breach

W_R = mass of the fuel in fuel rod [g]

N_R = number of fuel rods per assembly

N_A = number of assemblies

A_R = specific activity of fines emitted from cladding breach in fuel rod [Ci/g]

V = containment vessel void volume [cm³].

The activity density for isotopes characterized as volatile and gaseous is:

$$C_{\text{vol\&gas}} = C_{\text{vol}} + C_{\text{gas}} = \frac{N_R N_A f_B W_R (A_V f_V + A_G f_G)}{V}$$

where:

$C_{\text{vol\&gas}}$ = releasable activity concentration inside the containment vessel resulting from gases and volatiles released from cladding breaches [Ci/cm³]

C_{vol}	=	releasable activity concentration inside the containment vessel resulting from volatiles released from cladding breaches [Ci/cm ³]
C_{gas}	=	releasable activity concentration inside the containment vessel resulting from gases released from cladding breaches [Ci/cm ³]
W_R	=	mass of the fuel in a fuel rod [g]
N_R	=	number fuel rods per assembly
N_A	=	number of assemblies
f_B	=	fraction of rods that develop cladding breaches
A_v	=	specific activity of volatiles in fuel rod [Ci/g]
f_v	=	fraction of volatiles in fuel rod released if rod develops cladding breach
A_G	=	specific activity of gas in fuel rod [Ci/g]
f_G	=	fraction of gas that would escape from fuel rod that develops cladding breach
V	=	is the void volume inside containment vessel [cm ³].

Activity Values for Radionuclides

A_2 values for the design basis PWR and BWR fuel crud, gases and volatiles, and fuel fines are shown in Section 4.5.4, and summarized in Table 4.5-1 through Table 4.5-6. For those isotopes for which no specific A_2 value is specified, the generic values listed in 10 CFR 71, Table A-2, are applied. The A_2 value for mixtures of isotopes is calculated from:

$$A_2 = \frac{1}{\sum \frac{F_i}{A_2^i}}$$

where:

$$F_i = \frac{S_i}{S_n}$$

F_i = The fraction of isotope i with respect to the entire mixture

S_i = The activity isotope i (Curies)

S_n = The total group activity (Curies)

A mixture A_2 value is determined for gases, volatiles, fines, and crud. These A_2 values are then combined, using the same formula, to obtain a total cask mixture A_2 value. Based on the releasable curie content and the cask contents A_2 value, the allowable leak rate for the various spent fuel contents are summarized in Table 4.2-2.

Maximum Allowable Leak Rates

Using the methodology described above, the bounding maximum allowable leak rate for all of the NAC-LWT cask contents is calculated to be 1.32×10^{-6} cm³/sec. This leak rate analysis is based on the conservative assumption that 56% of the 25 high burnup fuel rods, or 14 fuel rods, fail in transport.

The results of the leak rate analysis of the high burnup fuel rods and the other NAC-LWT fuel contents are shown in Table 4.2-2. The allowable release rate for HEU MTR fuel is specified as it bounds the allowable release rate for MEU and LEU MTR fuel. Similarly, the allowable release rate for LEU DIDO fuel is specified, since it bounds the allowable release rate for HEU and MEU DIDO fuel. The evaluations of MTR and DIDO fuel are presented in Sections 4.1.1 and 4.5.7, respectively. Based on these results, a helium leak test value of 5.5×10^{-7} cm³/sec is used to demonstrate containment of the NAC-LWT spent fuel contents. As shown in Table 4.2-4, this test leak rate is conservative with respect to the calculated maximum allowable leak rate for the cask contents. A leaktight containment boundary is required for the transport of TPBAR contents.

The allowable release rate of the TRIGA fuel is more restrictive than for the design basis PWR or BWR assemblies because of the application of the postulated release fractions for light water reactor fuel to the metallic TRIGA fuel. This application is highly conservative as the metallic fuel is less subject to the release of volatile isotopes and fuel fines due to fabrication methods employed in making the fuel. Based on a report by General Atomics for Lockheed Martin Idaho Technologies Company, "Uranium-Zirconium Hydride Fuels for TRIGA Reactors," (UZR-28, June 1997) fission gas release from an unclad TRIGA element is less than 0.01% at a temperature of 400°C. The maximum accident temperature for the TRIGA cask is conservatively assumed to be 756°F (402°C) with air in the cask. The maximum calculated accident average cavity gas temperature is 574°F (301°C) as shown in Section 3.5.3.2. A conservative release fraction of 1% is employed in the containment evaluation. A 1% release represents the release fraction of the fuel at 800°C.

4.2.1.2 Correlation of Permissible Leak Rates to Air Standard

The maximum allowable release must be correlated to air standard leak rates, which depend on gas temperatures, pressures, and leak path. This correlation requires calculation of the capillary opening diameter through which the flow occurs. Depending on pressure and condition of the flow, two flow regimes are evaluated: continuum and molecular flow. Continuum flow and molecular flow equations are obtained from NUREG/CR-6487, Section 2. Continuum and molecular flow can occur simultaneously and are so treated in this analysis. Both continuum and molecular flow rate equations presented below are adjusted to upstream flow rate.

The continuum volumetric flow rate of the gas (cm³/sec), L_c , is given by:

$$L_c = \frac{2.48 \times 10^6 D^4}{8 \mu} (P_u - P_d) \frac{P_a}{P_u} = F_c (P_u - P_d) \frac{P_a}{P_u}$$

where:

L_c = continuum flow rate of gas at P_u [cm³/sec]

F_c = coefficient for continuum flow [cm³/atm-s]

D = capillary diameter [cm]

A = capillary length [cm]

μ = fluid viscosity [cP]

P_u = upstream pressure [atm] - pressure inside containment

P_d = downstream pressure [atm] - pressure outside containment

The molecular volumetric flow rate of the gas (cm³/sec), L_m , is given by:

$$L_m = \frac{3.81 \times 10^3 D^3}{8 A P_a} \sqrt{\frac{T}{M}} (P_u - P_d) \frac{P_a}{P_u} = F_m (P_u - P_d) \frac{P_a}{P_u}$$

where:

L_m = molecular volumetric flow rate of gas at P_u [cm³/sec]

F_m = coefficient for molecular flow [cm³/atm-s]

D = capillary diameter [cm]

T = gas temperature [K]

M = gas molecular weight [g/mole]

P_a = average pressure $(P_u + P_d)/2$ [atm]

P_u = upstream pressure [atm]

P_d = downstream pressure [atm]

A = capillary diameter [cm]

For this analysis, the gas temperature used for molecular flow analysis is identical to the upstream temperature.

Based on the maximum allowable leakage rate, the flow rate equations are solved for the capillary diameter. Air standard (reference) properties for air are then substituted into the flow equations to arrive at the air standard leakage rate (L_R) and leak test sensitivity. Standard conditions represent leakage at 298K, flowing from an upstream pressure of 1 atmosphere, to a

downstream pressure of 0.01 atmospheres. To complete the analysis, helium leak rates are calculated for the NAC-LWT limiting contents at standard conditions.

The cask pressure, P_u , is determined based on the pressure conditions for the design basis PWR fuel as described in Section 4.2.2. This pressure is conservative because the metallic fuel, including MTR, TRIGA and DIDO fuel, does not contain an initial charge of helium gas. The temperature applied is that for the type of fuel considered in the leak rate evaluation as shown in Table 4.2-3.

4.2.2 Pressurization of Containment Vessel

The maximum pressure in the cask during normal conditions of transport for the fissile material payloads is calculated by using the methodology presented in Section 3.4.4. Assumptions underlying this calculation are that during normal conditions of transport, 3% of the fuel rods may fail and that 30% of the fission gases in the rods are releasable. In addition, for LWR high burnup rods, 56% of the rods with oxide layers greater than 70 micrometers (14 rods) are assumed to fail during transport. This is conservative since fuel rods classified as damaged may have released fission and charge gases prior to transport. Failed rods are assumed to have released the fission gas prior to transport. The cask cavity is backfilled to 1 atm with 99.9% pure helium gas.

The gas volume (e.g., plenum and pellet to cladding gap) inside the fuel rods is conservatively neglected when calculating the cask free volume. The maximum normal conditions cavity pressure for the PWR fuel configuration is 1.99 atm. This pressure is conservatively applied to all the fuels (except in the 25 PWR/BWR high burnup fuel rod analysis) to establish the allowable leak rate. The pressure is conservative since the metallic fuels contain no initial charge of helium gas and release a lower percentage of fission product gases. The maximum normal condition cavity pressure used for the 25 intact PWR/BWR high burnup fuel rod analysis is 2.1 atm. For the 25 BWR/PWR rod analysis with 56% fuel rod failure, the maximum normal condition cavity pressure is 3.2 atm for the BWR analysis, and 3.0 atm for the PWR analysis, respectively.

Normal condition system maximum normal operating pressure (MNOP) for the transport of up to 300 production TPBARs (including up to 2 prefailed rods) is conservatively determined in Section 3.4.4.5 as 289 psig. The TPBAR normal condition pressure assumed clad failure of all 300 TPBARs during transport. The pressure for the second TPBAR content condition of 55 segmented TPBARs contained in a waste container is bounded by the 300 TPBAR MNOP.

4.2.3 Containment Criteria

The standard leak rate provided in Table 4.2-4 for fissile material shipments represents the maximum leak rate allowed if the seals were to be tested with air at an upstream pressure of 1 atm and a downstream pressure of 0.01 atm at a temperature of 25°C. This is the maximum allowable leak rate for the containment system fabrication verification and periodic verification leak tests described in Section 4.1, and in Chapter 8.

As specified in Section 4.1.2, the containment boundary is leak tested to 5.5×10^{-7} std cm³/sec (helium). The sensitivity for these tests is required by ANSI N14.5-1997 to be one-half the test leak rate, or 2.75×10^{-7} std cm³/sec (helium).

The standard leak rate for leaktight shipment per ANSI N14.5-1997 is 1×10^{-7} ref cm³/sec, which is equivalent to a helium leak rate of 2×10^{-7} std cm³/sec. Test sensitivity for the 1 atm to vacuum helium leak test for the leaktight containment boundary is 1×10^{-7} cm³/sec (helium). Leaktight containment boundary requirements are imposed on TPBAR shipments.

Table 4.2-1 Release Fractions: Normal and Accident Conditions

Radionuclide Origin	Fraction: Normal Conditions	Fraction: Accident Conditions
Fuel Assumed to Fail	0.03 ¹	1.0
Fission Gas Released ²	0.3	0.3
Volatiles Released	0.0002	0.0002
Fuel Mass Released as Fines	0.00003	0.00003
Crud Spallation ³	0.15	1.0

¹ 56% for > 70 micrometer oxide layer rod shipment.

² The release fraction from TRIGA and NRX fuel is taken as 0.01.

³ Applied only to BWR and PWR spent fuel.

Table 4.2-2 Allowable Release Rates for NAC-LWT Cask Contents: Normal Conditions

Fuel Type	Crud (Ci)	Gas (Ci)	Volatiles (Ci)	Fines (Ci)	Total (Ci)	A ₂ (Ci)	L _N (cm ³ /sec)
WE 15x15	4.397	36.144	1.173	0.400	42.114	36.603	3.56E-05
GE 7x7	42.808	24.611	0.827	0.275	68.521	15.525	6.41E-06
Metallic (NRX - 15 Intact Rods)	---	0.103	0.106	0.095	0.304	2.793	2.60E-04
Metallic (NRX -9 Failed Rods)	---	2.059	2.129	1.894	6.082	2.793	1.30E-05
25 PWR Rods	0.602	7.930	0.456	0.242	9.231	12.295	5.45E-05
MTR ¹	0.019	108.851	0.012	1.829	110.711	24.745	1.42E-05
DIDO ²	0.011	53.613	0.005	8.161	61.789	7.996	1.32E-05
TRIGA (Intact)	---	1.011	0.697	0.156	1.864	6.161	1.58E-04
TRIGA ³ (Failed)	---	14.086	9.711	2.179	25.976	6.161	1.13E-05
25 PWR Rods – 56% Failed	0.773	194.727	37.154	23.708	256.362	17.473	1.83E-06
25 BWR Rods – 56% Failed	9.236	293.314	44.234	26.349	373.133	19.828	1.32E-06

¹ As evaluated in Section 4.5.5, the listed values are for HEU MTR elements, which bound the LEU and MEU MTR fuel elements.

² As evaluated in Section 4.5.7, the listed values are for LEU DIDO assemblies, which bound the MEU and HEU DIDO fuel assemblies.

³ Assumes 84 intact elements and 56 failed elements in sealed cans.

Table 4.2-3 Cask Free Volumes and Pressures

Fuel Type	Pressure (atm)		Temperature (K)	Free Volume (10 ⁵ cm ³)
	Normal	Accident		
PWR	1.99 ¹	11.4 ¹	517.4	1.471
BWR	1.99 ²	11.4 ²	517.4	1.018
Metallic Fuel	1.99 ²	11.4 ²	405.2	1.018
MTR	1.99 ²	11.4 ²	470.2	2.293
DIDO	1.99 ²	11.4 ³	433.2	3.681
TRIGA	1.99 ²	11.4 ²	571.4 ²	1.717
GA IFM	N/A ⁶	N/A ⁶	403.2	3.354
25 PWR Rods – 56% Failed Fuel Fraction	3.0	4.3 ⁵	588.7 ⁴	0.9681
25 BWR Rods – 56% Failed Fuel Fraction	3.2	4.5 ⁵	588.7 ⁴	0.8932

¹ Based on Sections 3.4.4 and 3.5.4, the maximum calculated pressures for the PWR payload are 1.93 atm (28.3 psia) normal condition and 8.56 atm (125.8 psia) accident conditions. The higher pressures used in the analyses are conservative since a higher pressure will result in a smaller leak diameter and reduced leak test requirements.

² The maximum pressure for the PWR fuel is conservatively applied.

³ The temperature employed is approximately 4K lower than the maximum fuel clad temperature calculated. The fuel clad temperature is significantly higher than the average gas temperature in the cask. By combining the listed temperature with the cask maximum pressure (PWR fuel) conservative leak rates are calculated.

⁴ The normal condition temperature is conservatively applied to the 25 PWR and BWR high burnup rod analysis.

⁵ These pressures result from the 100% fuel rod failure plus the design basis fire accident.

⁶ Based on the lower temperature and larger free volume of the GA IFM, as compared to the other contents, the pressure, although not explicitly calculated, is lower than that calculated PWR and BWR fuel.

Table 4.2-4 Leak Rate and Leak Test Sensitivity - Normal Conditions

Fuel Type ¹	Assembly Type	Volumetric	Leak Rate (cm ³ / sec)			Test (helium) ²
		Activity (Ci/cm ³)	Allowable (L _N)	Allowable (air) (L _R)	Allowable (helium)	
BWR	GE 7x7	6.73E-04	6.41E-06	5.35E-06	7.66E-06	5.50E-07
TRIGA (Failed) ³	FLIP-LEU II	1.51E-04	1.13E-05	9.90E-06	1.36E-05	5.50E-07
MTR	HEU	4.83E-04	1.42E-05	1.19E-05	1.62E-05	5.50E-07
DIDO	LEU	1.68E-04	1.32E-05	1.46E-05	4.54E-06	5.50E-07
25 BWR Rods – 56% Failed Fuel Fraction	Exxon 7x7	4.18E-03	1.32E-06	6.39E-07	1.06E-06	5.50E-07

¹ The bounding TRIGA fuel element is the FLIP-LEU II.

² Containment Verification Leak Test. Test Sensitivity is 2.75E-07 std. cm³/sec (helium).

³ Assumes 84 intact TRIGA elements and 56 failed elements in sealed cans.

4.3 Containment Requirements for Hypothetical Accident Conditions

The 10 CFR 71 requirement for the release of radioactive material under hypothetical accident conditions is met by ensuring that the requirement is met for the bounding fissile material contents, 140 TRIGA fuel elements, 56 of which are characterized as failed. Calculation of the allowable release rate is provided in Section 4.3.2.

The structural integrity of the cask containment during hypothetical accident conditions is demonstrated in Section 2.7. Therefore, the cask containment is maintained under hypothetical accident conditions.

As shown in Table 4.3-2, the allowable release rate in the hypothetical accident condition is significantly larger than that for normal conditions of transport. Consequently, the bounding allowable leak rate is that for the failed TRIGA fuel as calculated in Section 4.2.1.

Containment for shipment of the TPBARs is demonstrated by leaktight testing to 1×10^{-7} ref cm³/sec. Per ANSI N14.5, the equivalent helium leakage rate for leaktight conditions is 2×10^{-7} cm³/sec.

PULSTAR fuel element specific analyses are compliant with B(U)F-96 requirements as documented in Section 4.5.8.

4.3.1 Fission Gas Products

The accident conditions for maximum fission gas release assumes 100% rod failure and also assume that 30% of the tritium and 30% of the ⁸⁵Kr are available for release to the cask cavity. In addition, 100% of the ⁶⁰Co in the crud on the design basis PWR and BWR fuel assemblies is conservatively assumed to be available for release as an aerosol. Due to the crud contamination of the BWR assembly, its allowable leak rate bounds that of the PWR fuel. The metallic fuels do not contain significant amounts of fission gas that are available for immediate release and do not have significant levels of crud. TRIGA fuel elements are assumed to release 1% of their fission gas products under accident conditions.

4.3.2 Containment of Radioactive Materials

The NAC-LWT cask is designed to maintain a release rate of less than 1 A₂/week for the hypothetical accident conditions, as required by 10 CFR 71.51. The A₂ for the mixed radionuclides considered to be available for release is determined by using the method described in 10 CFR 71, Appendix A. The release fractions for the various radionuclides found in the cask are obtained from NUREG/CR-6487 and are summarized in Table 4.2-1. The A₂ per week limit is not exceeded for any NAC-LWT contents, based on the leak test described in Section 4.1.3.

4.3.2.1 Calculation of Allowable Leak Rates

The allowable leak rates under hypothetical accident conditions are calculated by using the method described in Section 4.2.1.1 for normal conditions of transport. The total inventory of fission product gases, volatiles, fines, and crud are calculated by using the source terms generated by SAS2H. The assumed release fractions are shown in Table 4.2-1. Using the A_2 values from 10 CFR 71, Appendix A, the mixture A_2 values are determined for gas, volatile, fine, and crud mixtures for the bounding accident condition fuel contents (WE 15 × 15 PWR) as shown in Table 4.3-1. For the 25 PWR and BWR high burnup rod analysis, A_2 values were also determined and are reported in Table 4.3-3 (PWR) and Table 4.3-4 (BWR). The maximum allowable release rates are calculated by using the hypothetical accident condition allowable release limit:

$$R_A = L_A C_A \leq A_2 \times \text{week}^{-1} = A_2 \times 1.65 \times 10^{-6} \text{ sec}^{-1}$$

where:

L_A = volumetric gas leak rate [cm^3/s]

C_A = curies per unit volume (termed “activity density”) of the radioactive material that passes through the leak path [Ci/cm^3]

R_A = release rate for accident transport conditions

Assumptions underlying the calculations for the hypothetical accident conditions are that 100% of the fuel cladding fails and 100% of the crud is released. The mixture A_2 value for the hypothetical accident conditions is calculated using the methodology of Section 4.2.1.1, applying the accident condition release fractions of Table 4.2-1.

The calculated maximum allowable hypothetical accident condition leak rate for the design basis PWR and BWR spent fuel, and for metallic fuel rods and TRIGA fuel characterized as failed, are tabulated in Table 4.3-2. The calculated maximum allowable hypothetical accident condition leak rate for the 25 PWR and BWR high burnup rod analysis is also reported in Table 4.3-2.

4.3.2.2 Correlation of Allowable Leak Rates to Standard Leak Rates

The maximum allowable leak rates for the hypothetical accident conditions are corrected to standard leakage rates using the methodology described in Section 4.2.1.2. The results are tabulated in Table 4.3-2 for the design basis PWR and BWR spent fuel, MTR HEU elements, DIDO LEU assemblies and 140 TRIGA fuel elements, with 56 elements characterized as failed prior to loading in the cask.

4.3.2.3 Containment Criteria

For fissile material payloads evaluated, the allowable leak rates for the hypothetical accident conditions are much greater than those for the normal conditions of transport calculated in Section 4.2.1. Because the cask containment is demonstrated to be maintained under hypothetical accident conditions (Section 2.7), the maximum permissible leak rates for normal conditions of transport are more limiting and are, therefore, used for the establishment of the maximum allowable leak rates for the containment system fabrication and periodic verification leak tests. For TPBAR shipments, a leaktight containment boundary is maintained.

4.3.2.4 Tritium Permeation Rate of Seals for TPBAR Shipment

The release of tritium into the cask cavity from all 300 rods, 298 rods that are event-failed and 2 rods defined to be prefailed, has the potential of releasing a significant quantity of tritium ($> 1A_2$) into the cask cavity. As shown in the structural analysis, the lid and port cover seals retain their ability to provide cask closure during all accident conditions. To assure that the accident release limit of $1A_2/\text{week}$ is not exceeded under accident conditions the port and lid seal permeation rates are evaluated.

The formula for permeation through metal is:

$$PR = \Phi \times A / l \times (P_p)^{1/2}$$

where:

PR = equilibrium (steady-state) permeation rate in std cc (permeate) per sec

Φ = permeability in std cc (permeate) per second per material surface area per permeate partial pressure $1/2$ through a unit material thickness

A = material surface area that is "exposed" to the permeate

l = material thickness through which the permeate "passes"

P_p = upstream permeate partial pressure

The formula for permeability is:

$$\Phi = \Phi_0 \times \exp\left(-\frac{E_\Phi}{RT}\right)$$

where:

Φ = permeability as stated previously

Φ_0 = pre-exponential permeation factor in the same units as Φ

E_Φ/R = the activation energy of the permeation process, which has been 'normalized' by the universal gas constant

T = absolute temperature of the metal (K).

Combining the permeation equations with an activity density of 0.16 Ci/cc, resulting from the release of 55 Ci per event failed rod and 0.199 moles of tritiated water for each prefailed rods, and

T = 572K – Maximum accident temperature for the seals per Table 3.5-1

Φ_o = 7.42×10^{-2} [LLNL Report UCRL-53441] (stainless steel port seal),
 2.10×10^{-2} [Fusion Science and Technology] (inconel lid seal)

$E_{\Phi/R}$ = 7,700 (stainless steel port seal), 7490 [Fusion Science and Technology]
(inconel lid seal)

l = 0.012 inch for the port cover seal (only considering the stainless steel portion of the seal) and 0.032 inch for the lid seal

P_p = 0.15 atm – tritium partial pressure in the cask cavity based on the cask free volume, accident condition temperature, and a release of 55 Ci of tritium per event failed rod (conservative modeled as isotope not molecular tritium) and 0.199 moles of tritiated water from the prefailed rods)

yields an approximate release through seal permeation of 5 Ci/week compared to the allowable accident release rate of 1.1×10^3 Ci/week (1A₂/week based on an A₂ value for tritium of 1.1×10^3 Ci).

Actual permeation release rates would be significantly lower as the accident temperatures are short term, with elevated temperatures at the seal locations returning to normal condition temperatures within an hour of the fire.

Similar calculations are performed for the 55 equivalent TPBARs, in segments and debris, which may release up to 100% of the tritium contained in the pellets during transport. The pellet tritium content represents approximately 40% of the tritium quantity in the TPBAR. At NAC-LWT normal and accident conditions temperatures, the TPBAR components release tritium primarily as tritiated water with only a small fraction (maximum 2%) as gaseous tritium (see Appendix 1-B of Chapter 1). Gaseous tritium represents the basis for the seal permeation evaluation. During a one-year transport, an additional maximum 1% of the tritiated water may undergo radiolysis and dissociate. Conservatively applying a maximum 3% release rate to the 55 equivalent TPBAR total inventory of 66 grams (1.2 grams per rod) yields an inventory of 0.33 moles T₂. Seal permeation rates based on the conservative temperatures discussed in the previous paragraphs and a 3% tritium gas release are 6.5×10^{-6} Ci/hr, normal conditions, and 1.06 Ci/week, accident conditions. A gaseous release of over 90% of the 1.2 grams per rod tritium inventory is required to exceed normal condition allowables at the conservative seal temperature of 222°F. A 100% gaseous release and resulting tritium permeation through the cask seals meets accident condition limits. Reducing seal temperatures less than 5°F, to account for a significantly lower decay heat

payload (0.127 kW for the waste container TPBARs versus 1.05 kW on which the 222°F temperature is based), permits a normal condition release of 100% of the tritium in gaseous form while meeting the 10^{-6} A₂/hr allowable.

4.3.3 Tritium Contamination Issues

Precautions will be taken to minimize the risk of excessive contamination of NAC-LWT casks during the loading and unloading of TPBAR contents to ensure the reusability of the NAC-LWT casks for transport of non-TPBAR contents. In addition to ensuring the safe handling of TPBAR contents, additional cavity gas and internal and external removable contamination surveys for tritium contamination will be implemented at all TPBAR loading and unloading facilities. The specific monitoring methods and levels of contamination to which the cask surfaces must be decontaminated are defined in the TPBAR loading and unloading procedures in Chapter 7. In addition, the TPBAR procedures also include precautions for users to observe when loading, unloading and handling TPBARs.

The procedures and precautions comply with the recommended practices of NUREG-1609, Supplement 2. The results of previous loading and unloading experiences regarding the measurement of tritium gas and contamination levels are provided in the PNNL letter in Section 1.5, Appendix 1-G of this SAR.

NAC-LWT cask units used for TPBAR transports shall comply with the specified contamination levels, or other non-TPBAR users will be advised to incorporate tritium monitoring requirements into their survey procedures and radiological control program.

Table 4.3-1 A₂ Calculation for PWR Spent Fuel

	Crud	Gas	Volatiles	Fines	Total
Total Activity per Assembly (Ci)	2.931E+01	4.016E+03	1.955E+05	4.446E+05	6.441E+05
Releasable Activity per Cask (Ci)	2.931E+01	1.205E+03	3.910E+01	1.334E+01	1.287E+03
Cask Volumetric Activity (Ci/cm ³)	1.992E-04	8.188E-03	2.658E-04	9.065E-05	8.744E-03
A ₂ Value (Ci)	11.00000	281.42094	8.72766	0.81991	3.020E+02
Fraction of Activity	0.02278	0.93646	0.03039	0.01037	---
Fraction of Activity / A ₂ (1/Ci)	0.00207	0.00333	0.00348	0.01264	0.02152
Mixture A ₂ Value (Ci)					46.458

Table 4.3-2 Standard Leak Rates for Accident Conditions

Fuel Type	Assembly Type	Volumetric Activity (Ci/cm ³)	^{L_A} Allowable Leak Rate (cm ³ / sec)
BWR	GE 7x7	1.12E-02	3.88E-03
PWR	WE 15x15	8.74E-03	8.77E-03
MTR	HEU	1.64E-02	1.35E-03
DIDO	LEU	6.33E-03	1.20E-03
TRIGA (Includes Cans)	FLIP-LEU II	3.62E-04	2.81E-02
25 High Burnup PWR rods	CE 14x14 ¹	4.77E-03	6.02E-03
25 High Burnup BWR rods	Exxon 7x7 ¹	7.97E-03	3.91E-03

¹ Based upon these assemblies, but the active fuel lengths and rod lengths are extended to 150 inches.

Table 4.3-3 A₂ Calculation for 25 High Burnup PWR Spent Fuel Rods

	Crud	Gas	Volatiles	Fines	Total
Total Activity per Assembly (Ci)	5.150E+00	1.159E+03	3.317E+05	1.411E+06	1.744E+06
Releasable Activity per Cask (Ci)	5.150E+00	3.477E+02	6.635E+01	4.234E+01	4.616E+02
Cask Volumetric Activity (Ci/cm ³)	5.320E-05	3.592E-03	6.853E-04	4.373E-04	4.768E-03
A ₂ Value (Ci)	11.00000	283.63841	13.58800	2.12043	3.103E+02
Fraction of Activity	0.01116	0.75337	0.14374	0.09172	1.000
Fraction of Activity / A ₂ (1/Ci)	0.00101	0.00266	0.01058	0.04326	0.05751
Mixture A ₂ Value (Ci)					17.389

Table 4.3-4 A₂ Calculation for 25 High Burnup BWR Spent Fuel Rods

	Crud	Gas	Volatiles	Fines	Total
Total Activity per Assembly (Ci)	6.157E+01	1.746E+03	3.949E+05	1.568E+06	1.965E+06
Releasable Activity per Cask (Ci)	6.157E+01	5.238E+02	7.899E+01	4.705E+01	7.114E+02
Cask Volumetric Activity (Ci/cm ³)	6.894E-04	5.864E-03	8.844E-04	5.268E-04	7.965E-03
A ₂ Value (Ci)	11.00000	283.89694	13.28843	1.93498	3.101E+02
Fraction of Activity	0.08655	0.73627	0.11104	0.06614	—
Fraction of Activity / A ₂ (1/Ci)	0.00787	0.00259	0.00836	0.03418	0.05300
Mixture A ₂ Value (Ci)					18.868

4.4 Special Requirements

The NAC-LWT cask may contain damaged TRIGA fuel elements, or debris, in sealed failed fuel cans. The calculation of allowable and test leak rates for the sealed failed fuel can is similar to the calculation performed for the cask containment boundary. Testing of the cans as a containment boundary is not required per 10 CFR 71.

Table 4.4-1 includes the free volume, temperature, and pressure for the sealed failed fuel can under normal conditions of transport and the hypothetical accident conditions. The A_2 calculation plutonium content of the limiting TRIGA fuel element is listed in Table 4.4-2. Based on the listed conditions, Table 4.4-3 includes the allowable and air standard leak rate (L_R). The helium leak rate at standard conditions is $2.35 \times 10^{-6} \text{ cm}^3/\text{sec (He)}$.

Table 4.4-1 Transport Conditions for the TRIGA Sealed Failed Fuel Can

Transport Condition	Normal	Accident
Pressure (atm)	1.49	1.77
Temperature (K) ¹	571.4	679.8
Free Volume (cm ³)	1269	1269

Table 4.4-2 A₂ Calculation for Two Canned FLIP-LEU II Elements

	Crud	Gas	Volatiles	Fines	Total
Total Activity per Assembly (Ci)	---	2.407E+01	8.297E+02	1.241E+03	2.095E+03
Releasable Activity (Ci)	---	7.149E-01	4.928E-01	1.106E-01	1.318E+00
Volumetric Activity (Ci/cm ³)	---	5.632E-04	3.883E-04	8.714E-05	1.039E-03
A ₂ Value (Ci)	---	279.37074	11.08453	0.26789	2.907E+02
Fraction of Activity	---	0.54226	0.37384	0.08390	---
Fraction of Activity / A ₂ (1/Ci)	---	0.00194	0.03373	0.31319	0.34886
Mixture A ₂ Value (Ci)					2.867

Table 4.4-3 Normal and Accident Condition Leak Rates for the TRIGA Failed Fuel Can

Operating Condition	Vol. Activity Ci/cm ³	Leak Rates (cm ³ /sec)		
		Allowable	Air Standard	Test Sensitivity
Normal	6.994E-05	1.139E-06	1.505E-06	7.27E-07
Accident	6.994E-04	6.763E-03	8.694E-03	N/A



¹ The temperatures employed are approximately 4K lower than the maximum fuel clad temperatures calculated. The fuel clad temperature is significantly higher than the average gas temperature of the can. Employing the listed temperature provides bounding can pressures and leak rates.

4.5 Appendices

4.5.1 Tetrafluoroethylene O-Rings

This appendix contains the SAE International Aerospace Standard AS8791 (Figure 4.5-1), which prescribes the physical and chemical properties of the TFE O-rings. This document replaces Military Specification MIL-R-8791D. These O-rings have an unlimited shelf life.

Figure 4.5-1 SAE International Aerospace Standard AS8791

 <p>SAE The Engineering Society For Advancing Mobility Land Sea Air and Space® INTERNATIONAL 400 Commonwealth Drive, Warrendale, PA 15096-0001</p> <p>AEROSPACE STANDARD</p> <p>Submitted for recognition as an American National Standard</p>	 AS8791	
	Issued 1997-10	
<p>Retainer, Packing, Hydraulic, and Pneumatic, Tetrafluoroethylene Resin</p>		
<p style="text-align: center;">NOTICE</p> <p>This document has been taken directly from U.S. Military Specification MIL-R-8791D and contains only minor editorial and format changes required to bring it into conformance with the publishing requirements of SAE technical standards.</p> <p>The original Military Specification was adopted as an SAE standard under the provisions of the SAE Technical Standards Board (TSB) Rules and Regulations (TSB 001) pertaining to accelerated adoption of government specifications and standards. TSB rules provide for (a) the publication of portions of unrevised government specifications and standards without consensus voting at the SAE Committee level, (b) the use of the existing government specification or standard format, and (c) the exclusion of any qualified product list (QPL) sections.</p> <p>1. SCOPE:</p> <p>1.1 Scope:</p> <p>This specification covers tetrafluoroethylene resin (hereinafter referred to as "TFE") retainers intended for use in hydraulic and pneumatic system components as antiextrusion devices in conjunction with packings and gaskets (see 6.1).</p>		

SAE Technical Standards Board Rules provide that: "This report is published by SAE to advance the state of technical and engineering sciences. The use of this report is entirely voluntary, and its applicability and suitability for any particular use, including any patent infringement arising therefrom, is the sole responsibility of the user."

SAE reviews each technical report at least every five years at which time it may be reaffirmed, revised, or cancelled. SAE invites your written comments and suggestions.

Copyright 1997 Society of Automotive Engineers, Inc.
All rights reserved.

Printed in U.S.A.

QUESTIONS REGARDING THIS DOCUMENT:
TO PLACE A DOCUMENT ORDER:

(412) 772-8510
(412) 776-4870

FAX: (412) 776-0243
FAX: (412) 776-0790

Figure 4.5-1 SAE International Aerospace Standard AS8791 (Continued)

SAE AS8791	
2. APPLICABLE DOCUMENTS:	
2.1 Issue of Documents:	
The following documents, of the issue in effect on date of invitation for bids or request for proposal, form a part of this specification to the extent specified herein:	
SPECIFICATIONS	
FEDERAL	
PPP-B-566	Box, Folding, Paperboard
PPP-B-636	Box, Shipping, Fiberboard
PPP-B-640	Box, Fiberboard, Corrugated, Triple Wall
PPP-B-676	Boxes, Set-Up
MILITARY	
MIL-P-116	Preservation - Packaging, Methods of
MIL-B-117	Bags, Interior Packaging
MIL-P-7936	Parts and Equipment, Aeronautical, Preparation for Delivery
STANDARDS	
MILITARY	
MIL-STD-105	Sampling Procedures and Tables for Inspection by Attributes
MIL-STD-129	Marking for Shipment and Storage
MS27595	Retainer, Packing Backup, Continuous Ring, Tetrafluoroethylene
MS28773	Retainer, Packing Backup, Tetrafluoroethylene, Straight Thread Tube Fitting Boss
MS28774	Retainer, Packing Backup, Single Turn, Tetrafluoroethylene
MS28782	Retainer, Packing Backup, Teflon
MS28783	Ring, Gasket, Backup, Teflon
(Copies of specifications, standards, drawings, and publications required by contractors in connection with specific procurement functions should be obtained from the procuring activity or as directed by the contracting officer.)	

Figure 4.5-1 SAE International Aerospace Standard AS8791 (Continued)

SAE AS8791									
2.2	<p>Other Publications:</p> <p>The following documents form a part of this specification to the extent specified herein. Unless otherwise indicated, the issue in effect on date of invitation for bids or request for proposal shall apply.</p> <p>AMERICAN SOCIETY FOR TESTING AND MATERIALS</p> <table><tr><td>D 570</td><td>Method of Test for Water Absorption of Plastics (Tentative)</td></tr><tr><td>D 747</td><td>Method of Test for Stiffness in Flexure of Plastics (Tentative)</td></tr><tr><td>D 792</td><td>Method of Test for Specific Gravity of Plastics</td></tr><tr><td>D 1708</td><td>Plastics, Tensile Properties of, by Use of Microtensile Specimens</td></tr></table> <p>(Copies of ASTM publications may be obtained upon application to the American Society for Testing and Materials, 100 Barr Harbor Drive, West Conshohocken, PA 19428-2959.)</p>	D 570	Method of Test for Water Absorption of Plastics (Tentative)	D 747	Method of Test for Stiffness in Flexure of Plastics (Tentative)	D 792	Method of Test for Specific Gravity of Plastics	D 1708	Plastics, Tensile Properties of, by Use of Microtensile Specimens
D 570	Method of Test for Water Absorption of Plastics (Tentative)								
D 747	Method of Test for Stiffness in Flexure of Plastics (Tentative)								
D 792	Method of Test for Specific Gravity of Plastics								
D 1708	Plastics, Tensile Properties of, by Use of Microtensile Specimens								
3.	<p>REQUIREMENTS:</p>								
3.1	<p>Materials:</p> <p>The material shall be tetrafluoroethylene resin, hereinafter referred to as "TFE". Reprocessed TFE shall not be used. Bar stock and heavy wall tubing from which parts are machined shall be molded, sintered, baked, and annealed as specified below.</p>								
3.1.1	<p>Color: Color shall be uniformly white with no noticeable streaky or blotchy appearance. A slight brownish tint or presence of scattered brownish specks will not be considered detrimental. The surface shall have a waxy sheen. A dead chalklike appearance usually indicates porosity or other unsatisfactory properties. There shall be no noticeable grainy appearance.</p>								
3.2	<p>Data:</p> <p>Unless otherwise specified in the contract or order, no data is required by this specification or any of the documents referenced in Section 2 (see 6.2).</p>								
3.3	<p>Design and Construction:</p>								
3.3.1	<p>Shape and Dimensions: The shape and dimensions of the TFE retainers shall conform to MS27595, MS28773, MS28774, MS28782, and MS28783 as applicable (see 6.2).</p>								
3.4	<p>Physical Properties:</p> <p>The physical properties of the finished retainers and test specimens shall be uniform throughout and shall satisfy the following requirements, when tested as specified in 4.5.1.</p>								

Figure 4.5-1 SAE International Aerospace Standard AS8791 (Continued)

SAE AS8791	
3.4.1	Tensile Strength: The tensile strength shall be not less than 3,000 pounds per square inch (psi), when tested in accordance with 4.5.1.1.
3.4.2	Elongation: The elongation shall be not less than 75 percent before fracture, when tested in accordance with 4.5.1.2.
3.4.3	Stiffness: The stiffness shall be a minimum of 45,000 psi when tested in accordance with 4.5.1.3.
3.4.4	Water Absorption: There shall be no water absorption in excess of 0.005 percent or decrease of soluble matter, when tested in accordance with 4.5.1.4.
3.4.5	Dimensional Stability: The circumferential length of the finished retainer shall not change more than 0.002 inch per inch and the cross-sectional dimensions of TFE material shall conform to the applicable military standard when tested in accordance with 4.5.1.5.
3.4.6	Specific Gravity: The specific gravity value shall be 2.150 to 2.220, when tested in accordance with 4.5.1.6.
3.4.7	Porosity: The retainers shall exhibit no noticeable porosity, when tested in accordance with 4.5.1.7.
3.5	Workmanship:
3.5.1	Finish: Workmanship and finish of the end product shall be uniform in quality and condition. It shall be clean, smooth, and free from foreign materials and from imperfections detrimental to fabrication, appearance, or performance.
3.5.2	Fabrication: Retainers shall be cut from stock having diameters equal to those intended for the end product, if available. If stock material is not available, semifinished machine stock may be employed and processed in accordance with 3.4.5.
4.	QUALITY ASSURANCE PROVISIONS:
4.1	Responsibility for Inspection: Unless otherwise specified in the contract, the contractor is responsible for the performance of all inspection requirements as specified herein. Except as otherwise specified in the contract, the contractor may utilize his own facilities or any commercial laboratory acceptable to the Government. The Government reserves the right to perform any of the inspections set forth in the specification where such inspections are deemed necessary to insure supplies and services conform to prescribed requirements.

Figure 4.5-1 SAE International Aerospace Standard AS8791 (Continued)

SAE AS8791	
4.2	Sampling for Lot Acceptance: Samples shall be selected at random from each inspection lot in accordance with MIL-STD-105 as follows: a. Examination of product (4.4.1): Use inspection level II, and Acceptable Quality Level (AQL) 1.5 percent defective. b. Physical properties (4.5.1): Use inspection level S-2 and AQL 1.0 percent defective. 4.2.1 Inspection Lot: A lot shall consist of all TFE retainers of one type and size made from the same batch of material and submitted for inspection at the same time and place. 4.2.1.1 Batch: A batch shall be defined as the quantity of material received from the resin manufacturer assigned the same batch number. 4.2.1.2 Test Specimen: Specimens required for use in the elongation and tensile strength tests specified in this specification are obtained by cutting a sample specimen in a longitudinal direction from the TFE tubing. The tubing must be obtained from the same lot of material as the finished items. 4.3 Test Conditions: 4.3.1 Test Specimen: All test specimens, other than finished retainers, shall be prepared and conditioned as specified in the test referenced herein. 4.3.2 Standard Temperature: Unless otherwise specified, physical properties tests (4.5.1) shall be performed at room temperature of 75 °F ± 5 °F (24 °C). 4.4 Examinations: 4.4.1 Examination of Product: Each sample retainer shall be carefully examined to determine conformance to the requirements for workmanship (3.5), color (3.1.1), and dimensions (3.4.5). 4.4.2 Packaging, Packing, and Marking: Preparation for delivery shall be examined for conformance to Section 5. 4.5 Test Methods: 4.5.1 Physical Properties: 4.5.1.1 Tensile Strength: Specimens shall be tested in accordance with ASTM D 1708 at 1 inch per minute. The mean of (5) five values of ultimate tensile strength shall be reported.

Figure 4.5-1 SAE International Aerospace Standard AS8791 (Continued)

SAE AS8791	
4.5.1.2	Elongation: Tests shall be conducted in accordance with ASTM D 1708 at 1 inch per minute. The mean of (5) five values shall be reported.
4.5.1.3	Stiffness: The results of stiffness tests conducted in accordance with ASTM D 747 shall be a minimum of 45,000 psi.
4.5.1.4	Water Absorption: Sample retainers as required (4.2) shall be subjected to the water absorption tests, 24-hour procedure, as specified in ASTM D 570. The percent of increase or decrease of weight shall not exceed 0.005 percent.
4.5.1.5	Dimensional Stability: Sample retainers as required (4.2) shall be subjected to air aging for a minimum of 1 hour at 350 °F ± 10 °F (177 °C) and cooled to room temperature, and shall not have exhibited a change in circumferential length of more than 0.002 inch per inch.
4.5.1.6	Specific Gravity: Specific gravity shall be determined by ASTM D 792 on two finished retainers. The specific gravity value shall be 2.150 to 2.220.
4.5.1.7	Porosity: The sample part shall be dip- or brush-coated with suitable red dye penetrant. The coat shall be allowed to stand for 10 minutes and then shall be wiped off with a cloth saturated with solvent. Any retained dye, other than minor indications attributable to surface machining irregularities, is an indication of material porosity and shall be cause for rejection.
5.	PACKAGING:
5.1	Packaging:
	Packaging shall be level A or C in accordance with MIL-P-7936 as specified in the contract or order (see 6.2).
5.1.1	Level A packaging shall be Method III of MIL-P-116. Unless otherwise specified, 50 retainers of the same part number shall be arranged snugly side by side on a rigid cylindrical fiberboard, plastic, or metal case and retained at the ends by suitable plastic rings. Each unit shall be packaged within a container conforming to PPP-B-566 or PPP-B-676. Internal supports and centering devices shall be used on the core to prevent the retainers from contacting the inner surfaces of the container.

Figure 4.5-1 SAE International Aerospace Standard AS8791 (Continued)

SAE AS8791	
5.1.2	When two retainers per unit package are specified, packaging shall be Method III of MIL-P-116. Two retainers of the same part number shall be placed on a circular mandril or core fabricated of fiber, plastic, or metal. The outside diameter of the mandril shall effect a snug fit to the inside diameter of the retainers and shall be the approximate height of the two retainers combined. The mandril shall be affixed by the use of a contact cement, to a substantially oversized (no less than 1 1/2-inch clearance from all points of circumference) fiberboard stiffener pad. Caution shall be taken to prevent contamination of retainers by the cement. An additional fiberboard pad shall be placed over the top of the mandril, effecting a sandwich construction of the cushion pads and retainers. The two-cushion pads shall then be secured with pressure-sensitive tape across all four edges. The sandwiched pads containing the two retainers shall be inserted within a bag conforming to class "B" or "C" of MIL-B-117, or equivalent. Closure shall be accomplished by any suitable means.
5.2	Packing: Packing shall be level A, B, or C in accordance with MIL-P-7936, as specified in the contract or order (see 6.2).
5.2.1	Levels A and B: Intermediate packages of retainers shall be snugly packed in shipping containers conforming to PPP-B-636 or PPP-B-640, overseas type for level A, and domestic type for level B.
5.3	Marking of Shipment: In addition to any special marking required by the contract or order, unit packages, intermediate packages, and shipping containers shall be marked in accordance with MIL-STD-129.
6.	NOTES:
6.1	Intended Use: The retainers are intended for use in air, nitrogen, and hydraulic applications that contain fluids conforming to MIL-H-5606, MIL-H-6083, MIL-F-17111, MIL-L-17331, MIL-L-17672, MIL-H-19457, and MIL-H-83282 with no adverse effect on the properties of the fluid, packings, or metal contained in the system through the temperature range of -65 °F (-55 °C) to +275 °F (135 °C) at operating pressure from 0 to 3,000 psi continuous and 0 to 4,500 psi intermittent.
6.2	Ordering Data: Procurement documents should specify: a. Title, number, and date of this specification b. Data requirements (see 3.2) c. MS part number of the retainer desired (see 3.3.1) d. Levels of preservation, packaging, and packing required (see Section 5)

Figure 4.5-1 SAE International Aerospace Standard AS8791 (Continued)

SAE AS8791
<p data-bbox="323 527 583 552">6.3 Dimensional Stability:</p> <p data-bbox="376 579 1338 758">Prior to finish machining, all material should be annealed or dimensionally stabilized by being subjected to air aging for a minimum of 1 hour for each 0.250 inch of thickness, at 500 °F ± 25 °F (260 °C), and then cooled to room temperature at a rate of not less than 1 °F and not more than 3 °F per minute. The annealed material should be held at a temperature of 75 °F (24 °C) or above for at least 16 hours prior to machining. Machining and subsequent inspection should be accomplished at a temperature of 75 °F (24 °C) or above. Adequate tool cooling should be provided during machining so that the temperature of the tool does not exceed 350 °F (177 °C).</p> <p data-bbox="388 1633 1339 1684">PREPARED BY SAE SUBCOMMITTEE A-6C, FLUID POWER DISTRIBUTION ELEMENTS OF COMMITTEE A-6, AEROSPACE FLUID POWER ACTUATION & CONTROL TECHNOLOGIES</p>

4.5.2 Metallic O-Rings

This appendix contains the manufacturer's technical bulletins for the metallic O-rings.

Figure 4.5-2 Metallic O-Rings Technical Bulletin

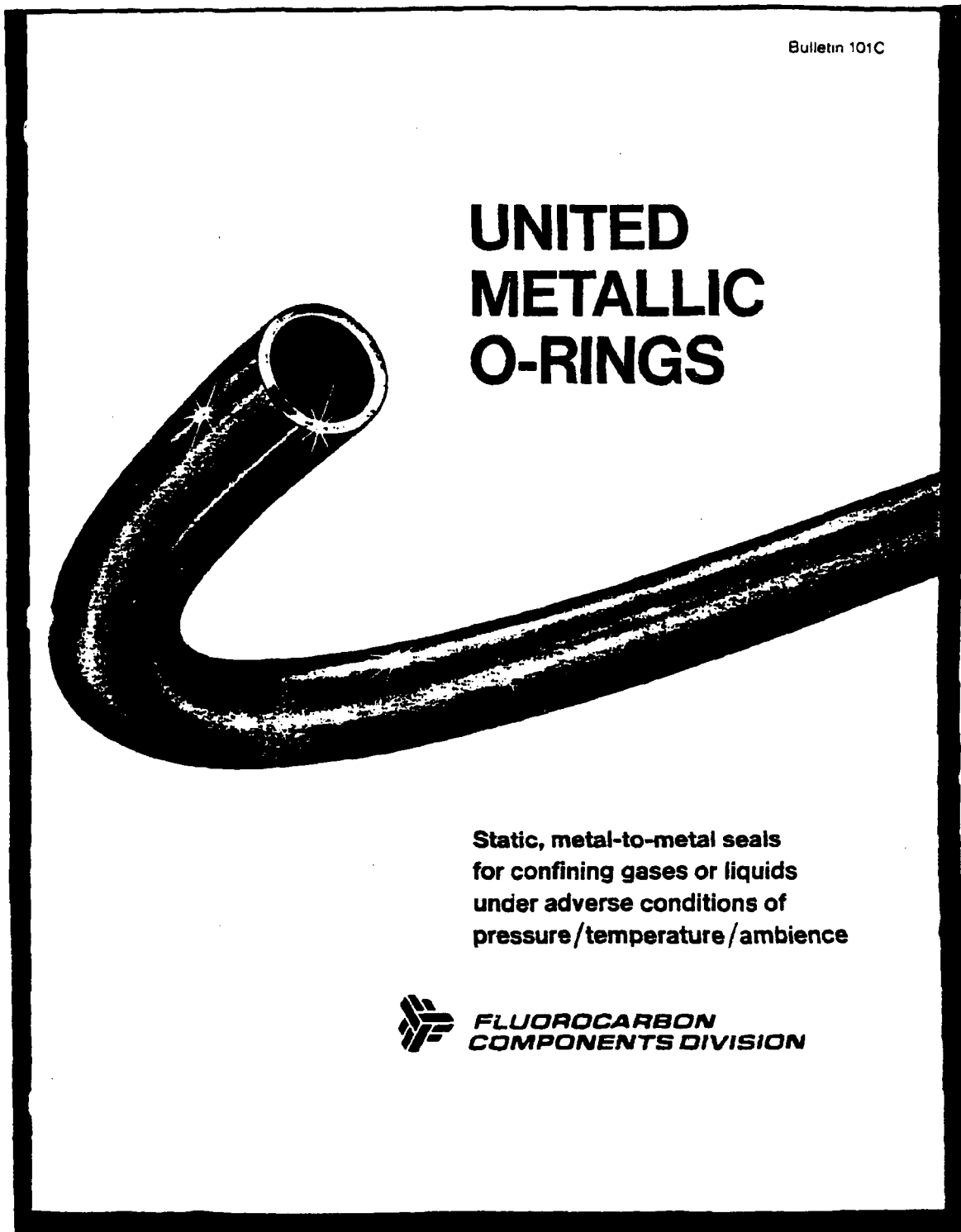


Figure 4.5-2 Metallic O-Rings Technical Bulletin (Continued)

United Metallic O-Rings

United Metallic O-Rings are designed to prevent leakage of gases or liquids under adverse sealing conditions. These static, metal-to-metal seals can withstand pressures from high vacuum to 100,000 psi (6,804 atm). They can endure continuous temperatures from -425°F up to $1,800^{\circ}\text{F}$ (-269°C to 982°C), or intermittent temperatures up to $3,000^{\circ}\text{F}$ ($1,650^{\circ}\text{C}$). They resist radiation, chlorides, corrosives, and other hostile environments. They will not deteriorate with age, either in use or in storage.

Design, Materials, Coatings, Sizes

United Metallic O-Rings, designated MOR, are made of metal tubing (or solid rod) which is formed into circular or other shapes and the two ends welded together. The O-Ring metal is stainless steel or other alloys. The O-Ring can be electroplated with silver, copper, indium, nickel, gold, lead or other metals, or it can be coated with Teflon. The flow of the finish material improves the sealing, especially under high pressure and/or vacuum. Since tensile strength and resilience of the seal are determined in part by metal temper, Fluorocarbon Components offers a choice of heat treating to material specification or tempering to customer specifications. Tubular or solid wire

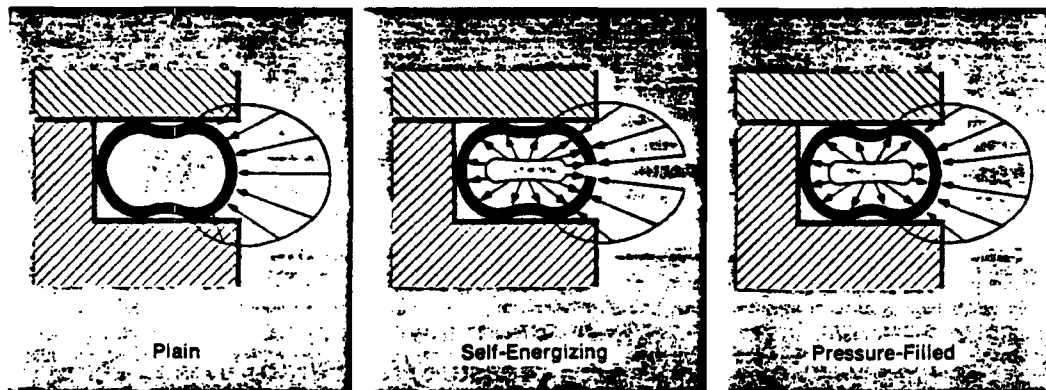
ings can be manufactured in sizes ranging up to 25 feet (7.6 m) or more in diameter, or as small as .250 inches (6.4 mm) OD.

Application Characteristics

The typical application places a Metallic O-Ring in axial compression between parallel faces which are square to the fluid passage or vessel axis. The seal is usually located in an open or closed groove in one face. It can also be located in a retainer, which eliminates the need for machining a groove (see description of retainers on page 8).

Upon compression to a predetermined fixed height, the seal tubing buckles slightly, resulting in two contact areas on the seal face and maximum contact stress between the seal and the mating faces. When the flange faces are closed, the O-Ring is under compression and tends to spring back against the flanges, thus exerting a positive sealing force. If the O-Ring is the self-energizing type, the pressure of the gas or liquid on the vented side energizes the seal and further increases the sealing force by pushing the seal against the flange face.

Types of Metallic O-Rings



Plain

(Not Self-Energizing or Pressure-Filled)

Made of metal tubing (or solid rod) in most metals. This type is the most economical O-Ring. It is designed for low to moderate pressure and vacuum conditions.

Self-Energizing

The inner periphery of the O-Ring is vented by small holes or a slot. The pressure inside the ring becomes

the same as in the system. Increasing the internal pressure increases sealing effectiveness.

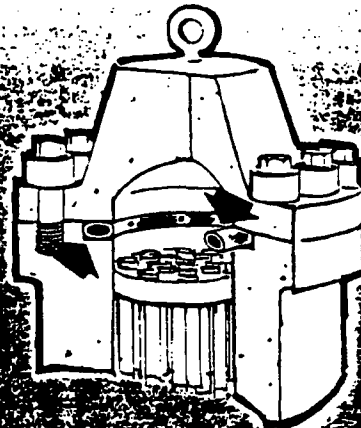
Pressure-Filled

Pressure-filled O-Rings are designed for a temperature range of 800°F to $2,000^{\circ}\text{F}$ (425°C to 1093°C). They cannot tolerate pressures as high as the self-energizing type. The ring is filled with an inert gas at about 600 psi (41 atm). At elevated temperatures, gas pressure increases, offsetting loss of strength in tubing and increasing sealing stress.

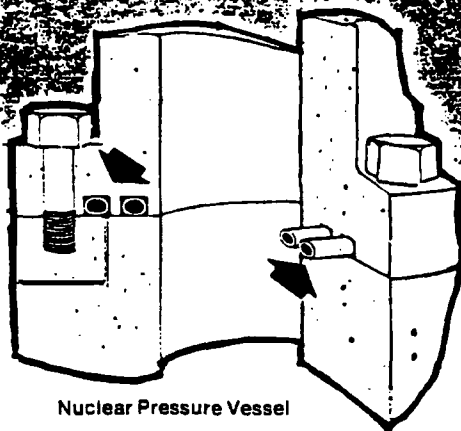
Figure 4.5-2 Metallic O-Rings Technical Bulletin (Continued)

Typical Applications

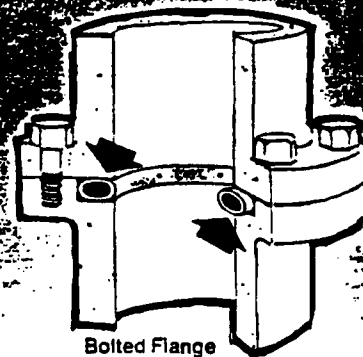
Metallic O-Rings have been used successfully in vacuum and high pressure systems, and in critical systems for hydraulic and lubricating oil, jet engine fuel, gasoline, rocket fuels, steam, liquid metals and combustion gas. They also provide positive, leak-proof seals in piping systems for chemical, petrochemical, oil and gas, and refining industries. Many reciprocating engines, gas turbines, compressors, heat exchangers, pressure vessels, injection molding machines, high pressure filters and other components rely on Metallic O-Rings for permanent, metal-to-metal seals. Several common applications are shown in the following illustrations.



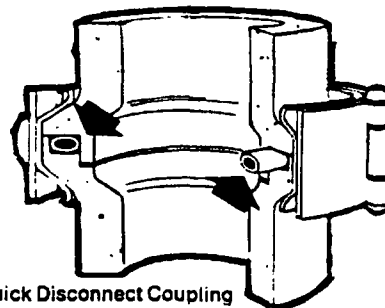
Heat Exchanger/Pressure Vessels



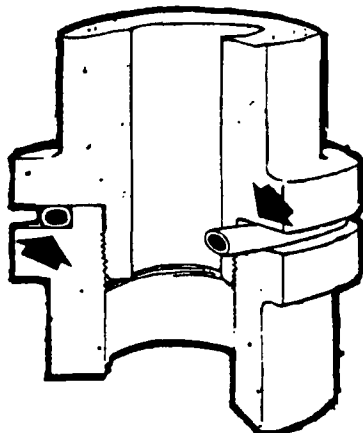
Nuclear Pressure Vessel



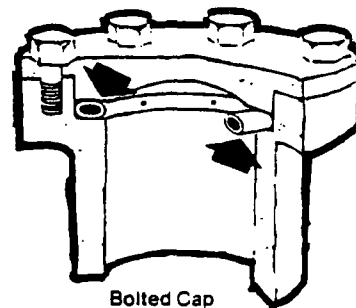
Bolted Flange



Quick Disconnect Coupling



External Pressure (Thread Joint)



Bolted Cap

Figure 4.5-2 Metallic O-Rings Technical Bulletin (Continued)

Metallic O-Ring Selection Guide

To select the proper Metallic O-Ring for a particular application, it is necessary to determine system pressure, temperature, and kind of fluid to be sealed.

1. O-Ring Type

Pressure determines if O-Ring should be self-energizing.

Pressure	O-Ring Type
Vacuum to 100 psi (6.81 atm)	Self-energizing not required
100 psi (6.81 atm and above)	Self-energizing desirable

2. O-Ring Material

Temperature determines basic O-Ring material.

Temperature	O-Ring Material
Cryogenics to 500° F. (260° C.)	321 Stainless steel
to 800° F. (427° C.)	Alloy 600
to 1800° F. (982° C.)	Alloy X-750
above 1800° F. (982° C.)	Consult Factory

3. O-Ring Size

Tubing diameter is determined by ring OD, compression force desired, and available space. See complete data for O-Ring size selection on pages 6 and 7.

4. Seal Load vs. Seal Ring Diameter

Curves on page 7 show the seal load vs. seal ring diameter to various tubing outer diameters and wall thickness for stainless steel tubing. For tubing made of Alloy 600, multiply loads shown by 1.1. For Alloy X-750, multiply by 1.4.

5. O-Ring Wall Thickness

The wall thickness should be selected to provide the proper yield under compression. The data on pages 6 and 7 include the practical wall thickness dimensions that may be used for each tube diameter. If plating is used, wall thickness for seals made with .125 inch (3.2mm) tubing and smaller should cause yielding of the plating at a load of 400 lb/in (7.14 kg/mm). For tubing over .125 inch (3.2mm) diameter, 800 lb/in (14.28 kg/mm) should be required. Teflon coatings on rings will yield at 100 lb/in (1.78 kg/mm).

6. Groove Dimensions

The proper dimensions and surface finish of the groove are as important in achieving a seal as the O-Ring itself. As a general guide in the preparation of joint surfaces, the

recommended groove dimensions for internal and external pressure applications are shown on page 5.

Should you need further guidance and our recommendations, submit the following information regarding your application: 1. Temperature and pressure ranges. 2. Space available. 3. Material. 4. Medium to be sealed. 5. Available compression load. 6. Sketch of proposed application.

7. Coating or Plating

Coating or plating of the O-Ring will provide adherence and ductility (softness) to conform to microscopic groove or flange irregularities.

For unplated seals, liquid leakage can be estimated by the following expression:

$$Q = \frac{5.0 \times 10^{-6} P}{\mu}$$

(Q=leakage cc/sec; P=pressure difference psi; and μ =liquid viscosity at operating conditions, centipoise.) If the resulting calculated leakage is 10^{-3} to 10^{-4} or less, actual leakage may be zero because of surface tension. If leakage occurs, it should be proportional to seal diameter, and in the above expression, multiplied by D/2. D=seal diameter. Actual leakage will probably be less than predicted.

For coated or plated seals, helium-leaktight joints may be made with proper O-Ring and coating or plating selections. Test results range from 10^{-3} to 10^{-4} cc/sec. and lower at one atmosphere differential. Recommended coating or plating materials are:

Temperature	Plating or Coating
Cryogenic to 500° F. (260° C.)	Teflon
to 1800° F. (982° C.)	Silver
to 2200° F. (1186° C.)	Nickel

See page 12 for other coatings and plating.

8. Sealing Surface Finish

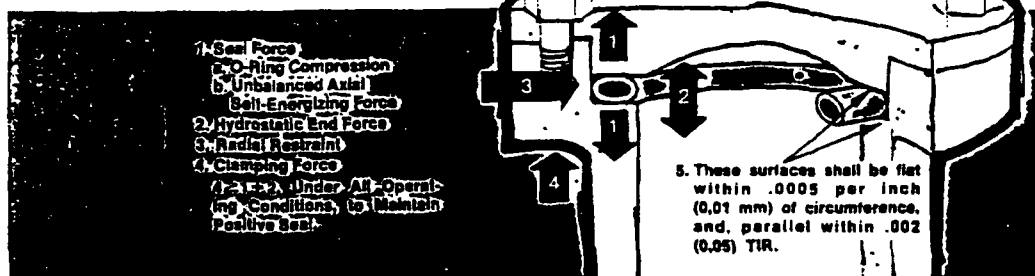
The groove and mating flange face must have a surface finish of 16 μ in. rms (0.4 μ mm) for bare rings, and 32-100 μ in. rms (0.8 μ -2.54 μ mm) for plated or coated rings.

For gas, vacuum and light liquid (water), a finish of 16 μ in. (0.4 μ mm) rms is recommended. For medium liquids (hydraulic oils) and heavy liquids (tar or polymers) a finish of 32 μ in. (0.8 μ mm) rms is recommended. Machining tool marks on groove or flange face must be concentric.

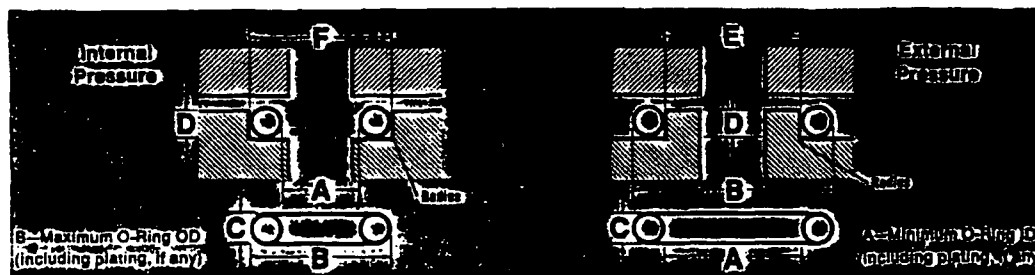
Seal surfaces should be free of dirt, grit or other foreign materials.

Figure 4.5-2 Metallic O-Rings Technical Bulletin (Continued)

9. Other Design Considerations



Recommended Groove Dimension



Internal Pressure			External Pressure			
C Tube Diameter Inches/mm	F Groove OD Inches/mm	D Groove Depth Inches/mm	Ring Tolerance A + .000 - .000 Inches/mm	E Groove ID Inches/mm	Minimize Groove Width Inches/mm	Springback* Inches/mm
.031	B + .004/.006	.020/.022	0.003	A - .004/.006	.042	.002
.08	B - 0.10/0.15	.050/.055	0.076	A - 0.10/0.15	1.07	0.05
.063	B + .004/.006	.042/.045	0.003	A - .004/.006	.085	.002
.16	B - 0.10/0.15	.107/.114	0.076	A - 0.10/0.15	2.16	0.05
.093	B + .005/.009	.065/.069	0.004	A - .005/.009	.112	.002
.24	B - 0.13/0.23	.165/.175	0.102	A - 0.13/0.23	2.80	0.05
.125	B + .007/.012	.090/.095	0.005	A - .007/.012	.144	.003
.32	B - 0.18/0.30	.223/.241	0.127	A - 0.18/0.30	3.66	0.08
.156	B + .008/.014	.115/.120	0.006	A - .008/.014	.182	.004
.40	B - 0.20/0.36	.292/.305	0.152	A - 0.20/0.36	4.46	0.10
.188	B + .009/.015	.145/.150	0.007	A - .009/.015	.220	.004
.48	B - 0.23/0.38	.358/.38	0.178	A - 0.23/0.38	5.59	0.10
.250	B + .011/.019	.195/.200	0.008	A - .011/.019	.290	.005
.94	B - 0.28/0.48	.495/.508	0.203	A - 0.28/0.48	7.37	0.13
.375	B + .014/.029	.295/.300	0.012	A - .014/.029	.445	.009
.95	B - 0.36/0.74	.749/.752	0.305	A - 0.36/0.74	11.3	0.23
.500	B + .020/.038	.415/.425	0.016	A - .020/.038	.645	.013
.127	B - 0.51/0.97	.054/.08	0.406	A - 0.51/0.97	16.7	0.33
.625	B + .020/.038	.520/.530	0.016	A - .020/.038	.780	.017
.159	B - 0.51/0.97	.132/.1346	0.406	A - 0.51/0.97	19.8	0.43

Dimensions in table above are for unplated rings. Increase groove depth for .031 inch (.8 mm) cross section rings by 2 times the plating or coating thickness of plated or coated rings.
Do not increase groove depth on plated or coated rings for cross section of .063 inch (1.6 mm) and larger.

*Springback figures for tube diameters up to .250 inch (6.4 mm) are for stainless steel. Springback for .375, .500 and .625 inch (9.5, 12.7 and 15.9 mm) tube diameters are for precipitation hardened Alloy 718. Other values for different materials are available.

Figure 4.5-2 Metallic O-Rings Technical Bulletin (Continued)

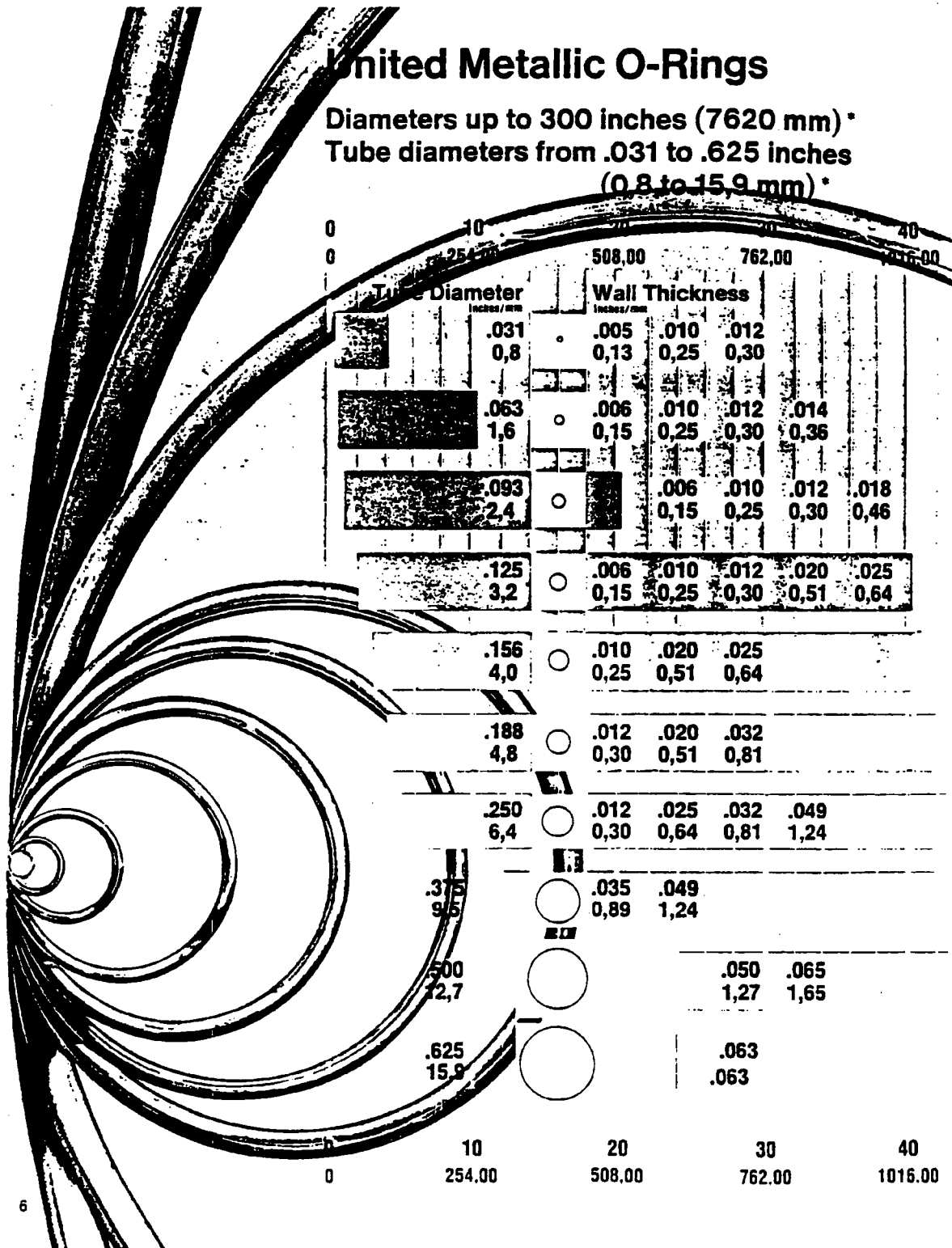
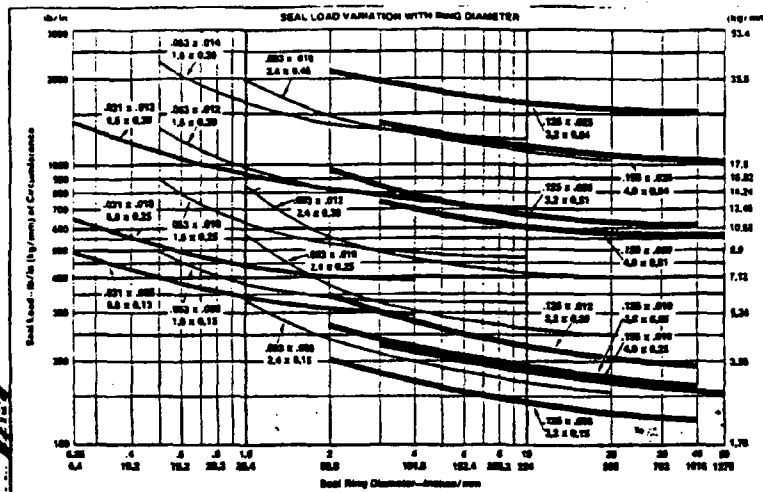


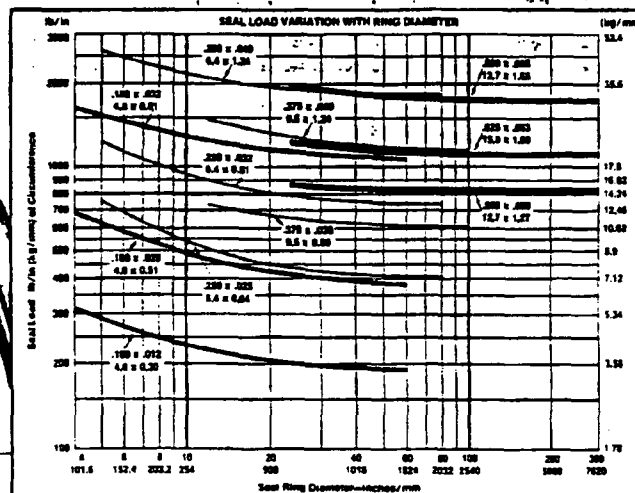
Figure 4.5-2 Metallic O-Rings Technical Bulletin (Continued)

Table I



Tables I and II are for 321 stainless steel tubing.
For tubing made of Alloy 800, multiply load by 1.2. For Alloy 600, multiply load by 1.1. For Alloy X-750, multiply by 1.0. For Alloy 718, multiply by 0.9.

Table II

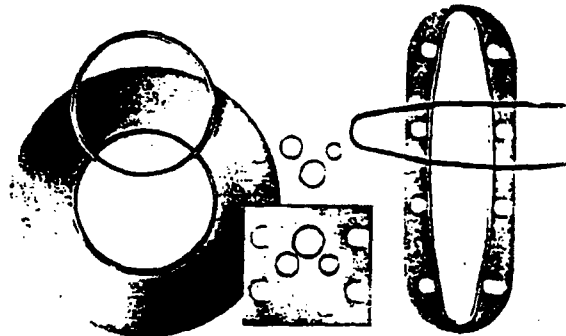


50	60	70	80	90	100	110
1270.00	1524.00	1778.00	2032.00	2286.00	2540.00	2794.00
Seal Ring Diameter—Inches/mm						

Figure 4.5-2 Metallic O-Rings Technical Bulletin (Continued)

Retainer Assemblies

Metallic O-Rings can be used with a metal retainer plate for mechanical back-up that serves the same function as the machined groove wall in conventional installations. Retainer assemblies may incorporate several Metallic O-Rings into one all metallic assembly. The O-Rings are press-fitted without cross-section distortion, are secured against dropout and are easily handled during field assignment or retrofit programs. The retainer plate furnishes the O-Ring compression limit, controls hoop tension of the O-Ring, simplifies surface finish operation, permits interchangeability of flanges, and applies to single or multiple O-Ring requirements. A selection of several standard assemblies is described below:



ASA/API Pipe Flange Seals

Metallic O-Rings offer static seal reliability and safety for installation or maintenance of piping. Over long periods of time, the all-metal construction of Fluorocarbon tubular Metallic O-Rings and retainer plates make them less susceptible to relaxation of sealing stresses—as compared to partially non-metallic gaskets.

In addition to their natural resilience characteristics, Metallic O-Rings provide the stability of a metal-to-metal pipe joint seal.

The natural springback of thin-wall metal tubing, and unique self-energizing design feature, create a balance of inside and outside forces which prevent collapse of the tube under pressure cycling. These same features allow Metallic O-Rings to respond to variations in sealing surface deflections without creep or cold flow and to accommodate high and low temperature cycling. For process plant piping, they withstand temperatures from cryogenic to 1,800° F (982° C.) and pressures from vacuum to 50,000 psi (3402 atm).

To maintain seal reliability, tubular Metallic O-Rings require less bolt stress than solid, fiber, flat metal, spiral wound or jacketed gaskets. Lower seal loads allow a greater bolt and flange safety factor for a given installation.

O-Rings and retainer plates are available for 250" to 24" (6.4 to 609.6 mm) pipe in all sizes of 150 to 2500 psi (10.2 to 170.1 atm) flat or raised face flanges.

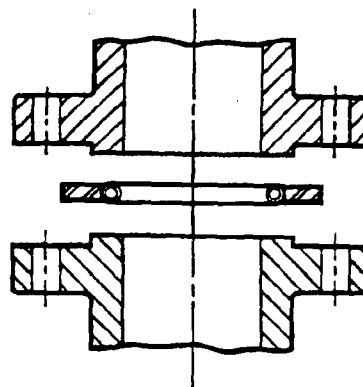
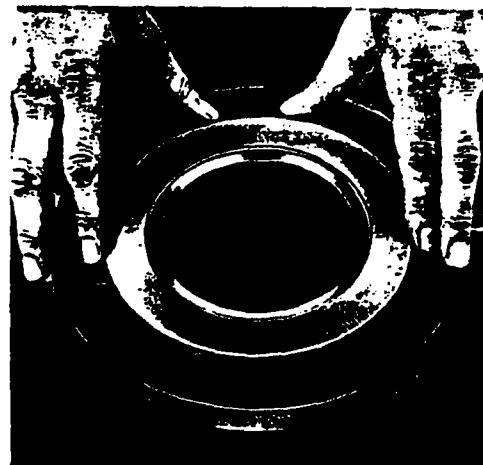
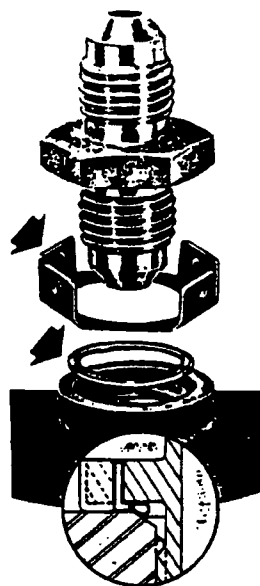


Figure 4.5-2 Metallic O-Rings Technical Bulletin (Continued)

Boss Seals

United Metallic FIT-O-SEAL for boss joints combines a stainless steel retainer and a press fit Metallic O-Ring. The unit is self-positioning, controls ring compression, and can be reused. It won't deteriorate with age and is not affected by environment. Existing boss can be easily retrofitted. It can seal fuels and chemicals from high vacuum to 10,000 psi (680 atm) or higher, and will endure continuous temperatures of -452° F. (-269° C.) to 1,800° F. (982° C.). Standard seal assembly available for MS33656 fitting to MS33649 boss. Modifications available.



Flange-O-Seal

The Metallic O-Ring is semi-fastened into the metal retainer. The assembly is used for sealing jet engine fuel lines and exotic missile fuel lines from -452° F. (-269° C.) to 1,800° F. (982° C.).

It can be used for steel fittings MS20757 thru MS20762 and MS33786 fitting installation. The following assemblies are available from stock:

Part No. U-700499	Part No. U-700520	A Dia. Inches / mm ± .025 (0.09)	B Inches / mm ± .005 (0.13)	B Inches / mm ± .005 (0.13)
-12	-12	.863 21.92	1.156 29.36	.210 5.33
-16	-16	1.113 28.27	1.312 33.32	.210 5.33
-17	-17	1.113 28.27	1.414 35.92	.271 6.88
-20	-20	1.425 36.2	1.656 42.06	.271 6.88
-24	-24	1.813 46.07	1.812 46.02	.271 6.88
-32	-32	2.300 58.42	2.375 60.33	.333 8.46

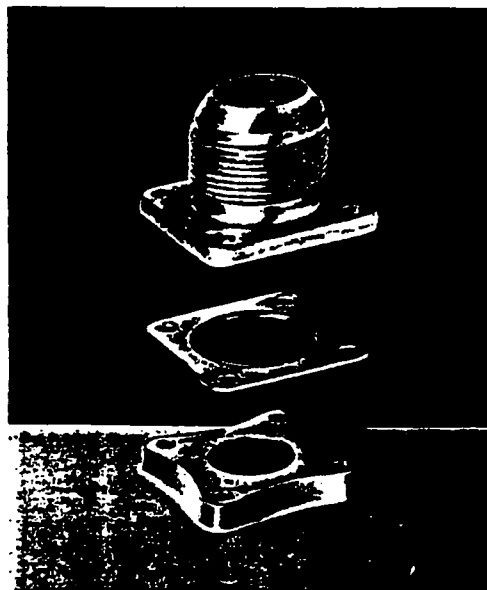
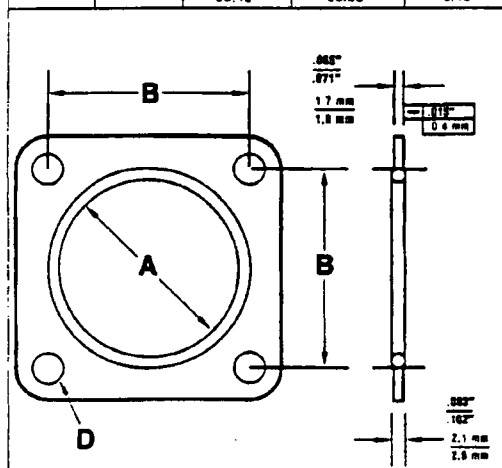


Figure 4.5-2 Metallic O-Rings Technical Bulletin (Continued)

Nuclear Pressure Vessel Seals

The principal application of United Metallic O-Rings in nuclear power plants is the sealing of reactor pressure-vessel heads. They are also specified for sealing applications on valves, steam generators, condensers, pumps, piping and other equipment components throughout the nuclear flow chart.

United O-Rings can easily meet the three major requirements of nuclear applications: high tempera-

ture ratings, high pressure ratings, and larger than average ring diameters (see Page 2 for specifics). United Metallic O-Rings offer other significant advantages in nuclear applications: they are not normally affected by damaging environments or corrosives; they don't deteriorate with age, even in storage, and they resist radiation and chlorides.

TABLE 1 O-Ring—Alloy 718—DEFLECTION and SPRINGBACK—Inches (mm)						
Load Force Unrestrained /linear inch Φ	.375 dia. x .038 wall (9.5 x 0.95)		.500 dia. x .050 wall (12.7 x 1.27)		.625 dia. x .063 wall (15.9 x 1.60)	
	2500 lb/in (45 kg/mm)		2500 lb/in (45 kg/mm)		4000 lb/in (71.5 kg/mm)	
Percentage	Deflection	Min. Springback	Deflection	Min. Springback	Deflection	Min. Springback
8%	.030 (0.76)	.009 (0.23)	.040 (1.02)	.013 (0.33)	.050 (1.27)	.017 (0.43)
10%	.037 (0.94)	.009 (0.23)	.050 (1.27)	.013 (0.33)	.062 (1.57)	.017 (0.43)
12%	.045 (1.14)	.009 (0.23)	.060 (1.52)	.013 (0.33)	.075 (1.91)	.017 (0.43)
16% *	.060 (1.52)	.009 (0.23)	.080 (2.03)	.013 (0.33)	.100 (2.54)	.017 (0.43)
17%	.064 (1.63)	.009 (0.23)	.085 (2.16)	.013 (0.33)	.106 (2.69)	.017 (0.43)

*Optimum compression percentage. 8 to 17% compression may be utilized with UAP Inconel 718. Load forces may vary slightly below 17% inch compression.

Media to be Sealed

Media in the nuclear power plant which United O-Rings can successfully seal include: ordinary (light) water, heavy water, boiling water, steam, borated water, carbon dioxide, helium, nitrogen, liquid metals including sodium, terphenyl and other phenyl fluids, and acids including boric acid.

Flange and Groove Details

United Metallic O-Rings do not require expensive groove preparation and, being flexible, are easily installed. On pressure vessel head seals, a machined groove is required, the groove diameter being determined by the location of vessel rings so that minimum lift-off exists.

The O-Ring OD must be sufficiently large so that upon compression, the ring will expand and contact the groove outer wall. This limits hoop tension of the ring and provides a backup that restricts radial outward movement of the ring when the vessel is pressurized. Groove should be sufficiently wide so that the O-Ring ID does not contact the inside wall when the ring is compressed. Groove depth controls the amount of compression and the amount of load required to seat the ring. Table 1 shows the amount of flange load required to seat the seal.

The O-Ring and groove dimensions for internal and external pressure applications may be determined from the data on page 5.

Materials and Plating

Alloy 718 is the O-Ring material of choice on most nuclear sealing applications. Inconel 706 is also available. Alloy 718 used in United O-Rings is annealed and age hardened, offers optimum strength and springback, and resists chlorides, radiation and corrosion. Type 304 stainless steel O-Rings are also offered for applications that are less critical and where a less expensive material will suffice.

Both Alloy 718 and Type 304 stainless steel O-Rings are available with silver plating of .004" — .006" (0.10 mm — 0.15 mm) thickness. Ring OD can be controlled to .010" (0.25 mm) total tolerance after silver plating. The silver plating assures good adherence and ductility (softness) to conform to groove irregularities. Nickel plating is recommended when sealing sodium.

O-Ring Fabrication

United Metallic O-Rings are fabricated by bending straight metal tubing into circular or other desired shapes. The two ends are welded together and the weld ground flush.

Where the proposed size of the fabricated O-Ring would prohibit shipping, the company offers on-site welding fabrication that meets the same quality standards as fabrication performed in our plant.

Figure 4.5-2 Metallic O-Rings Technical Bulletin (Continued)

Tube and Ring Dimensions

The three most common tube diameters used for nuclear applications are shown below with the recommended relationship of tube diameter and wall thickness to the O-Ring diameter. Other tube diameters are also available for nuclear applications. See pages 6 and 7.

TABLE 2

Tube Diameter Inches/mm	Wall Thickness Inches/mm	O-Ring Diameter Inches/mm
375 9.5	.038 1.0	Up to 180 Up to 4572
500 12.7	.050 1.3	120 to 260 3048 to 6604
625 15.9	.063 1.6	220 and up 5580 and up


TABLE 3

O-RING DIAMETER (Inches (mm))	No. Slots or Holes *
Up to 144 (3657.6)	8
144 (3657.6) and up	12

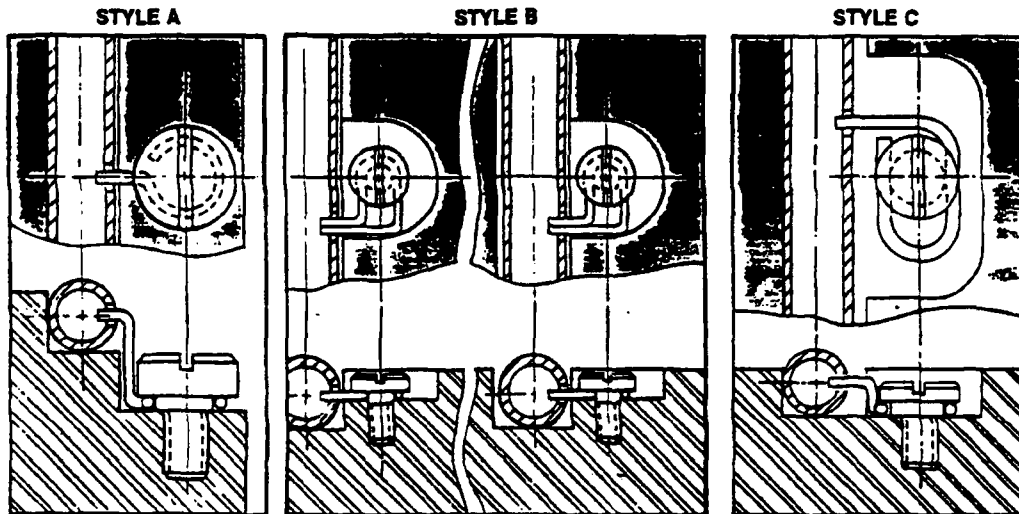
* unless otherwise specified

TABLE 4

SLOT or HOLE DIMENSIONS (Inches (mm))



E	.375 (9.5)	.500 (12.7)	.625 (15.9)
W	.038 (1.0)	.050 (1.3)	.063 (1.6)
S	.281 (7.1)	.375 (9.5)	.438 (11.1)
T	.125 (3.2)	.205 (5.2)	.256 (6.5)
D	.070 (1.8)	.093 (2.4)	.125 (3.2)



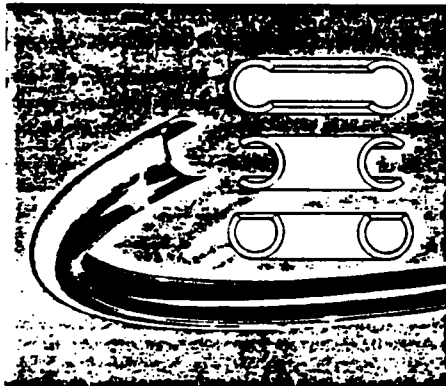
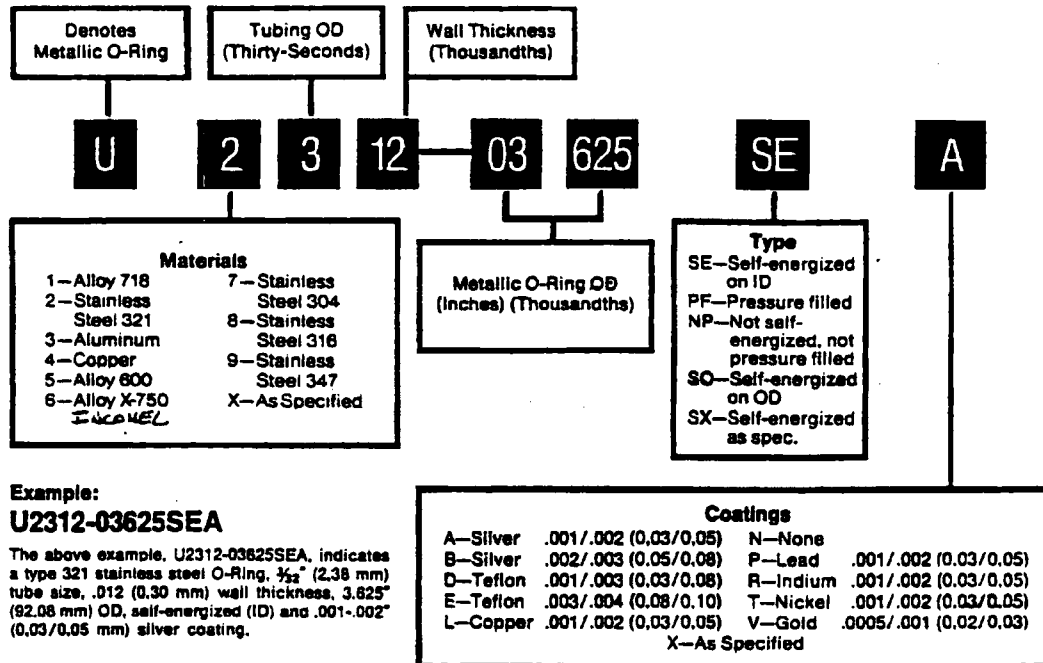
Retainer Clips

On nuclear pressure vessel heads, the rings are installed to the underside of the flange on the head. This requires clips to hold the rings in proper place and alignment during assembly of the head to the vessel. Slots are provided in the O-Ring to receive the retainer clips. In some instances the retainer clips are welded to the O-Ring. Instead of slots for retainer clips, drilled holes with additional self-energizing holes can be provided. The number of slots

or holes and their size varies in relation to the ring and tube diameters (see Tables 3 and 4). The data shown assures installation without excessive O-Ring buckling in the groove and without endangering O-Ring strength. Different clipping methods are available, depending on vessel design, for both single and double ring applications (see drawings above—styles A, B and C).

Figure 4.5-2 Metallic O-Rings Technical Bulletin (Continued)

How to Specify O-Rings



United Metallic C-Rings

United Metallic C-Rings (designated MCR) are designed for static sealing on machinery or equipment and are available for internal pressure, external pressure, or axial pressure ID/OD applications. Because C-Rings are designed with an open side on the pressure side of the installation, the seal is self-energizing. United C-Rings are offered in round or irregular shapes in a broad range of sizes from .126" (3.2 mm) OD x .032" (0.81 mm) free height to over 300" (7620 mm) OD x 2" (50.80 mm) free height. They are available in a wide variety of metal alloys and metallic or Teflon coatings. Sealing application temperature range is from cryogenic to 3,000° F. (1650° C.); pressure tolerances are from 10⁻¹⁰ torr to 100,000 psi (6.804 atm). Where customer requirements are large, the C-Ring provides the lowest unit price of any high performance seal on the market. Request Bulletin 102C.



**FLUOROCARBON
COMPONENTS DIVISION**

Post Office Box 9889/Columbia, South Carolina 29290

Phone: 803/783-1880 Telex: 57-3334

4.5.3 Viton® O-Rings

This appendix provides a description of the leak testing performed using the Viton® O-rings on the alternate port cover design at temperatures exceeding the manufacturer's elevated temperature limit. In addition, it also contains the Parker Seals Material Report on the Viton® material.

4.5.3.1 Alternate Port Cover O-Ring Elevated Temperature Leak Testing

The alternate port cover provides a Viton® O-ring face seal for the containment boundary. The alternate port cover bolts are torqued to 100 inch-pounds. When torqued as specified, the inner face of the alternate port cover will contact the sealing surface in the top forging and compress the Viton® O-ring to create a seal. To evaluate the Viton® O-ring performance at temperatures greater than 400°F, two test fixtures simulating the top forging of the cask and two alternate port covers were fabricated. Two assemblies were tested simultaneously to confirm that the test results were credible. A thermocouple was located within 0.063 inch of the centerline of the inner end O-ring and is the transducer used to report temperature during testing.

The O-ring used in conjunction with the alternate port cover is fabricated from a material with the trade name Viton®. The Viton® material is chosen because the operating temperature range for the material is low enough (-40°F) to satisfy the low temperature requirements for cask operations. The elevated temperature limit specified is 400°F. (The Parker Seals Material Report follows this test description.) Analyses presented in Section 3.5.1 show that the maximum post-fire accident temperature is 547°F.

NAC, with the aid of an independent laboratory, performed leak testing in excess of 550°F to demonstrate Viton's capability to perform at the elevated temperature and to determine the leak rate of the alternate port cover design at the elevated temperature. It was determined that the alternate port cover O-ring maintains its sealing capability at a temperature of 575°F after prolonged heating above 400°F. Testing was done in accordance with NAC Specification Number 315-S-09, Revision 0. Two fixtures were put into a thermal test chamber. All the fittings attached to the test assemblies were checked and confirmed leaktight. The assemblies were heated in a manner that conservatively approximates the fire-transient analysis and one fixture was held at a temperature above 550°F for more than 4 hours 37 minutes. The region inside the port cover was evacuated to below 2 psia, backfilled with helium at 0 psig, evacuated and backfilled again and then leak checked. The leak test procedure emulates the maintenance test of the port cover stated in Chapter 8, with one atmosphere of pressure acting on the O-ring during the test.

Data pertinent to the test:

	Test Assembly 16	Test Assembly 64	Fire-Transient
Time Above 400°F	~6:32 hours	~5:52 hours	4:37 hours
Time Above 550°F	~5:05 hours	~4:25 hours	0 hour
Maximum Seal Temperature	~575°F	~575°F	547°F

The test temperature of 550°F was selected because it approximates the maximum calculated O-ring temperature in the fire-transient analysis. The duration was selected because it is the calculated duration that the O-ring is above the manufacturer's maximum recommended O-ring temperature of 400°F. This results in a conservative test due to the slower heat-up rate of the oven compared to the heat-up rate of the port cover in the fire-transient analysis.

Each test assembly was leak checked after the temperature test, while at a temperature of approximately 575°F. The measured leak rate for each of the assemblies was less than 4.0×10^{-8} atm-cc/sec. In conclusion, the alternate port cover provides a leaktight seal, in accordance with ANSI N14.5, using Viton® O-rings at an elevated temperature.

Figure 4.5-3 Parker Seals Material Report on the Viton® Material

Sep-17-99 03:35P

P.01



Software Version: 2.0

9/17/99

Customer Identification

Company:	NAC International
Contact:	George Carver
Project Name:	
Address:	
City:	Zip Code:
State:	
Telephone No.:	770-447-1797 fax
Date/Time:	9-17-1999 15:27

Ordering Specifications

Application:	O-ring Only
Compound Number:	V0835-75
Size:	

Compound Information

Search Parameter

Material Selection Method:	Compound Search
Contained Media:	
Desired Temperature Range	
High:	
Low:	

Selected Material Information

Durometer (Shore A):	75
Polymer:	Fluorocarbon GLT - LOWTEMP COMPOUND.
Temperature	
Normal High:	400 °F
Extended High:	400 °F
Normal Low:	-40 °F
Color:	Black
Static Application Only:	No
Military Spec.:	MIL-R-83485
AMS NAS Spec.:	None
SAE/ASTM Spec.:	None

Seal Size Information

Sizing Selection Method:	Known: O-ring P/N. Search for: O-ring dimensions.
--------------------------	---

Figure 4.5-3 Parker Seals Material Report on the Viton® Material (Continued)

Sep-17-99 03:35P

P.02



Compound Data Sheet
O-Ring Division United States

MATERIAL REPORT

REPORT NUMBER: KJ0835
DATE: 10/10/89

TITLE: Test of Parker Compound V0835-75 to MIL-R-83485, Type I.

PURPOSE: To determine if V0835-75 meets MIL-R-83485, Type I.

CONCLUSION: V0835-75 meets the above specification.

Parker O-Ring Division
2380 Palumbo Drive
Lexington, Kentucky 40509
(606) 269-2351

Figure 4.5-3 Parker Seals Material Report on the Viton® Material (Continued)

Sep-17-99 03:35P

P. 03

REPORT DATA

Report Number: KJ0835

<u>ORIGINAL</u>	<u>MIL-R-83485 TYPE 1, O-RINGS & COMPRESSION SEALS</u>	<u>V0835-75 ACTUAL VALUES</u>
Specific Gravity	As determined	1.75
Hardness points	75 ± 5	78
Tensile Strength, psi. min.	1600	1708
Elongation, % min.	120	180
Temperature Retraction, 10% (TR-10), °F, max.	-20	-22
<u>AFTER AIR AGING, 70 HRS. @ 75° ± 5°F. Compression Set</u>		
% of original deflection, max.	25	— (14)
<u>AFTER AGING, 70 HRS. @ 75°F IN TT-S-735, TYPE III</u>		
Hardness Change, pts.	+5	77 (-1)
Tensile Strength decrease, % max.	30	1662 (-3)
Elongation decrease, % max.	20	165 (-8)
Volume change, % max.	1 to 10	— (+2)
<u>AFTER AIR AGING, 70 HRS. @ 528° ± 5°F</u>		
Hardness change, pts.	+5	78 (0)
Tensile Strength decrease, % max.	35	1136 (-33)
Elongation decrease, % max.	10	235 (+31)
Weight loss, % max.	12	— (-7)
<u>AFTER AIR AGING, 166 HRS @ 347° ± 5°F. COMPRESSION SET</u>		
% of original deflection, max.	25	— (15)
18 hrs. cooling		— (24)
<u>AFTER AIR AGING, 22 HRS @ 392° ± 5°F. COMPRESSION SET</u>		
% of original deflection, max.	20	— (11)

Figure 4.5-3 Parker Seals Material Report on the Viton® Material (Continued)

Sep-17-99 03:35P

P. 04

AFTER AGING, 70 HRS.
@ 347°MIL-R-83485
±5°F in AMS-3021

MIL-R-83485
TYPE 1, O-RINGS %
COMPRESSION SEALS

V0835-75
ACTUAL VALUES

Hardness change, pts
Tensile Strength decrease, %, max.
Elongation decrease, %, max.
Volume change, %
Compression set, % of
original deflection, max.
18 hr. cooling

+0, -15
35
20
1 to 20
10

73
1408 (-18)
171 (-5)
- (+15)
- 7
- 9

4.5.4 SAS2H Output and Group A₂ Values for Design Basis PWR, BWR, TRIGA, MTR and DIDO Fuel

SAS2H output is provided on a per assembly basis for Westinghouse 15×15 and GE 7×7 fuel assemblies, TRIGA FLIP-LEU II fuel elements and for MTR HEU fuel elements, 25 PWR rods, 25 BWR rods and DIDO LEU fuel assemblies in Table 4.5-1 through Table 4.5-21. The radionuclide inventory for the TRIGA fuel cluster rods is bounded by that of the design basis TRIGA fuel element. Radionuclides are grouped into fission gases, volatiles, and fines. Volatiles and gases are defined as those radionuclides listed in NUREG/CR-6487. All remaining radionuclides are grouped as fines. A₂ values were obtained from 10 CFR 71.

Table 4.5-1 Westinghouse 15×15 SAS2H Output and Group A₂ Value (Gas)

Isotope	Activity/Assembly (Ci)	Fraction of Source	Isotope A ₂ Value (Ci)	Isotope Fraction/A ₂ (Ci ⁻¹)	Group A ₂ (Ci)
H3	2.16E+02	5.83E-02	1100	4.89E-05	--
KR 85	3.80E+03	9.46E-01	270	3.50E-03	--
Total	4.02E+03	--	--	3.55E-03	281.35

Table 4.5-2 Westinghouse 15×15 SAS2H Output and Group A₂ Value (Volatiles)

Isotope	Activity/Assembly (Ci)	Fraction of Source	Isotope A ₂ Value (Ci)	Isotope Fraction/A ₂ (Ci ⁻¹)	Group A ₂ (Ci)
CS134	3.97E+04	2.03E-01	19	1.07E-02	--
CS137	5.17E+04	2.64E-01	16	1.62E-02	--
SR 89	1.46E+01	0.0	16	4.67E-06	--
SR 90	3.56E+04	0.182E-01	8.1	2.25E-02	--
RU103	1.73E+00	0.0	54	1.64E-07	--
RU106	6.85E+04	3.50E-01	5.4	6.49E-02	--
Total	1.96E+05	--	--	1.15E-01	8.73

Table 4.5-3 Westinghouse 15×15 SAS2H Output and Group A₂ Value (Fuel Fines)

Isotope	Activity/ Assembly (Ci)	Fraction of Source	Isotope A ₂ Value (Ci)	Isotope Fraction/A ₂ (Ci ⁻¹)	Group A ₂ (Ci)
TH234	1.51E-01	3.40E-07	8.1	4.19E-08	--
PA233	1.61E-01	3.62E-07	19	1.91E-08	--
PA234M	1.51E-01	3.40E-07	0.54	6.29E-07	--
U236	1.20E-01	2.70E-07	0.16	1.69E-06	--
U237	1.47E+00	3.31E-06	0.54	6.12E-06	--
U238	1.51E-01	3.40E-07	unlimited	---	--
NP237	1.61E-01	3.62E-07	0.054	6.71E-06	--
NP239	1.22E+01	2.74E-05	11	2.49E-06	--
PU236	3.91E-01	8.79E-07	0.081	1.09E-05	--
PU238	1.48E+03	3.33E-03	0.027	1.23E-01	--
PU239	1.48E+02	3.33E-04	0.027	1.23E-02	--
PU240	2.36E+02	5.31E-04	0.027	1.97E-02	--
PU241	6.13E+04	1.38E-01	1.6	8.62E-02	--
PU242	1.09E+00	2.45E-06	0.027	9.08E-05	--
AM241	2.74E+02	6.16E-04	0.027	2.28E-02	--
AM242M	5.58E+00	1.26E-05	0.027	4.65E-04	--
AM242	5.55E+00	1.25E-05	0.54	2.31E-05	--
AM243	1.22E+01	2.74E-05	0.027	1.02E-03	--
CM242	1.20E+03	2.70E-03	0.27	1.00E-02	--
CM243	1.29E+01	2.90E-05	0.027	1.07E-03	--
CM244	1.31E+03	2.95E-03	0.054	5.46E-02	--
CM245	1.13E-01	2.54E-07	0.024	1.06E-05	--
Y90	3.56E+04	8.01E-02	8.1	9.89E-03	--
Y91	7.66E+01	1.72E-04	16	1.08E-05	--
ZR93	5.87E-01	1.32E-06	unlimited	---	--
ZR95	2.36E+02	5.31E-04	22	2.41E-05	--
NB95	5.18E+02	1.17E-03	27	4.32E-05	--
NB95M	2.77E+00	6.23E-06	0.54	1.15E-05	--
TC99	6.71E+00	1.51E-05	24	6.29E-07	--
RH103M	1.73E+00	3.89E-06	1100	3.54E-09	--

Table 4.5-3 Westinghouse 15×15 SAS2H Output and Group A₂ Value (Fuel Fines)
(Continued)

Isotope	Activity/ Assembly (Ci)	Fraction of Source	Isotope A ₂ Value (Ci)	Isotope Fraction/A ₂ (Ci ⁻¹)	Group A ₂ (Ci)
RH106	6.85E+04	1.54E-01	0.54	2.85E-01	--
AG110	3.58E+00	8.05E-06	0.54	1.49E-05	--
AG110M	2.63E+02	5.92E-04	11	5.38E-05	--
CD113M	1.37E+01	3.08E-05	14	2.20E-06	--
SN119M	3.98E+00	8.95E-06	810	1.11E-08	--
SN121	9.09E-01	2.04E-06	0.54	3.79E-06	--
SN121M	1.17E+00	2.63E-06	24	1.10E-07	--
SN123	5.18E+00	1.17E-05	16	7.28E-07	--
SB125	2.36E+03	5.31E-03	27	1.97E-04	--
TE125M	5.76E+02	1.30E-03	24	5.40E-05	--
TE127	6.14E+01	1.38E-04	19	7.27E-06	--
TE127M	6.27E+01	1.41E-04	14	1.01E-05	--
BA137M	4.89E+04	1.10E-01	0.54	2.04E-01	--
CE144	8.32E+04	1.87E-01	5.4	3.47E-02	--
PR144	8.32E+04	1.87E-01	0.54	3.47E-01	--
PR144M	1.16E+03	2.61E-03	0.54	4.83E-03	--
PM146	1.63E+00	3.67E-06	0.54	6.79E-06	--
PM147	4.61E+04	1.04E-01	54	1.92E-03	--
SM151	1.73E+02	3.89E-04	270	1.44E-06	--
EU152	2.66E+00	5.89E-06	27	2.22E-07	--
GD153	9.72E-01	2.19E-06	240	9.11E-09	--
EU154	4.78E+03	1.08E-02	16	6.72E-04	--
EU155	2.76E+03	6.21E-03	81	7.66E-05	--
Total	4.45E+05	--	--	1.22E+00	0.82

Table 4.5-4 General Electric 7×7 SAS2H Output and Group A₂ Value (Gas)

Isotope	Activity/Assembly (Ci)	Fraction of Source	Isotope A ₂ Value (Ci)	Isotope Fraction/A ₂ (Ci ⁻¹)	Group A ₂ (Ci)
H3	7.73E+01	5.65E-02	1100	5.14E-05	--
KR 85	1.29E+03	9.43E-01	270	3.49E-03	--
Total	1.37E+03	--	--	3.55E-03	282.03

Table 4.5-5 General Electric 7×7 SAS2H Output and Group A₂ Value (Volatiles)

Isotope	Activity/Assembly (Ci)	Fraction of Source	Isotope A ₂ Value (Ci)	Isotope Fraction/A ₂ (Ci ⁻¹)	Group A ₂ (Ci)
CS134	1.33E+04	1.93E-01	19	1.02E-02	--
CS137	1.84E+04	2.67E-01	16	1.67E-02	--
SR 89	4.51E+00	6.55E-05	16	4.09E-06	--
SR 90	1.21E+04	1.76E-01	8.1	2.17E-02	--
RU103	5.90E-01	8.56E-06	54	1.59E-07	--
RU106	2.51E+04	3.64E-01	5.4	6.75E-02	--
Total	6.89E+04	--	--	1.16E-01	8.62

Table 4.5-6 General Electric 7x7 SAS2H Output and Group A₂ Value (Fuel Fines)

Isotope	Activity/ Assembly (Ci)	Fraction of Source	Isotope A ₂ Value (Ci)	Isotope Fraction/A ₂ (Ci ⁻¹)	Group A ₂ (Ci)
TH234	6.34E-02	4.15E-07	8.1	5.13E-08	--
PA233	5.08E-02	3.33E-07	19	1.75E-08	--
PA234M	6.34E-02	4.15E-07	0.54	7.69E-07	--
U236	3.79E-02	2.48E-07	0.16	1.55E-06	--
U237	5.04E-01	3.30E-06	0.54	6.12E-06	--
U238	6.34E-02	4.15E-07	unlimited	--	--
NP237	5.08E-02	3.33E-07	0.054	6.16E-06	--
NP239	4.52E+00	2.96E-05	11	2.69E-06	--
PU236	1.07E-01	7.01E-07	0.081	8.66E-06	--
PU238	4.80E+02	3.15E-03	0.027	1.16E-01	--
PU239	5.34E+01	3.50E-04	0.027	1.30E-02	--
PU240	9.99E+01	6.55E-04	0.027	2.42E-02	--
PU241	2.11E+04	1.38E-01	1.6	8.64E-02	--
PU242	4.25E-01	2.78E-06	0.027	1.03E-04	--
AM241	9.57E+01	6.27E-04	0.027	2.32E-02	--
AM242M	1.90E+00	1.24E-05	0.027	4.61E-04	--
AM242	1.89E+00	1.24E-05	0.54	2.29E-05	--
AM243	4.52E+00	2.96E-05	0.027	1.10E-03	--
CM242	4.30E+02	2.82E-03	0.27	1.04E-02	--
CM243	4.62E+00	3.03E-05	0.027	1.12E-03	--
CM244	4.82E+02	3.16E-03	0.054	5.85E-02	--
CM245	3.72E-02	2.44E-07	0.024	1.02E-05	--
Y 90	1.21E+04	7.93E-02	8.1	9.79E-03	--
Y 91	2.39E+01	1.57E-04	16	9.79E-06	--
ZR 93	2.04E-01	1.34E-06	unlimited	--	--
ZR 95	7.63E+01	5.00E-04	22	2.27E-05	--
NB 95	1.68E+02	1.10E-03	27	4.08E-05	--
NB 95M	8.97E-01	5.88E-06	0.54	1.09E-05	--
TC 99	2.39E+00	1.57E-05	24	6.53E-07	--
RH103M	5.89E-01	3.86E-06	1100	3.51E-09	--
RH106	2.51E+04	1.64E-01	0.54	3.05E-01	--
AG110	1.35E+00	8.85E-06	0.54	1.64E-05	--
AG110M	9.90E+01	6.49E-04	11	5.90E-05	--
CD113M	5.18E+00	3.39E-05	14	2.42E-06	--
SN119M	1.40E+00	9.17E-06	810	1.13E-08	--
SN121	3.46E-01	2.27E-06	0.54	4.20E-06	--
SN121M	4.46E-01	2.92E-06	24	1.22E-07	--

**Table 4.5-6 General Electric 7×7 SAS2H Output and Group A₂ Value (Fuel Fines)
(Continued)**

Isotope	Activity/ Assembly (Ci)	Fraction of Source	Isotope A ₂ Value (Ci)	Isotope Fraction/A ₂ (Ci ⁻¹)	Group A ₂ (Ci)
SN123	1.75E+00	1.15E-05	16	7.17E-07	--
SB125	8.66E+02	5.67E-03	27	2.10E-04	--
TE125M	2.12E+02	1.39E-03	24	5.79E-05	--
TE127	2.14E+01	1.40E-04	19	7.38E-06	--
TE127M	2.19E+01	1.43E-04	14	1.02E-05	--
BA137M	1.74E+04	1.14E-01	0.54	2.11E-01	--
CE144	2.73E+04	1.79E-01	5.4	3.31E-02	--
PR144	2.73E+04	1.79E-01	0.54	3.31E-01	--
PR144M	3.82E+02	2.50E-03	0.54	4.64E-03	--
PM146	5.15E-01	3.37E-06	0.54	6.25E-06	--
PM147	1.60E+04	1.05E-01	54	1.94E-03	--
SM151	5.76E+01	3.77E-04	270	1.40E-06	--
EU152	8.97E-01	5.88E-06	27	2.18E-07	--
GD153	3.69E-01	2.42E-06	240	1.01E-08	--
EU154	1.74E+03	1.14E-02	16	7.13E-04	--
EU155	9.69E+02	6.35E-03	81	7.84E-05	--
Total	1.53E+05		--	1.23E+00	0.81

Table 4.5-7 TRIGA (FLIP-LEU II) SAS2H Output and Group A₂ Value (Gas)

Isotope	Activity/ Assembly (Ci)	Fraction of Source	Isotope A ₂ Value (Ci)	Isotope Fraction/A ₂ (Ci ⁻¹)	Group A ₂ (Ci)
H3	1.07E+00	4.45E-02	1,100	4.04E-05	---
KR 85	2.30E+01	9.56E-01	270	3.54E-03	---
Total	2.41E+01	--	--	3.58E-03	279.37

Table 4.5-8 TRIGA (FLIP-LEU II) SAS2H Output and Group A₂ Value (Volatiles)

Isotope	Activity/ Assembly (Ci)	Fraction of Source	Isotope A ₂ Value (Ci)	Isotope Fraction/A ₂ (Ci ⁻¹)	Group A ₂ (Ci)
CS134	1.41E+02	1.70E-01	19	8.94E-03	---
CS135	4.12E-03	4.97E-06	27	1.84E-07	---
CS137	3.43E+02	4.13E-01	16	2.58E-02	---
SR 89	2.29E-03	2.76E-06	16	1.73E-07	---
SR 90	2.92E+02	3.52E-01	8.1	4.34E-02	---
RU106	5.37E+01	6.47E-02	5.4	1.20E-02	---
Total	8.30E+02	--	--	9.02E-02	11.08

Table 4.5-9 TRIGA (FLIP-LEU II) SAS2H Output and Group A₂ Value (Fuel Fines)

Isotope	Activity/ Assembly (Ci)	Fraction of Source	Isotope A ₂ Value (Ci)	Isotope Fraction/A ₂ (Ci ⁻¹)	Group A ₂ (Ci)
TH234	2.21E-04	1.78E-07	8.1	2.20E-08	---
PA233	1.56E-03	1.26E-06	19	6.61E-08	---
PA234M	2.21E-04	1.78E-07	0.54	3.30E-07	---
U232	2.24E-04	1.80E-07	0.0024	7.52E-05	---
U234	3.38E-04	2.72E-07	0.16	1.70E-06	---
U236	1.51E-03	1.22E-06	0.16	7.60E-06	---
U237	4.49E-03	3.62E-06	0.54	6.70E-06	---
U238	2.21E-04	1.78E-07	unlimited	---	---
NP237	1.56E-03	1.26E-06	0.054	2.33E-05	---
NP238	3.85E-04	3.10E-07	0.54	5.74E-07	---
NP239	5.03E-02	4.05E-05	11	3.68E-06	---
PU236	2.12E-03	1.71E-06	0.081	2.11E-05	---
PU238	1.66E+01	1.34E-02	0.027	4.95E-01	---
PU239	4.05E-01	3.26E-04	0.027	1.21E-02	---
PU240	5.34E-01	4.30E-04	0.027	1.59E-02	---
PU241	1.88E+02	1.51E-01	1.6	9.47E-02	---
PU242	4.18E-03	3.37E-06	0.027	1.25E-04	---
AM241	1.81E+00	1.46E-03	0.027	5.40E-02	---
AM242M	8.55E-02	6.89E-05	0.027	2.55E-03	---
AM242	8.51E-02	6.86E-05	0.54	1.27E-04	---
AM243	5.03E-02	4.05E-05	0.027	1.50E-03	---
CM242	2.88E+00	2.32E-03	0.27	8.59E-03	---
CM243	6.77E-02	5.45E-05	0.027	2.02E-03	---
CM244	5.29E+00	4.26E-03	0.054	7.89E-02	---
CM245	4.82E-04	3.88E-07	0.024	1.62E-05	---
Y 90	2.92E+02	2.35E-01	8.1	2.90E-02	---
Y 91	1.58E-02	1.27E-05	16	7.95E-07	---
ZR 93	5.27E-03	4.25E-06	unlimited	---	---
NB 93M	2.03E-03	1.64E-06	810	2.02E-09	---
ZR 95	4.98E-02	4.01E-05	22	1.82E-06	---
NB 95	1.10E-01	8.86E-05	27	3.28E-06	---
TC 99	5.24E-02	4.22E-05	24	1.76E-06	---
RH106	5.37E+01	4.33E-02	0.54	8.01E-02	---
AG110	2.63E-03	2.12E-06	0.54	3.92E-06	---

Table 4.5-9 TRIGA (FLIP-LEU II) SAS2H Output and Group A₂ Value (Fuel Fines)
(Continued)

Isotope	Activity/ Assembly (Ci)	Fraction of Source	Isotope A ₂ Value (Ci)	Isotope Fraction/A ₂ (Ci ⁻¹)	Group A ₂ (Ci)
AG110M	1.93E-01	1.55E-04	11	1.41E-05	---
CD113M	5.23E-02	4.21E-05	14	3.01E-06	---
SN119M	4.04E-03	3.25E-06	810	4.02E-09	---
SN121	4.05E-03	3.26E-06	0.54	6.04E-06	---
SN121M	5.22E-03	4.20E-06	24	1.75E-07	---
SN123	2.47E-03	1.99E-06	16	1.24E-07	---
SB125	4.11E+00	3.31E-03	27	1.23E-04	---
TE125M	1.00E+00	8.06E-04	24	3.36E-05	---
TE127	1.98E-02	1.59E-05	19	8.39E-07	---
TE127M	2.02E-02	1.63E-05	14	1.16E-06	---
BA137M	3.24E+02	2.61E-01	0.54	4.83E-01	---
CE144	8.88E+01	7.15E-02	5.4	1.32E-02	---
PR144	8.88E+01	7.15E-02	0.54	1.32E-01	---
PR144M	1.24E+00	9.99E-04	0.54	1.85E-03	---
PM146	4.30E-03	3.46E-06	0.54	6.41E-06	---
PM147	1.30E+02	1.05E-01	54	1.94E-03	---
SM151	8.64E-01	6.96E-04	270	2.58E-06	---
EU152	6.20E-02	4.99E-05	27	1.85E-06	---
GD153	8.69E-03	7.00E-06	240	2.92E-08	---
EU154	2.75E+01	2.22E-02	16	1.38E-03	---
EU155	1.29E+01	1.04E-02	81	1.28E-04	---
Total	1.24E+03	--	--	1.51E+00	0.66

Table 4.5-10 MTR HEU SAS2H Output and Group A₂ Value (Gas)

Isotope	Activity/ Assembly (Ci)	Fraction of Source	Isotope A ₂ Value (Ci)	Isotope Fraction/A ₂ (Ci ⁻¹)	Group A ₂ (Ci)
H3	3.19E+00	3.69E-02	1100	3.36E-05	---
KR 85	8.32E+01	9.63E-01	270	3.57E-03	---
Total	8.64E+01	--	--	3.60E-03	277.74

Table 4.5-11 MTR HEU SAS2H Output and Group A₂ Value (Volatiles)

Isotope	Activity/ Assembly (Ci)	Fraction of Source	Isotope A ₂ Value (Ci)	Isotope Fraction/A ₂ (Ci ⁻¹)	Group A ₂ (Ci)
CS134	9.14E+02	3.31E-01	19	1.74E-02	---
CS137	8.85E+02	3.21E-01	16	20.1E-02	---
SR89	3.26E-05	1.18E-08	16	7.39E-10	---
SR 90	8.47E+02	3.07E-01	8.1	3.79E-02	---
RU103	7.62E-08	2.76E-11	54	5.12E-13	---
RU106	1.12E+02	4.06E-02	5.4	7.52E-03	---
Total	2.76E+03	--	--	8.29E-02	12.06

Table 4.5-12 MTR HEU SAS2H Output and Group A₂ Value (Fuel Fines)

Isotope	Activity/ Assembly (Ci)	Fraction of Source	Isotope A ₂ Value (Ci)	Isotope Fraction/A ₂ (Ci ⁻¹)	Group A ₂ (Ci)
PA233	7.45E-03	2.19E-06	19	1.15E-07	---
U234	1.48E-03	4.34E-07	0.16	2.72E-06	---
U236	4.86E-03	1.43E-06	0.16	8.92E-06	---
U237	2.71E-03	7.96E-07	0.54	1.47E-06	---
NP237	7.45E-03	2.19E-06	0.054	4.05E-05	---
NP239	6.16E-02	1.81E-05	11	1.64E-06	---
PU236	6.07E-03	1.78E-06	0.081	2.20E-05	---
PU238	1.16E+02	3.41E-02	0.027	1.26E+00	---
PU239	1.84E-01	5.40E-05	0.027	2.00E-03	---
PU240	1.32E-01	3.88E-05	0.027	1.44E-03	---
PU241	1.13E+02	3.32E-02	1.6	2.07E-02	---
PU242	2.58E-03	7.57E-07	0.027	2.81E-05	---
AM241	8.39E-01	2.46E-04	0.027	9.12E-03	---
AM242M	5.54E-03	1.63E-06	0.027	6.02E-05	---
AM242	5.52E-03	1.62E-06	0.54	3.00E-06	---
AM243	6.16E-02	1.81E-05	0.027	6.70E-04	---
CM242	1.38E-01	4.05E-05	0.27	1.50E-04	---
CM243	4.80E-02	1.41E-05	0.027	5.22E-04	---
CM244	1.39E+01	4.08E-03	0.054	7.56E-02	---
CM245	3.41E-03	1.00E-06	0.024	4.17E-05	---
CM246	1.30E-03	3.82E-07	0.024	1.59E-05	---
BK249	4.27E-05	1.25E-08	8.1	1.55E-09	---
Y 90	8.47E+02	2.49E-01	8.1	3.07E-02	---
Y 91	6.14E-04	1.80E-07	16	1.13E-08	---
ZR 95	3.06E-03	8.98E-07	22	4.08E-08	---
NB 95	6.73E-03	1.98E-06	27	7.32E-08	---
NB 95M	3.60E-05	1.06E-08	0.54	1.96E-08	---
TC 99	1.03E-01	3.02E-05	24	1.26E-06	---
RH103M	7.60E-08	2.23E-11	1100	2.03E-14	---

Table 4.5-12 MTR HEU SAS2H Output and Group A₂ Value (Fuel Fines) (Continued)

Isotope	Activity/ Assembly (Ci)	Fraction of Source	Isotope A ₂ Value (Ci)	Isotope Fraction/A ₂ (Ci ⁻¹)	Group A ₂ (Ci)
RH106	1.12E+02	3.29E-02	0.54	6.09E-02	---
AG110	3.32E-03	9.75E-07	0.54	1.80E-06	---
AG110M	2.44E-01	7.16E-05	11	6.51E-06	---
CD113M	1.18E-01	3.46E-05	14	2.47E-06	---
SN119M	1.56E-02	4.58E-06	810	5.65E-09	---
SN123	2.47E-03	7.25E-07	16	4.53E-08	---
TE123M	5.98E-05	1.76E-08	27	6.50E-10	---
SB124	7.26E-07	2.13E-10	16	1.33E-11	---
SB125	1.60E+01	4.70E-03	27	1.74E-04	---
TE125M	3.92E+00	1.15E-03	24	4.80E-05	---
TE127	8.38E-03	2.46E-06	19	1.29E-07	---
TE127M	8.56E-03	2.51E-06	14	1.80E-07	---
TE129	2.72E-11	7.99E-15	16	4.99E-16	---
TE129M	4.25E-11	1.25E-14	11	1.13E-15	---
BA137M	8.36E+02	2.45E-01	0.54	4.55E-01	---
CE141	5.84E-10	1.71E-13	16	1.07E-14	---
CE144	4.48E+02	1.32E-01	5.4	2.44E-02	---
PR144	4.48E+02	1.32E-01	0.54	2.44E-01	---
PR144M	6.27E+00	1.84E-03	0.54	3.41E-03	---
PM147	3.10E+02	9.10E-02	54	1.69E-03	---
PM148	1.94E-10	5.70E-14	0.54	1.05E-13	---
PM148M	3.68E-09	1.08E-12	19	5.69E-14	---
SM151	3.12E+00	9.16E-04	270	3.39E-06	---
GD153	2.49E-03	7.31E-07	240	3.05E-09	---
EU154	8.10E+01	2.38E-02	16	1.49E-03	---
EU155	5.00E+01	1.47E-02	81	1.81E-04	---
TB160	6.34E-06	1.86E-09	16	1.16E-10	---
Total	3.41E+03	--	--	2.19E+00	0.46

Table 4.5-13 25 High Burnup BWR-Rod SAS2H Output and Group A₂ Value (Gas)

Isotope	Activity/ Assembly (Ci)	Fraction of Source	Isotope A ₂ Value (Ci)	Isotope Fraction/A ₂ (Ci ⁻¹)	Group A ₂ (Ci)
H 3	1.13E+02	6.49E-02	1100	5.90E-05	---
KR 85	1.63E+03	9.35E-01	270	3.46E-03	---
Total	1.75E+03			3.52E-03	283.90

Table 4.5-14 25 High Burnup BWR-Rod SAS2H Output and Group A₂ Value (Volatiles)

Isotope	Activity/ Assembly (Ci)	Fraction of Source	Isotope A ₂ Value (Ci)	Isotope Fraction/A ₂ (Ci ⁻¹)	Group A ₂ (Ci)
CS134	5.09E+04	1.29E-01	19	6.79E-03	---
CS136	1.30E+04	3.29E-02	14	2.35E-03	---
CS137	2.66E+04	6.74E-02	16	4.21E-03	---
SR 89	4.32E+04	1.09E-01	16	6.83E-03	---
SR 90	1.53E+04	3.88E-02	8.1	4.78E-03	---
RU103	1.54E+05	3.90E-01	54	7.22E-03	---
RU106	9.18E+04	2.33E-01	5.4	4.31E-02	---
Total	3.95E+05			7.53E-02	13.29

Table 4.5-15 25 High Burnup BWR-Rod SAS2H Output and Group A₂ Value (Fuel Fines)

Isotope	Activity/ Assembly (Ci)	Fraction of Source	Isotope A ₂ Value (Ci)	Isotope Fraction/A ₂ (Ci ⁻¹)	Group A ₂ (Ci)
U236	3.75E-02	2.39E-08	0.16	1.49E-07	---
U238	3.29E-02	2.09E-08	unlimited	---	---
NP237	7.35E-02	4.68E-08	0.054	8.67E-07	---
PU238	1.24E+03	7.91E-04	0.027	2.93E-02	---
PU239	2.94E+01	1.88E-05	0.027	6.95E-04	---
PU240	8.16E+01	5.20E-05	0.027	1.93E-03	---
PU241	1.72E+04	1.10E-02	1.6	6.87E-03	---
PU242	8.16E-01	5.20E-07	0.027	1.93E-05	---
AM241	2.01E+01	1.28E-05	0.027	4.75E-04	---
AM242M	1.55E+00	9.89E-07	0.027	3.66E-05	---
AM243	1.46E+01	9.34E-06	0.027	3.46E-04	---
CM242	1.18E+04	7.55E-03	0.27	2.80E-02	---
CM243	9.18E+00	5.86E-06	0.027	2.17E-04	---
CM244	4.92E+03	3.14E-03	0.054	5.81E-02	---
CM245	4.49E-01	2.86E-07	0.024	1.19E-05	---
CM246	5.31E-01	3.38E-07	0.024	1.41E-05	---
RB 86	3.74E+02	2.39E-04	14	1.71E-05	---
Y 90	1.63E+04	1.04E-02	8.1	1.28E-03	---
Y 91	6.28E+04	4.00E-02	16	2.50E-03	---
ZR 95	1.12E+05	7.12E-02	22	3.24E-03	---
NB 95	1.12E+05	7.16E-02	27	2.65E-03	---
NB 95M	1.27E+03	8.10E-04	0.54	1.50E-03	---
TC 99	2.76E+00	1.76E-06	24	7.33E-08	---
RH103M	1.54E+05	9.79E-02	1100	8.90E-05	---
RH106	9.74E+04	6.21E-02	0.54	1.15E-01	---
AG110	4.75E+04	3.03E-02	0.54	5.61E-02	---
AG110M	1.57E+03	9.99E-04	11	9.08E-05	---
CD113M	1.33E+01	8.49E-06	14	6.06E-07	---
CD115M	5.09E+01	3.24E-05	14	2.32E-06	---
SN119M	1.34E+01	8.52E-06	810	1.05E-08	---
SN123	5.36E+01	3.42E-05	16	2.13E-06	---
TE123M	6.68E+00	4.26E-06	27	1.58E-07	---

Table 4.5-15 25 High Burnup BWR-Rod SAS2H Output and Group A₂ Value (Fuel Fines)

(Continued)

Isotope	Activity/ Assembly (Ci)	Fraction of Source	Isotope A ₂ Value (Ci)	Isotope Fraction/A ₂ (Ci ⁻¹)	Group A ₂ (Ci)
SB124	2.14E+02	1.36E-04	16	8.52E-06	---
SB125	1.47E+03	9.37E-04	27	3.47E-05	---
TE125M	3.36E+02	2.14E-04	24	8.93E-06	---
TE127	8.57E+03	5.47E-03	19	2.88E-04	---
TE127M	1.49E+03	9.53E-04	14	6.81E-05	---
TE129	2.67E+04	1.70E-02	16	1.07E-03	---
TE129M	5.46E+03	3.48E-03	11	3.16E-04	---
BA137M	2.52E+04	1.61E-02	0.54	2.98E-02	---
BA140	1.34E+05	8.52E-02	8.1	1.05E-02	---
LA140	1.48E+05	9.47E-02	11	8.61E-03	---
CE141	1.21E+05	7.74E-02	16	4.84E-03	---
PR143	1.05E+05	6.67E-02	16	4.17E-03	---
CE144	9.39E+04	5.99E-02	5.4	1.11E-02	---
PR144	9.49E+04	6.05E-02	0.54	1.12E-01	---
PR144M	1.32E+03	8.43E-04	0.54	1.56E-03	---
PM146	1.10E+00	7.03E-07	0.54	1.30E-06	---
ND147	5.20E+04	3.32E-02	16	2.07E-03	---
PM147	1.43E+04	9.11E-03	54	1.69E-04	---
PM148	1.62E+04	1.03E-02	0.54	1.91E-02	---
PM148M	2.20E+03	1.41E-03	19	7.40E-05	---
SM151	5.20E+01	3.32E-05	270	1.23E-07	---
EU152	7.55E-01	4.81E-07	27	1.78E-08	---
GD153	9.39E+00	5.99E-06	240	2.49E-08	---
EU154	3.49E+03	2.23E-03	16	1.39E-04	---
EU155	2.25E+03	1.43E-03	81	1.77E-05	---
EU156	6.94E+04	4.42E-02	19	2.33E-03	---
TB160	4.40E+02	2.80E-04	16	1.75E-05	---
Total	1.57E+06			5.17E-01	1.93

Table 4.5-16 25 High Burnup PWR-Rod SAS2H Output and Group A₂ Value (Gas)

Isotope	Activity/ Assembly (Ci)	Fraction of Source	Isotope A ₂ Value (Ci)	Isotope Fraction/A ₂ (Ci ⁻¹)	Group A ₂ (Ci)
H 3	7.39E+01	6.37E-02	1100	5.79E-05	---
KR 85	1.09E+03	9.36E-01	270	3.47E-03	---
Total	1.16E+03			3.53E-03	283.64

Table 4.5-17 25 High Burnup PWR-Rod SAS2H Output and Group A₂ Value (Volatiles)

Isotope	Activity/ Assembly (Ci)	Fraction of Source	Isotope A ₂ Value (Ci)	Isotope Fraction/A ₂ (Ci ⁻¹)	Group A ₂ (Ci)
CS134	3.69E+04	1.11E-01	19	5.86E-03	---
CS136	9.38E+03	2.83E-02	14	2.02E-03	---
CS137	1.66E+04	5.01E-02	16	3.13E-03	---
SR 89	4.11E+04	1.24E-01	16	7.73E-03	---
SR 90	9.57E+03	2.89E-02	8.1	3.56E-03	---
RU103	1.40E+05	4.23E-01	54	7.83E-03	---
RU106	7.78E+04	2.35E-01	5.4	4.35E-02	---
Total	3.32E+05			7.36E-02	13.59

Table 4.5-18 25 High Burnup PWR-Rod SAS2H Output and Group A₂ Value (Fuel Fines)

Isotope	Activity/ Assembly (Ci)	Fraction of Source	Isotope A ₂ Value (Ci)	Isotope Fraction/A ₂ (Ci ⁻¹)	Group A ₂ (Ci)
U236	2.24E-02	1.59E-08	0.16	9.94E-08	---
U238	7.88E+02	5.59E-04	unlimited	---	---
NP237	4.80E-02	3.40E-08	0.054	6.30E-07	---
PU238	7.88E+02	5.59E-04	0.027	2.07E-02	---
PU239	1.99E+01	1.41E-05	0.027	5.22E-04	---
PU240	4.72E+01	3.34E-05	0.027	1.24E-03	---
PU241	1.20E+04	8.52E-03	1.6	5.32E-03	---
PU242	4.94E-01	3.50E-07	0.027	1.30E-05	---
AM241	1.01E+01	7.14E-06	0.027	2.64E-04	---
AM242M	8.25E-01	5.85E-07	0.027	2.17E-05	---
AM243	9.43E+00	6.68E-06	0.027	2.48E-04	---
CM242	7.94E+03	5.63E-03	0.27	2.08E-02	---
CM243	6.21E+00	4.40E-06	0.027	1.63E-04	---
CM244	3.07E+03	2.17E-03	0.054	4.03E-02	---
CM245	3.11E-01	2.20E-07	0.024	9.18E-06	---
CM246	3.15E-01	2.23E-07	0.024	9.31E-06	---
RB 86	3.07E+02	2.17E-04	14	1.55E-05	---
Y 89M	3.85E+00	2.73E-06	0.54	5.05E-06	---
Y 90	1.03E+04	7.32E-03	8.1	9.03E-04	---
Y 91	5.94E+04	4.21E-02	16	2.63E-03	---
ZR 95	1.04E+05	7.37E-02	22	3.35E-03	---
NB 95	1.05E+05	7.41E-02	27	2.74E-03	---
NB 95M	1.19E+03	8.40E-04	0.54	1.56E-03	---
TC 99	1.70E+00	1.21E-06	24	5.03E-08	---
RH103M	1.40E+05	9.92E-02	1100	9.02E-05	---
RH106	8.51E+04	6.03E-02	0.54	1.12E-01	---
AG110	4.15E+04	2.94E-02	0.54	5.44E-02	---
AG110M	1.24E+03	8.82E-04	11	8.02E-05	---
CD113M	8.11E+00	5.75E-06	14	4.11E-07	---
CD115M	4.52E+01	3.20E-05	14	2.29E-06	---
SN119M	1.06E+01	7.48E-06	810	9.23E-09	---
SN123	4.93E+01	3.49E-05	16	2.18E-06	---
TE123M	4.94E+00	3.50E-06	27	1.30E-07	---

Table 4.5-18 25 High Burnup PWR-Rod SAS2H Output and Group A₂ Value (Fuel Fines)
(continued)

Isotope	Activity/ Assembly (Ci)	Fraction of Source	Isotope A ₂ Value (Ci)	Isotope Fraction/A ₂ (Ci ⁻¹)	Group A ₂ (Ci)
SB124	1.78E+02	1.26E-04	16	7.86E-06	---
SB125	1.12E+03	7.93E-04	27	2.94E-05	---
TE125M	2.51E+02	1.78E-04	24	7.42E-06	---
TE127	7.83E+03	5.55E-03	19	2.92E-04	---
TE127M	1.36E+03	9.60E-04	14	6.86E-05	---
TE129	2.44E+04	1.73E-02	16	1.08E-03	---
TE129M	5.01E+03	3.55E-03	11	3.23E-04	---
BA137M	1.58E+04	1.12E-02	0.54	2.07E-02	---
BA140	1.24E+05	8.76E-02	8.1	1.08E-02	---
LA140	1.36E+05	9.61E-02	11	8.74E-03	---
CE141	1.12E+05	7.96E-02	16	4.98E-03	---
PR143	9.63E+04	6.82E-02	16	4.27E-03	---
CE144	8.75E+04	6.20E-02	5.4	1.15E-02	---
PR144	8.85E+04	6.27E-02	0.54	1.16E-01	---
PR144M	1.23E+03	8.72E-04	0.54	1.61E-03	---
PM146	8.71E-01	6.17E-07	0.54	1.14E-06	---
ND147	4.74E+04	3.36E-02	16	2.10E-03	---
PM147	1.03E+04	7.32E-03	54	1.36E-04	---
PM148	1.48E+04	1.05E-02	0.54	1.94E-02	---
PM148M	1.70E+03	1.21E-03	19	6.36E-05	---
SM151	3.61E+01	2.56E-05	270	9.47E-08	---
EU152	0.00E+00	0.00E+00	27	0.00E+00	---
GD153	5.06E+00	3.58E-06	240	1.49E-08	---
EU154	2.26E+03	1.60E-03	16	1.00E-04	---
EU155	1.49E+03	1.06E-03	81	1.30E-05	---
EU156	5.94E+04	4.21E-02	19	2.21E-03	---
TB160	3.38E+02	2.40E-04	16	1.50E-05	---
Total	1.41E+06			4.72E-01	2.12

Table 4.5-19 DIDO LEU SAS2H Output and Group A₂ Value (Gas)

Isotope	Activity/ Assembly (Ci)	Fraction of Source	Isotope A ₂ Value (Ci)	Isotope Fraction/A ₂ (Ci ⁻¹)	Group A ₂ (Ci)
H 3	1.47E+00	3.62E-02	1100	3.31E-05	---
KR 85	3.91E+01	9.64E-01	270	3.57E-03	---
Total	4.06E+01			3.6E-03	277.63

Table 4.5-20 DIDO LEU SAS2H Output and Group A₂ Value (Volatiles)

Isotope	Activity/ Assembly (Ci)	Fraction of Source	Isotope A ₂ Value (Ci)	Isotope Fraction/A ₂ (Ci ⁻¹)	Group A ₂ (Ci)
CS134	1.63E+02	1.41E-01	19	7.42E-03	---
CS137	3.73E+02	3.23E-01	16	2.04E-02	---
SR 89	2.93E+00	2.53E-03	16	1.12E-04	---
SR 90	3.59E+02	3.11E-01	8.1	3.87E-02	---
RU103	2.00E-01	1.73E-04	54	2.09E-06	---
RU106	2.58E+02	2.23E-01	5.4	4.03E-02	---
Total	1.16E+03			1.07E-01	9.36

Table 4.5-21 DIDO LEU SAS2H Output and Group A₂ Value (Fuel Fines)

Isotope	Activity/ Assembly (Ci)	Fraction of Source	Isotope A ₂ Value (Ci)	Isotope Fraction/A ₂ (Ci ⁻¹)	Group A ₂ (Ci)
TH231	8.99E-05	1.59E-08	0.54	3.15E-08	---
TH234	2.42E-04	4.29E-08	8.1	5.90E-09	---
PA233	3.31E-04	5.87E-08	19	3.37E-09	---
PA234M	2.42E-04	4.29E-08	0.54	8.85E-08	---
U235	8.99E-05	1.59E-08	unlimited	---	---
U236	1.34E-03	2.38E-07	0.16	1.58E-06	---
U237	9.63E-04	1.71E-07	0.54	3.57E-07	---
U238	2.42E-04	4.29E-08	unlimited	---	---
NP237	3.31E-04	5.87E-08	0.054	1.19E-06	---
NP239	1.22E-03	2.16E-07	11	2.28E-08	---
PU238	1.02E+00	1.81E-04	0.027	7.46E-03	---
PU239	2.02E-01	3.58E-05	0.027	1.47E-03	---
PU240	3.09E-01	5.48E-05	0.027	2.24E-03	---
PU241	4.03E+01	7.15E-03	1.6	5.00E-03	---
PU242	6.07E-04	1.08E-07	0.027	4.48E-06	---
AM241	1.25E-01	2.22E-05	0.027	9.57E-04	---
AM242M	5.80E-04	1.03E-07	0.027	4.55E-06	---
AM242	5.77E-04	1.02E-07	0.54	2.26E-07	---
AM243	1.22E-03	2.16E-07	0.027	9.31E-06	---
CM242	3.70E-01	6.56E-05	0.27	2.59E-04	---
CM243	7.38E-04	1.31E-07	0.027	5.75E-06	---
CM244	4.67E-02	8.28E-06	0.054	1.81E-04	---
Y 90	3.59E+02	6.37E-02	8.1	8.32E-03	---
Y 91	1.10E+01	1.95E-03	16	9.48E-05	---
ZR 95	2.27E+01	4.02E-03	22	1.45E-04	---
NB 95	5.01E+01	8.88E-03	27	2.61E-04	---
NB 95M	2.67E-01	4.73E-05	0.54	6.97E-05	---

Table 4.5-21 DIDO LEU SAS2H Output and Group A₂ Value (Fuel Fines) (Continued)

Isotope	Activity/ Assembly (Ci)	Fraction of Source	Isotope A ₂ Value (Ci)	Isotope Fraction/A ₂ (Ci ⁻¹)	Group A ₂ (Ci)
TC 99	5.29E-02	9.38E-06	24	4.14E-07	---
RH103M	2.00E-01	3.55E-05	1100	2.20E-08	---
RH106	2.58E+02	4.57E-02	0.54	8.65E-02	---
AG110M	2.29E-01	4.06E-05	11	3.78E-06	---
CD113M	3.96E-02	7.02E-06	14	5.33E-07	---
SN119M	2.00E-02	3.55E-06	810	4.38E-09	---
SN123	1.55E-01	2.75E-05	16	1.56E-06	---
SB125	1.30E+01	2.30E-03	27	8.91E-05	---
TE125M	3.17E+00	5.62E-04	24	2.44E-05	---
TE127	1.27E+00	2.25E-04	19	1.06E-05	---
TE127M	1.30E+00	2.30E-04	14	1.48E-05	---
BA137M	3.53E+02	6.26E-02	0.54	1.22E-01	---
CE141	3.69E-02	6.54E-06	16	2.54E-07	---
CE144	1.89E+03	3.35E-01	5.4	6.11E-02	---
PR144	1.89E+03	3.35E-01	0.54	6.11E-01	---
PR144M	2.65E+01	4.70E-03	0.54	8.58E-03	---
PM147	6.99E+02	1.24E-01	54	2.38E-03	---
SM151	6.24E-01	1.11E-04	270	4.39E-07	---
EU154	1.29E+01	2.29E-03	16	1.55E-04	---
EU155	5.06E+00	8.97E-04	81	1.19E-05	---
Total	5.64E+03			9.18E-01	1.09

4.5.5 Containment Analysis of MTR Fuel Elements

To support the shipment of MTR fuel elements that have localized aluminum cladding corrosion, or mechanical damage, DOE has prepared a set of reports titled "Bases for Containment Analysis for Transportation of Aluminum-Based Spent Nuclear Fuel" (WSRC-TR-98-00317) and "Impact of Degraded RA-3 Fuel Condition on Transportation to and Storage in SRS Basins" (WSRC-TR-2000-00152). Report WSRC-TR-98-00317 has been presented by DOE to the NRC, and subsequently requested by DOE to be used to justify the radionuclide activity concentrations for MTR fuel in the NAC-LWT cask. Report WSRC-TR-2000-00152 demonstrates that mechanical damage may be treated similarly to cladding corrosion, and that the controlling variable in the calculation is the surface area of fuel meat exposed. The information that follows relies heavily on the methodology and terminology presented in the WSRC reports.

MTR fuel elements are divided into three broad categories based on their initial enrichment. These categories are highly enriched (HEU), medium enriched (MEU), and low enriched (LEU). Each category was individually evaluated in Chapter 5 to determine minimum cool time as a function of burnup. Containment evaluations were performed for each of the fuel types at 30 watts at or above the maximum permissible burnup. The 30-watt pattern reflects full basket loads (seven elements per basket) and bounds the higher heat load HEU patterns. While higher fuel mass LEU elements (640 grams ^{235}U) produce larger radionuclide inventories on a per element basis than those employed in the following calculations, the high LEU mass basket is limited to four elements (refer to Chapter 6) and is, therefore, bounded by the evaluations shown. MTR fuel element content condition allowable leakage rates are bounded by the allowable release rates calculated for 25 high burnup BWR fuel rods (see Sections 4.2 and 4.5.6).

The activities and A_2 values together with the maximum allowable normal condition leak rate for each of the three fuel types are:

	<u>MTR LEU</u>	<u>MTR MEU</u>	<u>MTR HEU</u>
Fission Gas Ci	8.84E+01	9.43E+01	8.64E+01
Fission Gas A_2	2.78E+02	2.78E+02	2.78E+02
Volatiles Ci	2.79E+03	2.79E+03	2.76E+03
Volatiles A_2	1.05E+01	1.09E+0	1.21E+01
Fines Ci	5.36E+03	5.05E+03	3.41E+03
Fines A_2	9.56E-01	9.72E-01	4.56E-01
Allowable Leakage Rate (cm ³ /sec)	1.83E-05	1.94E-05	1.42E-05

The detailed evaluation of the bounding HEU MTR fuel element is shown in the following sections.

4.5.5.1 Definition of Variables

The following variables are utilized to determine the releasable quantity of radionuclides and the corresponding allowable leakage rate from the cask. These variables are defined either within the WSRC reports or are specific to the MTR fuel loading proposed for the NAC-LWT cask.

Fraction of Breached Fuel	f_b	0.10 (normal)	1.0 (accident)
Fission Gas Release Fraction	f_G	0.30 (normal)	1.0 (accident)
Volatile Release Fraction	f_v	1×10^{-6} (normal & accident)	
Fuel Meat Spallation Fraction	T_F	0.15 (normal)	1.0 (accident)
Crud Spallation Fraction	f_C	0.15 (normal)	1.0 (accident)
Depth of Corrosion Attack	P	5×10^{-4} cm	
Cask Free Volume	V_c	2.293×10^5 cm ³ (Table 4.2-3) ¹	
Number of MTR Assemblies	Assy	42 (maximum)	
Gas A ₂ Value	$A_{2 \text{ gas}}$	277.74 Ci (Table 4.5-10)	
Volatile A ₂ Value	$A_{2 \text{ vol}}$	12.06 Ci (Table 4.5-11)	
Fines A ₂ Value	$A_{2 \text{ fines}}$	0.46 Ci (Table 4.5-12)	
Crud A ₂ Value	$A_{2 \text{ crud}}$	0.27 Ci (WSRC Report, Section 5.4)	
Corrosion Fraction	0.5	(maximum design basis)	

¹ Free volume associated with 42 element basket with intact MTR fuel elements. Cask free volume would not be significantly reduced for the configuration of loose plates in an MTR plate canister, as the additional material of the can is offset by the lack of MTR fuel assembly hardware materials.

4.5.5.1.1 Calculation of MTR Fuel Element Surface Area

The physical data of the HEU design basis assembly are presented below and are based on the shielding and source term model presented in Chapter 5. The surface area of the element is calculated by using the exposed length and width of each of the plates in the design basis assembly, multiplying by two to account for each side of the plate, multiplying by the number of plates, then adding the area of the two side plates. Any variation in the fuel surface area will have a minimal impact on the result of the evaluation since the fuel element surface area is used only to calculate the crud radionuclide inventory, which is only a small fraction of the total inventory, as shown in Section 4.5.5.3.1. The following variables are defined for the design basis MTR fuel element.

Number of Fuel Plates	Plates = 23
Exposed Plate Width	Plate Width = 6.35 cm
Exposed Plate Length	Plate Length = 66.4 cm
Side Plate Width	Side Width = 7.5 cm
Side Plate Length	Side Length = 66.4 cm
Side Plate Thickness	Side Thickness = 0.475 cm

Using these variables, the total surface area of an MTR fuel element can be determined. This is calculated as follows, using the areas of the exposed fuel plates and the side plates.

Fuel Plate Area	Plate Area = $2 \times \text{Plate Width} \times \text{Plate Length}$
Side Plate Area	Side Area = $2 \times (\text{Side Width} + \text{Side Thick}) \times \text{Side Length}$
Total Surface Area	SA = Plates \times Plate Area + $2 \times$ Side Area SA = $2.15 \times 10^4 \text{ cm}^2$

4.5.5.1.2 Calculation of Exposed Meat Surface Area and Volume

To determine the releasable quantity of fuel fines, it is necessary to calculate the fuel meat surface area of the outermost two fuel plates, and the total fuel meat volume in the fuel element. The following variables are defined for the design basis MTR elements.

Fuel Meat Thickness per Plate	Meat Thickness = 0.051 cm
Fuel Meat Width per Plate	Meat Width = 6.35 cm
Fuel Meat Length per Plate	Meat Length = 65 cm

Using these variables, the outside surface area and total fuel meat volume of an MTR fuel element can be determined. This is calculated as follows, using the variables listed above.

Fuel Meat Surface Area on Outside Plates	Meat Area = $2 \times 2 \times \text{Meat Width} \times \text{Meat Length}$ Meat Area = $1.651 \times 10^3 \text{ cm}^2$
---	---

Fuel Meat Volume	$V_M = \text{Plates} \times \text{Meat Thick} \times \text{Meat Width} \times \text{Meat Length}$ $V_M = 484 \text{ cm}^3$
------------------	---

4.5.5.2 Calculation of Releasable Radionuclides

The following sections present the releasable quantities of radionuclides determined in accordance with the WSRC report and using the data defined in Section 4.1.1.1.

4.5.5.2.1 Fission Gas Radionuclide Inventory

Fission Gas Radionuclide Quantity	$A_G = 86.4 \text{ Ci}$	(Table 4.5-10)
-----------------------------------	-------------------------	----------------

Fission Gas Releasable Inventory	$R_{\text{gas}} = A_G \times \text{Assy} \times f_b \times f_G$ $R_{\text{gas}} = 109 \text{ Ci (normal)}$ $R_{\text{gas}} = 3628 \text{ Ci (accident)}$
----------------------------------	--

Fission Gas Activity Density	$C_{\text{gas}} = R_{\text{gas}} / V_C$ $C_{\text{gas}} = 4.75 \times 10^{-4} \text{ Ci/cm}^3 \text{ (normal)}$ $C_{\text{gas}} = 1.58 \times 10^{-2} \text{ Ci/cm}^3 \text{ (accident)}$
------------------------------	---

4.5.5.2.2 Volatile Radionuclide Inventory

Volatile Radionuclide Quantity	$A_V = 2.76 \times 10^3 \text{ Ci}$	(Table 4.5-11)
--------------------------------	-------------------------------------	----------------

Volatile Releasable Quantity	$R_{\text{vol}} = A_V \times \text{Assy} \times f_b \times f_V$ $R_{\text{vol}} = 0.012 \text{ Ci (normal)}$ $R_{\text{vol}} = 0.116 \text{ Ci (accident)}$
------------------------------	---

Volatile Activity Density	$C_{\text{vol}} = R_{\text{vol}} / V_C$ $C_{\text{vol}} = 5.05 \times 10^{-8} \text{ Ci/cm}^3 \text{ (normal)}$ $C_{\text{vol}} = 5.05 \times 10^{-7} \text{ Ci/cm}^3 \text{ (accident)}$
---------------------------	---

4.5.5.2.3 Fuel Fines Radionuclide Inventory

To calculate the fuel fines available for release, the total inventory of radionuclides in the spent fuel other than gases and volatiles is reduced by fractions accounting for the percentage of fuel that has

surface area corrosion or mechanical damage producing breached cladding. Section 5.1.3 of WSRC report WSRC-TR-98-00317 presents a basis for determining the bounding value of fuel element corrosion. Based on the worldwide examinations of MTR fuel elements utilized in the report, the worst-case extent of surface corrosion was 1%. However, for this analysis, the exposed surface area (ESA) is determined by multiplying a worst-case corrosion fraction of 50% by the surface area of the fuel meat in the outermost two fuel plates as calculated in Section 4.5.5.1.2. As described in Sections 4 and A.2.3 of WSRC report WSRC-TR-2000-0152, mechanical cladding damage exhibits the same properties of radionuclide release as corrosion damage. Therefore, this ESA is considered to be the fuel meat surface exposed by a combination of corrosion and/or mechanical damage.

Exposed Surface Area	$ESA = \text{Meat Area} \times \text{Corrosion Fraction}$ $ESA = 825.5 \text{ cm}^2 \text{ per element}$
Fuel Fines Radionuclide Quantity	$A_F = 3.41 \times 10^3 \text{ Ci} \quad (\text{Table 4.5-12})$
Fuel Fines Releasable Quantity	$R_{\text{fines}} = (A_F \times \text{Assy} \times P \times ESA \times f_b \times T_F) / V_M$ $R_{\text{fines}} = 1.829 \text{ Ci (normal)}$ $R_{\text{fines}} = 122 \text{ Ci (accident)}$
Fuel Fines Activity Density	$C_{\text{fines}} = R_{\text{fines}} / V_C$ $C_{\text{fines}} = 7.98 \times 10^{-6} \text{ Ci/cm}^3 \text{ (normal)}$ $C_{\text{fines}} = 5.32 \times 10^{-4} \text{ Ci/cm}^3 \text{ (accident)}$

4.5.5.2.4 Crud Radionuclide Inventory

Crud Surface Activity	$S_C = 1.39 \times 10^{-7} \text{ Ci/cm}^2 \text{ (WSRC Report, Section 5.4)}$
Crud Releasable Quantity	$R_{\text{crud}} = S_C \times \text{Assy} \times SA \times f_C$ $R_{\text{crud}} = 0.019 \text{ Ci (normal)}$ $R_{\text{crud}} = 0.13 \text{ Ci (accident)}$
Crud Activity Density	$C_{\text{crud}} = R_{\text{crud}} / V_C$ $C_{\text{crud}} = 8.22 \times 10^{-8} \text{ Ci/cm}^3 \text{ (normal)}$ $C_{\text{crud}} = 5.48 \times 10^{-7} \text{ Ci/cm}^3 \text{ (accident)}$

4.5.5.2.5 Total Radionuclide Inventory

Total Activity Density

$$C_{\text{total}} = C_{\text{gas}} + C_{\text{vol}} + C_{\text{fines}} + C_{\text{crud}}$$

$$C_{\text{total}} = 4.83 \times 10^{-4} \text{ Ci/cm}^3 \text{ (normal)}$$

$$C_{\text{total}} = 1.64 \times 10^{-2} \text{ Ci/cm}^3 \text{ (accident)}$$

4.5.5.3 Allowable Leak Rate Calculation

After the radionuclide activity concentrations have been determined for the four categories of releasable radionuclides, the allowable normal and accident condition leak rates can be determined in accordance with 10 CFR 71.51(a) requirements.

4.5.5.3.1 Equivalent A₂ Values

The activity fractions for each of the four categories are calculated by dividing the activity density of each by the total activity densities listed in Section 4.5.5.2.5. These fractions are listed below for normal and accident conditions (numbers do not total exactly to 1.0 due to rounding).

Activity Fraction	Symbol	Normal Conditions	Accident Conditions
Fission Gas	Fr _{gas}	0.983	0.967
Volatile	Fr _{vol}	1.05×10 ⁻⁴	3.09×10 ⁻⁵
Fuel Fines	Fr _{fines}	0.017	0.033
Crud	Fr _{crud}	1.70×10 ⁻⁴	3.35×10 ⁻⁵

To determine the equivalent A₂ value of the releasable radionuclides under normal and accident conditions, the activity fractions are divided by their respective mixture A₂ values as presented in Section 4.1.1.1, the resulting four values are summed, then inverted to determine the final value as presented below.

$$\text{Equivalent } A_2 \text{ Value} \quad A_2 = \frac{1}{\frac{Fr_{\text{gas}}}{A_{2 \text{ gas}}} + \frac{Fr_{\text{vol}}}{A_{2 \text{ vol}}} + \frac{Fr_{\text{fines}}}{A_{2 \text{ fines}}} + \frac{Fr_{\text{crud}}}{A_{2 \text{ crud}}}}$$

$$A_2 = 24.745 \text{ Ci (normal)}$$

$$A_2 = 13.349 \text{ Ci (accident)}$$

Using the values of activity density and A_2 values previously determined, the allowable leak rates can be determined for normal and accident conditions. The normal and accident condition release rates are defined below.

Accident Condition Allowable Release Rate R = 1 A₂/week
R = 2.207 × 10⁻⁵ Ci/sec (accident)

Next, the allowable release rates are converted to volumetric leak rates by dividing the allowable release rates by the total activity concentrations defined in Section 4.5.5.2.5.

Allowable Volumetric Leakage Rate $L = R / C_{\text{total}}$
 $L = 1.42 \times 10^{-5} \text{ cm}^3/\text{sec (normal)}$
 $L = 1.35 \times 10^{-3} \text{ cm}^3/\text{sec (accident)}$

For an allowable leak rate of $1.42 \times 10^{-5} \text{ cm}^3/\text{sec}$ (for HEU MTR fuel in normal conditions of transport), a helium leak from 1.99 atm to 1 atm at 470K, and a capillary length of 0.762 cm, the capillary diameter is calculated to be 0.000565 cm. Based on these capillary dimensions, and using the correlations in Section 4.2.1.2, the air standard leak rates and helium test leak rates are determined. The air standard leak rate is $1.19 \times 10^{-5} \text{ ref cm}^3/\text{sec}$, with a leak test sensitivity of $5.95 \times 10^{-6} \text{ ref cm}^3/\text{sec}$. The reference air leakage rate is converted to a helium leak rate at the same conditions (a leak from 1 atm to 0.01 atm at 298K). The equivalent helium leak rate is $1.62 \times 10^{-5} \text{ std cm}^3/\text{s (He)}$, with a sensitivity of $8.08 \times 10^{-6} \text{ std cm}^3/\text{s (He)}$.

This section presents the calculation for determining the maximum allowable leakage rate for the 25 BWR rods with a 56% fuel rod failure fraction, using the methodology presented in Section 4.2.1.2. This envelops rods placed in either a rod holder or a fuel assembly lattice. The allowable leak rate (L) of 1.32×10^{-6} cm³/sec is based on a normal condition maximum allowable leak rate of 10^{-6} A₂/hr, a cask contents A₂ value of 19.828, and an activity density of 4.178×10^{-3} Ci/cm³. The

activity density is the result of a releasable inventory of 373 Ci and a cask-free volume of 89,320 cm³. Based on the allowable leak rate, the cask operating conditions and seal configuration, the capillary diameter is determined by iteratively solving the continuum and molecular flow equations until the allowable leak rate is met.

$$L = 1.32 \times 10^{-6} \text{ cm}^3 / \text{sec} = L_c + L_m$$

The continuum volumetric flow rate of the gas (cm³/sec), L_c is given by:

$$L_c = \frac{2.48 \times 10^6 D^4}{a \mu} (P_u - P_d) \frac{P_a}{P_u} = F_c (P_u - P_d) \frac{P_a}{P_u}$$

where:

L_c = continuum flow rate of gas at P_u [cm³/sec]

D = capillary diameter [cm]

A = capillary length [cm] = 0.762

μ = fluid viscosity [cP] (He at 588K) = 0.0312

P_u = upstream pressure [atm] = 3.155

P_d = downstream pressure [atm] = 1.0

P_a = average pressure $(P_u + P_d)/2$ [atm] = 2.08

The molecular volumetric flow rate of the gas (cm³/sec), L_m is given by:

$$L_m = \frac{3.81 \times 10^3 D^3 \sqrt{\frac{T}{M}}}{a P_a} (P_u - P_d) \frac{P_a}{P_u} = F_m (P_u - P_d) \frac{P_a}{P_u}$$

where:

L_m = molecular volumetric flow rate of gas at P_u [cm³/sec]

D = capillary diameter [cm]

T = gas temperature [K] = 588

M = gas molecular weight [g/mole] = 4

P_a = average pressure $(P_u + P_d)/2$ [atm] = 2.08

P_u = upstream pressure [atm] = 3.155

P_d = downstream pressure [atm] = 1.0

$$a = \text{capillary length [cm]} = 0.762$$

Yielding a capillary diameter of:

$$D = 2.553 \times 10^{-4} \text{ cm}$$

Based on the calculated capillary diameter, air standard (reference) properties are then substituted into the flow equations to arrive at the air standard leakage rate (L_R). Standard conditions represent leakage at 298K, flowing from an upstream pressure of 1 atmosphere, to a downstream pressure of 0.01 atmospheres.

The continuum volumetric flow rate of the reference condition air (cm^3/sec), L_c , is given by:

$$L_c = \frac{2.48 \times 10^6 D^4}{a \mu} (P_u - P_d) \frac{P_a}{P_u} = F_c (P_u - P_d) \frac{P_a}{P_u}$$

where:

$$L_c = \text{continuum flow rate of gas at } P_u \text{ [cm}^3/\text{sec]}$$

$$D = \text{capillary diameter [cm]} = 2.553 \times 10^{-4}$$

$$A = \text{capillary length [cm]} = 0.762$$

$$\mu = \text{fluid viscosity [cP]} = 0.0185$$

$$P_u = \text{upstream pressure [atm]} = 1.00$$

$$P_d = \text{downstream pressure [atm]} = 0.01$$

$$P_a = \text{average pressure } (P_u + P_d)/2 \text{ [atm]} = 0.505$$

Using the above parameters, solving for L_c yields:

$$L_c = F_c (P_u - P_d) \frac{P_a}{P_u} = 7.502 \times 10^{-7} (1.0 - 0.01) \frac{0.505}{1.00}$$

$$L_c = 3.75 \times 10^{-7} \text{ ref cm}^3/\text{sec}$$

The molecular volumetric flow rate of the gas (cm^3/sec), L_m , is given by:

$$L_m = \frac{3.81 \times 10^3 D^3 \sqrt{\frac{T}{M}}}{a P_a} (P_u - P_d) \frac{P_a}{P_u} = F_m (P_u - P_d) \frac{P_a}{P_u}$$

where:

$$L_m = \text{molecular volumetric flow rate of gas at } P_u \text{ [cm}^3/\text{sec]}$$

$$\begin{aligned} D &= \text{capillary diameter [cm]} = 2.553 \times 10^{-4} \\ T &= \text{gas temperature [K]} = 298 \\ M &= \text{gas molecular weight [g/mole]} = 29 \\ P_a &= \text{average pressure } (P_u + P_d)/2 \text{ [atm]} = 0.505 \\ P_u &= \text{upstream pressure [atm]} = 1.00 \\ P_d &= \text{downstream pressure [atm]} = 0.01 \\ a &= \text{capillary diameter [cm]} = 0.762 \end{aligned}$$

Using these parameters, solving for L_m yields:

$$L_m = F_m (P_u - P_d) \frac{P_a}{P_u} = 5.280 \times 10^{-7} (1.00 - 0.01) \frac{0.505}{1.00}$$

$$L_m = 2.640 \times 10^{-7} \text{ ref cm}^3/\text{sec}$$

The reference air leakage rate (L_R) is calculated by summing L_m and L_c :

$$L_R = L_c + L_m = 3.751 \times 10^{-7} + 2.640 \times 10^{-7}$$

$$L_R = 6.390 \times 10^{-7} \text{ ref cm}^3/\text{sec}$$

To complete the analysis, helium leak rates are calculated at standard conditions (1.0 to 0.01 atm pressure drop at 298K).

For helium, the continuum volumetric flow rate of the helium gas (cm^3/sec), L_c , at standard conditions is given by:

$$L_c = \frac{2.48 \times 10^6 D^4}{a \mu} (P_u - P_d) \frac{P_a}{P_u} = F_c (P_u - P_d) \frac{P_a}{P_u}$$

where:

$$\begin{aligned} L_c &= \text{continuum flow rate of gas at } P_u \text{ [cm}^3/\text{sec]} \\ D &= \text{capillary diameter [cm]} = 2.553 \times 10^{-4} \\ A &= \text{capillary length [cm]} = 0.762 \\ \mu &= \text{fluid viscosity [cP]} = 0.0198 \end{aligned}$$

$$P_u = \text{upstream pressure [atm]} = 1.00$$

$$P_d = \text{downstream pressure [atm]} = 0.01$$

$$P_a = \text{average pressure } (P_u + P_d)/2 \text{ [atm]} = 0.505$$

Using the above parameters, solving for L_c yields:

$$L_c = F_c (P_u - P_d) \frac{P_a}{P_u} = 7.009 \times 10^{-7} (1.0 - 0.01) \frac{0.505}{1.00}$$

$$L_c = 3.504 \times 10^{-7} \text{ std cm}^3/\text{sec (He)}$$

The molecular volumetric flow rate of the gas (cm^3/sec), L_m , is given by:

$$L_m = \frac{3.81 \times 10^3 D^3 \sqrt{\frac{T}{M}}}{a P_a} (P_u - P_d) \frac{P_a}{P_u} = F_m (P_u - P_d) \frac{P_a}{P_u}$$

where:

$$L_m = \text{molecular volumetric flow rate of gas at } P_u \text{ [cm}^3/\text{sec]}$$

$$D = \text{capillary diameter [cm]} = 2.553 \times 10^{-4}$$

$$T = \text{gas temperature [K]} = 298$$

$$M = \text{gas molecular weight [g/mole]} = 4$$

$$P_a = \text{average pressure } (P_u + P_d)/2 \text{ [atm]} = 0.505$$

$$P_u = \text{upstream pressure [atm]} = 1.00$$

$$P_d = \text{downstream pressure [atm]} = 0.01$$

$$A = \text{capillary diameter [cm]} = 0.762$$

Using the these parameters, solving for L_m yields:

$$L_m = F_m (P_u - P_d) \frac{P_a}{P_u} = 1.422 \times 10^{-7} (1.00 - 0.01) \frac{0.505}{1.00}$$

$$L_m = 7.108 \times 10^{-7} \text{ std cm}^3/\text{sec (He)}$$

The helium leakage rate at standard conditions is calculated by summing L_m and L_c :

$$L_{\text{He}} = L_{\text{C}} + L_{\text{M}} = 3.504 \times 10^{-7} + 7.108 \times 10^{-7}$$

$$L_{\text{He}} = 1.061 \times 10^{-6} \text{ std cm}^3/\text{sec (He)}$$

4.5.7 Containment Analysis of DIDO Fuel Assemblies

The fuel meat and clad material composition for both MTR and DIDO are similar. MTR elements have been substituted for DIDO fuel assemblies in research reactors. Based on the material similarity and element interchangeability, the WSRC reports used in Section 4.5.5 to justify the radionuclide activity concentrations for MTR fuel are assumed to be applicable to DIDO fuel. The information that follows relies heavily on the methodology and terminology presented in the WSRC reports.

4.5.7.1 Definition of Variables

The following variables are utilized to determine the releasable quantity of radionuclides and the corresponding allowable leakage rate from the cask. These variables are defined either within the WSRC reports or are specific to the DIDO fuel loading proposed for the NAC-LWT cask.

Name	Variable	Normal Condition	Accident Condition
Fraction of Breached Fuel	f_b	0.10	1.0
Fission Gas Release Fraction	f_G	0.30	1.0
Volatile Release Fraction	f_V	1×10^{-6}	1×10^{-6}
Fuel Meat Spallation Fraction	T_F	0.15	1.0
Crud Spallation Fraction	f_C	0.15	1.0
Depth of Corrosion Attack	P	$5 \times 10^{-4} \text{ cm}$	
Cask Free Volume	V_c	$3.681 \times 10^5 \text{ cm}^3$ (Table 4.2-3)*	
Number of MTR Assemblies	Assy	42 (maximum)	
Gas A_2 Value	$A_{2 \text{ gas}}$	277.63 Ci (Table 4.5-19)	
Volatile A_2 Value	$A_{2 \text{ vol}}$	9.36 Ci (Table 4.5-20)	
Fines A_2 Value	$A_{2 \text{ fines}}$	1.09 Ci (Table 4.5-21)	
Crud A_2 Value	$A_{2 \text{ crud}}$	0.27 Ci (WSRC Report, Section 5.4)	
Corrosion Fraction	0.5	(maximum design basis)	

- * Free volume associated with 42 element basket with intact DIDO fuel assemblies.

4.5.7.1.1 Calculation of DIDO Fuel Assembly Surface Area

The physical data of the design basis assembly are presented in Figure 6.2.8-1 and Table 6.2.8-1. The surface area of the fuel assembly is calculated by using the dimensions of each of the four tubes in the design basis assembly. The following variables are defined for the design basis DIDO fuel assembly:

Tube OD₁ = 6.38 cm
 Tube OD₂ = 7.36 cm
 Tube OD₃ = 8.34 cm
 Tube OD₄ = 9.32 cm
 Tube Thickness = 0.150 cm
 Tube Height = 62.5 cm

Using these variables, the total surface area of a DIDO fuel assembly can be determined. This is calculated as follows:

Outer Tube Area_i = $\pi \times (\text{Tube OD}_i) \times \text{Tube Height}$
 Inner Tube Area_i = $\pi \times (\text{Tube OD}_i - (2 \times \text{Tube Thickness})) \times \text{Tube Height}$

Total Surface Area is calculated as:

$$SA = \sum_i \text{Outer Tube Area}_i + \text{Inner Tube Area}_i$$

$$SA = 1.21 \times 10^4 \text{ cm}^2$$

4.5.7.1.2 Calculation of Exposed Meat Surface Area and Volume

To determine the releasable quantity of fuel fines, it is necessary to calculate the fuel meat surface area of the outermost fuel tube, and the total fuel meat volume in the fuel element. The following variables are defined for the design basis DIDO fuel assembly presented in Table 6.2.8-1. Similar to the MTR evaluation, which only considered the outermost fuel plates in the calculation of exposed meat surface area, only the outer tube (Tube 4) is considered for DIDO fuel assemblies.

Fuel Meat Thickness per Tube, Meat Thick = 0.065 cm
 Fuel Meat Length per Tube, Meat Length = 60.0 cm
 Clad Thickness per Tube, Clad Thick = 0.0425 cm

Using these variables, the outside surface area and total fuel meat volume of the DIDO fuel assemblies can be determined. This is calculated as follows, using the variables previously listed.

Fuel Meat Surface Area (Tube 4)

$$\begin{aligned}\text{Meat Area} &= \pi \times (\text{Tube OD}_4 - \text{Clad Thick}) \times \text{Meat Length} + \pi \times (\text{Tube OD}_4 - \text{Tube} \\ &\quad \text{Thickness} + \text{Clad Thick}) \times \text{Meat Length} \\ \text{Meat Area} &= 3.485 \times 10^3 \text{ cm}^2\end{aligned}$$

Fuel Meat Volume

$$\begin{aligned}V_M &= \\ \sum_i \pi \times &\left[\left(\frac{\text{Tube OD}_i}{2} - \text{Clad Thick} \right)^2 - \left(\frac{\text{Tube OD}_i}{2} - \text{Tube Thickness} + \text{Clad Thick} \right)^2 \right] \times \text{Meat Length} \\ V_M &= 377.37 \text{ cm}^3\end{aligned}$$

4.5.7.2 Calculation of Releasable Radionuclides

The following sections present calculation of the releasable quantities of radionuclides determined in accordance with the WSRC report and using the data defined in Section 4.5.7.1.

4.5.7.2.1 Fission Gas Radionuclide Inventory

Fission Gas Radionuclide Quantity $A_G = 42.55 \text{ Ci}$ (Table 4.5-19)

Fission Gas Releasable Inventory $R_{\text{gas}} = A_G \times \text{Assy} \times f_b \times f_G$ [See variables presented in Section 4.5.7.1]

$$R_{\text{gas}} = 54 \text{ Ci (normal)}$$

$$R_{\text{gas}} = 1,787 \text{ Ci (accident)}$$

Fission Gas Activity Density

$$C_{\text{gas}} = R_{\text{gas}} / V_C$$

$$C_{\text{gas}} = 1.46 \times 10^{-4} \text{ Ci/cm}^3 \text{ (normal)}$$

$$C_{\text{gas}} = 4.85 \times 10^{-3} \text{ Ci/cm}^3 \text{ (accident)}$$

4.5.7.2.2 Volatile Radionuclide Inventory

Volatile Radionuclide Quantity $A_V = 1.21 \times 10^3 \text{ Ci}$ (Table 4.5-20)

Volatile Releasable Quantity $R_{\text{vol}} = A_V \times \text{Assy} \times f_b \times f_V$

$$R_{\text{vol}} = 0.005 \text{ Ci (normal)}$$

$$R_{\text{vol}} = 0.051 \text{ Ci (accident)}$$

Volatile Activity Density

$$C_{\text{vol}} = R_{\text{vol}} / V_C$$

$$C_{\text{vol}} = 1.38 \times 10^{-8} \text{ Ci/cm}^3 \text{ (normal)}$$

$$C_{\text{vol}} = 1.38 \times 10^{-7} \text{ Ci/cm}^3 \text{ (accident)}$$

4.5.7.2.3 Fuel Fines Radionuclide Inventory

To calculate the fuel fines available for release, the total inventory of radionuclides in the spent fuel other than gases and volatiles is reduced by fractions accounting for the percentage of fuel that has surface area corrosion and breached cladding. WSRC-TR-98-00317, Section 5.1.3, presents a basis for determining the bounding value of fuel element corrosion. Based on the worldwide examinations of MTR fuel elements utilized in the report, the worst-case extent of surface corrosion was 1%. However, for this analysis, the exposed surface area (ESA) is determined by multiplying a worst-case corrosion fraction of 50% by the surface area of the fuel meat in the outermost fuel tube (Tube 4) as calculated in Section 4.5.7.1.2. As described in Sections 4 and A.2.3 of WSRC report WSRC-TR-2000-00152, mechanical cladding damage exhibits the same properties of radionuclide release as corrosion damage. Therefore, this ESA will be considered to be the fuel meat surface exposed by a combination of corrosion and/or mechanical damage.

Exposed Surface Area

$$ESA = \text{Meat Area} \times \text{Corrosion Fraction}$$

[Meat areas are calculated in Section 4.5.7.1.2 and corrosion fraction is presented in Section 4.5.7.1]

$$ESA = 1743 \text{ cm}^2 \text{ per element}$$

Fuel Fines Radionuclide Quantity

$$A_F = 5.61 \times 10^3 \text{ Ci} \quad (\text{Table 4.5-21})$$

Fuel Fines Releasable Quantity

$$R_{\text{fines}} = (A_F \times \text{Assy} \times P \times ESA \times f_b \times T_F) / V_M$$

$$R_{\text{fines}} = 8.161 \text{ Ci (normal)}$$

$$R_{\text{fines}} = 544 \text{ Ci (accident)}$$

Fuel Fines Activity Density

$$C_{\text{fines}} = R_{\text{fines}} / V_C$$

$$C_{\text{fines}} = 2.22 \times 10^{-5} \text{ Ci/cm}^3 \text{ (normal)}$$

$$C_{\text{fines}} = 1.48 \times 10^{-3} \text{ Ci/cm}^3 \text{ (accident)}$$

4.5.7.2.4 Crud Radionuclide Inventory

Crud Surface Activity

$$S_C = 1.39 \times 10^{-7} \text{ Ci/cm}^2 \text{ (WSRC Report, Section 5.4)}$$

Crud Releasable Quantity

$$R_{\text{crud}} = S_C \times \text{Assy} \times SA \times f_C$$

$$R_{\text{crud}} = 0.011 \text{ Ci (normal)}$$

$$R_{\text{crud}} = 0.071 \text{ Ci (accident)}$$

Crud Activity Density

$$C_{\text{crud}} = R_{\text{crud}} / V_C$$

$$C_{\text{crud}} = 2.88 \times 10^{-8} \text{ Ci/cm}^3 \text{ (normal)}$$

$$C_{\text{crud}} = 1.92 \times 10^{-7} \text{ Ci/cm}^3 \text{ (accident)}$$

4.5.7.2.5 Total Radionuclide Inventory

Total Activity Density

$$C_{\text{total}} = C_{\text{gas}} + C_{\text{vol}} + C_{\text{fines}} + C_{\text{crud}}$$

$$C_{\text{total}} = 1.68 \times 10^{-4} \text{ Ci/cm}^3 \text{ (normal)}$$

$$C_{\text{total}} = 6.33 \times 10^{-3} \text{ Ci/cm}^3 \text{ (accident)}$$

4.5.7.3 Allowable Leak Rate Calculation

After the radionuclide activity concentrations have been determined for the four categories of releasable radionuclides, the allowable normal and accident condition leak rates can be determined in accordance with 10 CFR 71.51(a) requirements.

4.5.7.3.1 Equivalent A₂ Values

The activity fractions for each of the four categories are calculated by dividing the activity density of each by the total activity densities listed in Section 4.5.7.2.5. These fractions are listed below for normal and accident conditions (numbers do not total to 1.0 exactly due to rounding).

Name	Variable	Normal Conditions	Accident Conditions
Fission Gas Activity Fraction	Fr _{gas}	0.861	0.757
Volatile Activity Fraction	Fr _{vol}	8.19 × 10 ⁻⁵	2.17 × 10 ⁻⁵
Fuel Fines Activity Fraction	Fr _{fines}	0.132	0.233
Crud Activity Fraction	Fr _{crud}	1.71 × 10 ⁻⁴	3.03 × 10 ⁻⁵

To determine the equivalent A₂ value of the releasable radionuclides under normal and accident conditions, the activity fractions are divided by their respective mixture A₂ values as presented in Section 4.5.7.1, the resulting four values are summed, then inverted to determine the final value as presented below.

$$\text{Equivalent A}_2 \text{ Value } A_2 = \frac{1}{\frac{Fr_{\text{gas}}}{A_{2 \text{ gas}}} + \frac{Fr_{\text{vol}}}{A_{2 \text{ vol}}} + \frac{Fr_{\text{fines}}}{A_{2 \text{ fines}}} + \frac{Fr_{\text{crud}}}{A_{2 \text{ crud}}}}$$

$$A_2 = 7.996 \text{ Ci (normal)}$$

$$A_2 = 4.604 \text{ Ci (accident)}$$

4.5.7.3.2 Leak Rate Correlations

Using the values of activity density and A_2 values previously determined, the allowable leak rates can be determined for normal and accident conditions. The normal and accident condition release rates are defined below.

Normal Condition Allowable Release Rate	$R = 1 \times 10^{-6} A_2/\text{hr}$ $R = 2.221 \times 10^{-9} \text{ Ci/sec (normal)}$
---	--

Accident Condition Allowable Release Rate	$R = 1 A_2/\text{week}$ $R = 7.612 \times 10^{-6} \text{ Ci/sec (accident)}$
---	---

Next, the allowable release rates are converted to volumetric leak rates by dividing the allowable release rates by the total activity concentrations defined in Section 4.5.7.2.5.

Allowable Volumetric Leakage Rate	$L = R / C_{\text{total}}$ $L = 1.323 \times 10^{-5} \text{ cm}^3/\text{sec (normal)}$ $L = 1.202 \times 10^{-3} \text{ cm}^3/\text{sec (accident)}$
-----------------------------------	--

4.5.8 Containment Analysis for PULSTAR Fuel Elements

Internal pressure and containment evaluations are performed for the NAC-LWT with a PULSTAR fuel payload. Cask evaluations are performed for both a payload of 28 intact assemblies, and a mixed payload of 14 intact assemblies and 14 cans. Since the intact assembly volume is based on the assembly envelope and 25 elements are in each assembly, the internal pressure and containment calculations bound those for TRIGA fuel rod holders containing a 4×4 array of PULSTAR fuel elements.

Internal pressures are calculated using the Ideal Gas Law. The containment evaluation is performed according to ANSI N14.5 and NUREG/CR-6487 guidance and satisfies all 10 CFR 71 requirements for a B(U)F-96 cask designation.

Based on the postulated PULSTAR fuel payloads, internal pressure was calculated for the cask cavity. Contributors to the cask pressure are the rod backfill, fission gases, cask backfill and can backfill (where applicable). The cask, can and rods are all backfilled at 1 atm. System pressure and average gas temperature during normal and accident conditions are documented in Sections 3.4.4.5 and 3.5.4.4 and summarized in Table 4.5-22.

Radionuclide activities were taken from source term and shielding evaluation documented in Chapter 5. Radionuclide inventories for a design basis MTR basket cell payload of 25 elements are listed in Table 4.5-23 through Table 4.5-25. Radionuclides are separated into gas, volatile and fine sections. Also included in the tables are B(U)F-96 compliant isotope A_2 values and group average A_2 values. In addition to the fuel material radionuclides, a source surface contamination source is included in the analysis. Reference information on PULSTAR fuel surface contamination is not available. As the PULSTAR fuel rods are similar to LWR fuel rods, the maximum surface contamination available for LWR rods is applied. A $1254 \mu\text{Ci}/\text{cm}^2$ ^{60}Co activity at discharge (BWR value from PNL-6273) is conservatively applied to the fuel assembly rods and box surfaces. Combining the radionuclide inventories with release fractions from NUREG-1617 (applicable to the zirconium alloy-clad UO_2 PULSTAR fuel elements) yields the allowable leakage rates documented in Table 4.5-27.

The maximum allowable release rates are then transformed into standard leak rates, which depend on gas temperatures, pressures and leakage path. Flow correlations are obtained from Section 2 of NUREG/CR-6487. Continuum and molecular flow can occur simultaneously and are treated as such in this analysis. Normal condition temperatures are employed during air standard leak rate calculations of both normal and accident conditions. The use of normal condition temperature is conservative as an increase in gas temperature to accident condition levels raises gas viscosity, which, in turn, decreases the continuum dominated flow and increases the calculated capillary diameter. An increased capillary diameter, in turn, produces higher test leakage rates. Air standard and helium leakage rates and test leakage rates are listed in Table 4.5-28 for both intact and damaged fuel configurations.

For the cask, the limiting air standard leak rate for a PULSTAR fuel payload is $5.49\text{E-}06$ ref cm^3/sec , with a leak rate test sensitivity of $2.74\text{E-}06$ ref cm^3/sec . The mixed intact/canned cask payload is limiting. The reference air leakage rate is converted to helium cover gas leaking from 1 atm to 0.01 atm at 298K and results in a leak rate of $7.84\text{E-}06$ std cm^3/sec (He), with a test sensitivity of $3.92\text{E-}06$ std cm^3/sec (He).

Table 4.5-22 Pressure Summary for PULSTAR Fuel

Payload	Free Volume (liters)	Condition	Gas Temp. (°F)	Pressure		
				(atm)	(psia)	(psig)
28 Intact Assemblies	217.0	Normal	295	1.449	21.3	6.6
		Accident	394	2.3	34.0	19.3
14 Intact Assemblies; 14 Cans	233.0	Normal	295	1.8	27.2	12.5
		Accident	394	2.4	35.4	20.7

Table 4.5-23 PULSTAR Fuel SAS2H Output and Group A₂ Value (Gas)

Isotope	Activity/Assembly (Ci)	Fraction of Source	Isotope A ₂ Value (Ci)	Isotope Fraction/A ₂ (Ci ⁻¹)	Group A ₂ (Ci)
H 3	3.78E+00	4.49E-02	1100	4.08E-05	---
KR 85	8.04E+01	9.55E-01	270	3.54E-03	---
I131	4.58E-11	5.44E-13	19	2.86E-14	
Total	8.42E+01			3.58E-03	279.47

Table 4.5-24 PULSTAR Fuel SAS2H Output and Group A₂ Value (Volatiles)

Isotope	Activity/Assembly (Ci)	Fraction of Source	Isotope A ₂ Value (Ci)	Isotope Fraction/A ₂ (Ci ⁻¹)	Group A ₂ (Ci)
SR 89	1.66E+01	5.63E-03	16	3.52E-04	---
SR 90	8.78E+02	2.98E-01	8.1	3.67E-02	---
RU103	4.66E+00	1.58E-03	54	2.93E-05	---
RU106	5.67E+02	1.92E-01	5.4	3.56E-02	---
CS134	4.34E+02	1.47E-01	19	7.74E-03	---
CS136	8.23E-07	2.79E-10	14	1.99E-11	---
CS137	1.05E+03	3.56E-01	16	2.22E-02	---
Total	2.95E+03			1.03E-01	9.74

Table 4.5-25 PULSTAR Fuel SAS2H Output and Group A₂ Value (Fuel Fines)

Isotope	Activity/ Assembly (Ci)	Fraction of Source	Isotope A ₂ Value (Ci)	Isotope Fraction/A ₂ (Ci ⁻¹)	Group A ₂ (Ci)
TH234	4.12E-03	5.48E-07	8.1	6.77E-08	---
PA233	3.85E-03	5.12E-07	19	2.70E-08	---
PA234M	4.12E-03	5.48E-07	0.54	1.01E-06	---
U236	4.59E-03	6.11E-07	0.16	3.82E-06	---
U237	2.38E-02	3.17E-06	0.54	5.86E-06	---
U238	4.12E-03	5.48E-07	1E+60	5.48E-67	---
NP237	3.85E-03	5.12E-07	0.054	9.48E-06	---
NP238	1.83E-03	2.43E-07	0.54	4.51E-07	---
NP239	3.81E-02	5.07E-06	11	4.61E-07	---
PU236	4.99E-03	6.64E-07	0.081	8.20E-06	---
PU238	2.46E+01	3.27E-03	0.027	1.21E-01	---
PU239	5.71E+00	7.60E-04	0.027	2.81E-02	---
PU240	3.82E+00	5.08E-04	0.027	1.88E-02	---
PU241	9.95E+02	1.32E-01	1.6	8.27E-02	---
PU242	5.24E-03	6.97E-07	0.027	2.58E-05	---
AM241	6.88E+00	9.15E-04	0.027	3.39E-02	---
AM242M	4.07E-01	5.41E-05	0.027	2.01E-03	---
AM242	4.05E-01	5.39E-05	0.54	9.98E-05	---
AM243	3.81E-02	5.07E-06	0.027	1.88E-04	---
CM242	5.53E+01	7.36E-03	0.27	2.72E-02	---
CM243	1.02E-01	1.36E-05	0.027	5.03E-04	---
CM244	2.12E+00	2.82E-04	0.054	5.22E-03	---
RB 86	4.18E-06	5.56E-10	14	3.97E-11	---
Y 89M	1.55E-03	2.06E-07	0.54	3.82E-07	---
Y 90	8.78E+02	1.17E-01	8.1	1.44E-02	---
Y 91	4.17E+01	5.55E-03	16	3.47E-04	---
ZR 95	7.47E+01	9.94E-03	22	4.52E-04	---
NB 95	1.61E+02	2.14E-02	27	7.93E-04	---
NB 95M	8.79E-01	1.17E-04	0.54	2.17E-04	---
TC 99	1.54E-01	2.05E-05	24	8.54E-07	---
RH103M	4.65E+00	6.19E-04	1100	5.62E-07	---
RH106	5.67E+02	7.54E-02	0.54	1.40E-01	---
AG110	2.76E-02	3.67E-06	0.54	6.80E-06	---
AG110M	2.03E+00	2.70E-04	11	2.46E-05	---
CD113M	1.60E-01	2.13E-05	14	1.52E-06	---
CD115M	2.18E-03	2.90E-07	14	2.07E-08	---

Table 4.5-25 PULSTAR Fuel SAS2H Output and Group A₂ Value (Fuel Fines)
(Continued)

Isotope	Activity/ Assembly (Ci)	Fraction of Source	Isotope A ₂ Value (Ci)	Isotope Fraction/A ₂ (Ci ⁻¹)	Group A ₂ (Ci)
SN119M	4.50E-02	5.99E-06	810	7.39E-09	---
SN123	1.91E-01	2.54E-05	16	1.59E-06	---
SB124	1.77E-02	2.35E-06	16	1.47E-07	---
SB125	2.43E+01	3.23E-03	27	1.20E-04	---
TE125M	5.94E+00	7.90E-04	24	3.29E-05	---
TE127	2.58E+00	3.43E-04	19	1.81E-05	---
TE127M	2.64E+00	3.51E-04	14	2.51E-05	---
TE129	4.15E-02	5.52E-06	16	3.45E-07	---
TE129M	6.47E-02	8.61E-06	11	7.82E-07	---
XE131M	4.13E-08	5.49E-12	1100	4.99E-15	---
XE133	5.88E-18	7.82E-22	270	2.90E-24	---
BA136M	9.22E-08	1.23E-11	0.54	2.27E-11	---
BA137M	9.91E+02	1.32E-01	0.54	2.44E-01	---
BA140	9.59E-06	1.28E-09	8.1	1.58E-10	---
LA140	1.10E-05	1.46E-09	11	1.33E-10	---
CE141	1.54E+00	2.05E-04	16	1.28E-05	---
PR143	3.10E-05	4.12E-09	16	2.58E-10	---
CE144	1.35E+03	1.80E-01	5.4	3.33E-02	---
PR144	1.35E+03	1.80E-01	0.54	3.33E-01	---
PR144M	1.89E+01	2.51E-03	0.54	4.66E-03	---
ND147	1.42E-07	1.89E-11	16	1.18E-12	---
PM147	8.32E+02	1.11E-01	54	2.05E-03	---
PM148	1.30E-02	1.73E-06	0.54	3.20E-06	---
PM148M	2.46E-01	3.27E-05	19	1.72E-06	---
SM151	6.85E+00	9.11E-04	270	3.38E-06	---
EU152	6.30E-01	8.38E-05	27	3.10E-06	---
GD153	4.18E-02	5.56E-06	240	2.32E-08	---
EU154	6.28E+01	8.35E-03	16	5.22E-04	---
EU155	4.23E+01	5.63E-03	81	6.95E-05	---
EU156	8.09E-06	1.08E-09	19	5.66E-11	---
TB160	3.05E-02	4.06E-06	16	2.54E-07	---
TOTAL	7.52E+03			1.09E+00	0.91

Table 4.5-26 PULSTAR Fuel Containment Release Fractions

Component	Normal	Accident
Crud Spallation Fraction	0.15	1.0
Fuel Mass Fraction Released as Fines	3×10^{-5}	3×10^{-5}
Fraction of Fuel Rods developing Cladding Breach	0.03 ¹	1.0
Fraction of Volatiles Released due to Cladding Breach	2×10^{-4}	2×10^{-4}
Fraction of Gases Released due to Cladding Breach	0.3	0.3

Table 4.5-27 Containment Analysis Results for PULSTAR Fuel Payloads

Payload		Intact Fuel Normal	Mixed Normal	Intact Fuel Accident	Mixed Accident
Crud	(Ci)	52.3	52.3	348.5	348.5
Gas	(Ci)	21.2	364.2	707.1	707.1
Volatiles	(Ci)	0.5	8.5	16.5	16.5
Fines	(Ci)	0.2	3.2	6.3	6.3
Total	(Ci)	74.2	428.2	1078.5	1078.5
A ₂	(Ci)	14.6	40.8	25.2	25.2
L _N	(cm ³ /sec)	1.19E-05	6.18E-06	8.36E-03	8.98E-03

Table 4.5-28 PULSTAR Fuel Leakage Rate Calculation

Payload Operating Condition		Intact Normal	Mixed Normal	Intact Accident	Mixed Accident
Volumetric Activity	Ci/cm ³	3.42E-04	1.84E-03	4.97E-03	4.63E-03
Capillary Diameter	cm	6.29E-04	4.60E-04	2.80E-03	2.81E-03
Allowable Leakage Rate	(cm ³ /sec)	1.19E-05	6.18E-06	8.36E-03	8.98E-03
Air Standard Leakage Rate	(cm ³ /sec)	1.78E-05	5.49E-06	5.79E-03	5.89E-03
Test Sensitivity	(cm ³ /sec)	8.89E-06	2.74E-06	N/A	N/A
He Ref. Condition Leakage Rate	(cm ³ /sec)	2.36E-05	7.84E-06	6.02E-03	6.13E-03
He Test Sensitivity	(cm ³ /sec)	1.18E-05	3.92E-06	3.01E-03	3.06E-03

¹ Fraction developing breach for canned material is 1.0.

4.5.9 Metallic Face Seal

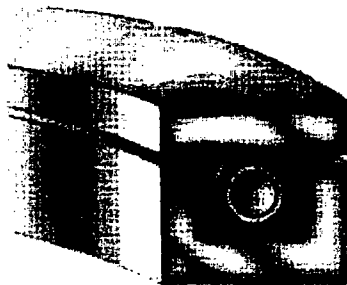
This appendix contains the specification that describes the properties of the metallic port cover face seal.

GENERAL INFORMATION

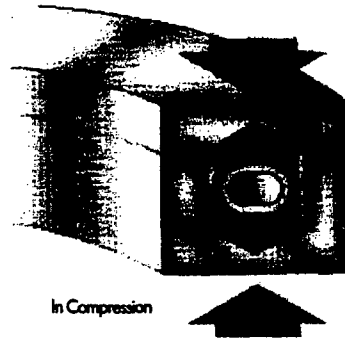
The Helicoflex® seal represents the leading edge in seal technology for high performance sealing applications. Today's extreme sealing requirements have rendered traditional seals & gaskets obsolete. If you can't afford the lost time associated with leaks, put your trust in the leader: Helicoflex®.

SEALING CONCEPT

The sealing principle of the Helicoflex® family of seals is based upon the plastic deformation of a jacket of greater ductility than the flange materials. This occurs between the sealing face of a flange and an elastic core composed of a close-wound helical spring. The spring is selected to have a specific compression resistance. During compression, the resulting specific pressure forces the jacket to yield and fill the flange imperfections while ensuring positive contact with the flange sealing faces. Each coil of the helical spring acts independently and allows the seal to conform to surface irregularities on the flange surface. This combination of elasticity and plasticity makes the Helicoflex seal the best overall performing seal in the industry.



Free State



In Compression

GENERAL CHARACTERISTICS

- Wide range of applications:
 - Dimensional: Diameters from 0.250 inches (6.3 mm) to over 300 inches (7.6 m)
Cross sections from 0.063 inches (1.6 mm) to over 0.625 inches (15.9 mm)
 - Temperature: Cryogenic to 1800 °F (982 °C)
 - Pressure: Ultra High Vacuum to 50,000 PSI (100,000 PSI under special conditions)
- Excellent springback: the spring energized Helicoflex is capable of compensating for flange distortions due to temperature and pressure cycling.
- Adaptable to a majority of standard flanges: ANSI, ISO, KF, ASA
- Suited to different types of assemblies:
 - metal/metal with groove
 - flat flanges with limiter/retainer
 - 3 face contact
- Extended shelf life
- Excellent resistance to corrosion and radiation
- Minimum relaxation: the Helicoflex's resilient spring compensates for relaxation ensuring positive seal contact.

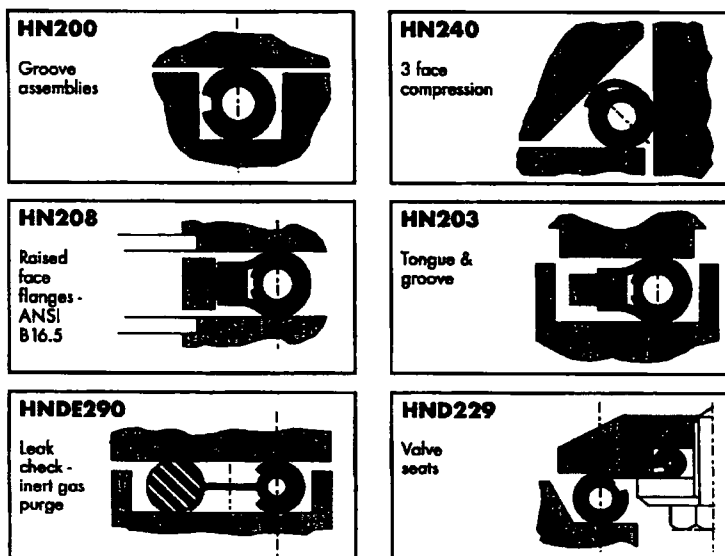
CLASSIFICATION OF SEAL TYPE



CONFIGURATION GUIDE

Cross Section Type	HN	single section
	HNR	ground spring for precise load control (Beta Spring)
	HNW	low load (Delta Seal)
	HND	tandem Helicoflex seals
	HNDE	tandem Helicoflex and elastomer seals note: "L" indicates internal limiter (ex: HLDE)
Jacket/Lining	1 = jacket only	
	2 = jacket with inner lining	
Jacket Orientation	0	1
	2	3
	4	5
	6	7
	8	9
Section Orientation	0	1
	2	3
	4	5
	6	7
	8	9

TYPICAL CONFIGURATIONS



Garlock Helicoflex

For Additional Information, Please Consult Our Engineering Staff
1-800-233-1722

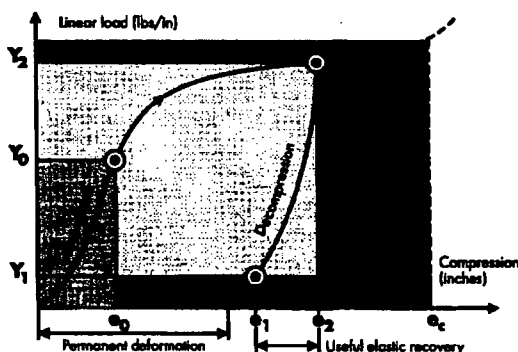
CHARACTERISTIC CURVE

The resilient characteristic of the Helicoflex® seal ensures useful elastic recovery during service. This elastic recovery permits the Helicoflex® seal to accommodate minor distortions in the flange assembly due to temperature and pressure cycling. For most sealing applications the Y_0 value will occur early in the compression curve and the Y_1 value will occur near the end of the decompression curve.

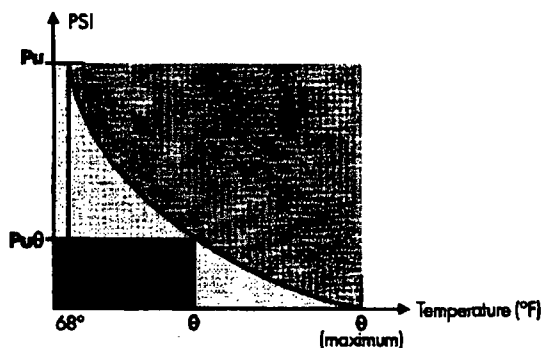
The compression and decompression cycle of the Helicoflex® seal is characterized by the gradual flattening of the compression curve. The decompression curve, which is distinct from the compression curve, is the result of a hysteresis effect and permanent deformation of the spring and jacket.

DEFINITION OF TERMS

- Y_0 - load on the compression curve above which leak rate is at required level
- Y_2 - load required to reach optimum compression e_2
- Y_1 - load on the decompression curve below which leak rate exceeds required level
- e_2 - optimum compression
- e_c - compression limit beyond which there is risk of damaging the spring



INTRINSIC POWER OF THE SEAL



The intrinsic power of the Helicoflex seal reflects its ability to maintain and hold system pressure for a given temperature at Y_2 and e_2 . This value is expressed as a specific pressure and is noted by the symbols P_u (room temperature) and $P_{u\theta}$ (at operating temperature). The influence of temperature on P_u is shown in the graph above. The tables on pages 10 and 11 give the values of P_u at 68°F (20°C), $P_{u\theta}$ at a given temperature and the maximum temperature where $P_{u\theta} = 0$.

DEFINITION OF CHARACTERISTIC VALUES

D_j	Mean reaction diameter of the seal. (For a double section seal, $D_j = D_{j1} + D_{j2}$)	_____ inches
Y_2	Linear load corresponding to e_2 compression	_____ lbs/inch
Y_1	Linear load on the seal to maintain sealing in service at low pressure ($-Y_{m1}$)	_____ lbs/inch
P_u	Intrinsic power of the seal under pressure at 68 °F (20 °C) when the reaction force of the seal is maintained at Y_2 , regardless of the operating conditions.	_____ PSI
$P_{u\theta}$	Value of P_u at temperature θ	_____ PSI
P	Operating or proof pressure Note: If $\frac{P}{P_u \text{ or } P_{u\theta}} > 1$, the definition of the seal must be modified This ratio must never exceed 1.	_____ PSI
Y_{m2}	Linear tightening load on the seal at room temperature to maintain sealing under pressure. $Y_{m2} = Y_2 \frac{P}{P_u}$	_____ lbs/inch
$Y_{m2\theta}$	Value of Y_{m2} at temperature θ . $Y_{m2\theta} = Y_2 \frac{P}{P_{u\theta}}$	_____ lbs/inch
E_t	Young's modulus of bolt material at 68 °F (20 °C)	_____ PSI
E_s	Young's modulus of bolt material at operating temperature	_____ PSI

LOAD CALCULATIONS

F_j	Total tightening load to compress the seal to the operating point ($Y_2; e_2$) $F_j = \pi \times D_j \times Y_2$	_____ lbs
F_f	Total hydrostatic end force $F_f = \pi/4 D_{j1}^2 \times P$ ($D_{j1} = D_j$ in case of a single section seal)	_____ lbs
F_m	Minimum total load to be maintained on the seal in service to preserve sealing. i.e. $F_m = \pi D_j Y_m$ where: Y_m = the greater of the two values: Y_{m1} or $Y_{m2\theta}$ (see note 1 below)	_____ lbs
F_s	Total load to be applied on the bolts to maintain sealing in service. $F_s = F_f + F_m$	_____ lbs
F_s^*	Increased value of F_s to compensate for Young's modulus at temperature $F_s^* = F_s E_t / E_s$	_____ lbs
F_B	LOAD TO BE APPLIED: If $F_s^* > F_j$ then $F_b = F_s^*$ If $F_j > F_s^*$ then $F_b = F_j$	_____ lbs

Note 1: wherever the working pressure is high and/or seal diameter is big, to such an extent that $P \cdot D_j \geq 32 Y_m$, in order to remain on the safe side, whatever the inaccuracy on the tightening load may be, it is recommended to take the F_j value in lieu of F_m for the calculation of F_s so that $F_s = F_f + F_j$.

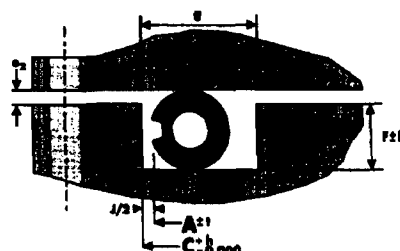
Note 2: this information is provided as a reference only.

Garlock Helicoflex

For Additional Information, Please Consult Our Engineering Staff
1-800-233-1722

5

Groove Design - Radial Pressure



CALCULATIONS

Groove Depth (F)	= Cross Section (CS) - e_2
Depth Tolerance (f)	= $e_2 \times 0.12$
Groove Width (g)	= See table below
Seal OD (A)	= Groove OD (C) - Clearance (J)
Groove Finish	= See table below
Flatness	= See table below

CLEARANCE AND MINIMUM GROOVE WIDTH

Seal Cross Section	Pressure < 300 psi (20 bar)		Pressure ≥ 300 psi (20 bar)	
	Clearance J	Min Groove Width g	Clearance J	Min Groove Width g
CS 0.059 to 0.134 1.5 to 3.4	J = e_2	$g > CS + 2e_2$	J = 0.012 J = 0.3	$g > CS + 2e_2$
0.138 to 0.272 3.5 to 6.9	J = e_2	$g > CS + 2e_2$	J = 0.020 J = 0.5	$g > CS + 2e_2$
0.276 to 0.390 7.0 to 9.9	J = e_2	$g > CS + 2e_2$	J = 0.028 J = 0.7	$g > CS + 2e_2$

SEAL / GROOVE TOLERANCES

Seal Diameter Range	Pressure < 300 psi (20 bar)		Pressure ≥ 300 psi (20 bar)	
	Seal Tolerance t	Groove Tolerance h	Seal Tolerance t	Groove Tolerance h
0.350 to 2.000 3.8 to 50.0	0.005 0.13	0.005 0.13	0.004 0.10	0.004 0.10
2.001 to 12.000 50.0 to 305.0	0.010 0.25	0.010 0.25	0.004 0.10	0.004 0.10
12.001 to 25.000 305.0 to 635.0	0.010 0.25	0.010 0.25	0.006 0.15	0.006 0.15
25.001 to 48.000 635.0 to 1220.0	0.015 0.38	0.015 0.38	0.008 0.20	0.008 0.20
48.001 to 72.000 1220.0 to 1830.0	0.020 0.51	0.015 0.38	0.010 0.25	0.008 0.20
> 72.000 > 1830.0	Consult our engineering staff		Consult our engineering staff	

SURFACE FINISH

Nr. ICA/CEA	N10	N9	N8	N7	N6	N5	N4
Ra in μm	12.5	6.3	3.2	1.6	0.8	0.4	0.2
Rt in μm	50	37	21	11	6.2	3.4	1.9
RMS	500	250	125	63	32	16	8
Aluminum							
Silver, copper, iron							
Nickel, stainless steel							

⊙ recommended ○ consult our engineering staff

Note: Machining/polishing marks must follow seal circumference

SHAPED SEALS

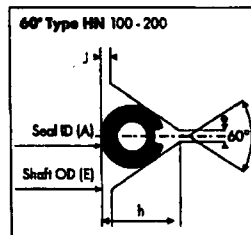
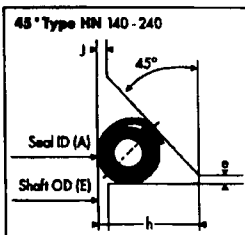
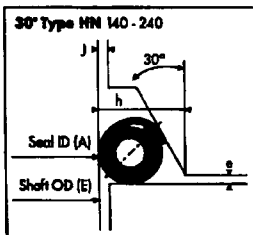
Groove Design: Contact our engineering staff for assistance in designing non-circular grooves.
Groove Finish: Most applications will require a finish of 16-32 RMS (0.4 to 0.8 Ra μm). All machining & polishing marks must follow seal circumference.
Min. Seal Radius: The minimum seal bending radius is six times the seal cross section (CS).
Seating Load: The load (Y2) to seat the seal is approximately 30% higher due to a slightly stiffer spring design.

FLATNESS

Seal Diameter Range	Amplitude	Tangential Slope	Radial Slope
0.350 to 20.000 10 to 500	0.008 0.2	1:1000	1:100
20.001 to 80.000 500 to 2000	0.016 0.4	2:1000	2:100

Dimensions in inches Dimensions in mm

THREE FACE COMPRESSION



$$E = \text{Shaft OD} \begin{matrix} +0.000 & +0.00 \\ -0.002 & -0.05 \end{matrix}$$

$$A = \text{Seal ID} \begin{matrix} +0.002 & +0.05 \\ -0.000 & -0.00 \end{matrix}$$

CALCULATIONS

Axial Load (Ya)	= $K \cdot Y2$
Shaft OD (E)	= Seal ID (A)
Clearance (J)	< CS / 10
Axial Compression (e)	= $a \cdot e2$
Cavity Finish	< 32 RMS (0.8 μ m)

COEFFICIENT VALUES

Coefficient	30°	45°	60°
a	2	1.4	1.15
K	0.9	1.2	1.4



"h" VALUES

Cross Section CS	30°				45°				60°			
	Aluminum Jacket		Other Jackets		Aluminum Jacket		Other Jackets		Aluminum Jacket		Other Jackets	
in mm	in	mm	in	mm	in	mm	in	mm	in	mm	in	mm
0.102 2.6	0.130 3.30	0.126 3.20	0.163 4.15	0.157 4.00	0.126 3.20	0.134 3.40						
0.126 3.2	0.157 4.00	0.157 4.00	0.199 5.05	0.199 5.05	0.157 4.00	0.165 4.20						
0.165 4.2	0.207 5.25	0.207 5.25	0.260 6.60	0.260 6.60	0.213 5.40	0.220 5.60						
0.205 5.2	0.260 6.60	0.260 6.60	0.327 8.30	0.327 8.30	0.272 6.90	0.280 7.10						
0.252 6.4	0.321 8.15	0.321 8.15	0.402 10.20	0.402 10.20	0.339 8.60	0.346 8.80						

Dimensions in inches Dimensions in mm

TARGET SEALING CRITERIA

The ultimate leak rate of a joint is a function of the seal design, flange design, bolting, surface finish and other factors. Helicoflex seals are designed to provide two levels of service: Helium Sealing or Bubble Sealing.

Helium Sealing: These Helicoflex seals are designed with a target Helium leak rate not to exceed 1×10^{-2} cc/sec.atm under a ΔP of 1 atmosphere. The ultimate leak rate will depend on the factors listed above.

Bubble Sealing: These Helicoflex seals are designed with a target air leak rate not to exceed 1×10^{-4} cc/sec.atm under a ΔP of 1 atmosphere.

Garlock Helicoflex

For Additional Information, Please Consult Our Engineering Staff
1-800-233-1722

7

CALCULATIONS ACCORDING TO CODES

	D.I.N. 2505 1990	A.S.M.E. Section VIII Division 1	CODAP 1995	Garlock Helicoflex CEFILAC
Operating load	$F_{ov} = \pi \cdot d_o \cdot k_o \cdot K_{ov}$	$W_{m0} = \pi \cdot b \cdot G \cdot y$	$F_A = \pi \cdot D_i \cdot J_E \cdot P_A$	
Hydrostatic force	$F_p = \pi \cdot \frac{(d_o)^2}{4} \cdot P$	$H = \pi \cdot \frac{G^2}{4} \cdot P$	$F_f = \pi \cdot \frac{(D_i)^2}{4} \cdot P$	
Minimum service load	$F_{m0} = \pi \cdot d_o \cdot k_o \cdot P$	$H_p = 2 \cdot b \cdot \pi \cdot G \cdot m \cdot P$	$F_i = 2 \cdot \pi \cdot D_i \cdot J_E \cdot m \cdot P$	
Minimum tightening load to apply on bolts	$F_{m0} = (1) F_{ov}$ $F_{m0} = (2) F_p + F_{m0}$ Use the greater of the two (1) or (2)	$W = (1) W_{m0}$ $(2) H + H_p = W_{m0}$ Use the greater of the two (1) or (2)	$F_s = (1) F_A$ $F_s = (2) F_f + F_i$ Use the greater of the two (1) or (2)	

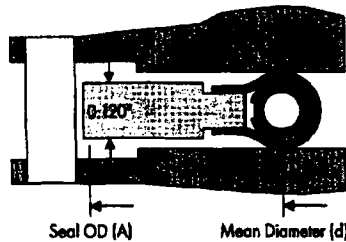
EQUIVALENT SYMBOLS

	D.I.N. 2505 1990	A.S.M.E. Section VIII Division 1	CODAP 1995	Garlock Helicoflex CEFILAC
Operating load	$F_{ov} = F_i$ $d_o = D_i$ $k_o \cdot K_{ov} = Y_s$ \downarrow $F_{ov} = \pi \cdot D_i \cdot Y_s$	$W_{m0} = F_i$ $b = 1$ $G = D_i$ $Y = Y_s$ \downarrow $W_{m0} = \pi \cdot D_i \cdot Y_s$	$F_A = F_i$ $D_i = D_i$ $J_E = 1$ $F_A = Y_s$ \downarrow $F_A = \pi \cdot D_i \cdot Y_s$	
Hydrostatic force	$F_p = F_f$ $d_o = D_i$ \downarrow $F_p = \pi \cdot \frac{(D_i)^2}{4} \cdot P$	$H = F_f$ $G = D_i$ \downarrow $H = \pi \cdot \frac{(D_i)^2}{4} \cdot P$	$F_f = F_f$ $D_i = D_i$ \downarrow $F_f = \pi \cdot \frac{(D_i)^2}{4} \cdot P$	
Minimum service load	$F_{m0} = F_m$ $d_o = D_i$ $k_o \cdot P = Y_m$ \downarrow $F_{m0} = \pi \cdot D_i \cdot Y_m$	$H_p = F_m$ $b = 1$ $G = D_i$ $2 \cdot m \cdot P = Y_m$ $m = \frac{Y_m}{2 \cdot P}$ \downarrow $H_p = \pi \cdot D_i \cdot Y_m$	$F_i = F_m$ $D_i = D_i$ $J_E = 1$ $2 \cdot m \cdot P = Y_m$ $m = \frac{Y_m}{2 \cdot P}$ \downarrow $F_i = \pi \cdot D_i \cdot Y_m$	
Minimum bolt load	$F_{m0} = F_B$ $F_{m0} = (1) F_i$ $F_{m0} = (2) F_f + F_m = F_s$ Use the greater of the two (1) or (2)	$W = F_B$ $W = (1) F_i$ $W = (2) F_f + F_m = F_s$ Use the greater of the two (1) or (2)	$F_s = F_B$ $F_s = (1) F_i$ $F_s = (2) F_f + F_m = F_s$ Use the greater of the two (1) or (2)	

Note: Due to its circular cross section, the Helicoflex seal exhibits a "line" load instead of an "area load" typical of traditional gaskets. As a result, "b", "G" and "Y" factors are not pertinent when applied to the Helicoflex seal. The above equivalent equations were developed to assist flange designers with their calculations.

ANSI B16.5 RAISED FACE FLANGE

The Helicoflex® HN208a is ideally suited for standard raised face flanges. The resilient nature of the seal allows it to compensate for the extremes of high temperature and pressure where traditional spiral wounds and double jacketed seals fail. The jacket and spring combination can be modified to meet most requirements of temperature and pressure. In addition, a large selection of jacket materials ensures chemical compatibility in corrosive and caustic media.



SEAL TYPE: HN208a

Jacket	Availability	Cross Section (inches)	Sealing Load (lbs/in)*	Recommended Flange Finish (RMS)
Aluminum	Standard	0.160	1150	63 - 125
Silver	Standard	0.160	1725	63 - 125
Copper	Standard	0.155	2250	63 - 125
Soft Iron	Optional	0.155	2250	32 - 63
Nickel	Standard	0.150	2800	32 - 63
Monel	Optional	0.150	2800	32 - 63
Hastelloy C	Optional	0.150	2800	32 - 63
Stainless Steel	Standard	0.150	3800	32 - 63
Alloy 600	Optional	0.150	3800	32 - 63
Alloy X750	Optional	0.150	4000	32 - 63
Titanium	Optional	0.150	4000	32 - 63

* Note: Sealing load only! Does not allow for hydrostatic end force. See page 5 for calculations.

SEAL DIMENSIONS

Nominal Diameter	Mean Diameter (d)	Seal OD (A)							
		150lb	300lb	400lb	600lb	900lb	1500lb	2500lb	
1/2	0.827	1.874	2.126	2.126	2.126	2.500	2.500	2.752	
3/4	1.102	2.252	2.626	2.626	2.626	2.752	2.752	3.000	
1	1.417	2.626	2.874	2.874	2.874	3.122	3.122	3.374	
1-1/4	1.890	3.000	3.252	3.252	3.252	3.500	3.500	4.126	
1-1/2	2.283	3.374	3.752	3.752	3.752	3.874	3.874	4.626	
2	2.913	4.126	4.374	4.374	4.374	5.626	5.626	5.752	
2-1/2	3.425	4.874	5.126	5.126	5.126	6.500	6.500	6.626	
3	4.173	5.374	5.874	5.874	5.874	6.626	6.874	7.752	
3-1/2	4.685	6.374	6.500	6.500	6.374	N/A	N/A	N/A	
4	5.256	6.874	7.126	7.000	7.626	8.126	8.252	9.252	
5	6.378	7.752	8.500	8.374	9.500	9.752	10.000	11.000	
6	7.500	8.752	9.874	9.752	10.500	11.413	11.126	12.500	
8	9.567	10.996	12.126	12.000	12.626	14.126	13.874	15.252	
10	11.693	13.374	14.252	14.126	15.752	17.126	17.126	18.760	
12	13.858	16.126	16.626	16.500	18.000	19.626	20.500	21.626	
14	15.098	17.752	19.126	19.000	19.374	20.500	22.752	N/A	
16	17.205	20.252	21.252	21.126	22.252	22.626	25.252	N/A	
18	19.567	21.626	23.500	23.374	24.126	25.126	27.752	N/A	
20	21.575	23.874	25.752	25.500	26.874	27.500	29.752	N/A	
24	25.728	28.252	30.500	30.252	31.126	32.996	35.500	N/A	

Note: Consult our engineering staff for other available sizes and materials.

Garlock Helicoflex

For Additional Information, Please Consult Our Engineering Staff
1-800-233-1722

9

Calculation Data - U.S. Customary

	HELIUM SEALING								BUBBLE SEALING					
Jacket Material	Cross Section In	e ₂ in	e ₃ in	Y ₂ lbs/inch	Y ₁ lbs/inch	Pu68 °F PSI	Pu392 °F PSI	Y ₂ lbs/inch	Y ₁ lbs/inch	Pu68 °F PSI	Pu392 °F PSI	Max Temp °F		
Aluminum	0.063	0.024	0.028	857	114	7250	N/A	514	114	5075	N/A	302		
	0.075	0.028	0.033	914	114	7540	N/A	571	114	5800	N/A	302		
	0.087	0.028	0.035	942	114	7685	N/A	600	114	5800	N/A	356		
	0.098	0.028	0.035	999	114	7975	725	657	114	6090	725	428		
	0.118	0.031	0.039	1056	143	7975	1450	742	114	6525	1450	482		
	0.138	0.031	0.039	1085	143	7975	2030	799	114	6815	2030	482		
	0.157	0.035	0.043	1142	143	8700	2465	857	114	7250	2465	536		
	0.177	0.035	0.047	1199	143	8700	2900	914	114	7540	2900	536		
	0.197	0.035	0.055	1256	171	9135	3190	971	143	7975	3190	572		
	0.217	0.035	0.063	1313	171	9425	3480	1028	143	8265	3480	608		
	0.236	0.039	0.071	1399	200	9715	3625	1113	171	8700	3625	644		
	0.276	0.039	0.087	1542	228	10150	4060	1171	200	9425	4060	644		
	0.315	0.039	0.102	1656	286	10440	4640	1285	228	9860	4495	680		
Silver	0.063	0.020	0.024	1142	171	9425	N/A	857	171	5800	N/A	464		
	0.075	0.024	0.028	1256	171	9425	N/A	857	171	5800	N/A	464		
	0.087	0.024	0.031	1313	200	10150	N/A	914	171	5800	580	536		
	0.098	0.028	0.035	1370	257	10875	1160	971	228	6525	725	536		
	0.118	0.031	0.039	1485	286	12325	2030	1028	257	7250	1305	572		
	0.138	0.031	0.039	1599	286	13775	3190	1085	257	7975	1885	572		
	0.157	0.031	0.043	1713	314	15225	3915	1142	286	8700	2320	662		
	0.177	0.031	0.043	1827	343	16675	4495	1256	286	10150	2755	698		
	0.197	0.031	0.051	1941	343	18125	5220	1313	286	11600	3190	698		
	0.217	0.031	0.055	2056	371	19575	5800	1428	343	13050	3625	752		
	0.236	0.035	0.067	2284	400	21750	6815	1542	343	15950	4350	842		
	0.276	0.035	0.079	2512	457	23200	7830	1713	371	18125	5220	842		
	0.315	0.035	0.094	2798	514	24650	8700	1999	400	20300	6090	932		
Copper Soft Iron, Mild Steels	0.063	0.020	0.024	1485	228	7250	1450	1085	171	5075	725	662		
	0.075	0.024	0.028	1599	286	7250	1995	1142	228	5075	870	662		
	0.087	0.024	0.031	1713	343	7975	1885	1256	286	5075	1160	680		
	0.098	0.028	0.035	1827	400	8700	2465	1313	343	5800	1450	716		
	0.118	0.028	0.039	1999	457	9425	2900	1428	400	5800	1748	716		
	0.138	0.028	0.039	2227	457	10150	3335	1542	400	6525	2175	752		
	0.157	0.031	0.043	2455	514	10150	3915	1656	457	6525	2465	788		
	0.177	0.031	0.043	2684	571	11600	4350	1827	457	6525	2755	842		
	0.197	0.031	0.051	2912	628	12325	4785	1884	514	7250	3045	842		
	0.217	0.031	0.055	3141	685	13050	5220	2056	571	7250	3335	896		
	0.236	0.035	0.067	3597	799	13775	5800	2284	571	7975	3770	968		
	0.276	0.035	0.079	4225	914	14500	6525	2627	628	8700	4205	968		
	0.315	0.035	0.094	4911	1085	15950	7105	3026	742	9425	4640	1022		
Nickel Monel Tantalum	0.063	0.016	0.020	1827	457	10150	1595	1142	343	5800	1015	716		
	0.075	0.020	0.024	1999	457	10440	2320	1256	343	6090	1305	716		
	0.087	0.020	0.028	2227	514	11020	3045	1313	400	6380	1740	788		
	0.098	0.024	0.031	2512	571	11890	3915	1542	400	6815	2320	842		
	0.118	0.024	0.035	2512	628	12615	4930	1713	457	7250	2900	896		
	0.138	0.024	0.035	2798	685	13485	5800	1941	514	7830	3335	932		
	0.157	0.028	0.039	3312	799	13920	6525	2170	571	8265	3915	1022		
	0.177	0.028	0.039	4111	857	15225	7540	2398	628	8700	4350	1112		
	0.197	0.028	0.043	4454	1028	15950	8265	2627	628	9425	4785	1202		
	0.217	0.028	0.051	4625	1142	16675	8990	2855	685	9715	5365	1202		
	0.236	0.031	0.063	N/A	N/A	N/A	N/A	3198	742	10440	5945	1202		
	0.276	0.031	0.071	N/A	N/A	N/A	N/A	3712	857	11310	6525	1202		
	0.315	0.031	0.083	N/A	N/A	N/A	N/A	4168	914	12035	7250	1202		
Stainless Steel Inconel Titanium	0.063	0.016	0.020	1999	571	13050	3625	1713	457	6815	870	788		
	0.075	0.020	0.024	2284	571	13195	3915	1827	457	7250	1160	788		
	0.087	0.020	0.028	2570	628	13340	4205	1999	514	7540	1595	896		
	0.098	0.024	0.031	2855	685	14065	4640	2170	571	8265	2175	932		
	0.118	0.024	0.035	3283	742	14500	5220	2427	628	8990	2900	932		
	0.138	0.024	0.035	3769	857	15080	5655	2684	742	9715	3625	1022		
	0.157	0.028	0.039	4283	971	15515	6090	2969	857	10440	4350	1112		
	0.177	0.028	0.039	4711	1256	15950	6525	3198	1028	11165	4930	1202		
	0.197	0.028	0.043	N/A	N/A	N/A	N/A	3426	1085	11890	5365	1292		
	0.217	0.028	0.051	N/A	N/A	N/A	N/A	3712	1142	12615	6090	1292		
	0.236	0.031	0.063	N/A	N/A	N/A	N/A	4111	1256	13630	6815	1292		
	0.276	0.031	0.071	N/A	N/A	N/A	N/A	4568	1485	14790	7540	1292		
	0.315	0.031	0.083	N/A	N/A	N/A	N/A	5139	1656	15660	8410	1292		

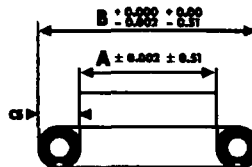
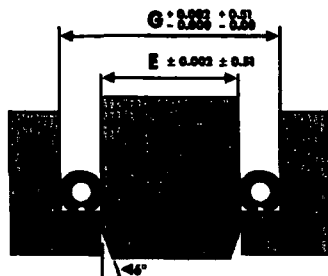
Calculation Data - Metric

Jacket Material	HELIUM SEALING								BUBBLE SEALING								Max Temp °C
	Cross Section mm	e ₂ mm	e _c mm	Y ₂ daN/cm	Y ₁ daN/cm	Pu20°C daN/cm ²	Pu@200°C daN/cm ²		Y ₂ daN/cm	Y ₁ daN/cm	Pu20°C daN/cm ²	Pu@200°C daN/cm ²					
Aluminum	1.6	0.6	0.7	150	20	30	N/A		90	20	35	N/A					150
	1.9	0.7	0.85	160	20	32	N/A		100	20	40	N/A					150
	2.2	0.7	0.9	165	20	33	N/A		105	20	40	N/A					160
	2.5	0.7	0.9	175	20	35	5		115	20	42	5					220
	3.0	0.8	1.0	185	25	35	10		130	20	45	10					250
	3.5	0.8	1.0	190	25	35	14		140	20	47	14					250
	4.0	0.9	1.1	200	25	40	17		150	20	50	17					280
	4.5	0.9	1.2	210	25	60	20		160	20	52	20					280
	5.0	0.9	1.4	220	30	63	22		170	25	53	22					300
	5.5	0.9	1.6	230	30	65	24		180	25	57	24					320
Silver	6.0	1.0	1.8	245	35	67	25		195	30	60	25					340
	7.0	1.0	2.2	270	40	70	28		205	35	65	28					340
	8.0	1.0	2.6	290	50	72	32		225	40	68	31					360
Copper Soft Iron Mild Steels	1.6	0.5	0.6	200	30	65	N/A		130	30	40	N/A					240
	1.9	0.6	0.7	220	30	65	N/A		150	30	40	N/A					240
	2.2	0.6	0.8	230	35	70	6		160	30	40	6					280
	2.5	0.7	0.9	240	45	75	8		170	40	45	5					280
	3.0	0.8	1.0	260	50	85	14		180	45	50	13					300
	3.5	0.8	1.0	280	50	95	22		190	45	55	13					300
	4.0	0.8	1.1	300	55	105	27		200	50	60	19					350
	4.5	0.8	1.1	320	60	115	31		220	50	70	19					370
	5.0	0.8	1.3	340	60	125	36		230	50	80	22					370
	5.5	0.8	1.4	360	65	135	40		250	60	90	25					400
Copper Soft Iron Mild Steels	6.0	0.9	1.7	400	70	150	47		270	60	110	30					450
	7.0	0.9	2.0	440	80	160	54		300	65	125	36					450
	8.0	0.9	2.4	480	90	170	60		350	70	140	42					500
Nickel Monel Titanium	1.6	0.5	0.6	260	40	50	10		190	30	35	5					350
	1.9	0.6	0.7	280	50	50	11		200	40	35	6					350
	2.2	0.6	0.8	300	60	55	13		220	50	35	8					360
	2.5	0.7	0.9	320	70	60	17		230	60	40	10					380
	3.0	0.7	1.0	350	80	65	20		250	70	40	12					380
	3.5	0.7	1.0	390	80	70	23		270	70	45	15					400
	4.0	0.8	1.1	430	90	70	27		290	80	45	17					420
	4.5	0.8	1.1	470	100	80	30		320	80	45	19					450
	5.0	0.8	1.3	510	110	85	33		330	90	50	21					450
	5.5	0.8	1.4	550	120	90	36		360	100	50	23					480
Nickel Monel Titanium	6.0	0.9	1.7	630	140	95	40		400	100	55	26					520
	7.0	0.9	2.0	740	160	100	45		460	110	60	29					520
	8.0	0.9	2.4	860	190	110	49		530	130	65	32					550
Stainless Steel Inconel Titanium	1.6	0.4	0.5	350	100	90	25		300	80	47	6					420
	1.9	0.5	0.6	400	100	91	27		320	80	50	8					420
	2.2	0.5	0.7	450	110	92	29		350	90	52	11					480
	2.5	0.6	0.8	500	120	97	32		380	100	57	15					500
	3.0	0.6	0.9	575	130	100	36		425	110	62	20					500
	3.5	0.6	0.9	660	150	104	39		470	130	67	25					550
	4.0	0.7	1.0	750	170	107	42		520	150	72	30					600
	4.5	0.7	1.0	825	220	110	45		560	180	77	34					650
	5.0	0.7	1.1	N/A	N/A	N/A	N/A		600	190	82	37					700
	5.5	0.7	1.3	N/A	N/A	N/A	N/A		650	200	87	42					700
Stainless Steel Inconel Titanium	6.0	0.8	1.6	N/A	N/A	N/A	N/A		720	220	94	47					700
	7.0	0.8	1.8	N/A	N/A	N/A	N/A		800	260	102	52					700
	8.0	0.8	2.1	N/A	N/A	N/A	N/A		900	290	108	58					700

Garlock Helicoflex

For Additional Information, Please Consult Our Engineering Staff
1-800-233-1722

RADIAL COMPRESSION



CALCULATIONS

Cavity OD (G)	= Seal OD (B)
Shaft OD (E)	= Seal ID (A) + 2 e ₃
Cavity Finish	< 32 RMS (0.8 um)
Axial Load	= Y _a

Notes: For best results, the cavity should be lubricated with a product that is compatible with the medium to be sealed.

CHARACTERISTIC VALUES

Aluminum Jacket						Silver Jacket						Nickel Jacket					
CS		e ₃		Y _a		CS		e ₃		Y _a		CS		e ₃		Y _a	
in	mm	in	mm	lb/in	daN/cm	in	mm	in	mm	lb/in	daN/cm	in	mm	in	mm	lb/in	daN/cm
0.063	1.60	0.012	0.30	109	19	0.063	1.60	0.010	0.25	170	30	0.063	1.60	0.008	0.20	228	40
0.102	2.60	0.014	0.35	137	24	0.102	2.60	0.012	0.30	195	34	0.102	2.60	0.010	0.25	308	54
0.118	3.00	0.016	0.40	154	27	0.122	3.10	0.014	0.35	206	36	0.126	3.20	0.012	0.30	343	60
0.157	4.00	0.020	0.50	183	32	0.165	4.20	0.018	0.45	228	40	0.165	4.20	0.016	0.40	434	76
0.200	5.10	0.020	0.50	206	36	0.205	5.20	0.018	0.45	263	46	0.205	5.20	0.016	0.40	525	92
0.260	6.60	0.024	0.60	235	41	0.244	6.20	0.020	0.50	308	54	0.252	6.40	0.018	0.45	640	112

Dimensions in inches Dimensions in mm

The technical data contained herein is by way of example and should not be relied on for any specific application. Garlock Helicoflex will be pleased to provide specific technical data or specifications with respect to any customer's particular applications. Use of the technical data or specifications contained herein without the express written approval of Garlock Helicoflex is at user's risk and Garlock Helicoflex

expressly disclaims responsibility for such use and the situation which may result therefrom. Garlock Helicoflex makes no warranty, express or implied, that utilization of the technology or products described herein will not infringe any patented or trademarked property rights of third parties. Garlock Helicoflex is constantly involved in engineering and development. Accordingly, Garlock Helicoflex reserves the

right to modify, at any time, the technology and product specifications contained herein. All technical data, specifications and other information contained herein is deemed to be the proprietary intellectual property of Garlock Helicoflex. No reproduction, copy or use thereof may be made without the express written consent of Garlock Helicoflex.

BFGoodrich

Garlock Helicoflex
PO Box 9889
2770 The Boulevard
Columbia, SC 29290 USA
Phone: 1-803-783-1880
Toll Free: 1-800-233-1722
Fax: 1-803-783-4279
www.helicoflex.com
www.garlock.net

Cefitac, S.A.
90 rue de la Roche-du-Geai
42029 Saint-Etienne, FRANCE
Phone: 011-33-4-77-43-51-00
Fax: 011-33-4-77-43-51-52

Garlock Sealing Technologies

Palmyra, NY, USA 1-315-597-4811
Paragould, AR, USA 1-870-239-4051
Houston, TX USA 1-281-459-7200
Sydney, Australia 61-2-9793-2511
São Paulo, Brazil 55-11-884-9680
Oakville, Canada 1-905-829-3200
Berkshire, England 44-1635-38509
Neuss, Germany 49-2131-3490
Seoul, Korea 822-554-6341
Mexico City, Mexico 52-5-567-7011
Singapore 65-284-7873

Fax: 1-315-597-3216
Fax: 1-870-239-4054
Fax: 1-281-458-0502
Fax: 61-2-9793-2544
Fax: 55-11-884-9680
Fax: 1-905-829-3333
Fax: 44-1635-569573
Fax: 49-2131-349-222
Fax: 822-554-6343
Fax: 52-5-368-0418
Fax: 65-284-6089

Catalog Reference: HEL 1

4.5.10 Containment Analysis of ANSTO Basket Payloads

Payloads evaluated in the ANSTO basket are spiral fuel assemblies similar in design to the DIDO assemblies discussed in Section 4.5.7, and MOATA plate bundles similar in design to MTR assemblies discussed in Section 4.5.5. The ANSTO basket is a slightly modified version of the DIDO basket, with each basket containing seven fuel tubes designed to hold one fuel assembly or plate bundle in each fuel tube.

Parameter	DIDO Basket	ANSTO Basket
Fuel Assembly Openings	7	7
Fuel Tube OD (inch)	4.25	4.375
Fuel Tube Wall Thickness (inch)	0.120	0.125

The DIDO basket contains aluminum heat transfer components, while the ANSTO basket contains additional support disks. Overall, there are no significant free volume differences between the empty cask assembly configurations.

MOATA plate bundles, while displacing more free volume than DIDO assemblies, are limited to maximum burnups of 30,000 MWd/MTU and a minimum cool time of 10 years, resulting in source terms a small fraction of the DIDO payloads evaluated in Section 4.5.7. MOATA plate bundles, therefore, do not represent a containment-limiting payload configuration.

Spiral fuel assemblies are limited to the cool time curve of the 18-watt MEU DIDO fuel assemblies. As demonstrated in Chapter 5, Section 5.3.15, this produces a significantly lower source for the spiral fuel than the 18-watt DIDO assembly. The lower source for the spiral fuel is attributed to a higher fissile material mass in the DIDO evaluation (190 g ^{235}U versus 160 g ^{235}U for the spiral fuel), at identical cool time and a maximum depletion of 70%, in conjunction with a lower DIDO enrichment (40 % ^{235}U for the MEU DIDO fuel versus 75% ^{235}U enrichment in the spiral fuel calculations). For containment evaluations, the higher heat load, 25-watt DIDO configuration was evaluated, providing additional margin for the spiral fuel assemblies. When compared to the DIDO payload, the spiral assembly payload, therefore, has a significantly lower source of radionuclides at a similar cask free volume. As a result, the DIDO fuel assembly containment evaluation bounds the spiral fuel.

Table of Contents

5	SHIELDING EVALUATION.....	5-1
5.1	Discussion and Results	5.1.1-1
5.1.1	NAC-LWT Contents	5.1.1-1
5.2	Gamma and Neutron Sources	5.2.1-1
5.2.1	ORIGEN 2.....	5.2.1-1
5.3	Model Specification	5.3.1-1
5.3.1	Description of Radial and Axial Shielding Configuration.....	5.3.1-1
5.3.2	Shield Regional Densities	5.3.2-1
5.3.3	Metallic Fuel Configuration.....	5.3.3-1
5.3.4	MTR Fuel Configuration	5.3.4-1
5.3.5	25 PWR Fuel Rods Configuration	5.3.5-1
5.3.6	TRIGA Fuel Element Model Specification and Shielding Evaluation	5.3.6-1
5.3.7	TRIGA Fuel Cluster Rod Model Specification and Shielding Evaluation	5.3.7-1
5.3.8	High Burnup PWR and BWR Rods Shielding Evaluation	5.3.8-1
5.3.9	DIDO Fuel Configuration	5.3.9-1
5.3.10	GA IFM Shielding Evaluation	5.3.10-1
5.3.11	High Burnup PWR and BWR Rods in a Fuel Assembly Lattice	5.3.11-1
5.3.12	Damaged High Burnup PWR and BWR Rods in a Rod Holder	5.3.12-1
5.3.13	TPBAR Shielding Evaluation	5.3.13-1
5.3.14	PULSTAR Fuel Configuration	5.3.14-1
5.3.15	Spiral Fuel Assembly Configuration.....	5.3.15-1
5.3.16	MOATA Plate Bundle Configuration	5.3.16-1
5.3.17	Irradiated Hardware Shielding Evaluation.....	5.3.17-1
5.4	Shielding Evaluation	5.4.1-1
5.4.1	Shielding Evaluation Codes.....	5.4.1-1

List of Figures

Figure 5.3.3-1	Three-Dimensional Radial Model.....	5.3.3-2
Figure 5.3.3-2	End-Fitting Model with Fuel	5.3.3-3
Figure 5.3.3-3	Lead Slump Accident – PWR Top End-Fitting	5.3.3-4
Figure 5.3.3-4	Lead Slump Accident – PWR Bottom End-Fitting.....	5.3.3-5
Figure 5.3.3-5	Lead Slump Accident – BWR Bottom End-Fitting	5.3.3-6
Figure 5.3.3-6	One-Dimensional Radial Calculational Model.....	5.3.3-7
Figure 5.3.4-1	MTR Fuel Evaluated Configurations	5.3.4-5
Figure 5.3.4-2	SAS4 Shielding Model for the MTR Fuel Basket in the NAC-LWT (Upper Half).....	5.3.4-6
Figure 5.3.4-3	Dose Rates 2 Meters from Transport Vehicle (30 W Uniform Loading).....	5.3.4-7
Figure 5.3.6-1	TRIGA Fuel Element One-Dimensional Bounding Radial Dose Rate - Normal Conditions of Transport - Curves and Data Points.....	5.3.6-7
Figure 5.3.6-2	TRIGA Fuel Element One-Dimensional Bounding Radial Dose Rate - Accident Condition - Curves and Data Points	5.3.6-8
Figure 5.3.6-3	TRIGA SAS4A Radial Model Geometry.....	5.3.6-9
Figure 5.3.6-4	TRIGA SAS4A Basket Model Geometry	5.3.6-10
Figure 5.3.6-5	TRIGA SAS4A Upper Half Model Geometry (Normal Condition – Shifted Fuel).....	5.3.6-11
Figure 5.3.6-6	TRIGA SAS4A Upper Half Model Geometry (Normal Condition).....	5.3.6-12
Figure 5.3.6-7	TRIGA SAS4A Lower Half Model Geometry (Normal and Accident Condition)	5.3.6-13
Figure 5.3.8-1	PWR Rod SAS2H Model	5.3.8-6
Figure 5.3.8-2	BWR 7×7 SAS2H Model Shown at 80,000 MWd/MTU	5.3.8-6
Figure 5.3.8-3	BWR 8×8 Rod SAS2H Model.....	5.3.8-7
Figure 5.3.8-4	PWR Rods Axial Burnup and Source Profiles	5.3.8-7
Figure 5.3.8-5	BWR Rods Axial Burnup and Source Profiles.....	5.3.8-8
Figure 5.3.9-1	SAS2H Input for HEU DIDO Fuel 70% ²³⁵ U Burnup and 18W Heat Load	5.3.9-5
Figure 5.3.9-2	SAS4 Fuel Gamma Input for HEU DIDO Fuel 70% ²³⁵ U Burnup and 18W Heat Load – Radial Biasing & Normal Transport Conditions	5.3.9-6
Figure 5.3.9-3	SAS4 Shielding Model for the DIDO Fuel Basket in the NAC-LWT (Upper Half).....	5.3.9-12
Figure 5.3.9-4	SAS4 Shielding Model for the DIDO Fuel Basket in the NAC-LWT (Section through Fuel)	5.3.9-13
Figure 5.3.9-5	DIDO LEU Cooling Time vs. Fuel Burnup Basket Module Loading Guidelines for Uniform Loading.....	5.3.9-14
Figure 5.3.9-6	DIDO MEU Cooling Time vs. Fuel Burnup Basket Module Loading Guidelines for Uniform Loading.....	5.3.9-14
Figure 5.3.9-7	DIDO HEU Cooling Time vs. Fuel Burnup Basket Module Loading Guidelines for Uniform Loading.....	5.3.9-15
Figure 5.3.9-8	DIDO LEU Element Cooling Time vs. ²³⁵ U % Depletion.....	5.3.9-15

List of Figures (continued)

Figure 5.3.9-9	DIDO MEU Element Cooling Time vs. ^{235}U % Depletion.....	5.3.9-16
Figure 5.3.9-10	DIDO HEU Element Cooling Time vs. ^{235}U % Depletion	5.3.9-16
Figure 5.3.9-11	Comparison of DIDO Element 25W Minimum Cool Time Curves as a Function of ^{235}U % Depletion	5.3.9-17
Figure 5.3.9-12	Bounding DIDO Element Minimum Cool Time vs. % ^{235}U Depletion...	5.3.9-17
Figure 5.3.9-13	18W DIDO HEU Fuel Predicted vs. Actual ^{235}U Depletion Loading Curve.....	5.3.9-18
Figure 5.3.10-1	ORIGEN-S Input for GA RERTR IFM	5.3.10-3
Figure 5.3.10-2	ORIGEN-S Input for GA HTGR IFM	5.3.10-4
Figure 5.3.10-3	SAS1 Input for GA RERTR IFM	5.3.10-5
Figure 5.3.10-4	SAS1 Input for GA HTGR IFM.....	5.3.10-6
Figure 5.3.10-5	GA IFM One-Dimensional Radial Model of NAC-LWT	5.3.10-7
Figure 5.3.10-6	One-Dimensional Radial Model of GA RERTR and HTGR IFM.....	5.3.10-8
Figure 5.3.11-1	PWR Lattice Axial Source Profiles	5.3.11-7
Figure 5.3.11-2	BWR Lattice Axial Source Profiles.....	5.3.11-7
Figure 5.3.11-3	MCBEND Model of NAC-LWT with Fuel Assembly Lattice – Axial Detail.....	5.3.11-8
Figure 5.3.11-4	MCBEND Model of NAC-LWT with Fuel Assembly Lattice – Radial Detail.....	5.3.11-9
Figure 5.3.11-5	Normal Condition Radial Surface Dose Rate Profile by Source Type – Fuel Assembly Lattice.....	5.3.11-10
Figure 5.3.11-6	Normal Condition Radial 2m Dose Rate Profile by Source Type – Fuel Assembly Lattice.....	5.3.11-10
Figure 5.3.11-7	Accident Condition Radial 1m Dose Rate Profile by Source Type – Fuel Assembly Lattice.....	5.3.11-11
Figure 5.3.11-8	MCBEND Input – High Burnup Fuel Lattice – Radial Fuel Gamma....	5.3.11-12
Figure 5.3.12-1	MCBEND Model of NAC-LWT with Damaged Fuel Rods – Axial Detail.....	5.3.12-6
Figure 5.3.12-2	MCBEND Model of NAC-LWT with Damaged Fuel Rods – Radial Detail.....	5.3.12-7
Figure 5.3.12-3	Normal Condition Axial Surface Dose Rate Profile by Source Type – Damaged Fuel Rods.....	5.3.12-8
Figure 5.3.12-4	Normal Condition Radial 2m Dose Rate Profile by Source Type – Damaged Fuel Rods.....	5.3.12-8
Figure 5.3.12-5	Accident Condition Radial 1m Dose Rate Profile by Source Type – Damaged Fuel Rods.....	5.3.12-9
Figure 5.3.12-6	Sample Input File for Damaged Fuel Evaluation.....	5.3.12-10
Figure 5.3.13-1	ORIGEN-S Input for TPBARs at 30 Days Cool Time	5.3.13-3
Figure 5.3.13-2	MCNP Input for 300 TPBARs at 30 Days Cool Time – Normal Conditions & Radial Biasing	5.3.13-4
Figure 5.3.13-3	MCNP Three-Dimensional Model of NAC-LWT with 300 TPBAR Payload – Radial Detail.....	5.3.13-8

List of Figures (continued)

Figure 5.3.13-4	MCNP Three-Dimensional Model of NAC-LWT with 300 TPBAR Payload - Axial Detail.....	5.3.13-9
Figure 5.3.13-5	Normal Condition Radial Surface Dose Rate Profile for 300 TPBAR Payload.....	5.3.13-10
Figure 5.3.13-6	Normal Condition Radial 2 Meter Dose Rate Profile for 300 TPBAR Payload.....	5.3.13-10
Figure 5.3.13-7	Accident Condition Radial 1 Meter Dose Rate Profile for 300 TPBAR Payload.....	5.3.13-11
Figure 5.3.14-1	PULSTAR Fuel Assembly	5.3.14-6
Figure 5.3.14-2	SAS2H Input for PULSTAR Fuel	5.3.14-7
Figure 5.3.14-3	MCNP Model of NAC-LWT with PULSTAR Fuel – Axial Detail	5.3.14-8
Figure 5.3.14-4	MCNP Model of NAC-LWT with PULSTAR Fuel – Radial Detail	5.3.14-9
Figure 5.3.14-5	Sample MCNP Input File for Minimum Height Canned PULSTAR Fuel	5.3.14-10
Figure 5.3.14-6	Normal Condition Axial Surface Dose Rate Profile by Source Type – Minimum Height Canned PULSTAR Fuel.....	5.3.14-14
Figure 5.3.14-7	Normal Condition Radial 2m Dose Rate Profile by Source Type – Minimum Height Canned PULSTAR Fuel.....	5.3.14-14
Figure 5.3.14-8	Accident Condition Radial 1m Dose Rate Profile by Source Type – Minimum Height Canned PULSTAR Fuel.....	5.3.14-15
Figure 5.3.15-1	SAS2H Input for Spiral Fuel 70% ²³⁵ U Depletion and 18-Watt Heat Load	5.3.15-3
Figure 5.3.15-2	Spiral Fuel versus MEU DIDO Gamma Spectrum Comparison (18 Watts, 70% Depletion).....	5.3.15-4
Figure 5.3.15-3	Minimum Cool Time Curve for 18-Watt Heat Load (Spiral Fuel and MEU DIDO)	5.3.15-5
Figure 5.3.16-1	SAS2H Input for the MOATA Plate Bundle	5.3.16-3
Figure 5.3.17-1	SAS2H Input for Irradiated Hardware (on a per kg Basis)	5.3.17-3
Figure 5.3.17-2	Sample SAS1 Input for Irradiated Hardware (Source 1 kg Material).....	5.3.17-4
Figure 5.3.17-3	Irradiated Hardware One-Dimensional Radial Model of NAC-LWT	5.3.17-5
Figure 5.3.17-4	Irradiated Hardware Normal Condition Surface Dose Rate as a Function of Irradiated Hardware Height	5.3.17-6
Figure 5.3.17-5	Irradiated Hardware Normal Condition 2 Meter Dose Rate as a Function of Irradiated Hardware Height	5.3.17-6
Figure 5.3.17-6	Irradiated Hardware Accident Condition 1 Meter Dose Rate as a Function of Irradiated Hardware Height	5.3.17-7

List of Tables

Table 5.1.1-1	Type, Form, Quantity and Potential Sources of Design Basis Fuel	5.1.1-6
Table 5.1.1-2	Design Basis Fuel for Shielding Evaluation	5.1.1-10
Table 5.1.1-3	Nuclear and Thermal Source Parameters.....	5.1.1-13
Table 5.1.1-4	Combined Dose Rates for Normal Operations Conditions	5.1.1-14
Table 5.1.1-5	Hypothetical Accident – Loss of Shielding Materials.....	5.1.1-15
Table 5.1.1-6	Hypothetical Accident –Lead Slump.....	5.1.1-16
Table 5.2.1-1	LOR-2 Input Data.....	5.2.1-3
Table 5.2.1-2	Photon Spectrum for Design Basis Fuel.....	5.2.1-5
Table 5.2.1-3	Fission Product Gas Inventory	5.2.1-6
Table 5.2.1-4	Design Basis Fuel Neutron Spectrum.....	5.2.1-7
Table 5.3.3-1	Source Material Compositions	5.3.3-8
Table 5.3.3-2	Shield Material Densities and Compositions	5.3.3-8
Table 5.3.4-1	Design Basis MTR Fuel Assembly Characteristics.....	5.3.4-8
Table 5.3.4-2	MTR Fuel Element Gamma Source Terms by Thermal Output – 380 grams ²³⁵ U	5.3.4-9
Table 5.3.4-3	MTR Fuel Element Neutron Source Terms by Thermal Output – 380 grams ²³⁵ U	5.3.4-10
Table 5.3.4-4	MTR Fuel Element Gamma Source Terms by Thermal Output – 460 grams ²³⁵ U	5.3.4-11
Table 5.3.4-5	MTR Fuel Element Neutron Source Terms by Thermal Output – 460 grams ²³⁵ U	5.3.4-12
Table 5.3.4-6	LEU MTR Hardware Source to Fuel Source Comparison.....	5.3.4-13
Table 5.3.4-7	HEU MTR Hardware Source to Fuel Comparison.....	5.3.4-14
Table 5.3.4-8	Material Densities for MTR Fuel Shielding Analysis.....	5.3.4-15
Table 5.3.4-9	LWT Cask Surface Total Dose Rates (Normal Conditions of Transport) .	5.3.4-16
Table 5.3.4-10	LWT Cask Plan of Conveyance Dose Rates (Normal Conditions of Transport)	5.3.4-16
Table 5.3.4-11	LWT Cask 2 Meter Off The Plane of Conveyance Dose Rates (Normal Conditions of Transport)	5.3.4-17
Table 5.3.4-12	LWT Cask 1 Meter From the Cask Surface Dose Rates (Normal Conditions of Transport)	5.3.4-17
Table 5.3.4-13	Axial Surface Dose Rates at Cask Lid (Normal Conditions of Transport)	5.3.4-18
Table 5.3.4-14	LWT Cask Dose Rates 5 Meters from the Cask Lid (Back of Tractor Cab) for Normal Conditions of Transport.....	5.3.4-19
Table 5.3.4-15	LWT Cask Dose Rates – 1 Meter from the Cask Surface (Hypothetical Accident Conditions).....	5.3.4-19
Table 5.3.5-1	25 PWR Fuel Rods Design Basis Fuel Source Spectra.....	5.3.5-2
Table 5.3.5-2	Material Densities for 25 Design Basis PWR Rods Fuel Shielding Analysis	5.3.5-3
Table 5.3.5-3	Cask Radial Dose Rates with 25 Design Basis PWR Fuel Rods (mrem/hr).....	5.3.5-4

List of Tables (continued)

Table 5.3.6-1	TRIGA Fuel Element Gamma Source Term - Normal Transport (ACPR, 86,100 MWd/MTU, 231 Days Cooling, 50% ²³⁵ U Depletion).....	5.3.6-14
Table 5.3.6-2	TRIGA Fuel Element Neutron Source Term - Normal Transport (ACPR, 86,100 MWd/MTU, 231 Days Cooling, 50% ²³⁵ U Depletion).....	5.3.6-15
Table 5.3.6-3	TRIGA Fuel Element Gamma Source Term - Accident Conditions (FLIP- LEU-II, 151,100 MWd/MTU, 908 Days Cooling, 80% ²³⁵ U Depletion)	5.3.6-16
Table 5.3.6-4	TRIGA Fuel Element Neutron Source Term - Accident Conditions (FLIP-LEU-II, 151,100 MWd/MTU, 908 Days Cooling, 80% ²³⁵ U Depletion)	5.3.6-17
Table 5.3.6-5	Material Densities for TRIGA Fuel Element Shielding Analysis.....	5.3.6-18
Table 5.3.7-1	TRIGA Fuel Cluster Rod Parameters	5.3.7-4
Table 5.3.7-2	Incoloy 800 Clad Composition	5.3.7-5
Table 5.3.7-3	Representative TRIGA Fuel Cluster Rod Gamma Spectra at 180 GWd/MTU and 1.849 Year Cool Time	5.3.7-6
Table 5.3.7-4	Representative TRIGA Fuel Cluster Rod Neutron Spectrum at 180 GWd/MTU and 1.849 Year Cool Time	5.3.7-7
Table 5.3.7-5	Fuel Basket Region Material Composition Used in Shielding Analysis	5.3.7-8
Table 5.3.7-6	Normal Condition Dose Response to Gammas for TRIGA Fuel Cluster Rods	5.3.7-9
Table 5.3.7-7	Normal Condition Dose Response to Neutrons for TRIGA Fuel Cluster Rods	5.3.7-9
Table 5.3.7-8	Accident Condition Dose Response to Gammas for TRIGA Fuel Cluster Rods.....	5.3.7-10
Table 5.3.7-9	Accident Condition Dose Response to Neutrons for TRIGA Fuel Cluster Rods.....	5.3.7-10
Table 5.3.7-10	TRIGA Fuel Cluster Rod Required Cool Time at Various Fuel Burnups ..	5.3.7-11
Table 5.3.8-1	High Burnup Fuel Rod Model Parameters.....	5.3.8-9
Table 5.3.8-2	High Burnup Fuel Assembly Model Parameters	5.3.8-9
Table 5.3.8-3	SCALE 27N18G Neutron Group Structure and ANSI Dose Factors	5.3.8-10
Table 5.3.8-4	SCALE 27N18G Gamma Group Structure and ANSI Dose Factors.....	5.3.8-11
Table 5.3.8-5	LWT Cask Total Decay Heat [kW] for 25 Rods at Various Cool Times ...	5.3.8-11
Table 5.3.8-6	PWR 80,000 MWd/MTU Fuel Model Neutron Source Term [n/sec/assy].....	5.3.8-12
Table 5.3.8-7	PWR 80,000 MWd/MTU Fuel Model Gamma Source Term [γ/sec/assy] ..	5.3.8-12
Table 5.3.8-8	BWR 7×7 60,000 MWd/MTU Fuel Model Neutron Source Term [n/sec/assy].....	5.3.8-13
Table 5.3.8-9	BWR 7×7 60,000 MWd/MTU Fuel Model Gamma Source Term [γ/sec/assy]	5.3.8-13
Table 5.3.8-10	BWR 7×7 70,000 MWd/MTU Fuel Model Neutron Source Term [n/sec/assy].....	5.3.8-14

List of Tables (continued)

Table 5.3.8-11	BWR 7×7 70,000 MWd/MTU Fuel Model Gamma Source Term [γ/sec/assy].....	5.3.8-14
Table 5.3.8-12	BWR 7×7 80,000 MWd/MTU Fuel Model Neutron Source Term [n/sec/assy]	5.3.8-15
Table 5.3.8-13	BWR 7×7 80,000 MWd/MTU Fuel Model Gamma Source Term [γ/sec/assy].....	5.3.8-15
Table 5.3.8-14	BWR 8×8 80,000 MWd/MTU Fuel Model Neutron Source Term [n/sec/assy]	5.3.8-16
Table 5.3.8-15	BWR 8×8 80,000 MWd/MTU Fuel Model Gamma Source Term [γ/sec/assy].....	5.3.8-16
Table 5.3.8-16	Fuel Axial Source Profile Parameters	5.3.8-17
Table 5.3.8-17	PWR Fuel Axial Source Profile	5.3.8-17
Table 5.3.8-18	BWR Fuel Axial Source Profile	5.3.8-18
Table 5.3.8-19	Fuel Region Homogenized Material Description [atom/b-cm].....	5.3.8-19
Table 5.3.8-20	Basket and Cask Shielding Material Composition [atom/b-cm].....	5.3.8-19
Table 5.3.8-21	Basket Model Parameters	5.3.8-20
Table 5.3.8-22	LWT Cask One-Dimensional Model for LWR High Burnup Rod Analysis	5.3.8-20
Table 5.3.8-23	LWT Cask Surface Neutron Dose Response Function	5.3.8-21
Table 5.3.8-24	LWT Cask Surface Gamma Dose Response Function	5.3.8-21
Table 5.3.8-25	LWT Cask 2m Neutron Dose Response Function	5.3.8-22
Table 5.3.8-26	LWT Cask 2m Gamma Dose Response Function	5.3.8-22
Table 5.3.8-27	Surface Dose Responses [mrem/hr] and Cask Decay Heat [kW] for Various Decay Times	5.3.8-23
Table 5.3.8-28	2m Dose Responses [mrem/hr] and Cask Decay Heat [kW] for Various Decay Times	5.3.8-24
Table 5.3.8-29	Loading Table for PWR and BWR High Burnup Rods Showing Minimum Required Cool Time as a Function of Burnup and Enrichment	5.3.8-25
Table 5.3.9-1	Design Basis DIDO Fuel Assembly Characteristics.....	5.3.9-19
Table 5.3.9-2	DIDO Fuel Assembly Gamma Source Terms by Thermal Output.....	5.3.9-20
Table 5.3.9-3	DIDO Fuel Assembly Neutron Source Terms by Thermal Output.....	5.3.9-21
Table 5.3.9-4	Material Densities for DIDO Fuel Shielding Analysis.....	5.3.9-22
Table 5.3.9-5	LWT Cask Surface Total Dose Rates - DIDO Fuel (Normal Conditions of Transport).....	5.3.9-23
Table 5.3.9-6	LWT Cask Plane of Conveyance Dose Rates – DIDO Fuel (Normal Conditions of Transport)	5.3.9-23
Table 5.3.9-7	LWT Cask 2 Meters Off the Plane of Conveyance Dose Rates – DIDO Fuel (Normal Conditions of Transport).....	5.3.9-24
Table 5.3.9-8	LWT Cask 1 Meter from the Cask Surface Dose Rates – DIDO Fuel (Normal Conditions of Transport).....	5.3.9-24

List of Tables (continued)

Table 5.3.9-9	Axial Surface Dose Rates at Cask Lid – DIDO Fuel (Normal Conditions of Transport).....	5.3.9-25
Table 5.3.9-10	LWT Cask Dose Rates - 5 Meters from the Cask Lid – DIDO Fuel (Back of Tractor Cab) for Normal Conditions of Transport.....	5.3.9-26
Table 5.3.9-11	LWT Cask Dose Rates - 1 Meter from the Radial Cask Surface – DIDO Fuel (Hypothetical Accident Conditions)	5.3.9-26
Table 5.3.10-1	GA IFM Activity Inventory as of January 1, 1996	5.3.10-9
Table 5.3.10-2	GA IFM Neutron and Gamma Spectra in SCALE Format.....	5.3.10-10
Table 5.3.10-3	GA IFM Primary and Secondary Enclosure Dimensions	5.3.10-11
Table 5.3.10-4	Elemental Constituents of GA IFM	5.3.10-12
Table 5.3.10-5	Material Compositions of GA IFM and NAC-LWT	5.3.10-13
Table 5.3.10-6	Combined Payload Radial Dose Rates for GA IFM	5.3.10-14
Table 5.3.11-1	MCBEND Standard 28 Group Neutron Boundaries.....	5.3.11-25
Table 5.3.11-2	MCBEND Standard 22 Group Gamma Boundaries	5.3.11-26
Table 5.3.11-3	BWR Fuel Assembly Lattice Three-Dimensional Model Parameters	5.3.11-27
Table 5.3.11-4	PWR Fuel Assembly Lattice Three-Dimensional Model Parameters.....	5.3.11-28
Table 5.3.11-5	Fuel Assembly Lattice SAS2H Burnup Parameters at 80,000 MWd/MTU	5.3.11-29
Table 5.3.11-6	B&W 15x15 80,000 MWd/MTU, 150 Day Cool Time Source Terms in MCBEND Format.....	5.3.11-30
Table 5.3.11-7	B&W 17x17 PWR 80,000 MWd/MTU, 150 Day Cool Time Source Terms in MCBEND Format.....	5.3.11-31
Table 5.3.11-8	CE 14x14 PWR 80,000 MWd/MTU, 150 Day Cool Time Source Terms in MCBEND Format.....	5.3.11-32
Table 5.3.11-9	Westinghouse 14x14 PWR 80,000 MWd/MTU, 150 Day Cool Time Source Terms in MCBEND Format	5.3.11-33
Table 5.3.11-10	Westinghouse 15x15 PWR 80,000 MWd/MTU, 150 Day Cool Time Source Terms in MCBEND Format	5.3.11-34
Table 5.3.11-11	Westinghouse 17x17 PWR 80,000 MWd/MTU, 150 Day Cool Time Source Terms in MCBEND Format	5.3.11-35
Table 5.3.11-12	BWR 7x7 80,000 MWd/MTU, 210 Day Cool Time Source Terms in MCBEND Format.....	5.3.11-36
Table 5.3.11-13	BWR 8x8 80,000 MWd/MTU, 150 Day Cool Time Source Terms in MCBEND Format.....	5.3.11-37
Table 5.3.11-14	PWR Fuel Lattice Axial Source Profile.....	5.3.11-38
Table 5.3.11-15	BWR Fuel Lattice Axial Source Profile	5.3.11-39
Table 5.3.11-16	BWR Fuel Assembly Lattice Fuel Region Homogenization	5.3.11-40
Table 5.3.11-17	PWR Fuel Assembly Lattice Fuel Region Homogenization.....	5.3.11-41
Table 5.3.11-18	Fuel Assembly Lattice Activated Hardware Region Homogenization	5.3.11-43
Table 5.3.11-19	Fuel Lattice Accident Condition Damaged Fuel Material Heights.....	5.3.11-44
Table 5.3.11-20	BWR Fuel Assembly Lattice Fuel Region Homogenized Material Description.....	5.3.11-44

List of Tables (continued)

Table 5.3.11-21	PWR Fuel Assembly Lattice Fuel Region Homogenized Material Description	5.3.11-45
Table 5.3.11-22	Basket and Cask Shielding Material Composition.....	5.3.11-45
Table 5.3.11-23	ANSI/ANS 6.1.1-1977 Neutron Flux-to-Dose Conversion Factors.....	5.3.11-46
Table 5.3.11-24	ANSI/ANS 6.1.1-1977 Gamma Flux-to-Dose Conversion Factors	5.3.11-47
Table 5.3.11-25	Maximum Radial Dose Rates for PWR and BWR Fuel Rods in an Irradiated Fuel Assembly Lattice.....	5.3.11-48
Table 5.3.11-26	Maximum Axial Dose Rates for PWR and BWR Fuel Rods in an Irradiated Fuel Assembly Lattice.....	5.3.11-48
Table 5.3.12-1	PWR Rods 80,000 MWd/MTU, 150 Day Cool Time Source Terms in MCBEND Format	5.3.12-20
Table 5.3.12-2	BWR 7x7 Rods 80,000 MWd/MTU, 210 Day Cool Time Source Terms in MCBEND Format	5.3.12-21
Table 5.3.12-3	BWR 8x8 Rods 80,000 MWd/MTU, 150 Day Cool Time Source Terms in MCBEND Format	5.3.12-22
Table 5.3.12-4	Fuel Region Homogenization for PWR Fuel Rods	5.3.12-23
Table 5.3.12-5	Fuel Region Homogenization for BWR 7x7 Fuel Rods	5.3.12-23
Table 5.3.12-6	Region Homogenization for BWR 8x8 Fuel Rods.....	5.3.12-24
Table 5.3.12-7	Intact/Damaged Fuel Mixture Composition Determinations	5.3.12-24
Table 5.3.12-8	Fuel Region Homogenized Material Description.....	5.3.12-25
Table 5.3.12-9	Maximum Radial Dose Rates for Damaged PWR and BWR Fuel Rods ..	5.3.12-26
Table 5.3.12-10	Maximum Axial Dose Rates for Damaged PWR and BWR Fuel Rods ..	5.3.12-26
Table 5.3.13-1	Single TPBAR Activity Inventory at 30 Days Cool Time	5.3.13-12
Table 5.3.13-2	TPBAR 30-Day Gamma Source Spectrum	5.3.13-13
Table 5.3.13-3	TPBAR Elemental Constituents	5.3.13-14
Table 5.3.13-4	Material Compositions of NAC-LWT for 300 TPBAR Payload	5.3.13-15
Table 5.3.13-5	Dose Rate Summary for 300 TPBARs at 30 Days Cool Time.....	5.3.13-16
Table 5.3.13-6	Reactor Operating Conditions for TPBAR Source Term Generation	5.3.13-17
Table 5.3.14-1	PULSTAR Fuel Geometry	5.3.14-16
Table 5.3.14-2	Source Term Generation Parameters for PULSTAR Fuel	5.3.14-16
Table 5.3.14-3	PULSTAR Fuel Assembly Neutron Source Term for 1 Year Cool Time ..	5.3.14-17
Table 5.3.14-4	PULSTAR Fuel Assembly Gamma Source Term for 1 Year Cool Time ..	5.3.14-18
Table 5.3.14-5	Intact Assembly Fuel Homogenization for PULSTAR Fuel	5.3.14-19
Table 5.3.14-6	Nominal Height Can Fuel Homogenization for PULSTAR Fuel.....	5.3.14-19
Table 5.3.14-7	Minimum Height Can Fuel Homogenization for PULSTAR Fuel.....	5.3.14-19
Table 5.3.14-8	Fuel Region Homogenized Material Description for PULSTAR Fuel ...	5.3.14-20
Table 5.3.14-9	Cask/Basket Material Descriptions for PULSTAR Fuel	5.3.14-20
Table 5.3.14-10	Maximum Radial Dose Rates for PULSTAR Fuel	5.3.14-21
Table 5.3.14-11	Maximum Axial Dose Rates for PULSTAR Fuel	5.3.14-21
Table 5.3.15-1	Spiral Fuel Assembly Characteristics.....	5.3.15-6
Table 5.3.15-2	Spiral Fuel Assembly Neutron and Gamma Source (18 Watt Heat Load) ..	5.3.15-7

List of Tables (continued)

Table 5.3.15-3	Spiral Fuel Assembly Source Comparison to DIDO MEU Fuel (70% Depletion and 18 Watts)	5.3.15-8
Table 5.3.15-4	Spiral Fuel Assembly Source Comparison to DIDO MEU Fuel (70% Depletion and Fixed 2.23-Year Cool Time)	5.3.15-9
Table 5.3.16-1	MOATA Plate Bundle Characteristics.....	5.3.16-4
Table 5.3.16-2	MOATA Plate Bundle Source Comparison.....	5.3.16-5
Table 5.3.17-1	Irradiated Hardware Gamma Spectra in SCALE Format (1 kg Activated Stainless Steel)	5.3.17-8
Table 5.3.17-2	Material Compositions of the NAC-LWT	5.3.17-9
Table 5.4.1-1	Discrete Axial Source Distribution.....	5.4.1-4
Table 5.4.1-2	Flux to Dose Conversion Factors.....	5.4.1-6

5 SHIELDING EVALUATION

The NAC-LWT cask utilizes a concentric cylindrical arrangement of steel, lead, steel and water to provide gamma shielding for the design basis fuel. The water-glycol solution in the neutron shield tank also provides neutron shielding. The water contains 1 weight percent (wt %) boron, which absorbs neutrons without producing significant secondary gamma radiation.

The PWR and BWR design basis shielding analysis uses the LOR-2 version of the ORIGEN-2 code to calculate radiation sources. The QAD-CG (Cain) and XSDRNPM (NUREG/CR-0200, Vol, 2, F3) codes are used to calculate the cask dose rates for normal operations and hypothetical accident conditions. The shielding analysis shows that the dose rates are below regulatory limits specified in 10 CFR 71.47 and 71.51 as well as IAEA Transportation Safety Standards (TS-R-1).

The PWR and BWR design basis shielding analyses were performed for a 0.25 inch thick neutron shield tank shell, while the actual fabricated thickness is only 0.24 inch (6mm). The shell thickness difference of 0.01 inch yields a maximum dose rate increase of only 2.4 percent, which gives lower dose rates than worst case tolerance analysis in this chapter. The analyses of this chapter, therefore, are valid.

The MTR design basis shielding analysis used the SCALE package. This included SAS2H (Herman) for source terms, and SAS4 (Tang) for three-dimensional shielding analysis. This evaluation is presented in Section 5.3.4. This shielding analysis shows that dose rates are below regulatory limits when the NAC-LWT contains up to 42 design basis MTR fuel elements with less than 210 watts of decay heat per basket.

The MTR shielding analysis explicitly calculated dose rates for LEU, MEU and HEU MTR fuel for a range of burnups and cool times to meet decay heat and dose rate limits. HEU fuel source terms were higher and thus the HEU fuel provides the most limiting dose rates for fixed decay heat limits.

The 25 PWR rod design basis shielding analysis used the SCALE package. This included SAS2H for source terms and SAS1 for one-dimensional radial shielding analysis. This analysis is presented in Section 5.3.5. This shielding analysis shows that the dose rates are below regulatory limits when the NAC-LWT contains up to 25 design basis PWR rods. A shielding evaluation of high burnup PWR and BWR fuel rods in a rod holder is presented in Section 5.3.8. Up to 25 PWR and BWR fuel rods are evaluated at burnups up to 80,000 MWd/MTU.

The NAC-LWT is evaluated for the transport of up to 140 TRIGA fuel elements or up to 560 TRIGA fuel cluster rods arranged in five (5) basket modules. This shielding evaluation uses the SCALE package with the SAS2H sequence for source term identification, and SAS4, also from

the SCALE package, to perform a three-dimensional shielding analysis. The analysis is presented in Section 5.3.6. The analysis shows that the dose rates are below the regulatory limits when the cask contains up to 140 TRIGA fuel elements each having a maximum decay heat of 7.5 W, or up to 560 TRIGA fuel cluster rods each having a maximum decay heat of 1.875 W.

There are two TRIGA basket configurations, non-poisoned and poisoned, as described in Section 1.2.3.1.2. Each TRIGA basket module consists of seven cells. The center cell of each non-poisoned basket module is blocked with a stainless steel plate. Consequently, only six (6) cells of each non-poisoned basket module are loaded with fuel. Because the shielding analyses assumes the center cell contains the bounding TRIGA fuel elements or TRIGA fuel cluster rods during the normal and accident conditions of transport; the evaluation of 140 fuel elements or 560 fuel cluster rods bounds the 120 fuel element / 480 fuel cluster rod configurations.

The DIDO design basis shielding analysis used the SCALE package. This included SAS2H (Herman) for source terms, and SAS4 (Tang) for three-dimensional shielding analysis. This evaluation is presented in Section 5.3.9. This shielding analysis shows that dose rates are below regulatory limits when the NAC-LWT contains up to 42 design basis DIDO fuel assemblies with two allowable heat loads per basket module, either 175 watts or 126 watts, dependent on the axial position of the fuel elements in the top basket.

The DIDO shielding analysis explicitly calculated dose rates for LEU, MEU and HEU DIDO fuel for a range of burnups and cool times to meet decay heat and dose rate limits. HEU fuel source terms were higher and thus the HEU fuel provides the most limiting dose rates for fixed decay heat limits.

The analysis of General Atomics (GA) Irradiated Fuel Material (IFM) used the SCALE package. The GA IFM consists of two Fuel Handling Units, one containing RERTR (an Incoloy clad TRIGA type fuel) and the other containing HTGR graphite matrix fuel material. The analysis included ORIGIN-S for source terms and SAS1 for one-dimensional radial shielding analysis. This evaluation is presented in Section 5.3.10. The shielding evaluation shows that dose rates are well below regulatory limits for a combined payload of the two Fuel Handling Units.

Up to 25 high burnup intact PWR or BWR fuel rods loaded into a fuel assembly lattice are analyzed in Section 5.3.11. Source terms were calculated using SAS2H with three-dimensional dose rates calculated using the MCBEND Monte Carlo transport code. Up to 14 high burnup damaged fuel rods may be loaded in a shipment of 25 PWR or BWR fuel rods, as demonstrated in Section 5.3.12. Damaged rods must be loaded in the rod holder. Source terms were calculated using SAS2H with three-dimensional dose rates calculated using the MCBEND Monte Carlo transport code.

An analysis of the content condition of 300 production Tritium Producing Burnable Absorber Rods (TPBARs) in a consolidation canister used the ORIGEN-S module of the SCALE package for source terms and the MCNP code package to calculate three-dimensional dose rates. This evaluation is presented in Section 5.3.13 and shows that dose rates are well below regulatory limits for normal and accident conditions. The second TPBAR content condition of 55 segmented TPBARs cooled for a minimum of 90 days is evaluated using the source terms determined by the ORIGEN-S module of the SCALE package. This evaluation readily shows compliance with the previously calculated regulatory dose rates for 300 production TPBARs cooled a minimum of 30 days.

A payload of up to 700 PULSTAR fuel elements is analyzed in Section 5.3.14. Source terms were calculated using SAS2H with three-dimensional dose rates calculated using the MCNP code. PULSTAR fuel elements may be loaded as assemblies in a 5×5 rectangular array; intact elements in a 4×4 fuel rod insert; or intact or damaged elements and nonfuel components of fuel assemblies in a can. Four 7-element MTR basket modules are stacked to form a 28 MTR basket in the cask cavity. The maximum cell loading is 25 elements.

A payload of up to 42 spiral fuel assemblies or 42 MOATA plate bundles in the ANSTO basket is analyzed in Section 5.3.15. Six 7-element ANSTO basket modules are stacked to form a 42-assembly payload in the cask cavity. Source terms were calculated using SAS2H. Due to similarities in the basket design to the DIDO basket and bounding source terms in the DIDO shielding evaluation, no shielding evaluations are required to demonstrate regulatory compliance.

5.1 Discussion and Results

The NAC-LWT cask is designed for the safe transport of spent nuclear fuel from various commercial nuclear installations and research reactors.

5.1.1 NAC-LWT Contents

The following contents constitute the design basis for transport in the NAC-LWT cask:

- one Westinghouse 15 × 15 Pressurized Water Reactor (PWR) assembly
- up to 25 PWR rods
- up to two General Electric 7 × 7 Boiling Water Reactor (BWR) assemblies
- fifteen intact metallic fuel rods or six failed metallic fuel rods
- up to 42 Materials Test Reactor (MTR) research reactor fuel elements
- up to 140 TRIGA fuel elements or up to 560 TRIGA fuel cluster rods
- up to 25 PWR or BWR high burnup (up to 80,000 MWd/MTU) fuel rods
- up to 42 DIDO research reactor fuel assemblies
- two General Atomics (GA) Irradiated Fuel Material (IFM) Fuel Handling Units
- up to 300 TPBARs (of which two can be prefailed)
- up to 55 TPBARs segmented during PIE and associated segmentation debris
- up to 700 PULSTAR fuel elements (intact or damaged)
- up to 42 spiral fuel assemblies
- up to 42 MOATA plate bundles

The high burnup PWR and BWR rods may be transported in three configurations: 1) a maximum of 25 intact fuel rods loaded in the rod holder; 2) a maximum of 25 fuel rods with up to 14 damaged fuel rods or rod fragments loaded in the rod holder; and 3) a maximum of 25 intact fuel rods housed in a fuel assembly lattice within the NAC-LWT PWR basket. The fuel assembly lattice may be irradiated up to an equivalent burnup of 80,000 MWd/MTU.

The metallic fuel consists of a single rod of uranium metal clad with aluminum. The intact metallic fuel rods are placed into a transport canister that will hold five intact rods. The cask can hold three transport canisters for a total of 15 intact metallic fuel rods. In the event the metallic fuel has failed or is suspected of having failed, each fuel rod is sealed in its own container. The failed metallic fuel is loaded into either one of the three holes in the metallic fuel basket or into one of the six openings in the failed metallic fuel basket.

MTR research reactor fuel elements are typically 33 to 57 inches long, including lower nozzle and upper handle. The fuel plates typically consist of U-Al, U₃O₈-Al, or USi-Al clad with aluminum. The fuel plates are held in a parallel arrangement with two thick aluminum slotted

pieces to form a fuel element. Standard fuel elements have between 10 and 23 fuel plates. The active fuel region is typically 22.75 inches in height, and the fuel meat is typically 0.023-inch thick. The highly enriched uranium (HEU) fuel has been analyzed conservatively with an enrichment of 90 wt % ^{235}U and fuel loading per element up to 380 g ^{235}U , with a separate analysis performed to accommodate up to 460 g ^{235}U . The design basis fuel parameters are provided in Table 5.1.1-1. The fuel characteristics are presented in Table 5.1.1-2. The dose rates produced from the design basis 470 g ^{235}U and 640 g ^{235}U LEU and 380 g ^{235}U MEU MTR fuel are bounded by the HEU MTR design basis fuel. Therefore, a mixed loading of LEU, MEU and HEU MTR fuel elements are also bounded by a full HEU MTR fuel element loading.

The source term characteristics of the design basis PWR fuel assembly, BWR fuel assembly, metallic rods, 25 PWR rods and MTR fuels are given in Table 5.1.1-3. The design basis PWR and BWR fuels require two years of cooling after discharge to meet the neutron and gamma source, and decay heat limits of the cask. The 25 design basis PWR rods burned to 60,000 MWd/MTU require 150 days of cooling. The design basis metallic fuel requires one year cooling. The design basis MTR fuel requires a variable number of years cooling, after discharge, to meet the decay heat limits of the cask. Loading configurations must conform to the limits stated in Section 7.1.5.

DIDO research reactor fuel elements typically consist of U-Al, U_3O_8 -Al, or U_3Si_2 -Al that is aluminum clad. The fuel elements are held in a concentric arrangement inside an outer aluminum cylinder to form a fuel assembly. Fuel assemblies have 4 fuel elements. The active fuel region is typically 23.6 inches in height, and the fuel meat is typically 0.026 inch thick. The highly enriched uranium (HEU) fuel has been analyzed with a minimum enrichment of 90 wt % ^{235}U and fuel loading per assembly up to 190 g ^{235}U . Low enriched (LEU) and medium enriched (MEU) assemblies are evaluated at 190 g ^{235}U with minimum enrichments of 19 and 40 wt % ^{235}U , respectively. The design basis fuel parameters are provided in Table 5.1.1-1. The fuel characteristics are presented in Table 5.1.1-2. As discussed in Section 5, the dose rates produced from the design basis LEU and MEU DIDO fuel are bounded by the HEU DIDO design basis fuel. Therefore, a mixed loading of LEU, MEU and HEU DIDO fuel assemblies is also bounded by a full HEU DIDO fuel assembly loading.

Two GA IFM Fuel Handling Units (packages) are intended for a single shipment in the NAC-LWT. The first package is composed of Reduced-Enrichment Research and Test Reactor (RERTR) type fuel, which is an Incoloy clad TRIGA fuel. The second is composed of High-Temperature Gas-Cooled Reactor (HTGR) type fuel. Each set of IFM is packaged into stainless steel weld-encapsulated primary and secondary enclosures. Design basis fuel parameters are summarized in Table 5.1.1-1, with fuel characteristics presented in Table 5.1.1-2. Design basis

source terms are provided in Table 5.1.1-3. NAC-LWT combined dose rates for GA IFM are bounded by the dose rates for PWR fuel shown in Table 5.1.1-4 through Table 5.1.1-6.

An inventory of up to 300 production TPBARs (of which two can be prefailed) is intended for multiple shipments in the NAC-LWT. A separate content condition is for the transport of up to 55 segmented TPBARs and associated segmentation debris from PIE contained in a waste container. Each TPBAR is a Type 316 stainless steel rod with a 0.381-inch outer diameter and a 0.336-inch inner diameter and a post-irradiation length of approximately 154 inches. Tritium is produced by irradiation of ^6Li . Design basis fuel parameters are summarized in Table 5.1.1-1 with characteristics presented in Table 5.1.1-2. Design basis source terms are provided in Table 5.1.1-3. NAC-LWT dose rates for the payloads of up to 300 production TPBARs in a consolidation canister, or up to 55 segmented TPBARs in the waste container, are bounded by the dose rates for PWR fuel shown in Table 5.1.1-4 through Table 5.1.1-6.

Source terms for the high burnup PWR and BWR rods are developed using the SCALE SAS2H code package. Cask dose rates are evaluated using the SCALE SAS1 shielding analysis sequence. Results presented in Section 5.3.8 give the required cool time for PWR and BWR rods as a function of burnup for up to 25 intact fuel rods loaded in the NAC-LWT rod holder. The results presented in Sections 5.3.11 and 5.3.12 demonstrate that dose rate limits are met for the shipment of fuel rods in an irradiated fuel assembly lattice and damaged fuel rods in a rod holder, respectively.

As can be seen from Table 5.1.1-3, the PWR fuel assembly has the largest source terms and was used as the design basis fuel for shielding analysis of PWR and BWR fuel in the NAC-LWT presented in this section. The metallic fuel shielding analysis is presented in Section 5.3.3. Metallic fuel is shipped with the neutron shield drained and the analysis reflects this. The MTR fuel shielding analysis is presented in Section 5.3.4. The design basis source terms for 25 PWR rods at 60,000 MWd/MTU are well below the design basis PWR fuel assembly. However, the self shielding of 25 PWR rods is less than the 204 rod design basis PWR fuel assembly. Thus, a shielding evaluation of 25 design basis PWR rods is presented in Section 5.3.5. Similarly, the self shielding for either the 25 high burnup PWR or BWR rods at 80,000 MWd/MTU is lower than that of the design basis assemblies. Shielding evaluations for these rods are presented in Sections 5.3.8, 5.3.11 and 5.3.12.

The transport of up to 140 TRIGA fuel elements is evaluated in Section 5.3.6. TRIGA fuel is a solid metal hydride, U-ZrH and may be high enriched (70%), or low enriched (20%). The fuel clad is either aluminum or stainless steel. TRIGA fuel is fabricated in several configurations, as described in Section 1.2.3.1, that vary in weight, active fuel length and overall length. The typical fuel element length and weight is 28.3 inches and 8.82 pounds. The fuel follower control

rod element (FFCR) establishes the upper bound weight (13.2 pounds) and length (approximately 45 inches). These elements can only be loaded in the top module of the TRIGA fuel basket. The design basis TRIGA fuel parameters are presented in Table 5.1.1-1 and Table 5.1.1-2. Source term characteristics are presented in Table 5.1.1-3. Cooling time for TRIGA fuel is variable, down to a minimum of 90 days, based on the time required for the decay heat to reach 7.5 watts. In addition, the transport of TRIGA fuel cluster rods is evaluated in Section 5.3.7. These rods are obtained from the disassembly of the 5x5 (25 rod) arrays comprising the cluster-type TRIGA fuel as shown in Figure 1.2-6. Only the shipment of the fuel cluster rods is analyzed here; no other activated components of the TRIGA cluster assembly are considered for shipment in this analysis. The TRIGA fuel cluster rod is considered to contain a maximum design-basis fuel mass of 452 g of U-ZrH with an H to Zr ratio of 1.6 and a total uranium mass fraction of 10%. The fuel is highly enriched (93 wt. % ^{235}U). The rods are clad in Incoloy 800 and contain upper and lower stainless steel end plugs with a mass of approximately 60.5 g each. For shipment, each rod is placed inside an aluminum tube (ID 0.625 in, OD 0.750 in), with 16 rods occupying each LWT basket opening for a total of up to 112 rods per basket or 560 rods per cask.

The basis for the dose rate evaluation of the TRIGA fuel cluster rods is a source term and one-dimensional shielding analysis in which the minimum cooling time required for the dose rates produced by the TRIGA fuel cluster rods to fall below the dose rates produced by the design basis TRIGA fuel elements. Cooling time results are determined at a large number of fuel burnup values (at approximately every 2.5% increment in ^{235}U depletion).

PULSTAR fuel elements are zirconium alloy-clad UO_2 pellets with a physical design characteristic as listed in Table 5.1.1-1 and Table 5.1.1-2. PULSTAR fuel assemblies are a 5x5 rectangular array of elements surrounded by a zirconium alloy box, with aluminum upper and lower fittings. The element pitch is nominally 0.524 x 0.606 inch. PULSTAR fuel elements are analyzed at a loading of 32 grams ^{235}U per element, an initial enrichment of 6 wt % ^{235}U , and 45% ^{235}U burnup. For conservatism, a cool time of one year from discharge is employed in the shielding analysis; a cool time of at least 1.5 years is required to meet the basket cell heat load limit of 30 W. Source term characteristics are presented in Table 5.1.1-3

Spiral fuel assemblies typically consist of 10 curved plates (also referred to as elements) of metallic U-Al fuel meat that is aluminum clad. The fuel elements are held in a spiral arrangement between an inner and outer aluminum cylinder to form a fuel assembly. The active fuel region is typically 60.325 cm in height, and the fuel meat is typically 0.061 cm thick. The elements are nominally enriched to 80 wt % ^{235}U and were conservatively evaluated at 75 wt % ^{235}U . Maximum fuel loading per assembly is evaluated at 160 g ^{235}U . The design basis fuel parameters are provided in Table 5.1.1-1. The fuel characteristics are presented in Table 5.1.1-2.

Applying MEU DIDO fuel assembly minimum cool time curves, which are based on a 40 wt % ^{235}U enriched 190 g ^{235}U fuel assembly, to the spiral fuel elements produces source terms that are bounded by the DIDO MEU fuel. Given similar basket designs, the dose rates produced by the spiral fuel elements are bounded by the MEU DIDO evaluation set.

MOATA fuel bundles consist of a maximum of 14 flat MTR type fuel plates. The fuel plates are composed of a metallic U-Al fuel meat that is aluminum clad. The fuel elements are held in place with aluminum outer plates and pins through the top and bottom of the plate stack in their shipment configuration. The plates are held in a typical MTR plate (12 plates per assembly) with a comb side plate configuration during reactor operations. The active fuel region is typically 58.4 cm in height, and the fuel meat is typically 0.1016-cm thick. The elements are nominally enriched to 90 wt % ^{235}U and were conservatively evaluated at 80 wt % ^{235}U . Maximum fuel loading per plate is evaluated at 25 g ^{235}U (nominal loading is 22 g ^{235}U). The design basis fuel parameters are provided in Table 5.1.1-1. The fuel characteristics are presented in Table 5.1.1-2. The gamma radiation source for the 14 fuel plate bundle is approximately 2% of the DIDO MEU assembly. Since the basket designs are similar, the dose rates produced by the plate bundle are bounded by the MEU DIDO evaluation set.

The shield materials are selected and arranged to minimize cask weight while maintaining overall shield effectiveness. Lead and steel are chosen as effective gamma radiation shields, and a water tank on the outside of the cask is provided to efficiently moderate and absorb the neutron radiation.

The total neutron and gamma dose rates calculated for the normal operations conditions are shown in Table 5.1.1-4. Note that the maximum dose rate is on the cask lid surfaces at the top end of the cask and does not exceed the design limit of 200 mrem/hour for the surface of the cask. The 10 CFR 71 limits of 10 mrem/hour at two meters from the cask surface and the design limit of 200 mrem/hour on the cask surface are met. Table 5.1.1-4 contains the total dose rates for the hypothetical accident conditions. These dose rates are well under the 49 CFR 173 limit of 1000 mrem/hour at one meter from the cask surface. The dose rates for the lead slump accident are shown in Table 5.1.1-5. These dose rates show that even with the lead slumped, the hypothetical accident dose rate limits have not been exceeded and the cask is safe for transport.

The cask surface fuel centerline normal operations and hypothetical accident dose rates calculated include neutrons and gammas originating from the fuel, neutrons and gammas scattered from the ground and secondary gammas resulting from neutron capture in the neutron shield. All of the other dose locations also include the contribution from the ^{60}Co in the end-fittings.

Table 5.1.1-1 Type, Form, Quantity and Potential Sources of Design Basis Fuel

<u>Fuel Type</u>	- PWR, Westinghouse 15 x 15
	- 3.7 wt % ²³⁵ U maximum initial enrichment
	- 35,000 MWd/MTU maximum burnup
	- 2.5 kW per assembly maximum decay heat
	- 2 years (or more) decay time after reactor discharge
<u>Fuel Form</u>	- Intact assemblies
<u>Quantity</u>	- 1 design basis fuel assembly
<u>Source of Fuel</u>	- Commercial PWR nuclear power reactors
<u>Transport Index</u>	- 35
<u>Fuel Type</u>	- BWR, General Electric 7 x 7
	- 4.0 wt % ²³⁵ U maximum initial enrichment
	- 30,000 MWd/MTU maximum burnup
	- 1.1 kW per assembly maximum decay heat, 2.2 kW per cask for 2 assemblies
	- 2 years (or more) decay time after reactor discharge
<u>Fuel Form</u>	- Intact assemblies
<u>Quantity</u>	- 2 design basis fuel assemblies
<u>Source of Fuel</u>	- Commercial BWR nuclear power reactors
<u>Transport Index</u>	- 35
<u>Fuel Type</u>	- High Burnup PWR or BWR rods
	- 5.0 wt % maximum ²³⁵ U initial enrichment
	- 80,000 MWd/MTU maximum average burnup
	- 2.3 kW /cask maximum decay heat
	- Minimum cool time dependent on burnup (See Table 5.3.8-29)
<u>Fuel Form</u>	- Intact rods in a fuel assembly lattice or rod holder and intact rods with up to 14 fuel rods classified as damaged in a rod holder
<u>Quantity</u>	- Up to 25
<u>Source of Fuel</u>	- Commercial PWR or BWR nuclear power reactor
<u>Transport Index</u>	- 36 (intact rods)
	28 (intact rods in a fuel assembly lattice)
	37 (intact rods with 14 rods classified as damaged)
<u>Fuel Type</u>	- Uranium metal fuel rods
	- Natural wt % ²³⁵ U
	- 1,600 MWd/MTU maximum burnup
	- 0.0357 kW per sound rod maximum decay heat, 0.54 kW per cask for 15 sound fuel rods
	- 1 year (or more) decay time after reactor discharge
<u>Fuel Form</u>	- Intact or encapsulated failed fuel rods
<u>Quantity</u>	- 15 design basis fuel rods, or 6 design basis failed fuel rods
<u>Source of Fuel</u>	- Research reactors
<u>Transport Index</u>	- 25

Table 5.1.1-1 Type, Form, Quantity and Potential Sources of Design Basis Fuel (cont'd)

<u>Fuel Type</u>	- Material Test Reactor (MTR) Fuel Elements
	- HEU: 90 wt % ²³⁵ U, Maximum burnup variable up to 660,000 MWd/MTU for 380 g ²³⁵ U and 577,500 MWd/MTU for 460 g ²³⁵ U
	- MEU: 40 wt % ²³⁵ U, Maximum burnup variable up to 293,300 MWd/MTU for 380 g ²³⁵ U
	- LEU: 19 wt % ²³⁵ U, Maximum burnup variable up to 139,300 MWd/MTU for 470 g ²³⁵ U and 640 g ²³⁵ U
	- 210 W per basket decay heat
	- Variable cool time down to 90 days using the procedure in Section 7.1.5
<u>Fuel Form</u>	- Intact aluminum clad parallel plates
<u>Quantity</u>	- Up to 42 fuel elements
<u>Source of Fuel</u>	- Research and Material Test Reactors
<u>Transport Index</u>	- 45
<u>Fuel Type</u>	- TRIGA Fuel Element
	- 20 to 70 wt % ²³⁵ U
	- 80% ²³⁵ U depletion (approximately 151 GWd/MTU for LEU fuel and 460 GWd/MTU HEU fuel)
	- 7.5 watts per element decay heat
	- Variable cool time down to 90 days
<u>Fuel Form</u>	- Aluminum or stainless steel (304) clad rods, intact, failed or as debris
<u>Quantity</u>	- Up to 140 fuel elements
<u>Source of Fuel</u>	- Test, Research and Isotope Reactors
<u>Transport Index</u>	- 25
<u>Fuel Type</u>	- TRIGA Fuel Cluster Rods
	- 93 wt % ²³⁵ U
	- 80% ²³⁵ U depletion (approximately 600 GWd/MTU)
	- 1.875 watts per rod decay heat
	- Variable cool time down to 90 days
<u>Fuel Form</u>	- Incoloy 800 clad rods, intact, failed or as debris
<u>Quantity</u>	- Up to 560 fuel rods
<u>Source of Fuel</u>	- Test, Research and Isotope Reactors
<u>Transport Index</u>	- 25
<u>Fuel Type</u>	- DIDO Fuel Assemblies
	- HEU: 90 wt % ²³⁵ U, Maximum burnup variable up to 577,460 MWd/MTU or 70% ²³⁵ U depletion
	- MEU: 40 wt % ²³⁵ U, Maximum burnup variable up to 256,650 MWd/MTU or 70% ²³⁵ U depletion
	- LEU: 19 wt % ²³⁵ U, Maximum burnup variable up to 121,910 MWd/MTU or 70% ²³⁵ U depletion
	- 175 or 126 W per basket decay heat
	- Variable cool time down to 180 days using the procedure in Section 7.1.4

Table 5.1.1-1 Type, Form, Quantity and Potential Sources of Design Basis Fuel (cont'd)

<u>Fuel Form</u>	- Intact aluminum clad concentric fuel tubes
<u>Quantity</u>	- Up to 42 fuel assemblies
<u>Source of Fuel</u>	- Research Reactors
<u>Transport Index</u>	- 40.1
<u>Fuel Type</u>	- General Atomics (GA) Irradiated Fuel Material (IFM)
	- RERTR (see activity inventory in Table 5.3.10-1)
	- HTGR (see activity inventory in Table 5.3.10-1)
	- <13.05 W
	- Transport after 1/1/96
<u>Fuel Form</u>	- RERTR: 13 intact TRIGA elements, 7 sectioned elements
	- HTGR: Spherical loose fuel particles, cylindrical fuel rods, 2 fuel pebbles
<u>Quantity</u>	- 1 Fuel Handling Unit holding RERTR IFM and 1 Fuel Handling Unit holding HTGR IFM
<u>Source of Fuel</u>	- Research reactors, commercial LWR reactors
<u>Transport Index</u>	- <1
<u>Maximum Activity</u>	- 3403 Ci
<u>Material Type</u>	- Tritium Producing Burnable Absorber Rods (TPBARs)
	- 3.35 W/TPBARs; 1.005 kW total ¹
	- 30 days minimum cool time
<u>Material Form</u>	- Type 316 stainless steel clad TPBARs
<u>Quantity</u>	- Up to 300 TPBARs (of which two can be prefailed)
<u>Source of Material</u>	- Commercial LWR reactors
<u>Transport Index</u>	- 22
<u>Maximum Activity</u>	- 12,800 Ci/TPBAR; 3,840,000 Ci total ¹
<u>Material Type</u>	- Tritium Producing Burnable Poison Rods (TPBARs)
	- 2.31 W/TPBAR, 127 W total
	- 90 days
<u>Material Form</u>	- Type 316 stainless steel clad TPBARs segmented for PIE
<u>Quantity</u>	- Up to 55 segmented TPBARs
<u>Source of Material</u>	- Commercial LWRs
<u>Transport Index</u>	- 22 ²
<u>Maximum Activity</u>	- 12,000 Ci/TPBAR, 665,500 Ci total

¹ Conservatively calculated for 30-day minimum cooling time. Actual minimum cooling period for thermal requirements is 90 days.

² Conservatively applied 300 TPBAR shipment transport index.

Table 5.1.1-1 Type, Form, Quantity and Potential Sources of Design Basis Fuel (cont'd)

<u>Fuel Type</u>	- PULSTAR Fuel Elements
	- 6 wt % ²³⁵ U
	- 32 grams ²³⁵ U per element
	- 45% ²³⁵ U depletion (burnup)
	- 210 W per basket decay heat (30 watts per basket cell) × 4 = 840W
	Minimum cool time from discharge of 1.5 years ¹
<u>Fuel Form</u>	- Intact assemblies; intact elements in fuel rod insert; canned intact or failed elements
<u>Quantity</u>	- Up to 700 elements (25 elements per cell)
<u>Sources of Fuel</u>	- Research reactors
<u>Transport Index</u>	- 25
<u>Fuel Type</u>	- Spiral Fuel Assemblies
	- 75 wt % ²³⁵ U, maximum burnup variable up to 70% ²³⁵ U depletion
	- 18 W per assembly , 126 W per basket (at given cool time and burnup limits, maximum heat load is 15.7 W per assembly or 110 W per basket)
	Variable cool time down to 270 days using the procedure in Section 7.1.4 for 18 W DIDO MEU fuel
<u>Fuel Form</u>	- Intact aluminum clad fuel plates within concentric aluminum inner and outer shells
<u>Quantity</u>	- Up to 42 fuel assemblies
<u>Sources of Fuel</u>	- Research reactors
<u>Transport Index</u>	- 40.1 (applied bounding MEU DIDO limit)
<u>Fuel Type</u>	- MOATA Plate Bundles
	- 80 wt % ²³⁵ U, maximum burnup variable up to a 30,000 MWd/MTU or 4.1% ²³⁵ U depletion
<u>Fuel Form</u>	- Intact aluminum-clad fuel plates
<u>Quantity</u>	- Up to 42 bundles
<u>Sources of Fuel</u>	- Research reactors
<u>Transport Index</u>	- 40.1 (applied bounding MEU DIDO limit)

¹ Conservatively evaluated at a one-year cool time and 38 watts per basket cell.

Table 5.1.1-2 Design Basis Fuel for Shielding Evaluation

Parameter	PWR	BWR	Metallic	MTR (HEU)	MTR (MEU)	MTR (LEU)	DIDO
Assembly Array	15 x 15	7 x 7	N/A	Parallel Plates	Parallel Plates	Parallel Plates	Fuel Tubes
Assembly or Element Weight (lbs)	1650	750	1805 (15 rods)	13.0 (max)	13.0 (max)	13.0 (max)	15.0 (max)
Assembly/Element/Rod Length (in)	162	176	120.5	25.23 ⁵	26.14 ⁵	26.14 ⁵	24.6
Active Fuel Length (in)	144	144	120.0	24.80	25.59	25.59	23.6
No. Rods per Assembly	204	49	N/A	N/A	N/A	N/A	N/A
No. of Plates per Element	N/A	N/A	N/A	23	23	23	4
Fuel Rod Diameter/Plate Thickness (in)	0.422	0.563	1.36	0.050	0.050	0.050	0.059
Clad Material	Zr-4	Zr-4	Al	Al	Al	Al	Al
Clad Thickness (in)	0.0243	0.032	0.080	0.0150	0.0150	0.0150	0.0167
Pellet Diameter/Meat Thickness (in)	0.3659	0.487	1.36	0.020	0.020	0.020	0.026
Fuel Material	UO ₂	UO ₂	U metal	U ₃ O ₈ -Al; U-Al; or U ₃ Si ₂ -Al	U ₃ O ₈ -Al; U-Al; or U ₃ Si ₂ -Al	U ₃ O ₈ -Al; U-Al; or U ₃ Si ₂ -Al	U ₃ O ₈ -Al; U-Al; or U ₃ Si ₂ -Al
Percent Theoretical Density	95	95	100	N/A	N/A	N/A	N/A
Enrichment (wt % ²³⁵ U)	3.7	4.0	Natural	90 ⁸	40 ⁸	19 ⁸	90 (HEU) 400 (MEU) 199 (LEU)
Maximum Average Burnup (MWd/MTU)	35,000	30,000	1,600	Variable up to 660,000 ^{2,9}	Variable up to 293,300 ²	Variable up to 139,300 ²	Variable up to 577,460 (HEU) 256,650 (MEU) 121,910 (LEU)
Minimum Cool Time	2 Years	2 Years	1 Year	Variable down to 90 days ²	Variable down to 90 days ²	Variable down to 90 days ²	Variable down to 180 days ¹⁰
U Weight (kg/assembly)	475	198	N/A	N/A	N/A	N/A	N/A
U Weight (kg/element)	N/A	N/A	54.5	0.422 0.511	0.950	2.4737 3.3684	0.2111 (HEU) 0.4750 (MEU) 1.0000 (LEU)
UO ₂ Weight (kg/assembly)	538.9	224.3	N/A	N/A	N/A	N/A	N/A

Notes:

- Up to 2 of the PWR rods may have a maximum average burnup of 65,000 MWd/MTU.
- Variable cool time down to 90 days using the procedure in Section 7.1.4.
- Design Basis normal condition source term is for ACPR fuel with 86,100 MWd/MTU (50% ²³⁵U depletion) and accident condition source term is for FLIP-LEU-II with 151,100 MWd/MTU (80% ²³⁵U depletion).
- Detailed fuel data is presented in Tables 1.2-1 and 6.2.5-1. The values presented here are the physical values for the bounding source terms of the ACPR and FLIP-LEU-II fuel types.
- For MTR fuel assemblies, which are cut to remove non-fuel bearing hardware prior to transport, a nominal 0.28 inch of non-fuel hardware will remain above and below the active fuel region to allow for fuel handling operations.
- Minimum cool time varies with burnup such that maximum decay heat is 1.875 watts/rod.
- Varies with burnup – see Table 5.3.8-29.
- For the shielding evaluation, lower values are conservatively assumed.
- Maximum burnup of 660,000 MWd/MTU for 380 g ²³⁵U and 577,500 MWd/MTU for 460 g ²³⁵U.
- Variable cool time down to 180 days using the procedure in Section 7.1.4.

Table 5.1.1-2 Design Basis Fuel for Shielding Evaluation (continued)

Parameter	PWR Rods	High B/U PWR Rods	High B/U BWR Rods	TRIGA ⁴	TRIGA Fuel Cluster Rods	TPBARs
Assembly Array	N/A	N/A	N/A	N/A	N/A	N/A
Assembly or Element Weight (lbs)	N/A	N/A	N/A	8.82 (nominal) 13.2 (max)		2.655
Assembly/Element/Rod Length (in)	162	162	176.1	45	31.0	153.035 (pre-irradiation)
Active Fuel Length (in)	144	150	150	15	22.5	N/A
No. Rods per Assembly per Shipment	25	25	25	1	1	300 Production or 55 Segmented
No. of Plates per Element	N/A	N/A	N/A	N/A	N/A	N/A
Fuel Rod Diameter/Plate Thickness (in)	0.422	0.440	0.570 (7x7) 0.4961 (other)	1.478	0.542	0.381
Clad Material	Zr-4	Zr-4	Zr-2	304SS	Incoloy 800	316 SS
Clad Thickness (in)	0.242	0.026	0.036 (7x7) 0.0343 (other)	0.02	0.016	0.0225
Pellet Diameter/Meat Thickness (in)	0.3659	0.3805	0.4900 (7x7) 0.4213 (other)	1.435 (max)	0.510	N/A
Fuel Material	UO ₂	UO ₂	UO ₂	U-ZrH	U-ZrH	N/A
Percent Theoretical Density	97	95	95	95	95	N/A
Enrichment (wt % ²³⁵ U)	5.0	5.0	5.0	20	93.3	N/A
Maximum Average Burnup (MWd/MTU)	60,000 ¹	80,000	60,000 – 80,000	ACPR 86,100 (50% ²³⁵ U) ³ FLIP-LEU-II 151,100 (80% ²³⁵ U) ³	Variable up to 600,000	N/A
Minimum Cool Time	150 (days)	150 days	Varies with burnup ⁷	ACPR 231 days FLIP-LEU-II 908 days	Varies with burnup ⁶	30 days for production TPBAR; 90 days for PIE TPBAR
U Weight (kg/assembly)	58.2	65.6	108.8 (7x7) 91.3 (other)	N/A	N/A	N/A
U Weight (kg/element)	N/A	N/A	N/A	ACPR 0.280 FLIP-LEU-II 0.824	0.0452	N/A
UO ₂ Weight (kg/assembly)	66.0	66.0	74.5	N/A	N/A	N/A

Notes:

- Up to 2 of the PWR rods may have a maximum average burnup of 65,000 MWd/MTU.
- Variable cool time down to 90 days using the procedure in Section 7.1.4.
- Design Basis normal condition source term is for ACPR fuel with 86,100 MWd/MTU (50% ²³⁵U depletion) and accident condition source term is for FLIP-LEU-II with 151,100 MWd/MTU (80% ²³⁵U depletion).
- Detailed fuel data is presented in Tables 1.2-1 and 6.2.5-1. The values presented here are the physical values for the bounding source terms of the ACPR and FLIP-LEU-II fuel types.
- For MTR fuel assemblies, which are cut to remove nonfuel-bearing hardware prior to transport, a nominal 0.28 inch of non-fuel hardware will remain above and below the active fuel region to allow for fuel handling operations.
- Minimum cool time varies with burnup such that maximum decay heat is 1.875 watts/rod.
- Varies with burnup – see Table 5.3.8-29.
- For the shielding evaluation, lower values are conservatively assumed.
- Maximum burnup of 660,000 MWd/MTU for 380 g ²³⁵U and 577,500 MWd/MTU for 460 g ²³⁵U.
- Variable cool time down to 180 days using the procedure in Section 7.1.4.

Table 5.1.1-2 Design Basis Fuel for Shielding Evaluation (continued)

Parameter	GA IFM RERTR	GA IFM HTGR	PULSTAR Fuel	Spiral Fuel Assembly	MOATA Plate Bundle
Assembly Array	N/A	N/A	5x5	Spiral Plates	Parallel Plates
Assembly or Element Weight (lbs)	23.73	23.52	45 (assembly); 1.3 (element)	7.9	13.6 ¹¹
Assembly/Element/Rod Length (in)	29.92	N/A	38 (assembly) 26.2 (element)	63.5 cm	58.4 cm ¹²
Active Fuel Length (in)	22.05	N/A	24.1	60.325 cm	58.4 cm
No. Rods per Assembly	13 intact; 7 sectioned	N/A	25	N/A	N/A
No. of Plates per Element	N/A	N/A	N/A	10	maximum 14
Fuel Rod Diameter/Plate Thickness (in)	0.543	N/A	0.47	0.147 cm	0.203 cm
Clad Material	Incoloy	N/A	Zirconium alloy	Al	Al
Clad Thickness (in)	0.031	N/A	0.0185	0.043 cm	N/A
Pellet Diameter/Meat Thickness (in)	0.512	N/A	0.423	0.061 cm	0.1016 cm
Fuel Material	U-ZrH	UC ₂ ; UCO; UO ₂ ; (Th,U)C ₂ ; or (Th,U)O ₂	UO ₂	U-Al	U-Al
Percent Theoretical Density	N/A	N/A	94.9% (nominal); 99.5% (analyzed)	N/A	N/A
Enrichment (wt % ²³⁵ U)	19.7	93.15 (maximum)	6	75	80
Maximum Average Burnup (MWd/MTU)	N/A	N/A	45	70% ²³⁵ U depletion	30,000 MWd/MTU 4.1% ²³⁵ U depletion
Minimum Cool Time	None	None	1.0 Year	see MEU DIDO	10 yr
U Weight (kg/assembly)	8.49	0.45	13.33	0.213 ¹³	0.4375 ¹⁴
U Weight (kg/element)	0.42	N/A	0.53	0.0213 ¹⁵	0.03125 ¹⁶
UO ₂ Weight (kg/assembly)	N/A	N/A	15.13	N/A	N/A

Notes: (cont'd)

11. For 14-fuel plate bundle.
12. Not available for in-core configuration. Analysis input restricted to active fuel length.
13. Based on a 160 g ²³⁵U fissile material load and listed enrichment.
14. Based on fuel mass per plate multiplied by 14 plates.
15. Based on 10 plates per assembly.
16. Based on 25 g ²³⁵U and listed enrichment.

Table 5.1.1-3 Nuclear and Thermal Source Parameters

Payload	Decay Heat (kW)	Gamma Source (MeV/sec) (g/sec)	Neutron Source (n/sec)	Top End-Fitting (g/sec)	Bottom End-Fitting (g/sec)
1 PWR Assembly	2.5	7.78E+15 1.27E+16	2.21E+08	1.49E+13	1.25E+13
2 BWR Assemblies	2.2	6.35E+15 1.04E+16	1.34E+08	1.16E+12	2.78E+12
15 Sound Metallic Fuel Rods ²	0.532	8.81E+14 4.37E+15	1.61E+05	N/A	N/A
6 Failed Metallic Fuel Rods ¹	0.03	3.53E+14 1.75E+15	6.44E+04	N/A	N/A
42 HEU MTR Elements ^{3,9}	1.26	-- 7.42E+15	1.40E+08	N/A ¹⁵	N/A ¹⁵
42 MEU MTR Elements ^{3,8}	1.26	-- 7.86E+15	2.88E+07	N/A ¹⁵	N/A ¹⁵
42 LEU MTR Elements ^{3,8,14}	1.26	-- 7.51E+15	3.96E+07	N/A ¹⁵	N/A ¹⁵
42 DIDO Assemblies ¹⁰	1.05	-- 6.07E+15	9.73E+04	N/A	N/A
25 PWR Rods ²	1.41	3.47E+15 8.39E+15	1.40E+08	N/A	N/A
TRIGA (140 Elements) ⁷ Normal Condition	1.05	2.15E+15 ⁴ 6.52E+15 ⁴	1.57E+06	Note 6	Note 6
TRIGA (140 Elements) ⁷ Accident Condition	1.05	2.60E+15 ⁵ 5.97E+15 ⁵	1.06E+08	Note 6	Note 6
General Atomics Irradiated Fuel Material	0.013	-- 3.429E+13	1.279E+04	Note 11	Note 11
300 Production TPBARs	1.005	5.030E+15 6.681E+15	N/A	N/A	N/A
55 PIE TPBARs	0.127	-- 7.54E+14	N/A	N/A	N/A
PULSTAR Fuel	1.05 ¹²	6.206E+15	2.115E+07	N/A	N/A
Spiral Fuel Assembly ¹³	0.756	-- 1.07E+14	4.54E+3	N/A	N/A
MOATA Plate Bundle	0.042	-- 2.2E+12	< 1E+3	N/A	N/A

Notes:

- Gamma and neutron source terms conservatively calculated based on design basis sound metallic fuel rods.
- 23 rods with 60,000 MWd/MTU burnup and two rods with 65,000 MWd/MTU burnup. Source terms as a function of cool time for the 80,000 MWd/MTU burnup PWR and BWR rods are presented in Section 5.3.8.
- Bounding values of the gamma and neutron source terms presented for 30W uniform loading for 80% burnup.
- Based on TRIGA ACPR fuel (86,100 MWd/MTU, 231 days cooling, 50% ²³⁵U depletion).
- Based on TRIGA FLIP-LEU-II fuel (151,100 MWd/MTU, 908 days cooling, 80% ²³⁵U depletion).
- Total hardware gamma is 7.64E+14 gamma/second for ACPR fuel (86,100 MWd/MTU, 231 days cooling, 50% ²³⁵U depletion).
- TRIGA Fuel Elements are the bounding values used in dose determination for TRIGA cluster rods fuel type.
- Moderator used is light water, H₂O.
- Moderator used is heavy water, D₂O.
- Bounding values of the gamma and neutron source terms presented for 25W uniform loading for 70% burnup HEU fuel.
- Hardware activation, including end-fitting sources, for the TRIGA elements included in the total gamma source for GA IFM.
- Cool time required to meet 30 watt per cell heat load limit is 1.5 years.
- Based on 18 W per assembly heat load.
- Fuel source represents maximum magnitude gamma source obtained from the 470 g ²³⁵U analysis, and the maximum neutron source obtained from the 640 g ²³⁵U analysis.
- A maximum 100 grams of cadmium may be included as part of the MTR fuel element or plate construction. Activation of the cadmium produces no significant source per Section 5.3.4.

Table 5.1.1-4 Combined Dose Rates for Normal Operations Conditions

(1 PWR assembly, 35,000 MWd/MTU, 2-year cool time)

Location	Detector I.D.	Radiation	Normal Dose Rate (mrem/hr)
Radial at 2 m from personnel barrier, Fuel midplane	1	Neutron	1.25
		Secondary Gamma	0.18
		Primary Gamma	<u>6.71</u>
		TOTAL	8.14
Radial surface, Fuel midplane	2	Neutron	6.53
		Secondary Gamma	1.37
		Primary Gamma	<u>43.44</u>
		TOTAL	51.34
Bottom surface, Axial centerline	3	Neutron	0.33
		Primary Gamma	35.51
		End-fitting Gamma	<u>17.02</u>
		TOTAL	52.86
Bottom at 2 m from impact limiter, Axial centerline	4	Neutron	0.03
		Primary Gamma	2.19
		End-fitting Gamma	<u>0.79</u>
		TOTAL	3.01
Top surface, Axial centerline	5	Neutron	0.12
		Primary Gamma	54.17
		End-fitting Gamma	<u>41.45</u>
		TOTAL	95.74
Top at 2 m from impact limiter, Axial centerline	6	Neutron	0.01
		Primary Gamma	3.82
		End-fitting Gamma	<u>2.17</u>
		TOTAL	6.00
Top at Cab	7	Neutron	0.00135
		Primary Gamma	0.47
		End-fitting Gamma	<u>0.25</u>
		TOTAL	0.72

Table 5.1.1-5 Hypothetical Accident – Loss of Shielding Materials

(1 PWR assembly, 35,000 MWd/MTU, 2-year cool time)

Location	Detector I.D.	Radiation	Normal Dose Rate (mrem/hr)
Radial surface, Fuel midplane, With neutron shield	8	Neutron	6.53
		Secondary Gamma	1.37
		Primary Gamma	<u>43.44</u>
		TOTAL	51.34
Radial surface, Fuel midplane, Without neutron shield	9	Neutron	177.13
		Secondary Gamma	0.39
		Primary Gamma	<u>75.00</u>
		TOTAL	252.52
Radial at 1 m from surface, Fuel midplane, Without neutron shield	10	Neutron	50.93
		Secondary Gamma	1.52
		Primary Gamma	<u>54.59</u>
		TOTAL	107.04

Table 5.1.1-6 Hypothetical Accident –Lead Slump

Location	Detector I.D.	Radiation	Normal Dose Rate (mrem/hr)
Radial at 1 m from surface, PWR top end-fitting	11	End-fitting Gamma	3.60
		TOTAL	3.60
Radial at 1 m from surface, PWR top end-fitting	12	End-fitting Gamma	1.31
		TOTAL	1.31
Radial at 1 m from surface, PWR top end-fitting	13	End-fitting Gamma	0.80
		TOTAL	0.80
Radial at 1 m from surface, PWR bottom end-fitting	14	End-fitting Gamma	0.01
		TOTAL	0.01
Radial at 1 m from surface, PWR bottom end-fitting	15	End-fitting Gamma	0.35
		TOTAL	0.35
Radial at 1 m from surface, PWR bottom end-fitting	16	End-fitting Gamma	1.48
		TOTAL	1.48
Radial at 1 m from surface, BWR bottom end-fitting	17	End-fitting Gamma	0.10
		TOTAL	0.10
Radial at 1 m from surface, BWR bottom end-fitting	18	End-fitting Gamma	0.54
		TOTAL	0.54
Radial at 1 m from surface, BWR bottom end-fitting	19	End-fitting Gamma	0.84
		TOTAL	0.84

5.2 Gamma and Neutron Sources

5.2.1 ORIGEN 2

ORIGEN2 is used to calculate the neutron and gamma source strengths. The LOR-2 version of ORIGEN2 in use at the Babcock and Wilcox (B&W) computing center is used for the PWR and BWR fuel because of the improved LWR nuclear data available for this version. The metallic fuel sources are calculated using ORIGEN2 with the CANDU library from Atomic Energy of Canada Limited in place of the LOR-2 library. ORIGEN2 also calculates the gamma spectrum and the concentration of radiologically important fission products such as ^3H , ^{131}Xe , ^{129}I , ^{85}Kr , ^{134}Cs and ^{137}Cs . The LOR-2 data for the design basis PWR assembly is given in Table 5.2.1-1. The gamma spectrum for the PWR assembly is shown in Table 5.2.1-2. Table 5.2.1-3 shows the fission product inventory of the PWR assembly.

Radionuclides other than ^{60}Co present as activation products have short half-lives resulting in rapid decay to negligible concentrations, or they emit soft X-rays or betas that cannot penetrate the cask shielding. The ^{60}Co is present in significant concentrations; it has a relatively long half-life; and it emits two energetic gammas per decay with a mean energy of 1.25 MeV. The ^{60}Co is, therefore, the only activation product considered.

The end-fitting activation is calculated by LOR-2 using a short, hard burnup cycle and a typical burnup cycle from Surry-2. The short cycle yielded the higher values that are used to assure conservatism. The input data for the activation of the end-fittings is also provided in Table 5.2.1-1. The densities used in ORIGEN are obtained by using the weights of inconel for the top and bottom end-fittings that are found in "Physical and Decay Characteristics of Commercial LWR Spent Fuel" (Roddy). Note also that there are 4694 grams of cobalt per metric ton of inconel. It is assumed that all of the cobalt is ^{59}Co . This assumption is conservative because it is the ^{59}Co neutron absorption that results in the formation of the ^{60}Co .

A Watt spectrum for ^{252}Cf is used to simulate the ^{242}Cm and the ^{244}Cm neutron spectra of the fuel. This equation is provided by Westinghouse as a part of the Extended Fuel Burnup Demonstration Program (DOE/ET34014-10).

The spectrum takes the form of:

$$X(E) = (0.37e^{-0.88E})\text{SINH}(\sqrt{2.0E})$$

where:

E is the neutron energy in MeV

Table 5.2.1-4 presents the evaluated source neutron spectrum used in the shielding analysis.

The analyses are performed with the limiting design basis fuel - the PWR assembly. However, any intact PWR, BWR or metallic fuel rods that do not exceed the thermal, reactivity and radiological characteristics of the design basis fuels shown in Table 5.1.1-3 are acceptable for transport in the NAC-LWT cask.

Table 5.2.1-1 LOR-2 Input Data

PWR Fuel	
Mass (kgU)	475.0
Enrichment (wt % ²³⁵ U)	3.7
Burnup (MWd)	16,625.0
(MWd/MTU)	35,000.0
Burnup Cycle	4 Cycles 405 full power days 60 day outages 10.262 MW at full power
Average Flux (n/cm ² – sec)	2.19 x 10 ¹³
PWR End-Fittings	
Masses (kg Inconel)	Top – 6.8 Bottom – 5.7
Concentration (g- ⁵⁹ Co/MT Inconel)	4694.0
Assembly Burnup (MWd)	16,625.0
(MWd/MTU)	35,000.0
Irradiation Cycle	3 Cycles 383 full power days 50 day outages 13.972 MW at full power
Average Flux (n/cm ² – sec)	2.95 x 10 ¹³

Table 5.2.1-1 LOR-2 Input Data (continued)

Masses (kg Inconel)	BWR End-Fittings
	Top – 2.0 Bottom – 4.8
Concentration (g- ⁵⁹ Co/MT Inconel)	4,694.0
Assembly Burnup (MWd) MWd/MTU)	5,580.0 30,000.0
Irradiation Cycle	4 Cycles 227 full power days 61 day outages 6.134 MW at full power
Average Flux (n/cm ² – sec)	3.28 x 10 ¹³

Table 5.2.1-2 Photon Spectrum for Design Basis Fuel

One PWR assembly with 35,000 MWd/MTU burnup and a 2-year cool time

Mean Energy (MeV)	Energy Source (MeV/Sec) Per Assembly	Total Source Per Assembly (Photons/Sec)
3.500	2.717×10^{10}	7.762×10^9
2.750	6.754×10^{11}	2.456×10^{11}
2.250	3.233×10^{13}	1.432×10^{13}
1.830	2.038×10^{13}	1.114×10^{13}
1.495	3.220×10^{14}	2.154×10^{14}
1.160	1.929×10^{14}	1.663×10^{14}
0.900	1.496×10^{14}	1.663×10^{14}
0.700	3.964×10^{15}	5.663×10^{15}
0.500	2.909×10^{15}	5.818×10^{15}
0.350	1.093×10^{14}	3.123×10^{14}
0.250	7.808×10^{13}	3.123×10^{14}
TOTALS	7.712×10^{15}	1.268×10^{16}

Table 5.2.1-3 Fission Product Gas Inventory

One PWR assembly with 35,000 MWd/MTU burnup and a 2-year cool time

Fission Product	Inventory – Curies/Assembly
Gases	
Tritium	203.2
Krypton-85	3,797.0
Xenon-131	Negligible
Iodine-129	Negligible
Total	4,000.2
Particulates	
Cesium-134	96,000
Cesium-137	50,000
Total	146,000

Table 5.2.1-4 Design Basis Fuel Neutron Spectrum

Group	Energy (eV)	n/cm ² - sec
1	0.20000 x 10 ⁸	1.39971 x 10 ⁻²
2	0.64340 x 10 ⁷	2.61998 x 10 ⁻¹
3	0.30000 x 10 ⁷	2.34004 x 10 ⁻¹
4	0.18500 x 10 ⁷	1.19993 x 10 ⁻¹
5	0.14000 x 10 ⁷	1.49064 x 10 ⁻¹
6	0.90000 x 10 ⁶	1.45953 x 10 ⁻¹
7	0.40000 x 10 ⁶	6.39921 x 10 ⁻²
8	0.10000 x 10 ⁶	9.00005 x 10 ⁻³
9	0.17000 x 10 ⁵	1.00002 x 10 ⁻³
10	0.30000 x 10 ⁴	1.00002 x 10 ⁻³
11	0.55000 x 10 ³	0.00000
12	0.10000 x 10 ³	0.00000
13	0.30000 x 10 ²	0.00000
14	0.10000 x 10 ²	0.00000
15	0.30500 x 10 ¹	0.00000
16	0.17700 x 10 ¹	0.00000
17	0.13000 x 10 ¹	0.00000
18	0.11300 x 10 ¹	0.00000
19	0.10000 x 10 ¹	0.00000
20	0.80000	0.00000
21	0.40000	0.00000
22	0.32500	0.00000
23	0.22500	0.00000
24	0.10000	0.00000
25	0.50000 x 10 ⁻¹	0.00000
26	0.30000 x 10 ⁻¹	0.00000
27	0.10000 x 10 ⁻⁴	0.00000

Note: Spectrum is normalized to 1 n/cm² - sec.

5.3 Model Specification

5.3.1 Description of Radial and Axial Shielding Configuration

The gamma radiation protection provided by the NAC-LWT cask is primarily in the form of solid shielding material, which totally surrounds the fuel. The principal components of gamma shielding in the cask body are the 0.75-inch inner steel shell, 5.75 inches of lead, a 1.20-inch outer steel shell, 5 inches of water, and a 0.24-inch (6mm) thick outside layer of steel surrounding the neutron shield. The bottom of the cask is a steel/lead/steel configuration, having an inner steel layer 4 inches thick, a 3-inch thick layer of lead, and an outside layer of steel 3.5 inches thick. The gamma shielding at the top of the cask consists of the closure lid, which does not contain lead, but is made up of 11.25 inches of stainless steel.

The principal neutron shielding is provided by a 5-inch water shield, which surrounds the fuel. The water contains boron to aid in shielding by suppressing the production of capture gammas in the water.

Dose points for normal operations conditions are chosen and placed in accordance with conditions specified in 10 CFR 71. Thus, dose points are placed at the fuel midplane on the surface of the neutron shield jacket and at 2 meters from the personnel barrier, as illustrated in Table 5.3.3-1. Dose points are also placed at the top and bottom at the centerline of the cask on the surface of the outer steel, at 2 meters from the personnel barrier and 197 inches (5 meters) from the surface at the top of the cask (to obtain dose rates directly behind the vehicle cab).

These dose points are shown in Figure 5.3.3-2. The dose points are placed at the surface and at 1 meter from the surface for the hypothetical accident, and at 1 meter from the surface at various points along the outside of the cask for the lead slump accident. Dose points for accident conditions are shown in Figure 5.3.3-1 and Figure 5.3.3-3 through Figure 5.3.3-5.

There is a void due to the contraction of the lead after the initial pour that is not taken into consideration in the shielding model. It is not included because even though the lead contracts, the mass of the lead remains constant. A void also exists between the aluminum of the basket and the cask, which does not significantly affect the shielding results.

The 3-dimensional model for normal transport conditions contains all of the shielding described previously in its proper configuration. (See Figure 5.3.3-1 and Figure 5.3.3-2 for details.) The 1-dimensional model for normal transport conditions contains the same shielding geometry, but uses an equivalent circularized source as shown in Figure 5.3.3-6. Some accident conditions will change the configuration of the model. In the loss of neutron shield accident, it is assumed that

the entire neutron shield is lost. This loss is represented by a void in place of the neutron shield; therefore, the configuration of the model does not change, only the material of the neutron shield.

This case is shown in Figure 5.3.3-1 as detector 9. In the lead slump accident, the cask is dropped on its end allowing the lead to fill the gap left between the steel and the lead from the lead pour. This creates a gap in the lead either on top or bottom, depending on cask orientation. The new gap changes the dimensions of the model as illustrated in Figure 5.3.3-3 through Figure 5.3.3-5.

5.3.2 Shield Regional Densities

Typical Westinghouse 15 x 15 PWR fuel assemblies have a mass of 459 kgU; however, a mass of 475 kgU is chosen for conservatism.

Table 5.3.3-1 contains detailed information on source compositions and densities. The source densities are obtained by multiplying the original fuel (UO₂) density by the volume fraction of fuel in the effective fuel region and the 95 percent theoretical density. The zirconium density is calculated by multiplying the original zirconium density by the volume fraction of zirconium in the effective fuel region. All shield materials and their densities are included in Table 5.3.3-2.

The steel, aluminum and iron densities are found in the Book of Standards, the Metals Handbook, Alcoa Aluminum Handbook, and Merritt's Standard Handbook for Civil Engineers.

The density of the water in the neutron shield is based on a water temperature of 250°F. This is conservative since the neutron shield never actually reaches this temperature. The water is less dense at higher temperatures; therefore, the calculated dose is higher than the actual dose at the normal operating temperature.

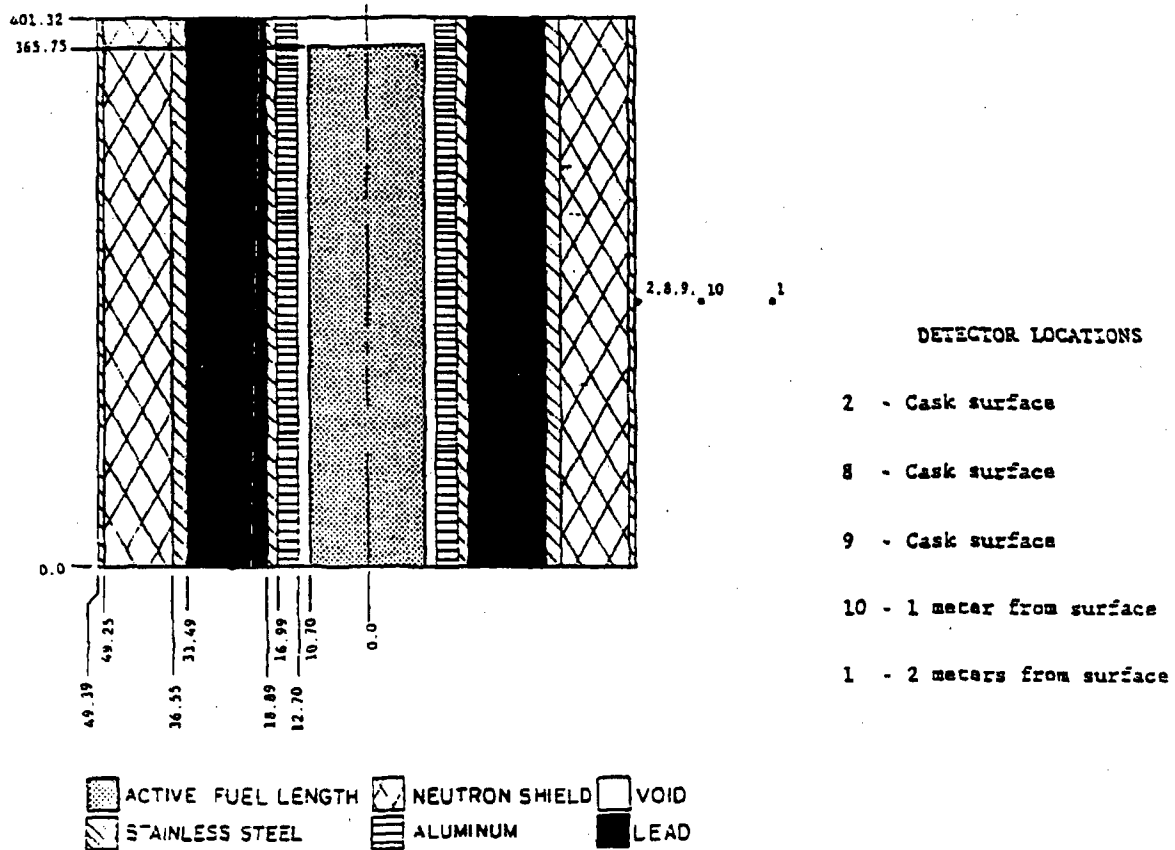
5.3.3 Metallic Fuel Configuration

The NAC-LWT cask is also evaluated for a configuration consisting of 15 metallic fuel rods in the cask with the neutron shield tank liquid drained and with the cask inside an International Shipping Organization container. The gamma and neutron sources for the metallic fuel configuration are 11.3 percent and 0.073 percent of the design basis PWR sources, respectively. The hypothetical accident dose rates for the metallic fuel may be obtained directly from the PWR hypothetical accident dose rates by multiplying the neutron and secondary gamma PWR values by a factor of 7.30×10^{-4} and the primary gamma PWR value by a factor of 0.113, as calculated from Table 5.1.1-3. The normal operations dose rates for the metallic fuel may be obtained from the PWR normal operations dose rates by applying the factors given above, but the lack of neutron shield tank fluid must be accounted for by ratioing the dose rates on the cask surface with and without the neutron shield liquid. These dose rates are given in Table 5.1.1-5. The loss of the neutron shield liquid results in a 27.1-fold increase in the neutron dose rate; however, the secondary gamma dose rate decreases by 71 percent. The primary gamma dose rate increases by 73 percent with the shield liquid removed. The cask radial dose rates at the fuel midplane, which result from this evaluation for the metallic fuel rods, are as follows:

	Normal Operations (2 meters from personnel barrier)	Hypothetical Accident (1 meter from cask surface)
Neutron	0.025 mrem/hr	0.037 mrem/hr
Secondary Gamma	0.000	0.001
Primary Gamma	<u>1.309</u>	<u>6.169</u>
Total	1.334 mrem/hr	6.207 mrem/hr

The metallic fuel rod dose rates for normal operations and hypothetical accident conditions are 17 and 6 percent of the PWR dose rates, respectively. These values are less than the regulatory limits; therefore, the metallic fuel rods are adequately shielded during transportation.

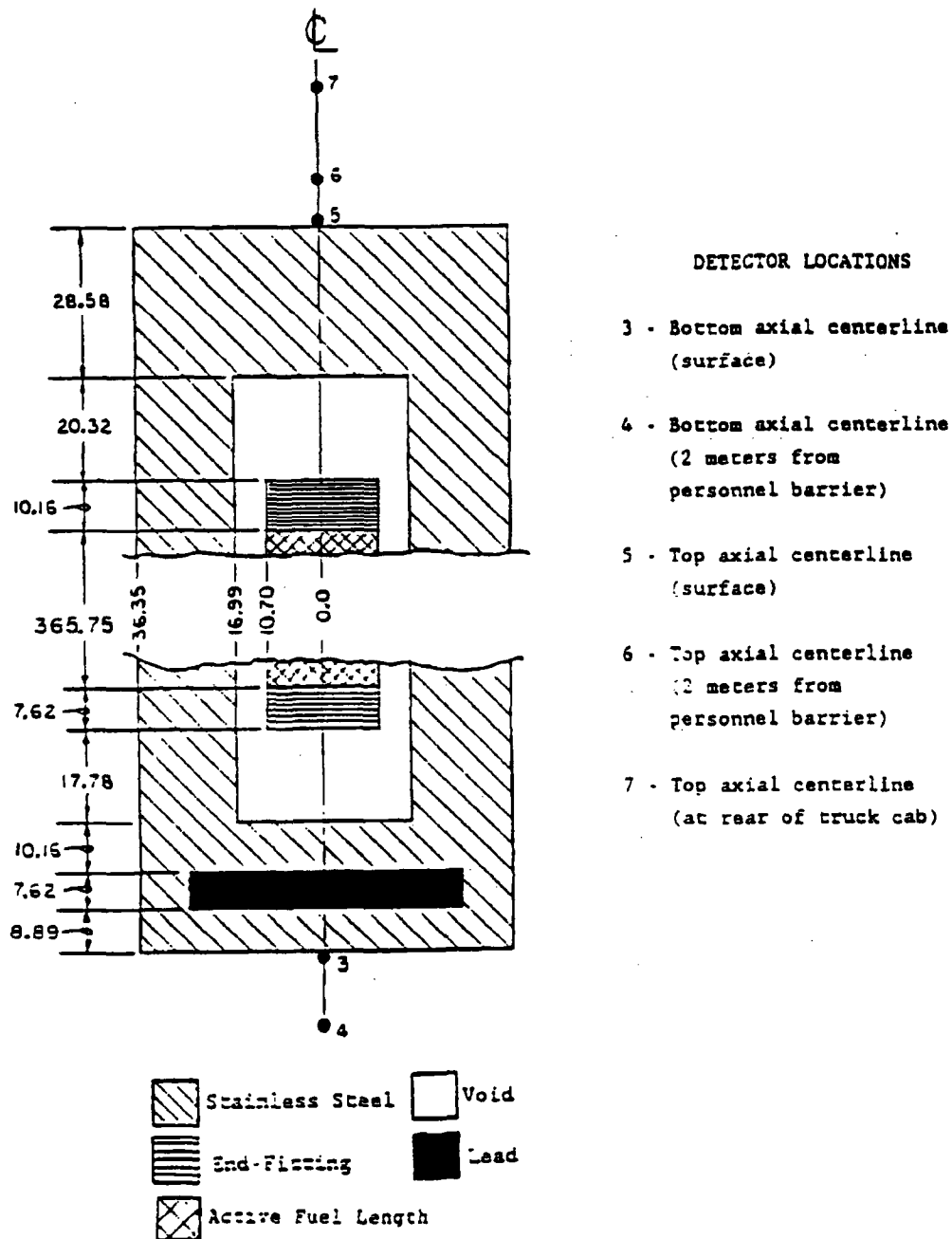
Figure 5.3.3-1 Three-Dimensional Radial Model



(Dimensions are in cm)

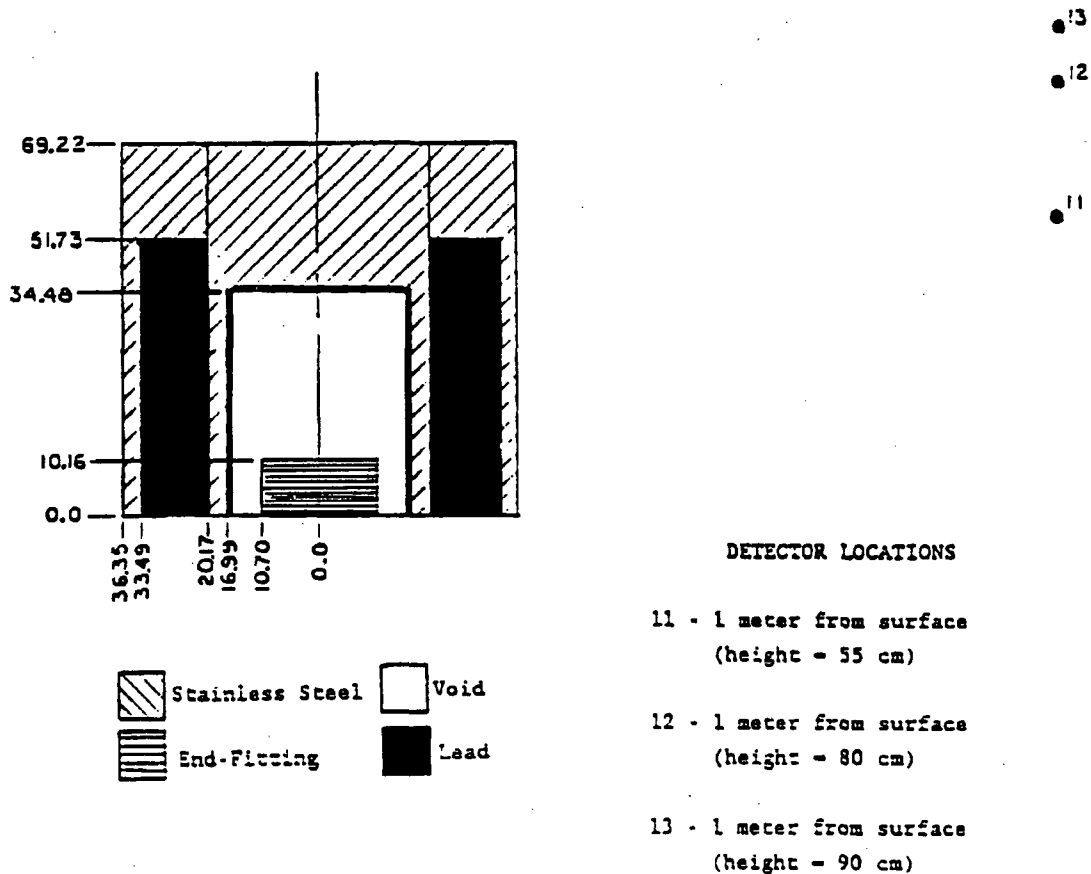
(In hypothetical accident condition, neutron shield is void.)

Figure 5.3.3-2 End-Fitting Model with Fuel



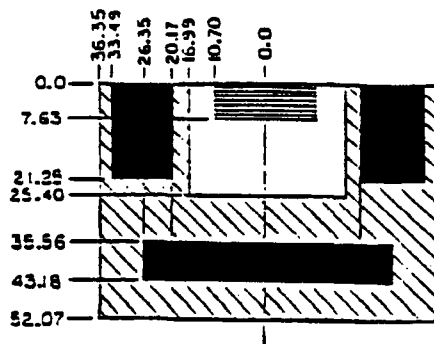
(Dimensions are in cm)

Figure 5.3.3-3 Lead Slump Accident – PWR Top End-Fitting



(Dimensions are in cm)

Figure 5.3.3-4 Lead Slump Accident – PWR Bottom End-Fitting



16

15

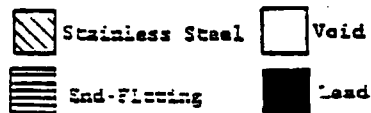
14

DETECTOR LOCATIONS

14 - 1 meter from surface
(height = 125 cm)

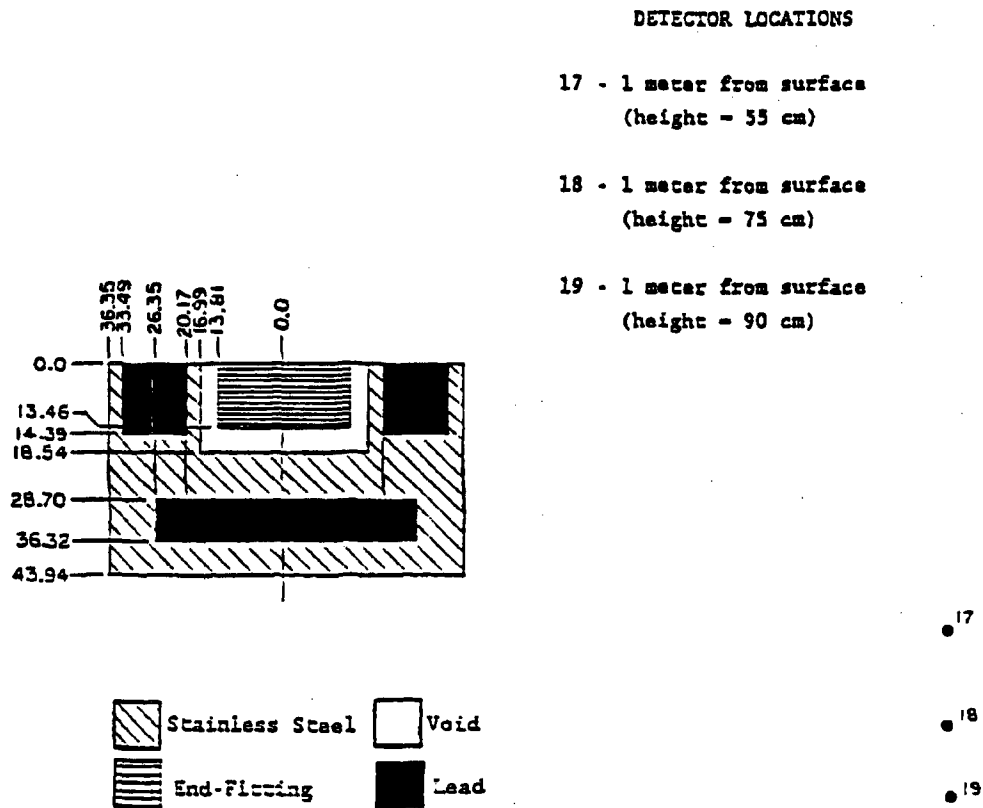
15 - 1 meter from surface
(height = 80 cm)

16 - 1 meter from surface
(height = 21.30 cm)



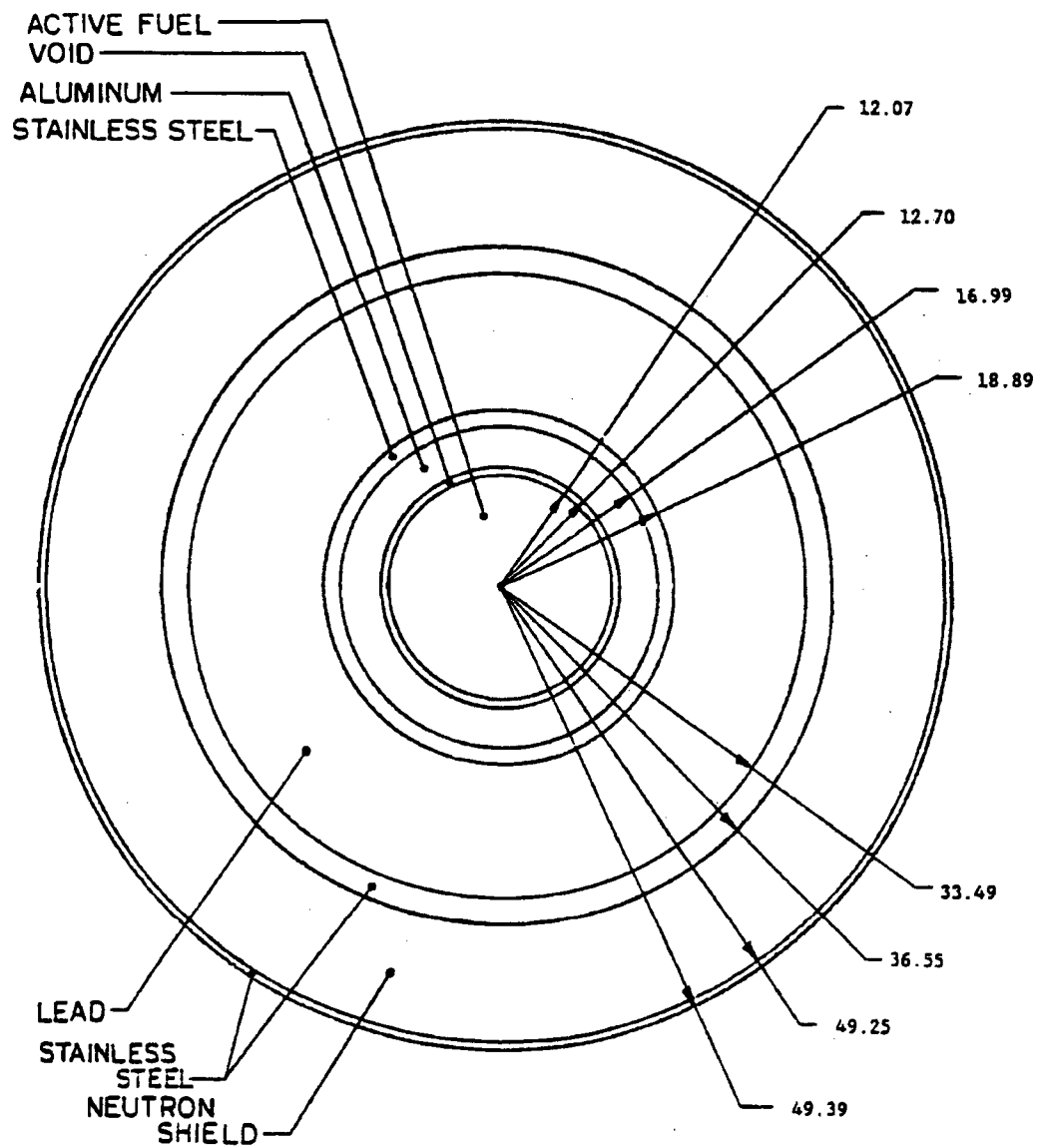
(Dimensions are in cm)

Figure 5.3.3-5 Lead Slump Accident – BWR Bottom End-Fitting



(Dimensions are in cm)

Figure 5.3.3-6 One-Dimensional Radial Calculational Model



(Dimensions are in cm)

Table 5.3.3-1 Source Material Compositions

QAD-CG

Element	U	O
Density, g/cc	2.759	0.370
Density, atoms/barn-cm	6.98E-3	1.39E-2

XSDRNPM

Isotope	²³⁵ U	²³⁸ U	¹⁶ O	Zr
Density, g/cc	0.1021	2.657	0.370	0.6344
Density, atoms/barn-cm	2.62E-4	6.73E-4	1.39E-2	4.18E-3

Table 5.3.3-2 Shield Material Densities and Compositions

Material	Element	QAD-CG (g/cc)	XSDRNPM (atom/barn-cm)
Aluminum	AL	2.7	6.026E-2
Stainless Steel	Fe	5.618	6.026E-2
	Cr	1.445	1.67E-2
	Ni	0.963	9.88E-3
Lead	Pb	11.35	3.29E-2
Neutron Shield	H	0.1046	5.73E-2
	O	0.8373	3.15E-2
	B	0.00184	1.108E-4

5.3.4 MTR Fuel Configuration

A maximum of 42 MTR fuel assemblies have been analyzed for transport in the LWT cask. This configuration consists of up to seven fuel assemblies placed radially in each of the six axial fuel basket modules. Two alternate configurations of MTR fuel assembly loading provide for loads of 35 assemblies in five basket modules or 28 assemblies in four basket modules.

LEU and MEU fuel is evaluated for a uniform loading of 30 W per fuel position, resulting in a basket module maximum of 210 W (or 1.26 kW per cask). To allow flexibility in loading either high burnup or short cooled HEU fuel, three possible fuel loading configurations are evaluated. The configurations are based on limiting the total heat load (and corresponding gamma/neutron source) in each basket module to a maximum of 210 W (1.26 kW per cask). Configuration 1 is the loading of three assemblies, having thermal outputs of 120, 70 and 20 watts, in close proximity, with the 120 W assembly occupying the center cell. Configuration 2 is the uniform loading of 7 MTR assemblies, each having a decay heat of 30 W. Configuration 3 has three assemblies in line across the center of the basket, as required by the loading procedure, with a maximum of 70 watts per assembly. These configurations are shown in Figure 5.3.4-1.

The shielding analysis evaluated all three MTR fuel types for variable burnup considering uniform basket loading for LEU and MEU fuel and the configurations above for HEU fuel. HEU fuel provides the limiting dose rates and, therefore, only the HEU results are discussed in detail. A comparison of dose rates at 2 meters from the transport vehicle is shown in Figure 5.3.4-3 for various LEU, MEU and HEU payloads. This figure demonstrates that HEU fuel bounds the LEU and MEU payloads. As discussed below, the HEU loading patterns produce significantly higher dose rates than those documented in Figure 5.3.4-3 for the uniform 30 W loading.

In order to present the limiting MTR dose rates, NAC performed a parametric study in which each of these configurations were examined using the SCALE 4.3 (ORNL,1995) SAS4 (Tang, 1995) computer code for shielding analysis and SAS2H (Herman, 1995) for source terms. The SAS4 sequence incorporates a FORTRAN coding modification that permits the determination of dose rate profiles along the axial and radial surfaces. This study established Configuration 1 as the bounding configuration, with respect to axial and radial dose rates. In the case of the radial evaluation, Configuration 1 is clearly limiting based on the concentrated source term. The axial evaluation concluded that Configurations 1 and 3 are statistically similar and bound Configuration 2. Configuration 1 is selected as the limiting MTR preferential loading configuration and is the load bases for the shielding analysis.

The MTR fuel assembly consists of plates held in a parallel arrangement by thick aluminum slotted side plates. The number of fuel plates range from 17 to 23 per assembly, and the analysis assumed the maximum 23 plate value for each of the three MTR fuel types.

The design basis MTR fuel assemblies were constructed using typical MTR parameters. The physical characteristics of the analyzed LEU, MEU and HEU fuel assemblies are shown in Table 5.3.4-1. The fueled section of the assembly consists of 23 plates of 0.050-inch thickness and two side plates 0.187-inch thick, which do not contain fuel. The fuel core of each fuel plate is a cermet of aluminum and U-Al, which is 0.020-inch thick. The 6061 aluminum cladding has a minimum thickness of 0.015-inch. The HEU fresh fuel load analyzed consists of either 380 grams or 460 grams of ^{235}U per assembly 90% enriched. The initial enrichment is used to encompass other HEU MTR fuel types.

The SAS2H sequence was used to determine the gamma and neutron source terms and decay heat loads for the evaluated MTR fuel assembly loading configurations. The SAS2H sequence includes the ORIGEN-S code and a 1D XSDRNPM model of the fuel assembly. ORIGEN-S performs fuel assembly depletion at specified operating conditions and calculates heat generation, gamma and neutron spectra for a given discharge isotopic composition as a function of out of reactor time (cooling time). The 1D model of the fuel assembly is used to collapse the 27 group neutron cross-section library (27GROUPNDF4) into three broad energy groups for the depletion calculation. The 1D model is based on an equivalent area representation of the fuel/moderator cell and surrounding structural regions. Average power is based on reactor maximum power divided by the number of assemblies in the core.

For the HEU fuel, separate analyses were performed for ^{235}U loadings of 380 grams and 460 grams. For the 380 gram ^{235}U loading, the maximum allowable burnup was 660,000 MWd/MTU. For the 460 gram ^{235}U loading, dose rates exceeding 10 CFR 71 limits were calculated at 660,000 MWd/MTU, so the burnup was limited to 577,500 MWd/MTU. Calculated dose rates are higher for the 380 gram ^{235}U loading at 660,000 MWd/MTU.

For the bounding HEU fuel with 380 grams ^{235}U , a series of 10 cases was run in which burnup was varied from a minimum of 82,500 MWd/MTU to a maximum of 660,000 MWd/MTU. Cooling times were considered from 30 days to 6.0 years. Because the cask is loaded based on the decay heat limits, no single design basis fuel assembly or loading configuration exists. Design basis photon and neutron source terms for MTR assemblies with decay heat loads of 20, 30, 70 and 120 watts are determined for the 660,000 MWd/MTU burnup case, which was bounding. The SAS2H results from these cases are used for the design basis photon and neutron source terms and are summarized in Table 5.3.4-2 and Table 5.3.4-3 for 380 grams ^{235}U and Table 5.3.4-4 and Table 5.3.4-5 for 460 grams ^{235}U . The material densities used

in the analysis are summarized in Table 5.3.4-8. Minimum cool time curves for the various MTR fuel and loading configurations are shown in Section 7.1.5.

MTR elements may contain a small amount of cadmium (maximum 100 grams Cd) in the form of nonfuel hardware. Table 5.3.4-6 and Table 5.3.4-7 contain comparisons of the cadmium light element gamma source compared to the U-Al fuel material gamma source. The light element source is produced during the SAS2H depletion analysis and applies 100% of the element flux levels. Included for comparison are HEU (460 gram) and LEU (640 gram) fuel types at the maximum allowed burnup (i.e., maximum activation) and cool times required to meet 30 watts (uniform heat load limit per element). Also shown are conservative comparisons of the design basis 30-watt fuel source to a 90-day-cooled Cd source. As shown in the comparison tables, the cadmium source is not significant to NAC-LWT cask shielding evaluations. The hardware gamma source of the cadmium represents less than 0.1% of the fuel gamma source at the required minimum cool time and less than 2% at the conservative 90-day-cooled Cd source. As the majority of the Cd source is at energy lines less than 0.5 MeV and does not penetrate the NAC-LWT cask shields, the actual effect on dose rates is even smaller than that indicated by the difference in total source magnitude.

Based on the MTR source term calculation, the (alpha, n) reactions in ^{27}Al and ^{28}Si are included in the MTR neutron source term. The (alpha, n) reactions in ^{27}Al and ^{28}Si increase the neutron source term by a factor of ~2.9. Consequently, a factor of 2.9 is applied to the MTR neutron source terms.

The SAS4 (Tang) sequence is used to calculate the dose rates at all points of interest. In this sequence, a 1D adjoint XSDRNPM model generates biasing parameters for a 3D MORSE Monte Carlo model of the NAC-LWT cask with the MTR fuel. SAS4 requires model symmetry about the active fuel midplane (midplane of the six basket modules in this case). A 3D Monte Carlo model is developed for the upper half of the cask. This model bounds the results for a lower half model as the cask has more shielding in the axial direction at the bottom end. The upper half model is shown in Figure 5.3.4-2. The model assumes that the fuel is at the highest point in the basket module, that the fuel is loaded in the same way axially in all of the modules, and it ignores the presence of the impact limiters. Detectors are placed at three radial locations of interest. These locations are: 1) cask surface; 2) one meter from the cask surface; and 3) at two meters from the edge of the cask conveyance.

5.3.4.1 Shielding Evaluation for MTR Fuel

This section presents the shielding analyses for normal conditions of transport, illustrates compliance with 10 CFR Part 71. In normal transport, the dose rate limits are:

- The dose rate on the surface of the package is less than 200 mrem/hr, except that localized dose rates up to 1000 mrem/hr are allowed if it is shown that the dose rate on the surface of the ISO enclosure is less than 200 mrem/hr.
- At 2 meters from the edge of the transport vehicle the dose rate is limited to 10 mrem/hr.
- The truck cab (defined as a point 5 meters from the NAC-LWT lid) dose rate is limited to 2 mrem/hr.

The dose rates for the bounding loading configuration (Configuration 1) are shown in Table 5.3.4-9, Table 5.3.4-10 and Table 5.3.4-11 for the cask surface, plane of conveyance, and at 2 meters from the edge of the conveyance, respectively. These dose rates are well below the regulatory limits. The dose rates at 1 meter from the cask surface are presented in Table 5.3.4-12, where the maximum dose rate defines the Transport Index (TI) for the cask.

The axial surface and the 5 meter (back of tractor cab) dose rates are shown in Table 5.3.4-13 and Table 5.3.4-14. Shielding provided by the impact limiter is conservatively neglected. The axial dose rates at the bottom of the cask are conservatively assumed to be equal to the dose rates reported at the top.

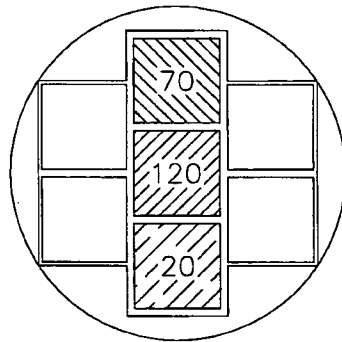
This evaluation shows that the NAC-LWT cask, with up to 42 MTR fuel assemblies, meets the shielding requirements of 10 CFR 71, 49 CFR 173, and IAEA Transportation Safety Standards (TS-R-1).

5.3.4.2 Accident Conditions of Transport

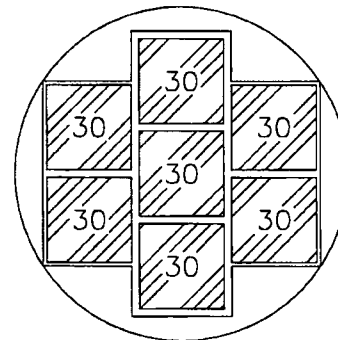
This section presents the accident condition shielding analyses. Under accident conditions, the NRC limits the package dose rate to 1000 mrem/hr at 1 meter off the package surface. The only accident condition examined in this section is the loss of the LWT liquid neutron shield.

This analysis examines Configuration 1 consistent with the limiting configuration analysis for normal conditions of transport presented in Section 5.3.4. The accident condition source terms are identical to the normal condition source terms. The accident condition results are presented in Table 5.3.4-15.

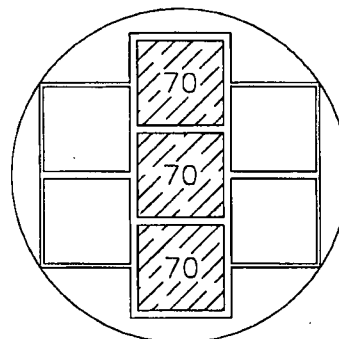
Figure 5.3.4-1 MTR Fuel Evaluated Configurations



CONFIGURATION 1



CONFIGURATION 2



CONFIGURATION 3

Figure 5.3.4-2 SAS4 Shielding Model for the MTR Fuel Basket in the NAC-LWT (Upper Half)

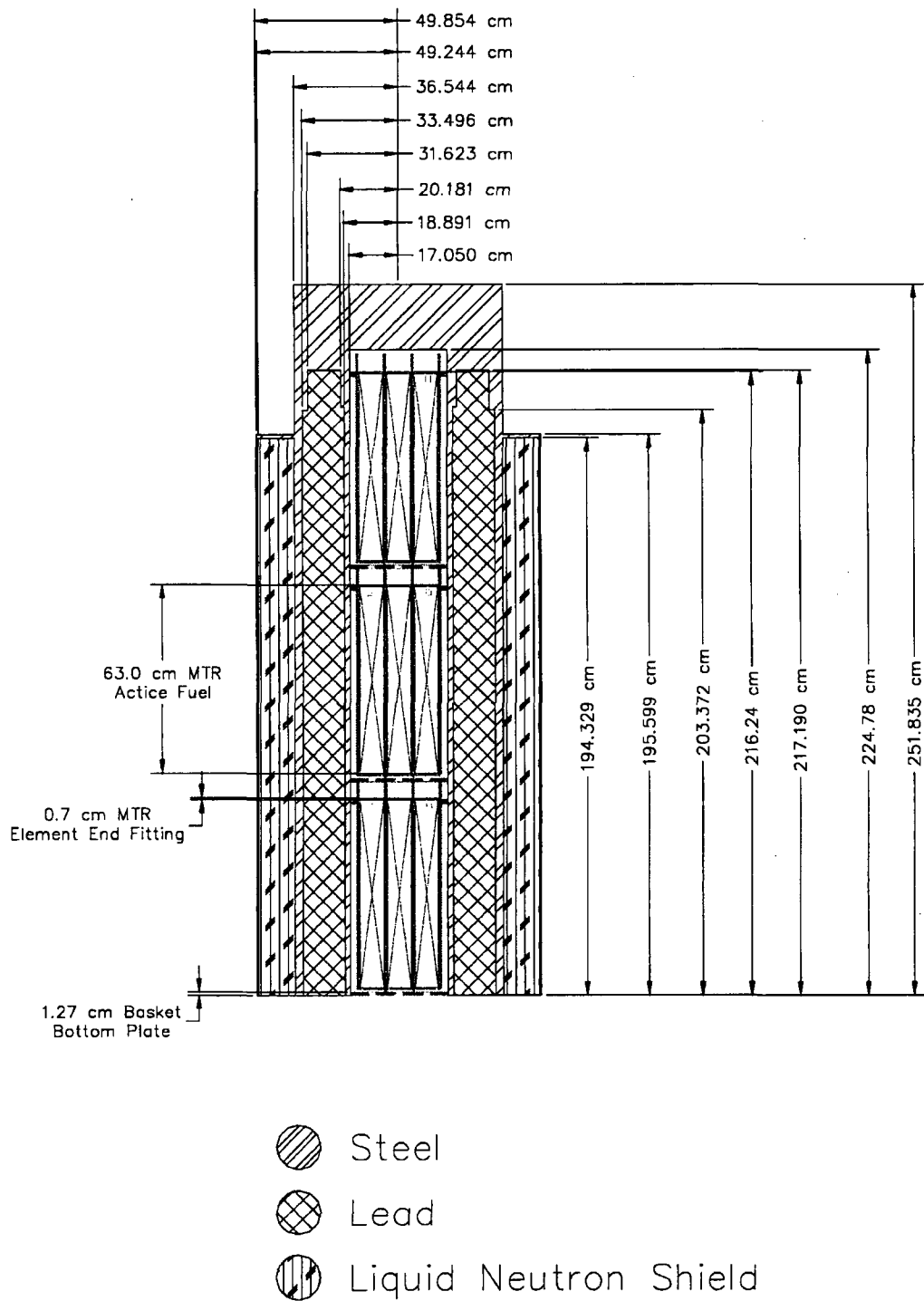


Figure 5.3.4-3 Dose Rates 2 Meters from Transport Vehicle (30 W Uniform Loading)

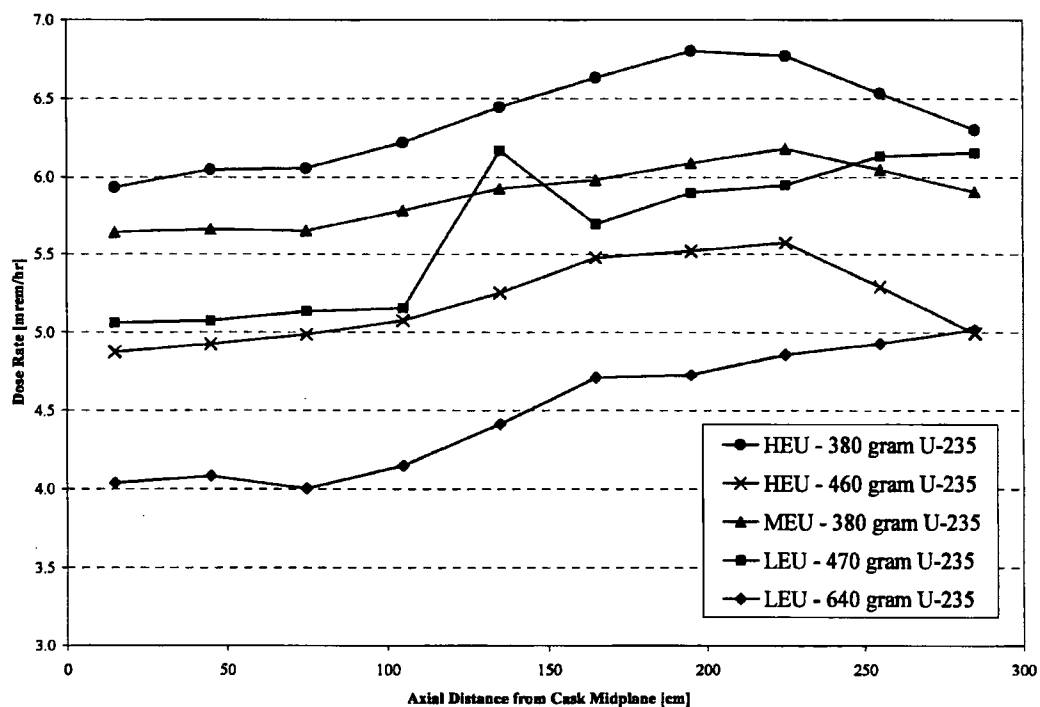


Table 5.3.4-1 Design Basis MTR Fuel Assembly Characteristics

Fuel Parameters	Units	HEU	MEU	LEU
Element Width	[cm]	7.6	7.6	7.6
Element Depth	[cm]	8.0	8.0	8.0
Side Plate Thickness	[cm]	0.475	0.475	0.475
Side Plate Depth	[cm]	7.5	7.5	7.5
Number of Plates		23	23	23
Plate Thickness	[cm]	0.127	0.127	0.127
Active Fuel Length	[cm]	63	65	65
Active Fuel Width	[cm]	6.35	6.35	6.35
Active Fuel Thickness	[cm]	0.051	0.051	0.051
Cut End Length	[cm]	0.7	0.7	0.7
Fuel Composition		U-Al	U-Al	U-Al
Wt % ²³⁵ U		90	40	19
Maximum ²³⁵ U per Fuel Assembly	[g]	380 ¹	380	470 ²
Wt % U in Fuel Composition		30	50	75

¹ HEU fuel was also analyzed at 460 grams of ²³⁵U per fuel element.

² LEU fuel was also analyzed at 640 grams of ²³⁵U per fuel element.

Table 5.3.4-2 MTR Fuel Element Gamma Source Terms by Thermal Output –
380 grams ²³⁵U

Burnup 660,000 MWd/MTU			MTR Assembly Thermal Output			
Group	E _{hi} (Mev)	E _{low} (Mev)	20 Watts	30 Watts	70 Watts	120 Watts
			2162 Days (g/sec)	1413 Days (g/sec)	581 Days (g/sec)	330 Days (g/sec)
1	10.00	8.00	1.63E+03	1.81E+03	2.08E+03	2.21E+03
2	8.00	6.50	7.69E+03	8.52E+03	9.79E+03	1.04E+04
3	6.50	5.00	3.92E+04	4.35E+04	4.99E+04	5.30E+04
4	5.00	4.00	9.77E+04	1.08E+05	1.24E+05	1.32E+05
5	4.00	3.00	3.30E+07	1.32E+08	6.24E+08	9.96E+08
6	3.00	2.50	2.81E+08	1.17E+09	5.84E+09	9.56E+09
7	2.50	2.00	2.45E+10	1.47E+11	1.09E+12	2.00E+12
8	2.00	1.66	6.34E+09	2.33E+10	1.32E+11	2.34E+11
9	1.66	1.33	5.93E+11	1.19E+12	3.01E+12	4.20E+12
10	1.33	1.00	1.87E+12	2.75E+12	5.21E+12	6.81E+12
11	1.00	0.80	8.36E+12	1.61E+13	3.47E+13	4.42E+13
12	0.80	0.60	4.21E+13	6.14E+13	1.14E+14	2.15E+14
13	0.60	0.40	1.70E+13	3.41E+13	7.83E+13	1.04E+14
14	0.40	0.30	9.18E+11	1.71E+12	7.11E+12	1.23E+13
15	0.30	0.20	1.42E+12	2.47E+12	9.38E+12	1.62E+13
16	0.20	0.10	5.22E+12	9.84E+12	4.12E+13	7.19E+13
17	0.10	0.05	6.33E+12	1.09E+13	4.07E+13	7.00E+13
18	0.05	0.01	2.19E+13	3.60E+13	1.26E+14	2.15E+14
Total	–	–	1.06E+14	1.77E+14	4.60E+14	7.61E+14

Table 5.3.4-3 MTR Fuel Element Neutron Source Terms by Thermal Output –
380 grams ^{235}U

Group	Burnup 660,000 MWd/MTU		MTR Assembly Thermal Output			
	E_{hi} (Mev)	E_{low} (Mev)	20 Watts	30 Watts	70 Watts	120 Watts
			2162 Days (n/sec)	1413 Days (n/sec)	581 Days (n/sec)	330Days (n/sec)
1	2.00E+01	6.43E+00	5.42E+04	6.06E+04	7.06E+04	7.52E+04
2	6.43E+00	3.00E+00	6.26E+05	6.98E+05	8.12E+05	8.67E+05
3	3.00E+00	1.85E+00	7.11E+05	7.90E+05	9.14E+05	9.74E+05
4	1.85E+00	1.40E+00	3.92E+05	4.37E+05	5.07E+05	5.39E+05
5	1.40E+00	9.00E-01	5.25E+05	5.86E+05	6.81E+05	7.24E+05
6	9.00E-01	4.00E-01	5.69E+05	6.36E+05	7.40E+05	7.87E+05
7	4.00E-01	1.00E-01	1.11E+05	1.24E+05	1.45E+05	1.54E+05
8	1.00E-01	1.70E-02	0.00E+00	0.00E+00	0.00E+00	0.00E+00
9	1.70E-02	3.00E-03	0.00E+00	0.00E+00	0.00E+00	0.00E+00
10	3.00E-03	5.50E-04	0.00E+00	0.00E+00	0.00E+00	0.00E+00
11	5.50E-04	1.00E-04	0.00E+00	0.00E+00	0.00E+00	0.00E+00
12	1.00E-04	3.00E-05	0.00E+00	0.00E+00	0.00E+00	0.00E+00
13	3.00E-05	1.00E-05	0.00E+00	0.00E+00	0.00E+00	0.00E+00
14	1.00E-05	3.05E-06	0.00E+00	0.00E+00	0.00E+00	0.00E+00
15	3.05E-06	1.77E-06	0.00E+00	0.00E+00	0.00E+00	0.00E+00
16	1.77E-06	1.30E-06	0.00E+00	0.00E+00	0.00E+00	0.00E+00
17	1.30E-06	1.13E-06	0.00E+00	0.00E+00	0.00E+00	0.00E+00
18	1.13E-06	1.00E-06	0.00E+00	0.00E+00	0.00E+00	0.00E+00
19	1.00E-06	8.00E-07	0.00E+00	0.00E+00	0.00E+00	0.00E+00
20	8.00E-07	4.00E-07	0.00E+00	0.00E+00	0.00E+00	0.00E+00
21	4.00E-07	3.25E-07	0.00E+00	0.00E+00	0.00E+00	0.00E+00
22	3.25E-07	2.25E-07	0.00E+00	0.00E+00	0.00E+00	0.00E+00
23	2.25E-07	1.00E-07	0.00E+00	0.00E+00	0.00E+00	0.00E+00
24	1.00E-07	5.00E-08	0.00E+00	0.00E+00	0.00E+00	0.00E+00
25	5.00E-08	3.00E-08	0.00E+00	0.00E+00	0.00E+00	0.00E+00
26	3.00E-08	1.00E-08	0.00E+00	0.00E+00	0.00E+00	0.00E+00
27	1.00E-08	0.00E+00	0.00E+00	0.00E+00	0.00E+00	0.00E+00
Total	–	–	2.99E+06	3.33E+06	3.87E+06	4.12E+06

Table 5.3.4-4 MTR Fuel Element Gamma Source Terms by Thermal Output –
460 grams ²³⁵U

Burnup 577,500 MWd/MTU			MTR Assembly Thermal Output			
Group	E _{hi} (Mev)	E _{low} (Mev)	20 Watts	30 Watts	70 Watts	120 Watts
			2247 Days (g/sec)	1467 Days (g/sec)	602 Days (g/sec)	341 Days (g/sec)
1	10.00	8.00	1.07E+03	1.16E+03	1.31E+03	1.40E+03
2	8.00	6.50	5.02E+03	5.48E+03	6.18E+03	6.59E+03
3	6.50	5.00	2.56E+04	2.80E+04	3.15E+04	3.36E+04
4	5.00	4.00	6.38E+04	6.97E+04	7.86E+04	8.38E+04
5	4.00	3.00	2.70E+07	1.15E+08	5.77E+08	9.39E+08
6	3.00	2.50	2.33E+08	1.02E+09	5.47E+09	9.13E+09
7	2.50	2.00	2.08E+10	1.34E+11	1.08E+12	2.03E+12
8	2.00	1.66	5.73E+09	2.12E+10	1.27E+11	2.30E+11
9	1.66	1.33	5.49E+11	1.12E+12	2.93E+12	4.14E+12
10	1.33	1.00	1.86E+12	2.73E+12	5.18E+12	6.81E+12
11	1.00	0.80	7.73E+12	1.52E+13	3.37E+13	4.34E+13
12	0.80	0.60	4.20E+13	6.08E+13	1.12E+14	2.09E+14
13	0.60	0.40	1.56E+13	3.21E+13	7.58E+13	1.02E+14
14	0.40	0.30	9.39E+11	1.68E+12	7.05E+12	1.24E+13
15	0.30	0.20	1.46E+12	2.44E+12	9.31E+12	1.63E+13
16	0.20	0.10	5.34E+12	9.69E+12	4.10E+13	7.28E+13
17	0.10	0.05	6.58E+12	1.09E+13	4.07E+13	7.09E+13
18	0.05	0.01	2.26E+13	3.60E+13	1.26E+14	2.17E+14
Total	--	--	1.05E+14	1.73E+14	4.55E+14	7.56E+14

Table 5.3.4-5 MTR Fuel Element Neutron Source Terms by Thermal Output –
460 grams ^{235}U

Group	Burnup 577,500 MWd/MTU		MTR Assembly Thermal Output			
	E_{hi} (Mev)	E_{low} (Mev)	20 Watts	30 Watts	70 Watts	120 Watts
			2247 Days (n/sec)	1467 Days (n/sec)	602 Days (n/sec)	341 Days (n/sec)
1	2.00E+01	6.43E+00	3.49E+04	3.83E+04	4.33E+04	4.61E+04
2	6.43E+00	3.00E+00	4.12E+05	4.50E+05	5.09E+05	5.46E+05
3	3.00E+00	1.85E+00	4.83E+05	5.24E+05	5.89E+05	6.29E+05
4	1.85E+00	1.40E+00	2.59E+05	2.83E+05	3.19E+05	3.38E+05
5	1.40E+00	9.00E-01	3.42E+05	3.74E+05	4.22E+05	4.48E+05
6	9.00E-01	4.00E-01	3.68E+05	4.03E+05	4.55E+05	4.84E+05
7	4.00E-01	1.00E-01	7.19E+04	7.87E+04	8.90E+04	9.47E+04
8	1.00E-01	1.70E-02	0.00E+00	0.00E+00	0.00E+00	0.00E+00
9	1.70E-02	3.00E-03	0.00E+00	0.00E+00	0.00E+00	0.00E+00
10	3.00E-03	5.50E-04	0.00E+00	0.00E+00	0.00E+00	0.00E+00
11	5.50E-04	1.00E-04	0.00E+00	0.00E+00	0.00E+00	0.00E+00
12	1.00E-04	3.00E-05	0.00E+00	0.00E+00	0.00E+00	0.00E+00
13	3.00E-05	1.00E-05	0.00E+00	0.00E+00	0.00E+00	0.00E+00
14	1.00E-05	3.05E-06	0.00E+00	0.00E+00	0.00E+00	0.00E+00
15	3.05E-06	1.77E-06	0.00E+00	0.00E+00	0.00E+00	0.00E+00
16	1.77E-06	1.30E-06	0.00E+00	0.00E+00	0.00E+00	0.00E+00
17	1.30E-06	1.13E-06	0.00E+00	0.00E+00	0.00E+00	0.00E+00
18	1.13E-06	1.00E-06	0.00E+00	0.00E+00	0.00E+00	0.00E+00
19	1.00E-06	8.00E-07	0.00E+00	0.00E+00	0.00E+00	0.00E+00
20	8.00E-07	4.00E-07	0.00E+00	0.00E+00	0.00E+00	0.00E+00
21	4.00E-07	3.25E-07	0.00E+00	0.00E+00	0.00E+00	0.00E+00
22	3.25E-07	2.25E-07	0.00E+00	0.00E+00	0.00E+00	0.00E+00
23	2.25E-07	1.00E-07	0.00E+00	0.00E+00	0.00E+00	0.00E+00
24	1.00E-07	5.00E-08	0.00E+00	0.00E+00	0.00E+00	0.00E+00
25	5.00E-08	3.00E-08	0.00E+00	0.00E+00	0.00E+00	0.00E+00
26	3.00E-08	1.00E-08	0.00E+00	0.00E+00	0.00E+00	0.00E+00
27	1.00E-08	0.00E+00	0.00E+00	0.00E+00	0.00E+00	0.00E+00
Total	–	–	1.97E+06	2.15E+06	2.43E+06	2.59E+06

Table 5.3.4-6 LEU MTR Hardware Source to Fuel Source Comparison

Group	E _{hi} (Mev)	E _{low} (Mev)	834 days Fuel (y/sec)	Cd at 834 days 100 g Cd (y/sec)	Cd Source % of Fuel Gamma	Cd at 90 days 100 g Cd (y/sec)	Cd Source % of Fuel Gamma
1	10.00	8.00	6.30E+02	0.00E+00	0.0%	0.00E+00	0.0%
2	8.00	6.50	2.97E+03	0.00E+00	0.0%	0.00E+00	0.0%
3	6.50	5.00	1.51E+04	0.00E+00	0.0%	0.00E+00	0.0%
4	5.00	4.00	3.78E+04	0.00E+00	0.0%	0.00E+00	0.0%
5	4.00	3.00	2.57E+08	4.49E-16	0.0%	1.80E-15	0.0%
6	3.00	2.50	2.16E+09	3.23E+00	0.0%	2.55E+01	0.0%
7	2.50	2.00	1.72E+11	1.19E+03	0.0%	9.38E+03	0.0%
8	2.00	1.66	3.60E+10	5.80E+04	0.0%	5.04E+05	0.0%
9	1.66	1.33	8.12E+11	7.57E+07	0.0%	6.35E+08	0.1%
10	1.33	1.00	2.68E+12	8.65E+05	0.0%	2.07E+09	0.1%
11	1.00	0.80	9.90E+12	2.11E+08	0.0%	5.66E+09	0.1%
12	0.80	0.60	6.14E+13	2.87E+08	0.0%	3.49E+09	0.0%
13	0.60	0.40	2.21E+13	2.13E+07	0.0%	3.12E+09	0.0%
14	0.40	0.30	2.36E+12	2.19E+08	0.0%	3.55E+09	0.2%
15	0.30	0.20	3.34E+12	8.06E+08	0.0%	5.78E+09	0.2%
16	0.20	0.10	1.27E+13	4.57E+09	0.0%	2.32E+10	0.2%
17	0.10	0.05	1.45E+13	1.17E+10	0.1%	3.88E+10	0.3%
18	0.05	0.01	4.76E+13	5.52E+10	0.1%	1.65E+11	0.3%
Total	—	—	1.78E+14	7.31E+10	0.0%	2.51E+11	0.1%

Table 5.3.4-7 HEU MTR Hardware Source to Fuel Comparison

Group	E _{hi} (Mev)	E _{low} (Mev)	1467 days Fuel (y/sec)	Cd at 1467days 100 g Cd (y/sec)	Cd Source % of Fuel Gamma	Cd at 90 days 100 g Cd (y/sec)	Cd Source % of Fuel Gamma
1	10.00	8.00	1.16E+03	0.00E+00	0.0%	0.00E+00	0.0%
2	8.00	6.50	5.48E+03	0.00E+00	0.0%	0.00E+00	0.0%
3	6.50	5.00	2.80E+04	0.00E+00	0.0%	0.00E+00	0.0%
4	5.00	4.00	6.97E+04	0.00E+00	0.0%	0.00E+00	0.0%
5	4.00	3.00	1.15E+08	8.77E-15	0.0%	1.14E-13	0.0%
6	3.00	2.50	1.02E+09	2.69E+00	0.0%	1.23E+02	0.0%
7	2.50	2.00	1.34E+11	9.89E+02	0.0%	4.52E+04	0.0%
8	2.00	1.66	2.12E+10	4.82E+04	0.0%	2.49E+06	0.0%
9	1.66	1.33	1.12E+12	6.30E+07	0.0%	3.66E+09	0.3%
10	1.33	1.00	2.73E+12	7.02E+05	0.0%	4.30E+10	1.6%
11	1.00	0.80	1.52E+13	1.75E+08	0.0%	9.22E+10	0.6%
12	0.80	0.60	6.08E+13	2.38E+08	0.0%	2.76E+10	0.0%
13	0.60	0.40	3.21E+13	4.54E+07	0.0%	5.33E+10	0.2%
14	0.40	0.30	1.68E+12	5.87E+08	0.0%	6.72E+10	4.0%
15	0.30	0.20	2.44E+12	2.16E+09	0.1%	1.01E+11	4.2%
16	0.20	0.10	9.69E+12	1.23E+10	0.1%	3.51E+11	3.6%
17	0.10	0.05	1.09E+13	3.01E+10	0.3%	5.20E+11	4.8%
18	0.05	0.01	3.60E+13	1.33E+11	0.4%	1.75E+12	4.9%
Total	--	--	1.73E+14	1.79E+11	0.1%	3.01E+12	1.7%

Table 5.3.4-8 Material Densities for MTR Fuel Shielding Analysis

Material	Element	Density [atom/barn-cm]
HEU Fuel (380 g ²³⁵ U)	AL	2.470E-02
	U-235	2.548E-04
	U-238	2.795E-05
HEU Fuel (460 g ²³⁵ U)	AL	2.590E-02
	U-235	3.075E-04
	U-238	3.373E-05
MEU Fuel	AL	2.432E-02
	U-235	2.460E-04
	U-238	3.643E-04
LEU Fuel	AL	2.361E-02
	U-235	3.051E-04
	U-238	1.284E-03
End Fitting	AL	2.634E-02
H ₂ O/Glycol	H	5.988E-02
	C	1.070E-02
	O	2.459E-02
Stainless Steel	CR	1.743E-02
	MN	1.736E-03
	FE	5.936E-02
	NI	7.721E-03
Lead	PB	3.297E-02

Table 5.3.4-9 LWT Cask Surface Total Dose Rates (Normal Conditions of Transport)

Band [cm]	LWT Cask Surface Radial Dose Rates (mrem/hr)							
	Gamma	FSD (%)	Neutron	FSD (%)	N-Gamma	FSD (%)	Total	FSD (%)
247	98.87	1.1	18.62	0.6	0.19	3.3	117.69	0.9
221	234.17	1.1	59.67	0.3	0.48	1.7	294.31	0.9
195	86.34	0.5	43.38	0.4	1.38	0.7	131.10	0.4
169	54.75	0.4	5.06	0.7	2.58	0.5	62.39	0.4
143	45.55	0.5	4.75	0.7	2.75	0.5	53.04	0.4
117	57.19	0.5	5.31	0.6	2.91	0.4	65.42	0.4
91	52.97	0.5	5.13	0.6	2.90	0.5	61.00	0.4
65	46.75	0.5	4.85	0.6	2.89	0.4	54.48	0.4
39	58.61	0.5	5.40	0.7	3.00	0.4	67.01	0.4
13	53.69	0.5	5.22	0.6	3.03	0.5	61.94	0.4

Maximum dose rate for 460 gram ^{235}U element is 267.1 mrem/hr at the 221 cm band.

Table 5.3.4-10 LWT Cask Plan of Conveyance Dose Rates (Normal Conditions of Transport)

Band [cm]	Conveyance Dose Rates (mrem/hr)							
	Gamma	FSD (%)	Neutron	FSD (%)	N-Gamma	FSD (%)	Total	FSD (%)
266	30.64	1.1	6.20	0.5	0.18	1.0	37.01	0.9
238	39.27	1.0	8.17	0.5	0.25	0.8	47.69	0.8
210	35.26	0.9	8.48	0.4	0.37	0.6	44.11	0.8
182	26.66	0.6	6.29	0.5	0.50	0.5	33.45	0.5
154	22.13	0.5	3.77	0.6	0.62	0.5	26.52	0.4
126	20.53	0.5	2.47	0.7	0.71	0.4	23.70	0.4
98	20.27	0.4	1.96	0.6	0.78	0.4	23.01	0.4
70	19.92	0.4	1.76	0.6	0.82	0.4	22.50	0.3
42	20.05	0.4	1.72	0.7	0.84	0.4	22.61	0.4
14	20.24	0.4	1.69	0.5	0.86	0.4	22.78	0.4

Maximum dose rate for 460 gram ^{235}U element is 43.8 mrem/hr at the 238 cm band.

Table 5.3.4-11 LWT Cask 2 Meter Off The Plane of Conveyance Dose Rates (Normal Conditions of Transport)

Band [cm]	2 Meters off the Vertical Plane of Conveyance Dose Rates (mrem/hr)							
	Gamma	FSD (%)	Neutron	FSD (%)	N-Gamma	FSD (%)	Total	FSD (%)
285	7.00	2.0	1.14	2.0	0.10	2.1	8.23	1.7
255	7.55	2.0	1.19	1.9	0.11	2.1	8.86	1.8
225	8.47	2.4	1.19	1.8	0.12	2.0	9.79	2.1
195	8.02	1.6	1.20	1.9	0.14	1.7	9.36	1.4
165	8.60	1.8	1.12	1.8	0.15	1.7	9.87	1.5
135	8.42	1.3	1.11	1.8	0.16	1.7	9.69	1.1
105	8.55	1.2	1.01	1.9	0.17	2.1	9.74	1.1
75	8.59	1.1	0.97	2.1	0.18	1.6	9.73	1.0
45	8.85	1.7	0.94	2.0	0.18	1.6	9.98	1.5
15	8.80	1.2	0.89	2.0	0.19	1.7	9.88	1.1

Maximum dose rate for 460 gram ²³⁵U element is 9.36 mrem/hr at the 195 cm band.

Table 5.3.4-12 LWT Cask 1 Meter From the Cask Surface Dose Rates (Normal Conditions of Transport)

Band [cm]	1 Meter off the Cask Dose Rates							
	Gamma	FSD (%)	Neutron	FSD (%)	N-Gamma	FSD (%)	Total	FSD (%)
285	17.95	1.0	3.86	0.6	0.14	0.9	21.96	0.8
255	25.73	1.1	4.98	0.5	0.20	0.8	30.90	0.9
225	25.83	1.0	5.58	0.4	0.27	0.6	31.68	0.8
195	23.06	0.8	5.03	0.5	0.35	0.6	28.45	0.7
165	19.06	0.6	3.69	0.5	0.44	0.5	23.18	0.5
135	17.24	0.5	2.54	0.6	0.51	0.4	20.29	0.4
105	16.68	0.4	1.90	0.6	0.57	0.4	19.16	0.4
75	16.44	0.4	1.60	0.6	0.61	0.4	18.65	0.4
45	16.33	0.4	1.47	0.7	0.63	0.4	18.42	0.4
15	16.38	0.4	1.40	0.5	0.65	0.4	18.43	0.3

Maximum dose rate for 460 gram ²³⁵U element is 29.5 mrem/hr at the 225 cm band.

Table 5.3.4-13 Axial Surface Dose Rates at Cask Lid (Normal Conditions of Transport)

Band [cm]	Cask Lid Dose Rates (mrem/hr) Directly Above the MTR Elements					
	Gamma	FSD (%)	Neutron	FSD (%)	Total	FSD (%)
28.5	16.19	0.8	16.82	7.2	33.01	3.7
25.5	25.34	0.9	19.95	7.9	45.53	3.5
22.5	35.61	0.8	24.84	5.8	60.55	2.4
19.5	48.48	0.8	29.90	6.5	78.43	2.5
16.5	63.02	0.8	41.88	24.9	105.20	9.9
13.5	80.35	0.9	38.04	7.9	118.46	2.6
10.5	103.64	0.9	44.71	14.1	148.35	4.3
7.5	126.16	0.9	51.17	10.1	177.41	3.0
4.5	147.50	1.2	41.19	10.5	188.70	2.5
1.5	158.66	2.5	52.57	26.1	211.23	6.8

Maximum dose rate for 460 gram ^{235}U element is 174.1 mrem/hr at the 1.5 cm band.

Table 5.3.4-14 LWT Cask Dose Rates 5 Meters from the Cask Lid (Back of Tractor Cab) for Normal Conditions of Transport

Band [cm]	5 Meter Dose Rates (mrem/hr)					
	Gamma	FSD (%)	Neutron	FSD (%)	Total	FSD (%)
84.38	0.47	1.6	0.12	13.9	0.59	3.1
73.13	0.49	1.6	0.11	12.4	0.61	2.6
61.88	0.49	1.8	0.12	16.3	0.61	3.5
50.63	0.51	2.1	0.13	19.0	0.65	4.2
39.38	0.53	2.4	0.12	18.8	0.65	3.9
28.13	0.54	3.0	0.10	23.1	0.64	4.4
16.88	0.55	3.6	0.07	28.2	0.62	4.6
5.63	0.54	5.8	0.14	51.6	0.68	11.5

Maximum dose rate for 460 gram ²³⁵U element is 0.62 mrem/hr at the 28.13 cm band.

Table 5.3.4-15 LWT Cask Dose Rates – 1 Meter from the Cask Surface (Hypothetical Accident Conditions)

Band [cm]	1 Meter Accident Dose Rates (mrem/hr)					
	Gamma	FSD (%)	Neutron	FSD (%)	Total	FSD (%)
285	21.38	5.2	9.78	0.4	31.18	3.5
255	33.72	13.5	13.90	0.3	47.63	9.6
225	31.01	3.0	19.15	0.3	50.19	1.9
195	30.50	2.9	24.55	0.2	55.08	1.6
165	29.36	3.5	29.32	0.2	58.71	1.7
135	29.51	3.0	33.11	0.2	62.66	1.4
105	28.68	3.4	35.67	0.2	64.38	1.5
75	29.52	4.3	37.51	0.2	67.07	1.9
45	28.49	2.2	38.59	0.2	67.12	0.9
15	27.74	1.2	39.24	0.2	67.02	0.5

Maximum dose rate for 460 gram ²³⁵U element is 54.5 mrem/hr at the 15 cm band.

5.3.5 25 PWR Fuel Rods Configuration

A maximum of 25 design basis PWR fuel rods has been analyzed for transport in the NAC-LWT. The design basis includes 23 fuel rods at 60,000 MWd/MTU burnup, 150 days cooling, and 2 fuel rods at 65,000 MWd/MTU burnup, 150 days cooling. The design basis neutron and gamma spectra are shown in Table 5.3.5-1. These source terms were generated using the SAS2H SCALE sequence on the NAC-LWT design basis PWR fuel assembly. Source terms were generated at 60,000 MWd/MTU, 150 days cooling and 65,000 MWd/MTU 150 days cooling. The PWR fuel assembly source terms were then rated by the number of rods, i.e., 23/204 for the 60,000 MWd/MTU case and 2/204 for the 65,000 MWd/MTU case.

SAS1, one-dimensional radial shielding analysis, was used to calculate surface and 2 meter dose rates from the edge of vehicle under normal and accident conditions of transport. The analyses considered an axial peaking factor of 1.12. The 1D radial shielding model consisted of a source region, 25 homogenized PWR rods, surrounded by a 0.12 inch thick canister followed by the cylindrical shield regions of the cask. The same conservative assumptions used in previous radial shielding analysis were applied, i.e., minimum shield dimensions, lead gap and 0.94 g/cc neutron shield solution density. The material densities used for the 25 PWR rod analyses are provided in Table 5.3.5-2.

As activated hardware will not be included in a shipment of the 25 design basis PWR rods, dose rates at the top and bottom surfaces as well as in the transition regions will be below regulatory limits.

The results of the shielding analysis are presented in Table 5.3.5-3. The calculated dose rates are below the regulatory limits of 200 mrem/hr at the surface and 10 mrem/hr at 2 meters from edge of vehicle under normal conditions, and 1000 mrem/hr at 1 meter from surface under accident conditions.

Table 5.3.5-1 25 PWR Fuel Rods Design Basis Fuel Source Spectra

Energy Group	Energy Range (MeV)		Neutrons/sec	Energy Group	Energy Range (MeV)		Photons/sec
1	6.43	20.00	2.539E+6	1	8.00	10.00	2.110E+15
2	3.00	6.43	3.039E+7	2	6.50	8.00	6.802E+14
3	1.85	3.00	3.318E+7	3	5.00	6.50	7.002E+14
4	1.40	1.85	1.799E+7	4	4.00	5.00	1.688E+14
5	0.90	1.40	2.425E+7	5	3.00	4.00	1.274E+14
6	0.40	0.90	2.653E+7	6	2.50	3.00	1.151E+15
7	0.10	0.40	5.200E+6	7	2.00	2.50	2.964E+15
8-27	0.10	1E-08		8	1.66	2.00	3.389E+14
Total			1.401E+8	9	1.33	1.66	9.132E+13
				10	1.00	1.33	3.848E+13
				11	0.80	1.00	3.719E+12
				12	0.60	0.80	1.443E+13
				13	0.40	0.60	2.832E+11
				14	0.30	0.40	3.052E+10
				15	0.20	0.30	4.684E+06
				15	0.10	0.20	1.879E+06
				17	0.05	0.10	3.686E+05
				18	0.01	0.05	7.824E+04
				Total			8.389E+15

Table 5.3.5-2 Material Densities for 25 Design Basis PWR Rods Fuel Shielding Analysis

Material	25 PWR Rods	H ₂ O/ Glycol	304 Stainless Steel	Lead
Density, g/cc	0.4422	0.944	7.920	11.350
Nuclide	atm/b-cm			
Uranium 235	5.983E-06			
Uranium 238	8.319E-04			
Zircaloy	4.390E-04			
Oxygen	1.675E-03	2.458E-02		
Hydrogen		5.987E-02		
Carbon		1.070E-02		
Iron			5.936E-02	
Chromium			1.743E-02	
Nickel			7.721E-03	
Manganese			1.736E-03	
Lead				3.299E-02

**Table 5.3.5-3 Cask Radial Dose Rates with 25 Design Basis PWR Fuel Rods
(mrem/hr)**

Source Term	Normal Conditions		Accident Conditions
	Surface	2 Meters from Vehicle Edge	1 Meter from Surface
Neutron	6.05	0.53	33.60
Primary Gamma	77.95	8.68	35.39
Secondary Gamma	3.14	0.19	0.45
Total	87.14	9.40	69.44

5.3.6 TRIGA Fuel Element Model Specification and Shielding Evaluation

A maximum of 140 TRIGA fuel elements are analyzed for transport in the LWT cask. This configuration consists of four (4) fuel elements placed in each of seven (7) cells in each of five (5) modules that form the TRIGA basket assembly. The five modules consist of a top, bottom and three intermediate units. All five of the modules must be installed in the cask cavity prior to transport. The maximum total decay heat load is 1.05 kW per cask, or 7.5 watts per element.

As described in Sections 5 and 5.1, the center cell of each non-poisoned TRIGA fuel module is blocked prohibiting the loading of the central fuel tube. Consequently, only 120 fuel elements are loaded into the TRIGA fuel basket in the nonpoisoned configuration. Evaluating the NAC-LWT for the transport of 140 elements in the poisoned basket configuration, utilizing all seven of the TRIGA basket module cells, is bounding as a larger gamma and neutron source is evaluated than would occur for only 120 elements.

The TRIGA fuel element is provided in several configurations. The fuel is a Uranium-Zirconium Hydride (U-ZrH) which is enriched to 20 wt % ^{235}U or 70 wt % ^{235}U . The fuel consists of U-ZrH pellets clad in a tube of either aluminum or stainless steel, depending on fuel type. The active fuel length is either 14 inches or 15 inches, depending on the fuel type. The basic parameters of the various fuel configurations are presented in Table 1.2-2.

For the shielding analysis, the fuel region material description is based on the aluminum clad element with an active fuel length of 14 inches. This element is chosen for the shielding evaluation because it provides the least self-shielding among the TRIGA fuel types considered. The contents of a single basket cell are represented by five homogenized axial zones: fuel, upper and lower reflector, and upper and lower end fixture. The material densities of the homogenized zones are given in Table 5.3.6-5.

5.3.6.1 TRIGA Fuel Element Source Terms

Each of the TRIGA fuel element types is evaluated using the SAS2H (Herman) sequence to establish the burnup and cool time that results in a decay heat power limit for each fuel element type of 7.5 watts. TRIGA fuel cluster rods are evaluated in Section 5.3.7. The fuel parameters determined by the 7.5 watts decay heat limit are used in a SCALE SAS1 one-dimensional shielding analysis to calculate the normal transport and accident condition dose rate for each fuel type. As described below, the TRIGA fuel elements that result in the highest dose rates for the transport conditions (ACPR for normal conditions, and FLIP-LEU-II for accident conditions) are selected as the bounding case, and are evaluated using SCALE SAS4 three-dimensional analysis

to establish the cask surface, one-meter and two-meter dose rates. These bounding source terms are presented in Table 5.1.1-3.

Figure 5.3.6-1 shows the one-dimensional dose rates at 2 meters from the edge of the conveyance for each fuel element under normal conditions of transport. Figure 5.3.6-2 shows the one-dimensional radial dose rate at 1 meter from the cask surface under hypothetical accident conditions. These figures provide a basis for comparison between fuel configurations, allowing the selection of a bounding fuel configuration. In normal conditions of transport, dose rates are dominated by contributions from gamma sources, and the limiting source term corresponds to that of the ACPR fuel type with 50% ^{235}U depletion (86.1 GWd/MTU). The total source includes a 5% uncertainty factor applied to the standard source value (SFA parameter), to more clearly bound the narrow range of dose rate variation observed among the various fuel configurations. Under accident conditions, in which a loss of the liquid neutron shield is assumed, neutron sources in fuel configurations at the high range of burnup are the chief contributor to dose rate. The accident conditions are analyzed on the basis of a low FLIP-LEU-II fuel element with 80% ^{235}U depletion (151.1 GWd/MTU). A three-dimensional analysis, which more accurately represents the cask shielding geometry, is applied to calculate dose rates at points of interest once the bounding fuel configuration is selected.

Source terms from activated fuel and non-fuel hardware are determined by computing the activation of a unit mass of stainless steel irradiated in the full core flux for the bounding fuel configuration using the SAS2H sequence. The stainless steel composition includes an assumed 1.2 g/kg concentration of ^{60}Co to bound the gamma dose contribution from ^{60}Co . Hardware source rates in each source region are determined by scaling this result by the mass of hardware present, and by a flux activation ratio intended to account for differences in the flux spectrum and intensity in the given source region. Material present in the reflector and end fixture regions is activated at a flux ratio of 0.1. Source rates from activated fuel cladding are computed using a flux ratio of 1.0. The resulting source terms are shown in Table 5.3.6-1 through Table 5.3.6-4. The reported spectra for the normal conditions analysis includes the 5% margin added to the source term. Hardware spectra are reported on a per kg basis.

Following conventional usage, TRIGA fuel element burnup is characterized in terms of the percent of ^{235}U atoms present in the fresh fuel element, which are depleted over the course of the fuel life. Depletion of ^{235}U refers to the net effect of all loss mechanisms, including in particular, parasitic absorption. In this analysis, values are determined by comparing the SAS2H-reported concentration of ^{235}U atoms at the beginning and end of the assumed irradiation period. The relation between ^{235}U depletion and burnup, measured in terms of energy per unit mass (MWd/MTU), depends on the initial enrichment of the fuel. Typically, for LEU (20% ^{235}U

enrichment) TRIGA fuel elements, an 80% ^{235}U depletion corresponds to 151,100 MWd/MTU. For HEU fuel (70% ^{235}U enrichment), an 80% ^{235}U depletion corresponds to 460,000 MWd/MTU.

5.3.6.2 TRIGA Fuel Element Model Description

The SCALE SAS4 Monte-Carlo shielding analysis sequence is used to compute dose rates exterior to the cask. The SAS4 sequence incorporates a validated FORTRAN coding modification that permits the determination of dose rate profiles along the axial and radial surfaces of cylindrical detectors surrounding the cask. SAS4 prepares input for and executes the MORSE Monte Carlo shielding analysis code, and automatically generates biasing parameters based on a one-dimensional XSDRNPM calculation. Because SAS4 requires model symmetry, both upper half and lower half three-dimensional models are developed.

The radial model dimensions are shown in Figure 5.3.6-3. Details of the TRIGA fuel basket are shown in Figure 5.3.6-4. The upper model dimensions are shown in Figure 5.3.6-5 and Figure 5.3.6-6, and the lower model dimensions are shown in Figure 5.3.6-7. The SAS4 model plane of symmetry is taken as the horizontal plane, which separates two baskets in the upper model and three baskets in the lower model.

Both normal and accident shielding analyses are performed using the upper and lower models. For the upper model, the fuel is shifted above the neutron shielding for both normal and accident conditions. Modeling the shifted fuel accounts for any potential sliding or shifting of the fuel.

The upper half model for normal conditions is presented in Figure 5.3.6-6. The upper half model with the shifted fuel is presented in Figure 5.3.6-5. For the lead slump accident, the fuel in the lower model is shifted above the neutron shield. For the lower model, under normal and accident conditions, the fuel is positioned as illustrated in Figure 5.3.6-7. Only one lower model is created because the dose rates are bounded by the upper half analysis, where the fuel is shifted above the neutron shielding. Each of these models incorporates the sources from the fuel gamma, fuel neutron, and fuel hardware.

Each of these models incorporates a discrete representation of the TRIGA fuel baskets. The borated steel plates in the poisoned basket configuration are omitted from the model, producing less shielding material in the basket region. The fuel region, basket module and cask material densities are provided in Table 5.3.6-5. To minimize self-shielding in the fuel, the fuel region modeled is based on the TRIGA AL14 aluminum clad fuel element. This element has the least mass of the fuel configurations considered, and its aluminum fixtures and cladding provide the least shielding. The source terms determined above are based on the stainless-steel clad element. This is conservative, since the aluminum end fixtures and cladding, and lower fuel mass provide

significantly less self shielding than the actual fuel. A full poisoned basket loading of 140 TRIGA fuel elements is modeled, which bounds the 120 element loading of the nonpoisoned basket.

Models for Normal Conditions of Transport

In normal conditions of transport the neutron shield is assumed intact and the impact limiters installed. For simplicity, the impact limiters are neglected in the SAS4 upper and lower half normal condition models. As previously stated, the upper half shielding models are reflected about the upper two baskets.

One axial model is created representing the upper half of the NAC-LWT cask loaded with design basis TRIGA fuel elements. This model is used to predict upper and lower axial dose rates under both normal and accident conditions. In order to address the worst case geometric configuration, the TRIGA fuel elements are translated to the upper most position, in their respective baskets.

There are two radial upper half shielding models. The first model evaluates the fuel in the neutral position (in contact with the basket bottom plate). The second upper half model examines the fuel elements translated to the upper most basket position to evaluate the point of least shielding. The point of least shielding occurs in the area directly above the lead gamma shield and consists of ~7.66 inches of steel. Only one lower half model is used because fuel element translation does not affect radial dose rates and the lower half axial dose rates are bounded by the upper half axial analysis.

Analysis of the intact fuel elements shipped directly in baskets bounds the transportation of fuel in both the screened and sealed cans. Cans may only be transported in the top or bottom basket modules. In all cases, the top model of the cask with intact fuel or cans placed in the upper most position (directly against the bottom of the lid) is the bounding case. The shipping geometry of fuel in screened cans is essentially identical to fuel shipped directly in baskets, with the added conservatism that the can limits axial placement of fuel in the basket. The shipping geometry for fuel in the failed fuel can is similar to the analyzed case. The differences are that cladding may not be intact and source material may be distributed throughout the can or concentrated at either end. The analysis with standard fuel placed in the upper most position closely approximates the unlikely situation of a sealed fuel can with the source material in the top of the can. The two-rod limit for sealed cans lowers the source term and adds conservatism. For both types of cans, the can wall provides additional shielding material conservatively neglected in the shielding analysis.

Models for Accident Conditions

Under the accident conditions, the liquid neutron shield and the impact limiters are conservatively assumed to be removed from the package. Two radial shielding models, one for the upper half and one for the lower half are used. The accident condition radial models are

identical to the normal condition models with the omission of the neutron shielding material. No axial models are required because the normal transport conditions models ignore the impact limiters and there is no neutron shielding in the axial direction. Consequently, there are no differences in the normal transport condition and the accident condition axial dose rates.

5.3.6.3 Shielding Evaluation for TRIGA Fuel Elements in Normal Conditions of Transport

The NAC-LWT is normally transported inside of an ISO container, but may be transported on a trailer with a personnel barrier. The sides of the ISO container are coincident with the edge of the transport trailer, and are the edge of the vehicle. Dose rates for the design basis 140 TRIGA fuel elements are reported at the cask (package) surface, at the edge of the vehicle (plane of conveyance), at one meter from the package, and at two meters from the edge of the vehicle. The one meter dose rate (25 mrem/hr) is the estimated TRIGA fuel configuration Transport Index.

Each of the three radial models (top, top/point of least shielding, bottom) were evaluated with the design basis source term. The maximum radial dose rates for a uniform configuration of design basis ACPR TRIGA fuel elements (86,100 MWd/MTU, 231 days cooled) with a heat load of 7.5 watts per assembly in normal conditions of transport are:

Detector Radial Plane	Dose Rate (mrem/hr)	Regulatory Limit (mrem/hr)
Cask (Package) Surface	258.78	1,000
Edge of Vehicle	38.02	200
1 Meter From Package	25	Transport Index
2 Meters From Edge of Vehicle	6.09	10

These dose rates are taken at positions radially away from the point of least shielding and are well below the regulatory limits. The point of least shielding corresponds to the area directly above the lead gamma shield. This analysis assumes the fuel elements are translated to the top of the cask cavity.

The axial locations of interest are contact with the cask surface, and the dose at two meters from the front edge of the vehicle, and at the rear of the truck cab. Shielding provided by the impact limiter is conservatively neglected. The axial dose rates from the bottom of the cask, which has slightly more shielding than the top of the cask, are conservatively assumed to be equal to the dose rates from the top of the cask. The maximum normal condition axial surface, two meter, and back of truck cab dose rates are:

Detector Axial Plane	Dose Rate (mrem/hr)	Regulatory Limit (mrem/hr)
Cask Surface (Lid)	123.81	1,000
2 Meters From Package	3.18	10
Back of Tractor Cab	0.61	2

The axial dose rates are also below the regulatory limit. Thus, the NAC-LWT with up to 140 TRIGA fuel elements meets the shielding requirements of 10 CFR 71, 49 CFR 173 and IAEA Transportation Safety Standards (TS-R-1) for normal conditions of transport.

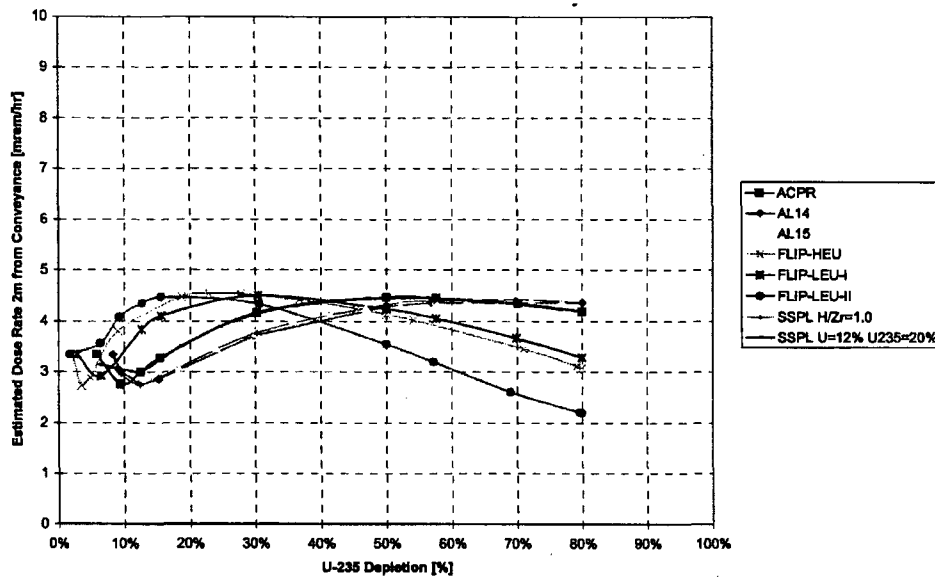
5.3.6.4 Shielding Evaluation for TRIGA Fuel Elements in Hypothetical Accident Conditions

The configuration of the TRIGA fuel elements and basket arrangement in the hypothetical accident conditions is the same as that for the normal conditions of transport. The accident conditions assume the loss of the neutron shield, which results in an increase in the neutron dose rates. The accident condition source terms are based upon the FLIP-LEU-II fuel. This fuel has a burnup of 151,100 MWd/MTU and a cool time of 908 days. The accident condition design basis source term differs from the normal condition source due to the significant higher neutron source, which dominates the dose rate when the neutron shield is assumed to be lost.

Two accident scenarios, loss of neutron shield and lead slump, are analyzed. The top/point of least shielding model was used to evaluate accident condition dose rates, since it produces the bounding normal condition doses. The loss of neutron shielding hypothetical accident condition dose rate at 1 meter from the package is 28.07 mrem/hr. The loss of lead (lead slump) hypothetical accident condition dose rate at one meter from the package, is 178.83 mrem/hr, which is well below the regulatory limit of 1,000 mrem/hr. The total dose due to both conditions simultaneously is 207 mrem/hr, which is still well below the regulatory limit. These hypothetical accident dose rates are summarized below. They are based upon the FLIP-LEU-II source terms (80% ^{235}U depleted) at a decay heat of 7.5 watts.

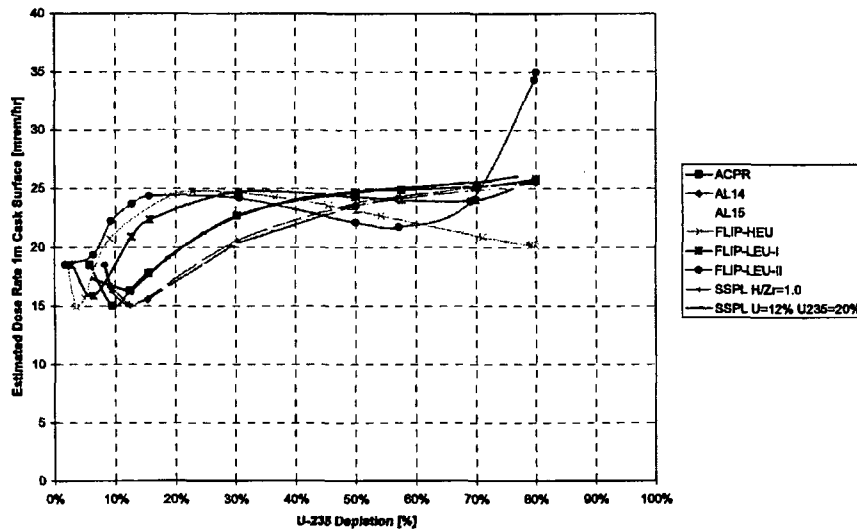
Accident Scenario	Dose Rate (at 1 meter mrem/hr)	Regulatory Limit (mrem/hr)
Loss of Neutron Shielding	28.07	1,000
Lead Slump	178.83	1,000
Total	207	1,000

Figure 5.3.6-1 TRIGA Fuel Element One-Dimensional Bounding Radial Dose Rate - Normal Conditions of Transport - Curves and Data Points



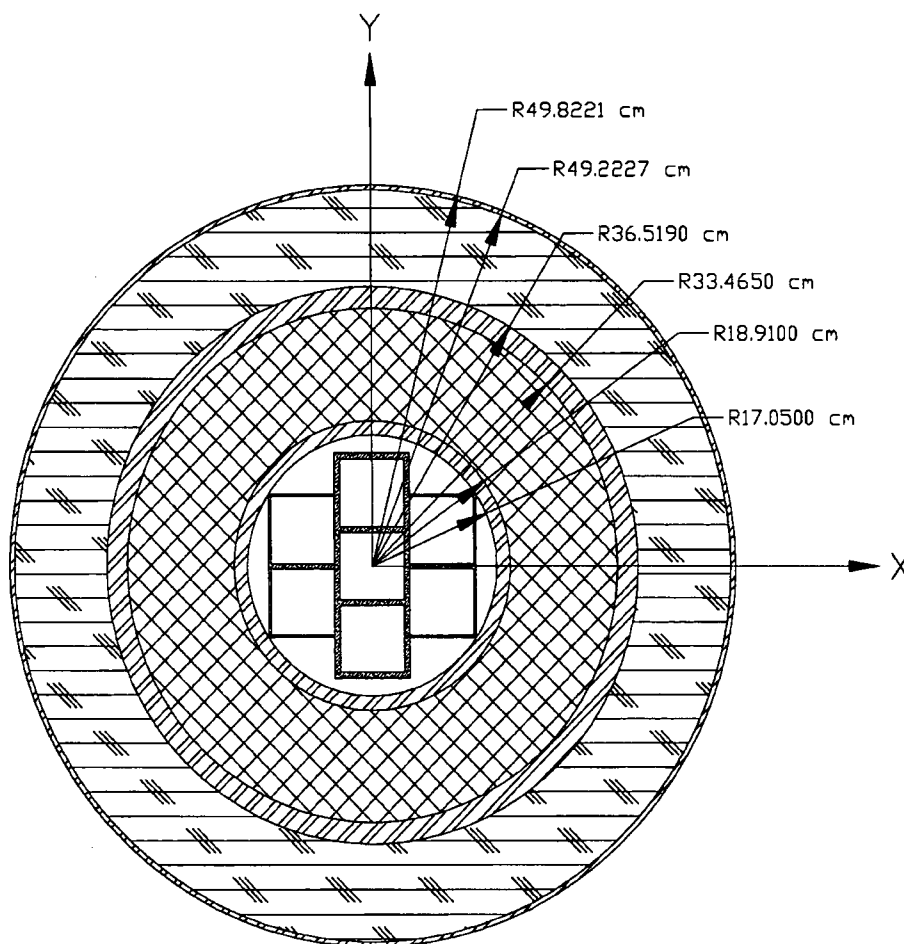
ACPR - U=12.0% - ²³⁵ U=20.0% - H/Zr=1.7 - 2370g	Burnup [GWd/MTU]	9	25	50	100	147
	²³⁵ U Depletion [%]	5.80	15.47	30.23	57.85	80.00
	Cool Time [d]	90.0	147.8	189.9	245.5	310.1
AL14 - U=8.5% - ²³⁵ U=20.0% - H/Zr=1.0 - 2350g	Burnup [GWd/MTU]	13	25	50	100	149
	²³⁵ U Depletion [%]	8.27	15.29	29.83	56.89	80.00
	Cool Time [d]	90.0	125.8	165.2	212.0	253.7
AL15 - U=8.5% - ²³⁵ U=20.0% - H/Zr=1.0 - 2412g	Burnup [GWd/MTU]	20	30	50	100	150
	²³⁵ U Depletion [%]	12.44	18.29	30.00	57.56	81.24
	Cool Time [d]	115.3	138.2	167.7	215.6	260.4
FLIP-HEU - U=8.5% - ²³⁵ U=70.0% - H/Zr=1.6 - 2420g	Burnup [GWd/MTU]	12	50	150	300	455
	²³⁵ U Depletion [%]	2.08	9.03	27.78	54.17	80.00
	Cool Time [d]	90.0	170.9	242.6	335.3	524.6
FLIP-LEU-I - U=20.0% - ²³⁵ U=20.0% - H/Zr=1.6 - 2650g	Burnup [GWd/MTU]	5	25	50	100	148
	²³⁵ U Depletion [%]	2.83	15.66	30.47	57.64	80.00
	Cool Time [d]	90.0	186.0	234.0	330.1	497.0
FLIP-LEU-II - U=30.0% - ²³⁵ U=20.0% - H/Zr=1.6 - 2890g	Burnup [GWd/MTU]	3	15	50	100	151
	²³⁵ U Depletion [%]	1.73	9.25	30.64	57.17	80.00
	Cool Time [d]	90.0	184.9	280.4	486.7	908.3
SSPL - U=8.5% - ²³⁵ U 20.0% - H/Zr=1.0 - 2410g	Burnup [GWd/MTU]	13	25	50	100	148
	²³⁵ U Depletion [%]	8.05	15.37	30.24	57.32	80.00
	Cool Time [d]	90.0	128.2	168.3	217.6	264.7
SSPL - U=12% - ²³⁵ U 20.0% - H/Zr=1.0 - 2334g	Burnup [GWd/MTU]	10	30	50	100	150
	²³⁵ U Depletion [%]	6.25	18.57	30.18	57.50	80.71
	Cool Time [d]	93.8	157.4	189.3	247.8	322.6

Figure 5.3.6-2 TRIGA Fuel Element One-Dimensional Bounding Radial Dose Rate - Accident Condition - Curves and Data Points



ACPR - U=12.0% - ²³⁵ U=20.0% - H/Zr=1.7 - 2370g	Burnup [GWd/MTU]	9	25	50	100	147
	²³⁵ U Depletion [%]	5.80	15.47	30.23	57.65	80.00
	Cool Time [d]	90.0	147.8	189.9	245.5	310.1
AL14 - U=8.5% - ²³⁵ U=20.0% - H/Zr=1.0 - 2350g	Burnup [GWd/MTU]	13	25	50	100	149
	²³⁵ U Depletion [%]	8.27	15.29	29.83	56.89	80.00
	Cool Time [d]	90.0	125.8	165.2	212.0	253.7
AL15 - U=8.5% - ²³⁵ U=20.0% - H/Zr=1.0 - 2412g	Burnup [GWd/MTU]	20	30	50	100	150
	²³⁵ U Depletion [%]	12.44	18.29	30.00	57.56	81.24
	Cool Time [d]	115.3	138.2	167.7	215.6	260.4
FLIP-HEU - U=8.5% - ²³⁵ U=70.0% - H/Zr=1.6 - 2420g	Burnup [GWd/MTU]	12	50	150	300	455
	²³⁵ U Depletion [%]	2.08	9.03	27.78	54.17	80.00
	Cool Time [d]	90.0	170.9	242.6	335.3	524.6
FLIP-LEU-I - U=20.0% - ²³⁵ U=20.0% - H/Zr=1.6 - 2650g	Burnup [GWd/MTU]	5	25	50	100	148
	²³⁵ U Depletion [%]	2.83	15.66	30.47	57.64	80.00
	Cool Time [d]	90.0	186.0	234.0	330.1	497.0
FLIP-LEU-II - U=30.0% - ²³⁵ U=20.0% - H/Zr=1.6 - 2890g	Burnup [GWd/MTU]	3	15	50	100	151
	²³⁵ U Depletion [%]	1.73	9.25	30.64	57.17	80.00
	Cool Time [d]	90.0	184.9	280.4	486.7	908.3
SSPL - U=8.5% - ²³⁵ U 20.0% - H/Zr=1.0 - 2410g	Burnup [GWd/MTU]	13	25	50	100	148
	²³⁵ U Depletion [%]	8.05	15.37	30.24	57.32	80.00
	Cool Time [d]	90.0	128.2	168.3	217.6	264.7
SSPL - U=12% - ²³⁵ U 20.0% - H/Zr=1.0 - 2334g	Burnup [GWd/MTU]	10	30	50	100	150
	²³⁵ U Depletion [%]	6.25	18.57	30.18	57.50	80.71
	Cool Time [d]	93.8	157.4	189.3	247.8	322.6

Figure 5.3.6-3 TRIGA SAS4A Radial Model Geometry






-  Steel
-  Lead
-  Liquid Neutron Shield

Figure 5.3.6-4 TRIGA SAS4A Basket Model Geometry

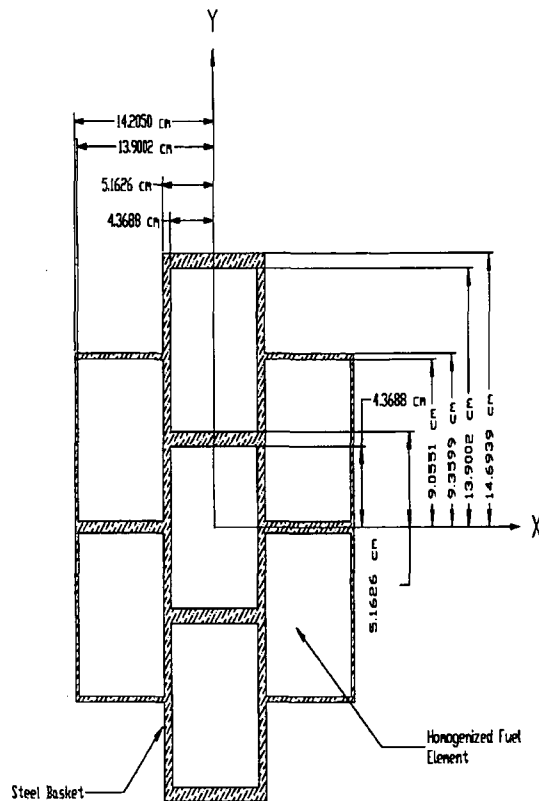
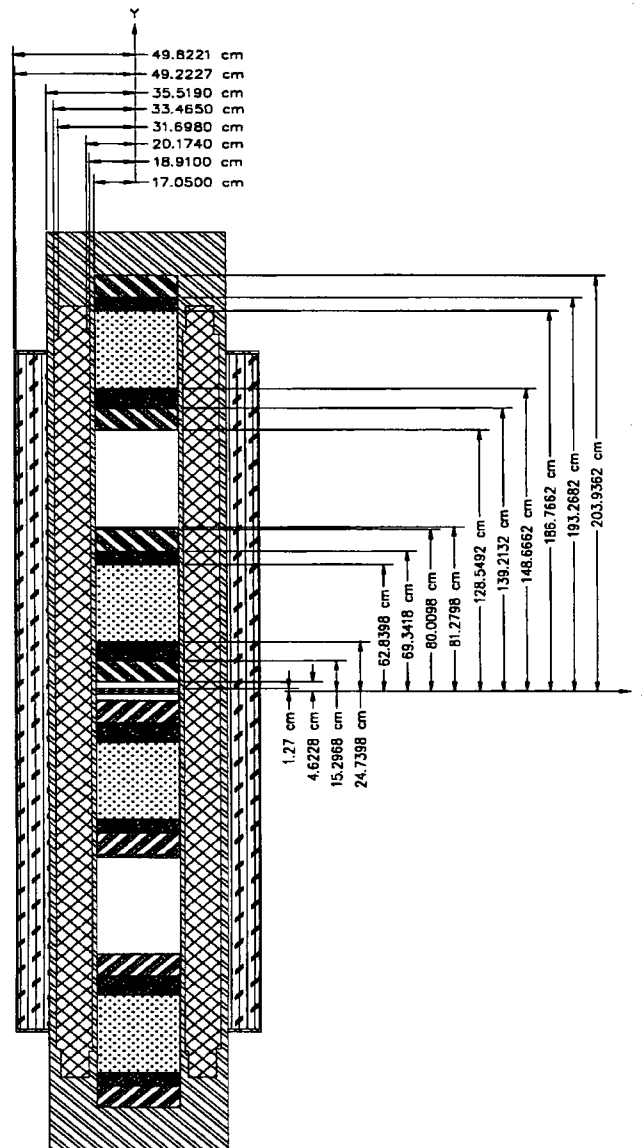


Figure 5.3.6-5 TRIGA SAS4A Upper Half Model Geometry (Normal Condition – Shifted Fuel)










-  Fixture
-  Reflector
-  Fuel
-  Steel
-  Lead
-  Liquid Neutron Shield
-  Void

Figure 5.3.6-6 TRIGA SAS4A Upper Half Model Geometry (Normal Condition)

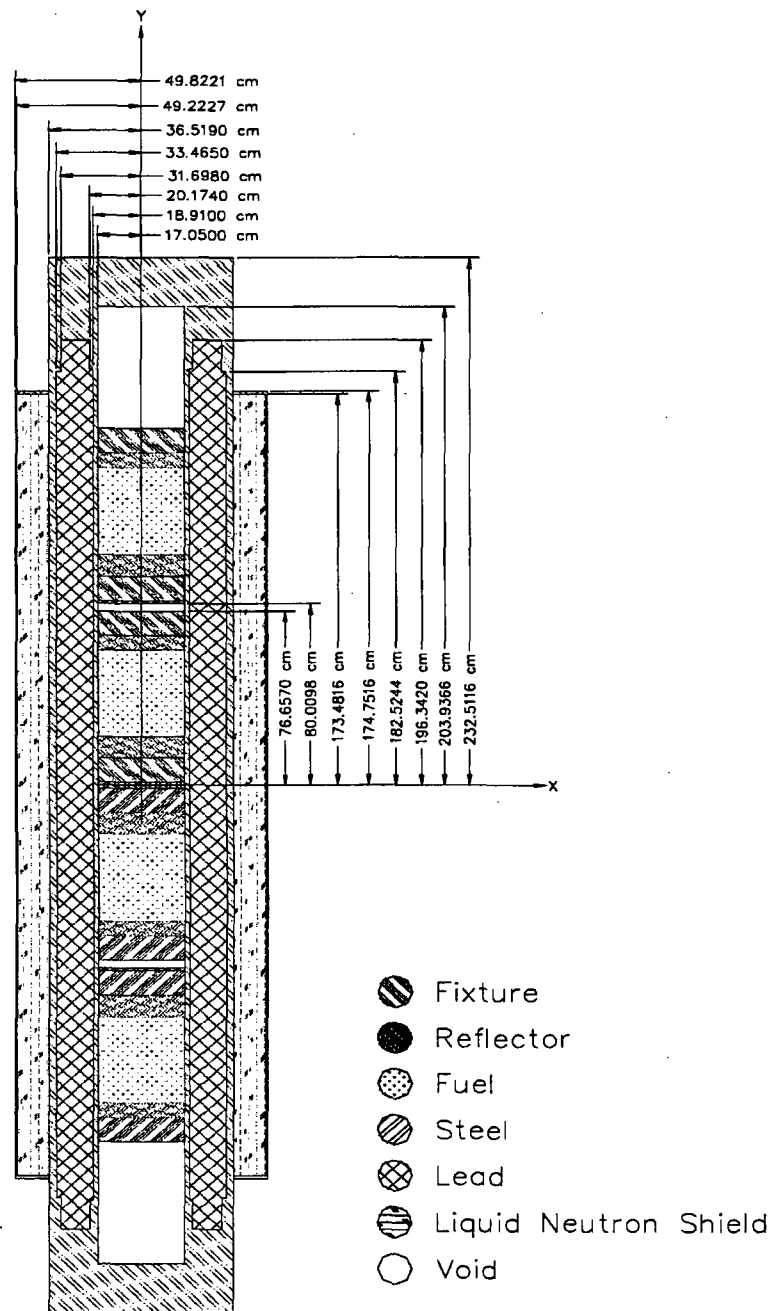


Figure 5.3.6-7 TRIGA SAS4A Lower Half Model Geometry (Normal and Accident Condition)

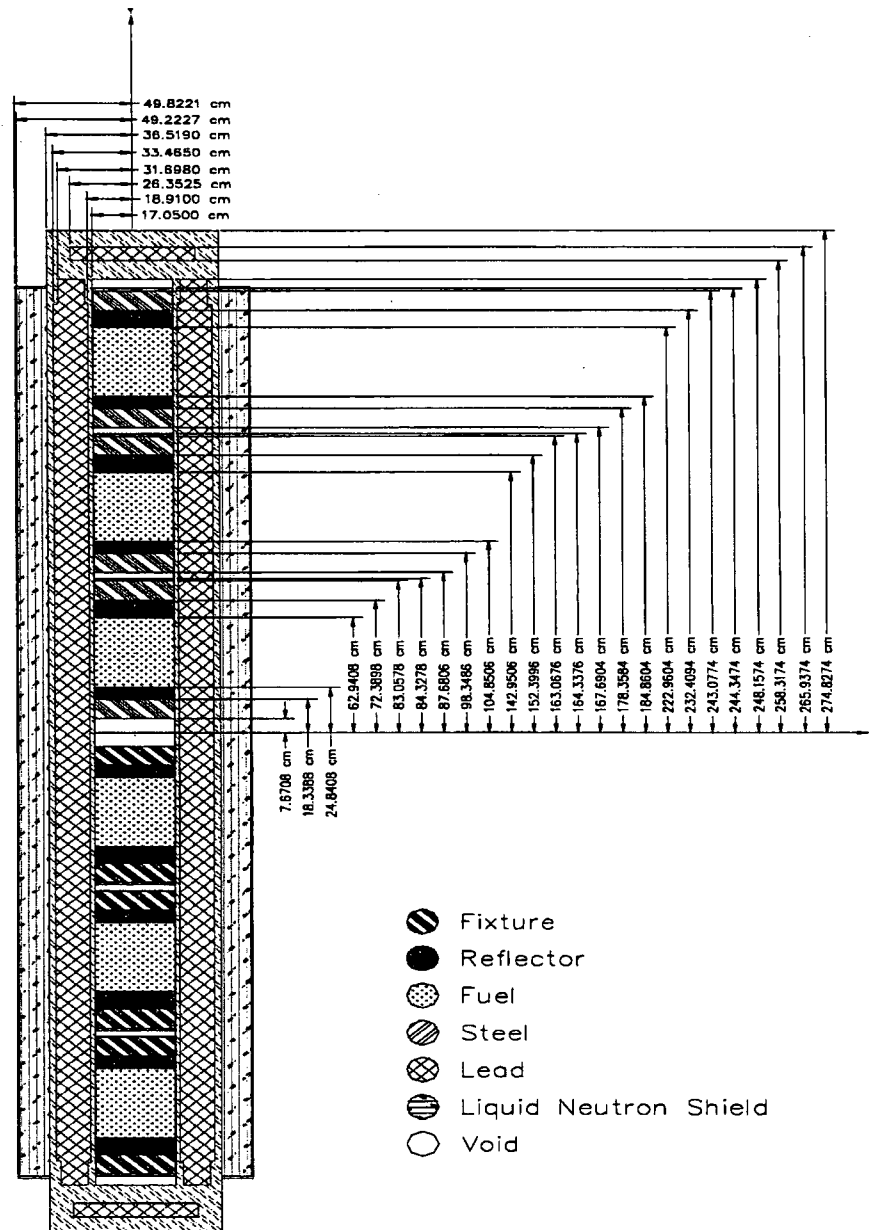


Table 5.3.6-1 TRIGA Fuel Element Gamma Source Term - Normal Transport (ACPR, 86,100 MWd/MTU, 231 Days Cooling, 50% ²³⁵U Depletion)

Group	Emin	Emax	Eav	Fuel Gamma		Hardware	
				g/s/assy	MeV/s	g/s/kg	MeV/s
1	8.00E+00	1.00E+01	9.00E+00	6.0391E+00	5.4352E+01	0.0000E+00	0.0000E+00
2	6.50E+00	8.00E+00	7.25E+00	2.8479E+01	2.0647E+02	0.0000E+00	0.0000E+00
3	5.00E+00	6.50E+00	5.75E+00	1.4544E+02	8.3628E+02	0.0000E+00	0.0000E+00
4	4.00E+00	5.00E+00	4.50E+00	3.6314E+02	1.6341E+03	0.0000E+00	0.0000E+00
5	3.00E+00	4.00E+00	3.50E+00	7.5826E+07	2.6539E+08	6.0459E-18	2.1161E-17
6	2.50E+00	3.00E+00	2.75E+00	7.2081E+08	1.9822E+09	3.7457E+04	1.0301E+05
7	2.00E+00	2.50E+00	2.25E+00	1.3883E+11	3.1237E+11	2.4157E+07	5.4353E+07
8	1.66E+00	2.00E+00	1.83E+00	1.6447E+10	3.0098E+10	7.3055E+08	1.3369E+09
9	1.33E+00	1.66E+00	1.50E+00	1.2858E+11	1.9223E+11	1.0179E+12	1.5218E+12
10	1.00E+00	1.33E+00	1.17E+00	2.4333E+11	2.8348E+11	3.6045E+12	4.1992E+12
11	8.00E-01	1.00E+00	9.00E-01	6.9542E+11	6.2588E+11	4.3345E+11	3.9011E+11
12	6.00E-01	8.00E-01	7.00E-01	1.4822E+13	1.0375E+13	5.2897E+07	3.7028E+07
13	4.00E-01	6.00E-01	5.00E-01	2.6894E+12	1.3447E+12	4.7499E+10	2.3750E+10
14	3.00E-01	4.00E-01	3.50E-01	8.9800E+11	3.1430E+11	5.9683E+09	2.0889E+09
15	2.00E-01	3.00E-01	2.50E-01	1.1708E+12	2.9270E+11	5.5248E+08	1.3812E+08
16	1.00E-01	2.00E-01	1.50E-01	5.1716E+12	7.7574E+11	4.2906E+09	6.4359E+08
17	5.00E-02	1.00E-01	7.50E-02	5.0445E+12	3.7834E+11	1.4319E+10	1.0739E+09
18	1.00E-02	5.00E-02	3.00E-02	1.5535E+13	4.6605E+11	6.7886E+10	2.0366E+09
Total				4.6554E+13	1.5394E+13	5.1972E+12	6.1423E+12

Table 5.3.6-2 TRIGA Fuel Element Neutron Source Term - Normal Transport (ACPR, 86,100 MWd/MTU, 231 Days Cooling, 50% ²³⁵U Depletion)

Group	Emin	Emax	Eav	Spectrum	
				n/s/assy	MeV/s
1	6.43E+00	2.00E+01	1.32E+01	1.7680E+02	2.3368E+03
2	3.00E+00	6.43E+00	4.72E+00	2.7350E+03	1.2901E+04
3	1.85E+00	3.00E+00	2.43E+00	3.0300E+03	7.3478E+03
4	1.40E+00	1.85E+00	1.63E+00	1.3370E+03	2.1726E+03
5	9.00E-01	1.40E+00	1.15E+00	1.7010E+03	1.9562E+03
6	4.00E-01	9.00E-01	6.50E-01	1.8430E+03	1.1980E+03
7	1.00E-01	4.00E-01	2.50E-01	3.6320E+02	9.0800E+01
8	1.70E-02	1.00E-01	5.85E-02	0	0
9	3.00E-03	1.70E-02	1.00E-02	0	0
10	5.50E-04	3.00E-03	1.78E-03	0	0
11	1.00E-04	5.50E-04	3.25E-04	0	0
12	3.00E-05	1.00E-04	6.50E-05	0	0
13	1.00E-05	3.00E-05	2.00E-05	0	0
14	3.05E-06	1.00E-05	6.52E-06	0	0
15	1.77E-06	3.05E-06	2.41E-06	0	0
16	1.30E-06	1.77E-06	1.53E-06	0	0
17	1.13E-06	1.30E-06	1.21E-06	0	0
18	1.00E-06	1.13E-06	1.06E-06	0	0
19	8.00E-07	1.00E-06	9.00E-07	0	0
20	4.00E-07	8.00E-07	6.00E-07	0	0
21	3.25E-07	4.00E-07	3.63E-07	0	0
22	2.25E-07	3.25E-07	2.75E-07	0	0
23	1.00E-07	2.25E-07	1.62E-07	0	0
24	5.00E-08	1.00E-07	7.50E-08	0	0
25	3.00E-08	5.00E-08	4.00E-08	0	0
26	1.00E-08	3.00E-08	2.00E-08	0	0
27	1.00E-11	1.00E-08	5.01E-09	0	0
Total				1.1190E+04	2.8003E+04

**Table 5.3.6-3 TRIGA Fuel Element Gamma Source Term - Accident Conditions
(FLIP-LEU-II, 151,100 MWd/MTU, 908 Days Cooling, 80% ²³⁵U
Depletion)**

Group	Emin	Emax	Eav	Fuel Gamma		Hardware	
				g/s/assy	MeV/s	g/s/kg	MeV/s
1	8.00E+00	1.00E+01	9.00E+00	4.2483E+02	3.8235E+03	0.0000E+00	0.0000E+00
2	6.50E+00	8.00E+00	7.25E+00	2.0012E+03	1.4509E+04	0.0000E+00	0.0000E+00
3	5.00E+00	6.50E+00	5.75E+00	1.0204E+04	5.8673E+04	0.0000E+00	0.0000E+00
4	4.00E+00	5.00E+00	4.50E+00	2.5433E+04	1.1445E+05	0.0000E+00	0.0000E+00
5	3.00E+00	4.00E+00	3.50E+00	5.4231E+07	1.8981E+08	3.8494E-16	1.3473E-15
6	2.50E+00	3.00E+00	2.75E+00	4.5053E+08	1.2390E+09	4.1493E+04	1.1411E+05
7	2.00E+00	2.50E+00	2.25E+00	2.8353E+10	6.3794E+10	2.6759E+07	6.0208E+07
8	1.66E+00	2.00E+00	1.83E+00	7.1432E+09	1.3072E+10	1.1986E+06	2.1934E+06
9	1.33E+00	1.66E+00	1.50E+00	1.9911E+11	2.9767E+11	1.1276E+12	1.6858E+12
10	1.00E+00	1.33E+00	1.17E+00	7.5382E+11	8.7820E+11	3.9929E+12	4.6517E+12
11	8.00E-01	1.00E+00	9.00E-01	2.5223E+12	2.2701E+12	8.5366E+10	7.6829E+10
12	6.00E-01	8.00E-01	7.00E-01	1.5741E+13	1.1019E+13	4.7974E+06	3.3582E+06
13	4.00E-01	6.00E-01	5.00E-01	5.3998E+12	2.6999E+12	9.1500E+07	4.5750E+07
14	3.00E-01	4.00E-01	3.50E-01	5.0638E+11	1.7723E+11	2.1537E+08	7.5380E+07
15	2.00E-01	3.00E-01	2.50E-01	7.4180E+11	1.8545E+11	1.6448E+08	4.1120E+07
16	1.00E-01	2.00E-01	1.50E-01	2.7773E+12	4.1660E+11	3.3013E+09	4.9520E+08
17	5.00E-02	1.00E-01	7.50E-02	3.2348E+12	2.4261E+11	1.3678E+10	1.0259E+09
18	1.00E-02	5.00E-02	3.00E-02	1.0747E+13	3.2241E+11	6.8944E+10	2.0683E+09
Total				4.2659E+13	1.8587E+13	5.2923E+12	6.4181E+12

**Table 5.3.6-4 TRIGA Fuel Element Neutron Source Term - Accident Conditions
(FLIP-LEU-II, 151,100 MWd/MTU, 908 Days Cooling, 80% ²³⁵U
Depletion)**

Group	Emin	Emax	Eav	Spectrum	
				n/s/assy	MeV/s
1	6.43E+00	2.00E+01	1.32E+01	1.3810E+04	1.8253E+05
2	3.00E+00	6.43E+00	4.72E+00	1.6000E+05	7.5472E+05
3	1.85E+00	3.00E+00	2.43E+00	1.7970E+05	4.3577E+05
4	1.40E+00	1.85E+00	1.63E+00	9.9250E+04	1.6128E+05
5	9.00E-01	1.40E+00	1.15E+00	1.3320E+05	1.5318E+05
6	4.00E-01	9.00E-01	6.50E-01	1.4470E+05	9.4055E+04
7	1.00E-01	4.00E-01	2.50E-01	2.8330E+04	7.0825E+03
8	1.70E-02	1.00E-01	5.85E-02	0	0
9	3.00E-03	1.70E-02	1.00E-02	0	0
10	5.50E-04	3.00E-03	1.78E-03	0	0
11	1.00E-04	5.50E-04	3.25E-04	0	0
12	3.00E-05	1.00E-04	6.50E-05	0	0
13	1.00E-05	3.00E-05	2.00E-05	0	0
14	3.05E-06	1.00E-05	6.52E-06	0	0
15	1.77E-06	3.05E-06	2.41E-06	0	0
16	1.30E-06	1.77E-06	1.53E-06	0	0
17	1.13E-06	1.30E-06	1.21E-06	0	0
18	1.00E-06	1.13E-06	1.06E-06	0	0
19	8.00E-07	1.00E-06	9.00E-07	0	0
20	4.00E-07	8.00E-07	6.00E-07	0	0
21	3.25E-07	4.00E-07	3.63E-07	0	0
22	2.25E-07	3.25E-07	2.75E-07	0	0
23	1.00E-07	2.25E-07	1.62E-07	0	0
24	5.00E-08	1.00E-07	7.50E-08	0	0
25	3.00E-08	5.00E-08	4.00E-08	0	0
26	1.00E-08	3.00E-08	2.00E-08	0	0
27	1.00E-11	1.00E-08	5.01E-09	0	0
Total				7.5900E+05	1.7886E+06

Table 5.3.6-5 Material Densities for TRIGA Fuel Element Shielding Analysis

Material ¹	Mixture ID	SCALE SCL Name	Density [g/cm ³]	SCALE Isotope	Density [a/barn-cm]
Active Fuel Region Homogenized Densities (4 TRIGA Elements)	1	U	0.275	URANIUM-235	1.408E-04
				URANIUM-238	5.559E-04
		ZR	2.925	ZIRCONIUM	1.931E-02
		H	0.032	HYDROGEN	1.931E-02
Upper Graphite Reflector	2	AL	0.124	ALUMINUM	2.767E-03
		C	1.310	CARBON-12	6.575E-02
End Fixtures	3	AL	0.344	ALUMINIUM	2.767E-03
Lower Graphite Reflector	4	AL	0.124	ALUMINIUM	2.767E-03
		C	1.310	CARBON-12	6.575E-02
Stainless Steel 304	5	SS304	7.920	CHROMIUM (SS304)	1.743E-02
				MANGANESE	1.736E-03
				IRON (SS304)	5.936E-02
				NICKEL (SS304)	7.721E-03
Neutron Shield (Ethylene Glycol, Water)	6	-	0.9437	HYDROGEN	5.988E-02
				CARBON-12	1.070E-02
				OXYGEN-16	2.459E-02
Lead Shielding	7	LEAD	11.344	LEAD	3.297E-02

¹ Borated stainless steel plates omitted from poisoned basket models for conservatism.

5.3.7 TRIGA Fuel Cluster Rod Model Specification and Shielding Evaluation

TRIGA fuel cluster rods are shown to comply with regulatory dose rate limits by determining the cool time required for the fuel to fall below the design basis TRIGA element-type dose rates. Source terms for the fuel cluster rods are determined using the SCALE SAS2H (Herman) code at various fuel burnup values. The resulting source spectra are then decayed using the ORIGEN-S code, and a one-dimensional shielding analysis is conducted at each decay step using the SCALE SAS1 code. For each burnup considered, the resulting set of cool time and dose rate values are interpolated to find the cool time required for the fuel to meet the maximum design basis dose rate. A final ORIGEN-S calculation is performed at this cool time in order to compute the source spectra at the required decay time.

For consistency, the one-dimensional dose rate computed for the fuel cluster rods are compared with one-dimensional dose rates for the design basis TRIGA fuel elements. Both normal condition and accident condition dose rates are considered, and the maximum cool time required to meet both limits is reported. Further, since the TRIGA fuel cluster rods have approximately the same end-fitting mass as the element-type fuel, the comparison is made on the basis of fuel radiation sources alone.

The maximum computed one-dimensional dose rate at 2 meters from the conveyance for the normal condition TRIGA fuel element analysis is 4.5 mrem/hr. The more accurate three-dimensional analysis predicts a dose rate at the same location of 3.18 mrem/hr. Hence, the one-dimensional analysis provides a conservative estimate of computed dose rates. Similarly, in the loss of neutron shielding hypothetical accident scenario, the maximum computed one-dimensional dose rate for the design basis fuel is 35 mrem/hr and the three-dimensional result is 28.07 mrem/hr.

Section 5.3.7.1 presents the SAS2H source term model for the TRIGA fuel cluster rods. Section 5.3.7.2 discusses the methodology used to compute one-dimensional dose rates for each burnup and cool time case. The resulting required cool times for the fuel cluster rods are presented in Section 5.3.7.3.

5.3.7.1 TRIGA Fuel Cluster Rod Source Terms

The SAS2H description of the TRIGA fuel cluster rods is based on the material and dimensional parameters given in Table 5.3.7-1. The irradiation parameters are based on a nominal 14 MW TRIGA reactor operating with 29 cluster-type assemblies consisting of 25 rods each. For each burnup case, the required exposure time is computed at this fixed power level. This

conservatively assumes that all fuel irradiation occurs during the period immediately prior to fuel discharge. Representative gamma and neutron source terms are summarized in Table 5.3.7-3 and Table 5.3.7-4.

The Incoloy 800 (density 7.94 g/cm^3) clad material composition is given in Table 5.3.7-2. A cobalt impurity concentration of 1.2 g/kg is assumed. No cobalt is listed in the manufacturer specifications for this material.

5.3.7.2 TRIGA Fuel Cluster Rod One-Dimensional Dose Rate Analysis

The task of computing one-dimensional dose rates for the dozens of source terms developed in this analysis is simplified by the use of a dose response methodology. In this approach, a dose rate response function is computed at various detector locations outside the cask. The response function for a location gives the contribution to the total dose rate from an unit source strength in each energy group. Hence, the computation of a response function involves the solution of a one-dimensional problem for each energy group in the spectrum. Here, 18 gamma responses and 7 neutron responses are computed. Only seven neutron responses are required because the spent fuel neutron spectrum is non-zero only in the first seven groups.

For the one-dimensional response calculations, the LWT basket region is represented as a homogenized smear of the fuel, fuel tube, and basket structural materials. The resulting composition of the smear is shown in Table 5.3.7-5. The basket smear is homogenized on the basis of a cylinder of radius 14.329 cm and height 279.40 cm (5 times the active fuel height).

With these response functions, the dose rate at the corresponding detector location is determined for any given burnup and cool time combination by simply multiplying the fuel source spectrum by the appropriate response function. The SCALE SAS1 sequence is used to develop dose rate response functions. The computed response functions are shown in Table 5.3.7-6 through Table 5.3.7-9.

5.3.7.3 TRIGA Fuel Cluster Rod Required Cool Times

The cool time results for the TRIGA fuel cluster rods are shown in Table 5.3.7-10. The cool time required to meet each individual limit is shown along with the maximum cool time which ensures that all limits are met. The "Active" column indicates the constraint, which provides the limiting cool time for each burnup case.

The cooling times presented in Table 5.3.7-10 are based on in core burnup occurring over a conservatively short time period. Higher burnup values are expected to occur over significantly longer time periods, producing lower decay heat and radiation source terms than these design basis values. Therefore, a TRIGA fuel cluster rod may be loaded into the cask if the decay heat

is less than 1.875 watts, and the full load of TRIGA fuel rods as prepared for shipment meets the dose limits of 10 CFR 71.47.

Table 5.3.7-1 TRIGA Fuel Cluster Rod Parameters

Parameter	[in]	[cm]
Overall length	30.130	76.530
Fuel height	22.000	55.880
Fuel diameter	0.510	1.295
U mass fraction	10%	-
²³⁵ U enrichment	93%	-
Fuel mass [g]	452	-
H to Zr ratio	1.6	-
Cladding thickness	0.016	0.041
Clad diameter	0.542	1.377
Clad material	Incoloy 800	-
Tube ID	0.625	1.588
Tube OD	0.750	1.905
Tube material	aluminum	-
Power [MW]	0.0193	-
Number cycles	4	-
Down time between cycles [d]	10	-
Exposure [d]	varies	-

Table 5.3.7-2 Incoloy 800 Clad Composition

$\rho=7.94 \text{ g/cm}^3$ Isotope	Mass Fraction	Number Density [atm/b-cm]
NI	0.3250	2.6479E-02
FE	0.4182	3.5803E-02
CR	0.2100	1.9312E-02
C	0.0010	3.9846E-04
MN	0.0150	1.3055E-03
S	0.0002	2.2369E-05
SI	0.0100	1.7025E-03
CU	0.0075	5.5949E-04
CO	0.0012	9.7361E-05
AL	0.0060	1.0633E-03
TI	0.0060	5.9920E-04

Table 5.3.7-3 Representative TRIGA Fuel Cluster Rod Gamma Spectra at 180 GWd/MTU and 1.849 Year Cool Time

Group	Emin	Emax	Eav	Fuel Gamma		Hardware	
				g/s/assy	MeV/s	g/s/kg	MeV/s
1	8.00E+00	1.00E+01	9.00E+00	1.4212E-02	1.2791E-01	0.0000E+00	0.0000E+00
2	6.50E+00	8.00E+00	7.25E+00	6.7907E-02	4.9233E-01	0.0000E+00	0.0000E+00
3	5.00E+00	6.50E+00	5.75E+00	3.5339E-01	2.0320E+00	0.0000E+00	0.0000E+00
4	4.00E+00	5.00E+00	4.50E+00	9.0065E-01	4.0529E+00	0.0000E+00	0.0000E+00
5	3.00E+00	4.00E+00	3.50E+00	1.0364E+07	3.6274E+07	3.5727E-18	1.2504E-17
6	2.50E+00	3.00E+00	2.75E+00	1.0850E+08	2.9838E+08	1.6385E+04	4.5059E+04
7	2.00E+00	2.50E+00	2.25E+00	3.0979E+10	6.9703E+10	1.0567E+07	2.3776E+07
8	1.66E+00	2.00E+00	1.83E+00	3.1495E+09	5.7636E+09	1.8569E+07	3.3981E+07
9	1.33E+00	1.66E+00	1.50E+00	2.5716E+10	3.8445E+10	4.4527E+11	6.6568E+11
10	1.00E+00	1.33E+00	1.17E+00	4.2575E+10	4.9600E+10	1.5767E+12	1.8369E+12
11	8.00E-01	1.00E+00	9.00E-01	1.2408E+11	1.1167E+11	1.7069E+11	1.5362E+11
12	6.00E-01	8.00E-01	7.00E-01	1.2152E+12	8.5064E+11	3.0983E+06	2.1688E+06
13	4.00E-01	6.00E-01	5.00E-01	4.1234E+11	2.0617E+11	1.2124E+09	6.0620E+08
14	3.00E-01	4.00E-01	3.50E-01	1.9145E+11	6.7008E+10	9.1743E+07	3.2110E+07
15	2.00E-01	3.00E-01	2.50E-01	2.4647E+11	6.1618E+10	7.4893E+07	1.8723E+07
16	1.00E-01	2.00E-01	1.50E-01	1.0963E+12	1.6445E+11	1.3355E+09	2.0033E+08
17	5.00E-02	1.00E-01	7.50E-02	1.0786E+12	8.0895E+10	5.4483E+09	4.0862E+08
18	1.00E-02	5.00E-02	3.00E-02	3.3334E+12	1.0000E+11	2.7289E+10	8.1867E+08
Total				7.8004E+12	1.8063E+12	2.2281E+12	2.6583E+12

Table 5.3.7-4 Representative TRIGA Fuel Cluster Rod Neutron Spectrum at 180 GWd/MTU and 1.849 Year Cool Time

Group	Emin	Emax	Eav	Fuel Neutron	
				n/s/assy	MeV/s
1	6.43E+00	2.00E+01	1.32E+01	4.0380E-01	5.3370E+00
2	3.00E+00	6.43E+00	4.72E+00	1.1840E+01	5.5849E+01
3	1.85E+00	3.00E+00	2.43E+00	2.4980E+01	6.0577E+01
4	1.40E+00	1.85E+00	1.63E+00	8.1070E+00	1.3174E+01
5	9.00E-01	1.40E+00	1.15E+00	6.7800E+00	7.7970E+00
6	4.00E-01	9.00E-01	6.50E-01	5.0610E+00	3.2897E+00
7	1.00E-01	4.00E-01	2.50E-01	9.6100E-01	2.4025E-01
8-27				0	0
Total				5.8133E+01	1.4626E+02

Table 5.3.7-5 Fuel Basket Region Material Composition Used in Shielding Analysis

Isotope	Number Density [a/b-cm]
HYDROGEN	1.3121E-02
CARBON-12	1.1803E-05
ALUMINUM	9.1431E-03
SILICON	5.0432E-05
SULFUR	8.8350E-07
TITANIUM	1.7750E-05
CHROMIUM	5.7206E-04
CHROMIUM(SS304)	2.9885E-03
MANGANESE	3.3640E-04
IRON	1.0607E-03
IRON(SS304)	1.0178E-02
COBALT-59	2.8841E-06
NICKEL	7.8439E-04
NICKEL(SS304)	1.3239E-03
COPPER	1.6574E-05
ZIRCONIUM	8.2001E-03
URANIUM-235	3.3466E-04
URANIUM-238	2.4871E-05

Table 5.3.7-6 Normal Condition Dose Response to Gammas for TRIGA Fuel Cluster Rods

Conveyance+2m Response to Gammas [mrem/hr per 10 ¹⁰ g/sec/cm ³]			
Gamma Group	Neutron	Gamma	Total
1	0.0000E+00	9.1398E+02	9.1398E+02
2	0.0000E+00	1.1721E+03	1.1721E+03
3	0.0000E+00	1.2700E+03	1.2700E+03
4	0.0000E+00	1.1962E+03	1.1962E+03
5	0.0000E+00	9.7074E+02	9.7074E+02
6	0.0000E+00	6.3202E+02	6.3202E+02
7	0.0000E+00	3.4587E+02	3.4587E+02
8	0.0000E+00	1.3598E+02	1.3598E+02
9	0.0000E+00	4.0645E+01	4.0645E+01
10	0.0000E+00	5.0418E+00	5.0418E+00
11	0.0000E+00	1.7609E-01	1.7609E-01
12	0.0000E+00	2.3171E-03	2.3171E-03
13	0.0000E+00	7.5558E-08	7.5558E-08
14	0.0000E+00	1.2157E-18	1.2157E-18
15	0.0000E+00	5.6115E-50	5.6115E-50
16	0.0000E+00	0.0000E+00	0.0000E+00
17	0.0000E+00	0.0000E+00	0.0000E+00
18	0.0000E+00	0.0000E+00	0.0000E+00

Table 5.3.7-7 Normal Condition Dose Response to Neutrons for TRIGA Fuel Cluster Rods

Conveyance+2m Response to Neutrons [mrem/hr per 10 ¹⁰ n/sec/cm ³]			
Neutron Group	Neutron	N-Gamma	Total
1	1.4395E+07	3.2079E+06	1.7602E+07
2	8.9074E+06	3.0520E+06	1.1959E+07
3	8.3977E+06	3.1016E+06	1.1499E+07
4	7.0780E+06	3.1793E+06	1.0257E+07
5	6.4960E+06	3.2394E+06	9.7354E+06
6	6.2823E+06	3.3839E+06	9.6662E+06
7	6.9926E+06	3.6484E+06	1.0641E+07

Table 5.3.7-8 Accident Condition Dose Response to Gammas for TRIGA Fuel Cluster Rods

Accident 1m Response to Gammas [mrem/hr per 10^{10} g/sec/cm ³]			
Gamma Group	Neutron	Gamma	Total
1	0.0000E+00	2.5730E+03	2.5730E+03
2	0.0000E+00	3.3184E+03	3.3184E+03
3	0.0000E+00	3.6238E+03	3.6238E+03
4	0.0000E+00	3.4422E+03	3.4422E+03
5	0.0000E+00	2.8144E+03	2.8144E+03
6	0.0000E+00	1.8454E+03	1.8454E+03
7	0.0000E+00	1.0152E+03	1.0152E+03
8	0.0000E+00	4.0124E+02	4.0124E+02
9	0.0000E+00	1.2051E+02	1.2051E+02
10	0.0000E+00	1.5045E+01	1.5045E+01
11	0.0000E+00	5.2812E-01	5.2812E-01
12	0.0000E+00	6.9991E-03	6.9991E-03
13	0.0000E+00	2.3068E-07	2.3068E-07
14	0.0000E+00	3.6734E-18	3.6734E-18
15	0.0000E+00	1.7451E-49	1.7451E-49
16	0.0000E+00	0.0000E+00	0.0000E+00
17	0.0000E+00	0.0000E+00	0.0000E+00
18	0.0000E+00	0.0000E+00	0.0000E+00

Table 5.3.7-9 Accident Condition Dose Response to Neutrons for TRIGA Fuel Cluster Rods

Accident 1m Response to Neutrons [mrem/hr per 10^{10} n/sec/cm ³]			
Neutron Group	Neutron	N-Gamma	Total
1	6.3928E+08	1.6717E+06	6.4095E+08
2	5.8145E+08	1.2754E+06	5.8273E+08
3	5.9195E+08	1.1720E+06	5.9312E+08
4	5.8819E+08	1.1480E+06	5.8933E+08
5	5.8510E+08	1.1548E+06	5.8625E+08
6	5.7267E+08	1.2334E+06	5.7391E+08
7	5.6579E+08	1.4931E+06	5.6728E+08

Table 5.3.7-10 TRIGA Fuel Cluster Rod Required Cool Time at Various Fuel Burnups

Burnup [GWd/MTU]	Depletion [% ²³⁵ U]	Cool Time Required to Reach Limit [d] ¹				Active
		DecayHeat (1.875 W)	Accident (35 mrem/hr)	Normal (4.5 mrem/hr)	MAX	
20	2.86%	158.9	90.0	90.0	158.9	DecayHeat
30	4.05%	201.0	90.0	90.0	201.0	DecayHeat
40	5.48%	233.2	90.0	90.0	233.2	DecayHeat
50	6.91%	259.7	91.5	235.0	259.7	DecayHeat
60	8.33%	283.1	95.6	295.9	295.9	Normal
70	9.76%	305.1	100.0	352.2	352.2	Normal
80	10.95%	325.9	104.9	400.3	400.3	Normal
90	12.38%	345.7	110.4	442.2	442.2	Normal
100	13.81%	365.3	117.1	479.3	479.3	Normal
110	15.24%	385.4	125.4	512.2	512.2	Normal
120	16.43%	404.0	135.9	541.8	541.8	Normal
130	17.86%	422.8	149.3	568.8	568.8	Normal
140	19.29%	441.0	165.4	593.5	593.5	Normal
150	20.71%	460.2	182.8	616.2	616.2	Normal
160	21.91%	476.7	200.1	637.3	637.3	Normal
170	23.33%	495.1	216.7	657.0	657.0	Normal
180	24.76%	510.4	232.2	675.3	675.3	Normal
190	26.19%	527.6	246.7	692.6	692.6	Normal
200	27.38%	544.3	260.2	708.9	708.9	Normal
225	30.71%	583.9	290.6	746.3	746.3	Normal
250	34.29%	621.0	316.7	779.6	779.6	Normal
275	37.62%	656.5	339.5	810.1	810.1	Normal
300	40.95%	690.4	359.8	838.4	838.4	Normal
325	44.29%	724.1	378.3	865.3	865.3	Normal
350	47.62%	757.4	395.1	891.1	891.1	Normal
375	50.95%	790.7	410.8	916.4	916.4	Normal
400	54.05%	824.0	425.7	941.4	941.4	Normal
425	57.38%	858.8	439.9	966.5	966.5	Normal
450	60.71%	892.7	453.8	992.2	992.2	Normal
475	63.81%	931.2	467.7	1018.8	1018.8	Normal
500	67.14%	969.9	481.7	1046.8	1046.8	Normal
525	70.24%	1006.0	496.2	1076.6	1076.6	Normal
550	73.33%	1049.6	511.3	1108.8	1108.8	Normal
575	76.55%	1096.6	527.6	1144.5	1144.5	Normal
600	79.60%	1145.0	545.5	1184.3	1184.3	Normal

¹ These values provide a conservative, maximum possible cooling time necessary to meet the maximum allowable decay heat or design basis TRIGA fuel element external dose rate calculations. Actual TRIGA fuel cluster rods may require shorter cooling times to meet the 1.875 watt/rod decay heat limit and 10 CFR 71.47 external dose rate limits.

5.3.8 High Burnup PWR and BWR Rods Shielding Evaluation

Results of a shielding and decay heat source analysis for up to 25 high burnup PWR or BWR fuel rods are presented in this section. The rods have burnups up to 80,000 MWd/MTU. The results are presented in terms of the cool time required for 25 rods to meet package surface and 2 meter dose rate limits and a cask total decay heat limit of 2.1 kW for BWR rods and 2.3 kW for PWR rods.

Consistent with the analysis performed for the lower burnup PWR rods, the shielding analysis is performed using the one-dimensional SCALE SAS1 shielding analysis sequence. Source terms are generated based on a limiting description of PWR and BWR fuel rods using the SCALE SAS2H code.

The PWR analysis is based on a single limiting description of a PWR fuel rod which bounds rods from all PWR assembly array sizes. Two BWR rod models are employed. The first is based on a limiting description of rods from 7×7 array size assemblies. The results for this case indicate that the highest burnup BWR 7×7 rods require greater than 150 days cool time before shipment. Hence, a second BWR fuel rod model is developed which bounds rods from 8×8 and larger array size fuel assemblies. The results for this model indicate that up to 25 rods from these assemblies can be shipped at the maximum burnup of 80,000 MWd/MTU after 150 days cool time.

5.3.8.1 High Burnup PWR and BWR Rods Source Terms

The limiting rod descriptions are determined by developing a hybrid fuel rod model, which contains a conservatively bounding uranium loading. For a given burnup, the bounding uranium mass leads to bounding decay heat and radiation source terms. Fuel rod model parameters are shown in Table 5.3.8-1. In the BWR model, fuel rods from 7×7 array size assemblies are treated as a special case, since their significantly higher mass loadings lead to required extended cool times, which would unnecessarily penalize BWR rods from larger array size assemblies, which have a significantly lower mass per rod and correspondingly lower radiation and decay heat source terms. The BWR 7×7 fuel rod model bounds all rods from 7×7 array size BWR assemblies, and the BWR 8×8 fuel rod model bounds rods from all 8×8 and larger (i.e., 9×9, 10×10) BWR assemblies.

SAS2H models of the three fuel rod models are developed based on the cycle parameters shown in Table 5.3.8-2. The rod exposure is conservatively assumed to occur over a typical number of reactor operating cycles: three for the PWR rods and four for the BWR rods. In addition, in order to achieve the high fuel burnups, assembly powers are conservatively increased rather than extending cycle lengths. A down time of 60 days between cycles is assumed. Fuel rods are evaluated at an initial enrichment of 4.0 wt % ²³⁵U. This enrichment is expected to be a lower

bound for fuel burned as high as 80,000 MWd/MTU. The SAS2H models for each rod type are shown in Figure 5.3.8-1 through Figure 5.3.8-3. The SCALE 27N18G library is employed here; the energy group structure of this library is shown in Table 5.3.8-3 and Table 5.3.8-4 along with the ANSI flux-to-dose-rate conversion factors employed in the shielding analysis.

The resulting decay heat source terms for 25 rods of each fuel type are shown in Table 5.3.8-5. The BWR 7×7 rods are analyzed at 60, 70, and 80 GWd/MTU burnup. Neutron and gamma radiation source spectra for the various fuel types are shown in Table 5.3.8-6 through Table 5.3.8-15 at various cool times. Note that the neutron source spectrum is non-zero only in the highest seven energy groups; hence, the remaining energy groups are omitted from the tables.

5.3.8.1.1 Axial Source Profile

The description of the PWR and BWR rods axial source profile is based on bounding axial burnup profiles observed for fuel at much lower burnups. This description is conservative because the higher burned fuel of interest here will have a substantially lower axial peaking factor. The PWR and BWR axial burnup and source profiles are shown in Figure 5.3.8-4 and Figure 5.3.8-5, respectively. Values are tabulated in Table 5.3.8-17 and Table 5.3.8-18.

The computed relation between source rate S and burnup B :

$$S = aB^b$$

implies that, in general, the average source rate is not equal to the source rate at the average burnup. The exponent b is determined based on SAS2H analyses of various fuel assemblies at different burnups. A value of 4.22 is used for neutron source rate variation in both PWR and BWR fuel types. The exponent for photon source rates has been determined to be 1.0.

Two scaling quantities are of interest. First, since SAS2H analyses are conducted at the average assembly burnup, a scale factor is required to relate the assembly average source rate to the source rate at the average burnup:

$$r = \frac{\bar{S}}{S(\bar{B})} = \frac{\frac{a}{H} \int B^b dz}{a\bar{B}^b}$$

where H is the height of the fuel region. With the burnup profile normalized to one, this becomes

$$r = \frac{1}{H} \int B^b dz$$

The integral is evaluated numerically using the trapezoid rule, and the resulting scale factors are shown in Table 5.3.8-16. The second scaling parameter is the ratio of the peak to average source rate.

$$s = \frac{S(B_{\max})}{\bar{S}}$$

This parameter is also shown in Table 5.3.8-16.

5.3.8.2 High Burnup PWR and BWR Rods Shielding Model

A homogenized description of the LWT cask payload and basket structural materials is developed for use in the one-dimensional shielding model. The fuel region is a homogenized smear of the fuel rods and the stainless steel insert tubes (1.7463 cm OD with 0.0711 cm wall thickness). Resulting homogenized material compositions are provided in Table 5.3.8-19.

Outside the homogenized fuel region, the remaining basket materials are represented as concentric rings of stainless steel, aluminum or void regions. The radii of the rings are chosen to conserve the cross sectional area of the material present in each region.

Table 5.3.8-21 shows the key basket model parameters required to develop the concentric radial model. Material compositions for the basket and cask materials are shown in Table 5.3.8-20. The resulting one-dimensional model of the LWT cask including basket and payload is shown in Table 5.3.8-22.

SAS1 shielding models are developed for each fuel type based on the one-dimensional model shown in Table 5.3.8-22. Neutron and gamma dose rates are evaluated for each fuel type and for each decay time shown in Table 5.3.8-6 through Table 5.3.8-15. Dose rates are evaluated using a dose response methodology.

5.3.8.2.1 Dose Response Methodology

In order to avoid the significant effort required to prepare and execute dozens of one-dimensional cases for all fuel configurations and burnups under consideration, a unique device is employed which permits the ready calculation of dose rates at a given location by use of a dose rate response function. The dose rate response function for a given source type at a given detector location is a collection of values, one for each energy group, each of which gives the contribution to the dose rate at a specific detector location from a unit source strength in that energy group. With this response function, the dose rate, d , at the corresponding detector location is determined for any given fuel type simply by vector multiplying the unnormalized source spectrum, f , by the response function, r .

The dose rate response function is computed by solving a series of one-dimensional cases, one for each energy group, with a unit source strength in each energy group. In practice, the source

strength is normalized to some large value (here, $10^{10}/\text{cm}^3/\text{sec}$) in order to avoid numeric underflow in the calculation.

The resulting cask surface and 2m response functions for the various fuel types analyzed here are shown in Table 5.3.8-23 through Table 5.3.8-26.

The results of multiplying the computed dose response functions by the various spectra shown in the tables are dose rates associated with the source at the average assembly burnup. These computed dose rates are then scaled by the ratio of the average source to the source at the average burnup, as tabulated in Table 5.3.8-16. At 2m from the cask, this result is an accurate estimate of the dose rate since the axial source peaking factor does not have a significant effect on dose rates at this distance from the cask. On the surface, however, the computed dose rates are further scaled by the peak-to-average source ratio in order to more accurately capture the peak axial surface dose rate.

5.3.8.3 High Burnup PWR and BWR Rods Shielding Evaluation

Table 5.3.8-27 and Table 5.3.8-28 summarize the computed dose rates as a function of cool time for each fuel type at the surface and 2m from the edge of the cask conveyance. Each table also includes the cask total decay heat.

The surface dose rate results are well below the regulatory limit of 200 mrem/hr for all fuel types at burnups up to 80,000 MWd/MTU and for cool times greater than 150 days. Hence, the normal condition surface dose rates do not impose any restrictions on the suitability of fuel for shipment.

The 2m dose rate results are limited to 10.0 mrem/hr. Hence, the results in Table 5.3.8-28 indicate that all fuels except the BWR 7×7 at 80,000 MWd/MTU lead to 2m dose rates below 9.0 mrem/hr at 150 days cool time. The BWR 7×7 fuel requires 180 days cool time to fall below 9.0 mrem/hr.

Finally, the cask decay heat limit of 2.1 kW/cask (BWR) and 2.3 kW/cask (PWR) further constrains the minimum cool time requirements. Based on the tabulated results, all fuel except the BWR 7×7 can be shipped at 150 days cool time. The BWR 7×7 at 60,000 MWd/MTU requires 210 days cool time, at 70,000 requires 240 days cool time, and at 80,000 MWd/MTU requires 270 days cool time based on decay heat source alone.

Combining the constraints for surface and 2m dose rate and cask total decay heat, the loading table shown in Table 5.3.8-29 is obtained.

Accident dose rates were not explicitly calculated for the 80 GWd/MTU PWR and BWR fuel rods. The accident dose rate for the 60 GWd/MTU PWR rods was reported in Section 5.3.5 as 69.44 mrem/hr at 1 meter from the cask. Conservatively applying a fuel mass ratio of the maximum 80 GWd/MTU payload to the 60 GWd/MTU payload (108.8/65.6), and the neutron

dose rate scaling factor ($[80/60]^{4.22}$) results in a maximum dose rate less than 400 mrem/hr. This conservative estimate is significantly lower than the 1000 mrem/hr limit.

Figure 5.3.8-1 PWR Rod SAS2H Model

```
=SAS2H      PARM=(HALT06,SKIPSHIPDATA)
PWR 4.0 W/O U235, 80000 MWD/MTU UP TO 1 YEAR COOLING
27GROUPNDF4 LATTICECELL
UO2         1 0.95 811 92235 4.0 92238 96.0 END
ZIRCALLOY   2 1.0 620 END
H2O         3 DEN=0.725 1.0 570 END
ARBMB-BORMOD 0.725 1 1 0 0 5000 100 3 550.0E-6 570 END
END COMP
SQUAREPITCH 1.473 0.9665 1 3 1.118 2 0.986 0 END
NPIN/ASSM=176 FUELENGTH=389.9 NCYCLE=3 NLIB/CYC=2 PRINTLEVEL=6
INPLEVEL=2 NUMZONES=4 END
3 1.3589 2 1.4605 3 1.6623 500 5.2039
POWER=19.36 BURN=636.4 DOWN=60.0 END
POWER=19.36 BURN=636.4 DOWN=60.0 END
POWER=19.36 BURN=636.4 DOWN=0.0 END
END
```

Figure 5.3.8-2 BWR 7x7 SAS2H Model Shown at 80,000 MWd/MTU

```
=SAS2H      PARM=(HALT08,SKIPSHIPDATA)
BWR/4-6 7x7 4.0 W/O U235 80,000 MWD/MTU, 40% VOID, UP TO 1 YEAR
COOLING
27GROUPNDF4 LATTICECELL
UO2         1 0.95 840 92235 4.0 92238 96.0 END
ZIRCALLOY   2 1.0 620. END
H2O 3 DEN=0.446 1.0 562. END
H2O 4 DEN=0.743 1.0 553. END
ZIRCALLOY   5 1.0 553 END
H2O 6 DEN=0.446 1.0 562. END
END COMP
SQUAREPITCH 1.8745 1.2446 1 3 1.448 2 1.265 0 END
NPIN/ASSM=49 FUELENGTH=389.9 NCYCLES=4 NLIB/CYC=2 PRINTLEVEL=6
INPLEVEL=2 NUMZONES=5 END
1 0.001 500 7.403 6 7.564 5 7.793 4 8.598
POWER=5.85 BURN=730.0 DOWN=60 END
POWER=5.85 BURN=730.0 DOWN=60 END
POWER=5.85 BURN=730.0 DOWN=60 END
POWER=5.85 BURN=730.0 DOWN=0.0 END
```

Figure 5.3.8-3 BWR 8x8 Rod SAS2H Model

```
=SAS2H      PARM=(HALT08,SKIPSHIPDATA)
BWR/4-6 8x8 4.0 W/O U235 80,000 MWD/MTU, 40% VOID,  UP TO 1 YEAR
COOLING
'LEVEL 2 INPUT FROM 790-4002
27GROUPNDF4 LATTICECELL
UO2        1 0.95 840 92235 4.0 92238 96.0 END
ZIRCALLOY 2 1.0 620. END
H2O 3 DEN=0.446 1.0 562. END
H2O 4 DEN=0.743 1.0 553. END
ZIRCALLOY 5 1.0 553 END
H2O 6 DEN=0.446 1.0 562. END
END COMP
SQUAREPITCH 1.626 1.0701 1 3 1.260 2 1.086 0 END
NPIN/ASSM=63 FUELENGTH=389.9 NCYCLES=4 NLIB/CYC=2 PRINTLEVEL=6
INPLEVEL=2 NUMZONES=7 END
4 0.540 5 0.620 6 0.917 500 7.337 6 7.564 5 7.793 4 8.598
POWER=5.56 BURN=730.0 DOWN=60 END
POWER=5.56 BURN=730.0 DOWN=60 END
POWER=5.56 BURN=730.0 DOWN=60 END
POWER=5.56 BURN=730.0 DOWN=0.0 END
END
```

Figure 5.3.8-4 PWR Rods Axial Burnup and Source Profiles

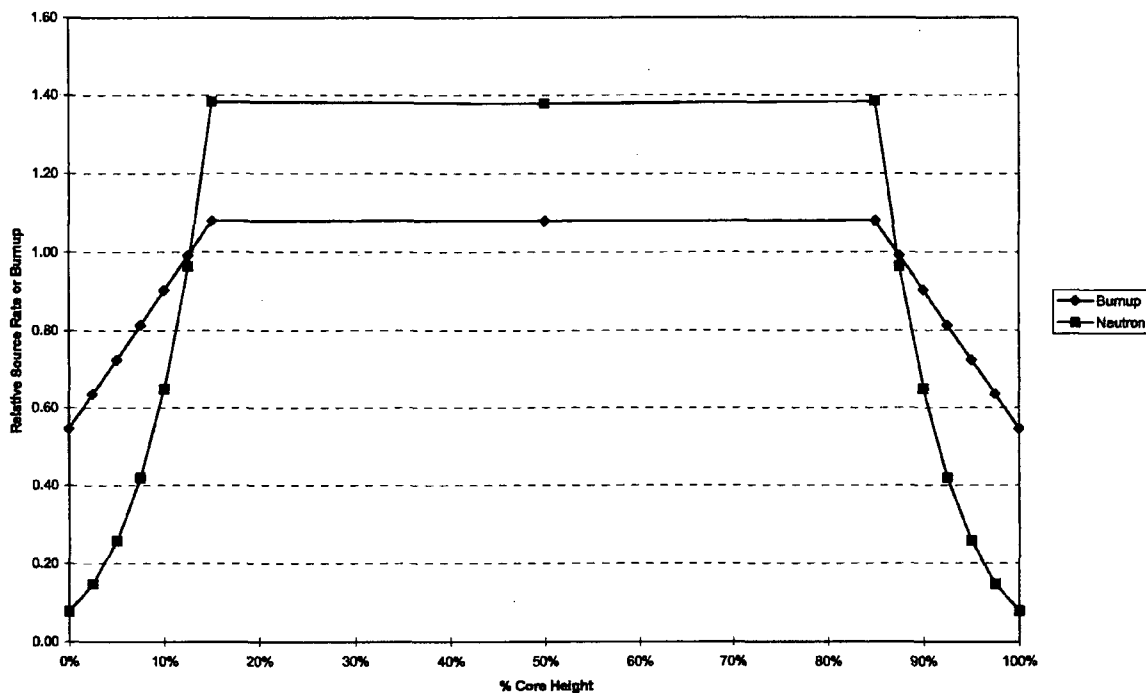


Figure 5.3.8-5 BWR Rods Axial Burnup and Source Profiles

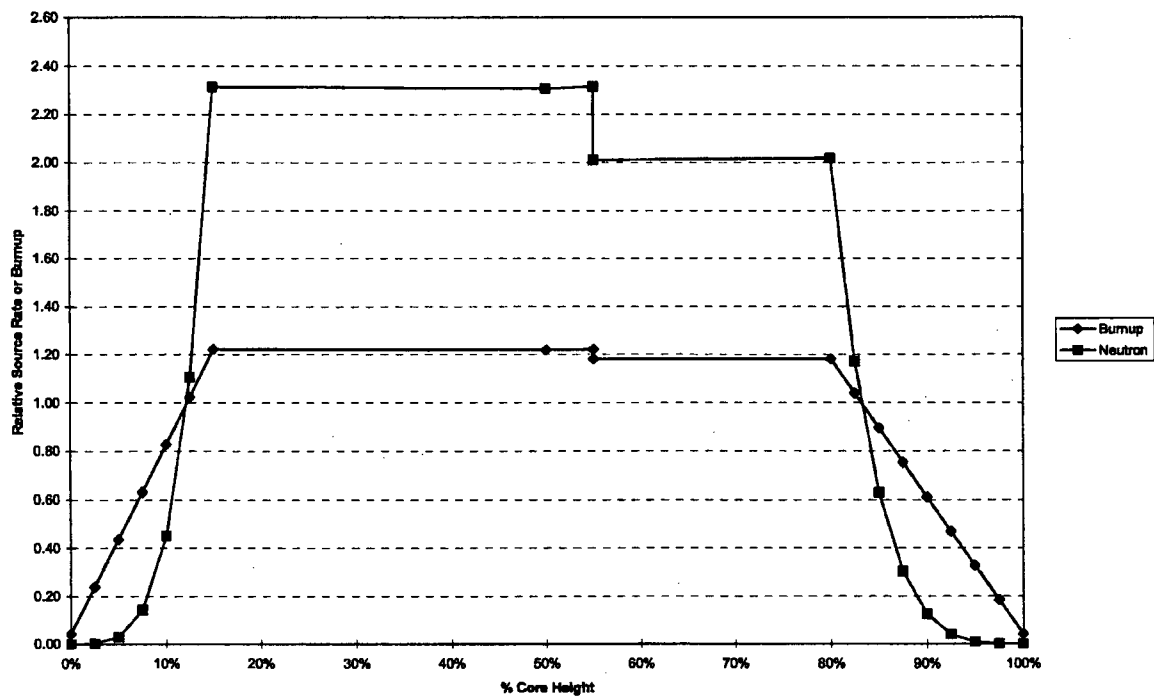


Table 5.3.8-1 High Burnup Fuel Rod Model Parameters

Parameter	Unit	PWR	BWR 7×7	BWR 8×8
Version		Hybrid	Hybrid	Hybrid
% Theoretical Density	[%]	95%	95%	95%
Clad		Zirc-4	Zirc-4	Zirc-2
Max Assy Loading	[MTU]	0.4620	0.2133	0.2028
Fuel Rods		176	49	63
Pitch	[cm]	1.4730	1.8750	1.6260
Rod Diam	[cm]	1.1180	1.4480	1.2600
Clad Inner Diam	[cm]	0.9860	1.2650	1.0860
Pellet Diam	[cm]	0.9665	1.2446	1.0701
Active Length	[cm]	389.9	389.9	389.9
Mass Density	[kg/cm]	1.185	0.547	0.520
	[g/cm/rod]	6.733	11.165	8.256

Table 5.3.8-2 High Burnup Fuel Assembly Model Parameters

Fuel Type	Burnup [MWd/MTU]	Number Cycles	Assy Power [MW]	Cycle Length [d]
PWR	80,000	3	19.36	636.4
BWR 7×7	60,000	4	5.85	547.0
BWR 7×7	70,000	4	5.85	638.1
BWR 7×7	80,000	4	5.85	730.0
BWR 8×8	80,000	4	5.56	730.0

Table 5.3.8-3 SCALE 27N18G Neutron Group Structure and ANSI Dose Factors

Group	Lower E [MeV]	Upper E [MeV]	Avg E [MeV]	Dose Factor [(rem/hr)/(n/cm ² /s)]
1	6.43E+00	2.00E+01	1.32E+01	1.49E-04
2	3.00E+00	6.43E+00	4.72E+00	1.45E-04
3	1.85E+00	3.00E+00	2.43E+00	1.27E-04
4	1.40E+00	1.85E+00	1.63E+00	1.28E-04
5	9.00E-01	1.40E+00	1.15E+00	1.30E-04
6	4.00E-01	9.00E-01	6.50E-01	1.03E-04
7	1.00E-01	4.00E-01	2.50E-01	5.12E-05
8	1.70E-02	1.00E-01	5.85E-02	1.23E-05
9	3.00E-03	1.70E-02	1.00E-02	3.84E-06
10	5.50E-04	3.00E-03	1.78E-03	3.72E-06
11	1.00E-04	5.50E-04	3.25E-04	4.02E-06
12	3.00E-05	1.00E-04	6.50E-05	4.29E-06
13	1.00E-05	3.00E-05	2.00E-05	4.47E-06
14	3.05E-06	1.00E-05	6.52E-06	4.57E-06
15	1.77E-06	3.05E-06	2.41E-06	4.56E-06
16	1.30E-06	1.77E-06	1.53E-06	4.52E-06
17	1.13E-06	1.30E-06	1.21E-06	4.49E-06
18	1.00E-06	1.13E-06	1.06E-06	4.47E-06
19	8.00E-07	1.00E-06	9.00E-07	4.43E-06
20	4.00E-07	8.00E-07	6.00E-07	4.33E-06
21	3.25E-07	4.00E-07	3.63E-07	4.20E-06
22	2.25E-07	3.25E-07	2.75E-07	4.10E-06
23	1.00E-07	2.25E-07	1.62E-07	3.84E-06
24	5.00E-08	1.00E-07	7.50E-08	3.67E-06
25	3.00E-08	5.00E-08	4.00E-08	3.67E-06
26	1.00E-08	3.00E-08	2.00E-08	3.67E-06
27	1.00E-11	1.00E-08	5.01E-09	3.67E-06

Table 5.3.8-4 SCALE 27N18G Gamma Group Structure and ANSI Dose Factors

Group	Lower E [MeV]	Upper E [MeV]	Avg E [MeV]	Dose Factor [(rem/hr)/(γ/cm ² /s)]
1	8.00E+00	1.00E+01	9.00E+00	8.77E-06
2	6.50E+00	8.00E+00	7.25E+00	7.48E-06
3	5.00E+00	6.50E+00	5.75E+00	6.37E-06
4	4.00E+00	5.00E+00	4.50E+00	5.41E-06
5	3.00E+00	4.00E+00	3.50E+00	4.62E-06
6	2.50E+00	3.00E+00	2.75E+00	3.96E-06
7	2.00E+00	2.50E+00	2.25E+00	3.47E-06
8	1.66E+00	2.00E+00	1.83E+00	3.02E-06
9	1.33E+00	1.66E+00	1.50E+00	2.63E-06
10	1.00E+00	1.33E+00	1.17E+00	2.21E-06
11	8.00E-01	1.00E+00	9.00E-01	1.83E-06
12	6.00E-01	8.00E-01	7.00E-01	1.52E-06
13	4.00E-01	6.00E-01	5.00E-01	1.17E-06
14	3.00E-01	4.00E-01	3.50E-01	8.76E-07
15	2.00E-01	3.00E-01	2.50E-01	6.31E-07
16	1.00E-01	2.00E-01	1.50E-01	3.83E-07
17	5.00E-02	1.00E-01	7.50E-02	2.67E-07
18	1.00E-02	5.00E-02	3.00E-02	9.35E-07

Table 5.3.8-5 LWT Cask Total Decay Heat [kW] for 25 Rods at Various Cool Times

Fuel Type	Burnup [MWd/MTU]	Decay Time [d]						
		150	180	210	240	270	300	365
PWR	80,000	2.25	2.05	1.87	1.73	1.62	1.52	1.35
BWR 7×7	60,000	2.40	2.17	1.98	1.83	1.70	1.59	1.39
BWR 7×7	70,000	2.61	2.38	2.18	2.02	1.89	1.78	1.58
BWR 7×7	80,000	2.80	2.57	2.37	2.21	2.07	1.96	1.75
BWR 8×8	80,000	2.06	1.89	1.75	1.63	1.53	1.44	1.29

Table 5.3.8-6 PWR 80,000 MWd/MTU Fuel Model Neutron Source Term [n/sec/assy]

Group	Decay Time [d]						
	150	180	210	240	270	300	365
1	8.1050E+07	8.0010E+07	7.9030E+07	7.8110E+07	7.7240E+07	7.6400E+07	7.4730E+07
2	9.2480E+08	9.1140E+08	8.9880E+08	8.8710E+08	8.7610E+08	8.6570E+08	8.4510E+08
3	1.0070E+09	9.9240E+08	9.7890E+08	9.6620E+08	9.5430E+08	9.4310E+08	9.2080E+08
4	5.6830E+08	5.6090E+08	5.5400E+08	5.4740E+08	5.4130E+08	5.3540E+08	5.2360E+08
5	7.7310E+08	7.6320E+08	7.5400E+08	7.4520E+08	7.3690E+08	7.2900E+08	7.1320E+08
6	8.4670E+08	8.3590E+08	8.2570E+08	8.1610E+08	8.0700E+08	7.9830E+08	7.8090E+08
7	1.6590E+08	1.6370E+08	1.6170E+08	1.5980E+08	1.5800E+08	1.5630E+08	1.5290E+08
Total	4.3670E+09	4.3080E+09	4.2520E+09	4.2000E+09	4.1510E+09	4.1040E+09	4.0110E+09

Table 5.3.8-7 PWR 80,000 MWd/MTU Fuel Model Gamma Source Term [γ/sec/assy]

Group	Decay Time [d]						
	150	180	210	240	270	300	365
1	2.3232E+06	2.2933E+06	2.2655E+06	2.2394E+06	2.2149E+06	2.1918E+06	2.1458E+06
2	1.0942E+07	1.0801E+07	1.0670E+07	1.0547E+07	1.0432E+07	1.0323E+07	1.0106E+07
3	5.5776E+07	5.5059E+07	5.4390E+07	5.3764E+07	5.3175E+07	5.2619E+07	5.1514E+07
4	1.3897E+08	1.3719E+08	1.3552E+08	1.3396E+08	1.3249E+08	1.3110E+08	1.2835E+08
5	4.2790E+11	4.0245E+11	3.8014E+11	3.5939E+11	3.3983E+11	3.2136E+11	2.8470E+11
6	3.8055E+12	3.3306E+12	3.0956E+12	2.9155E+12	2.7535E+12	2.6020E+12	2.3025E+12
7	1.5053E+14	1.3842E+14	1.2854E+14	1.1969E+14	1.1155E+14	1.0400E+14	8.9386E+13
8	5.0113E+13	4.5330E+13	4.1850E+13	3.8948E+13	3.6392E+13	3.4088E+13	2.9742E+13
9	4.9111E+14	4.5948E+14	4.3646E+14	4.1614E+14	3.9727E+14	3.7955E+14	3.4454E+14
10	1.0333E+15	9.8515E+14	9.4552E+14	9.1017E+14	8.7765E+14	8.4736E+14	7.8780E+14
11	4.2618E+15	4.1142E+15	3.9785E+15	3.8505E+15	3.7284E+15	3.6117E+15	3.3748E+15
12	3.1096E+16	2.6322E+16	2.2653E+16	1.9844E+16	1.7692E+16	1.6036E+16	1.3594E+16
13	1.4249E+16	1.2805E+16	1.1793E+16	1.1042E+16	1.0449E+16	9.9572E+15	9.0869E+15
14	1.4614E+15	1.3614E+15	1.2732E+15	1.1934E+15	1.1206E+15	1.0535E+15	9.2448E+14
15	1.9165E+15	1.7798E+15	1.6605E+15	1.5544E+15	1.4588E+15	1.3717E+15	1.2061E+15
16	7.6172E+15	6.8766E+15	6.3117E+15	5.8531E+15	5.4626E+15	5.1189E+15	4.4821E+15
17	7.6978E+15	7.1504E+15	6.6731E+15	6.2484E+15	5.8655E+15	5.5167E+15	4.8539E+15
18	2.3353E+16	2.1519E+16	1.9991E+16	1.8675E+16	1.7514E+16	1.6472E+16	1.4518E+16
Total	9.3381E+16	8.3560E+16	7.5891E+16	6.9749E+16	6.4717E+16	6.0505E+16	5.3295E+16

**Table 5.3.8-8 BWR 7x7 60,000 MWd/MTU Fuel Model Neutron Source Term
[n/sec/assy]**

Group	Decay Time [d]						
	150	180	210	240	270	300	365
1	1.0720E+07	1.0520E+07	1.0340E+07	1.0180E+07	1.0040E+07	9.9050E+06	9.6580E+06
2	1.2660E+08	1.2370E+08	1.2110E+08	1.1880E+08	1.1670E+08	1.1470E+08	1.1120E+08
3	1.3820E+08	1.3500E+08	1.3220E+08	1.2970E+08	1.2750E+08	1.2540E+08	1.2160E+08
4	7.5740E+07	7.4310E+07	7.3020E+07	7.1860E+07	7.0800E+07	6.9850E+07	6.8050E+07
5	1.0230E+08	1.0050E+08	9.8780E+07	9.7260E+07	9.5880E+07	9.4630E+07	9.2290E+07
6	1.1190E+08	1.0990E+08	1.0800E+08	1.0640E+08	1.0490E+08	1.0350E+08	1.0090E+08
7	2.1940E+07	2.1530E+07	2.1170E+07	2.0840E+07	2.0550E+07	2.0280E+07	1.9770E+07
Total	5.8740E+08	5.7550E+08	5.6470E+08	5.5500E+08	5.4630E+08	5.3830E+08	5.2350E+08

**Table 5.3.8-9 BWR 7x7 60,000 MWd/MTU Fuel Model Gamma Source Term
[γ/sec/assy]**

Group	Decay Time [d]						
	150	180	210	240	270	300	365
1	3.2931E+05	3.2274E+05	3.1683E+05	3.1151E+05	3.0671E+05	3.0237E+05	2.9427E+05
2	1.5512E+06	1.5202E+06	1.4924E+06	1.4673E+06	1.4447E+06	1.4242E+06	1.3860E+06
3	7.9088E+06	7.7507E+06	7.6086E+06	7.4806E+06	7.3651E+06	7.2606E+06	7.0658E+06
4	1.9710E+07	1.9315E+07	1.8961E+07	1.8642E+07	1.8353E+07	1.8092E+07	1.7606E+07
5	1.1468E+11	1.0776E+11	1.0177E+11	9.6205E+10	9.0967E+10	8.6019E+10	7.6202E+10
6	1.0391E+12	8.9960E+11	8.3400E+11	7.8498E+11	7.4121E+11	7.0037E+11	6.1963E+11
7	4.5886E+13	4.2337E+13	3.9344E+13	3.6637E+13	3.4138E+13	3.1817E+13	2.7325E+13
8	1.3614E+13	1.2407E+13	1.1497E+13	1.0722E+13	1.0033E+13	9.4069E+12	8.2168E+12
9	1.3126E+14	1.2257E+14	1.1646E+14	1.1113E+14	1.0619E+14	1.0154E+14	9.2359E+13
10	3.0058E+14	2.8714E+14	2.7599E+14	2.6605E+14	2.5694E+14	2.4847E+14	2.3186E+14
11	1.1408E+15	1.1018E+15	1.0661E+15	1.0324E+15	1.0003E+15	9.6961E+14	9.0725E+14
12	9.4684E+15	7.9625E+15	6.8088E+15	5.9289E+15	5.2583E+15	4.7452E+15	3.9979E+15
13	3.8994E+15	3.4870E+15	3.2005E+15	2.9896E+15	2.8249E+15	2.6892E+15	2.4513E+15
14	4.3090E+14	4.0087E+14	3.7459E+14	3.5098E+14	3.2950E+14	3.0980E+14	2.7208E+14
15	5.6889E+14	5.2746E+14	4.9163E+14	4.6001E+14	4.3166E+14	4.0596E+14	3.5735E+14
16	2.3056E+15	2.0775E+15	1.9047E+15	1.7652E+15	1.6471E+15	1.5436E+15	1.3528E+15
17	2.3068E+15	2.1396E+15	1.9949E+15	1.8672E+15	1.7526E+15	1.6488E+15	1.4525E+15
18	7.0478E+15	6.4851E+15	6.0194E+15	5.6207E+15	5.2710E+15	4.9585E+15	4.3763E+15
Total	2.7661E+16	2.4647E+16	2.2305E+16	2.0441E+16	1.8923E+16	1.7662E+16	1.5527E+16

**Table 5.3.8-10 BWR 7x7 70,000 MWd/MTU Fuel Model Neutron Source Term
[n/sec/assy]**

Group	Decay Time [d]						
	150	180	210	240	270	300	365
1	2.0300E+07	2.0020E+07	1.9760E+07	1.9520E+07	1.9290E+07	1.9090E+07	1.8680E+07
2	2.3450E+08	2.3060E+08	2.2700E+08	2.2370E+08	2.2070E+08	2.1800E+08	2.1260E+08
3	2.5560E+08	2.5140E+08	2.4760E+08	2.4400E+08	2.4080E+08	2.3780E+08	2.3210E+08
4	1.4280E+08	1.4070E+08	1.3890E+08	1.3720E+08	1.3560E+08	1.3410E+08	1.3120E+08
5	1.9370E+08	1.9100E+08	1.8860E+08	1.8630E+08	1.8420E+08	1.8220E+08	1.7840E+08
6	2.1200E+08	2.0910E+08	2.0640E+08	2.0390E+08	2.0160E+08	1.9940E+08	1.9520E+08
7	4.1540E+07	4.0960E+07	4.0430E+07	3.9940E+07	3.9490E+07	3.9060E+07	3.8230E+07
Total	1.1000E+09	1.0840E+09	1.0690E+09	1.0550E+09	1.0420E+09	1.0300E+09	1.0060E+09

**Table 5.3.8-11 BWR 7x7 70,000 MWd/MTU Fuel Model Gamma Source Term
[γ/sec/assy]**

Group	Decay Time [d]						
	150	180	210	240	270	300	365
1	6.0324E+05	5.9443E+05	5.8638E+05	5.7897E+05	5.7215E+05	5.6585E+05	5.5368E+05
2	2.8412E+06	2.7998E+06	2.7618E+06	2.7269E+06	2.6948E+06	2.6650E+06	2.6077E+06
3	1.4485E+07	1.4273E+07	1.4079E+07	1.3901E+07	1.3737E+07	1.3586E+07	1.3293E+07
4	3.6093E+07	3.5565E+07	3.5082E+07	3.4638E+07	3.4229E+07	3.3851E+07	3.3121E+07
5	1.2918E+11	1.2149E+11	1.1474E+11	1.0848E+11	1.0258E+11	9.7000E+10	8.5934E+10
6	1.1503E+12	1.0061E+12	9.3500E+11	8.8057E+11	8.3162E+11	7.8586E+11	6.9541E+11
7	4.5889E+13	4.2245E+13	3.9241E+13	3.6544E+13	3.4060E+13	3.1754E+13	2.7290E+13
8	1.5067E+13	1.3671E+13	1.2642E+13	1.1778E+13	1.1013E+13	1.0322E+13	9.0142E+12
9	1.5436E+14	1.4472E+14	1.3769E+14	1.3149E+14	1.2572E+14	1.2029E+14	1.0955E+14
10	3.4479E+14	3.2983E+14	3.1746E+14	3.0640E+14	2.9622E+14	2.8673E+14	2.6805E+14
11	1.3888E+15	1.3419E+15	1.2988E+15	1.2579E+15	1.2190E+15	1.1817E+15	1.1059E+15
12	1.0027E+16	8.5551E+15	7.4228E+15	6.5551E+15	5.8895E+15	5.3763E+15	4.6175E+15
13	4.5056E+15	4.0651E+15	3.7549E+15	3.5230E+15	3.3394E+15	3.1861E+15	2.9133E+15
14	4.5235E+14	4.2171E+14	3.9475E+14	3.7041E+14	3.4818E+14	3.2773E+14	2.8843E+14
15	5.9741E+14	5.5540E+14	5.1883E+14	4.8637E+14	4.5715E+14	4.3055E+14	3.8002E+14
16	2.3773E+15	2.1503E+15	1.9773E+15	1.8369E+15	1.7174E+15	1.6122E+15	1.4174E+15
17	2.4086E+15	2.2405E+15	2.0940E+15	1.9640E+15	1.8467E+15	1.7400E+15	1.5374E+15
18	7.3510E+15	6.7875E+15	6.3182E+15	5.9142E+15	5.5579E+15	5.2383E+15	4.6398E+15
Total	2.9670E+16	2.6649E+16	2.4287E+16	2.2395E+16	2.0843E+16	1.9542E+16	1.7314E+16

Table 5.3.8-12 BWR 7x7 80,000 MWd/MTU Fuel Model Neutron Source Term
[n/sec/assy]

Group	Decay Time [d]						
	150	180	210	240	270	300	365
1	3.8790E+07	3.8290E+07	3.7810E+07	3.7350E+07	3.6920E+07	3.6500E+07	3.5660E+07
2	4.4140E+08	4.3500E+08	4.2900E+08	4.2330E+08	4.1790E+08	4.1280E+08	4.0260E+08
3	4.8040E+08	4.7340E+08	4.6690E+08	4.6080E+08	4.5500E+08	4.4950E+08	4.3850E+08
4	2.7180E+08	2.6820E+08	2.6480E+08	2.6160E+08	2.5850E+08	2.5560E+08	2.4970E+08
5	3.6990E+08	3.6510E+08	3.6060E+08	3.5630E+08	3.5220E+08	3.4820E+08	3.4020E+08
6	4.0520E+08	4.0000E+08	3.9500E+08	3.9020E+08	3.8570E+08	3.8140E+08	3.7260E+08
7	7.9380E+07	7.8340E+07	7.7360E+07	7.6430E+07	7.5540E+07	7.4690E+07	7.2970E+07
Total	2.0870E+09	2.0580E+09	2.0310E+09	2.0060E+09	1.9820E+09	1.9590E+09	1.9120E+09

Table 5.3.8-13 BWR 7x7 80,000 MWd/MTU Fuel Model Gamma Source Term
[γ/sec/assy]

Group	Decay Time [d]						
	150	180	210	240	270	300	365
1	1.0954E+06	1.0813E+06	1.0680E+06	1.0555E+06	1.0437E+06	1.0325E+06	1.0100E+06
2	5.1590E+06	5.0924E+06	5.0300E+06	4.9710E+06	4.9153E+06	4.8625E+06	4.7566E+06
3	2.6298E+07	2.5959E+07	2.5640E+07	2.5340E+07	2.5056E+07	2.4786E+07	2.4246E+07
4	6.5524E+07	6.4678E+07	6.3884E+07	6.3135E+07	6.2427E+07	6.1755E+07	6.0409E+07
5	1.4025E+11	1.3197E+11	1.2467E+11	1.1787E+11	1.1145E+11	1.0540E+11	9.3384E+10
6	1.2350E+12	1.0871E+12	1.0118E+12	9.5327E+11	9.0040E+11	8.5091E+11	7.5306E+11
7	4.5796E+13	4.2083E+13	3.9076E+13	3.6393E+13	3.3924E+13	3.1634E+13	2.7203E+13
8	1.6213E+13	1.4660E+13	1.3531E+13	1.2592E+13	1.1766E+13	1.1023E+13	9.6211E+12
9	1.7524E+14	1.6472E+14	1.5685E+14	1.4984E+14	1.4331E+14	1.3717E+14	1.2500E+14
10	3.8063E+14	3.6437E+14	3.5095E+14	3.3895E+14	3.2788E+14	3.1755E+14	2.9718E+14
11	1.6124E+15	1.5582E+15	1.5081E+15	1.4608E+15	1.4155E+15	1.3722E+15	1.2842E+15
12	1.0580E+16	9.1279E+15	8.0071E+15	7.1444E+15	6.4791E+15	5.9627E+15	5.1894E+15
13	5.0278E+15	4.5657E+15	4.2366E+15	3.9878E+15	3.7884E+15	3.6203E+15	3.3179E+15
14	4.6875E+14	4.3760E+14	4.1008E+14	3.8518E+14	3.6237E+14	3.4135E+14	3.0088E+14
15	6.1935E+14	5.7682E+14	5.3964E+14	5.0652E+14	4.7661E+14	4.4932E+14	3.9734E+14
16	2.4314E+15	2.2052E+15	2.0320E+15	1.8908E+15	1.7703E+15	1.6639E+15	1.4664E+15
17	2.4876E+15	2.3184E+15	2.1705E+15	2.0386E+15	1.9194E+15	1.8105E+15	1.6032E+15
18	7.5934E+15	7.0287E+15	6.5564E+15	6.1482E+15	5.7870E+15	5.4621E+15	4.8515E+15
Total	3.1441E+16	2.8406E+16	2.6022E+16	2.4101E+16	2.2517E+16	2.1181E+16	1.8871E+16

**Table 5.3.8-14 BWR 8x8 80,000 MWd/MTU Fuel Model Neutron Source Term
[n/sec/assy]**

Group	Decay Time [d]						
	150	180	210	240	270	300	365
1	3.5570E+07	3.5120E+07	3.4700E+07	3.4290E+07	3.3910E+07	3.3540E+07	3.2800E+07
2	4.0480E+08	3.9910E+08	3.9380E+08	3.8870E+08	3.8390E+08	3.7940E+08	3.7040E+08
3	4.4060E+08	4.3450E+08	4.2870E+08	4.2320E+08	4.1810E+08	4.1320E+08	4.0340E+08
4	2.4930E+08	2.4610E+08	2.4310E+08	2.4020E+08	2.3750E+08	2.3490E+08	2.2970E+08
5	3.3930E+08	3.3500E+08	3.3100E+08	3.2710E+08	3.2350E+08	3.2000E+08	3.1300E+08
6	3.7160E+08	3.6690E+08	3.6250E+08	3.5830E+08	3.5430E+08	3.5050E+08	3.4270E+08
7	7.2790E+07	7.1870E+07	7.1000E+07	7.0170E+07	6.9380E+07	6.8630E+07	6.7120E+07
Total	1.9140E+09	1.8890E+09	1.8650E+09	1.8420E+09	1.8210E+09	1.8000E+09	1.7590E+09

**Table 5.3.8-15 BWR 8x8 80,000 MWd/MTU Fuel Model Gamma Source Term
[γ/sec/assy]**

Group	Decay Time [d]						
	150	180	210	240	270	300	365
1	1.0111E+06	9.9843E+05	9.8657E+05	9.7541E+05	9.6486E+05	9.5486E+05	9.3484E+05
2	4.7618E+06	4.7023E+06	4.6464E+06	4.5938E+06	4.5441E+06	4.4971E+06	4.4027E+06
3	2.4273E+07	2.3970E+07	2.3685E+07	2.3417E+07	2.3163E+07	2.2923E+07	2.2442E+07
4	6.0480E+07	5.9723E+07	5.9013E+07	5.8344E+07	5.7712E+07	5.7114E+07	5.5915E+07
5	1.3406E+11	1.2615E+11	1.1916E+11	1.1266E+11	1.0654E+11	1.0075E+11	8.9259E+10
6	1.1796E+12	1.0388E+12	9.6696E+11	9.1101E+11	8.6048E+11	8.1319E+11	7.1969E+11
7	4.3512E+13	3.9982E+13	3.7126E+13	3.4578E+13	3.2233E+13	3.0058E+13	2.5849E+13
8	1.5435E+13	1.3964E+13	1.2896E+13	1.2005E+13	1.1222E+13	1.0515E+13	9.1811E+12
9	1.6587E+14	1.5590E+14	1.4845E+14	1.4181E+14	1.3563E+14	1.2981E+14	1.1830E+14
10	3.6038E+14	3.4497E+14	3.3223E+14	3.2084E+14	3.1033E+14	3.0051E+14	2.8115E+14
11	1.5243E+15	1.4731E+15	1.4258E+15	1.3810E+15	1.3382E+15	1.2973E+15	1.2140E+15
12	1.0033E+16	8.6556E+15	7.5925E+15	6.7743E+15	6.1433E+15	5.6535E+15	4.9201E+15
13	4.7720E+15	4.3323E+15	4.0194E+15	3.7827E+15	3.5932E+15	3.4334E+15	3.1462E+15
14	4.4637E+14	4.1676E+14	3.9060E+14	3.6690E+14	3.4520E+14	3.2519E+14	2.8665E+14
15	5.8943E+14	5.4903E+14	5.1370E+14	4.8221E+14	4.5375E+14	4.2778E+14	3.7831E+14
16	2.3111E+15	2.0962E+15	1.9316E+15	1.7974E+15	1.6829E+15	1.5817E+15	1.3939E+15
17	2.3651E+15	2.2044E+15	2.0638E+15	1.9384E+15	1.8250E+15	1.7215E+15	1.5243E+15
18	7.2203E+15	6.6839E+15	6.2352E+15	5.8471E+15	5.5038E+15	5.1949E+15	4.6141E+15
Total	2.9848E+16	2.6967E+16	2.4704E+16	2.2881E+16	2.1376E+16	2.0107E+16	1.7912E+16

Table 5.3.8-16 Fuel Axial Source Profile Parameters

Type	Burnup Peak to Average	Source	Exponent b	Average Source to Average Burnup	Source Peak to Average
PWR	1.08	Neutron	4.22	1.125	1.230
		Gamma	1.00	1.000	1.080
BWR	1.22	Neutron	4.22	1.582	1.463
		Gamma	1.00	1.000	1.220

Table 5.3.8-17 PWR Fuel Axial Source Profile

% Core Height	Burnup Profile	Photon Source	Neutron Source
0.00%	0.5470	0.5470	7.840E-02
2.50%	0.6358	0.6358	1.479E-01
5.00%	0.7247	0.7247	2.569E-01
7.50%	0.8135	0.8135	4.185E-01
10.00%	0.9023	0.9023	6.481E-01
12.50%	0.9912	0.9912	9.633E-01
15.00%	1.0800	1.0800	1.384E+00
50.00%	1.0790	1.0790	1.378E+00
85.00%	1.0800	1.0800	1.384E+00
87.50%	0.9912	0.9912	9.633E-01
90.00%	0.9023	0.9023	6.481E-01
92.50%	0.8135	0.8135	4.185E-01
95.00%	0.7247	0.7247	2.569E-01
97.50%	0.6358	0.6358	1.479E-01
100.00%	0.5470	0.5470	7.840E-02

Table 5.3.8-18 BWR Fuel Axial Source Profile

% Core Height	Burnup Profile	Photon Source	Neutron Source
0.00%	0.0430	0.0430	1.711E-06
2.50%	0.2392	0.2392	2.388E-03
5.00%	0.4353	0.4353	2.991E-02
7.50%	0.6315	0.6315	1.437E-01
10.00%	0.8277	0.8277	4.501E-01
12.50%	1.0238	1.0238	1.105E+00
15.00%	1.2200	1.2200	2.314E+00
50.00%	1.2190	1.2190	2.306E+00
55.00%	1.2200	1.2200	2.314E+00
55.01%	1.1800	1.1800	2.011E+00
80.00%	1.1810	1.1810	2.018E+00
82.50%	1.0379	1.0379	1.170E+00
85.00%	0.8958	0.8958	6.284E-01
87.50%	0.7536	0.7536	3.031E-01
90.00%	0.6115	0.6115	1.255E-01
92.50%	0.4694	0.4694	4.110E-02
95.00%	0.3272	0.3272	8.970E-03
97.50%	0.1851	0.1851	8.104E-04
100.00%	0.0430	0.0430	1.711E-06

Table 5.3.8-19 Fuel Region Homogenized Material Description [atom/b-cm]

SCALE Isotope	Number Density [atom/b-cm]		
	PWR	BWR 7x7	BWR 8x8
OXYGEN-16	1.04184E-02	1.72764E-02	1.27718E-02
CHROMIUM(SS304)	1.99453E-03	1.99453E-03	1.99453E-03
MANGANESE	1.98706E-04	1.98706E-04	1.98706E-04
IRON(SS304)	6.79292E-03	6.79292E-03	6.79292E-03
NICKEL(SS304)	8.83557E-04	8.83557E-04	8.83557E-04
ZIRCONIUM ALLOY	2.88833E-03	5.16316E-03	4.24529E-03
URANIUM-234	2.86507E-07	4.75102E-07	3.51224E-07
URANIUM-235	3.75064E-05	6.21953E-05	4.59785E-05
URANIUM-238	5.17142E-03	8.57554E-03	6.33956E-03

Table 5.3.8-20 Basket and Cask Shielding Material Composition [atom/b-cm]

Material	SCALE Isotope	Number Density [atom/b-cm]
Aluminum	ALUMINUM	6.03066E-02
Stainless Steel 304	CHROMIUM(SS304)	1.74286E-02
	MANGANESE	1.73633E-03
	IRON(SS304)	5.93579E-02
	NICKEL(SS304)	7.72070E-03
Lead	LEAD	3.29690E-02
Neutron Shield	HYDROGEN	5.99351E-02
	CARBON-12	1.07197E-02
	OXYGEN-16	2.46077E-02

Table 5.3.8-21 Basket Model Parameters

Parameter	Outer Dimension		Thickness	
	[in]	[cm]	[in]	[cm]
Array size	3.5600	9.0424	-	-
Fuel pin insert tube	0.6875	1.7463	0.0280	0.0711
Internal spacer	3.9350	9.9949	0.1875	0.4763
Void	5.0000	12.7000	0.5325	1.3526
Weldment tube	5.5000	13.9700	0.2500	0.6350
Void	5.7500	14.6050	0.1250	0.3175
Insert wall	8.5000	21.5900	1.3750	3.4925
Basket opening	8.8800	22.5552	-	-

Table 5.3.8-22 LWT Cask One-Dimensional Model for LWR High Burnup Rod Analysis

Model Region	Material	Outer Radius[cm]
Rod array	Fuel	5.1016
Spacer	SS304	5.6390
Spacer void	Void	7.1652
Weldment wall	SS304	7.8817
Weldment void	Void	8.2400
Insert wall	Aluminum	12.1809
Insert void	Void	12.7254
Basket	Aluminum	16.9863
Inner shell	SS304	18.8214
Lead Shield	Lead	33.2890
Lead Gap	Void	33.4264
Outer Shell	SS304	36.3728
Neutron Shield	Neutron Shield	49.0728
Shield Shell	SS304	49.1338

Table 5.3.8-23 LWT Cask Surface Neutron Dose Response Function

Surface Neutron Dose Response [(mrem/hr)/(10 ¹⁰ n/cm ² /sec)]			
Group	PWR	BWR-7x7	BWR-8x8
1	2.7193E+07	2.6380E+07	2.6835E+07
2	1.6896E+07	1.6513E+07	1.6726E+07
3	1.5997E+07	1.5593E+07	1.5829E+07
4	1.2227E+07	1.1960E+07	1.2127E+07
5	1.0406E+07	1.0101E+07	1.0295E+07
6	8.3940E+06	8.2487E+06	8.3427E+06
7	6.2803E+06	6.1775E+06	6.2441E+06

Table 5.3.8-24 LWT Cask Surface Gamma Dose Response Function

Surface Gamma Dose Response [(mrem/hr)/(10 ¹⁰ γ/cm ² /sec)]			
Group	PWR	BWR-7X7	BWR-8X8
1	1.2725E+03	1.0022E+03	1.1584E+03
2	1.6222E+03	1.2839E+03	1.4795E+03
3	1.7521E+03	1.3907E+03	1.5995E+03
4	1.6430E+03	1.3055E+03	1.5002E+03
5	1.3176E+03	1.0457E+03	1.2020E+03
6	8.4261E+02	6.6508E+02	7.6670E+02
7	4.5052E+02	3.5272E+02	4.0845E+02
8	1.7075E+02	1.3183E+02	1.5387E+02
9	4.8503E+01	3.6807E+01	4.3389E+01
10	5.5182E+00	4.0692E+00	4.8783E+00
11	1.6030E-01	1.1350E-01	1.3927E-01
12	1.5868E-03	1.0805E-03	1.3561E-03
13	1.4339E-08	9.2536E-09	1.1975E-08
14	5.4441E-25	3.3976E-25	4.4798E-25
15	0.0000E+00	0.0000E+00	0.0000E+00
16	0.0000E+00	0.0000E+00	0.0000E+00
17	0.0000E+00	0.0000E+00	0.0000E+00
18	0.0000E+00	0.0000E+00	0.0000E+00

Table 5.3.8-25 LWT Cask 2m Neutron Dose Response Function

2m Neutron Dose Response [(mrem/hr)/(10 ⁻⁶ n/cm ² /sec)]			
Group	PWR	BWR-7X7	BWR-8X8
1	2.3145E+06	2.2330E+06	2.2792E+06
2	1.3767E+06	1.3396E+06	1.3604E+06
3	1.2981E+06	1.2593E+06	1.2821E+06
4	9.5362E+05	9.2901E+05	9.4445E+05
5	7.8702E+05	7.6091E+05	7.7751E+05
6	6.0300E+05	5.9196E+05	5.9909E+05
7	4.2815E+05	4.2161E+05	4.2585E+05

Table 5.3.8-26 LWT Cask 2m Gamma Dose Response Function

2m Gamma Dose Response [(mrem/hr)/(10 ⁻⁶ γ/cm ² /sec)]			
Group	PWR	BWR-7X7	BWR-8X8
1	1.6112E+02	1.2688E+02	1.4667E+02
2	2.0395E+02	1.6141E+02	1.8600E+02
3	2.1743E+02	1.7261E+02	1.9851E+02
4	2.0052E+02	1.5935E+02	1.8310E+02
5	1.5806E+02	1.2547E+02	1.4421E+02
6	9.9064E+01	7.8207E+01	9.0147E+01
7	5.2070E+01	4.0775E+01	4.7212E+01
8	1.9335E+01	1.4930E+01	1.7425E+01
9	5.3870E+00	4.0885E+00	4.8193E+00
10	5.9731E-01	4.4050E-01	5.2806E-01
11	1.6841E-02	1.1924E-02	1.4631E-02
12	1.6212E-04	1.1039E-04	1.3855E-04
13	1.4138E-09	9.1234E-10	1.1807E-09
14	5.2387E-26	3.2694E-26	4.3107E-26
15	0.0000E+00	0.0000E+00	0.0000E+00
16	0.0000E+00	0.0000E+00	0.0000E+00
17	0.0000E+00	0.0000E+00	0.0000E+00
18	0.0000E+00	0.0000E+00	0.0000E+00

Table 5.3.8-27 Surface Dose Responses [mrem/hr] and Cask Decay Heat [kW] for Various Decay Times

Fuel	Burnup [GWd/MTU]	Source	Decay Time [d]						
			150	180	210	240	270	300	365
PWR	80	Neutron	35.2	34.7	34.3	33.8	33.4	33.0	32.3
		Gamma	53.1	49.0	45.8	43.0	40.4	38.0	33.3
		Total	88.3	83.7	80.1	76.8	73.8	71.1	65.6
		Heat	2.3	2.0	1.9	1.7	1.6	1.5	1.3
BWR 7x7	80	Neutron	98.6	97.2	96.0	94.7	93.6	92.5	90.3
		Gamma	53.6	49.5	46.4	43.6	41.0	38.6	34.0
		Total	152.2	146.8	142.3	138.3	134.6	131.1	124.3
		Heat	2.8	2.6	2.4	2.2	2.1	2.0	1.8
	70	Neutron	52.1	51.3	50.6	49.9	49.3	48.7	47.6
		Gamma	51.4	47.5	44.4	41.7	39.3	36.9	32.4
		Total	103.5	98.8	95.0	91.6	88.5	85.6	80.0
		Heat	2.6	2.4	2.2	2.0	1.9	1.8	1.6
	60	Neutron	27.9	27.3	26.8	26.3	25.9	25.5	24.8
		Gamma	48.8	45.1	42.2	39.5	37.1	34.9	30.6
		Total	76.7	72.4	68.9	65.8	63.0	60.4	55.4
		Heat	2.4	2.2	2.0	1.8	1.7	1.6	1.4
BWR 8x8	80	Neutron	71.4	70.4	69.5	68.6	67.8	67.1	65.5
		Gamma	46.2	42.7	39.9	37.5	35.3	33.3	29.3
		Total	117.5	113.1	109.5	106.2	103.2	100.4	94.9
		Heat	2.1	1.9	1.7	1.6	1.5	1.4	1.3

Table 5.3.8-28 2m Dose Responses [mrem/hr] and Cask Decay Heat [kW] for Various Decay Times

Fuel	Burnup [GWd/MTU]	Source	Decay Time [d]						
			150	180	210	240	270	300	365
PWR	80	Neutron	2.3	2.2	2.2	2.2	2.1	2.1	2.1
		Gamma	5.6	5.2	4.8	4.5	4.3	4.0	3.5
		Total	7.9	7.4	7.0	6.7	6.4	6.1	5.6
		Heat	2.3	2.0	1.9	1.7	1.6	1.5	1.3
BWR 7x7	80	Neutron	5.3	5.2	5.1	5.1	5.0	5.0	4.8
		Gamma	5.0	4.6	4.3	4.1	3.8	3.6	3.2
		Total	10.3	9.8	9.5	9.2	8.8	8.6	8.0
		Heat	2.8	2.6	2.4	2.2	2.1	2.0	1.8
	70	Neutron	2.8	2.8	2.7	2.7	2.6	2.6	2.6
		Gamma	4.8	4.4	4.2	3.9	3.7	3.4	3.0
		Total	7.6	7.2	6.9	6.6	6.3	6.1	5.6
		Heat	2.6	2.4	2.2	2.0	1.9	1.8	1.6
	60	Neutron	1.5	1.5	1.4	1.4	1.4	1.4	1.3
		Gamma	4.6	4.2	3.9	3.7	3.5	3.3	2.9
		Total	6.1	5.7	5.4	5.1	4.9	4.6	4.2
		Heat	2.4	2.2	2.0	1.8	1.7	1.6	1.4
BWR 8x8	80	Neutron	3.8	3.8	3.7	3.7	3.6	3.6	3.5
		Gamma	4.3	4.0	3.7	3.5	3.3	3.1	2.7
		Total	8.1	7.8	7.5	7.2	6.9	6.7	6.3
		Heat	2.1	1.9	1.7	1.6	1.5	1.4	1.3

Table 5.3.8-29 Loading Table for PWR and BWR High Burnup Rods Showing Minimum Required Cool Time as a Function of Burnup and Enrichment

Fuel Type	Burnup, b	Minimum Cool Time
	[GWd/MTU]	[d]
PWR	$b \leq 80$	150
BWR 7×7	$b \leq 60$	210
	$60 < b \leq 70$	240
	$70 < b \leq 80$	270
BWR 8×8 ¹	$b \leq 80$	150

¹ Includes rods from all larger BWR assembly arrays (e.g., 9×9, 10×10).

5.3.9 DIDO Fuel Configuration

A maximum of 42 DIDO fuel assemblies has been analyzed for transport in the LWT cask. The fuel assemblies are configured in 6 basket modules with one fuel assembly loaded in each of the 7 cells in each basket module. The cells in each basket module are arranged with one center cell [tube structure] surrounded by 6 other cells.

LEU, MEU and HEU fuels are evaluated for a uniform loading of 18W and 25W per fuel position. However, if any assemblies greater than 18W are to be loaded into the cask, the active fuel for the assemblies in the top basket must be physically restricted from moving any closer than a minimum of 3.7 inches (9.3 cm) to the cask lid. Thus, basket module maximum heat loads of 175W (1.05 kW per cask – uniform 25W per assembly) or 126W (0.756 kW per cask – uniform 18W per assembly) are permissible. Only uniform loading configurations are considered.

The shielding analysis evaluated all three DIDO fuel types for variable burnup considering uniform basket loading for LEU, MEU, and HEU fuel at heat loads of both 18W and 25W. Fuel assemblies with heat loads between 18W and 25W were analyzed with their axial location restricted to maintain the required offset from the cask lid. There are no height restrictions in the other five baskets in the cask load.

If there is no axial restriction to fuel assembly position in the top basket, the fuel assemblies can have active fuel exposed beyond the radial lead shield. This geometric effect makes the 18W heat load pattern more limiting, with higher dose rates than those calculated for the 25W pattern. At a distance of 2 meters from the conveyance radial surface, the 18W pattern provided a maximum dose rate of 9.72 mrem/hr compared with a maximum dose rate of 8.90 mrem/hr, for the 25W pattern. Thus, the 18W pattern is used as the load basis for the shielding analysis. Furthermore, the HEU fuel provided the highest dose rates 2 meters from the conveyance surface over the enrichment range analyzed.

The DIDO fuel assembly consists of four tubes of varying diameter, each nested within the larger diameter tube, clipped together at each end to form a cylindrical assembly. The design basis fuel assemblies were constructed using typical DIDO parameters. The physical characteristics of the analyzed LEU, MEU and HEU fuel assemblies are shown in Table 5.3.9-1. The active fuel section of the assembly consists of four tubes of 0.150-cm thickness. The fuel core of each fuel tube is a cermet of aluminum and U-Al, which is 0.065-cm thick. The 6061 aluminum cladding has a thickness of 0.0425 cm. All three enrichments are analyzed with a maximum loading of 190 grams of ^{235}U per assembly.

The SAS2H sequence was used to determine the gamma and neutron source terms and decay heat loads for the DIDO fuel assembly loading configurations evaluated. The SAS2H sequence includes the ORIGEN-S code and a 1-D XSDRNP model of the fuel assembly. ORIGEN-S performs fuel assembly depletion at specified operating conditions and calculates heat generation, gamma and neutron spectra for a given discharge isotopic composition as a function of out of reactor time (cooling time). The 1-D model of the fuel assembly is used to collapse the 27-group neutron cross section library (27GROUPNDF4) into three broad energy groups for the depletion calculation. The 1-D model is based on an equivalent area representation of the fuel/moderator cell and surrounding structural regions. Average power is based on reactor maximum power divided by the number of assemblies in the core. Assembly burnup is modeled in four cycles of equal length with 30 days of down time between cycles. This burnup description bounds typical research reactor use, where fuel is burned over a period of years or even decades to achieve the optimal discharge burnup. The SAS2H input for the 18W, 70% depleted, HEU cask is shown in Figure 5.3.9-1.

For the bounding HEU fuel, a series of seven cases were run in which burnup was varied from a minimum of 82,490 MWd/MTU to a maximum of 577,460 MWd/MTU. Cooling times were considered from 90 days to 3.5 years. Because the cask is loaded based on the decay heat limits, no single design basis fuel assembly or loading configuration exists. Design basis photon and neutron source terms for DIDO assemblies with decay heat loads of 18 and 25 watts are determined for the 577,460 MWd/MTU burnup case, which was bounding. The SAS2H results from these cases are used for the design basis photon and neutron source terms and are summarized in Table 5.3.9-2 and Table 5.3.9-3. The material densities used in the analysis are summarized in Table 5.3.9-4.

Minimum cool times as a function of burnup in MWd/MTU are shown in Figure 5.3.9-5 through Figure 5.3.9-7 for both 18 and 25 watt loading patterns.

In addition to loading curves in terms of MWd/MTU, loading curves with terms of ^{235}U % depletion as the independent variable are generated. Use of these curves will provide a more meaningful measure of loadability of the cask based on elements having different (but bounded) fuel parameters. While both MWd/MTU and percent depletion curves produce loading times meeting cask dose and heat load limits, each of the curves contains inherent conservatism that may result in significant variations in minimum cool time required for any specific fuel element. There is no restriction on cask users as to which of the curves to apply at loading.

Loading curves are based on the results of SAS2H runs with a minimum (lower) enrichment limit to maximize source generation. A fuel assembly containing a higher than modeled initial enrichment (wt % ^{235}U), at the same ^{235}U loading (grams), contains less total uranium and,

therefore, will yield a higher MWd/MTU value for the same energy production (MWd). Based on MWd/MTU loading curves, the higher MWd/MTU value, in turn, requires an increase in cool time without a significant change in source. Loading curves based on % ^{235}U depletion circumvent this potential applicability problem for fuel with significantly higher enrichment than the one employed in the source generation.

Loading curves as a function of % ^{235}U depletion are shown for LEU, MEU and HEU DIDO fuel in Figure 5.3.9-8 through Figure 5.3.9-10. As demonstrated in Figure 5.3.9-11 for the 25 W loading pattern, the use of ^{235}U % depletion rather than burnup yields almost overlapping curves for the three modeled enrichments. To reduce the number of curves applicable to DIDO fuels, a bounding loading curve for the 18 and 25 watt loading patterns is generated and shown in Figure 5.3.9-12.

Note that the loading curves shown in this section are based on a fixed energy conversion factor of 0.9166 MWd produced per gram ^{235}U consumed. This factor represents the classical recoverable energy generated by ^{235}U thermal fission. Actual depletion in the SAS2H sequence may differ from the analysis input factor. As demonstrated in Figure 5.3.9-13 for DIDO HEU fuel, the application of a constant conversion factor to determine percent depletion minimum cool time curves results in a conservative (i.e., longer) longer minimum cool time (i.e., the predicted minimum cool time curve, based on a constant conversion factor, is higher than the SAS2H generated, "actual" depletion curve).

The SAS2H DIDO source term calculation does not directly account for the (alpha, n) reactions in ^{27}Al and ^{28}Si . Based on MTR evaluations with a similar fuel meat composition, the (alpha, n) reactions in ^{27}Al and ^{28}Si increase the neutron source term by a factor of ~2.9. Consequently, a factor of 2.9 is applied to the DIDO neutron source terms.

The SAS4 (Tang) sequence is used to calculate the dose rates at all points of interest. In this sequence, a 1-D adjoins XSDRNPM model generates biasing parameters for a 3-D MORSE Monte Carlo model of the NAC-LWT cask with the DIDO fuel. SAS4 requires model symmetry about the active fuel midplane (midplane of the six basket modules in this case). A 3-D Monte Carlo model is developed for the upper half of the cask. This model bounds the results for a lower half model as the cask has more shielding in the axial direction at the bottom end. The upper half model is shown in Figure 5.3.9-3. The model assumes that the fuel is at the highest point permissible in the basket module, that the fuel is loaded in the same way axially in all of the modules, and it ignores the presence of the impact limiters. Detectors are placed at three radial locations of interest. These locations are: 1) cask surface; 2) one meter from the cask surface; and 3) at two meters from the edge of the cask conveyance. A radial SAS4A input for the 18W heat load pattern is shown in Figure 5.3.9-2 and Figure 5.3.9-4. SAS4B is a version of SAS4 developed by NAC to

model surface detectors and to improve solution convergence testing. The improved convergence test criteria reduces geometric tracing area and improves computational efficiency.

5.3.9.1 Shielding Evaluation for DIDO Fuel

This section presents the shielding analyses for normal conditions of transport and illustrates compliance with 10 CFR Part 71. In normal transport, the dose rate limits are:

- The dose rate on the surface of the package is less than 200 mrem/hr, except that localized dose rates up to 1000 mrem/hr are allowed if it is shown that the dose rate on the surface of the ISO enclosure is less than 200 mrem/hr.
- At 2 meters from the edge of the transport vehicle the dose rate is limited to 10 mrem/hr.
- The truck cab (defined as a point 5 meters from the NAC-LWT lid) dose rate is limited to 2 mrem/hr.

The dose rates for the 18W heat load are shown in Table 5.3.9-5, Table 5.3.9-6 and Table 5.3.9-7 for the cask surface, plane of conveyance, and at 2 meters from the edge of the conveyance, respectively. These dose rates are well below the regulatory limits. The dose rates at 1 meter from the cask surface are presented in Table 5.3.9-8, where the maximum dose rate defines the Transport Index for the cask.

The axial surface and the 5 meter (back of tractor cab) dose rates are shown in Table 5.3.9-9 and Table 5.3.9-10. Shielding provided by the impact limiter is conservatively neglected. The axial dose rates at the bottom of the cask are conservatively assumed to be equal to the dose rates reported at the top.

This evaluation shows that the NAC-LWT cask, with up to 42 DIDO fuel assemblies, meets the shielding requirements of 10 CFR 71, 49 CFR 173, and IAEA Transportation Safety Standards (TS-R-1).

5.3.9.2 Accident Conditions of Transport

This section presents the accident condition shielding analyses. Under accident conditions, the NRC limits the package dose rate to 1000 mrem/hr at 1 meter off the package surface. The only accident condition examined in this section is the loss of the LWT liquid neutron shield.

This analysis examines the 18W heat load consistent with the limiting configuration analysis for normal conditions of transport presented in Section 5.3.4. The accident condition source terms are identical to the normal condition source terms. The accident condition results are presented in Table 5.3.9-11.

Figure 5.3.9-1 SAS2H Input for HEU DIDO Fuel 70% ²³⁵U Burnup and 18W Heat Load

```
=SAS2H          PARM=(HALT04,SKIPSHIPDATA)
Heu DIDO FUEL 70% U235 BURNUP - 190g - 18w Heat
Load
27GROUPNDF4 LATTICECELL
URANIUM 1 DEN=0.559 1.0 373 92235 90.00 92238
10.00 END
AL 1 DEN=1.678 1.0 373 END
AL      2 1.0 323 END
D2O     3 DEN=1.0948 1.0 313 END
END COMP
SYMMSLABCELL 0.980 0.065 1 3 0.15 2 END
NPIN=4 FUEL=60 VOLF=377.368 NCYC=4 NLIB=1
PRIN=6 INPL=2 NUMZ=5 NUMH=0
3 2.625 500 5.075 3 5.1 2 5.25 3 8.598
POWER=0.3846 BURN=79.24 DOWN=30 END
POWER=0.3846 BURN=79.24 DOWN=30 END
POWER=0.3846 BURN=79.24 DOWN=30 END
POWER=0.3846 BURN=79.24 DOWN=90 END
END
```

Figure 5.3.9-2 SAS4 Fuel Gamma Input for HEU DIDO Fuel 70% ²³⁵U Burnup and 18W Heat Load – Radial Biasing & Normal Transport Conditions

```

=SAS4B          PARM='SIZE=1000000'
NAC - LWT WITH DIDO Heu FUEL, Radial, UPPER HALF, Normal , Config2, 18w, Gamma
27N-18COUPLE INFHOMMEDIUM
'Material Description for LWT Shielding Analysis - DIDO Heu Fuel
URANIUM        1 0.0021 293 92235 90.00 92238 10.00 END
AL              1 0.1401 END
AL              4 1.0 END
ARBMGLYC        0.9437 3 0 1 0 6012 2 1001 6 8016 2 5 0.584 END
H2O             5 0.4160 END
SS304           6 1.0 END
PB              7 1.0 END
END COMP
IDR=0          ITY=2          IZM=7          FRD=14.3          END
15.455         16.986         18.910         33.465         36.519         49.219         49.818         END
1 0 6 7 6 5 6          END
XEND
TIM=10000      NST=2000      NIT=8000      ISO=0      ICS=4      RAN=15270511
'Gamma Spectrum for 70% Burnup - 190g Heu @18w - 42 assemblies
SFA=4.4083E+15  IGO=4 END
SOE 27Z        6.6997E-01    3.1836E+00    1.6438E+01    4.1542E+01    1.2913E+08
1.3269E+09     3.5795E+11     3.7376E+10     4.0544E+11     7.9798E+11     2.9979E+12
1.9642E+13     7.9847E+12     2.3166E+12     3.0158E+12     1.3247E+13     1.3145E+13
4.1016E+13          END
CSF            49.82
121.92
149.82
321.92
END
CSL            0.0          260
0.0          280
0.0          300
0.0          300
END
CSD            10          1
10           1
10           1
10           1
END
SXY 1          -15.46       15.46       -15.46       15.46       0.00       222.01
17.00         1.0          1.0          1.0          END
GEND
NAC-LWT CASK - 42 DIDO FUEL ELEMENTS - UPPER HALF MODEL
0 0 1 0
' Fuel Cell 1
RCC 1          0.0000       0.0000       -11.9474     2*0.0       23.8948     4.6600
RCC 2          0.0000       0.0000       -13.1974     2*0.0       26.3948     4.6600
RCC 3          0.0000       0.0000       -73.1974     2*0.0       146.3948    4.6600
RCC 4          0.0000       0.0000       -74.4474     2*0.0       148.8948    4.6600
RCC 5          0.0000       0.0000       -86.3948     2*0.0       172.7896    4.6600
RCC 6          0.0000       0.0000       -87.6448     2*0.0       175.2896    4.6600
RCC 7          0.0000       0.0000       -147.6448    2*0.0       295.2896    4.6600
RCC 8          0.0000       0.0000       -148.8948    2*0.0       297.7896    4.6600
RCC 9          0.0000       0.0000       -160.7600    2*0.0       321.5200    4.6600
RCC 10         0.0000       0.0000       -162.0100    2*0.0       324.0200    4.6600
RCC 11         0.0000       0.0000       -222.0100    2*0.0       444.0200    4.6600
RCC 12         0.0000       0.0000       -223.2600    2*0.0       446.5200    4.6600
' Fuel Cell 3
RCC 13         10.7950     0.0000       -11.9474     2*0.0       23.8948     4.6600
RCC 14         10.7950     0.0000       -13.1974     2*0.0       26.3948     4.6600
RCC 15         10.7950     0.0000       -73.1974     2*0.0       146.3948    4.6600
RCC 16         10.7950     0.0000       -74.4474     2*0.0       148.8948    4.6600
RCC 17         10.7950     0.0000       -86.3948     2*0.0       172.7896    4.6600
RCC 18         10.7950     0.0000       -87.6448     2*0.0       175.2896    4.6600
RCC 19         10.7950     0.0000       -147.6448    2*0.0       295.2896    4.6600
RCC 20         10.7950     0.0000       -148.8948    2*0.0       297.7896    4.6600
RCC 21         10.7950     0.0000       -160.7600    2*0.0       321.5200    4.6600
RCC 22         10.7950     0.0000       -162.0100    2*0.0       324.0200    4.6600
RCC 23         10.7950     0.0000       -222.0100    2*0.0       444.0200    4.6600
RCC 24         10.7950     0.0000       -223.2600    2*0.0       446.5200    4.6600
' Fuel cell 6
RCC 25         -10.7950     0.0000       -11.9474     2*0.0       23.8948     4.6600
RCC 26         -10.7950     0.0000       -13.1974     2*0.0       26.3948     4.6600
RCC 27         -10.7950     0.0000       -73.1974     2*0.0       146.3948    4.6600
RCC 28         -10.7950     0.0000       -74.4474     2*0.0       148.8948    4.6600
RCC 29         -10.7950     0.0000       -86.3948     2*0.0       172.7896    4.6600
RCC 30         -10.7950     0.0000       -87.6448     2*0.0       175.2896    4.6600
RCC 31         -10.7950     0.0000       -147.6448    2*0.0       295.2896    4.6600
RCC 32         -10.7950     0.0000       -148.8948    2*0.0       297.7896    4.6600
RCC 33         -10.7950     0.0000       -160.7600    2*0.0       321.5200    4.6600
RCC 34         -10.7950     0.0000       -162.0100    2*0.0       324.0200    4.6600
RCC 35         -10.7950     0.0000       -222.0100    2*0.0       444.0200    4.6600
RCC 36         -10.7950     0.0000       -223.2600    2*0.0       446.5200    4.6600
' Fuel cell 7
RCC 37         -5.3975     9.3487       -11.9474     2*0.0       23.8948     4.6600
RCC 38         -5.3975     9.3487       -13.1974     2*0.0       26.3948     4.6600
RCC 39         -5.3975     9.3487       -73.1974     2*0.0       146.3948    4.6600
RCC 40         -5.3975     9.3487       -74.4474     2*0.0       148.8948    4.6600

```

Figure 5.3.9-2 SAS4 Fuel Gamma Input for HEU DIDO Fuel 70% ²³⁵U Burnup and 18W Heat Load – Radial Biasing & Normal Transport Conditions (continued)

RCC 41	-5.3975	9.3487	-86.3948	2*0.0	172.7896	4.6600
RCC 42	-5.3975	9.3487	-87.6448	2*0.0	175.2896	4.6600
RCC 43	-5.3975	9.3487	-147.6448	2*0.0	295.2896	4.6600
RCC 44	-5.3975	9.3487	-148.8948	2*0.0	297.7896	4.6600
RCC 45	-5.3975	9.3487	-160.7600	2*0.0	321.5200	4.6600
RCC 46	-5.3975	9.3487	-162.0100	2*0.0	324.0200	4.6600
RCC 47	-5.3975	9.3487	-222.0100	2*0.0	444.0200	4.6600
RCC 48	-5.3975	9.3487	-223.2600	2*0.0	446.5200	4.6600
Fuel cell 5						
RCC 49	-5.3975	-9.3487	-11.9474	2*0.0	23.8948	4.6600
RCC 50	-5.3975	-9.3487	-13.1974	2*0.0	26.3948	4.6600
RCC 51	-5.3975	-9.3487	-73.1974	2*0.0	146.3948	4.6600
RCC 52	-5.3975	-9.3487	-74.4474	2*0.0	148.8948	4.6600
RCC 53	-5.3975	-9.3487	-86.3948	2*0.0	172.7896	4.6600
RCC 54	-5.3975	-9.3487	-87.6448	2*0.0	175.2896	4.6600
RCC 55	-5.3975	-9.3487	-147.6448	2*0.0	295.2896	4.6600
RCC 56	-5.3975	-9.3487	-148.8948	2*0.0	297.7896	4.6600
RCC 57	-5.3975	-9.3487	-160.7600	2*0.0	321.5200	4.6600
RCC 58	-5.3975	-9.3487	-162.0100	2*0.0	324.0200	4.6600
RCC 59	-5.3975	-9.3487	-222.0100	2*0.0	444.0200	4.6600
RCC 60	-5.3975	-9.3487	-223.2600	2*0.0	446.5200	4.6600
Fuel cell 2						
RCC 61	5.3975	9.3487	-11.9474	2*0.0	23.8948	4.6600
RCC 62	5.3975	9.3487	-13.1974	2*0.0	26.3948	4.6600
RCC 63	5.3975	9.3487	-73.1974	2*0.0	146.3948	4.6600
RCC 64	5.3975	9.3487	-74.4474	2*0.0	148.8948	4.6600
RCC 65	5.3975	9.3487	-86.3948	2*0.0	172.7896	4.6600
RCC 66	5.3975	9.3487	-87.6448	2*0.0	175.2896	4.6600
RCC 67	5.3975	9.3487	-147.6448	2*0.0	295.2896	4.6600
RCC 68	5.3975	9.3487	-148.8948	2*0.0	297.7896	4.6600
RCC 69	5.3975	9.3487	-160.7600	2*0.0	321.5200	4.6600
RCC 70	5.3975	9.3487	-162.0100	2*0.0	324.0200	4.6600
RCC 71	5.3975	9.3487	-222.0100	2*0.0	444.0200	4.6600
RCC 72	5.3975	9.3487	-223.2600	2*0.0	446.5200	4.6600
Fuel cell 4						
RCC 73	5.3975	-9.3487	-11.9474	2*0.0	23.8948	4.6600
RCC 74	5.3975	-9.3487	-13.1974	2*0.0	26.3948	4.6600
RCC 75	5.3975	-9.3487	-73.1974	2*0.0	146.3948	4.6600
RCC 76	5.3975	-9.3487	-74.4474	2*0.0	148.8948	4.6600
RCC 77	5.3975	-9.3487	-86.3948	2*0.0	172.7896	4.6600
RCC 78	5.3975	-9.3487	-87.6448	2*0.0	175.2896	4.6600
RCC 79	5.3975	-9.3487	-147.6448	2*0.0	295.2896	4.6600
RCC 80	5.3975	-9.3487	-148.8948	2*0.0	297.7896	4.6600
RCC 81	5.3975	-9.3487	-160.7600	2*0.0	321.5200	4.6600
RCC 82	5.3975	-9.3487	-162.0100	2*0.0	324.0200	4.6600
RCC 83	5.3975	-9.3487	-222.0100	2*0.0	444.0200	4.6600
RCC 84	5.3975	-9.3487	-223.2600	2*0.0	446.5200	4.6600
EMPTY CELLS						
Center (Position 1)						
RCC 85	0.0000	0.0000	-1.2700	2*0.0	2.5400	5.0927
RCC 86	0.0000	0.0000	-74.4474	2*0.0	148.8948	5.0927
RCC 87	0.0000	0.0000	-75.7174	2*0.0	151.4348	5.0927
RCC 88	0.0000	0.0000	-148.8948	2*0.0	297.7896	5.0927
RCC 89	0.0000	0.0000	-150.1648	2*0.0	300.3296	5.0927
RCC 90	0.0000	0.0000	-224.7800	2*0.0	449.5600	5.0927
Position 3 (Right)						
RCC 91	10.7950	0.0000	-1.2700	2*0.0	2.5400	5.0927
RCC 92	10.7950	0.0000	-74.4474	2*0.0	148.8948	5.0927
RCC 93	10.7950	0.0000	-75.7174	2*0.0	151.4348	5.0927
RCC 94	10.7950	0.0000	-148.8948	2*0.0	297.7896	5.0927
RCC 95	10.7950	0.0000	-150.1648	2*0.0	300.3296	5.0927
RCC 96	10.7950	0.0000	-224.7800	2*0.0	449.5600	5.0927
Position 6 (Left)						
RCC 97	-10.7950	0.0000	-1.2700	2*0.0	2.5400	5.0927
RCC 98	-10.7950	0.0000	-74.4474	2*0.0	148.8948	5.0927
RCC 99	-10.7950	0.0000	-75.7174	2*0.0	151.4348	5.0927
RCC 100	-10.7950	0.0000	-148.8948	2*0.0	297.7896	5.0927
RCC 101	-10.7950	0.0000	-150.1648	2*0.0	300.3296	5.0927
RCC 102	-10.7950	0.0000	-224.7800	2*0.0	449.5600	5.0927
Position 7 (Upper left)						
RCC 103	-5.3975	9.3487	-1.2700	2*0.0	2.5400	5.0927
RCC 104	-5.3975	9.3487	-74.4474	2*0.0	148.8948	5.0927
RCC 105	-5.3975	9.3487	-75.7174	2*0.0	151.4348	5.0927
RCC 106	-5.3975	9.3487	-148.8948	2*0.0	297.7896	5.0927
RCC 107	-5.3975	9.3487	-150.1648	2*0.0	300.3296	5.0927
RCC 108	-5.3975	9.3487	-224.7800	2*0.0	449.5600	5.0927
Position 5 (Lower left)						
RCC 109	-5.3975	-9.3487	-1.2700	2*0.0	2.5400	5.0927
RCC 110	-5.3975	-9.3487	-74.4474	2*0.0	148.8948	5.0927
RCC 111	-5.3975	-9.3487	-75.7174	2*0.0	151.4348	5.0927
RCC 112	-5.3975	-9.3487	-148.8948	2*0.0	297.7896	5.0927
RCC 113	-5.3975	-9.3487	-150.1648	2*0.0	300.3296	5.0927
RCC 114	-5.3975	-9.3487	-224.7800	2*0.0	449.5600	5.0927
Position 2 (Upper right)						
RCC 115	5.3975	9.3487	-1.2700	2*0.0	2.5400	5.0927
RCC 116	5.3975	9.3487	-74.4474	2*0.0	148.8948	5.0927
RCC 117	5.3975	9.3487	-75.7174	2*0.0	151.4348	5.0927
RCC 118	5.3975	9.3487	-148.8948	2*0.0	297.7896	5.0927
RCC 119	5.3975	9.3487	-150.1648	2*0.0	300.3296	5.0927
RCC 120	5.3975	9.3487	-224.7800	2*0.0	449.5600	5.0927
Position 4 (Lower right)						
RCC 121	5.3975	-9.3487	-1.2700	2*0.0	2.5400	5.0927
RCC 122	5.3975	-9.3487	-74.4474	2*0.0	148.8948	5.0927
RCC 123	5.3975	-9.3487	-75.7174	2*0.0	151.4348	5.0927
RCC 124	5.3975	-9.3487	-148.8948	2*0.0	297.7896	5.0927

Figure 5.3.9-2 SAS4 Fuel Gamma Input for HEU DIDO Fuel 70% ²³⁵U Burnup and 18W Heat Load – Radial Biasing & Normal Transport Conditions (continued)

RCC 125	5.3975	-9.3487	-150.1648	2*0.0	300.3296	5.0927
RCC 126	5.3975	-9.3487	-224.7800	2*0.0	449.5600	5.0927
BOTTOM PLATE HOLES						
RCC 127	0.0000	0.0000	-300.0000	2*0.0	600.0000	1.2700
RCC 128	10.7950	0.0000	-300.0000	2*0.0	600.0000	1.2700
RCC 129	-10.7950	0.0000	-300.0000	2*0.0	600.0000	1.2700
RCC 130	-5.3975	9.3487	-300.0000	2*0.0	600.0000	1.2700
RCC 131	-5.3975	-9.3487	-300.0000	2*0.0	600.0000	1.2700
RCC 132	5.3975	9.3487	-300.0000	2*0.0	600.0000	1.2700
RCC 133	5.3975	-9.3487	-300.0000	2*0.0	600.0000	1.2700
OUTER BASKET STEEL						
RCC 134	0.0000	0.0000	-223.2600	2*0.0	446.5200	5.3975
RCC 135	10.7950	0.0000	-223.2600	2*0.0	446.5200	5.3975
RCC 136	-10.7950	0.0000	-223.2600	2*0.0	446.5200	5.3975
RCC 137	-5.3975	9.3487	-223.2600	2*0.0	446.5200	5.3975
RCC 138	-5.3975	-9.3487	-223.2600	2*0.0	446.5200	5.3975
RCC 139	5.3975	9.3487	-223.2600	2*0.0	446.5200	5.3975
RCC 140	5.3975	-9.3487	-223.2600	2*0.0	446.5200	5.3975
Interior fuel element regions						
RCC 141	0.0000	0.0000	-223.2600	2*0.0	446.5200	3.0400
RCC 142	10.7950	0.0000	-223.2600	2*0.0	446.5200	3.0400
RCC 143	-10.7950	0.0000	-223.2600	2*0.0	446.5200	3.0400
RCC 144	-5.3975	9.3487	-223.2600	2*0.0	446.5200	3.0400
RCC 145	-5.3975	-9.3487	-223.2600	2*0.0	446.5200	3.0400
RCC 146	5.3975	9.3487	-223.2600	2*0.0	446.5200	3.0400
RCC 147	5.3975	-9.3487	-223.2600	2*0.0	446.5200	3.0400
LWT SHIELDS						
RCC 148	0.0000	0.0000	-224.7800	0.0000	0.0000	449.5600
RCC 149	0.0000	0.0000	-224.7800	0.0000	0.0000	449.5600
RCC 150	0.0000	0.0000	-203.3720	0.0000	0.0000	406.7440
RCC 151	0.0000	0.0000	-217.1900	0.0000	0.0000	434.3800
RCC 152	0.0000	0.0000	-217.1900	0.0000	0.0000	434.3800
RCC 153	0.0000	0.0000	-253.3590	0.0000	0.0000	506.7180
RCC 154	0.0000	0.0000	-194.3290	0.0000	0.0000	388.6580
RCC 155	0.0000	0.0000	-195.5990	0.0000	0.0000	391.1980
DETECTOR PLANES						
RCC 156	0.0000	0.0000	-352.4680	0.0000	0.0000	704.9360
RCC 157	0.0000	0.0000	-452.4680	0.0000	0.0000	904.9360
RCC 158	0.0000	0.0000	-552.4680	0.0000	0.0000	1104.9360
RCC 159	0.0000	0.0000	-600.0000	0.0000	0.0000	1200.0000
OUTER WORLD						
RCC 160	0.0000	0.0000	-652.4680	0.0000	0.0000	1304.9360
RCC 161	0.0000	0.0000	-752.4680	0.0000	0.0000	1504.9360
END						
Element in Position 1						
BP1	+85	-127				
HO1	+85	+127				
GP1	+1	-85				
EF1	+2	-1	-141			
FU1	+3	-2	-141			
EF1	+4	-3	-141			
BP2	+87	-86	-127			
HO2	+87	-86	+127			
GP2	+5	-87				
EF2	+6	-5	-141			
FU2	+7	-6	-141			
EF2	+8	-7	-141			
BP3	+89	-88	-127			
HO3	+89	-88	+127			
GP3	+9	-89				
EF3	+10	-9	-141			
FU3	+11	-10	-141			
EF3	+12	-11	-141			
TU1	OR	+86	-85	-4		
OR	+88	-87	-8			
OR	+90	-89	-12			
OR	+2	-1	+141			
OR	+3	-2	+141			
OR	+4	-3	+141			
OR	+5	-5	+141			
OR	+7	-6	+141			
OR	+8	-7	+141			
OR	+10	-9	+141			
OR	+11	-10	+141			

Figure 5.3.9-2 SAS4 Fuel Gamma Input for HEU DIDO Fuel 70% ²³⁵U Burnup and 18W Heat Load – Radial Biasing & Normal Transport Conditions (continued)

	OR	+12	-11	+141
Element in Position 3				
BP1		+91	-128	
HO1		+91	+128	
GP1		+13	-91	
EF1		+14	-13	-142
FU1		+15	-14	-142
EF1		+16	-15	-142
Element in Position 4				
BP2		+93	-92	-128
HO2		+93	-92	+128
GP2		+17	-93	
EF2		+18	-17	-142
FU2		+19	-18	-142
EF2		+20	-19	-142
Element in Position 5				
BP3		+95	-94	-128
HO3		+95	-94	+128
GP3		+21	-95	
EF3		+22	-21	-142
FU3		+23	-22	-142
EF3		+24	-23	-142
TU1	OR	+92	-91	-16
Element in Position 6				
BP1		+97	-129	
HO1		+97	+129	
GP1		+25	-97	
EF1		+26	-25	-143
FU1		+27	-26	-143
EF1		+28	-27	-143
Element in Position 7				
BP2		+99	-98	-129
HO2		+99	-98	+129
GP2		+29	-99	
EF2		+30	-29	-143
FU2		+31	-30	-143
EF2		+32	-31	-143
Element in Position 8				
BP3		+101	-100	-129
HO3		+101	-100	+129
GP3		+33	-101	
EF3		+34	-33	-143
FU3		+35	-34	-143
EF3		+36	-35	-143
TU1	OR	+98	-97	-28
Element in Position 9				
BP1		+100	-99	-32
HO1		+102	-101	-36
GP1		+26	-25	+143
EF1		+27	-26	+143
FU1		+28	-27	+143
EF1		+30	-29	+143
BP2		+31	-30	+143
HO2		+32	-31	+143
GP2		+34	-33	+143
EF2		+35	-34	+143
FU2		+36	-35	+143
Element in Position 10				
BP3		+103	-130	
HO3		+103	+130	
GP3		+37	-103	
EF3		+38	-37	-144
FU3		+39	-38	-144
EF3		+40	-39	-144
BP2		+105	-104	-130
HO2		+105	-104	+130
GP2		+41	-105	
EF2		+42	-41	-144
FU2		+43	-42	-144
EF2		+44	-43	-144
BP3		+107	-106	-130
HO3		+107	-106	+130
GP3		+45	-107	
EF3		+46	-45	-144
FU3		+47	-46	-144
EF3		+48	-47	-144
TU1	OR	+104	-103	-40
Element in Position 11				
BP1		+106	-105	-44
HO1		+108	-107	-48
GP1		+38	-37	+144
EF1		+39	-38	+144
FU1		+40	-39	+144
EF1		+42	-41	+144
BP2		+43	-42	+144
HO2		+44	-43	+144
GP2		+46	-45	+144

Figure 5.3.9-2 SAS4 Fuel Gamma Input for HEU DIDO Fuel 70% ²³⁵U Burnup and 18W Heat Load – Radial Biasing & Normal Transport Conditions (continued)

OR	+47	-46	+144
OR	+48	-47	+144
Element in Position 5			
BP1	+109	-131	
HO1	+109	+131	
GP1	+49	-109	
EF1	+50	-49	-145
FU1	+51	-50	-145
EF1	+52	-51	-145
,			
BP2	+111	-110	-131
HO2	+111	-110	+131
GP2	+53	-111	
EF2	+54	-53	-145
FU2	+55	-54	-145
EF2	+56	-55	-145
,			
BP3	+113	-112	-131
HO3	+113	-112	+131
GP3	+57	-113	
EF3	+58	-57	-145
FU3	+59	-58	-145
EF3	+60	-59	-145
TU1	OR	+110	-109 -52
OR	+112	-111	-56
OR	+114	-113	-60
OR	+50	-49	+145
OR	+51	-50	+145
OR	+52	-51	+145
OR	+54	-53	+145
OR	+55	-54	+145
OR	+56	-55	+145
OR	+58	-57	+145
OR	+59	-58	+145
OR	+60	-59	+145
,			
Element in Position 2			
BP1	+115	-132	
HO1	+115	+132	
GP1	+61	-115	
EF1	+62	-61	-146
FU1	+63	-62	-146
EF1	+64	-63	-146
,			
BP2	+117	-116	-132
HO2	+117	-116	+132
GP2	+65	-117	
EF2	+66	-65	-146
FU2	+67	-66	-146
EF2	+68	-67	-146
,			
BP3	+119	-118	-132
HO3	+119	-118	+132
GP3	+69	-119	
EF3	+70	-69	-146
FU3	+71	-70	-146
EF3	+72	-71	-146
,			
TU1	OR	+116	-115 -64
OR	+118	-117	-68
OR	+120	-119	-72
OR	+62	-61	+146
OR	+63	-62	+146
OR	+64	-63	+146
OR	+66	-65	+146
OR	+67	-66	+146
OR	+68	-67	+146
OR	+70	-69	+146
OR	+71	-70	+146
OR	+72	-71	+146
,			
Element in Position 4			
BP1	+121	-133	
HO1	+121	+133	
GP1	+73	-121	
EF1	+74	-73	-147
FU1	+75	-74	-147
EF1	+76	-75	-147
BP2	+123	-122	-133
HO2	+123	-122	+133
GP2	+77	-123	
EF2	+78	-77	-147
FU2	+79	-78	-147
EF2	+80	-79	-147
,			
BP3	+125	-124	-133
HO3	+125	-124	+133
GP3	+81	-125	
EF3	+82	-81	-147
FU3	+83	-82	-147
EF3	+84	-83	-147
,			
TU1	OR	+122	-121 -76
OR	+124	-123	-80
OR	+126	-125	-84
OR	+74	-73	+147
OR	+75	-74	+147
OR	+76	-75	+147
OR	+78	-77	+147
OR	+79	-78	+147

Figure 5.3.9-2 SAS4 Fuel Gamma Input for HEU DIDO Fuel 70% ²³⁵U Burnup and
18W Heat Load – Radial Biasing & Normal Transport Conditions
(continued)

```

OR      +80      -79      +147
OR      +82      -81      +147
OR      +83      -82      +147
OR      +84      -83      +147
.
. BASKET
.
BSK      OR      +134      -90
OR      +135      -96
OR      +136      -102
OR      +137      -108
OR      +138      -114
OR      +139      -120
OR      +140      -126
.
. LWT SHIELDS
.
CAV      +148
-134      -135      -136      -137      -138      -139      -140
-90      -96
-102      -108      -114      -120      -126      -132
IST      +149      -148
RPB      +150      -149
TPB      +152      -151      -150
OST      OR      +153      -152      -151      -150      -149
OR      +151      -150      -149
RNS      +154      -153
NNS      +155      -154      -153
.
. DETECTOR PLANES
.
DE1      +156      -155      -153
DE2      +157      -156
DE3      +158      -157
DE4      +159      -158
.
. OUTER WORLD
.
INV      +160      -159
OUV      +161      -160
END
141R1 2 1 2 1 2 1
147R0
.
. DIDO FUEL ELEMENTS
.
6 1000 1000 4 1 4 6 1000 1000 4 1 4 6 1000 1000 4 1 4 1000
6 1000 1000 4 1 4 6 1000 1000 4 1 4 6 1000 1000 4 1 4 1000
6 1000 1000 4 1 4 6 1000 1000 4 1 4 6 1000 1000 4 1 4 1000
6 1000 1000 4 1 4 6 1000 1000 4 1 4 6 1000 1000 4 1 4 1000
6 1000 1000 4 1 4 6 1000 1000 4 1 4 6 1000 1000 4 1 4 1000
6 1000 1000 4 1 4 6 1000 1000 4 1 4 6 1000 1000 4 1 4 1000
6 1000 1000 4 1 4 6 1000 1000 4 1 4 6 1000 1000 4 1 4 1000
.
. BASKET
.
6
.
. LWT CASK
.
1000      6      7      7      6      5      6
.
. DETECTORS
.
4R1000
.
. WORLDS
.
1000 0
0 0
0
END

```


Figure 5.3.9-3 SAS4 Shielding Model for the DIDO Fuel Basket in the NAC-LWT
(Upper Half)

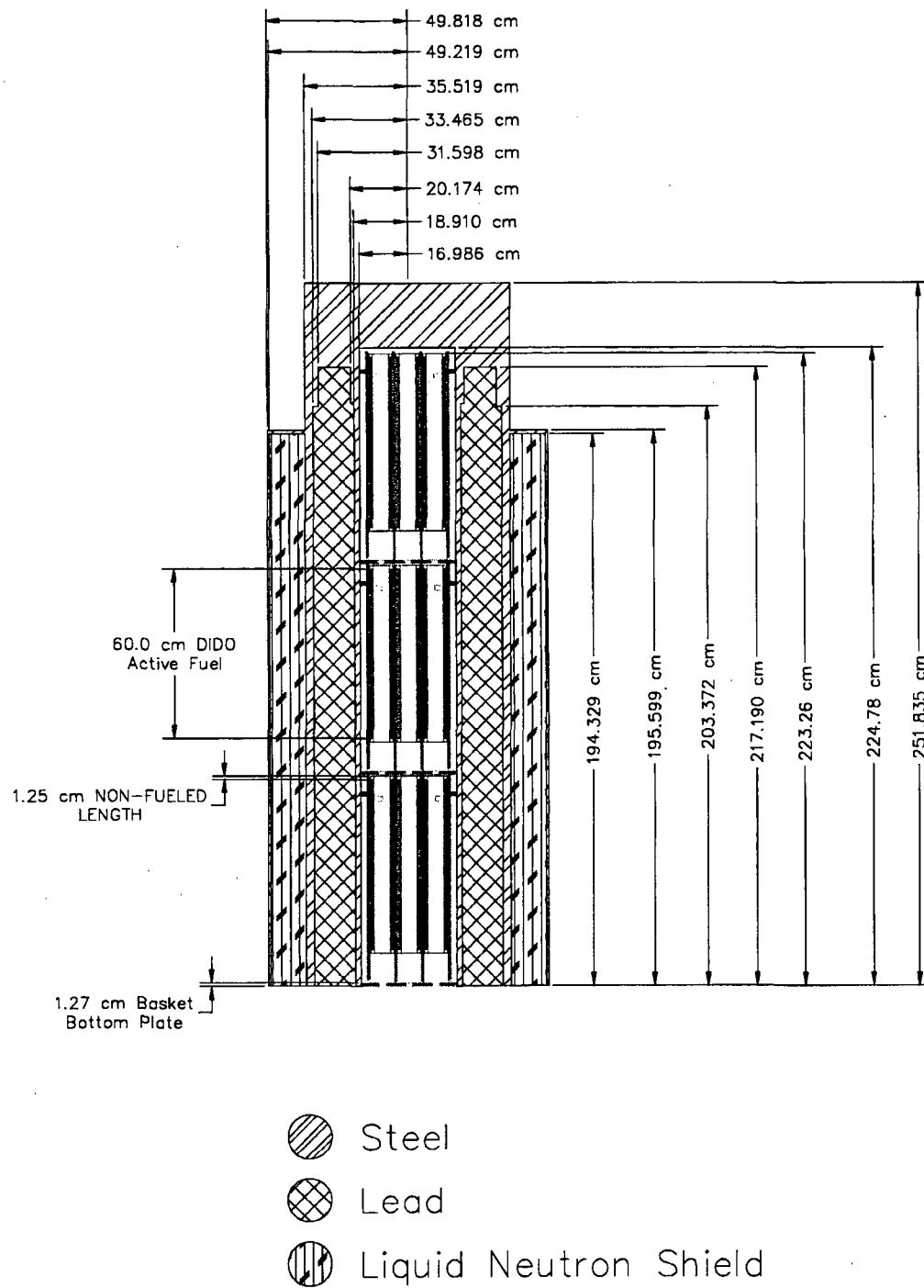


Figure 5.3.9-4 SAS4 Shielding Model for the DIDO Fuel Basket in the NAC-LWT
(Section through Fuel)

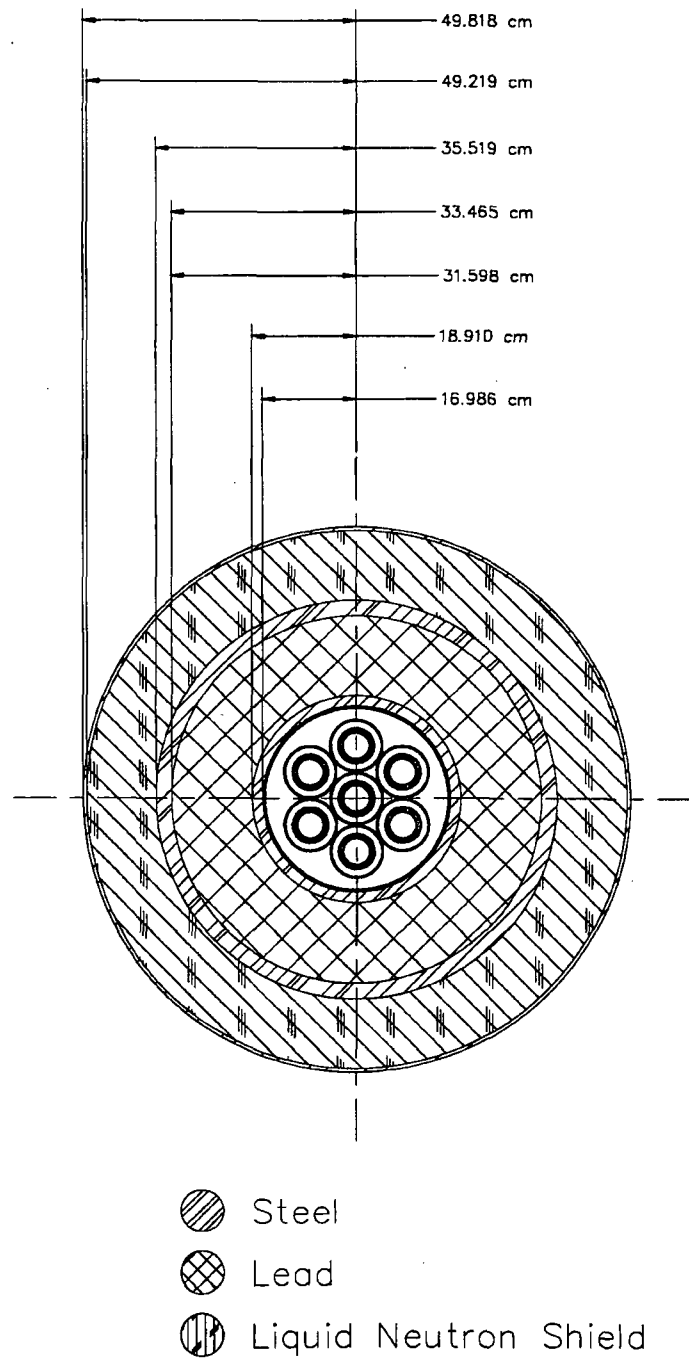


Figure 5.3.9-5 DIDO LEU Cooling Time vs. Fuel Burnup Basket Module Loading Guidelines for Uniform Loading

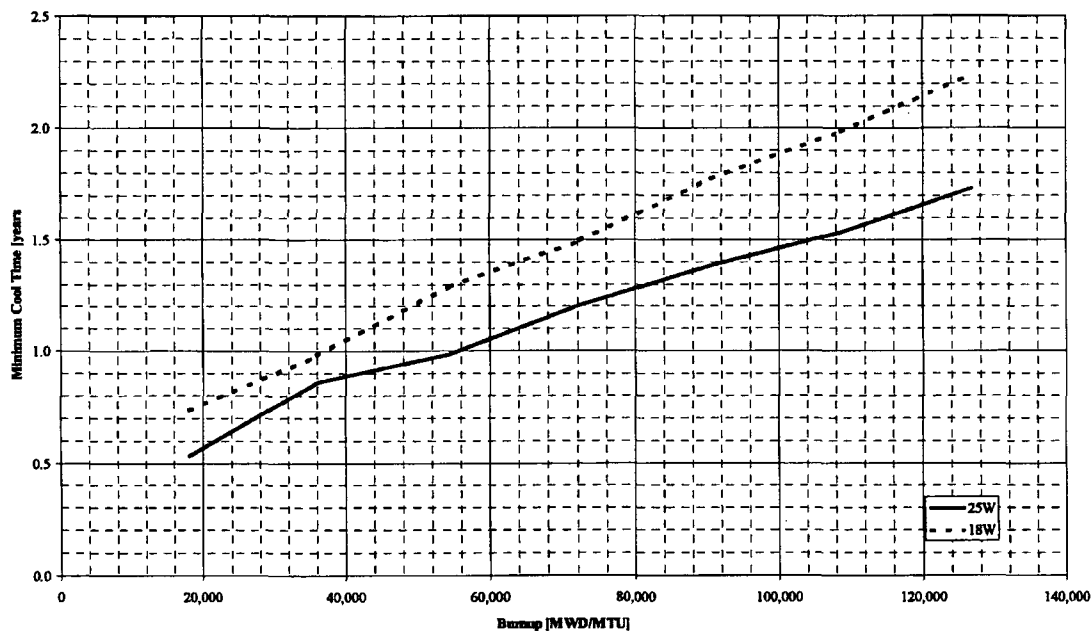


Figure 5.3.9-6 DIDO MEU Cooling Time vs. Fuel Burnup Basket Module Loading Guidelines for Uniform Loading

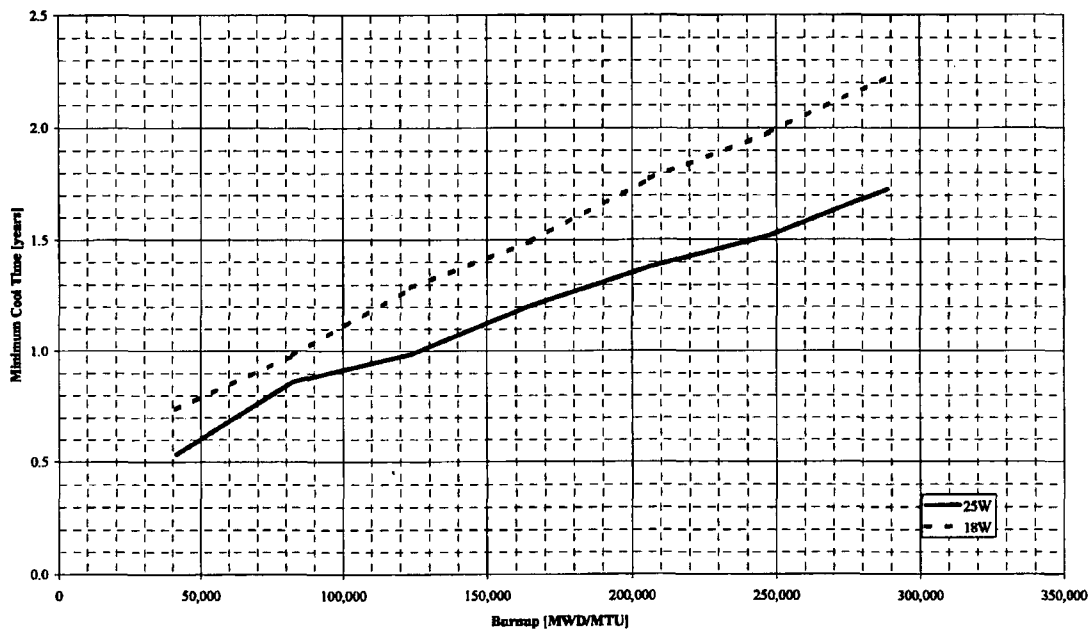


Figure 5.3.9-7 DIDO HEU Cooling Time vs. Fuel Burnup Basket Module Loading Guidelines for Uniform Loading

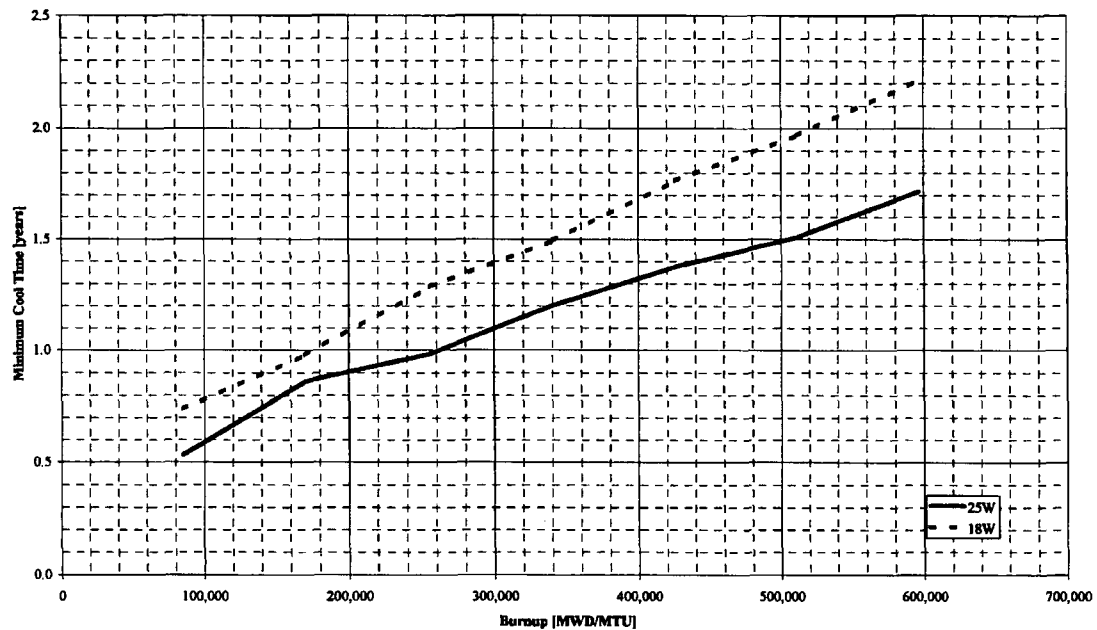


Figure 5.3.9-8 DIDO LEU Element Cooling Time vs. ^{235}U % Depletion

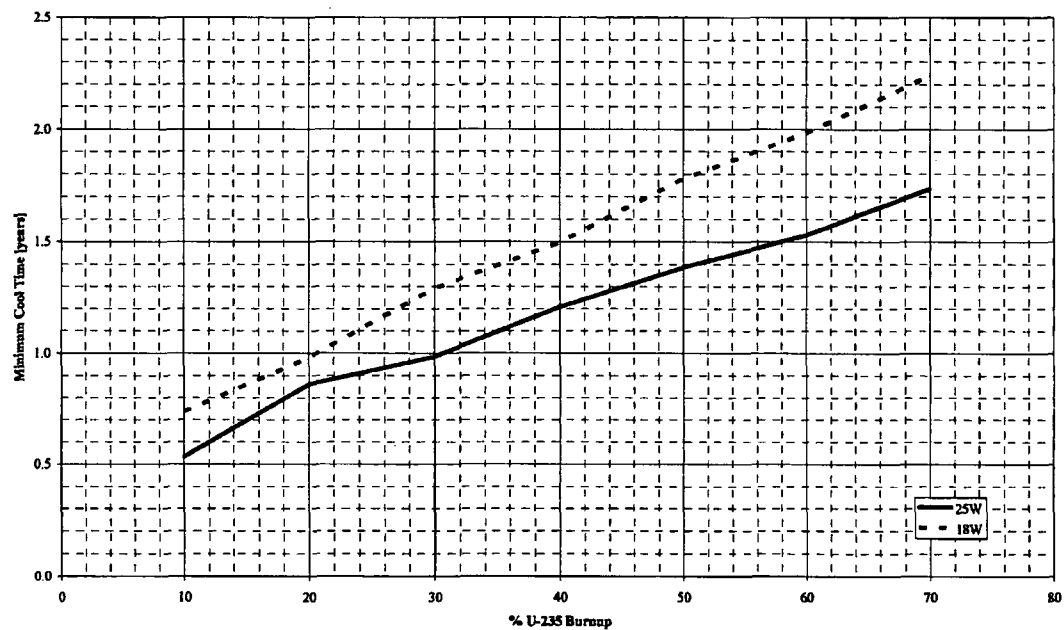


Figure 5.3.9-9 DIDO MEU Element Cooling Time vs. ^{235}U % Depletion

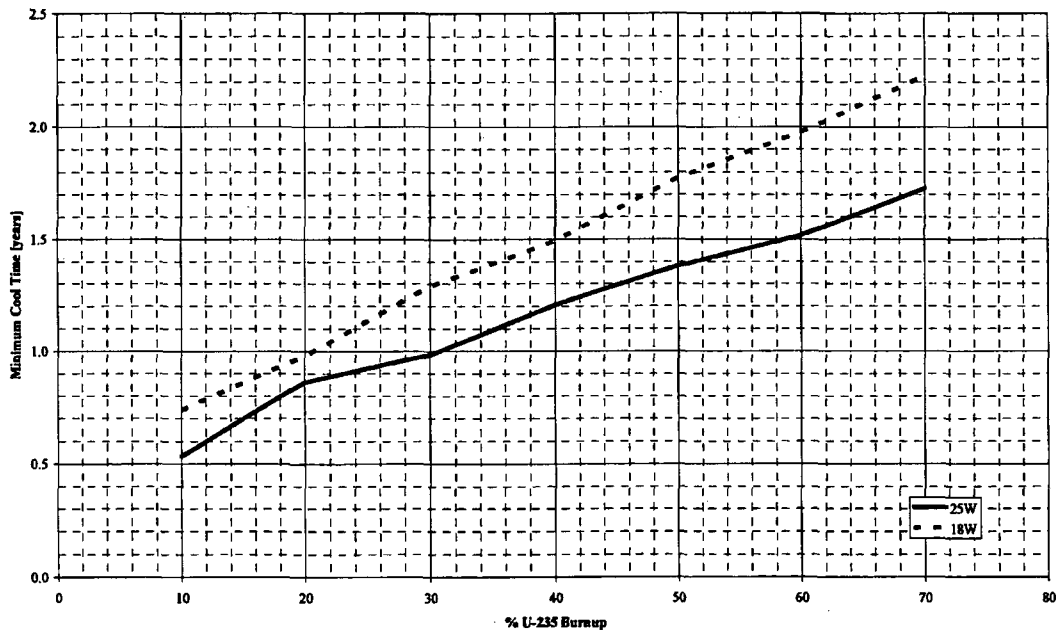


Figure 5.3.9-10 DIDO HEU Element Cooling Time vs. ^{235}U % Depletion

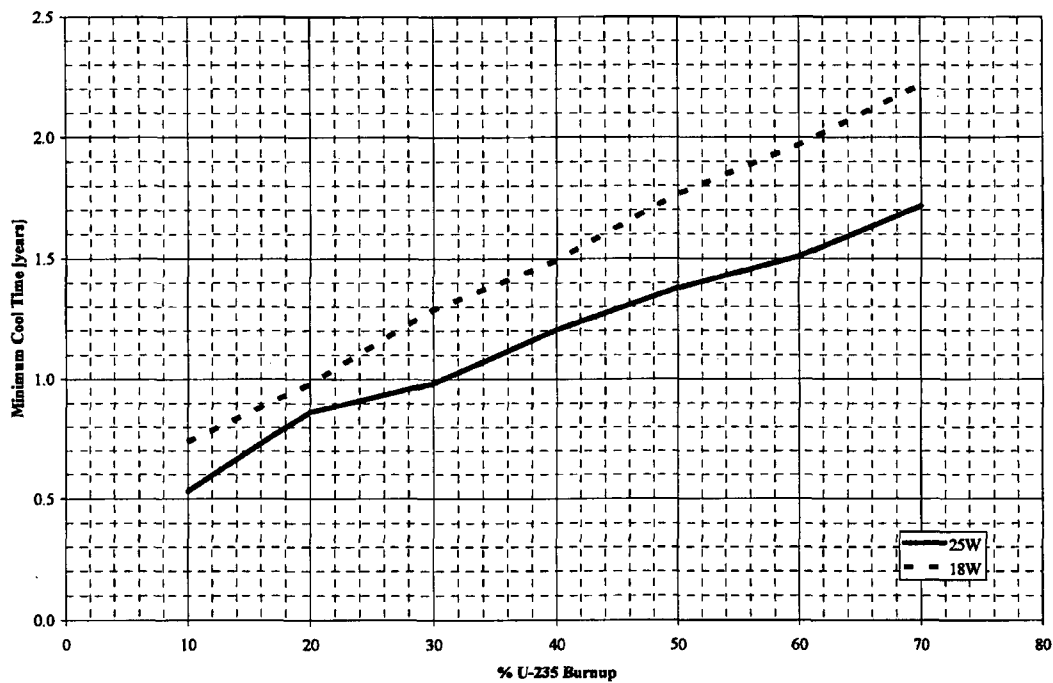


Figure 5.3.9-11 Comparison of DIDO Element 25W Minimum Cool Time Curves as a Function of ^{235}U % Depletion

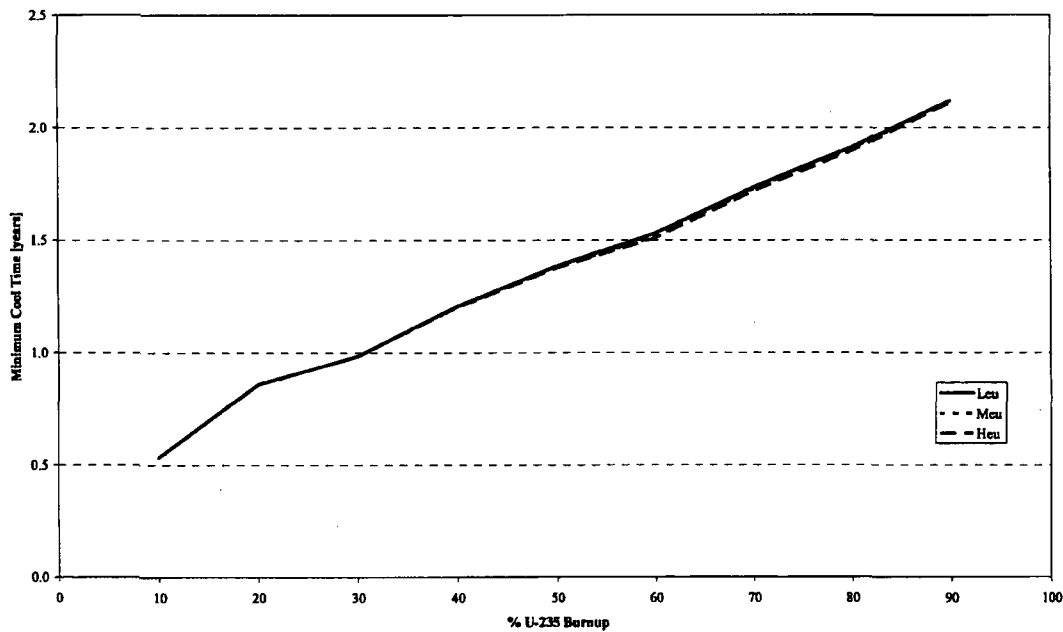


Figure 5.3.9-12 Bounding DIDO Element Minimum Cool Time vs. % ^{235}U Depletion

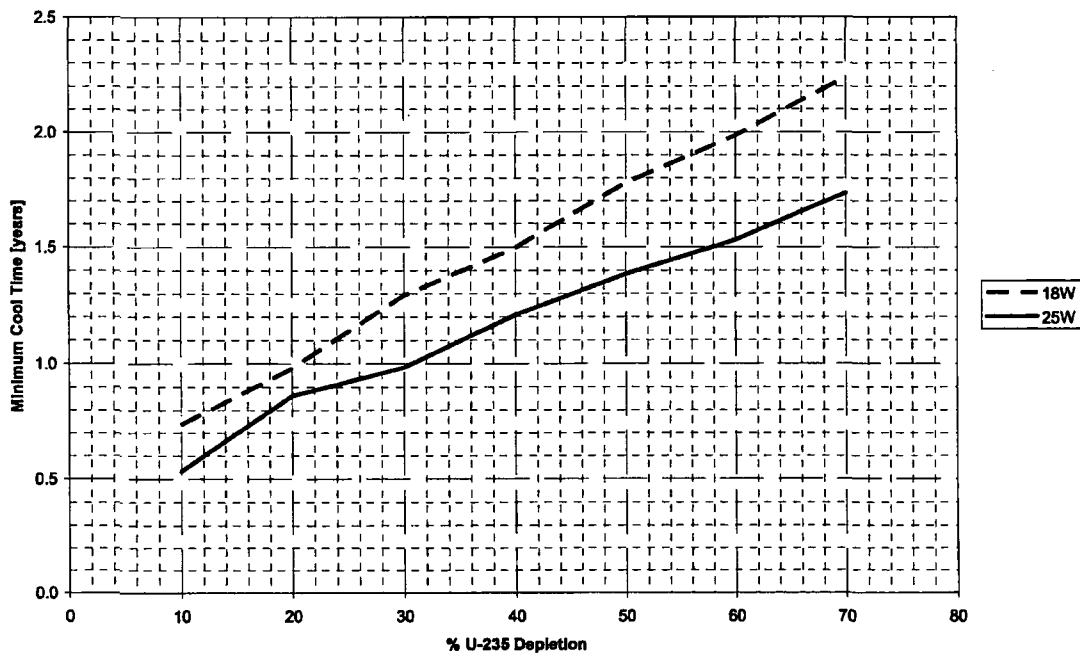


Figure 5.3.9-13 18W DIDO HEU Fuel Predicted vs. Actual ^{235}U Depletion Loading Curve

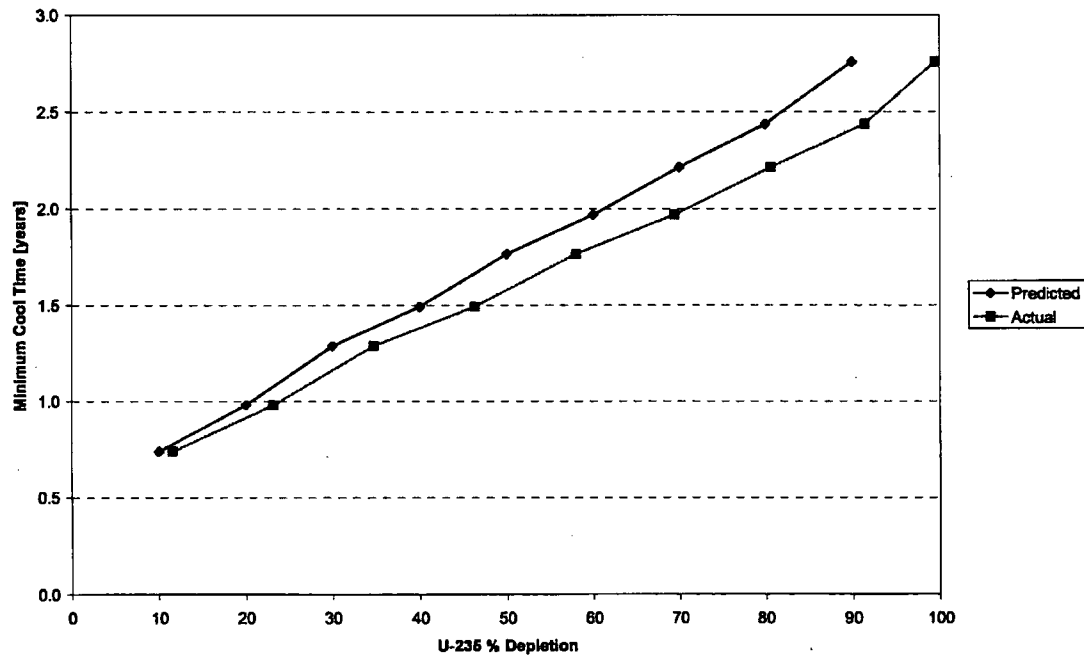


Table 5.3.9-1 Design Basis DIDO Fuel Assembly Characteristics

Fuel Parameters	Units	LEU	MEU	HEU
Tube 1 outer diameter	[cm]	6.38	6.38	6.38
Tube 2 outer diameter	[cm]	7.36	7.36	7.36
Tube 3 outer diameter	[cm]	8.34	8.34	8.34
Tube 4 outer diameter	[cm]	9.32	9.32	9.32
Aluminum plate outer diameter	[cm]	10.5	10.5	10.5
Aluminum outer plate thickness	[cm]	0.15	0.15	0.15
Clad thickness	[cm]	0.0425	0.0425	0.0425
Tube thickness	[cm]	0.15	0.15	0.15
Fuel meat thickness	[cm]	0.065	0.065	0.065
Active fuel length	[cm]	60.0	60.0	60.0
Total assembly length	[cm]	62.5	62.5	62.5
Tube pitch	[cm]	0.98	0.98	0.98
Fuel assembly pitch	[cm]	15.24	15.24	15.24
Fuel composition		U-Al	U-Al	U-Al
Weight percent ²³⁵ U		19%	40%	90%
Maximum ²³⁵ U per fuel assembly	[g]	190.0	190.0	190.0
U wt % in fuel composition		65%	40%	25%
Assembly power level	[MW]	0.3846	0.3846	0.3846
Mass of uranium	[g]	1000.0	475.0	211.1

Note: Active fuel in the top basket is restricted to a minimum distance below the cask lid of 3.7 inches (9.3 cm) in the 25 W pattern and to 1.1 inches (2.8 cm) below the lid in the 18 W pattern.

Table 5.3.9-2 DIDO Fuel Assembly Gamma Source Terms by Thermal Output

HEU Burnup 577,460 MWd/MTU			Assembly Thermal Output	
Group	E _{hi} (Mev)	E _{low} (Mev)	18 Watts	25 Watts
			809 Days (g/sec)	627 Days (g/sec)
1	10.00	8.00	6.70E-01	7.45E-01
2	8.00	6.50	3.18E+00	3.54E+00
3	6.50	5.00	1.64E+01	1.82E+01
4	5.00	4.00	4.15E+01	4.60E+01
5	4.00	3.00	1.29E+08	1.81E+08
6	3.00	2.50	1.33E+09	1.91E+09
7	2.50	2.00	3.58E+11	5.56E+11
8	2.00	1.66	3.74E+10	5.60E+10
9	1.66	1.33	4.05E+11	5.58E+11
10	1.33	1.00	7.98E+11	1.01E+12
11	1.00	0.80	3.00E+12	3.64E+12
12	0.80	0.60	1.96E+13	2.39E+13
13	0.60	0.40	7.98E+12	1.01E+13
14	0.40	0.30	2.32E+12	3.37E+12
15	0.30	0.20	3.02E+12	4.36E+12
16	0.20	0.10	1.32E+13	1.95E+13
17	0.10	0.05	1.31E+13	1.89E+13
18	0.05	0.01	4.10E+13	5.85E+13
Total	—	—	1.05E+14	1.45E+14

Table 5.3.9-3 DIDO Fuel Assembly Neutron Source Terms by Thermal Output

HEU Burnup 577,460 MWd/MTU			Assembly Thermal Output	
Group	E _{hi} (Mev)	E _{low} (Mev)	18 Watts	25 Watts
			809 Days (n/sec)	627 Days (n/sec)
1	2.00E+01	6.43E+00	2.03E+01	2.25E+01
2	6.43E+00	3.00E+00	4.44E+02	4.78E+02
3	3.00E+00	1.85E+00	8.47E+02	8.84E+02
4	1.85E+00	1.40E+00	3.02E+02	3.18E+02
5	1.40E+00	9.00E-01	2.83E+02	3.04E+02
6	9.00E-01	4.00E-01	2.38E+02	2.61E+02
7	4.00E-01	1.00E-01	4.57E+01	5.02E+01
8	1.00E-01	1.70E-02	-	-
9	1.70E-02	3.00E-03	-	-
10	3.00E-03	5.50E-04	-	-
11	5.50E-04	1.00E-04	-	-
12	1.00E-04	3.00E-05	-	-
13	3.00E-05	1.00E-05	-	-
14	1.00E-05	3.05E-06	-	-
15	3.05E-06	1.77E-06	-	-
16	1.77E-06	1.30E-06	-	-
17	1.30E-06	1.13E-06	-	-
18	1.13E-06	1.00E-06	-	-
19	1.00E-06	8.00E-07	-	-
20	8.00E-07	4.00E-07	-	-
21	4.00E-07	3.25E-07	-	-
22	3.25E-07	2.25E-07	-	-
23	2.25E-07	1.00E-07	-	-
24	1.00E-07	5.00E-08	-	-
25	5.00E-08	3.00E-08	-	-
26	3.00E-08	1.00E-08	-	-
27	1.00E-08	0.00E+00	-	-
Total	-	-	2.18E+03	2.32E+03

Table 5.3.9-4 Material Densities for DIDO Fuel Shielding Analysis

Material	Element	Density [atom/barn-cm]
HEU Fuel	AL	8.449E-03
	U-235	9.225E-05
	U-238	1.012E-05
MEU Fuel	AL	8.793E-03
	U-235	9.371E-05
	U-238	1.388E-04
LEU Fuel	AL	8.045E-03
	U-235	9.366E-05
	U-238	3.943E-04
End Fitting	AL	6.031E-02
H ₂ O/Glycol	H	5.988E-02
	C	1.070E-02
	O	2.459E-02
Stainless Steel	CR	1.743E-02
	MN	1.736E-03
	FE	5.936E-02
	NI	7.721E-03
Lead	PB	3.297E-02

Table 5.3.9-5 LWT Cask Surface Total Dose Rates - DIDO Fuel (Normal Conditions of Transport)

Band [cm]	LWT Cask Surface Radial Dose Rates (mrem/hr)							
	Gamma	FSD (%)	Neutron	FSD (%)	N-Gamma	FSD (%)	Total	FSD (%)
247	141.20	8.8	0.03	1.2	0.00	10.8	141.23	8.8
221	403.40	9.7	0.11	0.7	0.00	4.2	403.51	9.7
195	95.33	3.1	0.07	0.8	0.00	1.1	95.41	3.1
169	41.29	1.6	0.01	1.1	0.00	0.8	41.30	1.6
143	41.22	2.6	0.01	1.2	0.00	0.8	41.23	2.6
117	51.37	1.7	0.01	1.0	0.00	0.7	51.38	1.7
91	40.01	3.1	0.01	1.2	0.00	0.8	40.02	3.1
65	41.88	2.0	0.01	1.1	0.00	0.7	41.89	2.0
39	53.01	5.6	0.01	1.0	0.00	0.7	53.02	5.6
13	30.15	1.8	0.01	1.2	0.00	0.8	30.16	1.8

Table 5.3.9-6 LWT Cask Plane of Conveyance Dose Rates – DIDO Fuel (Normal Conditions of Transport)

Band [cm]	Conveyance Dose Rates (mrem/hr)							
	Gamma	FSD (%)	Neutron	FSD (%)	N-Gamma	FSD (%)	Total	FSD (%)
266	42.13	7.1	0.01	1.0	0.00	1.5	42.14	7.1
238	63.12	8.6	0.01	0.9	0.00	2.8	63.14	8.6
210	53.01	8.3	0.01	0.9	0.00	1.1	53.03	8.3
182	33.35	6.3	0.01	0.9	0.00	0.9	33.36	6.3
154	22.69	4.8	0.01	1.1	0.00	0.8	22.70	4.8
126	19.16	4.1	0.00	1.2	0.00	0.7	19.17	4.1
98	17.32	2.1	0.00	1.3	0.00	0.7	17.32	2.1
70	16.45	3.8	0.00	1.0	0.00	0.7	16.45	3.8
42	15.73	2.1	0.00	0.9	0.00	0.7	15.73	2.1
14	14.39	2.0	0.00	1.0	0.00	0.7	14.39	2.0

Table 5.3.9-7 LWT Cask 2 Meters Off the Plane of Conveyance Dose Rates – DIDO Fuel (Normal Conditions of Transport)

Band [cm]	2 Meters off the Vertical Plane of Conveyance Dose Rates (mrem/hr)							
	Gamma	FSD (%)	Neutron	FSD (%)	N-Gamma	FSD (%)	Total	FSD (%)
285	9.61	10.6	0.00	1.3	0.00	2.5	9.61	10.6
255	9.72	6.2	0.00	1.2	0.00	1.0	9.72	6.2
225	9.05	5.9	0.00	1.3	0.00	1.0	9.05	5.9
195	9.20	6.2	0.00	1.2	0.00	1.0	9.20	6.2
165	8.77	8.8	0.00	1.2	0.00	0.9	8.77	8.8
135	7.74	4.6	0.00	1.2	0.00	1.0	7.74	4.6
105	7.75	6.3	0.00	1.2	0.00	0.9	7.75	6.3
75	6.94	4.6	0.00	1.1	0.00	0.9	6.95	4.6
45	6.67	4.3	0.00	1.2	0.00	0.9	6.67	4.3
15	6.55	3.7	0.00	1.2	0.00	0.8	6.56	3.7

Table 5.3.9-8 LWT Cask 1 Meter from the Cask Surface Dose Rates – DIDO Fuel (Normal Conditions of Transport)

Band [cm]	1 Meter off the Cask Dose Rates							
	Gamma	FSD (%)	Neutron	FSD (%)	N-Gamma	FSD (%)	Total	FSD (%)
285	24.58	6.8	0.01	1.0	0.00	1.4	24.59	6.8
255	37.66	8.5	0.01	0.9	0.00	2.7	37.67	8.5
225	40.09	7.2	0.01	1.0	0.00	1.0	40.10	7.2
195	31.65	8.4	0.01	1.0	0.00	1.0	31.66	8.4
165	21.85	5.5	0.01	1.0	0.00	0.8	21.86	5.5
135	16.74	4.1	0.00	1.1	0.00	0.8	16.75	4.1
105	15.29	4.1	0.00	1.2	0.00	0.7	15.29	4.1
75	13.98	3.6	0.00	1.1	0.00	0.7	13.98	3.6
45	12.97	2.1	0.00	1.1	0.00	0.7	12.97	2.1
15	12.14	1.8	0.00	1.1	0.00	0.6	12.14	1.8

Table 5.3.9-9 Axial Surface Dose Rates at Cask Lid – DIDO Fuel (Normal Conditions of Transport)

Band [cm]	Cask Lid Dose Rates (mrem/hr) Directly Above the DIDO Assemblies					
	Gamma	FSD (%)	Neutron	FSD (%)	Total	FSD (%)
28.5	21.28	1.2	0.03	4.5	21.31	1.2
25.5	34.06	1.2	0.04	4.2	34.10	1.2
22.5	50.79	1.1	0.05	4.5	50.84	1.1
19.5	72.98	1.8	0.06	7.1	73.04	1.8
16.5	88.35	1.1	0.07	5.4	88.42	1.1
13.5	110.20	1.2	0.07	4.4	110.27	1.2
10.5	129.10	1.4	0.08	4.2	129.18	1.4
7.5	145.30	1.5	0.09	7.3	145.39	1.5
4.5	155.70	2.1	0.09	6.0	155.79	2.1
1.5	159.50	2.9	0.09	11.3	159.59	2.9

Table 5.3.9-10 LWT Cask Dose Rates - 5 Meters from the Cask Lid – DIDO Fuel (Back of Tractor Cab) for Normal Conditions of Transport

Band [cm]	5 Meter Dose Rates (mrem/hr)					
	Gamma	FSD (%)	Neutron	FSD (%)	Total	FSD (%)
84.38	0.63	2.4	0.00	9.2	0.63	2.4
73.13	0.68	2.9	0.00	10.2	0.68	2.9
61.88	0.72	3.2	0.00	11.1	0.72	3.2
50.63	0.70	3.2	0.00	12.7	0.70	3.2
39.38	0.79	3.9	0.00	13.6	0.79	3.9
28.13	0.77	4.6	0.00	15.6	0.77	4.6
16.88	0.76	6.9	0.00	21.0	0.76	6.9
5.63	0.90	9.4	0.00	37.9	0.90	9.4

Table 5.3.9-11 LWT Cask Dose Rates - 1 Meter from the Radial Cask Surface – DIDO Fuel (Hypothetical Accident Conditions)

Band [cm]	1 Meter Accident Dose Rates (mrem/hr)					
	Gamma	FSD (%)	Neutron	FSD (%)	Total	FSD (%)
285	24.57	5.4	0.02	0.8	24.59	5.4
255	37.09	5.1	0.02	0.6	37.11	5.1
225	39.60	4.9	0.03	0.5	39.63	4.9
195	32.57	3.2	0.04	0.5	32.61	3.2
165	30.21	9.9	0.04	0.5	30.25	9.9
135	23.86	1.5	0.05	0.4	23.91	1.5
105	22.68	1.5	0.05	0.4	22.73	1.5
75	22.10	2.0	0.05	0.4	22.15	2.0
45	21.16	2.3	0.05	0.4	21.21	2.3
15	21.77	9.0	0.05	0.4	21.82	9.0

5.3.10 GA IFM Shielding Evaluation

Two General Atomics (GA) Irradiated Fuel Material (IFM) Fuel Handling Units (packages) are analyzed for transport in the LWT cask. One IFM package is composed of Reduced-Enrichment Research and Test Reactor (RERTR) type TRIGA fuel. The other is composed of High-Temperature Gas-Cooled Reactor (HTGR) type fuel. Each set of IFM is packaged into stainless steel weld-encapsulated primary and secondary enclosures.

Source terms for each IFM package are calculated using the activity inventories determined by GA as of January 1, 1996. The activity inventory for each package is input into ORIGEN-S, which outputs gamma and neutron spectra in the SCALE 27-group neutron and 18-group gamma structures. A radial one-dimensional shielding analysis is performed using SAS1 for each fuel type independently, with bounding dose rates determined by combining the results for each IFM package.

Table 5.3.10-1 gives the activity inventory for the isotopes in each IFM package. The inventory includes the hardware activation components of the RERTR IFM. Hardware activation for HTGR IFM is not significant. Using the table, ORIGEN-S inputs are created for each fuel type in order to produce gamma and neutron spectra in the SCALE energy group format. ORIGEN-S input is shown in Figure 5.3.10-1 and Figure 5.3.10-2 for RERTR and HTGR IFM, respectively. The resulting spectra are summarized in Table 5.3.10-2.

The geometric description of the fuel is based on the IFM enclosure dimensions and the constituent element masses for each fuel type. Based on the primary enclosure dimensions shown in Table 5.3.10-3, fuel volumes of 7140 and 9555 cm³ are calculated for RERTR and HTGR IFM, respectively. Using these volumes, a density is calculated for each of the constituent elements as shown in Table 5.3.10-4. Material compositions are given in Table 5.3.10-5. Note that the erbium in the TRIGA fuel matrix is not modeled in SAS1.

SAS1 input for RERTR and HTGR IFM is shown in Figure 5.3.10-3 and Figure 5.3.10-4, respectively. No credit is taken for NAC-LWT basket materials or geometry, and the homogenized fuel is centered in the cask cavity. Source strengths are input on a volumetric basis. The same conservative assumptions used in previous radial shielding analysis were applied—i.e., minimum shield dimensions, lead gap, a 0.94 g/cm³ neutron shield solution density, and no boron in the neutron shield solution. In the accident analysis, the neutron shield is modeled as void. Dimensional sketches of the modeled geometry are shown in Figure 5.3.10-5 and Figure 5.3.10-6.

Dose rates for a combined payload of RERTR and HTGR IFM are shown in Table 5.3.10-6. Dose rates are well below regulatory limits at the surface and 2 meters from the truck bed. The transport index, based on the normal conditions dose rate at 1 meter from the package, is less than 1.

Due to the minimal radial dose rates calculated for a combined payload of the GA IFM and the significant amount of stainless steel axial shielding in the NAC-LWT, axial dose rates are expected to be minimal and well below regulatory limits.

Figure 5.3.10-1 ORIGEN-S Input for GA RERTR IFM

```
#ORIGENS
0$$$ A11 71 E T
DECAY CASE
3$$$ 21 1 1 27 A16 4 A33 18 E T
35$$$ 0 T
54$$$ A8 1 E
56$$$ A2 1 A6 1 A10 0 A13 28 A14 5 A15 3 E
57** 0 E T
GA IFM
RERTR FHU NUCLIDE ACTIVITY INVENTORY AS OF 1/1/96
60** 1.E-20
61** F1E-20
65$$$
'GRAM-ATOMS   GRAMS   CURIES   WATTS-ALL   WATTS-GAMMA
3Z   3R1   3R1   3R1   3Z   6Z
3Z   3R1   3R1   3R1   3Z   6Z
3Z   3R1   3R1   3R1   3Z   6Z
81$$$ 2 0 26 1 E
82$$$ 2
83** 1.E+7      8.E+6      6.5E+6      5.E+6      4.E+6
      3.E+6      2.5E+6      2.E+6      1.66E+6     1.33E+6
      1.E+6      8.E+5      6.E+5      4.E+5      3.E+5
      2.E+5      1.E+5      5.E+4      1.E+4
84** 2.E+7      6.434E+6     3.E+6      1.85E+6     1.4E+6
      9.E+5      4.E+5      1.E+5      1.7E+4      3.E+3
      5.5E+2      1.E+2      3.E+1      1.E+1      3.04999E+0
      1.77E+0     1.29999E+0     1.12999E+0     1.E+0      8.E-1
      4.E-1      3.25E-1     2.25E-1     9.999985E-2  5.E-2
      3.E-2      9.999998E-3     1.E-5
73$$$ 250540 260550 270600 280590 280630 430990 922330
      922340 922350 922360 922380 932370 942390 942400
      942410 942420 10030 360850 380900 390900 441060
      511250 551340 551370 611470 621510 631540 631550
74** 1.15E-02 3.06E+01 2.46E+00 3.30E-01 3.96E+01 1.40E-01 1.71E-07
      3.91E-04 7.39E-04 5.61E-03 8.58E-04 2.48E-03 1.30E+00 1.35E+00
      2.84E+02 3.35E-03 2.50E+00 5.86E+01 7.60E+02 7.60E+02 6.67E-01
      4.18E+00 2.29E+01 8.26E+02 9.44E+01 3.35E+00 2.39E+01 6.71E+00
75$$$ 6R1 10R2 12R3 T
RERTR FHU NUCLIDE ACTIVITY INVENTORY AS OF 1/1/96
56$$$ FD T
END
```

Figure 5.3.10-2 ORIGEN-S Input for GA HTGR IFM

```
#ORIGENS
05$ A11 71 E T
DECAY CASE
35$ 21 1 1 27 A16 4 A33 18 E T
35$ 0 T
54$ A8 1 E
56$ A2 1 A6 1 A10 0 A13 22 A14 5 A15 3 E
57** 0 E T
GA IFM
HTGR FNU NUCLIDE ACTIVITY INVENTORY AS OF 1/1/96
60** 1.E-20
61** F1E-20
65$
'GRAM-ATOMS GRAMS CURIES WATTS-ALL WATTS-GAMMA
3Z 3R1 3R1 3R1 3Z 6Z
3Z 3R1 3R1 3R1 3Z 6Z
3Z 3R1 3R1 3R1 3Z 6Z
81$ 2 0 26 1 E
82$ 2
83** 1.E+7 8.E+6 6.5E+6 5.E+6 4.E+6
3.E+6 2.5E+6 2.E+6 1.66E+6 1.33E+6
1.E+6 8.E+5 6.E+5 4.E+5 3.E+5
2.E+5 1.E+5 5.E+4 1.E+4
84** 2.E+7 6.434E+6 3.E+6 1.85E+6 1.4E+6
9.E+5 4.E+5 1.E+5 1.7E+4 3.E+3
5.5E+2 1.E+2 3.E+1 1.E+1 3.04999E+0
1.77E+0 1.29999E+0 1.12999E+0 1.E+0 8.E-1
4.E-1 3.25E-1 2.25E-1 9.999985E-2 5.E-2
3.E-2 9.99998E-3 1.E-5
73$ 10030 360850 380900 390900 511250 551340 551370
611470 621510 631540 631550 902320 922330 922340
922350 922360 922380 942380 942390 942400 942410
942420
74** 3.04E-01 9.19E+00 1.52E+02 1.52E+02 1.15E-01 3.62E-01 1.57E+02
2.59E+00 1.28E+00 1.52E+00 1.49E-01 2.10E-04 2.92E-01 3.13E-02
2.27E-04 1.04E-03 3.84E-06 2.91E+00 1.71E-02 1.91E-02 3.14E+00
1.08E-04
75$ 11R3 11R2 T
HTGR FNU NUCLIDE ACTIVITY INVENTORY AS OF 1/1/96
56$ F0 T
END
```

Figure 5.3.10-3 SAS1 Input for GA RERTR IFM

```
=SAS1
GA FHU - RERTR Source at 1/1/96 - Nrm Model
27N-18COUPLE      INFROMMEDIUM
ZR 1 DEN=0.9413 1.0 END
U 1 DEN=0.5393 1.0 END
H 1 DEN=0.0162 1.0 END
C 1 DEN=0.0022 1.0 END
FE 1 DEN=0.2387 1.0 END
NI 1 DEN=0.1287 1.0 END
CR 1 DEN=0.1067 1.0 END
MN 1 DEN=0.0043 1.0 END
MO 1 DEN=0.0024 1.0 END
AL      2 1.0 END
SS304   3 1.0 END
PB      4 1.0 END
AREMGLYC 0.9437 3 0 1 0 6012 2 1001 6 8016 2 5 .585 END
H2O      5 0.4160 END
END COMP
END

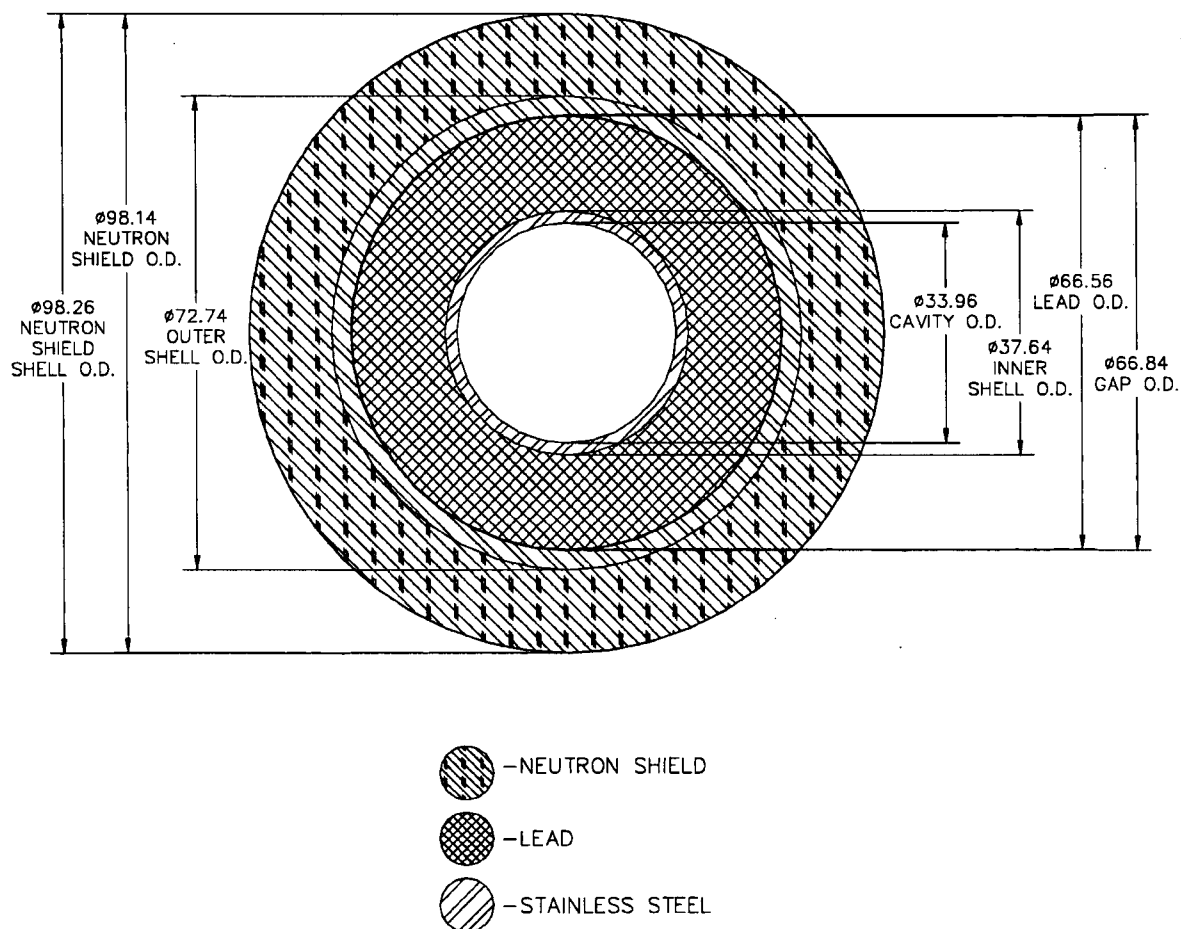
RERTR FHU IN THE NAC-LWT - NEUTRON SOURCE
CYLINDRICAL
1 5.0927 30 -1 0 0.0 1.327E+00 0.0
3 5.3975 4 0
0 5.7277 1 0
3 6.0325 4 0
0 16.9863 1 0
3 18.8214 4 0
4 33.2890 60 0
0 33.4264 1 0
3 36.3728 12 0
5 49.0728 30 0
3 49.1338 4 0
END ZONE
1.440E+02 2.064E+03 2.687E+03 1.239E+03 1.498E+03 1.540E+03
3.009E+02
38Z
DY=87.63 NDETEC=5
READ XSDOSE
87.63 49.1338 43.815 149.1338 87.63 249.1338 43.815
321.92 43.815 349.1338 43.815
END
LAST
RERTR FHU IN THE NAC-LWT - GAMMA SOURCE
CYLINDRICAL
1 5.0927 30 -1 0 0.0 0.0 4.093E+09
3 5.3975 4 0
0 5.7277 1 0
3 6.0325 4 0
0 16.9863 1 0
3 18.8214 4 0
4 33.2890 60 0
0 33.4264 1 0
3 36.3728 12 0
5 49.0728 30 0
3 49.1338 4 0
END ZONE
27Z
5.132E+00 2.423E+01 1.239E+02 3.100E+02 9.223E+02 2.523E+03
9.580E+07 1.893E+09 9.706E+10 6.854E+11 7.046E+11 1.311E+12
1.376E+12 7.350E+11 1.081E+12 3.565E+12 4.901E+12 1.477E+13
DY=87.63 NDETEC=5
READ XSDOSE
87.63 49.1338 43.815 149.1338 87.63 249.1338 43.815
321.92 43.815 349.1338 43.815
END
```

Figure 5.3.10-4 SAS1 Input for GA HTGR IFM

```
=SAS1
GA FHU - HTGR Source at 1/1/96 - Nrm Model
27N-18COUPLE INPHOMMEDIUM
C 1 DEN=0.7405 1.0 END
TH 1 DEN=0.2048 1.0 END
SI 1 DEN=0.1474 1.0 END
U 1 DEN=0.0214 1.0 END
O 1 DEN=0.0023 1.0 END
AL 2 1.0 END
SS304 3 1.0 END
PB 4 1.0 END
AREMGLYC 0.9437 3 0 1 0 6012 2 1001 6 8016 2 5 .585 END
H2O 5 0.4160 END
END COMP
END

HTGR FHU IN THE NAC-LWT - NEUTRON SOURCE
CYLINDRICAL
1 5.7277 30 -1 0 0.0 3.474E-01 0.0
3 6.0325 4 0
0 6.3627 1 0
3 6.6675 4 0
0 16.9863 1 0
3 18.8214 4 0
4 33.2890 60 0
0 33.4264 1 0
3 36.3728 12 0
5 49.0728 30 0
3 49.1338 4 0
END ZONE
1.130E+01 6.522E+02 1.627E+03 4.790E+02 3.328E+02 1.835E+02
3.334E+01
382
DY=92.71 NDETEC=5
READ XSDOSE
92.71 49.1338 46.355 149.1338 92.71 249.1338 46.355
321.92 46.355 349.1338 46.355
END
LAST
HTGR FHU IN THE NAC-LWT - GAMMA SOURCE
CYLINDRICAL
1 5.7277 30 -1 0 0.0 0.0 5.299E+08
3 6.0325 4 0
0 6.3627 1 0
3 6.6675 4 0
0 16.9863 1 0
3 18.8214 4 0
4 33.2890 60 0
0 33.4264 1 0
3 36.3728 12 0
5 49.0728 30 0
3 49.1338 4 0
END ZONE
27Z
4.344E-01 2.119E+00 1.135E+01 2.979E+01 9.356E+01 1.094E+02
1.896E+07 3.731E+08 3.877E+09 4.080E+10 4.055E+10 7.294E+10
1.162E+11 1.454E+11 2.067E+11 6.573E+11 9.500E+11 2.829E+12
DY=92.71 NDETEC=5
READ XSDOSE
92.71 49.1338 46.355 149.1338 92.71 249.1338 46.355
321.92 46.355 349.1338 46.355
END
```

Figure 5.3.10-5 GA IFM One-Dimensional Radial Model of NAC-LWT



Dimensions in cm.

Figure 5.3.10-6 One-Dimensional Radial Model of GA RERTR and HTGR IFM

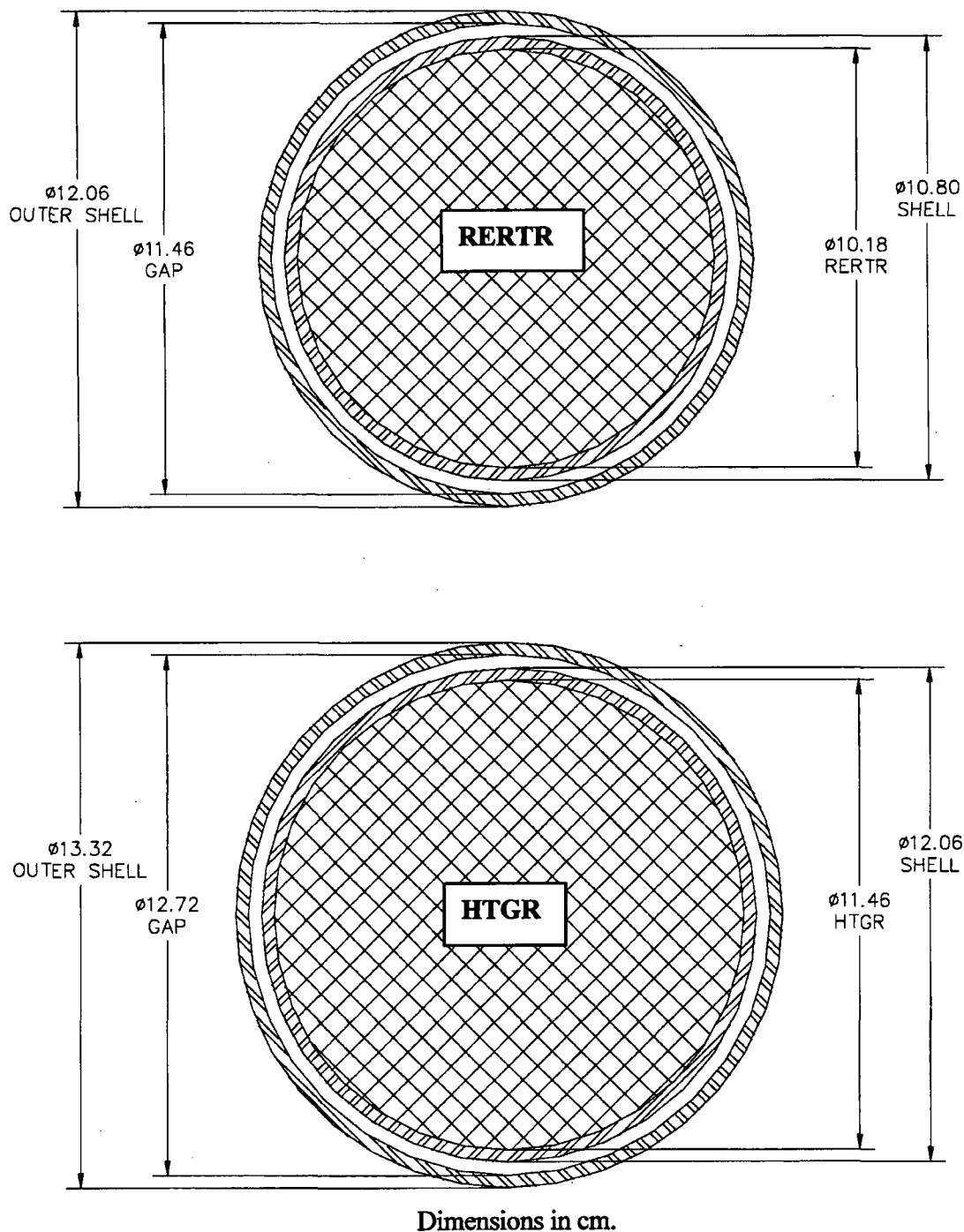


Table 5.3.10-1 GA IFM Activity Inventory as of January 1, 1996

Isotope	Activity [Ci]	
	RERTR	HTGR
³ H	2.50E+00	3.04E-01
⁵⁴ Mn	1.15E-02	—
⁵⁵ Fe	3.06E+01	—
⁶⁰ Co	2.46E+00	—
⁵⁹ Ni	3.30E-01	—
⁶³ Ni	3.96E+01	—
⁸⁵ Kr	5.86E+01	9.19E+00
⁹⁰ Sr	7.60E+02	1.52E+02
⁹⁰ Y	7.60E+02	1.52E+02
⁹⁹ Tc	1.40E-01	—
¹⁰⁶ Ru	6.67E-01	—
¹²⁵ Sb	4.18E+00	1.15E-01
¹³⁴ Cs	2.29E+01	3.62E-01
¹³⁷ Cs	8.26E+02	1.57E+02
¹⁴⁷ Pm	9.44E+01	2.59E+00
¹⁵¹ Sm	3.35E+00	1.28E+00
¹⁵⁴ Eu	2.39E+01	1.52E+00
¹⁵⁵ Eu	6.71E+00	1.49E-01
²³² Th	—	2.10E-04
²³³ U	1.71E-07	2.92E-01
²³⁴ U	3.91E-04	3.13E-02
²³⁵ U	7.39E-04	2.27E-04
²³⁶ U	5.61E-03	1.04E-03
²³⁸ U	8.58E-04	3.84E-06
²³⁷ Np	2.48E-03	—
²³⁸ Pu	—	2.91E+00
²³⁹ Pu	1.30E+00	1.71E-02
²⁴⁰ Pu	1.35E+00	1.91E-02
²⁴¹ Pu	2.84E+02	3.14E+00
²⁴² Pu	3.35E-03	1.08E-04
Total	2920	483

Table 5.3.10-2 GA IFM Neutron and Gamma Spectra in SCALE Format

Energy Group	HTGR IFM		RERTR IFM	
	[neutron/sec]	[gamma/sec]	[neutron/sec]	[gamma/sec]
1	1.130E+01	4.344E-01	1.440E+02	5.132E+00
2	6.522E+02	2.119E+00	2.064E+03	2.423E+01
3	1.627E+03	1.135E+01	2.687E+03	1.239E+02
4	4.790E+02	2.979E+01	1.239E+03	3.100E+02
5	3.328E+02	9.356E+01	1.498E+03	9.223E+02
6	1.835E+02	1.094E+02	1.540E+03	2.523E+03
7	3.334E+01	1.896E+07	3.009E+02	9.580E+07
8	0.000E+00	3.731E+08	0.000E+00	1.893E+09
9	0.000E+00	3.877E+09	0.000E+00	9.706E+10
10	0.000E+00	4.080E+10	0.000E+00	6.854E+11
11	0.000E+00	4.055E+10	0.000E+00	7.046E+11
12	0.000E+00	7.294E+10	0.000E+00	1.311E+12
13	0.000E+00	1.162E+11	0.000E+00	1.376E+12
14	0.000E+00	1.454E+11	0.000E+00	7.350E+11
15	0.000E+00	2.067E+11	0.000E+00	1.081E+12
16	0.000E+00	6.573E+11	0.000E+00	3.565E+12
17	0.000E+00	9.500E+11	0.000E+00	4.901E+12
18	0.000E+00	2.829E+12	0.000E+00	1.477E+13
19	0.000E+00		0.000E+00	
20	0.000E+00		0.000E+00	
21	0.000E+00		0.000E+00	
22	0.000E+00		0.000E+00	
23	0.000E+00		0.000E+00	
24	0.000E+00		0.000E+00	
25	0.000E+00		0.000E+00	
26	0.000E+00		0.000E+00	
27	0.000E+00		0.000E+00	
Total	3.319E+03	5.063E+12	9.473E+03	2.922E+13

Table 5.3.10-3 GA IFM Primary and Secondary Enclosure Dimensions

Description	Value [in]
RERTR Primary Enclosure Interior Height	34.50
RERTR Primary Enclosure OD	4.25
RERTR Secondary Enclosure OD	4.75
RERTR Enclosure Wall Thickness	0.12
HTGR Primary Enclosure Interior Height	36.50
HTGR Primary Enclosure OD	4.75
HTGR Secondary Enclosure OD	5.25
HTGR Enclosure Wall Thickness	0.12

Table 5.3.10-4 Elemental Constituents of GA IFM

Fuel Type	Element	Mass [g]	Density [g/cc]
RERTR	ZR	6721.1	0.9413
	U	3850.66	0.5393
	H	116.02	0.0162
	ER	63.32	0.0089
	C	15.44	0.0022
	FE	1704.5	0.2387
	NI	919.1	0.1287
	CR	761.7	0.1067
	MN	30.8	0.0043
	MO	17.3	0.0024
	Total	14199.94	1.9888
HTGR	C	7075.55	0.7405
	TH	1956.87	0.2048
	SI	1408.37	0.1474
	U	204.81	0.0214
	O	22.40	0.0023
	Total	10668.00	1.1165

Table 5.3.10-5 Material Compositions of GA IFM and NAC-LWT

Material	SCALE Isotope/Element	Number Density [atom/b-cm]
RERTR Fuel	HYDROGEN	9.68035E-03
	CARBON-12	1.10406E-04
	CHROMIUM	1.23580E-03
	MANGANESE	4.71352E-05
	IRON	2.57407E-03
	NICKEL	1.32065E-03
	ZIRCONIUM	6.21428E-03
	MOLYBDENUM	1.50647E-05
	URANIUM-234	7.50436E-08
	URANIUM-235	9.82391E-06
	URANIUM-238	1.35453E-03
HTGR Fuel	CARBON-12	3.71616E-02
	OXYGEN-16	8.66191E-05
	SILICON	3.16060E-03
	THORIUM-232	5.31533E-04
	URANIUM-234	2.97781E-09
	URANIUM-235	3.89823E-07
	URANIUM-238	5.37492E-05
Stainless Steel	CHROMIUM (SS304)	1.74286E-02
	MANGANESE	1.73633E-03
	IRON (SS304)	5.93579E-02
	NICKEL (SS304)	7.72070E-03
Lead	LEAD	3.29690E-02
Neutron Shield	HYDROGEN	5.99351E-02
	CARBON-12	1.07197E-02
	OXYGEN-16	2.46077E-02

Table 5.3.10-6 Combined Payload Radial Dose Rates for GA IFM

Condition	Source	Surface [mrem/hr]	1 meter [mrem/hr]	2 meter [mrem/hr]
Normal	Neutron	1.7E-03	1.7E-04	4.3E-05
	Gamma	4.8E-01	6.1E-02	1.9E-02
	Total	4.8E-01	6.1E-02	1.9E-02
Accident	Neutron	2.0E-02	2.4E-03	6.1E-04
	Gamma	7.0E-01	1.0E-01	3.3E-02
	Total	7.2E-01	1.0E-01	3.4E-02

5.3.11 High Burnup PWR and BWR Rods in a Fuel Assembly Lattice

Results of a shielding analysis for up to 25 high burnup PWR or BWR intact fuel rods in a fuel assembly lattice are presented in this section. The rods have burnups up to 80,000 MWd/MTU. The fuel assembly lattice hardware is assumed to have been activated by an 80,000 MWd/MTU average burnup fuel assembly. Based on the minimum cool times developed in Section 5.3.8 for intact fuel in the rod holder, maximum dose rates are calculated to demonstrate that the 10 CFR 71 dose rate limits are not exceeded.

Dose rates are calculated using the MCBEND three-dimensional Monte Carlo transport code. Source terms are calculated using the SAS2H module of the SCALE package, with ORIGEN-S used to rebin the gamma-ray and neutron spectra onto the 22-group and 28-group structures required by MCBEND.

5.3.11.1 High Burnup PWR and BWR Rod and Lattice Source Terms

A total of eight fuel assembly models are employed in the analysis. BWR 7×7 and 8×8 fuel pin parameters are taken from the analysis in Section 5.3.8, with additional lattice parameters taken from a survey of BWR fuel assembly data. The six PWR fuel assembly models are based on the most prevalent designs that fit within the NAC-LWT cavity. Based on the PWR fuel characteristics in Table 1.2-5, B&W 15×15 and 17×17, CE 14×14, and Westinghouse (WE) 14×14, 15×15, and 17×17 bounding fuel assembly models are created based on maximizing uranium loading (MTU). The use of specific assembly types in the analysis allows modeling of the as-loaded axial positioning of the lattice, as determined by the assembly-specific spacer lengths defined in the License drawings.

Three-dimensional fuel assembly parameters are defined in Table 5.3.11-3 and Table 5.3.11-4 for BWR and PWR fuel lattices, respectively. SAS2H models are created based on the parameters in Table 5.3.11-5, and assume 95% theoretical density UO₂. Source terms employed in this analysis are identical to those employed in Section 5.3.8. The SAS2H-generated source spectra are rebinned, using ORIGEN-S, onto the standard 28 group neutron and 22 group gamma scheme used in MCBEND as shown in Table 5.3.11-1 and Table 5.3.11-2, respectively.

Gamma, and neutron, and hardware source terms in MCBEND format are presented in Table 5.3.11-6 through Table 5.3.11-13 for PWR and BWR fuel. PWR and BWR 8×8 fuel types are analyzed at 80,000 MWd/MTU and 150 days cool time. Based on the results in Section 5.3.8, the minimum cool time for BWR 7×7 fuel is 210 days for a maximum burnup of 60,000 MWd/MTU; BWR 7×7 fuel is conservatively analyzed at 80,000 MWd/MTU and 210 days cool time.

Activated fuel assembly hardware source terms are found by multiplying the source strength from 1 kilogram by the kilograms of steel or inconel material in the active fuel, plenum, upper end fitting or lower end fitting regions, and by multiplying by a regional flux ratio. The regional flux ratio accounts for the effects of both magnitude and spectrum variation on hardware activation. These ratios are based on empirical data (Luksic). Within the active fuel region, this ratio is unity. A flux ratio of 0.2 is applied to hardware regions directly adjacent to the active core region (i.e., upper and lower plenum), and a flux ratio of 0.1 is applied to hardware regions once removed from the active core region (i.e., upper and lower end fitting region). For BWR fuel, the recommended lower end fitting flux ratio is 0.15 (Luksic).

The analyzed hardware source terms for BWR fuel are based on the maximum values in each source region determined in a survey of BWR assembly data. Maximum values are shown in Table 5.3.11-3. The BWR 7×7 hardware inventory reflects the maximum for 7×7 assemblies and the BWR 8×8 hardware inventory reflects the maximum for 8×8, 9×9, and 10×10 assemblies. The analyzed hardware source terms for PWR fuel are based on the values specific to each assembly type, shown in Table 5.3.11-4. Based on the modeled source regions discussed in Section 5.3.11.3, the lower nozzle (end-fitting) hardware inventories in Table 5.3.11-4 reflect the combination of lower nozzle and lower plenum (if present) masses.

The effect of subcritical neutron multiplication is not directly computed in the MCBEND analysis, due to difficulties in adequately biasing the calculation. Instead, neutron source rates are scaled by a subcritical multiplication factor based on the system multiplication factor, k_{eff} :

$$\text{Scale Factor} = \frac{1}{1 - k_{\text{eff}}}$$

For the dry cask conditions of transport, calculated system k_{eff} is 0.06 for BWR fuel and is 0.05 for PWR fuel, with resulting scale factors of 1.0638 and 1.0526, respectively. These scale factors are included in the source strength input unit in MCBEND.

5.3.11.2 Axial Source Profile

The axial source profiles employed in MCBEND for PWR fuel are identical to those employed in Section 5.3.8.1.1. The 1.22 peaking factor for BWR fuel employed in Section 5.3.8.1.1 represents a bounding shape for fuel assembly burnups up to 35,000 MWd/MTU. A 1.15 peak represents an expected bounding value for burnups greater than 60,000 MWd/MTU and is employed here. Based on the indicated burnup profiles for PWR and BWR fuel, the ratio of average source to average burnup is unity (1) for fuel gamma sources. It is 1.13 and 1.31 for PWR and BWR neutron sources, respectively. Profiles are input by evaluating the source multiplier in each axial bin. By default, no internal normalization of the profile is performed.

Profiles are shown graphically in Figure 5.3.11-1 and Figure 5.3.11-2 and Table 5.3.11-14 and Table 5.3.11-15.

5.3.11.3 High Burnup PWR and BWR Rod and Lattice Shielding Model

MCBEND three-dimensional shielding analysis allows detailed modeling of the fuel, basket, and cask shield configurations. For the fuel rod sources, some fuel rod detail is homogenized in the model to simplify model input and improve computational efficiency. Thus, the three-dimensional models represent the various fuel assembly source regions as homogenized zones within the fuel assembly lattice width, but explicitly model the axial extent of the source regions. The basket and cask body details are explicitly modeled, including the axial extents described by the License Drawings.

The geometric description of a MCBEND model is based on the combinatorial geometry system embedded in the code. In this system, bodies such as cylinders and rectangular parallelepipeds, and their logical intersections and unions, are used to describe the extent of material zones.

MCBEND employs an automated biasing technique for the Monte Carlo calculation based on a three-dimensional adjoint diffusion calculation. Mesh cells for the adjoint solution are selected based on half value thicknesses for each material.

Fuel Assembly Model (Lattice and 25 Fuel Rods)

Based on the fuel parameters provided in Table 5.3.11-3 and Table 5.3.11-4, homogenized treatments of fuel assembly source regions are developed. The homogenized fuel assembly is represented in the model as a stack of boxes with width equal to the fuel assembly width. The height of each box corresponds to the modeled height of the corresponding assembly region.

The active fuel region homogenizations for the analyzed fuel types shown in Table 5.3.11-16 and Table 5.3.11-17 are based on the detailed three-dimensional data in Table 5.3.11-3 and Table 5.3.11-4. Components of the fuel assembly homogenization are subdivided to account for the various area fractions present in the homogenized fuel assembly description. "Interstitial" refers to the space within the fuel assembly array defined by the lattice pitch but outside the fuel rods. "Void" refers to the pellet to clad gap. Combined with the fuel rod clad and fuel material, the void accounts for the total fuel region volume. The clad region is zirconium alloy (density 6.55 g/cm³) for all fuel types. For PWR fuel, the guide and instrument tube volumes are also considered in the fuel assembly homogenization. The activated steel/inconel in the active fuel region (Table 5.3.11-18) is added to the fuel material description as a final step.

Fuel assembly nonfuel regions are homogenized as shown in Table 5.3.11-18, based on the model parameters in Table 5.3.11-3 and Table 5.3.11-4. The only material included in the homogenized region is stainless steel. Volume fractions of material are based on the modeled

regional volume and the volume of stainless steel as computed from the modeled mass and density (7.92 g/cm^3 for stainless steel).

Damaged Fuel Model

Under hypothetical accident conditions, the high burnup rods in the fuel assembly lattice are assumed to reconfigure towards the upper region of the NAC-LWT cavity. Modeling the source in this location maximizes gamma streaming above the radial lead shield and neutron flux above the liquid neutron shield.

For each fuel type, a conservative compaction fraction is assumed in order to model all of the UO_2 above the upper elevation of the basket in the case of PWR fuel and above the PWR insert in the case of BWR fuel. Compaction fractions of 70% for BWR fuel and 50% for PWR fuel were employed to meet this height restriction. Based on these compaction fractions and the amount of UO_2 in 25 rods for each fuel type, damaged fuel heights are calculated as shown in Table 5.3.11-19.

Basket Model

For a given fuel type, the MCBEND description of the basket elements forms a common sub-model employed in the analysis. The key feature of the model is the detailed representation of the PWR basket. The BWR model adds the PWR insert required for shipment of a BWR fuel assembly in the PWR basket.

MCBEND NAC-LWT Model

The three-dimensional model of the NAC-LWT cask containing design basis fuel assemblies is based on the following features:

Normal conditions:

- Radial neutron shield and shield shell
- Aluminum impact limiters with 0.5 g/cm^3 density (calculated based on the impact limiter weight and dimensions) and diameter equal to the neutron shield shell diameter

Accident conditions:

- Removal of radial neutron shield and shield shell
- Loss of upper and lower impact limiters

Common to both the normal and accident conditions models is a 0.1374 cm gap between the lead outer diameter and the cask outer shell. For BWR fuel, the top of the fuel assembly is modeled flush with the top of the NAC-LWT cask cavity. For PWR fuel, the assembly-specific PWR

assembly spacer length is considered, yielding an offset ranging from 3.92 inches (9.96 cm) to 12.26 inches (31.14 cm) from the fuel assembly top to the top of the NAC-LWT cask cavity.

Detailed model parameters used in creating the three-dimensional model are taken directly from the License Drawings. Elevations associated with the three-dimensional features are established with respect to the center bottom of the NAC-LWT cask cavity for the MCBEND combinatorial model. The three-dimensional NAC-LWT models are shown in Figure 5.3.11-3 and Figure 5.3.11-4 for the modeled B&W 15×15 PWR lattice. A sample MCBEND input file for the PWR lattice evaluation is provided in Figure 5.3.11-8.

Shield Regional Densities

Based on the homogenization, the resulting active fuel regional densities are shown in Table 5.3.11-20 and Table 5.3.11-21. Material compositions for remaining structural and shield materials, as well as the BWR and PWR damaged fuel definitions, are shown in Table 5.3.11-22. Compositions for fuel assembly non-fuel regions are equivalent to the stainless steel composition in Table 5.3.11-22 scaled by the material volume fractions shown in Table 5.3.11-18.

5.3.11.4 High Burnup PWR and BWR Rod and Lattice Shielding Evaluation

The shielding evaluation is performed using MCBEND. As described in Section 5.3.11.2, the evaluation includes the effect of fuel burnup peaking on fuel neutron and gamma source terms.

The MCBEND shielding model described in Section 5.3.11.3 is utilized with the source terms described in Section 5.3.11.1 to estimate the dose rate profiles at various distances from the side, top and bottom of the cask for both normal and accident conditions. The method of solution is continuous energy Monte Carlo with an adjoint diffusion solution for generating importance meshes. Radial biasing is performed within the MCBEND code to estimate dose rates on the side of the cask. Axial biasing is performed to estimate dose rates on the top and bottom of the cask.

The MCBEND code has been validated against various classical shielding problems, including fast and thermal neutron sources penetrating through single material slab geometries of iron, graphite and water. The validation suite also includes fast neutron transmission through alternating slabs of iron and water. Of particular interest is a benchmark of MCBEND to gamma and neutron dose rates outside a metal transport cask, where agreement between measurement and calculation is within 20% for the majority of dose locations.

MCBEND results are calculated using the JEF2.2 neutron cross-section library and the ANSWERS gamma library.

MCBEND Flux-to-Dose Conversion Factors

The ANSI/ANS 6.1.1-1977 flux-to-dose rate conversion factors are employed in the MCBEND analysis. The ANSI/ANS gamma and neutron dose conversion factors are shown in Table 5.3.11-23 and Table 5.3.11-24. The number of energy/conversion factor pairs was increased to 133 neutron and 371 gamma pairs by a log-log interpolation scheme indicated as appropriate in ANSI/ANS 6.1.1-1977.

Three-Dimensional Dose Rates for High Burnup Fuel

Table 5.3.11-25 and Table 5.3.11-26 summarize the computed dose rates for each fuel type at the tabulated distances and transport conditions (normal and accident).

Normal condition radial surface dose rates for PWR and BWR fuel are in excess of 200 mrem/hr, necessitating an exclusive use designation for the NAC-LWT. The maximum dose rate, calculated for BWR 7×7 fuel, is dominated by the upper nozzle (end fitting) component, which comprises approximately 80% of the maximum dose rate. The axial elevation of the maximum dose rate is above the lead gamma shield. The dose rate profile is shown in Figure 5.3.11-5.

The normal condition maximum radial 2-meter dose rate is 9.9 mrem/hr, calculated for B&W 15×15 fuel. At this distance, the fuel gamma component contributes approximately 74% of the maximum. The maximum dose rate occurs near the fuel midplane, as shown Figure 5.3.11-6.

Accident condition radial 1-meter dose rates for all three fuel types are below the 1,000 mrem/hr limit. The maximum dose rate, calculated for BWR 7×7 fuel, is dominated by the damaged fuel neutron and damaged fuel gamma components, which each contribute approximately 47% towards the maximum. The axial elevation of the maximum dose rate is coincident with the top of the NAC-LWT cavity, the location of the damaged fuel material volume. The dose rate profile is shown in Figure 5.3.11-7

As shown in Table 5.3.11-26, axial surface dose rates are well below limits for PWR and BWR fuel. Significant margin is present for the normal condition 2-meter and accident condition 1-meter dose rate limits.

Figure 5.3.11-1 PWR Lattice Axial Source Profiles

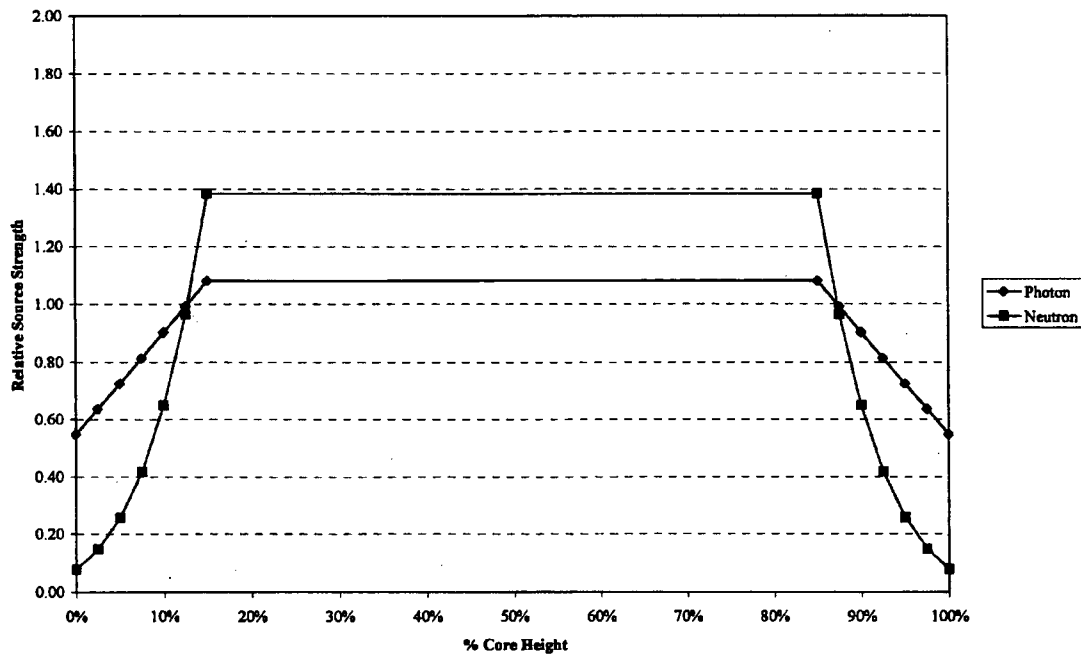


Figure 5.3.11-2 BWR Lattice Axial Source Profiles

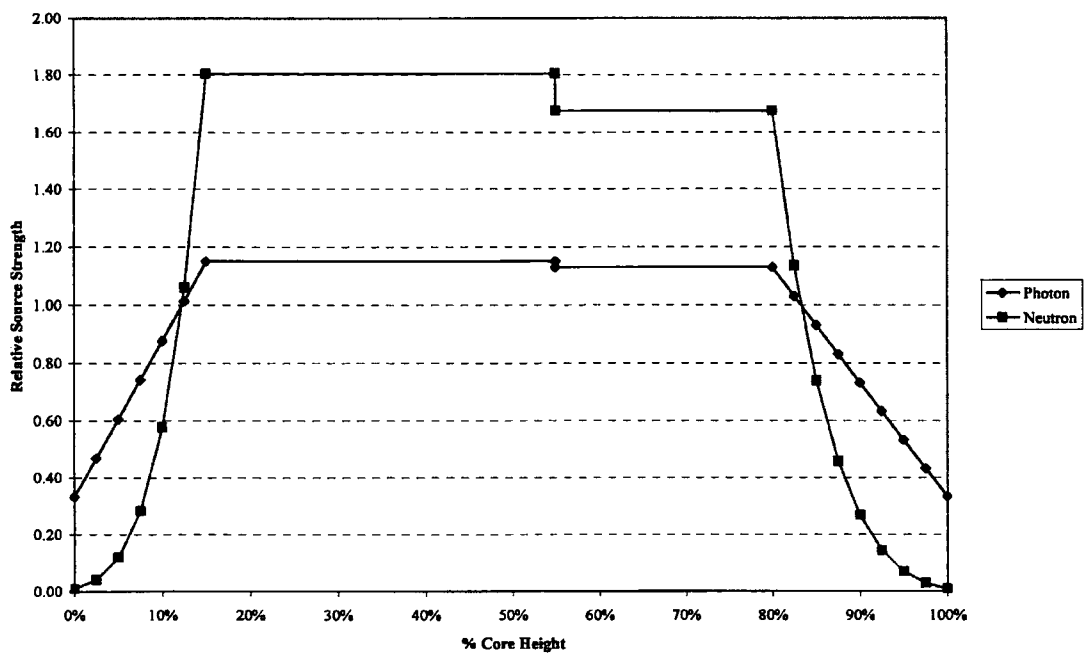
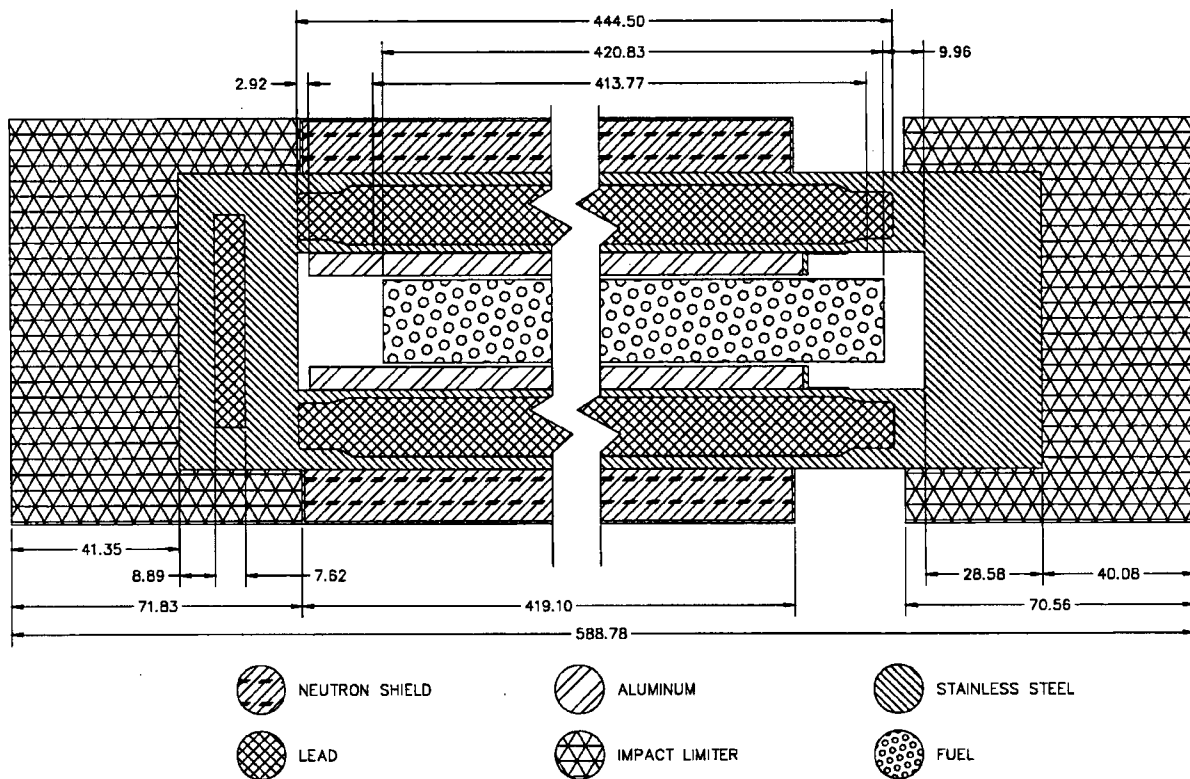


Figure 5.3.11-3 MCBEND Model of NAC-LWT with Fuel Assembly Lattice – Axial Detail



Dimensions in cm.

Figure 5.3.11-4 MCBEND Model of NAC-LWT with Fuel Assembly Lattice – Radial Detail

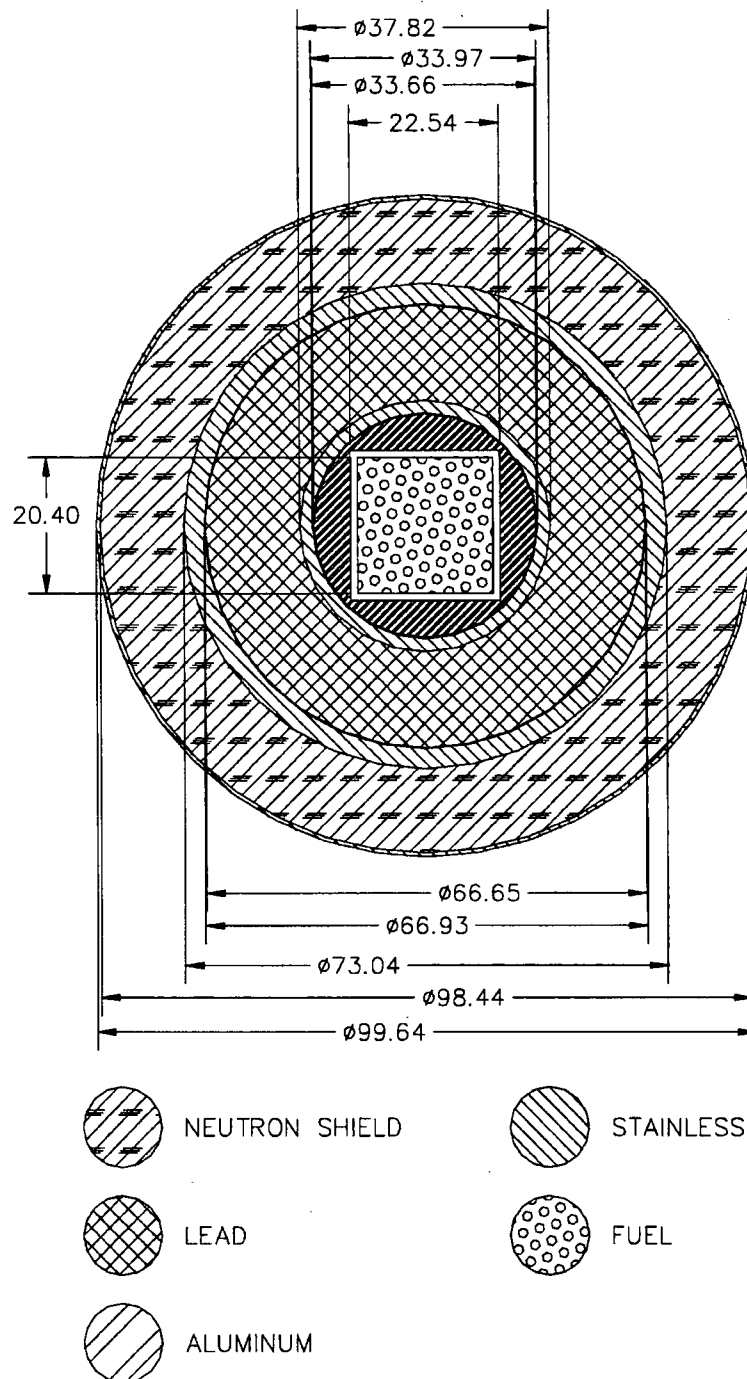


Figure 5.3.11-5 Normal Condition Radial Surface Dose Rate Profile by Source Type – Fuel Assembly Lattice

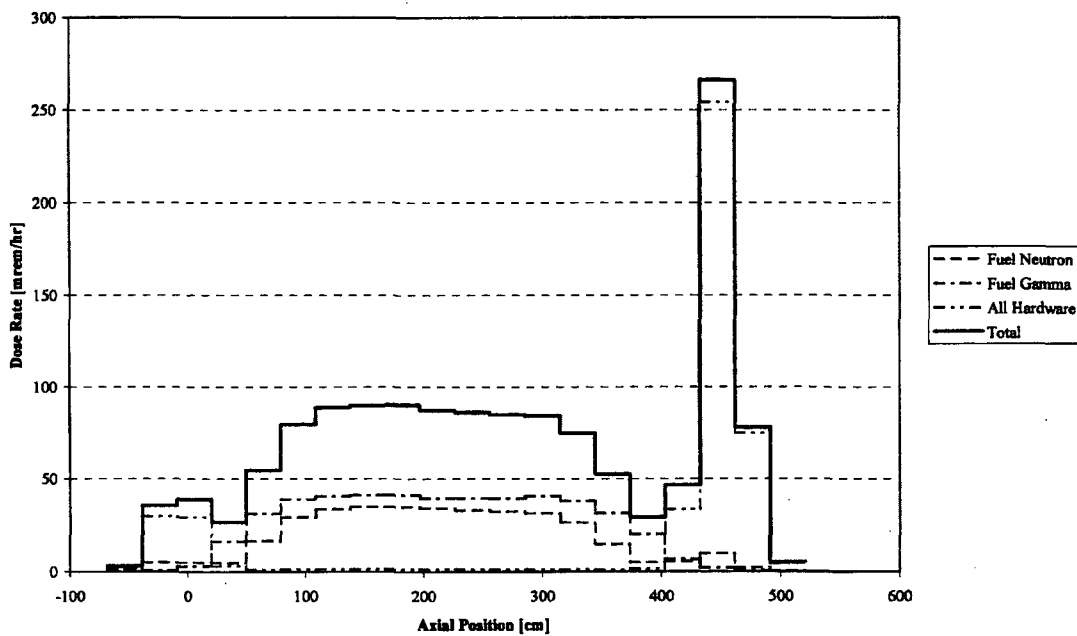


Figure 5.3.11-6 Normal Condition Radial 2m Dose Rate Profile by Source Type – Fuel Assembly Lattice

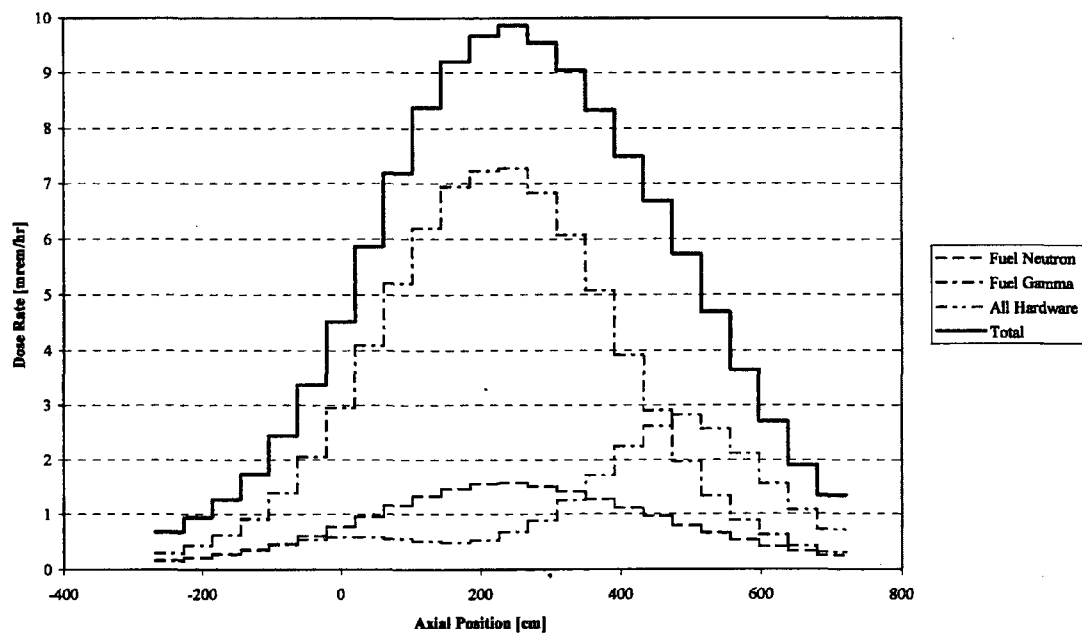


Figure 5.3.11-7 Accident Condition Radial 1m Dose Rate Profile by Source Type –
Fuel Assembly Lattice

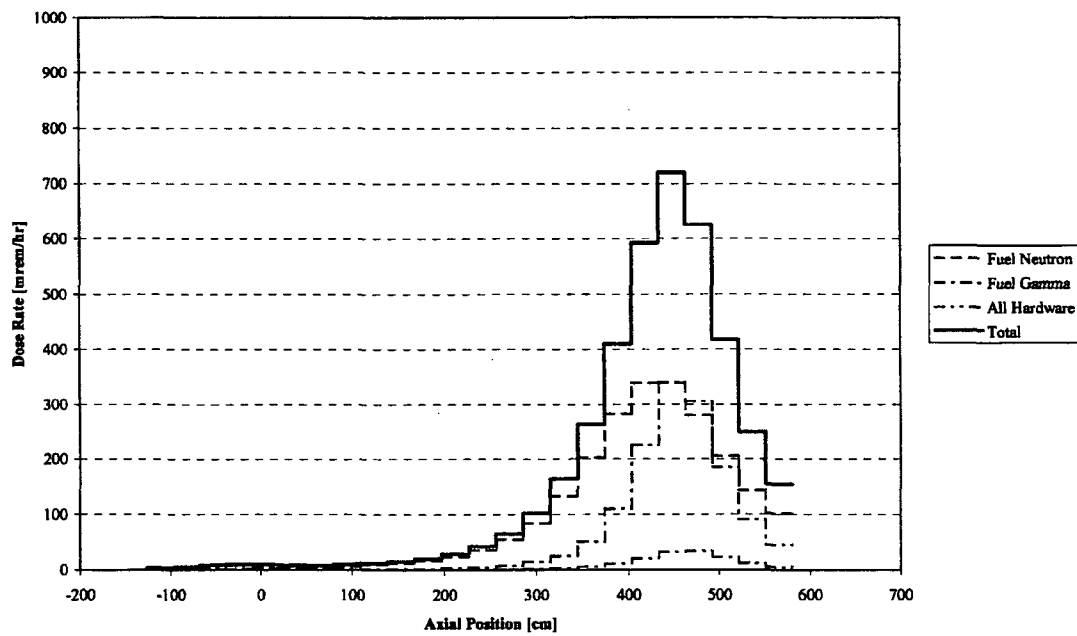


Figure 5.3.11-8 MCBEND Input – High Burnup Fuel Lattice – Radial Fuel Gamma

```

columns 1 200
*
* LWT Cask - lwtNmRadFg_bw15b_80b40e150d
* Normal Transport Conditions
* Model Revision v1.9.2
*
*
* Parameters
*
@samps = 10000000
*
* Unit 1 Control Data
*
begin control data
  run
  sample limit @samps
  time limit 1000m
  seeds 76008 97592
  chime every (@samps/10) samples
  report interim results
  sbd 30s
  dump intervals 1
end
*
* Unit 3 Output Control
*
*begin output control
* suppress inflows
*end
*
* Unit 4 Material Geometry
*
begin material geometry
* LWR Fuel Assembly - Class 2 - bw15b - B&W15 (Mark B2)
PART 1 NEST
BOX M2 0.0000 0.0000 0.0000 21.6814 21.6814 18.4087 ! lower nozzle
BOX M1 S 0.0000 0.0000 0.0000 21.6814 21.6814 384.1687 ! fuel
BOX M4 0.0000 0.0000 0.0000 21.6814 21.6814 395.6050 ! top plenum
BOX M3 0.0000 0.0000 0.0000 21.6814 21.6814 420.6875 ! upper nozzle
* PWR Fuel Basket v1.9
PART 2
BOX 1 -10.8407 -10.8407 21.4757 21.6814 21.6814 420.6875 ! Fuel assembly
BOX 2 -11.2713 -11.2713 0.0000 22.5425 22.5425 442.1632 ! Fuel assembly void
ZROD 3 0.0000 0.0000 2.9210 16.8275 410.2100 ! Basket
BOX 4 -11.6743 -11.6743 413.1310 23.3487 23.3487 1.2700 ! Flange inner
ZROD 5 0.0000 0.0000 413.1310 16.8351 1.2700 ! Flange outer
ZROD 6 0.0000 0.0000 414.4010 16.5100 9.8552 ! Ring inner
ZROD 7 0.0000 0.0000 414.4010 16.8351 9.8552 ! Ring outer
ZP 8 433.3012 ! Cut plane
ZROD 9 0.0000 0.0000 0.0000 16.8351 452.1200 ! Container
ZONES
/FuelAssy/ P1 +1
/FuelAssyVoid/ M0 +2 -1 -8
/Basket/ M7 +3 -2
/FlangeVoid/ M0 +4 -2
/Flange/ M9 +5 -4
/RingVoid/ M0 +6 -2
/Ring/ M9 +7 -6
/Void/ M0 +8 +9 -1
/Container/ M0 +9 -2 -3 -5 -7 -8
VOLUMES UNITY
* PWR Fuel Basket in Cask Cavity v1.9
PART 3
ZROD 1 0.0000 0.0000 0.0000 16.8351 452.1200 ! PWR basket
ZROD 2 0.0000 0.0000 0.0000 16.9863 452.1200 ! Cavity
ZONES
/PWRBasket/ P2 +1
/Cavity/ M0 +2 -1
VOLUMES UNITY
* LWT Cask Normal Conditions v1.9
PART 4
ZROD 1 0.0000 0.0000 -26.6700 36.5189 507.3650 ! Lwt
ZROD 2 0.0000 0.0000 -26.6700 36.5189 26.6700 ! Bottom
ZROD 3 0.0000 0.0000 0.0000 16.9863 452.1200 ! Cavity
ZROD 4 0.0000 0.0000 -17.7800 26.3525 7.6200 ! Bottom gamma shield
ZROD 5 0.0000 0.0000 0.0000 20.1740 444.5000 ! Lead id - taper
ZROD 6 0.0000 0.0000 0.0000 31.5976 444.5000 ! Lead od - taper
ZROD 7 0.0000 0.0000 13.8176 18.9103 416.8648 ! Lead id
ZROD 8 0.0000 0.0000 13.8176 33.3271 416.8648 ! Lead od
ZROD 9 0.0000 0.0000 13.8176 33.4645 416.8648 ! Lead gap
ZROD 10 0.0000 0.0000 3.8100 49.8183 419.1000 ! Neutron shield shell
ZROD 11 0.0000 0.0000 5.0800 49.2189 416.5600 ! Neutron shield
ZROD 12 0.0000 0.0000 450.2150 49.8183 70.5612 ! Upper limiter
ZROD 13 0.0000 0.0000 -68.0212 49.8183 71.8312 ! Lower limiter
ZROD 14 0.0000 0.0000 -68.0212 49.8183 588.7974 ! Container
ZONES
/BotPb/ M8 +4

```

Figure 5.3.11-8 MCBEND Input – High Burnup Fuel Lattice – Radial Fuel Gamma

```

/Cavity/      P3      +3
/Bottom/      M9      +2      -4
/OuterShell/  M9      +1      -2      -6      -9      -3
/InnerShellTaper/ M9      +5      -8      -3
/InnerShell/  M9      +7      -3
/Lead/        M8      +8      -7
/LeadTaper/   M8      +6      -5      -8
/LeadGap/     M0      +9      -8
/NeutronShield/ M6      +11     -1
/NSShell/     M9      +10     -1     -11
/UpperLimiter/ M10     +12     -1
/LowerLimiter/ M10     +13     -1
/Exterior/    M0      +14     -1     -10     -12     -13
VOLUMES UNITY
* LWT Cask Detector Description v1.9
PART 5
* Radial Detector DRA (Surface) Bodies
ZROD 1 0.0000 0.0000 -68.0212 49.8183 588.7974
ZROD 2 0.0000 0.0000 -68.0212 50.8183 29.4399
ZROD 3 0.0000 0.0000 -38.5813 50.8183 29.4399
ZROD 4 0.0000 0.0000 -9.1415 50.8183 29.4399
ZROD 5 0.0000 0.0000 20.2984 50.8183 29.4399
ZROD 6 0.0000 0.0000 49.7383 50.8183 29.4399
ZROD 7 0.0000 0.0000 79.1782 50.8183 29.4399
ZROD 8 0.0000 0.0000 108.6180 50.8183 29.4399
ZROD 9 0.0000 0.0000 138.0579 50.8183 29.4399
ZROD 10 0.0000 0.0000 167.4978 50.8183 29.4399
ZROD 11 0.0000 0.0000 196.9376 50.8183 29.4399
ZROD 12 0.0000 0.0000 226.3775 50.8183 29.4399
ZROD 13 0.0000 0.0000 255.8174 50.8183 29.4399
ZROD 14 0.0000 0.0000 285.2572 50.8183 29.4399
ZROD 15 0.0000 0.0000 314.6971 50.8183 29.4399
ZROD 16 0.0000 0.0000 344.1370 50.8183 29.4399
ZROD 17 0.0000 0.0000 373.5769 50.8183 29.4399
ZROD 18 0.0000 0.0000 403.0167 50.8183 29.4399
ZROD 19 0.0000 0.0000 432.4566 50.8183 29.4399
ZROD 20 0.0000 0.0000 461.8965 50.8183 29.4399
ZROD 21 0.0000 0.0000 491.3363 50.8183 29.4399
* Radial Detector DRAA (SurfaceAzi) Bodies
ZROD 22 0.0000 0.0000 -69.0212 50.8183 590.7974
* Band 1 Bodies
ZSEC 23 0.0000 0.0000 444.5000 50.8183 51.8183 36.1950 0.0000 12.0000
ZSEC 24 0.0000 0.0000 444.5000 50.8183 51.8183 36.1950 12.0000 24.0000
ZSEC 25 0.0000 0.0000 444.5000 50.8183 51.8183 36.1950 24.0000 36.0000
ZSEC 26 0.0000 0.0000 444.5000 50.8183 51.8183 36.1950 36.0000 48.0000
ZSEC 27 0.0000 0.0000 444.5000 50.8183 51.8183 36.1950 48.0000 60.0000
ZSEC 28 0.0000 0.0000 444.5000 50.8183 51.8183 36.1950 60.0000 72.0000
ZSEC 29 0.0000 0.0000 444.5000 50.8183 51.8183 36.1950 72.0000 84.0000
ZSEC 30 0.0000 0.0000 444.5000 50.8183 51.8183 36.1950 84.0000 96.0000
ZSEC 31 0.0000 0.0000 444.5000 50.8183 51.8183 36.1950 96.0000 108.0000
ZSEC 32 0.0000 0.0000 444.5000 50.8183 51.8183 36.1950 108.0000 120.0000
ZSEC 33 0.0000 0.0000 444.5000 50.8183 51.8183 36.1950 120.0000 132.0000
ZSEC 34 0.0000 0.0000 444.5000 50.8183 51.8183 36.1950 132.0000 144.0000
ZSEC 35 0.0000 0.0000 444.5000 50.8183 51.8183 36.1950 144.0000 156.0000
ZSEC 36 0.0000 0.0000 444.5000 50.8183 51.8183 36.1950 156.0000 168.0000
ZSEC 37 0.0000 0.0000 444.5000 50.8183 51.8183 36.1950 168.0000 180.0000
ZSEC 38 0.0000 0.0000 444.5000 50.8183 51.8183 36.1950 180.0000 192.0000
ZSEC 39 0.0000 0.0000 444.5000 50.8183 51.8183 36.1950 192.0000 204.0000
ZSEC 40 0.0000 0.0000 444.5000 50.8183 51.8183 36.1950 204.0000 216.0000
ZSEC 41 0.0000 0.0000 444.5000 50.8183 51.8183 36.1950 216.0000 228.0000
ZSEC 42 0.0000 0.0000 444.5000 50.8183 51.8183 36.1950 228.0000 240.0000
ZSEC 43 0.0000 0.0000 444.5000 50.8183 51.8183 36.1950 240.0000 252.0000
ZSEC 44 0.0000 0.0000 444.5000 50.8183 51.8183 36.1950 252.0000 264.0000
ZSEC 45 0.0000 0.0000 444.5000 50.8183 51.8183 36.1950 264.0000 276.0000
ZSEC 46 0.0000 0.0000 444.5000 50.8183 51.8183 36.1950 276.0000 288.0000
ZSEC 47 0.0000 0.0000 444.5000 50.8183 51.8183 36.1950 288.0000 300.0000
ZSEC 48 0.0000 0.0000 444.5000 50.8183 51.8183 36.1950 300.0000 312.0000
ZSEC 49 0.0000 0.0000 444.5000 50.8183 51.8183 36.1950 312.0000 324.0000
ZSEC 50 0.0000 0.0000 444.5000 50.8183 51.8183 36.1950 324.0000 336.0000
ZSEC 51 0.0000 0.0000 444.5000 50.8183 51.8183 36.1950 336.0000 348.0000
ZSEC 52 0.0000 0.0000 444.5000 50.8183 51.8183 36.1950 348.0000 360.0000
* Radial Detector DRB (1ft) Bodies
ZROD 53 0.0000 0.0000 -98.5012 81.2983 649.7574
ZROD 54 0.0000 0.0000 -98.5012 81.2983 32.4879
ZROD 55 0.0000 0.0000 -66.0133 81.2983 32.4879
ZROD 56 0.0000 0.0000 -33.5255 81.2983 32.4879
ZROD 57 0.0000 0.0000 -1.0376 81.2983 32.4879
ZROD 58 0.0000 0.0000 31.4503 81.2983 32.4879
ZROD 59 0.0000 0.0000 63.9382 81.2983 32.4879
ZROD 60 0.0000 0.0000 96.4260 81.2983 32.4879
ZROD 61 0.0000 0.0000 128.9139 81.2983 32.4879
ZROD 62 0.0000 0.0000 161.4018 81.2983 32.4879
ZROD 63 0.0000 0.0000 193.8896 81.2983 32.4879
ZROD 64 0.0000 0.0000 226.3775 81.2983 32.4879
ZROD 65 0.0000 0.0000 258.8654 81.2983 32.4879
ZROD 66 0.0000 0.0000 291.3532 81.2983 32.4879
ZROD 67 0.0000 0.0000 323.8411 81.2983 32.4879
ZROD 68 0.0000 0.0000 356.3290 81.2983 32.4879
ZROD 69 0.0000 0.0000 388.8169 81.2983 32.4879
ZROD 70 0.0000 0.0000 421.3047 81.2983 32.4879
ZROD 71 0.0000 0.0000 453.7926 81.2983 32.4879
ZROD 72 0.0000 0.0000 486.2805 81.2983 32.4879
ZROD 73 0.0000 0.0000 518.7683 81.2983 32.4879

```

Figure 5.3.11-8 MCBEND Input – High Burnup Fuel Lattice – Radial Fuel Gamma

* Radial Detector DRC (1m) Bodies									
ZROD	74	0.0000	0.0000	-168.0212	149.8183	788.7974			
ZROD	75	0.0000	0.0000	-168.0212	150.8183	32.8666			
ZROD	76	0.0000	0.0000	-135.1546	150.8183	32.8666			
ZROD	77	0.0000	0.0000	-102.2881	150.8183	32.8666			
ZROD	78	0.0000	0.0000	-69.4215	150.8183	32.8666			
ZROD	79	0.0000	0.0000	-36.5550	150.8183	32.8666			
ZROD	80	0.0000	0.0000	-3.6884	150.8183	32.8666			
ZROD	81	0.0000	0.0000	29.1782	150.8183	32.8666			
ZROD	82	0.0000	0.0000	62.0447	150.8183	32.8666			
ZROD	83	0.0000	0.0000	94.9113	150.8183	32.8666			
ZROD	84	0.0000	0.0000	127.7778	150.8183	32.8666			
ZROD	85	0.0000	0.0000	160.6444	150.8183	32.8666			
ZROD	86	0.0000	0.0000	193.5109	150.8183	32.8666			
ZROD	87	0.0000	0.0000	226.3775	150.8183	32.8666			
ZROD	88	0.0000	0.0000	259.2441	150.8183	32.8666			
ZROD	89	0.0000	0.0000	292.1106	150.8183	32.8666			
ZROD	90	0.0000	0.0000	324.9772	150.8183	32.8666			
ZROD	91	0.0000	0.0000	357.8437	150.8183	32.8666			
ZROD	92	0.0000	0.0000	390.7103	150.8183	32.8666			
ZROD	93	0.0000	0.0000	423.5769	150.8183	32.8666			
ZROD	94	0.0000	0.0000	456.4434	150.8183	32.8666			
ZROD	95	0.0000	0.0000	489.3100	150.8183	32.8666			
ZROD	96	0.0000	0.0000	522.1765	150.8183	32.8666			
ZROD	97	0.0000	0.0000	555.0431	150.8183	32.8666			
ZROD	98	0.0000	0.0000	587.9096	150.8183	32.8666			
* Radial Detector DRD (2m) Bodies									
ZROD	99	0.0000	0.0000	-268.0212	249.8183	988.7974			
ZROD	100	0.0000	0.0000	-268.0212	250.8183	41.1999			
ZROD	101	0.0000	0.0000	-226.8213	250.8183	41.1999			
ZROD	102	0.0000	0.0000	-185.6214	250.8183	41.1999			
ZROD	103	0.0000	0.0000	-144.4215	250.8183	41.1999			
ZROD	104	0.0000	0.0000	-103.2216	250.8183	41.1999			
ZROD	105	0.0000	0.0000	-62.0217	250.8183	41.1999			
ZROD	106	0.0000	0.0000	-20.8219	250.8183	41.1999			
ZROD	107	0.0000	0.0000	20.3780	250.8183	41.1999			
ZROD	108	0.0000	0.0000	61.5779	250.8183	41.1999			
ZROD	109	0.0000	0.0000	102.7778	250.8183	41.1999			
ZROD	110	0.0000	0.0000	143.9777	250.8183	41.1999			
ZROD	111	0.0000	0.0000	185.1776	250.8183	41.1999			
ZROD	112	0.0000	0.0000	226.3775	250.8183	41.1999			
ZROD	113	0.0000	0.0000	267.5774	250.8183	41.1999			
ZROD	114	0.0000	0.0000	308.7773	250.8183	41.1999			
ZROD	115	0.0000	0.0000	349.9772	250.8183	41.1999			
ZROD	116	0.0000	0.0000	391.1771	250.8183	41.1999			
ZROD	117	0.0000	0.0000	432.3770	250.8183	41.1999			
ZROD	118	0.0000	0.0000	473.5769	250.8183	41.1999			
ZROD	119	0.0000	0.0000	514.7767	250.8183	41.1999			
ZROD	120	0.0000	0.0000	555.9766	250.8183	41.1999			
ZROD	121	0.0000	0.0000	597.1765	250.8183	41.1999			
ZROD	122	0.0000	0.0000	638.3764	250.8183	41.1999			
ZROD	123	0.0000	0.0000	679.5763	250.8183	41.1999			
* Radial Detector DRE (2m+Convey) Bodies									
ZROD	124	0.0000	0.0000	-269.0212	321.9200	990.7974			
ZROD	125	0.0000	0.0000	-268.0212	322.9200	41.1999			
ZROD	126	0.0000	0.0000	-226.8213	322.9200	41.1999			
ZROD	127	0.0000	0.0000	-185.6214	322.9200	41.1999			
ZROD	128	0.0000	0.0000	-144.4215	322.9200	41.1999			
ZROD	129	0.0000	0.0000	-103.2216	322.9200	41.1999			
ZROD	130	0.0000	0.0000	-62.0217	322.9200	41.1999			
ZROD	131	0.0000	0.0000	-20.8219	322.9200	41.1999			
ZROD	132	0.0000	0.0000	20.3780	322.9200	41.1999			
ZROD	133	0.0000	0.0000	61.5779	322.9200	41.1999			
ZROD	134	0.0000	0.0000	102.7778	322.9200	41.1999			
ZROD	135	0.0000	0.0000	143.9777	322.9200	41.1999			
ZROD	136	0.0000	0.0000	185.1776	322.9200	41.1999			
ZROD	137	0.0000	0.0000	226.3775	322.9200	41.1999			
ZROD	138	0.0000	0.0000	267.5774	322.9200	41.1999			
ZROD	139	0.0000	0.0000	308.7773	322.9200	41.1999			
ZROD	140	0.0000	0.0000	349.9772	322.9200	41.1999			
ZROD	141	0.0000	0.0000	391.1771	322.9200	41.1999			
ZROD	142	0.0000	0.0000	432.3770	322.9200	41.1999			
ZROD	143	0.0000	0.0000	473.5769	322.9200	41.1999			
ZROD	144	0.0000	0.0000	514.7767	322.9200	41.1999			
ZROD	145	0.0000	0.0000	555.9766	322.9200	41.1999			
ZROD	146	0.0000	0.0000	597.1765	322.9200	41.1999			
ZROD	147	0.0000	0.0000	638.3764	322.9200	41.1999			
ZROD	148	0.0000	0.0000	679.5763	322.9200	41.1999			
* Radial Detector DREE (2m+ConveyAzi) Bodies									
ZROD	149	0.0000	0.0000	-270.0212	322.9200	992.7974			
* Band 1 Bodies									
ZSEC	150	0.0000	0.0000	444.5000	322.9200	323.9200	46.1950	0.0000	12.0000
ZSEC	151	0.0000	0.0000	444.5000	322.9200	323.9200	46.1950	12.0000	24.0000
ZSEC	152	0.0000	0.0000	444.5000	322.9200	323.9200	46.1950	24.0000	36.0000
ZSEC	153	0.0000	0.0000	444.5000	322.9200	323.9200	46.1950	36.0000	48.0000
ZSEC	154	0.0000	0.0000	444.5000	322.9200	323.9200	46.1950	48.0000	60.0000
ZSEC	155	0.0000	0.0000	444.5000	322.9200	323.9200	46.1950	60.0000	72.0000
ZSEC	156	0.0000	0.0000	444.5000	322.9200	323.9200	46.1950	72.0000	84.0000
ZSEC	157	0.0000	0.0000	444.5000	322.9200	323.9200	46.1950	84.0000	96.0000
ZSEC	158	0.0000	0.0000	444.5000	322.9200	323.9200	46.1950	96.0000	108.0000
ZSEC	159	0.0000	0.0000	444.5000	322.9200	323.9200	46.1950	108.0000	120.0000
ZSEC	160	0.0000	0.0000	444.5000	322.9200	323.9200	46.1950	120.0000	132.0000
ZSEC	161	0.0000	0.0000	444.5000	322.9200	323.9200	46.1950	132.0000	144.0000

Figure 5.3.11-8 MCBEND Input – High Burnup Fuel Lattice – Radial Fuel Gamma

ZSEC	162	0.0000	0.0000	444.5000	322.9200	323.9200	46.1950	144.0000	156.0000
ZSEC	163	0.0000	0.0000	444.5000	322.9200	323.9200	46.1950	156.0000	168.0000
ZSEC	164	0.0000	0.0000	444.5000	322.9200	323.9200	46.1950	168.0000	180.0000
ZSEC	165	0.0000	0.0000	444.5000	322.9200	323.9200	46.1950	180.0000	192.0000
ZSEC	166	0.0000	0.0000	444.5000	322.9200	323.9200	46.1950	192.0000	204.0000
ZSEC	167	0.0000	0.0000	444.5000	322.9200	323.9200	46.1950	204.0000	216.0000
ZSEC	168	0.0000	0.0000	444.5000	322.9200	323.9200	46.1950	216.0000	228.0000
ZSEC	169	0.0000	0.0000	444.5000	322.9200	323.9200	46.1950	228.0000	240.0000
ZSEC	170	0.0000	0.0000	444.5000	322.9200	323.9200	46.1950	240.0000	252.0000
ZSEC	171	0.0000	0.0000	444.5000	322.9200	323.9200	46.1950	252.0000	264.0000
ZSEC	172	0.0000	0.0000	444.5000	322.9200	323.9200	46.1950	264.0000	276.0000
ZSEC	173	0.0000	0.0000	444.5000	322.9200	323.9200	46.1950	276.0000	288.0000
ZSEC	174	0.0000	0.0000	444.5000	322.9200	323.9200	46.1950	288.0000	300.0000
ZSEC	175	0.0000	0.0000	444.5000	322.9200	323.9200	46.1950	300.0000	312.0000
ZSEC	176	0.0000	0.0000	444.5000	322.9200	323.9200	46.1950	312.0000	324.0000
ZSEC	177	0.0000	0.0000	444.5000	322.9200	323.9200	46.1950	324.0000	336.0000
ZSEC	178	0.0000	0.0000	444.5000	322.9200	323.9200	46.1950	336.0000	348.0000
ZSEC	179	0.0000	0.0000	444.5000	322.9200	323.9200	46.1950	348.0000	360.0000
* World									
ZROD	180	0.0000	0.0000	-320.0212	372.9200	1092.7974			
* External Void									
ZROD	181	0.0000	0.0000	-370.0212	422.9200	1192.7974			
ZONES									
/LWTcask/ P4 +1									
* Detector DRA (Surface)									
/DRA01/	M0	+2	-1						
/DRA02/	M0	+3	-1						
/DRA03/	M0	+4	-1						
/DRA04/	M0	+5	-1						
/DRA05/	M0	+6	-1						
/DRA06/	M0	+7	-1						
/DRA07/	M0	+8	-1						
/DRA08/	M0	+9	-1						
/DRA09/	M0	+10	-1						
/DRA10/	M0	+11	-1						
/DRA11/	M0	+12	-1						
/DRA12/	M0	+13	-1						
/DRA13/	M0	+14	-1						
/DRA14/	M0	+15	-1						
/DRA15/	M0	+16	-1						
/DRA16/	M0	+17	-1						
/DRA17/	M0	+18	-1						
/DRA18/	M0	+19	-1						
/DRA19/	M0	+20	-1						
/DRA20/	M0	+21	-1						
/Void/	M0	+22	-1						
		-2	-3	-4	-5	-6	-7		
		-8	-9	-10	-11	-12	-13		
		-14	-15	-16	-17	-18	-19		
		-20	-21						
* Detector DRAA (SurfaceAzi)									
/DRAA0101/	M0	+23							
/DRAA0102/	M0	+24							
/DRAA0103/	M0	+25							
/DRAA0104/	M0	+26							
/DRAA0105/	M0	+27							
/DRAA0106/	M0	+28							
/DRAA0107/	M0	+29							
/DRAA0108/	M0	+30							
/DRAA0109/	M0	+31							
/DRAA0110/	M0	+32							
/DRAA0111/	M0	+33							
/DRAA0112/	M0	+34							
/DRAA0113/	M0	+35							
/DRAA0114/	M0	+36							
/DRAA0115/	M0	+37							
/DRAA0116/	M0	+38							
/DRAA0117/	M0	+39							
/DRAA0118/	M0	+40							
/DRAA0119/	M0	+41							
/DRAA0120/	M0	+42							
/DRAA0121/	M0	+43							
/DRAA0122/	M0	+44							
/DRAA0123/	M0	+45							
/DRAA0124/	M0	+46							
/DRAA0125/	M0	+47							
/DRAA0126/	M0	+48							
/DRAA0127/	M0	+49							
/DRAA0128/	M0	+50							
/DRAA0129/	M0	+51							
/DRAA0130/	M0	+52							
/Void/	M0	+53	-22						
		-23	-24	-25	-26	-27	-28		
		-29	-30	-31	-32	-33	-34		
		-35	-36	-37	-38	-39	-40		
		-41	-42	-43	-44	-45	-46		
		-47	-48	-49	-50	-51	-52		
* Detector DRB (1ft)									
/DRB01/	M0	+54	-53						
/DRB02/	M0	+55	-53						
/DRB03/	M0	+56	-53						
/DRB04/	M0	+57	-53						

Figure 5.3.11-8 MCBEND Input – High Burnup Fuel Lattice – Radial Fuel Gamma

/DRB05/	M0	+58	-53				
/DRB06/	M0	+59	-53				
/DRB07/	M0	+60	-53				
/DRB08/	M0	+61	-53				
/DRB09/	M0	+62	-53				
/DRB10/	M0	+63	-53				
/DRB11/	M0	+64	-53				
/DRB12/	M0	+65	-53				
/DRB13/	M0	+66	-53				
/DRB14/	M0	+67	-53				
/DRB15/	M0	+68	-53				
/DRB16/	M0	+69	-53				
/DRB17/	M0	+70	-53				
/DRB18/	M0	+71	-53				
/DRB19/	M0	+72	-53				
/DRB20/	M0	+73	-53				
/Void/	M0	+74	-53				
		-54	-55	-56	-57	-58	-59
		-60	-61	-62	-63	-64	-65
		-66	-67	-68	-69	-70	-71
		-72	-73				
* Detector DRC (1m)							
/DRC01/	M0	+75	-74				
/DRC02/	M0	+76	-74				
/DRC03/	M0	+77	-74				
/DRC04/	M0	+78	-74				
/DRC05/	M0	+79	-74				
/DRC06/	M0	+80	-74				
/DRC07/	M0	+81	-74				
/DRC08/	M0	+82	-74				
/DRC09/	M0	+83	-74				
/DRC10/	M0	+84	-74				
/DRC11/	M0	+85	-74				
/DRC12/	M0	+86	-74				
/DRC13/	M0	+87	-74				
/DRC14/	M0	+88	-74				
/DRC15/	M0	+89	-74				
/DRC16/	M0	+90	-74				
/DRC17/	M0	+91	-74				
/DRC18/	M0	+92	-74				
/DRC19/	M0	+93	-74				
/DRC20/	M0	+94	-74				
/DRC21/	M0	+95	-74				
/DRC22/	M0	+96	-74				
/DRC23/	M0	+97	-74				
/DRC24/	M0	+98	-74				
/Void/	M0	+99	-74				
		-75	-76	-77	-78	-79	-80
		-81	-82	-83	-84	-85	-86
		-87	-88	-89	-90	-91	-92
		-93	-94	-95	-96	-97	-98
* Detector DRD (2m)							
/DRD01/	M0	+100	-99				
/DRD02/	M0	+101	-99				
/DRD03/	M0	+102	-99				
/DRD04/	M0	+103	-99				
/DRD05/	M0	+104	-99				
/DRD06/	M0	+105	-99				
/DRD07/	M0	+106	-99				
/DRD08/	M0	+107	-99				
/DRD09/	M0	+108	-99				
/DRD10/	M0	+109	-99				
/DRD11/	M0	+110	-99				
/DRD12/	M0	+111	-99				
/DRD13/	M0	+112	-99				
/DRD14/	M0	+113	-99				
/DRD15/	M0	+114	-99				
/DRD16/	M0	+115	-99				
/DRD17/	M0	+116	-99				
/DRD18/	M0	+117	-99				
/DRD19/	M0	+118	-99				
/DRD20/	M0	+119	-99				
/DRD21/	M0	+120	-99				
/DRD22/	M0	+121	-99				
/DRD23/	M0	+122	-99				
/DRD24/	M0	+123	-99				
/Void/	M0	+124	-99				
		-100	-101	-102	-103	-104	-105
		-106	-107	-108	-109	-110	-111
		-112	-113	-114	-115	-116	-117
		-118	-119	-120	-121	-122	-123
* Detector DRE (2m+Convey)							
/DRE01/	M0	+125	-124				
/DRE02/	M0	+126	-124				
/DRE03/	M0	+127	-124				
/DRE04/	M0	+128	-124				
/DRE05/	M0	+129	-124				
/DRE06/	M0	+130	-124				
/DRE07/	M0	+131	-124				
/DRE08/	M0	+132	-124				
/DRE09/	M0	+133	-124				
/DRE10/	M0	+134	-124				
/DRE11/	M0	+135	-124				

Figure 5.3.11-8 MCBEND Input – High Burnup Fuel Lattice – Radial Fuel Gamma

```

/DRE12/ M0 +136 -124
/DRE13/ M0 +137 -124
/DRE14/ M0 +138 -124
/DRE15/ M0 +139 -124
/DRE16/ M0 +140 -124
/DRE17/ M0 +141 -124
/DRE18/ M0 +142 -124
/DRE19/ M0 +143 -124
/DRE20/ M0 +144 -124
/DRE21/ M0 +145 -124
/DRE22/ M0 +146 -124
/DRE23/ M0 +147 -124
/DRE24/ M0 +148 -124
/Void/ M0 +149 -124
          -125 -126 -127 -128 -129 -130
          -131 -132 -133 -134 -135 -136
          -137 -138 -139 -140 -141 -142
          -143 -144 -145 -146 -147 -148
* Detector DREE (2m+ConveyAzi)
/DREE0101/ M0 +150
/DREE0102/ M0 +151
/DREE0103/ M0 +152
/DREE0104/ M0 +153
/DREE0105/ M0 +154
/DREE0106/ M0 +155
/DREE0107/ M0 +156
/DREE0108/ M0 +157
/DREE0109/ M0 +158
/DREE0110/ M0 +159
/DREE0111/ M0 +160
/DREE0112/ M0 +161
/DREE0113/ M0 +162
/DREE0114/ M0 +163
/DREE0115/ M0 +164
/DREE0116/ M0 +165
/DREE0117/ M0 +166
/DREE0118/ M0 +167
/DREE0119/ M0 +168
/DREE0120/ M0 +169
/DREE0121/ M0 +170
/DREE0122/ M0 +171
/DREE0123/ M0 +172
/DREE0124/ M0 +173
/DREE0125/ M0 +174
/DREE0126/ M0 +175
/DREE0127/ M0 +176
/DREE0128/ M0 +177
/DREE0129/ M0 +178
/DREE0130/ M0 +179
/Void/ M0 +180 -149
          -150 -151 -152 -153 -154 -155
          -156 -157 -158 -159 -160 -161
          -162 -163 -164 -165 -166 -167
          -168 -169 -170 -171 -172 -173
          -174 -175 -176 -177 -178 -179
/ExtVoid/ M-2000 +181 -180
Volumes
          1.0 20*9.3077E+03 1.0 30*3.8903E+02 1.0 20*1.6493E+04
          1.0 24*3.1042E+04 1.0 24*6.4799E+04 1.0 24*8.3464E+04
          1.0 30*3.1291E+03 1.0 1.0
end
*
* Unit 5 Splitting Geometry for Radial Detectors - Gamma
*
begin splitting geometry
  r 15 fill 0.0000
    n 4 16.9863
    n 1 18.9103
    n 6 33.3271
    n 1 36.5189
    n 1 49.2189
    n 1 49.8183
    n 1 54.8183
  z 29 fill -73.0212
    n 1 -68.0212
    n 1 -26.6700
    n 1 -17.7800
    n 1 -10.1600
    n 1 0.0000
    n 1 39.8844
    n 13 405.6444
    n 3 417.0807
    n 4 452.1200
    n 1 480.6950
    n 1 520.7762
    n 1 525.7762
end
*
* Unit 6 - Source Geometry for Fuel Gamma

```

Figure 5.3.11-8 MCBEND Input – High Burnup Fuel Lattice – Radial Fuel Gamma

```

begin source geometry
  x 1 -10.84072 10.84072
  y 1 -10.84072 10.84072
  z 13
    39.8844 49.0284 58.1724 67.3164 76.4604 85.6044
    94.7484 350.7804 359.9244 369.0684 378.2124 387.3564
    396.5004 405.6444
end
*
* Unit 7
*
begin energy data
  gamma dice
  importance standard 22 groups
  scoring as importance
  simple source histogram weighting automatic
end

*
* Unit 8 Importance Map - Radial
*
begin importance map
  calculate
  targets 20
  part 5
  zones
    2 3 4 5 6
    7 8 9 10 11
    12 13 14 15 16
    17 18 19 20 21
  strengths
    2*100.0 2*100.0 2*50.0 2*50.0 2*10.0
    2*10.0 2*50.0 2*50.0 2*100.0 2*100.0

  defer mixing
  void density 0.10
  track
  ! coupled source
  ! write gamma importances to 32
  ! write unformatted file to 31
  ! use method d
end

*
* Unit 9 Scoring Data - Radial
*
begin scoring data
  flux
  part 5
  from 2 to 21 ! DRA
  from 23 to 52 ! DRAA
  from 54 to 73 ! DRB
  from 75 to 98 ! DRC
  from 100 to 123 ! DRD
  from 125 to 148 ! DRE
  from 150 to 179 ! DREE
  responses sos ditto
  contributions to responses ditto
  ! score distribution for response
  ! weight distribution total
end

*
* Unit 10 Response Data
*
begin response data
  * Scaled to mrem/hr
  /ansi ans-6.1.1-1977 photon flux-dose conversion factors - mcnp table h.2 - mrem/
  function pairs
    1.5000E+01 1.3300E-02
    1.4787E+01 1.3142E-02
    1.4577E+01 1.2985E-02
    1.4370E+01 1.2831E-02
    1.4166E+01 1.2678E-02
    1.3964E+01 1.2528E-02
    1.3766E+01 1.2379E-02
    1.3570E+01 1.2231E-02
    1.3377E+01 1.2086E-02
    1.3187E+01 1.1942E-02
    1.3000E+01 1.1800E-02
    1.2785E+01 1.1641E-02
    1.2573E+01 1.1483E-02
    1.2365E+01 1.1328E-02
    1.2160E+01 1.1175E-02
    1.1958E+01 1.1025E-02
    1.1760E+01 1.0876E-02
    1.1565E+01 1.0729E-02
    1.1374E+01 1.0584E-02
    1.1185E+01 1.0441E-02
    1.1000E+01 1.0300E-02
    1.0781E+01 1.0136E-02
    1.0567E+01 9.9740E-03
    1.0357E+01 9.8149E-03

```

Figure 5.3.11-8 MCBEND Input – High Burnup Fuel Lattice – Radial Fuel Gamma

1.0152E+01	9.6583E-03
9.9499E+00	9.5043E-03
9.7522E+00	9.3526E-03
9.5585E+00	9.2035E-03
9.3686E+00	9.0566E-03
9.1824E+00	8.9122E-03
9.0000E+00	8.7700E-03
8.8374E+00	8.6521E-03
8.6777E+00	8.5358E-03
8.5210E+00	8.4211E-03
8.3670E+00	8.3079E-03
8.2158E+00	8.1962E-03
8.0674E+00	8.0861E-03
7.9216E+00	7.9774E-03
7.7785E+00	7.8701E-03
7.6380E+00	7.7644E-03
7.5000E+00	7.6600E-03
7.4214E+00	7.6031E-03
7.3436E+00	7.5467E-03
7.2666E+00	7.4907E-03
7.1905E+00	7.4351E-03
7.1151E+00	7.3799E-03
7.0406E+00	7.3251E-03
6.9668E+00	7.2707E-03
6.8937E+00	7.2167E-03
6.8215E+00	7.1632E-03
6.7500E+00	7.1100E-03
6.6983E+00	7.0721E-03
6.6469E+00	7.0344E-03
6.5959E+00	6.9969E-03
6.5454E+00	6.9596E-03
6.4952E+00	6.9225E-03
6.4454E+00	6.8856E-03
6.3960E+00	6.8489E-03
6.3469E+00	6.8124E-03
6.2983E+00	6.7761E-03
6.2500E+00	6.7400E-03
6.1981E+00	6.7021E-03
6.1466E+00	6.6643E-03
6.0956E+00	6.6268E-03
6.0450E+00	6.5895E-03
5.9948E+00	6.5524E-03
5.9450E+00	6.5155E-03
5.8956E+00	6.4788E-03
5.8467E+00	6.4423E-03
5.7981E+00	6.4061E-03
5.7500E+00	6.3700E-03
5.6979E+00	6.3331E-03
5.6463E+00	6.2963E-03
5.5952E+00	6.2598E-03
5.5445E+00	6.2235E-03
5.4943E+00	6.1874E-03
5.4446E+00	6.1515E-03
5.3953E+00	6.1158E-03
5.3464E+00	6.0803E-03
5.2980E+00	6.0451E-03
5.2500E+00	6.0100E-03
5.2244E+00	5.9887E-03
5.1990E+00	5.9674E-03
5.1737E+00	5.9462E-03
5.1485E+00	5.9251E-03
5.1235E+00	5.9041E-03
5.0985E+00	5.8831E-03
5.0737E+00	5.8622E-03
5.0490E+00	5.8414E-03
5.0245E+00	5.8207E-03
5.0000E+00	5.8000E-03
4.9744E+00	5.7797E-03
4.9490E+00	5.7594E-03
4.9236E+00	5.7393E-03
4.8985E+00	5.7192E-03
4.8734E+00	5.6991E-03
4.8485E+00	5.6792E-03
4.8237E+00	5.6593E-03
4.7990E+00	5.6394E-03
4.7744E+00	5.6197E-03
4.7500E+00	5.6000E-03
4.6975E+00	5.5619E-03
4.6455E+00	5.5240E-03
4.5941E+00	5.4863E-03
4.5433E+00	5.4490E-03
4.4931E+00	5.4118E-03
4.4434E+00	5.3750E-03
4.3942E+00	5.3384E-03
4.3456E+00	5.3020E-03
4.2975E+00	5.2659E-03
4.2500E+00	5.2300E-03
4.1971E+00	5.1886E-03
4.1449E+00	5.1474E-03
4.0934E+00	5.1066E-03
4.0425E+00	5.0662E-03
3.9922E+00	5.0260E-03
3.9425E+00	4.9862E-03

Figure 5.3.11-8 MCBEND Input – High Burnup Fuel Lattice – Radial Fuel Gamma

3.8935E+00	4.9467E-03
3.8451E+00	4.9075E-03
3.7972E+00	4.8686E-03
3.7500E+00	4.8300E-03
3.6967E+00	4.7863E-03
3.6442E+00	4.7429E-03
3.5924E+00	4.7000E-03
3.5414E+00	4.6574E-03
3.4911E+00	4.6152E-03
3.4415E+00	4.5734E-03
3.3926E+00	4.5320E-03
3.3444E+00	4.4910E-03
3.2968E+00	4.4503E-03
3.2500E+00	4.4100E-03
3.2019E+00	4.3683E-03
3.1546E+00	4.3269E-03
3.1079E+00	4.2860E-03
3.0619E+00	4.2454E-03
3.0166E+00	4.2052E-03
2.9720E+00	4.1655E-03
2.9280E+00	4.1260E-03
2.8847E+00	4.0870E-03
2.8420E+00	4.0483E-03
2.8000E+00	4.0100E-03
2.7793E+00	3.9906E-03
2.7588E+00	3.9713E-03
2.7384E+00	3.9520E-03
2.7182E+00	3.9329E-03
2.6981E+00	3.9138E-03
2.6782E+00	3.8949E-03
2.6585E+00	3.8760E-03
2.6388E+00	3.8573E-03
2.6193E+00	3.8386E-03
2.6000E+00	3.8200E-03
2.5569E+00	3.7780E-03
2.5146E+00	3.7364E-03
2.4729E+00	3.6953E-03
2.4319E+00	3.6547E-03
2.3917E+00	3.6145E-03
2.3520E+00	3.5747E-03
2.3131E+00	3.5354E-03
2.2747E+00	3.4965E-03
2.2371E+00	3.4580E-03
2.2000E+00	3.4200E-03
2.1563E+00	3.3744E-03
2.1135E+00	3.3293E-03
2.0715E+00	3.2849E-03
2.0303E+00	3.2410E-03
1.9900E+00	3.1978E-03
1.9504E+00	3.1551E-03
1.9117E+00	3.1130E-03
1.8737E+00	3.0714E-03
1.8365E+00	3.0304E-03
1.8000E+00	2.9900E-03
1.7553E+00	2.9381E-03
1.7118E+00	2.8872E-03
1.6693E+00	2.8371E-03
1.6279E+00	2.7879E-03
1.5875E+00	2.7395E-03
1.5481E+00	2.6920E-03
1.5096E+00	2.6453E-03
1.4722E+00	2.5994E-03
1.4356E+00	2.5543E-03
1.4000E+00	2.5100E-03
1.3537E+00	2.4512E-03
1.3089E+00	2.3937E-03
1.2656E+00	2.3376E-03
1.2237E+00	2.2828E-03
1.1832E+00	2.2293E-03
1.1441E+00	2.1771E-03
1.1062E+00	2.1260E-03
1.0696E+00	2.0762E-03
1.0342E+00	2.0275E-03
1.0000E+00	1.9800E-03
9.7793E-01	1.9477E-03
9.5635E-01	1.9160E-03
9.3525E-01	1.8848E-03
9.1461E-01	1.8541E-03
8.9443E-01	1.8238E-03
8.7469E-01	1.7941E-03
8.5539E-01	1.7649E-03
8.3651E-01	1.7361E-03
8.1805E-01	1.7078E-03
8.0000E-01	1.6800E-03
7.8939E-01	1.6633E-03
7.7892E-01	1.6467E-03
7.6859E-01	1.6303E-03
7.5839E-01	1.6141E-03
7.4833E-01	1.5980E-03
7.3841E-01	1.5821E-03
7.2861E-01	1.5663E-03
7.1895E-01	1.5507E-03
7.0941E-01	1.5353E-03

Figure 5.3.11-8 MCBEND Input – High Burnup Fuel Lattice – Radial Fuel Gamma

7.0000E-01	1.5200E-03
6.9483E-01	1.5118E-03
6.8970E-01	1.5037E-03
6.8461E-01	1.4955E-03
6.7955E-01	1.4875E-03
6.7454E-01	1.4795E-03
6.6956E-01	1.4715E-03
6.6461E-01	1.4635E-03
6.5971E-01	1.4557E-03
6.5483E-01	1.4478E-03
6.5000E-01	1.4400E-03
6.4482E-01	1.4318E-03
6.3968E-01	1.4236E-03
6.3458E-01	1.4155E-03
6.2952E-01	1.4075E-03
6.2450E-01	1.3994E-03
6.1952E-01	1.3915E-03
6.1458E-01	1.3835E-03
6.0968E-01	1.3756E-03
6.0482E-01	1.3678E-03
6.0000E-01	1.3600E-03
5.9480E-01	1.3507E-03
5.8965E-01	1.3415E-03
5.8454E-01	1.3324E-03
5.7948E-01	1.3233E-03
5.7446E-01	1.3142E-03
5.6948E-01	1.3053E-03
5.6455E-01	1.2964E-03
5.5966E-01	1.2875E-03
5.5481E-01	1.2787E-03
5.5000E-01	1.2700E-03
5.4478E-01	1.2596E-03
5.3962E-01	1.2493E-03
5.3450E-01	1.2391E-03
5.2943E-01	1.2290E-03
5.2440E-01	1.2190E-03
5.1943E-01	1.2090E-03
5.1450E-01	1.1991E-03
5.0962E-01	1.1893E-03
5.0479E-01	1.1796E-03
5.0000E-01	1.1700E-03
4.9476E-01	1.1607E-03
4.8957E-01	1.1514E-03
4.8444E-01	1.1422E-03
4.7937E-01	1.1331E-03
4.7434E-01	1.1241E-03
4.6937E-01	1.1151E-03
4.6445E-01	1.1062E-03
4.5958E-01	1.0974E-03
4.5477E-01	1.0887E-03
4.5000E-01	1.0800E-03
4.4473E-01	1.0701E-03
4.3952E-01	1.0603E-03
4.3438E-01	1.0506E-03
4.2929E-01	1.0409E-03
4.2426E-01	1.0314E-03
4.1930E-01	1.0220E-03
4.1439E-01	1.0126E-03
4.0953E-01	1.0033E-03
4.0474E-01	9.9411E-04
4.0000E-01	9.8500E-04
3.9469E-01	9.7374E-04
3.8946E-01	9.6260E-04
3.8429E-01	9.5160E-04
3.7920E-01	9.4072E-04
3.7417E-01	9.2996E-04
3.6920E-01	9.1933E-04
3.6431E-01	9.0882E-04
3.5947E-01	8.9843E-04
3.5470E-01	8.8815E-04
3.5000E-01	8.7800E-04
3.4465E-01	8.6531E-04
3.3937E-01	8.5279E-04
3.3418E-01	8.4046E-04
3.2907E-01	8.2831E-04
3.2404E-01	8.1633E-04
3.1908E-01	8.0453E-04
3.1420E-01	7.9290E-04
3.0939E-01	7.8143E-04
3.0466E-01	7.7014E-04
3.0000E-01	7.5900E-04
2.9458E-01	7.4511E-04
2.8926E-01	7.3147E-04
2.8403E-01	7.1809E-04
2.7890E-01	7.0495E-04
2.7386E-01	6.9205E-04
2.6891E-01	6.7938E-04
2.6405E-01	6.6695E-04
2.5928E-01	6.5474E-04
2.5460E-01	6.4276E-04
2.5000E-01	6.3100E-04
2.4448E-01	6.1661E-04
2.3909E-01	6.0255E-04

Figure 5.3.11-8 MCBEND Input – High Burnup Fuel Lattice – Radial Fuel Gamma

```

2.3381E-01      5.8881E-04
2.2865E-01      5.7538E-04
2.2361E-01      5.6226E-04
2.1867E-01      5.4943E-04
2.1385E-01      5.3690E-04
2.0913E-01      5.2466E-04
2.0451E-01      5.1269E-04
2.0000E-01      5.0100E-04
1.9433E-01      4.8721E-04
1.8882E-01      4.7380E-04
1.8346E-01      4.6076E-04
1.7826E-01      4.4808E-04
1.7321E-01      4.3575E-04
1.6829E-01      4.2376E-04
1.6352E-01      4.1210E-04
1.5888E-01      4.0075E-04
1.5438E-01      3.8973E-04
1.5000E-01      3.7900E-04
1.4404E-01      3.6809E-04
1.3832E-01      3.5749E-04
1.3282E-01      3.4720E-04
1.2754E-01      3.3721E-04
1.2247E-01      3.2750E-04
1.1761E-01      3.1807E-04
1.1293E-01      3.0892E-04
1.0845E-01      3.0002E-04
1.0414E-01      2.9139E-04
1.0000E-01      2.8300E-04
9.6496E-02      2.8039E-04
9.3115E-02      2.7781E-04
8.9852E-02      2.7526E-04
8.6704E-02      2.7272E-04
8.3666E-02      2.7021E-04
8.0734E-02      2.6772E-04
7.7906E-02      2.6526E-04
7.5176E-02      2.6282E-04
7.2542E-02      2.6040E-04
7.0000E-02      2.5800E-04
6.7684E-02      2.6103E-04
6.5444E-02      2.6410E-04
6.3279E-02      2.6721E-04
6.1185E-02      2.7035E-04
5.9161E-02      2.7353E-04
5.7203E-02      2.7675E-04
5.5311E-02      2.8000E-04
5.3481E-02      2.8330E-04
5.1711E-02      2.8663E-04
5.0000E-02      2.9000E-04
4.7510E-02      3.1092E-04
4.5144E-02      3.3335E-04
4.2896E-02      3.5740E-04
4.0760E-02      3.8318E-04
3.8730E-02      4.1083E-04
3.6801E-02      4.4047E-04
3.4968E-02      4.7224E-04
3.3227E-02      5.0631E-04
3.1572E-02      5.4284E-04
3.0000E-02      5.8200E-04
2.8879E-02      7.0502E-04
2.4082E-02      8.5404E-04
2.1577E-02      1.0346E-03
1.9332E-02      1.2532E-03
1.7321E-02      1.5181E-03
1.5518E-02      1.8390E-03
1.3904E-02      2.2277E-03
1.2457E-02      2.6986E-03
1.1161E-02      3.2690E-03
1.0000E-02      3.9600E-03
end

*
* Unit 13 Hole Data
*
*begin hole data
*   < hole
*end

*
* Unit 15 Source Strength - Fuel Gamma
*
* UMS Class 2 - bw15b - Bw15 (Mark BZ) - 80 GWD/MTU - 150 Day - Fuel Gamma - Direct
begin source strength
component      5.8160E-06      ! 1/volFue (1/1.7194E+05)
component      1.2019E-01      ! 25 rods / 208 assy rods
component      x      1.0
component      y      1.0
component      z
5.9142E-01      6.8025E-01      7.6908E-01      8.5792E-01      9.4675E-01      1.0356E+00
1.0800E+00      1.0356E+00      9.4675E-01      8.5792E-01      7.6908E-01      6.8025E-01
5.9142E-01
component      energy
0.0000E+00      1.2045E+05      2.3297E+06      1.0972E+07      5.5933E+07      1.3937E+08
3.6008E+11      3.1872E+12      1.2156E+14      4.1653E+13      1.4690E+14      5.5783E+14

```

Figure 5.3.11-8 MCBEND Input – High Burnup Fuel Lattice – Radial Fuel Gamma

```

7.0383E+14  3.9476E+15  2.7006E+16  1.2622E+16  1.2169E+15  1.6044E+15
6.3406E+15  6.4499E+15  1.2726E+16  9.5931E+15

end

*
* Unit 16 Simple Source Weights
*
*begin source weights
*
*end

*
* Unit 31 Tabular Output
*
begin tabular output
/Case lwtNrmRadFg_bw15b_80b40e150d - Det DRA - Surface - Response/
response interim
number some 1
region from 31 to 50
output to file also
/Case lwtNrmRadFg_bw15b_80b40e150d - Det DRB - 1ft - Response/
response
number some 1
region from 83 to 102
output to file also
/Case lwtNrmRadFg_bw15b_80b40e150d - Det DRC - 1m - Response/
response
number some 1
region from 104 to 127
output to file also
/Case lwtNrmRadFg_bw15b_80b40e150d - Det DRE - 2m+Convey - Response/
response interim
number some 1
region from 154 to 177
output to file also
end

*
* Unit 32 Material Specification
*
begin material specification
type gamma
normalise
nmixtures 2
weight mixture 1
u235 3.5260E-02
u238 8.4624E-01
o 1.1850E-01
atoms mixture 2
h 6.6667E-01
o 3.3333E-01

*
* Materials List - Common Materials - vl.2
*
mmaterials 11
volume ! Homogenized fuel
material 1
mixture 1 density 10.4120 prop 3.6613E-02 ! UO2 mixture at 4%
void prop 1.6877E-03 ! Gap
zircalloy density 6.5500 prop 1.7120E-02 ! Tube, clad
void prop 9.4458E-01 ! Interstitial, inside tubes
stainless 3041 steel density 7.9200 prop 0.0000E+00 ! Hardware
volume ! Lower Nozzle Material
material 2
stainless 3041 steel density 7.9200 prop 0.1501
void prop 0.8499
volume ! Upper Nozzle Material
material 3
stainless 3041 steel density 7.9200 prop 0.1152
void prop 0.8848
volume ! Upper Plenum Material
material 4
stainless 3041 steel density 7.9200 prop 0.0465
void prop 0.9535
volume ! Water
material 5
mixture 2 density 0.9982 prop 1.0000 ! mixH2O
atoms ! Water/Glycol
material 6 density 0 ! 0 means atom/b-cm
h prop 5.9880E-02
c prop 1.0701E-02
o prop 2.4589E-02
volume ! Aluminum
material 7
aluminium prop 1.0000
volume ! Lead
material 8
pb density 11.3440 prop 1.0000
volume ! Stainless Steel 304
material 9
stainless 3041 steel density 7.9200 prop 1.0000
volume ! Impact limiter
material 10

```

Figure 5.3.11-8 MCBEND Input – High Burnup Fuel Lattice – Radial Fuel Gamma

```
aluminium      density  0.4997  prop  1.0000
volume
material      11
mixture       1  density  10.4120  prop  0.5000  ! UO2 mixture at 4%
void          prop    0.5000
end
```

Table 5.3.11-1 MCBEND Standard 28 Group Neutron Boundaries

Group	E Lower [MeV]	E Upper [MeV]	E Average [MeV]
1	1.360E+01	1.460E+01	1.410E+01
2	1.250E+01	1.360E+01	1.305E+01
3	1.125E+01	1.250E+01	1.188E+01
4	1.000E+01	1.125E+01	1.063E+01
5	8.250E+00	1.000E+01	9.125E+00
6	7.000E+00	8.250E+00	7.625E+00
7	6.070E+00	7.000E+00	6.535E+00
8	4.720E+00	6.070E+00	5.395E+00
9	3.680E+00	4.720E+00	4.200E+00
10	2.870E+00	3.680E+00	3.275E+00
11	1.740E+00	2.870E+00	2.305E+00
12	6.400E-01	1.740E+00	1.190E+00
13	3.900E-01	6.400E-01	5.150E-01
14	1.100E-01	3.900E-01	2.500E-01
15	6.740E-02	1.100E-01	8.870E-02
16	2.480E-02	6.740E-02	4.610E-02
17	9.120E-03	2.480E-02	1.696E-02
18	2.950E-03	9.120E-03	6.035E-03
19	9.610E-04	2.950E-03	1.956E-03
20	3.540E-04	9.610E-04	6.575E-04
21	1.660E-04	3.540E-04	2.600E-04
22	4.810E-05	1.660E-04	1.071E-04
23	1.600E-05	4.810E-05	3.205E-05
24	4.000E-06	1.600E-05	1.000E-05
25	1.500E-06	4.000E-06	2.750E-06
26	5.500E-07	1.500E-06	1.025E-06
27	7.090E-08	5.500E-07	3.105E-07
28	1.000E-11	7.090E-08	3.546E-08

Table 5.3.11-2 MCBEND Standard 22 Group Gamma Boundaries

Group	E Lower [MeV]	E Upper [MeV]	E Average [MeV]
1	1.200E+01	1.400E+01	1.300E+01
2	1.000E+01	1.200E+01	1.100E+01
3	8.000E+00	1.000E+01	9.000E+00
4	6.500E+00	8.000E+00	7.250E+00
5	5.000E+00	6.500E+00	5.750E+00
6	4.000E+00	5.000E+00	4.500E+00
7	3.000E+00	4.000E+00	3.500E+00
8	2.500E+00	3.000E+00	2.750E+00
9	2.000E+00	2.500E+00	2.250E+00
10	1.660E+00	2.000E+00	1.830E+00
11	1.440E+00	1.660E+00	1.550E+00
12	1.220E+00	1.440E+00	1.330E+00
13	1.000E+00	1.220E+00	1.110E+00
14	8.000E-01	1.000E+00	9.000E-01
15	6.000E-01	8.000E-01	7.000E-01
16	4.000E-01	6.000E-01	5.000E-01
17	3.000E-01	4.000E-01	3.500E-01
18	2.000E-01	3.000E-01	2.500E-01
19	1.000E-01	2.000E-01	1.500E-01
20	5.000E-02	1.000E-01	7.500E-02
21	2.000E-02	5.000E-02	3.500E-02
22	1.000E-02	2.000E-02	1.500E-02

Table 5.3.11-3 BWR Fuel Assembly Lattice Three-Dimensional Model Parameters

Parameter	BWR 7x7	BWR 8x8
Lower Nozzle Height [cm]	18.76	18.76
Active Fuel Region Height [cm]	389.90	389.90
Upper Plenum Height [cm]	19.74	19.74
Upper Nozzle Height [cm]	19.05	19.05
Fuel Rod Diameter [cm]	1.4480	1.2600
Fuel Clad Thickness [cm]	0.0915	0.0870
Fuel Pellet Diameter [cm]	1.2446	1.0701
Array Size	7	8
Fuel Rod Pitch [cm]	1.8750	1.6260
Fuel Assembly Height [cm]	447.45	447.45
Fuel Assembly Width [cm]	14.02	14.02
Number of Fuel Pins	49	63
Lower Nozzle Mass [kg]	4.700	4.700
Incore Hardware Mass [kg]	2.030	0.330
Upper Plenum Mass [kg]	2.830	2.858
Upper Nozzle Mass [kg]	3.520	2.080

Table 5.3.11-4 PWR Fuel Assembly Lattice Three-Dimensional Model Parameters

Parameter	B&W 15×15	B&W 17×17	CE 14×14	West. 14×14	West. 15×15	West. 17×17
Lower Nozzle Height [cm]	18.41	19.12	12.53	8.69	10.76	8.60
Active Fuel Region Height [cm]	365.76	363.22	347.98	368.81	365.76	365.76
Upper Plenum Height [cm]	8.11	8.82	21.66	14.71	16.46	15.90
Upper Nozzle Height [cm]	28.41	29.76	16.60	13.45	12.82	15.63
Fuel Rod Diameter [cm]	1.0922	0.9627	1.1176	1.0719	1.0719	0.9500
Fuel Clad Thickness [cm]	0.0673	0.0597	0.0660	0.0572	0.0615	0.0572
Fuel Pellet Diameter [cm]	0.9362	0.8230	0.9563	0.9332	0.9294	0.8192
Array Size	15	17	14	14	15	17
Fuel Rod Pitch [cm]	1.4427	1.2751	1.4732	1.4122	1.4300	1.2598
Fuel Assembly Height [cm]	420.69	420.93	398.78	405.66	405.80	405.89
Fuel Assembly Width [cm]	21.68	21.68	20.96	19.72	21.40	21.40
Number of Fuel Pins	208	264	176	179	204	264
Number of Guide Tubes	16	24	4	16	20	24
Guide Tube OD [cm]	1.2522	1.0668	2.8321	1.2205	1.2294	1.2243
Guide Tube Thickness [cm]	0.0406	0.0445	0.1016	0.0864	0.0381	0.0381
Number of Instrument Tubes	1	1	1	1	1	1
Instrument Tube OD [cm]	1.2522	1.0668	2.8321	1.2205	1.2294	1.2243
Instrument Tube Thickness [cm]	0.0406	0.0381	0.1016	0.0864	0.0381	0.0381
Lower Nozzle Mass [kg]	10.290	7.130	5.000	7.893	5.440	5.900
Incore Hardware Mass [kg]	0.000	4.270	1.360	0.862	1.030	1.016
Upper Plenum Mass [kg]	1.980	1.560	7.980	5.684	3.680	5.310
Upper Nozzle Mass [kg]	10.760	18.130	6.180	9.890	7.850	7.850

Note: Listed assembly types are representative of the main core configurations employing assembly lattices transportable in the NAC-LWT and are not assembly-vendor specific.

Table 5.3.11-5 Fuel Assembly Lattice SAS2H Burnup Parameters at 80,000 MWd/MTU

Fuel Type	Pellet Diameter [cm]	Active Length [cm]	# Fuel Pins	Calculated MTU [MTU]	Assembly Power [MW]	Number of Cycles	Cycle Length [days]
BWR 7×7	1.2446	389.90	49	0.2133	4.68	5	730.00
BWR 8×8	1.0701	389.90	63	0.2028	4.44	5	730.00
B&W 15×15	0.9362	365.76	208	0.4807	15.66	4	613.93
B&W 17×17	0.8230	363.22	264	0.4681	17.67	4	529.87
CE 14×14	0.9563	347.98	176	0.4037	13.07	4	618.06
WE 14×14	0.9332	368.81	179	0.4144	13.07	4	634.40
WE 15×15	0.9294	365.76	204	0.4646	15.55	4	597.54
WE 17×17	0.8192	365.76	264	0.4671	17.67	4	528.65

Table 5.3.11-6 B&W 15x15 80,000 MWd/MTU, 150 Day Cool Time Source Terms in MCBEND Format

Group	Neutron [n/sec/assy]	Gamma [γ/sec/assy]	Hardware [γ/sec/kg]
1	0.000E+00	0.0000E+00	0.0000E+00
2	2.872E+05	1.2045E+05	0.0000E+00
3	1.197E+06	2.3297E+06	0.0000E+00
4	3.973E+06	1.0972E+07	0.0000E+00
5	1.247E+07	5.5933E+07	0.0000E+00
6	3.350E+07	1.3937E+08	0.0000E+00
7	5.785E+07	3.6008E+11	2.1915E-14
8	1.932E+08	3.1872E+12	1.7869E+05
9	3.321E+08	1.2156E+14	1.1524E+08
10	4.504E+08	4.1653E+13	5.1389E+09
11	1.052E+09	1.4690E+14	1.7618E+03
12	1.640E+09	5.5783E+14	1.0917E+13
13	4.286E+08	7.0383E+14	1.1507E+13
14	1.487E+08	3.9476E+15	3.2449E+12
15	2.157E+03	2.7006E+16	3.6269E+08
16	0.000E+00	1.2622E+16	3.3409E+11
17	0.000E+00	1.2169E+15	1.1626E+11
18	0.000E+00	1.6044E+15	3.5724E+09
19	0.000E+00	6.3406E+15	2.3610E+10
20	0.000E+00	6.4499E+15	7.3282E+10
21	0.000E+00	1.2726E+16	1.9462E+11
22	0.000E+00	9.5931E+15	2.2439E+11
23	0.000E+00		
24	0.000E+00		
25	0.000E+00		
26	0.000E+00		
27	0.000E+00		
28	0.000E+00		
Total	4.354E+09	8.3082E+16	2.6645E+13

Table 5.3.11-7 B&W 17x17 PWR 80,000 MWd/MTU, 150 Day Cool Time Source Terms
in MCBEND Format

Group	Neutron [n/sec/assy]	Gamma [γ/sec/assy]	Hardware [γ/sec/kg]
1	0.000E+00	0.0000E+00	0.0000E+00
2	2.759E+05	1.1608E+05	0.0000E+00
3	1.150E+06	2.2451E+06	0.0000E+00
4	3.817E+06	1.0574E+07	0.0000E+00
5	1.198E+07	5.3905E+07	0.0000E+00
6	3.218E+07	1.3431E+08	0.0000E+00
7	5.557E+07	3.9352E+11	2.3952E-14
8	1.856E+08	3.4957E+12	1.8611E+05
9	3.191E+08	1.3560E+14	1.2003E+08
10	4.330E+08	4.5731E+13	5.3749E+09
11	1.011E+09	1.5996E+14	1.8456E+03
12	1.575E+09	5.7162E+14	1.1370E+13
13	4.117E+08	7.4715E+14	1.1985E+13
14	1.428E+08	4.0794E+15	3.5336E+12
15	2.091E+03	2.9120E+16	3.7931E+08
16	0.000E+00	1.3405E+16	3.4944E+11
17	0.000E+00	1.3364E+15	1.3403E+11
18	0.000E+00	1.7573E+15	3.7376E+09
19	0.000E+00	6.9698E+15	2.4666E+10
20	0.000E+00	7.0599E+15	7.6490E+10
21	0.000E+00	1.3906E+16	2.0306E+11
22	0.000E+00	1.0475E+16	2.3406E+11
23	0.000E+00		
24	0.000E+00		
25	0.000E+00		
26	0.000E+00		
27	0.000E+00		
28	0.000E+00		
Total	4.183E+09	8.9773E+16	2.7920E+13

Table 5.3.11-8 CE 14x14 PWR 80,000 MWd/MTU, 150 Day Cool Time Source Terms in MCBEND Format

Group	Neutron [n/sec/assy]	Gamma [γ/sec/assy]	Hardware [γ/sec/kg]
1	0.000E+00	0.0000E+00	0.0000E+00
2	2.371E+05	9.9541E+04	0.0000E+00
3	9.877E+05	1.9252E+06	0.0000E+00
4	3.279E+06	9.0674E+06	0.0000E+00
5	1.029E+07	4.6222E+07	0.0000E+00
6	2.765E+07	1.1517E+08	0.0000E+00
7	4.774E+07	3.0376E+11	2.2126E-14
8	1.595E+08	2.6846E+12	1.8758E+05
9	2.736E+08	1.0140E+14	1.2097E+08
10	3.704E+08	3.4996E+13	4.8198E+09
11	8.669E+08	1.2255E+14	1.6615E+03
12	1.353E+09	4.6029E+14	1.1460E+13
13	3.537E+08	5.8686E+14	1.2079E+13
14	1.227E+08	3.2738E+15	3.0780E+12
15	1.730E+03	2.2459E+16	3.4254E+08
16	0.000E+00	1.0531E+16	3.1336E+11
17	0.000E+00	1.0194E+15	1.3181E+11
18	0.000E+00	1.3424E+15	3.4375E+09
19	0.000E+00	5.2910E+15	2.3798E+10
20	0.000E+00	5.3863E+15	7.5509E+10
21	0.000E+00	1.0630E+16	2.0185E+11
22	0.000E+00	8.0135E+15	2.3335E+11
23	0.000E+00		
24	0.000E+00		
25	0.000E+00		
26	0.000E+00		
27	0.000E+00		
28	0.000E+00		
Total	3.590E+09	6.9255E+16	2.7606E+13

Table 5.3.11-9 Westinghouse 14x14 PWR 80,000 MWd/MTU, 150 Day Cool Time
Source Terms in MCBEND Format

Group	Neutron [n/sec/assy]	Gamma [γ/sec/assy]	Hardware [γ/sec/kg]
1	0.000E+00	0.0000E+00	0.0000E+00
2	2.491E+05	1.0438E+05	0.0000E+00
3	1.038E+06	2.0189E+06	0.0000E+00
4	3.446E+06	9.5086E+06	0.0000E+00
5	1.081E+07	4.8472E+07	0.0000E+00
6	2.905E+07	1.2078E+08	0.0000E+00
7	5.017E+07	3.0153E+11	2.1414E-14
8	1.675E+08	2.6680E+12	1.7451E+05
9	2.881E+08	1.0164E+14	1.1254E+08
10	3.910E+08	3.4881E+13	5.1766E+09
11	9.130E+08	1.2353E+14	1.7716E+03
12	1.422E+09	4.7718E+14	1.0662E+13
13	3.717E+08	5.9547E+14	1.1238E+13
14	1.289E+08	3.3649E+15	3.2285E+12
15	1.886E+03	2.2792E+16	3.6470E+08
16	0.000E+00	1.0676E+16	3.3654E+11
17	0.000E+00	1.0201E+15	1.0845E+11
18	0.000E+00	1.3463E+15	3.5740E+09
19	0.000E+00	5.3205E+15	2.3322E+10
20	0.000E+00	5.4166E+15	7.1937E+10
21	0.000E+00	1.0691E+16	1.9069E+11
22	0.000E+00	8.0605E+15	2.1970E+11
23	0.000E+00		
24	0.000E+00		
25	0.000E+00		
26	0.000E+00		
27	0.000E+00		
28	0.000E+00		
Total	3.777E+09	7.0024E+16	2.6088E+13

**Table 5.3.11-10 Westinghouse 15x15 PWR 80,000 MWd/MTU, 150 Day Cool Time
Source Terms in MCBEND Format**

Group	Neutron [n/sec/assy]	Gamma [γ/sec/assy]	Hardware [γ/sec/kg]
1	0.000E+00	0.0000E+00	0.0000E+00
2	2.752E+05	1.1553E+05	0.0000E+00
3	1.147E+06	2.2345E+06	0.0000E+00
4	3.807E+06	1.0524E+07	0.0000E+00
5	1.194E+07	5.3649E+07	0.0000E+00
6	3.209E+07	1.3368E+08	0.0000E+00
7	5.542E+07	3.5682E+11	2.2624E-14
8	1.851E+08	3.1587E+12	1.8341E+05
9	3.180E+08	1.2047E+14	1.1829E+08
10	4.310E+08	4.1248E+13	5.0837E+09
11	1.008E+09	1.4482E+14	1.7466E+03
12	1.571E+09	5.4122E+14	1.1205E+13
13	4.106E+08	6.9042E+14	1.1811E+13
14	1.424E+08	3.8450E+15	3.2481E+12
15	2.048E+03	2.6544E+16	3.5960E+08
16	0.000E+00	1.2387E+16	3.3051E+11
17	0.000E+00	1.2039E+15	1.2551E+11
18	0.000E+00	1.5857E+15	3.5639E+09
19	0.000E+00	6.2649E+15	2.3914E+10
20	0.000E+00	6.3691E+15	7.4770E+10
21	0.000E+00	1.2564E+16	1.9900E+11
22	0.000E+00	9.4694E+15	2.2964E+11
23	0.000E+00		
24	0.000E+00		
25	0.000E+00		
26	0.000E+00		
27	0.000E+00		
28	0.000E+00		
Total	4.170E+09	8.1775E+16	2.7257E+13

Table 5.3.11-11 Westinghouse 17x17 PWR 80,000 MWd/MTU, 150 Day Cool Time
Source Terms in MCBEND Format

Group	Neutron [n/sec/assy]	Gamma [γ/sec/assy]	Hardware [γ/sec/kg]
1	0.000E+00	0.0000E+00	0.0000E+00
2	2.760E+05	1.1608E+05	0.0000E+00
3	1.150E+06	2.2451E+06	0.0000E+00
4	3.818E+06	1.0574E+07	0.0000E+00
5	1.198E+07	5.3902E+07	0.0000E+00
6	3.219E+07	1.3431E+08	0.0000E+00
7	5.559E+07	3.9282E+11	2.4111E-14
8	1.856E+08	3.4903E+12	1.8520E+05
9	3.193E+08	1.3558E+14	1.1944E+08
10	4.333E+08	4.5679E+13	5.4313E+09
11	1.012E+09	1.5991E+14	1.8636E+03
12	1.576E+09	5.7191E+14	1.1314E+13
13	4.118E+08	7.4675E+14	1.1926E+13
14	1.429E+08	4.0797E+15	3.5687E+12
15	2.098E+03	2.9120E+16	3.8295E+08
16	0.000E+00	1.3398E+16	3.5311E+11
17	0.000E+00	1.3353E+15	1.3207E+11
18	0.000E+00	1.7560E+15	3.7644E+09
19	0.000E+00	6.9673E+15	2.4688E+10
20	0.000E+00	7.0565E+15	7.6320E+10
21	0.000E+00	1.3899E+16	2.0242E+11
22	0.000E+00	1.0469E+16	2.3323E+11
23	0.000E+00		
24	0.000E+00		
25	0.000E+00		
26	0.000E+00		
27	0.000E+00		
28	0.000E+00		
Total	4.185E+09	8.9745E+16	2.7841E+13

Table 5.3.11-12 BWR 7x7 80,000 MWd/MTU, 210 Day Cool Time Source Terms in MCBEND Format

Group	Neutron [n/sec/assy]	Gamma [γ/sec/assy]	Hardware [γ/sec/kg]
1	0.000E+00	0.0000E+00	0.0000E+00
2	1.289E+05	5.3159E+04	0.0000E+00
3	5.370E+05	1.0281E+06	0.0000E+00
4	1.783E+06	4.8422E+06	0.0000E+00
5	5.594E+06	2.4683E+07	0.0000E+00
6	1.503E+07	6.1499E+07	0.0000E+00
7	2.595E+07	1.0195E+11	1.8206E-14
8	8.671E+07	8.2657E+11	1.6514E+05
9	1.481E+08	3.1183E+13	1.0650E+08
10	1.994E+08	1.1011E+13	2.2830E+09
11	4.690E+08	3.9966E+13	7.9373E+02
12	7.354E+08	1.9668E+14	1.0089E+13
13	1.923E+08	2.1866E+14	1.0635E+13
14	6.669E+07	1.3365E+15	1.8380E+12
15	8.453E+02	6.9578E+15	1.7082E+08
16	0.000E+00	3.6581E+15	1.4845E+11
17	0.000E+00	3.3622E+14	2.2220E+10
18	0.000E+00	4.4552E+14	1.9205E+09
19	0.000E+00	1.6749E+15	1.7265E+10
20	0.000E+00	1.7956E+15	6.0694E+10
21	0.000E+00	3.5384E+15	1.6698E+11
22	0.000E+00	2.6583E+15	1.9530E+11
23	0.000E+00		
24	0.000E+00		
25	0.000E+00		
26	0.000E+00		
27	0.000E+00		
28	0.000E+00		
Total	1.947E+09	2.2900E+16	2.3177E+13

Table 5.3.11-13 BWR 8x8 80,000 MWd/MTU, 150 Day Cool Time Source Terms in
MCBEND Format

Group	Neutron [n/sec/assy]	Gamma [γ/sec/assy]	Hardware [γ/sec/kg]
1	0.000E+00	0.0000E+00	0.0000E+00
2	1.204E+05	4.9995E+04	0.0000E+00
3	5.016E+05	9.6694E+05	0.0000E+00
4	1.665E+06	4.5540E+06	0.0000E+00
5	5.225E+06	2.3215E+07	0.0000E+00
6	1.404E+07	5.7842E+07	0.0000E+00
7	2.424E+07	1.0937E+11	1.6861E-14
8	8.098E+07	9.5997E+11	1.7019E+05
9	1.387E+08	3.4649E+13	1.0975E+08
10	1.874E+08	1.2514E+13	3.9517E+09
11	4.394E+08	4.5081E+13	1.3631E+03
12	6.870E+08	1.9612E+14	1.0397E+13
13	1.796E+08	2.2814E+14	1.0959E+13
14	6.230E+07	1.3467E+15	2.2905E+12
15	8.288E+02	8.5500E+15	2.8268E+08
16	0.000E+00	4.0807E+15	2.5692E+11
17	0.000E+00	3.6453E+14	9.8102E+10
18	0.000E+00	4.8432E+14	2.8804E+09
19	0.000E+00	1.8933E+15	2.0793E+10
20	0.000E+00	1.9461E+15	6.7247E+10
21	0.000E+00	3.8683E+15	1.8082E+11
22	0.000E+00	2.9183E+15	2.0962E+11
23	0.000E+00		
24	0.000E+00		
25	0.000E+00		
26	0.000E+00		
27	0.000E+00		
28	0.000E+00		
Total	1.821E+09	2.5969E+16	2.4488E+13

Table 5.3.11-14 PWR Fuel Lattice Axial Source Profile

% Core Height	Burnup Profile	Photon Source	Neutron Source
0.00%	0.5470	0.5470	7.840E-02
2.50%	0.6358	0.6358	1.479E-01
5.00%	0.7247	0.7247	2.569E-01
7.50%	0.8135	0.8135	4.185E-01
10.00%	0.9023	0.9023	6.481E-01
12.50%	0.9912	0.9912	9.633E-01
15.00%	1.0800	1.0800	1.384E+00
85.00%	1.0800	1.0800	1.384E+00
87.50%	0.9912	0.9912	9.633E-01
90.00%	0.9023	0.9023	6.481E-01
92.50%	0.8135	0.8135	4.185E-01
95.00%	0.7247	0.7247	2.569E-01
97.50%	0.6358	0.6358	1.479E-01
100.00%	0.5470	0.5470	7.840E-02

Table 5.3.11-15 BWR Fuel Lattice Axial Source Profile

% Core Height	Burnup Profile	Photon Source	Neutron Source
0.00%	0.3329	0.3329	9.637E-03
2.50%	0.4690	0.4690	4.098E-02
5.00%	0.6052	0.6052	1.202E-01
7.50%	0.7414	0.7414	2.829E-01
10.00%	0.8776	0.8776	5.764E-01
12.50%	1.0138	1.0138	1.060E+00
15.00%	1.1500	1.1500	1.804E+00
55.00%	1.1500	1.1500	1.804E+00
80.00%	1.1300	1.1300	1.675E+00
82.50%	1.0304	1.0304	1.135E+00
85.00%	0.9307	0.9307	7.386E-01
87.50%	0.8311	0.8311	4.580E-01
90.00%	0.7314	0.7314	2.672E-01
92.50%	0.6318	0.6318	1.440E-01
95.00%	0.5321	0.5321	6.980E-02
97.50%	0.4325	0.4325	2.910E-02
100.00%	0.3329	0.3329	9.637E-03

Table 5.3.11-16 BWR Fuel Assembly Lattice Fuel Region Homogenization

Fuel Type	Component	Volume Fraction of Components			
		UO ₂	Void	Clad	Interstitial
BWR 7×7	Fuel	1.5483E-01			
	Gap		5.1172E-03		
	Clad			4.9625E-02	
	Interstitial				7.9043E-01
	Total	1.5483E-01	5.1172E-03	4.9625E-02	7.9043E-01
BWR 8×8	Fuel	1.1446E-01			
	Gap		3.4266E-03		
	Clad			4.0802E-02	
	Interstitial				8.4131E-01
	Total	1.1446E-01	3.4266E-03	4.0802E-02	8.4131E-01

Table 5.3.11-17 PWR Fuel Assembly Lattice Fuel Region Homogenization

Fuel Type	Component	Volume Fraction of Components			
		UO ₂	Void	Clad	Interstitial
B&W 15×15	Fuel	3.6613E-02			
	Gap		1.6877E-03		
	Clad			1.1526E-02	
	Guide Tube			5.2650E-03	
	Instrument Tube			3.2906E-04	
	Inside Tubes				3.8943E-02
	Interstitial				9.0564E-01
	Total	3.6613E-02	1.6877E-03	1.7120E-02	9.4458E-01
B&W 17×17	Fuel	2.8289E-02			
	Gap		1.4142E-03		
	Clad			9.0051E-03	
	Guide Tube			7.2888E-03	
	Instrument Tube			2.6193E-04	
	Inside Tubes				3.9985E-02
	Interstitial				9.1376E-01
	Total	2.8289E-02	1.4142E-03	1.6556E-02	9.5374E-01
CE 14×14	Fuel	4.0893E-02			
	Gap		2.5363E-03		
	Clad			1.2421E-02	
	Guide Tube			7.9391E-03	
	Instrument Tube			1.9848E-03	
	Inside Tubes				6.1806E-02
	Interstitial				8.7242E-01
	Total	4.0893E-02	2.5363E-03	2.2345E-02	9.3423E-01

Table 5.3.11-17 PWR Fuel Assembly Lattice Fuel Region Homogenization (continued)

Fuel Type	Component	Volume Fraction of Components			
		UO ₂	Void	Clad	Interstitial
West. 14×14	Fuel	4.3979E-02	2.3284E-03		
	Gap				
	Clad			1.1715E-02	
	Guide Tube			1.2662E-02	
	Instrument Tube			7.9139E-04	
	Inside Tubes				3.7699E-02
	Interstitial				8.9083E-01
	Total	4.3979E-02	2.3284E-03	2.5168E-02	9.2852E-01
West. 15×15	Fuel	3.7044E-02	1.5755E-03		
	Gap				
	Clad			1.0655E-02	
	Guide Tube			6.2288E-03	
	Instrument Tube			3.1144E-04	
	Inside Tubes				4.7905E-02
	Interstitial				8.9628E-01
	Total	3.7044E-02	1.5755E-03	1.7195E-02	9.4419E-01
West. 17×17	Fuel	2.8764E-02	1.1712E-03		
	Gap				
	Clad			8.7489E-03	
	Guide Tube			7.4392E-03	
	Instrument Tube			3.0997E-04	
	Inside Tubes				5.6502E-02
	Interstitial				8.9706E-01
	Total	2.8764E-02	1.1712E-03	1.6498E-02	9.5357E-01

Table 5.3.11-18 Fuel Assembly Lattice Activated Hardware Region Homogenization

Fuel Type	Region	Mass SS [kg/assy]	SS Volume [cm ³ /assy]	Height [cm]	Volume [cm ³ /assy]	Volume Fraction
B&W 15×15	Lower Nozzle	10.29	1.2992E+03	18.4087	8.6536E+03	1.5014E-01
	Fuel Hardware	0.00	0.0000E+00	365.7600	1.7194E+05	0.0000E+00
	Upper Plenum	1.98	2.5000E+02	11.4364	5.3761E+03	4.6503E-02
	Upper Nozzle	10.76	1.3586E+03	25.0825	1.1791E+04	1.1522E-01
B&W 17×17	Lower Nozzle	7.13	9.0025E+02	19.1230	8.9894E+03	1.0015E-01
	Fuel Hardware	4.27	5.3914E+02	363.2200	1.7074E+05	3.1576E-03
	Upper Plenum	1.56	1.9697E+02	14.6920	6.9065E+03	2.8520E-02
	Upper Nozzle	18.13	2.2891E+03	23.8906	1.1231E+04	2.0383E-01
CE 14×14	Lower Nozzle	5.00	6.3131E+02	12.5349	5.5042E+03	1.1470E-01
	Fuel Hardware	1.36	1.7172E+02	347.9800	1.5280E+05	1.1238E-03
	Upper Plenum	7.98	1.0076E+03	25.7251	1.1296E+04	8.9196E-02
	Upper Nozzle	6.18	7.8030E+02	12.5400	5.5065E+03	1.4171E-01
West. 14×14	Lower Nozzle	7.89	9.9659E+02	8.6944	3.3804E+03	2.9482E-01
	Fuel Hardware	0.86	1.0884E+02	368.8080	1.4339E+05	7.5902E-04
	Upper Plenum	5.68	7.1762E+02	19.2710	7.4926E+03	9.5778E-02
	Upper Nozzle	9.89	1.2487E+03	8.8900	3.4564E+03	3.6128E-01
West. 15×15	Lower Nozzle	5.44	6.8687E+02	10.7607	4.9266E+03	1.3942E-01
	Fuel Hardware	1.03	1.3005E+02	365.7600	1.6746E+05	7.7663E-04
	Upper Plenum	3.68	4.6465E+02	20.2654	9.2781E+03	5.0080E-02
	Upper Nozzle	7.85	9.9116E+02	9.0170	4.1283E+03	2.4009E-01
West. 17×17	Lower Nozzle	5.90	7.4495E+02	8.5979	3.9382E+03	1.8916E-01
	Fuel Hardware	1.02	1.2828E+02	365.7600	1.6754E+05	7.6571E-04
	Upper Plenum	5.31	6.7045E+02	22.2123	1.0174E+04	6.5897E-02
	Upper Nozzle	7.85	9.9116E+02	9.3218	4.2698E+03	2.3213E-01
BWR 7×7	Lower Nozzle	4.70	5.9343E+02	18.7579	3.6848E+03	1.6105E-01
	Fuel Hardware	2.03	2.5631E+02	389.9000	7.6592E+04	3.3465E-03
	Upper Plenum	2.83	3.5738E+02	19.7385	3.8774E+03	9.2169E-02
	Upper Nozzle	3.52	4.4444E+02	19.0500	3.7422E+03	1.1877E-01
BWR 8×8	Lower Nozzle	4.70	5.9343E+02	18.7579	3.6848E+03	1.6105E-01
	Fuel Hardware	0.33	4.1667E+01	389.9000	7.6592E+04	5.4401E-04
	Upper Plenum	2.86	3.6082E+02	19.7385	3.8774E+03	9.3055E-02
	Upper Nozzle	2.08	2.6263E+02	19.0500	3.7422E+03	7.0180E-02

Table 5.3.11-19 Fuel Lattice Accident Condition Damaged Fuel Material Heights

Assembly	Axial Extent [cm]
B&W 15×15	18.82
B&W 17×17	11.85
CE 14×14	14.04
Westinghouse 14×14	14.17
Westinghouse 15×15	13.93
Westinghouse 17×17	10.82
BWR 7×7	24.41
BWR 8×8	18.05

Table 5.3.11-20 BWR Fuel Assembly Lattice Fuel Region Homogenized Material Description

Element	Number Density [atom/b-cm]	
	BWR 7×7	BWR 8×8
U	3.60E-03	2.66E-03
O	7.20E-03	5.33E-03
ZR	2.10E-03	1.73E-03
SN	2.47E-05	2.03E-05
FE	2.19E-04	4.01E-05
CR	5.90E-05	1.21E-05
NI	2.21E-05	3.81E-06
HF	1.10E-07	9.02E-08

Table 5.3.11-21 PWR Fuel Assembly Lattice Fuel Region Homogenized Material Description

Element	Number Density [atom/b-cm]					
	B&W 15×15	B&W 17×17	CE 14×14	WE 14×14	WE 15×15	WE 17×17
U	8.51E-04	6.57E-04	9.50E-04	1.02E-03	8.61E-04	6.68E-04
O	1.70E-03	1.32E-03	1.90E-03	2.05E-03	1.72E-03	1.34E-03
ZR	7.26E-04	7.02E-04	9.48E-04	1.07E-03	7.29E-04	7.00E-04
SN	8.53E-06	8.25E-06	1.11E-05	1.25E-05	8.57E-06	8.22E-06
FE	2.42E-06	2.02E-04	7.42E-05	5.15E-05	5.15E-05	5.07E-05
CR	1.30E-06	5.34E-05	2.03E-05	1.44E-05	1.41E-05	1.39E-05
NI	1.15E-07	2.06E-05	7.46E-06	5.10E-06	5.16E-06	5.09E-06
HF	3.78E-08	3.66E-08	4.94E-08	5.56E-08	3.80E-08	3.65E-08

Table 5.3.11-22 Basket and Cask Shielding Material Composition

Material	Element	Number Density [atom/b-cm]
Aluminum	AL	6.02626E-02
Stainless Steel 304	FE	6.31986E-02
	CR	1.65112E-02
	NI	6.50094E-03
Lead	PB	3.29706E-02
Neutron Shield	H	5.98800E-02
	C	1.07010E-02
	O	2.45890E-02
Impact Limiter	AL	1.11530E-02
BWR Damaged Fuel	U	1.62614E-02
	O	3.25085E-02
PWR Damaged Fuel	U	1.16153E-02
	O	2.32204E-02

Table 5.3.11-23 ANSI/ANS 6.1.1-1977 Neutron Flux-to-Dose Conversion Factors

Energy [MeV]	Response [(rem/hr)/(n/cm²/sec)]
20.0	2.27E-04
14.0	2.08E-04
10.0	1.47E-04
7.0	1.47E-04
5.0	1.56E-04
2.5	1.25E-04
1.0	1.32E-04
5.0E-01	9.26E-05
1.0E-01	2.17E-05
1.0E-02	3.56E-06
1.0E-03	3.76E-06
1.0E-04	4.18E-06
1.0E-05	4.54E-06
1.0E-06	4.46E-06
1.0E-07	3.67E-06
2.5E-08	3.67E-06

Table 5.3.11-24 ANSI/ANS 6.1.1-1977 Gamma Flux-to-Dose Conversion Factors

Energy, E [MeV]	Response [(rem/hr)/(γ/cm ² /sec)]	Energy, E [MeV]	Response [(rem/hr)/(γ/cm ² /sec)]
15.0	1.33E-05	1.0	1.98E-06
13.0	1.18E-05	0.8	1.68E-06
11.0	1.03E-05	0.7	1.52E-06
9.0	8.77E-06	0.65	1.44E-06
7.5	7.66E-06	0.6	1.36E-06
6.75	7.11E-06	0.55	1.27E-06
6.25	6.74E-06	0.5	1.17E-06
5.75	6.37E-06	0.45	1.08E-06
5.25	6.01E-06	0.4	9.85E-07
5.0	5.80E-06	0.35	8.78E-07
4.75	5.60E-06	0.3	7.59E-07
4.25	5.23E-06	0.25	6.31E-07
3.75	4.83E-06	0.2	5.01E-07
3.25	4.41E-06	0.15	3.79E-07
2.8	4.01E-06	0.1	2.83E-07
2.6	3.82E-06	0.07	2.58E-07
2.2	3.42E-06	0.05	2.90E-07
1.8	2.99E-06	0.03	5.82E-07
1.4	2.51E-06	0.01	3.96E-06

Table 5.3.11-25 Maximum Radial Dose Rates for PWR and BWR Fuel Rods in an Irradiated Fuel Assembly Lattice

Fuel Type	Dose Rate [mrem/hr]				
	Normal Surface	Normal 1 foot	Normal 1 meter	Normal 2 meter	Accident 1 meter
B&W 15×15	157	54.7	26.2	9.9	683
B&W 17×17	204	69.4	24.8	9.6	670
CE 14×14	98	54.3	27.0	9.6	653
Westinghouse 14×14	105	52.4	26.0	9.7	664
Westinghouse 15×15	100	53.9	26.5	9.8	665
Westinghouse 17×17	82	46.0	23.1	8.5	653
BWR 7×7	267	83.0	27.6	8.9	720
BWR 8×8	200	63.2	21.2	7.5	663

Table 5.3.11-26 Maximum Axial Dose Rates for PWR and BWR Fuel Rods in an Irradiated Fuel Assembly Lattice

Fuel Type	Dose Rate [mrem/hr]			
	Normal – Surface		Accident – 1 meter	
	Top	Bottom	Top	Bottom
B&W 15×15	13.9	7.4	147	2.1
B&W 17×17	13.2	7.0	146	1.9
CE 14×14	9.7	8.3	148	1.5
Westinghouse 14×14	12.6	7.0	152	1.8
Westinghouse 15×15	12.6	8.5	157	2.4
Westinghouse 17×17	12.0	8.5	145	2.6
BWR 7×7	8.0	4.5	166	2.2
BWR 8×8	7.9	4.3	155	2.1

5.3.12 Damaged High Burnup PWR and BWR Rods in a Rod Holder

Results of a shielding analysis for up to 25 high burnup PWR or BWR fuel rods with a maximum of 14 damaged fuel rods are presented in this section. The 14 damaged fuel rods are assumed to fail during transport. The rods have burnups up to 80,000 MWd/MTU. Based on the minimum cool times developed in Section 5.3.8, maximum dose rates are calculated to demonstrate that dose rate limits are not exceeded.

Dose rates are calculated using the MCBEND three-dimensional Monte Carlo transport code. Source terms are calculated using the SAS2H module of the SCALE package, with ORIGEN-S used to rebin the gamma-ray and neutron spectra onto the 22-group and 28-group structures required by MCBEND.

5.3.12.1 Damaged PWR and BWR Rods Source Terms

Source terms employed in this analysis are identical to those employed in Section 5.3.8 above. The SAS2H-generated source spectra are rebinned onto the standard 28-group neutron and 22-group gamma scheme used in MCBEND as shown in Table 5.3.11-1 and Table 5.3.11-2, respectively.

Source terms in MCBEND format are presented in Table 5.3.12-1 through Table 5.3.12-3 for PWR and BWR fuel. PWR and BWR 8x8 fuel types are analyzed at 80,000 MWd/MTU and 150 days cool time. Based on the results in Section 5.3.8, the minimum cool time for BWR 7x7 fuel is 210 days for a maximum burnup of 60,000 MWd/MTU; BWR 7x7 fuel is conservatively analyzed at 80,000 MWd/MTU and 210 days cool time.

The effect of subcritical neutron multiplication is not directly computed in the MCBEND analysis, due to difficulties in adequately biasing the calculation. Instead, neutron source rates are scaled by a subcritical multiplication factor based on the system multiplication factor, k_{eff} :

$$\text{Scale Factor} = \frac{1}{1 - k_{\text{eff}}}$$

For the dry cask conditions of transport, calculated k_{eff} is 0.06 for BWR fuel and 0.05 for PWR fuel, with resulting scale factors of 1.0638 and 1.0526, respectively. These scale factors are included in the source strength input unit in MCBEND.

5.3.12.2 Axial Source Profile

The axial source profiles employed in MCBEND for PWR and BWR fuel are identical to those employed in Section 5.3.11.2. Profiles are input by evaluating the fraction of source in each axial bin. By default, no internal normalization of the profile is performed. The discrete axial profile

is applied to the intact rods. A uniform source is applied to the damaged fuel concentrated at the top of the cask. The nonlinear impact of burnup on the total neutron source strength is accounted for in both the damaged and intact fuel regions.

5.3.12.3 High Burnup PWR and BWR Rods Shielding Model

MCBEND three-dimensional shielding analysis allows detailed modeling of the fuel, basket, and cask shield configurations. For the fuel rod sources, some fuel rod detail is homogenized in the model to simplify model input and improve computational efficiency. Thus, the three-dimensional models represent the various fuel assembly source regions as homogenized zones within the rod holder, but explicitly model the axial extent of the source regions. The basket and cask body details are explicitly modeled, including the axial extents described by the License Drawings.

The geometric description of a MCBEND model is based on the combinatorial geometry system embedded in the code. In this system, bodies such as cylinders and rectangular parallelepipeds, and their logical intersections and unions, are used to describe the extent of material zones.

MCBEND employs an automated biasing technique for the Monte Carlo calculation based on a three-dimensional adjoint diffusion calculation. Mesh cells for the adjoint solution are selected based on half value thicknesses for each material.

Fuel Rod Model

Based on the fuel parameters provided in Section 5.3.8, and the rod holder cross-sectional detail provided by the License Drawings, homogenized treatments of fuel rod source regions are developed. The homogenized fuel rods are represented in the model as a stack of boxes with width equal to the rod holder interior width. The height of each box corresponds to the modeled height of the corresponding source region.

The intact fuel region homogenizations are shown in Table 5.3.12-4 through Table 5.3.12-6, based on a homogenization area of 81.765 cm^2 . Components of the fuel homogenization are subdivided to account for the various area fractions present in the homogenized fuel description. "Interstitial" refers to the space within the rod holder canister but outside the 5×5 tube array. "Insert void" refers to the space inside the rod holder tubes but outside the fuel rods. "Gap" refers to the pellet to clad gap. All three regions are assigned a void material as part of the shielding evaluation since the cask cavity is dry during all transport conditions. Combined with the fuel rod clad, fuel material, and tube materials, the void accounts for the total fuel region volume. The clad region is zirconium alloy (density 6.55 g/cm^3) for both PWR and BWR fuel.

Failed fuel is considered by filling the void space between the top of the intact fuel and the rod holder can lid ($2.70\text{E}+03 \text{ cm}^3$) with UO_2 at a 50% volume fraction. For all three fuel types, this volume corresponds to less than 14 fuel rods. Therefore, an additional source region is modeled, which considers a mixture of damaged fuel and intact fuel homogenized over the height required to yield the appropriate volume difference. The area available for failed fuel in this mixture region is 50% of the void space within the pin holder can excluding the pellet-clad gap. The mixture calculations are summarized in Table 5.3.12-7.

For conservatism, the input description differs in the analysis of the three source regions described above. For the intact fuel mixture, the source region is the entire active fuel height (389.9 cm) with the remaining space above (33.01 cm) filled with damaged fuel. No credit is taken for the self-shielding of intact and damaged fuel spanning at the top of the active fuel region, and no credit is taken for the reduction in active fuel source required for the dispersion of 14 rods. Thus, the total source evaluated is 39 rods.

Basket Model

For a given fuel type, the MCBEND description of the basket elements forms a common sub-model employed in the analysis. The key features of the model are the detailed representation of pin canister, PWR insert, and PWR basket.

MCBEND NAC-LWT Model

The three-dimensional model of the NAC-LWT cask containing design basis fuel assemblies is based on the following features:

Normal conditions:

- Radial neutron shield and shield shell
- Aluminum impact limiters with 0.5 g/cm^3 density (calculated based on the impact limiter weight and dimensions) and diameter equal to the neutron shield shell diameter

Accident conditions:

- Removal of radial neutron shield and shield shell
- Loss of upper and lower impact limiters

Common to both the normal and accident conditions models is a 0.1374 cm gap between the lead outer diameter and the cask outer shell. The elevation of the source regions is controlled such that the offset of the rod holder canister from the bottom of the NAC-LWT cask cavity is not more than 2.05 inches (5.21 cm) based on the cavity, spacer and rod holder dimensions. This conservatively shifts the failed fuel source to the top of the cask cavity where, as shown in Figure 5.3.10-6, the least radial shielding is located.

Detailed model parameters used in creating the three-dimensional model are taken directly from the License Drawings. Elevations associated with the three-dimensional features are established with respect to the center bottom of the NAC-LWT cask cavity for the MCBEND combinatorial model. The three-dimensional NAC-LWT models are shown in Figure 5.3.12-1 and Figure 5.3.12-2. A sample input file for the damaged fuel evaluation is provided in Figure 5.3.12-6.

Shield Regional Densities

Based on the homogenization described for the fuel rod model, the resulting fuel regional densities are shown in Table 5.3.12-8. Material compositions for structural and shield materials are shown in Table 5.3.11-22.

5.3.12.4 Damaged High Burnup PWR and BWR Rods Shielding Evaluation

Calculational Methods

The shielding evaluation is performed using MCBEND. As described in Section 5.3.12.2, the evaluation includes the effect of fuel burnup peaking on fuel neutron and gamma source terms.

The MCBEND shielding model described in Section 5.3.12.3 is utilized with the source terms described in Section 5.3.12.1 to estimate the dose rate profiles at various distances from the side, top and bottom of the cask for both normal and accident conditions. The method of solution is continuous energy Monte Carlo with an adjoint diffusion solution for generating importance meshes. Radial biasing is performed within the MCBEND code to estimate dose rates on the side of the cask. Axial biasing is performed to estimate dose rates on the top and bottom of the cask.

The MCBEND code has been validated against various classical shielding problems, including fast and thermal neutron sources penetrating through single material slab geometries of iron, graphite and water. The validation suite also includes fast neutron transmission through alternating slabs of iron and water. Of particular interest is a benchmark of MCBEND to gamma and neutron dose rates outside a metal transport cask, where agreement between measurement and calculation is within 20% for the majority of dose locations.

MCBEND results are calculated using the JEF2.2 neutron cross-section library and the ANSWERS gamma library.

MCBEND Flux-to-Dose Conversion Factors

The ANSI/ANS 6.1.1-1977 flux-to-dose rate conversion factors are employed in the MCBEND analysis. The ANSI/ANS gamma and neutron dose conversion factors are shown in Table 5.3.11-23 and Table 5.3.11-24. The number of energy/conversion factor pairs was increased to

133 neutron and 371 gamma pairs by a log-log interpolation scheme indicated as appropriate in ANSI/ANS 6.1.1-1977.

Three-Dimensional Dose Rates for High Burnup Fuel

Table 5.3.12-9 and Table 5.3.12-10 summarize the computed dose rates for each fuel type at the tabulated distances and transport conditions (normal and accident). The highest calculated radial dose rates at the surface and 2-meter locations under normal conditions are for BWR 8×8 and PWR rods, respectively. The highest calculated radial dose rates at 1 meter from the cask under accident conditions are for BWR 7×7 rods.

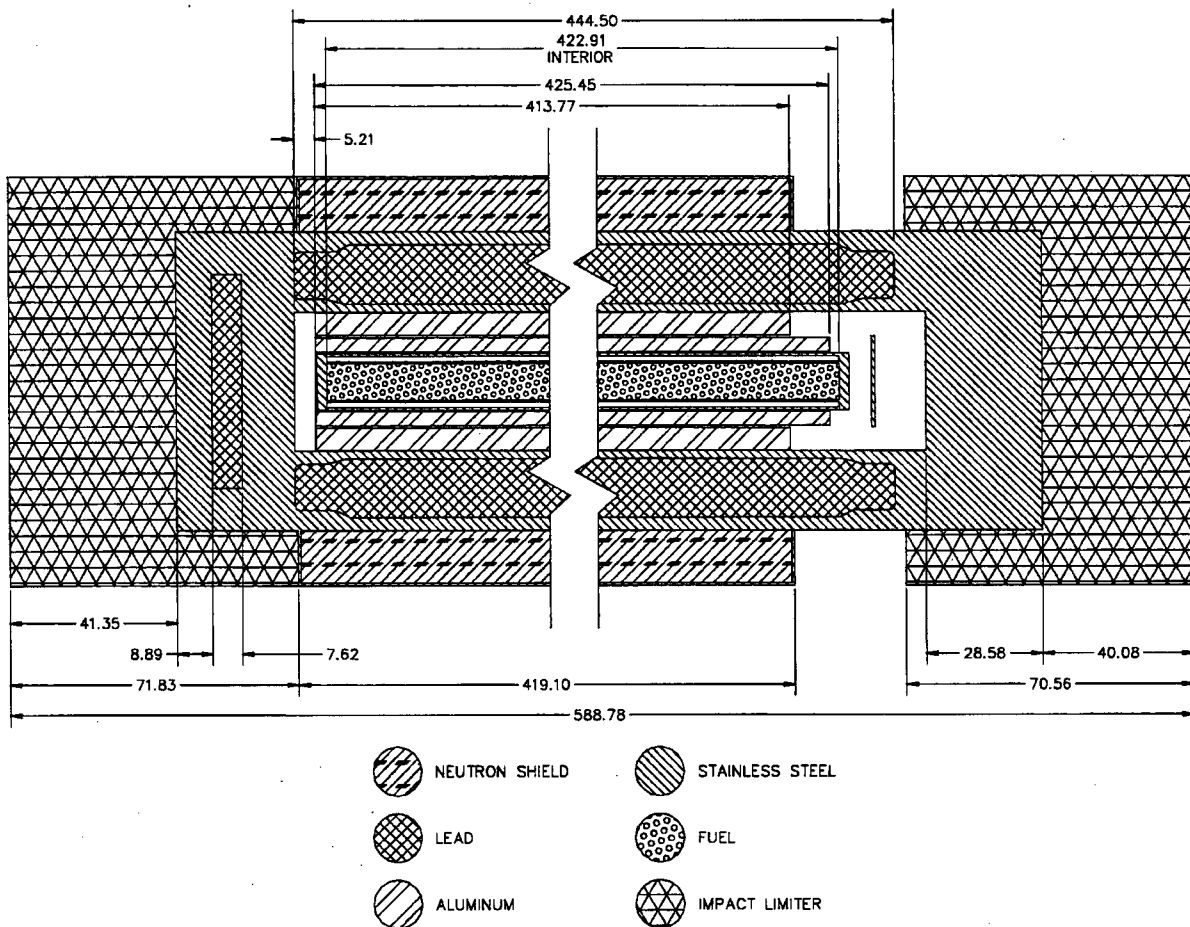
Normal condition radial surface dose rates for all three fuel types are in excess of 200 mrem/hr, necessitating an exclusive use designation for the NAC-LWT. The maximum dose rate is dominated by the damaged fuel neutron component, which comprises approximately 74% of the maximum dose rate. The axial elevation of the maximum dose rate is above the neutron shield. The dose rate profile is shown in Figure 5.3.12-3.

The normal condition maximum radial 2-meter dose rate is 9.8 mrem/hr. At this distance, the damaged fuel neutron component contributes approximately 34% of the maximum. The dose rate profile is skewed towards the top of cask, as shown Figure 5.3.12-4.

Accident condition radial 1-meter dose rates for all three fuel types are well below the 1,000 mrem/hr limit. The maximum dose rate is dominated by the intact fuel neutron component, which contributes approximately 68% towards the maximum. The dose rate profile is shown in Figure 5.3.12-5.

As shown in Table 5.3.12-10, axial surface dose rates are well below limits for all three fuel types. Significant margin is present for the normal condition 2-meter and accident condition 1-meter dose rate limits.

Figure 5.3.12-1 MCBEND Model of NAC-LWT with Damaged Fuel Rods – Axial Detail



Dimensions in cm.

Note: Spacer, rod holder handle and basket bottom weldment material are not included in the model. The spacing provided by these components is maintained in the model.

Figure 5.3.12-2 MCBEND Model of NAC-LWT with Damaged Fuel Rods – Radial Detail

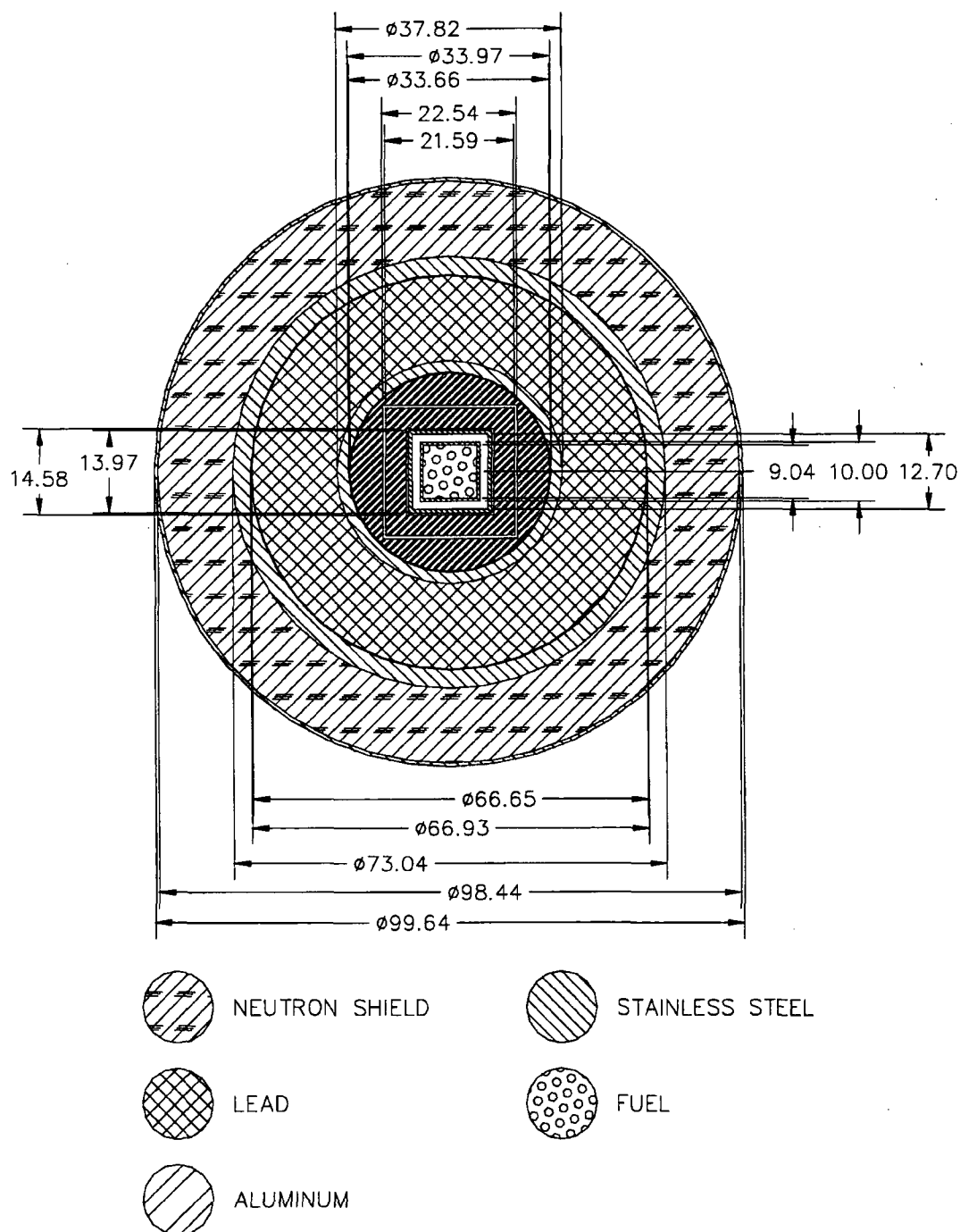


Figure 5.3.12-3 Normal Condition Axial Surface Dose Rate Profile by Source Type – Damaged Fuel Rods

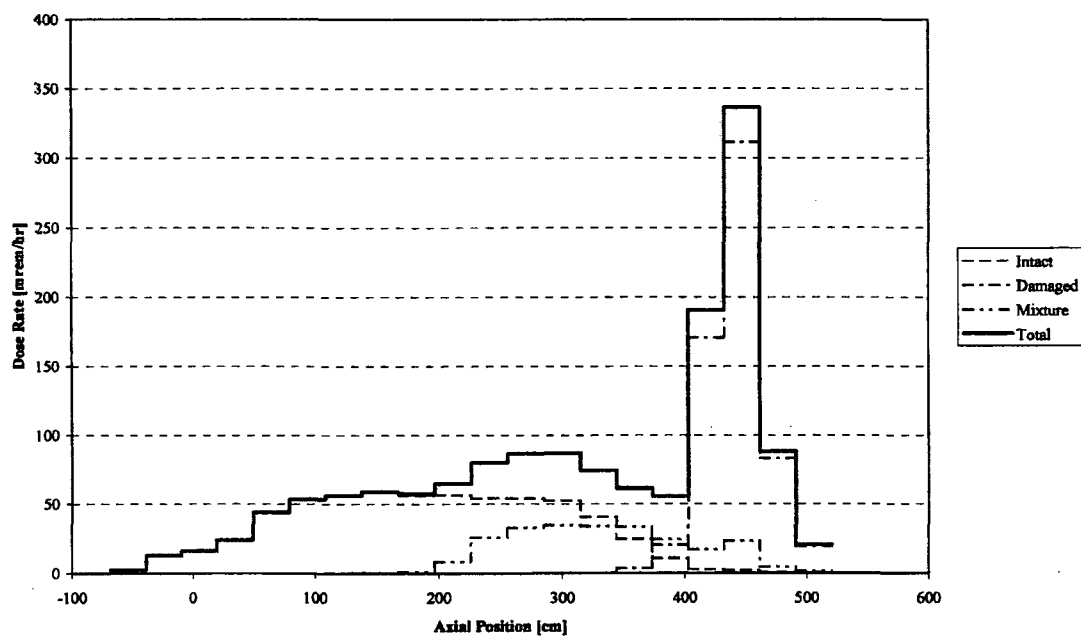


Figure 5.3.12-4 Normal Condition Radial 2m Dose Rate Profile by Source Type – Damaged Fuel Rods

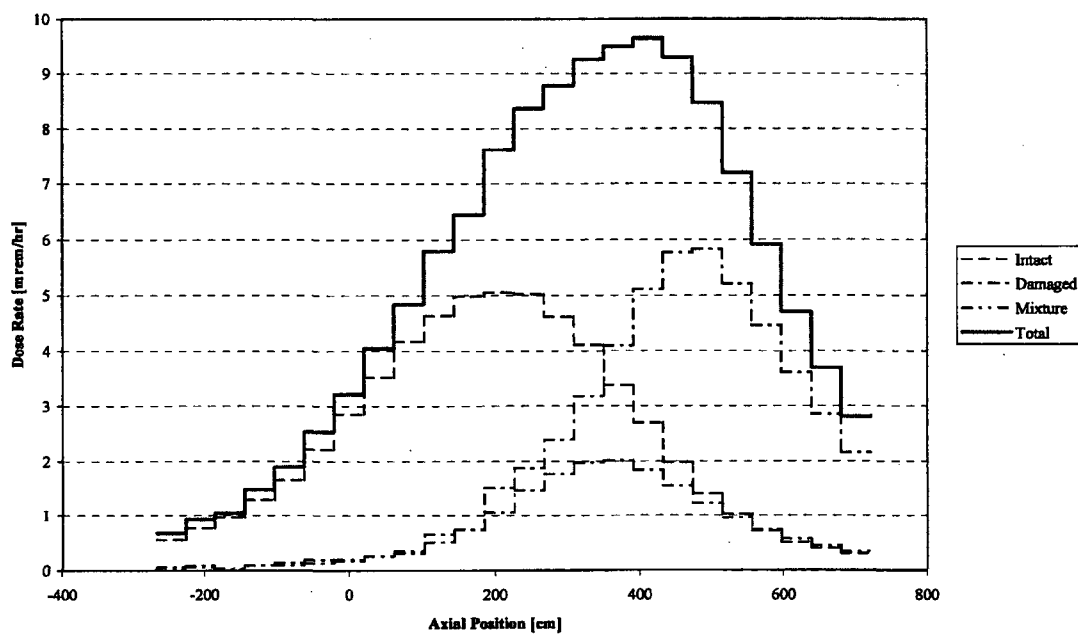


Figure 5.3.12-5 Accident Condition Radial 1m Dose Rate Profile by Source Type –
Damaged Fuel Rods

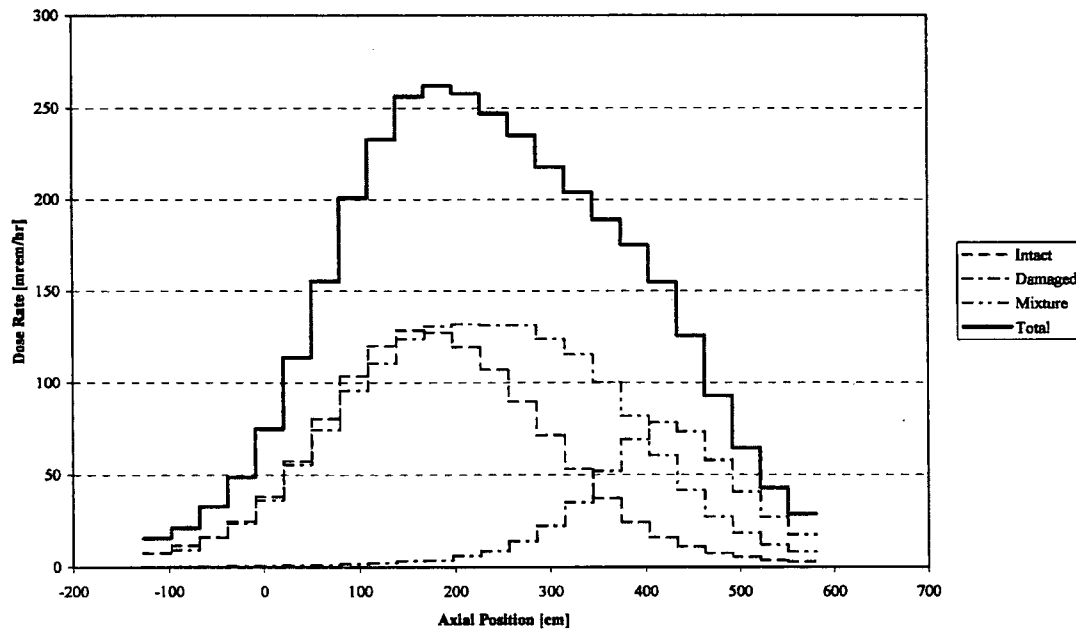


Figure 5.3.12-6 Sample Input File for Damaged Fuel Evaluation

```

columns 1 200
*
* LWT Cask - b7Dmg_80b40e210d
* Normal Transport Conditions
* Damaged Rods Condition Normal(25) Damaged(14)
* BWR 7x7 Rods 80 GWD/MTU 4.0 wt. % 210 days Cool Time
* Fuel Neutron Source
* Radial Detector Positions
* Model Revision v2.7.2
*
*
* Parameters
*
@samps = 1000000
*
* Unit 1 Control Data
*
begin control data
run
sample limit @samps
time limit 1000m
seeds 92356 84336
chime every (@samps/10) samples
report interim results
sbd 30s
dump intervals 1
end

*
* Unit 3 Output Control
*
*begin output control
* suppress inflows
*end

*
* Unit 4 Material Geometry
*
begin material geometry
* LWT Cask Normal Conditions v2.7
PART 1
ZROD 1 0.0000 0.0000 -26.6700 36.5189 507.3650 ! Lwt
ZROD 2 0.0000 0.0000 -26.6700 36.5189 26.6700 ! Bottom
ZROD 3 0.0000 0.0000 0.0000 16.9863 452.1200 ! Cavity
ZROD 4 0.0000 0.0000 -17.7800 26.3525 7.6200 ! Bottom gamma shield
ZROD 5 0.0000 0.0000 0.0000 20.1740 444.5000 ! Lead id - taper
ZROD 6 0.0000 0.0000 0.0000 31.5976 444.5000 ! Lead od - taper
ZROD 7 0.0000 0.0000 13.8176 18.9103 416.8648 ! Lead id
ZROD 8 0.0000 0.0000 13.8176 33.3271 416.8648 ! Lead od
ZROD 9 0.0000 0.0000 13.8176 33.4645 416.8648 ! Lead gap
ZROD 10 0.0000 0.0000 3.8100 49.8183 419.1000 ! Neutron shield shell
ZROD 11 0.0000 0.0000 5.0800 49.2189 416.5600 ! Neutron shield
ZROD 12 0.0000 0.0000 450.2150 49.8183 70.5612 ! Upper limiter
ZROD 13 0.0000 0.0000 -68.0212 49.8183 71.8312 ! Lower limiter
ZROD 14 0.0000 0.0000 -68.0212 49.8183 588.7974 ! Container
ZONES
/Bottom/ M4 +4
/Cavity/ P2 +3
/Bottom/ M5 +2 -4 -2 -6 -9 -3
/OuterShell/ M5 +1 -2 -6 -9 -3
/InnerShellTaper/ M5 +5 -8 -3
/InnerShell/ M5 +7 -3
/Lead/ M4 +8 -7
/LeadTaper/ M4 +6 -5 -8
/LeadGap/ M0 +9 -8
/NeutronShield/ M2 +11 -1
/NSShell/ M5 +10 -11 -1
/UpperLimiter/ M9 +12 -1
/LowerLimiter/ M9 +13 -1
/Exterior/ M0 +14 -1 -10 -12 -13
VOLUMES UNITY
* Cask Cavity for Rods Model v2.7
PART 2
ZROD 1 0.0000 0.0000 0.0000 16.8275 433.1970 ! PWR basket
ZROD 2 0.0000 0.0000 438.7850 11.1760 0.9525 ! Spacer plate
ZROD 3 0.0000 0.0000 0.0000 16.9863 452.1200 ! Cavity
ZONES
/PWRBasket/ P3 +1
/Spacer/ M5 +2
/Cavity/ M0 +3 -2 -1
VOLUMES UNITY
* PWR Basket for Rods Model v2.7
PART 3
BOX 1 -11.2713 -11.2713 5.2070 22.5425 22.5425 427.9900 ! Internal cavity
ZROD 2 0.0000 0.0000 0.0000 16.8275 5.2070 ! Bottom offset
ZROD 3 0.0000 0.0000 0.0000 16.8275 415.4170 ! Basket walls
ZROD 4 0.0000 0.0000 0.0000 16.8275 433.1970 ! Basket void
ZONES
/PWR Insert/ P4 +1
/Offset/ M0 +2
/Basket/ M3 +3 -2 -1
/Basket/ M0 +4 -3 -2 -1
VOLUMES UNITY

```

Figure 5.3.12-6 Sample Input File for Damaged Fuel Evaluation (Continued)

```
* PWR Insert for Rods Model v2.7
PART 4
BOX 1 -7.2898 -7.2898 1.2700 14.5796 14.5796 426.7200 ! PWR Insert cavity
BOX 2 -10.7950 -10.7950 0.0000 21.5900 21.5900 425.4500 ! PWR Insert body
BOX 3 -11.2713 -11.2713 0.0000 22.5425 22.5425 427.9900 ! PWR Insert void
ZONES
/Can Weldment/ P5 +1
/PWR Insert Body/ M3 +2 -1
/Container/ M0 +3 -2 -1
VOLUMES UNITY
* Can Weldment for Rods Model v2.7
PART 5
BOX 1 -4.5212 -4.5212 2.5400 9.0424 9.0424 422.9100 ! Internal cavity
BOX 2 -4.9975 -4.9975 2.5400 9.9949 9.9949 419.7350 ! Internal spacer
BOX 3 -6.3500 -6.3500 2.5400 12.7000 12.7000 420.3700 ! Can weldment cavity
BOX 4 -6.9850 -6.9850 0.0000 13.9700 13.9700 2.5400 ! Can weldment base
BOX 5 -6.9850 -6.9850 0.0000 13.9700 13.9700 422.9100 ! Can weldment body
BOX 6 -6.9850 -6.9850 0.0000 13.9700 13.9700 425.4500 ! Can weldment flange
BOX 7 -6.9850 -6.9850 0.0000 13.9700 13.9700 426.7200 ! Can weldment lid
BOX 8 -7.2898 -7.2898 0.0000 14.5796 14.5796 426.7200 ! PWR Insert cavity
ZONES
/Fuel Insert/ P6 +1
/Internal Spacer/ M5 +2 -1
/Can Weldment void/ M0 +3 -2 -1
/Can Weldment base/ M5 +4
/Can Weldment body/ M5 +5 -4 -3 -1
/Can Weldment flange/ M5 +6 -5 -1
/Can Weldment lid/ M5 +7 -6
/Container/ M0 +8 -7
VOLUMES UNITY
* Rods Model Fuel Insert v2.7
PART 6 NEST
BOX M6 0.0000 0.0000 0.0000 9.0424 9.0424 0.0001 ! Intact fuel
BOX M6 0.0000 0.0000 0.0000 9.0424 9.0424 389.9000 ! Intact fuel
BOX M7 S 0.0000 0.0000 0.0000 9.0424 9.0424 422.9100 ! Damaged fuel
* LWT Cask Detector Description v2.7
PART 7
* Radial Detector DRA (Surface) Bodies
ZR0D 1 0.0000 0.0000 -68.0212 49.8183 588.7974
ZR0D 2 0.0000 0.0000 -68.0212 50.8183 29.4399
ZR0D 3 0.0000 0.0000 -38.5813 50.8183 29.4399
ZR0D 4 0.0000 0.0000 -9.1415 50.8183 29.4399
ZR0D 5 0.0000 0.0000 20.2984 50.8183 29.4399
ZR0D 6 0.0000 0.0000 49.7383 50.8183 29.4399
ZR0D 7 0.0000 0.0000 79.1782 50.8183 29.4399
ZR0D 8 0.0000 0.0000 108.6180 50.8183 29.4399
ZR0D 9 0.0000 0.0000 138.0579 50.8183 29.4399
ZR0D 10 0.0000 0.0000 167.4978 50.8183 29.4399
ZR0D 11 0.0000 0.0000 196.9376 50.8183 29.4399
ZR0D 12 0.0000 0.0000 226.3775 50.8183 29.4399
ZR0D 13 0.0000 0.0000 255.8174 50.8183 29.4399
ZR0D 14 0.0000 0.0000 285.2572 50.8183 29.4399
ZR0D 15 0.0000 0.0000 314.6971 50.8183 29.4399
ZR0D 16 0.0000 0.0000 344.1370 50.8183 29.4399
ZR0D 17 0.0000 0.0000 373.5769 50.8183 29.4399
ZR0D 18 0.0000 0.0000 403.0167 50.8183 29.4399
ZR0D 19 0.0000 0.0000 432.4566 50.8183 29.4399
ZR0D 20 0.0000 0.0000 461.8965 50.8183 29.4399
ZR0D 21 0.0000 0.0000 491.3363 50.8183 29.4399
* Radial Detector DRAA (SurfaceAzi) Bodies
ZR0D 22 0.0000 0.0000 -69.0212 50.8183 590.7974
* Band 1 Bodies
ZSEC 23 0.0000 0.0000 444.5000 50.8183 51.8183 36.1950 0.0000 12.0000
ZSEC 24 0.0000 0.0000 444.5000 50.8183 51.8183 36.1950 12.0000 24.0000
ZSEC 25 0.0000 0.0000 444.5000 50.8183 51.8183 36.1950 24.0000 36.0000
ZSEC 26 0.0000 0.0000 444.5000 50.8183 51.8183 36.1950 36.0000 48.0000
ZSEC 27 0.0000 0.0000 444.5000 50.8183 51.8183 36.1950 48.0000 60.0000
ZSEC 28 0.0000 0.0000 444.5000 50.8183 51.8183 36.1950 60.0000 72.0000
ZSEC 29 0.0000 0.0000 444.5000 50.8183 51.8183 36.1950 72.0000 84.0000
ZSEC 30 0.0000 0.0000 444.5000 50.8183 51.8183 36.1950 84.0000 96.0000
ZSEC 31 0.0000 0.0000 444.5000 50.8183 51.8183 36.1950 96.0000 108.0000
ZSEC 32 0.0000 0.0000 444.5000 50.8183 51.8183 36.1950 108.0000 120.0000
ZSEC 33 0.0000 0.0000 444.5000 50.8183 51.8183 36.1950 120.0000 132.0000
ZSEC 34 0.0000 0.0000 444.5000 50.8183 51.8183 36.1950 132.0000 144.0000
ZSEC 35 0.0000 0.0000 444.5000 50.8183 51.8183 36.1950 144.0000 156.0000
ZSEC 36 0.0000 0.0000 444.5000 50.8183 51.8183 36.1950 156.0000 168.0000
ZSEC 37 0.0000 0.0000 444.5000 50.8183 51.8183 36.1950 168.0000 180.0000
ZSEC 38 0.0000 0.0000 444.5000 50.8183 51.8183 36.1950 180.0000 192.0000
ZSEC 39 0.0000 0.0000 444.5000 50.8183 51.8183 36.1950 192.0000 204.0000
ZSEC 40 0.0000 0.0000 444.5000 50.8183 51.8183 36.1950 204.0000 216.0000
ZSEC 41 0.0000 0.0000 444.5000 50.8183 51.8183 36.1950 216.0000 228.0000
ZSEC 42 0.0000 0.0000 444.5000 50.8183 51.8183 36.1950 228.0000 240.0000
ZSEC 43 0.0000 0.0000 444.5000 50.8183 51.8183 36.1950 240.0000 252.0000
ZSEC 44 0.0000 0.0000 444.5000 50.8183 51.8183 36.1950 252.0000 264.0000
ZSEC 45 0.0000 0.0000 444.5000 50.8183 51.8183 36.1950 264.0000 276.0000
ZSEC 46 0.0000 0.0000 444.5000 50.8183 51.8183 36.1950 276.0000 288.0000
ZSEC 47 0.0000 0.0000 444.5000 50.8183 51.8183 36.1950 288.0000 300.0000
ZSEC 48 0.0000 0.0000 444.5000 50.8183 51.8183 36.1950 300.0000 312.0000
ZSEC 49 0.0000 0.0000 444.5000 50.8183 51.8183 36.1950 312.0000 324.0000
ZSEC 50 0.0000 0.0000 444.5000 50.8183 51.8183 36.1950 324.0000 336.0000
ZSEC 51 0.0000 0.0000 444.5000 50.8183 51.8183 36.1950 336.0000 348.0000
ZSEC 52 0.0000 0.0000 444.5000 50.8183 51.8183 36.1950 348.0000 360.0000
* Radial Detector DRB (1ft) Bodies
```


Figure 5.3.12-6 Sample Input File for Damaged Fuel Evaluation (Continued)

ZROD	53	0.0000	0.0000	-98.5012	80.2983	649.7574
ZROD	54	0.0000	0.0000	-98.5012	81.2983	32.4879
ZROD	55	0.0000	0.0000	-66.0133	81.2983	32.4879
ZROD	56	0.0000	0.0000	-33.5255	81.2983	32.4879
ZROD	57	0.0000	0.0000	-1.0376	81.2983	32.4879
ZROD	58	0.0000	0.0000	31.4503	81.2983	32.4879
ZROD	59	0.0000	0.0000	63.9382	81.2983	32.4879
ZROD	60	0.0000	0.0000	96.4260	81.2983	32.4879
ZROD	61	0.0000	0.0000	128.9139	81.2983	32.4879
ZROD	62	0.0000	0.0000	161.4018	81.2983	32.4879
ZROD	63	0.0000	0.0000	193.8896	81.2983	32.4879
ZROD	64	0.0000	0.0000	226.3775	81.2983	32.4879
ZROD	65	0.0000	0.0000	258.8654	81.2983	32.4879
ZROD	66	0.0000	0.0000	291.3532	81.2983	32.4879
ZROD	67	0.0000	0.0000	323.8411	81.2983	32.4879
ZROD	68	0.0000	0.0000	356.3290	81.2983	32.4879
ZROD	69	0.0000	0.0000	388.8169	81.2983	32.4879
ZROD	70	0.0000	0.0000	421.3047	81.2983	32.4879
ZROD	71	0.0000	0.0000	453.7926	81.2983	32.4879
ZROD	72	0.0000	0.0000	486.2805	81.2983	32.4879
ZROD	73	0.0000	0.0000	518.7683	81.2983	32.4879
* Radial Detector DRC (1m) Bodies						
ZROD	74	0.0000	0.0000	-168.0212	149.8183	788.7974
ZROD	75	0.0000	0.0000	-168.0212	150.8183	32.8666
ZROD	76	0.0000	0.0000	-135.1546	150.8183	32.8666
ZROD	77	0.0000	0.0000	-102.2881	150.8183	32.8666
ZROD	78	0.0000	0.0000	-69.4215	150.8183	32.8666
ZROD	79	0.0000	0.0000	-36.5550	150.8183	32.8666
ZROD	80	0.0000	0.0000	-3.6884	150.8183	32.8666
ZROD	81	0.0000	0.0000	29.1782	150.8183	32.8666
ZROD	82	0.0000	0.0000	62.0447	150.8183	32.8666
ZROD	83	0.0000	0.0000	94.9113	150.8183	32.8666
ZROD	84	0.0000	0.0000	127.7778	150.8183	32.8666
ZROD	85	0.0000	0.0000	160.6444	150.8183	32.8666
ZROD	86	0.0000	0.0000	193.5109	150.8183	32.8666
ZROD	87	0.0000	0.0000	226.3775	150.8183	32.8666
ZROD	88	0.0000	0.0000	259.2441	150.8183	32.8666
ZROD	89	0.0000	0.0000	292.1106	150.8183	32.8666
ZROD	90	0.0000	0.0000	324.9772	150.8183	32.8666
ZROD	91	0.0000	0.0000	357.8437	150.8183	32.8666
ZROD	92	0.0000	0.0000	390.7103	150.8183	32.8666
ZROD	93	0.0000	0.0000	423.5769	150.8183	32.8666
ZROD	94	0.0000	0.0000	456.4434	150.8183	32.8666
ZROD	95	0.0000	0.0000	489.3100	150.8183	32.8666
ZROD	96	0.0000	0.0000	522.1765	150.8183	32.8666
ZROD	97	0.0000	0.0000	555.0431	150.8183	32.8666
ZROD	98	0.0000	0.0000	587.9096	150.8183	32.8666
* Radial Detector DRD (2m) Bodies						
ZROD	99	0.0000	0.0000	-268.0212	249.8183	988.7974
ZROD	100	0.0000	0.0000	-268.0212	250.8183	41.1999
ZROD	101	0.0000	0.0000	-226.8213	250.8183	41.1999
ZROD	102	0.0000	0.0000	-185.6214	250.8183	41.1999
ZROD	103	0.0000	0.0000	-144.4215	250.8183	41.1999
ZROD	104	0.0000	0.0000	-103.2216	250.8183	41.1999
ZROD	105	0.0000	0.0000	-62.0217	250.8183	41.1999
ZROD	106	0.0000	0.0000	-20.8219	250.8183	41.1999
ZROD	107	0.0000	0.0000	20.3780	250.8183	41.1999
ZROD	108	0.0000	0.0000	61.5779	250.8183	41.1999
ZROD	109	0.0000	0.0000	102.7778	250.8183	41.1999
ZROD	110	0.0000	0.0000	143.9777	250.8183	41.1999
ZROD	111	0.0000	0.0000	185.1776	250.8183	41.1999
ZROD	112	0.0000	0.0000	226.3775	250.8183	41.1999
ZROD	113	0.0000	0.0000	267.5774	250.8183	41.1999
ZROD	114	0.0000	0.0000	308.7773	250.8183	41.1999
ZROD	115	0.0000	0.0000	349.9772	250.8183	41.1999
ZROD	116	0.0000	0.0000	391.1771	250.8183	41.1999
ZROD	117	0.0000	0.0000	432.3770	250.8183	41.1999
ZROD	118	0.0000	0.0000	473.5769	250.8183	41.1999
ZROD	119	0.0000	0.0000	514.7767	250.8183	41.1999
ZROD	120	0.0000	0.0000	555.9766	250.8183	41.1999
ZROD	121	0.0000	0.0000	597.1765	250.8183	41.1999
ZROD	122	0.0000	0.0000	638.3764	250.8183	41.1999
ZROD	123	0.0000	0.0000	679.5763	250.8183	41.1999
* Radial Detector DRE (2m+Convey) Bodies						
ZROD	124	0.0000	0.0000	-269.0212	321.9200	990.7974
ZROD	125	0.0000	0.0000	-268.0212	322.9200	41.1999
ZROD	126	0.0000	0.0000	-226.8213	322.9200	41.1999
ZROD	127	0.0000	0.0000	-185.6214	322.9200	41.1999
ZROD	128	0.0000	0.0000	-144.4215	322.9200	41.1999
ZROD	129	0.0000	0.0000	-103.2216	322.9200	41.1999
ZROD	130	0.0000	0.0000	-62.0217	322.9200	41.1999
ZROD	131	0.0000	0.0000	-20.8219	322.9200	41.1999
ZROD	132	0.0000	0.0000	20.3780	322.9200	41.1999
ZROD	133	0.0000	0.0000	61.5779	322.9200	41.1999
ZROD	134	0.0000	0.0000	102.7778	322.9200	41.1999
ZROD	135	0.0000	0.0000	143.9777	322.9200	41.1999
ZROD	136	0.0000	0.0000	185.1776	322.9200	41.1999
ZROD	137	0.0000	0.0000	226.3775	322.9200	41.1999
ZROD	138	0.0000	0.0000	267.5774	322.9200	41.1999
ZROD	139	0.0000	0.0000	308.7773	322.9200	41.1999
ZROD	140	0.0000	0.0000	349.9772	322.9200	41.1999
ZROD	141	0.0000	0.0000	391.1771	322.9200	41.1999
ZROD	142	0.0000	0.0000	432.3770	322.9200	41.1999
ZROD	143	0.0000	0.0000	473.5769	322.9200	41.1999

Figure 5.3.12-6 Sample Input File for Damaged Fuel Evaluation (Continued)

```

ZROD      144      0.0000      0.0000      514.7767      322.9200      41.1999
ZROD      145      0.0000      0.0000      555.9766      322.9200      41.1999
ZROD      146      0.0000      0.0000      597.1765      322.9200      41.1999
ZROD      147      0.0000      0.0000      638.3764      322.9200      41.1999
ZROD      148      0.0000      0.0000      679.5763      322.9200      41.1999
* Radial Detector DREE (2m+ConveyAzi) Bodies
ZROD      149      0.0000      0.0000      -270.0212      322.9200      992.7974
* Band 1 Bodies
ZSEC      150      0.0000      0.0000      444.5000      322.9200      323.9200      46.1950      0.0000      12.0000
ZSEC      151      0.0000      0.0000      444.5000      322.9200      323.9200      46.1950      12.0000      24.0000
ZSEC      152      0.0000      0.0000      444.5000      322.9200      323.9200      46.1950      24.0000      36.0000
ZSEC      153      0.0000      0.0000      444.5000      322.9200      323.9200      46.1950      36.0000      48.0000
ZSEC      154      0.0000      0.0000      444.5000      322.9200      323.9200      46.1950      48.0000      60.0000
ZSEC      155      0.0000      0.0000      444.5000      322.9200      323.9200      46.1950      60.0000      72.0000
ZSEC      156      0.0000      0.0000      444.5000      322.9200      323.9200      46.1950      72.0000      84.0000
ZSEC      157      0.0000      0.0000      444.5000      322.9200      323.9200      46.1950      84.0000      96.0000
ZSEC      158      0.0000      0.0000      444.5000      322.9200      323.9200      46.1950      96.0000      108.0000
ZSEC      159      0.0000      0.0000      444.5000      322.9200      323.9200      46.1950      108.0000      120.0000
ZSEC      160      0.0000      0.0000      444.5000      322.9200      323.9200      46.1950      120.0000      132.0000
ZSEC      161      0.0000      0.0000      444.5000      322.9200      323.9200      46.1950      132.0000      144.0000
ZSEC      162      0.0000      0.0000      444.5000      322.9200      323.9200      46.1950      144.0000      156.0000
ZSEC      163      0.0000      0.0000      444.5000      322.9200      323.9200      46.1950      156.0000      168.0000
ZSEC      164      0.0000      0.0000      444.5000      322.9200      323.9200      46.1950      168.0000      180.0000
ZSEC      165      0.0000      0.0000      444.5000      322.9200      323.9200      46.1950      180.0000      192.0000
ZSEC      166      0.0000      0.0000      444.5000      322.9200      323.9200      46.1950      192.0000      204.0000
ZSEC      167      0.0000      0.0000      444.5000      322.9200      323.9200      46.1950      204.0000      216.0000
ZSEC      168      0.0000      0.0000      444.5000      322.9200      323.9200      46.1950      216.0000      228.0000
ZSEC      169      0.0000      0.0000      444.5000      322.9200      323.9200      46.1950      228.0000      240.0000
ZSEC      170      0.0000      0.0000      444.5000      322.9200      323.9200      46.1950      240.0000      252.0000
ZSEC      171      0.0000      0.0000      444.5000      322.9200      323.9200      46.1950      252.0000      264.0000
ZSEC      172      0.0000      0.0000      444.5000      322.9200      323.9200      46.1950      264.0000      276.0000
ZSEC      173      0.0000      0.0000      444.5000      322.9200      323.9200      46.1950      276.0000      288.0000
ZSEC      174      0.0000      0.0000      444.5000      322.9200      323.9200      46.1950      288.0000      300.0000
ZSEC      175      0.0000      0.0000      444.5000      322.9200      323.9200      46.1950      300.0000      312.0000
ZSEC      176      0.0000      0.0000      444.5000      322.9200      323.9200      46.1950      312.0000      324.0000
ZSEC      177      0.0000      0.0000      444.5000      322.9200      323.9200      46.1950      324.0000      336.0000
ZSEC      178      0.0000      0.0000      444.5000      322.9200      323.9200      46.1950      336.0000      348.0000
ZSEC      179      0.0000      0.0000      444.5000      322.9200      323.9200      46.1950      348.0000      360.0000
* World
ZROD      180      0.0000      0.0000      -320.0212      372.9200      1092.7974
* External Void
ZROD      181      0.0000      0.0000      -370.0212      422.9200      1192.7974

ZONES
/LWTCask/ P1      +1
* Detector DRA (Surface)
/DRA01/ MO      +2      -1
/DRA02/ MO      +3      -1
/DRA03/ MO      +4      -1
/DRA04/ MO      +5      -1
/DRA05/ MO      +6      -1
/DRA06/ MO      +7      -1
/DRA07/ MO      +8      -1
/DRA08/ MO      +9      -1
/DRA09/ MO      +10     -1
/DRA10/ MO      +11     -1
/DRA11/ MO      +12     -1
/DRA12/ MO      +13     -1
/DRA13/ MO      +14     -1
/DRA14/ MO      +15     -1
/DRA15/ MO      +16     -1
/DRA16/ MO      +17     -1
/DRA17/ MO      +18     -1
/DRA18/ MO      +19     -1
/DRA19/ MO      +20     -1
/DRA20/ MO      +21     -1
/Void/ MO      +22     -1
          -2      -3      -4      -5      -6      -7
          -8      -9      -10     -11     -12     -13
          -14     -15     -16     -17     -18     -19
          -20     -21

* Detector DRAA (SurfaceAzi)
/DRAA0101/ MO      +23
/DRAA0102/ MO      +24
/DRAA0103/ MO      +25
/DRAA0104/ MO      +26
/DRAA0105/ MO      +27
/DRAA0106/ MO      +28
/DRAA0107/ MO      +29
/DRAA0108/ MO      +30
/DRAA0109/ MO      +31
/DRAA0110/ MO      +32
/DRAA0111/ MO      +33
/DRAA0112/ MO      +34
/DRAA0113/ MO      +35
/DRAA0114/ MO      +36
/DRAA0115/ MO      +37
/DRAA0116/ MO      +38
/DRAA0117/ MO      +39
/DRAA0118/ MO      +40
/DRAA0119/ MO      +41
/DRAA0120/ MO      +42
/DRAA0121/ MO      +43
/DRAA0122/ MO      +44

```

Figure 5.3.12-6 Sample Input File for Damaged Fuel Evaluation (Continued)

```

/DRAA0123/      M0      +45
/DRAA0124/      M0      +46
/DRAA0125/      M0      +47
/DRAA0126/      M0      +48
/DRAA0127/      M0      +49
/DRAA0128/      M0      +50
/DRAA0129/      M0      +51
/DRAA0130/      M0      +52
/Void/          M0      +53      -22
                -23      -24      -25      -26      -27      -28
                -29      -30      -31      -32      -33      -34
                -35      -36      -37      -38      -39      -40
                -41      -42      -43      -44      -45      -46
                -47      -48      -49      -50      -51      -52

* Detector DRB (1ft)
/DRB01/         M0      +54      -53
/DRB02/         M0      +55      -53
/DRB03/         M0      +56      -53
/DRB04/         M0      +57      -53
/DRB05/         M0      +58      -53
/DRB06/         M0      +59      -53
/DRB07/         M0      +60      -53
/DRB08/         M0      +61      -53
/DRB09/         M0      +62      -53
/DRB10/         M0      +63      -53
/DRB11/         M0      +64      -53
/DRB12/         M0      +65      -53
/DRB13/         M0      +66      -53
/DRB14/         M0      +67      -53
/DRB15/         M0      +68      -53
/DRB16/         M0      +69      -53
/DRB17/         M0      +70      -53
/DRB18/         M0      +71      -53
/DRB19/         M0      +72      -53
/DRB20/         M0      +73      -53
/Void/          M0      +74      -53
                -54      -55      -56      -57      -58      -59
                -60      -61      -62      -63      -64      -65
                -66      -67      -68      -69      -70      -71
                -72      -73

* Detector DRC (1m)
/DRC01/         M0      +75      -74
/DRC02/         M0      +76      -74
/DRC03/         M0      +77      -74
/DRC04/         M0      +78      -74
/DRC05/         M0      +79      -74
/DRC06/         M0      +80      -74
/DRC07/         M0      +81      -74
/DRC08/         M0      +82      -74
/DRC09/         M0      +83      -74
/DRC10/         M0      +84      -74
/DRC11/         M0      +85      -74
/DRC12/         M0      +86      -74
/DRC13/         M0      +87      -74
/DRC14/         M0      +88      -74
/DRC15/         M0      +89      -74
/DRC16/         M0      +90      -74
/DRC17/         M0      +91      -74
/DRC18/         M0      +92      -74
/DRC19/         M0      +93      -74
/DRC20/         M0      +94      -74
/DRC21/         M0      +95      -74
/DRC22/         M0      +96      -74
/DRC23/         M0      +97      -74
/DRC24/         M0      +98      -74
/Void/          M0      +99      -74
                -75      -76      -77      -78      -79      -80
                -81      -82      -83      -84      -85      -86
                -87      -88      -89      -90      -91      -92
                -93      -94      -95      -96      -97      -98

* Detector DRD (2m)
/DRD01/         M0      +100     -99
/DRD02/         M0      +101     -99
/DRD03/         M0      +102     -99
/DRD04/         M0      +103     -99
/DRD05/         M0      +104     -99
/DRD06/         M0      +105     -99
/DRD07/         M0      +106     -99
/DRD08/         M0      +107     -99
/DRD09/         M0      +108     -99
/DRD10/         M0      +109     -99
/DRD11/         M0      +110     -99
/DRD12/         M0      +111     -99
/DRD13/         M0      +112     -99
/DRD14/         M0      +113     -99
/DRD15/         M0      +114     -99
/DRD16/         M0      +115     -99
/DRD17/         M0      +116     -99
/DRD18/         M0      +117     -99
/DRD19/         M0      +118     -99
/DRD20/         M0      +119     -99
/DRD21/         M0      +120     -99
/DRD22/         M0      +121     -99
/DRD23/         M0      +122     -99

```

Figure 5.3.12-6 Sample Input File for Damaged Fuel Evaluation (Continued)

```

/DRD24/ M0 +123 -99
/Void/ M0 +124 -99
          -100 -101 -102 -103 -104 -105
          -106 -107 -108 -109 -110 -111
          -112 -113 -114 -115 -116 -117
          -118 -119 -120 -121 -122 -123

* Detector DRE (2m+Convey)
/DRE01/ M0 +125 -124
/DRE02/ M0 +126 -124
/DRE03/ M0 +127 -124
/DRE04/ M0 +128 -124
/DRE05/ M0 +129 -124
/DRE06/ M0 +130 -124
/DRE07/ M0 +131 -124
/DRE08/ M0 +132 -124
/DRE09/ M0 +133 -124
/DRE10/ M0 +134 -124
/DRE11/ M0 +135 -124
/DRE12/ M0 +136 -124
/DRE13/ M0 +137 -124
/DRE14/ M0 +138 -124
/DRE15/ M0 +139 -124
/DRE16/ M0 +140 -124
/DRE17/ M0 +141 -124
/DRE18/ M0 +142 -124
/DRE19/ M0 +143 -124
/DRE20/ M0 +144 -124
/DRE21/ M0 +145 -124
/DRE22/ M0 +146 -124
/DRE23/ M0 +147 -124
/DRE24/ M0 +148 -124
/Void/ M0 +149 -124
          -125 -126 -127 -128 -129 -130
          -131 -132 -133 -134 -135 -136
          -137 -138 -139 -140 -141 -142
          -143 -144 -145 -146 -147 -148

* Detector DRE (2m+ConveyAzi)
/DRE0101/ M0 +150
/DRE0102/ M0 +151
/DRE0103/ M0 +152
/DRE0104/ M0 +153
/DRE0105/ M0 +154
/DRE0106/ M0 +155
/DRE0107/ M0 +156
/DRE0108/ M0 +157
/DRE0109/ M0 +158
/DRE0110/ M0 +159
/DRE0111/ M0 +160
/DRE0112/ M0 +161
/DRE0113/ M0 +162
/DRE0114/ M0 +163
/DRE0115/ M0 +164
/DRE0116/ M0 +165
/DRE0117/ M0 +166
/DRE0118/ M0 +167
/DRE0119/ M0 +168
/DRE0120/ M0 +169
/DRE0121/ M0 +170
/DRE0122/ M0 +171
/DRE0123/ M0 +172
/DRE0124/ M0 +173
/DRE0125/ M0 +174
/DRE0126/ M0 +175
/DRE0127/ M0 +176
/DRE0128/ M0 +177
/DRE0129/ M0 +178
/DRE0130/ M0 +179
/Void/ M0 +180 -149
          -150 -151 -152 -153 -154 -155
          -156 -157 -158 -159 -160 -161
          -162 -163 -164 -165 -166 -167
          -168 -169 -170 -171 -172 -173
          -174 -175 -176 -177 -178 -179

/ExtVoid/ M-2000 +181 -180
Volumes
          1.0 20*9.3077E+03 1.0 30*3.8903E+02 1.0 20*1.6493E+04
          1.0 24*3.1042E+04 1.0 24*6.4799E+04 1.0 24*8.3464E+04
          1.0 30*3.1291E+03 1.0 1.0

end

*
* Unit 5 Splitting Geometry for Radial Detectors - Neutron
*
begin splitting geometry
r 18 fill 0.0000
n 5 6.3939
n 1 12.1809
n 1 16.9863
n 1 18.9103
n 2 33.3271
n 1 36.5189
n 5 49.2189
n 1 49.8183
n 1 50.8183

```

Figure 5.3.12-6 Sample Input File for Damaged Fuel Evaluation (Continued)

```

z 36 fill -73.0212
      n 1 -68.0212
      n 2 -26.6700
      n 2 -17.7800
      n 2 -10.1600
      n 2 0.0000
      n 1 7.1120
      n 1 10.9220
      n 16 400.8220
      n 3 452.1200
      n 4 480.6950
      n 1 520.7762
      n 1 525.7762
end

*
* Unit 6 - Source Geometry - Damaged Rods
*
begin source geometry
x 1 -4.5212 4.5212
y 1 -4.5212 4.5212
z 1 398.9170 431.9270
end

*
* Unit 7
*
begin energy data
neutron
thermal treatment none
importance standard 28 groups
scoring as importance
simple source histogram weighting automatic
end

*
* Unit 8 Importance Map - Radial
*
begin importance map
calculate
targets 20
part 7
zones
  2 3 4 5 6
  7 8 9 10 11
  12 13 14 15 16
  17 18 19 20 21
strengths
  1.0E+00 1.0E+00 1.0E+00 1.0E+00 1.0E+00
  1.0E+00 1.0E+00 1.0E+00 1.0E+00 1.0E+00
  1.0E+00 1.0E+00 1.0E+01 1.0E+01 1.0E+02
  1.0E+02 1.0E+02 1.0E+02 1.0E+02 1.0E+02
defer mixing
void density 0.10
track
! coupled source
! write gamma importances to 32
! write unformatted file to 31
! use method d
end

*
* Unit 9 Scoring Data - Radial
*
begin scoring data
flux
part 7
from 2 to 21 ! DRA
from 23 to 52 ! DRAA
from 54 to 73 ! DRB
from 75 to 98 ! DRC
from 100 to 123 ! DRD
from 125 to 148 ! DRE
from 150 to 179 ! DREE
responses sos ditto
contributions to responses ditto
! score distribution for response
! weight distribution total
end

*
* Unit 10 Response Data
*
begin response data
* Scale to mrem/hr
/ncrp38 - ansi ans-6.1.1-1977 neutron flux-dose conversion factors - mcnr table h.1 - mrem/
function pairs
  2.0000E+01 2.2700E-01
  1.9299E+01 2.2502E-01
  1.8623E+01 2.2307E-01
  1.7970E+01 2.2112E-01
  1.7341E+01 2.1920E-01
  1.6733E+01 2.1729E-01
  1.6147E+01 2.1540E-01

```

Figure 5.3.12-6 Sample Input File for Damaged Fuel Evaluation (Continued)

1.5581E+01	2.1353E-01
1.5035E+01	2.1167E-01
1.4508E+01	2.0983E-01
1.4000E+01	2.0800E-01
1.3537E+01	2.0090E-01
1.3089E+01	1.9405E-01
1.2656E+01	1.8743E-01
1.2237E+01	1.8104E-01
1.1832E+01	1.7486E-01
1.1441E+01	1.6889E-01
1.1062E+01	1.6313E-01
1.0696E+01	1.5757E-01
1.0342E+01	1.5219E-01
1.0000E+01	1.4700E-01
7.0000E+00	1.4700E-01
6.7684E+00	1.4788E-01
6.5444E+00	1.4876E-01
6.3279E+00	1.4964E-01
6.1185E+00	1.5054E-01
5.9161E+00	1.5143E-01
5.7203E+00	1.5234E-01
5.5311E+00	1.5324E-01
5.3481E+00	1.5416E-01
5.1711E+00	1.5508E-01
5.0000E+00	1.5600E-01
4.6652E+00	1.5258E-01
4.3528E+00	1.4924E-01
4.0613E+00	1.4597E-01
3.7893E+00	1.4277E-01
3.5355E+00	1.3964E-01
3.2988E+00	1.3658E-01
3.0779E+00	1.3359E-01
2.8717E+00	1.3066E-01
2.6794E+00	1.2780E-01
2.5000E+00	1.2500E-01
2.2811E+00	1.2568E-01
2.0814E+00	1.2637E-01
1.8991E+00	1.2706E-01
1.7329E+00	1.2775E-01
1.5811E+00	1.2845E-01
1.4427E+00	1.2915E-01
1.3164E+00	1.2986E-01
1.2011E+00	1.3057E-01
1.0960E+00	1.3128E-01
1.0000E+00	1.3200E-01
9.3303E-01	1.2740E-01
8.7055E-01	1.2296E-01
8.1225E-01	1.1868E-01
7.5786E-01	1.1455E-01
7.0711E-01	1.1056E-01
6.5975E-01	1.0671E-01
6.1557E-01	1.0299E-01
5.7435E-01	9.9404E-02
5.3589E-01	9.5942E-02
5.0000E-01	9.2600E-02
4.2567E-01	8.0093E-02
3.6239E-01	6.9276E-02
3.0852E-01	5.9919E-02
2.6265E-01	5.1826E-02
2.2361E-01	4.4827E-02
1.9037E-01	3.8772E-02
1.6207E-01	3.3536E-02
1.3797E-01	2.9006E-02
1.1746E-01	2.5089E-02
1.0000E-01	2.1700E-02
7.9433E-02	1.8112E-02
6.3096E-02	1.5117E-02
5.0119E-02	1.2617E-02
3.9811E-02	1.0531E-02
3.1623E-02	8.7893E-03
2.5119E-02	7.3359E-03
1.9953E-02	6.1228E-03
1.5849E-02	5.1104E-03
1.2589E-02	4.2653E-03
1.0000E-02	3.5600E-03
7.9433E-03	3.5795E-03
6.3096E-03	3.5991E-03
5.0119E-03	3.6189E-03
3.9811E-03	3.6387E-03
3.1623E-03	3.6586E-03
2.5119E-03	3.6787E-03
1.9953E-03	3.6988E-03
1.5849E-03	3.7191E-03
1.2589E-03	3.7395E-03
1.0000E-03	3.7600E-03
7.9433E-04	3.8000E-03
6.3096E-04	3.8405E-03
5.0119E-04	3.8814E-03
3.9811E-04	3.9227E-03
3.1623E-04	3.9644E-03
2.5119E-04	4.0066E-03
1.9953E-04	4.0493E-03
1.5849E-04	4.0924E-03
1.2589E-04	4.1360E-03

Figure 5.3.12-6 Sample Input File for Damaged Fuel Evaluation (Continued)

```

1.0000E-04      4.1800E-03
7.9433E-05      4.2147E-03
6.3096E-05      4.2496E-03
5.0119E-05      4.2849E-03
3.9811E-05      4.3204E-03
3.1623E-05      4.3563E-03
2.5119E-05      4.3924E-03
1.9953E-05      4.4289E-03
1.5849E-05      4.4656E-03
1.2589E-05      4.5026E-03
1.0000E-05      4.5400E-03
7.9433E-06      4.5319E-03
6.3096E-06      4.5239E-03
5.0119E-06      4.5159E-03
3.9811E-06      4.5078E-03
3.1623E-06      4.4998E-03
2.5119E-06      4.4918E-03
1.9953E-06      4.4839E-03
1.5849E-06      4.4759E-03
1.2589E-06      4.4679E-03
1.0000E-06      4.4600E-03
7.9433E-07      4.3739E-03
6.3096E-07      4.2894E-03
5.0119E-07      4.2066E-03
3.9811E-07      4.1254E-03
3.1623E-07      4.0458E-03
2.5119E-07      3.9677E-03
1.9953E-07      3.8910E-03
1.5849E-07      3.8159E-03
1.2589E-07      3.7423E-03
1.0000E-07      3.6700E-03
2.5000E-08      3.6700E-03

end

*
* Unit 13 Hole Data
*
*begin hole data
* < hole
*end

*
* Unit 15 Source Strength - Fuel Neutron
*
* DMS BWR 7x7 ~ 80 GWD/MTU - 210 Day - Fuel Neutron - Direct
begin source strength
component      1.0638E+00      ! Subcritical multiplication factor
component      4.3023E-05      ! 1/rodeFuelParamActiveVolume
component      5.0000E-01      ! volFrac fuel in damaged src region
component      1.3069E+00      ! (Avg Src Rate)/(Src at Avg BU)
component      x      1.0
component      y      1.0
component      z      1.0
component      energy
0.0000E+00      1.3440E+05      5.6010E+05      1.8600E+06      5.8350E+06      1.5680E+07
2.7070E+07      9.0440E+07      1.5440E+08      2.0770E+08      4.8880E+08      7.6690E+08
2.0050E+08      6.9560E+07      8.5080E+02      0.0000E+00      0.0000E+00      0.0000E+00
0.0000E+00      0.0000E+00      0.0000E+00      0.0000E+00      0.0000E+00      0.0000E+00
0.0000E+00      0.0000E+00      0.0000E+00      0.0000E+00      0.0000E+00      0.0000E+00

end

*
* Unit 16 Simple Source Weights
*
*begin source weights
*
*end

*
* Unit 31 Tabular Output
*
begin tabular output
/Case lwtNrmRadFn_b7Dmg_80b40e210d - Det DRA - Surface - Response/
response      interim
number      some      1
region      from      37      to      56
output to file      also
/Case lwtNrmRadFn_b7Dmg_80b40e210d - Det DRB - 1ft - Response/
response
number      some      1
region      from      89      to      108
output to file      also
/Case lwtNrmRadFn_b7Dmg_80b40e210d - Det DRC - 1m - Response/
response
number      some      1
region      from      110      to      133
output to file      also
/Case lwtNrmRadFn_b7Dmg_80b40e210d - Det DRE - 2m+Convey - Response/
response      interim
number      some      1
region      from      160      to      183
output to file      also

end

```

Figure 5.3.12-6 Sample Input File for Damaged Fuel Evaluation (Continued)

```
*
* Unit 32 Material Specification
*
begin material specification
type dice
normalise
nmixtures 2
atoms mixture 1
  h 6.6667E-01
  o 3.3333E-01
weight mixture 2
  u235 3.5260E-02
  u238 8.4624E-01
  o 1.1850E-01
*
* Materials List - Common Materials - v1.2
*
nmaterials 10
volume
material 1 ! Water
  mixture 1 density 0.9982 prop 1.0000 ! mixH2O
atoms
material 2 ! Water/Glycol
  density 0 ! 0 means atom/b-cm
  h 5.9880E-02
  c 1.0701E-02
  o 2.4589E-02
volume
material 3 ! Aluminum
  aluminium prop 1.0000
volume
material 4 ! Lead
  pb density 11.3440 prop 1.0000
volume
material 5 ! Stainless Steel 304
  stainless 3041 steel density 7.9200 prop 1.0000
volume
material 6 ! Intact fuel rods
  mixture 2 density 10.4120 prop 3.7198E-01 ! UO2 mixture at 4%
  zircalloy density 6.5500 prop 1.1922E-01 ! Tube, clad
  stainless 3041 steel density 7.9200 prop 1.1444E-01 ! Insert tubes
  void prop 3.9436E-01 ! Interstitial, inside tubes
volume
material 7 ! Damaged fuel rods
  mixture 2 density 10.4120 prop 5.0000E-01 ! UO2 mixture at 4%
  void prop 5.0000E-01 ! Void
volume
material 8 ! Intact/damaged mixture
  mixture 2 density 10.4120 prop 3.7198E-01 ! UO2 mixture at 4%
  zircalloy density 6.5500 prop 1.1922E-01 ! Tube, clad
  stainless 3041 steel density 7.9200 prop 1.1444E-01 ! Insert tubes
  void prop 1.2294E-02 ! Pellet/clad gap
  mixture 2 density 10.4120 prop 1.9103E-01 ! UO2 mixture at 4%
  void prop 1.9103E-01 ! Void
volume
material 9 ! Aluminum
  aluminium density 0.4997 prop 1.0000
volume
material 10 ! Upper Plenum (rods model)
  stainless 3041 steel density 7.9200 prop 4.7048E-02 ! Springs
  zircalloy density 6.5500 prop 1.1922E-01 ! Tube, clad
  void prop 8.3373E-01
end
```


Table 5.3.12-1 PWR Rods 80,000 MWd/MTU, 150 Day Cool Time Source Terms in MCBEND Format

Group	Neutron [n/sec/assy]	Gamma [γ/sec/assy]
1	0.000E+00	0.0000E+00
2	2.883E+05	1.2008E+05
3	1.201E+06	2.3224E+06
4	3.989E+06	1.0938E+07
5	1.251E+07	5.5757E+07
6	3.363E+07	1.3893E+08
7	5.807E+07	4.2785E+11
8	1.939E+08	3.8050E+12
9	3.327E+08	1.5052E+14
10	4.501E+08	5.0107E+13
11	1.054E+09	1.7429E+14
12	1.645E+09	5.9067E+14
13	4.302E+08	7.9464E+14
14	1.492E+08	4.2613E+15
15	2.040E+03	3.1093E+16
16	0.000E+00	1.4248E+16
17	0.000E+00	1.4613E+15
18	0.000E+00	1.9163E+15
19	0.000E+00	7.6165E+15
20	0.000E+00	7.6971E+15
21	0.000E+00	1.5136E+16
22	0.000E+00	1.1383E+16
23	0.000E+00	
24	0.000E+00	
25	0.000E+00	
26	0.000E+00	
27	0.000E+00	
28	0.000E+00	
Total	4.365E+09	9.6575E+16

Table 5.3.12-2 BWR 7x7 Rods 80,000 MWd/MTU, 210 Day Cool Time Source Terms
in MCBEND Format

Group	Neutron [n/sec/assy]	Gamma [γ/sec/assy]
1	0.000E+00	0.0000E+00
2	1.344E+05	5.5172E+04
3	5.601E+05	1.0671E+06
4	1.860E+06	5.0255E+06
5	5.835E+06	2.5617E+07
6	1.568E+07	6.3827E+07
7	2.707E+07	1.2463E+11
8	9.044E+07	1.0115E+12
9	1.544E+08	3.9067E+13
10	2.077E+08	1.3527E+13
11	4.888E+08	4.8042E+13
12	7.669E+08	2.1590E+14
13	2.005E+08	2.5366E+14
14	6.956E+07	1.5077E+15
15	8.508E+02	8.0050E+15
16	0.000E+00	4.2354E+15
17	0.000E+00	4.0998E+14
18	0.000E+00	5.3950E+14
19	0.000E+00	2.0315E+15
20	0.000E+00	2.1700E+15
21	0.000E+00	4.2503E+15
22	0.000E+00	3.1923E+15
23	0.000E+00	
24	0.000E+00	
25	0.000E+00	
26	0.000E+00	
27	0.000E+00	
28	0.000E+00	
Total	2.029E+09	2.6913E+16

Table 5.3.12-3 BWR 8x8 Rods 80,000 MWd/MTU, 150 Day Cool Time Source Terms in MCBEND Format

Group	Neutron [n/sec/assy]	Gamma [γ/sec/assy]
1	0.000E+00	0.0000E+00
2	1.265E+05	5.2227E+04
3	5.270E+05	1.0101E+06
4	1.750E+06	4.7573E+06
5	5.489E+06	2.4251E+07
6	1.475E+07	6.0423E+07
7	2.547E+07	1.3401E+11
8	8.507E+07	1.1792E+12
9	1.456E+08	4.3500E+13
10	1.965E+08	1.5430E+13
11	4.610E+08	5.4550E+13
12	7.216E+08	2.1638E+14
13	1.887E+08	2.6602E+14
14	6.544E+07	1.5238E+15
15	8.372E+02	1.0031E+16
16	0.000E+00	4.7704E+15
17	0.000E+00	4.4625E+14
18	0.000E+00	5.8927E+14
19	0.000E+00	2.3105E+15
20	0.000E+00	2.3645E+15
21	0.000E+00	4.6764E+15
22	0.000E+00	3.5252E+15
23	0.000E+00	
24	0.000E+00	
25	0.000E+00	
26	0.000E+00	
27	0.000E+00	
28	0.000E+00	
Total	1.912E+09	3.0834E+16

Table 5.3.12-4 Fuel Region Homogenization for PWR Fuel Rods

Region	Material Area [cm ²]			
	UO ₂	Zirconium Alloy	SS304	Void
Fuel	1.8341E+01	–	–	–
Gap	–	–	–	7.4758E-01
Clad	–	5.4532E+00	–	–
Insert Void	–	–	–	2.5976E+01
Insert Tubes	–	–	9.3569E+00	–
Interstitial	–	–	–	2.1890E+01
Total	1.8341E+01	5.4532E+00	9.3569E+00	4.8614E+01
Vol Frac	2.2432E-01	6.6693E-02	1.1444E-01	5.9455E-01

Table 5.3.12-5 Fuel Region Homogenization for BWR 7×7 Fuel Rods

Region	Material Area [cm ²]			
	UO ₂	Zirconium Alloy	SS304	Void
Fuel	3.0415E+01	–	–	–
Gap	–	–	–	1.0052E+00
Clad	–	9.7483E+00	–	–
Insert Void	–	–	–	9.3491E+00
Insert Tubes	–	–	9.3569E+00	–
Interstitial	–	–	–	2.1890E+01
Total	3.0415E+01	9.7483E+00	9.3569E+00	3.2245E+01
Vol Frac	3.7198E-01	1.1922E-01	1.1444E-01	3.9436E-01

Table 5.3.12-6 Region Homogenization for BWR 8x8 Fuel Rods

Region	Material Area [cm ²]			
	UO ₂	Zirconium Alloy	SS304	Void
Fuel	2.2484E+01	--	--	--
Gap	--	--	--	6.7313E-01
Clad	--	8.0151E+00	--	--
Insert Void	--	--	--	1.9345E+01
Insert Tubes	--	--	9.3569E+00	--
Interstitial	--	--	--	2.1890E+01
Total	2.2484E+01	8.0151E+00	9.3569E+00	4.1909E+01
Vol Frac	2.7499E-01	9.8026E-02	1.1444E-01	5.1255E-01

Table 5.3.12-7 Intact/Damaged Fuel Mixture Composition Determinations

Parameter	PWR	BWR 7x7	BWR 8x8
Damaged Volume [cm ³]	1.3495E+03	1.3495E+03	1.3495E+03
14 Rod Volume [cm ³]	4.0047E+03	6.6410E+03	4.9093E+03
# Rods in Top	4.7	2.8	3.8
# Rods in Mixture	9.3	11.2	10.2
Mixture Volume [cm ³]	2.6552E+03	5.2914E+03	3.5598E+03
Void Area for Mixture [cm ²]	4.7866E+01	3.1239E+01	4.1236E+01
Mixture Height [cm]	110.9438	338.7657	172.6549

Table 5.3.12-8 Fuel Region Homogenized Material Description

Material	Element	Number Density [atom/b-cm]		
		PWR	BWR 7x7	BWR 8x8
Intact Fuel	U	5.21106E-03	8.64130E-03	6.38813E-03
	O	1.04340E-02	1.73044E-02	1.27948E-02
	ZR	2.82841E-03	5.05606E-03	4.15721E-03
	SN	3.32411E-05	5.94217E-05	4.88579E-05
	FE	7.24185E-03	7.24929E-03	7.24626E-03
	CR	1.89459E-03	1.89858E-03	1.89696E-03
	NI	7.44414E-04	7.44769E-04	7.44623E-04
	HF	1.47386E-07	2.63468E-07	2.16629E-07
Damaged Fuel	U	2.32306E-02	2.32306E-02	2.32306E-02
	O	4.64408E-02	4.64408E-02	4.64408E-02
Intact/Damaged Mixture	U	1.69811E-02	1.61676E-02	1.63750E-02
	O	3.39706E-02	3.23574E-02	3.27679E-02
	ZR	3.99892E-03	6.25005E-03	5.55893E-03
	SN	4.69975E-05	7.34541E-05	6.53316E-05
	FE	1.02388E-02	8.96120E-03	9.68953E-03
	CR	2.67865E-03	2.34693E-03	2.53657E-03
	NI	1.05248E-03	9.20646E-04	9.95692E-04
	HF	2.08380E-07	3.25685E-07	2.89671E-07

Table 5.3.12-9 Maximum Radial Dose Rates for Damaged PWR and BWR Fuel Rods

Fuel Type	Dose Rate [mrem/hr]				
	Normal Surface	Normal 1 foot	Normal 1 meter	Normal 2 meter	Accident 1 meter
PWR	321.2	126.6	36.5	9.8	223.5
BWR 7×7	324.0	123.4	34.3	9.6	394.0
BWR 8×8	336.9	128.4	35.2	9.6	304.2

Table 5.3.12-10 Maximum Axial Dose Rates for Damaged PWR and BWR Fuel Rods

Fuel Type	Dose Rate [mrem/hr]			
	Normal – Surface		Accident – Surface	
	Top	Bottom	Top	Bottom
PWR	27.5	4.9	192.1	34.7
BWR 7×7	28.6	4.7	196.2	32.3
BWR 8×8	29.4	3.6	203.1	24.5

5.3.13 TPBAR Shielding Evaluation

The content condition of up to 300 production TPBARs (of which two can be prefailed) loaded into a consolidation canister and cooled a minimum of 30 days is analyzed for transport in the NAC-LWT cask. A second NAC-LWT content condition is evaluated and is shown to be conservatively bounded by the reported results for the 300 TPBARs. The second content condition is for the transport of up to 55 segmented TPBARs and associated segmentation debris from PIE loaded in a welded waste container and cooled a minimum of 90 days.

A production TPBAR source spectrum is calculated using the activity inventory for a cool time of 30 days from reactor discharge. Source spectra are generated using ORIGEN 2.1 with the PWRU cross-section library. Reactor operating conditions used to generate the activity inventory are summarized in Table 5.3.13-6 (also see Chapter 1, Appendix 1-C). The activity inventory is input into ORIGEN-S, which outputs a gamma spectrum in the 22-group spectrum employed in the analysis.

Table 5.3.13-1 (also see Chapter 1, Appendix 1-C) gives the activity inventory for a single TPBAR at 30 days cool time. Using the table, an ORIGEN-S input is created in order to produce a gamma spectrum in the employed 22-group format. ORIGEN-S input is shown in Figure 5.3.13-1; the resulting spectrum is summarized in Table 5.3.13-2. In the MCNP analysis, a uniform peaking factor of 1.15 is applied over the entire TPBAR length to bound the actual discharge irradiation profile. The application of the peaking factor results in a source of $7.683\text{E}+15$ photons/sec being employed in the analysis.

The geometric description of the TPBARs is based on the consolidation canister cavity width of 8.15 inches, the modeled TPBAR height of 154 inches, and a TPBAR mass of 1.25 kg/rod. Based on these dimensions, a homogenized source region is modeled, with a material density of 2.24 g/cm^3 . The material description in MCNP is based on the element masses given in Table 5.3.13-3 (also see Chapter 1, Appendix 1-C), which also summarizes the resultant number densities of each element. Table 5.3.13-3 contains trace elements contained in the TPBAR components, such as uranium in the Zircaloy clad. The listed TPBAR mass and activation source represent a bounding source description and is larger than the structural bounding weight of 1.2 kg/rod.

The NAC-LWT cavity model explicitly considers the axial position of the TPBARs and the consolidation canister as determined by the basket upper and lower fittings and the TPBAR spacer. The TPBARs are modeled at their highest position in the cask cavity, which is the difference of the cavity height, TPBAR height, and spacer height. The resultant axial offset

positions the rods 11.87 inches from the cavity bottom and 12.13 inches from the cavity top. For conservatism, the cavity model considers only the extents of the upper and lower basket fittings and the basket spacer; these regions are modeled as voids. Radial shielding in the cavity is provided by the 0.135-inch thick consolidation canister and the aluminum basket shell.

MCNP input for the normal conditions model with radial biasing is shown in Figure 5.3.13-2; sketches of key radial and axial dimensions are shown in Figure 5.3.13-3 and Figure 5.3.13-4, respectively. In the accident analysis, the neutron shield and shell are conservatively modeled as void. Material descriptions of the NAC-LWT constituent volumes are summarized in Table 5.3.13-4.

Normal and hypothetical accident condition radial and axial maximum and average dose rates for a payload of 300 production TPBARs at 30 days cool time are shown in Table 5.3.13-5. Dose rates are below regulatory limits at the surface and 2 meters from the truck bed. The transport index, based on the normal conditions dose rate at 1 meter from the package, is 22. Significant margin exists to the 1000 mrem/hr 1 meter hypothetical accident condition dose rate limit.

The significantly smaller source term of 55 segmented TPBARs cooled for a minimum of 90 days is bounded by the source term of 300 TPBARs cooled 30 days and the associated dose analysis reported herein. The 55 segmented TPBAR dose rates will be significantly below the regulatory limits for normal conditions of transport and hypothetical accident conditions. The transport index applied to this content is 22.

Figure 5.3.13-5 through Figure 5.3.13-7 show radial dose rate profiles under normal and hypothetical accident conditions.

Dose conversion and quality factors used in the analysis are those from ANSI/ANS-6.1.1-1977.

The three-dimensional Monte Carlo code MCNP (version 4C) is employed in the shielding analysis (ORNL). Significant validation literature is available on MCNP and it represents an industry standard tool for spent fuel cask evaluations. Confirmatory calculations against other validated shielding codes (SCALE and MCBEND) on NAC casks have further validated the use of MCNP for shielding evaluations of the NAC-LWT.

Figure 5.3.13-1 ORIGEN-S Input for TPBARs at 30 Days Cool Time

```
#ORIGENS
0$$ A11 71 E T
DECAY CASE
3$$ 21 1 1 28 A16 4 A33 22 E T
35$$ 0 T
54$$ A8 1 E
56$$ A2 1 A6 1 A10 0 A13 84 A14 5 A15 3 E
57** 0 E T
TPBAR Spectrum Generation
Cool Time of 30 Days
60** 1.E-20
61** F1E-20
65$$
'GRAM-ATOMS GRAMS CURIES WATTS-ALL WATTS-GAMMA
21R1
21R1
21R1
81$$ 2 0 26 1 E
82$$ 2
83** 1.40E+7 1.20E+7 1.00E+7 8.00E+6 6.50E+6
5.00E+6 4.00E+6 3.00E+6 2.50E+6 2.00E+6
1.66E+6 1.44E+6 1.22E+6 1.00E+6 8.00E+5
6.00E+5 4.00E+5 3.00E+5 2.00E+5 1.00E+5
5.00E+4 2.00E+4 1.00E+4
84** 1.460E+7 1.350E+7 1.250E+7 1.125E+7 1.000E+7
8.500E+6 7.000E+6 6.070E+6 4.720E+6 3.680E+6
2.870E+6 1.740E+6 6.000E+5 3.900E+5 1.100E+5
6.740E+4 2.480E+4 9.120E+3 2.950E+3 9.610E+2
3.540E+2 1.660E+2 4.810E+1 1.600E+1 4.000E+0
1.500E+0 5.500E-1 7.090E-2 0.000E+0
73$$ 10030 60140 110240 150320 160350 180370 180390
190420 200410 200450 200470 210460 210470 240510
250540 260550 260590 270580 270600 280590 280630
280660 290640 290660 300650 330760 340750 350820
380890 390891 390900 390910 400890 400930 400950
400970 410920 410931 410940 410950 410951 410960
410970 410971 420930 420990 430990 441030 481150
481151 491131 491140 491141 501130 501171 501191
501210 501211 501230 501250 511220 511240 511250
511260 521231 521251 551310 561310 561330 561331
561351 571400 711770 721750 721810 731820 731830
741810 741850 741870 741880 751860 751880 761910
74** 1.15E+04 1.42E-03 1.65E-13 3.38E-01 1.15E-02 2.40E-01 9.49E-03
8.34E-12 7.51E-05 2.84E-01 4.66E-06 6.78E-03 1.76E-05 5.44E+02
3.98E+01 2.12E+02 1.39E+01 2.15E+02 3.57E+01 1.68E-01 2.29E+01
1.38E-07 1.04E-16 1.38E-07 3.87E-03 4.25E-07 7.77E-01 2.25E-08
5.48E-02 4.18E-06 1.30E-03 1.46E-01 4.18E-06 1.13E-04 5.12E+01
1.65E-11 6.34E-02 4.02E-06 4.76E-04 6.50E+01 3.80E-01 9.19E-11
1.78E-11 1.57E-11 1.04E-03 5.11E-02 4.36E-05 2.14E-03 2.27E-07
1.28E-04 1.14E+00 9.13E-02 9.54E-02 1.14E+00 2.63E+00 7.89E+00
4.66E-08 5.53E-04 4.22E-01 4.21E-01 2.99E-04 1.43E-02 1.66E+00
1.56E-02 2.65E-03 3.40E-01 2.34E-02 9.53E-03 7.40E-04 1.95E-09
4.49E-10 1.86E-07 1.99E-04 2.59E-02 6.06E-01 9.33E+00 1.12E+00
5.16E-03 1.69E-01 2.99E-09 1.31E-02 4.66E-04 1.33E-02 1.73E-05
75$$ 84R1 T
TPBAR Spectrum Generation - Cool Time of 30 Days
56$$ F0 T
END
```

Figure 5.3.13-2 MCNP Input for 300 TPBARs at 30 Days Cool Time – Normal Conditions & Radial Biasing

```

NAC-LWT Cask - Tpbars_030d - Normal Transport Conditions
C Radial Biasing - Fuel Gamma Source
C Cells - TPBARs in Consolidation Canister & Basket - v1.4
1 1 -2.1515 -1 u=2 $ TPBARs
2 0 -2 +1 u=2 $ Can void
3 6 -7.9200 -3 +2 u=2 $ Consol. Can
4 0 -4 +3 +1 u=2 $ Basket void
5 4 -2.7000 -5 +4 -6 u=2 $ Basket shell
6 0 -6 +5 u=2 $ Void
7 0 +6 u=2 $ Outside
C Cells - LWT Cask Normal Conditions v1.4
8 5 -11.3440 -10 u=1 $ BotPb
9 0 -9 fill=2 u=1 $ Cavity
10 6 -7.9200 -8 +10 u=1 $ Bottom
11 6 -7.9200 -7 +8 +12 +15 +9 u=1 $ OuterShell
12 6 -7.9200 -11 +14 +9 u=1 $ InnerShellTaper
13 6 -7.9200 -13 +9 u=1 $ InnerShell
14 5 -11.3440 -14 +13 u=1 $ Lead
15 5 -11.3440 -12 +11 +14 u=1 $ LeadTaper
16 0 -15 +14 u=1 $ LeadGap
17 3 -0.9669 -17 +7 u=1 $ NeutronShield
18 6 -7.9200 -16 +7 +17 u=1 $ MSShell
19 7 -0.4997 -18 +7 u=1 $ UpperLimiter
20 7 -0.4997 -19 +7 u=1 $ LowerLimiter
21 0 -20 +7 +16 +18 +19 u=1 $ Container
22 0 +20 u=1 $ Outside
C Detector Cells - Radial Biasing
100 0 -100 fill=1 $ Surface
200 0 -200 +100 $ 1ft
300 0 -300 +200 $ 1m
400 0 -400 +300 $ 2m
500 0 -500 +400 $ 2m+Convey
600 0 +500 $ Exterior
C Surfaces - TPBARs in Consolidation Canister & Basket - v1.4
1 RPP -10.3505 10.3505 -10.3505 10.3505 30.1498 421.3098 $ TPBARs
2 RPP -10.3505 10.3505 -10.3505 10.3505 17.7800 383.5400 $ Consol. can inner
3 RPP -10.6934 10.6934 -10.6934 10.6934 17.7800 383.5400 $ Consol. can outer
4 RPP -11.2713 11.2713 -11.2713 11.2713 17.7800 427.9900 $ Basket void
5 RPP -12.5413 12.5413 -12.5413 12.5413 17.7800 427.9900 $ Basket shell
6 CZ 16.8275 $ Basket OD
C Surfaces - LWT Cask Normal Conditions v1.4
7 RCC 0.0000 0.0000 -26.6700 0.0000 0.0000 507.3650 36.5189 $ Lwt
8 RCC 0.0000 0.0000 -26.6700 0.0000 0.0000 26.6700 36.5189 $ Bottom
9 RCC 0.0000 0.0000 0.0000 0.0000 0.0000 452.1200 16.9863 $ Cavity
10 RCC 0.0000 0.0000 -17.7800 0.0000 0.0000 7.6200 26.3525 $ Bottom gamma shield
11 RCC 0.0000 0.0000 0.0000 0.0000 0.0000 444.5000 20.1740 $ Lead id - taper
12 RCC 0.0000 0.0000 0.0000 0.0000 0.0000 444.5000 31.5976 $ Lead od - taper
13 RCC 0.0000 0.0000 13.8176 0.0000 0.0000 416.8648 18.9103 $ Lead id
14 RCC 0.0000 0.0000 13.8176 0.0000 0.0000 416.8648 33.3271 $ Lead od
15 RCC 0.0000 0.0000 13.8176 0.0000 0.0000 416.8648 33.4645 $ Lead gap
16 RCC 0.0000 0.0000 3.8100 0.0000 0.0000 419.1000 49.8183 $ Neutron shield shell
17 RCC 0.0000 0.0000 5.0800 0.0000 0.0000 416.5600 49.2189 $ Neutron shield
18 RCC 0.0000 0.0000 450.2150 0.0000 0.0000 70.5612 49.8183 $ Upper limiter
19 RCC 0.0000 0.0000 -68.0212 0.0000 0.0000 71.8312 49.8183 $ Lower limiter
20 RCC 0.0000 0.0000 -68.0212 0.0000 0.0000 588.7974 49.8183 $ Container
C Radial Detector DRA (Surface)
100 RCC 0.0000 0.0000 -68.1212 0.0000 0.0000 588.9974 49.9183
101 PZ -38.6713
102 PZ -9.2215
103 PZ 20.2284
104 PZ 49.6783
105 PZ 79.1282
106 PZ 108.5780
107 PZ 138.0279
108 PZ 167.4778
109 PZ 196.9276
110 PZ 226.3775
111 PZ 255.8274
112 PZ 285.2772
113 PZ 314.7271
114 PZ 344.1770
115 PZ 373.6269
116 PZ 403.0767
117 PZ 432.5266
118 PZ 461.9765
119 PZ 491.4263
C Radial Detector DRB (1ft)
200 RCC 0.0000 0.0000 -98.6012 0.0000 0.0000 649.9574 80.2983
201 PZ -66.1033
202 PZ -33.6055
203 PZ -1.1076
204 PZ 31.3903
205 PZ 63.8882
206 PZ 96.3860
207 PZ 128.8839
208 PZ 161.3818
209 PZ 193.8796
210 PZ 226.3775
211 PZ 258.8754
212 PZ 291.3732
213 PZ 323.8711
214 PZ 356.3690
215 PZ 388.8669
216 PZ 421.3647

```

Figure 5.3.13-2 MCNP Input for 300 TPBARs at 30 Days Cool Time – Normal
Conditions & Radial Biasing (Continued)

```

217 PZ 453.8626
218 PZ 486.3605
219 PZ 518.8583
C Radial Detector DRC (1m)
300 RCC 0.0000 0.0000 -168.1212 0.0000 0.0000 788.9974 149.8183
301 PZ -135.2463
302 PZ -102.3714
303 PZ -69.4965
304 PZ -36.6216
305 PZ -3.7467
306 PZ 29.1282
307 PZ 62.0030
308 PZ 94.8779
309 PZ 127.7528
310 PZ 160.6277
311 PZ 193.5026
312 PZ 226.3775
313 PZ 259.2524
314 PZ 292.1273
315 PZ 325.0022
316 PZ 357.8771
317 PZ 390.7520
318 PZ 423.6269
319 PZ 456.5017
320 PZ 489.3766
321 PZ 522.2515
322 PZ 555.1264
323 PZ 588.0013
C Radial Detector DRD (2m)
400 RCC 0.0000 0.0000 -268.1212 0.0000 0.0000 988.9974 249.8183
401 PZ -226.9130
402 PZ -185.7048
403 PZ -144.4965
404 PZ -103.2883
405 PZ -62.0801
406 PZ -20.8719
407 PZ 20.3364
408 PZ 61.5446
409 PZ 102.7528
410 PZ 143.9611
411 PZ 185.1693
412 PZ 226.3775
413 PZ 267.5857
414 PZ 308.7940
415 PZ 350.0022
416 PZ 391.2104
417 PZ 432.4186
418 PZ 473.6269
419 PZ 514.8351
420 PZ 556.0433
421 PZ 597.2515
422 PZ 638.4598
423 PZ 679.6680
C Radial Detector DRE (2m+Convey)
500 RCC 0.0000 0.0000 -269.1212 0.0000 0.0000 990.9974 321.9200
501 PZ -227.8296
502 PZ -186.5381
503 PZ -145.2465
504 PZ -103.9550
505 PZ -62.6634
506 PZ -21.3719
507 PZ 19.9197
508 PZ 61.2113
509 PZ 102.5028
510 PZ 143.7944
511 PZ 185.0859
512 PZ 226.3775
513 PZ 267.6691
514 PZ 308.9606
515 PZ 350.2522
516 PZ 391.5437
517 PZ 432.8353
518 PZ 474.1269
519 PZ 515.4184
520 PZ 556.7100
521 PZ 598.0015
522 PZ 639.2931
523 PZ 680.5846
C
C Materials List - Common Materials - v1.4
C
C Homogenized TPBARs
m1 3000 -2.138E+01 $ Li
26000 -3.500E+02 $ Fe
24000 -1.020E+02 $ Cr
28000 -3.350E+02 $ Ni
8000 -1.020E+02 $ O
13000 -8.660E+01 $ Al
33000 -2.750E-01 $ As
5000 -1.140E-02 $ B
56000 -1.680E-01 $ Ba
6000 -7.120E-01 $ C
20000 -8.400E-01 $ Ca
48000 -1.080E-04 $ Cd

```

Figure 5.3.13-2 MCNP Input for 300 TPBARs at 30 Days Cool Time – Normal Conditions & Radial Biasing (Continued)

```

27000 -2.870E-01 $ Co
29000 -2.370E-01 $ Cu
1000 -5.380E-03 $ H
72000 -2.150E-02 $ Hf
19000 -1.050E+00 $ K
12000 -4.240E-01 $ Mg
25000 -1.130E+01 $ Mn
42000 -1.700E+01 $ Mo
7000 -7.370E-02 $ N
11000 -1.050E+00 $ Na
41000 -2.830E-01 $ Nb
15000 -2.260E-01 $ P
82000 -8.400E-02 $ Pb
16000 -5.650E-02 $ S
34000 -7.350E-02 $ Se
14000 -6.360E+00 $ Si
50000 -3.660E+00 $ Sn
73000 -1.130E-01 $ Ta
22000 -1.080E-02 $ Ti
23000 -2.830E-01 $ V
74000 -2.150E-02 $ W
40000 -2.100E+02 $ Zr
92000 -7.530E-04 $ U

C Water
m2 1001 6.6667E-01 $ H
8016 3.3333E-01 $ O
mt2 lwtr.01
C Water/Glycol
m3 1001 -1.03651E-01
8016 -6.75619E-01
6000 -2.20730E-01

C Aluminum
m4 13027 -1.0
C Lead
m5 82000 -1.0
C Stainless Steel 304
m6 26000 -0.695
24000 -0.190
28000 -0.095
25000 -0.020

C Aluminum Honeycomb Impact Limiter
m7 13027 -1.0
nomu $ No subcritical multiplication
C
C Cell Importances
C
imp:p 1 26r 0
C
C Source Definition - Fuel Gamma - Tpbars_030d
C
sdef x=d1 y=d2 z=d3 erg=d4
si1 -10.3505 10.3505
sp1 0 1
si2 -10.3505 10.3505
sp2 0 1
si3 30.1498 421.3098
sp3 0 1
si4 1.000E-02 2.000E-02 5.000E-02 1.000E-01 2.000E-01 3.000E-01
4.000E-01 6.000E-01 8.000E-01 1.000E+00 1.220E+00 1.440E+00
1.660E+00 2.000E+00 2.500E+00 3.000E+00 4.000E+00 5.000E+00
6.500E+00 8.000E+00 1.000E+01 1.200E+01 1.400E+01
sp4 0.0000E+00 3.0175E+11 4.7611E+11 4.4009E+11 2.9577E+11 1.0398E+11
1.8282E+12 2.5002E+12 4.6571E+12 8.5647E+12 1.6438E+12 1.4198E+12
1.5788E+08 3.8151E+10 2.2794E+08 4.3234E+04 1.8781E+00 4.8373E-08
0.0000E+00 0.0000E+00 0.0000E+00 0.0000E+00 0.0000E+00 0.0000E+00

mode p
nps 40000000
C
C ANSI/ANS-6.1.1-1977 - Gamma Flux-to-Dose Conversion Factors
C (mrem/hr)/(photons/cm2-sec)
C
de0 0.01 0.03 0.05 0.07 0.1 0.15 0.2
0.25 0.3 0.35 0.4 0.45 0.5 0.55
0.6 0.65 0.7 0.8 1 1.4 1.8
2.2 2.6 2.8 3.25 3.75 4.25 4.75
5 5.25 5.75 6.25 6.75 7.5 9
11 13 15
df0 3.96E-03 5.82E-04 2.90E-04 2.58E-04 2.83E-04 3.79E-04 5.01E-04
6.31E-04 7.59E-04 8.78E-04 9.85E-04 1.08E-03 1.17E-03 1.27E-03
1.36E-03 1.44E-03 1.52E-03 1.68E-03 1.98E-03 2.51E-03 2.99E-03
3.42E-03 3.82E-03 4.01E-03 4.41E-03 4.83E-03 5.23E-03 5.60E-03
5.80E-03 6.01E-03 6.37E-03 6.74E-03 7.11E-03 7.66E-03 8.77E-03
1.03E-02 1.18E-02 1.33E-02
C
C Weight Window Generation - Radial
C
wwg 2 0 0 0
wwp:p 5 3 5 0 -1 0
mesh geom=cyl ref=0 0 226 origin=0.1 0.1 -568
imesh 15.1 17.0 18.9 33.3 36.5 49.2 49.8 549.8
iints 5 1 1 5 1 1 1 1
jmesh 500 541 550 558 568 598 989 1020 1049 1089 1589
jints 1 1 1 1 1 1 1 1 1 1 1
kmesh 0.5 1

```

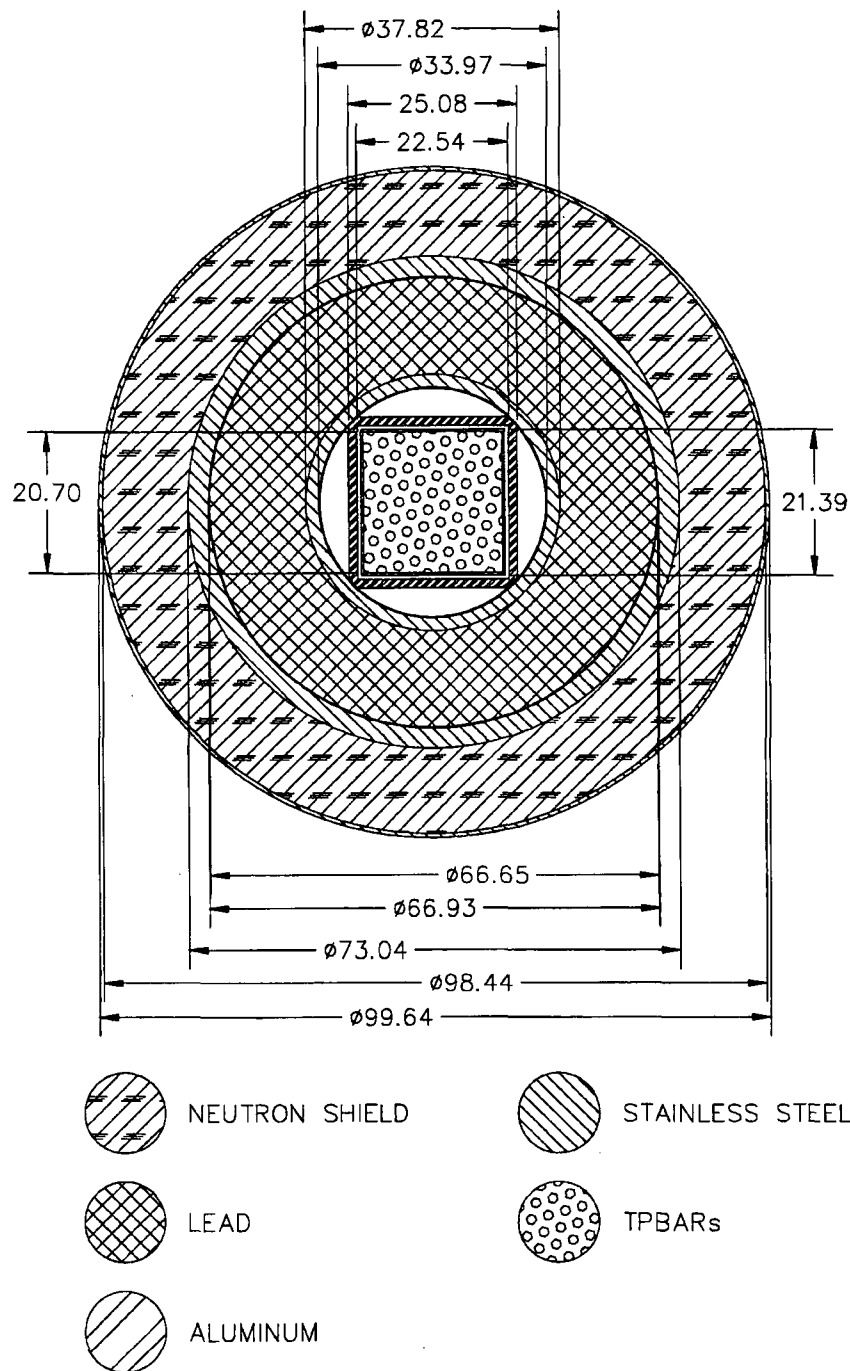
Figure 5.3.13-2 MCNP Input for 300 TPBARs at 30 Days Cool Time – Normal
Conditions & Radial Biasing (Continued)

```

kints 1 1
wvge:p 1e-3 1 20
fc2 Radial Surface Tally
f2:p 100.1
fm2 7.6832E+15
fs2 -101 -102 -103 -104 -105 -106
    -107 -108 -109 -110 -111 -112
    -113 -114 -115 -116 -117 -118
    -119 T
tf2
fc12 Radial 1ft Tally
f12:p 200.1
fm12 7.6832E+15
fs12 -201 -202 -203 -204 -205 -206
    -207 -208 -209 -210 -211 -212
    -213 -214 -215 -216 -217 -218
    -219 T
tf12
fc22 Radial 1m Tally
f22:p 300.1
fm22 7.6832E+15
fs22 -301 -302 -303 -304 -305 -306
    -307 -308 -309 -310 -311 -312
    -313 -314 -315 -316 -317 -318
    -319 -320 -321 -322 -323 T
tf22
fc32 Radial 2m Tally
f32:p 400.1
fm32 7.6832E+15
fs32 -401 -402 -403 -404 -405 -406
    -407 -408 -409 -410 -411 -412
    -413 -414 -415 -416 -417 -418
    -419 -420 -421 -422 -423 T
tf32
fc42 Radial 2m+Convey Tally
f42:p 500.1
fm42 7.6832E+15
fs42 -501 -502 -503 -504 -505 -506
    -507 -508 -509 -510 -511 -512
    -513 -514 -515 -516 -517 -518
    -519 -520 -521 -522 -523 T
tf42
C
C
C Print Control
C
prdmp -30 -60 1 2
print

```

Figure 5.3.13-3 MCNP Three-Dimensional Model of NAC-LWT with 300 TPBAR Payload – Radial Detail



Dimensions in cm.

Figure 5.3.13-4 MCNP Three-Dimensional Model of NAC-LWT with 300 TPBAR Payload - Axial Detail

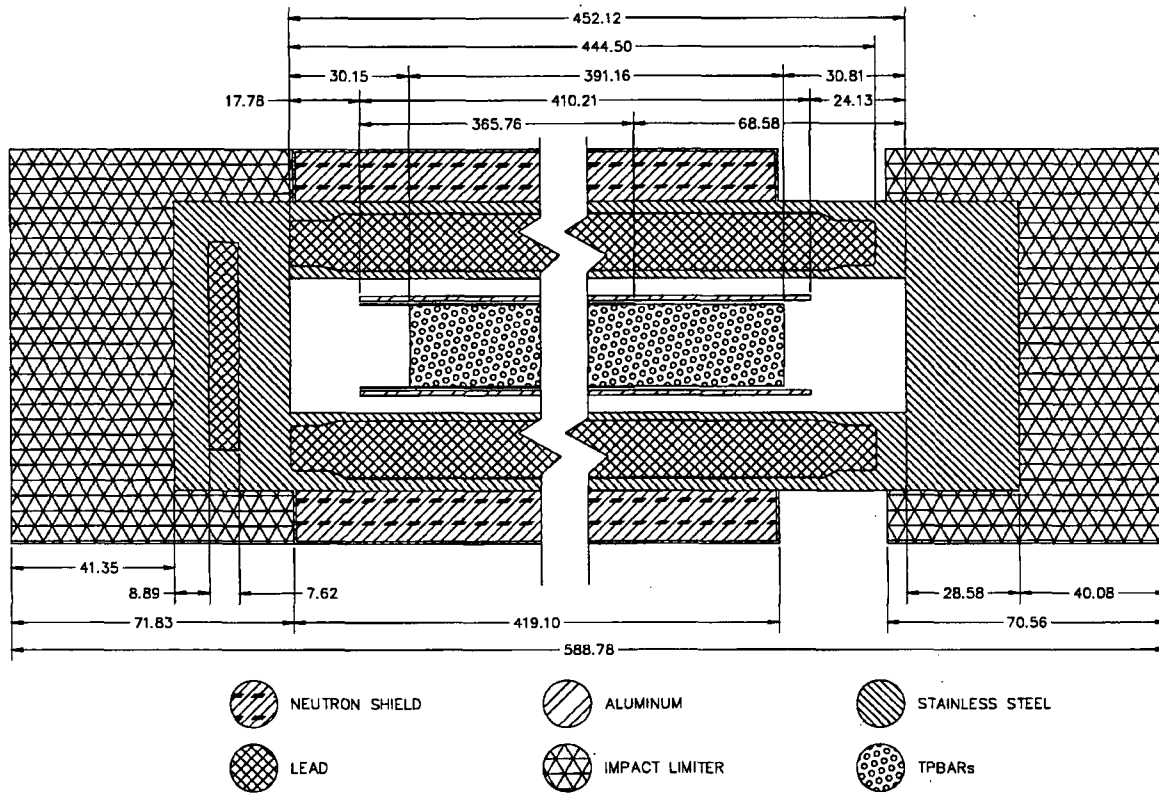


Figure 5.3.13-5 Normal Condition Radial Surface Dose Rate Profile for 300 TPBAR Payload

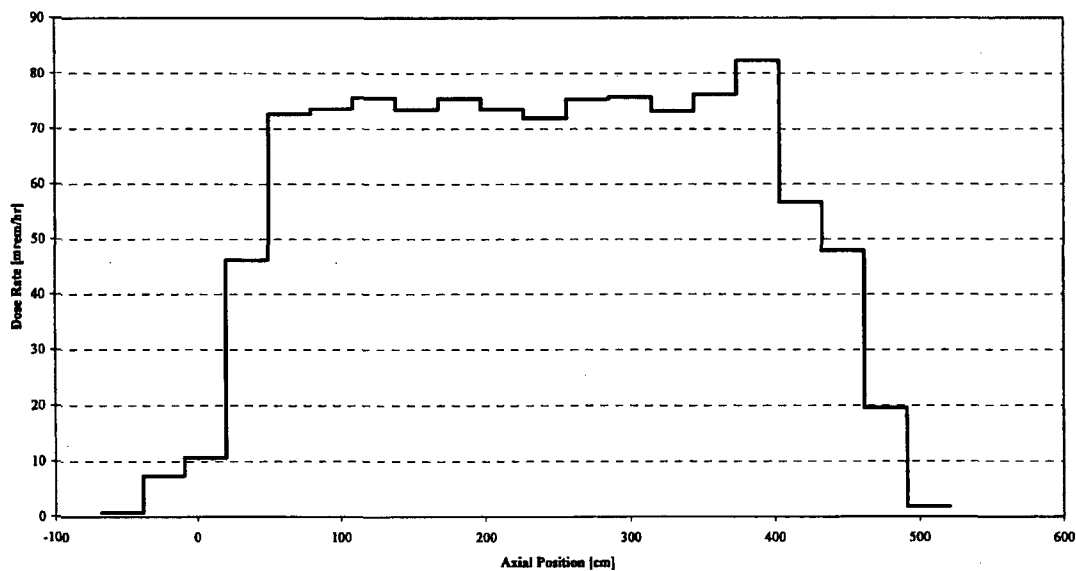
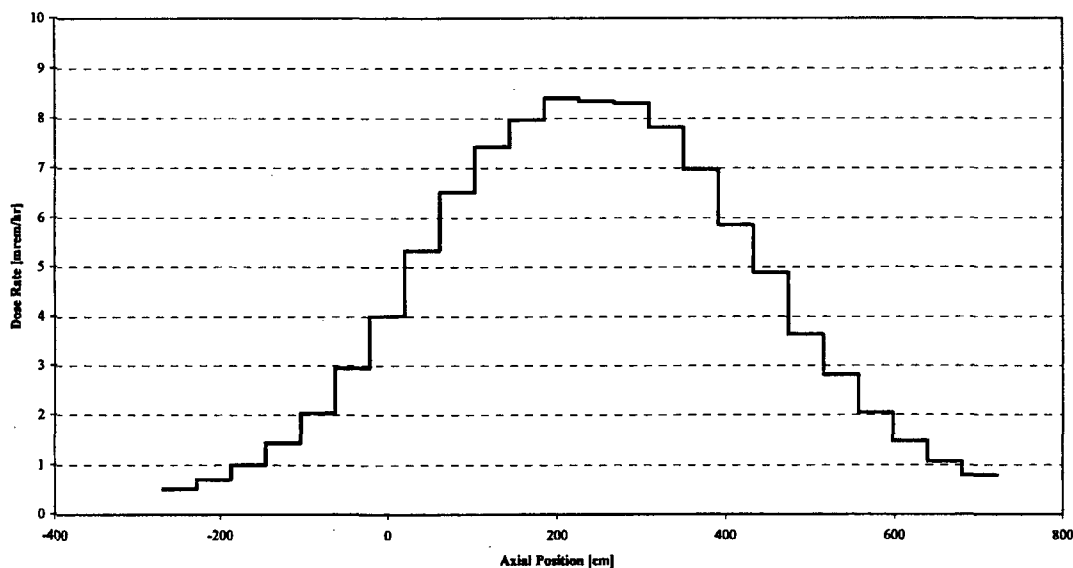


Figure 5.3.13-6 Normal Condition Radial 2 Meter Dose Rate Profile for 300 TPBAR Payload



**Figure 5.3.13-7 Accident Condition Radial 1 Meter Dose Rate Profile for 300 TPBAR
Payload**

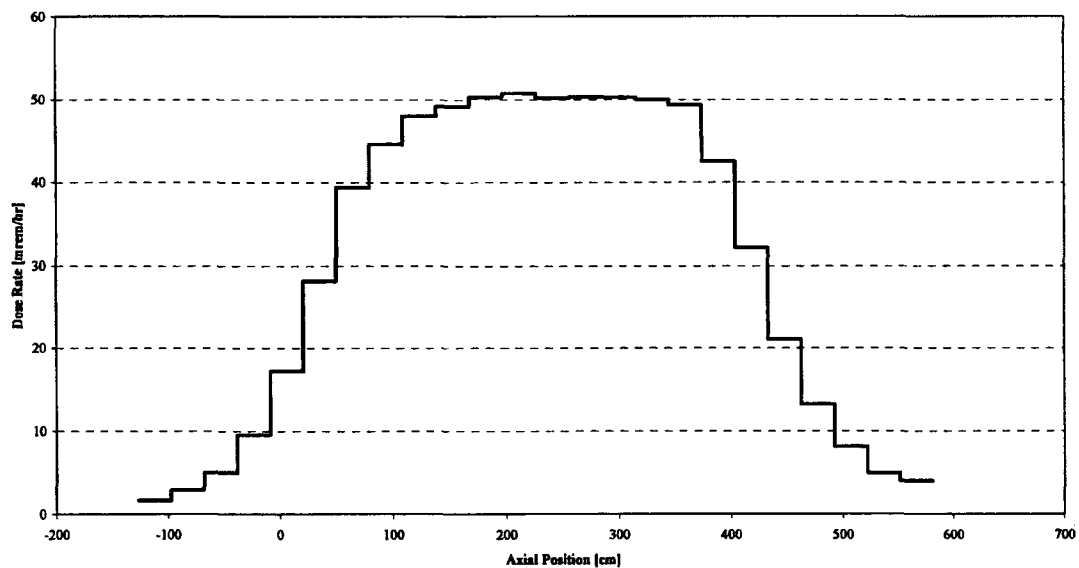


Table 5.3.13-1 Single TPBAR Activity Inventory at 30 Days Cool Time

Isotope	Activity [Ci]	Isotope	Activity [Ci]
³ H	1.15E+04	^{97m} Nb	1.57E-11
¹⁴ C	1.42E-03	⁹³ Mo	1.04E-03
²⁴ Na	1.65E-13	⁹⁹ Mo	5.11E-02
³² P	3.38E-01	⁹⁹ Tc	4.36E-05
³⁵ S	1.15E-02	¹⁰³ Ru	2.14E-03
³⁷ Ar	2.40E-01	¹¹⁵ Cd	2.27E-07
³⁹ Ar	9.49E-03	^{115m} Cd	1.28E-04
⁴² K	8.34E-12	^{113m} In	1.14E+00
⁴¹ Ca	7.51E-05	¹¹⁴ In	9.13E-02
⁴⁵ Ca	2.84E-01	^{114m} In	9.54E-02
⁴⁷ Ca	4.66E-06	¹¹³ Sn	1.14E+00
⁴⁶ Sc	6.78E-03	^{117m} Sn	2.63E+00
⁴⁷ Sc	1.76E-05	^{119m} Sn	7.89E+00
⁵¹ Cr	5.44E+02	¹²¹ Sn	4.66E-08
⁵⁴ Mn	3.98E+01	^{121m} Sn	5.53E-04
⁵⁵ Fe	2.12E+02	¹²³ Sn	4.22E-01
⁵⁹ Fe	1.39E+01	¹²⁵ Sn	4.21E-01
⁵⁸ Co	2.15E+02	¹²² Sb	2.99E-04
⁶⁰ Co	3.57E+01	¹²⁴ Sb	1.43E-02
⁵⁹ Ni	1.68E-01	¹²⁵ Sb	1.66E+00
⁶³ Ni	2.29E+01	¹²⁶ Sb	1.56E-02
⁶⁶ Ni	1.38E-07	^{123m} Te	2.65E-03
⁶⁴ Cu	1.04E-16	^{125m} Te	3.40E-01
⁶⁶ Cu	1.38E-07	¹³¹ Cs	2.34E-02
⁶⁵ Zn	3.87E-03	¹³¹ Ba	9.53E-03
⁷⁶ As	4.25E-07	¹³³ Ba	7.40E-04
⁷⁵ Se	7.77E-01	^{133m} Ba	1.95E-09
⁸² Br	2.25E-08	^{135m} Ba	4.49E-10
⁸⁹ Sr	5.48E-02	¹⁴⁰ La	1.86E-07
^{89m} Y	4.18E-06	¹⁷⁷ Lu	1.99E-04
⁹⁰ Y	1.30E-03	¹⁷⁵ Hf	2.59E-02
⁹¹ Y	1.46E-01	¹⁸¹ Hf	6.06E-01
⁸⁹ Zr	4.18E-06	¹⁸² Ta	9.33E+00
⁹³ Zr	1.13E-04	¹⁸³ Ta	1.12E+00
⁹⁵ Zr	5.12E+01	¹⁸¹ W	5.16E-03
⁹⁷ Zr	1.65E-11	¹⁸⁵ W	1.69E-01
⁹² Nb	6.34E-02	¹⁸⁷ W	2.99E-09
^{93m} Nb	4.02E-06	¹⁸⁸ W	1.31E-02
⁹⁴ Nb	4.76E-04	¹⁸⁶ Re	4.66E-04
⁹⁵ Nb	6.50E+01	¹⁸⁸ Re	1.33E-02
^{95m} Nb	3.80E-01	¹⁹¹ Os	1.73E-05
⁹⁶ Nb	9.19E-11	Total	1.28E+04
⁹⁷ Nb	1.78E-11		

Table 5.3.13-2 TPBAR 30-Day Gamma Source Spectrum

Energy Group	E _{Lower} [MeV]	E _{Upper} [MeV]	Source [gamma/sec/TPBAR]
1	1.200E+01	1.400E+01	0.000E+00
2	1.000E+01	1.200E+01	0.000E+00
3	8.000E+00	1.000E+01	0.000E+00
4	6.500E+00	8.000E+00	0.000E+00
5	5.000E+00	6.500E+00	0.000E+00
6	4.000E+00	5.000E+00	4.837E-08
7	3.000E+00	4.000E+00	1.878E+00
8	2.500E+00	3.000E+00	4.323E+04
9	2.000E+00	2.500E+00	2.279E+08
10	1.660E+00	2.000E+00	3.815E+10
11	1.440E+00	1.660E+00	1.579E+08
12	1.220E+00	1.440E+00	1.420E+12
13	1.000E+00	1.220E+00	1.644E+12
14	8.000E-01	1.000E+00	8.565E+12
15	6.000E-01	8.000E-01	4.657E+12
16	4.000E-01	6.000E-01	2.500E+12
17	3.000E-01	4.000E-01	1.828E+12
18	2.000E-01	3.000E-01	1.040E+11
19	1.000E-01	2.000E-01	2.958E+11
20	5.000E-02	1.000E-01	4.401E+11
21	2.000E-02	5.000E-02	4.761E+11
22	1.000E-02	2.000E-02	3.018E+11
Total			2.227E+13

Table 5.3.13-3 TPBAR Elemental Constituents

Nuclide	Mass[g]	Number Density [atom/b-cm]
Li	2.14E+01	3.3198E-03
Fe	3.50E+02	6.7548E-03
Cr	1.02E+02	2.1143E-03
Ni	3.10E+02	5.6925E-03
O	1.02E+02	6.8712E-03
Al	8.66E+01	3.4592E-03
As	2.75E-01	3.9560E-06
B	1.14E-02	1.1365E-06
Ba	1.68E-01	1.3185E-06
C	7.05E-01	6.3261E-05
Ca	8.40E-01	2.2589E-05
Cd	1.08E-04	1.0355E-09
Co	2.87E-01	5.2487E-06
Cu	2.37E-01	4.0197E-06
H	5.38E-03	5.7530E-06
Hf	2.15E-02	1.2982E-07
K	1.05E+00	2.8944E-05
Mg	4.24E-01	1.8802E-05
Mn	1.13E+01	2.2168E-04
Mo	1.70E+01	1.9098E-04
N	7.37E-02	5.6709E-06
Na	1.05E+00	4.9224E-05
Nb	2.83E-01	3.2830E-06
P	2.26E-01	7.8639E-06
Pb	8.40E-02	4.3694E-07
S	5.65E-02	1.8991E-06
Se	7.35E-02	1.0032E-06
Si	6.36E+00	2.4406E-04
Sn	3.66E+00	3.3229E-05
Ta	1.13E-01	6.7305E-07
Ti	1.08E-02	2.4317E-07
V	2.83E-01	5.9874E-06
W	2.15E-01	1.2605E-07
Zr	1.86E+02	2.1975E-03
U	7.53E-04	3.4095E-09
Total	1.25E+03	3.2074E-02

Table 5.3.13-4 Material Compositions of NAC-LWT for 300 TPBAR Payload

Material	Density [g/cm ³]	MCNP Isotope/Element	Mass Fraction	Number Density [atom/b-cm]
Neutron Shield	9.6690E-01	Hydrogen	1.0365E-01	5.9884E-02
		Oxygen-16	6.7562E-01	2.4595E-02
		Carbon	2.2073E-01	1.0701E-02
Aluminum	2.7000E+00	Aluminum-27	1.0000E+00	6.0262E-02
Lead	1.1344E+01	Lead	1.0000E+00	3.2970E-02
Stainless Steel	7.9200E+00	Iron	6.9500E-01	5.9357E-02
		Chromium	1.9000E-01	1.7428E-02
		Nickel	9.5000E-02	7.6845E-03
		Manganese	2.0000E-02	1.7363E-03
Impact Limiters	4.9970E-01	Aluminum-27	1.0000E+00	1.1153E-02

Table 5.3.13-5 Dose Rate Summary for 300 TPBARs at 30 Days Cool Time

Transport Condition	Dose Rate Location	Maximum		Average	
		[mrem/hr]	FSD	[mrem/hr]	FSD
Normal	Side Surface of Cask	82.3	1.8%	54.5	2.4%
	Top Surface of Cask	14.2	3.7%	7.5	4.2%
	Bottom Surface of Cask	3.8	3.9%	2.0	4.3%
	Side 1m	21.6	1.2%	12.0	1.5%
	2m from Truck - Radial	8.4	1.0%	4.3	1.3%
	2m from Top	0.6	3.5%	0.3	7.5%
	2m from Bottom	0.2	3.6%	0.1	8.9%
Accident	Side Surface of Cask	253.7	2.1%	178.6	2.6%
	Top Surface of Cask	110.7	3.5%	45.3	4.9%
	Bottom Surface of Cask	29.5	4.7%	11.2	6.7%
	Side 1m	50.8	1.2%	30.1	1.7%
	Top 1m	6.9	2.9%	2.7	6.1%
	Bottom 1m	1.8	3.8%	0.7	5.5%

Table 5.3.13-6 Reactor Operating Conditions for TPBAR Source Term Generation

Parameter	Value
Mass of U [kg/assembly]	462
Number of Assemblies	193
Reactor Power [MW]	3,459
Irradiation Time [days]	510
Maximum Assembly Burnup [MWd/MTU]	29,700
²³⁵ U enrichment [wt %]	3.000
Mass ²³⁵ U [g/MTU]	30,000
Mass ²³⁸ U [g/MTU]	970,000
Assembly Specific Power [MW/MTU]	58.24
Radial Assembly Peaking Factor	1.50

5.3.14 PULSTAR Fuel Configuration

Results of a shielding analysis for up to 700 PULSTAR fuel elements in the LWT cask are presented in this section. Maximum dose rates are calculated to demonstrate that dose rate limits of 10 CFR 71.47 are not exceeded.

Dose rates are calculated using the MCNP three-dimensional transport code. Source terms are calculated using the SAS2H module of the SCALE package, with ORIGEN-S used to rebin the gamma-ray and neutron spectra onto the 22-group and 28-group structures employed in the evaluation.

5.3.14.1 PULSTAR Fuel Source Term

Source terms are calculated to bound the irradiation history of the PULSTAR fuel elements. Fuel element and assembly geometry is summarized in Figure 5.3.14-1 and Table 5.3.14-1. Inputs for irradiation and material parameters required by SAS2H are given in Table 5.3.14-2. Using these parameters, and a fission yield of 0.9166 MWd/g ^{235}U , the single cycle irradiation time is 4583 days (12.5 years). The calculated UO_2 density is 99% of theoretical.

At lower enrichments, a reduced fissile mass must be specified to yield a calculated UO_2 density of 100% or less. Given a fixed cool time and burnup specified as a percentage of ^{235}U rather than a fixed exposure (in MWd/MTU), the evaluated parameters are bounding.

SAS2H input is shown in Figure 5.3.14-2. Neutron and gamma source terms for a cool time of 1 year from discharge are presented in Table 5.3.14-3 and Table 5.3.14-4, respectively. These source terms are very conservative in that the resulting calculated assembly heat load is 37.67 W. A cool time of 1.5 years is required for the assembly heat load to be below the basket cell limit of 30 W.

The effect of subcritical neutron multiplication is not directly computed in the MCNP analysis, due to difficulties in adequately biasing the calculation. Instead, neutron source rates are scaled by a subcritical multiplication factor based on the system multiplication factor, k_{eff} :

$$\text{Scale Factor} = \frac{1}{1 - k_{\text{eff}}}$$

For the dry cask conditions of transport, the calculated k_{eff} is significantly less than 0.4. Conservatively applying this k_{eff} yields a scale factor of 1.6667, which is included in the tally cards in MCNP.

5.3.14.2 PULSTAR Fuel Shielding Model

MCNP three-dimensional shielding analysis allows detailed modeling of the fuel, basket, and cask shield configurations. Some fuel rod detail is homogenized in the model to simplify model input and improve computational efficiency. The basket and cask body details are explicitly modeled, including the axial extents described by the License Drawings.

The geometric description of a MCNP model is based on the combinatorial geometry system embedded in the code. In this system, bodies such as cylinders and rectangular parallelepipeds, and their logical intersections and unions, are used to describe the extent of material zones.

Source Models

Based on the possible basket cell loadings of PULSTAR fuel, three source models are employed to bound all hypothetical configurations of the fuel. The first model considers an intact assembly, with the 5×5 array of fuel elements homogenized and surrounded by the assembly zirconium alloy box. The axial extents of the upper and lower assembly fittings are modeled as void to simulate the spacing of assemblies vertically within each basket. The fuel assembly model bounds a model of 16 elements placed within the 4×4 fuel rod insert and loaded into a basket cell due to both a larger source (25 vs. 16 elements) and less shielding (the insert tubes will offer a slight improvement in shielding). The fuel homogenization, shown in Table 5.3.14-5, is based on an area bounded by the assembly zirconium alloy box. The source height is the active fuel height, 24.1 inches.

The second and third source models both consider 25 canned elements. Bounding can cavity dimensions of 3.3-inch width × 30-inch height were chosen to maximize the source volume. The second and third source models are based on modeling 25 elements over either a 30-inch height or a 9.23-inch height. The latter is calculated by fixing the can opening width to 3.3 inches and calculating the minimum height needed to accommodate the volume of 25 elements, 1,647 cm³. In both of the can models, no credit is taken for the can wall, lid, or bottom structure, and the source regions are moved to their highest axial location within each basket. This serves to maximize source at the point of minimum radial shielding in the cask. Source region homogenizations for the canned element models are shown in Table 5.3.14-6 and Table 5.3.14-7.

Basket Model

For a given fuel type, the MCNP description of the basket stack forms a common sub-model employed in the analysis. The key features of the model are the detailed representation of the basket structural members, base plates, and support plates.

MCNP NAC-LWT Model

The three-dimensional model of the NAC-LWT cask is based on the following features.

Normal conditions:

- Radial neutron shield and shield shell
- Aluminum impact limiters with 0.5 g/cm³ density (calculated based on the impact limiter weight and dimensions) and diameter equal to the neutron shield shell diameter

Accident conditions:

- Removal of radial neutron shield and shield shell
- Loss of upper and lower impact limiters

Common to both the normal and accident conditions models is a 0.1374 cm gap between the lead outer diameter and the cask outer shell. As stated previously, the elevation of the source regions is set at its maximum axial extent. This conservatively shifts the failed fuel source to the top of the cask cavity where, as shown in Figure 5.3.14-3, the least radial shielding is located.

Detailed model parameters used in creating the three-dimensional model are taken directly from the License Drawings. Elevations associated with the three-dimensional features are established with respect to the center bottom of the NAC-LWT cask cavity for the MCNP combinatorial model. The three-dimensional NAC-LWT models are shown in Figure 5.3.14-3 and Figure 5.3.14-4. The axial model shows the minimum source height for canned fuel. Similar models are constructed for intact assemblies and the nominal source height for canned fuel. A sample input file is provided in Figure 5.3.14-5.

Shield Regional Densities

Based on the homogenization described for each source model the fuel rod model, the resulting fuel regional densities are shown in Table 5.3.14-8. Material compositions for structural and shield materials are shown in Table 5.3.14-9.

5.3.14.3 PULSTAR Fuel Shielding Evaluation

Calculational Methods

The shielding evaluation is performed using MCNP.

The MCNP shielding model described in Section 5.3.14.2 is utilized with the source terms described in Section 5.3.14.1 to estimate the dose rate profiles at various distances from the side, top and bottom of the cask for both normal and accident conditions. The method of solution is continuous energy Monte Carlo with a Monte Carlo based weight window generator to accelerate code convergence. Weight window and problem convergence is verified by the 10 statistical

checks performed by MCNP. Radial or axial biasing is performed depending on the desired dose location.

Significant validation literature is available for MCNP as it is an industry standard tool for spent fuel cask evaluations. Available literature covers a range of shielding penetration problems ranging from slab geometry to spent fuel cask geometries. Confirmatory calculations against other validated shielding codes (SCALE and MCBEND) on NAC casks have further validated the use of MCNP for shielding evaluations.

MCNP Flux-to-Dose Conversion Factors

The ANSI/ANS 6.1.1-1977 flux-to-dose rate conversion factors are employed in the MCNP analysis. The ANSI/ANS gamma and neutron dose conversion factors are shown in Table 5.3.11-23 and Table 5.3.11-24.

Three-Dimensional Dose Rates for PULSTAR Fuel

Table 5.3.14-10 and Table 5.3.14-11 summarize the computed dose rates for each source model at the tabulated distances and transport conditions (normal and accident). The highest calculated radial dose rates for normal conditions are for the minimum source height can model.

Calculated normal condition radial surface dose rates are in excess of 200 mrem/hr, necessitating an exclusive use designation for the NAC-LWT. The maximum dose rate is dominated by the gamma component, which comprises approximately 93% of the maximum dose rate. The axial elevation of the maximum dose rate is above the radial lead shield. The dose rate profile is shown in Figure 5.3.14-6.

The normal condition maximum radial 2-meter dose rate is 5.2 mrem/hr. The dose rate profile is skewed towards the top of cask, as shown Figure 5.3.14-7.

Accident condition radial 1-meter dose rates for all three source models are well below the 1,000 mrem/hr limit. The maximum dose rate is dominated by the gamma component, which contributes approximately 89% towards the maximum. The dose rate profile is shown in Figure 5.3.14-8.

As shown in Table 5.3.14-11, axial surface dose rates are well below limits for all three source models. Significant margin is present for the normal condition 2-meter and accident condition 1-meter dose rate limits.

Note that a full cask load (28 basket cells) of canned elements is not an allowable payload (refer to Chapter 6). To justify a mixed loading of intact assemblies in the two intermediate baskets and canned elements in the top and bottom baskets, the 2 meter dose rates for the intact fuel source model and minimum source height canned model are summed. The maximum radial dose

rate (at 2 meters) for the summed profiles is 6.5 mrem/hr, well below the 10 mrem/hr regulatory limit. Dose rates for the fuel assembly model peak at the cask midplane, while the can model peaks above the lead shield. The maximum 6.5 mrem/hr dose rate is, therefore, slightly lower than the sum of the individual maximum dose rates reported in Table 5.3.14-10.

Figure 5.3.14-1 PULSTAR Fuel Assembly

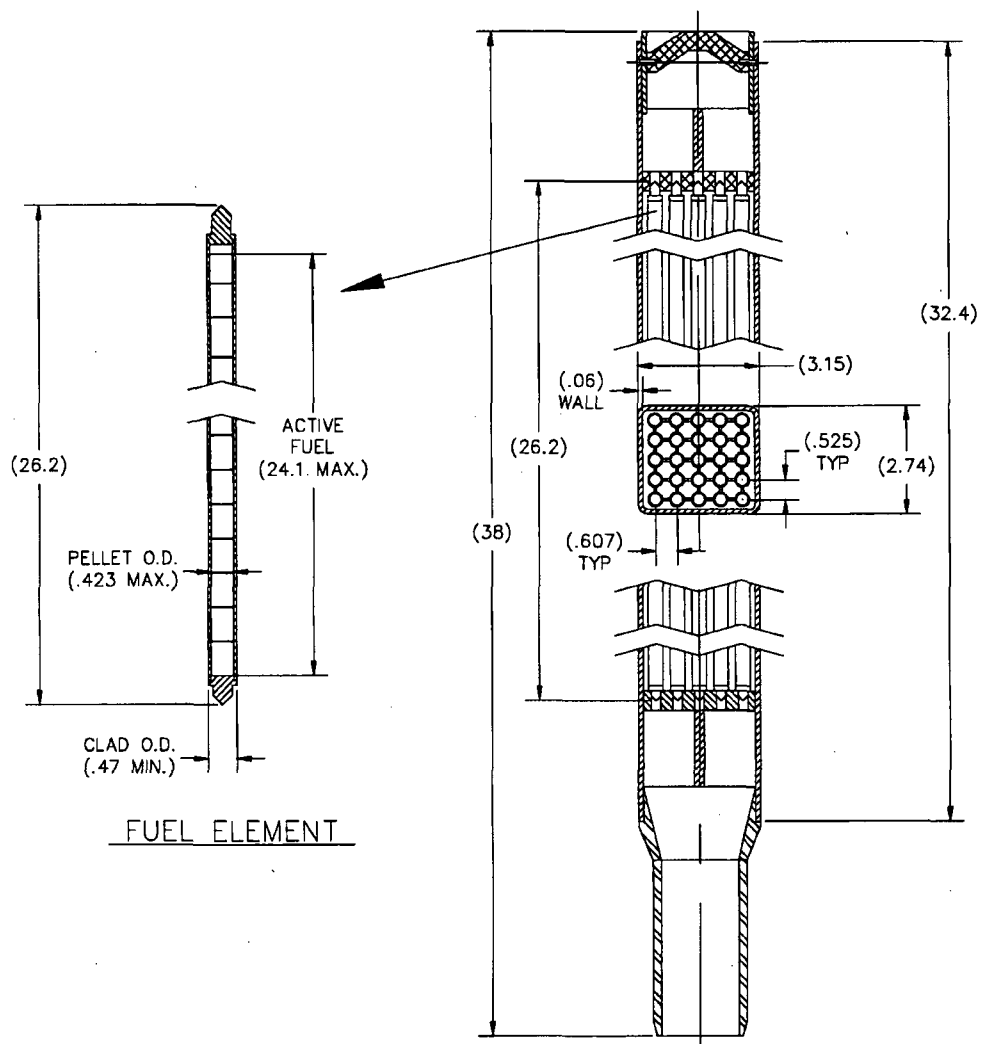


Figure 5.3.14-2 SAS2H Input for PULSTAR Fuel

```
=SAS2H      PARM=(HALT05,SKIPSHIPDATA)
PULSTAR Assembly, 50% burnup, 6 wt % U-235
27GROUPNDF4 LATTICECELL
UO2        1 0.99 633.15 92235 6.0 92238 94.0 END
ZIRCALLOY  2 1.0 433.15 END
H2O        3 1.0 333.15 END
ZIRCALLOY  4 1.0 333.15 END
END COMP
SQUAREPITCH 1.4313 1.0744 1 3 1.1938 2 1.0998 0 END
NPIN=25 FUEL=61.214 NCYC=1 NLIB=5 PRIN=6 LIGH=5
INPL=2 NUMZ=5 END
3 0.0001 500 4.0377 3 4.0378 4 4.2101 3 4.2675
POWER=0.0800 BURN=4583.0000 DOWN=91.3125 END
FE 0.6738 CR 0.1900 NI 0.1150 MN 0.0200 CO 0.0012
END
```

Note: Target burnup for this case is 50% ^{235}U . Cycle length is based on only generating power from thermal fission of ^{235}U . Due to fissile actinide buildup, actual depletion of ^{235}U for this case is 46%.

Figure 5.3.14-3 MCNP Model of NAC-LWT with PULSTAR Fuel – Axial Detail

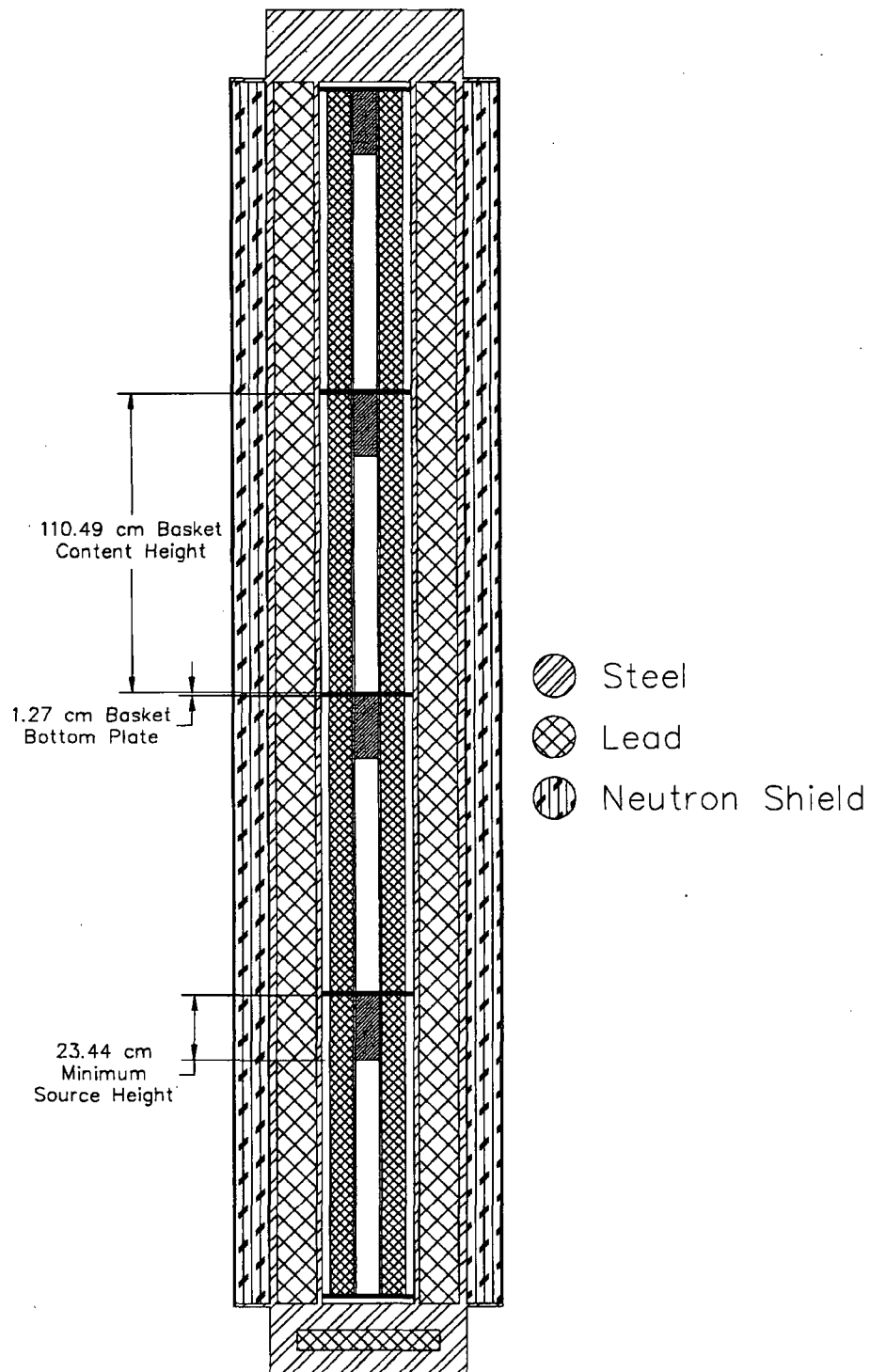


Figure 5.3.14-4 MCNP Model of NAC-LWT with PULSTAR Fuel – Radial Detail

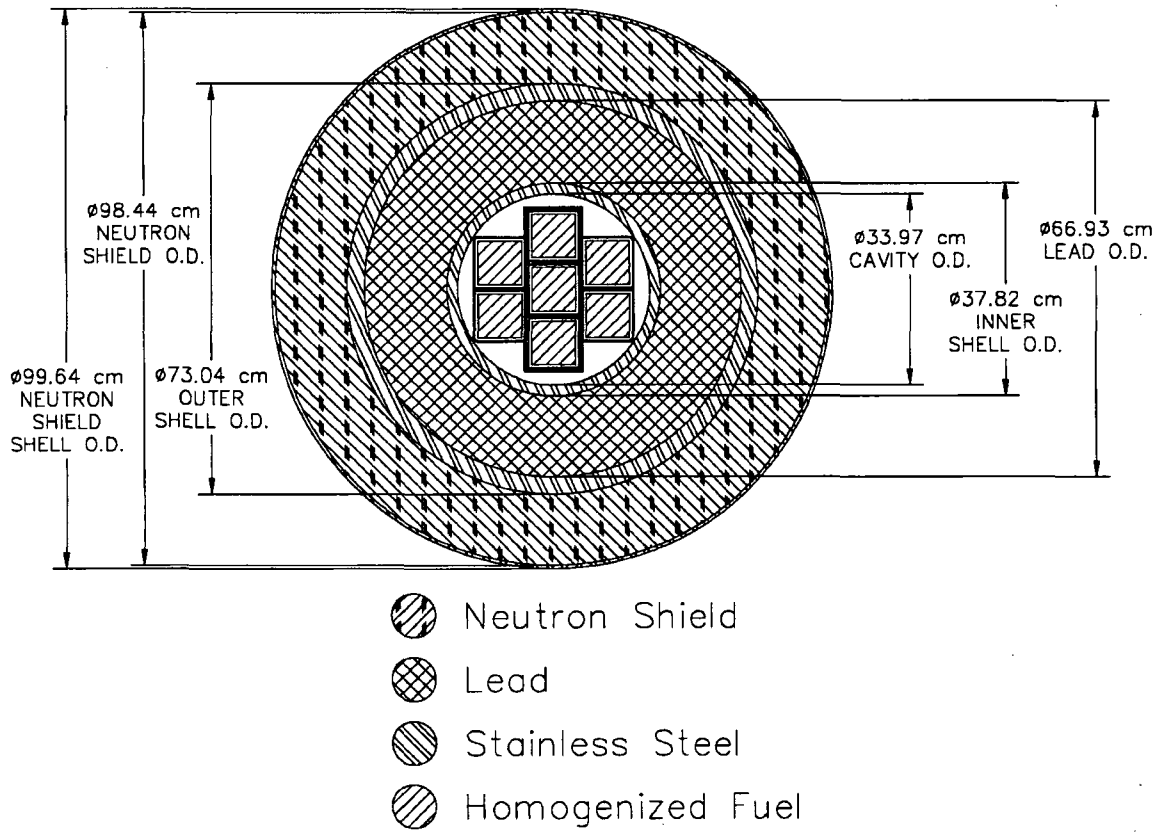


Figure 5.3.14-5 Sample MCNP Input File for Minimum Height Canned PULSTAR Fuel

```

NAC-LWT Cask - Cmin_50b50e01y - Normal Transport Conditions
C Radial Biasing - Fuel Gamma Source
C Canned Homogenized Fuel - Cells
1 1 -10.2184 -1 u=5 $ Can
2 0 +1 u=5 $ Outside
C Cells - MTR 7 Element Basket
7 6 -7.9400 -6 +9 +10 +11 +12 +13 +14 +15 u=4 $ Base plate
8 6 -7.9400 -7 +16 +20 u=4 $ Support plate
9 6 -7.9400 -8 +16 +20 u=4 $ Support plate
10 6 -7.9400 -16 +17 #7 #8 #9 u=4 $ Center column
11 6 -7.9400 -18 #7 #8 #9 u=4 $ Center divider upper
12 6 -7.9400 -19 #7 #8 #9 u=4 $ Center divider lower
13 6 -7.9400 -20 +21 +16 #7 #8 #9 u=4 $ Small side
14 6 -7.9400 -22 #7 #8 #9 u=4 $ Left divider
15 6 -7.9400 -23 #7 #8 #9 u=4 $ Right divider
16 0 #7 #8 #9 #10 #11 #12 #13 #14 #15 u=4 $ Void
C Cells - Basket Cavity
17 0 -1 fill=5 trcl = ( 0.0000 0.0000 88.3239 ) u=3 $ CC
18 like 17 but fill=5 trcl = ( 0.0000 9.5250 88.3239 ) u=3 $ UC
19 like 17 but fill=5 trcl = ( 0.0000 -9.5250 88.3239 ) u=3 $ LC
20 like 17 but fill=5 trcl = ( -9.5250 4.6990 88.3239 ) u=3 $ UL
21 like 17 but fill=5 trcl = ( -9.5250 -4.6990 88.3239 ) u=3 $ LL
22 like 17 but fill=5 trcl = ( 9.5250 4.6990 88.3239 ) u=3 $ UR
23 like 17 but fill=5 trcl = ( 9.5250 -4.6990 88.3239 ) u=3 $ LR
24 0 #17 #18 #19 #20 #21 #22 #23 fill=4 u=3 $ Void
C Cells - LWT Cavity
25 0 -31 fill=3 ( 0.0000 0.0000 3.8100 ) u=2
26 0 -32 fill=3 ( 0.0000 0.0000 115.5700 ) u=2
27 0 -33 fill=3 ( 0.0000 0.0000 227.3300 ) u=2
28 0 -34 fill=3 ( 0.0000 0.0000 339.0900 ) u=2
29 0 #25 #26 #27 #28 u=2
C Cells - LWT Cask Normal Conditions
30 5 -11.344 -38 u=1 $ BotPb
31 0 -37 fill=2 u=1 $ Cavity
32 6 -7.9400 -35 -36 +38 u=1 $ Bottom
33 6 -7.9400 -35 +36 +40 +43 +37 u=1 $ OuterShell
34 6 -7.9400 -39 +42 +37 u=1 $ InnerShellTaper
35 6 -7.9400 -41 +37 u=1 $ InnerShell
36 5 -11.344 -42 +41 u=1 $ Lead
37 5 -11.344 -40 +39 +42 u=1 $ LeadTaper
38 0 -43 +42 u=1 $ LeadGap
39 3 -0.9669 -45 +35 u=1 $ NeutronShield
40 6 -7.9400 -44 +35 +45 u=1 $ NSShell
41 7 -0.4997 -46 +35 u=1 $ UpperLimiter
42 7 -0.4997 -47 +35 u=1 $ LowerLimiter
43 0 -48 +35 +44 +46 +47 u=1 $ Container
44 0 +48 u=1 $ Outside
C Detector Cells - Radial Biasing
100 0 -100 fill=1 $ Surface
200 0 -200 +100 $ 1ft
300 0 -300 +100 +200 $ 1m
400 0 -400 +100 +200 +300 $ 2m
500 0 -500 +100 +200 +300 +400 $ 2m+Convey
600 0 +100 +200 +300 +400 +500 $ Exterior
C Canned Homogenized Fuel - Surfaces
1 RPP -4.1910 4.1910 -4.1910 0.0000 23.4361 $ Can
C Surfaces - MTR 7 Element Basket
6 RCC 0.0000 0.0000 0.0000 0.0000 0.0000 1.2700 16.8466 $ Base plate
7 RCC 0.0000 0.0000 52.0700 0.0000 0.0000 1.2700 16.8466 $ Support plate
8 RCC 0.0000 0.0000 104.1400 0.0000 0.0000 1.2700 16.8466 $ Support plate
9 CZ 1.2700 $ Hole CC
10 C/Z 0.0000 9.5250 1.2700 $ Hole UC
11 C/Z 0.0000 -9.5250 1.2700 $ Hole LC
12 C/Z -9.5250 4.6990 1.2700 $ Hole UL
13 C/Z -9.5250 -4.6990 1.2700 $ Hole LL
14 C/Z 9.5250 4.6990 1.2700 $ Hole UR
15 C/Z 9.5250 -4.6990 1.2700 $ Hole LR
16 RPP -5.1604 5.1604 -14.6939 14.6939 1.2700 111.7600 $ Center column outer
17 RPP -4.3667 4.3667 -13.9002 13.9002 1.2700 111.7600 $ Center column inner
18 RPP -4.3667 4.3667 4.3688 5.1626 1.2700 111.7600 $ Center divider upper
19 RPP -4.3667 4.3667 -5.1626 -4.3688 1.2700 111.7600 $ Center divider lower
20 RPP -14.1986 14.1986 -9.3599 9.3599 1.2700 111.7600 $ Small side outer
21 RPP -13.8938 13.8938 -9.0551 9.0551 1.2700 111.7600 $ Small side inner
22 RPP -13.8938 -5.1604 -0.3175 0.3175 1.2700 111.7600 $ Left divider
23 RPP 5.1604 13.8938 -0.3175 0.3175 1.2700 111.7600 $ Right divider
C Surfaces - LWT Cavity
31 RCC 0.0000 0.0000 3.8100 0.0000 0.0000 111.7600 16.8467 $ Basket
32 RCC 0.0000 0.0000 115.5700 0.0000 0.0000 111.7600 16.8467 $ Basket
33 RCC 0.0000 0.0000 227.3300 0.0000 0.0000 111.7600 16.8467 $ Basket
34 RCC 0.0000 0.0000 339.0900 0.0000 0.0000 111.7600 16.8467 $ Basket
C Surfaces - LWT Cask Normal Conditions
35 RCC 0.0000 0.0000 -26.6700 0.0000 0.0000 507.3650 36.5189 $ Lwt
36 RCC 0.0000 0.0000 -26.6700 0.0000 0.0000 26.6700 36.5189 $ Bottom
37 RCC 0.0000 0.0000 0.0000 0.0000 0.0000 452.1200 16.9863 $ Cavity
38 RCC 0.0000 0.0000 -17.7800 0.0000 0.0000 7.6200 26.3525 $ Bottom gamma shield
39 RCC 0.0000 0.0000 0.0000 0.0000 0.0000 444.5000 20.1740 $ Lead id - taper
40 RCC 0.0000 0.0000 0.0000 0.0000 0.0000 444.5000 31.5976 $ Lead od - taper
41 RCC 0.0000 0.0000 13.8176 0.0000 0.0000 416.8648 18.9103 $ Lead id
42 RCC 0.0000 0.0000 13.8176 0.0000 0.0000 416.8648 33.3271 $ Lead od
43 RCC 0.0000 0.0000 13.8176 0.0000 0.0000 416.8648 33.4645 $ Lead gap
44 RCC 0.0000 0.0000 3.8100 0.0000 0.0000 419.1000 49.8183 $ Neutron shield shell
45 RCC 0.0000 0.0000 5.0800 0.0000 0.0000 416.5600 49.2189 $ Neutron shield
46 RCC 0.0000 0.0000 450.2150 0.0000 0.0000 70.5612 49.8183 $ Upper limiter
47 RCC 0.0000 0.0000 -68.0212 0.0000 0.0000 71.8312 49.8183 $ Lower limiter

```

Figure 5.3.14-5 Sample MCNP Input File for Minimum Height Canned PULSTAR Fuel

```

48 RCC 0.0000 0.0000 -68.0212 0.0000 0.0000 588.7974 49.8183 $ Container
C Radial Detector DRA (Surface)
100 RCC 0.0000 0.0000 -68.1212 0.0000 0.0000 588.9974 49.9184
101 PZ -38.6713
102 PZ -9.2215
103 PZ 20.2284
104 PZ 49.6783
105 PZ 79.1282
106 PZ 108.5780
107 PZ 138.0279
108 PZ 167.4778
109 PZ 196.9276
110 PZ 226.3775
111 PZ 255.8274
112 PZ 285.2772
113 PZ 314.7271
114 PZ 344.1770
115 PZ 373.6269
116 PZ 403.0767
117 PZ 432.5266
118 PZ 461.9765
119 PZ 491.4263
C Radial Detector DRB (1ft)
200 RCC 0.0000 0.0000 -98.6012 0.0000 0.0000 649.9574 80.2984
201 PZ -66.1033
202 PZ -33.6055
203 PZ -1.1076
204 PZ 31.3903
205 PZ 63.8882
206 PZ 96.3860
207 PZ 128.8839
208 PZ 161.3818
209 PZ 193.8796
210 PZ 226.3775
211 PZ 258.8754
212 PZ 291.3732
213 PZ 323.8711
214 PZ 356.3690
215 PZ 388.8669
216 PZ 421.3647
217 PZ 453.8626
218 PZ 486.3605
219 PZ 518.8583
C Radial Detector DRC (1m)
300 RCC 0.0000 0.0000 -168.1212 0.0000 0.0000 788.9974 149.8184
301 PZ -135.2463
302 PZ -102.3714
303 PZ -69.4965
304 PZ -36.6216
305 PZ -3.7467
306 PZ 29.1282
307 PZ 62.0030
308 PZ 94.8779
309 PZ 127.7528
310 PZ 160.6277
311 PZ 193.5026
312 PZ 226.3775
313 PZ 259.2524
314 PZ 292.1273
315 PZ 325.0022
316 PZ 357.8771
317 PZ 390.7520
318 PZ 423.6269
319 PZ 456.5017
320 PZ 489.3766
321 PZ 522.2515
322 PZ 555.1264
323 PZ 588.0013
C Radial Detector DRD (2m)
400 RCC 0.0000 0.0000 -268.1212 0.0000 0.0000 988.9974 249.8184
401 PZ -226.9130
402 PZ -185.7048
403 PZ -144.4965
404 PZ -103.2883
405 PZ -62.0801
406 PZ -20.8719
407 PZ 20.3364
408 PZ 61.5446
409 PZ 102.7528
410 PZ 143.9611
411 PZ 185.1693
412 PZ 226.3775
413 PZ 267.5857
414 PZ 308.7940
415 PZ 350.0022
416 PZ 391.2104
417 PZ 432.4186
418 PZ 473.6269
419 PZ 514.8351
420 PZ 556.0433
421 PZ 597.2515
422 PZ 638.4598
423 PZ 679.6680

```

Figure 5.3.14-5 Sample MCNP Input File for Minimum Height Canned PULSTAR Fuel

```

C Radial Detector DRE (2m+Convey)
500 RCC 0.0000 0.0000 -269.1212 0.0000 0.0000 990.9974 321.9200
501 PZ -227.8296
502 PZ -186.5381
503 PZ -145.2465
504 PZ -103.9550
505 PZ -62.6634
506 PZ -21.3719
507 PZ 19.9197
508 PZ 61.2113
509 PZ 102.5028
510 PZ 143.7944
511 PZ 185.0859
512 PZ 226.3775
513 PZ 267.6691
514 PZ 308.9606
515 PZ 350.2522
516 PZ 391.5437
517 PZ 432.8353
518 PZ 474.1269
519 PZ 515.4184
520 PZ 556.7100
521 PZ 598.0015
522 PZ 639.2931
523 PZ 680.5846

C
C Materials List
C
C Homogenized UO2 Fuel
m1 92235 -4.7547E-02 40000 -9.9220E-02 24000 -1.0101E-04
    92238 -7.4491E-01 50000 -1.5152E-03 7014 -5.0507E-05
    8016 -1.0653E-01 26000 -1.2627E-04

C Water
m2 1001 6.6667E-01 8016 3.3333E-01
mt2 lwtr.01
C Water/Glycol
m3 1001 -1.03651E-01 8016 -6.75619E-01 6000 -2.20730E-01
C Aluminum
m4 13027 -1.0
C Lead
m5 82000 -1.0
C Stainless Steel 304
m6 26000 -0.695 24000 -0.190 28000 -0.095
    25055 -0.020
C Aluminum Honeycomb Impact Limiter
m7 13027 -1.0
C Zircaloy
m8 40000 -9.8225E-01 50000 -1.5000E-02 26000 -1.2500E-03
    24000 -1.0000E-03 7014 -5.0000E-04
nonu $ No subcritical multiplication
C
C Cell Importances
imp:p 1 44r 0
C
C Source Definition - Fuel Gamma
C 50% burnup, 6 wt % U-235, 1-year cool time, 32 g U-235 per rod, 37.67 W/assy
sdef x=d1 y=d2 z=d3 erg=d4 cell=100:31:d5:d6:1
si1 -4.1910 4.1910
sp1 0 1
si2 -4.1910 4.1910
sp2 0 1
si3 0.0000 23.4361
sp3 0 1
si4 1.000E-02 2.000E-02 5.000E-02 1.000E-01 2.000E-01 3.000E-01
    4.000E-01 6.000E-01 8.000E-01 1.000E+00 1.220E+00 1.440E+00
    1.660E+00 2.000E+00 2.500E+00 3.000E+00 4.000E+00 5.000E+00
    6.500E+00 8.000E+00 1.000E+01 1.200E+01 1.400E+01
sp4 0.0000E+00 3.1584E+13 4.4346E+13 2.1659E+13 2.0132E+13 5.0486E+12
    3.7916E+12 2.1998E+13 6.1006E+13 8.1897E+12 1.5636E+12 1.4912E+12
    3.3074E+11 7.9476E+10 4.1847E+11 4.9183E+09 5.8148E+08 2.4473E+04
    9.8056E+03 1.9207E+03 4.0738E+02 2.1050E+01 0.0000E+00
si5 1 25 26 27 28
sp5 1.0 1.0 1.0 1.0
si6 1 17 18 19 20 21 22 23
sp6 1.0 1.0 1.0 1.0 1.0 1.0 1.0
mode p
nps 40000000
C
C ANSI/ANS-6.1.1-1977 - Gamma Flux-to-Dose Conversion Factors
C (mrem/hr)/(photons/cm2-sec)
de0 0.01 0.03 0.05 0.07 0.1 0.15 0.2
    0.25 0.3 0.35 0.4 0.45 0.5 0.55
    0.6 0.65 0.7 0.8 1 1.4 1.8
    2.2 2.6 2.8 3.25 3.75 4.25 4.75
    5 5.25 5.75 6.25 6.75 7.5 9
    11 13 15
df0 3.96E-03 5.82E-04 2.90E-04 2.58E-04 2.83E-04 3.79E-04 5.01E-04
    6.31E-04 7.59E-04 8.78E-04 9.85E-04 1.08E-03 1.17E-03 1.27E-03
    1.36E-03 1.44E-03 1.52E-03 1.68E-03 1.98E-03 2.51E-03 2.99E-03
    3.42E-03 3.82E-03 4.01E-03 4.41E-03 4.83E-03 5.23E-03 5.60E-03
    5.80E-03 6.01E-03 6.37E-03 6.74E-03 7.11E-03 7.66E-03 8.77E-03
    1.03E-02 1.18E-02 1.33E-02
C

```

Figure 5.3.14-5 Sample MCNP Input File for Minimum Height Canned PULSTAR Fuel

```

C Weight Window Generation - Radial
wwg 2 0 0 0 0
wwp:p 5 3 5 0 -1 0
mesh geom=cyl ref=0 13 316 origin=0.1 0.1 -568
      imesh 16.8 17.0 18.9 33.3 36.5 49.2 49.8 549.8
      iints 1 1 1 5 1 1 1 1
      jmesh 500 541 550 558 568 659 1019 1020 1049 1089 1589
      jint 1 1 1 1 1 1 1 1 1 1
      kmesh 1
      kints 1
wwge:p 1e-3 1 20
fc2 Radial Surface Tally
f2:p +100.1
fm2 6.20620E+15
fs2 -101 -102 -103 -104 -105 -106
     -107 -108 -109 -110 -111 -112
     -113 -114 -115 -116 -117 -118
     -119 T
tf2
fc12 Radial 1ft Tally
f12:p +200.1
fm12 6.20620E+15
fs12 -201 -202 -203 -204 -205 -206
     -207 -208 -209 -210 -211 -212
     -213 -214 -215 -216 -217 -218
     -219 T
tf12
fc22 Radial 1m Tally
f22:p +300.1
fm22 6.20620E+15
fs22 -301 -302 -303 -304 -305 -306
     -307 -308 -309 -310 -311 -312
     -313 -314 -315 -316 -317 -318
     -319 -320 -321 -322 -323 T
tf22
fc32 Radial 2m Tally
f32:p +400.1
fm32 6.20620E+15
fs32 -401 -402 -403 -404 -405 -406
     -407 -408 -409 -410 -411 -412
     -413 -414 -415 -416 -417 -418
     -419 -420 -421 -422 -423 T
tf32
fc42 Radial 2m+Convey Tally
f42:p +500.1
fm42 6.20620E+15
fs42 -501 -502 -503 -504 -505 -506
     -507 -508 -509 -510 -511 -512
     -513 -514 -515 -516 -517 -518
     -519 -520 -521 -522 -523 T
tf42
C
C Print Control
prtmp -30 -60 1 2
print
C Random Number Generator
rand gen=2 seed=19073486328125 stride=152917 hist=1

```

Figure 5.3.14-6 Normal Condition Axial Surface Dose Rate Profile by Source Type – Minimum Height Canned PULSTAR Fuel

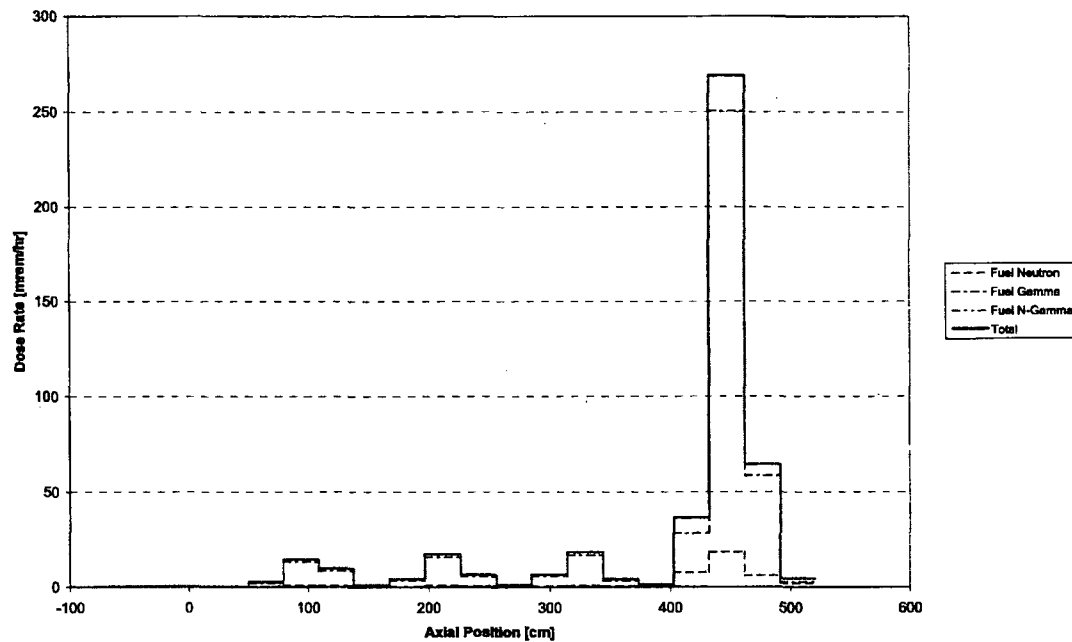
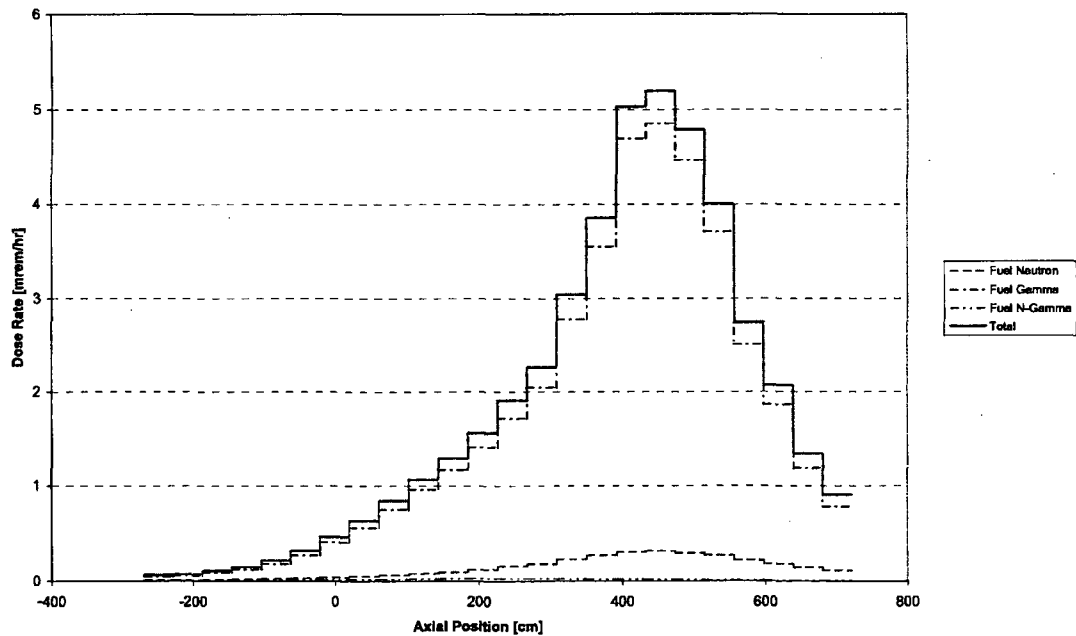


Figure 5.3.14-7 Normal Condition Radial 2m Dose Rate Profile by Source Type – Minimum Height Canned PULSTAR Fuel



**Figure 5.3.14-8 Accident Condition Radial 1m Dose Rate Profile by Source Type –
Minimum Height Canned PULSTAR Fuel**

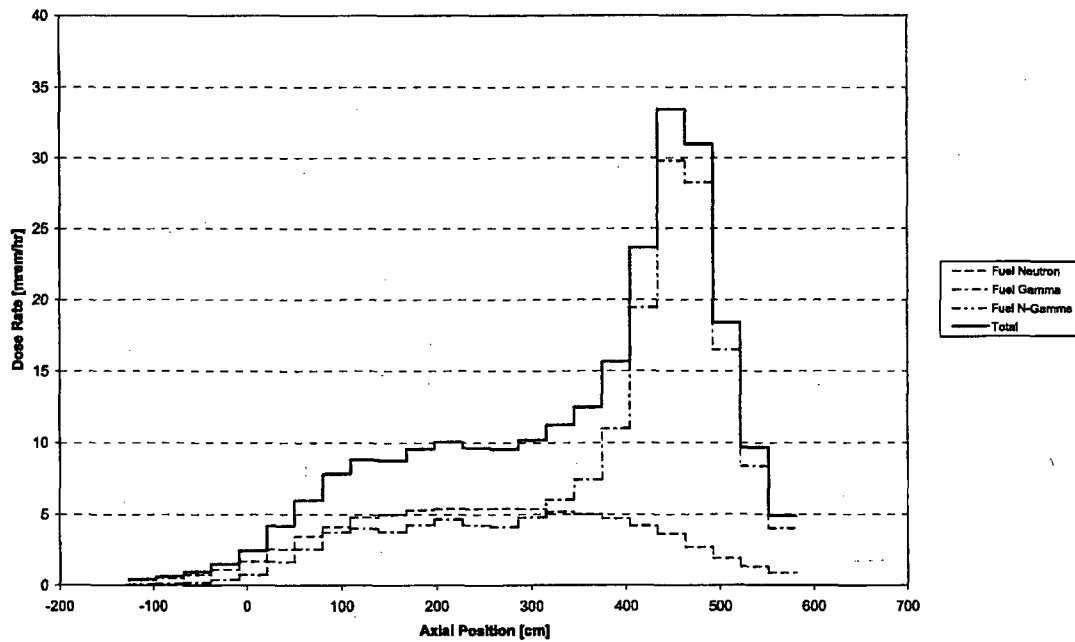


Table 5.3.14-1 PULSTAR Fuel Geometry

Parameter	Value
Pellet Diameter (inch)	0.423
Clad Thickness (inch)	0.0185
Rod Diameter (inch)	0.47
Rod Pitch (inch)	0.606×0.524
Active Fuel Length (inch)	24.1
Assembly Width (inch)	3.15×2.74
Zirconium Alloy Box Thickness (inch)	0.06
Lower Fitting Height (inch)	5.4
Upper Fitting Height (inch)	8.5
Assembly Height (inch)	38

Table 5.3.14-2 Source Term Generation Parameters for PULSTAR Fuel

Parameter	Value
²³⁵ U Mass Per Rod (grams)	32
Assembly Power (MW/assy)	0.08
Initial Enrichment (wt % ²³⁵ U)	6.0
Burnup (% ²³⁵ U) ¹	45
Moderator/Box Temperature (K)	333.15
Clad Temperature (K)	433.15
Fuel Temperature (K)	633.15

¹ Target burnup was 50% depletion. Due to fissile material build-up, actual depletion is 46%. A maximum 45% depletion is conservatively applied in the fuel limits.

Table 5.3.14-3 PULSTAR Fuel Assembly Neutron Source Term for 1 Year Cool Time

Group	E Lower [MeV]	E Upper [MeV]	Source [neutrons/sec]
1	1.360E+01	1.460E+01	0.000E+00
2	1.250E+01	1.360E+01	4.387E+01
3	1.125E+01	1.250E+01	1.828E+02
4	1.000E+01	1.125E+01	6.036E+02
5	8.250E+00	1.000E+01	1.897E+03
6	7.000E+00	8.250E+00	5.130E+03
7	6.070E+00	7.000E+00	8.887E+03
8	4.720E+00	6.070E+00	2.932E+04
9	3.680E+00	4.720E+00	6.083E+04
10	2.870E+00	3.680E+00	1.004E+05
11	1.740E+00	2.870E+00	2.023E+05
12	6.400E-01	1.740E+00	2.571E+05
13	3.900E-01	6.400E-01	6.590E+04
14	1.100E-01	3.900E-01	2.289E+04
15	6.740E-02	1.100E-01	2.636E+00
16	2.480E-02	6.740E-02	0.000E+00
17	9.120E-03	2.480E-02	0.000E+00
18	2.950E-03	9.120E-03	0.000E+00
19	9.610E-04	2.950E-03	0.000E+00
20	3.540E-04	9.610E-04	0.000E+00
21	1.660E-04	3.540E-04	0.000E+00
22	4.810E-05	1.660E-04	0.000E+00
23	1.600E-05	4.810E-05	0.000E+00
24	4.000E-06	1.600E-05	0.000E+00
25	1.500E-06	4.000E-06	0.000E+00
26	5.500E-07	1.500E-06	0.000E+00
27	7.090E-08	5.500E-07	0.000E+00
28	1.000E-11	7.090E-08	0.000E+00
Total			7.555E+05

Table 5.3.14-4 PULSTAR Fuel Assembly Gamma Source Term for 1 Year Cool Time

Group	E Lower [MeV]	E Upper [MeV]	Source [photons/sec]
1	1.20E+01	1.40E+01	0.0000E+00
2	1.00E+01	1.20E+01	2.1050E+01
3	8.00E+00	1.00E+01	4.0738E+02
4	6.50E+00	8.00E+00	1.9207E+03
5	5.00E+00	6.50E+00	9.8056E+03
6	4.00E+00	5.00E+00	2.4473E+04
7	3.00E+00	4.00E+00	5.8148E+08
8	2.50E+00	3.00E+00	4.9183E+09
9	2.00E+00	2.50E+00	4.1847E+11
10	1.66E+00	2.00E+00	7.9476E+10
11	1.44E+00	1.66E+00	3.3074E+11
12	1.22E+00	1.44E+00	1.4912E+12
13	1.00E+00	1.22E+00	1.5636E+12
14	8.00E-01	1.00E+00	8.1897E+12
15	6.00E-01	8.00E-01	6.1006E+13
16	4.00E-01	6.00E-01	2.1998E+13
17	3.00E-01	4.00E-01	3.7916E+12
18	2.00E-01	3.00E-01	5.0486E+12
19	1.00E-01	2.00E-01	2.0132E+13
20	5.00E-02	1.00E-01	2.1659E+13
21	2.00E-02	5.00E-02	4.4346E+13
22	1.00E-02	2.00E-02	3.1584E+13
Total			2.2165E+14

Table 5.3.14-5 Intact Assembly Fuel Homogenization for PULSTAR Fuel

Component	Area	Area	Volume Fraction of Components		
	[cm ²]	Fraction	UO ₂	Void	Clad
Fuel	2.2666E+01	4.4255E-01	4.4255E-01		
Gap	1.0844E+00	2.1172E-02		2.1172E-02	
Clad	4.2324E+00	8.2637E-02			8.2637E-02
Void	2.3234E+01	4.5364E-01		4.5364E-01	
Total	5.1217E+01	1.0000E+00	4.4255E-01	4.7481E-01	8.2637E-02

Table 5.3.14-6 Nominal Height Can Fuel Homogenization for PULSTAR Fuel

Component	Volume	Volume	Volume Fraction of Components		
	[cm ³]	Fraction	UO ₂	Void	Clad
Fuel	1.3875E+03	2.5917E-01	2.5917E-01		
Clad	2.5908E+02	4.8394E-02			4.8394E-02
Void	3.7071E+03	6.9244E-01		6.9244E-01	
Total	5.3537E+03	1.0000E+00	2.5917E-01	6.9244E-01	4.8394E-02

Table 5.3.14-7 Minimum Height Can Fuel Homogenization for PULSTAR Fuel

Component	Volume	Volume	Volume Fraction of Components		
	[cm ³]	Fraction	UO ₂	Void	Clad
Fuel	1.3875E+03	8.4265E-01	8.4265E-01		
Clad	2.5908E+02	1.5735E-01			1.5735E-01
Void	0.0000E+00	0.0000E+00		0.0000E+00	
Total	1.6466E+03	1.0000E+00	8.4265E-01	0.0000E+00	1.5735E-01

Table 5.3.14-8 Fuel Region Homogenized Material Description for PULSTAR Fuel

Element	Model Number Density [atom/b-cm]		
	Assembly (5.37 g/cm ³)	Nominal Height Can (3.14 g/cm ³)	Minimum Height Can (10.22 g/cm ³)
²³⁵ U	6.5376E-04	3.8286E-04	1.2448E-03
Zr	3.5151E-03	2.0585E-03	6.6930E-03
Cr	6.2782E-06	3.6767E-06	1.1954E-05
²³⁸ U	1.0113E-02	5.9224E-03	1.9256E-02
Sn	4.1250E-05	2.4157E-05	7.8543E-05
N	1.1657E-05	6.8263E-06	2.2195E-05
O	2.1525E-02	1.2605E-02	4.0984E-02
Fe	7.3071E-06	4.2792E-06	1.3913E-05

Table 5.3.14-9 Cask/Basket Material Descriptions for PULSTAR Fuel

Material	Element	Density [g/cm ³]	Number Density [atom/b-cm]
Stainless Steel 304	Fe	7.94	5.9505E-02
	Cr		1.7472E-02
	Ni		7.7392E-03
	Mn		1.7407E-03
Lead	Pb	11.34	3.2967E-02
Neutron Shield	H	0.97	5.9884E-02
	O		2.4595E-02
	C		1.0701E-02
Impact Limiter	Al	0.50	1.1153E-02
Zirconium alloy	Zr	6.56	4.2537E-02
	Sn		4.9917E-04
	Fe		8.8422E-05
	Cr		7.5976E-05
	N		1.4106E-04

Table 5.3.14-10 Maximum Radial Dose Rates for PULSTAR Fuel

Source Model	Dose Rate [mrem/hr]				
	Normal Surface	Normal 1 meter	Normal 2 meter	Accident Surface	Accident 1 meter
Assembly	24.3	4.5	1.7	108	15.5
Nominal Can	222	21.8	5.1	430	32.0
Minimum Can	269	24.6	5.2	511	33.4

Table 5.3.14-11 Maximum Axial Dose Rates for PULSTAR Fuel

Source Model	Dose Rate [mrem/hr]			
	Normal – Surface		Accident – Surface	
	Top	Bottom	Top	Bottom
Assembly	2.5	0.9	18.4	6.3
Nominal Can	7.8	0.7	73.3	5.0
Minimum Can	11.6	0.1	81.1	1.0

5.3.15 Spiral Fuel Assembly Configuration

A maximum payload of 42 spiral fuel assemblies has been analyzed for transport in the LWT cask. The fuel assemblies are configured in six ANSTO basket modules with one fuel assembly loaded in each of the seven cells in each basket module. The cells in each basket module are arranged with one center cell (fuel tube structure) surrounded by six other cells.

Assemblies are evaluated for a uniform loading of 18W, matching the lower of the DIDO heat load allowables, and at sources matching the MEU DIDO fuel burnup minimum cool time curve. Thus, basket module maximum heat loads of 126W (0.756 kW per cask) are permissible. Only uniform loading configurations are considered.

The spiral fuel assembly consists of curved fuel plates located within an inner and outer concentric aluminum shell. The physical characteristics of the analyzed spiral assembly are shown in Table 5.3.15-1. The active fuel section of the assembly consists of 10 plates. The fuel core of each fuel plate is an alloy of aluminum and uranium. The assembly is evaluated at a bounding maximum fissile material mass of 160 grams ^{235}U per assembly and a minimum enrichment of 75 wt % ^{235}U .

The SAS2H sequence was used to determine the gamma and neutron source terms and decay heat loads for the spiral assembly. The SAS2H sequence includes the ORIGEN-S code and a 1-D XSDRNP model of the fuel assembly. ORIGEN-S performs fuel assembly depletion at specified operating conditions and calculates heat generation, gamma and neutron spectra for a given discharge isotopic composition as a function of out of reactor time (cooling time). The 1-D model of the fuel assembly is used to collapse the 27-group neutron cross-section library (27GROUPNDF4) into three broad energy groups for the depletion calculation. The 1-D model is based on an equivalent area representation of the fuel/moderator cell and surrounding structural regions. Average power is based on reactor maximum power divided by the number of assemblies in the core. Assembly burnup is modeled in four cycles of equal length with 30 days of down time between cycles. This burnup description bounds typical research reactor use, where fuel is burned over a period of years or even decades to achieve the optimal discharge burnup. The SAS2H input for the 18W, 70% depleted case is shown in Figure 5.3.15-1. The SAS2H input contains relevant operating parameters such as power density and number of days of irradiation, in addition to the material compositions employed.

A series of seven cases were run in which burnup was varied from a depletion of 10% to 70%. Cooling times were considered from 90 days to 3.5 years. Because the cask is loaded based on the decay heat limits at various depletion steps, no single loading configuration exists.

Design basis gamma and neutron source terms for the spiral assembly with decay heat loads of 18 watts are listed in Table 5.3.15-2. A source comparison by energy line, total source, and for the energy lines significant to the shielding evaluations is shown in Table 5.3.15-3. Energy line comparisons are also illustrated in Figure 5.3.15-2. Source comparisons are made at the 70% depletion level, which was shown to be bounding for DIDO type fuel evaluations. Source terms are similar to those of the DIDO assembly with slightly lower sources at the shielding-controlling energy lines.

A cool time curve comparison for the DIDO MEU and spiral fuel assemblies is included in Figure 5.3.15-3. The spiral fuel requires less time to meet the 18-watt heat load level per element than the MEU DIDO element. To illustrate the additional source margin for spiral fuel assemblies when applying the MEU DIDO fuel cool time figure, spectrums are generated at the DIDO limited cool time values. As indicated in Table 5.3.15-4, a significant source margin exists when restricting the spiral assembly to DIDO minimum cool times.

The ANSTO basket is a slightly modified version of the DIDO basket, with each basket containing seven tubes designed to hold one fuel assembly in each tube. ANSTO fuel tubes are slightly larger in diameter and thickness.

Parameter	DIDO Basket	ANSTO Basket
Fuel Assembly Openings	7	7
Fuel Tube OD (inch)	4.25	4.375
Fuel Tube Wall Thickness (inch)	0.120	0.125

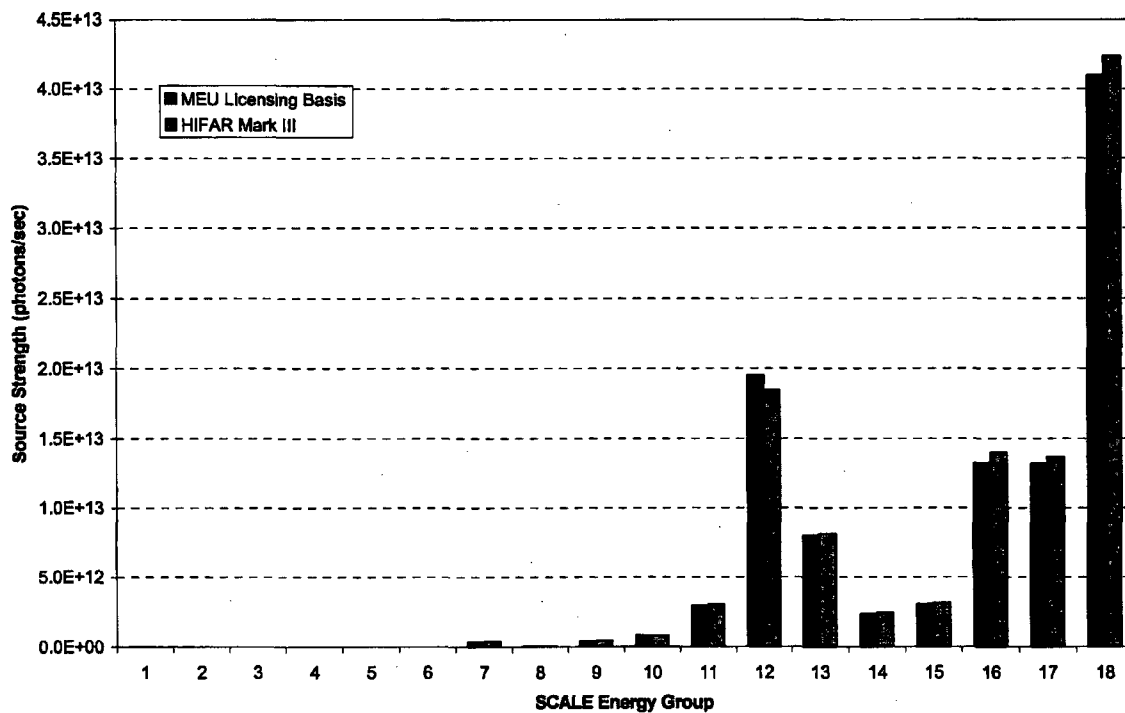
The DIDO basket contains aluminum heat transfer components, while the ANSTO basket contains additional support disks. The aluminum heat transfer components were not included in the DIDO shielding evaluations.

Combining a lower spiral fuel assembly source with a similar basket design demonstrates that DIDO shielding evaluations, and the dose rates produced by the evaluations, bound those expected from the spiral fuel shipments.

Figure 5.3.15-1 SAS2H Input for Spiral Fuel 70% ²³⁵U Depletion and 18-Watt Heat Load

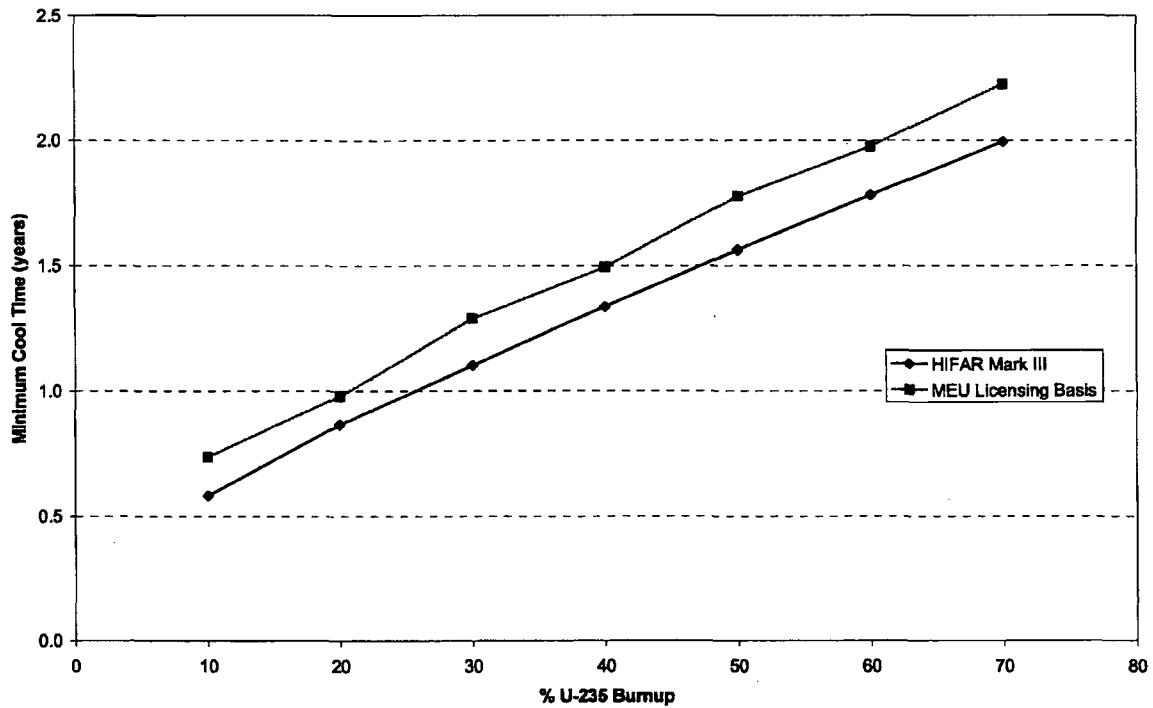
```
=SAS2H          PARM=(HALT04,SKIPSHIPDATA)
HIFAR Mark III Fuel, 70% U-235 BURNUP, 160g, 18W
27GROUPNDF4 LATTICECELL
URANIUM 1 DEN=0.965 1.0 373 92235 75.00 92238 25.00 END
AL 1 DEN=1.575 1.0 373 END
AL      2 1.0 323 END
D2O     3 DEN=1.0948 1.0 313 END
END COMP
SYMMSLABCELL 0.634 0.0489 1 3 0.1439 2 END
NPIN=3 FUEL=60.325 VOLF=220.957 NCYC=4 NLIB=1
PRIN=6 INPL=2 NUMZ=5 NUMH=0
3 2.91 2 3.0225 500 4.925 2 5.08 3 8.598
POWER=0.4000 BURN=64.16 DOWN=30 END
POWER=0.4000 BURN=64.16 DOWN=30 END
POWER=0.4000 BURN=64.16 DOWN=30 END
POWER=0.4000 BURN=64.16 DOWN=90 END
END
=ORIGENS
0$$$ A4 21 A8 26 A10 51 71 E
1$$$ 1 1T
COOLING TO 729 DAYS AND FISSION PRODUCT GAMMA REBIN
3$$$ 21 0 1 A33 -86 E
54$$$ A8 1 E T
35$$$ 0 T
56$$$ 0 1 A13 -2 4 3 E
57** 90 E T
COOLING TO 729 DAYS AND FISSION PRODUCT GAMMA REBIN
SINGLE REACTOR ASSEMBLY
60** 729
65$$$ A4 1 A7 1 A10 1 A25 1 A28 1 A31 1 A46 1 A49 1 A52 1 E
61** F.0001
81$$$ 2 51 26 1 E
82$$$ F6 T
FISSION PRODUCT GAMMA SPECTRA IN SCALE 18 GROUPS
56$$$ F0 T
END
=ORIGENS
0$$$ A4 21 A8 26 A10 51 71 E
1$$$ 1 1T
COOLING TO 729 DAYS AND ACTINIDE GAMMA REBIN
3$$$ 21 0 1 A33 -86 E
54$$$ A8 1 E T
35$$$ 0 T
56$$$ 0 1 A13 -2 4 3 E
57** 90 E T
COOLING TO 729 DAYS AND ACTINIDE GAMMA REBIN
SINGLE REACTOR ASSEMBLY
60** 729
65$$$ A4 1 A7 1 A10 1 A25 1 A28 1 A31 1 A46 1 A49 1 A52 1 E
61** F.0001
81$$$ 2 51 26 1 E
82$$$ F5 T
ACTINIDE GAMMA SPECTRA IN SCALE 18 GROUPS
56$$$ F0 T
END
```


Figure 5.3.15-2 Spiral Fuel versus MEU DIDO Gamma Spectrum Comparison
(18 Watts, 70% Depletion)



Note: HIFAR Mark III type designation refers to spiral fuel. MEU licensing basis refers to DIDO MEU fuels as discussed in Section 5.3.9.

Figure 5.3.15-3 Minimum Cool Time Curve for 18-Watt Heat Load (Spiral Fuel and MEU DIDO)



Note: HIFAR Mark III type designation refers to spiral fuel. MEU licensing basis refers to DIDO MEU fuels as discussed in Section 5.3.9.

Table 5.3.15-1 Spiral Fuel Assembly Characteristics

Parameter	Unit	Value
Inner Aluminum Plate ID	[cm]	5.82
Inner Aluminum Plate OD	[cm]	6.045
Outer Aluminum Plate ID	[cm]	9.85
Outer Aluminum Plate OD	[cm]	10.16
Number of Fuel Plates		10
Active Fuel Width ¹	[cm]	6
Active Fuel Thickness ²	[cm]	0.061
Active Fuel Length	[cm]	60.325
Plate Width ³	[cm]	7.33
Plate Thickness ⁴	[cm]	0.147
Total Element Length	[cm]	63.5
Plate Pitch ⁵	[cm]	0.6342
Minimum Enrichment (wt % ²³⁵ U)		75%
Maximum ²³⁵ U per Fuel Assembly	[g]	160
Modeled Assembly Power Level	[MW]	0.4000
U wt % in Fuel Composition		38%
Mass of Uranium	[g]	213.3
Fuel Composition		U-Al

¹ In conjunction with fuel meat thickness used to calculate total fuel meat volume. Fuel meat thickness adjusted to conserve fuel meat volume.

² Adjusted to 0.0489 cm to conserve volume (mass).

³ In conjunction with plate thickness used to calculate total plate volume. Fuel plate thickness is then adjusted to conserve plate volume (H/U ratio).

⁴ Adjusted to 0.1439 cm to conserve volume (mass) and H/U ratio.

⁵ Modeled pitch represents a set of three concentric cylinders. Uniform set of three fuel cylinders preserves H/U ratio within 2%.

Table 5.3.15-2 Spiral Fuel Assembly Neutron and Gamma Source (18 Watt Heat Load)

Spiral Fuel Neutron Spectra @ 18W - [n/sec/assembly]							
Percent Burnup							
Group ¹	10	20	30	40	50	60	70
1	2.01E-01	8.64E-01	2.29E+00	5.08E+00	1.09E+01	2.48E+01	6.22E+01
2	4.74E+00	1.82E+01	4.79E+01	1.05E+02	2.13E+02	4.33E+02	9.49E+02
3	9.08E+00	3.24E+01	8.42E+01	1.83E+02	3.64E+02	7.04E+02	1.42E+03
4	3.11E+00	1.16E+01	3.02E+01	6.63E+01	1.36E+02	2.77E+02	6.07E+02
5	2.84E+00	1.12E+01	2.95E+01	6.51E+01	1.36E+02	2.93E+02	6.88E+02
6	2.36E+00	9.86E+00	2.61E+01	5.78E+01	1.23E+02	2.75E+02	6.77E+02
7	4.54E-01	1.91E+00	5.05E+00	1.12E+01	2.39E+01	5.33E+01	1.32E+02
Total	2.28E+01	8.60E+01	2.25E+02	4.94E+02	1.01E+03	2.06E+03	4.54E+03

Spiral Fuel Gamma Spectra @ 18W - [g/sec/assembly]							
Percent Burnup							
Group	10	20	30	40	50	60	70
1	7.09E-03	3.01E-02	7.96E-02	1.75E-01	3.69E-01	8.12E-01	1.99E+00
2	3.38E-02	1.43E-01	3.78E-01	8.29E-01	1.75E+00	3.84E+00	9.38E+00
3	1.75E-01	7.37E-01	1.95E+00	4.27E+00	8.99E+00	1.97E+01	4.81E+01
4	4.44E-01	1.86E+00	4.91E+00	1.08E+01	2.26E+01	4.96E+01	1.20E+02
5	5.99E+07	9.49E+07	1.19E+08	1.33E+08	1.40E+08	1.42E+08	1.42E+08
6	8.09E+08	1.07E+09	1.31E+09	1.44E+09	1.49E+09	1.49E+09	1.45E+09
7	2.49E+11	3.71E+11	4.33E+11	4.51E+11	4.43E+11	4.21E+11	3.89E+11
8	2.30E+10	3.49E+10	4.15E+10	4.40E+10	4.41E+10	4.28E+10	4.05E+10
9	1.60E+11	2.43E+11	3.00E+11	3.38E+11	3.65E+11	3.91E+11	4.22E+11
10	2.69E+11	3.75E+11	4.60E+11	5.32E+11	6.03E+11	6.85E+11	7.89E+11
11	3.24E+11	5.99E+11	9.21E+11	1.31E+12	1.75E+12	2.29E+12	2.99E+12
12	6.20E+13	4.01E+13	2.59E+13	1.87E+13	1.63E+13	1.66E+13	1.84E+13
13	4.05E+12	3.41E+12	3.94E+12	4.76E+12	5.69E+12	6.77E+12	8.11E+12
14	1.60E+12	2.16E+12	2.48E+12	2.60E+12	2.61E+12	2.54E+12	2.43E+12
15	2.16E+12	2.81E+12	3.20E+12	3.34E+12	3.36E+12	3.28E+12	3.15E+12
16	1.04E+13	1.28E+13	1.45E+13	1.52E+13	1.51E+13	1.47E+13	1.40E+13
17	9.47E+12	1.23E+13	1.39E+13	1.45E+13	1.46E+13	1.43E+13	1.37E+13
18	2.97E+13	3.76E+13	4.25E+13	4.45E+13	4.48E+13	4.40E+13	4.24E+13
Total	1.20E+14	1.13E+14	1.09E+14	1.06E+14	1.06E+14	1.06E+14	1.07E+14

¹ SCALE 4.3 27N-18G energy structure

Table 5.3.15-3 Spiral Fuel Assembly Source Comparison to DIDO MEU Fuel (70% Depletion and 18 Watts)

Group ¹	g/sec/assy			Group Energy	MeV/sec/assy		
	Spiral Fuel	DIDO MEU	% Diff	Avg. (MeV)	Spiral Fuel	DIDO MEU	% Diff
1	1.9854E+00	3.6156E+00	82%	9.000E+06	1.7869E+07	3.2540E+07	82%
2	9.3816E+00	1.7064E+01	82%	7.250E+06	6.8017E+07	1.2371E+08	82%
3	4.8053E+01	8.7244E+01	82%	5.750E+06	2.7630E+08	5.0165E+08	82%
4	1.2037E+02	2.1810E+02	81%	4.500E+06	5.4167E+08	9.8145E+08	81%
5	1.4171E+08	1.5823E+08	12%	3.500E+06	4.9599E+14	5.5381E+14	12%
6	1.4525E+09	1.5502E+09	7%	2.750E+06	3.9944E+15	4.2631E+15	7%
7	3.8868E+11	3.5325E+11	-9%	2.250E+06	8.7453E+17	7.9481E+17	-9%
8	4.0475E+10	3.9342E+10	-3%	1.830E+06	7.4069E+16	7.1996E+16	-3%
9	4.2164E+11	3.9960E+11	-5%	1.495E+06	6.3035E+17	5.9740E+17	-5%
10	7.8942E+11	8.0635E+11	2%	1.165E+06	9.1967E+17	9.3940E+17	2%
11	2.9876E+12	2.8948E+12	-3%	9.000E+05	2.6888E+18	2.6053E+18	-3%
12	1.8425E+13	1.9469E+13	6%	7.000E+05	1.2898E+19	1.3628E+19	6%
13	8.1110E+12	7.9993E+12	-1%	5.000E+05	4.0555E+18	3.9997E+18	-1%
14	2.4273E+12	2.3302E+12	-4%	3.500E+05	8.4956E+17	8.1557E+17	-4%
15	3.1458E+12	3.0292E+12	-4%	2.500E+05	7.8645E+17	7.5730E+17	-4%
16	1.3951E+13	1.3197E+13	-5%	1.500E+05	2.0927E+18	1.9796E+18	-5%
17	1.3677E+13	1.3157E+13	-4%	7.500E+04	1.0258E+18	9.8678E+17	-4%
18	4.2400E+13	4.0972E+13	-3%	3.000E+04	1.2720E+18	1.2292E+18	-3%
Total	1.0676E+14	1.0464E+14	-2%	—	2.8171E+19	2.8410E+19	1%
>= .7 MeV	2.3054E+13	2.3964E+13	4%	—	1.8089E+19	1.8642E+19	3%
>= .5 MeV	3.1165E+13	3.1963E+13	3%	—	2.2145E+19	2.2642E+19	2%
Group 11-13	2.9524E+13	3.0363E+13	3%	—	1.9642E+19	2.0233E+19	3%

¹ SCALE 4.3 27N-18G energy structure

Table 5.3.15-4 Spiral Fuel Assembly Source Comparison to DIDO MEU Fuel (70% Depletion and Fixed 2.23-Year Cool Time)

Group ¹	DIDO MEU g/sec/assy	Spiral Fuel g/sec/assy
1	3.62E+00	1.91E+00
2	1.71E+01	9.03E+00
3	8.72E+01	4.63E+01
4	2.18E+02	1.16E+02
5	1.58E+08	1.21E+08
6	1.55E+09	1.23E+09
7	3.53E+11	3.17E+11
8	3.93E+10	3.36E+10
9	4.00E+11	3.65E+11
10	8.06E+11	7.10E+11
11	2.89E+12	2.73E+12
12	1.95E+13	1.71E+13
13	8.00E+12	7.29E+12
14	2.33E+12	2.05E+12
15	3.03E+12	2.66E+12
16	1.32E+13	1.17E+13
17	1.32E+13	1.16E+13
18	4.10E+13	3.61E+13
Total	1.05E+14	9.26E+13
% difference		15%

¹ SCALE 4.3 27N-18G energy structure

5.3.16 MOATA Plate Bundle Configuration

A maximum payload of 42 MOATA plate bundles has been analyzed for transport in the NAC-LWT cask. The fuel assemblies are configured in six ANSTO basket modules with one plate bundle loaded in each of the seven cells in each basket module. The cells in each basket module are arranged with one center cell (fuel tube structure) surrounded by six other cells.

Plate bundles are evaluated at a maximum depletion of 4.1 wt % ^{235}U (equivalent to 30,000 MWd/MTU for the modeled bundle) at a minimum cool time of 10 years (reactor shutdown in 1995). This produces a heat load less than 1 watt per bundle. Thus, basket module maximum heat loads of 7 W (42 W per cask) are permissible from a shielding perspective. Maximum heat load is evaluated as 3 W in the thermal evaluation sections. Given the low source terms discussed later in this section, increased source terms associated with a 3 W heat load level would not approach licensing limits for sources within the NAC-LWT cask.

The plate bundles consist of flat fuel plates sandwiched between two thick nonfuel aluminum plates. The physical characteristics of the analyzed plate bundle are shown in Table 5.3.16-1. The active fuel section of the assembly consists of a maximum of 14 plates. The fuel core of each fuel plate is an alloy of aluminum and uranium. The assembly is evaluated at a bounding maximum fissile material mass of 25 grams ^{235}U per plate and a minimum enrichment of 80 wt % ^{235}U .

The SAS2H sequence was used to determine the gamma and neutron source terms and decay heat loads for the spiral assembly (see Figure 5.3.16-1). The SAS2H sequence includes the ORIGEN-S code and a 1-D XSDRNPM model of the fuel assembly. ORIGEN-S performs fuel assembly depletion at specified operating conditions and calculates heat generation, gamma and neutron spectra for a given discharge isotopic composition as a function of out of reactor time (cooling time). The 1-D model of the fuel assembly is used to collapse the 27-group neutron cross-section library (27GROUPNDF4) into three broad energy groups for the depletion calculation. The 1-D model is based on an equivalent area representation of the fuel/moderator cell and surrounding structural regions. Average power is based on reactor maximum power divided by the number of assemblies in the core. Assembly burnup is modeled in four cycles of equal length with 30 days of down time between cycles. This burnup description bounds typical research reactor use, where fuel is burned over a period of years or even decades to achieve the optimal discharge burnup. The SAS2H input for the plate bundle is shown in Figure 5.3.16-1. During in-core operations, the MOATA fuel assembly falls under the MTR headings, as discussed in Section 5.3.4, and is typically configured with 12 fuel plates and comb aluminum side plates. Standard MTR characteristics are assigned to the assembly for in-core use, with source terms adjusted to represent a 14-plate fuel bundle. The SAS2H input contains relevant

operating parameters such as power density and number of days of irradiation, in addition to the material compositions employed.

The design basis photon (gamma) source term for the plate bundle is listed in Table 5.3.16-2 with a source comparison by energy line and total source to the MEU DIDO results. Gamma source terms are approximately 2% of those calculated for the MEU DIDO assembly. There is no significant neutron source associated with the low burnup plate bundle material.

The ANSTO basket is a slightly modified version of the DIDO basket, with each basket containing seven tubes designed to hold one fuel assembly (element) in each tube. ANSTO fuel tubes are slightly larger in diameter and thickness.

Parameter	DIDO Basket	ANSTO Basket
Fuel Assembly Openings	7	7
Fuel Tube OD (inch)	4.25	4.375
Fuel Tube Wall Thickness (inch)	0.120	0.125

The DIDO basket contains aluminum heat transfer components, while the ANSTO basket contains additional support disks. The aluminum heat transfer components were not included in the DIDO shielding evaluations.

Combining a significantly lower plate bundle source with a similar basket design demonstrates that DIDO shielding evaluations, and the dose rates produced by the evaluations, bound those expected from the plate bundle.

Figure 5.3.16-1 SAS2H Input for the MOATA Plate Bundle

```
=SAS2H      PARM=(HALT04,SKIPSHIPDATA)
MOATA MARK II ASSEMBLY, 300 g U-235
27GROUPNDF4 LATTICECELL
URANIUM 1 DEN=0.753 1.0 373 92235 80.00 92238 20.00 END
AL      1 DEN=2.702 1.0 373 END
AL      2 1.0 323 END
H2O     3 1.0 313 END
AL      4 0.7258 313 END
H2O     4 0.2742 313 END
END COMP
SYMMSLABCELL 0.667 0.1016 1 3 0.203 2 END
NPIN=12 FUEL=58.4 VOLF=497.697 NCYC=1 NLIB=4
PRIN=6 INPL=2 NUMZ=3 NUMH=0
3 0.01 500 4.2190 4 4.3992
POWER=0.0083 BURN=1350.00 DOWN=1461 END
END
=ORIGENS
0$$$ A4 21 A8 26 A10 51 71 E
1$$$ 1 1T
COOLING TO 10 YEARS AND FISSION PRODUCT GAMMA REBIN
3$$$ 21 0 1 A33 -86 E
54$$$ A8 1 E T
35$$$ 0 T
56$$$ 0 1 A13 -2 5 3 E
57** 4.0 E T
COOLING TO 10 YEARS AND FISSION PRODUCT GAMMA REBIN
SINGLE REACTOR ASSEMBLY
60** 10
65$$$ A4 1 A7 1 A10 1 A25 1 A28 1 A31 1 A46 1 A49 1 A52 1 E
61** F.01
81$$$ 2 51 26 1 E
82$$$ F6 T
FISSION PRODUCT GAMMA SPECTRA IN SCALE 18 GROUPS
56$$$ F0 T
END
=ORIGENS
0$$$ A4 21 A8 26 A10 51 71 E
1$$$ 1 1T
COOLING TO 10 YEARS AND ACTINIDE GAMMA REBIN
3$$$ 21 0 1 A33 -86 E
54$$$ A8 1 E T
35$$$ 0 T
56$$$ 0 1 A13 -2 5 3 E
57** 4.0 E T
COOLING TO 10 YEARS AND ACTINIDE GAMMA REBIN
SINGLE REACTOR ASSEMBLY
60** 10
65$$$ A4 1 A7 1 A10 1 A25 1 A28 1 A31 1 A46 1 A49 1 A52 1 E
61** F.01
81$$$ 2 51 26 1 E
82$$$ F5 T
ACTINIDE GAMMA SPECTRA IN SCALE 18 GROUPS
56$$$ F0 T
END
```

Table 5.3.16-1 MOATA Plate Bundle Characteristics

Parameter	Unit	Value
Element Width ¹	[cm]	7.6
Element Depth ¹	[cm]	8
Side Plate Thickness ²	[cm]	0.203
Side Plate Depth ¹	[cm]	7.5
Number of Plates (in-core operation)		12
Plate Thickness	[cm]	0.203
Active Fuel Length	[cm]	58.4
Active Fuel Width	[cm]	6.99
Active Fuel Thickness	[cm]	0.1016
Plate Pitch ³	[cm]	0.667
Fuel Composition		U-Al-Alloy
Weight Percent ²³⁵ U		80
Maximum ²³⁵ U per Plate	[g]	25
U wt % in Fuel Composition		18%
Modeled Element Power Level	[MW]	0.00833
Mass of Uranium (per Assembly/12 Plates)	[kg]	0.375

¹ Used in SAS2H input for in-core operations. Based on typical MTR dimensions for similar fuel.

² Applied fuel plate dimension.

³ Calculated based on 12 fuel plates and the assembly dimensions obtained from the MTR evaluations.

Table 5.3.16-2 MOATA Plate Bundle Source Comparison

Group ¹	MOATA Plate Bundle	DIDO MEU	Factor
	y/sec/assy	y/sec/assy	
1	4.0723E-03	3.6156E+00	9E+02
2	1.9549E-02	1.7064E+01	9E+02
3	1.0240E-01	8.7244E+01	9E+02
4	2.6282E-01	2.1810E+02	8E+02
5	3.5099E+04	1.5823E+08	5E+03
6	2.9504E+05	1.5502E+09	5E+03
7	2.3606E+07	3.5325E+11	1E+04
8	8.5904E+07	3.9342E+10	5E+02
9	5.9393E+08	3.9960E+11	7E+02
10	3.2031E+09	8.0635E+11	3E+02
11	5.3494E+09	2.8948E+12	5E+02
12	1.0244E+12	1.9469E+13	2E+01
13	2.5891E+10	7.9993E+12	3E+02
14	3.2239E+10	2.3302E+12	7E+01
15	4.4973E+10	3.0292E+12	7E+01
16	1.4315E+11	1.3197E+13	9E+01
17	2.1309E+11	1.3157E+13	6E+01
18	7.2597E+11	4.0972E+13	6E+01
Total	2.2190E+12	1.0464E+14	5E+01

¹ SCALE 4.3 27N-18G energy structure

5.3.17 Irradiated Hardware Shielding Evaluation

Irradiated hardware is evaluated for transport in the LWT cask. The irradiated hardware represents a potentially significant gamma source when compared to fuel material payloads due to the high energy spectrum feasible from activated materials. Typical irradiated hardware is irradiated steel where cobalt activation, and subsequent ^{60}Co decay, produces two gamma rays, each over 1 MeV in energy.

A source term for typical irradiated hardware is established by activating one kilogram of stainless steel with a 1.2 g/kg cobalt impurity in a PWR in-core neutron spectrum (PWR fuel assembly burnup to 45,000 MWd/MTU at a 3.5 wt % ^{235}U initial enrichment, followed by a 90-day cool time). This material will represent a baseline to establish source limits in terms of gammas per second and energy per second (γ/s and MeV/s). The gamma source activity is determined in the SCALE 27-group neutron and 18-group gamma structures using the SAS2H sequence of SCALE 4.3. The activated hardware may contain surface contamination (including actinides), but this component has no significant effect on cask surface dose rates compared to the activated material itself and is, therefore, neglected from the analysis. The SAS2H input for the gamma source generation is listed in Figure 5.3.17-1. The resulting gamma spectrum is summarized in Table 5.3.17-1.

A radial one-dimensional shielding analysis is performed using SAS1 with a void source region. A void source region is by default conservative since it neglects the substantial self-shielding of the activated hardware. A sample radial SAS1 input for irradiated hardware evaluations is shown in Figure 5.3.17-2 with material compositions for the cask given in Table 5.3.17-2. Note that various irradiated hardware heights (and two radial configurations) are evaluated using SAS1. The buckling height in each case is set to the source region height of the particular analysis. The same conservative assumptions used in previous radial shielding analysis were applied, i.e., minimum shield dimensions, lead gap, a $0.94 \text{ g}/\text{cm}^3$ neutron shield solution density, and no boron in the neutron shield solution. In the accident analysis, the neutron shield is modeled as void. A one-dimensional sketch of the modeled cask geometry is shown in Figure 5.3.17-3. As demonstrated in the shielding evaluations for various other payloads (e.g., fuel skeleton with activated hardware), the axial dose of the NAC-LWT cask is not limiting. Therefore, only radial dose rates are evaluated in this section.

SAS1 dose rates are calculated using the SAS2H-generated gamma source (1 kg activated hardware). Dose rates are then scaled up to represent an increased source with a magnitude of $2 \times 10^{14} \gamma/\text{sec}$ or $2.2 \times 10^{14} \text{ MeV}/\text{sec}$ (equivalent of 10 kg of the SAS2H activated stainless).

This source represents a radionuclide content of approximately 8.9×10^3 Ci, with a ^{60}Co portion of 2×10^3 Ci. Normal condition transport cask surface and 2 meter dose rates, as well as accident condition 1 meter dose rates, are plotted in Figure 5.3.17-4 through Figure 5.3.17-6 for the increased source. Dose rates are well below regulatory limits at the surface (300 mrem/hr) and 2 meters from the truck bed (7.6 mrem/hr). The transport index, based on the normal condition of transport dose rate at 1 meter from the package, is less than 35.

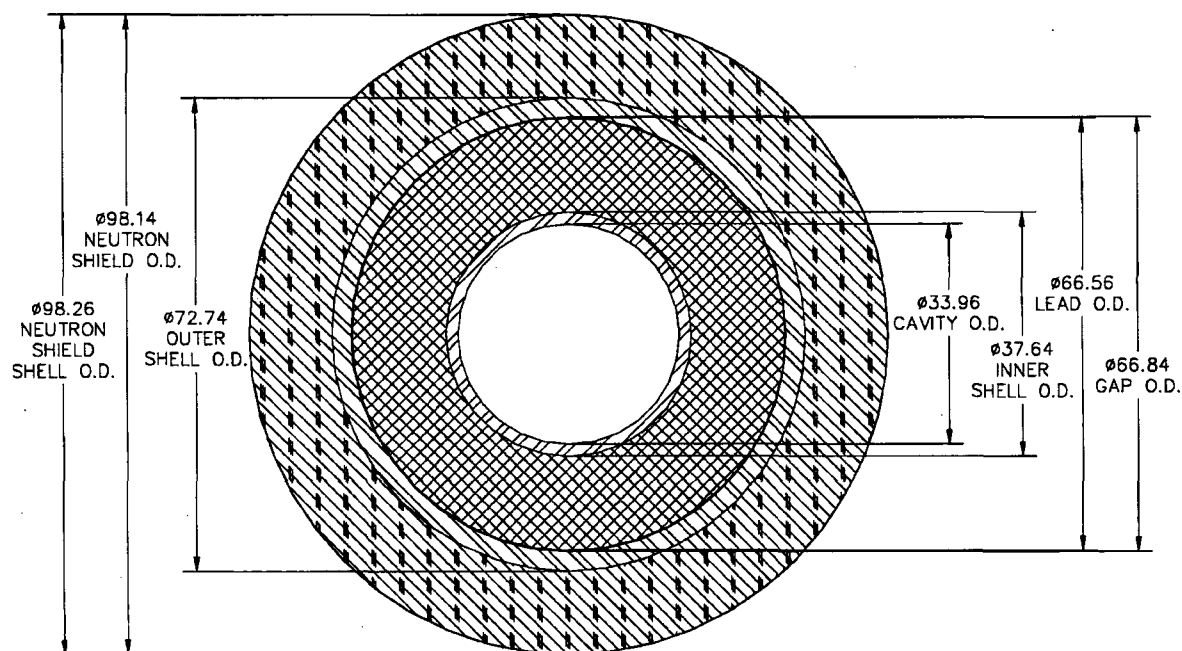
Figure 5.3.17-1 SAS2H Input for Irradiated Hardware (on a per kg Basis)




```
=SAS2H      PARM=(HALT03,SKIPSHIPDATA)
WEST 15X15 3.5 WT % U235, 45000 MWd/MTU 5.0-10.0 YEAR COOLING
27GROUPNDF4 LATTICECELL
UO2      1 0.95 900 92235 3.5 92238 96.5 END
ZIRCALLOY 2 1.0 620 END
H2O      3 DEN=0.725 1.0 580 END
AREM-BORMOD 0.725 1 1 0 0 5000 100 3 550.0E-6 580 END
END COMP
SQUAREPITCH 1.43 0.9294 1 3 1.0719 2 0.9489 0 END
NPIN=204 FUEL=365.76 NCYC=3 NLIB=1 PRIN=6 LIGH=5
INPL=1 NUMH=20 NUMI=1 ORTU=0.6922 SRTU=0.6541 END
POWER=16.28 BURN=428.0692 DOWN=60.0 END
POWER=16.28 BURN=428.0692 DOWN=60.0 END
POWER=16.28 BURN=428.0692 DOWN=0.0 END
FE 0.672 CR 0.190 NI 0.115 MN 0.020 CO 0.0012
END
=ORIGENS
O$$ A4 21 A8 26 A10 51 71 E
1$$ 1 1T
COOLING 0.25-4 YEARS AND LIGHT ELEMENT GAMMA REBIN
3$$ 21 0 1 A33 -86 E
54$$ A8 1 E T
35$$ 0 T
56$$ 0 6 A13 -2 5 3 E
57** 0.0 E T
COOLING 0.25-4 YEARS AND LIGHT ELEMENT GAMMA REBIN
SINGLE REACTOR ASSEMBLY
60** 0.25 0.5 0.75 1.0 1.5 2.0
65$$ A4 1 A7 1 A10 1 A25 1 A28 1 A31 1 A46 1 A49 1 A52 1 E
61** F.01
81$$ 2 51 26 1 E
82$$ F4 T
LIGHT ELEMENT SCALE GROUP STRUCTURE
LIGHT ELEMENT SCALE GROUP STRUCTURE
LIGHT ELEMENT SCALE GROUP STRUCTURE
LIGHT ELEMENT SCALE GROUP STRUCTURE
LIGHT ELEMENT SCALE GROUP STRUCTURE
LIGHT ELEMENT SCALE GROUP STRUCTURE
56$$ F0 T
END
```

Figure 5.3.17-2 Sample SAS1 Input for Irradiated Hardware (Source 1 kg Material)

```
SAS1
Irradiated Hardware - Nrm Model - 16 cm Radius Source - 150cm Height Source
27N-18COUPLE      INFHOMMEDIUM
AL      2      1.0 END
SS304   3      1.0 END
PB      4      1.0 END
ARBMGLYC 0.9437 3 0 1 0 6012 2 1001 6 8016 2 5 .585 END
H2O     5      0.4160 END
END COMP
END
LAST
Irradiated Hardware in the NAC-LWT - GAMMA SOURCE
CYLINDRICAL
0  8  30  -1  0  0.0  0.0  6.678E+08
0 16.9863  1  0
3 18.8214  4  0
4 33.2890 60  0
0 33.4264  1  0
3 36.3728 12  0
5 49.0728 30  0
3 49.1338  4  0
END ZONE
27Z
0.000E+00 0.000E+00 0.000E+00 0.000E+00 2.631E-15 1.195E+05
7.709E+07 9.199E+09 3.249E+12 1.150E+13 3.950E+12 6.266E+08
5.980E+11 4.581E+11 5.615E+09 2.643E+10 6.543E+10 2.763E+11
DY=150 NDETEC=5
READ XSDOSE
150 49.1338 75 149.1338 75 249.1338 75
321.92 75 349.1338 75
END
```

Figure 5.3.17-3 Irradiated Hardware One-Dimensional Radial Model of NAC-LWT



-  - NEUTRON SHIELD
-  - LEAD
-  - STAINLESS STEEL

Dimensions in cm.

Figure 5.3.17-4 Irradiated Hardware Normal Condition Surface Dose Rate as a Function of Irradiated Hardware Height

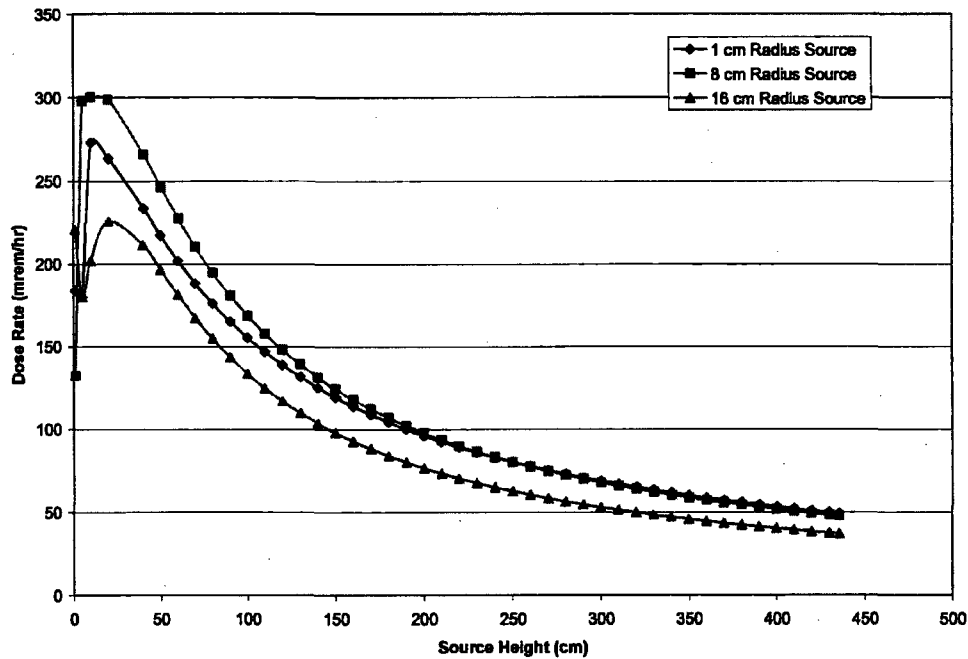


Figure 5.3.17-5 Irradiated Hardware Normal Condition 2 Meter Dose Rate as a Function of Irradiated Hardware Height

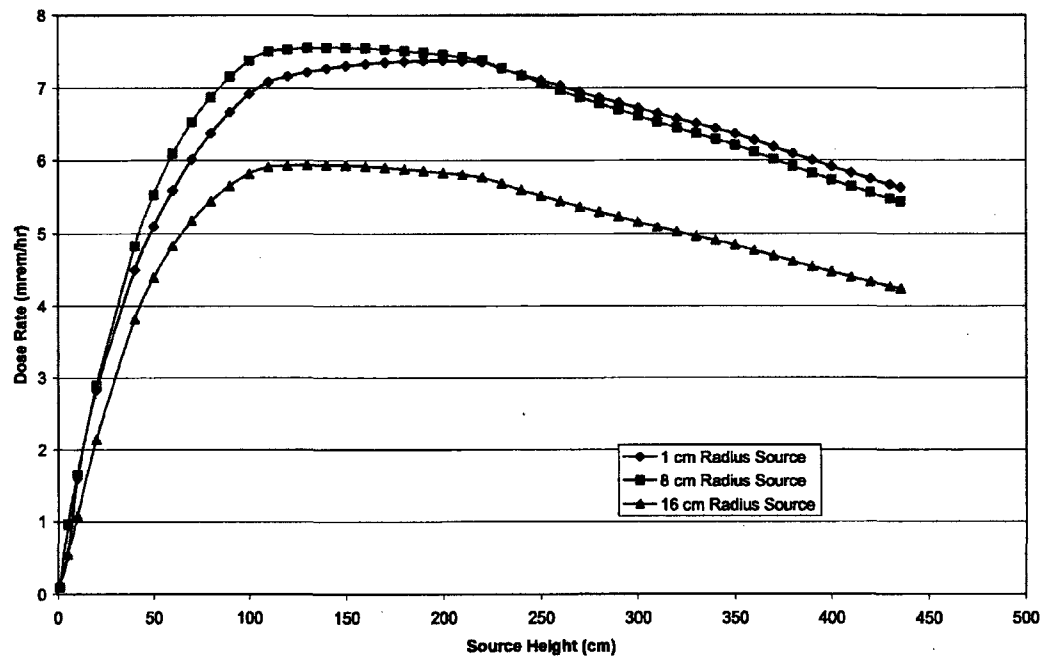


Figure 5.3.17-6 Irradiated Hardware Accident Condition 1 Meter Dose Rate as a Function of Irradiated Hardware Height

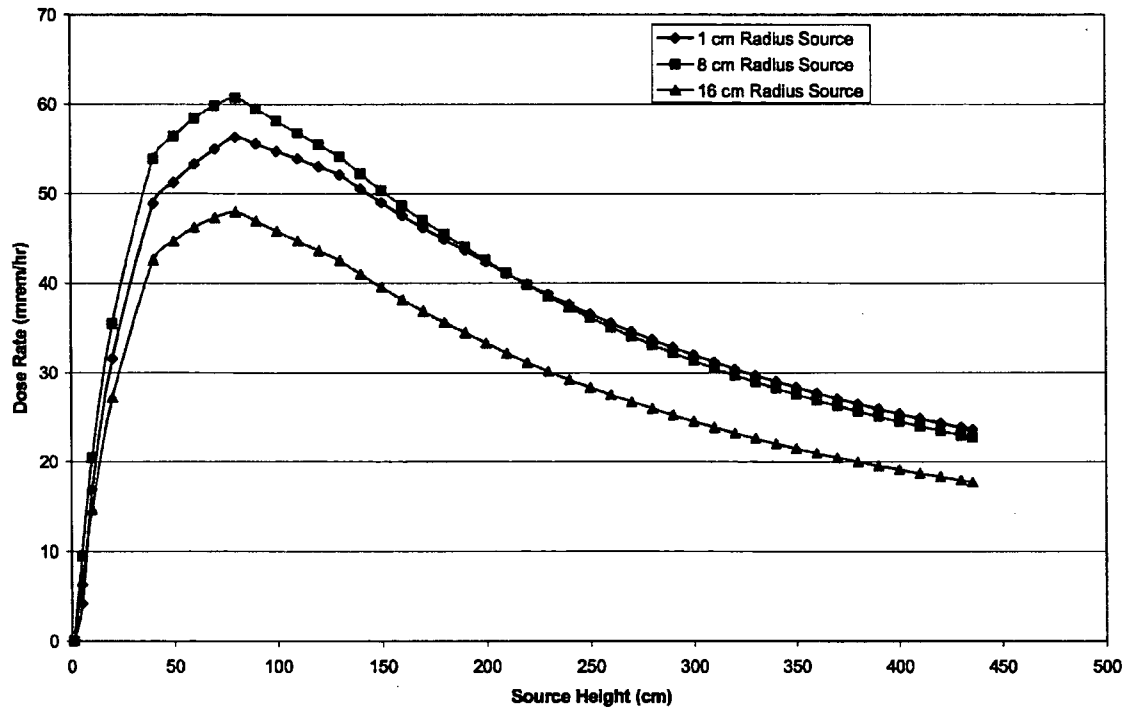


Table 5.3.17-1 Irradiated Hardware Gamma Spectra in SCALE Format (1 kg Activated Stainless Steel)

Energy Group	Source	
	[gamma/sec]	[MeV/sec]
1	0.000E+00	0.000E+00
2	0.000E+00	0.000E+00
3	0.000E+00	0.000E+00
4	0.000E+00	0.000E+00
5	2.631E-15	9.209E-15
6	1.195E+05	3.287E+05
7	7.709E+07	1.735E+08
8	9.199E+09	1.683E+10
9	3.249E+12	4.857E+12
10	1.150E+13	1.340E+13
11	3.950E+12	3.555E+12
12	6.266E+08	4.386E+08
13	5.980E+11	2.990E+11
14	4.581E+11	1.603E+11
15	5.615E+09	1.404E+09
16	2.643E+10	3.964E+09
17	6.543E+10	4.907E+09
18	2.763E+11	8.290E+09
Total	2.014E+13	2.231E+13

Table 5.3.17-2 Material Compositions of the NAC-LWT

Material	SCALE Isotope/Element	Number Density [atom/b-cm]
Stainless Steel	CHROMIUM (SS304)	1.74286E-02
	MANGANESE	1.73633E-03
	IRON (SS304)	5.93579E-02
	NICKEL (SS304)	7.72070E-03
Lead	LEAD	3.29690E-02
Neutron Shield	HYDROGEN	5.99351E-02
	CARBON-12	1.07197E-02
	OXYGEN-16	2.46077E-02

5.4 Shielding Evaluation

5.4.1 Shielding Evaluation Codes

The two codes used in the shielding evaluation of the NAC-LWT cask are XSDRNPM (NUREG/CR-0200, Vol. 2, F3) and QAD-CG (Cain). XSDRNPM is a 1-dimensional multigroup code developed by Oak Ridge National Laboratories (ORNL) for reactivity calculations. In this case, it is used to perform shielding analysis by solving the Boltzmann transport equation including anisotropic scattering by the discrete ordinates method. In this analysis, the P_3S_8 approximation is used for a more accurate dose rate calculation. The SCALE (NUREG/CR-0200) 27N/18G group coupled neutron-gamma cross section master library is processed through NITAWL (NUREG/CR-0200, Vol. 2, F2) and XSDRNPM for self-shielding resonance treatment and cell weighting. This step is necessary to generate the working data library required as input for XSDRNPM to perform dose rate calculations. The QAD-CG combinatorial geometry version of QAD was also developed at ORNL. It is a 3-dimensional computer code that is used extensively in industry and yields good results for gamma-ray calculations and usually satisfactory results for neutron calculations. The code uses buildup factors based on the Goldstein and Wilkins moments method calculations for gamma-ray transport in an infinite homogeneous medium. The code uses Capo's fit to the Goldstein-Wilkins data with bivariate polynomial expressions to calculate the approximate buildup factors as a function of the gamma-ray energy and the number of mean free paths from the source to the detector. The buildup factor selected for all of the shielding calculations in this case is for iron, which yields conservative results. For neutron dose calculations, the code uses either a modified Albert-Welton kernel or kernels obtained from the moments method solution of the Boltzmann transport equation. With the moments method kernels, the neutron spectrum penetrating a shield is determined on the basis of the equivalent length of a reference material between the source point and the receiver point.

XSDRNPM has been shown to be an accurate shielding code, but it has geometrical limitations. To perform calculations with XSDRNPM, a flat source distribution along the fuel axial direction and an equivalent circularized cylindrical source core are used. For the design basis Westinghouse 15×15 PWR assembly, the fuel area is 458.05 square centimeters, which yields an effective radius of 12.07 centimeters, as shown in Figure 5.3.3-6. In actuality, an axial source distribution (Figure 3.4-2) exists, which introduces higher dose rates at the peak axial source location. Also, the circularized core underestimates the dose at points where the real source region is nearer the cask surface.

QAD-CG is used to correct for the axial source distribution and the three-dimensional effects of geometry. Calculations are done with QAD for a three-dimensional model with an axial source distribution (Table 5.4.1-1) and for a 1-dimensional model with a flat source distribution. The flux to dose conversion factors for these models are found in the Radiological Health Handbook and are listed in Table 5.4.1-2. The buildup factor used for both of these models is for iron, since it has the largest number of mean free paths. The detector points are placed on the surface for the flat source distribution and at 2 meters from the personnel barrier for the axial source distribution. This gives a 3-dimensional to 1-dimensional correction factor, which is applied to the XSDRNPM results to calculate the actual dose. This method is used to calculate the dose rates from the side of the cask, at the surface, and at 2 meters from the personnel barrier (Table 5.1.1-4).

For the radial dose rates, an additional correction factor is applied to account for scattering. Schaeffer's Reactor Engineering for Nuclear Engineers is used to determine the scattering factors of 5 percent for primary and secondary gammas and 45 percent for neutrons. These values are found in tables 7.10 and 7.18 (Schaeffer) generated using total albedos. The use of total albedos rather than differential albedos is conservative, since total albedos take into account scattering angles that do not allow radiation to reach the detector point. It is also important to note that since this is high energy radiation, the probability of it scattering through large angles is very low.

The end-fitting calculations are straight forward. To calculate the end-fitting gamma as well as the fuel contribution to the dose rates at the ends of the cask, a simple QAD-CG model is used. The model is an arrangement of stacked disks and uses a flat source distribution so that a correction factor is not necessary. The various contributions are added together to obtain the total dose rate. The dose rates are included in Table 5.1.1-4.

The dose rates for a loss of the neutron shield are calculated using both XSDRNPM and QAD-CG. XSDRNPM is used to calculate a ratio of the dose rate on the surface with the neutron shield to the dose rate without the neutron shield. QAD-CG is used to calculate a 3-dimensional to 1-dimensional geometrical correction factor. The QAD-CG dose points are located on the surface, with a flat source distribution, and at 1 meter using an axial source distribution (Figure 3.4-2). The dose rates at 1 meter without the neutron shield are obtained by multiplying the normal operations dose rate at the surface by the 3-dimensional to 1-dimensional geometric correction factor. This product is then multiplied by the ratio of dose rates without water to with water, to obtain the hypothetical accident dose rate at 1 meter. The dose rate at 1 meter from the surface of the cask for this accident is 77.5 mrem/hour (Table 5.1.1-5), which is well below the limits of 49 CFR 173.

The lead slump accident is analyzed using QAD-CG. Models are created for the top and bottom end-fittings of a PWR and the bottom end-fitting of a BWR. The BWR bottom end-fitting is analyzed since it is bigger and has a larger ^{60}Co source than the PWR bottom end-fitting. It also sits closer to the bottom of the cask and, therefore, closer to the lead slump than the PWR bottom end-fitting. The analysis is not performed for the BWR top end-fitting because it is smaller and, therefore, has a lower source strength than the BWR bottom end-fitting. Detector points are placed at various positions along the outside of the cask in order to determine if the lead "window" that could be created during the cask drop would have adverse shielding consequences. The resulting dose rates are presented in Table 5.1.1-6.

For completeness, a normal transport conditions shielding analysis is performed for the NAC-LWT cask, which takes into account the shell tolerances found in the license drawings (Section 1.4). The method used is identical to the one used for the fuel radial calculations; however, neutrons and secondary gammas are not recalculated because a small reduction in the lead thickness would not significantly affect either the neutrons or the secondary gammas. The lead density in this analysis was determined by multiplying the maximum density at room temperature (11.35 g/cc) by a ratio of the volume of lead at 620°F to the volume of lead at room temperature (335,779.9/339,930.5). A thermal insulator is used to preclude lead melt during the 10 CFR 71 hypothetical fire accident. The displacement of the lead by the thermal insulator is also taken into account. The dose rate, accounting for tolerances and thermal insulator, is 8.93 mrem/hour at the fuel midplane, 2 meters from the personnel barrier, an increase of only 0.79 mrem/hour. Therefore, under normal transport conditions, with the tolerances and the thermal insulator taken into account, the cask is within the limits of 10 CFR 71.

Table 5.4.1-1 Discrete Axial Source Distribution

Axial Location Above Bottom of Active Fuel Length (cm)	Relative Axial Source Strength	Axial Location Above Bottom of Active Fuel Length (cm)	Relative Axial Source Strength
0.0	0.35	99.72	1.20
5.54	0.45	105.26	1.20
11.08	0.563	110.80	1.20
16.62	0.685	116.34	1.20
22.16	0.768	121.88	1.20
27.70	0.843	127.42	1.20
33.24	0.909	132.96	1.20
38.78	0.965	138.50	1.20
44.32	1.015	144.04	1.20
49.86	1.039	149.58	1.20
55.40	1.074	155.12	1.20
60.94	1.103	160.66	1.20
66.48	1.128	166.20	1.20
72.02	1.148	171.74	1.20
77.56	1.166	177.28	1.20
83.10	1.175	182.82	1.20
88.64	1.20	188.36	1.20
94.18	1.20	193.90	1.187

Table 5.4.1-1 Discrete Axial Source Distribution (Continued)

Axial Location Above Bottom of Active Fuel Length (cm)	Relative Axial Source Strength	Axial Location Above Bottom of Active Fuel Length (cm)	Relative Axial Source Strength
199.44	1.175	288.08	1.04
204.98	1.175	293.62	0.934
210.52	1.175	299.16	0.88
216.06	1.175	304.70	0.88
221.60	1.152	310.24	0.88
227.14	1.14	315.78	0.88
232.68	1.14	321.32	0.88
238.22	1.14	326.86	0.88
243.76	1.14	332.40	0.839
249.30	1.14	337.94	0.769
254.84	1.14	343.48	0.665
260.38	1.089	349.02	0.591
265.92	1.04	354.56	0.513
271.46	1.04	360.10	0.523
277.00	1.04	365.75	0.301
282.54	1.04		

Table 5.4.1-2 Flux to Dose Conversion Factors

Energy (MeV)	Flux-to-Dose
0.35	5.13E-4
0.452	8.00E-4
0.79	1.52E-3
0.90	1.67E-3
1.25	2.17E-3
1.29	2.38E-3
1.58	2.63E-3
1.74	2.86E-3
2.35	3.45E-3

Table of Contents

6	CRITICALITY EVALUATION	6-1
6.1	Discussion and Results	6.1-1
6.2	Package Fuel Loading	6.2-1
6.2.1	PWR Fuel Assemblies	6.2.1-1
6.2.2	BWR Fuel Assemblies	6.2.2-1
6.2.3	MTR Fuel Elements	6.2.3-1
6.2.4	PWR and BWR Rods in a Rod Holder or Fuel Assembly Lattice	6.2.4-1
6.2.5	TRIGA Fuel Elements	6.2.5-1
6.2.6	TRIGA Fuel Cluster Rods	6.2.6-1
6.2.7	Metallic Fuel Rods	6.2.7-1
6.2.8	DIDO Fuel Assemblies	6.2.8-1
6.2.9	General Atomics Irradiated Fuel Material	6.2.9-1
6.2.10	PULSTAR Fuel Elements	6.2.10-1
6.2.11	Spiral Fuel Assemblies	6.2.11-1
6.2.12	MOATA Plate Bundles	6.2.12-1
6.3	Criticality Model Specifications	6.3.1-1
6.3.1	PWR Fuel Assemblies	6.3.1-1
6.3.2	BWR Fuel Assemblies	6.3.2-1
6.3.3	MTR Fuel Elements	6.3.3-1
6.3.4	PWR and BWR Rods in a Rod Holder or Fuel Assembly Lattice	6.3.4-1
6.3.5	TRIGA Fuel Elements and Cluster Rods	6.3.5-1
6.3.6	DIDO Fuel Assemblies	6.3.6-1
6.3.7	General Atomics Irradiated Fuel Material	6.3.7-1
6.3.8	PULSTAR Fuel Contents	6.3.8-1
6.3.9	ANSTO Basket Payload	6.3.9-1
6.4	Criticality Calculations	6.4.1-1
6.4.1	PWR Fuel Assemblies	6.4.1-1
6.4.2	BWR Fuel Assemblies	6.4.2-1
6.4.3	MTR Fuel Elements	6.4.3-1
6.4.4	PWR and BWR Rods in a Rod Holder or Fuel Assembly Lattice	6.4.4-1
6.4.5	TRIGA Fuel Elements	6.4.5-1
6.4.6	TRIGA Fuel Cluster Rods	6.4.6-1
6.4.7	DIDO Fuel Assemblies	6.4.7-1
6.4.8	General Atomics Irradiated Fuel Material	6.4.8-1
6.4.9	PULSTAR Fuel Contents	6.4.9-1
6.4.10	ANSTO Basket Payloads	6.4.10-1
6.5	Critical Benchmarks	6.5.1-1
6.5.1	PWR and BWR Fuel Assemblies	6.5.1-1
6.5.2	MTR and DIDO Fuel Elements	6.5.2-1
6.5.3	TRIGA Fuel Elements	6.5.3-1

Note: See separate Section 6.6 for Appendices to this chapter.

List of Figures

Figure 6.2.3-1	Design Basis HFBR MTR Fuel Element.....	6.2.3-2
Figure 6.2.5-1	Aluminum Clad TRIGA Fuel Element.....	6.2.5-2
Figure 6.2.5-2	Stainless Steel Clad TRIGA Fuel Element	6.2.5-3
Figure 6.2.6-1	TRIGA Fuel Cluster Rod Details	6.2.6-2
Figure 6.2.8-1	DIDO Fuel Assembly	6.2.8-2
Figure 6.2.10-1	PULSTAR Fuel Assembly	6.2.10-2
Figure 6.2.11-1	Spiral Fuel Assembly Cross-Section Sketch	6.2.11-2
Figure 6.2.12-1	MOATA Plate Bundle Sketch.....	6.2.12-2
Figure 6.3.1-1	KENO-Va Model of the NAC-LWT Cask Model with PWR Basket and 15×15 PWR Assembly	6.3.1-4
Figure 6.3.1-2	KENO-Va Model of the NAC-LWT Cask with PWR Basket and Westinghouse 17×17 OFA Assembly	6.3.1-5
Figure 6.3.2-1	KENO-Va Model of the NAC-LWT Cask Model with BWR Basket and 2 Exxon 9×9-2/80 Assemblies	6.3.2-3
Figure 6.3.3-1	KENO-Va Fuel/Basket Unit Cell Model for MTR Fuel	6.3.3-4
Figure 6.3.3-2	KENO-Va Model of NAC-LWT Cask with MTR Fuel	6.3.3-5
Figure 6.3.3-3	Intermediate MTR 42 Basket Module.....	6.3.3-6
Figure 6.3.3-4	Full Length NAC-LWT Cask Model with 42 MTR Fuel Elements.....	6.3.3-7
Figure 6.3.3-5	MTR Fuel Basket Module Loading Pattern	6.3.3-8
Figure 6.3.4-1	Triangular Pitch Lattice Formation of 25 PWR Rods.....	6.3.4-4
Figure 6.3.4-2	KENO-Va Model of the NAC-LWT Cask with 25 PWR Rods.....	6.3.4-5
Figure 6.3.4-3	Maximum Reactivity Triangular Pitch Lattice Formation of Damaged Fuel Rods.....	6.3.4-6
Figure 6.3.4-4	KENO-Va Model of the NAC-LWT Cask with Damaged Fuel Rods – Radial Detail.....	6.3.4-7
Figure 6.3.4-5	KENO-Va Model of the NAC-LWT Cask with Damaged Fuel Rods – Axial Detail	6.3.4-8
Figure 6.3.5-1	Fuel Rod Handling Insert for TRIGA Fuel Cluster Rods.....	6.3.5-5
Figure 6.3.5-2	Fuel/Basket Unit Cell Model for TRIGA Fuel Elements.....	6.3.5-6
Figure 6.3.5-3	NAC-LWT Cask with TRIGA Fuel, Nonpoisoned Basket - Radial View...	6.3.5-7
Figure 6.3.5-4	KENO-Va Model of NAC-LWT with Poisoned Basket – Radial View	6.3.5-8
Figure 6.3.5-5	NAC-LWT Cask Model with TRIGA Fuel Elements, Nonpoisoned Basket - Axial View	6.3.5-9
Figure 6.3.5-6	Full Length NAC-LWT Cask Model with TRIGA Fuel Elements, Nonpoisoned Basket - Axial View	6.3.5-10
Figure 6.3.6-1	Intermediate DIDO 42 Basket Module.....	6.3.6-3
Figure 6.3.6-2	KENO-Va DIDO Fuel in Fuel Tube and Basket Cross-Section.....	6.3.6-4
Figure 6.3.6-3	KENO-Va Model of NAC-LWT Cask Cross-Section with DIDO Fuel	6.3.6-5
Figure 6.3.6-4	Full Length NAC-LWT Cask Model with 42 DIDO Fuel Assemblies	6.3.6-6
Figure 6.3.7-1	PICTURE Representation of NAC-LWT Cavity with ‘Rectangular’ Array of GA IFM TRIGA Elements.....	6.3.7-2

List of Figures (continued)

Figure 6.3.7-2	PICTURE Representation of NAC-LWT Cavity with 'Square' Array of GA IFM TRIGA Elements.....	6.3.7-2
Figure 6.3.7-3	KENO-Va Model of NAC-LWT Cask Cross-Section with GA IFM.....	6.3.7-3
Figure 6.3.8-1	PICTURE Representation of NAC-LWT Cavity with PULSTAR Assemblies	6.3.8-3
Figure 6.3.8-2	PICTURE Representation of NAC-LWT Cavity with PULSTAR Elements in 4x4 Rod Insert.....	6.3.8-3
Figure 6.3.8-3	PICTURE Representation of NAC-LWT Cavity with Canned Discrete PULSTAR Elements.....	6.3.8-4
Figure 6.3.8-4	PICTURE Representation of NAC-LWT Cavity with Canned Homogenized PULSTAR Elements.....	6.3.8-4
Figure 6.3.8-5	KENO-Va Model of NAC-LWT Cask Cross-Section with 28 MTR 7-Element Basket	6.3.8-5
Figure 6.3.8-6	Finite Length KENO-Va Model of NAC-LWT Cask with 700 PULSTAR Fuel Elements.....	6.3.8-6
Figure 6.3.9-1	Intermediate ANSTO Basket Module.....	6.3.9-3
Figure 6.3.9-2	KENO-Va ANSTO Payloads and Basket Cross-Section.....	6.3.9-4
Figure 6.3.9-3	KENO-Va Model of NAC-LWT Cask Cross-Section with ANSTO Basket.....	6.3.9-5
Figure 6.4.3.1	Cask Interior Moderator Density and Blocked Cell Study Results.....	6.4.3-16
Figure 6.4.4-1	Maximum Reactivity Pitch Determination for Damaged BWR Rod Arrays – Water Exterior.....	6.4.4-8
Figure 6.4.4-2	Maximum Reactivity Pitch Determination for Damaged PWR Rod Arrays – Water Exterior.....	6.4.4-8
Figure 6.4.4-3	Maximum Reactivity Determination for Homogenized UO ₂ /Water Mixture.....	6.4.4-9
Figure 6.4.5-1	Finite Cask Array Reactivity versus Fuel Zirconium Mass (Dry Cask Cavity).....	6.4.5-14
Figure 6.4.5-2	Finite Cask Array Reactivity versus H/Zr Ratio (Dry Cask Cavity).....	6.4.5-14
Figure 6.4.5-3	Finite Cask Array Reactivity versus Fuel Mass (Study of ZrH Displacement of Fissile Material for a Fixed Fuel Geometry).....	6.4.5-15
Figure 6.4.5-4	Intact Fuel Optimum Moderator Study – 70 wt % ²³⁵ U Various Zirconium Masses.....	6.4.5-15
Figure 6.4.5-5	Detailed Intact Fuel Optimum Moderator Study – H/Zr Ratio, Fuel Element Characteristics and Location Varied.....	6.4.5-16
Figure 6.4.5-6	Screened and Sealed Can Optimum Moderator Study – Maximum Reactivity Fuel Configuration – 70 wt % ²³⁵ U Steel Clad.....	6.4.5-16
Figure 6.4.5-7	Screened and Sealed Can Debris Height Study – Maximum Reactivity Fuel Configuration – 70 wt % ²³⁵ U Steel Clad	6.4.5-17
Figure 6.4.5-8	Screened Can – 4 Elements per Can – Maximum Reactivity Fuel Configuration – 70 wt % ²³⁵ U Steel Clad	6.4.5-17

List of Figures (continued)

Figure 6.4.9-1	PICTURE Schematic of Modified PULSTAR Fuel Assembly Alignment Configuration.....	6.4.9-5
Figure 6.4.9-2	PULSTAR Intact Assembly Model Moderator Density Study Graphical Results	6.4.9-6
Figure 6.4.10-1	Spiral Fuel - Moderator Density Plot	6.4.10-7
Figure 6.4.10-2	MOATA Plate Bundle -Moderator Density Plot.....	6.4.10-8
Figure 6.5.1-1	KENO-Va Validation—27 Group Library Results: Frequency Distribution of k_{eff} Values	6.5.1-6
Figure 6.5.1-2	KENO-Va Validation—27-Group Library Results: k_{eff} versus Enrichment	6.5.1-7
Figure 6.5.1-3	KENO-Va Validation—27-Group Library Results: k_{eff} versus Rod Pitch...	6.5.1-8
Figure 6.5.1-4	KENO-Va Validation—27-Group Library Results: k_{eff} versus H/U Volume Ratio	6.5.1-9
Figure 6.5.1-5	KENO-Va Validation—27-Group Library Results: k_{eff} versus Average Group of Fission.....	6.5.1-10

Note: See separate Section 6.6 for Appendices to this chapter, along with the List of Figures for the Appendices.

List of Tables

Table 6.2.1-1	B&W, CE and Westinghouse PWR Fuel Assembly Data	6.2.1-2
Table 6.2.1-2	Exxon/ANF PWR Fuel Assembly Data.....	6.2.1-3
Table 6.2.2-1	GE BWR Fuel Assembly Data.....	6.2.2-2
Table 6.2.2-2	Exxon BWR Fuel Assembly Data	6.2.2-2
Table 6.2.2-3	BWR Fuel Assembly Data.....	6.2.2-3
Table 6.2.3-1	Characteristics of Design Basis HEU MTR Fuels	6.2.3-3
Table 6.2.3-2	Characteristics of Design Basis LEU MTR Fuel	6.2.3-6
Table 6.2.3-3	Characteristics of Design Basis MEU MTR Fuel	6.2.3-7
Table 6.2.5-1	Characteristics of Design Basis TRIGA Fuels Elements.....	6.2.5-4
Table 6.2.5-2	Characteristics of Design Basis TRIGA Fuels -Fuel Compositions	6.2.5-5
Table 6.2.6-1	Characteristics of Design-Basis TRIGA Fuel Cluster Rods	6.2.6-3
Table 6.2.6-2	Characteristics of Design-Basis TRIGA Fuel Cluster Rods - Fuel Compositions	6.2.6-3
Table 6.2.7-1	Characteristics of Design-Basis Metallic Fuel Rods.....	6.2.7-2
Table 6.2.8-1	Characteristics of DIDO Fuel Assemblies	6.2.8-3
Table 6.2.8-2	DIDO Fuel Assembly Tolerances	6.2.8-3
Table 6.2.9-1	GA IFM RERTR/TRIGA Fuel Parameters.....	6.2.9-3
Table 6.2.9-2	GA IFM RERTR/TRIGA Fuel Composition.....	6.2.9-3
Table 6.2.9-3	GA IFM RERTR/TRIGA Clad Composition	6.2.9-3
Table 6.2.9-4	GA IFM Elemental Constituents.....	6.2.9-4
Table 6.2.9-5	GA IFM Primary and Secondary Enclosure Dimensions	6.2.9-4
Table 6.2.10-1	PULSTAR Fuel Characteristics	6.2.10-3
Table 6.2.11-1	Spiral Fuel Assemblies Characteristics.....	6.2.11-3
Table 6.2.11-2	Spiral Fuel Assemblies Tolerances Applied	6.2.11-3
Table 6.2.12-1	MOATA Plate Bundle Characteristics	6.2.12-3
Table 6.2.12-2	MOATA Plate Bundle Tolerances Applied	6.2.12-4
Table 6.3.1-1	Compositions and Number Densities Used in the Criticality Analysis of PWR Fuel Assemblies	6.3.1-6
Table 6.3.2-1	Compositions and Number Densities Used in the Criticality Analysis of BWR Fuel Assemblies.....	6.3.2-4
Table 6.3.3-1	Composition Densities Used in Criticality Analysis of MTR Fuel.....	6.3.3-9
Table 6.3.4-1	Compositions and Number Densities Used in the Criticality Analysis of PWR and BWR Rods	6.3.4-9
Table 6.3.5-1	Sample Compositions and Number Densities Used in Criticality Analysis of TRIGA Fuel Elements	6.3.5-11
Table 6.3.5-2	Compositions and Number Densities Used in Criticality Analysis of TRIGA Fuel Cluster Rods.....	6.3.5-12
Table 6.3.6-1	DIDO Fuel Parameters.....	6.3.6-7
Table 6.3.6-2	DIDO Basket and Cask Parameters.....	6.3.6-8
Table 6.3.6-3	Composition Densities Used in Criticality Analysis of DIDO Fuel	6.3.6-9
Table 6.3.7-1	Composition Densities Used in Criticality Analysis of GA IFM.....	6.3.7-4
Table 6.3.8-1	Composition Densities Used in Criticality Analysis of PULSTAR Fuel	6.3.8-7
Table 6.3.9-1	ANSTO Basket and Cask Parameters	6.3.9-6

List of Tables (continued)

Table 6.3.9-2	Composition Densities Used in Criticality Analysis of ANSTO Basket Payload	6.3.9-7
Table 6.4.1-1	PWR Fuel Assembly at 3.7% Enrichment Most Reactive Assembly Results	6.4.1-5
Table 6.4.1-2	PWR Fuel Assembly at 3.5% Enrichment Most Reactive Assembly Results	6.4.1-6
Table 6.4.1-3	Westinghouse 17×17 OFA Assembly Geometric Tolerances and Mechanical Perturbations Results	6.4.1-7
Table 6.4.1-4	Exxon 15×15 Geometric Tolerances and Mechanical Perturbations Results	6.4.1-7
Table 6.4.1-5	Reactivity with Design Basis PWR Fuel vs. Basket Moderator Density, Normal Conditions	6.4.1-8
Table 6.4.1-6	Reactivity with Design Basis PWR Fuel vs. Basket Moderator Density, Accident Conditions	6.4.1-9
Table 6.4.1-7	PWR Single Package 10 CFR 71.55(b)(3) Evaluation k_{eff} Summary for 3.5% Enrichment	6.4.1-10
Table 6.4.1-8	PWR Single Package 10 CFR 71.55(b)(3) Evaluation k_{eff} Summary for 3.7% Enrichment	6.4.1-10
Table 6.4.2-1	BWR Most Reactive Assembly Analysis Results	6.4.2-5
Table 6.4.2-2	BWR Basket Tolerances.....	6.4.2-6
Table 6.4.2-3	BWR Fuel Assembly Geometric Tolerances and Mechanical Perturbations Results	6.4.2-7
Table 6.4.2-4	Reactivity with BWR Fuel vs. Basket Moderator Density, Normal Conditions, Array of 20 Casks	6.4.2-8
Table 6.4.2-5	Reactivity with BWR Fuel vs. Basket Moderator Density, Accident Conditions, Array of 20 Casks	6.4.2-9
Table 6.4.2-6	BWR Single Package 10 CFR 71.55(b)(3) Evaluation k_{eff} Summary	6.4.2-10
Table 6.4.3-1	Fuel/Basket Unit Cell k_{eff} versus MTR Fuel Element Type	6.4.3-17
Table 6.4.3-2	Cask k_{eff} versus Fuel Plate Spacing	6.4.3-17
Table 6.4.3-3	MTR Basket Geometric Tolerances	6.4.3-18
Table 6.4.3-4	MTR Basket/Intact Fuel Element Geometric Tolerances and Mechanical Perturbations Results	6.4.3-18
Table 6.4.3-5	MTR Basket/Optimally Spaced Fuel Plates Geometric Tolerances and Mechanical Perturbations Results	6.4.3-18
Table 6.4.3-6	Reactivity with MTR Fuel vs. Basket Moderator Density, Normal Conditions, Dry Exterior, Infinite Array of Casks	6.4.3-19
Table 6.4.3-7	Reactivity with MTR Fuel vs. Basket Moderator Density, Accident Conditions, Dry Exterior, Infinite Array of Casks	6.4.3-20
Table 6.4.3-8	MTR Fuel Element Rotation Perturbation Study	6.4.3-21
Table 6.4.3-9	MTR Basket/Center Fuel Element Perturbation Study	6.4.3-21
Table 6.4.3-10	Mixed HEU/LEU MTR Fuel Perturbation Study	6.4.3-21
Table 6.4.3-11	MTR Single Package 10 CFR 71.55(b)(3) Evaluation k_{eff} Summary	6.4.3-21
Table 6.4.3-12	MTR Fuel Uranium Weight Percentage Perturbations	6.4.3-22

List of Tables (continued)

Table 6.4.3-13	MEU MTR Unit Cell k_{eff} Comparison (Enrichment Variation)	6.4.3-22
Table 6.4.3-14	MEU MTR Basket k_{eff} Comparison (Plate Location).....	6.4.3-23
Table 6.4.3-15	Physical Characteristics of McMaster MTR Fuels	6.4.3-23
Table 6.4.3-16	Reactivity of Various Parameter Variations for 10-Plate McMaster Element	6.4.3-24
Table 6.4.3-17	Reactivity of Various Parameter Variations for 18-Plate McMaster Element	6.4.3-24
Table 6.4.3-18	MTR Limiting Fuel Configurations.....	6.4.3-25
Table 6.4.3-19	Initial Fuel Configurations for MTR Bounding Evaluations	6.4.3-25
Table 6.4.3-20	Reactivity Impact of Parameter Variations in the Finite Cask Model	6.4.3-26
Table 6.4.3-21	Baseline MTR Bounding Configurations	6.4.3-27
Table 6.4.3-22	High Fissile Mass MTR Fuel – Bounding Parameter Analysis.....	6.4.3-28
Table 6.4.3-23	MTR High Fissile Content Loading Evaluation (460 g ^{235}U).....	6.4.3-29
Table 6.4.3-24	LEU MTR Active Fuel Width Increase Evaluation.....	6.4.3-29
Table 6.4.3-25	Summary of LEU MTR Bounding Configurations.....	6.4.3-30
Table 6.4.3-26	Summary of Previous Bounding Configurations for Use in High Mass LEU Calculations.....	6.4.3-31
Table 6.4.3-27	High Fissile Mass LEU (32 g ^{235}U per Plate) Analysis Results.....	6.4.3-32
Table 6.4.3-28	LEU High Fissile Mass Bounding Configuration.....	6.4.3-33
Table 6.4.3-29	Cask Interior Moderator Density and Blocked Cell Study Results.....	6.4.3-34
Table 6.4.4-1	NAC-LWT Cask with 25 PWR Rods, k_{eff} versus Fuel Rod Pitch, 5.0 wt % ^{235}U Initial Enrichment	6.4.4-10
Table 6.4.4-2	Reactivity with 25 PWR Rods vs. Basket Moderator Density, Normal Conditions, Infinite Array of Casks	6.4.4-11
Table 6.4.4-3	Reactivity with 25 PWR Rods vs. Basket Moderator Density, Accident Conditions, Infinite Array of Casks	6.4.4-12
Table 6.4.4-4	PWR Rods, Single Package 10 CFR 71.55(b)(3) Evaluation k_{eff} Summary	6.4.4-13
Table 6.4.4-5	NAC-LWT Cask with 25 BWR rods, k_{eff} versus Fuel Rod Pitch, 5.0 wt % ^{235}U Initial Enrichment	6.4.4-13
Table 6.4.4-6	Reactivity with 25 BWR Rods vs. Basket Moderator Density, Normal Conditions, Infinite Array of Casks	6.4.4-14
Table 6.4.4-7	Reactivity with 25 BWR Rods vs. Basket Moderator Density, Accident Conditions, Infinite Array of Casks	6.4.4-15
Table 6.4.4-8	BWR Rods, Single Package 10 CFR 71.55(b)(3) Evaluation k_{eff} Summary	6.4.4-16
Table 6.4.4-9	Maximum Reactivity Pitch Determination for 25 BWR Rods – Water Exterior.....	6.4.4-16
Table 6.4.4-10	Maximum Reactivity Pitch Determination for 25 PWR Rods – Water Exterior.....	6.4.4-17
Table 6.4.4-11	Maximum Reactivity Pitch Determination for 37 BWR Rods – Water Exterior.....	6.4.4-17

List of Tables (continued)

Table 6.4.4-12	Maximum Reactivity Pitch Determination for 37 PWR Rods – Water Exterior	6.4.4-18
Table 6.4.4-13	Maximum Reactivity Pitch Determination for 61 BWR Rods – Water Exterior	6.4.4-18
Table 6.4.4-14	Maximum Reactivity Pitch Determination for 61 PWR Rods – Water Exterior	6.4.4-19
Table 6.4.4-15	Maximum Reactivity Pitch Determination for 61 BWR Rods – Void Exterior	6.4.4-19
Table 6.4.4-16	Maximum Reactivity Pitch Determination for 61 PWR Rods – Void Exterior	6.4.4-20
Table 6.4.4-17	Maximum Reactivity Pitch Determination for 61 BWR Rods – Void Exterior and Preferential Flooding of Cask Cavity	6.4.4-20
Table 6.4.4-18	Maximum Reactivity Pitch Determination for 61 PWR Rods – Void Exterior and Preferential Flooding of Cask Cavity	6.4.4-21
Table 6.4.4-19	Damaged Rod Array Area Calculation – Flooded Cask Cavity	6.4.4-21
Table 6.4.4-20	Damaged Rod Array Area Calculation – Preferential Flooding	6.4.4-22
Table 6.4.4-21	Maximum Reactivity Determination for Homogenized UO_2 / Water Mixture	6.4.4-22
Table 6.4.4-22	Homogenized UO_2 /Water Cask Cavity Moderator Density Study Results - Void Exterior	6.4.4-22
Table 6.4.4-23	Homogenized UO_2 /Water Cask Cavity Moderator Density Study Results - Water Exterior	6.4.4-23
Table 6.4.4-24	Homogenized UO_2 /Water Exterior Moderator Density Study Results – Void Cask Cavity	6.4.4-23
Table 6.4.4-25	Homogenized UO_2 /Water Exterior Moderator Density Study Results – Water Cask Cavity	6.4.4-24
Table 6.4.4-26	Single Cask Containment Reflected Results Comparison for Homogenized UO_2 /Water Model	6.4.4-24
Table 6.4.5-1	Parametric Study – Fuel / Basket k_{eff} versus TRIGA Fuel Element Type, Nonpoisoned Basket	6.4.5-18
Table 6.4.5-2	Parametric Study – Cask k_{eff} versus TRIGA Fuel Element Type, Poisoned Basket	6.4.5-19
Table 6.4.5-3	Axially Infinite Cask k_{eff} with TRIGA Fuel Elements- Fuel Element Placement Perturbations, Nonpoisoned Basket	6.4.5-20
Table 6.4.5-4	Axially Infinite Cask k_{eff} with TRIGA Fuel Elements - Fuel Element Placement Perturbations, Poisoned Basket	6.4.5-20
Table 6.4.5-5	Axially Infinite Cask k_{eff} with TRIGA Fuel Elements – Basket Manufacturing Tolerance Perturbations, Nonpoisoned Basket	6.4.5-21
Table 6.4.5-6	Axially Infinite Cask k_{eff} with TRIGA Fuel Elements – Basket Manufacturing Tolerance Perturbations, Poisoned Basket	6.4.5-21
Table 6.4.5-7	Screened Can Preferential Flooding and Partial Loading Reactivity Evaluations for TRIGA Fuel Elements, Nonpoisoned and Poisoned Baskets	6.4.5-22

List of Tables (continued)

Table 6.4.5-8	Sealed Can Preferential Flooding and Partial Loading Reactivity Evaluations for TRIGA Fuel Elements, Nonpoisoned and Poisoned Baskets	6.4.5-23
Table 6.4.5-9	Summary of Most Reactive Configurations, TRIGA Fuel Elements, Nonpoisoned Basket.....	6.4.5-24
Table 6.4.5-10	Summary of Most Reactive Configurations, TRIGA Fuel Elements, Poisoned Basket	6.4.5-24
Table 6.4.5-11	Reactivity Results for TRIGA Fuel Elements, Sealed Cans, Normal Conditions, Nonpoisoned Basket	6.4.5-25
Table 6.4.5-12	Reactivity Results for TRIGA Fuel Elements, Sealed Cans, Accident Conditions, Nonpoisoned Basket	6.4.5-26
Table 6.4.5-13	Reactivity Results for TRIGA Fuel Elements, Screened Cans, Normal Conditions, Poisoned Basket	6.4.5-27
Table 6.4.5-14	Reactivity Results for TRIGA Fuel Elements, Screened Cans, Accident Conditions, Poisoned Basket	6.4.5-28
Table 6.4.5-15	Single Package 10 CFR 71.55(b)(3) Evaluation k_{eff} Summary, TRIGA Fuel Element, Nonpoisoned Basket	6.4.5-29
Table 6.4.5-16	Single Package 10 CFR 71.55(b)(3) Evaluation k_{eff} Summary, TRIGA Fuel Element, Poisoned Basket.....	6.4.5-29
Table 6.4.5-17	Fuel Element Physical Characteristics Evaluation.....	6.4.5-30
Table 6.4.5-18	Element Variation to Reduce k_s Below 0.95.....	6.4.5-31
Table 6.4.5-19	General Model Configuration – Dry to Wet System Reactivity Changes, 70 wt % ^{235}U Stainless Steel Clad Fuel - Nominal Fuel Parameters	6.4.5-31
Table 6.4.5-20	Primary Fuel Type Reactivity Comparison – Accident Conditions Eight-Cask Array (No Cans)	6.4.5-32
Table 6.4.5-21	Normal Condition Maximum System Reactivities (No Cans)	6.4.5-32
Table 6.4.6-1	Cask k_{eff} with TRIGA Fuel Cluster Rods – Fuel Rod Placement Perturbations, Nonpoisoned Basket	6.4.6-7
Table 6.4.6-2	Cask k_{eff} with TRIGA Fuel Cluster Rods – Fuel Rod Placement Perturbations, Poisoned Basket.....	6.4.6-7
Table 6.4.6-3	Axially Infinite Cask k_{eff} with TRIGA Fuel Cluster Rods – Basket and Insert Manufacturing Tolerance Perturbations, Nonpoisoned Basket.....	6.4.6-8
Table 6.4.6-4	Axially Infinite Cask k_{eff} with TRIGA Fuel Cluster Rods – Basket and Insert Manufacturing Tolerance Perturbations, Poisoned Basket	6.4.6-9
Table 6.4.6-5	Sealed Can Preferential Flooding and Partial Loading Reactivity Evaluations for TRIGA Fuel Rod Clusters, Nonpoisoned Basket	6.4.6-10
Table 6.4.6-6	Sealed Can Preferential Flooding and Partial Loading Reactivity Evaluations for TRIGA Fuel Rod Clusters, Poisoned Basket	6.4.6-10
Table 6.4.6-7	Summary of Most Reactive Configurations, TRIGA Fuel Cluster Rods, Nonpoisoned Basket.....	6.4.6-11
Table 6.4.6-8	Summary of Most Reactive Configurations, TRIGA Fuel Cluster Rods, Poisoned Basket.....	6.4.6-11

List of Tables (continued)

Table 6.4.6-9	Reactivity Results for TRIGA Fuel Cluster Rods, Sealed Cans, Normal Conditions, Nonpoisoned Basket.....	6.4.6-12
Table 6.4.6-10	Reactivity Results for TRIGA Fuel Cluster Rods, Sealed Can, Accident Conditions, Nonpoisoned Basket.....	6.4.6-13
Table 6.4.6-11	Reactivity Results for TRIGA Fuel Cluster Rods, Sealed Cans, Normal Conditions, Poisoned Basket.....	6.4.6-14
Table 6.4.6-12	Reactivity Results for TRIGA Fuel Cluster Rods, Sealed Cans, Accident Conditions, Poisoned Basket.....	6.4.6-15
Table 6.4.6-13	Single Package 10 CFR 71.55(b)(3) Evaluation k_{eff} Summary, TRIGA Fuel Cluster Rod, Nonpoisoned Basket	6.4.6-16
Table 6.4.6-14	Single Package 10 CFR 71.55(b)(3) Evaluation k_{eff} Summary, TRIGA Fuel Cluster Rod, Poison Basket.....	6.4.6-16
Table 6.4.6-15	Increased Fuel Dimensional Parameter k_{eff} Summary, TRIGA Fuel Cluster Rod, Nonpoisoned Basket.....	6.4.6-17
Table 6.4.7-1	Normal Condition HEU, LEU, MEU DIDO Evaluation.....	6.4.7-7
Table 6.4.7-2	HEU DIDO Accident Evaluation – Radial Shift and Exterior Moderator Density Variation.....	6.4.7-8
Table 6.4.7-3	DIDO Heat Shunt and Aluminum Shell Evaluation Results.....	6.4.7-8
Table 6.4.7-4	DIDO Basket Geometric Tolerance Study Results	6.4.7-8
Table 6.4.7-5	DIDO Fuel Assembly Tolerance Study Results.....	6.4.7-9
Table 6.4.7-6	DIDO Fuel Maximum Reactivity Combinations	6.4.7-10
Table 6.4.7-7	Moderator Density Study for the Infinite Array of Casks (Nominal Fuel and Basket Configuration).....	6.4.7-11
Table 6.4.7-8	DIDO Single Package 10 CFR 71.55(b)(3) Evaluation k_{eff} Summary	6.4.7-12
Table 6.4.7-9	DIDO Fuel Assembly Tolerance Study Results (Reduced Clad Thickness)	6.4.7-12
Table 6.4.7-10	DIDO Fuel Maximum Reactivity Combinations (Reduced Clad Thickness)	6.4.7-12
Table 6.4.7-11	DIDO Fuel Maximum Reactivity Combinations (Reduced Clad and Maximum Pitch).....	6.4.7-13
Table 6.4.7-12	DIDO Bounding Configurations	6.4.7-14
Table 6.4.8-1	GA IFM Payload Evaluation Result Summary	6.4.8-5
Table 6.4.8-2	GA IFM TRIGA Rectangular Array Pitch Evaluation Result Summary	6.4.8-6
Table 6.4.8-3	GA IFM TRIGA Square Array Pitch Evaluation Result Summary.....	6.4.8-6
Table 6.4.8-4	GA IFM Interior Moderator Density Evaluation Result Summary	6.4.8-7
Table 6.4.8-5	GA IFM HTGR Matrix Moderator Density Evaluation Result Summary ...	6.4.8-8
Table 6.4.8-6	GA IFM Exterior Moderator Density Evaluation Result Summary	6.4.8-9
Table 6.4.8-7	GA IFM Partial Flooding Comparison Result Summary	6.4.8-10
Table 6.4.8-8	GA IFM Partial Flooding Interior Moderator Density, Void Exterior Result Summary	6.4.8-10
Table 6.4.8-9	GA IFM Partial Flooding Interior Moderator Density, Water Exterior Result Summary	6.4.8-11

List of Tables (continued)

Table 6.4.8-10	GA IFM Partial Flooding Exterior Moderator Density, Void Interior Result Summary	6.4.8-12
Table 6.4.8-11	GA IFM Partial Flooding Exterior Moderator Density, Water Interior Result Summary	6.4.8-13
Table 6.4.8-12	GA IFM Partial Flooding Single Cask Result Comparison	6.4.8-13
Table 6.4.8-13	GA IFM Damaged TRIGA Fuel Result Summary	6.4.8-14
Table 6.4.9-1	PULSTAR Intact Assembly Shift Results	6.4.9-7
Table 6.4.9-2	PULSTAR Intact Assembly Mechanical Perturbation Results	6.4.9-7
Table 6.4.9-3	PULSTAR Intact Assembly Lattice Moderator Ratio Results	6.4.9-8
Table 6.4.9-4	PULSTAR Canned Intact Element Results	6.4.9-8
Table 6.4.9-5	PULSTAR Canned Homogenized Element Results	6.4.9-9
Table 6.4.9-6	PULSTAR Maximum Reactivity Summary	6.4.9-10
Table 6.4.10-1	Spiral Fuel Assembly - Base Data Comparisons	6.4.10-9
Table 6.4.10-2	Spiral Fuel Assembly - Basket Tolerance Evaluations	6.4.10-10
Table 6.4.10-3	Spiral Fuel Assembly - Fuel Tolerance Evaluations	6.4.10-11
Table 6.4.10-4	Spiral Fuel Assembly - Moderator Density Variations	6.4.10-12
Table 6.4.10-5	Spiral Fuel Assembly - Maximum Reactivity Case Summary	6.4.10-13
Table 6.4.10-6	MOATA Plate Bundle - Base Data Comparisons	6.4.10-14
Table 6.4.10-7	MOATA Plate Bundle - Basket Tolerance Evaluations	6.4.10-15
Table 6.4.10-8	MOATA Plate Bundle - Fuel Tolerance Evaluations	6.4.10-16
Table 6.4.10-9	MOATA Plate Bundle - Moderator Density Variations	6.4.10-17
Table 6.4.10-10	MOATA Plate Bundle - Maximum Reactivity Case Summary	6.4.10-18
Table 6.5.1-1	KENO-Va and 27-Group Library Validation Statistics	6.5.1-11
Table 6.5.2-1	Criticality Results for High Enrichment Uranium Systems	6.5.2-3

6 CRITICALITY EVALUATION

The NAC-LWT cask is designed to transport either 1 pressurized water reactor (PWR) assembly; up to 25 intact PWR or BWR rods in a rod holder or fuel assembly lattice; up to 25 PWR or BWR fuel rods with a maximum of 14 of the rods classified as damaged in a rod holder; 2 boiling water reactor (BWR) assemblies; 15 sound metallic fuel rods; 6 failed metallic fuel rods; up to 42 high enriched uranium (HEU), medium enriched uranium (MEU) or low enriched uranium (LEU) Materials Test Reactor (MTR) fuel elements, or DIDO fuel assemblies; up to 140 TRIGA fuel elements; two packages of General Atomics Irradiated Fuel Material (GA IFM); up to 560 TRIGA fuel cluster rods; 1 consolidation canister with up to 300 TPBARs (including up to 2 damaged TPBARs); up to 700 PULSTAR fuel elements; up to 42 spiral fuel assemblies; or up to 42 MOATA plate bundles. This chapter illustrates that all packages meet the requirements of parts 71.55, 71.59 and 71.71 of 10 CFR 71.

In accordance with the requirements of 10 CFR 71.59 (b), the NAC-LWT cask is assigned a Criticality Safety Index (CSI) for criticality control for the authorized contents as follows: 100 for PWR assemblies; 5 for BWR assemblies; 12.5 for DIDO assemblies; 0 for metallic fuel, TPBARs, spiral fuel assemblies; MOATA plate bundles, high burnup PWR or BWR rods with up to 14 damaged rods, MTR elements, TRIGA fuel elements loaded into a poisoned basket, TRIGA fuel cluster rods, TRIGA payloads with screened cans containing up to four TRIGA elements in a nonpoisoned basket, and GA IFM packages. The CSI for PULSTAR fuel is 0 for a payload of intact elements and 33.4 for a mixed payload of intact and damaged elements.

6.1 Discussion and Results

Analyses are performed on the NAC-LWT cask for one PWR assembly and two BWR assemblies. Both PWR and BWR packages are examined for normal transport conditions and hypothetical accident conditions. The hypothetical accident conditions are modeled with the fuel at its most reactive credible configuration. The design of the cask and the fuel basket is such that, under all conditions, the highest neutron multiplication factor with correction for bias and uncertainty is less than 0.95. Analyses to demonstrate conformance to this criterion include (1) no dissolved boron in the neutron shield tank, thus improving the shield tank neutron reflection; (2) no structural material present in the assembly; and (3) no dissolved boron in the cask cavity or surrounding loading or storage area. No credit is included for burnup or for the buildup of fission product neutron poisons.

Analyses are performed for the NAC-LWT cask with the most limiting single PWR assembly and also for the most limiting BWR assemblies. Sections 6.3.1 and 6.3.2 present the methods (CSAS25) and KENO-Va models used in the analysis for each of these respective fuel assemblies. Sections 6.4.1 and 6.4.2 present the criticality analysis results for the PWR and BWR fuel assemblies, respectively. The maximum PWR fuel enrichment is set at 3.7 wt % ^{235}U , but it was found that certain PWR fuel assemblies were required to be limited to a maximum uranium enrichment of 3.5 wt % ^{235}U . Thus, two design-basis PWR assemblies were consequently selected. Namely, a design basis case with the uranium enrichment limited to 3.7 wt % ^{235}U and a second design basis case for those assemblies with the uranium enrichment limited to 3.5 wt % ^{235}U .

Analyses are performed on the NAC-LWT with fuel baskets designed to transport up to 42 MTR research reactor fuel elements. Shipment of MTR loose fuel plates is evaluated inside an MTR plate canister. Section 6.3.2 presents the methods (CSAS25) and KENO-Va models used in the analysis. Section 6.4.3 presents the criticality analysis results of the NAC-LWT loaded with MTR fuel. Section 6.5.2 presents the validation of CSAS25 for use in criticality evaluations of MTR fuel. Criticality of the NAC-LWT cask with the most limiting MTR fuel assembly type and basket configuration is evaluated. The fuel assemblies are assumed to be unburned. An infinite array of casks of infinite axial extent is analyzed. The cask/basket configuration is examined for normal transport and accident conditions. Both normal and accident conditions consider variation in moderator density inside and outside the cask as well as the spacing between casks. Reactivity penalties for mechanical perturbations are also considered. The results show that the k_{eff} of an infinite array of NAC-LWT casks with the most limiting MTR fuel and at optimum interspersed moderation is always below 0.95 including the method bias, method uncertainty, Monte Carlo uncertainty and penalties due to mechanical perturbations.

Analyses are performed on the NAC-LWT with up to 25 PWR or BWR fuel rods of 5.0 wt % ^{235}U initial enrichment. Separate evaluations are performed for a payload consisting of only intact rods in a rod holder, a payload including up to 14 damaged rods in a rod holder, and rods in a fuel assembly lattice. Section 6.3.3 presents the methods (CSAS25) and KENO-Va model used in the rod holder or fuel assembly lattice analyses. Section 6.4.4 presents the criticality analysis results of the NAC-LWT loaded with up to 25 PWR or BWR fuel rods in either a rod holder or a fuel assembly lattice. The system reactivity of the NAC-LWT with up to 25 PWR or BWR fuel rods in intact (rod holder or lattice) or damaged configurations is evaluated as a function of rod pitch. Damaged fuel evaluations include the removal of clad and fuel and moderator mixture studies. The fuel is assumed to be fresh, i.e., no burnup credit. An infinite array of casks is analyzed. Variation of moderator density inside and outside the cask also is considered. The results show that the k_{eff} of an infinite array of NAC-LWT casks at optimum fuel rod pitch and at optimum interspersed moderation is significantly below 0.95 including the method bias, method uncertainty and Monte Carlo uncertainty.

Poisoned and nonpoisoned basket configurations of the NAC-LWT cask are evaluated for TRIGA fuel elements with up to 70 wt % ^{235}U initial enrichment and TRIGA fuel cluster rods with up to 93.3 wt % ^{235}U initial enrichment. The placement of sealed canisters in the top and bottom baskets of the cask is also evaluated to permit the transport of failed TRIGA fuel. Section 6.3.4 presents the methods (CSAS25) and the models used in the analyses. Section 6.4.5 presents the criticality analysis results for the NAC-LWT cask loaded with TRIGA fuel elements, while Section 6.4.6 presents the results for TRIGA fuel cluster rods. The fuel is assumed to be fresh (unirradiated) and the effects of burnable absorbers are conservatively ignored. An infinite array of casks is analyzed. Variation of moderator density inside and outside the cask is considered. Variation of geometrical configurations are also analyzed, including the tolerances of the TRIGA basket materials and fuel element positioning, to determine the most reactive configuration. The results show that the k_{eff} of an array of NAC-LWT casks with TRIGA fuel at optimum fuel element pitch, geometrical configuration, and optimum moderation is always below 0.95, including corrections for bias and uncertainty. An infinite cask array is evaluated for the poisoned and nonpoisoned TRIGA cluster rod baskets and the poisoned TRIGA fuel element basket, while a finite cask array is applied to the nonpoisoned TRIGA fuel element evaluations.

Analyses are performed on the NAC-LWT with fuel baskets designed to transport up to 42 DIDO fuel assemblies. Section 6.3.6 presents the methods (CSAS25) and KENO-VA models used in the analysis. Section 6.4.7 presents the criticality analysis results of the NAC-LWT loaded with DIDO fuel. Section 6.5.2 presents the validation of CSAS25 for use in criticality evaluations of DIDO fuel. Criticality of the NAC-LWT cask with the most limiting DIDO fuel assembly type (HEU) and basket configuration is evaluated. The fuel elements are assumed to be unburned.

An infinite array of casks of infinite axial extent is analyzed. The cask/basket configuration is examined for normal transport and accident conditions. Variations in moderator density inside and outside the cask are evaluated. Reactivity penalties for mechanical perturbations are also considered. The results show that the bias adjusted k_{eff} of an infinite array of NAC-LWT casks with the most limiting DIDO fuel under accident conditions at optimum interspersed moderation (void) is above 0.95. Limiting the accident array to a maximum of eight casks results in a k_{eff} below 0.95 including the method bias, method uncertainty, Monte Carlo uncertainty and penalties due to mechanical perturbations.

Analyses are performed of the NAC-LWT with a fuel basket designed to transport two Fuel Handling Units (packages) of General Atomics (GA) Irradiated Fuel Material (IFM). The first IFM package is composed of Reduced-Enrichment Research and Test Reactor (RERTR) type TRIGA fuel and the second is composed of High-Temperature Gas-cooled Reactor (HTGR) type fuel. Each set of IFM is packaged into stainless steel weld-encapsulated primary and secondary enclosures. Section 6.3.8 presents the methods (CSAS25) and KENO-Va models used in the analyses. Section 6.4.8 presents the criticality analysis results of the two GA IFM packages in the NAC-LWT. Section 6.5.3 presents the validation of CSAS25 for use in criticality evaluations of TRIGA fuel, which is deemed relevant for the GA IFM as discussed in Section 6.4.8. Criticality of the NAC-LWT cask with GA IFM is evaluated using pre-irradiation material compositions. No credit is taken for the basket structure axially or radially, and an infinite array of casks of infinite axial extent is analyzed. Variations in moderator density inside and outside the cask are evaluated, as well as the partial flooding of the IFM packages. The results show that the bias adjusted k_{eff} of an infinite array of NAC-LWT casks under accident conditions at optimum internal and interstitial moderation is less than 0.95, including corrections for bias and uncertainty. Maximum reactivity is obtained with flooded IFM packages, a void NAC-LWT cavity, and a void exterior.

The metallic fuel rods are not analyzed because the metallic fuel is at natural enrichment, and cannot become critical without the presence of heavy water (Paxton).

Criticality evaluations for the NAC-LWT loaded with TPBARs (Tritium Producing Burnable Absorber Rods) are not required because the TPBARs do not contain fissile material and, therefore, cannot form a critical configuration.

Analyses are performed of the NAC-LWT with a stack of four 28 MTR 7-element modules with a PULSTAR fuel element payload. PULSTAR fuel assemblies are comprised of a 5x5 rectangular fuel element array surrounded by a Zircaloy box with aluminum upper and lower fittings. The fuel elements are Zircaloy-clad UO_2 pellets conservatively evaluated at an enrichment of 6.5 wt % ^{235}U . PULSTAR fuel assemblies may be loaded directly into the module

cells. Individual intact PULSTAR fuel elements may be loaded into either a 4×4 fuel rod insert, or one of two PULSTAR cans. The can loadings are only permissible in the top and base modules. Damaged PULSTAR fuel elements or debris must be loaded into either of the cans. Section 6.3.7 presents the methods (CSAS25) and KENO-Va models used in the analyses. Section 6.4.9 presents the criticality analyses results of the various permissible loading configurations. Section 6.5.1-1 presents the validation of CSAS25 for use in criticality evaluations of PWR and BWR fuel, which is deemed relevant for PULSTAR fuel as discussed in Section 6.4.9. Criticality is evaluated using pre-irradiation material compositions. The basket structure axial and radial extents are explicitly modeled in a cask of finite axial extent. Cask arrays analyzed are dependent on the payload of either intact fuel or a mixed loading of intact fuel and canned elements. Variations in moderator density inside and outside the cask are evaluated, as well as the preferential flooding of the cans. The results show that the bias adjusted k_{eff} under accident conditions at optimum internal and interstitial moderation is less than 0.95, including corrections for bias and uncertainty. Maximum reactivity is obtained for a preferentially flooded cask containing two modules baskets of intact fuel assemblies and two modules of cans (each can contains 25 damaged fuel elements). Preferential flooding in this case is a void NAC-LWT cavity, flooded fuel cans, and a void cask exterior (including a void neutron shield).

Analyses are performed on the NAC-LWT with ANSTO fuel baskets designed to transport up to 42 spiral fuel assemblies, 42 MOATA plate bundles, or a combination of spiral assembly baskets and plate bundle baskets. Section 6.3.8 presents the methods (CSAS25) and KENO-VA models used in the analysis. Section 6.4.10 presents the criticality analysis results of the NAC-LWT loaded with spiral fuel assemblies or plate bundles. Section 6.5.2 presents the validation of CSAS25 for use in criticality evaluations of the ANSTO basket. Criticality of the NAC-LWT cask with the most limiting fuel characteristics and basket configuration is evaluated. The fuel elements are assumed to be unburned. An infinite array of casks in both the radial and axial extent is analyzed. The cask/basket configuration is examined for normal transport and accident conditions. Variations in moderator density inside and outside the cask are evaluated. Reactivity penalties for mechanical perturbations are also considered. The results show that the bias adjusted k_{eff} of an infinite array of NAC-LWT casks with the most-limiting ANSTO basket payload under normal and accident conditions at optimum interspersed moderation (void) is below 0.95.

6.2 Package Fuel Loading

The NAC-LWT cask can safely transport 1 PWR assembly, up to 25 intact PWR or BWR rods in a rod holder or fuel assembly lattice, up to 25 PWR or BWR rods with up to 14 of the fuel rods classified as damaged in a rod holder, 2 BWR assemblies, 15 sound metallic fuel rods, 6 failed metallic fuel rods, up to 42 MTR fuel elements, up to 140 TRIGA fuel elements, up to 560 TRIGA fuel cluster rods, up to 42 DIDO fuel assemblies, two General Atomics Irradiated Fuel Material packages, up to 300 TPBARs (of which two can be damaged), up to 700 PULSTAR fuel elements, up to 42 spiral fuel assemblies, or up to 42 MOATA plate bundles. The characteristics for payloads containing fissile material are presented in the following sections. Fresh fuel is conservative because the fuel becomes less reactive as burnup increases. Burnable poisons, such as the gadolinium rods sometimes used in BWR assemblies, are ignored for conservatism.

TPBARs are stainless steel clad rods containing LiAlO_2 absorber pellets and nickel-plated Zircaloy getter tube or nickel-plated zirconium (NPZ) alloy spacer tubes with no absorber pellets. The TPBARs do not contain any fissile material.

6.2.1 PWR Fuel Assemblies

Table 6.2.1-1 and Table 6.2.1-2 contain the geometry data for the PWR assemblies. Relevant dimensions are in three categories: Fuel Rod, Guide Tube and Instrument Tube. Fuel rod data includes the number of fuel rods, pitch, diameter, clad thickness, clad material, pellet diameter and active fuel length. The guide tube and instrument tube geometry sections include the number of tubes, tube diameter, tube thickness and tube material.

Table 6.2.1-1 B&W, CE and Westinghouse PWR Fuel Assembly Data

Fuel Type/ Parameter	B&W 15x15 Mark B4	B&W 17x17 Mark C	CE 14x14	CE 16x16 SYS 80	West 14x14 Std	West 14x14 OFA	West 15x15	West 17x17	West 17x17 OFA
Fuel Rod Data									
# Rods	208	264	176	236	179	179	204	264	264
Pin Pitch (in)	0.568	0.502	0.58	0.506	0.556	0.556	0.563	0.496	0.496
Rod Dia. (in)	0.43	0.379	0.44	0.382	0.422	0.4	0.422	0.374	0.36
Clad Thick. (in)	0.0265	0.024	0.028	0.025	0.0225	0.0243	0.0242	0.0225	0.0225
Clad Mat.	Zirc	Zirc	Zirc	Zirc	Zirc	Zirc	Zirc	Zirc	Zirc
Pellet Dia. (in)	0.3686	0.3232	0.3765	0.325	0.3674	0.3444	0.3659	0.3225	0.3088
Act. Length (in)	144	143	137	150	145.2	144	144	144	144
Guide Tube Data									
# Tubes	16	24	5	5	16	N/A	16	24	24
Tube Dia. (in)	0.53	0.465	1.15	0.98	0.539	N/A	0.545	0.482	0.482
Tube Thick. (in)	0.016	0.0175	0.04	0.035	0.034	N/A	0.015	0.016	0.016
Tube Mat.	Zirc	Zirc	Zirc	Zirc	Zirc	Zirc	Zirc	Zirc	Zirc
Instrument Tube Data									
# Inst. Tubes	1	1	0	0	1	N/A	1	1	1
Tube Dia. (in)	0.493	0.42	----	----	0.539	N/A	0.545	0.482	0.482
Tube Thick. (in)	0.026	0.015	----	----	0.034	N/A	0.015	0.016	0.016
Tube Mat.	Zirc	Zirc	----	----	Zirc	N/A	Zirc	Zirc	Zirc

N/A – Not Available. Westinghouse 14×14 standard data used in analysis.

Table 6.2.1-2 Exxon/ANF PWR Fuel Assembly Data

Fuel Type/ Parameter	Ex/ANF 14×14 WE	Ex/ANF 15×15 WE	Ex/ANF 17×17 WE	Ex/ANF 14×14 CE
Fuel Rod Data				
# Rods	179	204	264	176
Pin Pitch (in)	0.556	0.563	0.496	0.58
Rod Dia. (in)	0.424	0.424	0.36	0.44
Clad Thick. (in)	0.03	0.03	0.025	0.031
Clad Mat.	Zirc	Zirc	Zirc	Zirc
Pellet Dia. (in)	0.3505	0.3565	0.303	0.37
Act. Length (in)	142	144	144	134
Guide Tube Data				
# Tubes	N/A	20	24	4
Tube Dia. (in)	N/A	0.544	0.48	1.115
Tube Thick. (in)	N/A	0.017	0.016	0.036
Tube Mat.	N/A	Zirc	Zirc	Zirc
Instrument Tube Data				
# Inst. Tubes	N/A	1	1	1
Tube Dia. (in)	N/A	0.544	0.48	1.115
Tube Thick. (in)	N/A	0.017	0.016	0.036
Tube Mat. (in)	N/A	Zirc	Zirc	Zirc

N/A – Not Available. Westinghouse 14×14 standard data used in analysis.

6.2.2 BWR Fuel Assemblies

Table 6.2.2-1 through Table 6.2.2-3 contains the geometry data for the BWR assemblies. Relevant dimensions are in three categories: Fuel Rod, Water Rod and Channel. Fuel rod data includes the number of fuel rods, pitch, clad inner radius, clad outer radius, clad material, pellet radius and active fuel length. The water rod and channel geometry sections include the number of water rods, rod radii, rod and channel thickness and material.

Table 6.2.2-1 GE BWR Fuel Assembly Data

Parameter	GE 7×7	GE 8×8-1	GE 8×8-2	GE 8×8-4	GE 9×9
Fuel Rod					
Pellet Rad. (cm)	0.6058	0.5283	0.5207	0.5200	0.4775
Clad Inner Rad. (cm)	0.6210	0.5398	0.5321	0.5350	0.4890
Clad Outer Rad. (cm)	0.7150	0.6261	0.6134	0.6150	0.5600
Clad Material	Zircaloy	Zircaloy	Zircaloy	Zircaloy	Zircaloy
Pitch / 2 (cm)	0.9373	0.8128	0.8128	0.8100	0.7190
Zircaloy Water Rod					
Inner Rad. (cm)	—	0.5398	0.6744	0.5370	1.5000
Outer Rad. (cm)	—	0.6261	0.7506	0.6150	1.6000
Zircaloy Channel 80 Mil					
Inner Dim. (cm)	±6.7031	±6.7031	±6.7031	±6.7500	±6.7900
Outer Dim. (cm)	±6.9063	±6.9063	±6.9063	±6.9500	±6.9500
Thickness (cm)	0.2032	0.2032	0.2032	0.2000	0.1600
Zircaloy Channel 100 Mil					
Inner Dim. (cm)	N/A	±6.7031	±6.7031	N/A	N/A
Outer Dim. (cm)	N/A	±6.9571	±6.9571	N/A	N/A
Thickness (cm)	N/A	0.2540	0.2540	N/A	N/A
Zircaloy Channel 120 Mil					
Inner Dim. (cm)	N/A	±6.7031	N/A	N/A	N/A
Outer Dim. (cm)	N/A	±7.0079	N/A	N/A	N/A
Thickness (cm)	N/A	0.3048	N/A	N/A	N/A

N/A – Not Applicable. See Table 6.2.2-3 for combinations of fuel/channel.

Table 6.2.2-2 Exxon BWR Fuel Assembly Data

Parameter	Exxon 7×7	Exxon 8×8-1	Exxon 8×8-2	Exxon 9×9
Fuel Rod				
Pellet Rad. (cm)	0.6223	0.5137	0.5137	0.4528
Clad Inner Rad. (cm)	0.6325	0.5232	0.5232	0.4623
Clad Outer Rad. (cm)	0.7239	0.6147	0.6147	0.5385
Clad Material	Zircaloy	Zircaloy	Zircaloy	Zircaloy
Pitch / 2 (cm)	0.9373	0.8141	0.8141	0.7264
Zircaloy Channel ≤80 Mil				
Inner Width (cm)	6.7031	6.7031	6.7031	6.8000

Table 6.2.2-3 BWR Fuel Assembly Data

Assembly Type	Number Rods		Channel Thickness	Active Fuel Length (in)
	Fuel	Water		
Exxon 9x9	79	2	80 Mil	150
Exxon 9x9	79	2	2mm	150
Exxon 9x9	74	2	2mm	150
GE 8x8	62	2	80 Mil	150
GE 8x8	62	2	100 Mil	150
GE 9x9	74	2	80 Mil	150
GE 7x7	49	0	80 Mil	146
Exxon 8x8-2	62	2	80 Mil	150
GE 8x8	60	4	2mm	150
GE 9x9	79	2	2mm	150
Exxon 8x8-1	63	1	80 Mil	145.2
GE 9x9	79	2	80 Mil	150
Exxon 7x7	49	0	80 Mil	144
GE 8x8	63	1	120 Mil	146
GE 8x8	63	1	100 Mil	146
GE 8x8	63	1	80 Mil	146

6.2.3 MTR Fuel Elements

The NAC-LWT MTR basket designs can transport up to 42 MTR research reactor fuel elements. This configuration consists of seven fuel elements placed radially in each of four, five or six axial fuel basket segments. The analysis provided herein is bounding for all MTR element loading configurations.

An MTR fuel element comprises fuel plates held in a parallel arrangement by thick aluminum slotted side plates. The number of fuel plates range from 10 to 23 per element. The fuel plates have a fuel meat composed of either $\text{U}_3\text{O}_8\text{-Al}$, U-Al or USi-Al . The listed fuel enrichment ranges up to slightly greater than 93 wt % ^{235}U . Thus, initial criticality analysis is performed at a nominal 93 wt % ^{235}U with a reactivity penalty of ± 1 wt % ^{235}U applied to allow for enrichment variation up to 94 wt % and with a reactivity penalty of ± 5 grams per element to allow for loading variation up to 355 grams per element.

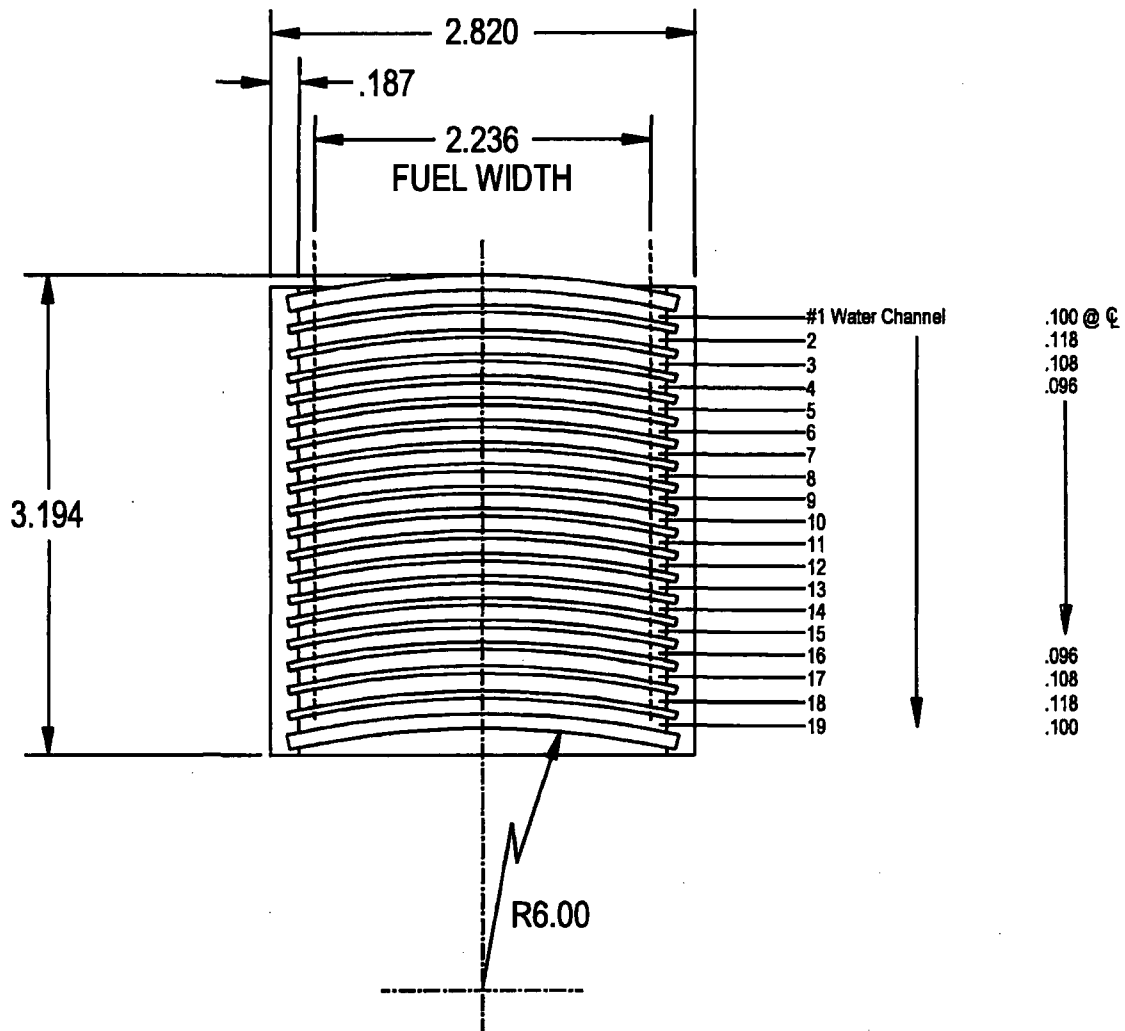
Figure 6.2.3-1 shows a cross-sectional view of the design basis MTR fuel element. The various design basis HEU, LEU and MEU MTR fuel characteristics are shown in Table 6.2.3-1, Table 6.2.3-2 and Table 6.2.3-3, respectively. The High Flux Beam Reactor (HFBR) is modeled in the criticality analysis as the design basis MTR fuel element design, and is shown in

Figure 6.2.3-1. The listed fuel dimensions are extended to arrive at bounding fuel configurations in Section 6.4.3.

The bounding fuel dimensions provide for loading MTR fuel elements containing up to a maximum ^{235}U content of 460 grams (20 grams per plate in 23 plates), and LEU specific loads up to 736 grams ^{235}U (32 grams per plate in 23 plates). Total ^{235}U content of the fuel elements modeled in the criticality evaluations may exceed that used in the Chapter 5 shielding analysis. For cases containing a lower fissile material content in the shielding evaluations, the lower value represents the cask payload limit.

MTR fuel plates can also be transported. The loose plates are placed inside an MTR plate canister prior to placement into the NAC-LWT MTR basket. The number of fuel plates in each canister is restricted to that of an equivalent MTR fuel element.

Figure 6.2.3-1 Design Basis HFBR MTR Fuel Element



(18) INNER FUEL PLATES, 23 3/4" LONG, .050" THICK
FUEL ALLOY CORE 22 3/4" LONG, .021 THICK
CLADDING .0145" THICK. TOTAL U²³⁵ CONTENT - 351 g
OUTER ALUMINUM PLATES .100" THICK

Table 6.2.3-1 Characteristics of Design Basis HEU MTR Fuels

Reactor ^{1/} Fuel Parameters	HFBR	ORR #1	ORR #2	OWR	BSR	NISTR ³	THOR
Element Length (cm)	145.4	97.5	97.5	108.31	94.3	34	100.3
Element Width (cm)	7.2	7.6	7.6	7.7	7.6	7.6	7.6
Element Depth (cm)	8.2	8.0	8.0	8.4	8.4	8.3	7.7
Side Plate Thickness (cm)	0.475	0.475	0.475	0.475	0.475	0.475	0.51
No. of Plates	18+2 Al	19	19	19	19	17+2 Al	10
Plate Thickness (cm)	0.127	0.127	0.127	0.127	0.129	0.127	0.251
Active Fuel Length (cm)	57.8	60.0	60.0	61.2	59.8	28.0	60.0
Active Fuel Width (cm)	5.72	6.35	6.35	6.47	6.3	6.35	6.0
Active Fuel Thickness (cm)	0.053	0.051	0.051	0.051	0.051	0.051	0.175
Clad Thickness (cm)	0.037	0.038	0.038	0.038	0.038	0.038	0.038
Water Channel Thickness (cm)	0.244 ²	0.295	0.295	0.295	0.295	0.295	0.51
Fuel Composition	U ₃ O ₈ -Al	U-Al	U ₃ O ₈ -Al	U ₃ O ₈ -Al	U-Al ⁴	U ₃ O ₈ -Al	U-Al
Wt % ²³⁵ U (nominal) ⁵	93	93	93	93	93	93	93
²³⁵ U per Fuel Element (grams)	351	202	285	232	223	181.05	140
²³⁵ U per Plate (grams)	19.5	10.6	15	12.21	11.7	10.65	14
U Density (g U/cm ³)	1.197	0.59	0.83	0.60	0.66	1.25	0.23
U in Fuel Composition (wt %)	30	20	25	25	20	30	8

Notes:

1. Reactors:

HFBR - High Flux Beam Reactor, Brookhaven USA

ORR - Oak Ridge Research Reactor, Oak Ridge USA

OWR - Omega West Reactor, Los Alamos USA

BSR - Bulk Shielding Reactor, Oak Ridge USA

NISTR - National Institute of Standards Test Reactor, Washington D.C. USA

THOR - Tsing Hua Open-Pool Reactor, Hsinchu, Taiwan

2. Variable outer plate spacing.

3. Fuel element cut in half. Two half-sections are loaded into each basket cell.

4. Two plates in some fuel elements contain U₃O₈.

5. Maximum 94 wt % enrichment analyzed in Section 6.4.3.4 for conservatism.

Table 6.2.3-1 Characteristics of Design Basis HEU MTR Fuels (continued)

Reactor/ Fuel Parameters	GRR #1 (NUKEM)	GRR #2 (US Nuc)	GRR #3 (CERCA)	ASTRA	SAPFIR #1	SAPFIR #2	PRR
Element Length (cm)	95.0	95.0	95.0	87.3	87.3	87.3	100.3
Element Width (cm)	7.6	7.6	7.6	7.6	7.6	7.6	7.6
Element Depth (cm)	8.0	8.0	8.0	8.0	8.0	8.0	7.6
Side Plate Thickness (cm)	0.45	0.45	0.45	0.45	0.45	0.45	0.47
No. of Plates	19	18	18	23	23	23	18
Plate Thickness (cm)	0.127	0.127	0.152	0.127	0.127	0.127	0.152
Active Fuel Length (cm)	60.	60.	60.	62.5	62.5	62.5	62.2
Active Fuel Width (cm)	6.3	6.3	6.3	6.28	6.28	6.28	6.12
Active Fuel Thickness (cm)	0.051	0.051	0.050	0.051	0.051	0.051	0.1016
Clad Thickness (cm)	0.038	0.038	0.051	0.038	0.038	0.038	0.0254
Water Channel Thickness (cm)	0.295	0.315	0.290	0.223	0.223	0.223	0.279
Fuel Composition	U-Al	U-Al	U-Al	U-Al	U-Al	U ₃ Si ₂ -Al	U-Al
Wt % ²³⁵ U (nominal)	93	93	93	93	90	93	94
²³⁵ U per Fuel Element (grams)	180.5	187.2	180.9	281	281	281	247
²³⁵ U per Plate (grams)	9.5	10.4	10.05	12.2	12.2	12.2	13.7
U Density (g U/cm ³)	0.53	0.58	0.57	0.66	0.68	0.66	0.378
U in Fuel Composition (wt %)	20	20	20	20	20	20	12.5

Notes:

1. Reactors:

GRR - Greek Research Reactor, Greece

ASTRA - Adapter Schwimmbecken Tank Reaktor, Austria

SAPFIR - Research Reactor, Switzerland

PRR - Philippine Research Reactor, Philippines

Table 6.2.3-1 Characteristics of Design Basis HEU MTR Fuels (continued)

Reactor/ Fuel Parameters	PRR (Mod)	CNEA #1	CNEA #2	CNEA (Hybrid)
Element Length (cm)	100.3	88.0	88.0	88.0
Element Width (cm)	7.6	7.62	7.6	7.62
Element Depth (cm)	8.03	8.4	8.4	8.4
Side Plate Thickness (cm)	0.47	0.52	0.49	0.49
No. of Plates	19	19	19	19
Plate Thickness (cm)	0.1496	0.130 ± 0.015	0.140 (+0.05, -0.02)	0.108
Active Fuel Length (cm)	62.2	61.5 ± 1.0	61.5 ± 1.0	60.5
Active Fuel Width (cm)	6.12	6.0 ± 0.13	5.9 (+0.05, -0.0)	6.15
Active Fuel Thickness (cm)	0.1016	0.052 ± 0.003	0.056 ± 0.003	0.060
Clad Thickness (cm)	0.024	0.039	0.042 ± 0.006	0.024
Water Channel Thickness (cm)	0.279	0.312 ± 0.015	0.302 (+0.05, -0.02)	0.334
Fuel Composition	U-Al	U-Al	U-Al	U-Al
Wt % ²³⁵ U (nominal)	94	90 ± 1	90 ± 1	91
²³⁵ U per Fuel Element (grams)	262	148.2 ± 5.7	200.1 ± 10.1	218.5
²³⁵ U per Plate (grams)	13.7	7.8 ± 0.3	10.53 ± 0.53	11.5
U Density (g U/cm ³)	0.378	0.452 (+0.071, -0.061)	0.576 (+0.081, -0.075)	0.566
U in Fuel Composition (wt %)	12.5	15.0% ± 0.6%	18.3% ± 0.9%	20.5%
Fuel Meat Al Alloy Weight (g)	102.02	49.1	52.3	49.0

Notes:

1. Reactors:

PRR (Mod) – NAC modified PRR fuel element – 19 plates and reduced clad thickness (0.024 cm).

CNEA – Comision Nacional De Energia Atomica.

CNEA (Hybrid) – NAC modified CNEA element containing maximum reactivity dimensions from the two CNEA plate/element types.

Table 6.2.3-2 Characteristics of Design Basis LEU MTR Fuel

Reactor/ Fuel Parameters	BSR	ZPRL	THOR	RSG- GAS	IEA-R1
Element Length (cm)	97.5	100.3	100.3	N/A	N/A
Element Width (cm)	7.8	7.7	7.62	7.7	7.7
Element Depth (cm)	8.4	7.7	7.73	7.7	7.7
Side Plate Thickness (cm)	0.475	0.477	0.510	0.477	0.477
Number of Plates	19	10	10	21	18
Plate Thickness (cm)	0.127	0.251	0.251	0.130	0.150
Active Fuel Length (cm)	60	60	60	60	60
Active Fuel Width (cm)	6.35	6	6	6.275	6
Active Fuel Thickness (cm)	0.051	0.175	0.175	0.064	0.084
Clad Thickness (cm)	0.038	0.038	0.038	0.033	0.033
Water Channel Thickness (cm)	0.295	0.5356	0.510	0.2724	0.3138
Fuel Composition	U ₃ Si ₂ -Al	U-Al	U-Al	U ₃ O ₈ -Al	U-Al
Weight Percent ²³⁵ U (wt %)	19.75	20	20	19.75	20
²³⁵ U per Fuel Element (grams)	340	210	210	271	180
²³⁵ U per Plate (grams)	17.9	21	21	13	10
U Density (grams U/cm ³)	4.66	0.64	0.64	3	1.8
U in Fuel Composition (wt %)	74	40	40	57	40

Notes:

1. Reactors:

BSR – Bulk Shielding Reactor, ORNL

ZPRL – ZPRL Research Reactor Facility, Taiwan

THOR – Tsing Hua Open-Pool Reactor, Hsinchu, Taiwan

RSG-GAS - National Center for Research and Technology, Serpong, Indonesia

IEA-R1 – IEA-R1 Facility, Brazil

Table 6.2.3-3 Characteristics of Design Basis MEU MTR Fuel

Reactor ^{1/} Fuel Parameters	ASTRA	MEUG
Element Length (cm)	68.65 (cut)	— ²
Element Width (cm)	7.61	7.61
Element Depth (cm)	8.05	8.05
Side Plate Thickness (cm)	0.45	0.45
Number of Plates	23	23
Plate Thickness (cm)	0.127	0.127
Active Fuel Length (cm)	60.0	60.0
Active Fuel Width (cm)	6.275	6.275
Active Fuel Thickness (cm)	0.051	0.053
Clad Thickness (cm)	0.038/0049	0.037
Water Channel Thickness (cm)	0.221 ³	0.221 ³
Fuel Composition	UAl _x -Al	UAl _x -Al ⁴
Weight Percent ²³⁵ U (wt %)	45%	20%-80%
²³⁵ U per Fuel Element (grams)	320	333.5
²³⁵ U per Plate (grams)	13.9	14.5
U Density (grams U/cm ³)	1.63	0.91-2.08
U in Fuel Composition (wt %)	63	38-87

Notes:

- Reactors:
ASTRA – Adaptierter Schwimmbecken Tank Reactor Austria
MEUG – Modified ASTRA MEU fuel element parameters
- Not required for infinite length criticality evaluation.
- Channel thickness was not included in reference information. Indicated channel thickness is the result of assuming a constant channel between all plates and one-half the channel beyond the outer plates.
- Based on a constant fuel mass and material thickness, the fuel material composition (ex. U₃O₈, UAl_x, USi₂) will not have a significant impact on the reactivity of the system.

6.2.4 PWR and BWR Rods in a Rod Holder or Fuel Assembly Lattice

The NAC-LWT cask may transport up to 25 intact PWR or BWR fuel rods in a fuel rod holder or fuel assembly lattice. Up to 14 of 25 PWR or BWR fuel rods in a fuel rod holder may be classified as damaged.

6.2.4.1 Intact PWR or BWR Rods in a Rod Holder or Fuel Assembly Lattice

To bound all PWR and BWR rods that may be transported in the NAC-LWT cask, rods with a maximum enrichment of 5.0 wt % ^{235}U were analyzed. Characteristics of the design basis PWR rods are presented in Table 6.2.1-1 and Table 6.2.1-2. Characteristics of the design basis BWR rods are presented in Table 6.2.2-1, Table 6.2.2-2 and Table 6.2.2-3. Given an infinite length rod and an enrichment of 5.0 wt % ^{235}U as the basis for this analysis, the most reactive PWR and BWR rod has the greatest fissile mass, i.e. the rod with the largest pellet radius. Therefore, the rod used in the CE 14×14 assembly was chosen as the most reactive PWR fuel rod and the rod used in the Exxon 7×7 assembly was chosen as the most reactive BWR fuel rod. A maximum of 25 PWR or BWR rods were used in the analysis.

6.2.4.2 Damaged PWR or BWR Rods in a Rod Holder

The evaluation of the damaged fuel rods uses the bounding fuel characteristics for the intact fuel rod condition as described in Section 6.2.4.1, but assumes that up to 14 of the fuel rods are classified as damaged. Fuel transported in this configuration must be in a fuel rod holder. The fuel rod used in the CE 14×14 assembly was chosen as the most reactive PWR fuel rod, and the rod used in the Exxon 7×7 assembly was chosen as the most reactive BWR fuel rod.

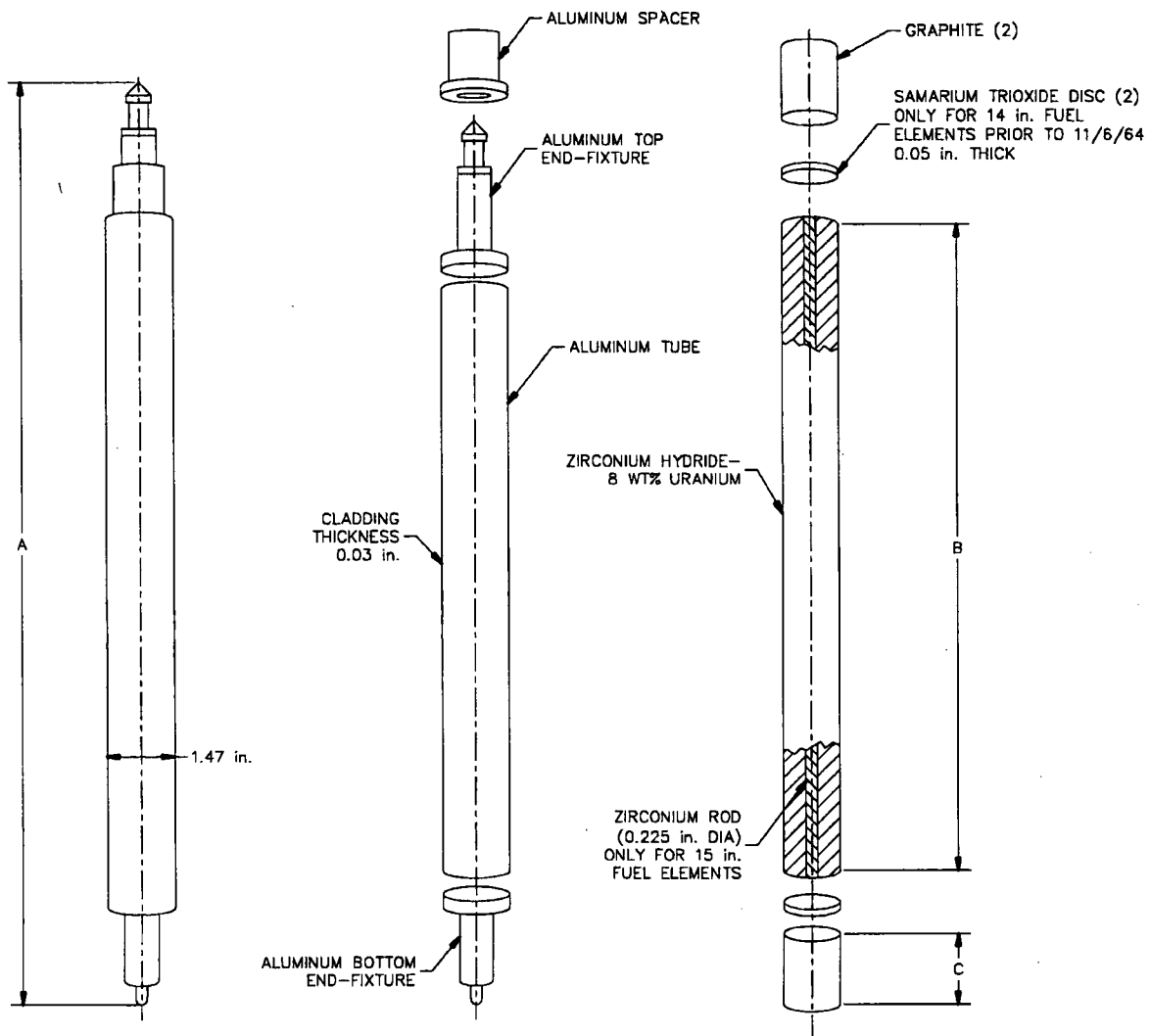
6.2.5 TRIGA Fuel Elements

The NAC-LWT TRIGA non-poisoned and poisoned basket designs can transport up to 140 TRIGA fuel elements. These configurations contain sets of up to 4 intact TRIGA fuel elements. Each set of elements is placed in the cells of the five TRIGA basket modules. In the non-poisoned configuration, the central cell of each module is blocked to prohibit the placement of fuel elements in that location. The NAC-LWT TRIGA basket design can also accommodate sets of four follower control rod (FFCR) elements per cell in the top module. The TRIGA base and top basket modules can accommodate screened failed fuel cans or sealed failed fuel cans for TRIGA failed fuel or fuel debris. The screened failed fuel can is able to hold up to four intact TRIGA fuel elements. The sealed failed fuel can is limited to the equivalent content of two TRIGA fuel elements.

Figure 6.2.5-1 and Figure 6.2.5-2 show typical TRIGA aluminum and stainless steel clad fuel elements, respectively (Tomsio). The various design basis TRIGA fuel element characteristics are shown in Table 6.2.5-1 and Table 6.2.5-2. The TRIGA fuel matrix is a solid uranium-zirconium-hydride metal alloy in which the zirconium-hydride moderator is homogeneously combined with the enriched uranium into pellets. Uranium enrichment in the TRIGA fuel elements is either 20 wt % or 70 wt %. The fuel pellets are loaded into cylindrical rods approximately 1.5 inches in diameter and 30 inches long. Sections of graphite are placed above and below the active fuel section of the TRIGA fuel elements. TRIGA fuel elements can be aluminum clad or stainless steel clad. The FFCR TRIGA fuel element is 45 inches long and has a 15 inch U-ZrH active fuel region with a slightly smaller diameter than 1.5 inches, a 15-inch boron carbide upper section and 6 inch void lower section.

As shown in Figure 6.4.5-1, the design basis TRIGA fuel element type for criticality evaluations is the stainless steel clad element with the FLIP composition enriched to 70 wt % ^{235}U (HEU) and with 137 grams ^{235}U per element. This fuel element design bounds all the other TRIGA fuel elements under consideration, including the stainless steel clad FLIP LEU-II fuel element enriched to 20 wt % ^{235}U and with 169 grams ^{235}U per element. The FFCR elements are also bounded by the design basis TRIGA fuel element.

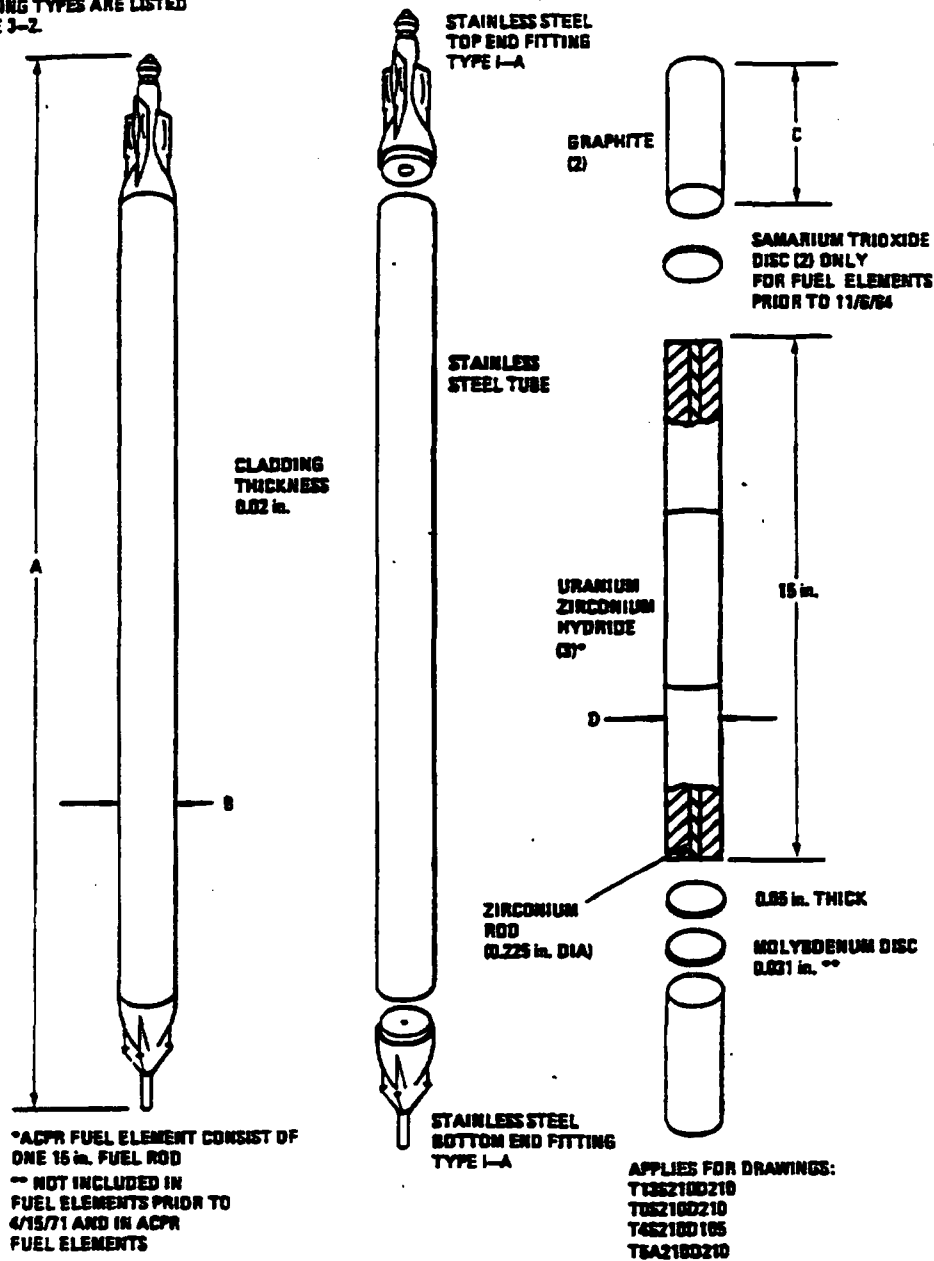
Figure 6.2.5-1 Aluminum Clad TRIGA Fuel Element



TRIGA Fuel Type	A (in.)	B (in.)	C (in.)
Original - 14 in.	28.37	14.0	3.95
Original - 15 in.	28.3	15.0	3.53

Figure 6.2.5-2 Stainless Steel Clad TRIGA Fuel Element

NOTE:
APPLICABLE DIMENSIONS "A-D"
AND FITTING TYPES ARE LISTED
ON TABLE 3-2.



TRIGA Fuel Type	A (in.)	B (in.)	C (in.)	D(in.)
Standard - streamline	29.68	1.478	2.56 ⁽²⁾	1.435
Standard - plain	28.9	1.478	3.42	1.435
ACPR ⁽¹⁾	28.89	1.478	3.45	1.40

- (1) Annular Core Pulse Reactor
(2) Lower graphite is 3.72 inches

Table 6.2.5-1 Characteristics of Design Basis TRIGA Fuels Elements

Element Type	Al Clad	ACPR⁽¹⁾	Steel Clad	Fuel Follower Standard Control Rod⁽⁶⁾
Element Diameter (in.)	1.47	1.478	1.478	1.355
Element Length(in.)	28.4 ⁽²⁾ 28.3 ⁽³⁾	28.89	29.7 ⁽⁴⁾ 28.9 ⁽⁵⁾	45
Active Length (in.)	14 ⁽²⁾ 15 ⁽³⁾	15	15	15
Graphite Reflector (in.)	3.53	3.45	2.56, 3.72 ⁽⁴⁾ 3.42 ⁽⁵⁾	-
Graphite Diameter	1.41	1.40	1.435	-
Reflector (2) Mass (g)	450	450	450	-
End Fitting Mass (g)	140	530	530	290
Clad Material	Al	SS304	SS304	SS304
Clad Thickness (in.)	0.03	0.02	0.02	0.02
Clad Mass (g)	140	270	270	462
Fuel Material	U-ZrH	U-ZrH	U-ZrH	U-ZrH
Pellet Diameter (in.)	1.41	1.40	1.435	1.311 ⁽⁷⁾
Central Hole (in.)	0.25	0.25	0.25	0.25
Filling Rod Mat'l	Zirc	Zirc	Zirc	Zirc
Filling Rod Dia. (in.)	0.225	0.225	0.225	0.225

Notes:

1. Annular Core Pulse Reactor.
2. Al clad fuel with 14-inch active fuel has no central hole with Zircaloy rod.
3. Al clad fuel 15-inch active fuel has a central hole with Zircaloy rod.
4. Steel clad standard streamline fuel has 2.56 and 3.72-inch upper and lower graphite reflectors.
5. Steel clad standard plain fuel has 3.42-inch upper and lower graphite reflectors.
6. Fuel follower control rod has an uppermost 6.5-inch air void section, a 15-inch boron carbide upper section, a 15-inch UZrH fuel section, and 5.88-inch lower void section.
7. Fuel meat diameter.

Table 6.2.5-2 Characteristics of Design Basis TRIGA Fuels -Fuel Compositions

Element Type	Al Clad	Steel Clad					Fuel Follower Control Rod		
		ACPR	Stand.	FLIP	FLIP LEU-I	FLIP LEU-II	Stand.	FLIP LEU-I	ACPR
U in Fuel (max. wt %)	8.5	12.5	12	8.5	20	31	8.5	8.5	12.5
²³⁸ U- Mass (g)	164	224	164	59	403	676	150	387	224
²³⁵ U in U (wt %)	20	20	20	70	20	20	20	20	20
²³⁵ U-Mass (g)	41	56	41	137	101	169	38	97	56
H to Zr Ratio	1.0	1.7	1 - 1.7	1.6	1.6	1.6	1.6	1.6	1.7
Zr Mass (g)	2300	1962	2300	2060	1988	1886	2004	1908	1962

Note:

1. FLIP - Fuel Life Improvement Program

6.2.6 TRIGA Fuel Cluster Rods

The NAC-LWT TRIGA non-poisoned and poisoned basket designs can transport up to 560 TRIGA fuel cluster rods. These configurations contain sets of up to 16 intact TRIGA fuel cluster rods within an insert. Each set of elements is placed in the cells of the five TRIGA basket modules. In the non-poisoned configuration, the central cell of each module is blocked to prohibit the placement of fuel elements in that location. The NAC-LWT TRIGA basket design can also accommodate sets of four follower control rod (FFCR) elements per cell in the top module. The TRIGA base and top basket modules can accommodate sealed failed fuel cans containing failed TRIGA fuel cluster rods or debris. The sealed failed fuel can is limited to the equivalent content of six TRIGA fuel cluster rods.

Figure 6.2.6-1 shows details of typical TRIGA fuel cluster rods (Tomsio). The design-basis TRIGA fuel cluster rod characteristics are shown in Table 6.2.6-1 and Table 6.2.6-2. The TRIGA fuel matrix is a solid uranium-zirconium-hydride metal alloy in which the zirconium-hydride moderator is homogeneously combined with the enriched uranium into pellets. Uranium enrichment in the TRIGA fuel cluster rods is 93.3 wt %. The fuel pellets are loaded into cylindrical rods approximately 0.5 inch in diameter and 30 inches long. TRIGA cluster rods are clad with Incoloy 800 material.

Figure 6.2.6-1 TRIGA Fuel Cluster Rod Details

TRIGA FUEL CLUSTER

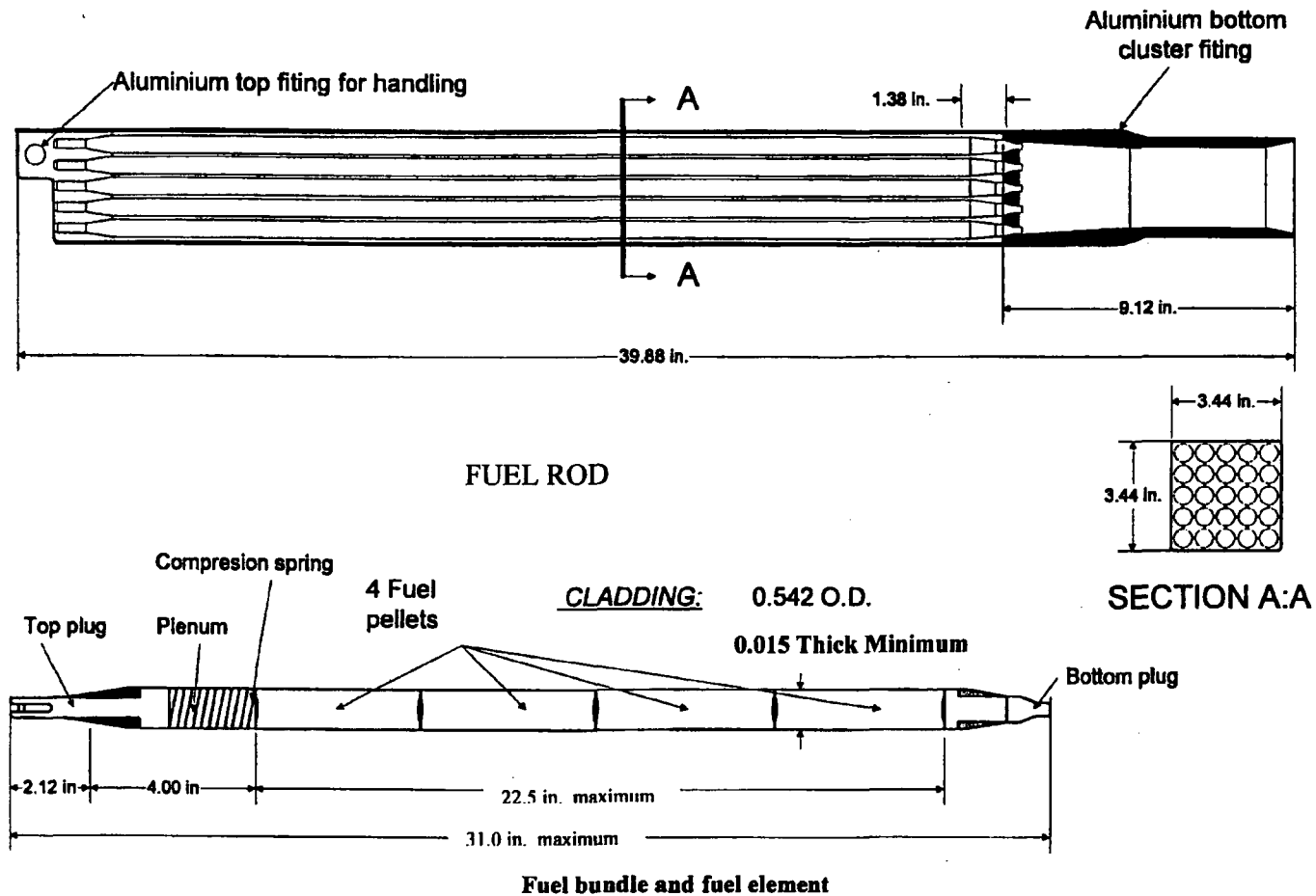


Table 6.2.6-1 Characteristics of Design-Basis TRIGA Fuel Cluster Rods

Element Type	TRIGA Fuel Cluster Rod
Element Diameter (in.)	0.542
Element Length (in.)	30.13
Active Length (in.)	22
End Fitting Mass (g)	121
Clad Material	Incoloy 800
Clad Thickness (in.)	0.016
Clad Mass (g)	210
Fuel Material	U-ZrH
Pellet Diameter (in.)	0.51

Table 6.2.6-2 Characteristics of Design-Basis TRIGA Fuel Cluster Rods - Fuel Compositions

Parameter	Value
U in Fuel (wt %)	10.2
²³⁸ U Mass (g)	3
²³⁵ U in U (wt %)	93.3
²³⁵ U Mass (g)	42
H to Zr Ratio	1.6
Zr Mass (g)	380

6.2.7 Metallic Fuel Rods

The design characteristics of the metallic fuel rods are shown in Table 6.2.7-1. As stated in Section 6.1, no criticality analyses are performed for these contents because naturally enriched uranium cannot become critical in light water.

Table 6.2.7-1 Characteristics of Design-Basis Metallic Fuel Rods

Parameter	Metallic
Assembly Rod Array	N/A
Assembly Weight, lbs	1,805 (15 rods)
Fuel Rod Length, in	120.5
Active Fuel Length, in	120.0
Number of Fuel Rods/Assembly	N/A
Fuel Rod Diameter, in	1.36
Cladding Material	Al
Cladding Thickness, in	0.080
Pellet Diameter, in	1.36
Fuel Cell Pitch, in	N/A
Pellet Material	Uranium metal
Theoretical Density percent	100
Maximum Initial Enrichment wt % ²³⁵ U	Natural
Design-basis Burnup, MWd/MTU	1,600
Weight of Uranium, kg/assembly	54.5
Weight of UO ₂ , kg/assembly	N/A

6.2.8 DIDO Fuel Assemblies

The NAC-LWT DIDO fuel basket module design can transport up to 42 DIDO research reactor fuel assemblies in six fuel basket modules. This configuration consists of seven fuel assemblies per basket, one placed in a center tube and one in each of six peripheral tubes. The analysis provided herein is bounding for all DIDO fuel assembly loading configurations.

A DIDO fuel assembly is comprised of four annular fuel elements that may be crimped at a common point after the assembly is cut to size. The fuel elements have a fuel meat composed of either U_3O_8 -Al, U_3Si_2 -Al, or U_3Si_2 in an aluminum matrix dispersing material. While data available did not indicate U-Al mixture, it will be enveloped by the evaluation shown in Section 6.4.7. Highly enriched, medium enriched and low enriched assemblies are available at maximum enrichments of 93 wt % ^{235}U , 45 wt % ^{235}U and 20 wt % ^{235}U , respectively. HEU fuel assemblies are conservatively evaluated at 94 wt % ^{235}U . Figure 6.2.8-1 shows a view of the DIDO fuel assembly. Nominal characteristics for the DIDO fuel assemblies are shown in Table 6.2.8-1. Uranium weight percent in the fuel composition is indicated as 57.5, 33.7, and 18.4 weight percent for the HEU, MEU and LEU fuel, respectively. The listed fuel dimensions are extended by the tolerances shown in Table 6.2.8-2 to arrive at bounding fuel configurations in Section 6.4.3.

Figure 6.2.8-1 DIDO Fuel Assembly

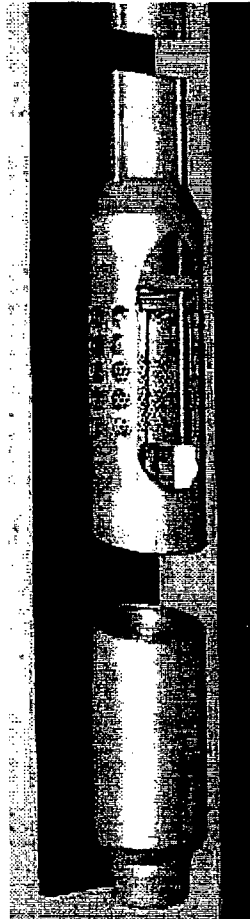


Table 6.2.8-1 Characteristics of DIDO Fuel Assemblies

Fuel Parameters	Units	U ₃ Si ₂ -Al	U ₃ Si ₂	U ₃ O ₈
Tube 1 outer diameter	[cm]	6.395	6.38	6.38
Tube 1 ²³⁵ U	[g]	36.0	35.67	35.67
Tube 2 outer diameter	[cm]	7.375	7.36	7.36
Tube 2 ²³⁵ U	[g]	42.0	41.88	41.88
Tube 3 outer diameter	[cm]	8.355	8.34	8.34
Tube 3 ²³⁵ U	[g]	48.0	48.09	48.09
Tube 4 outer diameter	[cm]	9.335	9.32	9.32
Tube 4 ²³⁵ U	[g]	54.0	54.36	54.36
Clad thickness	[cm]	0.048	0.0425	0.0425
Tube thickness	[cm]	0.146	0.15	0.15
Fuel meat thickness	[cm]	0.050	0.065	0.065
Active fuel length	[cm]	60.90	60.0	60.0
Total element length	[cm]	66.04	62.5	62.5
²³⁵ U per fuel assembly	[g]	180.0	180.0	180.0

Table 6.2.8-2 DIDO Fuel Assembly Tolerances

Description	Units	Value
Fuel Tube Diameter	[cm]	0.20
Plate Thickness	[cm]	0.02
Clad Thickness	[cm]	0.01
Fuel Cylinder Pitch	[cm]	0.02
Active Fuel Length	[cm]	1.25
Fuel Element Length	[cm]	1.00
²³⁵ U per Fuel Assembly	[g]	10.00
U wt % in Fuel Composition		5

6.2.9 General Atomics Irradiated Fuel Material

The NAC-LWT General Atomics (GA) Irradiated Fuel Material (IFM) basket module is designed to transport two IFM packages, also referred to as Fuel Handling Units (FHUs). The module is placed in the top of the NAC-LWT cavity with a bottom spacer to facilitate unloading of the IFM packages.

The two GA IFM FHUs are intended for a single shipment in the NAC-LWT. The first IFM FHU contains a Reduced-Enrichment Research and Test Reactor (RERTR) type fuel and the second contains a High-Temperature Gas-cooled Reactor (HTGR) type fuel. Each FHU consists of stainless steel weld-encapsulated primary and secondary enclosures that contain the GA IFM.

The RERTR IFM is comprised of 20 irradiated TRIGA fuel elements; 13 of the elements are intact and the remaining seven have been previously sectioned for examination purposes. The component segments of each sectioned element have been collected into separate aluminum tubes with crimped ends. Since the TRIGA elements are loaded in both intact and sectioned configurations, two models of the TRIGA fuel are considered: 1) intact elements in a regular array, and 2) fuel homogenization within the confines of the RERTR primary enclosure. The latter model is used to demonstrate system subcriticality for a damaged package.

Parameters characterizing the RERTR/TRIGA fuel elements are shown in Table 6.2.9-1. Three distinct mass loadings of uranium were used in the 20 TRIGA elements: 20, 30 and 45 wt % U; the average mass of the fueled portion of these elements is 551 g with an enrichment of 19.7 wt % ^{235}U . The overall mass fractions of the 20 elements are given in Table 6.2.9-2 and the composition of the incoloy clad is given in Table 6.2.9-3. For a homogenized (damaged) fuel description, equivalent densities calculated for each of the RERTR/TRIGA elemental constituents are shown in Table 6.2.9-4. The volume inside the RERTR primary enclosure is 436 in³ (7140 cm³).

The HTGR IFM is comprised of fuel in four forms: fuel particles (kernels), fuel particles (coatings), fuel compacts (rods), and fuel pebbles. Fuel kernels are solid, spheridized, high-temperature sintered fully-densified, ceramic kernel substrate, composed of: UC_2 , UCO , UO_2 , $(\text{Th,U})\text{C}_2$, or $(\text{Th,U})\text{O}_2$. The as-manufactured enrichment of the HTGR fuel varies from ~10.0 to 93.15 wt % ^{235}U . Fuel coatings are solid, spheridized, isotropic, discrete multi-layered fuel particle coatings with chemical composition including pyrolytic-carbon (PyC) and silicon carbide (SiC). Fuel compacts are multi-coated ceramic fuel particles, bound in solid, cylindrical, injection-molded, high-temperature heat-treated compacts. The fuel compact matrix is composed of carbonized graphite shim, coke, and graphite powder. Fuel pebbles are multi-coated fuel

particles, bound in solid, spherical injection-molded, high-temperature heat-treated pebbles. The fully-cured binding matrix is composed of carbonized graphite shim, coke and graphite powder.

The HTGR material composition is provided for the entire IFM package as shown in Table 6.2.9-4. Based on the dimensions of the stainless steel cylinders encapsulating both the RERTR and HTGR material, shown in Table 6.2.9-5, equivalent densities calculated for each of the HTGR elemental constituents are also shown in Table 6.2.9-4. The volume inside the HTGR primary enclosure is 583 in³ (9,555 cm³).

Table 6.2.9-1 GA IFM RERTR/TRIGA Fuel Parameters

Description	Unit	Value
Fuel OD	[cm]	1.3
Fuel Length	[cm]	56.0
Clad OD	[cm]	1.38
Clad Thickness	[cm]	0.041
Element Length	[cm]	76.0
Number of Elements		20
Enrichment	[wt % ²³⁵ U]	19.7

Table 6.2.9-2 GA IFM RERTR/TRIGA Fuel Composition

Constituent	Mass Fraction [wt %]
Zr	62.42
U	35.77
H	1.08
Er	0.59
C	0.14

Table 6.2.9-3 GA IFM RERTR/TRIGA Clad Composition

Constituent	Mass Fraction [wt %]
Fe	40
Ni	35
Cr	25

Table 6.2.9-4 GA IFM Elemental Constituents

Fuel Type	Element	Mass [g]	Density [g/cc]
RERTR	Zr	6721.1	0.9413
	U	3850.66	0.5393
	H	116.02	0.0162
	Er	63.32	0.0089
	C	15.44	0.0022
	Fe	1704.5	0.2387
	Ni	919.1	0.1287
	Cr	761.7	0.1067
	Mn	30.8	0.0043
	Mo	17.3	0.0024
	Total	14199.94	1.9888
HTGR	C	7075.55	0.7405
	Th	1956.87	0.2048
	Si	1408.37	0.1474
	U	204.81	0.0214
	O	22.40	0.0023
	Total	10668.00	1.1165

Table 6.2.9-5 GA IFM Primary and Secondary Enclosure Dimensions

Description	Value [in]
RERTR Primary Enclosure Interior Height	34.50
RERTR Primary Enclosure OD	4.25
RERTR Secondary Enclosure OD	4.75
RERTR Enclosure Wall Thickness	0.12
HTGR Primary Enclosure Interior Height	36.50
HTGR Primary Enclosure OD	4.75
HTGR Secondary Enclosure OD	5.25
HTGR Enclosure Wall Thickness	0.12

6.2.10 PULSTAR Fuel Elements

Four 28 MTR 7-element modules are stacked in the NAC-LWT cavity to accommodate PULSTAR fuel elements. PULSTAR fuel elements (rods) may be loaded as either loose rods or intact fuel assemblies. PULSTAR fuel elements are zirconium-alloy-clad UO_2 pellets with an analyzed enrichment of 6.5 wt % ^{235}U . PULSTAR fuel assemblies are a 5×5 rectangular array of elements surrounded by a zirconium alloy box with aluminum upper and lower fittings.

Possible loading configurations for PULSTAR fuel elements are listed below.

- intact assemblies loaded directly into any 28 MTR module cell
- up to 16 intact elements loaded in the 4×4 TRIGA fuel rod insert (rod insert is placed into a module cell),
- up to 25 intact or damaged (failed) elements and nonfuel components of fuel assemblies in the PULSTAR can, or (failed fuel or screened can)

Damaged fuel elements may include severe fuel damage, i.e., fuel debris.

PULSTAR fuel element and assembly characteristics are summarized in Table 6.2.10-1. A sketch of a PULSTAR fuel assembly is shown in Figure 6.2.10-1.

Figure 6.2.10-1 PULSTAR Fuel Assembly

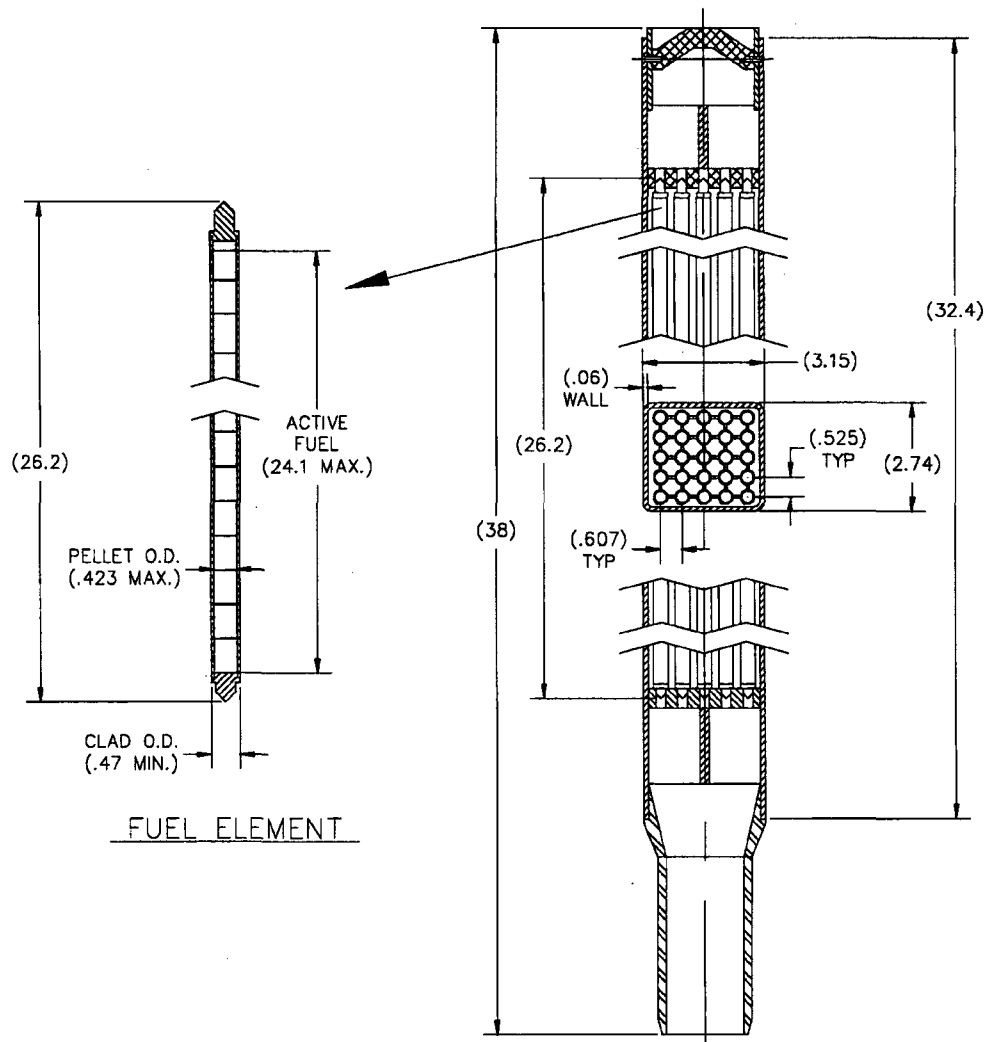


Table 6.2.10-1 PULSTAR Fuel Characteristics

Description	Value [in]
Maximum Pellet Diameter (inch)	0.423
Minimum Clad Thickness (inch)	0.0185
Minimum Element (Rod) Diameter (inch)	0.470
Maximum Active Fuel Height (inch)	24.1
Fuel Element (Rod) Length (inch)	26.2
Rod Pitch (inch)	0.525×0.607
Assembly Length	38 inch
Box Width	2.745×3.155
Box Thickness	0.06
Maximum Enrichment (wt % ^{235}U)	6.5
Maximum ^{235}U Content per Element (g)	33
No. of Element (Rods) per Assembly	25

6.2.11 Spiral Fuel Assemblies

The NAC-LWT ANSTO fuel basket module design can transport up to 42 spiral fuel assemblies in six fuel basket modules. This configuration consists of seven fuel assemblies per basket, one placed in a center fuel tube and one in each of six peripheral fuel tubes.

A spiral fuel assembly is comprised of 10 curved fuel plates in a spiral pattern located in the annulus formed by two concentric aluminum sleeves. The assembly top and bottom sections may be cropped outside the fuel region to allow the fuel assembly to fit within the basket cavity. The fuel elements have a fuel meat composed of U-Al alloy. Nominal enrichment for the assembly is 80 wt % ^{235}U enriched. The assemblies are evaluated up to 85 wt % ^{235}U enriched. Figure 6.2.11-1 shows a cross-section view of the spiral fuel assembly. Nominal characteristics for the spiral assemblies are shown in Table 6.2.11-1. The listed fuel dimensions are extended by the tolerances shown in Table 6.2.11-2 to arrive at bounding fuel configurations in Section 6.4.10.

Figure 6.2.11-1 Spiral Fuel Assembly Cross-Section Sketch

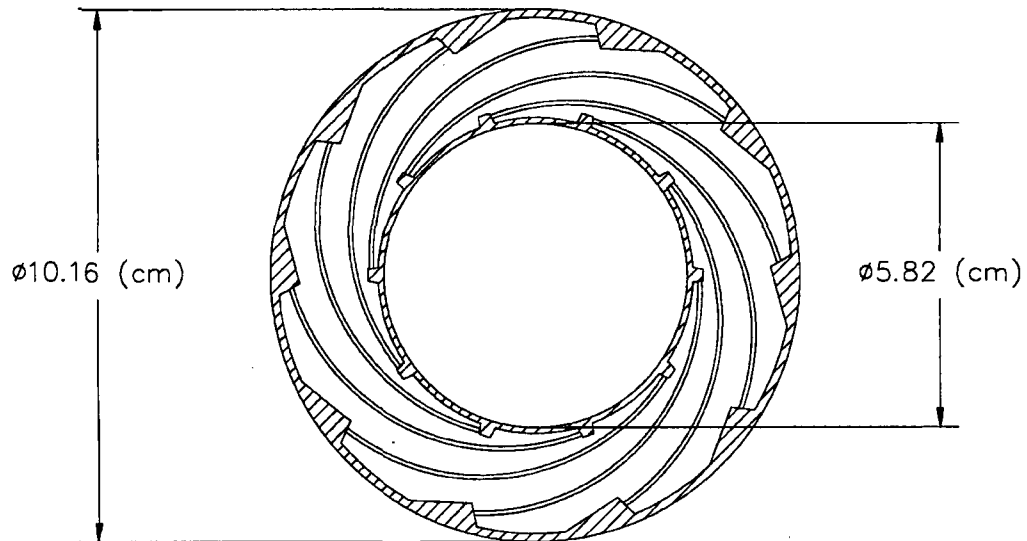


Table 6.2.11-1 Spiral Fuel Assemblies Characteristics

Fuel Parameters	Units	Value
Number of plates		10
Inner aluminum plate ID	[cm]	5.82
Inner aluminum plate OD	[cm]	6.045
Outer aluminum plate ID	[cm]	9.85
Outer aluminum plate OD	[cm]	10.16
Fuel length	[cm]	60.325
Active Fuel Width	[cm]	6.0
Active Fuel Thickness	[cm]	0.061
Plate Width	[cm]	7.33
Plate Thickness	[cm]	0.147
Total element length	[cm]	63.5
Fuel Material		U-Al
Clad Material		Al
Enrichment (wt % ²³⁵ U)		80%
Maximum ²³⁵ U per Assembly (nominal)	[g]	150.0
U wt % in Fuel Composition		38%
Mass of uranium (calculated)	[g]	176.5

Table 6.2.11-2 Spiral Fuel Assemblies Tolerances Applied

Fuel Parameters	Units	Value
Plate Thickness	[cm]	0.02
Clad Thickness	[cm]	0.020
Active Fuel Length	[cm]	1.25
Fuel Element Length	[cm]	1.00
²³⁵ U per Fuel Assembly	[g]	10.00
²³⁵ U wt % in U		5%
U wt % in Fuel Composition		20%

6.2.12 MOATA Plate Bundles

The NAC-LWT ANSTO fuel basket module design can transport up to 42 MOATA plate bundles in six fuel basket modules. This configuration consists of seven fuel assemblies per basket, one placed in a center fuel tube and one in each of six peripheral fuel tubes.

A plate bundle is comprised of a maximum 14 flat fuel plates sandwiched between two thick, nonfuel, aluminum side plates. The plates are pinned together at the top and bottom, outside the active fuel region, and the plates are separated by spacer disks. The fuel elements have a fuel meat composed of U-Al alloy. Nominal enrichment for the assembly is 90 wt % ^{235}U enriched. The assemblies are evaluated up to 92 wt % ^{235}U enriched. Figure 6.2.12-1 shows cross-section views of the plate bundle. Nominal characteristics for the plate bundle are shown in Table 6.2.12-1. The listed fuel dimensions are extended by the tolerances shown in Table 6.2.12-2 to arrive at bounding fuel configurations in Section 6.4.10.

Figure 6.2.12-1 MOATA Plate Bundle Sketch

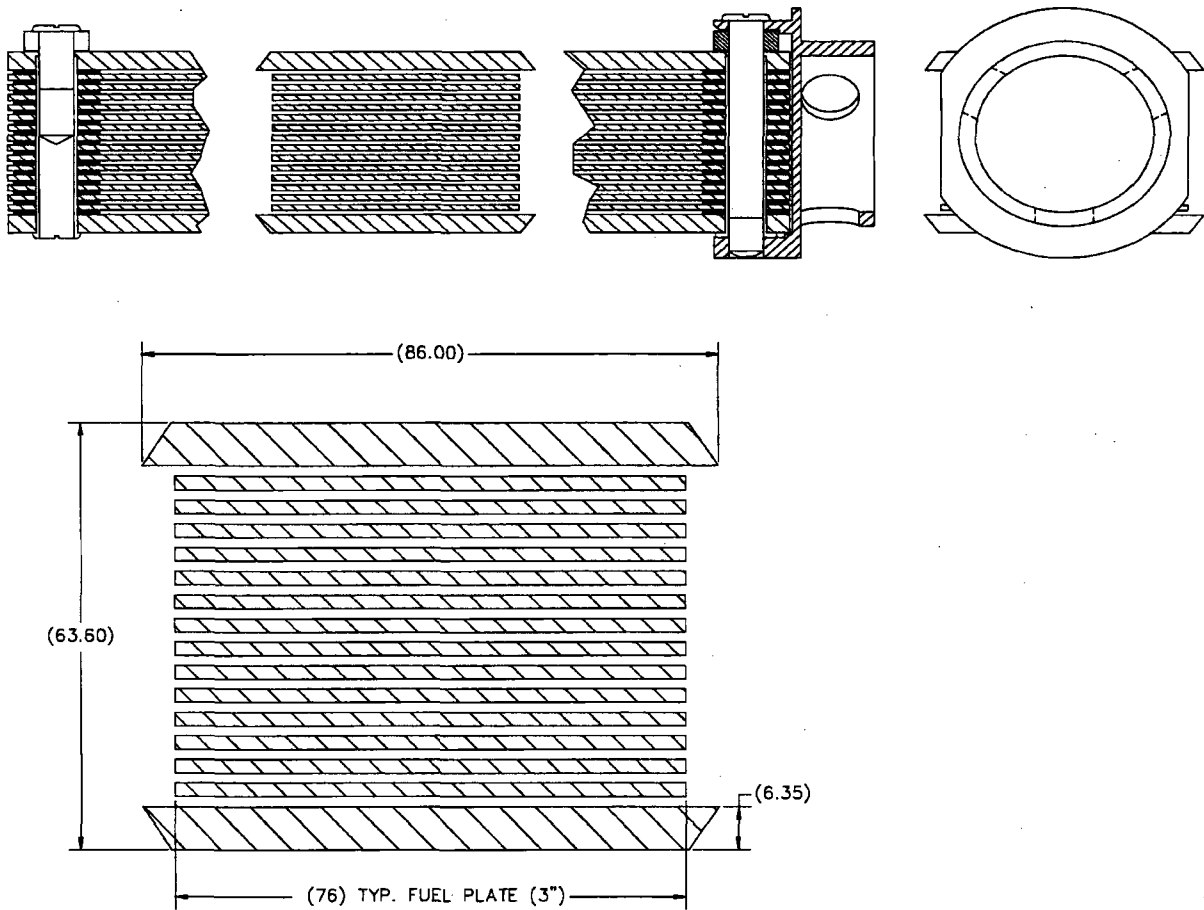


Table 6.2.12-1 MOATA Plate Bundle Characteristics

Fuel Parameters	Units	Value
Maximum Number of Plates		14
Plate Thickness	[cm]	0.2032
Plate Width		7.62
Total element length	[cm]	66.04
Clad thickness	[cm]	0.05
Fuel Meat Thickness (min)	[cm]	0.1032
Active Fuel Width	[cm]	6.985
Active Fuel Length	[cm]	58.42
Plate Spacer Thickness	[cm]	0.15
Side Plate Thickness	[cm]	0.635
Side Plate Width	[cm]	7.87 ¹
Angle Cut-Back (degrees)		30
Fuel Composition		U-Al-alloy
Enrichment wt % ²³⁵ U		90%
Maximum ²³⁵ U per Plate (nominal)	[g]	22.0
U wt % in Fuel (Calculated)		18%
Mass of uranium - Calculated	[g]	23.9
Assembly Width (Y) – Calculated ²	[cm]	7.87
Assembly Depth (X) - Calculated	[cm]	6.36

¹ Nominal width of “long side” is 8.60 cm. Listed value is “short side” to account for 30-degree chamfer.

² Assembly width and depth are calculated values based on the size of the plate stack-up. Circular plate bundle end-fittings and the “chamfered” side plates will minimize movement of fuel within the tube opening.

Table 6.2.12-2 MOATA Plate Bundle Tolerances Applied

Fuel Parameters	Units	Value
Plate Thickness	[cm]	0.00508
Plate Width	[cm]	0.0381
Fuel Element Length	[cm]	0.0381
Clad Thickness	[cm]	N/A
Active Fuel Width (calculated) ¹	[cm]	0.3175
Active Fuel Length	[cm]	1.27
Spacer Thickness	[cm]	0.03
Side Plate Thickness	[cm]	0.02
Side Plate Width	[cm]	0.02
²³⁵ U per plate	[g]	0.30
Enrichment wt % ²³⁵ U		2%
U wt % in Fuel Composition		10%

¹ Tolerance applied is one-half the difference between plate width and active fuel width.

6.3 Criticality Model Specifications

This section describes the models that are used in the criticality analyses for the NAC-LWT cask. The models presented are for cask loadings of one PWR assembly, two BWR assemblies, up to 42 HEU, MEU or LEU, MTR elements, up to 42 HEU, MEU or LEU DIDO assemblies, up to 140 TRIGA fuel elements, up to 560 TRIGA fuel cluster rods, two General Atomics Irradiated Fuel Material packages, 25 intact PWR or BWR rods in a rod holder or fuel assembly lattice, 25 PWR or BWR fuel rods with up to 14 of the fuel rods classified as damaged in a fuel rod holder, up to 700 PULSTAR fuel elements, up to 42 spiral fuel assemblies, or up to 42 MOATA plate bundles. The models are analyzed separately under normal operations and hypothetical accident conditions to ensure that all possible configurations are subcritical. The metallic fuel rods are not analyzed since this fuel is not enriched and cannot achieve criticality in light water.

6.3.1 PWR Fuel Assemblies

This section describes the methodology and the models used in the criticality analysis of the NAC-LWT cask with the design basis PWR assemblies. The methodology uses a 27 group neutron cross section library (27GROUPNDF4) and KENO-Va to determine the multiplication factor, k_{eff} , of the system. The models presented utilize configurations of the various PWR assemblies in the basket and the NAC-LWT cask.

The calculational methodology is the SCALE, CSAS25 criticality analysis sequence (Petrie). This sequence includes a material information processor (Landers), cross section and resonance treatment processing with the NITAWL code (Greene) and KENO-Va (Petrie) criticality analysis. The material information processor in the SCALE package calculates nuclide number densities for standard and non-standard compositions. The NITAWL code prepares a working library and performs resonance treatments on ^{235}U and ^{238}U . The KENO-Va code is used to model the PWR assemblies, basket and cask body of the NAC-LWT. KENO-Va uses Monte Carlo techniques to track neutrons through the geometry and determine the multiplication factor, k_{eff} , of the system. In these analyses, approximately 300 batches of 1000 neutrons per batch are tracked through the system.

6.3.1.1 Description of Calculational Models

Since it is planned to transport many types of PWR fuel assemblies in the NAC-LWT cask, a determination of the most limiting, i.e., highest k_{eff} , assembly must be made for criticality purposes. KENO-Va models of the assemblies in Table 6.2.1-1 and Table 6.2.1-2 are evaluated to determine the most limiting PWR assembly. This determination was first performed at a

Revision 38

uranium enrichment of 3.7 wt % ^{235}U . The assembly with the highest reactivity, not exceeding 0.95 while accounting for bias statistical uncertainties, was then selected as the most limiting assembly for a uranium enrichment of 3.7 wt % ^{235}U . Those assemblies exceeding 0.95 were reexamined at a uranium enrichment of 3.5 wt % ^{235}U . A most limiting assembly was likewise selected for this uranium enrichment. The KENO-Va models developed to select the most limiting assemblies incorporate a single PWR fuel assembly in the fuel basket and the NAC-LWT cask as shown in Figure 6.3.1-1 and Figure 6.3.1-2. These KENO-Va models incorporate water at 1 g/cc modeled between the fuel rods, in the basket holes surrounding the assemblies, in the neutron shield, and in the cask exterior. An active fuel length of 12 ft was utilized in constructing the KENO-Va PWR assembly models. The ends were reflected with water for the most reactive assembly analysis and with actual cask materials for the NCT and HAC moderator studies. The assemblies, the aluminum PWR basket, and the cask with radial shield regions are explicitly represented. There are no homogenizations of fuel, moderator or basket. In addition, water albedo boundary conditions were utilized as the boundary conditions for the cask exterior. The most limiting assembly analysis was performed with both a dry and a wet fuel pellet to clad gap.

The most limiting assembly models were analyzed to determine their most reactive configurations due to geometrical tolerances and mechanical perturbations. The models were analyzed under accident conditions with water at 1 g/cc modeled between the fuel rods, in the basket holes surrounding the assemblies, in the neutron shield, and in the cask exterior. The most reactive configuration analysis incorporates the more reactive of the wet or dry gap configurations.

As shown in Section 6.4.1, the most limiting PWR fuel assemblies for 3.7 and 3.5 wt % ^{235}U enrichments were determined to be the Exxon ANF 15×15 and the Westinghouse 17×17 OFA fuel assemblies, respectively. The most reactive configurations are the nominal configuration for the Exxon ANF 15×15 assembly and the maximum basket opening for the Westinghouse 17×17 OFA assembly. The material properties used in the model are shown in Table 6.3.1-1.

These KENO-Va models of the most limiting assemblies in their most reactive configurations were then analyzed to determine the effects moderator variations in the cavity and outside the cask under normal conditions and inside the neutron shield tank under accident conditions. The k_{eff} results for single casks loaded with the most limiting design basis PWR assemblies for both 3.5 and 3.7 wt % ^{235}U are always below 0.95 including all biases and uncertainties.

6.3.1.2 Package Regional Densities

The composition densities (g/cc) and nuclide number densities (atm/b-cm) calculated by the material information processor and used in the subsequent criticality analyses are shown in Table 6.3.1-1.

Figure 6.3.1-1 KENO-Va Model of the NAC-LWT Cask Model with PWR Basket and 15×15 PWR Assembly

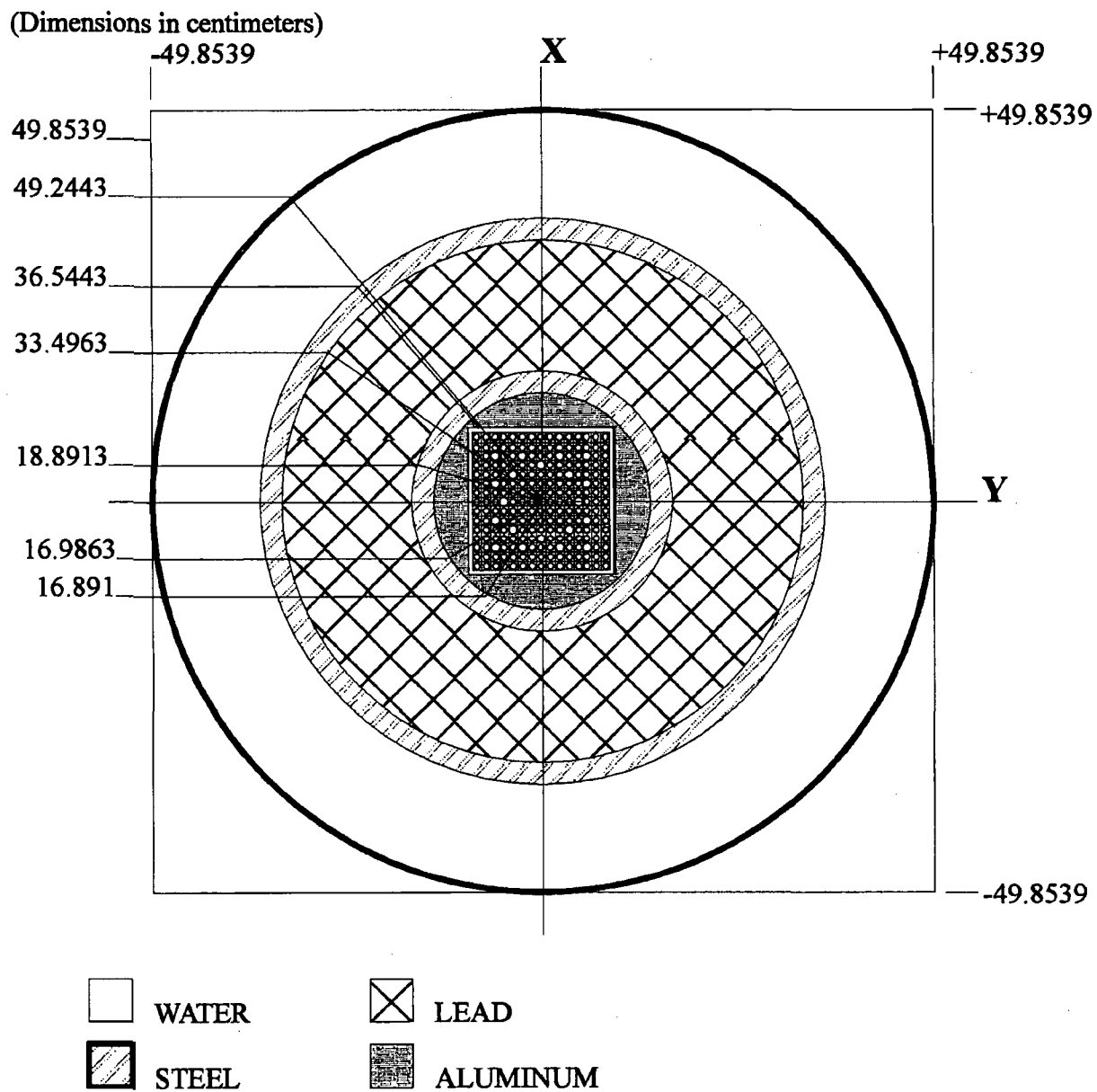


Figure 6.3.1-2 KENO-Va Model of the NAC-LWT Cask with PWR Basket and Westinghouse 17×17 OFA Assembly

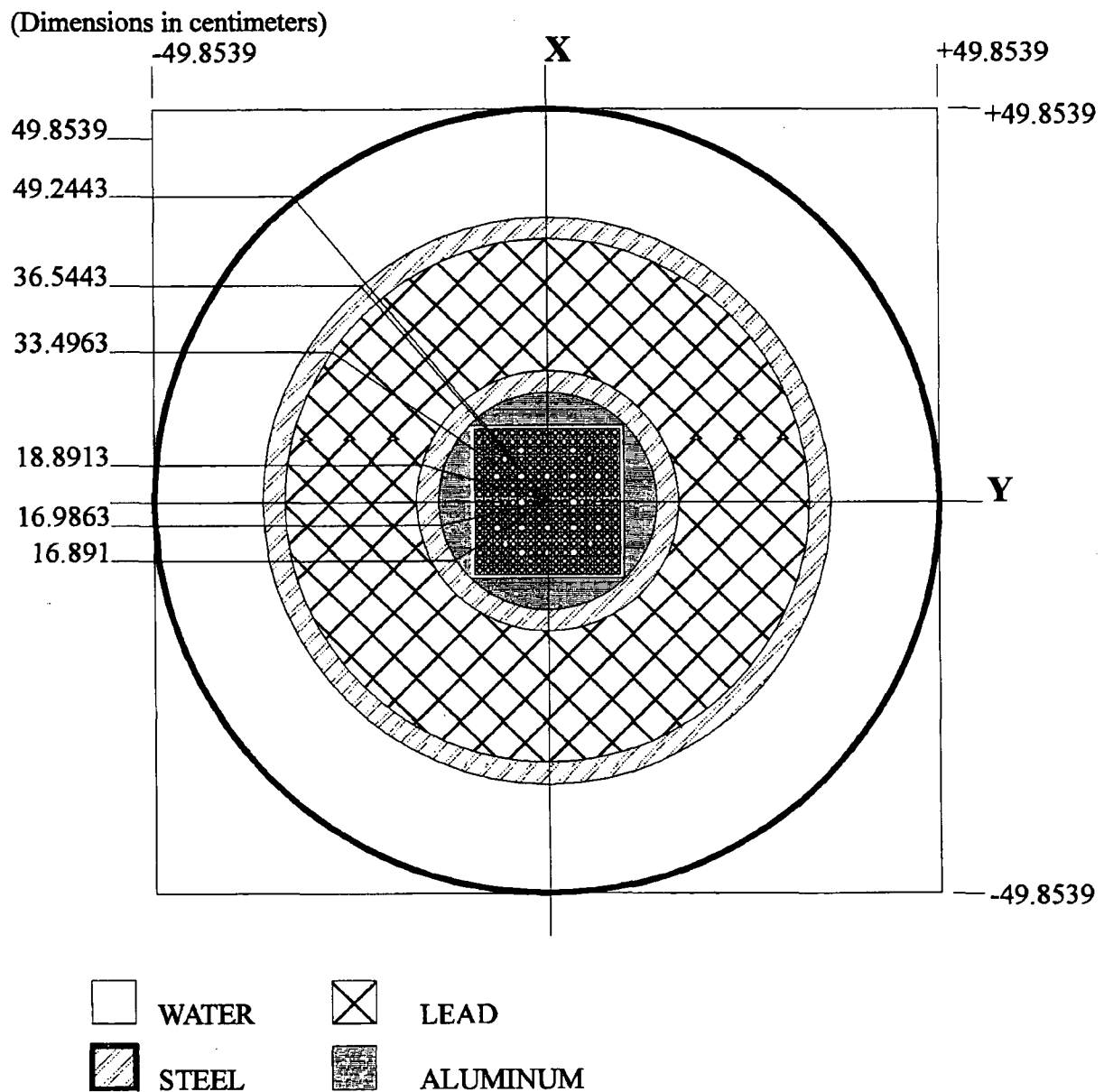


Table 6.3.1-1 Compositions and Number Densities Used in the Criticality Analysis of PWR Fuel Assemblies

Material	3.7% Enriched UO ₂	3.5% Enriched UO ₂	Zr	H ₂ O	304 Stainless Steel	Pb	Al
Density, g/cc	10.412	10.412	6.49	0.998	7.920	11.344	2.702
Nuclide	atm/b-cm						
²³⁵ U	8.701E-4	8.231E-4					
²³⁸ U	2.236E-2	2.241E-2					
Oxygen	4.646E-2	4.646E-2		3.338E-2			
Hydrogen				6.677E-2			
Zirconium			4.285E-2				
Iron					5.936E-2		
Chromium					1.743E-2		
Nickel					7.721E-3		
Manganese					1.736E-3		
Lead						3.297E-2	
Aluminum							6.031E-2

6.3.2 BWR Fuel Assemblies

This section describes the methodology and the models used in the criticality analysis of the NAC-LWT cask with the design basis BWR assemblies. The methodology uses a 27 group neutron cross section library (27GROUPNDF4) and KENO-Va to determine the multiplication factor, k_{eff} , of the system. The models presented utilize configurations of the various BWR assemblies in the basket and the NAC-LWT cask.

The calculation methodology is the SCALE, CSAS25 criticality analysis sequence (Petrie, June 1990). This sequence includes a material information processor (Landers), cross section and resonance treatment processing with the NITAWL code (Greene) and KENO-Va (Petrie, August 1990) criticality analysis. The material information processor in the SCALE package calculates nuclide number densities for standard and non-standard compositions. The NITAWL code prepares a working library and performs resonance treatments on ^{235}U and ^{238}U . The KENO-Va code is used to model the BWR assemblies, basket and cask body of the NAC-LWT. KENO-Va uses the Monte Carlo technique to track neutrons through the geometry and determine the multiplication factor, k_{eff} , of the system. In these analyses, approximately 300 batches of 1000 neutrons per batch are tracked through the system.

6.3.2.1 Description of Computational Models

Since it is planned to transport different BWR assemblies in the NAC-LWT cask, a determination of the most limiting, i.e., higher k_{eff} , assembly must be made for criticality purposes. KENO-Va models of the assemblies in Table 6.2.2-1 and Table 6.2.2-2 are evaluated to determine the most limiting assembly. The KENO-Va models incorporate a mid-fuel slice of two identical BWR assemblies in the BWR basket and the NAC-LWT cask as shown in Figure 6.3.2-1. The most limiting assembly analysis is performed for accident conditions with water at 1 g/cc modeled between the fuel rods and in the basket holes surrounding the assemblies. In addition, the neutron shield and cask exterior contain no water. The analysis is performed with these conditions with a dry and a wet clad gap. Reflecting boundary conditions are imposed on the sides, top and bottom of the KENO-Va CUBOID containing the loaded cask simulating an infinite array with no axial leakage. This produces the k_{eff} of an infinite array of BWR assemblies in the basket and cask. The most limiting assembly is the model that produces the highest k_{eff} . The most limiting assembly model is analyzed to determine its most reactive configuration due to geometric tolerances and mechanical perturbations. The model is analyzed for accident conditions with water at 1 g/cc modeled between the fuel rods and in the basket holes surrounding the assemblies. In addition, the neutron shield and cask exterior contain no

water. The most reactive configuration analysis incorporates the more reactive of the wet or dry gap configurations. The material properties used in the model are shown in Table 6.2.3-1.

A finite array KENO-Va model of the NAC-LWT cask with the design basis BWR fuel is developed from the KENO-Va model of the most limiting assembly in the most reactive configuration. As shown in Section 6.4.2, the Exxon 9×9 assembly with two water rods and an 80 mil channel (Ex 9×9-2/80) is the most limiting assembly and the nominal configuration is the most reactive configuration for the NAC-LWT cask with the two assembly BWR basket design. In the finite array model, the fuel assemblies, aluminum BWR basket, and the cask with radial shield regions are explicitly modeled. Twenty casks are placed on a triangular pitch in a KENO-Va region using the HOLE instruction. Finally, a CUBOID surrounds the array of casks. The KENO-Va model has an axial extent of ± 10 cm, but with reflecting boundary conditions imposed on top and bottom, the model is effectively infinite in axial extent. The water moderator is allowed to vary in the cavity and outside the cask under normal conditions and is allowed to vary inside the neutron shield tank under accident conditions. Cask center-to-center spacing is varied by adjusting the HOLE positions of the casks. The optimally moderated, most reactive configuration is then evaluated without the assembly channel to verify subcriticality in this arrangement. The k_{eff} results of this finite array model are always below 0.95, including all biases and uncertainties.

6.3.2.2 Package Regional Densities

The composition densities (g/cc) and nuclide number densities (atm/b-cm) calculated by the material information processor and used in the subsequent criticality analyses are shown in Table 6.3.2-1.

Figure 6.3.2-1 KENO-Va Model of the NAC-LWT Cask Model with BWR Basket and 2 Exxon 9×9-2/80 Assemblies

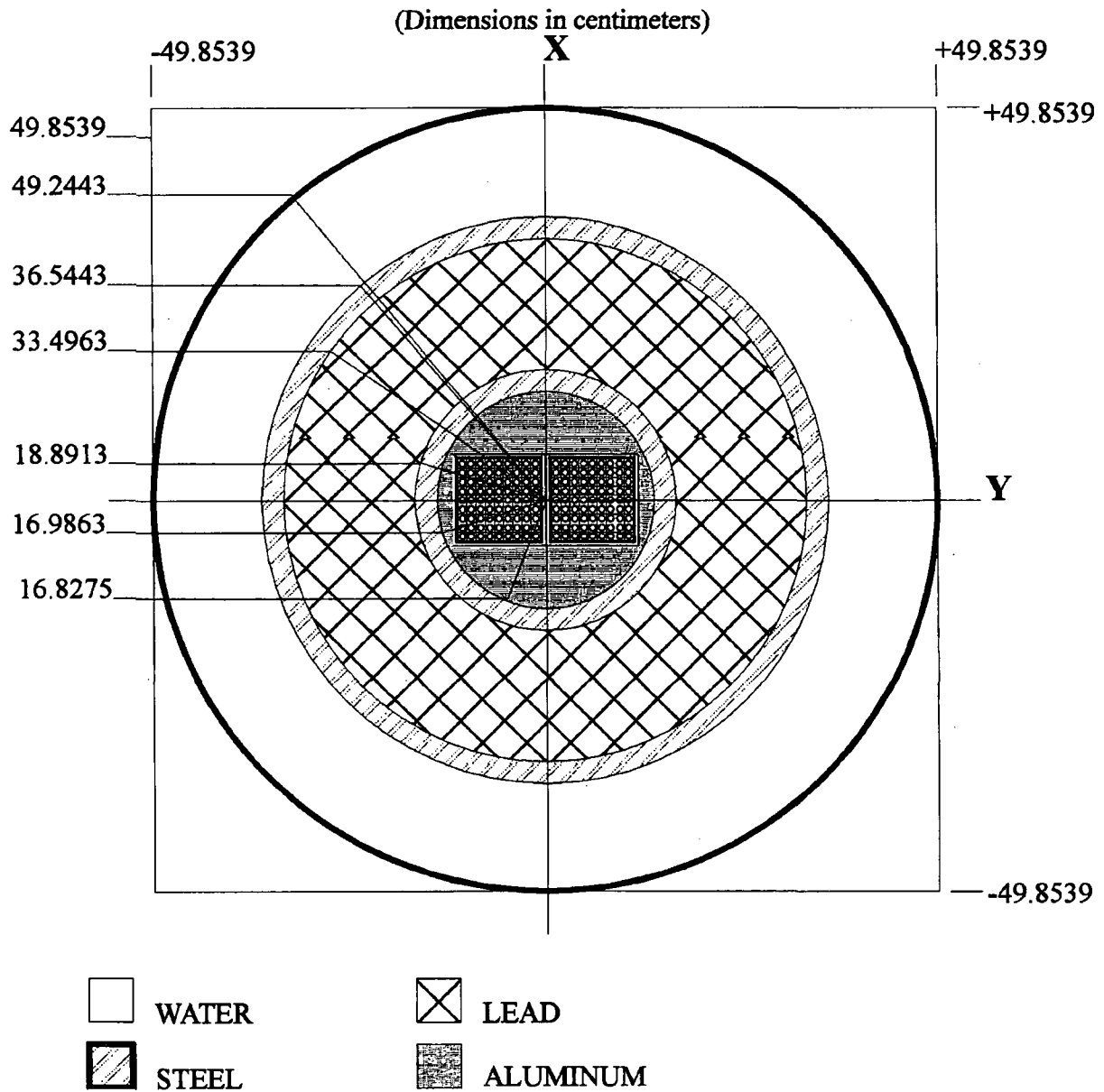


Table 6.3.2-1 Compositions and Number Densities Used in the Criticality Analysis of BWR Fuel Assemblies

Material	4.0% Enriched UO ₂	Zircaloy	H ₂ O	304 Stainless Steel	Pb	Al
Density, g/cc	10.412	6.56	0.9982	7.920	11.344	2.702
Nuclide	atm/b-cm					
²³⁵ U	9.406E-4					
²³⁸ U	2.229E-2					
Oxygen	4.646E-2		3.338E-2			
Hydrogen			6.677E-2			
Zircaloy		4.331E-2				
Iron				5.936E-2		
Chromium				1.743E-2		
Nickel				7.721E-3		
Manganese				1.736E-3		
Lead					3.297E-2	
Aluminum						6.031E-2

6.3.3 MTR Fuel Elements

6.3.3.1 Description of Calculational Models

Since it is planned to transport many types of MTR fuel elements in the NAC-LWT, a determination of the most limiting, i.e., higher k_{eff} , element must be made for criticality purposes. Primary candidates for the most limiting element from the MTR elements in Table 6.2.3-1 through Table 6.2.3-3 are selected for analysis. Limiting elements are primarily selected based on fissile material content. After establishing trends in reactivity versus the elements' physical characteristics, bounding element characteristics are defined.

Evaluations are performed with three distinct fuel element models. First stage evaluations compare reactivities between intact fuel element types in an infinite array of basket unit cells. The second phase of the evaluations employs a basket model representing a cross section of the cask at infinite height and is used to establish maximum reactivity basket configurations and moderator densities. Finally, the limiting fuel element parameters are defined by a three-dimensional cask model containing six baskets.

In the KENO-Va fuel/basket unit cell analysis, a unit cell of the fuel element and the basket is modeled. This includes the fuel element in a 3.44" \times 3.44" (8.738 cm \times 8.738 cm) opening surrounded by a 5/16" (0.7938 cm) web. Water at 1 g/cc is modeled between the fuel plates and in the basket hole surrounding the fuel element as shown in Figure 6.3.3-1. Reflecting boundary conditions are imposed on the sides, top and bottom simulating an infinite array with no axial leakage. This produces the k_{eff} of an infinite array of fuel elements and basket cells without modeling the entire basket and cask.

The KENO-Va model of the NAC-LWT cask with the design basis MTR fuel is derived from a radial slice of the NAC-LWT at the active fuel region as shown in Figure 6.3.3-2. As described in Section 6.4.3.1, the HFBR fuel element is selected as the most limiting assembly for the seven element basket design. The KENO-Va model has an axial extent of ± 10 cm, but with reflecting boundary conditions imposed on top and bottom, the model is effectively infinite in axial extent. The fuel elements, steel basket and cask with radial shield regions are explicitly represented. There are no homogenizations of fuel, moderator or basket. A CUBOID surrounds the casks with reflecting boundary conditions imposed on the sides, top and bottom simulating an infinite array of infinite axial extent. Moderator (H_2O) is allowed to vary in the cavity and outside the cask under normal conditions and, also, is allowed to vary inside the neutron shield tank under accident conditions. Cask center-to-center spacing is varied by adjusting the X-Y spacing of the CUBOID surrounding the cask. The k_{eff} results of this infinite array model are always below

0.95 including all biases and uncertainties. Because the integrity of MTR fuel is not assured, the fuel plates of an element may assume a more optimum configuration during accident conditions. Therefore, KENO-Va models of the NAC-LWT cask with MTR element plates optimally spaced within the limits of the basket opening are analyzed to verify that the HFBR element is the most limiting MTR element.

The full cask models are identical in cross section to the axially infinite cask models, but rather than axially reflecting an active fuel elevation section of a basket module, six basket modules are stacked into an array. The module chosen for stacking is the intermediate basket module. While axial extents differ from the bottom and top modules, the basket horizontal cross section is identical in all modules. Axial variations are associated with the stacking of the units, with all units containing the 0.5-inch thick base plate. Figure 6.3.3-3 displays a side view of the intermediate module, with Figure 6.3.3-4 showing this basket module stacked six high inside the NAC-LWT. The cask bottom weldment and lid enclose the basket module array with its associated radial shielding. Reflecting boundary conditions on all sides simulate an infinite array of casks. This model neglects the impact limiters that would provide additional spacing between casks, and models the cask under accident conditions with the neutron shield voided.

As discussed in Section 6.4.3.10, the accident, optimum plate pitch configuration bounds the configuration of loose plates in the MTR plate canister. Therefore, no separate models are constructed for the loose plate evaluation.

For high fissile material payloads, the MTR basket may require partial loading. Figure 6.3.3-5 contains a basket layout with each potential loading position numbered to correlate the analysis in Section 6.4.3 to allowed loading locations. The model construction for partially loaded baskets is identical to that of the fully loaded basket with the exception of cask interior moderator material being assigned to the basket opening rather than an array of fuel plates and the side plates. The basket opening not occupied by a fuel element may be blocked to physically prevent loading of an element. The spacer consists of an aluminum tube, evaluated at an outer diameter of 3.25 inches and a 1/8-inch thickness, with a rectangular aluminum top plate. For baskets containing multiple fuel types, the SCALE material information processor input DAN and RES variables are provided for the fuel material not included in the LATTICECELL description. The Dancoff factors are extracted from LATTICECELL calculations of the single fuel type runs.

6.3.3.2 Package Regional Densities

The composition densities (g/cc) and nuclide number densities (atm/b-cm) calculated by the SCALE material information processor for a range of elements evaluated in subsequent criticality

analyses are shown in Table 6.3.3-1. Additional material densities may be obtained from the sample input/output files provided in Section 6.6.

Figure 6.3.3-1 KENO-Va Fuel/Basket Unit Cell Model for MTR Fuel
(Dimensions in Centimeters)

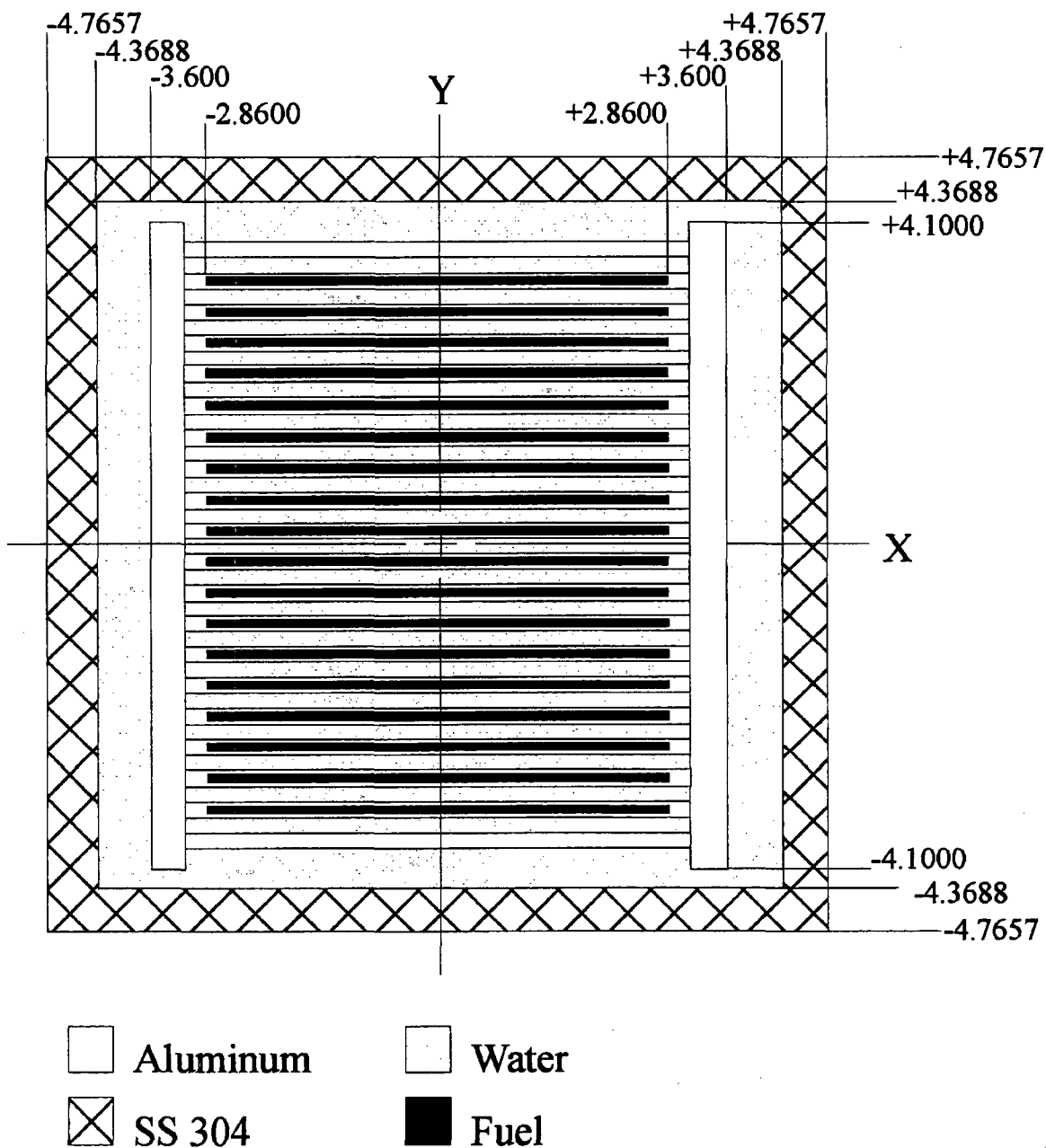


Figure 6.3.3-2 KENO-Va Model of NAC-LWT Cask with MTR Fuel

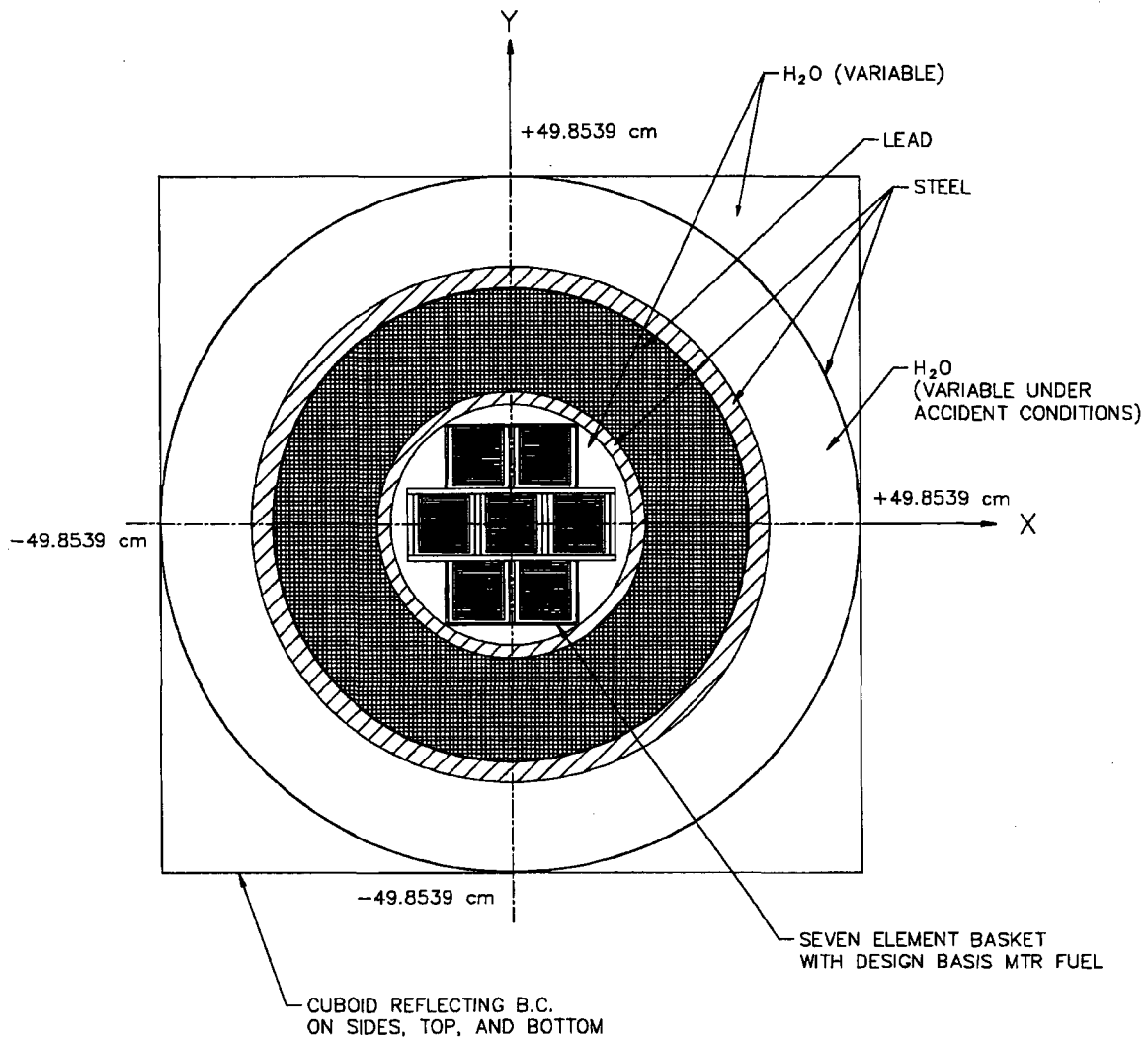


Figure 6.3.3-3 Intermediate MTR 42 Basket Module

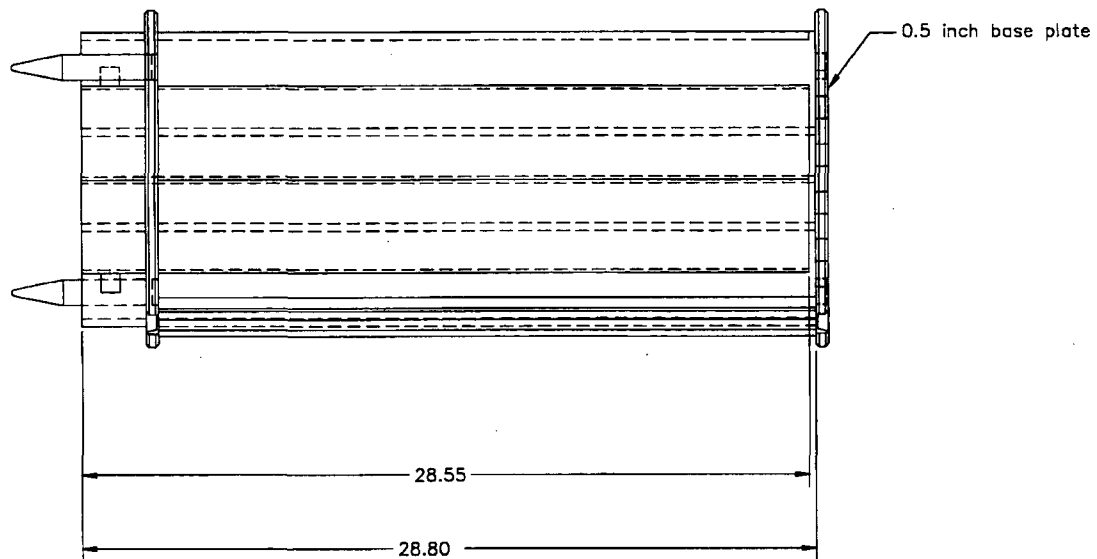


Figure 6.3.3-4 Full Length NAC-LWT Cask Model with 42 MTR Fuel Elements

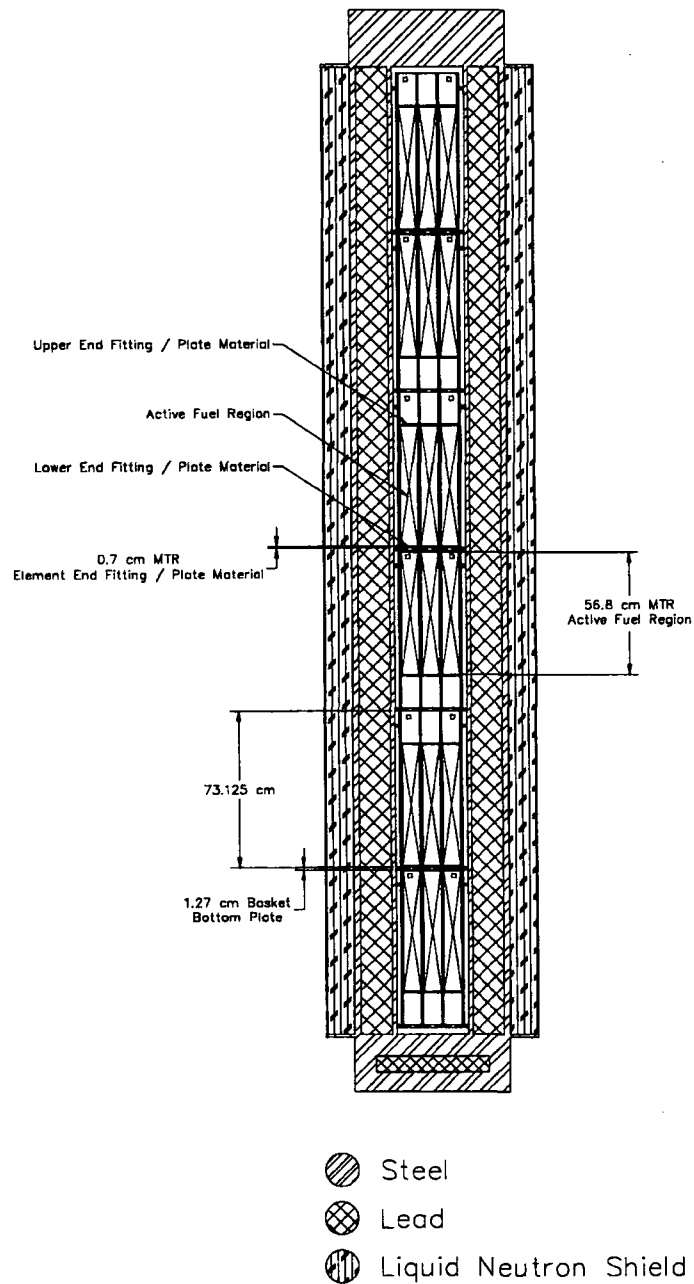


Figure 6.3.3-5 MTR Fuel Basket Module Loading Pattern

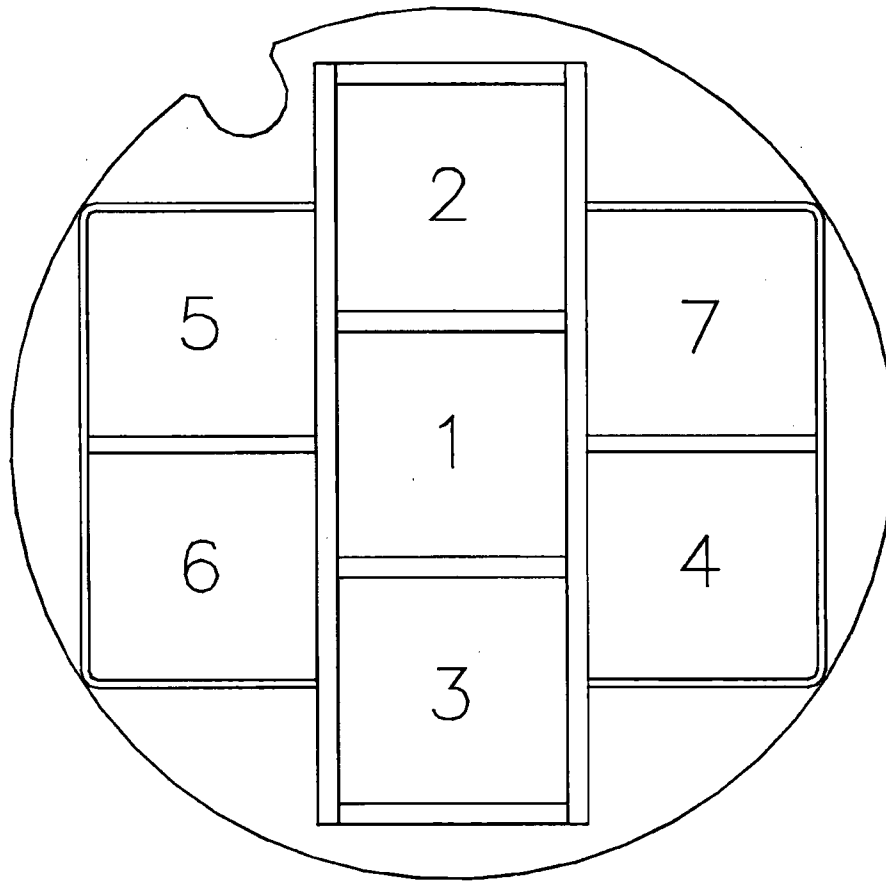


Table 6.3.3-1 Composition Densities Used in Criticality Analysis of MTR Fuel

Material	HFBR U ₃ O ₈ -Al	ORR U ₃ O ₈ -Al	GRR U-Al	IEA-R1 U-Al	THOR HEU U-Al	THOR LEU U-Al	RSG- GAS U ₃ O ₈ -Al	BSR U ₃ Si ₂	ZPRL U-Al
Density, g/cc	3.99	3.32	2.90	4.10	2.90	4.10	4.80	5.01	4.10
Nuclide	atm/b-cm								
Uranium 235	2.852-3	1.978-3	1.382-3	8.493E-4	5.683E-4	8.542E-4	1.366E-3	2.358E-3	8.542E-4
Uranium 238	2.120-4	1.470-4	1.027-4	3.354E-3	4.12E-5	3.373E-3	5.480E-3	9.460E-3	3.373E-3
Silicon								7.505E-3	
Aluminum	5.630-2	5.222-2	5.178-2	5.502E-2	5.950E-2	5.499E-2	3.713E-2		5.499E-2
Oxygen	8.142-3	5.662-3					1.826E-2		

Material	RSG- GAS Clad	Al Clad	H ₂ O	304 Stainless Steel	Pb	ASTRA ¹ UAl _x -A	MEUG UAl _x -A 35 wt %	CNEA U-Al	PRR U-Al
Density, g/cc	2.7	2.699	0.998	7.920	11.350	1.57	2.08	2.76	3.03
Nuclide	atm/b-cm								
Uranium 235						1.786E-3	1.862E-3	1.320E-3	9.113E-4
Uranium 238						2.205E-3	3.415E-3	1.289E-4	5.743E-5
Magnesium	9.916E-4								
Aluminum	5.892E-2	6.024E-2				5.303E-2	5.303E-2	4.900E-2	5.911E-2
Oxygen			6.675E-2						
Hydrogen			3.338E-2						
Iron				5.936E-2					
Chromium				1.743E-2					
Nickel				7.721E-3					
Manganese				1.736E-3					
Lead					3.299E-2				

¹ Based on 0.053 cm fuel meat width.

6.3.4 PWR and BWR Rods in a Rod Holder or Fuel Assembly Lattice

The NAC-LWT cask may transport up to 25 intact PWR or BWR fuel rods that are in a fuel rod holder or fuel assembly lattice. Up to 14 of 25 PWR or BWR fuel rods in a fuel rod holder may be classified as damaged.

6.3.4.1 Intact PWR or BWR Rods in a Rod Holder or Fuel Assembly Lattice

This section describes the methodology and the models used in the criticality analysis of the NAC-LWT with 25 design basis PWR or BWR rods in a rod holder or fuel assembly lattice. The methodology uses the CSAS25 criticality sequence from the SCALE 4.3 computer code package with the 27-group END/B-IV cross-section set. CSAS25 is the control sequence for the Material Information Processor (MIP), BONAMI, NITAWL-II and KENO-Va computer codes. The Material Information Processor generates number densities and prepares the geometry data for the resonance self shielding calculation. BONAMI and NITAWL-II calculate the resonance corrected cross sections in AMPX working format. KENO-Va uses the Monte Carlo technique to calculate the k_{eff} of a system. In these analyses, approximately 300 batches of 1000 neutrons per batch are tracked through the system.

Description of Calculational Models

The KENO-Va model of the NAC-LWT with 25 intact PWR or BWR fuel rods includes a triangular lattice formation of design basis rods centered in the cask cavity. No credit is taken for geometry control provided by either the rod holder or the fuel assembly lattice. The fuel rods, cask cavity and radial shields are explicitly modeled as shown in Figure 6.3.4-2. The KENO-Va model has two UNITS. UNIT 1 represents a PWR or BWR rod cell. It uses concentric CYLINDERS to model the fuel pellet, clad gap, and the cladding of the fuel rod. UNIT 2 is the GLOBAL UNIT containing CYLINDERS that model the cask, cavity, steel liners, and shields. There are 25 HOLES placed in the cask cavity with X, Y, and Z coordinates that place rods in a triangular lattice position. The cask outer CYLINDER is surrounded by a CUBOID, and reflecting boundary conditions are imposed on the sides, top and bottom which simulates an infinite array of casks of infinite length. Adjusting the X-Y spacing of the CUBOID surrounding the cask varies cask center-to-center spacing. The material properties used in the model are shown in Table 6.3.4-1.

To determine the optimum configuration, cask k_{eff} is studied as a function of fuel rod pitch within the cask cavity. This is done by changing the coordinates of the rod HOLES. Twenty different pitch values that range from the most compact configuration to the most dispersed configuration are evaluated. Figure 6.3.4-1 shows a simplified view of the cask with three different

configurations. The analysis is performed for accident conditions with water at 1 g/cc modeled between the fuel rods, in the cask cavity surrounding the rods. In addition, the neutron shield and cask exterior contain no water. The analysis is performed with these conditions with a dry and a wet clad gap.

An infinite array KENO-Va model of the NAC-LWT cask with 25 PWR or BWR fuel rods at the optimum pitch is used to evaluate the reactivity of the cask. The water moderator is allowed to vary in the cavity and outside the cask under normal conditions and is allowed to vary inside the neutron shield tank under accident conditions. Cask center-to-center spacing is varied by adjusting the dimensions of the CUBOID surrounding the cask. The k_{eff} results of this infinite array model are always below 0.95 including all biases and uncertainties.

Package Regional Densities

The composition densities (g/cc) and nuclide number densities (atm/b-cm) calculated by the material information processor and used in the subsequent criticality analyses are shown in Table 6.3.4-1.

6.3.4.2 Damaged PWR and BWR Rods in a Rod Holder

This section describes the methodology and the models used in the criticality analysis of the NAC-LWT with 25 PWR or BWR rods, up to 14 of which may be damaged. Although the NAC-LWT payload is limited to 14 damaged fuel rods in a 25-rod shipment, the analysis conservatively considers all 25 rods as failing during transport.

The methodology uses the CSAS25 criticality sequence from the SCALE 4.3 computer code package with the 27-group ENDF/B-IV cross-section set. CSAS25 is the control sequence for the Material Information Processor, BONAMI, NITAWL-II and KENO-Va computer codes. The Material Information Processor generates number densities and prepares the geometry data for the resonance self-shielding calculation. BONAMI and NITAWL-II calculate the resonance corrected cross-sections in AMPX working format. KENO-Va uses the Monte Carlo technique to calculate the k_{eff} of a system. In these analyses, approximately 300 batches of 1,000 neutrons per batch are tracked through the system.

Description of Calculational Models

Two calculational models were employed to evaluate the NAC-LWT system reactivity with damaged fuel rods.

The first model explicitly models unclad UO_2 rods in a triangular pitch. System reactivity is maximized by increasing the number of fuel rods while decreasing the rod diameter to conserve

Revision 38

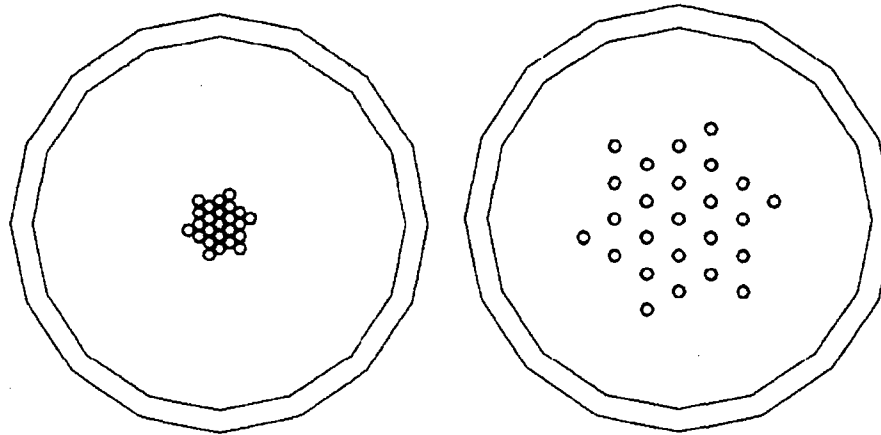
fuel area in the infinite height model (i.e., reflective boundary conditions are placed on the active fuel region). Fuel rod arrays of 25, 37 and 61 rods are considered. The latter two arrays are hexagonal with no lattice vacancies. For each of the three postulated rod arrays, the maximum reactivity pitch is determined for both PWR and BWR rods. System reactivity is determined using an axially infinite cask model in an infinite cask array. In establishing the trend of increasing reactivity with larger rod arrays, k_{eff} values for the explicit rod cases are calculated with full density water in the cask interior, exterior, and neutron shield. Void exterior and void neutron shield (accident) conditions are considered for the 61 rod array in addition to preferential flooding of the cask cavity. The maximum reactivity configuration for 61 rods (with an active fuel cross-sectional area equivalent to 25 intact rods) is shown in Figure 6.3.4-3. Fuel rod arrays with greater than 61 rods are not considered. As demonstrated in Section 0, increasing the number of fuel rods modeled increases the cross-sectional area of the most reactive lattice. The cross-sectional area required for the 61-rod array exceeds the area available in the interior of the rod holder and, therefore, represents a bounding, conservative configuration.

The second model considers a homogenized mixture of UO_2 and water with a square cross-section and finite axial height within the NAC-LWT fuel rod holder. The square cross-sectional area of the rod holder is conservatively based on the exterior width of the rod holder, 13.97 cm. Based on the maximum BWR pellet diameter and fuel length of 150 inches, the finite axial height of the fuel mixture is calculated based on various UO_2 volume fractions. The UO_2 volume fraction is varied until the maximum reactivity is determined. System reactivity is determined using an infinite cask array with a periodic reflection axial boundary condition. Given the limiting UO_2 /water fuel material description, water moderation variations are considered in the cask cavity (outside the rod holder), the cask exterior, and the cask neutron shield. The neutron shield material definition is tied to the exterior moderator definition; a void exterior includes a void neutron shield. Thus, the accident condition of loss of neutron shielding is explicitly modeled when the exterior moderator is set to void. Figure 6.3.4-4 and Figure 6.3.4-5 give dimensions of the maximum reactivity homogenized mixture configuration of finite extent.

Package Regional Densities

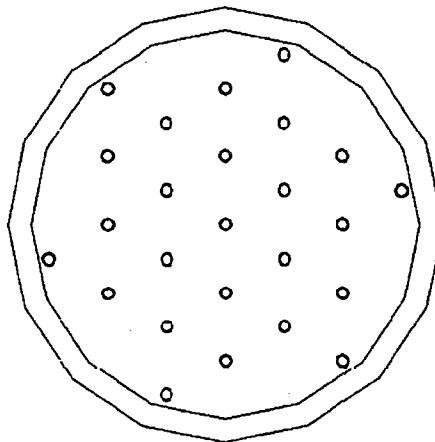
The composition densities (g/cc) and nuclide number densities (atm/b-cm) calculated by the material information processor and used in the subsequent criticality analyses are identical to those shown for intact fuel evaluations, Table 6.3.4-1. Additional material densities may be obtained from the sample input/output file provided in Section 6.6.10.

Figure 6.3.4-1 Triangular Pitch Lattice Formation of 25 PWR Rods



(a) Smallest Pitch

(b) Optimum Pitch



(c) Maximum Pitch

Figure 6.3.4-2 KENO-Va Model of the NAC-LWT Cask with 25 PWR Rods
(Dimensions in centimeters)

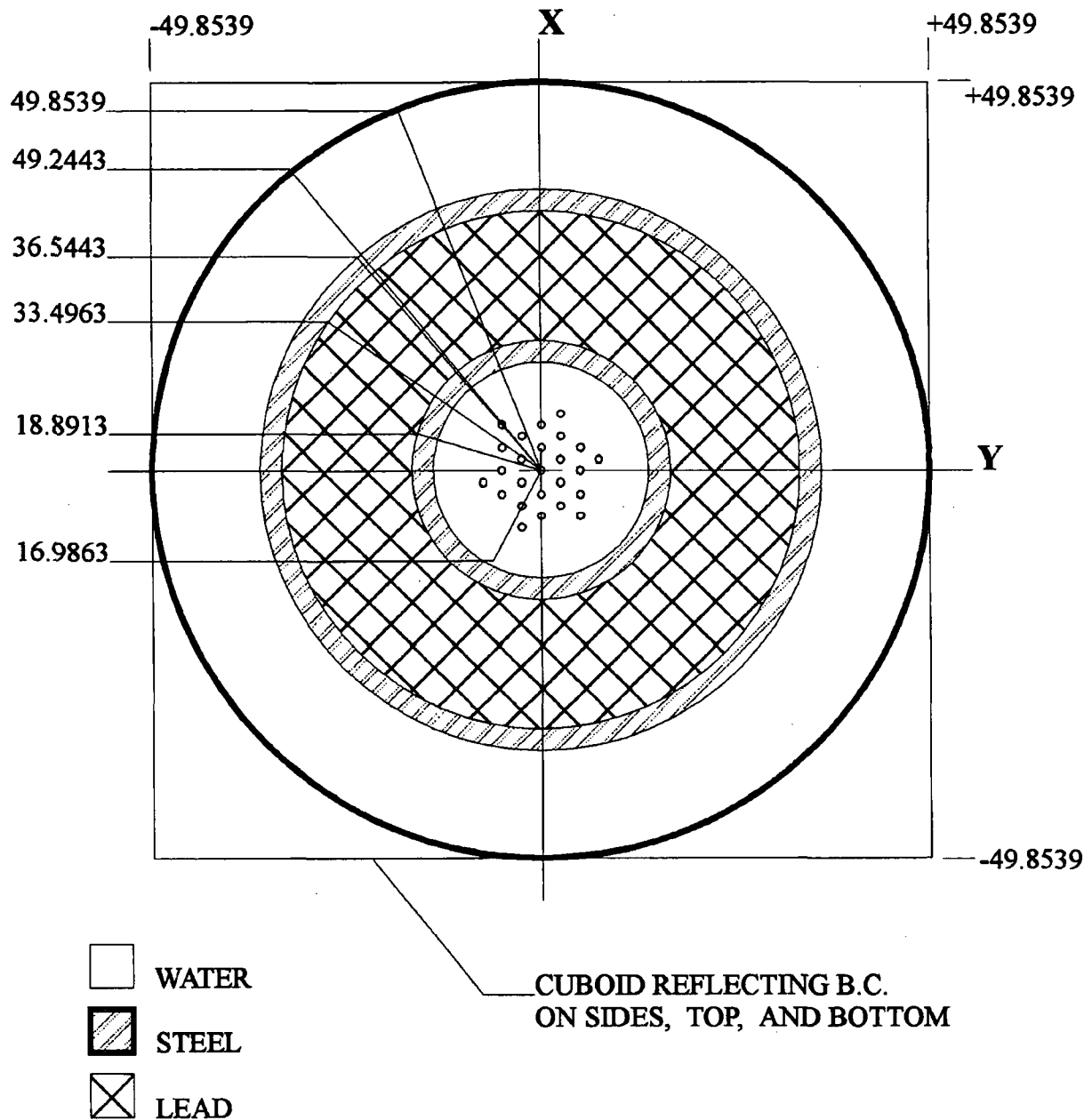


Figure 6.3.4-3 Maximum Reactivity Triangular Pitch Lattice Formation of Damaged Fuel Rods

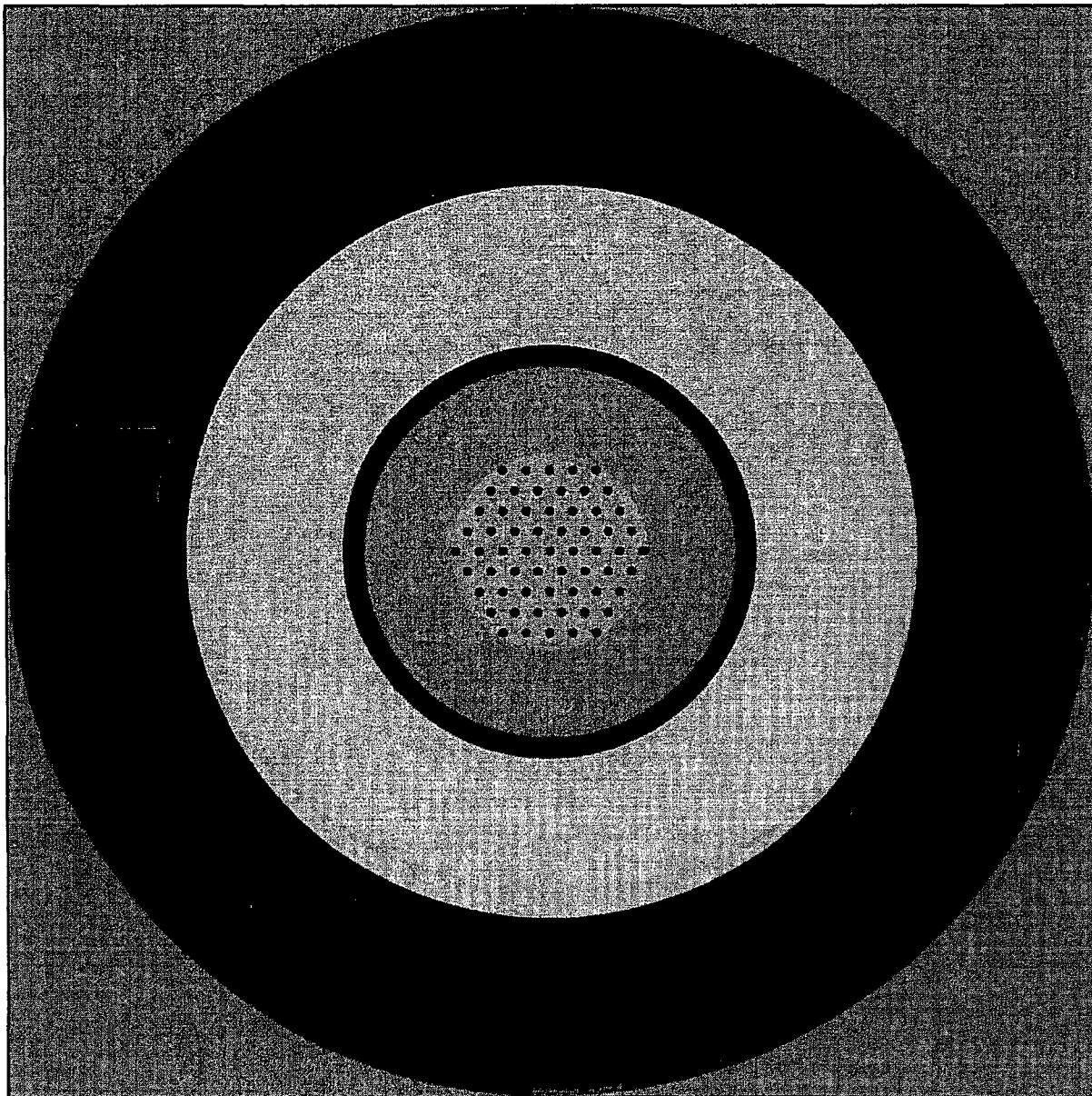
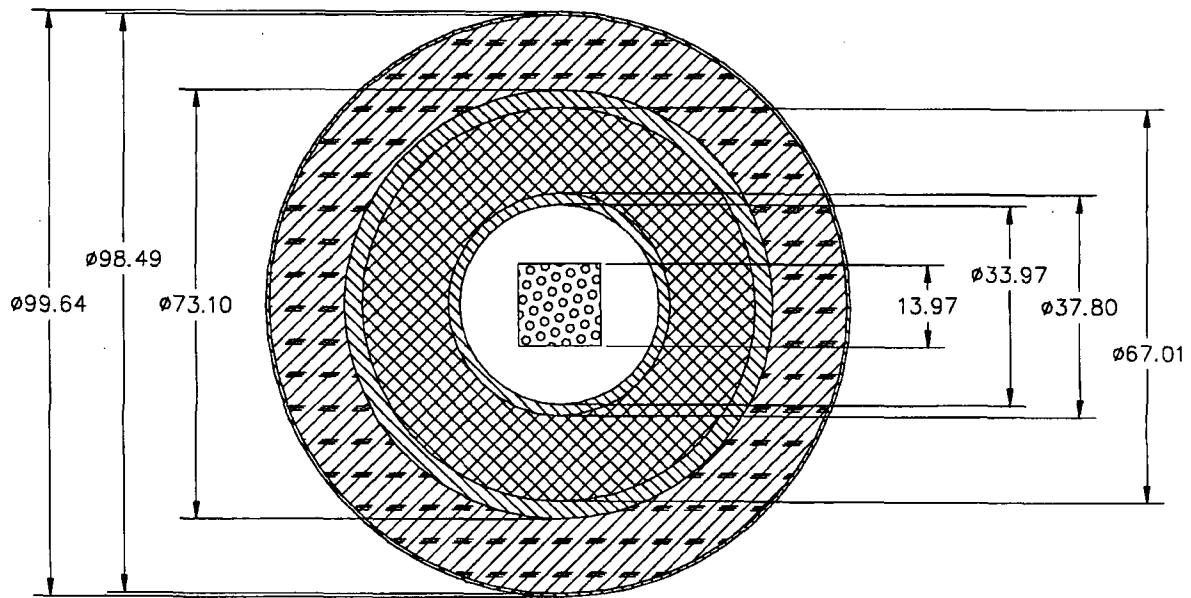


Figure 6.3.4-4 KENO-Va Model of the NAC-LWT Cask with Damaged Fuel Rods –
Radial Detail



NEUTRON SHIELD



STAINLESS STEEL



LEAD



FUEL/WATER

(Dimensions in centimeters)

Figure 6.3.4-5 KENO-Va Model of the NAC-LWT Cask with Damaged Fuel Rods – Axial Detail

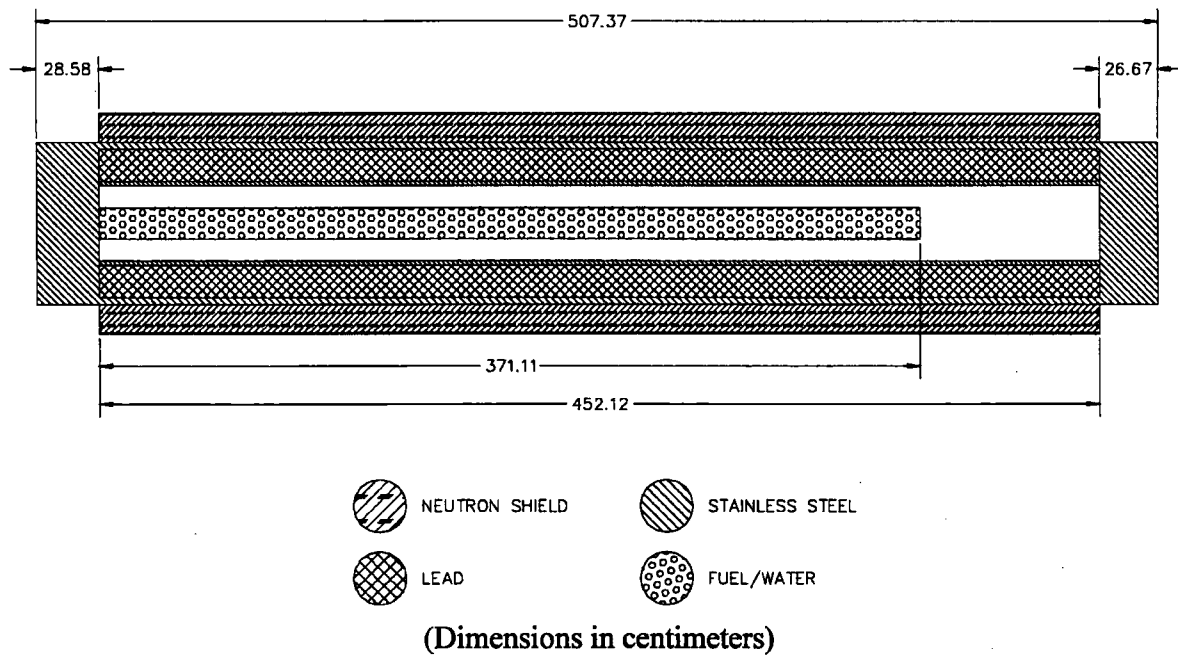


Table 6.3.4-1 Compositions and Number Densities Used in the Criticality Analysis of PWR and BWR Rods

Material	5.0% Enriched UO ₂	Zirconium Alloy	H ₂ O	304 Stainless Steel	Pb	Al
Density, g/cc	10.412	6.56	0.9982	7.920	11.344	2.702
Nuclide	atm/b-cm					
Uranium 235	1.176E-3					
Uranium 238	2.206E-2					
Oxygen	4.647E-2		3.338E-2			
Hydrogen			6.677E-2			
Zirconium Alloy		4.331E-2				
Iron				5.936E-2		
Chromium				1.743E-2		
Nickel				7.721E-3		
Manganese				1.736E-3		
Lead					3.297E-2	
Aluminum						6.031E-2

6.3.5 TRIGA Fuel Elements and Cluster Rods

As previously described, TRIGA fuel elements and fuel cluster rods may be transported in nonpoisoned or poisoned TRIGA basket modules. The following sections detail the analyses performed on these four combinations of design-basis TRIGA fuel types and basket configurations. Nonpoisoned basket designs are analyzed with a maximum of 120 TRIGA fuel elements, or 480 TRIGA fuel cluster rods, while the poisoned basket designs are analyzed with a maximum of 140 TRIGA fuel elements or 560 TRIGA fuel cluster rods.

6.3.5.1 Description of Calculational Models

6.3.5.1.1 TRIGA Fuel Element Methodology

To evaluate the nonpoisoned basket with TRIGA fuel elements, three models are utilized: a fuel/basket unit cell containing four intact TRIGA fuel elements, an axially infinite length cask model and a full cask model. Each of the two NAC-LWT cask models contains up to four TRIGA fuel elements, or screened or sealed cans, in each of the six peripheral TRIGA basket cells. In the case of the axially infinite cask model, a single basket module is surrounded by the cask radial shields and is axially reflected to simulate an infinite length cask. In the case of the full cask model, the NAC-LWT cask is represented with five TRIGA basket modules in the cavity surrounded by the cask radial and axial shields. In this model, the axial shields include an explicit representation of the cask lid and bottom forging. The fuel/basket unit cell model is used to determine the bounding TRIGA fuel element type (Section 6.4.5.1). The cask models are used to determine the maximum k_{eff} of the cask under normal and accident conditions with the bounding fuel element type (Section 6.4.5.2). The infinite length cask model is employed in the criticality evaluation of the intact TRIGA fuel elements in the most reactive basket configuration (Section 6.4.5.3). The full cask model is employed in the criticality evaluation of TRIGA basket modules with failed fuel (top and bottom baskets only) in the NAC-LWT cask under normal and accident conditions (Section 6.4.5.4). A finite cask array is employed in the revised TRIGA fuel element characteristics section (Section 6.4.5.6). The finite cask array model uses the same length cask model developed for the infinite array calculation. However, rather than applying reflective (mirror) boundary conditions to the single cask unit, the cask unit is placed into an 8 (or 4)-cask close-packed configuration.

To evaluate the poisoned basket with TRIGA fuel elements, the non-poisoned axially infinite length cask and full cask models are modified to include the borated stainless steel poison plates. Again, the infinite length cask model is used to evaluate intact TRIGA fuel elements in the most reactive basket configuration (Section 6.4.5.2) and the full cask model is used to evaluate the

basket modules with failed fuel (top and bottom baskets only) in the most reactive basket configuration (Section 6.4.5.3). In the poisoned basket, the central cell, in addition to the six peripheral basket cells, contains intact fuel elements, or (top and bottom baskets only) screened or sealed cans. The bounding TRIGA fuel element type in the non-poisoned basket is verified as the bounding element in the poisoned basket with the axially infinite length cask model.

6.3.5.1.2 TRIGA Fuel Cluster Rod Methodology

To evaluate the nonpoisoned basket with the TRIGA fuel cluster rods, two models are utilized: an axially infinite length cask model and a full cask model. The axially infinite cask model is a single basket module with up to 16 TRIGA fuel cluster rods in a fuel pin handling insert (Figure 6.3.5-1) in the six peripheral basket openings. The single basket module is surrounded by the cask radial shields and is axially reflected to simulate an infinite length cask. The infinite length cask model is employed in the criticality evaluation of the intact TRIGA fuel cluster rods in the most reactive basket configuration (Section 6.4.6.1). The full cask model, used to evaluate failed fuel, contains five TRIGA basket modules in the cavity surrounded by the cask radial and axial shields (Section 6.4.6.2). The three central modules contain intact TRIGA fuel cluster rods in the peripheral openings, and the peripheral openings of the top and bottom modules contain sealed failed fuel cans with up to six rods of TRIGA fuel cluster rod active fuel material. In this model, the axial shields include an explicit representation of the cask lid and bottom forging. The cask models are used to determine the maximum k_{eff} of the cask under normal and accident conditions (Section 6.4.6.3).

To evaluate the poisoned basket with TRIGA fuel cluster rods, the non-poisoned axially infinite length cask and full cask models are modified to include borated stainless steel poison plates. Again, the infinite length cask model is used to evaluate intact TRIGA fuel cluster rods in the most reactive basket configuration (Section 6.4.6.1) and the full cask model is used to evaluate the basket modules with failed fuel (top and bottom baskets only) in the most reactive basket configuration (Section 6.4.6.2). In the poisoned basket, the central cell, in addition to the six peripheral basket cells, contains intact fuel elements, or sealed cans (top and bottom baskets only) with up to six rods of TRIGA fuel cluster rod active fuel material.

6.3.5.1.3 TRIGA Fuel Element Parametric Study Models

For the parametric evaluation of the most reactive TRIGA fuel element, a unit cell of fuel elements and the basket is modeled for each TRIGA fuel element type (Figure 6.2.5-2). This includes four fuel elements in a 3.44-inch (8.738 cm) square opening surrounded by a 5/16-inch (0.7938 cm) web. The models are evaluated dry and with water at 1 g/cc in the basket opening.

Reflecting boundary conditions are imposed on the sides, top and bottom simulating an infinite array with no axial leakage. These models were used to determine which of TRIGA fuel element types is most reactive. The most reactive type was then used as the design-basis element in subsequent analyses for normal conditions of transport and hypothetical accident conditions. Combinations of fuel were also analyzed to ensure that fuel enrichment combinations would be bounded by the design-basis loading and enrichment.

6.3.5.1.4 Infinite Axial Length Cask Model

The infinite length models of the NAC-LWT cask with the TRIGA fuel basket are presented in Figure 6.3.5-3 through Figure 6.3.5-5. These models represent TRIGA baskets loaded with up to 24 (non-poisoned) or 28 (poisoned) TRIGA fuel elements, or 480 (nonpoisoned) or 560 (poisoned) TRIGA fuel cluster rods surrounded by the NAC-LWT radial shields. Since the nonpoisoned TRIGA basket center location is blocked, no fuel elements are present in this location. The models are surrounded by a CUBOID with reflecting boundary conditions imposed on the sides, top and bottom, simulating an infinite array of casks with an infinite axial extent. Water moderator density is allowed to vary in the cavity and outside the cask under normal conditions, and also is allowed to vary inside the neutron shield tank under accident conditions. Cask center-to-center spacing is varied by adjusting the X-Y spacing of the CUBOID surrounding the cask.

6.3.5.1.5 Full Cask Model

The full cask models are similar to the axially infinite cask models, but rather than axially reflecting single basket modules, five basket module arrays are created (Figure 6.3.5-6). The basket module arrays are enclosed by the modeling of the cask body and the lid. The CUBOID surrounding the cask is surrounded by reflecting boundary conditions on all sides simulating an infinite array of casks. For cask configurations including cans, screened or sealed failed fuel cans are placed into the appropriate openings of the top and bottom basket. The appropriate openings of the three intermediate baskets are filled with uncanned TRIGA fuel elements. Appropriate openings consist of peripheral openings for nonpoisoned baskets and all openings for poisoned baskets. Moderator variations, including preferential flooding of the screened cans and sealed cans, are evaluated.

6.3.5.1.6 Finite Cask Array Model

The finite cask array model is similar to the infinite array model, but rather than axially and radially reflecting the finite length cask, the KENO-Va HOLE function is used to place a number of casks (either 4 or 8, depending on the configuration evaluated) into a close-packed

configuration. The CUBOID surrounding the cask array is reflected by the use of an H₂O reflector card to maximize neutron reflection back into the system.

6.3.5.2 Package Regional Densities

The composition densities (g/cc) and nuclide number densities (atm/b-cm) calculated by the material information processor and used in the subsequent criticality analyses are shown in Table 6.3.5-1.

Since the SCALE standard composition library does not contain U-ZrH as a standard composition, number densities (atm/barn-cm) were calculated based on dimensional and gram load data from Table 6.2.5-2 (Tomsio). Hydrogen atom densities were calculated based on stoichiometric Zr-H or Zr₅H₈ for the base evaluations. For TRIGA elements in a nonpoisoned basket, variations in ZrH_x composition with a hydrogen-to-zirconium ratio up to the maximum possible (2.0) were evaluated. The homogenized end fitting volume fractions were based on the SCALE default Type 304 stainless steel density and dimensional and gram load data from Table 6.2.5-1. A sample set of TRIGA fuel element number densities used in the criticality analyses is shown in Table 6.3.6-1 and the design basis TRIGA fuel cluster rod number densities are presented in Table 6.3.5-2.

In all criticality models, the fuel elements are explicitly represented. In the case of the TRIGA fuel elements, an explicit 15-inch (38.1 cm) active fuel region of U-ZrH is modeled including 3.42 inches (8.687 cm) of graphite reflector segments above and below the active fuel. TRIGA fuel cluster rods have an active fuel length of 22 inches. All fuel elements are modeled as explicit nested CYLINDERS, but due to their unusual geometry, the TRIGA fuel element end fittings and the spring loaded section of the plenum in the TRIGA fuel cluster rods are modeled as homogenized stainless steel and water. With the exception of the homogenization of fuel debris within the sealed failed fuel cans to represent the worse case damage to the fuel, this is the only homogenization in the geometry.

Figure 6.3.5-1 Fuel Rod Handling Insert for TRIGA Fuel Cluster Rods

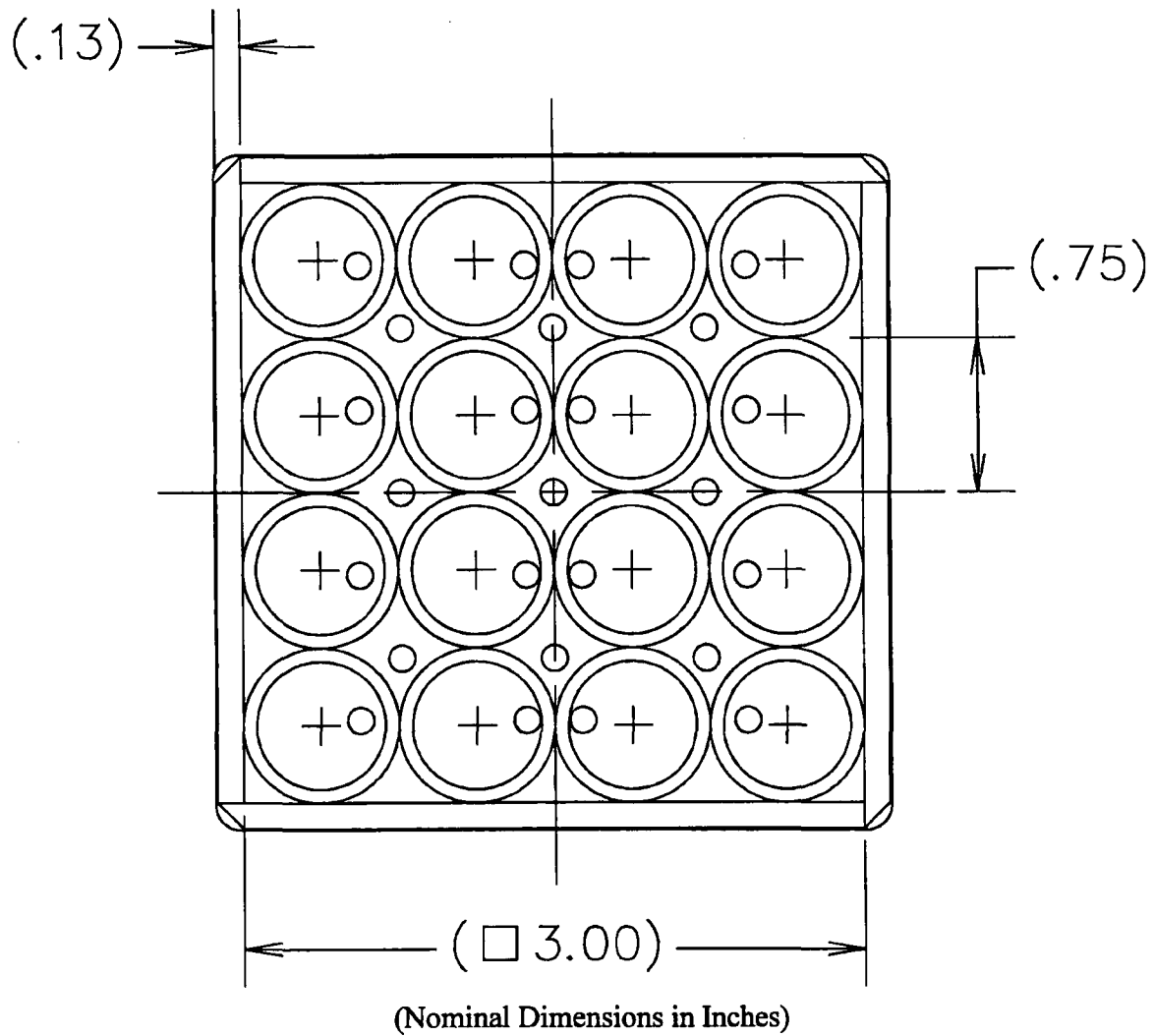
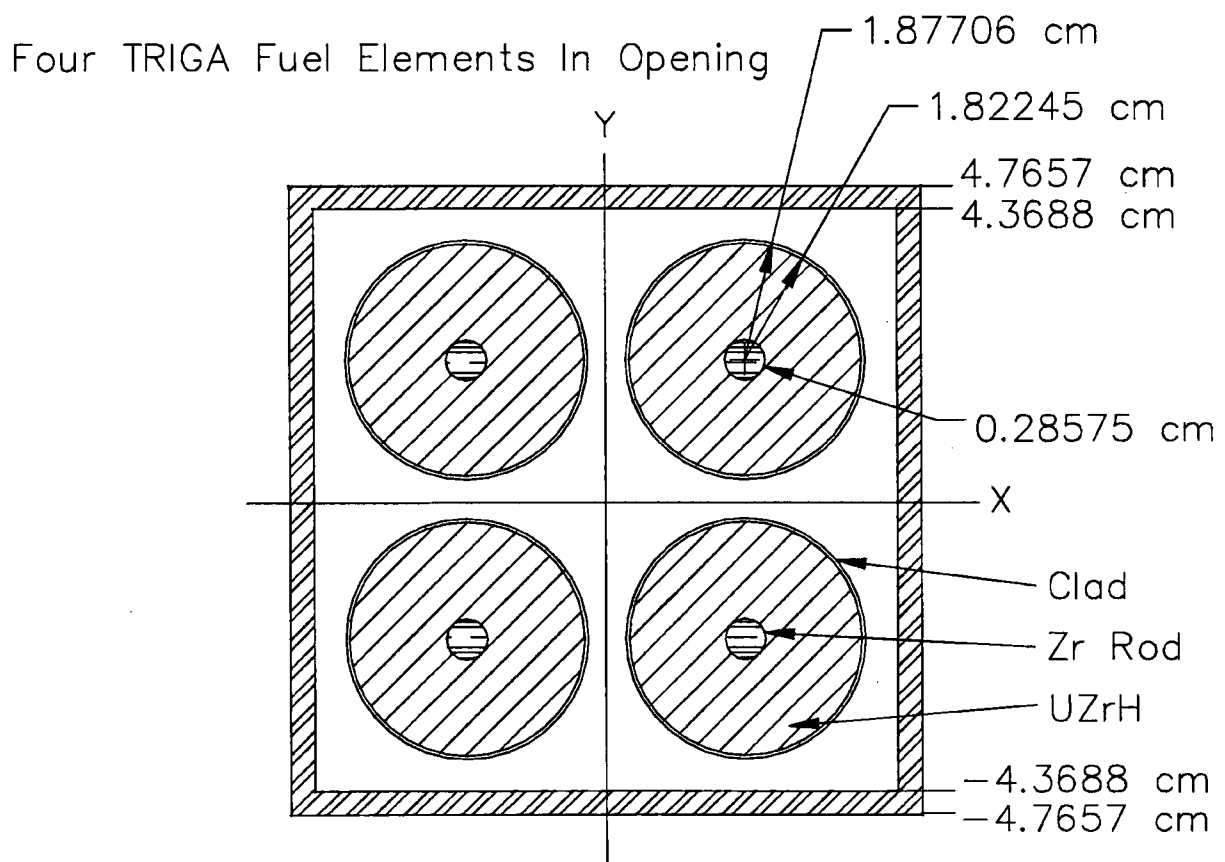


Figure 6.3.5-2 Fuel/Basket Unit Cell Model for TRIGA Fuel Elements



Reflecting Boundary Conditions
on sides top and bottom

Figure 6.3.5-3 NAC-LWT Cask with TRIGA Fuel, Nonpoisoned Basket - Radial View

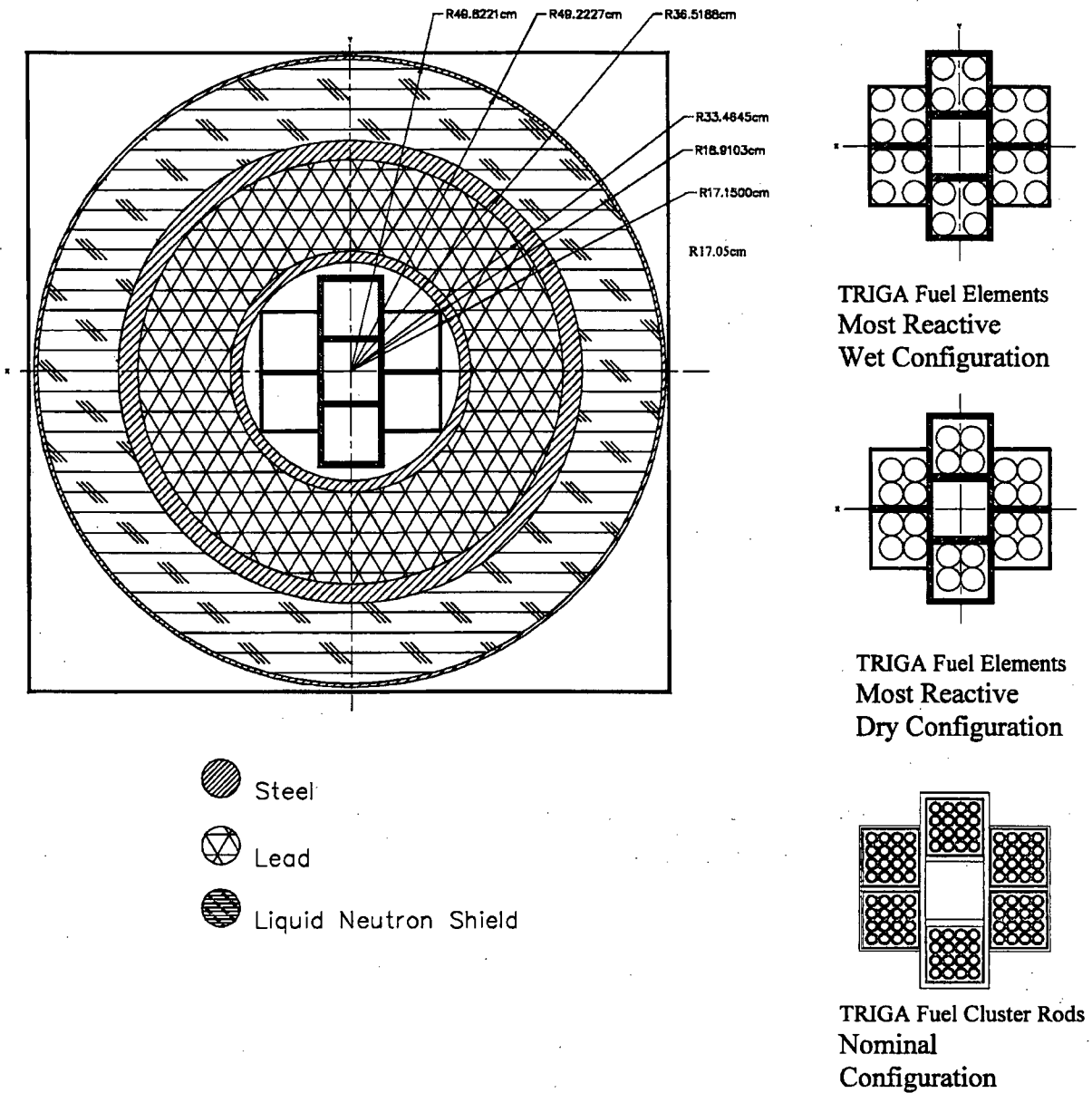
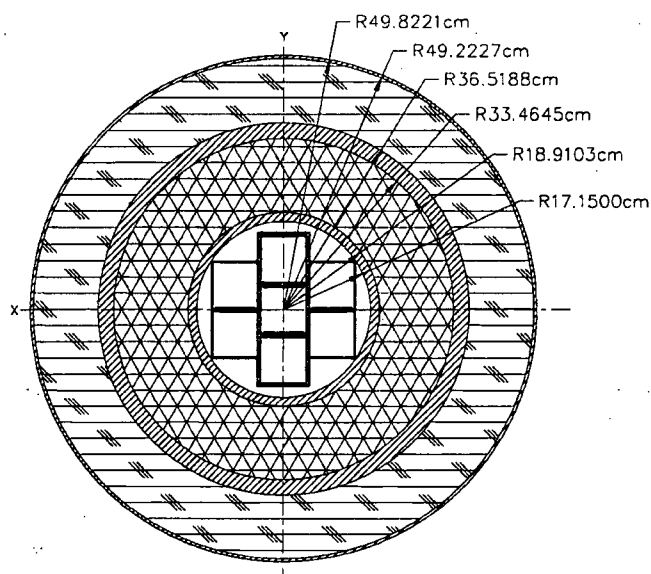
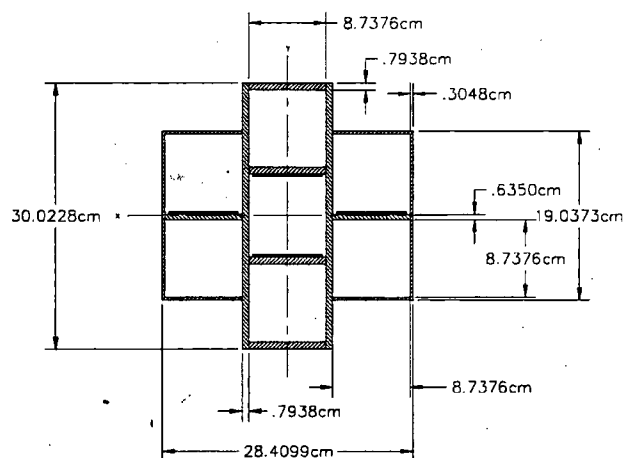




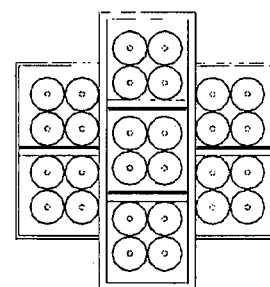


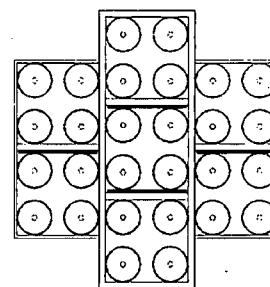
Figure 6.3.5-4 KENO-Va Model of NAC-LWT with Poisoned Basket - Radial View



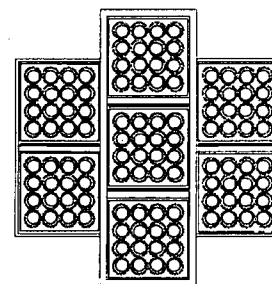
-  Steel
-  Lead
-  Liquid Neutron Shield
-  Borated Steel Plate



TRIGA Fuel Elements
Most Reactive Dry Configuration



TRIGA Fuel Elements
Most Reactive Wet Configuration



TRIGA Fuel Rods
Nominal Configuration

Figure 6.3.5-5 NAC-LWT Cask Model with TRIGA Fuel Elements, Nonpoisoned Basket - Axial View

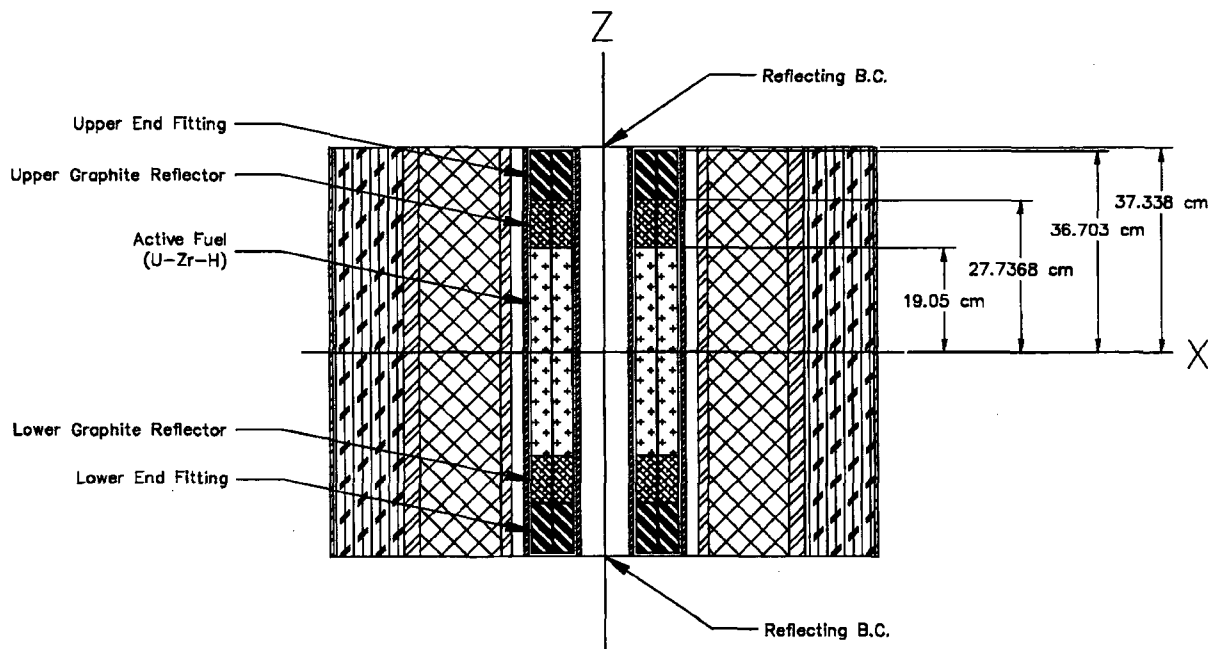


Figure 6.3.5-6 Full Length NAC-LWT Cask Model with TRIGA Fuel Elements, Nonpoisoned Basket - Axial View

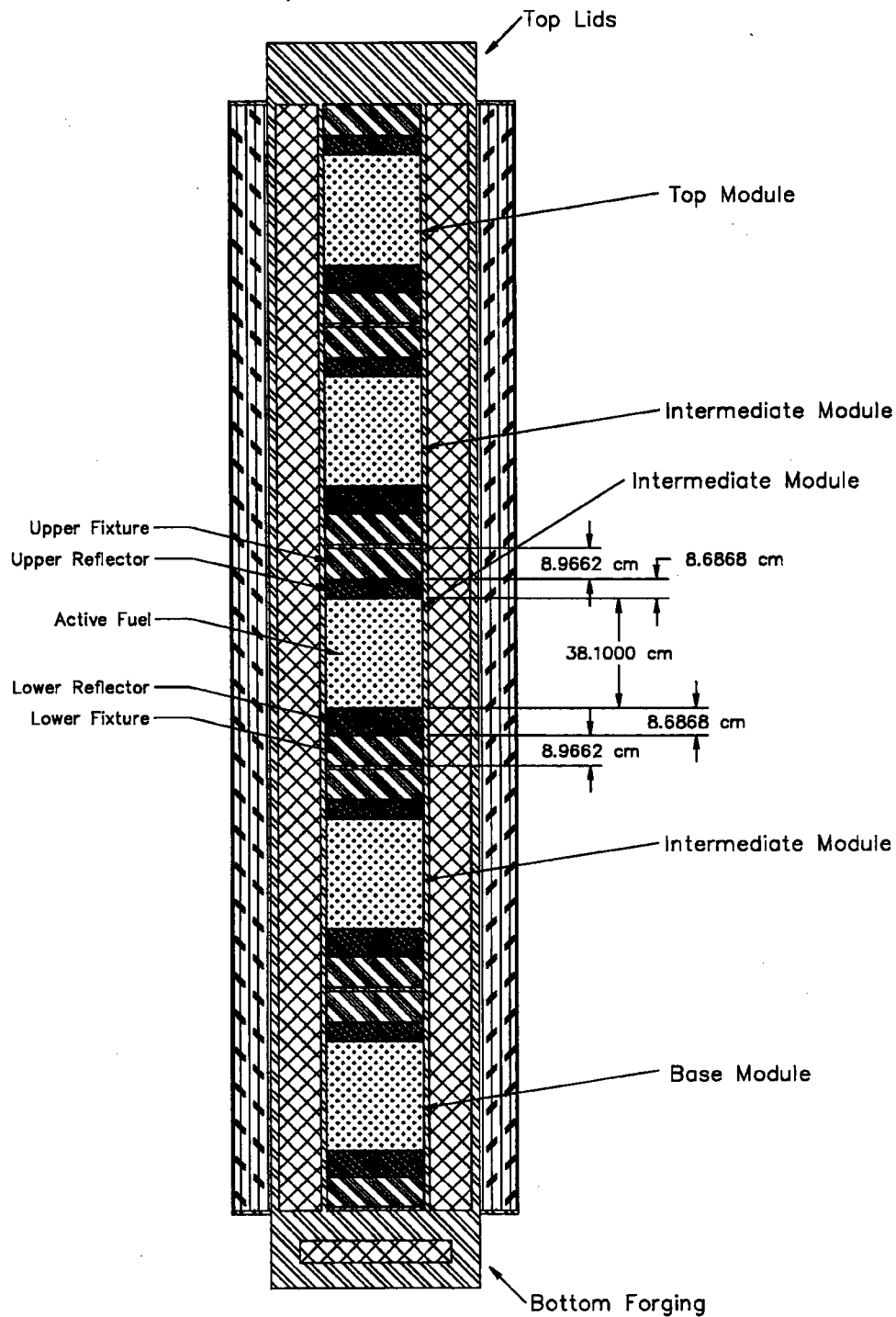


Table 6.3.5-1 Sample Compositions and Number Densities Used in Criticality Analysis of TRIGA Fuel Elements

Material	FLIP Fuel U-Zr-H	Aluminum	H ₂ O	304 Stainless Steel	Graphite	Lead
Density, g/cc	--	2.70	0.998	7.920	2.1	11.350
Nuclide				atm/barn-cm		
Uranium 235	9.053E-4	--	--	--	--	--
Uranium 238	3.849E-4	--	--	--	--	--
Zirconium	3.446E-2	--	--	--	--	--
Hydrogen	5.514E-2	--	3.338E-2	--	--	--
Oxygen	--	--	6.675E-2	--	--	--
Carbon	--	--	--	--	1.054E-1	--
Aluminum	--	6.024E-2	--	--	--	--
Iron	--	--	--	5.936E-2	--	--
Chromium	--	--	--	1.743E-2	--	--
Nickel	--	--	--	7.721E-3	--	--
Manganese	--	--	--	1.736E-3	--	--
Lead	--	--	--	--	--	3.297E-2

Table 6.3.5-2 Compositions and Number Densities Used in Criticality Analysis of TRIGA Fuel Cluster Rods

Material	U-Zr-H	Aluminum Insert	H ₂ O	304 Stainless Steel	Lead
Density, g/cc	--	2.70	0.998	7.920	11.350
Nuclide	atm/barn-cm				
Uranium 235	1.46137E-03	--	--	--	--
Uranium 238	1.03065E-04	--	--	--	--
Zirconium	3.40686E-02	--	--	--	--
Hydrogen	5.35638E-02	--	3.338E-2	--	--
Oxygen	--	--	6.675E-2	--	--
Carbon	--	--	--	--	--
Aluminum	--	6.024E-2	--	--	--
Iron	--	--	--	5.936E-2	--
Chromium	--	--	--	1.743E-2	--
Nickel	--	--	--	7.721E-3	--
Manganese	--	--	--	1.736E-3	--
Lead	--	--	--	--	3.297E-2

6.3.6 DIDO Fuel Assemblies

6.3.6.1 Description of Calculational Models

Since it is planned to transport many types of DIDO fuel assemblies in the NAC-LWT, a determination of the most limiting, i.e., highest k_{eff} , assembly must be made for criticality purposes. Fuel parameters in Table 6.3.6-1 are employed for the evaluations of HEU, MEU and LEU types and are based on the data presented in Table 6.2.8-1. The tolerances in Table 6.2.8-2 are used in trending reactivity versus the assembly's physical characteristics and produce a bounding fuel assembly characteristic set.

Evaluations are performed with two distinct models. The first stage evaluates reactivity in an infinite array of casks by modeling a single cask with mirrored boundary conditions. The second phase of the evaluations employs a finite array of eight casks. The basket and cask models constructed for the DIDO assembly evaluations are based on the dimensions listed in Table 6.3.6-2.

The KENO-Va model of the NAC-LWT cask with DIDO fuel is centered on a stack of six DIDO baskets. The cask radial shields surround the basket stack. The basket stack surrounded by shields has the lid and bottom weldment added. The module chosen for stacking is the intermediate basket module. While axial extents differ from the bottom and top modules, the basket horizontal cross section is identical in all modules. Axial variations are associated with the stacking of the units, with all units containing the 0.5-inch thick base plate. Figure 6.3.6-1 displays a side view of the intermediate module. A cross-section of the basket with fuel tubes numbered one through seven and the aluminum shell is shown in Figure 6.3.6-2. Two assumptions were made in the DIDO model due to limitation in the KENO-Va input structure and complexity of the model: (1) the heat transfer shunts are modeled as a set of three small cylinders versus a rectangular bar and (2) the aluminum shell is modeled over the full extent of the tube, neglecting the intermediate steel disk. An evaluation is provided in Section 6.4.7 to demonstrate that each of these assumptions is conservative. Figure 6.3.6-2 also includes a sketch of the two types of fuel configurations evaluated shown in a cross-section, loose and crimped cylinders. The "loose" cylinder configuration spaces the fuel at a constant pitch identical to that of the element during in-core configuration. The second configuration represents the fuel in a "crimped" configuration. For fuel shipment, the assembly can be cut and individual cylinders may be crimped. A radial sketch of the basket cross-section in the cask is shown in Figure 6.3.6-3. Figure 6.3.6-4 shows this basket module stacked six high inside the NAC-LWT. Reflecting boundary conditions on all sides simulate an infinite array of casks. This model

neglects the impact limiters that would provide additional spacing between casks, and models the cask under accident conditions with the neutron shield voided.

Tubes comprising the basket structure are defined to be stainless steel per licensing drawings. Aluminum tubes are evaluated in the DIDO calculation sets. This evaluation provides significant conservatism in the calculation, as stainless steel contains significant absorber nuclides while aluminum has no significant effect on system reactivity (beyond volume displacement).

The eight-cask array places the casks in a tight triangular pitch configuration. Seven casks are located in a tight cylindrical arrangement similar to that employed in the basket. The eighth cask is placed in a triangular pitch to the lower right corner of the seven cask array.

6.3.6.2 Package Regional Densities

The composition densities (g/cc) and nuclide number densities (atm/b-cm) calculated by the SCALE material information processor for a range of assemblies evaluated in subsequent criticality analyses are shown in Table 6.3.6-3. Displayed are the HEU, MEU and LEU material densities for the nominal fuel cylinders. Additional material densities may be obtained from the sample input/output files provided in Section 6.6.8.

Figure 6.3.6-1 Intermediate DIDO 42 Basket Module

(Dimensions in inches)

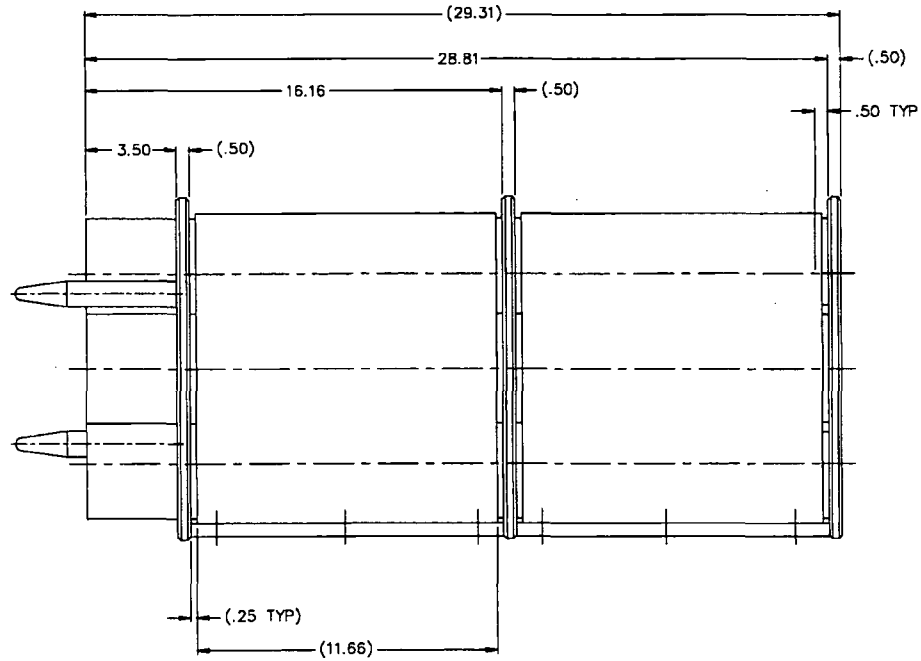


Figure 6.3.6-2 KENO-Va DIDO Fuel in Fuel Tube and Basket Cross-Section

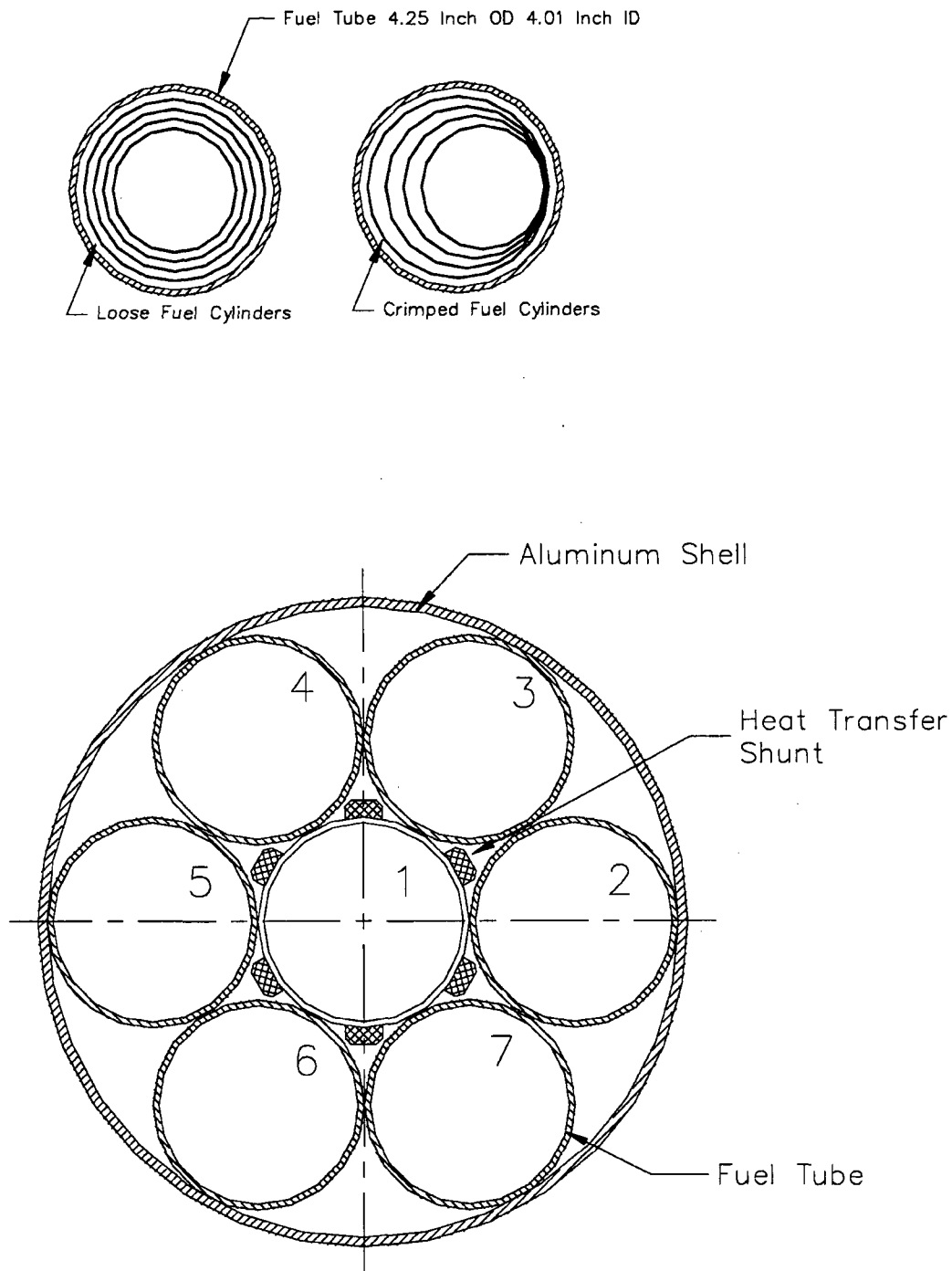
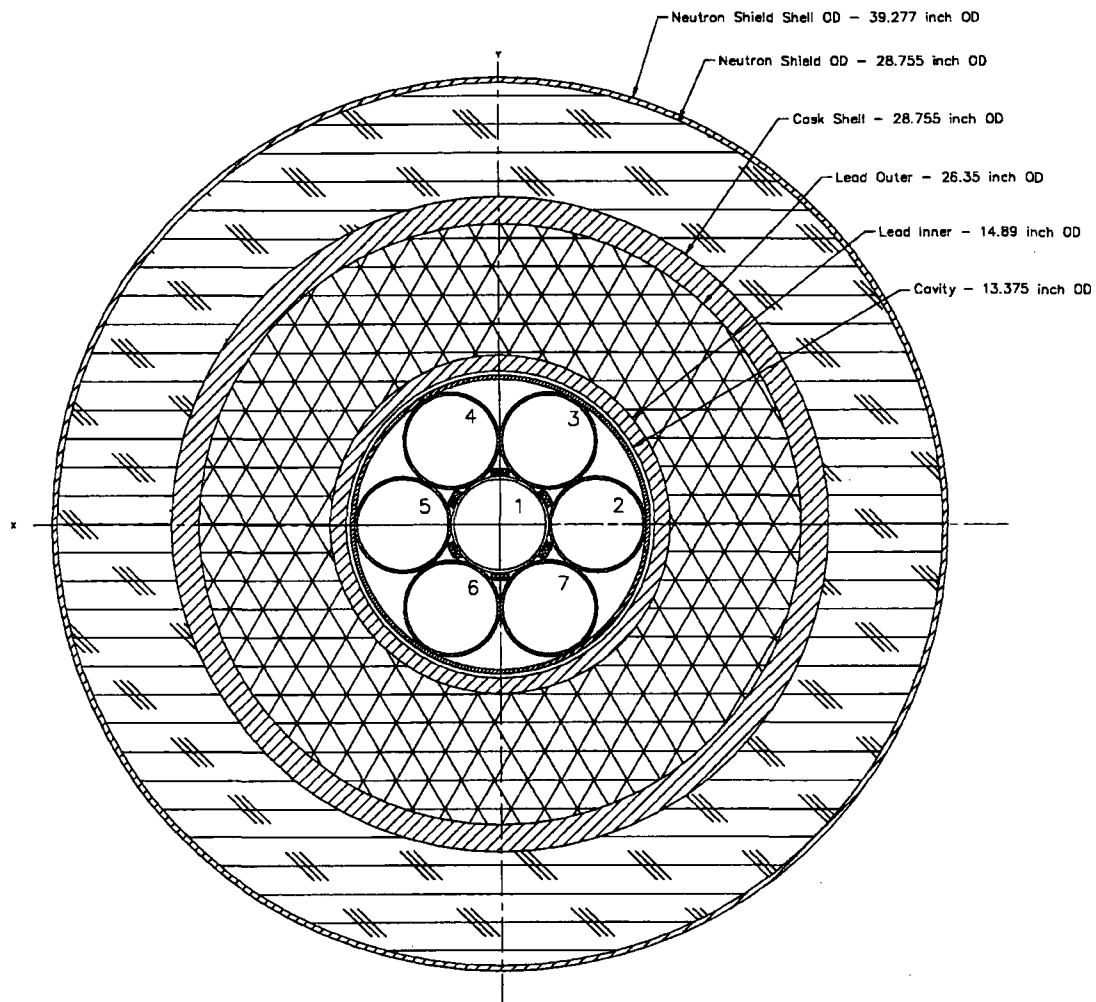


Figure 6.3.6-3 KENO-Va Model of NAC-LWT Cask Cross-Section with DIDO Fuel






-  Steel
-  Lead
-  Liquid Neutron Shield

Figure 6.3.6-4 Full Length NAC-LWT Cask Model with 42 DIDO Fuel Assemblies

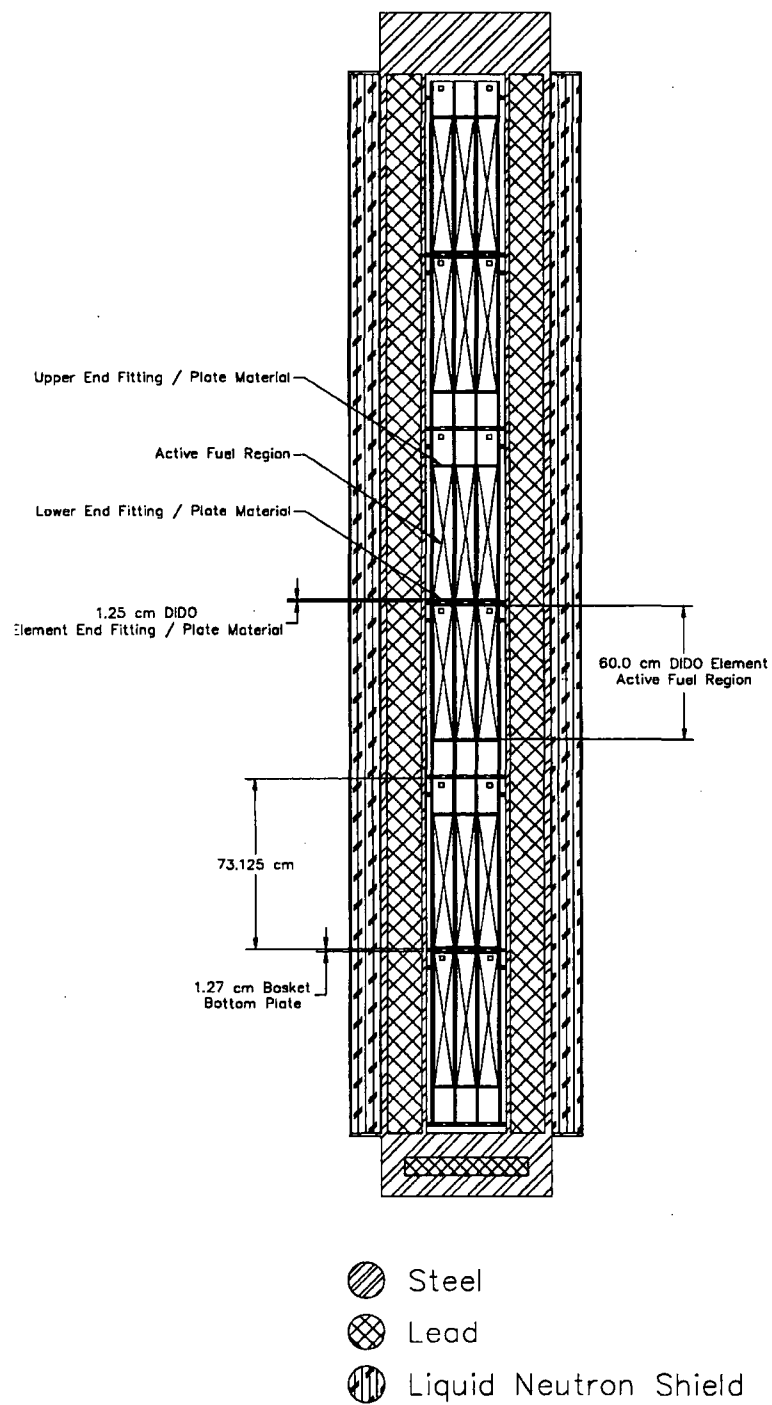


Table 6.3.6-1 DIDO Fuel Parameters

Fuel Parameters	Units	Value
Tube 1 Outer Diameter	[cm]	6.38
Tube 2 Outer Diameter	[cm]	7.36
Tube 3 Outer Diameter	[cm]	8.34
Tube 4 Outer Diameter	[cm]	9.32
Clad Thickness	[cm]	0.0425
Tube Thickness	[cm]	0.15
Fuel Meat Thickness	[cm]	0.065
Active Fuel Length	[cm]	60
Total Element Length	[cm]	62.5
Tube Pitch	[cm]	—
Fuel Composition		U-Al
Weight Percent ²³⁵ U		Note 1
Maximum ²³⁵ U per Fuel Assembly	[g]	180.0
U wt % in Fuel Composition		Note 1
Mass of Uranium	[g]	Note 1

Note:

1. ²³⁵U weight percent, uranium mass and weight percent of uranium in the fuel meat are dependent on the enrichment type evaluated and tolerances employed.

Table 6.3.6-2 DIDO Basket and Cask Parameters

Description	Dimension [in]
Fuel tube outer diameter	4.250
Fuel tube wall thickness	0.120
Fuel tube outer diameter tolerance (maximum)	0.015
Fuel tube outer diameter tolerance (minimum)	0.025
Fuel tube thickness tolerance (maximum)	22%
Fuel tube thickness tolerance (minimum)	0%
Outer ring tube location diameter	8.500
Tube location angle	60.000
Fuel basket outer diameter	13.265
Fuel basket base plate thickness	0.500
Fuel basket base plate thickness tolerance	0.020
Basket bottom plate hole size	1.000
Aluminum shell thickness	0.188
Aluminum shunt width	0.750
Aluminum shunt depth	0.375
Basket cavity height	28.81
Basket cavity height tolerance	0.060
Cask cavity diameter	13.375
Lead shield inner diameter	14.890
Lead shield outer diameter	26.350
Lead shield outer diameter of taper	24.880
Cask outer diameter	28.755
Cask lid thickness	11.250
Bottom forging thickness	10.500
Bottom forging lead insert diameter	20.750
Bottom forging lead insert thickness	3.000
Offset bottom of cask to lead	3.500
Neutron shield thickness	5.000
Neutron shield tank skin	0.236
Number of baskets per cask	6.000

Table 6.3.6-3 Composition Densities Used in Criticality Analysis of DIDO Fuel

Material	HEU U-Al	MEU U-Al	LEU U-Al
Density, g/cc	U=0.501 Al=2.250	U=1.060,Al=2.085	U=2.415,Al=1.786
Nuclide	Atoms/barn-cm		
Uranium 235	1.222-3	1.222-3	1.222-3
Uranium 238	7.702-5	1.475-3	4.900-3

Material	Al Clad	H ₂ O	304 Stainless Steel	Pb	H ₂ O/ Glycol
Density, g/cc	2.702	0.998	7.920	11.350	0.9437
Nuclide	Atoms/barn-cm				
Aluminum	6.031E-2				
Oxygen		3.338E-2			2.459E-2
Hydrogen		6.675E-2			5.988E-2
Iron			5.936E-2		
Chromium			1.743E-2		
Nickel			7.721E-3		
Manganese			1.736E-3		
Lead				3.299E-2	
Carbon					1.070E-2

6.3.7 General Atomics Irradiated Fuel Material

6.3.7.1 Description of Calculational Models

Criticality evaluations are performed for three payload combinations: RERTR (TRIGA) fuel only, HTGR fuel only, and both RERTR and HTGR fuel. The results of these analyses show which fuel material is most reactive and establish a basis for choosing a reactivity bias for the combined system. In the models of either RERTR or HTGR fuel, the radial detail of the basket tubes is included. In the combined payload model, the basket tubes are conservatively not modeled, and the RERTR and HTGR enclosures (Fuel Handling Units (FHUs)) intersect tangentially at the centerline of the cask cavity.

The KENO-Va model of the NAC-LWT cask with a combined payload of GA IFM is axially infinite in height, with the active fuel length of the TRIGA elements chosen as the modeled axial extent. Note that two pitch scenarios are evaluated for the 20 TRIGA fuel elements. This first scenario places the elements in a 4×5 rectangular array, as shown in Figure 6.3.7-1, and is denoted as 'Rectangular' in the result tables in Section 6.4.8. The second scenario places 16 elements in a 4×4 array with the remaining four elements inserted in the center of each face on a triangular pitch as shown in Figure 6.3.7-2. For convenience, this scenario is denoted as 'Square' in the result tables in Section 6.4.8. The centerline parameters are calculated as a function of pitch. The HTGR fuel matrix is a homogenized cylinder with outer diameter equal to the inner diameter of the HTGR primary enclosure. The two IFM enclosures intersect tangentially at the centerline of the cask cavity and are surrounded by the cask radial shields. A sketch of the cross-section in the cask is shown in Figure 6.3.7-3. Reflecting boundary conditions on all sides simulate an infinite array of casks. The neutron shield material definition is tied to the exterior moderator definition; a void exterior includes a void neutron shield. Thus, the accident condition of loss of neutron shielding is explicitly modeled when the exterior moderator is set to void.

6.3.7.2 Package Regional Densities

The composition densities (g/cc) and nuclide number densities (atm/b-cm) calculated by the SCALE material information processor are shown in Table 6.3.7-1. Two material descriptions exist for the RERTR/TRIGA fuel: 1) intact fuel with clad, and 2) homogenized fuel without clad.

Figure 6.3.7-1 PICTURE Representation of NAC-LWT Cavity with 'Rectangular' Array of GA IFM TRIGA Elements

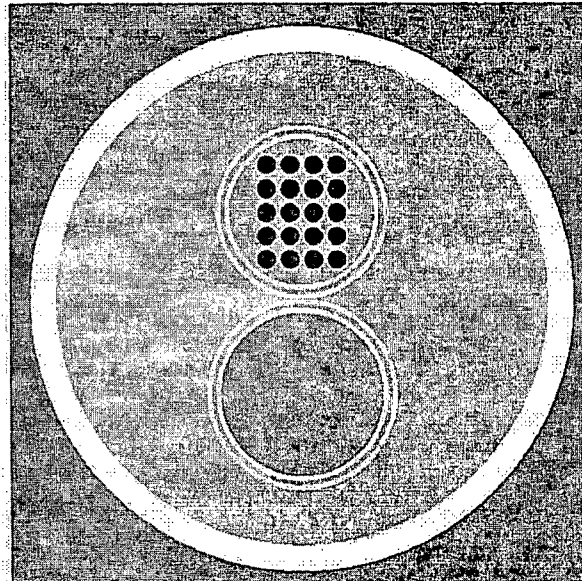


Figure 6.3.7-2 PICTURE Representation of NAC-LWT Cavity with 'Square' Array of GA IFM TRIGA Elements

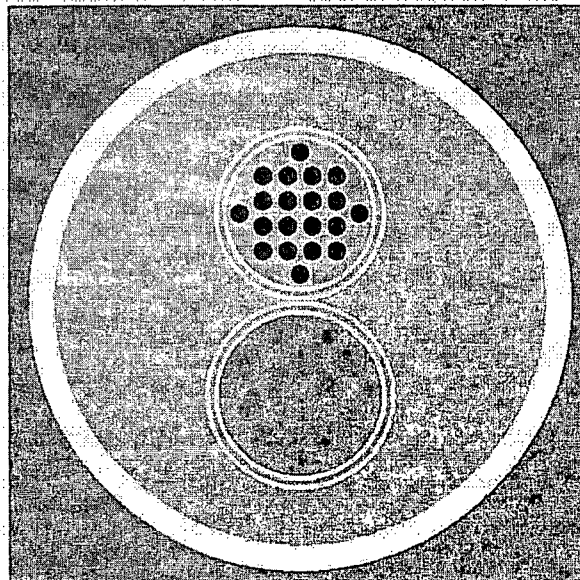
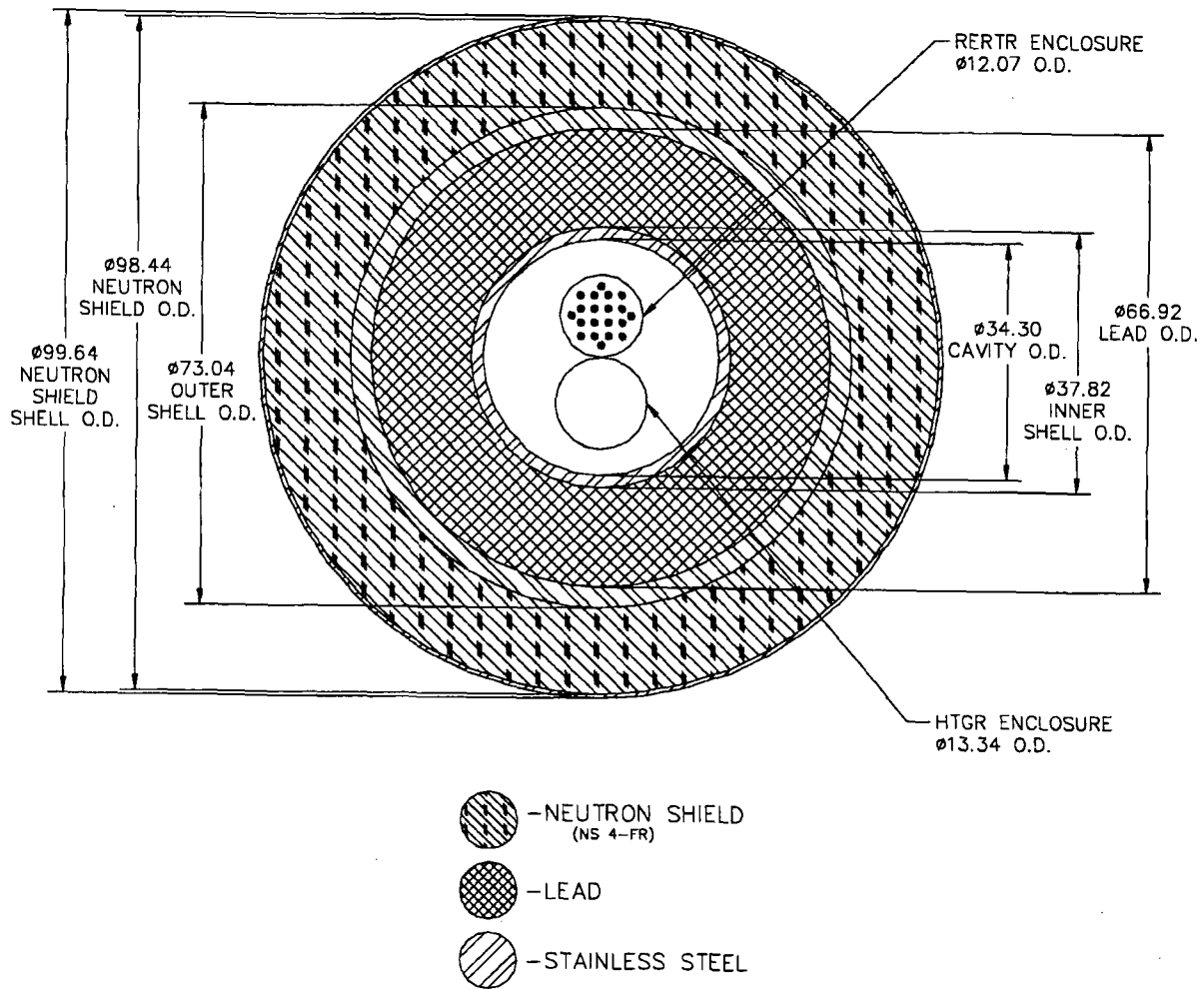


Figure 6.3.7-3 KENO-Va Model of NAC-LWT Cask Cross-Section with GA IFM



[Dimensions in cm]

Table 6.3.7-1 Composition Densities Used in Criticality Analysis of GA IFM

Material	Intact RERTR Fuel	Intact RERTR Clad	Homog. RERTR Fuel	HTGR Fuel	H ₂ O	304 Stainless Steel	Pb
Density, g/cc	7.409	7.940	1.499	1.116	0.998	7.920	11.344
Nuclide	Atoms/barn-cm						
Hydrogen	4.779E-02		9.717E-03		6.677E-02		
Carbon	5.199E-04		1.084E-04	3.716E-02			
Zirconium	3.052E-02		6.214E-03				
Uranium-235	1.337E-03		2.722E-04	5.117E-05			
Uranium-238	5.382E-03		1.096E-03	3.719E-06			
Chromium		2.298E-02				1.743E-02	
Iron		3.424E-02				5.936E-02	
Nickel		2.850E-02				7.721E-03	
Oxygen				8.810E-05	3.338E-02		
Silicon				3.160E-03			
Thorium				5.315E-04			
Manganese						1.736E-03	
Lead							3.297E-02

6.3.8 PULSTAR Fuel Contents

6.3.8.1 Description of Calculational Models

Four types of basket loadings are considered in the criticality evaluation: (1) intact assemblies loaded directly into the module cell, (2) up to 16 intact elements loaded in the 4×4 fuel rod holder, (3) up to 25 intact or damaged (failed) elements in the PULSTAR failed fuel can, or (4) up to 25 intact or damaged (failed) elements in the PULSTAR screened can. For the evaluation of the canned fuel elements, both discrete and homogenized fuel descriptions are employed.

Fuel elements are modeled using the parameters in Section 6.2.10. Using a conservatively selected enrichment of 6.5 wt % ^{235}U and a loading of 33 grams ^{235}U per element, the calculated UO_2 density is 10.38 g/cm^3 . The assembly is modeled as a 25-element rectangular rod array with no credit is taken for the assembly upper and lower fittings. The modeled height for intact elements is 26.2 inches, which includes the active fuel height of 24.1 inches and upper and lower end caps. No element (rod) plenum space is modeled.

A bounding can cavity dimension of 3.3-inch width × 30-inch height is chosen to bound the PULSTAR can dimensions. Neither canister wall nor end-plates are included in the model. The 3.3-inch cavity is wider than physically feasible in the minimum 3.38-inch basket opening when adding in the canister wall thicknesses.

PULSTAR fuel evaluations rely on base models developed for the MTR fuel reactivity calculations, as the PULSTAR elements are placed in the 28 MTR basket configuration with spacers. No credit for spacers is taken in the PULSTAR fuel calculations. Base PULSTAR fuel evaluations are performed with minimum basket opening and minimum basket plate thickness, fuel centered within each basket cell, fuel assemblies axially centered in the basket, a flooded cask cavity, and a void cask exterior. Infinite cask arrays are used where possible, with a reduced array specified when necessary to maintain system reactivity below licensing limits.

MTR KENO models are modified to include the PULSTAR fuel assemblies, fuel rod holder and cans. Models are configured to evaluate basket mechanical perturbations and payload radial and axial shifting. Can, cask cavity, neutron shield and cask exterior models are defined as separate materials to allow optimum moderator density and preferential flooding studies.

As indicated in Section 6.2.10, PULSTAR fuel assemblies are rectangular, not square; therefore, assembly alignment (rotation), dubbed 'Xlong' and 'Ylong', is evaluated.

Revision 38

The four types of basket loadings are illustrated in Figure 6.3.8-1 through Figure 6.3.8-4. Dimensioned model sketches with cask materials are shown in Figure 6.3.8-5 and Figure 6.3.8-6. The axial view shows the highest reactivity payload combination of cans and intact fuel assemblies shifted “alternating” into close contact. Note that no spacers are included in the model.

6.3.8.2 Package Regional Densities

The composition densities (g/cc) and nuclide number densities (atm/b-cm) calculated by the SCALE material information processor are shown in Table 6.3.8-1.

Figure 6.3.8-1 PICTURE Representation of NAC-LWT Cavity with PULSTAR Assemblies

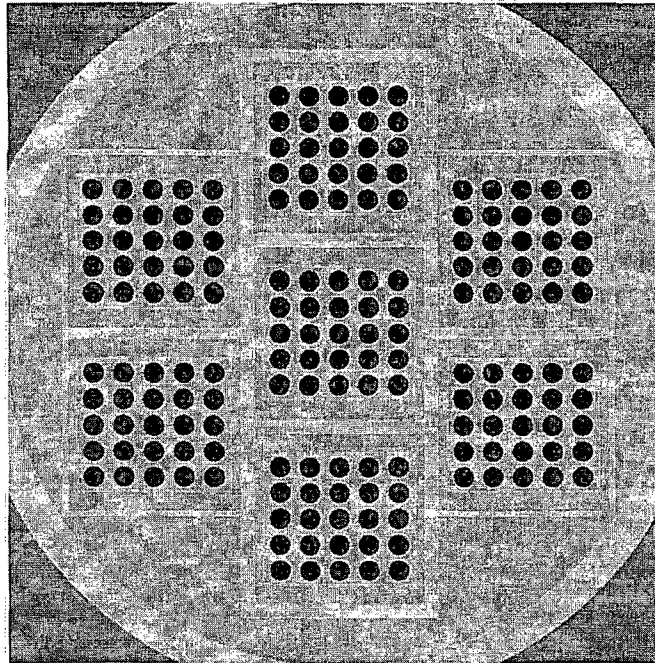


Figure 6.3.8-2 PICTURE Representation of NAC-LWT Cavity with PULSTAR Elements in 4x4 Rod Insert

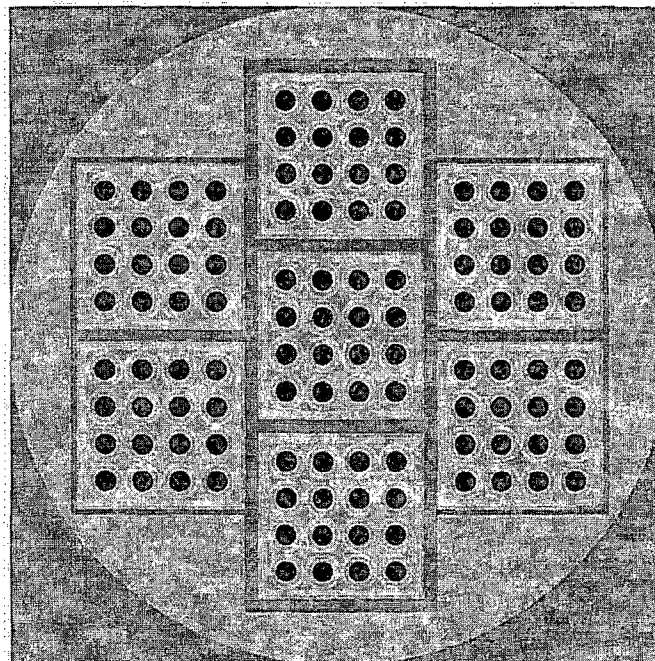


Figure 6.3.8-3 PICTURE Representation of NAC-LWT Cavity with Canned Discrete PULSTAR Elements

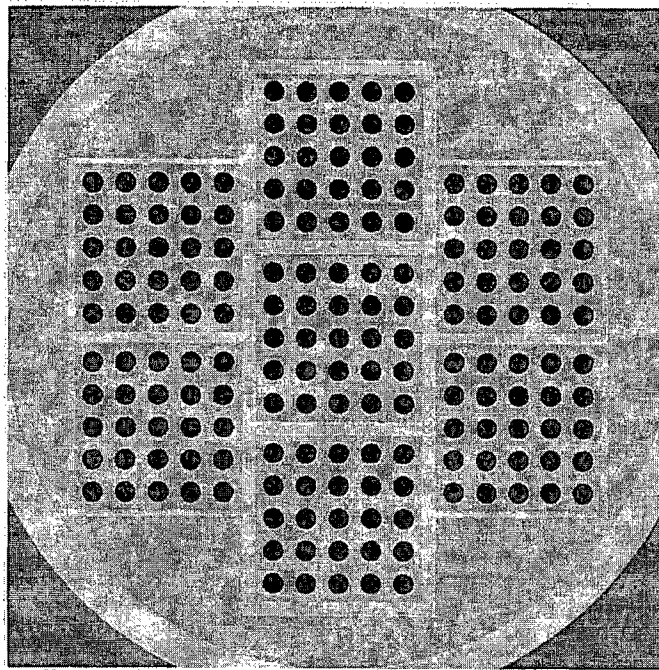
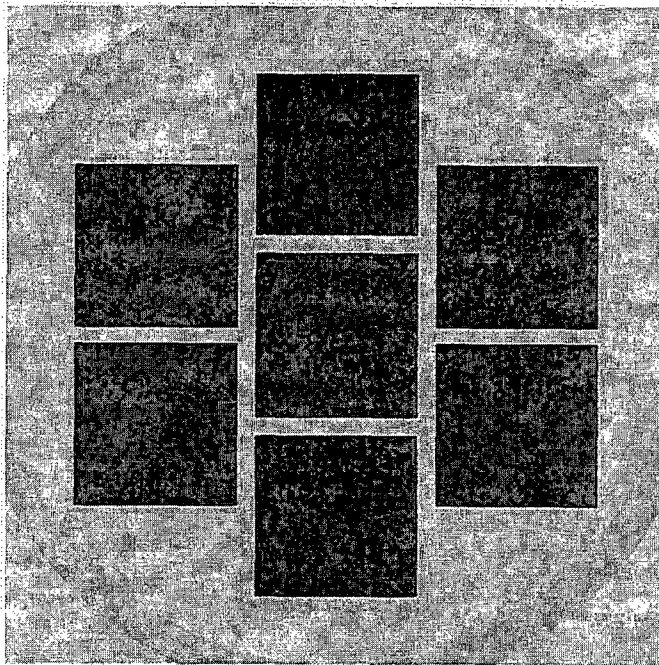
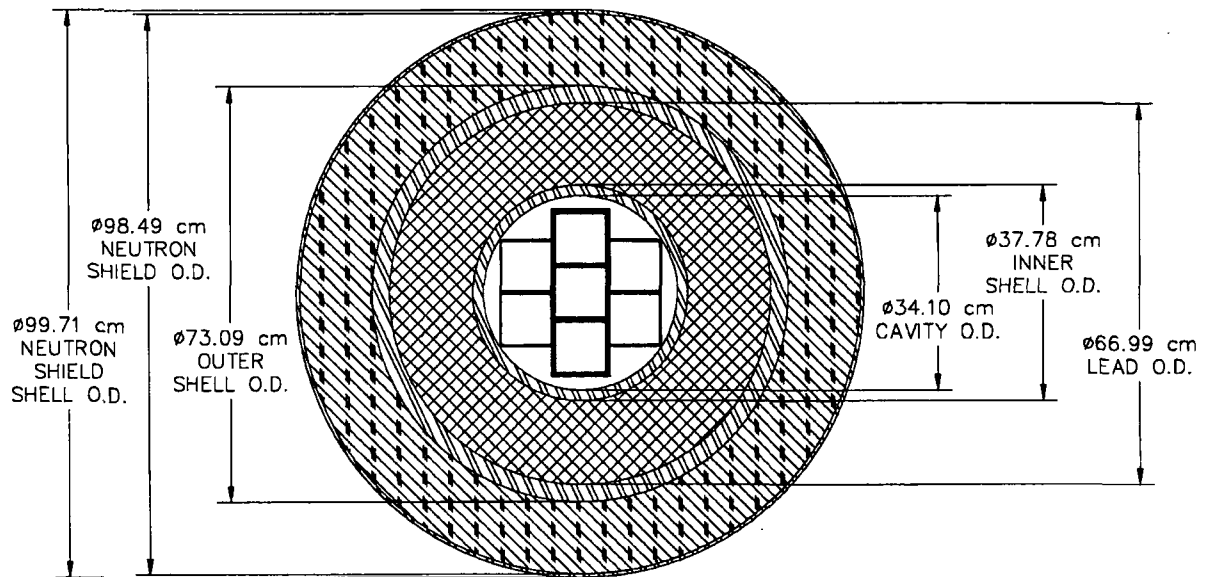


Figure 6.3.8-4 PICTURE Representation of NAC-LWT Cavity with Canned Homogenized PULSTAR Elements



**Figure 6.3.8-5 KENO-Va Model of NAC-LWT Cask Cross-Section with 28 MTR
7-Element Basket**






-  Neutron Shield
-  Lead
-  Stainless Steel

Figure 6.3.8-6 Finite Length KENO-Va Model of NAC-LWT Cask with 700 PULSTAR Fuel Elements

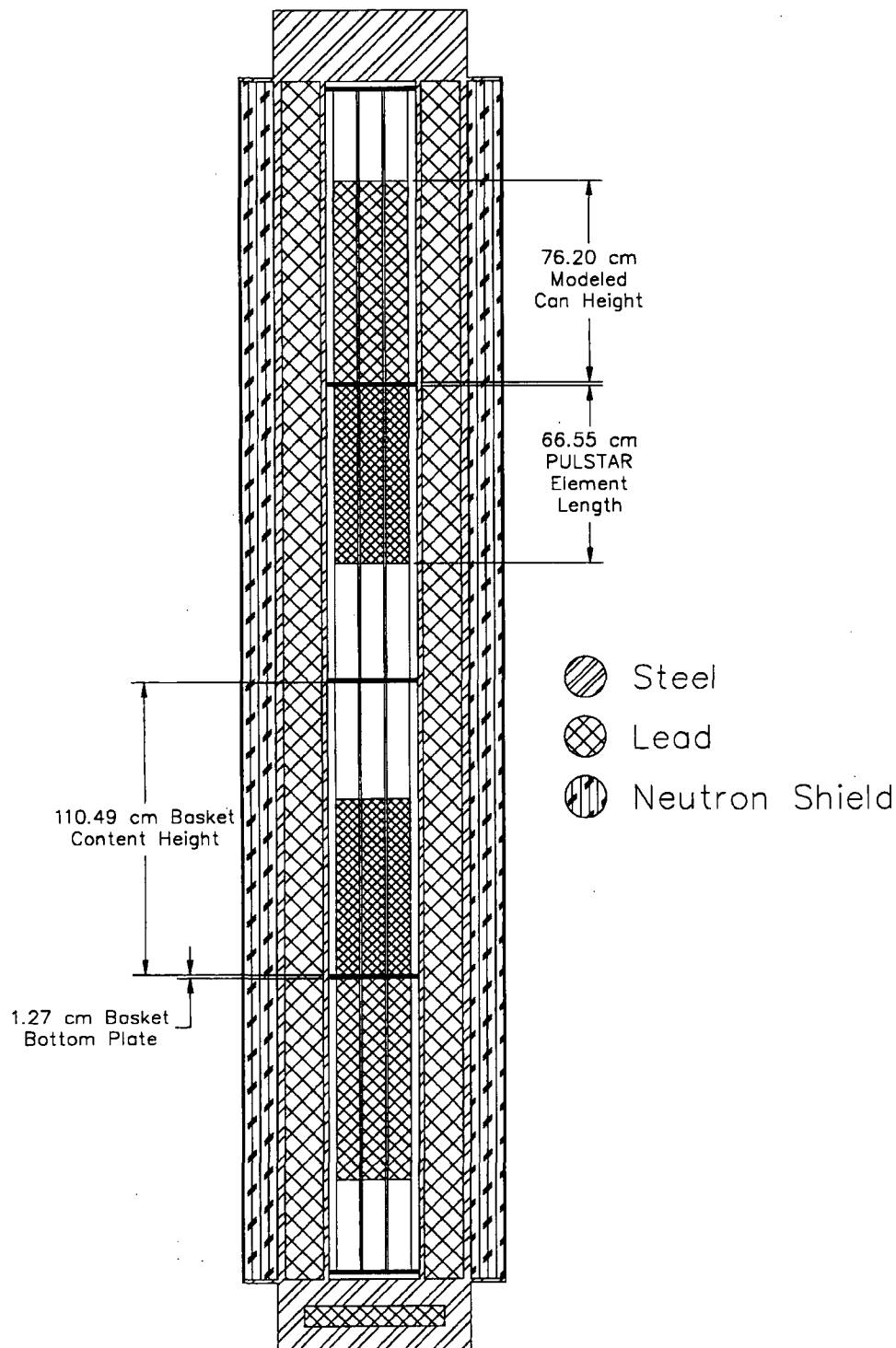


Table 6.3.8-1 Composition Densities Used in Criticality Analysis of PULSTAR Fuel

Material	Intact PULSTAR Fuel	Intact PULSTAR Clad	Homog. PULSTAR Fuel	H ₂ O	304 Stainless Steel	Pb
Density, g/cc	10.38	6.56	3.013.01	0.998	7.920	11.344
Nuclide	Atoms/barn-cm					
Hydrogen				6.677E-02		
Oxygen	4.633E-02			3.338E-02		
Uranium-235	1.524E-03		3.950E-04			
Uranium-238	2.164E-02		5.610E-03			
Zircaloy		4.331E-02	2.096E-03			
Chromium					1.743E-02	
Iron					5.936E-02	
Nickel					7.721E-03	
Manganese					1.736E-03	
Lead						3.297E-02

6.3.9 ANSTO Basket Payload

6.3.9.1 Description of Calculational Models

Fuel parameters in Table 6.2.11-1, spiral fuel assembly, and Table 6.2.12-1, MOATA plate bundle, are employed to build criticality models for the payloads within the NAC-LWT ANSTO baskets. The fuel tolerances in Table 6.2.11-2 and Table 6.2.12-2 are used in trending reactivity versus the assembly's physical characteristics and produce a bounding fuel assembly characteristic set.

Evaluations are performed with an infinite array of casks by modeling a single cask with mirrored boundary conditions. An additional evaluation is performed to demonstrate that a single cask, with containment boundary fully reflected by water, is subcritical with a reactivity below that of the bounding accident configuration array. The ANSTO basket and NAC-LWT cask models are based on the dimensions listed in Table 6.3.9-1 and are identical to the DIDO basket with the exception of slightly larger and thicker fuel tubes and the removal of the aluminum heat transfer components in the basket.

The KENO-Va model of the NAC-LWT cask with the spiral fuel assembly and plate bundle is centered on a stack of six ANSTO baskets. The cask radial shields surround the basket stack. The basket stack, surrounded by shields, has the lid and bottom weldment added. The module chosen for stacking is the intermediate basket module. While axial extents differ from the bottom and top modules, the basket horizontal cross-section is identical in all modules. Axial variations are associated with the stacking of the units, with all units containing the 0.5-inch thick base plate. Figure 6.3.9-1 displays a side view of the intermediate module. A cross-section of the basket with fuel tubes numbered one through seven is shown in Figure 6.3.9-2. To simplify model construction, the six steel disks surrounding the tubes are not included in the model. They represent a minor amount of parasitic absorber outside the fuel region and, therefore, will have no significant effect on system reactivity. Figure 6.3.9-2 also includes a sketch of the two types of payload included in the cask. Note that the MOATA plate bundle side plates are modeled without chamfers, allowing additional space for the bundle to move within the tube and allowing a closer approach to adjoining plate bundles than feasible in the as-built assembly configuration. Assembly end-fittings are also not modeled, allowing a significantly closer approach of fuel material in the alternating shifted payload. Structural evaluations of the plate bundle have demonstrated that the as-built configuration of the bundle is maintained through all normal and accident conditions. Structural evaluations of the spiral fuel assembly demonstrate that the inner and outer shells will maintain their geometry. Since the fuel plates of the spiral assembly are locked into tabs attached to the shells, they will also retain their

configuration. To bound a possible reconfiguration of spiral assembly fuel plates within the annular regions, criticality evaluations are performed for variations in fuel locations beyond those feasible by assembly fabrication. Included in the fuel sketches are images of the spiral fuel assembly as-built and the model approximation of three annular fuel rings. A radial sketch of the cask cross-section is shown in Figure 6.3.9-3. The axial stack of baskets is identical to that of the DIDO baskets as shown in Figure 6.3.6-4, with differences limited to payload height. Reflecting boundary conditions on all sides simulate an infinite array of casks. This model neglects the impact limiters that would provide additional spacing between casks, and models the cask under accident conditions with the neutron shield voided.

6.3.9.2 Package Regional Densities

The composition densities (g/cc) and nuclide number densities (atm/b-cm) calculated by the SCALE material information processor for the nominal characteristic ANSTO payloads used in subsequent criticality analyses are shown in Table 6.3.9-2.

Figure 6.3.9-1 Intermediate ANSTO Basket Module

(Dimensions in inches)

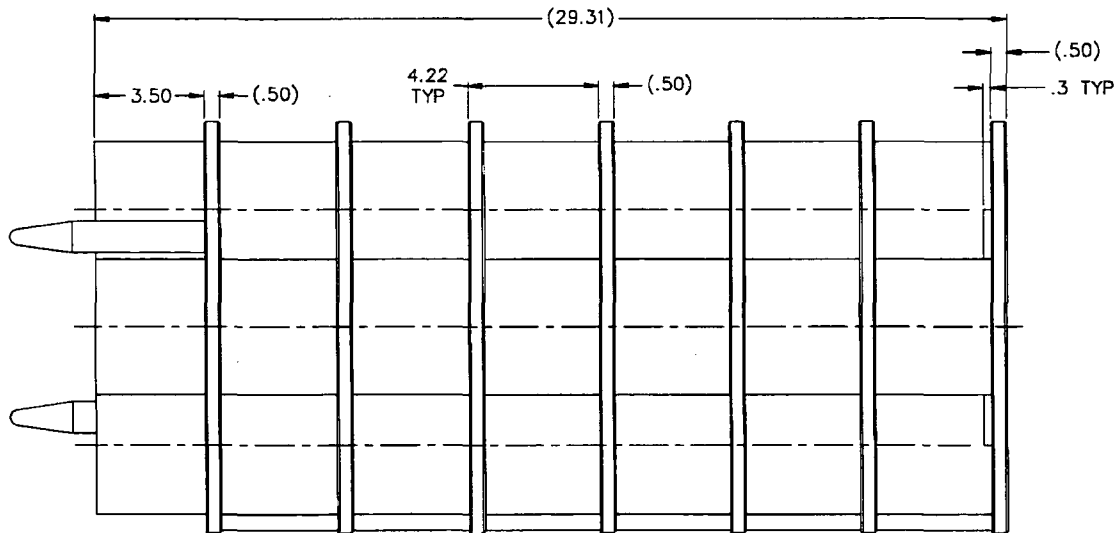
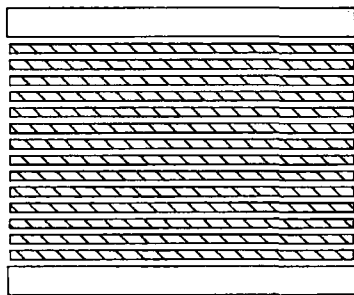
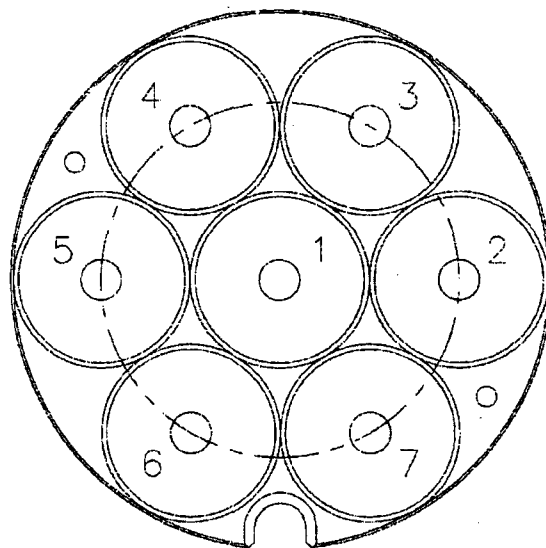


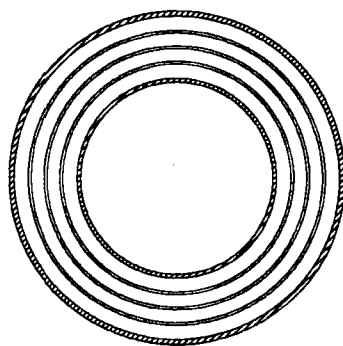
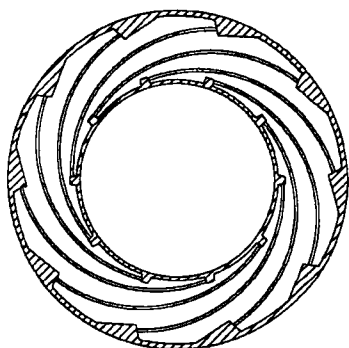
Figure 6.3.9-2 KENO-Va ANSTO Payloads and Basket Cross-Section



MOATA Plate Bundle Model



ANSTO Basket



Spiral Fuel Assembly Model

Figure 6.3.9-3 KENO-Va Model of NAC-LWT Cask Cross-Section with ANSTO Basket

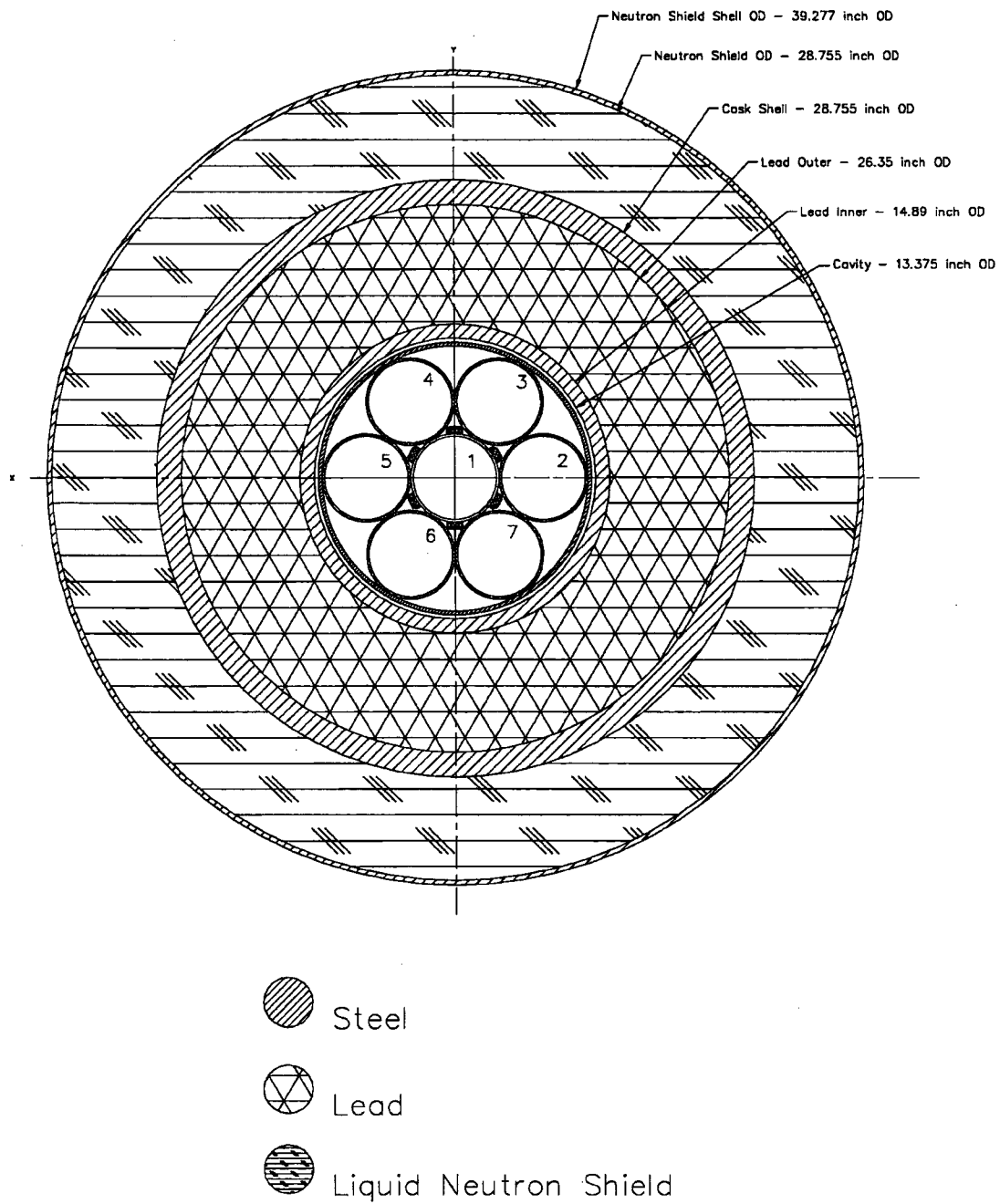


Table 6.3.9-1 ANSTO Basket and Cask Parameters

Description	Dimension [in]
Fuel tube outer diameter	4.375
Fuel tube wall thickness	0.125
Fuel tube outer diameter tolerance (maximum)	0.015
Fuel tube outer diameter tolerance (minimum)	0.025
Fuel tube thickness tolerance (maximum)	22%
Fuel tube thickness tolerance (minimum)	0%
Tube location angle (degrees)	60
Fuel basket outer diameter	13.265
Fuel basket base plate thickness	0.500
Fuel basket base plate thickness tolerance	0.020
Basket bottom plate hole size	1.000
Basket cavity height	28.81
Basket cavity height tolerance	0.060
Cask cavity diameter	13.375
Lead shield inner diameter	14.890
Lead shield outer diameter	26.350
Lead shield outer diameter of taper	24.880
Cask outer diameter	28.755
Cask lid thickness	11.250
Bottom forging thickness	10.500
Bottom forging lead insert diameter	20.750
Bottom forging lead insert thickness	3.000
Offset bottom of cask to lead	3.500
Neutron shield thickness	5.000
Neutron shield tank skin	0.236
Number of baskets per cask	6

Table 6.3.9-2 Composition Densities Used in Criticality Analysis of ANSTO Basket Payloads

Material	Sprial Assembly U-Al	MOATA Plate Bundles U-Al
Density, g/cc	U=0.847 Al=1.382	U=0.567, Al=2.517
Nuclide	Atoms/barn-cm	
Uranium 235	1.85E-03	1.34E-03
Uranium 238	3.21E-04	1.15E-04
Al	3.08E-02	5.62E-02

Material	Al Clad	H ₂ O	304 Stainless Steel	Pb	H ₂ O/ Glycol
Density, g/cc	2.702	0.998	7.920	11.350	0.9437
Nuclide	Atoms/barn-cm				
Aluminum	6.031E-2				
Oxygen		3.338E-2			2.459E-2
Hydrogen		6.675E-2			5.988E-2
Iron			5.936E-2		
Chromium			1.743E-2		
Nickel			7.721E-3		
Manganese			1.736E-3		
Lead				3.299E-2	
Carbon					1.070E-2

Note: Fuel material density and composition values are based on nominal fuel dimensions, mass and enrichment. Values used in the CSAS models vary due to tolerances applied to the fuel material specification and/or dimension.

6.4 Criticality Calculations

The criticality calculations for the contents to be transported in the NAC-LWT are described in Sections 6.4.1 through 6.4.10.

6.4.1 PWR Fuel Assemblies

This section presents the criticality analysis for the NAC-LWT cask with the PWR fuel assembly and basket configuration. Criticality analyses of this single assembly arrangement for the most limiting assembly type were performed to satisfy the criticality safety requirements of 10 CFR Parts 71.55 and 71.59 as well as IAEA Transportation Safety Standards (TS-R-1). In these analyses, the bounding PWR fuel assembly was determined for uranium enrichments of 3.7 and 3.5 wt % ^{235}U . Single casks loaded separately with the two design basis PWR fuel assemblies were studied for criticality under both normal and accident conditions. The reactivity effects associated with mechanical and geometric perturbations of the PWR fuel assembly and the basket opening are quantified. The analyses demonstrate that, including all calculational and mechanical uncertainties, the NAC-LWT cask remains subcritical under both normal and accident conditions for all PWR assemblies similar in construction and enrichment to those described herein.

6.4.1.1 Design Basis PWR Fuel Assembly

The k_{eff} values of a single NAC-LWT cask with the PWR fuel assemblies shown in Table 6.2.1-1 and Table 6.2.1-2 are given in Table 6.4.1-1. These results assume a uranium enrichment limit of 3.7 wt % ^{235}U and that full density water is present in the fuel clad gap. As seen in the table, the PWR assembly with the highest reactivity not exceeding 0.95 with uncertainties and bias per Section 6.4.1.6 was found to be the Exxon 15×15ANF WE assembly. Thus, this assembly was selected as the most limiting assembly for a uranium enrichment limit of 3.7 wt % ^{235}U . This assembly will serve as the basis to demonstrate that the CE 14×14, CE 16×16, Exxon 14×14 CE, Exxon 14×14 WE, Westinghouse 14×14, and the Westinghouse 14×14 OFA are sufficiently subcritical under both normal and accident conditions with an enrichment limit of 3.7 wt % ^{235}U .

The PWR fuel assemblies with k_s reactivities exceeding 0.95 were reanalyzed with a uranium enrichment limit of 3.5 wt % ^{235}U . The reactivities of a single NAC-LWT cask with these PWR assemblies and a uranium enrichment of 3.5 wt % ^{235}U are shown in Table 6.4.1-2. From this table it is shown that the reactivity of all re-analyzed assemblies were below the 0.95 limit and that the Westinghouse 17×17 OFA assembly is the most reactive. Consequently, this assembly was selected as the most limiting assembly for a uranium enrichment of 3.5 wt % ^{235}U . This fuel

assembly will serve as the basis to demonstrate that the B&W 15×15, B&W 17×17, Exxon 17×17 WE, Westinghouse 15×15, and the Westinghouse 17×17 assemblies are sufficiently subcritical under both normal and accident conditions with an enrichment limit of 3.5 wt % ²³⁵U.

6.4.1.2 PWR Fuel Perturbation Studies

The criticality evaluation for the NAC-LWT cask with the design basis PWR assemblies includes studying geometric tolerances and mechanical perturbations. The tolerances and perturbations are independently evaluated for the limiting PWR assemblies at uranium enrichments of 3.5 and 3.7 wt % ²³⁵U. The following perturbations and tolerances are analyzed:

I. Mechanical Perturbation

A. Fuel movement in the basket

II. Geometric Tolerances

A. Basket opening size

The geometric tolerance associated with the manufacture of the PWR basket is an opening tolerance of 8.88 ± 0.03 inches. Mechanical perturbations, i.e., fuel movement within the basket, arise from the gap between the assembly and the basket opening.

The effect of these tolerances and perturbations on the reactivity of the most limiting PWR fuel assemblies in the NAC-LWT cask is shown in the results presented in Table 6.4.1-3 and Table 6.4.1-4. Table 6.4.1-3 shows that there is one perturbed configuration with a larger reactivity than the nominal design configuration of the Westinghouse 17×17 OFA fuel assembly. However, the increase in reactivity was not statistically significant, i.e., less than 2σ . Thus, the nominal configuration, i.e. a centered assembly with nominal basket dimensions, of the Westinghouse 17×17 OFA PWR is the most reactive configuration of the most limiting PWR assembly for a uranium enrichment limit of 3.5 wt % ²³⁵U. This configuration serves as the design basis and is retained for subsequent moderator density variation studies.

For the Exxon 15×15 ANF WE fuel assembly, the effect of geometrical and mechanical perturbations is presented in Table 6.4.1-4. Analysis of the results reveals that the maximum basket opening causes a statistically significant increase, i.e., $>2\sigma$, on reactivity. This configuration serves as the design basis and is retained for subsequent normal and accident condition, moderator density variation studies at the 3.7 wt % enrichment limit.

6.4.1.3 Normal Condition Moderator Density Evaluations

Table 6.4.1-5 presents the cask k_{eff} for the most reactive normal condition configuration as a function of moderator density inside and outside a single cask for enrichment limits of 3.5 and 3.7 wt % ^{235}U . The results show an increase in reactivity with increasing internal moderator density. This indicates that moderator density changes due to increasing temperature have a negative reactivity effect. Low density moderation inside or outside of the cask does not produce abrupt increases in reactivity in comparison to other density values. The calculations show that k_{eff} does not vary significantly when varying external water with constant full density internal moderator. Because external water density does not affect reactivity within statistical limits, the most reactive case is chosen to be internal and external moderator density at 1.0 g/cc. The k_{eff} in this case for 3.5 and 3.7 wt % ^{235}U are 0.9279 ± 0.0014 and 0.9288 ± 0.0014 , respectively. The k_{eff} for the normal condition cask with a dry cavity is very subcritical, i.e., ~ 0.15 and is insensitive to external moderator density variations.

6.4.1.4 Accident Condition Moderator Density Evaluations

Table 6.4.1-6 shows the cask k_{eff} for the most reactive accident condition configuration as a function of moderator density variation in the cavity, neutron shield tank and outside a single cask for enrichment limits of 3.5 and 3.7 wt % ^{235}U . Again, the results show an increase in reactivity with increasing internal moderator density. Low density moderation inside or outside of the cask does not produce abrupt increases in reactivity in comparison to other density values. The calculations show that the k_{eff} for the accident condition with a dry cavity, neutron shield and exterior is very subcritical, i.e., ~ 0.16 . The most reactive case occurs with the moderator density at 1.0 g/cc in the cavity and the neutron shield tank as well as outside. The k_{eff} in this case for 3.5 and 3.7 wt % ^{235}U are 0.9325 ± 0.0013 and 0.9320 ± 0.0013 , respectively.

6.4.1.5 Single Package Evaluations

To satisfy 10 CFR 71.55(b)(3), an analysis of the reflection of the containment system (inner shell) by water is performed on a single wet cask. Successive replacement of the cask radial shields with water reflection is also evaluated. The results of this evaluation can be seen in Table 6.4.1-7 and Table 6.4.1-8. The reactivity of the system drops as each radial shield of the cask is replaced by water, $k_{\text{eff}} = 0.9251 \pm 0.013$ and $k_{\text{eff}} = 0.9295 \pm 0.0013$ for 3.5 and 3.7 wt % ^{235}U , respectively for the full cask surrounded by water to $k_{\text{eff}} = 0.8372 \pm 0.013$ and $k_{\text{eff}} = 0.8363 \pm 0.0014$ for 3.5 and 3.7 wt % ^{235}U , respectively, for the inner shell surrounded by water.

6.4.1.6 Conclusion

A calculation of k_s under normal and accident conditions can now be made based on the previous results and based on the KENO-Va validation statistics presented in Section 6.5.1 for low enriched uranium fuel. The value k_s is calculated based on the KENO-Va Monte Carlo average plus any biases and uncertainties associated with the methods and the modeling, i.e.:

$$k_s = k_{\text{eff}} + 2\sigma_{\text{mc}} + \Delta k_{\text{Bias}} + \Delta k_{\text{BU}}$$

In the validation presented in Section 6.5.1, a bias of 0.0052 (allowance for under prediction of k_{eff}) and a 95/95 method uncertainty of ± 0.0087 was determined. With this bias and uncertainty, the equation for k_s becomes:

$$k_s = k_{\text{eff}} + 2\sigma_{\text{mc}} + 0.0052 + 0.0087$$

Thus, $k_s = 0.9446$ and $k_s = 0.9455$ for 3.5 and 3.7 wt % ^{235}U , respectively, under normal conditions for a single NAC-LWT cask with a design basis PWR assembly, and a flooded basket cavity and exterior. Both are below the 0.95 regulatory limit. Under accident conditions, $k_s = 0.9490$ and $k_s = 0.9485$ for 3.5 and 3.7 wt % ^{235}U , respectively, for a single NAC-LWT cask with a design basis PWR assembly with a flooded basket cavity, neutron shield and exterior.

For both normal and accident conditions, the calculated k_{eff} values, after correction for biases and uncertainties, are below the 0.95 limit. The analyses demonstrate that, including all calculational and mechanical uncertainties, a single NAC-LWT cask with PWR fuel assemblies remains subcritical under normal and accident conditions.

Table 6.4.1-1 PWR Fuel Assembly at 3.7% Enrichment Most Reactive Assembly Results

PWR Fuel	k_{eff} (Dry Gap)	σ (Dry Gap)	k_{eff} (Wet Gap)	σ (Wet Gap)	k_s
W17×17 OFA	N/A	N/A	0.9428	0.0013	0.9593
W15×15	N/A	N/A	0.9407	0.0014	0.9574
B&W 15×15	N/A	N/A	0.9385	0.0014	0.9552
Ex17×17 WE	N/A	N/A	0.9381	0.0013	0.9546
B&W 17×17	N/A	N/A	0.9378	0.0014	0.9545
W17×17	N/A	N/A	0.9375	0.0013	0.9540
Ex15×15 WE	0.9246	0.0013	0.9321	0.0014	0.9488
CE16×16	0.9106	0.0013	0.9117	0.0014	0.9284
CE14×14	0.9059	0.0013	0.9103	0.0014	0.9270
Ex14×14 CE	0.9033	0.0014	0.9087	0.0013	0.9252
W14×14 OFA	0.8959	0.0014	0.9026	0.0014	0.9193
W14×14	0.8919	0.0014	0.9016	0.0013	0.9181
Ex14×14 WE	0.8805	0.0014	0.8944	0.0014	0.9111

Table 6.4.1-2 PWR Fuel Assembly at 3.5% Enrichment Most Reactive Assembly Results

PWR Fuel	k_{eff} (Dry Gap)	σ (Dry Gap)	k_{eff} (Wet Gap)	σ (Wet Gap)	k_s (Wet Gap)
W17×17 OFA	0.9279	0.0013	0.9326	0.0013	0.9491
B&W 17×17	0.9212	0.0013	0.9314	0.0013	0.9479
Ex17×17 WE	0.9248	0.0012	0.9309	0.0014	0.9476
W15×15	0.9235	0.0012	0.9303	0.0013	0.9468
W17×17	0.9208	0.0013	0.9284	0.0014	0.9451
B&W 15×15	0.9202	0.0013	0.9278	0.0014	0.9445

Table 6.4.1-3 Westinghouse 17×17 OFA Assembly Geometric Tolerances and Mechanical Perturbations Results

Configuration	k_{eff}	σ	$k_{eff} + 2\sigma$
Nominal Configuration	0.9326	0.0013	0.9352
Max. Basket Opening	0.9315	0.0013	0.9341
Min. Basket Opening	0.9342	0.0014	0.9370
Assembly on Side	0.9306	0.0014	0.9334
Assembly in Corner	0.9298	0.0014	0.9326

Table 6.4.1-4 Exxon 15×15 Geometric Tolerances and Mechanical Perturbations Results

Configuration	k_{eff}	σ	$k_{eff} + 2\sigma$
Nominal Configuration	0.9321	0.0014	0.9349
Max. Basket Opening	0.9353	0.0013	0.9379
Min. Basket Opening	0.9316	0.0014	0.9344
Assembly on Side	0.9294	0.0013	0.9320
Assembly in Corner	0.9286	0.0013	0.9312

Table 6.4.1-5 Reactivity with Design Basis PWR Fuel vs. Basket Moderator Density, Normal Conditions

Moderator Density	3.5% Enrichment	3.7% Enrichment
Dry Exterior, Vary Internal Density		
0.0000	0.1496 ± 0.0003	0.1561 ± 0.0003
0.0010	0.1502 ± 0.0003	0.1571 ± 0.0004
0.0100	0.1584 ± 0.0003	0.1656 ± 0.0004
0.0250	0.1733 ± 0.0004	0.1795 ± 0.0004
0.0500	0.1995 ± 0.0005	0.2069 ± 0.0005
0.0750	0.2292 ± 0.0005	0.2347 ± 0.0006
0.1000	0.2588 ± 0.0006	0.2645 ± 0.0006
0.2000	0.3822 ± 0.0009	0.3849 ± 0.0009
0.4000	0.5927 ± 0.0011	0.5926 ± 0.0011
0.6000	0.7417 ± 0.0014	0.7399 ± 0.0013
0.8000	0.8465 ± 0.0013	0.8492 ± 0.0015
0.9000	0.8923 ± 0.0013	0.8896 ± 0.0013
1.0000	0.9279 ± 0.0014	0.9288 ± 0.0014
Wet Interior, Vary External Density		
0.0000	0.9279 ± 0.0014	0.9288 ± 0.0014
0.0010	0.9295 ± 0.0013	0.9284 ± 0.0013
0.0100	0.9251 ± 0.0013	0.9266 ± 0.0013
0.0250	0.9292 ± 0.0013	0.9255 ± 0.0012
0.0500	0.9277 ± 0.0013	0.9297 ± 0.0014
0.0750	0.9284 ± 0.0013	0.9241 ± 0.0014
0.1000	0.9260 ± 0.0013	0.9248 ± 0.0013
0.2000	0.9247 ± 0.0014	0.9289 ± 0.0013
0.4000	0.9254 ± 0.0013	0.9268 ± 0.0013
0.6000	0.9265 ± 0.0013	0.9282 ± 0.0012
0.8000	0.9285 ± 0.0013	0.9271 ± 0.0013
0.9000	0.9266 ± 0.0014	0.9286 ± 0.0013
1.0000	0.9251 ± 0.0013	0.9244 ± 0.0012
Vary Interior and Exterior Density Simultaneously		
0.0000	0.1496 ± 0.0003	0.1561 ± 0.0003
0.0010	0.1508 ± 0.0004	0.1576 ± 0.0004
0.0100	0.1583 ± 0.0004	0.1644 ± 0.0004
0.0250	0.1737 ± 0.0004	0.1784 ± 0.0004
0.0500	0.2004 ± 0.0005	0.2062 ± 0.0005
0.0750	0.2293 ± 0.0006	0.2341 ± 0.0006
0.1000	0.2599 ± 0.0006	0.2637 ± 0.0006
0.2000	0.3834 ± 0.0009	0.3851 ± 0.0009
0.4000	0.5909 ± 0.0011	0.5942 ± 0.0011
0.6000	0.7398 ± 0.0012	0.7416 ± 0.0012
0.8000	0.8486 ± 0.0013	0.8487 ± 0.0014
0.9000	0.8886 ± 0.0014	0.8926 ± 0.0013
1.0000	0.9251 ± 0.0013	0.9244 ± 0.0012

Table 6.4.1-6 Reactivity with Design Basis PWR Fuel vs. Basket Moderator Density, Accident Conditions

Moderator Density	3.5% Enrichment	3.7% Enrichment
Dry Exterior, Vary Internal Density		
0.0000	0.1554± 0.0004	0.1637± 0.0004
0.0010	0.1561± 0.0004	0.1632± 0.0003
0.0100	0.1649± 0.0004	0.1737± 0.0004
0.0250	0.1808± 0.0004	0.1883± 0.0005
0.0500	0.2096± 0.0005	0.2159± 0.0005
0.0750	0.2390± 0.0006	0.2464± 0.0006
0.1000	0.2683± 0.0007	0.2767± 0.0007
0.2000	0.3928± 0.0009	0.3985± 0.0009
0.4000	0.5975± 0.0012	0.5995± 0.0012
0.6000	0.7462± 0.0012	0.7478± 0.0012
0.8000	0.8510± 0.0014	0.8535± 0.0014
0.9000	0.8936± 0.0012	0.8946± 0.0014
1.0000	0.9300± 0.0012	0.9296± 0.0014
Wet Interior, Vary External Density		
0.0000	0.9300± 0.0012	0.9296± 0.0014
0.0010	0.9283± 0.0014	0.9281± 0.0013
0.0100	0.9295± 0.0012	0.9303± 0.0013
0.0250	0.9304± 0.0014	0.9305± 0.0014
0.0500	0.9313± 0.0014	0.9330± 0.0013
0.0750	0.9291± 0.0013	0.9334± 0.0013
0.1000	0.9308± 0.0014	0.9326± 0.0013
0.2000	0.9303± 0.0013	0.9308± 0.0013
0.4000	0.9325± 0.0013	0.9319± 0.0013
0.6000	0.9310± 0.0013	0.9331± 0.0014
0.8000	0.9293± 0.0014	0.9317± 0.0013
0.9000	0.9303± 0.0013	0.9322± 0.0014
1.0000	0.9325± 0.0013	0.9320± 0.0013
Vary Interior and Exterior Density Simultaneously		
0.0000	0.1554± 0.0004	0.1637± 0.0004
0.0010	0.1566± 0.0004	0.1642± 0.0004
0.0100	0.1659± 0.0004	0.1740± 0.0004
0.0250	0.1826± 0.0004	0.1918± 0.0004
0.0500	0.2135± 0.0005	0.2220± 0.0006
0.0750	0.2450± 0.0006	0.2523± 0.0006
0.1000	0.2781± 0.0007	0.2840± 0.0006
0.2000	0.4035± 0.0010	0.4059± 0.0010
0.4000	0.6045± 0.0012	0.6071± 0.0012
0.6000	0.7518± 0.0012	0.7519± 0.0013
0.8000	0.8556± 0.0013	0.8572± 0.0013
0.9000	0.8988± 0.0013	0.8991± 0.0014
1.0000	0.9325± 0.0013	0.9335± 0.0013

Table 6.4.1-7 PWR Single Package 10 CFR 71.55(b)(3) Evaluation k_{eff} Summary for 3.5% Enrichment

Description	$k_{eff} \pm \sigma$	$k_{eff} + 2\sigma$
Single Cask / Inner Shell Reflected with H ₂ O	0.8372 ± 0.0013	0.8398
Single Cask / Inner Shell and Lead Reflected with H ₂ O	0.9165 ± 0.0013	0.9191
Single Cask / Inner Shell, Lead & Outer Shell Reflected with H ₂ O	0.9260 ± 0.0014	0.9288
Single Intact Cask Reflected with H ₂ O	0.9251 ± 0.0013	0.9277

Table 6.4.1-8 PWR Single Package 10 CFR 71.55(b)(3) Evaluation k_{eff} Summary for 3.7% Enrichment

Description	$k_{eff} \pm \sigma$	$k_{eff} + 2\sigma$
Single Cask / Inner Shell Reflected with H ₂ O	0.8363 ± 0.0014	0.8391
Single Cask / Inner Shell and Lead Reflected with H ₂ O	0.9184 ± 0.0014	0.9212
Single Cask / Inner Shell, Lead & Outer Shell Reflected with H ₂ O	0.9280 ± 0.0013	0.9306
Single Intact Cask Reflected with H ₂ O	0.9295 ± 0.0013	0.9321

6.4.2 BWR Fuel Assemblies

This section presents the criticality analyses for the NAC-LWT cask with the BWR assembly and basket configuration. Criticality analyses of the two assembly arrangement with the most limiting assembly type are performed to satisfy the criticality safety requirements of 10 CFR Parts 71.55 and 71.59 as well as IAEA Transportation Safety Standards (TS-R-1). In this analysis, the bounding BWR assembly type is determined, and an array of 20 NAC-LWT casks loaded with this design basis BWR assembly is studied for criticality under both normal and accident conditions. Spacing between the casks and moderator density in the cavity, neutron shield tank, and outside is varied to determine the maximum k_{eff} . The reactivity effects of mechanical and geometric perturbations on the assemblies and the basket are quantified. The analyses demonstrate that, including all calculational and mechanical uncertainties, the NAC-LWT remains subcritical under both normal and accident conditions for all BWR assemblies similar in construction to those described herein.

6.4.2.1 Design Basis BWR Fuel Assembly

The k_{eff} values for infinite arrays of BWR assemblies in the basket and cask are shown in Table 6.4.2-1. The arrays contain an infinite number of infinitely long, fully loaded BWR casks on a square pitch with surfaces touching. Conditions include water at 1 g/cc between the fuel rods and in the basket holes surrounding the assemblies. The neutron shield and cask exterior do not contain water. In addition, the results are reported for wet and dry clad gap configurations. As seen in the table, the Exxon 9×9 assembly with two water rods and an 80 mil channel (Ex 9×9-2/80) is more reactive than the other assembly types. Thus, the Ex 9×9-2/80 assembly is the most limiting, i.e., bounding, BWR assembly.

6.4.2.2 BWR Fuel Perturbation Studies

The criticality evaluation of the NAC-LWT cask with the basket loaded with design basis BWR assemblies includes studying geometric tolerances and mechanical perturbations. The tolerances and perturbations are independently evaluated for the most reactive BWR assembly, i.e., the Ex 9×9-2/80. The following perturbations and tolerances are analyzed:

I. Mechanical Perturbation

A. Fuel movement in the basket

II. Geometric Tolerances

A. Basket opening size

B. Basket divider plate thickness

The geometric tolerances associated with the manufacture of the BWR basket are listed in Table 6.4.2-2. Mechanical perturbations, i.e., fuel movement within the basket, arise from the gap between the fuel and the basket tube. The most reactive configuration analysis that evaluates these effects is performed for an infinite array of casks loaded with the design basis Ex 9×9-2/80 assembly and accident conditions with water at 1 g/cc modeled between the fuel rods, in the clad gap, and in the basket holes surrounding the assemblies. The neutron shield and cask exterior do not contain water.

The effect of these tolerances and perturbations on the reactivity of BWR assemblies in the BWR basket and NAC-LWT cask is shown in the results presented in Table 6.4.2-3. This table shows that the perturbations do not have a statistically significant, i.e. greater than 2σ , differential in k_{eff} than the nominal case. Thus, the most reactive configuration of BWR assemblies in the basket and cask is the nominal configuration with centered assemblies and nominal basket dimensions. This configuration with the Ex 9×9-2/80 assemblies is utilized in subsequent normal and accident condition moderator density variation analyses.

6.4.2.3 Normal Condition Moderator Density Evaluations

Table 6.4.2-4 presents the cask k_{eff} for the most reactive normal condition configuration as a function of moderator density inside and outside the cask. An array of 20 casks on a triangular pitch is modeled at three cask pitches: touching (99.7 cm), 2-foot surface-to-surface (160.7 cm), and ISO-container spacing (242.84 cm). Moderator density is varied from 1.0 g/cc to 0.0 g/cc and for normal conditions. In addition, it is assumed that the neutron shield is filled with water. The results show an increase in reactivity with increasing internal moderator density. This indicates that moderator density changes due to increasing temperature have a negative reactivity effect. Low density moderation inside or outside of the cask does not produce abrupt increases in reactivity in comparison to other density values. The calculations show that cask pitch has no significant impact on the reactivity of the cask array under normal conditions and that k_{eff} does not vary significantly when varying external moderator with constant full density internal moderator. Because external moderator does not affect reactivity within statistical limits, the most reactive case is chosen with both internal and external moderator density at 1.0 g/cc. The k_{eff} in this case is 0.8447 ± 0.0014 . The k_{eff} for the normal condition cask array with a dry cavity is very subcritical, i.e., ~ 0.15 and is insensitive to external moderator density variations.

6.4.2.4 Accident Condition Moderator Density Evaluations

Table 6.4.2-5 shows the cask k_{eff} for the most reactive accident condition configuration as a function of moderator density variation in the cavity, neutron shield tank and outside the cask. Again, three cask spacings are presented: touching (99.7 cm), 2-foot surface-to-surface (160.7 cm), and the ISO-container spacing (242.84 cm). Moderator density is varied from 1.0 g/cc to 0.0 g/cc. For accident conditions it is assumed that the neutron shield tank is punctured and that the moderator density in the tank is the same as the exterior moderator density. Again, the results show an increase in reactivity with increasing internal moderator density. Low density moderation inside or outside of the cask does not produce abrupt increases in reactivity in comparison to other density values. The calculations show that cask pitch does affect reactivity when the neutron shield is empty and that the k_{eff} for the accident condition cask array with a dry cavity, neutron shield and exterior is very subcritical, i.e., ~ 0.24 . The most reactive case occurs with casks touching and the moderator density at 1.0 g/cc in the cavity and at 0.0 g/cc in the neutron shield tank as well as exterior. The k_{eff} in this case is 0.9232 ± 0.0013 . Finally, this configuration has been modified to remove the channel. The resulting k_{eff} is 0.9292 ± 0.0012 .

6.4.2.5 Single Package Evaluations

To satisfy 10 CFR 71.55(b)(3), an analysis of the reflection of the containment system (inner shell) by water is performed on a single wet cask. Successive replacement of the cask radial shields with water reflection is also evaluated. The reactivity of the system drops as each radial shield of the cask is replaced by water, from a $k_{\text{eff}} = 0.8413 \pm 0.0014$ ($k_s = 0.8580$) for the full cask surrounded by water, to a $k_{\text{eff}} = 0.7411 \pm 0.0014$ ($k_s = 0.7578$) for the inner shell surrounded by water. The results of this evaluation can be seen in Table 6.4.2-6.

6.4.2.6 Conclusion

A calculation of k_s under normal and accident conditions can now be made based on the previous results and based on the KENO-Va validation statistics presented in Section 6.5.1 for low enriched uranium fuel. The value k_s is calculated based on the KENO-Va Monte Carlo average plus any biases and uncertainties associated with the methods and the modeling, i.e.:

$$k_s = k_{\text{eff}} + 2\sigma_{\text{mc}} + \Delta k_{\text{Bias}} + \Delta k_{\text{BU}}$$

In the validation presented in Section 6.5.1, a bias of 0.0052 (allowance for under prediction of k_{eff}) and a 95/95 method uncertainty of ± 0.0087 was determined. With this bias and uncertainty, the equation for k_s becomes:

$$k_s = k_{\text{eff}} + 2\sigma_{\text{mc}} + 0.0052 + 0.0087$$

Thus, $k_s = 0.8614$ under normal conditions for an array of 20 NAC-LWT casks fully loaded with BWR design basis fuel and a flooded basket cavity and exterior. This is below the 0.95 regulatory limit. Under accident conditions, $k_s = 0.9455$ for an array of 20 NAC-LWT casks fully loaded with BWR design basis fuel and with a flooded basket cavity and dry neutron shield and exterior.

For both normal and accident conditions, the calculated k_{eff} values, after correction for biases and uncertainties, are below the 0.95 limit. The analyses demonstrate that, including all calculational and mechanical uncertainties, an array of 20 NAC-LWT casks with BWR fuel remains subcritical under normal and accident conditions.

Table 6.4.2-1 BWR Most Reactive Assembly Analysis Results

Assembly Type	Number Rods		Channel Thickness	Dry Gap		Wet Gap	
	Fuel	Water		k_{eff}	σ	k_{eff}	σ
Exxon 9x9	79	2	80 Mil	0.9687	0.0013	0.9766	0.0013
Exxon 9x9	79	2	2mm	0.9711	0.0012	0.9728	0.0013
Exxon 9x9	74	2	2mm	0.9686	0.0013	0.9718	0.0012
GE 8x8	62	2	80 Mil	0.9651	0.0014	0.9711	0.0013
GE 8x8	62	2	100 Mil	0.9643	0.0013	0.9696	0.0013
GE 9x9	74	2	80 Mil	0.9636	0.0013	0.9686	0.0012
GE 7x7	49	0	80 Mil	0.9601	0.0012	0.9682	0.0013
Exxon 8x8 -2	62	2	80 Mil	0.9647	0.0013	0.9672	0.0013
GE 8x8	60	4	2mm	0.9613	0.0013	0.9669	0.0014
GE 9x9	79	2	2mm	0.9609	0.0014	0.9666	0.0012
Exxon 8x8 -1	63	1	80 Mil	0.9585	0.0012	0.9661	0.0013
GE 9x9	79	2	80 Mil	0.9604	0.0014	0.9657	0.0013
Exxon 7x7	49	0	80 Mil	0.9585	0.0013	0.9645	0.0012
GE 8x8	63	1	120 Mil	0.9557	0.0012	0.9641	0.0012
GE 8x8	63	1	100 Mil	0.9597	0.0013	0.9632	0.0012
GE 8x8	63	1	80 Mil	0.9616	0.0013	0.9631	0.0012

Table 6.4.2-2 BWR Basket Tolerances

Component	Dimension / Tolerance
Basket Diameter	13.25 in
Basket Opening	5.75 ± 0.02 in
1/8" Plate Thickness	0.125 / -0.0045 in

**Table 6.4.2-3 BWR Fuel Assembly Geometric Tolerances and Mechanical Perturbations
Results**

Configuration	k_{eff}	σ
Nominal Configuration	0.9746	0.0013
Assemblies Moved Out	0.9761	0.0013
Assemblies Moved in Close	0.9654	0.0013
Assemblies on Opposite Sides	0.9711	0.0013
Assemblies on Opposite Corners	0.9737	0.0012
Max. Basket Opening	0.9731	0.0013
Min. Basket Opening	0.9754	0.0013
Min. Basket Plate Thickness	0.9739	0.0013

Table 6.4.2-4 Reactivity with BWR Fuel vs. Basket Moderator Density, Normal Conditions, Array of 20 Casks

Moderator Density	Casks Touching	2 Foot Surf.-to-Surf.	ISO Container 242.84 cm Pitch
Dry Exterior, Vary Internal Density			
0.0000	0.1428 ± 0.0003	0.1425 ± 0.0003	0.1421 ± 0.0003
0.0010	0.1433 ± 0.0004	0.1435 ± 0.0003	0.1432 ± 0.0003
0.0100	0.1508 ± 0.0003	0.1506 ± 0.0004	0.1495 ± 0.0004
0.0250	0.1630 ± 0.0004	0.1632 ± 0.0004	0.1628 ± 0.0004
0.0500	0.1861 ± 0.0005	0.1857 ± 0.0005	0.1854 ± 0.0005
0.0750	0.2096 ± 0.0005	0.2107 ± 0.0005	0.2104 ± 0.0005
0.1000	0.2358 ± 0.0006	0.2359 ± 0.0006	0.2357 ± 0.0006
0.2000	0.3398 ± 0.0008	0.3413 ± 0.0008	0.3408 ± 0.0008
0.4000	0.5272 ± 0.0011	0.5248 ± 0.0011	0.5265 ± 0.0012
0.6000	0.6673 ± 0.0012	0.6673 ± 0.0013	0.6652 ± 0.0013
0.8000	0.7666 ± 0.0013	0.7685 ± 0.0012	0.7684 ± 0.0013
0.9000	0.8107 ± 0.0013	0.8095 ± 0.0013	0.8113 ± 0.0013
1.0000	0.8464 ± 0.0013	0.8412 ± 0.0012	0.8451 ± 0.0014
Wet Interior, Vary External Density			
0.0000	0.8449 ± 0.0013	0.8442 ± 0.0013	0.8441 ± 0.0013
0.0010	0.8441 ± 0.0013	0.8435 ± 0.0014	0.8438 ± 0.0013
0.0100	0.8423 ± 0.0014	0.8437 ± 0.0013	0.8437 ± 0.0013
0.0250	0.8447 ± 0.0014	0.8434 ± 0.0013	0.8429 ± 0.0013
0.0500	0.8438 ± 0.0014	0.8434 ± 0.0013	0.8436 ± 0.0013
0.0750	0.8446 ± 0.0014	0.8445 ± 0.0015	0.8439 ± 0.0014
0.1000	0.8441 ± 0.0014	0.8431 ± 0.0013	0.8429 ± 0.0012
0.2000	0.8437 ± 0.0014	0.8474 ± 0.0013	0.8434 ± 0.0014
0.4000	0.8445 ± 0.0014	0.8435 ± 0.0013	0.8444 ± 0.0014
0.6000	0.8444 ± 0.0013	0.8427 ± 0.0013	0.8437 ± 0.0013
0.8000	0.8457 ± 0.0013	0.8463 ± 0.0013	0.8439 ± 0.0014
0.9000	0.8429 ± 0.0013	0.8439 ± 0.0013	0.8447 ± 0.0012
1.0000	0.8447 ± 0.0014	0.8450 ± 0.0013	0.8447 ± 0.0012
Vary Interior and Exterior Density Simultaneously			
0.0000	0.1428 ± 0.0003	0.1425 ± 0.0003	0.1425 ± 0.0003
0.0010	0.1434 ± 0.0003	0.1431 ± 0.0003	0.1437 ± 0.0003
0.0100	0.1505 ± 0.0004	0.1502 ± 0.0004	0.1501 ± 0.0004
0.0250	0.1625 ± 0.0004	0.1631 ± 0.0004	0.1630 ± 0.0004
0.0500	0.1860 ± 0.0004	0.1856 ± 0.0005	0.1862 ± 0.0004
0.0750	0.2107 ± 0.0005	0.2100 ± 0.0005	0.2109 ± 0.0006
0.1000	0.2351 ± 0.0006	0.2354 ± 0.0006	0.2362 ± 0.0006
0.2000	0.3403 ± 0.0008	0.3402 ± 0.0008	0.3418 ± 0.0009
0.4000	0.5280 ± 0.0011	0.5271 ± 0.0010	0.5264 ± 0.0011
0.6000	0.6658 ± 0.0013	0.6641 ± 0.0013	0.6646 ± 0.0012
0.8000	0.7696 ± 0.0013	0.7681 ± 0.0014	0.7692 ± 0.0013
0.9000	0.8093 ± 0.0013	0.8090 ± 0.0013	0.8087 ± 0.0013
1.0000	0.8446 ± 0.0013	0.8433 ± 0.0014	0.8446 ± 0.0015

Table 6.4.2-5 Reactivity with BWR Fuel vs. Basket Moderator Density, Accident Conditions, Array of 20 Casks

Moderator Specific Gravity	Casks Touching	2 Foot Surface-to-Surface	ISO 242.84 cm Pitch
Dry Exterior, Vary Internal Density			
0.0000	0.2355 ± 0.0004	0.1849 ± 0.0004	0.1665 ± 0.0004
0.0010	0.2371 ± 0.0004	0.1854 ± 0.0004	0.1681 ± 0.0004
0.0100	0.2479 ± 0.0005	0.1940 ± 0.0004	0.1768 ± 0.0004
0.0250	0.2659 ± 0.0005	0.2105 ± 0.0005	0.1915 ± 0.0005
0.0500	0.2962 ± 0.0006	0.2387 ± 0.0006	0.2166 ± 0.0005
0.0750	0.3271 ± 0.0007	0.2677 ± 0.0006	0.2444 ± 0.0006
0.1000	0.3603 ± 0.0007	0.2970 ± 0.0006	0.2718 ± 0.0007
0.2000	0.4750 ± 0.0009	0.4096 ± 0.0009	0.3814 ± 0.0009
0.4000	0.6534 ± 0.0011	0.5911 ± 0.0011	0.5638 ± 0.0011
0.6000	0.7791 ± 0.0012	0.7212 ± 0.0013	0.6986 ± 0.0012
0.8000	0.8606 ± 0.0013	0.8151 ± 0.0013	0.7950 ± 0.0013
0.9000	0.8970 ± 0.0013	0.8519 ± 0.0014	0.8337 ± 0.0013
1.0000	0.9232 ± 0.0013	0.8822 ± 0.0014	0.8668 ± 0.0013
Wet Interior, Vary External Density			
0.0000	0.9200 ± 0.0012	0.8812 ± 0.0012	0.8678 ± 0.0013
0.0010	0.9220 ± 0.0012	0.8816 ± 0.0014	0.8622 ± 0.0014
0.0100	0.9060 ± 0.0013	0.8690 ± 0.0014	0.8564 ± 0.0014
0.0250	0.8869 ± 0.0013	0.8602 ± 0.0014	0.8491 ± 0.0014
0.0500	0.8719 ± 0.0014	0.8522 ± 0.0014	0.8511 ± 0.0013
0.0750	0.8653 ± 0.0013	0.8498 ± 0.0013	0.8509 ± 0.0012
0.1000	0.8604 ± 0.0014	0.8520 ± 0.0013	0.8506 ± 0.0014
0.2000	0.8513 ± 0.0013	0.8486 ± 0.0014	0.8506 ± 0.0012
0.4000	0.8501 ± 0.0013	0.8507 ± 0.0013	0.8501 ± 0.0013
0.6000	0.8512 ± 0.0013	0.8498 ± 0.0013	0.8512 ± 0.0014
0.8000	0.8494 ± 0.0013	0.8504 ± 0.0014	0.8501 ± 0.0013
0.9000	0.8498 ± 0.0013	0.8486 ± 0.0013	0.8515 ± 0.0013
1.0000	0.8528 ± 0.0014	0.8513 ± 0.0013	0.8500 ± 0.0013
Vary Interior and Exterior Density Simultaneously			
0.0000	0.2364 ± 0.0005	0.1841 ± 0.0004	0.1672 ± 0.0004
0.0010	0.2357 ± 0.0005	0.1855 ± 0.0004	0.1671 ± 0.0004
0.0100	0.2318 ± 0.0005	0.1856 ± 0.0004	0.1709 ± 0.0004
0.0250	0.2279 ± 0.0005	0.1895 ± 0.0004	0.1777 ± 0.0004
0.0500	0.2345 ± 0.0006	0.2051 ± 0.0005	0.1999 ± 0.0005
0.0750	0.2495 ± 0.0006	0.2284 ± 0.0006	0.2254 ± 0.0006
0.1000	0.2688 ± 0.0007	0.2541 ± 0.0007	0.2530 ± 0.0006
0.2000	0.3641 ± 0.0009	0.3563 ± 0.0008	0.3594 ± 0.0008
0.4000	0.5410 ± 0.0011	0.5400 ± 0.0011	0.5417 ± 0.0011
0.6000	0.6790 ± 0.0013	0.6759 ± 0.0013	0.6763 ± 0.0012
0.8000	0.7771 ± 0.0013	0.7756 ± 0.0013	0.7767 ± 0.0013
0.9000	0.8157 ± 0.0014	0.8152 ± 0.0013	0.8199 ± 0.0014
1.0000	0.8519 ± 0.0013	0.8495 ± 0.0013	0.8505 ± 0.0013

Table 6.4.2-6 BWR Single Package 10 CFR 71.55(b)(3) Evaluation k_{eff} Summary

Description	$k_{eff} \pm \sigma$	$k_{eff} + 2\sigma$
Single Cask / Inner Shell Reflected with H ₂ O	0.7411 ± 0.0014	0.7439
Single Cask / Inner Shell and Lead Reflected with H ₂ O	0.8331 ± 0.0013	0.8357
Single Cask / Inner Shell, Lead & Outer Shell Reflected with H ₂ O	0.8417 ± 0.0014	0.8445
Single Intact Cask Reflected with H ₂ O	0.8413 ± 0.0014	0.8441

6.4.3 MTR Fuel Elements

This section presents the criticality analyses for the NAC-LWT with the MTR fuel element and basket configuration. Criticality analyses of the seven element arrangement with the most limiting assembly type are performed with the SCALE 4.3 CSAS sequence to satisfy the criticality safety requirements of 10 CFR Parts 71.55 and 71.59 as well as IAEA Transportation Safety Standards (TS-R-1). In this analysis, the bounding MTR fuel element type is determined, and an infinite array of NAC-LWT casks loaded with this design basis MTR fuel is studied for criticality under normal and accident conditions. Spacing between the casks and moderator density in the cavity, neutron shield tank and outside is varied to determine the maximum k_{eff} . The reactivity effects of partial basket loading, loss of fuel integrity and mechanical and geometric perturbations of the fuel elements and basket plate material are quantified. The analyses demonstrate that, including all calculational and mechanical uncertainties, the NAC-LWT remains subcritical under normal and accident conditions for all MTR fuel elements that are bounded in enrichment and fissile uranium loading by the design basis assembly.

6.4.3.1 Design Basis MTR Fuel Element

The fuel/basket unit cell k_{eff} values for the HEU and LEU MTR element types are shown in Table 6.4.3-1. The results show that the HEU ORR #2, HEU HFBR and the LEU BSR fuel elements are significantly more reactive than the other element types. In addition, these three element types have the highest fissile loadings, as listed in Table 6.2.3-1 and Table 6.2.3-2. Furthermore, a study of the reactivity of the highest fissile uranium loading HEU (HFBR) and LEU (BSR) elements as a function of the spacing between fuel plates is performed, as shown in Table 6.4.3-2. As shown, the HFBR fuel element is the most reactive when the plates are free to expand to their maximum possible pitch with the basket opening, as is postulated to occur under accident conditions. Also, it is shown that the HFBR element is most reactive with its full load of 18 fuel plates. The greater spacing allowed by fewer fuel plates is shown to be less reactive. Because of this and the minor difference between the other fuel types for intact elements, the HFBR element is chosen as the design basis for further analyses.

6.4.3.2 MTR Fuel Perturbation Studies

The criticality evaluation of the NAC-LWT cask with the baskets fully loaded with design basis HFBR MTR fuel elements includes studying geometric tolerances, mechanical perturbations, moderator (H_2O) density variation and spacing variation between casks. Moderator density is varied from 1.0 g/cc to 0.0 g/cc. Cask center-to-center spacing is varied from touching (99.7 cm

cask pitch) to ISO-container array spacing (242.84 cm cask pitch). Under normal conditions it is assumed that the neutron shield is filled with water and the fuel element plate spacing is intact. Under accident conditions it is assumed that the fuel element plate spacing is at its most reactive within each basket opening, the neutron shield tank is punctured, and that the moderator density in the tank is the same as the exterior moderator density.

As shown in Table 6.4.3-2, k_{eff} varies significantly with plate spacing. This is because the intact HFBR fuel element is undermoderated. The largest possible pitch of the HFBR fuel plates within the MTR basket, 0.4572 cm, yields the greatest k_{eff} . Hypothetical accident condition analyses utilize fuel plates with this pitch spacing.

Geometric tolerances and mechanical perturbations are independently evaluated for intact HFBR elements during normal conditions, and optimally spaced HFBR fuel plates during accident conditions. The following perturbations and tolerances are analyzed:

I. Mechanical Perturbation

A. Fuel movement in the basket

II. Geometric Tolerances

A. Basket opening size

B. Basket steel plate thickness

The geometric tolerances associated with the manufacture of the MTR basket are listed in Table 6.4.3-3. Mechanical perturbations, i.e., fuel movement within the basket, arise from the gap between the MTR fuel and the basket tube.

The effect of these tolerances and perturbations on the reactivity of intact elements in the MTR basket and NAC-LWT cask is shown in the results presented in Table 6.4.3-4. This table shows there are three perturbations that have a higher k_{eff} than the nominal case. Two of these cases, "elements moved in close" and "elements moved in closest," are mechanical perturbations. These perturbations correspond to moving the outer elements toward the center element first on one axis and then on two axes, i.e., the top and bottom two elements are first moved down and up, respectively and then moved into the corners nearest to the center of the basket. The complementary configurations are labeled "elements moved out" and "elements moved out farthest," i.e., the top and bottom two elements are first moved up and down, respectively, and then moved into the corners farthest from the center of the basket. Since only one of these mechanical perturbations can occur at a time, the configuration with the greatest reactivity, "elements moved in close" is selected as a significant perturbation. The third case, "basket plate minimum thickness," is a geometric perturbation and is also selected as a significant

Revision 38

perturbation. The most reactive configuration of intact elements includes the impact of fuel movement, with the elements moved in close, and the impact of geometric tolerances, by using the minimum basket plate thickness. This configuration is utilized in the subsequent normal condition moderator density variation analyses.

The results of the mechanical and geometric perturbations for the optimally spaced fuel plates are shown in Table 6.4.3-5. This table shows that there are two perturbations that have a higher k_{eff} than the nominal case. The “minimum basket plate thickness” configuration is a geometric perturbation and the “plates moved in” configuration is a mechanical perturbation. Because the expanded plates cannot move in the vertical direction, the “plates moved in” configuration corresponds to moving the plate bundles on the horizontal axis towards the basket centerline. Conversely, the less reactive “plates moved out” configuration corresponds to moving the plate bundles away from the centerline. The most reactive configuration of optimally spaced fuel plates includes the impact of fuel movement, with the plates moved in, and the impact of geometric tolerances, by using the minimum basket plate thickness. This configuration is utilized in the subsequent hypothetical accident condition moderator density variation analyses. It should be noted that the maximum basket opening perturbation results do not exceed the nominal case by a statistically significant margin and is, therefore, not considered a part of the most reactive configuration.

6.4.3.3 MTR Fuel Moderator Density Criticality Evaluations for Normal Conditions

Table 6.4.3-6 presents the cask k_{eff} for the most reactive normal condition configuration as a function of moderator density inside and outside the cask. An infinite array of casks is modeled at three cask pitches: touching (99.7 cm), 2-foot surface-to-surface (160.7 cm), and ISO-container spacing (242.84 cm). The results show a monotonic increase in reactivity with increasing internal moderator density. This indicates that moderator density changes due to increasing temperature have a negative reactivity effect. Low density moderation inside or outside of the cask does not produce abrupt increases in reactivity in comparison to other density values. The calculations show that cask pitch has no significant impact on the reactivity of the cask array under normal conditions and that k_{eff} does not vary significantly when varying external moderator with constant full density internal moderator. Because external moderator does not affect reactivity within statistical limits, the most reactive case is chosen with both internal and external moderator density at 1.0 g/cc. The k_{eff} in this case is 0.8107 ± 0.0024 . The k_{eff} for the normal condition cask array with a dry cavity is very subcritical, i.e., ~ 0.07 and is insensitive to external moderator density variations.

The effect of partial basket loading on cask k_{eff} under normal conditions is investigated to determine if increased moderation might offset the loss of fuel loading. In this model, the central basket location is empty and filled with water instead of fuel. Also, the outer fuel elements are moved closer to the center. Moderator density is varied from 1.0 g/cc to 0.01 g/cc. The results are shown in the last column of Table 6.4.3-6. These results show the same basic increase in reactivity with increasing moderator density, and a level of k_{eff} consistently below that calculated for the fully loaded basket cases.

6.4.3.4 MTR Fuel Moderator Density Criticality Evaluations for Accident Conditions

Table 6.4.3-7 shows the cask k_{eff} for the most reactive accident condition configuration as a function of moderator density variation in the cavity, neutron shield tank and outside the cask. Again, three cask spacings are presented: touching (99.7 cm), 2-foot surface-to-surface (160.7 cm), and the ISO-container spacing (242.84 cm). Again, the results show a monotonic increase in reactivity with increasing internal moderator density. Low density moderation inside or outside of the cask does not produce abrupt increases in reactivity in comparison to other density values. The calculations show that cask pitch and exterior moderator density variation does significantly affect reactivity when the neutron shield is empty and that the k_{eff} for the accident condition cask array with a dry cavity, neutron shield and exterior is very subcritical, i.e., ~ 0.31 . The most reactive case occurs with casks touching and the moderator density at 1.0 g/cc in the cavity and at 0.0 g/cc in the neutron shield tank as well as outside. The k_{eff} in this case is 0.9005 ± 0.0021 . To address the potential for slightly higher enrichments and fissile uranium loadings, this most reactive case has been analyzed with 94 wt % ^{235}U enrichment and 355 grams ^{235}U per element. The resulting k_{eff} is 0.9021 ± 0.0020 .

6.4.3.5 Element Rotation

No controls are placed on the orientation, i.e., plate direction, of MTR elements within a basket opening. Thus, different orientations of MTR elements in the fuel basket are possible. To model this situation, unit cells from the HFBR unit cell analysis are stacked in a 3×3 array. The elements are arranged in several combinations with vacuum boundary conditions. It can be seen in Table 6.4.3-8 that the differences in reactivity of the different orientations are not statistically significant. Therefore, using a single element orientation in the analysis of MTR fuel is sufficient to model all permutations of element orientation.

6.4.3.6 Center Fuel Element Perturbation

The most reactive configurations of intact elements and expanded plates was developed with a nominally positioned, i.e., centered, central element or plate. To verify that these are the most reactive configurations, perturbations of the central component's position have been performed. The results are contained in Table 6.4.3-9. As seen in the table, the reactivity of the perturbations under normal conditions (intact fuel elements) do not vary by a statistically significant margin. Under accident conditions (optimum spaced plates), moving the central element decreases reactivity. Therefore, it is reasonable to utilize a centered central fuel element for the criticality evaluations.

6.4.3.7 Mixing HEU and LEU MTR Fuel

LEU and HEU fuel elements may be mixed within an MTR basket module. To model this situation, the unit cell models for HFBR and RSG-GAS fuel elements are stacked in a 3×3 array in a KENO-Va model. The RSG-GAS fuel element is selected because, as shown in Table 6.4.3-1

Table 6.4.3-1 has a relatively high reactivity, but the reactivity is sufficiently lower than the HEU to allow the impact of mixing HEU and LEU elements within the model to be more readily apparent. The fuels are arranged in several combinations within the array with vacuum boundary conditions. It can be seen in Table 6.4.3-10 that the reactivities of the different combinations of the HEU and LEU fuel elements within the model show a trend for lower reactivity with increasing number of LEU fuel elements within the model. Therefore, the mixing of HEU and LEU MTR fuels is bounded by the analysis of HFBR MTR fuel.

6.4.3.8 Uranium Weight Fraction in Fuel Meat

MTR fuel "meat" material is composed of a mixture of the uranium metal, or uranium oxide/silicide, with an aluminum alloying material. The design basis fuel parameters listed in Table 6.2.3-1 and Table 6.2.3-2 include the weight fraction of uranium in the fuel meat. This fraction may vary from the nominal values presented in the tables due to the manufacturing process for the fuel material. Based on the limiting maximum uranium quantities specified for the fuel and the fuel meat volume, the quantity and density of the aluminum in the meat may be calculated. The aluminum densities in the sheet are typically greater than 90% of aluminum's natural density of 2.7 g/cm³. Since the MTR fuel plates are manufactured from a combination of U-metal, U₃O₈, or U₃Si₂ and aluminum, some variations in the nominal uranium weight fraction reported in Table 6.2.3-1 and Table 6.2.3-2 are expected. A sensitivity study is, therefore,

performed on the uranium weight fraction of five types of MTR fuel elements chosen for their bounding configuration (i.e., HEU thin, medium, and thick fuel meat thickness, and LEU thin and thick fuel meat thickness). Because each MTR fuel element type contains effective aluminum densities within 10% of theoretical, the evaluations concentrate on the reactivity effect of reducing the aluminum weight percent while utilizing a fixed maximum uranium mass and enrichment for each fuel element type. This serves to vary the uranium weight fraction in the fuel meat, while maintaining the uranium mass in the fuel element at its fixed maximum value. For a given uranium mass and fuel meat volume, it is expected that reducing the mass of aluminum in the fuel meat volume would serve to increase reactivity by reducing potential neutron absorbers from the system.

The perturbation study of the aluminum weight fraction on reactivity was performed with the infinite lattice cell model used to establish the bounding fuel types as described in Section 6.4.3.1. As shown in Table 6.4.3-12, the reactivity of the system is relatively unaffected by an decrease in the uranium weight percent. For the bounding reactivity MTR fuel element (HFBR), a 50% reduction in aluminum density resulted in an increase in reactivity of less than $0.005 \Delta k$. This compares to a reactivity margin of 0.025 below 0.95 for the highest reactivity MTR fuel element as reported in Section 6.4.3.10. All cases studied resulted in reactivity increases of less than $0.02 \Delta k$, as reported in Table 6.4.3-12. The maximum reactivity increases occurred for the PRR and THOR MTR fuel element designs, which considered aluminum weight fraction reductions of as much as one-third that of the nominal fuel meat. Both the PRR and THOR fuel element designs have reactivities significantly below that of the design basis HFBR fuel element and do not exceed the reactivity of the HFBR element even at the low aluminum densities. Therefore it is concluded that for a fixed uranium mass in the fuel meat, the aluminum weight fraction does not have a significant effect on the bounding reactivity of the MTR fuel elements in the NAC-LWT.

6.4.3.9 Single Package Criticality Evaluation

To satisfy 10 CFR 71.55(b)(3), an analysis of the reflection of the containment system (inner shell) by water is performed on a single wet cask. Successive replacement of the cask radial shields with water reflection is also evaluated (Table 6.4.3-11). The reactivity of the system drops as each radial shield of the cask is replaced by water, from a $k_{\text{eff}} = 0.8094 \pm 0.0021$ ($k_s = 0.8317$) for the full cask surrounded by water, to a $k_{\text{eff}} = 0.7682 \pm 0.0021$ ($k_s = 0.7905$) for the inner shell surrounded by water.

6.4.3.10 MTR Loose Fuel Plate Evaluation

Loose MTR fuel plates may be shipped inside the NAC-LWT using an MTR plate canister. The canister consists of four rectangular aluminum side plates, and top and bottom lids, forming a 2.82 inch by 2.95 inch opening. Two parallel side plates are 0.25 inch (0.635 cm) thick with the remaining two side plates at 0.125-inch (0.3175 cm) thickness. The loose plates are inserted into the canister, which in turn is placed into one of the seven MTR basket openings. The number of fuel plates in each canister is restricted to those of an intact MTR fuel element. By restricting the number of plates to those of an intact fuel element, the criticality evaluation considering optimum pitch of the expanded MTR element, shown in Section 6.4.3.1 and Table 6.4.3-2, is applicable.

While intact, the MTR plate canister restricts the loose fuel plate pitch to a significantly smaller envelope than the basket opening (3.44 inch) employed in the evaluation shown in Table 6.4.3-2. Since the evaluation results in Table 6.4.3-2 indicate an increase in reactivity up to the maximum fuel plate pitch possible in the basket opening, the reactivity of the MTR plate canister configuration will be significantly lower than that of the uncanistered payload.

Also considered for criticality analysis is a loose plate canister configuration in which the canister plate separates. This configuration is bounded by the accident evaluation of MTR fuel plates where the two MTR element side plates separate from the fuel plates. The accident evaluation of MTR plates is the highest reactivity case for MTR fuel and models the maximum fuel plate pitch obtainable in an MTR basket cell. The additional two canister plates running parallel to the fuel plates restrict the maximum plate pitch possible in the canister opening. The reduced pitch reduces the reactivity of the system.

6.4.3.11 Code Bias and Code Bias Uncertainty Adjustments

A calculation of k_s under normal and accident conditions can now be made based on the previous results and based on the SCALE 4.3 CSAS sequence KENO-Va validation statistics presented in Section 6.5.2 for high enriched uranium fuel. The value k_s is calculated based on the KENO-Va Monte Carlo average plus any biases and uncertainties associated with the methods and the modeling, i.e.:

$$k_s = k_{eff} + \Delta k_{Bias} + \Delta k_{BU} + 2\sigma_{MC} \leq 0.95$$

In the validation presented in Section 6.5.2, a bias of -0.0044 (allowance for overprediction of k_{eff}) and a 95/95 method uncertainty of ± 0.0181 was determined. For added conservatism, the -0.0044 bias correction is neglected. With these biases and uncertainties, the equation for k_s becomes:

$$k_s = k_{eff} + 0.0181 + 2\sigma_{MC}$$

Thus, $k_s = 0.8336$ under normal conditions for an infinite array of NAC-LWT casks with a full load of HFBR design basis fuel elements, and a flooded basket cavity and exterior. Both are below the 0.95 regulatory limit. Under accident conditions, $k_s = 0.9242$ for an infinite array of NAC-LWT casks with a full load of 94 wt % / 355 g ^{235}U per element HFBR fuel with plates expanded to their maximum pitch within the basket, and with a flooded basket cavity and dry neutron shield and exterior.

For both normal and accident conditions, the calculated k_{eff} values, after correction for biases and uncertainties, are well below the 0.95 limit. The analyses demonstrate that, including all calculational and mechanical uncertainties, an infinite array of NAC-LWT casks with MTR fuel remains subcritical under normal and accident conditions.

6.4.3.12 Bounding Physical Characteristics for MTR Fuel Elements

The purpose of this section is to document an extended licensing envelope for the NAC-LWT cask. This is accomplished by constructing and evaluating an MTR element with a set of physical characteristics bounding the fuel inventory previously documented, with margin for manufacturing tolerance and expected variations in nominal element characteristics. Since this composite fuel element is expected to significantly increase the maximum reactivity of the NAC-LWT MTR configuration, a finite cask model is constructed. The existing evaluations employed an infinite element length model, which by its nature, contained a significant conservative margin that will be required to maximize the MTR payload fissile material quantities.

To establish bounding fuel element criteria, the analysis trends in Sections 6.4.3.1 through 6.4.3.10 are reviewed. Where necessary, additional analysis is performed to establish reactivity trends on the physical parameters of the elements.

Sections 6.4.3.1 through 6.4.3.4 demonstrate that MTR elements in their intact configuration are undermoderated, and that increased reactivity is achieved by maximizing plate pitch and total fissile material mass. The evaluations also showed that the maximum reactivity basket configuration for the loose fuel plates is obtained by modeling minimum basket plate thickness and fuel plates moved toward the basket center. Fuel element rotation and shifting of the center fuel element in the basket opening have been shown not to impact reactivity of the system significantly. Section 6.4.8 documents the impact of varying the uranium weight fraction at a fixed fissile mass. As the uranium weight fraction increases and the aluminum mass decreases, the system reactivity increases.

To support the addition of MEU fuel elements to the allowable content description, an infinite array of MEU elements was evaluated in the infinite basket cell model. The results of this evaluation, shown in Table 6.4.3-13, show that increasing the ^{235}U enrichment at a fixed fissile mass raises system reactivity. Table 6.4.3-14 demonstrates that the MEU element evaluated ($k_{\text{eff}} = 0.8312$) is lower in reactivity than the HFBR design basis element in the intact configuration ($k_{\text{eff}} = 0.8471$). When evaluating the MEU element in the axially infinite basket model, containing 7 elements inside the radial shields, a maximum reactivity was obtained by maximizing plate pitch (see Table 6.4.3-14). This is consistent with the HEU and LEU evaluations shown in previous sections. The MEU evaluation also demonstrated that moving fuel plates against the basket plates (Configuration B) for a maximum pitch increases reactivity over the configuration with fuel plates separated from the basket plates by a water gap.

Reactivity trends as a function of plate pitch, fuel meat thickness, and fuel plate thickness were obtained from an infinite basket cell model containing McMaster HEU MTR elements. Physical characteristics of the McMaster HEU fuels are provided in Table 6.4.3-15. The McMaster fuel evaluation results shown in Table 6.4.3-16 and Table 6.4.3-17 document that maximizing plate pitch, decreasing plate thickness, and increasing plate fuel meat thickness produce increases in reactivity. The evaluation also showed increases in reactivity as the result of maximizing the active fuel width.

Based on the above listed trends, the following fuel plate characteristics result in a maximum reactivity configuration.

1. Minimum clad thickness (implies maximum fuel thickness for a given plate thickness)
2. Minimum plate thickness
3. Maximum active fuel width
4. Maximum fuel mass
5. Maximum enrichment (reduces parasitic absorption in ^{238}U)
6. Minimum side plate width/length (increases moderator volume in basket cell)
7. Maximum fissile material density (at a fixed geometry, increasing fissile material mass will increase reactivity)
8. Reducing the number of fuel plates at a fixed fissile material mass per plate decreases reactivity (i.e., the increase in reactivity produced by raising the H/U ratio is offset by the decrease in fissile mass)

No trend to active fuel height is available from previous evaluations. Larger active fuel heights increase reactivity due to improved fuel to moderator ratios, but also lead to separating of the fissile material masses in the finite height basket models. The impact of active fuel height variations is, therefore, evaluated later in this section. To apply the above characteristics to the

MTR elements listed in Section 6.2, a set of hybrid bounding element definitions is as shown in Table 6.4.3-18. Limits are established for HEU and LEU elements. MEU element characteristics are enveloped by the HEU fuel characteristics. Various modifications of the listed parameters are addressed in later sections of this evaluation. Modifications to the parameters are made to demonstrate that the listed value is either bounding or provides a maximum licensing envelope value. Little information is available on the tolerances associated with the fuel element parameters; therefore, the larger the envelope, the more likely that any given element will fall within the licensing basis.

Based on the information listed in Table 6.4.3-17 and the analysis trends discussed above, an initial data set with margins in the parameters for tolerances and normal variations in element characteristics is compiled for 94 wt % ^{235}U enriched fuel. The resulting data set is shown in Table 6.4.3-19. The listed data does not represent a bounding configuration for all fuel types, but does represent a starting configuration from which bounding limits for the various fuel types may be determined. The bounding configurations may contain combinations of lower fissile mass per plate, lower enrichment, varying active fuel width or height, a lower number of fuel plates or reduced enrichment. The fuel plate pitch is determined by spacing the plates to the maximum extent, with the outer fuel plates resting on the basket plates. The resulting basket model serves as the basis for all remaining evaluations.

Results for all MTR criticality evaluations performed in this calculation package are listed in Table 6.4.3-20 and have been divided into matrix cases A through I. Each set (or individual case for certain evaluations) is designed to investigate a potential perturbation of the system or to provide a new group of limiting cask parameters.

Based on the results of analysis documented in Sets A through I, the NAC-LWT MTR cask containing up to 42 elements remains within the subcritical margin ($k_s \leq 0.95$) under the conditions listed in Table 6.4.3-21. Note that the further evaluations documented in Sections 6.4.3.13 and 6.4.3.14 provide additional allowed configurations for MTR fuel elements loaded into the NAC-LWT.

Sets A and B

Set A cases determine the most reactive placement of the fuel plates axially within the basket openings. As shown, the maximum reactivity is obtained by shifting plates toward the adjoining basket (i.e., three groups of two baskets). Set B employs the most reactive shifted scenario and varies the active fuel height. While the fuel plates are undermoderated, increasing the active fuel height serves to separate fissile material in the two baskets. As shown in the result table, the effect of separating the fissile material dominates the undermoderated state of the plates

Revision 38

themselves and results in the minimum height model (56 cm) being bounding. Differences in reactivity for both sets of cases (Δk_{eff}) are taken from the 56 cm active fuel height shifted model.

Sets C, D and E

As shown in the Set B evaluation, the maximum bias adjusted reactivity of the NAC-LWT with the MTR containing 20 g ^{235}U per plate is significantly above the 0.95 limit. Set C, therefore, performs a fissile material study to determine the maximum amount of ^{235}U that may be placed in each plate. To remain below a k_s of 0.95, the plates are limited to 18 g ^{235}U each. Evaluating the fuel at a lower enrichment (50 wt % ^{235}U) shows that the HEU (94 wt % ^{235}U) is bounding. To demonstrate that a lower number of plates in the cask is less reactive at the 18 g ^{235}U limit, Set D evaluates a reduced number of plates at maximum (optimal) pitch. Reactivity for these cases is significantly lower than that of the 23-plate case. Set E evaluates various perturbations to the input parameters of the model to demonstrate that the given input is bounding. As shown, there is no significant impact of uranium weight percent changes, modeling an aluminum extension to the width of the fuel plate, or shifting of the aluminum side plates within the plane of the basket. Reactivity decreases with a decreasing plate pitch, an extension of the element length by unfueled plate or end fitting, or changes to the plate thickness by either increasing the fuel core material thickness or the clad thickness. Reactivity increases by decreasing the element side plate thickness, and decreases significantly when inserting two additional aluminum plates approximating the configuration with a loose fuel plate canister inserted into the model. Differences in reactivity (Δk_{eff}) for set C, D, and E are taken from the 56 cm active fuel height shifted model with 18 g ^{235}U .

Set F

Not all MTR fuel plates contain less than 18 g ^{235}U . The HFBR fuel, in particular, contains up to 19.5 g ^{235}U per plate but is limited to 18 fuel plates. An analysis is therefore performed with a bounding 19 plate and 20 g ^{235}U per plate model. The k_s for this system is below 0.95.

Set G

A limited quantity of MTR plates exist with an active fuel width greater than the 6.6 cm evaluated. Therefore, additional analysis is performed at a 7.3 cm active fuel width. Based on the evaluation of an 18 g ^{235}U per plate model, the reactivity of this system is significantly higher than that of the 6.6 cm width case. Therefore, fissile quantity per plate is restricted to 16.5 g ^{235}U .

Set H

Low enriched uranium fuel (LEU) can reach a per plate loading up to 21 g ^{235}U . Therefore, evaluations at 7.3 cm and 6.6 cm active fuel width are performed with 23 plates at 22 g of LEU material (maximum 25 wt % ^{235}U). The 7.3 cm active fuel width resulted in a reactivity higher than the allowed limit. The 22 g ^{235}U plates of LEU material are, therefore, restricted to a maximum active fuel width of 6.6 cm.

Set I

NISTR fuel presents an exception to the standard MTR fuel element, since each plate has two fuel sections that are separated by a short section of non fuel-bearing aluminum. These plates may be cut at the aluminum strip, with both sections inserted into a basket opening. This evaluation demonstrates that both an intact and cut element would remain below the licensing limits at 22 grams per plate.

6.4.3.13 MTR Fuel Elements with High Fissile Material Loading

This section determines the requirements for loading a high fissile material content MTR fuel element with up to 20 g ^{235}U per plate (460 g ^{235}U per element based on 23 plates). Section 6.4.3.12 has demonstrated that the HEU fuel is more reactive than LEU and MEU fuel. Therefore, only the HEU fuel is evaluated in this section. Additional evaluations are provided with the limiting characteristics of an HEU MTR element containing up to 21 g ^{235}U per plate.

The models employed are similar to those of Section 6.4.3.12 with any differences originating in the modified minimum plate thickness and the amount of axial non-active fuel region material (or spacer material) in the basket. Section 6.4.3.12 relied on a minimum plate thickness of 0.115 cm and a minimum 0.7 cm offset of the active fuel region to the end of the fuel element. The offset of 0.7 cm assured an active fuel region separation of 2.67 cm (2 x 0.7 cm plus the 1.27 cm base plate). Section 6.4.3.12 analyses have shown that increasing the axial separation distance between the fissile material or increasing plate thickness will decrease system reactivity. Both of these effects are taken credit for in the evaluation of the high fissile material loaded MTR element. The minimum plate thickness and element axial end region hardware length are adjusted until k_s is below 0.95.

Evaluations for various amounts of axial hardware material reveal that with only this change, a minimum 4 cm offset, 8 cm total hardware (spacer material) must be provided for the system reactivity to remain below 0.95 (Table 6.4.3-23). Similarly, Table 6.4.3-23 shows that increasing the fuel plate thickness to 0.123 cm (1.23 mm) is insufficient by itself to reduce reactivity below 0.95. A combination of 2 cm of hardware at the top and bottom of the element, for a total of 4

cm fuel element hardware, in combination with the 0.123 cm minimum plate thickness produces the required result. While the model employed a symmetric 2 cm fuel plate extension on each end of the active fuel region, any combination of top or bottom hardware or basket spacer material resulting in a 4 cm total is sufficient to assure criticality safety. Based on this evaluation, it is permissible to load a 460 g ^{235}U element, provided that the fuel plates are at minimum 0.123 cm in thickness and that cropping of the fuel element or basket spacer material assures 4 cm axial element material separating the active fuel region. Note that 4 cm of fuel element or spacer material plus the 1.27 cm basket base plate result in a total 5.27 cm of axial separation for the limiting configuration. An enhanced fuel characteristic set is generated and shown in Table 6.4.3-22 to reflect the requirements for loading of the increased fissile material element.

At 21g ^{235}U per plate, additional loading constraint must be applied. The evaluations of the 21g ^{235}U per plate HEU elements are based on the 0.7 cm minimum offset of the active fuel region and decrease the number of plates per element and/or increase the plate minimum thickness. The results of this evaluation are added to Table 6.4.3-23 with a bounding set of fuel characteristics added to Table 6.4.3-22.

6.4.3.14 LEU MTR Fuel Elements with Increased Active Fuel Width and/or Increased Fissile Material Mass

Increased Active Fuel Width

This section determines the requirements for loading LEU fuel elements with an active fuel width larger than 6.6 cm. Section 6.4.3.12 has demonstrated an active fuel width of 7.3 cm yields a k_s of greater than 0.95. This section extends the licensing envelope to a maximum active fuel width of 7.0, 7.1 or 7.15 cm for LEU fuel.

The models employed are similar to those of Section 6.4.3.12 with differences originating in the modifications made in active fuel width, plate thickness, ^{235}U loading per plate, active fuel height, and number of fuel plates.

The 7.0 cm active fuel width evaluation shows that plate thickness, ^{235}U loading per plate, and active fuel height adjustments were sufficient to reduce system reactivity below 0.95. Evaluations of the 7.1 cm active fuel width envelope relied on changes in the number of fuel plates and plate thickness. Extending the active fuel width to 7.15 cm required an increased plate minimum thickness (0.119 cm) in conjunction with a decreased number of fuel plates, increased minimum active fuel height, or decreased fissile material load per plate. Evaluation results are shown in

Table 6.4.3-24. A summary of the allowable LEU fuel characteristics is shown in Table 6.4.3-25.

Increased Fissile Material Mass

LEU fuel elements may contain a ^{235}U content of up to 32 grams per plate. Based on the analysis trends observed in the previous sections, a full cask load of elements containing fissile material significantly above 22 grams per plate will exceed safety limits. Additional analyses are, therefore, performed limiting the contents of the basket module with 32 gram ^{235}U plates to four elements per basket. The center row of elements (locations 1, 2 and 3 in Figure 6.3.3-5) are not loaded. The LEU plate characteristics applied are a maximum 7.3 cm active fuel width, a minimum 56 cm fuel height, and a minimum 0.115 cm plate thickness. Twenty-three plate elements are modeled.

Table 6.4.3-27 contains the results of the criticality evaluations with the revised model. Each of the bounding MTR configurations (summarized in Table 6.4.3-26) is evaluated at full load and with a partial load in the top and bottom baskets. A single fuel type is included in this analysis set. As shown in the Table 6.4.3-26, the system reactivity of the 32 grams ^{235}U per plate element (Case 25%-J) is above safety limits for both full and partially loaded top and bottom baskets (k_s must be less than 0.95). Partially loading the top and bottom baskets reduces system reactivity by approximately 0.01 Δk across all fuel types. Loading the high fissile mass (high reactivity) 32 g ^{235}U per plate LEU elements in a partially loaded basket, and locating the partially loaded baskets at the top and bottom of the basket stack have no significant effect on system reactivities — i.e., system reactivity is controlled by the adjacent (cask center) baskets containing higher reactivity, fully loaded baskets.

An evaluation of six baskets with four elements per basket of the 32 grams ^{235}U per plate LEU fuel element results in a k_{eff} of approximately 0.7. This clearly demonstrates that removing three elements from the basket reduces the basket reactivity significantly, and that replacing any fully loaded basket by the partially loaded high fissile material content element basket is bounded by the evaluations of a fully loaded (42 element) cask configuration.

Loading of the high fissile material elements is, therefore, allowed provided that the elements meet the characteristics of Table 6.4.3-28, including the limitation that any basket containing LEU MTR plates above 22 grams ^{235}U must be limited to four elements (or an equivalent number of fuel plates in a plate canister) with no fuel material in basket openings 1, 2 and 3 per Figure 6.3.3-5.

The specified (partially loaded) basket configuration relies on the moderator in the center basket row to neutronicallly separate the fissile material in the outer sections. As moderator density in

the cask decreases, neutronic interaction among the high fissile mass LEU elements in the outer basket sections will increase. Because previous evaluations have demonstrated that the MTR element reactivity rapidly decreases as moderator density is decreased, it is, therefore, not expected that reduced moderator density will result in a system reactivity increase. To provide quantitative support to this conclusion, moderator density studies are performed for the system with partially loaded baskets located at the top and bottom of the stack, for a system with partially loaded baskets in the cask center baskets, and for a system containing six partially loaded baskets. The partially loaded baskets contain the high fissile mass LEU elements, while the fully loaded baskets contain the maximum reactivity HEU elements ("94%-D").

As demonstrated in Figure 6.4.3-1 and Table 6.4.3-29, maximum reactivity is achieved by a fully moderated cask interior for all conditions. Figure 6.4.3-1 also contains the results of a full set of moderator density evaluations for a system containing cell blocks that will physically prevent elements from being loaded into baskets containing high fissile mass LEU elements. The block body is composed of an aluminum tube and an aluminum top plate. As the length of the block depends on the type of MTR basket employed, and the tube represents the majority of the block mass (the top plate occupies less than three cubic inches), only the tube portion of the block is included in the model. As shown in the moderator density plot, Figure 6.4.3-1, and the result summary in Table 6.4.3-29, there is no effect from the insertion of the cell block on the models containing both full and partially loaded baskets, and only a minor effect on the lower reactivity models containing all partially loaded baskets.

6.4.3.15 MTR Payload Criticality Safety Index

Evaluations included in Sections 6.4.3.1 through 6.4.3.14 demonstrate that the bias and uncertainty adjusted reactivity (k_s) for an infinite array of NAC-LWT casks containing MTR fuel elements remains below 0.95. Therefore, the Criticality Safety Index (CSI) for all MTR payloads is 0.

Figure 6.4.3-1 Cask Interior Moderator Density and Blocked Cell Study Results

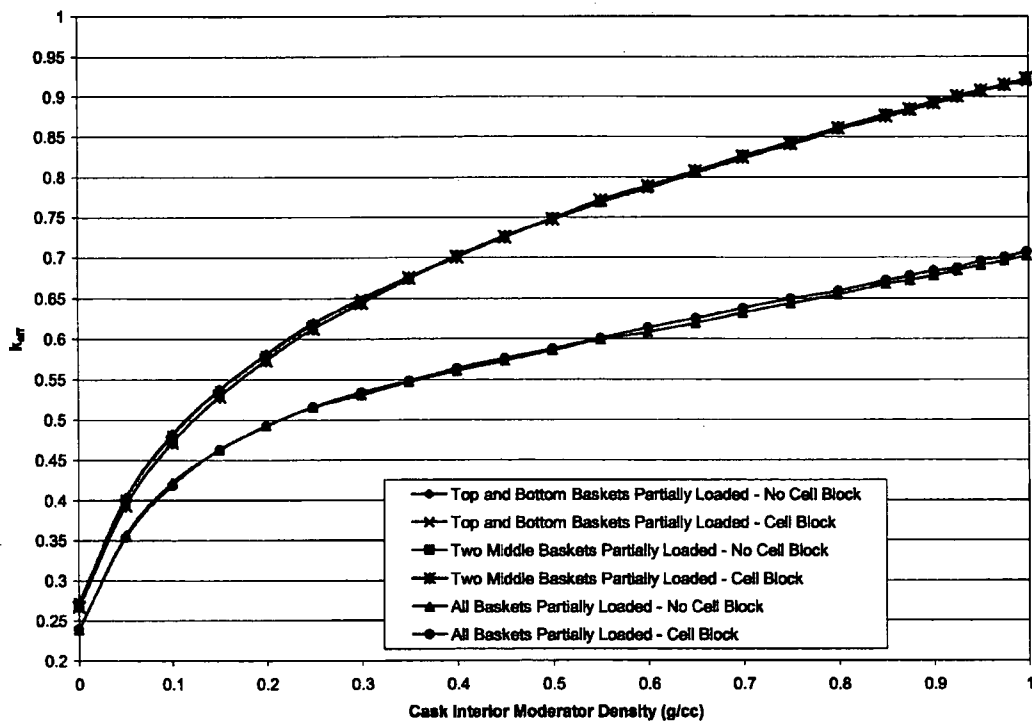


Table 6.4.3-1 Fuel/Basket Unit Cell k_{eff} versus MTR Fuel Element Type

MTR Type	Plate Pitch (cm)	²³⁵ U Loading (grams)	$k_{eff} \pm \sigma$
HEU ORR	0.422	285	1.2475 ± 0.0025
LEU BSR	0.422	340	1.2486 ± 0.0022
HEU HFBR	0.371 ¹	351	1.2396 ± 0.0022
HEU NISTR	0.422 ²	362	1.1808 ± 0.0027
LEU RSG-GAS	0.369	271	1.1502 ± 0.0033
HEU PRR	0.432	247	1.1594 ± 0.0027
LEU THOR	0.761	210	1.0600 ± 0.0032
LEU ZPRL	0.776	210	1.0596 ± 0.0030
LEU IEA-R1	0.431	180	1.0219 ± 0.0039
HEU THOR	0.761	140	0.9479 ± 0.0039
GRR	0.442	187.2	1.0982 ± 0.0037

1. Variable outer plate spacing.
2. Two half-sections stacked together in the basket cell. Section cuts are a minimum of 1 inch from active fuel on each end.

Table 6.4.3-2 Cask k_{eff} versus Fuel Plate Spacing

Fuel Type	# of Fuel Plates	Pitch (cm)	k_{eff}	σ	$k_{eff} + 2\sigma$
HFBR	13	0.6330*	0.7901	0.0034	0.7969
	14	0.5878*	0.8120	0.0036	0.8192
	15	0.5486*	0.8161	0.0040	0.8241
	16	0.5142*	0.8341	0.0034	0.8409
	17	0.4840*	0.8398	0.0030	0.8458
	18	0.4572*	0.8471	0.0033	0.8537
	18	0.3708	0.7918	0.0043	0.8004
	18	0.2921	0.7131	0.0040	0.7211
	18	0.2250	0.6462	0.0039	0.6540
	18	0.1270	0.5166	0.0035	0.5236
BSR	19	0.4782	0.8375	0.0027	0.8429
	19	0.3878	0.7967	0.0029	0.8027

- * Maximum possible spacing of fuel and end plates of HFBR fuel element within basket opening.

Table 6.4.3-3 MTR Basket Geometric Tolerances

Component	Dimension / Tolerance
Basket Opening	3.44 inch + 0.04 / - 0.06 inch
5/16 inch Plate Thickness	0.3125 nom. / 0.28 inch min.
1/4 inch Plate Thickness	0.25 nom. / 0.24 inch min.
11 Gauge Sheet	0.12 inch min.

Table 6.4.3-4 MTR Basket/Intact Fuel Element Geometric Tolerances and Mechanical Perturbations Results

Configuration	k_{eff}	σ	$k_{eff} + 2\sigma$
Elements Moved in Close	0.8023	0.0021	0.8065
Min. Basket Plate Thickness	0.8014	0.0032	0.8078
Elements Moved in Closest	0.7969	0.0021	0.8011
Nominal Configuration	0.7943	0.0031	0.8005
Elements Resting on Basket	0.7928	0.0020	0.7968
Max. Basket Opening	0.7898	0.0035	0.7960
Min. Basket Opening	0.7931	0.0032	0.7995
Elements Moved Out	0.7759	0.0019	0.7797
Elements Moved Out Furthest	0.7667	0.0020	0.7707

Table 6.4.3-5 MTR Basket/Optimally Spaced Fuel Plates Geometric Tolerances and Mechanical Perturbations Results

Configuration	k_{eff}	σ	$k_{eff} + 2\sigma$
Min. Basket Plate Thickness	0.8585	0.0035	0.8655
Plates Moved In	0.8577	0.0020	0.8617
Nominal Configuration	0.8471	0.0033	0.8537
Max. Basket Opening	0.8485	0.0037	0.8559
Min. Basket Opening	0.8406	0.0031	0.8468
Plates Moved Out	0.8290	0.0019	0.8328

Table 6.4.3-6 Reactivity with MTR Fuel vs. Basket Moderator Density, Normal Conditions, Dry Exterior, Infinite Array of Casks

Moderator Density	Casks Touching	2 Foot Surf.-to-Surf.	ISO Container 242.84 cm Pitch	Touching, Center Position Empty
Dry Exterior, Vary Internal Density				
0.0000	0.0705 ± 0.0004	0.0700 ± 0.0004	0.0716 ± 0.0004	N/A
0.0010	0.0728 ± 0.0004	0.0725 ± 0.0004	0.0722 ± 0.0004	N/A
0.0100	0.0912 ± 0.0006	0.0910 ± 0.0005	0.0912 ± 0.0005	0.0793 ± 0.0010
0.0250	0.1227 ± 0.0007	0.1231 ± 0.0007	0.1246 ± 0.0008	N/A
0.0500	0.1789 ± 0.0009	0.1795 ± 0.0009	0.1779 ± 0.0009	0.1612 ± 0.0018
0.0750	0.2285 ± 0.0011	0.2294 ± 0.0011	0.2292 ± 0.0011	N/A
0.1000	0.2741 ± 0.0012	0.2772 ± 0.0013	0.2771 ± 0.0012	0.2513 ± 0.0025
0.2000	0.4207 ± 0.0016	0.4211 ± 0.0016	0.4178 ± 0.0017	0.3886 ± 0.0032
0.4000	0.5868 ± 0.0019	0.5861 ± 0.0018	0.5864 ± 0.0019	0.5170 ± 0.0037
0.6000	0.6831 ± 0.0021	0.6792 ± 0.0020	0.6817 ± 0.0019	0.5829 ± 0.0037
0.8000	0.7511 ± 0.0020	0.7515 ± 0.0020	0.7539 ± 0.0020	0.6289 ± 0.0041
0.9000	0.7830 ± 0.0019	0.7773 ± 0.0021	0.7827 ± 0.0020	N/A
1.0000	0.8072 ± 0.0019	0.8105 ± 0.0020	0.8102 ± 0.0019	0.6639 ± 0.0041
Wet Interior, Vary External Density				
0.0000	0.8139 ± 0.0021	0.8067 ± 0.0020	0.8080 ± 0.0022	N/A
0.0010	0.8116 ± 0.0020	0.8128 ± 0.0020	0.8136 ± 0.0023	N/A
0.0100	0.8108 ± 0.0021	0.8061 ± 0.0019	0.8085 ± 0.0022	N/A
0.0250	0.8078 ± 0.0019	0.8107 ± 0.0021	0.8074 ± 0.0021	N/A
0.0500	0.8066 ± 0.0022	0.8082 ± 0.0020	0.8072 ± 0.0020	N/A
0.0750	0.8113 ± 0.0020	0.8054 ± 0.0022	0.8082 ± 0.0022	N/A
0.1000	0.8097 ± 0.0020	0.8075 ± 0.0019	0.8081 ± 0.0019	N/A
0.2000	0.8133 ± 0.0020	0.8075 ± 0.0023	0.8087 ± 0.0020	N/A
0.4000	0.8096 ± 0.0018	0.8113 ± 0.0020	0.8087 ± 0.0018	N/A
0.6000	0.8110 ± 0.0018	0.8098 ± 0.0020	0.8103 ± 0.0020	N/A
0.8000	0.8072 ± 0.0023	0.8108 ± 0.0019	0.8096 ± 0.0018	N/A
0.9000	0.8133 ± 0.0021	0.8080 ± 0.0021	0.8069 ± 0.0020	N/A
1.0000	0.8107 ± 0.0024	0.8096 ± 0.0022	0.8103 ± 0.0021	N/A
Vary Interior and Exterior Density Simultaneously				
0.0000	0.0705 ± 0.0004	0.0700 ± 0.0004	0.0716 ± 0.0004	N/A
0.0010	0.0736 ± 0.0004	0.0724 ± 0.0005	0.0733 ± 0.0004	N/A
0.0100	0.0906 ± 0.0005	0.0909 ± 0.0005	0.0895 ± 0.0005	N/A
0.0250	0.1239 ± 0.0007	0.1244 ± 0.0007	0.1245 ± 0.0007	N/A
0.0500	0.1774 ± 0.0008	0.1774 ± 0.0009	0.1778 ± 0.0009	N/A
0.0750	0.2291 ± 0.0011	0.2272 ± 0.0010	0.2307 ± 0.0010	N/A
0.1000	0.2750 ± 0.0011	0.2741 ± 0.0012	0.2753 ± 0.0013	N/A
0.2000	0.4204 ± 0.0016	0.4215 ± 0.0016	0.4187 ± 0.0015	N/A
0.4000	0.5809 ± 0.0018	0.5829 ± 0.0018	0.5825 ± 0.0019	N/A
0.6000	0.6833 ± 0.0020	0.6811 ± 0.0021	0.6802 ± 0.0020	N/A
0.8000	0.7547 ± 0.0020	0.7521 ± 0.0019	0.7495 ± 0.0022	N/A
0.9000	0.7821 ± 0.0021	0.7822 ± 0.0018	0.7828 ± 0.0021	N/A
1.0000	0.8107 ± 0.0024	0.8096 ± 0.0022	0.8103 ± 0.0021	N/A

Table 6.4.3-7 Reactivity with MTR Fuel vs. Basket Moderator Density, Accident Conditions, Dry Exterior, Infinite Array of Casks

Moderator Specific Gravity	Casks Touching	2 Foot Surface-to-Surface	ISO 242.84 cm Pitch
Dry Exterior, Vary Internal Density			
0.0000	0.3126 ± 0.0009	0.1031 ± 0.0005	0.1000 ± 0.0005
0.0010	0.3169 ± 0.0009	0.1071 ± 0.0005	0.1024 ± 0.0005
0.0100	0.3493 ± 0.0010	0.1316 ± 0.0006	0.1266 ± 0.0006
0.0250	0.3980 ± 0.0010	0.1720 ± 0.0008	0.1686 ± 0.0007
0.0500	0.4629 ± 0.0011	0.2343 ± 0.0010	0.2336 ± 0.0010
0.0750	0.5152 ± 0.0013	0.2910 ± 0.0010	0.2845 ± 0.0012
0.1000	0.5592 ± 0.0015	0.3425 ± 0.0012	0.3335 ± 0.0013
0.2000	0.6643 ± 0.0018	0.4836 ± 0.0014	0.4830 ± 0.0016
0.4000	0.7625 ± 0.0019	0.6440 ± 0.0018	0.6424 ± 0.0019
0.6000	0.8138 ± 0.0021	0.7390 ± 0.0019	0.7367 ± 0.0020
0.8000	0.8598 ± 0.0021	0.8138 ± 0.0021	0.8061 ± 0.0021
0.9000	0.8777 ± 0.0022	0.8428 ± 0.0021	0.8411 ± 0.0019
1.0000	0.9005 ± 0.0021	0.8717 ± 0.0021	0.8690 ± 0.0019
Wet Interior, Vary External Density			
0.0000	0.9005 ± 0.0021	0.8694 ± 0.0021	0.8739 ± 0.0020
0.0010	0.8975 ± 0.0020	0.8686 ± 0.0023	0.8680 ± 0.0022
0.0100	0.8851 ± 0.0022	0.8673 ± 0.0020	0.8683 ± 0.0021
0.0250	0.8737 ± 0.0022	0.8648 ± 0.0022	0.8671 ± 0.0020
0.0500	0.8709 ± 0.0020	0.8656 ± 0.0021	0.8648 ± 0.0022
0.0750	0.8681 ± 0.0020	0.8648 ± 0.0020	0.8658 ± 0.0020
0.1000	0.8645 ± 0.0019	0.8614 ± 0.0020	0.8618 ± 0.0020
0.2000	0.8625 ± 0.0020	0.8632 ± 0.0021	0.8616 ± 0.0021
0.4000	0.8625 ± 0.0020	0.8601 ± 0.0022	0.8594 ± 0.0019
0.6000	0.8592 ± 0.0021	0.8589 ± 0.0020	0.8591 ± 0.0021
0.8000	0.8600 ± 0.0020	0.8611 ± 0.0020	0.8589 ± 0.0021
0.9000	0.8629 ± 0.0020	0.8599 ± 0.0022	0.8584 ± 0.0021
1.0000	0.8606 ± 0.0023	0.8591 ± 0.0022	0.8602 ± 0.0020
Vary Interior and Exterior Density Simultaneously			
0.0000	0.3126 ± 0.0009	0.1031 ± 0.0005	0.1000 ± 0.0005
0.0010	0.2985 ± 0.0008	0.1054 ± 0.0005	0.1025 ± 0.0005
0.0100	0.2306 ± 0.0008	0.1270 ± 0.0006	0.1245 ± 0.0007
0.0250	0.2097 ± 0.0009	0.1579 ± 0.0008	0.1594 ± 0.0008
0.0500	0.2286 ± 0.0010	0.2072 ± 0.0010	0.2092 ± 0.0009
0.0750	0.2640 ± 0.0011	0.2534 ± 0.0011	0.2533 ± 0.0012
0.1000	0.2996 ± 0.0011	0.2963 ± 0.0012	0.2972 ± 0.0012
0.2000	0.4348 ± 0.0015	0.4337 ± 0.0015	0.4332 ± 0.0017
0.4000	0.6048 ± 0.0017	0.6066 ± 0.0020	0.6037 ± 0.0018
0.6000	0.7126 ± 0.0021	0.7144 ± 0.0020	0.7134 ± 0.0019
0.8000	0.7960 ± 0.0019	0.7892 ± 0.0022	0.7984 ± 0.0022
0.9000	0.8295 ± 0.0020	0.8303 ± 0.0021	0.8289 ± 0.0021
1.0000	0.8606 ± 0.0023	0.8591 ± 0.0022	0.8602 ± 0.0020

Table 6.4.3-8 MTR Fuel Element Rotation Perturbation Study

Case	k_{eff}	σ	$k_{eff} + 2\sigma$
All Horizontal Plates	0.6011	0.0027	0.6065
Corners-Only Horizontal	0.6033	0.0025	0.6083
Corners-Only Vertical	0.6045	0.0027	0.6099
All Vertical Plates	0.6053	0.0027	0.6107

Table 6.4.3-9 MTR Basket/Center Fuel Element Perturbation Study

Fuel Type	Center Element Configuration	k_{eff}	σ	$k_{eff} + 2\sigma$
Intact Elements	Centered	0.8107	0.0020	0.8147
Intact Elements	Corner	0.8066	0.0021	0.8108
Intact Elements	Right	0.8122	0.0021	0.8164
Intact Elements	Up	0.8133	0.0021	0.8175
Expanded Plates	Centered	0.8606	0.0023	0.8652
Expanded Plates	Right	0.8547	0.0019	0.8585

Table 6.4.3-10 Mixed HEU/LEU MTR Fuel Perturbation Study

Case	k_{eff}	σ	$k_{eff} + 2\sigma$
9 HEU	0.6011	0.0027	0.6065
8 HEU 1 LEU centered	0.6033	0.0030	0.6093
6 HEU 3 LEU center row	0.5976	0.0030	0.6036
4 HEU 5 LEU + pattern	0.5894	0.0026	0.5946
8 LEU 1 HEU centered	0.5789	0.0027	0.5843
9 LEU	0.5685	0.0025	0.5735

Table 6.4.3-11 MTR Single Package 10 CFR 71.55(b)(3) Evaluation k_{eff} Summary

Description	$k_{eff} \pm \sigma$	$k_{eff} + 2\sigma$
Single Cask / Inner Shell Reflected with H ₂ O	0.7682 ± 0.0021	0.7724
Single Cask / Inner Shell and Lead Reflected with H ₂ O	0.8043 ± 0.0021	0.8085
Single Cask / Inner Shell, Lead & Outer Shell Reflected with H ₂ O	0.8047 ± 0.0022	0.8091
Single Intact Cask Reflected with H ₂ O	0.8094 ± 0.0021	0.8136

Table 6.4.3-12 MTR Fuel Uranium Weight Percentage Perturbations

Fuel Type	U wt % ⁽¹⁾	Effective Al Density (g/cm ³)	% of Theoretical Al Density	k_{eff}	Δk_{eff}
HEU HFBR	30% ⁽²⁾	2.58	96%	1.2396 ± 0.0022	n/a
	45%	1.25	46%	1.2426 ± 0.0027	0.0030
HEU PRR	12.5% ⁽²⁾	2.65	98%	1.1594 ± 0.0027	n/a
	18.75%	1.64	61%	1.1679 ± 0.0025	0.0085
	33%	0.77	28%	1.1763 ± 0.0024	0.0169
HEU THOR	8.0% ⁽²⁾	2.67	99%	0.9479 ± 0.0039	n/a
	12%	1.75	65%	0.9530 ± 0.0035	0.0051
	20%	0.95	35%	0.9647 ± 0.0035	0.0168
LEU THOR	40% ⁽²⁾	2.46	91%	1.0600 ± 0.0032	n/a
	50%	1.64	61%	1.0628 ± 0.0035	0.0028
	60%	1.09	41%	1.0718 ± 0.0036	0.0118
LEU IEA	40% ⁽²⁾	2.47	91%	1.0219 ± 0.0039	n/a
	50%	1.64	61%	1.0266 ± 0.0036	0.0047
	60%	1.09	40%	1.0272 ± 0.0042	0.0053

Notes:

(1) Uranium in Fuel Composition (wt %)

(2) nominal value

n/a – not applicable

Table 6.4.3-13 MEU MTR Unit Cell k_{eff} Comparison (Enrichment Variation)

Description	k_{eff}	σ
13.91 g ²³⁵ U - 44.44 wt % ²³⁵ U – Al Clad	1.2476	0.0008
13.91 g ²³⁵ U - 44.44 wt % ²³⁵ U – AlMg Clad	1.2475	0.0008
14.5 g ²³⁵ U – 35 wt % ²³⁵ U – Al Clad	1.2501	0.0008
14.5 g ²³⁵ U – 50 wt % ²³⁵ U – Al Clad	1.2642	0.0008
14.5 g ²³⁵ U – 80 wt % ²³⁵ U – Al Clad	1.2844	0.0008

Table 6.4.3-14 MEU MTR Basket k_{eff} Comparison (Plate Location)

Number of Plates	Configuration ⁽¹⁾	k_{eff}	σ
23	A	0.8242	0.0011
22	A	0.8230	0.0010
21	A	0.8176	0.0010
23	B	0.8312	0.0010
22	B	0.8265	0.0010
21	B	0.8206	0.0010

Note:

1. Configuration A places the outer fuel plates separated from the basket plates by a space equal to one-half the spacing between the interior plates. Configuration B places the plates directly against the basket plates.

Table 6.4.3-15 Physical Characteristics of McMaster MTR Fuels

Fuel Parameters	10 Plate	18 Plate
Element Width (cm)	7.61	7.61
Element Depth (cm)	8.03	8.23
Side Plate Thickness (cm)	0.48 (0.19 inch)	0.48
No. of Plates	10	18
Plate Thickness (cm)	0.153 ± 0.005	0.127 ± 0.005
Active Fuel Length (cm)	61.0	59.1 to 60.0
Active Fuel Width (cm)	7.3	5.92 to 6.54
Active Fuel Thickness (cm)	0.051	0.0508
Clad Thickness (cm)	0.05 ± 0.008	0.038 ± 0.008
Plate Pitch	0.319 ± 0.004 inch	0.442 ± 0.004 cm
Fuel Composition	U-Al	U-Al
Wt % ^{235}U (nominal)	93.1 ± 0.1	93.1 ± 0.1
^{235}U per Fuel Element (g)	161.4 ± 0.1	212.1 ± 6
^{235}U per Plate (g)	16.0 ± 0.48	12.25 ± 0.37
Alloy per Plate (Al) (g)	58.9	50.4

Table 6.4.3-16 Reactivity of Various Parameter Variations for 10-Plate McMaster Element

k_{eff}	σ	$k_{eff}+2\sigma$	Δk_{eff}	$\Delta k_{eff}/\sigma$	Description
1.11679	0.00083	1.11845	-	-	nominal fuel (0.153 cm plate, 0.051 cm meat, 0.8103 cm pitch)
1.11451	0.00077	1.11605	-0.00240	-3.1	decreased pitch -0.010 cm
1.11975	0.00078	1.12131	0.00286	3.7	increased pitch +0.010 cm
1.12042	0.00079	1.12200	0.00069	0.9	max pitch and decreased plate thickness - 0.008
1.12020	0.00080	1.12180	0.00049	0.6	max pitch and increased plate thickness +0.008
1.11680	0.00080	1.11840	-0.00291	-3.6	max pitch/min plate thickness and decreased fuel meat thick. (0.029 cm)
1.12154	0.00080	1.12314	0.00183	2.3	max pitch/min plate thickness and increased fuel meat thick. (0.061 cm)
1.12346	0.00081	1.12508	0.00377	4.7	max pitch/min plate thickness and increased fuel meat thick. (0.077 cm)
1.13520	0.00080	1.13680	0.01549	19.4	max pitch/min plate thickness and increased fuel meat thick. (0.145 cm)

Table 6.4.3-17 Reactivity of Various Parameter Variations for 18-Plate McMaster Element

k_{eff}	σ	$k_{eff}+2\sigma$	Δk_{eff}	$\Delta k_{eff}/\sigma$	Description
1.17730	0.00111	1.17952	-	-	nominal fuel (0.127 cm plate, 0.051 cm meat, 0.8103 cm pitch)
1.17068	0.00117	1.17302	-0.00650	-5.6	decreased pitch -0.010 cm
1.17810	0.00112	1.18034	0.00082	0.7	increased pitch +0.010 cm
1.17956	0.00119	1.18194	0.00160	1.3	max pitch and decreased plate thickness - 0.008
1.17753	0.00117	1.17987	-0.00047	-0.4	max pitch and increased plate thickness +0.008
1.17646	0.00114	1.17874	-0.00160	-1.4	max pitch/min plate thickness and decreased fuel meat thick. (0.029 cm)
1.18002	0.00117	1.18236	0.00202	1.7	max pitch/min plate thickness and increased fuel meat thick. (0.061 cm)
1.19393	0.00116	1.19625	0.01591	13.7	max pitch/min plate thickness and increased fuel meat thick. (0.119 cm)
1.15124	0.00122	1.15368	-0.02584	-21.2	nominal case at minimum active fuel width (5.92 cm)

Table 6.4.3-18 MTR Limiting Fuel Configurations

Parameter	HEU/MEU	LEU
Min. side plate thickness (cm)	0.45	0.475
Min. side plate length (cm)	7.6	7.62
Min. plate thickness (cm)	0.122	0.127
Min. clad thickness (cm)	0.024	0.033
Maximum number of fuel plates	23	21
²³⁵ U content per plate (g)	19.5	21
Enrichment (wt % ²³⁵ U)	94	20
Max. Active Width (cm)	6.54 ⁽¹⁾	6.0
Max. Active Fuel Height (cm)	62.5	60.0
Max. Uranium Wt %	50 ⁽²⁾	74

Notes:

1. A 7.3 cm active fuel width is modeled for reduced fissile material mass (²³⁵U) and/or a reduced number of fuel plates.
2. Based on MEU fuel.

Table 6.4.3-19 Initial Fuel Configurations for MTR Bounding Evaluations

Variable	Value
Min. side plate thickness (cm)	0.40
Min. side plate length (cm)	7.5
Min. plate thickness (cm)	0.115
Min. clad thickness (cm)	0.020
Maximum number of fuel plates	23
²³⁵ U content per plate (g)	21
Enrichment (wt % ²³⁵ U)	94
Max. Active Width (cm)	6.6
Max. Active Fuel Height (cm)	65
Max. Uranium Wt %	50
Element/Plate Material Above/Below Active Fuel (cm)	0.7

Table 6.4.3-20 Reactivity Impact of Parameter Variations in the Finite Cask Model

Set	Number of Plates	²³⁵ U per Plate (g)	U wt %	²³⁵ U wt %	Fuel Width (cm)	Fuel Height (cm)	Additional Description of File Parameters	k _{eff}	σ	k _{eff} +2σ	k _s	Δk	Δk _{eff} /σ
A	23	20	50%	94%	6.6	65.0	Plates at bottom	0.91822	0.00093	0.92008	0.93818	-0.01358	-14.6
	23	20	50%	94%	6.6	65.0	Axial shift to cask center	0.92549	0.00094	0.92737	0.94547	-0.00631	-6.7
	23	20	50%	94%	6.6	65.0	Axial shift alternating	0.93180	0.00091	0.93362	0.95172	-	-
B	23	20	50%	94%	6.6	56.0	Alternating shift (a.s.)	0.94724	0.00091	0.94906	0.96716	0.01544	17.0
	23	20	50%	94%	6.6	60.0	Alternating shift	0.94157	0.00092	0.94341	0.96151	0.00977	10.6
	23	20	50%	94%	6.6	71.752	Alternating shift	0.93015	0.00092	0.93199	0.95009	-0.00165	-1.8
C	23	30	50%	94%	6.6	56.0	Alternating shift	1.01772	0.00097	1.01966	1.03776	0.09128	94.1
	23	19	50%	94%	6.6	56.0	Alternating shift	0.93739	0.00091	0.93921	0.95731	0.01095	12.0
	23	18	50%	94%	6.6	56.0	Alternating shift	0.92644	0.00093	0.92830	0.94640	-	-
	23	17	50%	94%	6.6	56.0	Alternating shift	0.91468	0.00099	0.91666	0.93476	-0.01176	-11.9
	23	18	50%	50%	6.6	56.0	a.s.; MEU Core	0.90732	0.00092	0.90916	0.92726	-0.01912	-20.8
D	21	18	50%	94%	6.6	56.0	Alternating shift	0.91806	0.00092	0.91990	0.93800	-0.00838	-9.1
	19	18	50%	94%	6.6	56.0	Alternating shift	0.90657	0.00097	0.90851	0.92661	-0.01987	-20.5
E	23	18	75%	94%	6.6	56.0	Alternating shift	0.92567	0.00091	0.92749	0.94559	-0.00077	-0.8
	23	18	30%	94%	6.6	56.0	Alternating shift	0.92753	0.00097	0.92947	0.94757	0.00109	1.1
	23	18	50%	94%	6.6	56.0	a.s.; pitch -0.02 cm	0.91104	0.00096	0.91296	0.93106	-0.01540	-16.0
	23	18	50%	94%	6.6	56.0	a.s.; pitch -0.04 cm	0.89691	0.00095	0.89881	0.91691	-0.02953	-31.1
	23	18	50%	94%	6.6	56.0	a.s.; side plate lateral shift	0.92711	0.00094	0.92899	0.94709	0.00067	0.7
	23	18	50%	94%	6.6	56.0	a.s.; side plates 0.5 cm	0.92357	0.00093	0.92543	0.94353	-0.00287	-3.1
	23	18	50%	94%	6.6	56.0	a.s.; side plates 0.3 cm	0.92975	0.00093	0.93161	0.94971	0.00331	3.6
	23	18	50%	94%	6.6	56.0	a.s.; canister plates added	0.89768	0.00193	0.90154	0.91964	-0.02876	-14.9
	23	18	50%	94%	6.6	56.0	a.s.; clad width +1cm	0.92573	0.00097	0.92767	0.94577	-0.00071	-0.7
	23	18	50%	94%	6.6	56.0	a.s.; clad length +4cm	0.91304	0.00094	0.91492	0.93302	-0.01340	-14.3
	23	18	50%	94%	6.6	56.0	a.s.; plate 0.125, clad 0.025	0.91525	0.00094	0.91713	0.93523	-0.01119	-11.9
	23	18	50%	94%	6.6	56.0	a.s.; plate 0.115, clad 0.020	0.91405	0.00094	0.91593	0.93403	-0.01239	-13.2
F	19	20	50%	94%	6.6	56.0	Alternating shift	0.92822	0.00096	0.93014	0.94824	-	-
G	23	18	50%	94%	7.3	56.0	Alternating shift	0.94448	0.00090	0.94628	0.96438	-	-
	23	17	50%	94%	7.3	56.0	Alternating shift	0.93237	0.00092	0.93421	0.95231	-	-
	23	16.5	50%	94%	7.3	56.0	Alternating shift	0.92550	0.00094	0.92738	0.94548	-	-
H	23	22	75%	25%	7.3	56.0	Alternating shift; LEU Core	0.94090	0.00091	0.94272	0.96082	-	-
	23	22	75%	25%	6.6	56.0	Alternating shift; LEU Core	0.91993	0.00092	0.92177	0.93987	-	-
I	34	11	50%	94%	6.6	26.0	Alternating shift	0.87068	0.00094	0.87256	0.89066	-	-
	34	11	50%	94%	6.6	30.0	Alternating shift	0.87146	0.00095	0.87336	0.89146	-	-
	17	22	50%	94%	6.6	26.0	Fuel split by 2 cm spacer	0.92616	0.00091	0.92798	0.94608	-	-

Table 6.4.3-21 Baseline MTR Bounding Configurations

Parameter ⁽¹⁾	Generic	NISTR ⁽²⁾
Plate thickness	≥ 0.115 cm	≥ 0.115 cm
Clad thickness	≥ 0.02 cm	≥ 0.02 cm
Number of fuel plates	≤ 23 ⁽³⁾	≤ 17
²³⁵ U content per plate	≤ 18 g ^(3,4,5)	≤ 22 g
Enrichment wt % ²³⁵ U	≤ 94 ⁽⁴⁾	≤ 94
Active width	≤ 6.6 cm ⁽⁵⁾	≤ 6.6 cm
Active fuel height	≥ 56 cm	≥ 54 cm
Maximum reactivity (k _s)	0.9482	0.9461

Notes:

- ¹ Loose fuel plates meeting the requirements in this table must be loaded into a MTR plate canister.
- ² Fuel plates may be cut in half with each half limited to 11 g ²³⁵U and an active fuel length between 27 and 30 cm.
- ³ At a 19 fuel plate maximum, the plates are limited to 20 g ²³⁵U per plate.
- ⁴ LEU fuel plate with up to 22 g ²³⁵U may be loaded at a maximum enrichment of 25 wt % ²³⁵U.
- ⁵ At a maximum active fuel width of 7.3 cm, the plates are limited to 16.5 g ²³⁵U.

Table 6.4.3-22 High Fissile Mass MTR Fuel – Bounding Parameter Analysis

Parameter	Variation From Baseline (Generic) MTR		
	Increased Plate Thickness and Fissile Mass ¹	Increased Plate Thickness and Fissile Mass and Decreased Number of Plates	Increased Fissile Mass and Decreased Number of Plates
Plate thickness [cm]	≥ 0.123	≥ 0.200	≥ 0.115
Clad thickness [cm]	≥ 0.02	≥ 0.02	≥ 0.02
Number of fuel plates	≤ 23	≤ 19	≤ 17
²³⁵ U content per plate [g]	≤ 20	≤ 21	≤ 21
Enrichment [wt % ²³⁵ U]	≤ 94	≤ 94	≤ 94
Active Width [cm]	≤ 6.6	≤ 6.6	≤ 6.6
Active Fuel Height [cm]	≥ 56	≥ 56	≥ 56
Maximum reactivity (k _s)	0.9488	0.8753	0.9451

¹ Requires a minimum 4 cm of fuel element hardware (or spacer material) separating the fuel segments axially.

Table 6.4.3-23 MTR High Fissile Content Loading Evaluation (460 g ²³⁵U)

Number of Plates	²³⁵ U per Plate (g)	Fuel Width (cm)	Fuel Height (cm)	Plate Thickness (cm)	Offset (cm)	k _{eff}	σ	k _{eff} +2σ	k _s	Δk
23	20.0	6.6	56.0	0.115	0.7	0.94724	0.00091	0.94906	0.96716	--
23	20.0	6.6	56.0	0.115	1.7	0.94161	0.00093	0.94347	0.96157	-0.00563
23	20.0	6.6	56.0	0.115	2.0	0.93810	0.00094	0.93998	0.95808	-0.00914
23	20.0	6.6	56.0	0.115	3.0	0.93339	0.00112	0.93563	0.95373	-0.01385
23	20.0	6.6	56.0	0.115	4.0	0.92770	0.00107	0.92984	0.94794	-0.01954
23	20.0	6.6	56.0	0.123	0.7	0.93729	0.00095	0.93919	0.95729	-0.00995
23	20.0	6.6	56.0	0.123	1.7	0.93036	0.00093	0.93222	0.95032	-0.01688
23	20.0	6.6	56.0	0.123	2.0	0.92883	0.00093	0.93069	0.94879	-0.01841
19	21.0	6.6	56.0	0.200	0.7	0.85540	0.0093	0.85726	0.87526	--
17	21.0	6.6	56.0	0.115	0.7	0.92509	0.0095	0.92699	0.94509	--

Table 6.4.3-24 LEU MTR Active Fuel Width Increase Evaluation

Number of Plates	²³⁵ U per Plate (g)	U wt %	²³⁵ U wt %	Fuel Width (cm)	Fuel Height (cm)	Plate Thickness (cm)	k _{eff}	σ	k _{eff} +2σ	k _s
23	22.0	75%	25%	6.6	56.0	0.115	0.91993	0.00092	0.92177	0.93987
23	22.0	75%	25%	7.0	56.0	0.115	0.93387	0.00093	0.93573	0.95383
23	22.0	75%	25%	7.0	56.0	0.119	0.92717	0.00090	0.92897	0.94707
23	21.5	75%	25%	7.0	56.0	0.115	0.92915	0.00087	0.93089	0.94899
23	22.0	75%	25%	7.0	63.0	0.115	0.92154	0.00087	0.92328	0.94138
17	22.0	75%	25%	7.1	56.0	0.115	0.90885	0.00093	0.91071	0.92881
23	22.0	75%	25%	7.1	56.0	0.200	0.81898	0.00089	0.82076	0.83886
23	22.0	75%	25%	7.15	56.0	0.119	0.93169	0.00086	0.93341	0.95151
22	22.0	75%	25%	7.15	56.0	0.119	0.92981	0.00092	0.93165	0.94975
23	21.5	75%	25%	7.15	56.0	0.119	0.92662	0.00090	0.92842	0.94652
23	22.0	75%	25%	7.15	61.0	0.119	0.92512	0.00091	0.92694	0.94504

Table 6.4.3-25 Summary of LEU MTR Bounding Configurations

Parameter	LEU Baseline	7.0 cm Active Width			7.1 cm Active Width		7.15 cm Active Width		
		Plate Thickness	²³⁵ U Content	Active Length	Plate Thickness	Number of Plates	Number of Plates	²³⁵ U Content	Active Length
Plate thickness [cm]	≥ 0.115	≥ 0.119	≥ 0.115	≥ 0.115	≥ 0.200	≥ 0.115	≥ 0.119	≥ 0.119	≥ 0.119
Clad thickness [cm]	≥ 0.02	≥ 0.02	≥ 0.02	≥ 0.02	≥ 0.02	≥ 0.02	≥ 0.02	≥ 0.02	≥ 0.02
Number of fuel plates	≤ 23	≤ 23	≤ 23	≤ 23	≤ 23	≤ 17	≤ 22	≤ 23	≤ 23
²³⁵ U content per plate [g]	≤ 22	≤ 22	≤ 21.5	≤ 22	≤ 22	≤ 22	≤ 22	≤ 21.5	≤ 22
Enrichment [wt % ²³⁵ U]	≤ 25	≤ 25	≤ 25	≤ 25	≤ 25	≤ 25	≤ 25	≤ 25	≤ 25
Active Width [cm]	≤ 6.6	≤ 7.0	≤ 7.0	≤ 7.0	≤ 7.1	≤ 7.1	≤ 7.15	≤ 7.15	≤ 7.15
Active Fuel Height [cm]	≥ 56	≥ 56	≥ 56	≥ 63	≥ 56	≥ 56	≥ 56	≥ 56	≥ 61
Maximum reactivity (k _s)	0.93987	0.94707	0.94899	0.94138	0.83886	0.92881	0.94975	0.94652	0.94504

Table 6.4.3-26 Summary of Previous Bounding Configurations for Use in High Mass LEU Calculations

Fuel ID	Plate thickness [cm]	Clad thickness [cm]	Number of fuel plates	²³⁵ U per plate [g]	Enrichment [wt % ²³⁵ U]	Active Width [cm]	Active Height [cm]	Fuel Offset [cm]
25%-A	0.115	0.02	23	22	25	6.6	56	0.7
25%-B	0.119	0.02	23	22	25	7	56	0.7
25%-C	0.115	0.02	23	21.5	25	7	56	0.7
25%-D	0.115	0.02	23	22	25	7	63	0.7
25%-E	0.2	0.02	23	22	25	7.1	56	0.7
25%-F	0.115	0.02	17	22	25	7.1	56	0.7
25%-G	0.119	0.02	22	22	25	7.15	56	0.7
25%-H	0.119	0.02	23	21.5	25	7.15	56	0.7
25%-I	0.119	0.02	23	22	25	7.15	61	0.7
25%-J ¹	0.115	0.02	23	32	25	7.3	56	0.7
94%-A	0.115	0.02	23	18	94	6.6	56	0.7
94%-B	0.115	0.02	19	20	94	6.6	56	0.7
94%-C	0.115	0.02	23	16.5	94	7.3	56	0.7
94%-D	0.123	0.02	23	20	94	6.6	56	2.0
94%-E	0.2	0.02	19	21	94	6.6	56	0.7
94%-F	0.115	0.02	17	21	94	6.6	56	0.7

Note: All configurations previously evaluated as bounding are included with the exception of NISTR fuel plates. The split plate design adds an additional model complexity not required in the evaluations. The LEU high fissile mass analysis scope is designed to demonstrate that the addition of a partially loaded basket to the previous payloads is bounded by the maximum reactivities already documented. Conclusions drawn from the remaining payloads are applicable to the NISTR fuel.

¹ Content added in Section 6.4.3.14

Table 6.4.3-27 High Fissile Mass LEU (32 g ^{235}U per Plate) Analysis Results

Fuel ID ⁽¹⁾	Same Fuel All Baskets				32 g ^{235}U PBL ⁽²⁾ - 7.3 cm Width		
	Full Load		Partial Top/Bottom		k_{eff}	Full Load	Partial Load
	k_{eff}	Dancoff Factor	k_{eff}	Δk		Δk	Δk
25%-A	0.92134	0.50241715	0.91073	-0.011	0.91254	-0.009	0.002
25%-B	0.92813	0.50706971	0.91656	-0.012	0.91521	-0.013	-0.001
25%-C	0.92913	0.50241715	0.91915	-0.010	0.91769	-0.011	-0.001
25%-D	0.92391	0.50241715	0.91091	-0.013	0.91053	-0.013	0.000
25%-E	0.81720	0.61588436	0.80189	-0.015	0.80451	-0.013	0.003
25%-F	0.91075	0.36430386	0.89951	-0.011	0.89608	-0.015	-0.003
25%-G	0.92995	0.48636374	0.91938	-0.011	0.91798	-0.012	-0.001
25%-H	0.92940	0.50706971	0.91356	-0.016	0.91640	-0.013	0.003
25%-I	0.92533	0.50706971	0.90939	-0.016	0.91298	-0.012	0.004
25%-J ⁽³⁾	0.99842	0.50241715	0.98432	-0.014	--	--	--
94%-A	0.92885	0.50241715	0.91645	-0.012	0.91873	-0.010	0.002
94%-B	0.92823	0.41448367	0.91949	-0.009	0.91825	-0.010	-0.001
94%-C	0.92533	0.50241715	0.91439	-0.011	0.91572	-0.010	0.001
94%-D	0.93162	0.51188898	0.91978	-0.012	0.92071	-0.011	0.001
94%-E	0.85605	0.50536168	0.84241	-0.014	0.84414	-0.012	0.002
94%-F	0.92381	0.36430386	0.91394	-0.010	0.91466	-0.009	0.001

Notes:

- (1) Fuel ID is the identifier for the fuel material contained in all baskets for the cases containing one fuel type, and for the fuel material in the middle baskets for cases containing two fuel types.
- (2) Partial basket loading (PBL) in the top and bottom baskets. Partially loaded baskets contain four 32 g ^{235}U per plate LEU elements per basket loaded in locations 4, 5, 6 and 7 per Figure 6.3.3-5.
- (3) LEU fuel material of 32 g ^{235}U per plate, up to 23 plates.

Table 6.4.3-28 LEU High Fissile Mass Bounding Configuration

Parameter	Value
Number of Elements per Basket	4
Plate thickness [cm]	≥ 0.115
Clad thickness [cm]	≥ 0.02
Number of fuel plates	≤ 23
²³⁵ U content per plate [g]	≤ 32
Enrichment [wt % ²³⁵ U]	≤ 25
Active Width [cm]	≤ 7.3
Active Fuel Height [cm]	≥ 56

Table 6.4.3-29 Cask Interior Moderator Density and Blocked Cell Study Results

Water Density (g/cc)	k_{eff} - No Block in Cells			k_{eff} - Cells Blocked		
	Top/Bottom	Middle	All	Top/Bottom	Middle	All
0.0001	0.27234	0.26713	0.23817	0.27245	0.26739	0.23954
0.05	0.40294	0.39430	0.35646	0.40162	0.39373	0.35399
0.1	0.48197	0.47202	0.42209	0.48063	0.47190	0.41877
0.15	0.53747	0.52908	0.46242	0.53688	0.52916	0.46267
0.2	0.58102	0.57382	0.49272	0.57990	0.57397	0.49199
0.25	0.61913	0.61263	0.51513	0.61741	0.61234	0.51569
0.3	0.64772	0.64313	0.53051	0.64984	0.64416	0.53452
0.35	0.67598	0.67399	0.54706	0.67618	0.67494	0.54860
0.4	0.70176	0.70168	0.56069	0.70205	0.70071	0.56383
0.45	0.72644	0.72472	0.57294	0.72649	0.72528	0.57630
0.5	0.74703	0.74779	0.58607	0.74782	0.74773	0.58752
0.55	0.76761	0.76773	0.59845	0.76797	0.77091	0.60062
0.6	0.78894	0.78853	0.60810	0.78536	0.78906	0.61363
0.65	0.80652	0.80700	0.61890	0.80456	0.80727	0.62501
0.7	0.82463	0.82581	0.63197	0.82236	0.82511	0.63753
0.75	0.83955	0.84342	0.64340	0.84073	0.84144	0.64965
0.8	0.85813	0.86053	0.65486	0.86006	0.86031	0.65927
0.85	0.87370	0.87748	0.66785	0.87507	0.87554	0.67184
0.875	0.88346	0.88416	0.67243	0.88172	0.88412	0.67783
0.9	0.89071	0.89426	0.67804	0.89148	0.89217	0.68348
0.925	0.89848	0.89942	0.68416	0.89951	0.90069	0.68737
0.95	0.90695	0.90763	0.69048	0.90568	0.90782	0.69599
0.975	0.91266	0.91418	0.69592	0.91351	0.91492	0.70057
0.9982	0.92071	0.92323	0.70202	0.91870	0.92264	0.70720

6.4.4 PWR and BWR Rods in a Rod Holder or Fuel Assembly Lattice

The NAC-LWT cask may transport up to 25 intact PWR or BWR fuel rods that are in a fuel rod holder or fuel assembly lattice. Up to 14 of 25 PWR or BWR fuel rods in a fuel rod holder may be classified as damaged.

6.4.4.1 Intact PWR and BWR Rods in a Rod Holder or Fuel Assembly Lattice

This section presents the criticality analysis for the NAC-LWT with up to 25 PWR or 25 BWR fuel rods of up to 5.0 wt % ^{235}U initial enrichment. No credit is taken for geometry control that is provided by the rod holder and no rod positions are specified for the rods in the lattice. Since various fuel rod arrangements may be shipped, the criticality of the PWR and BWR rods in the NAC-LWT cask cavity is studied to determine the optimum pitch and, therefore, the maximum k_{eff} for the cask. Both PWR and BWR studies evaluate rods unrestrained in the cavity. No credit is taken for any basket structure.

Cask k_{eff} versus rod fuel rod pitch is shown in Table 6.4.4-1 for the PWR analysis and Table 6.4.4-5 for the BWR study. The rod pitch, which corresponds to center-to-center spacing in a triangular and most reactive lattice formation, is varied from 1.128 cm to 5.997 cm. The limits 1.1278 cm and 5.997 cm correspond to the most compact and the most dispersed PWR rod formations in a triangular pitch, respectively. Due to the larger rod diameter, the BWR range is from 1.640 cm to 5.228 cm. These evaluations are based on an infinite array of casks with water at 1 g/cc between the fuel rods and in the basket cavity. The neutron shield and cask exterior do not contain water and the results are reported for wet and dry clad gap configurations. Table 6.4.4-1 and Table 6.4.4-5 show that a broad peak in k_{eff} occurs in the rod pitch range from 2.5 to 3.5 cm for the PWR rods and 3.0 to 4.0 for the BWR rods, and that there is no statistically significant difference between wet gap and dry gap reactivities. Therefore, the most reactive configuration is chosen for the PWR rod system with a wet gap and a pitch of 2.922 cm and $k_{\text{eff}} = 0.6082 \pm 0.0035$. The BWR rod most reactive configuration occurs at a pitch of 3.691 cm and a dry gap $k_{\text{eff}} = 0.7045 \pm 0.0033$. These pitches will be used in the subsequent moderator studies.

25 PWR or BWR Rods Moderator Density Criticality Evaluations for Normal Conditions

With the fuel rods at optimum pitch (2.922 cm, PWR, or 3.691 cm, BWR), Table 6.4.4-2 and Table 6.4.4-6 present the cask k_{eff} as a function of moderator density inside and outside the cask.

An infinite array of casks on a square pitch is modeled at three cask pitches: touching (99.7 cm), 2-foot surface-to-surface (160.7 cm), and ISO-container spacing (242.84 cm). The water

moderator density is varied from 1.0 g/cc to 0.0 g/cc, and for normal conditions it is assumed that the clad gap is dry and the neutron shield is filled with water. The results show an increase in reactivity with increasing internal moderator density. This indicates that moderator density changes due to increasing temperature have a negative reactivity effect. Low density moderation inside or outside of the cask does not produce abrupt increases in reactivity in comparison to other density values. There is no optimum at low density as expected from an undermoderated system. The calculations show that cask pitch has no significant impact on the reactivity of the cask array under normal conditions and that k_{eff} does not vary significantly when varying external moderator with constant full density internal moderator. For the PWR cases, the external moderator does not affect reactivity within statistical limits, and the most reactive case is chosen with both internal and external moderator density at 1.0 g/cc. The k_{eff} in this case is 0.6070 ± 0.0033 . Similarly, the most reactive BWR case is for a fully moderated interior, but a dry exterior, resulting in a k_{eff} of 0.7045 ± 0.0038 . The external moderator does not affect reactivity since the fully moderated exterior case produces a slightly lower k_{eff} that is within statistics. For both the PWR and BWR analysis, the k_{eff} for the normal condition cask array with a dry cavity is very subcritical, i.e. $\sim <0.1$ and is insensitive to external moderator density variations.

Thus, up to 25 PWR or BWR rods with 5.0 wt % ^{235}U initial enrichment are acceptable in the NAC-LWT cask. An infinite array of casks with optimum interspersed moderation has been analyzed and the NAC-LWT cask with up to 25 PWR or BWR fuel rod of up to 5.0 wt % ^{235}U remains subcritical in all of the normal transport and accident conditions.

25 PWR or BWR Rods Moderator Density Criticality Evaluations for Accident Conditions

With the fuel rods at optimum pitch, Table 6.4.4-3 (PWR) and Table 6.4.4-7 (BWR) show the cask k_{eff} for the most reactive accident condition configuration as a function of moderator density variation in the cavity, neutron shield tank and outside the cask. Again, three cask spacings are presented: touching (99.7 cm), 2-foot surface-to-surface (160.7 cm), and the ISO-container spacing (242.84 cm). Moderator density is varied from 1.0 g/cc to 0.0 g/cc. For accident conditions it is assumed that the clad gap contains full density water and that the neutron shield tank is punctured and the moderator density in the tank is the same as the exterior moderator density. Again, the results show an increase in reactivity with increasing internal moderator density. Low density moderation inside or outside of the cask does not produce abrupt increases in reactivity in comparison to other density values. For both the PWR and BWR analyses, the calculations show that cask pitch does affect reactivity and that the k_{eff} for the accident condition cask array with a dry cavity, neutron shield and exterior is very subcritical, i.e. is less than 0.20. Reactivity is dominated by full density internal moderator. All other variations do not affect reactivity significantly. Therefore, the most reactive PWR case is chosen with casks touching

and the moderator density at 1.0 g/cc in the cavity and at 0.0 g/cc in the neutron shield tank as well as exterior. The k_{eff} in this case is 0.6077 ± 0.0030 . Likewise, the most reactive BWR case is chosen with casks that are 242.82 cm apart (ISO case) and the moderator density at 1.0 g/cc in the cavity and at 0.0 g/cc in the neutron shield tank as well as exterior. The k_{eff} in this case is 0.7135 ± 0.0033 .

Single Package Criticality Evaluation

To satisfy 10 CFR 71.55(b)(3), an analysis of the reflection of the containment system (inner shell) by water is performed on a single wet cask. Successive replacement of the cask radial shields with water reflection is also evaluated. The reactivity of the PWR system does not vary with statistical significance as each radial shield of the cask is replaced by water, from a $k_{\text{eff}} = 0.6008 \pm 0.0034$ ($k_s = 0.6215$) for the full cask surrounded by water, to a $k_{\text{eff}} = 0.6001 \pm 0.0030$ ($k_s = 0.6200$) for the inner shell surrounded by water. BWR results are k_{eff} s of 0.6932 and 0.6943 for a full cask reflected and the inner shell water reflected, respectively. The results from this evaluation can be seen in Table 6.4.4-4 (PWR) and Table 6.4.4-8 (BWR).

Conclusion

A calculation of k_s under normal and accident conditions can now be made based on the previous results and based on the KENO-Va validation statistics presented in Section 6.5.1 for low enriched uranium fuel. The value k_s is calculated based on the KENO-Va Monte Carlo average plus any biases and uncertainties associated with the methods and the modeling, i.e.:

$$k_s = k_{\text{eff}} + 2\sigma_{\text{mc}} + \Delta k_{\text{Bias}} + \Delta k_{\text{BU}}$$

In the validation presented in Section 6.5.1, a bias of 0.0052 (allowance for under prediction of k_{eff}) and a 95/95 method uncertainty of ± 0.0087 was determined. With this bias and uncertainty, the equation for k_s becomes:

$$k_s = k_{\text{eff}} + 2\sigma_{\text{mc}} + 0.0052 + 0.0087$$

Thus, $k_s = 0.6275$ under normal conditions for an infinite array of NAC-LWT casks loaded with 25 PWR design basis fuel rods and a flooded basket cavity and exterior. This is below the 0.95 regulatory limit. Under accident conditions, $k_s = 0.6276$ for an infinite array of NAC-LWT casks loaded with 25 PWR design basis fuel rods and with a flooded basket cavity and dry neutron shield and exterior.

Under normal conditions, $k_s = 0.7251$ for an infinite array of NAC-LWT casks loaded with 25 BWR design basis fuel rods and a flooded basket cavity and a dry exterior. This is below the 0.95 regulatory limit. Under accident conditions, $k_s = 0.7340$ for an infinite array of NAC-LWT

casks loaded with 25 BWR design basis fuel rods and with a flooded basket cavity and dry neutron shield and exterior.

For both normal and accident conditions, the calculated k_{eff} values, after correction for biases and uncertainties, are below the 0.95 limit. The analyses demonstrate that, including all calculational and mechanical uncertainties, an infinite array of NAC-LWT casks with 25 PWR or BWR fuel rods remains subcritical under normal and accident conditions.

For both normal and accident conditions, the calculated k_{eff} values, after correction for biases and uncertainties, are below the 0.95 limit. The analyses demonstrate that, including all calculational and mechanical uncertainties, an infinite array of NAC-LWT casks with 25 PWR fuel remains subcritical under normal and accident conditions.

6.4.4.2 Damaged PWR and BWR Rods in a Rod Holder

This section presents the criticality analysis for the NAC-LWT with 25 PWR or BWR fuel rods of up to 5.0 wt % ^{235}U initial enrichment classified as damaged. Although the contents is limited to 14 damaged fuel rods in a 25-rod shipment, the analysis conservatively considers all 25 rods as failing during transport. No credit is taken for any parasitic absorption in the basket, fuel can or rod holder structure. Credit is taken for the rod holder weldment to contain the fissile material during water-fuel mixture studies. Criticality analyses are performed to satisfy the criticality safety requirements of 10 CFR Parts 71.55 and 71.59, as well as IAEA Transportation Safety Standards (TS-R-1). A single cask evaluation is also performed to comply with 10CFR71.55(b)(3). The analyses demonstrate that, including all calculational and mechanical uncertainties, the NAC-LWT is subcritical during normal and accident conditions with up to 25 damaged PWR or BWR rods.

Damaged Fuel Rod Evaluation – Heterogeneous (Rod) Configurations

Damaged fuel rods are evaluated in heterogeneous configurations by analyzing unclad fuel rods in a triangular pitch. Removing the cladding conservatively removes any potential parasitic absorbers while increasing the available volume for water moderator. Three rod arrays are considered: 25 rods, 37 rods, and 61 rods. The latter two arrays are complete hexagonal arrays. The limiting pitch is determined for each PWR and BWR array. The fuel region cross-sectional area is conserved in each of the configurations. The fuel rod radii for the various arrays are summarized in Table 6.4.4-19.

Water Exterior Evaluations

As shown in Table 6.4.4-9 through Table 6.4.4-14 and Figure 6.4.4-1 and Figure 6.4.4-2, the system reactivity increases as the number of rods is increased. As the number of rods increases,

Revision 38

so does the cross-sectional area occupied by the rod array. Since the canister provides a limited cross-sectional area for the rod array, evaluations for arrays larger than 61 rods are not required.

Based on the can outer width of 5.5 inches (13.97 cm), the can cross-sectional area is 195.16 cm². Using the rod radius, rod pitch, and number of rods, the area of an enclosing hexagon is calculated for each of the three PWR and BWR arrays, shown in Table 6.4.4-19. This area is compared to the can area. For both BWR and PWR fuel, the 37-rod array results in an enclosing area that is larger than the can. A further increase in the cross-sectional lattice area, required for maximum reactivity, is seen in the 61-rod array. Therefore, the use of a 61-rod array is bounding for the NAC-LWT with no larger arrays requiring analysis.

Void Exterior/Preferential Flooding Evaluations

To increase the coupling of adjacent casks in the infinite array, system reactivity is evaluated for two additional scenarios: void exterior with fully flooded cask cavity and void exterior with preferentially flooded cask cavity. Preferential flooding removes the cask interior moderator outside the fuel rod lattice providing for increased neutronic interaction between casks in the infinite array. The 61-rod hexagonal array is employed.

As shown in Table 6.4.4-15 and Table 6.4.4-16, the void exterior, completely flooded cask cavity, scenario produced slightly higher reactivities than the scenario containing a water cask exterior. This is the result of increased neutronic interaction between casks and indicates the need for preferential flooding evaluations.

The preferential flooding model encloses the 61-rod array in a fully flooded cylinder with the remaining cask cavity filled with the exterior moderator material. This allows the array to remain flooded while voiding from the remaining cask cavity space, the neutron shield and cask exterior. A range of rod pitches is evaluated for both BWR and PWR fuel to determine the maximum reactivity pitch in this configuration. Given the increased neutronic interaction between casks, the most reactive rod pitch of the previously evaluated isolated cask changes. A check is also made to determine whether the modeled array remains conservative with respect to the envelope of the rod holder.

As shown in Table 6.4.4-17 and Table 6.4.4-18, system reactivity is much higher given the preferential flooding scenario. As shown in Table 6.4.4-20, the 61-rod array remains conservative for BWR fuel under the preferential flooding scenario. A 61-rod array of PWR fuel at its most reactive pitch produces a cross sectional area slightly smaller than that produced by the rod holder exterior (186.9 cm² versus 195.2 cm² calculated for the canister). However, the area calculation takes no credit for the rod holder wall material and fuel rod tube insert, which

reduce the available cross-sectional area significantly. A larger array of PWR fuel rods (with reduced diameter) is, therefore, not investigated.

Single Cask Evaluation

10 CFR 71.55(b)(3) requires an evaluation of the NAC-LWT with the containment system fully reflected by water. The containment for the NAC-LWT is the cask inner shell. While no operating condition results in a removal of the cask outer shell and lead gamma shield, the most reactive preferential flooding case for BWR fuel is reevaluated by removing the lead and outer shells (including neutron shield), and reflecting the system by water at full density on the X and Y faces (the Z boundary condition remains mirrored). The results of this analysis, a $k_s = 0.60117$, demonstrates that the system reactivity of the single cask, with containment fully reflected, is significantly below regulatory limits.

Homogenized Fuel/Water Evaluation

A homogenized mixture of UO_2 and water is analyzed in a finite axial model with an infinite array of casks. The width chosen for the fuel homogenization, 13.97 cm, is conservative in that the fuel material must be enclosed by the inner dimension of the rod holder.

Given the maximum fuel volume for 25 BWR fuel rods, 11588 cm^3 , and a UO_2 volume fraction, the height of the homogenized mixture of UO_2 and water is calculated. For a UO_2 volume fraction of 0.16, the cross-sectional area of UO_2 is 31.23 cm^2 ($195.16 \text{ cm}^2 \times 0.16$) and the resultant axial extent is 371.11 cm. The fuel mixture is modeled at the top of the cask cavity.

The limiting UO_2 volume fraction is calculated using a void cask cavity (i.e., preferential flooding), cask exterior and neutron shield to maximize neutron interaction in the cask array. As shown in Table 6.4.4-21 and Figure 6.4.4-3, the maximum reactivity is calculated with a UO_2 volume fraction of 16 percent.

Four sets of moderator density studies are performed, as shown in Table 6.4.4-22 through Table 6.4.4-25. The studies all serve to demonstrate the maximum reactivity configuration of the voided cask cavity and cask exterior. All cases with a voided cask exterior also have a voided neutron shield; thus, the accident condition of loss of neutron shield is explicitly considered.

Single Cask Evaluation

10 CFR 71.55(b)(3) requires an evaluation of the NAC-LWT with the containment system fully reflected by water. The containment for the NAC-LWT is the cask inner shell. While no operating condition results in a removal of the cask outer shell and lead gamma shield, each of the partial flooding cases is reevaluated by removing the lead and outer shells (including neutron shield), and reflecting the system by full density water on the X and Y faces. The results of this

analysis are shown in Table 6.4.4-26 and demonstrate that the system reactivity decreases with the removal of the lead, outer shell and neutron shield reflectors.

Code Bias and Code Bias Uncertainty Adjustments

A calculation of k_s under normal and accident conditions can now be made based on the results for the heterogeneous rod and the homogenized fuel/water evaluations. Since the fuel rod (heterogeneous) configuration resulted in a significantly higher k_{eff} than the homogeneous configuration the KENO-Va validation statistics presented in Section 6.5.1 for low enriched uranium fuel are applied. The value k_s is calculated based on the KENO-Va Monte Carlo average plus any biases and uncertainties associated with the methods and the modeling, i.e.:

$$k_s = k_{eff} + 2\sigma_{mc} + \Delta k_{Bias} + \Delta k_{BU}$$

In the validation presented in Section 6.5.1, a bias of 0.0052 (allowance for under prediction of k_{eff}) and a 95/95 method uncertainty of ± 0.0087 were determined. With this bias and uncertainty, the equation for k_s becomes:

$$k_s = k_{eff} + 2\sigma_{mc} + 0.0052 + 0.0087$$

Each of the resulting tables for arrays of damaged fuel rods, Table 6.4.4-19 through Table 6.4.4-26, includes the calculated k_s . Mixtures with significantly lower k_{eff} results are not limiting.

Under accident conditions (i.e., dry neutron shield) and preferential flooding, $k_s = 0.89950$ for an infinite array of NAC-LWT casks loaded with 25 BWR design basis damaged fuel rods. The calculated k_s for PWR fuel rods is 0.77156.

The calculated k_{eff} values, after correction for biases and uncertainties, are below the 0.95 limit. The analyses demonstrate that, including all calculational and mechanical uncertainties, an infinite array of NAC-LWT casks with 25 PWR or BWR damaged fuel rods remains subcritical under normal and accident conditions.

**Figure 6.4.4-1 Maximum Reactivity Pitch Determination for Damaged BWR Rod Arrays
– Water Exterior**

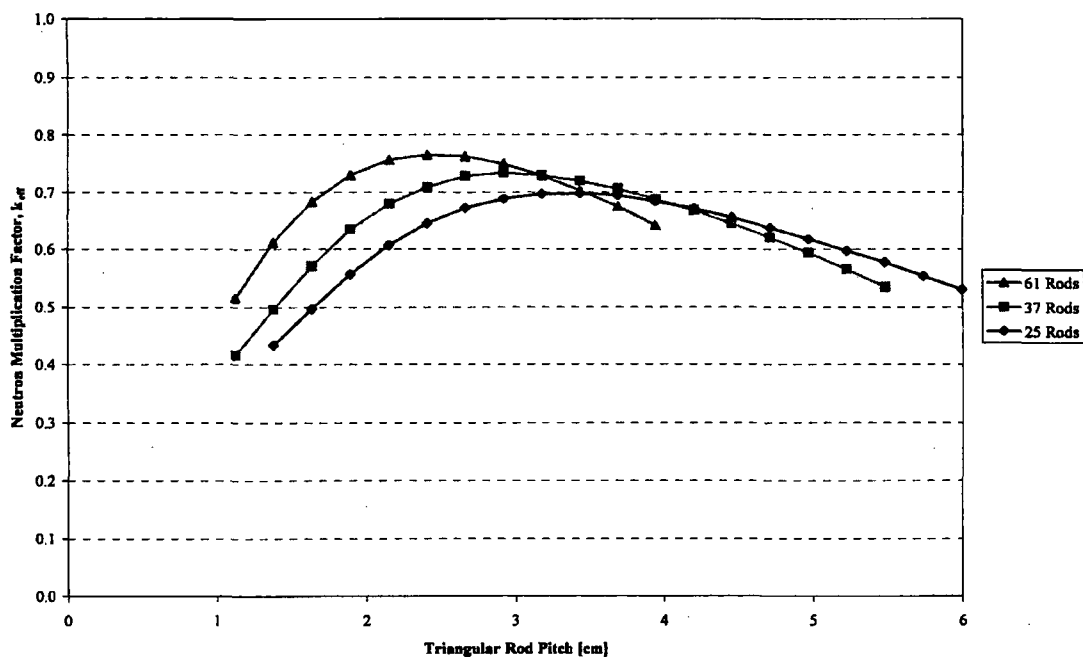


**Figure 6.4.4-2 Maximum Reactivity Pitch Determination for Damaged PWR Rod Arrays
– Water Exterior**

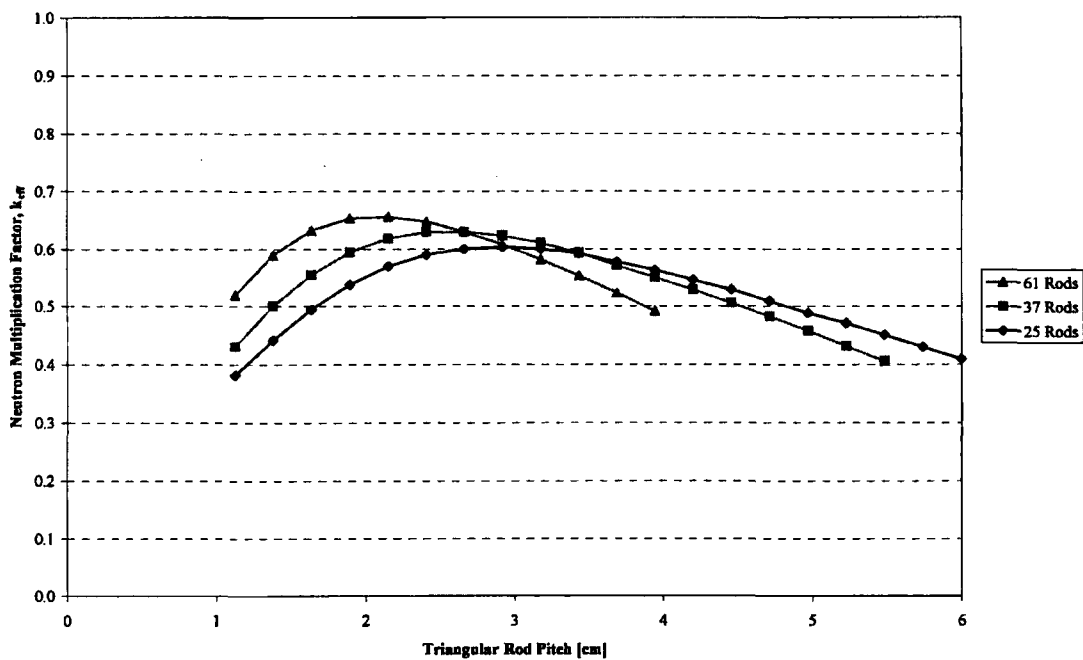


Figure 6.4.4-3 Maximum Reactivity Determination for Homogenized UO_2 /Water Mixture

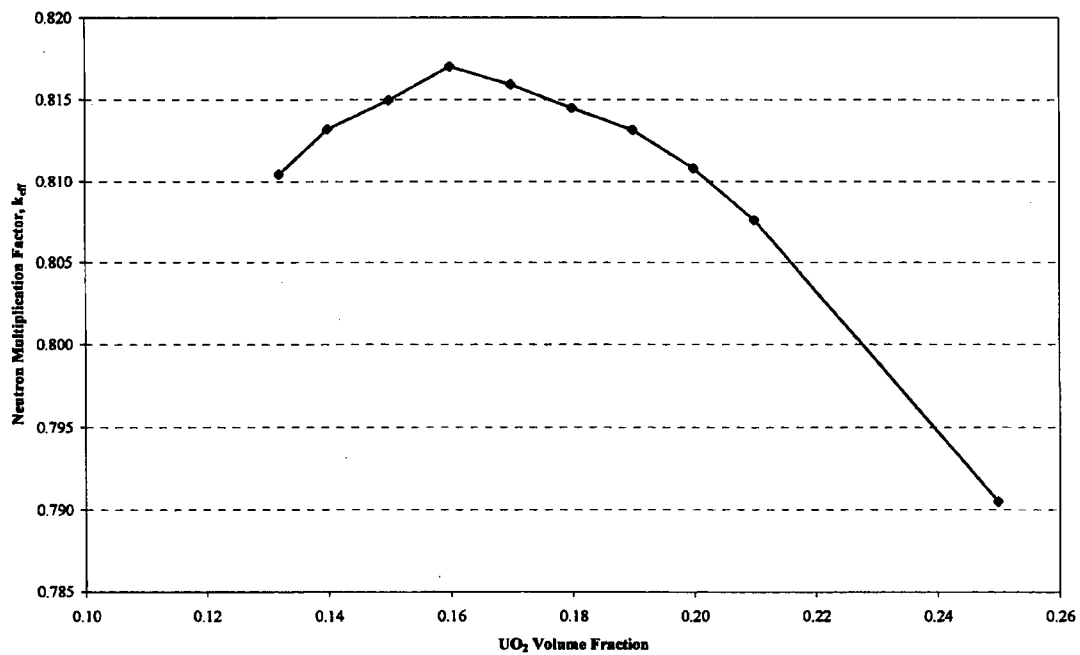


Table 6.4.4-1 NAC-LWT Cask with 25 PWR Rods, k_{eff} versus Fuel Rod Pitch, 5.0 wt % ^{235}U Initial Enrichment

Fuel Rod Pitch (cm)	Cask $k_{eff} \pm \sigma$ Wet Gap	Cask $k_{eff} \pm \sigma$ Dry Gap
1.12769	0.3581 ± 0.0027	0.3577 ± 0.0029
1.38399	0.4150 ± 0.0030	0.4167 ± 0.0033
1.64029	0.4757 ± 0.0032	0.4705 ± 0.0034
1.89659	0.5250 ± 0.0039	0.5268 ± 0.0032
2.15289	0.5578 ± 0.0035	0.5588 ± 0.0035
2.40919	0.5841 ± 0.0034	0.5801 ± 0.0035
2.66539	0.6018 ± 0.0033	0.6030 ± 0.0034
2.92169	0.6082 ± 0.0035	0.6037 ± 0.0035
3.17799	0.6037 ± 0.0034	0.6102 ± 0.0035
3.43429	0.5988 ± 0.0033	0.6002 ± 0.0033
3.69059	0.5838 ± 0.0034	0.5847 ± 0.0035
3.94689	0.5743 ± 0.0036	0.5725 ± 0.0033
4.20319	0.5610 ± 0.0032	0.5582 ± 0.0027
4.45949	0.5415 ± 0.0028	0.5464 ± 0.0036
4.71579	0.5217 ± 0.0027	0.5286 ± 0.0026
4.97209	0.5113 ± 0.0028	0.5109 ± 0.0028
5.22839	0.4858 ± 0.0026	0.4885 ± 0.0032
5.48459	0.4756 ± 0.0026	0.4763 ± 0.0030
5.74089	0.4562 ± 0.0029	0.4564 ± 0.0029
5.99719	0.4402 ± 0.0029	0.4385 ± 0.0028

Table 6.4.4-2 Reactivity with 25 PWR Rods vs. Basket Moderator Density, Normal Conditions, Infinite Array of Casks

Moderator Density	Casks Touching	2 Foot Surface-to-Surface	ISO Container 242.84 cm Pitch
Dry Exterior, Vary Internal Density			
0.0000	0.0413 ± 0.0004	0.0410 ± 0.0004	0.0410 ± 0.0005
0.0010	0.0414 ± 0.0005	0.0419 ± 0.0004	0.0421 ± 0.0004
0.0100	0.0483 ± 0.0005	0.0477 ± 0.0006	0.0488 ± 0.0005
0.0250	0.0652 ± 0.0008	0.0664 ± 0.0008	0.0645 ± 0.0008
0.0500	0.1026 ± 0.0014	0.1036 ± 0.0012	0.1051 ± 0.0012
0.0750	0.1429 ± 0.0017	0.1424 ± 0.0016	0.1453 ± 0.0015
0.1000	0.1845 ± 0.0021	0.1828 ± 0.0019	0.1860 ± 0.0022
0.2000	0.3075 ± 0.0029	0.3053 ± 0.0027	0.3070 ± 0.0026
0.4000	0.4296 ± 0.0033	0.4237 ± 0.0034	0.4265 ± 0.0036
0.6000	0.4959 ± 0.0036	0.4988 ± 0.0037	0.4931 ± 0.0030
0.8000	0.5615 ± 0.0035	0.5562 ± 0.0038	0.5560 ± 0.0034
0.9000	0.5823 ± 0.0035	0.5868 ± 0.0033	0.5866 ± 0.0036
1.0000	0.6056 ± 0.0036	0.6002 ± 0.0035	0.6030 ± 0.0030
Wet Interior, Vary External Density			
0.0000	0.5993 ± 0.0031	0.6027 ± 0.0036	0.6035 ± 0.0036
0.0010	0.5976 ± 0.0036	0.6021 ± 0.0034	0.6028 ± 0.0035
0.0100	0.6079 ± 0.0036	0.6052 ± 0.0037	0.6005 ± 0.0035
0.0250	0.6050 ± 0.0036	0.6034 ± 0.0033	0.6027 ± 0.0036
0.0500	0.6003 ± 0.0030	0.6005 ± 0.0034	0.6100 ± 0.0036
0.0750	0.6072 ± 0.0036	0.6009 ± 0.0033	0.5996 ± 0.0035
0.1000	0.6042 ± 0.0036	0.6038 ± 0.0036	0.5995 ± 0.0030
0.2000	0.6032 ± 0.0035	0.6034 ± 0.0035	0.6016 ± 0.0036
0.4000	0.6050 ± 0.0031	0.6032 ± 0.0031	0.5987 ± 0.0034
0.6000	0.6025 ± 0.0032	0.6071 ± 0.0037	0.6003 ± 0.0031
0.8000	0.5975 ± 0.0030	0.6045 ± 0.0034	0.6040 ± 0.0030
0.9000	0.5993 ± 0.0034	0.6033 ± 0.0039	0.6082 ± 0.0037
1.0000	0.6037 ± 0.0037	0.5970 ± 0.0033	0.6036 ± 0.0033
Vary Interior and Exterior Density Simultaneously			
0.0000	0.0407 ± 0.0005	0.0405 ± 0.0004	0.0409 ± 0.0004
0.0010	0.0418 ± 0.0004	0.0411 ± 0.0004	0.0418 ± 0.0005
0.0100	0.0480 ± 0.0005	0.0481 ± 0.0005	0.0488 ± 0.0005
0.0250	0.0669 ± 0.0008	0.0656 ± 0.0008	0.0649 ± 0.0007
0.0500	0.1051 ± 0.0012	0.1002 ± 0.0013	0.1034 ± 0.0012
0.0750	0.1415 ± 0.0016	0.1430 ± 0.0016	0.1464 ± 0.0018
0.1000	0.1850 ± 0.0020	0.1865 ± 0.0022	0.1826 ± 0.0019
0.2000	0.3014 ± 0.0025	0.3043 ± 0.0028	0.3011 ± 0.0027
0.4000	0.4245 ± 0.0030	0.4246 ± 0.0033	0.4193 ± 0.0032
0.6000	0.5022 ± 0.0037	0.4916 ± 0.0036	0.4998 ± 0.0031
0.8000	0.5567 ± 0.0034	0.5551 ± 0.0029	0.5550 ± 0.0034
0.9000	0.5865 ± 0.0035	0.5810 ± 0.0031	0.5725 ± 0.0033
1.0000	0.6070 ± 0.0033	0.6012 ± 0.0032	0.6012 ± 0.0034

Table 6.4.4-3 Reactivity with 25 PWR Rods vs. Basket Moderator Density, Accident Conditions, Infinite Array of Casks

Moderator Specific Gravity	Casks Touching	2 Foot Surface-to-Surface	ISO 242.84 cm Pitch
Dry Exterior, Vary Internal Density			
0.0000	0.1127 ± 0.0008	0.1135 ± 0.0008	0.1125 ± 0.0006
0.0010	0.1158 ± 0.0007	0.1161 ± 0.0007	0.1149 ± 0.0007
0.0100	0.1365 ± 0.0009	0.1377 ± 0.0009	0.1355 ± 0.0009
0.0250	0.1782 ± 0.0013	0.1778 ± 0.0012	0.1761 ± 0.0013
0.0500	0.2438 ± 0.0019	0.2392 ± 0.0018	0.2401 ± 0.0019
0.0750	0.2971 ± 0.0021	0.2974 ± 0.0021	0.2982 ± 0.0022
0.1000	0.3442 ± 0.0028	0.3404 ± 0.0027	0.3392 ± 0.0025
0.2000	0.4417 ± 0.0034	0.4417 ± 0.0030	0.4381 ± 0.0035
0.4000	0.4958 ± 0.0031	0.4941 ± 0.0032	0.4852 ± 0.0036
0.6000	0.5290 ± 0.0033	0.5228 ± 0.0034	0.5297 ± 0.0037
0.8000	0.5701 ± 0.0036	0.5689 ± 0.0034	0.5667 ± 0.0031
0.9000	0.5952 ± 0.0034	0.5842 ± 0.0030	0.5853 ± 0.0034
1.0000	0.6045 ± 0.0033	0.6040 ± 0.0032	0.6101 ± 0.0032
Wet Interior, Vary External Density			
0.0000	0.6008 ± 0.0033	0.6057 ± 0.0032	0.6047 ± 0.0034
0.0010	0.6053 ± 0.0033	0.6023 ± 0.0031	0.6046 ± 0.0036
0.0100	0.6010 ± 0.0033	0.6031 ± 0.0030	0.6036 ± 0.0032
0.0250	0.6058 ± 0.0035	0.6056 ± 0.0034	0.6002 ± 0.0029
0.0500	0.6052 ± 0.0035	0.5996 ± 0.0036	0.6028 ± 0.0037
0.0750	0.5991 ± 0.0035	0.6043 ± 0.0032	0.6017 ± 0.0034
0.1000	0.6022 ± 0.0037	0.6007 ± 0.0033	0.6081 ± 0.0036
0.2000	0.5975 ± 0.0033	0.6064 ± 0.0034	0.6016 ± 0.0032
0.4000	0.6063 ± 0.0038	0.6020 ± 0.0032	0.6090 ± 0.0035
0.6000	0.6063 ± 0.0032	0.6024 ± 0.0032	0.6014 ± 0.0035
0.8000	0.6044 ± 0.0035	0.6016 ± 0.0035	0.6018 ± 0.0034
0.9000	0.6010 ± 0.0033	0.6069 ± 0.0029	0.6041 ± 0.0035
1.0000	0.5986 ± 0.0031	0.6024 ± 0.0038	0.6060 ± 0.0034
Vary Interior and Exterior Density Simultaneously			
0.0000	0.1136 ± 0.0006	0.1110 ± 0.0006	0.1134 ± 0.0007
0.0010	0.1100 ± 0.0006	0.0985 ± 0.0007	0.0825 ± 0.0006
0.0100	0.0989 ± 0.0008	0.0696 ± 0.0007	0.0556 ± 0.0007
0.0250	0.1031 ± 0.0010	0.0769 ± 0.0010	0.0670 ± 0.0008
0.0500	0.1312 ± 0.0013	0.1090 ± 0.0013	0.1037 ± 0.0014
0.0750	0.1628 ± 0.0019	0.1483 ± 0.0018	0.1453 ± 0.0016
0.1000	0.1977 ± 0.0021	0.1854 ± 0.0020	0.1853 ± 0.0020
0.2000	0.3101 ± 0.0029	0.3018 ± 0.0025	0.3069 ± 0.0028
0.4000	0.4269 ± 0.0029	0.4287 ± 0.0032	0.4225 ± 0.0035
0.6000	0.4965 ± 0.0033	0.4952 ± 0.0035	0.4983 ± 0.0038
0.8000	0.5606 ± 0.0032	0.5614 ± 0.0035	0.5572 ± 0.0035
0.9000	0.5803 ± 0.0032	0.5782 ± 0.0037	0.5837 ± 0.0036
1.0000	0.6077 ± 0.0030	0.6011 ± 0.0037	0.5974 ± 0.0036

Table 6.4.4-4 PWR Rods, Single Package 10 CFR 71.55(b)(3) Evaluation k_{eff} Summary

Description	$k_{eff} \pm \sigma$	$k_{eff} + 2\sigma$
Single Cask / Inner Shell Reflected with H ₂ O	0.6001 ± 0.0030	0.6061
Single Cask / Inner Shell and Lead Reflected with H ₂ O	0.6079 ± 0.0036	0.6151
Single Cask / Inner Shell, Lead & Outer Shell Reflected with H ₂ O	0.6020 ± 0.0031	0.6082
Single Intact Cask Reflected with H ₂ O	0.6008 ± 0.0034	0.6076

Table 6.4.4-5 NAC-LWT Cask with 25 BWR rods, k_{eff} versus Fuel Rod Pitch, 5.0 wt % ²³⁵U Initial Enrichment

Fuel Rod Pitch (cm)	Cask $k_{eff} \pm \sigma$ Wet Gap			Cask $k_{eff} \pm \sigma$ Dry Gap		
1.64029	0.45706	±	0.00286	0.45873	±	0.00342
1.89659	0.52452	±	0.00385	0.52673	±	0.00355
2.15289	0.58707	±	0.00413	0.57828	±	0.00381
2.40919	0.62675	±	0.00393	0.62288	±	0.00333
2.66539	0.66556	±	0.00348	0.66648	±	0.00382
2.92169	0.68714	±	0.00383	0.68098	±	0.00317
3.17799	0.69181	±	0.00380	0.70311	±	0.00372
3.43429	0.69862	±	0.00368	0.70173	±	0.00300
3.69059	0.70297	±	0.00367	0.70447	±	0.00333
3.94689	0.69617	±	0.00347	0.69925	±	0.00329
4.20319	0.68521	±	0.00315	0.68556	±	0.00301
4.45949	0.67665	±	0.00369	0.6743	±	0.00337
4.71579	0.65473	±	0.00331	0.66008	±	0.00322
4.97209	0.64283	±	0.00344	0.64691	±	0.00330
5.22839	0.62652	±	0.00300	0.62668	±	0.00293

Table 6.4.4-6 Reactivity with 25 BWR Rods vs. Basket Moderator Density, Normal Conditions, Infinite Array of Casks

Moderator Specific Gravity	Casks Touching			2 Foot Surface-to-Surface			ISO 242.82 cm		
Dry Exterior. Vary Internal Density									
0.0000	0.05656	+ OR -	0.00055	0.05605	+ OR -	0.00059	0.05682	+ OR -	0.00057
0.0010	0.05819	+ OR -	0.00054	0.05788	+ OR -	0.00052	0.05871	+ OR -	0.00055
0.0100	0.06800	+ OR -	0.00062	0.06777	+ OR -	0.00073	0.06698	+ OR -	0.00065
0.0250	0.09072	+ OR -	0.00091	0.09067	+ OR -	0.00099	0.09127	+ OR -	0.00093
0.0500	0.13923	+ OR -	0.00146	0.13684	+ OR -	0.00140	0.13990	+ OR -	0.00125
0.0750	0.18606	+ OR -	0.00191	0.18738	+ OR -	0.00173	0.18799	+ OR -	0.00184
0.1000	0.23476	+ OR -	0.00216	0.23439	+ OR -	0.00210	0.23364	+ OR -	0.00212
0.2000	0.38517	+ OR -	0.00344	0.37607	+ OR -	0.00269	0.37838	+ OR -	0.00317
0.4000	0.53477	+ OR -	0.00344	0.53398	+ OR -	0.00357	0.53238	+ OR -	0.00399
0.6000	0.61570	+ OR -	0.00363	0.61111	+ OR -	0.00332	0.61508	+ OR -	0.00342
0.8000	0.66499	+ OR -	0.00388	0.66829	+ OR -	0.00360	0.66555	+ OR -	0.00367
0.9000	0.67966	+ OR -	0.00366	0.68529	+ OR -	0.00334	0.68097	+ OR -	0.00328
1.0000	0.69240	+ OR -	0.00386	0.70201	+ OR -	0.00364	0.69756	+ OR -	0.00346
Moderator Specific Gravity	Casks Touching			2 Foot Surface-to-Surface			ISO 242.82 cm		
Wet Interior. Vary External Density									
0.0000	0.69610	+ OR -	0.00339	0.69135	+ OR -	0.00338	0.69935	+ OR -	0.00329
0.0010	0.70161	+ OR -	0.00391	0.70301	+ OR -	0.00358	0.69066	+ OR -	0.00388
0.0100	0.69020	+ OR -	0.00397	0.69402	+ OR -	0.00352	0.70044	+ OR -	0.00329
0.0250	0.69884	+ OR -	0.00379	0.69871	+ OR -	0.00389	0.70458	+ OR -	0.00381
0.0500	0.69110	+ OR -	0.00349	0.69663	+ OR -	0.00384	0.69940	+ OR -	0.00326
0.0750	0.69634	+ OR -	0.00374	0.70282	+ OR -	0.00323	0.69400	+ OR -	0.00373
0.1000	0.69592	+ OR -	0.00367	0.69793	+ OR -	0.00317	0.69605	+ OR -	0.00352
0.2000	0.69566	+ OR -	0.00323	0.69491	+ OR -	0.00368	0.69803	+ OR -	0.00339
0.4000	0.69463	+ OR -	0.00382	0.69520	+ OR -	0.00331	0.70063	+ OR -	0.00348
0.6000	0.69541	+ OR -	0.00364	0.69413	+ OR -	0.00337	0.69327	+ OR -	0.00354
0.8000	0.69669	+ OR -	0.00329	0.69355	+ OR -	0.00380	0.69196	+ OR -	0.00365
0.9000	0.69587	+ OR -	0.00348	0.70373	+ OR -	0.00343	0.70134	+ OR -	0.00335
1.0000	0.70298	+ OR -	0.00377	0.70245	+ OR -	0.00365	0.69863	+ OR -	0.00333
Moderator Specific Gravity	Casks Touching			2 Foot Surface-to-Surface			ISO 242.82 cm		
Vary Interior and Exterior Density Simultaneously									
0.0000	0.05730	+ OR -	0.00053	0.05650	+ OR -	0.00052	0.05718	+ OR -	0.00049
0.0010	0.05797	+ OR -	0.00060	0.05815	+ OR -	0.00056	0.05839	+ OR -	0.00059
0.0100	0.06703	+ OR -	0.00062	0.06801	+ OR -	0.00070	0.06772	+ OR -	0.00074
0.0250	0.09224	+ OR -	0.00088	0.09213	+ OR -	0.00091	0.09063	+ OR -	0.00087
0.0500	0.14064	+ OR -	0.00150	0.13757	+ OR -	0.00153	0.13709	+ OR -	0.00145
0.0750	0.18790	+ OR -	0.00202	0.18714	+ OR -	0.00212	0.18650	+ OR -	0.00176
0.1000	0.23532	+ OR -	0.00225	0.23607	+ OR -	0.00229	0.23225	+ OR -	0.00256
0.2000	0.38056	+ OR -	0.00314	0.38750	+ OR -	0.00297	0.37600	+ OR -	0.00334
0.4000	0.53150	+ OR -	0.00323	0.53738	+ OR -	0.00338	0.53434	+ OR -	0.00372
0.6000	0.61988	+ OR -	0.00371	0.61154	+ OR -	0.00338	0.61457	+ OR -	0.00380
0.8000	0.66446	+ OR -	0.00377	0.66538	+ OR -	0.00334	0.66393	+ OR -	0.00362
0.9000	0.68590	+ OR -	0.00405	0.68149	+ OR -	0.00338	0.68109	+ OR -	0.00357
1.0000	0.70435	+ OR -	0.00312	0.69210	+ OR -	0.00383	0.69897	+ OR -	0.00348

Table 6.4.4-7 Reactivity with 25 BWR Rods vs. Basket Moderator Density, Accident Conditions, Infinite Array of Casks

Moderator Specific Gravity	Casks Touching			2 Foot Surface-to-Surface			ISO 242.82 cm		
Dry Exterior, Vary Internal Density									
0.0000	0.16678	+ OR -	0.00082	0.16532	+ OR -	0.00081	0.16417	+ OR -	0.00076
0.0010	0.16927	+ OR -	0.00092	0.16818	+ OR -	0.00076	0.16919	+ OR -	0.00083
0.0100	0.19533	+ OR -	0.00098	0.19554	+ OR -	0.00111	0.19714	+ OR -	0.00108
0.0250	0.24529	+ OR -	0.00150	0.24317	+ OR -	0.00136	0.24647	+ OR -	0.00156
0.0500	0.32172	+ OR -	0.00192	0.32000	+ OR -	0.00171	0.32349	+ OR -	0.00190
0.0750	0.38479	+ OR -	0.00267	0.38527	+ OR -	0.00234	0.38571	+ OR -	0.00253
0.1000	0.44132	+ OR -	0.00298	0.43394	+ OR -	0.00301	0.43722	+ OR -	0.00262
0.2000	0.56027	+ OR -	0.00330	0.56105	+ OR -	0.00321	0.55792	+ OR -	0.00334
0.4000	0.62723	+ OR -	0.00380	0.63534	+ OR -	0.00388	0.62068	+ OR -	0.00368
0.6000	0.65834	+ OR -	0.00371	0.65642	+ OR -	0.00342	0.65566	+ OR -	0.00399
0.8000	0.68180	+ OR -	0.00370	0.67879	+ OR -	0.00333	0.68134	+ OR -	0.00369
0.9000	0.69219	+ OR -	0.00333	0.69177	+ OR -	0.00348	0.69876	+ OR -	0.00338
1.0000	0.70574	+ OR -	0.00346	0.70062	+ OR -	0.00308	0.70613	+ OR -	0.00336
Moderator Specific Gravity	Casks Touching			2 Foot Surface-to-Surface			ISO 242.82 cm		
Wet Interior, Vary External Density									
0.0000	0.70485	+ OR -	0.00350	0.70537	+ OR -	0.00380	0.71353	+ OR -	0.00333
0.0010	0.70559	+ OR -	0.00330	0.70379	+ OR -	0.00376	0.70277	+ OR -	0.00317
0.0100	0.69932	+ OR -	0.00319	0.69971	+ OR -	0.00303	0.69208	+ OR -	0.00359
0.0250	0.69882	+ OR -	0.00378	0.69308	+ OR -	0.00346	0.69471	+ OR -	0.00343
0.0500	0.69939	+ OR -	0.00409	0.68428	+ OR -	0.00368	0.69751	+ OR -	0.00374
0.0750	0.69777	+ OR -	0.00369	0.69635	+ OR -	0.00352	0.69247	+ OR -	0.00358
0.1000	0.70068	+ OR -	0.00317	0.69051	+ OR -	0.00326	0.70317	+ OR -	0.00354
0.2000	0.69652	+ OR -	0.00304	0.69519	+ OR -	0.00337	0.69979	+ OR -	0.00329
0.4000	0.69578	+ OR -	0.00351	0.70041	+ OR -	0.00331	0.69308	+ OR -	0.00310
0.6000	0.69367	+ OR -	0.00362	0.69188	+ OR -	0.00404	0.69766	+ OR -	0.00327
0.8000	0.70330	+ OR -	0.00363	0.69912	+ OR -	0.00373	0.70236	+ OR -	0.00344
0.9000	0.69400	+ OR -	0.00340	0.69387	+ OR -	0.00385	0.69551	+ OR -	0.00386
1.0000	0.69902	+ OR -	0.00350	0.69844	+ OR -	0.00344	0.70029	+ OR -	0.00335
Moderator Specific Gravity	Casks Touching			2 Foot Surface-to-Surface			ISO 242.82 cm		
Vary Interior and Exterior Density Simulataneously									
0.0000	0.16499	+ OR -	0.00076	0.16534	+ OR -	0.00084	0.16534	+ OR -	0.00084
0.0010	0.15978	+ OR -	0.00082	0.11798	+ OR -	0.00081	0.11798	+ OR -	0.00081
0.0100	0.14066	+ OR -	0.00100	0.07981	+ OR -	0.00085	0.07981	+ OR -	0.00085
0.0250	0.14370	+ OR -	0.00128	0.09501	+ OR -	0.00100	0.09501	+ OR -	0.00100
0.0500	0.17380	+ OR -	0.00174	0.13825	+ OR -	0.00129	0.13825	+ OR -	0.00129
0.0750	0.21261	+ OR -	0.00179	0.19305	+ OR -	0.00197	0.19305	+ OR -	0.00197
0.1000	0.25648	+ OR -	0.00229	0.23437	+ OR -	0.00233	0.23437	+ OR -	0.00233
0.2000	0.38917	+ OR -	0.00323	0.37995	+ OR -	0.00299	0.37995	+ OR -	0.00299
0.4000	0.53569	+ OR -	0.00371	0.52997	+ OR -	0.00334	0.52997	+ OR -	0.00334
0.6000	0.61450	+ OR -	0.00367	0.61391	+ OR -	0.00352	0.61391	+ OR -	0.00352
0.8000	0.66387	+ OR -	0.00329	0.66631	+ OR -	0.00384	0.66631	+ OR -	0.00384
0.9000	0.68209	+ OR -	0.00360	0.68136	+ OR -	0.00384	0.68136	+ OR -	0.00384
1.0000	0.69742	+ OR -	0.00378	0.68992	+ OR -	0.00387	0.68992	+ OR -	0.00387

Table 6.4.4-8 BWR Rods, Single Package 10 CFR 71.55(b)(3) Evaluation k_{eff} Summary

Description	$k_{eff} \pm \sigma$			$k_{eff} + 2 \sigma$
Single Cask/ Inner Shell H ₂ O Reflected	0.69428	\pm	0.00368	0.70164
Single Cask/ Inner Shell & Lead H ₂ O Reflected	0.69355	\pm	0.00397	0.70149
Single Cask/ Inner Shell, Lead, & Outer Shell H ₂ O Reflected	0.69532	\pm	0.00373	0.70278
Single Cask H ₂ O Reflected	0.69322	\pm	0.00381	0.70084

Table 6.4.4-9 Maximum Reactivity Pitch Determination for 25 BWR Rods – Water Exterior

Cask Cavity (g/cc)	Exterior (g/cc)	Pitch (cm)	k_{eff}	σ	k_s	$k_{eff}+2\sigma$	Δk	$\Delta k/\sigma$
1	1	1.3840	0.43688	0.00070	0.45218	0.43828	-0.26228	-374.7
1	1	1.6403	0.49775	0.00076	0.51317	0.49927	-0.20129	-264.9
1	1	1.8966	0.55826	0.00078	0.57372	0.55982	-0.14074	-180.4
1	1	2.1529	0.60670	0.00083	0.62226	0.60836	-0.09220	-111.1
1	1	2.4092	0.64459	0.00080	0.66009	0.64619	-0.05437	-68.0
1	1	2.6654	0.67337	0.00081	0.68889	0.67499	-0.02557	-31.6
1	1	2.9217	0.68893	0.00084	0.70451	0.69061	-0.00995	-11.8
1	1	3.1780	0.69768	0.00080	0.71318	0.69928	-0.00128	-1.6
1	1	3.4343	0.69896	0.00080	0.71446	0.70056	—	—
1	1	3.6906	0.69337	0.00077	0.70881	0.69491	-0.00565	-7.3
1	1	3.9469	0.68509	0.00075	0.70049	0.68659	-0.01397	-18.6
1	1	4.2032	0.66997	0.00075	0.68537	0.67147	-0.02909	-38.8
1	1	4.4595	0.65593	0.00074	0.67131	0.65741	-0.04315	-58.3
1	1	4.7158	0.63801	0.00076	0.65343	0.63953	-0.06103	-80.3
1	1	4.9721	0.61716	0.00072	0.63250	0.61860	-0.08196	-113.8
1	1	5.2284	0.59692	0.00070	0.61222	0.59832	-0.10224	-146.1
1	1	5.4846	0.57611	0.00073	0.59147	0.57757	-0.12299	-168.5
1	1	5.7409	0.55318	0.00068	0.56844	0.55454	-0.14602	-214.7
1	1	5.9972	0.53013	0.00070	0.54543	0.53153	-0.16903	-241.5

Table 6.4.4-10 Maximum Reactivity Pitch Determination for 25 PWR Rods – Water Exterior

Cask Cavity (g/cc)	Exterior (g/cc)	Pitch (cm)	k_{eff}	σ	k_s	$k_{eff}+2\sigma$	Δk	$\Delta k/\sigma$
1	1	1.1277	0.38430	0.00070	0.39960	0.38570	-0.21964	-313.8
1	1	1.3840	0.44279	0.00072	0.45813	0.44423	-0.16111	-223.8
1	1	1.6403	0.49656	0.00077	0.51200	0.49810	-0.10724	-139.3
1	1	1.8966	0.53980	0.00073	0.55516	0.54126	-0.06408	-87.8
1	1	2.1529	0.56950	0.00075	0.58490	0.57100	-0.03434	-45.8
1	1	2.4092	0.59041	0.00078	0.60587	0.59197	-0.01337	-17.1
1	1	2.6654	0.60073	0.00077	0.61617	0.60227	-0.00307	-4.0
1	1	2.9217	0.60380	0.00077	0.61924	0.60534	–	–
1	1	3.1780	0.59904	0.00074	0.61442	0.60052	-0.00482	-6.5
1	1	3.4343	0.59206	0.00078	0.60752	0.59362	-0.01172	-15.0
1	1	3.6906	0.57836	0.00069	0.59364	0.57974	-0.02560	-37.1
1	1	3.9469	0.56256	0.00068	0.57782	0.56392	-0.04142	-60.9
1	1	4.2032	0.54640	0.00070	0.56170	0.54780	-0.05754	-82.2
1	1	4.4595	0.52823	0.00069	0.54351	0.52961	-0.07573	-109.8
1	1	4.7158	0.51025	0.00067	0.52549	0.51159	-0.09375	-139.9
1	1	4.9721	0.49011	0.00068	0.50537	0.49147	-0.11387	-167.5
1	1	5.2284	0.47064	0.00066	0.48586	0.47196	-0.13338	-202.1
1	1	5.4846	0.45036	0.00063	0.46552	0.45162	-0.15372	-244.0
1	1	5.7409	0.42865	0.00062	0.44379	0.42989	-0.17545	-283.0
1	1	5.9972	0.40918	0.00059	0.42426	0.41036	-0.19498	-330.5

Table 6.4.4-11 Maximum Reactivity Pitch Determination for 37 BWR Rods – Water Exterior

Cask Cavity (g/cc)	Exterior (g/cc)	Pitch (cm)	k_{eff}	σ	k_s	$k_{eff}+2\sigma$	Δk	$\Delta k/\sigma$
1	1	1.1277	0.41793	0.00067	0.43317	0.41927	-0.31608	-471.8
1	1	1.3840	0.49679	0.00073	0.51215	0.49825	-0.23710	-324.8
1	1	1.6403	0.57355	0.00077	0.58899	0.57509	-0.16026	-208.1
1	1	1.8966	0.63372	0.00081	0.64924	0.63534	-0.10001	-123.5
1	1	2.1529	0.67993	0.00087	0.69557	0.68167	-0.05368	-61.7
1	1	2.4092	0.71022	0.00085	0.72582	0.71192	-0.02343	-27.6
1	1	2.6654	0.72818	0.00082	0.74372	0.72982	-0.00553	-6.7
1	1	2.9217	0.73371	0.00082	0.74925	0.73535	–	–
1	1	3.1780	0.73076	0.00082	0.74630	0.73240	-0.00295	-3.6
1	1	3.4343	0.72100	0.00078	0.73646	0.72256	-0.01279	-16.4
1	1	3.6906	0.70690	0.00076	0.72232	0.70842	-0.02693	-35.4
1	1	3.9469	0.68847	0.00081	0.70399	0.69009	-0.04526	-55.9
1	1	4.2032	0.66618	0.00075	0.68158	0.66768	-0.06767	-90.2
1	1	4.4595	0.64430	0.00073	0.65966	0.64576	-0.08959	-122.7
1	1	4.7158	0.61821	0.00071	0.63353	0.61963	-0.11572	-163.0
1	1	4.9721	0.59337	0.00073	0.60873	0.59483	-0.14052	-192.5
1	1	5.2284	0.56602	0.00068	0.58128	0.56738	-0.16797	-247.0
1	1	5.4846	0.53531	0.00068	0.55057	0.53667	-0.19868	-292.2

Table 6.4.4-12 Maximum Reactivity Pitch Determination for 37 PWR Rods – Water Exterior

Cask Cavity (g/cc)	Exterior (g/cc)	Pitch (cm)	k_{eff}	σ	k_s	$k_{eff}+2\sigma$	Δk	$\Delta k/\sigma$
1	1	1.1277	0.43247	0.00068	0.44773	0.43383	-0.19855	-292.0
1	1	1.3840	0.50187	0.00077	0.51731	0.50341	-0.12897	-167.5
1	1	1.6403	0.55749	0.00078	0.57295	0.55905	-0.07333	-94.0
1	1	1.8966	0.59561	0.00081	0.61113	0.59723	-0.03515	-43.4
1	1	2.1529	0.61842	0.00078	0.63388	0.61998	-0.01240	-15.9
1	1	2.4092	0.62864	0.00079	0.64412	0.63022	-0.00216	-2.7
1	1	2.6654	0.63084	0.00077	0.64628	0.63238	–	–
1	1	2.9217	0.62153	0.00072	0.63687	0.62297	-0.00941	-13.1
1	1	3.1780	0.60939	0.00072	0.62473	0.61083	-0.02155	-29.9
1	1	3.4343	0.59297	0.00070	0.60827	0.59437	-0.03801	-54.3
1	1	3.6906	0.57112	0.00067	0.58636	0.57246	-0.05992	-89.4
1	1	3.9469	0.54994	0.00067	0.56518	0.55128	-0.08110	-121.0
1	1	4.2032	0.52793	0.00069	0.54321	0.52931	-0.10307	-149.4
1	1	4.4595	0.50588	0.00065	0.52108	0.50718	-0.12520	-192.6
1	1	4.7158	0.48106	0.00066	0.49628	0.48238	-0.15000	-227.3
1	1	4.9721	0.45664	0.00063	0.47180	0.45790	-0.17448	-277.0
1	1	5.2284	0.43149	0.00061	0.44661	0.43271	-0.19967	-327.3
1	1	5.4846	0.40582	0.00062	0.42096	0.40706	-0.22532	-363.4

Table 6.4.4-13 Maximum Reactivity Pitch Determination for 61 BWR Rods – Water Exterior

Cask Cavity (g/cc)	Exterior (g/cc)	Pitch (cm)	k_{eff}	σ	k_s	$k_{eff}+2\sigma$	Δk	$\Delta k/\sigma$
1	1	1.1277	0.52008	0.00072	0.53542	0.52152	-0.24512	-340.4
1	1	1.3840	0.61379	0.00081	0.62931	0.61541	-0.15123	-186.7
1	1	1.6403	0.68471	0.00083	0.70027	0.68637	-0.08027	-96.7
1	1	1.8966	0.73218	0.00083	0.74774	0.73384	-0.03280	-39.5
1	1	2.1529	0.75701	0.00082	0.77255	0.75865	-0.00799	-9.7
1	1	2.4092	0.76498	0.00083	0.78054	0.76664	–	–
1	1	2.6654	0.76171	0.00078	0.77717	0.76327	-0.00337	-4.3
1	1	2.9217	0.74933	0.00075	0.76473	0.75083	-0.01581	-21.1
1	1	3.1780	0.72877	0.00074	0.74415	0.73025	-0.03639	-49.2
1	1	3.4343	0.70376	0.00073	0.71912	0.70522	-0.06142	-84.1
1	1	3.6906	0.67540	0.00072	0.69074	0.67684	-0.08980	-124.7
1	1	3.9469	0.64190	0.00069	0.65718	0.64328	-0.12336	-178.8

Table 6.4.4-14 Maximum Reactivity Pitch Determination for 61 PWR Rods – Water Exterior

Cask Cavity (g/cc)	Exterior (g/cc)	Pitch (cm)	k_{eff}	σ	k_s	$k_{eff}+2\sigma$	Δk	$\Delta k/\sigma$
1	1	1.1277	0.52230	0.00075	0.53770	0.52380	-0.13379	-178.4
1	1	1.3840	0.58974	0.00078	0.60520	0.59130	-0.06629	-85.0
1	1	1.6403	0.63319	0.00083	0.64875	0.63485	-0.02274	-27.4
1	1	1.8966	0.65233	0.00077	0.66777	0.65387	-0.00372	-4.8
1	1	2.1529	0.65607	0.00076	0.67149	0.65759	–	–
1	1	2.4092	0.64753	0.00076	0.66295	0.64905	-0.00854	-11.2
1	1	2.6654	0.63012	0.00072	0.64546	0.63156	-0.02603	-36.2
1	1	2.9217	0.60859	0.00073	0.62395	0.61005	-0.04754	-65.1
1	1	3.1780	0.58257	0.00070	0.59787	0.58397	-0.07362	-105.2
1	1	3.4343	0.55274	0.00066	0.56796	0.55406	-0.10353	-156.9
1	1	3.6906	0.52407	0.00066	0.53929	0.52539	-0.13220	-200.3
1	1	3.9469	0.49246	0.00062	0.50760	0.49370	-0.16389	-264.3

Table 6.4.4-15 Maximum Reactivity Pitch Determination for 61 BWR Rods – Void Exterior

Cask Cavity (g/cc)	Exterior (g/cc)	Pitch (cm)	k_{eff}	σ	k_s	$k_{eff}+2\sigma$	Δk	$\Delta k/\sigma$
1	0	1.1277	0.52156	0.00075	0.53696	0.52306	-0.25209	-336.1
1	0	1.3840	0.61695	0.00083	0.63251	0.61861	-0.15654	-188.6
1	0	1.6403	0.68835	0.00083	0.70391	0.69001	-0.08514	-102.6
1	0	1.8966	0.73509	0.00085	0.75069	0.73679	-0.03836	-45.1
1	0	2.1529	0.76248	0.00083	0.77804	0.76414	-0.01101	-13.3
1	0	2.4092	0.77355	0.00080	0.78905	0.77515	–	–
1	0	2.6654	0.77146	0.00079	0.78694	0.77304	-0.00211	-2.7
1	0	2.9217	0.76267	0.00075	0.77807	0.76417	-0.01098	-14.6
1	0	3.1780	0.74480	0.00072	0.76014	0.74624	-0.02891	-40.2
1	0	3.4343	0.72517	0.00073	0.74053	0.72663	-0.04852	-66.5
1	0	3.6906	0.70227	0.00069	0.71755	0.70365	-0.07150	-103.6
1	0	3.9469	0.67451	0.00071	0.68983	0.67593	-0.09922	-139.7

Table 6.4.4-16 Maximum Reactivity Pitch Determination for 61 PWR Rods – Void Exterior

Cask Cavity (g/cc)	Exterior (g/cc)	Pitch (cm)	k_{eff}	σ	k_s	$k_{eff}+2\sigma$	Δk	$\Delta k/\sigma$
1	0	1.1277	0.52341	0.00079	0.53889	0.52499	-0.13907	-176.0
1	0	1.3840	0.59319	0.00077	0.60863	0.59473	-0.06933	-90.0
1	0	1.6403	0.63388	0.00079	0.64936	0.63546	-0.02860	-36.2
1	0	1.8966	0.65655	0.00078	0.67201	0.65811	-0.00595	-7.6
1	0	2.1529	0.66256	0.00075	0.67796	0.66406	—	—
1	0	2.4092	0.65394	0.00072	0.66928	0.65538	-0.00868	-12.1
1	0	2.6654	0.63865	0.00070	0.65395	0.64005	-0.02401	-34.3
1	0	2.9217	0.61660	0.00069	0.63188	0.61798	-0.04608	-66.8
1	0	3.1780	0.59274	0.00066	0.60796	0.59406	-0.07000	-106.1
1	0	3.4343	0.56934	0.00065	0.58454	0.57064	-0.09342	-143.7
1	0	3.6906	0.54287	0.00064	0.55805	0.54415	-0.11991	-187.4
1	0	3.9469	0.51595	0.00063	0.53111	0.51721	-0.14685	-233.1

Table 6.4.4-17 Maximum Reactivity Pitch Determination for 61 BWR Rods – Void Exterior and Preferential Flooding of Cask Cavity

Cask Cavity (g/cc)	Exterior (g/cc)	Pitch (cm)	k_{eff}	σ	k_s	$k_{eff}+2\sigma$	Δk	$\Delta k/\sigma$
0	0	1.1277	0.53776	0.00070	0.55306	0.53916	-0.34644	-494.9
0	0	1.3840	0.70636	0.00077	0.72180	0.70790	-0.17770	-230.8
0	0	1.6403	0.81018	0.00082	0.82572	0.81182	-0.07378	-90.0
0	0	1.8966	0.86442	0.00079	0.87990	0.86600	-0.01960	-24.8
0	0	2.1529	0.88400	0.00080	0.89950	0.88560	—	—
0	0	2.4092	0.87897	0.00077	0.89441	0.88051	-0.00509	-6.6
0	0	2.6654	0.86184	0.00079	0.87732	0.86342	-0.02218	-28.1
0	0	2.9217	0.83244	0.00073	0.84780	0.83390	-0.05170	-70.8
0	0	3.1780	0.79468	0.00071	0.81000	0.79610	-0.08950	-126.1
0	0	3.4343	0.75931	0.00070	0.77461	0.76071	-0.12489	-178.4
0	0	3.6906	0.71973	0.00073	0.73509	0.72119	-0.16441	-225.2

Table 6.4.4-18 Maximum Reactivity Pitch Determination for 61 PWR Rods – Void Exterior and Preferential Flooding of Cask Cavity

Cask Cavity (g/cc)	Exterior (g/cc)	Pitch (cm)	k_{eff}	σ	k_s	$k_{eff}+2\sigma$	Δk	$\Delta k/\sigma$
0	0	1.1277	0.55291	0.00071	0.56823	0.55433	-0.20333	-286.4
0	0	1.3840	0.67194	0.00076	0.68736	0.67346	-0.08420	-110.8
0	0	1.6403	0.73270	0.00078	0.74816	0.73426	-0.02340	-30.0
0	0	1.8966	0.75614	0.00076	0.77156	0.75766	—	—
0	0	2.1529	0.75121	0.00076	0.76663	0.75273	-0.00493	-6.5
0	0	2.4092	0.73087	0.00076	0.74629	0.73239	-0.02527	-33.3
0	0	2.6654	0.70242	0.00072	0.71776	0.70386	-0.05380	-74.7
0	0	2.9217	0.66618	0.00068	0.68144	0.66754	-0.09012	-132.5
0	0	3.1780	0.62965	0.00067	0.64489	0.63099	-0.12667	-189.1
0	0	3.4343	0.59036	0.00065	0.60556	0.59166	-0.16600	-255.4
0	0	3.6906	0.55310	0.00063	0.56826	0.55436	-0.20330	-322.7

Table 6.4.4-19 Damaged Rod Array Area Calculation – Flooded Cask Cavity

	Number	Fuel	Pitch	Rod Radius	# Rods	Diameter	Area _{Max}
Moderation	of Rods	Type	[cm]	[cm]	Max	[cm]	[cm ²]
Water Cavity	25	BWR	3.434	0.622	5	14.98	168.3
Water Exterior		PWR	2.922	0.478	5	12.64	119.9
Water Cavity	37	BWR	2.922	0.512	7	18.55	258.2
Water Exterior		PWR	2.665	0.393	7	16.78	211.1
Water Cavity	61	BWR	2.409	0.398	9	20.07	302.1
Water Exterior		PWR	2.153	0.306	9	17.84	238.6

Table 6.4.4-20 Damaged Rod Array Area Calculation – Preferential Flooding

	Number	Fuel	Pitch	Rod Radius	# Rods	Diameter	Area _{Hex}
Moderation	of Rods	Type	[cm]	[cm]	Max	[cm]	[cm ²]
Partially Flooded Cavity	61	BWR	2.153	0.398	9	18.02	243.5
Void Exterior		PWR	1.897	0.306	9	15.78	186.9

Table 6.4.4-21 Maximum Reactivity Determination for Homogenized UO₂/Water Mixture

Cask Cavity (g/cc)	Exterior (g/cc)	UO ₂ Vol Frac	k _{eff}	σ	k _{eff} +2σ	Δk	Δk/σ
0	0	0.132	0.81043	0.00075	0.81193	-0.00665	-8.9
0	0	0.14	0.81319	0.00075	0.81469	-0.00389	-5.2
0	0	0.15	0.81495	0.00071	0.81637	-0.00221	-3.1
0	0	0.16	0.81702	0.00078	0.81858	–	–
0	0	0.17	0.81592	0.00076	0.81744	-0.00114	-1.5
0	0	0.18	0.81448	0.00078	0.81604	-0.00254	-3.3
0	0	0.19	0.81315	0.00079	0.81473	-0.00385	-4.9
0	0	0.20	0.81080	0.00080	0.81240	-0.00618	-7.7

**Table 6.4.4-22 Homogenized UO₂/Water Cask Cavity Moderator Density Study
Results - Void Exterior**

Cask Cavity (g/cc)	Exterior (g/cc)	UO ₂ Vol Frac	k _{eff}	σ	k _{eff} +2σ	Δk	Δk/σ
0.0	0	0.16	0.81702	0.00078	0.81858	–	–
0.1	0	0.16	0.80234	0.00078	0.80390	-0.01468	-18.8
0.2	0	0.16	0.79078	0.00083	0.79244	-0.02614	-31.5
0.3	0	0.16	0.77986	0.00082	0.78150	-0.03708	-45.2
0.4	0	0.16	0.77082	0.00084	0.77250	-0.04608	-54.9
0.5	0	0.16	0.76440	0.00086	0.76612	-0.05246	-61.0
0.6	0	0.16	0.75856	0.00081	0.76018	-0.05840	-72.1
0.7	0	0.16	0.75823	0.00079	0.75981	-0.05877	-74.4
0.8	0	0.16	0.75812	0.00079	0.75970	-0.05888	-74.5
0.9	0	0.16	0.75836	0.00080	0.75996	-0.05862	-73.3
1.0	0	0.16	0.76077	0.00085	0.76247	-0.05611	-66.0

**Table 6.4.4-23 Homogenized UO₂/Water Cask Cavity Moderator Density Study
Results - Water Exterior**

Cask Cavity (g/cc)	Exterior (g/cc)	UO ₂ Vol Frac	k _{eff}	σ	k _{eff} +2σ	Δk	Δk/σ
0.0	1	0.16	0.65512	0.00078	0.65668	-0.10233	-131.2
0.1	1	0.16	0.68935	0.00083	0.69101	-0.06800	-81.9
0.2	1	0.16	0.70977	0.00084	0.71145	-0.04756	-56.6
0.3	1	0.16	0.72173	0.00084	0.72341	-0.03560	-42.4
0.4	1	0.16	0.72868	0.00079	0.73026	-0.02875	-36.4
0.5	1	0.16	0.73455	0.00083	0.73621	-0.02280	-27.5
0.6	1	0.16	0.73958	0.00081	0.74120	-0.01781	-22.0
0.7	1	0.16	0.74478	0.00082	0.74642	-0.01259	-15.4
0.8	1	0.16	0.74887	0.00084	0.75055	-0.00846	-10.1
0.9	1	0.16	0.75191	0.00082	0.75355	-0.00546	-6.7
1.0	1	0.16	0.75743	0.00079	0.75901	--	--

**Table 6.4.4-24 Homogenized UO₂/Water Exterior Moderator Density Study Results –
Void Cask Cavity**

Cask Cavity (g/cc)	Exterior (g/cc)	UO ₂ Vol Frac	k _{eff}	σ	k _{eff} +2σ	Δk	Δk/σ
0	0.0	0.16	0.81702	0.00078	0.81858	--	--
0	0.1	0.16	0.66923	0.00081	0.67085	-0.14773	-182.4
0	0.2	0.16	0.65897	0.00080	0.66057	-0.15801	-197.5
0	0.3	0.16	0.65619	0.00078	0.65775	-0.16083	-206.2
0	0.4	0.16	0.65607	0.00078	0.65763	-0.16095	-206.3
0	0.5	0.16	0.65449	0.00079	0.65607	-0.16251	-205.7
0	0.6	0.16	0.65513	0.00081	0.65675	-0.16183	-199.8
0	0.7	0.16	0.65479	0.00077	0.65633	-0.16225	-210.7
0	0.8	0.16	0.65445	0.00077	0.65599	-0.16259	-211.2
0	0.9	0.16	0.65591	0.00081	0.65753	-0.16105	-198.8
0	1.0	0.16	0.65512	0.00078	0.65668	-0.16190	-207.6

Table 6.4.4-25 Homogenized UO₂/Water Exterior Moderator Density Study Results – Water Cask Cavity

Cask Cavity (g/cc)	Exterior (g/cc)	UO ₂ Vol Frac	k _{eff}	σ	k _{eff} +2σ	Δk	Δk/σ
1	0.0	0.16	0.76077	0.00085	0.76247	–	–
1	0.1	0.16	0.75700	0.00085	0.75870	-0.00377	-4.4
1	0.2	0.16	0.75719	0.00080	0.75879	-0.00368	-4.6
1	0.3	0.16	0.75696	0.00081	0.75858	-0.00389	-4.8
1	0.4	0.16	0.75430	0.00083	0.75596	-0.00651	-7.8
1	0.5	0.16	0.75574	0.00081	0.75736	-0.00511	-6.3
1	0.6	0.16	0.75516	0.00080	0.75676	-0.00571	-7.1
1	0.7	0.16	0.75480	0.00085	0.75650	-0.00597	-7.0
1	0.8	0.16	0.75601	0.00084	0.75769	-0.00478	-5.7
1	0.9	0.16	0.75542	0.00081	0.75704	-0.00543	-6.7
1	1.0	0.16	0.75743	0.00079	0.75901	-0.00346	-4.4

Table 6.4.4-26 Single Cask Containment Reflected Results Comparison for Homogenized UO₂/Water Model

Cask Configuration	Cask Cavity (g/cc)	Exterior (g/cc)	UO ₂ Vol Frac	k _{eff}	σ	k _{eff} +2σ	Δk	Δk/σ
Array	0	0	0.16	0.81702	0.00078	0.81858	–	–
Single	0	0	0.16	0.50369	0.00076	0.50521	-0.31337	-412.3
Array	1	0	0.16	0.76077	0.00085	0.76247	–	–
Single	1	0	0.16	0.74882	0.00085	0.75052	-0.01195	-14.1
Array	1	1	0.16	0.75743	0.00079	0.75901	–	–
Single	1	1	0.16	0.75043	0.00080	0.75203	-0.00698	-8.7
Array	0	1	0.16	0.65512	0.00078	0.65668	–	–
Single	0	1	0.16	0.54351	0.00078	0.54507	-0.11161	-143.1

6.4.5 TRIGA Fuel Elements

This section presents the criticality evaluation for TRIGA fuel elements in the NAC-LWT with non-poisoned and poisoned basket modules for intact and failed fuel. In the non-poisoned configuration, up to 120 intact TRIGA fuel elements can be transported in the NAC-LWT cask. In the poisoned configuration, up to 140 intact TRIGA elements can be transported in the NAC-LWT cask. Up to four TRIGA fuel elements can be contained in screened canisters. Up to two failed TRIGA fuel elements can be contained in sealed canisters. The analyses are performed to satisfy the requirements of 10 CFR Parts 71.55 and 71.59 as well as IAEA Transportation Safety Standards (TS-R-1).

The most reactive TRIGA fuel element type in the NAC-LWT TRIGA basket is evaluated in Section 6.4.5.1. The most reactive basket and intact fuel configurations, including both geometric perturbations and manufacturing tolerances, under wet and dry conditions are evaluated in Section 6.4.5.2. The most reactive cask configuration with three baskets of intact design-basis TRIGA fuel and two baskets of fuel, either in screened cans or in sealed cans, is evaluated under normal and accident conditions in Section 6.4.5.3. Preferential flooding of the screened and sealed failed fuel cans is also evaluated. The maximum k_{eff} of the NAC-LWT cask loaded with design-basis TRIGA fuel is evaluated under normal and accident conditions in Section 6.4.5.4. A single package evaluation, in accordance with 10 CFR 71.55(b)(3), is performed in Section 6.4.5.5. The analyses demonstrate that, including all calculational and mechanical uncertainties, the NAC-LWT cask remains subcritical ($k_s < 0.95$) under normal and accident conditions.

Any combination of TRIGA fuel element types can be placed in the NAC-LWT TRIGA baskets. TRIGA fuel cluster rods are analyzed as separate loadings in Section 6.4.6 and will not be shipped with TRIGA fuel elements.

6.4.5.1 Most Reactive TRIGA Fuel Element

Of the four main types of TRIGA fuel elements (Table 6.2.5-1), three (aluminum clad, stainless steel clad, and FFCR) are explicitly analyzed to determine which element is bounding in terms of criticality. The ACPR fuel element and fuel follower control rod types are eliminated from consideration due to their low ^{235}U loading. For steel clad fuel, the standard, and FLIP LEU-I compositions (Table 6.2.5-2) are also eliminated from further consideration due to their low ^{235}U loading. These element types are bounded by this analysis. The two types of Al clad fuel elements, each with 20 wt % ^{235}U loading are analyzed, and the two types of stainless steel clad elements (standard streamlined and standard plain) both enriched to either 20 wt % or 70 wt % in

Revision 38

^{235}U are analyzed. The FFCR element is analyzed with FLIP LEU-I composition enriched to 20 wt % ^{235}U .

6.4.5.1.1 Nonpoisoned Basket Most Reactive TRIGA Fuel Element Evaluation

The parametric evaluation of the TRIGA fuel element types for the nonpoisoned basket is performed with the fuel/basket unit cell infinite array model. The reactivities of the seven candidate fuel types are presented in Table 6.4.5-1. The results show that the stainless steel clad, standard plain, TRIGA fuel element with FLIP composition at 70 wt % ^{235}U is the most reactive of all TRIGA fuel element types. Table 6.4.5-1 also includes the results for several combinations of steel FLIP LEU (20 wt % ^{235}U) and FLIP HEU (70 wt % ^{235}U) which are bounded by the results for four 70 wt % ^{235}U elements per basket cell.

6.4.5.1.2 Poisoned Basket Most Reactive TRIGA Fuel Element Evaluation

The parametric evaluation of TRIGA fuel element types for the poisoned basket is performed with an infinite cask array model. The reactivity of the candidate fuel types is presented in Table 6.4.5-2. Again, the results show that the stainless steel clad, standard plain, TRIGA fuel element with FLIP composition at 70 wt % ^{235}U is the most reactive of all TRIGA fuel element types, and combinations of steel FLIP LEU (20 wt % ^{235}U) and FLIP HEU (70 wt % ^{235}U) are bounded by the results for four 70 wt % ^{235}U elements per basket cell. Because of the low relative reactivity of the 14-inch aluminum clad and FFCR (Table 6.4.5-1) elements, it is not necessary to re-analyze these elements.

6.4.5.1.3 Summary of Most Reactive TRIGA Fuel Element Evaluation

The stainless steel clad, standard plain, TRIGA fuel element with FLIP composition at 70 wt % ^{235}U is the most reactive of all TRIGA fuel element types in the poisoned and non-poisoned baskets. Four of these elements in basket openings bound the other element types and any combination with other such elements. This TRIGA fuel element type and the TRIGA fuel cluster rods will be utilized in subsequent evaluations of the NAC-LWT cask with poisoned and non-poisoned baskets.

6.4.5.2 Most Reactive Fuel Element and Basket Configurations

The primary basket tolerances affecting system reactivity are geometric tolerances, including the positioning of the fuel elements in the cell opening, the size of the cell opening; and manufacturing tolerances, including the thickness of the steel plate dividing the basket openings. The effect of these tolerances is evaluated sequentially in this section.

6.4.5.2.1 Geometric Perturbations

The TRIGA fuel elements are held in place by basket modules. Each cell opening in the basket module can contain up to four TRIGA fuel elements. The TRIGA fuel elements are not constrained in the opening and, therefore, may shift to any location in the opening. Wet and dry conditions of the TRIGA fuel are evaluated to determine the most reactive fuel element and basket configuration.

Table 6.4.5-3 and Table 6.4.5-4 show the nonpoisoned and poisoned axially infinite basket cask k_{eff} with design-basis TRIGA fuel elements. The effects evaluated in the tables include fuel element movement and partial loading in wet and dry basket openings.

For each basket configuration, the most reactive wet configuration contains four design-basis TRIGA fuel elements moved outward to the corners of each cell opening, with $k_{\text{eff}} = 0.83468 \pm 0.00101$ and 0.87874 ± 0.00123 for nonpoisoned and poisoned basket configurations, respectively. Although the reactivity of the non-poisoned basket configurations with three fuel elements in a cell are similar to that with four rods, the four rod configuration is selected as the most reactive because it contains the greatest amount of ^{235}U . The wet configuration maximizes the moderation between TRIGA fuel elements within the wet cavity and is referred to as the wet configuration for TRIGA fuel elements.

The most reactive dry configuration, with no water in the neutron shield, contains four design-basis TRIGA fuel elements touching in each opening and moved inward to the basket center with $k_{\text{eff}} = 0.93434 \pm 0.00115$ and 0.88969 ± 0.00122 for nonpoisoned and poisoned basket configurations, respectively. This dry configuration minimizes the neutron leakage of TRIGA fuel elements within the dry basket and is referred to as the dry configuration for TRIGA fuel elements. The partial loading evaluations show a general decrease in reactivity with a decreasing number of fuel elements.

6.4.5.2.2 Manufacturing Tolerance Perturbations

In addition to geometric tolerances, the wet and dry configurations were evaluated to determine the effect of manufacturing tolerances. The dimensional ranges of the plate materials used to construct the basket openings are 0.28 inch minimum/0.3125 inch maximum for the center plate, 0.24 inch minimum/0.295 inch maximum for the outside divider plate, and 0.12 inch minimum/0.13 inch maximum for the outside plate. The cell opening is checked during fabrication to ensure a minimum cell opening of 3.38 inches square, and a maximum cell opening size of 3.48 inches square. The most reactive configurations based on geometric tolerances are utilized in this analysis.

Table 6.4.5-5 and Table 6.4.5-6 show the nonpoisoned and poisoned basket, cask k_{eff} with design-basis TRIGA fuel elements. The effects evaluated in the tables include perturbations on basket plate thickness and basket opening size. For the nonpoisoned basket, within statistical limits, the most reactive wet and dry configurations contain baskets with the minimum stainless steel thickness divider plates. The reactivity of these wet and dry configurations are $k_{\text{eff}} = 0.86861 \pm 0.00094$ and $k_{\text{eff}} = 0.90501 \pm 0.00109$, respectively. Furthermore, the most reactive dry configuration for manufacturing tolerances contains the minimum basket opening, $k_{\text{eff}} = 0.90817 \pm 0.00105$. For the poisoned basket configuration, the perturbations do not significantly increase reactivity.

6.4.5.3 Sealed and Screened Cans Criticality Evaluation

Criticality calculations were performed in screened and sealed failed fuel cans in the top and base basket modules of the cask. Three cases are examined for each basket combination, an all dry system, a full wet system, and a preferentially wet system with water only in the screened or sealed failed fuel can. Fuel in sealed cans is modeled both homogeneously, heterogeneously, and with partial loadings. The three central modules contain intact fuel in the most reactive wet or dry configurations, as appropriate, as determined in Section 6.4.5.2. The reactivities of the failed fuel combinations are compared to the reactivities of respective intact fuel configurations, and moderator density studies are performed on the most reactive configurations in Section 6.4.5.4.

6.4.5.3.1 Screened Failed Fuel Can Evaluations

Table 6.4.5-7 shows the results of the preferential flooding and partial loading studies of the screened failed fuel can configurations with design-basis TRIGA fuel elements in non-poisoned and poisoned baskets. As seen in the table, the most reactive configurations for the NAC-LWT cask containing screened cans with TRIGA fuel elements is an infinite array of casks with dry cavities, loaded with preferentially flooded screened cans, with each can containing four fuel elements in the corners of the cans. The most reactive poisoned configuration also contains the maximum can opening size.

The reactivity, k_{eff} , for the nonpoisoned and poisoned configurations is 0.90926 ± 0.00126 and 0.90224 ± 0.00128 , respectively. The reactivity of the screened cans in the nonpoisoned basket configuration is bounded by the sealed can evaluations presented in Section 6.4.5.3.2.

6.4.5.3.2 Sealed Failed Fuel Can Evaluations

Table 6.4.5-8 shows the results of the preferential flooding and partial loading studies of the sealed failed fuel can configurations with TRIGA fuel elements in non-poisoned and poisoned baskets. Included in the sealed can evaluations are homogenous fuel/moderator mixture cases,

representing fuel debris, with the mixture either being solid (no water), filling one half of the can or filling the whole can. Cases are evaluated for the solid in the mixture both with and without graphite.

As seen in the table, the most reactive configuration for the NAC-LWT cask with the non-poisoned basket containing sealed cans is for an infinite array of casks with dry cavities loaded with preferentially flooded, maximum diameter, sealed cans, each can containing a homogeneous mixture of water and the fissile material equivalent to two TRIGA fuel elements. The most reactive nonpoisoned configuration is $k_{\text{eff}} = 0.91355 \pm 0.00119$. The “Wet Cask / Wet Can, Elements Out” case for the non-poisoned basket was not analyzed because the reactivity of the element configurations is significantly lower than the homogenized mixture configurations.

The most reactive poisoned basket configuration is selected as the case containing flooded cask and cans with elements touching the can wall. The reactivity, k_{eff} , for this configuration is 0.88574 ± 0.00130 . Since the screened can reactivity presented in Section 6.4.5.3.1 is higher, this configuration is bounded.

6.4.5.4 Moderator Density Criticality Evaluations for Intact TRIGA Fuel Elements

The evaluations for normal and accident conditions include moderator density variations in the cask cavity and external environment to the cask. One evaluation is performed for each basket (non-poisoned / poisoned) combination. Table 6.4.5-9 and Table 6.4.5-10 show the most reactive configurations for these combinations as determined in Section 6.4.5.3. The tables contain results for infinite axial length models for the intact fuel and finite axial length models with cask end caps for failed fuel. Comparing the reactivity of the more conservative infinite models with finite models is acceptable, provided the result with the highest k_{eff} is always selected. Alternately, converting conservative infinite axial length models to finite axial length models is equally acceptable.

As seen in Table 6.4.5-9, $k_{\text{eff}} = 0.93434 \pm 0.00115$ for the most reactive dry configuration with intact, TRIGA fuel elements in the non-poisoned basket. When reevaluated as a finite axial length cask model with end caps, the resulting $k_{\text{eff}} = 0.89731 \pm 0.00117$. As a result, the most reactive configuration of TRIGA fuel elements in the nonpoisoned basket becomes the configuration with two baskets with sealed cans preferentially flooded with a dry cask, $k_{\text{eff}} = 0.91355 \pm 0.00119$. This configuration is chosen for further moderator density variation evaluations. As seen in Table 6.4.5-10, the most reactive configuration of TRIGA fuel elements in the poisoned basket contains two screened cans preferentially flooded with a dry cask. This configuration is chosen for moderator density variations. Results of the moderator density

Revision 38

variation cases for normal and accident conditions for the two basket configurations are presented in Table 6.4.5-11 through Table 6.4.6-14.

As seen in Table 6.4.5-12, the most reactive configuration for the TRIGA fuel elements in the nonpoisoned basket contains two baskets with sealed cans, preferentially flooded, under accident conditions with no water in the cask interior, neutron shield, or exterior, $k_{\text{eff}} = 0.9136 \pm 0.0012$. Per Section 6.5.3, this corresponds to $k_s = 0.9328$.

As seen in Table 6.4.5-14, the most reactive configuration for the TRIGA fuel elements in the poisoned basket, contains two baskets with sealed cans, preferentially flooded, under accident conditions with no water in the cask interior, neutron shield, or exterior, $k_{\text{eff}} = 0.9022 \pm 0.0015$. Per Section 6.5.3, this corresponds to $k_s = 0.9220$.

6.4.5.5 Single Package Criticality Evaluation

To satisfy 10 CFR 71.55(b)(3), an analysis of the reflection of the containment system (inner shell) by water is performed on a single wet cask. Successive replacement of the cask radial shields with water reflection is also evaluated for each basket (nonpoisoned/poisoned) combination. As seen in Table 6.4.5-15 and Table 6.4.5-16, the reactivity of the system drops as each radial shield of the cask is replaced by water from the full cask surrounded by water, to the inner shell surrounded by water.

6.4.5.6 Revised TRIGA Fuel Element Characteristics for Nonpoisoned Baskets

The purpose of this section is to demonstrate reactivity results for a revised set of TRIGA fuel element characteristics.

The analysis is broken into three subsections. The first section establishes a minimum number of fuel characteristics meeting criticality safety limits for intact fuel (cask shipments with no cans). The next section evaluates severely damaged TRIGA fuel, including debris, in sealed and screened cans. The last section contains the evaluations for a screened can containing TRIGA elements with potential clad damage, but meeting structural requirements for transport. Unless otherwise indicated, all models represent the accident condition cask (i.e., no neutron shield) in a finite cask array of eight casks.

6.4.5.6.1 Intact Fuel Elements (No Can)

Basic TRIGA fuel element characteristics affecting system reactivity are itemized in the following paragraphs, with a qualitative description as to their effect on system reactivity.

Revision 38

Following the qualitative description are the result discussions of the KENO-Va calculations for the individual parameters.

Enrichment

TRIGA fuel elements are constructed at two basic enrichment levels (20 wt % and 70 wt % ^{235}U).

Fissile Material Mass

Maximum fissile material mass for each enrichment/fuel clad material combination is assigned to the models. Maximum fissile material mass will result in maximum system reactivity.

Zirconium Mass and Hydrogen-to-Zirconium (H/Zr) Ratio

The combination of zirconium mass and the H/Zr ratio determines the quantity of moderator (hydrogen) within the fuel matrix. Previous evaluations indicate that increasing the moderator quantity has the potential to increase system reactivity (i.e., the fuel element itself is under-moderated). Therefore, maximum system reactivity is obtained from a H/Zr ratio of 2.0 (maximum for zirconium hydride) and a maximum fuel zirconium content (limited by the fuel region volume).

Rod Diameter

Modifying rod diameter at a fixed fuel geometry and mass has a small negative effect for stainless steel clad elements, as it increases clad volume (stainless steel is a parasitic absorber). There is no significant effect on aluminum clad fuel. A secondary effect of a rod diameter increase is the separation of the fuel in the dry cavity cask case and reduction in water between elements in the wet cavity cask case. Both result in minor negative reactivity trends.

When allowing the fuel to expand to the clad inner surface, a maximum rod OD allows for additional moderator (in the form of ZrH), which more than offsets the minor reactivity effects discussed previously and, therefore, represents a bounding configuration.

Clad Thickness

Reducing clad thickness removes parasitic absorber for the stainless steel clad fuel element. At a fixed outer diameter, reduced clad thickness provides additional rod interior volume. For a fixed fuel mass, the reactivity effect of a reduced clad thickness is, therefore, limited to the parasitic absorber removal while, at a maximum fuel mass, the reduced thickness clad provides volume for additional ZrH.

Fuel Outer and Inner Diameter

Inner and outer fuel diameters have no effect on system reactivity at a fixed fuel mass. Maximum outer diameter (i.e., contact with the clad) and minimum inner diameter (i.e., contact with the center zirconium rod where applicable) provide for additional ZrH volume and, therefore, represent a bounding configuration.

Central Zirconium Rod Diameter

A change in the diameter of the central zirconium rod at a fixed fuel geometry has no significant system reactivity effect, as it involves neutronically transparent material. A minimum zirconium rod is bounding for the modified fuel dimensions (maximum ZrH).

Active Fuel Length

The reactivity variations associated with the active fuel length have distinctly different trends when considering a system at a fixed (nominal) ZrH quantity and for a system maximizing the ZrH quantity. At a fixed ZrH quantity, the minimum active fuel height compacts the fissile material region (potentially above theoretical density) and, therefore, increases system reactivity. At the maximum ZrH quantity, the effect of a compacted (reduced leakage) fuel region is offset by the reduced moderator ratio in the fuel region, resulting in a slight decrease in reactivity for a dry cask cavity and no statistically resolvable effect for a wet cask cavity (bounding for the finite array of casks modeled). Therefore, active fuel length variations have no significant effects on the highest system reactivity cases containing maximum ZrH.

Zirconium Content and H/Zr Ratio

The effect of zirconium mass changes at a fixed H/Zr ratio of 1.6 is illustrated in Figure 6.4.5-1 for a finite cask array of eight casks. Similar reactivity changes as a function of H/Zr ratio are shown in Figure 6.4.5-2. Both figures clearly demonstrate that maximum zirconium quantity and H/Zr ratio are bounding for the system. Analysis trends hold true for both wet and dry cask cavity cases. Note that the 20% enriched material curve indicates a higher reactivity than the 70% enriched curve for the H/Zr ratio study (dry cask cavity). This is the result of specifying an artificially high zirconium content of the fuel material. The composition for the 20 wt % rod with 2,300 grams of zirconium in the fuel results in a ZrH_x density of approximately 6.9 g/cm³, well above the actual density of 5.61 g/cm³. The 2,300 grams base value is obtained from a fuel element with only 41 grams of ²³⁵U versus 167 grams in the design basis element. Figure 6.4.5-3 demonstrates that a maximum fissile material content is bounding for fuel containing the maximum ZrH content feasible at a maximum H/Zr ratio of 2.0.

At the maximum ZrH quantity possible in the fuel rod, the 70 wt % case is bounding as demonstrated in Table 6.4.5-20 and discussed later in this section.

Maximum Reactivity Fuel Element Configuration

Fuel assembly characteristics are evaluated by allowing:

- Rod diameter to reach a maximum of 1.5 inches
- Clad to be reduced to 0.0001 cm (essentially a no clad case, allowing the basic KENO cells to be retained within the input file structure)
- Fuel outer diameter to be maximized into contact with the clad inner surface and be minimized by 0.1 inch (arbitrary value chosen for study purposes)
- Fuel inner diameter to be minimized into contact with the zirconium center rod (no maximum was evaluated as analysis trends all indicate a reduced fuel volume to be bounding)
- Zirconium inner rod to be reduced (minimum) to a 0.0001 cm radius (essentially a "no inner rod" case with the KENO cell for the rod retained) or increased (maximum) to contact the fuel inner diameter
- Active fuel length to be varied by 0.5 inch

As shown in Table 6.4.5-17, maximum system reactivity is achieved for a fuel element with the following characteristics:

- Maximum zirconium content

Calculated based on the physical dimensions of the fuel region and zirconium hydride at full density (occupying all nonuranium volume)

- Maximum H/Zr atom ratio (2.0)

Based on the H/Zr ratio study in the previous section having determined a maximum H/Zr ratio to be bounding for wet and dry cask configurations, all fuel element physical characteristic studies applied the maximum ratio of 2.0.

- Maximum rod outer diameter of 1.5 inches

Fixed fuel mass cases show a slight decrease in reactivity due to the additional clad volume (stainless steel) associated with a larger fuel rod at a constant clad thickness. When considering increased fuel diameter and the associated increase in volume for zirconium hydride, a maximum rod diameter is bounding.

- Minimum clad thickness

Provides a significant increase in reactivity as the result of reduced parasitic absorber and increased volume for the fuel. Note that bias adjusted reactivities for a 0.0001 cm clad case

exceed a 0.95 limit. Further evaluations documented in Table 6.4.5-18 indicate a model containing a 0.01 inch clad is sufficient to demonstrate reactivity below the 0.95 limit. This model change is adopted for the screened and sealed can evaluations.

- Maximum fuel outer diameter, minimum inner diameter and a minimum (removed) central rod

All three properties increase the potential fuel volume and, therefore, provide additional ZrH volume.

- No significant reactivity effect of fuel length for the bounding (wet) fuel configurations

The maximum active fuel length is specified to be a bounding configuration as it provides the largest amount of integral fuel moderator (ZrH) to the system.

Optimum Moderation, Fuel Element Location and Basket Manufacturing Tolerances

Reference criticality calculations for TRIGA fuel in either an infinite basket cell or infinite cask array configuration indicate that maximum system reactivity is obtained from a dry cask cavity with fuel elements shifted toward the basket center in a minimum opening size basket. Finite cask array calculations on the fuel parameters evaluated herein indicate that this configuration is not bounding for a finite cask array. Water in the model not only thermalizes neutrons to support reactions with the fissile material, but also absorbs neutrons. Since the TRIGA elements contain moderator in the fuel matrix, independent of the water in the element-to-basket gaps, an infinite array of casks provides significant neutronic interactions on a dry cask basis. In the finite array models, the additional neutrons supplied by other casks are significantly reduced, resulting in a system with a water cavity being bounding.

A sample evaluation of reactivity trends as a function of model configuration is shown in Table 6.4.5-19. The data demonstrate a sharp drop-off in reactivity as the number of fuel units is reduced (infinite basket unit cell to finite cask model, to finite cask array, and finally to a single cask model) for a dry cask, while reactivity for a wet cask remains relatively constant across array sizes. Initial reactivity studies for the 70 wt % enriched steel clad fuel at various moderator quantities (accomplished by varying fuel zirconium quantity at a fixed H/Zr ratio) confirm that system reactivity increases with increased moderator density, but levels off at densities above 0.5 g/cm³ (see Figure 6.4.5-4). At this level, increased moderation between elements in a basket opening is offset by reduced interaction between the basket opening, baskets in the cask, and casks in the array. Detailed moderator density studies for the system considering various fuel element moderator quantities (adjusted by H/Zr ratio), TRIGA element configuration (nominal and most reactive element), rod locations (shifted in – optimal for dry system; shifted to basket

corners – optimal for wet system), and basket opening size (minimum and maximum) are illustrated in Figure 6.4.5-5. These studies demonstrate that maximum reactivity is the result of:

- Fully moderated cask cavity (water density 1 g/cm³)
- Most reactive element configuration defined in the previous section
- Shifted out (to basket corners) fuel elements

No significant changes in reactivity occurred as the result of basket opening size changes for a fully flooded (maximum reactivity) basket configuration.

Maximum Intact Fuel Reactivity and Criticality Safety Index

Based on a 1.5-inch maximum rod diameter, a minimum clad thickness of 0.01 inch, a conservatively removed central zirconium rod, and a maximum ZrH content system, reactivities are calculated for each of the primary TRIGA fuel types. Results for the analyses are listed in Table 6.4.5-20. Maximum bias adjusted reactivity (k_s) for the revised TRIGA fuel description is 0.94842 ($k_{eff} = 0.93024 \pm 0.00069$) under accident conditions with a cask array limited to eight casks (CSI = 12.5). Table 6.4.5-4 also illustrates the large reactivity increase associated with the move from a nominal fuel element to the bounding configuration specified here.

The normal condition (intact neutron shield) maximum reactivity for the system is shown in Table 6.4.5-21 for an infinite cask array. Therefore, the CSI for intact fuel shipments is 12.5.

6.4.5.6.2 Screened and Sealed Can Criticality Evaluations for Severely Damaged Fuel (Up to Two Elements per Can)

The NAC-LWT system may be loaded with screened or sealed cans in the top and bottom basket modules. The sealed can was previously evaluated for a damaged content of up to two equivalent intact rods. Based on an accident cask condition (i.e., no neutron shield), reactivity evaluations for a finite array of eight casks are repeated in this section for the revised TRIGA fuel element definition. In addition, the screened can is similarly evaluated to contain up to two equivalent intact rods.

Screened and sealed can reactivity evaluations are performed at various cask cavity and can moderator combinations for a solid fuel material and for a fuel mixture filling the can cavity. The results plotted in Figure 6.4.5-6 demonstrate that the reactivity of the system is controlled by the uncanned baskets with no significant feedback from the can locations regardless of can fuel height or moderator fraction. Note that the can contents are limited to the equivalent of two fuel elements, while uncanned basket locations contain up to four rods. Similar results are obtained from a study of debris height at various can moderator densities as shown in Figure 6.4.5-7. The study demonstrates no statistically significant effect of debris height on system reactivity.

Revision 38

Maximum system reactivity was calculated at a k_{eff} of 0.93159 ± 0.00066 for a k_s of 0.94971 after adjusting for a calculation bias uncertainty of 0.0168 (code bias is an approximately 0.02 Δk over-prediction and is, therefore, set to 0 for the bias adjusted reactivity). This reactivity is not statistically different from that of the intact fuel. Since an eight-cask array was modeled under accident conditions, the system CSI is 12.5.

Maximum normal condition reactivity for an infinite array of casks containing cans with up to two TRIGA elements worth of fuel material is 0.92351 ± 0.00071 (wet cask and can).

The overall system CSI for casks containing cans with up to four fuel elements per can, including fuel debris, is 12.5.

6.4.5.6.3 Screened Can Criticality Evaluations (Four Elements per Can – Elements Retaining Structural Integrity)

The NAC-LWT system may be loaded with screened cans in the top and bottom basket modules. The screened can was previously evaluated for a content of up to four TRIGA elements that may be damaged (but retain their structural integrity for transport). Based on an accident cask condition (i.e., no neutron shield), reactivity evaluations for a finite array of casks are repeated in this section for the revised TRIGA fuel element definition.

Reactivity evaluations are performed at various cask cavity and can moderator combinations for four elements per can in an eight-cask array. The results plotted in Figure 6.4.5-8 demonstrate that the maximum reactivity is achieved by a dry cask cavity with a full density, preferentially flooded can. Bias adjusted reactivity for this system is slightly above 0.95. Evaluations are, therefore, repeated for a four-cask array (CSI = 25) with the corresponding results added to the Figure 6.4.5-8 plot. Maximum system reactivity for the four-cask array is k_{eff} of 0.92798 ± 0.00070 for a k_s of 0.94618. Moderator condition for the maximum reactivity case is a wet (1 g/cm^3) cask and wet can at 0.4 g/cm^3 moderator density (note that there is no statistically significant change in system reactivity as a function of can cavity moderator density).

Maximum normal condition reactivity for an infinite array of casks containing the screened cans with four TRIGA elements is 0.92484 ± 0.00068 (wet cask/wet can).

The overall system CSI for casks containing cans with up to four fuel elements per can, including fuel debris, is 25.

6.4.5.6.4 Revised Fuel Parameter Reactivity Summary

The reactivity evaluation of the NAC-LWT cask containing up to 120 TRIGA elements demonstrates that subcritical margin ($k_s \leq 0.95$) can be maintained under the following condition:

Parameter	Value
Maximum Number of Elements per Basket	4
Openings	
Fuel Material	U-ZrH _x
Rod Diameter	≤ 1.5 inches
Clad Thickness	≥ 0.01 inch
²³⁵ U Content per Element	≤ 41 g (20% enriched fuel – Al Clad)
	≤ 137 g (20% enriched fuel – SS Clad)
	≤ 169 g (70% enriched fuel – SS Clad)
Maximum Reactivity (k _s)	0.949

Due to limitations on the array size for accident conditions, the criticality safety index (CSI) for the package is 12.5 for loading of intact fuel and screened and sealed cans containing up to two fuel elements (in any condition, including severely damaged fuel and debris). Screened cans containing up to four elements are permitted with a CSI of 25. The four elements in the screened can may contain clad damage provided the elements maintain structural integrity through normal and accident conditions.

6.4.5.7 Conclusion

Thus, including all calculational and mechanical uncertainties, an infinite array of NAC-LWT casks remains sub-critical, and is below the 0.95 limit, corrected for bias and uncertainty, under normal and accident conditions with:

Nonpoisoned Baskets:

1. 120 TRIGA fuel elements.
2. Screened cans each with four TRIGA fuel elements, retaining structural integrity (top and bottom baskets only).
3. Sealed and screened cans (top and bottom baskets only) with two severely failed TRIGA fuel elements.

Poisoned Baskets:

1. 140 TRIGA fuel elements.
2. Screened cans each with four TRIGA fuel elements (top and bottom baskets only).
3. Sealed cans (top and bottom baskets only) with two TRIGA fuel elements.

Figure 6.4.5-1 Finite Cask Array Reactivity versus Fuel Zirconium Mass (Dry Cask Cavity)

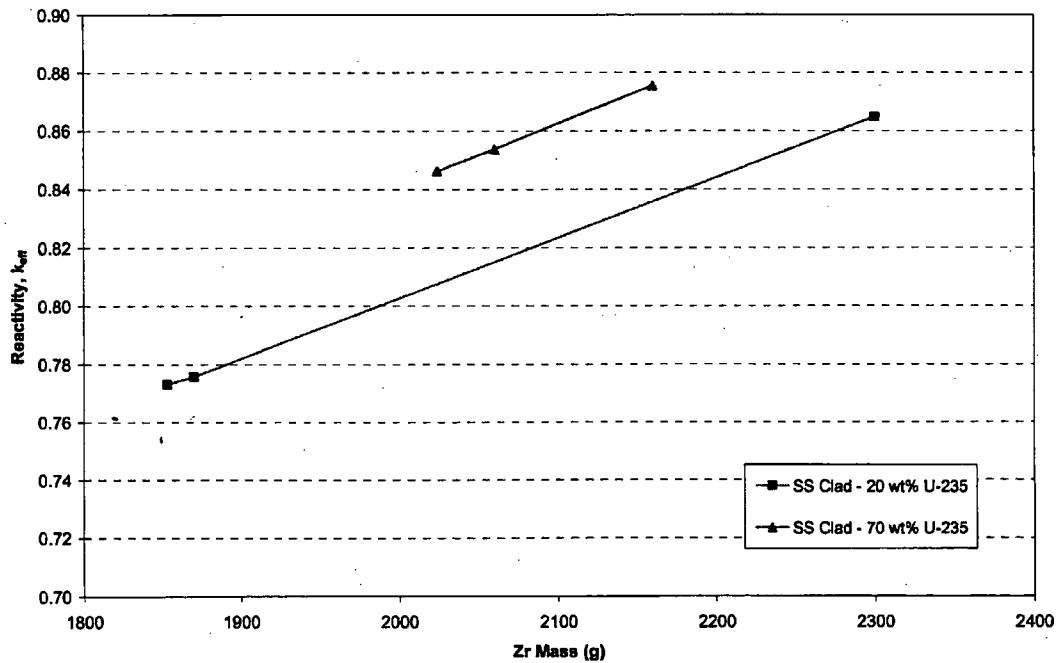


Figure 6.4.5-2 Finite Cask Array Reactivity versus H/Zr Ratio (Dry Cask Cavity)

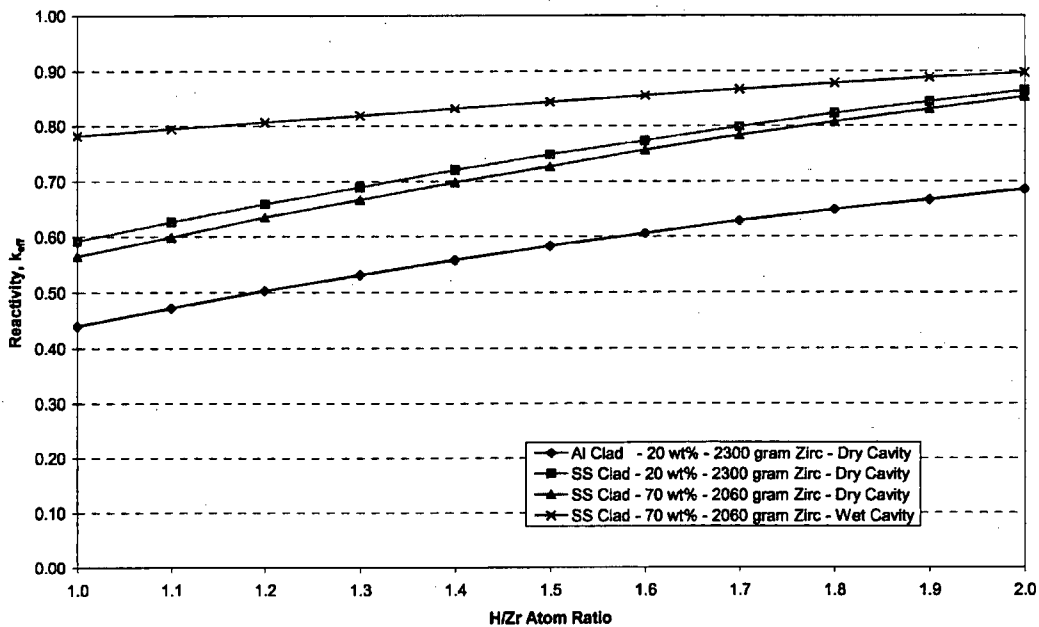


Figure 6.4.5-3 Finite Cask Array Reactivity versus Fuel Mass (Study of ZrH Displacement of Fissile Material for a Fixed Fuel Geometry)

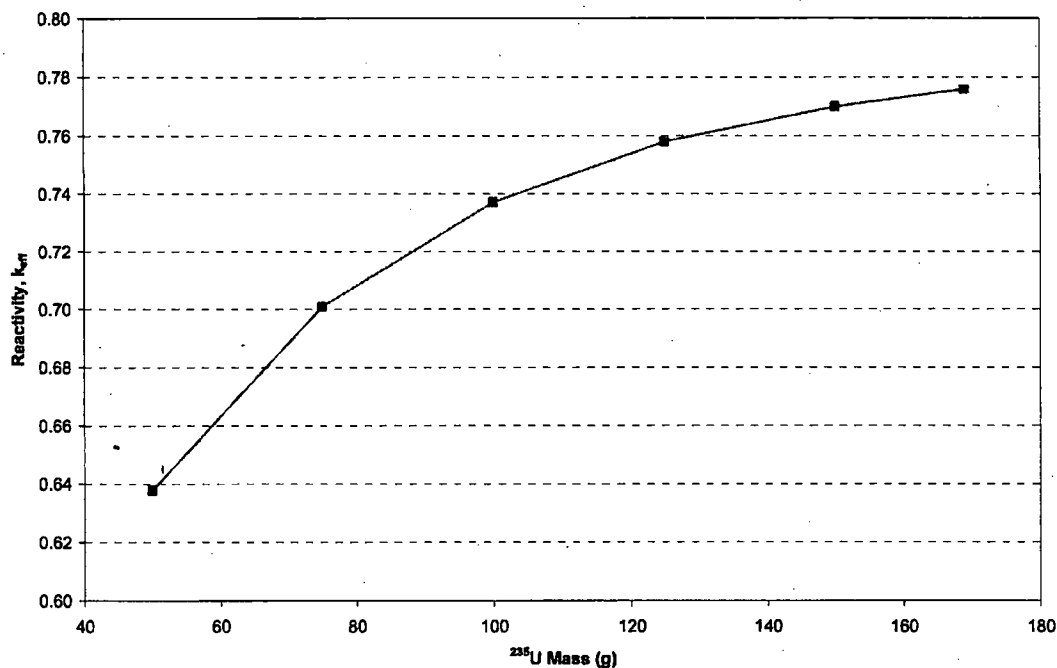


Figure 6.4.5-4 Intact Fuel Optimum Moderator Study – 70 wt % ^{235}U Various Zirconium Masses

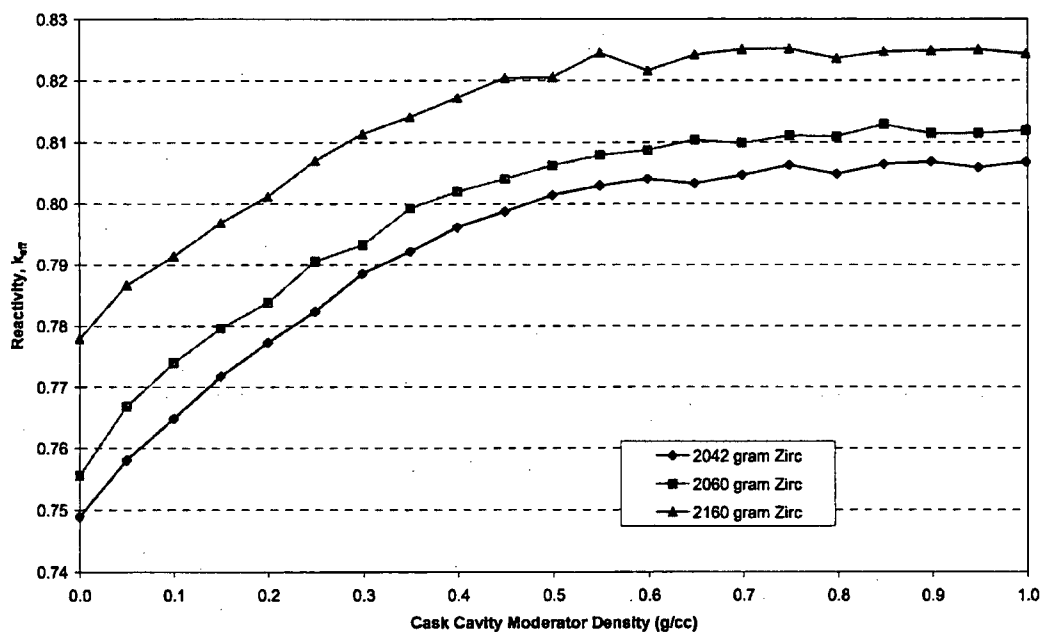


Figure 6.4.5-5 Detailed Intact Fuel Optimum Moderator Study – H/Zr Ratio, Fuel Element Characteristics and Location Varied

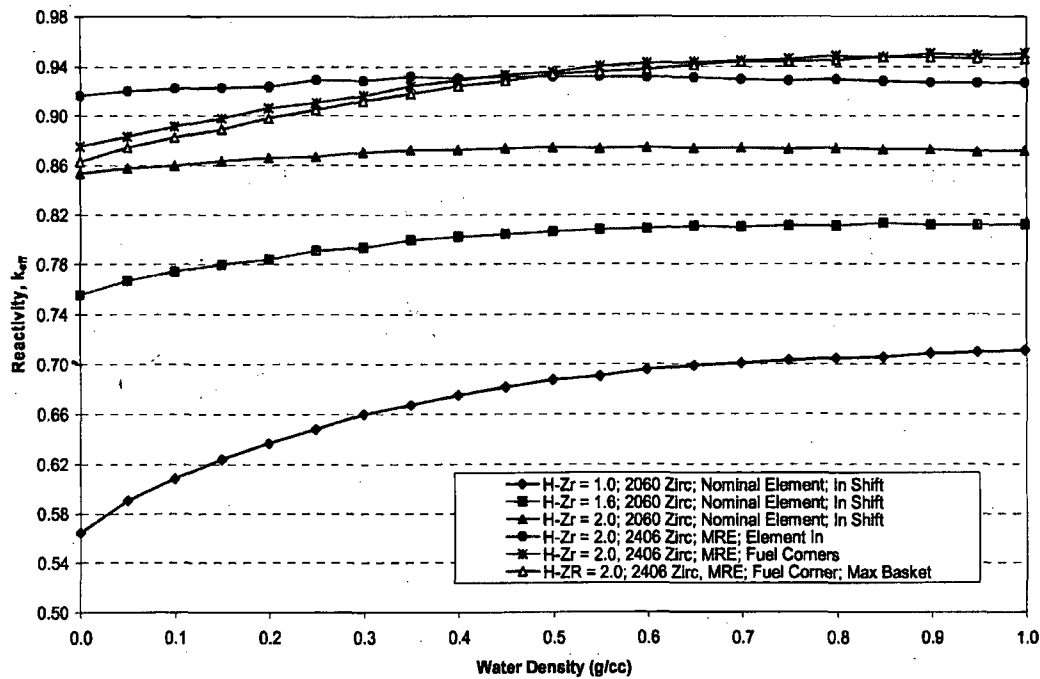
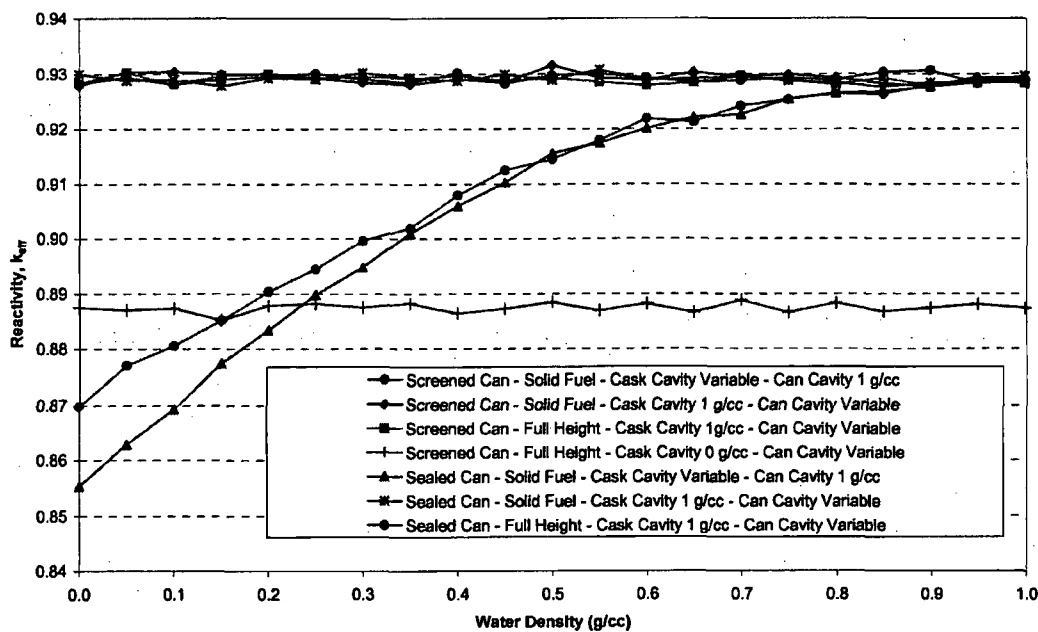
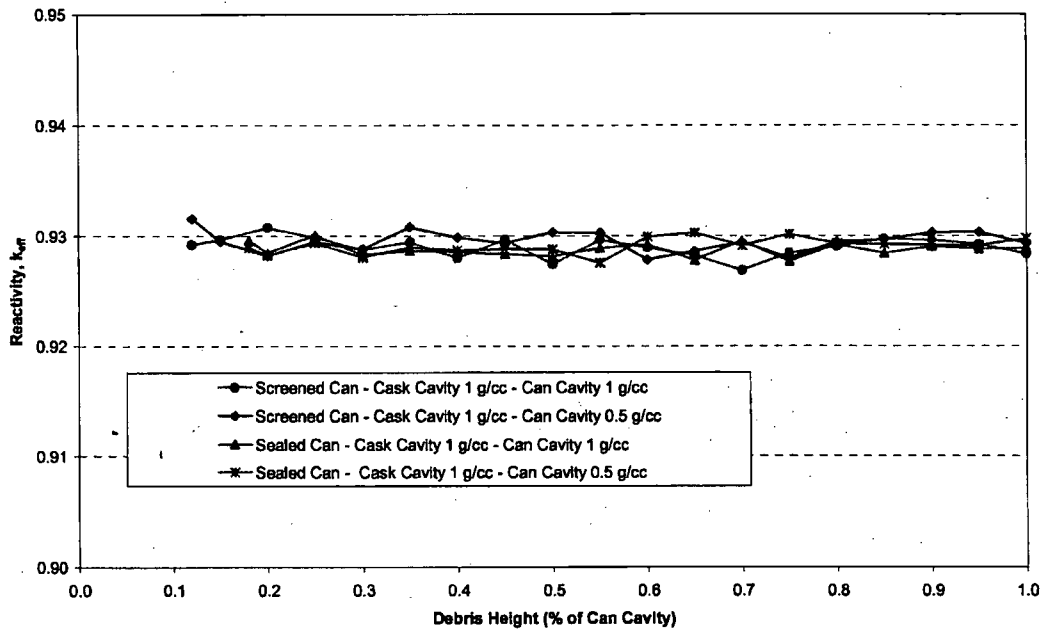


Figure 6.4.5-6 Screened and Sealed Can Optimum Moderator Study – Maximum Reactivity Fuel Configuration – 70 wt % ^{235}U Steel Clad



**Figure 6.4.5-7 Screened and Sealed Can Debris Height Study – Maximum Reactivity
Fuel Configuration – 70 wt % ^{235}U Steel Clad**



**Figure 6.4.5-8 Screened Can – 4 Elements per Can – Maximum Reactivity Fuel
Configuration – 70 wt % ^{235}U Steel Clad**

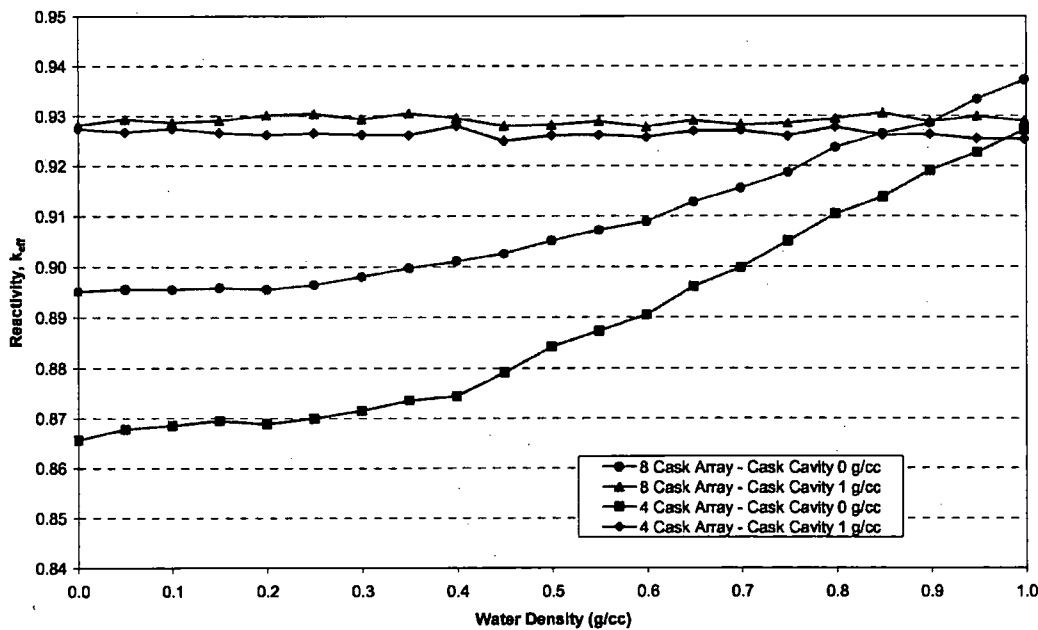


Table 6.4.5-1 Parametric Study – Fuel / Basket k-infinity versus TRIGA Fuel Element Type, Nonpoisoned Basket

(Infinite Array of Nonpoisoned TRIGA Basket Cells with Four (4) Elements)

Fuel Element Type	Initial U Content wt %	Total U grams	²³⁵ U wt %	Wet Case Results K(infinity) ± σ	Dry Case Results k(infinity) ± σ
Original Al Clad 14 inch Active Fuel	8-8.5	205	20.0	1.01740 ± 0.00081	1.04129 ± 0.00066
Original Al Clad 15 inch Active Fuel	8-8.5	205	20.0	1.00636 ± 0.00081	1.02634 ± 0.00065
Stand. Streamlined Steel Clad 15 inch Active Fuel (FLIP)	8.5	196	70.0	1.33900 ± 0.00094	1.43012 ± 0.00078
Stand. Plain Steel Clad 15 Active Fuel (FLIP)	8.5	196	70.0	1.33969 ± 0.00097	1.43009 ± 0.00077
Stand. Streamlined Steel Clad FLIP-LEU-II	30.6	845	20.0	1.28517 ± 0.00087	1.31180 ± 0.00073
Stand. Plain Steel Clad FLIP-LEU-II	30.6	845	20.0	1.28512 ± 0.00088	1.31198 ± 0.00072
FFCR Element FLIP-LEU-I	20.0	484	20.0	1.16407 ± 0.00086	1.23186 ± 0.00071
1-70 wt % ²³⁵ U + 3-20 wt % ²³⁵ U	--	--	--	1.30429 ± 0.00091	1.34060 ± 0.00071
3-70 wt % ²³⁵ U + 1-20 wt % ²³⁵ U	--	--	--	1.32896 ± 0.00092	1.40083 ± 0.00077
2-70 wt % ²³⁵ U + 2-20 wt % ²³⁵ U	--	--	--	1.31601 ± 0.00094	1.37156 ± 0.00076

LEU Low Enriched Uranium

FLIP Fuel Life Improvement Program

FFCR Fuel Follower Control Rod

* Resonance treatment for two different fuel types is included.

**Table 6.4.5-2 Parametric Study – Cask k_{eff} versus TRIGA Fuel Element Type,
Poisoned Basket**

Fuel Element Type	Initial U Content wt %	Total U grams	²³⁵ U wt %	Wet Case Results $k_{eff} \pm \sigma$	Dry Case Results $K_{eff} \pm \sigma$
Original Al Clad 15 inch Active Fuel	8-8.5	205	20.0	0.58906 ± 0.00097	0.47118 ± 0.00076
Stand. Streamlined Steel Clad 15 inch Active Fuel (FLIP)	8.5	196	70.0	0.86504 ± 0.00134	0.85705 ± 0.00112
Stand. Plain Steel Clad 15 Active Fuel (FLIP)	8.5	196	70.0	0.86647 ± 0.00137	0.86610 ± 0.00115
Stand. Streamlined Steel Clad FLIP-LEU-II	30.6	845	20.0	0.83413 ± 0.00130	0.80073 ± 0.00103
Stand. Plain Steel Clad FLIP-LEU-II	30.6	845	20.0	0.83604 ± 0.00127	0.80492 ± 0.00099
1-70 wt % ²³⁵ U + 3-20 wt % ²³⁵ U	--	--	--	0.84391 ± 0.00133	0.81589 ± 0.00101
3-70 wt % ²³⁵ U + 1-20 wt % ²³⁵ U	--	--	--	0.85826 ± 0.00131	0.84917 ± 0.00108
2-70 wt % ²³⁵ U + 2-20 wt % ²³⁵ U	--	--	--	0.85162 ± 0.00129	0.83177 ± 0.00103

Table 6.4.5-3 Axially Infinite Cask k_{eff} with TRIGA Fuel Elements- Fuel Element Placement Perturbations, Nonpoisoned Basket

Basket Configuration	Wet Case Results $k_{eff} \pm \sigma$	Dry Case Results $k_{eff} \pm \sigma$
Elements Touching, Moved In	-	0.93434 ± 0.00115
Elements Touching, Centered	0.77382 ± 0.00109	0.92672 ± 0.00185
Elements Out	0.83468 ± 0.00101	0.90817 ± 0.00105
Elements Centered, Quadrants	0.81340 ± 0.00107	-
Three - 70 wt % ^{235}U Elements (Equilateral)	0.83646 ± 0.00112	-
Three - 70 wt % ^{235}U Elements (in corner)	0.83579 ± 0.00101	0.80629 ± 0.00110
Three - 70 wt % ^{235}U Elements (Isosceles)	0.83468 ± 0.00101	-
Two - 70 wt % ^{235}U Elements (Center)	0.67480 ± 0.00097	0.63503 ± 0.00108
One - 70 wt % ^{235}U Elements (Center)	0.44428 ± 0.00091	-

Table 6.4.5-4 Axially Infinite Cask k_{eff} with TRIGA Fuel Elements - Fuel Element Placement Perturbations, Poisoned Basket

Basket Configuration	Wet Case Results $k_{eff} \pm \sigma$	Dry Case Results $k_{eff} \pm \sigma$
Elements Touching, Moved In	-	0.88969 ± 0.00122
Elements Touching, Centered	0.82705 ± 0.00136	0.87833 ± 0.00122
Elements Touching, Moved Out	-	0.87871 ± 0.00112
Elements Centered, Quadrants	0.86647 ± 0.00134	0.86610 ± 0.00115
Elements Out	0.87874 ± 0.00123	0.85348 ± 0.00114
27 Elements, Touching	0.85014 ± 0.00131	0.66829 ± 0.00114
27 Elements, Corners	0.84686 ± 0.00124	-
26 Elements, Touching	0.82959 ± 0.00124	0.64354 ± 0.00117
26 Elements, Corners	0.81959 ± 0.00126	-
21 Elements, Touching	0.70693 ± 0.00127	0.55021 ± 0.00110
21 Elements, Corners	0.73134 ± 0.00133	-
14 Elements, Touching	0.58154 ± 0.00136	0.39354 ± 0.00097
14 Elements, Corners	0.55112 ± 0.00117	-

Table 6.4.5-5 Axially Infinite Cask k_{eff} with TRIGA Fuel Elements – Basket Manufacturing Tolerance Perturbations, Nonpoisoned Basket

Basket Configuration	Wet Case Results w/ Dry Neutron Shield $k_{eff} \pm \sigma$	Dry Case Results $k_{eff} \pm \sigma$
Base Case ¹	0.86190 ± 0.00089^3	0.90053 ± 0.00115^4
Thin SS Plates	0.86861 ± 0.00094	0.90501 ± 0.00109
Maximum Basket Opening ²	0.86864 ± 0.00097	0.90023 ± 0.00107
Minimum Basket Opening ²	0.86489 ± 0.00091	0.90817 ± 0.00105

Notes:

1. Both wet and dry base case configurations include elements out to corners of basket openings.
2. Incorporates minimum thickness stainless steel, basket divider plates.
3. Comparable to the “elements out,” $k_{eff} = 0.83468 \pm 0.00101$, configuration of Table 6.4.5-3 except the neutron shield is dry.
4. Incorporates the “elements out” configuration.

Table 6.4.5-6 Axially Infinite Cask k_{eff} with TRIGA Fuel Elements – Basket Manufacturing Tolerance Perturbations, Poisoned Basket

Basket Configuration	Wet Case Results $k_{eff} \pm \sigma$	Dry Case Results $k_{eff} \pm \sigma$
Base Case ¹	0.87874 ± 0.00123	0.88969 ± 0.00122
Minimum Opening ²	0.87832 ± 0.00127	0.89054 ± 0.00107
Increased Central Opening ²	0.87981 ± 0.00133	0.88722 ± 0.00118
Increased Exterior Openings ²	0.87875 ± 0.00134	0.88998 ± 0.00120
Increased Central Opening, Decreased Exterior Openings ²	0.87475 ± 0.00134	0.88724 ± 0.00116

Notes:

1. Most reactive configurations from Table 6.4.5-4.
2. Incorporates minimum thickness stainless steel, basket divider plates.

Table 6.4.5-7 Screened Can Preferential Flooding and Partial Loading Reactivity Evaluations for TRIGA Fuel Elements, Nonpoisoned and Poisoned Baskets

Description	$k_{eff} \pm \sigma$ Nonpoisoned Basket	$k_{eff} \pm \sigma$ Poisoned Basket
Wet Cask / Wet Can	0.84040 ± 0.00132	0.88010 ± 0.00139
Dry Cask / Dry Can	0.89383 ± 0.00120	0.86228 ± 0.00128
Dry Cask / Wet Can – Elements To Center of Cask	0.89778 ± 0.00124	0.88272 ± 0.00124
Dry Cask / Wet Can – Elements To Center of Can	0.89435 ± 0.00124	0.87727 ± 0.00124
Dry Cask / Wet Can – Elements Quadrant Centered	0.89821 ± 0.00129	0.88737 ± 0.00123
Dry Cask / Wet Can – Elements in Corners	0.90926 ± 0.00126	0.89957 ± 0.00118
Dry Cask / Wet Can – Elements in Corners, Max. Can	0.90673 ± 0.00123	0.90224 ± 0.00128
18 Elements per Basket Module	0.84896 ± 0.00121	0.82527 ± 0.00114
12 Elements per Basket Module	0.82532 ± 0.00125	0.80281 ± 0.00119

Table 6.4.5-8 Sealed Can Preferential Flooding and Partial Loading Reactivity Evaluations for TRIGA Fuel Elements, Nonpoisoned and Poisoned Baskets

Description	$k_{\text{eff}} \pm \sigma$ Nonpoisoned Basket	$k_{\text{eff}} \pm \sigma$ Poisoned Basket
Wet Cask / Wet Can, Elements Out	-	0.88574 ± 0.00130
Wet Cask / Wet Can	0.84331 ± 0.00129	0.88036 ± 0.00125
Dry Cask / Dry Can	0.85693 ± 0.00121	0.83021 ± 0.00118
Dry Cask / Wet Can	0.84376 ± 0.00129	0.78084 ± 0.00114
2 Rods per Can - 3 Five Inch Fuel Pellets	0.84346 ± 0.00128	0.88212 ± 0.00133
Mixture Solid (No Moderator)- 2 Rods Per Can	0.87512 ± 0.00122	0.88371 ± 0.00125
Mixture Half Can Height - 2 Rods Per Can	0.90691 ± 0.00212	0.88564 ± 0.00146
Mixture Full Can Height - 2 Rods Per Can	0.91088 ± 0.00106	0.88411 ± 0.00129
Mixture - Solid (No Moderator) - 1 Rod Per Can	0.85868 ± 0.00132	0.88472 ± 0.00131
Mixture - Half Can Height - 1 Rod Per Can	0.87411 ± 0.00117	0.88204 ± 0.00130
Mixture - Full Can Height - 1 Rod Per Can	0.85913 ± 0.00117	0.88477 ± 0.00142
2 Rods Per Can + Graphite – Solid	0.87208 ± 0.00117	0.88616 ± 0.00138
2 Rods Per Can + Graphite – Full Can Height	0.89867 ± 0.00118	0.88431 ± 0.00129
Increased Can Diameter (+0.02 inch) ¹	0.91355 ± 0.00119	0.88436 ± 0.00138

Note:

1. The increased can diameter cases were analyzed using the most reactive cases for each basket configuration (nonpoisoned / poisoned). The “Wet Cask / Wet Can, Elements Out” case was selected for the poisoned basket configuration due to the lack of statistically significant differences in the above reported results.

Table 6.4.5-9 Summary of Most Reactive Configurations, TRIGA Fuel Elements, Nonpoisoned Basket

	Wet	Dry	Preferential
Intact Fuel	0.86861 ± 0.00094	0.93434 ± 0.00115^1	-
Screened Fuel Cans	0.84040 ± 0.00132	0.89383 ± 0.00120	0.90926 ± 0.00126
Sealed Fuel Cans	0.84331 ± 0.00129	0.85693 ± 0.00121	0.91355 ± 0.00199

Note:

1. As reported in Section 6.4.5.4, this case is reevaluated with a finite axial length model, making the preferentially flooded, sealed can case the most reactive.

Table 6.4.5-10 Summary of Most Reactive Configurations, TRIGA Fuel Elements, Poisoned Basket

	Wet	Dry	Preferential
Intact Fuel	0.87874 ± 0.00123	0.88969 ± 0.00122	-
Screened Fuel Cans	0.88010 ± 0.00139	0.86228 ± 0.00128	0.90224 ± 0.00128
Sealed Fuel Cans	0.88574 ± 0.00130	0.83021 ± 0.00118	0.88564 ± 0.00146

Table 6.4.5-11 Reactivity Results for TRIGA Fuel Elements, Sealed Cans, Normal Conditions, Nonpoisoned Basket

Moderator SG	Casks Touching ($k_{eff} \pm \sigma$)	8 Foot Center-To-Center ($k_{eff} \pm \sigma$)
Dry Exterior, Vary Internal Density		
0.00000	0.7239 \pm 0.0012	0.7203 \pm 0.0012
0.00100	0.7205 \pm 0.0012	0.7212 \pm 0.0012
0.00178	0.7231 \pm 0.0013	0.7201 \pm 0.0012
0.00316	0.7216 \pm 0.0012	0.7202 \pm 0.0012
0.00562	0.7227 \pm 0.0012	0.7181 \pm 0.0012
0.01000	0.7234 \pm 0.0012	0.7224 \pm 0.0012
0.01780	0.7205 \pm 0.0012	0.7223 \pm 0.0013
0.03160	0.7249 \pm 0.0012	0.7242 \pm 0.0012
0.05620	0.7263 \pm 0.0012	0.7285 \pm 0.0012
0.10000	0.7295 \pm 0.0012	0.7303 \pm 0.0012
0.17800	0.7446 \pm 0.0012	0.7415 \pm 0.0012
0.31600	0.7674 \pm 0.0012	0.7647 \pm 0.0013
0.56200	0.7887 \pm 0.0013	0.7884 \pm 0.0013
0.70000	0.7977 \pm 0.0014	0.7961 \pm 0.0014
0.80000	0.8009 \pm 0.0013	0.7974 \pm 0.0013
0.90000	0.8000 \pm 0.0013	0.8008 \pm 0.0012
1.00000	0.8020 \pm 0.0013	0.8022 \pm 0.0014
Optimally Moderated Cask Interior (SG = 1.0), Vary External Density		
0.00000	0.8020 \pm 0.0013	0.8022 \pm 0.0013
0.00100	0.8013 \pm 0.0014	0.8010 \pm 0.0013
0.00178	0.7993 \pm 0.0014	0.8003 \pm 0.0013
0.00316	0.8017 \pm 0.0014	0.8024 \pm 0.0013
0.00562	0.8041 \pm 0.0014	0.8002 \pm 0.0013
0.01000	0.8018 \pm 0.0013	0.8032 \pm 0.0013
0.01780	0.8025 \pm 0.0013	0.8018 \pm 0.0013
0.03160	0.8001 \pm 0.0013	0.8023 \pm 0.0013
0.05620	0.8004 \pm 0.0014	0.7993 \pm 0.0013
0.10000	0.8008 \pm 0.0012	0.8000 \pm 0.0013
0.17800	0.8018 \pm 0.0014	0.8019 \pm 0.0013
0.31600	0.8034 \pm 0.0014	0.8019 \pm 0.0013
0.56200	0.7996 \pm 0.0013	0.8025 \pm 0.0013
0.70000	0.8018 \pm 0.0014	0.8026 \pm 0.0014
0.80000	0.8013 \pm 0.0013	0.8009 \pm 0.0013
0.90000	0.7998 \pm 0.0013	0.8009 \pm 0.0012
1.00000	0.8019 \pm 0.0015	0.8003 \pm 0.0013
Vary Internal and External Density Simultaneously		
0.00000	0.7239 \pm 0.0012	0.7203 \pm 0.0013
0.00100	0.7212 \pm 0.0012	0.7192 \pm 0.0012
0.00178	0.7210 \pm 0.0011	0.7236 \pm 0.0012
0.00316	0.7202 \pm 0.0012	0.7217 \pm 0.0012
0.00562	0.7225 \pm 0.0012	0.7218 \pm 0.0012
0.01000	0.7229 \pm 0.0012	0.7236 \pm 0.0012
0.01780	0.7230 \pm 0.0012	0.7239 \pm 0.0012
0.03160	0.7253 \pm 0.0013	0.7236 \pm 0.0012
0.05620	0.7273 \pm 0.0012	0.7261 \pm 0.0013
0.10000	0.7311 \pm 0.0012	0.7296 \pm 0.0013
0.17800	0.7439 \pm 0.0013	0.7429 \pm 0.0012
0.31600	0.7634 \pm 0.0013	0.7650 \pm 0.0013
0.56200	0.7882 \pm 0.0014	0.7898 \pm 0.0013
0.70000	0.7950 \pm 0.0014	0.7941 \pm 0.0012
0.80000	0.7950 \pm 0.0013	0.7973 \pm 0.0013
0.90000	0.7984 \pm 0.0012	0.8002 \pm 0.0012
1.00000	0.8000 \pm 0.0013	0.8029 \pm 0.0014

Table 6.4.5-12 Reactivity Results for TRIGA Fuel Elements, Sealed Cans, Accident Conditions, Nonpoisoned Basket

Moderator SG	Casks Touching ($k_{eff} \pm \sigma$)	8 Foot Center-To-Center ($k_{eff} \pm \sigma$)
Dry Exterior and Neutron Shield, Vary Internal Moderator		
0.00000	0.9136 \pm 0.0012	0.9057 \pm 0.0011
0.00100	0.9119 \pm 0.0012	0.9054 \pm 0.0011
0.00178	0.9101 \pm 0.0012	0.9041 \pm 0.0011
0.00316	0.9110 \pm 0.0011	0.9040 \pm 0.0011
0.00562	0.9095 \pm 0.0012	0.9046 \pm 0.0011
0.01000	0.9059 \pm 0.0012	0.8999 \pm 0.0012
0.01780	0.9021 \pm 0.0012	0.8979 \pm 0.0012
0.03160	0.8965 \pm 0.0012	0.8908 \pm 0.0011
0.05620	0.8842 \pm 0.0013	0.8793 \pm 0.0012
0.10000	0.8660 \pm 0.0012	0.8622 \pm 0.0012
0.17800	0.8432 \pm 0.0012	0.8419 \pm 0.0012
0.31600	0.8275 \pm 0.0013	0.8222 \pm 0.0012
0.56200	0.8185 \pm 0.0013	0.8153 \pm 0.0014
0.70000	0.8144 \pm 0.0013	0.8124 \pm 0.0013
0.80000	0.8140 \pm 0.0013	0.8091 \pm 0.0013
0.90000	0.8154 \pm 0.0012	0.8082 \pm 0.0013
1.00000	0.8117 \pm 0.0013	0.8081 \pm 0.0013
Optimally Moderated Internal (SG = 0.0), Vary Neutron Shield and Exterior		
0.00000	0.9136 \pm 0.0012	0.9057 \pm 0.0011
0.00100	0.8950 \pm 0.0011	0.8208 \pm 0.0012
0.00178	0.8887 \pm 0.0011	0.7931 \pm 0.0012
0.00316	0.8732 \pm 0.0012	0.7651 \pm 0.0012
0.00562	0.8505 \pm 0.0012	0.7454 \pm 0.0011
0.01000	0.8210 \pm 0.0011	0.7311 \pm 0.0012
0.01780	0.7957 \pm 0.0012	0.7233 \pm 0.0012
0.03160	0.7655 \pm 0.0012	0.7192 \pm 0.0011
0.05620	0.7432 \pm 0.0012	0.7195 \pm 0.0013
0.10000	0.7325 \pm 0.0013	0.7177 \pm 0.0012
0.17800	0.7252 \pm 0.0011	0.7206 \pm 0.0012
0.31600	0.7216 \pm 0.0012	0.7213 \pm 0.0012
0.56200	0.7211 \pm 0.0012	0.7211 \pm 0.0012
0.70000	0.7199 \pm 0.0012	0.7190 \pm 0.0012
0.80000	0.7213 \pm 0.0012	0.7184 \pm 0.0012
0.90000	0.7183 \pm 0.0013	0.7196 \pm 0.0012
1.00000	0.7189 \pm 0.0011	0.7194 \pm 0.0013
Vary Interior, Exterior and Neutron Shield Simultaneously		
0.00000	0.9136 \pm 0.0012	0.9057 \pm 0.0011
0.00100	0.8964 \pm 0.0012	0.8189 \pm 0.0012
0.00178	0.8879 \pm 0.0011	0.7913 \pm 0.0013
0.00316	0.8726 \pm 0.0012	0.7673 \pm 0.0013
0.00562	0.8496 \pm 0.0011	0.7459 \pm 0.0012
0.01000	0.8223 \pm 0.0012	0.7345 \pm 0.0012
0.01780	0.7903 \pm 0.0012	0.7237 \pm 0.0012
0.03160	0.7685 \pm 0.0012	0.7223 \pm 0.0011
0.05620	0.7504 \pm 0.0012	0.7242 \pm 0.0012
0.10000	0.7415 \pm 0.0013	0.7296 \pm 0.0012
0.17800	0.7445 \pm 0.0013	0.7404 \pm 0.0013
0.31600	0.7674 \pm 0.0013	0.7658 \pm 0.0013
0.56200	0.7904 \pm 0.0013	0.7898 \pm 0.0013
0.70000	0.7972 \pm 0.0014	0.7936 \pm 0.0014
0.80000	0.7969 \pm 0.0013	0.7956 \pm 0.0014
0.90000	0.8003 \pm 0.0013	0.8007 \pm 0.0013
1.00000	0.8000 \pm 0.0013	0.8013 \pm 0.0013

Table 6.4.5-13 Reactivity Results for TRIGA Fuel Elements, Screened Cans, Normal Conditions, Poisoned Basket

Moderator SG	Casks Touching ($k_{eff} \pm \sigma$)	8 Foot Center-To-Center ($k_{eff} \pm \sigma$)
Dry Exterior, Vary Internal Density		
0.00000	0.8376 \pm 0.0018	0.8381 \pm 0.0017
0.00100	0.8408 \pm 0.0017	0.8418 \pm 0.0016
0.00178	0.8408 \pm 0.0018	0.8412 \pm 0.0018
0.00316	0.8390 \pm 0.0017	0.8432 \pm 0.0016
0.00562	0.8371 \pm 0.0017	0.8399 \pm 0.0017
0.01000	0.8420 \pm 0.0017	0.8397 \pm 0.0018
0.01780	0.8383 \pm 0.0017	0.8419 \pm 0.0017
0.03160	0.8413 \pm 0.0017	0.8427 \pm 0.0017
0.05620	0.8466 \pm 0.0017	0.8448 \pm 0.0017
0.10000	0.8433 \pm 0.0016	0.8479 \pm 0.0017
0.17800	0.8510 \pm 0.0017	0.8502 \pm 0.0017
0.31600	0.8497 \pm 0.0016	0.8505 \pm 0.0016
0.56200	0.8453 \pm 0.0017	0.8484 \pm 0.0017
0.70000	0.8444 \pm 0.0016	0.8464 \pm 0.0017
0.80000	0.8321 \pm 0.0017	0.8432 \pm 0.0017
0.90000	0.8458 \pm 0.0017	0.8437 \pm 0.0017
1.00000	0.8527 \pm 0.0017	0.8540 \pm 0.0017
Optimally Moderated Cask Interior (SG = 1.0), Vary External Density		
0.00000	0.8527 \pm 0.0017	0.8540 \pm 0.0017
0.00100	0.8482 \pm 0.0018	0.8513 \pm 0.0016
0.00178	0.8532 \pm 0.0017	0.8513 \pm 0.0016
0.00316	0.8516 \pm 0.0017	0.8531 \pm 0.0017
0.00562	0.8546 \pm 0.0017	0.8539 \pm 0.0017
0.01000	0.8521 \pm 0.0018	0.8517 \pm 0.0019
0.01780	0.8528 \pm 0.0018	0.8515 \pm 0.0018
0.03160	0.8543 \pm 0.0017	0.8526 \pm 0.0017
0.05620	0.8506 \pm 0.0018	0.8503 \pm 0.0017
0.10000	0.8523 \pm 0.0018	0.8542 \pm 0.0016
0.17800	0.8507 \pm 0.0018	0.8478 \pm 0.0016
0.31600	0.8539 \pm 0.0017	0.8518 \pm 0.0016
0.56200	0.8545 \pm 0.0017	0.8525 \pm 0.0017
0.70000	0.8512 \pm 0.0017	0.8534 \pm 0.0017
0.80000	0.8548 \pm 0.0017	0.8529 \pm 0.0017
0.90000	0.8523 \pm 0.0016	0.8522 \pm 0.0017
1.00000	0.8540 \pm 0.0018	0.8523 \pm 0.0017
Vary Internal and External Density Simultaneously		
0.00000	0.8376 \pm 0.0018	0.8381 \pm 0.0017
0.00100	0.8396 \pm 0.0017	0.8382 \pm 0.0017
0.00178	0.8404 \pm 0.0016	0.8404 \pm 0.0017
0.00316	0.8430 \pm 0.0016	0.8413 \pm 0.0017
0.00562	0.8448 \pm 0.0017	0.8391 \pm 0.0016
0.01000	0.8400 \pm 0.0017	0.8398 \pm 0.0017
0.01780	0.8419 \pm 0.0017	0.8424 \pm 0.0018
0.03160	0.8394 \pm 0.0017	0.8439 \pm 0.0017
0.05620	0.8437 \pm 0.0017	0.8385 \pm 0.0017
0.10000	0.8477 \pm 0.0017	0.8477 \pm 0.0017
0.17800	0.8502 \pm 0.0017	0.8469 \pm 0.0017
0.31600	0.8463 \pm 0.0017	0.8494 \pm 0.0018
0.56200	0.8484 \pm 0.0017	0.8513 \pm 0.0017
0.70000	0.8471 \pm 0.0017	0.8459 \pm 0.0018
0.80000	0.8440 \pm 0.0017	0.8462 \pm 0.0016
0.90000	0.8429 \pm 0.0017	0.8451 \pm 0.0017
1.00000	0.8540 \pm 0.0018	0.8523 \pm 0.0017

Table 6.4.5-14 Reactivity Results for TRIGA Fuel Elements, Screened Cans, Accident Conditions, Poisoned Basket

Moderator SG	Casks Touching ($k_{eff} \pm \sigma$)	8 Foot Center-To-Center ($k_{eff} \pm \sigma$)
Dry Exterior and Neutron Shield, Vary Internal Moderator		
0.00000	0.9022 \pm 0.0015	0.9015 \pm 0.0016
0.00100	0.9019 \pm 0.0016	0.9022 \pm 0.0016
0.00178	0.8998 \pm 0.0016	0.9003 \pm 0.0016
0.00316	0.8992 \pm 0.0016	0.9009 \pm 0.0016
0.00562	0.8995 \pm 0.0017	0.9015 \pm 0.0017
0.01000	0.8998 \pm 0.0017	0.8956 \pm 0.0017
0.01780	0.8979 \pm 0.0017	0.9003 \pm 0.0017
0.03160	0.8966 \pm 0.0018	0.8946 \pm 0.0016
0.05620	0.8949 \pm 0.0015	0.8889 \pm 0.0015
0.10000	0.8893 \pm 0.0018	0.8844 \pm 0.0017
0.17800	0.8843 \pm 0.0018	0.8822 \pm 0.0016
0.31600	0.8772 \pm 0.0017	0.8765 \pm 0.0016
0.56200	0.8635 \pm 0.0018	0.8640 \pm 0.0017
0.70000	0.8586 \pm 0.0017	0.8657 \pm 0.0017
0.80000	0.8620 \pm 0.0016	0.8594 \pm 0.0016
0.90000	0.8622 \pm 0.0016	0.8600 \pm 0.0017
1.00000	0.8662 \pm 0.0017	0.8629 \pm 0.0018
Optimally Moderated Internal (SG = 0.0), Vary Neutron Shield and Exterior		
0.00000	0.9022 \pm 0.0015	0.9015 \pm 0.0016
0.00100	0.8970 \pm 0.0016	0.8644 \pm 0.0017
0.00178	0.8910 \pm 0.0016	0.8596 \pm 0.0018
0.00316	0.8862 \pm 0.0015	0.8542 \pm 0.0016
0.00562	0.8789 \pm 0.0016	0.8457 \pm 0.0016
0.01000	0.8687 \pm 0.0015	0.8438 \pm 0.0017
0.01780	0.8618 \pm 0.0017	0.8409 \pm 0.0018
0.03160	0.8539 \pm 0.0016	0.8386 \pm 0.0017
0.05620	0.8482 \pm 0.0017	0.8403 \pm 0.0018
0.10000	0.8427 \pm 0.0015	0.8381 \pm 0.0017
0.17800	0.8433 \pm 0.0017	0.8418 \pm 0.0016
0.31600	0.8424 \pm 0.0018	0.8405 \pm 0.0018
0.56200	0.8422 \pm 0.0017	0.8391 \pm 0.0017
0.70000	0.8438 \pm 0.0017	0.8399 \pm 0.0016
0.80000	0.8429 \pm 0.0018	0.8407 \pm 0.0017
0.90000	0.8423 \pm 0.0017	0.8445 \pm 0.0016
1.00000	0.8398 \pm 0.0016	0.8383 \pm 0.0017
Vary Interior, Exterior and Neutron Shield Simultaneously		
0.00000	0.9022 \pm 0.0015	0.9015 \pm 0.0016
0.00100	0.8948 \pm 0.0016	0.8662 \pm 0.0016
0.00178	0.8932 \pm 0.0017	0.8577 \pm 0.0016
0.00316	0.8881 \pm 0.0016	0.8524 \pm 0.0017
0.00562	0.8762 \pm 0.0016	0.8429 \pm 0.0017
0.01000	0.8722 \pm 0.0017	0.8431 \pm 0.0017
0.01780	0.8628 \pm 0.0016	0.8412 \pm 0.0017
0.03160	0.8586 \pm 0.0016	0.8450 \pm 0.0017
0.05620	0.8533 \pm 0.0017	0.8448 \pm 0.0018
0.10000	0.8496 \pm 0.0017	0.8458 \pm 0.0017
0.17800	0.8494 \pm 0.0017	0.8489 \pm 0.0017
0.31600	0.8500 \pm 0.0017	0.8459 \pm 0.0017
0.56200	0.8489 \pm 0.0018	0.8488 \pm 0.0018
0.70000	0.8443 \pm 0.0017	0.8463 \pm 0.0017
0.80000	0.8459 \pm 0.0017	0.8407 \pm 0.0018
0.90000	0.8421 \pm 0.0017	0.8483 \pm 0.0017
1.00000	0.8540 \pm 0.0018	0.8504 \pm 0.0019

Table 6.4.5-15 Single Package 10 CFR 71.55(b)(3) Evaluation k_{eff} Summary, TRIGA Fuel Element, Nonpoisoned Basket

Description	$k_{eff} \pm \sigma$	k_s
Single Cask / Inner Shell Reflected with H ₂ O	0.80664 ± 0.00136	0.82616
Single Cask / Inner Shell and Lead Reflected with H ₂ O	0.84194 ± 0.00130	0.86134
Single Cask / Inner Shell, Lead & Outer Shell Reflected with H ₂ O	0.84398 ± 0.00128	0.86334
Single Intact Cask Reflected with H ₂ O	0.84446 ± 0.00126	0.86392

Table 6.4.5-16 Single Package 10 CFR 71.55(b)(3) Evaluation k_{eff} Summary, TRIGA Fuel Element, Poisoned Basket

Description	$k_{eff} \pm \sigma$	k_s
Single Cask / Inner Shell Reflected with H ₂ O	0.85480 ± 0.00135	0.87430
Single Cask / Inner Shell and Lead Reflected with H ₂ O	0.87788 ± 0.00136	0.89740
Single Cask / Inner Shell, Lead & Outer Shell Reflected with H ₂ O	0.88369 ± 0.00133	0.90315
Single Intact Cask Reflected with H ₂ O	0.88117 ± 0.00131	0.90059

Table 6.4.5-17 Fuel Element Physical Characteristics Evaluation

Parameter							Cask Cavity Moderator Condition/Fuel Location							
							Dry - In Shift		0.5 g/cc - In Shift		1 g/cc - In Shift		1 g/cc - Shifted Out	
Fuel Rod OD	Clad Thickness	Fuel OD	Fuel ID	Active Fuel Length	Zirc Interior Rod OD	Zirc Mass (gram)	k_{eff}	$\Delta k/\sigma$	k_{eff}	$\Delta k/\sigma$	k_{eff}	$\Delta k/\sigma$	k_{eff}	$\Delta k/\sigma$
Nominal	Nominal	Nominal	Nominal	Nominal	Nominal	2059	0.85521	-	0.87591	-	0.87217	-	0.89939	-
Max	Nominal	Nominal	Nominal	Nominal	Nominal	2059	0.85102	-2.8	0.87063	-5.6	0.86795	-4.4	0.89480	-4.8
Nominal	Min	Nominal	Nominal	Nominal	Nominal	2059	0.85966	6.2	0.88920	14.0	0.89067	19.4	0.92184	23.3
Nominal	Nominal	Min	Nominal	Nominal	Nominal	1765	0.78425	-72.2	0.82168	-58.1	0.82388	-51.7	0.85987	-42.6
Nominal	Nominal	Max	Nominal	Nominal	Nominal	2068	0.85611	2.6	0.87530	-0.6	0.87327	1.2	0.90107	1.8
Nominal	Nominal	Nominal	Min	Nominal	Nominal	2071	0.85409	0.4	0.87776	2.0	0.87334	1.2	0.90196	2.7
Nominal	Nominal	Nominal	Nominal	Min	Nominal	1988	0.84974	-4.2	0.87304	-3.0	0.87192	-0.3	0.89885	-0.6
Nominal	Nominal	Nominal	Nominal	Max	Nominal	2129	0.85762	4.2	0.87705	1.2	0.87078	-1.5	0.89995	0.6
Nominal	Nominal	Nominal	Nominal	Nominal	Min	2059	0.85370	0.0	0.87322	-2.8	0.87095	-1.3	0.89785	-1.6
Nominal	Nominal	Nominal	Nominal	Nominal	Max	2059	0.85360	-0.1	0.87502	-0.9	0.87125	-1.0	0.89966	0.3
Nominal	Min	Max	Nominal	Nominal	Nominal	2191	0.88846	36.9	0.91259	37.9	0.91057	39.6	0.93977	42.6
Max	Min	Max	Nominal	Nominal	Nominal	2261	0.89797	46.7	0.92086	47.8	0.91631	44.9	0.94365	46.4
Max	Min	Max	Nominal	Nominal	Min	2261	0.89729	45.3	0.92035	46.6	0.91583	46.1	0.94260	44.9
Max	Min	Max	Min	Nominal	Min	2327	0.91165	60.7	0.92950	55.7	0.92648	56.0	0.94983	51.3
Max	Min	Max	Min	Max	Min	2406	0.91646	66.2	0.93183	57.7	0.92716	56.3	0.95048	52.7
Max	Min	Max	Min	Min	Min	2248	0.90919	58.1	0.92962	57.1	0.92491	54.8	0.95030	52.2

Table 6.4.5-18 Element Variation to Reduce k_s Below 0.95

Variation	k_{eff}	σ	k_s	Δk
Base	0.95048	0.00069	0.9687	
Single Cask	0.94221	0.00068	0.9604	-0.00827
Min Clad 0.01 inch	0.93007	0.00068	0.9482	-0.02041
Center rod 0.1 inch	0.94559	0.00066	0.9637	-0.00489
Center Rod 0.1 inch and Clad 0.01 inch	0.92465	0.00069	0.9428	-0.02583

Table 6.4.5-19 General Model Configuration – Dry to Wet System Reactivity Changes, 70 wt % ^{235}U Stainless Steel Clad Fuel - Nominal Fuel Parameters

Model Type	Fuel Material	Dry Interior		Wet Interior		Dry to Wet	Dry to Wet
		k_{eff}	σ	k_{eff}	σ	Δk	$\Delta k/\sigma$
Unit Cell	2060 g Zirc 1.6 H/Zr	1.43854	0.0007 4	1.34434	0.00088	-0.0942	-82
Unit Cell	2060 g Zirc 2.0 H/Zr	1.47297	0.0007 2	1.37063	0.00095	-0.1023	-86
Infinite Cask Array	2060 g Zirc 1.6 H/Zr	0.91389	0.0005 8	0.82201	0.00069	-0.0919	-102
Infinite Cask Array	2060 g Zirc 2.0 H/Zr	0.99893	0.0006 0	0.87887	0.00069	-0.1201	-131
Finite Cask Array	2060 g Zirc 2.0 H/Zr	0.85371	0.0006 8	0.87160	0.00067	0.0179	19
Single Cask	2060 g Zirc 1.6 H/Zr	0.69491	0.0005 9	0.80561	0.00066	0.1107	125

Table 6.4.5-20 Primary Fuel Type Reactivity Comparison¹ – Accident Conditions Eight-Cask Array (No Cans)

Fuel Type	Cask Cavity Moderator	Fuel Characteristics	Rod Location	k_{eff}	σ	k_s	$\Delta k/\sigma$
Al Clad	Dry	Nominal	Shifted In	0.61831	0.00053	0.63617	-
14 inch	Wet	Nominal	Shifted In	0.67516	0.00056	0.69308	73.7
	Wet	Most Reactive	Shifted In	0.68914	0.00056	0.70706	91.9
	Wet	Most Reactive	Shifted Out	0.68690	0.00054	0.70478	90.7
Al Clad -	Dry	Nominal	Shifted In	0.60606	0.00051	0.62388	-
15 inch	Wet	Nominal	Shifted In	0.66104	0.00058	0.67900	71.2
	Wet	Most Reactive	Shifted In	0.68272	0.00055	0.70062	102.2
	Wet	Most Reactive	Shifted Out	0.67985	0.00052	0.69769	101.3
SS Clad -	Dry	Nominal	Shifted In	0.77575	0.00058	0.79371	-
20% Enriched	Wet	Nominal	Shifted In	0.82684	0.00064	0.84492	59.2
	Wet	Most Reactive	Shifted In	0.86114	0.00061	0.87916	101.4
	Wet	Most Reactive	Shifted Out	0.89909	0.00064	0.91717	142.8
SS Clad	Dry	Nominal	Shifted In	0.85521	0.00068	0.87337	-
70% Enriched	Wet	Nominal	Shifted In	0.87217	0.00067	0.89031	17.8
	Wet	Most Reactive	Shifted In	0.90587	0.00069	0.92405	52.3
	Wet	Most Reactive	Shifted Out	0.93024	0.00069	0.94842	77.4

Table 6.4.5-21 Normal Condition Maximum System Reactivities (No Cans)²

Array Size	Neutron Shield	Cask Cavity	Fuel Config	k_{eff}	σ	k_s
Infinite	Yes	Dry	MRE	0.84554	0.00066	0.86366
Infinite	Yes	Wet	MRE	0.92398	0.00068	0.94214

¹ Fueled follower rods are not evaluated separately as their physical characteristics and fuel compositions are bounded by a stainless steel clad 20% enriched element.

² Most reactive element configuration as documented under accident conditions.

6.4.6 TRIGA Fuel Cluster Rods

This section presents the criticality evaluation for the NAC-LWT with nonpoisoned and poisoned basket modules for intact and failed TRIGA fuel cluster rods. In the nonpoisoned configuration, up to 480 intact TRIGA fuel cluster rods can be transported in the NAC-LWT cask. In the poisoned configuration, up to 560 intact TRIGA fuel cluster rods can be transported in the NAC-LWT cask. Up to six TRIGA fuel cluster rods can be contained in sealed canisters. The analyses are performed to satisfy the requirements of 10 CFR Parts 71.55 and 71.59, as well as IAEA Transportation Safety Standards (TS-R-1).

The design basis TRIGA fuel cluster rod is evaluated for the most reactive basket and intact fuel configurations, including both geometric perturbations and manufacturing tolerances, under wet and dry conditions in Section 6.4.6.1. The most reactive cask configuration with three baskets of intact design-basis TRIGA fuel and two baskets of fuel in sealed cans, is evaluated under normal and accident conditions in Section 6.4.6.2. Preferential flooding of the sealed failed fuel cans is also evaluated. The maximum k_{eff} of the NAC-LWT cask loaded with design-basis TRIGA fuel cluster rods is evaluated under normal and accident conditions in Section 6.4.6.3. A single package evaluation, in accordance with 10 CFR 71.55(b)(3), is performed in Section 6.4.6.4. The analyses demonstrate that, including all calculational and mechanical uncertainties, the NAC-LWT cask remains subcritical ($k_s < 0.95$) under normal and accident conditions.

6.4.6.1 Most Reactive Fuel and Basket Configurations

The primary basket tolerances affecting system reactivity are geometric tolerances, including the positioning of the fuel cluster rods and aluminum tube insert in the cell opening, the size of the cell opening; and manufacturing tolerances, including the thickness of the steel plate dividing the basket openings. The effect of these tolerances is evaluated sequentially in this section.

6.4.6.1.1 Geometric Perturbations

The TRIGA fuel cluster rods are held in place by basket modules and a fuel rod insert (Figure 6.2.6-1) with a welded, 4×4 array of 0.75-inch OD aluminum tubes. The TRIGA fuel cluster rods, one per insert tube, may shift to any location in a tube. Wet and dry conditions of the TRIGA fuel cluster rods are evaluated to determine the most reactive fuel and basket configuration.

Table 6.4.6-1 and Table 6.4.6-2 show the cask k_{eff} for the nonpoisoned and poisoned baskets with TRIGA fuel cluster rods. The effects evaluated in the tables include fuel movement within the fuel rod inserts and partial loadings under wet and dry moderation conditions.

Revision 38

The most reactive wet configuration contains 16 TRIGA fuel cluster rods moved outward from the center of each 4×4 insert array and the inserts moved to the center of the basket with $k_{\text{eff}} = 0.7571 \pm 0.0025$ and 0.7995 ± 0.0026 , for the nonpoisoned and poisoned basket configurations, respectively. This wet configuration maximizes the moderation between TRIGA fuel cluster rods within wet inserts and maximizes the interaction between inserts. It is referred to as the wet configuration for TRIGA fuel cluster rods.

The dry configuration selected as most reactive, including no water in the neutron shield, contains 16 TRIGA fuel cluster rods moved inward to the center of each 4×4 insert array and the inserts moved to the center of the basket with $k_{\text{eff}} = 0.8047 \pm 0.0020$ and 0.7489 ± 0.0019 for the non-poisoned and poisoned basket configurations, respectively. This dry configuration minimizes the neutron leakage of TRIGA fuel cluster rods within the dry basket and is referred to as the dry configuration.

Finally, the effect of partial fuel element loading was examined. Table 6.4.6-1 and Table 6.4.6-2 show that partial loading of the elements in the basket generally serves to decrease the reactivity for both the wet and dry poisoned and non-poisoned baskets. Although the case with one rod removed from the wet, nonpoisoned basket has a higher k_{eff} than the most reactive full load configuration, the difference in k_{eff} values is significantly less than 2σ . This makes the result statistically insignificant, and the full loading cases can be selected for further evaluation as stated above.

6.4.6.1.2 Manufacturing Tolerance Perturbations

The manufacturing tolerance analyses were performed by sequentially analyzing perturbations to the most reactive configurations from Section 6.4.6.1.1 and retaining appropriate perturbations. First, the effect of reducing the basket plate thickness was examined. Table 6.4.6-3 and Table 6.4.6-4 show that, for the non-poisoned and poisoned baskets, reducing the thickness of the basket plates increases the reactivity of the system. Thus, this configuration is utilized for the subsequent analyses.

Next, the dimensional tolerances of the aluminum tube inserts were evaluated. Three different cases were examined. The first case examined an increase in the aluminum tube diameter, while retaining the nominal thickness, the second case examined a decrease in the aluminum tube diameter while retaining the nominal wall thickness, and the third case examined the effect of reducing the aluminum tube thickness. The results presented in Table 6.4.6-3 and Table 6.4.6-4 show that, for the non-poisoned and poisoned basket configurations, the highest k_{eff} values are obtained for the aluminum tubes at maximum diameter, and for the dry case with the aluminum tubes at minimum thickness. While these cases produced the highest values of k_{eff} , it should be

noted that the differences between these results and the previous case is insignificant because they are within 2σ of one another.

After incorporating the previously described modifications, the effect of minimizing the basket insert opening was examined. As shown in Table 6.4.6-3 and Table 6.4.6-4, this perturbation results in equal or higher k_{eff} values for 3 of the 4 cases, with the dry, non-poisoned case resulting in a slight decrease in k_{eff} . As previously described, these differences are considered insignificant because they differ by less than 2σ . Nevertheless, because this perturbation is expected to increase the interaction between the individual baskets, it is retained in the most reactive configuration for further analysis.

Therefore, the most reactive case for intact fuel in the poisoned basket is selected as a wet configuration consisting of the following features: fuel elements moved away from the center of the aluminum center, aluminum insert moved towards the basket center, minimum divider plate thickness, minimum basket opening, and maximum aluminum tube insert diameter. The resulting reactivity for this system is, $k_{\text{eff}} = 0.8025 \pm 0.0025$. Likewise, the most reactive case for intact fuel in the non-poisoned basket is selected as a dry configuration consisting of the following features: fuel elements moved toward the center of the aluminum insert, aluminum insert moved towards the basket center, minimum divider plate thickness, and minimum basket opening. The resulting reactivity for this system is, $k_{\text{eff}} = 0.8129 \pm 0.0021$.

6.4.6.2 Sealed Cans Criticality Evaluation

Criticality calculations were performed for sealed failed fuel cans in the top and base basket modules of the cask. Three cases are examined for each basket combination, an all dry system, a full wet system, and a preferentially wet system with water only in the sealed failed fuel can. Fuel in sealed cans is modeled homogeneously, heterogeneously, and with partial loadings. The three central modules contain intact fuel in the most reactive wet or dry configurations, as appropriate, as determined in Section 6.4.5.2. The reactivities of the failed fuel combinations are compared to the reactivities of respective intact fuel configurations, and moderator density studies are performed on the most reactive configurations in Section 6.4.6.3.

Table 6.4.6-5 and Table 6.4.6-6 show the results of the preferential flooding and partial loading studies of the sealed failed fuel can configurations with TRIGA fuel cluster rods in nonpoisoned and poisoned baskets. Each sealed can contains up to six equivalent TRIGA fuel cluster rods. The most reactive cases for the non-poisoned and poisoned baskets contain maximum outer diameter, preferential wet sealed fuel cans filled with a homogeneous mixture of fuel material

and water. The most reactive non-poisoned and poisoned cases are $k_{\text{eff}} = 0.8669 \pm 0.0022$ and $k_{\text{eff}} = 0.8384 \pm 0.0021$, respectively.

6.4.6.3 Moderator Density Criticality Evaluations for TRIGA Fuel Cluster Rods

The evaluations for normal and accident conditions include moderator density variations in the cask cavity and external environment to the cask. One evaluation is performed for each basket (non-poisoned / poisoned) combination. Table 6.4.6-7 and Table 6.4.6-8 show the most reactive configurations for these combinations as determined in Section 6.4.6.2. The tables contain results for infinite axial length models for the intact fuel and finite models with cask end caps for failed fuel. Comparing the reactivity of the more conservative infinite models with finite models is acceptable, provided the result with the highest k_{eff} is always selected. Alternately, converting infinite models to finite models is equally acceptable.

As seen in Table 6.4.6-7 and Table 6.4.6-8, the most reactive non-poisoned and poisoned basket configurations with TRIGA fuel cluster rods contain two baskets with sealed cans preferentially flooded with a dry cask, $k_{\text{eff}} = 0.8669 \pm 0.0022$ and $k_{\text{eff}} = 0.8384 \pm 0.0021$, respectively. These configurations are chosen for moderator density variations.

Results of the moderator density variation cases for normal and accident conditions for the non-poisoned and poisoned basket configurations are presented in Table 6.4.6-9 through Table 6.4.6-12.

As seen in Table 6.4.6-10, the most reactive configuration for the TRIGA fuel cluster rods in the non-poisoned basket, analyzed conservatively without end caps, contains 5 baskets with intact fuel under accident conditions with no water in the cask interior, neutron shield, or exterior, $k_{\text{eff}} = 0.8756 \pm 0.0023$. Per Section 6.5.3, this corresponds to $k_s = 0.8970$.

As seen in Table 6.4.6-12, the most reactive configuration for the TRIGA fuel cluster rods in the poisoned basket, contains two baskets with maximum diameter sealed cans, preferentially flooded, under accident conditions with no water in the cask interior, neutron shield, or exterior, $k_{\text{eff}} = 0.8399 \pm 0.0021$. Per Section 6.5.3, this corresponds to $k_s = 0.8609$.

6.4.6.4 Single Package Criticality Evaluation

To satisfy 10 CFR 71.55(b)(3), an analysis of the reflection of the containment system (inner shell) by water is performed on a single wet cask. Successive replacement of the cask radial shields with water reflection is also evaluated for each basket (poisoned/nonpoisoned) configuration. As seen in Table 6.4.6-13 and Table 6.4.6-14, the reactivity of the system drops as

each radial shield of the cask is replaced by water, from the full cask surrounded by water, to the inner shell surrounded by water.

6.4.6.5 Increased Fuel Dimensional / Mass Parameter Evaluation

The TRIGA fuel cluster rod contents evaluated previously in this section, and as presented in Table 6.2.6-1 and Table 6.2.6-2, are based on design basis nominal dimensional and compositional values. To ensure that criticality safety is maintained for parameter values slightly different from those listed in the tables, a set of calculations is performed with increased active fuel length, increased fuel pellet diameter, decreased cladding thickness, and corresponding increases in the uranium and zirconium masses due to the increased volume.

Calculations are performed for two cases based on the most reactive configuration presented in Section 6.4.6.3, which is for the nonpoisoned basket configuration. In each case, the active fuel length is increased to 22.5 inches, the cladding thickness is decreased to 0.015 inch, and the pellet diameter is set at 0.52 inch for the first case, then 0.53 inch for the second case. The results are presented in Table 6.4.6-15.

As seen in the results, the increase in fuel pellet diameter up to 0.53 inch results in an increase in k_s of less than 1.5%. The resulting value is well below the 0.95 limit. Additionally, the increasing reactivity trend is indicative that the increase in fuel pellet diameter results in an increase in reactivity. The increased active fuel height, retaining the overall height the same, results in more fissile material, and reduces the axial gap between the fissile material in each basket. Finally, reducing the cladding thickness increases the reactivity of the system in two ways, increasing the moderator volume and allowing the fuel cluster rods to shift closer to the center of each cluster rod insert. This shifted configuration was demonstrated to be the most reactive intact rod configuration in Section 6.4.6.1.1.

6.4.6.6 Conclusion

Thus, including all calculational and mechanical uncertainties, an infinite array of NAC-LWT casks remains sub-critical, and is below the 0.95 limit, corrected for bias and uncertainty, under normal and accident conditions with:

Nonpoisoned Baskets:

1. 480 TRIGA fuel cluster rods,
2. Sealed cans (top and bottom baskets only) with up to six TRIGA fuel cluster rods and remainder of baskets filled with intact fuel.

Poisoned Baskets:

1. 560 TRIGA fuel cluster rods,
2. Sealed cans (top and bottom baskets only) with up to six TRIGA fuel cluster rods and remainder of baskets filled with intact fuel.

Increased Fuel Parameters:

1. Maximum Fuel Pellet Diameter – 0.53 inch
2. Minimum Cladding Thickness – 0.015 inch
3. Maximum Active Fuel Height – 22.5 inches
4. Maximum Uranium Mass – 48.6 grams
5. Maximum ^{235}U Mass – 45.4 grams
6. Maximum Zirconium Mass – 421 grams

Table 6.4.6-1 Cask k_{eff} with TRIGA Fuel Cluster Rods – Fuel Rod Placement Perturbations, Nonpoisoned Basket

Basket Configuration	Wet Case Results $k_{eff} \pm \sigma$	Dry Case Results $k_{eff} \pm \sigma$
Nominal Centered Fuel and AI Insert	0.7340 ± 0.0026	0.8001 ± 0.0019
Elements Moved To AI Insert Center	0.7110 ± 0.0027	0.8076 ± 0.0019
Elements Moved Away From AI Insert Center	0.7458 ± 0.0026	0.8005 ± 0.0020
AI Insert Moved To Basket Center ¹	0.7571 ± 0.0025	0.8047 ± 0.0020
AI Insert Moved Away From Basket Center ¹	0.7391 ± 0.0025	0.8027 ± 0.0020
1 Rod Removed From Each AI Insert	0.7576 ± 0.0026	0.7782 ± 0.0020
2 Rods Removed From Each AI Insert	0.7558 ± 0.0024	0.7503 ± 0.0020
3 Rods Removed From Each AI Insert	0.7414 ± 0.0022	-

Note:

¹ The most reactive fuel positioning is retained.

Table 6.4.6-2 Cask k_{eff} with TRIGA Fuel Cluster Rods – Fuel Rod Placement Perturbations, Poisoned Basket

Basket Configuration	Wet Case Results $k_{eff} \pm \sigma$	Dry Case Results $k_{eff} \pm \sigma$
Nominal Centered Fuel and AI Insert	0.7809 ± 0.0026	0.7435 ± 0.0020
Elements Moved To AI Insert Center	0.7654 ± 0.0025	0.7501 ± 0.0019
Elements Moved Away From AI Insert Center	0.7922 ± 0.0027	0.7468 ± 0.0020
AI Insert Moved To Basket Center ¹	0.7995 ± 0.0026	0.7489 ± 0.0019
AI Insert Moved Away From Basket Center ¹	0.7914 ± 0.0027	0.7476 ± 0.0022
1 Rod Removed From Each AI Insert	0.7956 ± 0.0027	0.7163 ± 0.0019
2 Rods Removed From Each AI Insert	0.7882 ± 0.0026	0.6831 ± 0.0019
3 Rods Removed From Each AI Insert	0.7764 ± 0.0026	-

Note:

¹ The most reactive fuel in tube motion is retained.

Table 6.4.6-3 Axially Infinite Cask k_{eff} with TRIGA Fuel Cluster Rods – Basket and Insert Manufacturing Tolerance Perturbations, Nonpoisoned Basket

Basket Configuration	Wet Case Results $k_{eff} \pm \sigma$	Dry Case Results $k_{eff} \pm \sigma$
Base Case ¹	0.7571 ± 0.0025	0.8047 ± 0.0020
Thin SS Basket Plates	0.7652 ± 0.0025	0.8140 ± 0.0020
Maximum Al Insert Tube Diameter ²	0.7653 ± 0.0027	0.8146 ± 0.0022
Minimum Al Insert Tube Diameter ²	0.7487 ± 0.0025	0.8084 ± 0.0019
Minimum Al Insert Tube Thickness ²	0.7625 ± 0.0026	0.8157 ± 0.0021
Minimum Basket Opening ²	0.7682 ± 0.0026 ³	0.8129 ± 0.0021

Notes:

- ¹ Most reactive configurations as determined in Section 6.4.6.1.1.
- ² Incorporates minimum thickness stainless steel, basket divider plates.
- ³ Maximum aluminum tube diameter.

Table 6.4.6-4 Axially Infinite Cask k_{eff} with TRIGA Fuel Cluster Rods – Basket and Insert Manufacturing Tolerance Perturbations, Poisoned Basket

Basket Configuration	Wet Case Results $k_{eff} \pm \sigma$	Dry Case Results $k_{eff} \pm \sigma$
Base Case ¹	0.7995 ± 0.0026	0.7489 ± 0.0019
Thin SS Basket Plates	0.8019 ± 0.0024	0.7513 ± 0.0020
Maximum Al Insert Tube Diameter ²	0.8055 ± 0.0027	0.7512 ± 0.0019
Minimum Al Insert Tube Diameter ²	0.7969 ± 0.0026	0.7507 ± 0.0018
Minimum Al Insert Tube Thickness ²	0.7995 ± 0.0023	0.7518 ± 0.0019
Minimum Basket Opening ²	0.8025 ± 0.0025 ³	0.7518 ± 0.0018 ⁴

Notes:

- ¹ Most reactive configurations as determined in Section 6.4.6.1.1.
- ² Incorporates minimum thickness stainless steel, basket divider plates.
- ³ Maximum aluminum tube diameter.
- ⁴ Minimum aluminum tube thickness.

Table 6.4.6-5 Sealed Can Preferential Flooding and Partial Loading Reactivity Evaluations for TRIGA Fuel Rod Clusters, Nonpoisoned Basket

Description	$k_{eff} \pm \sigma$ Dry Cask/Dry Can	$k_{eff} \pm \sigma$ Wet Cask/Wet Can	$k_{eff} \pm \sigma$ Dry Cask/Wet Can
1 Solid Fuel Lump	0.7184 ± 0.0025	0.7654 ± 0.0024	0.6954 ± 0.0022
2 Solid Fuel Lumps	0.7053 ± 0.0021	0.7546 ± 0.0025	0.6721 ± 0.0020
3 Solid Fuel Lumps	0.6946 ± 0.0022	0.7597 ± 0.0025	0.6704 ± 0.0022
4 Solid Fuel Lumps	0.6983 ± 0.0020	0.7672 ± 0.0026	0.6714 ± 0.0023
5 Solid Fuel Lumps	0.6995 ± 0.0024	0.7620 ± 0.0028	0.6723 ± 0.0022
Mixture Full Can Height	0.6917 ± 0.0021	0.7592 ± 0.0024	0.8669 ± 0.0022
Mixture Half Can Height	0.6932 ± 0.0021	0.7582 ± 0.0025	0.7226 ± 0.0022
Mixture Full Can Height, 50 % mass	0.6807 ± 0.0022	0.7606 ± 0.0025	0.7416 ± 0.0021

Table 6.4.6-6 Sealed Can Preferential Flooding and Partial Loading Reactivity Evaluations for TRIGA Fuel Rod Clusters, Poisoned Basket

Description	$k_{eff} \pm \sigma$ Dry Cask/Dry Can	$k_{eff} \pm \sigma$ Wet Cask/Wet Can	$k_{eff} \pm \sigma$ Dry Cask/Wet Can
1 Solid Fuel Lump	0.6957 ± 0.0022	0.7937 ± 0.0025	0.6662 ± 0.0020
2 Solid Fuel Lumps	0.6704 ± 0.0021	0.7942 ± 0.0026	0.6405 ± 0.0022
3 Solid Fuel Lumps	0.6610 ± 0.0020	0.7959 ± 0.0026	0.6389 ± 0.0019
4 Solid Fuel Lumps	0.6592 ± 0.0020	0.7986 ± 0.0025	0.6389 ± 0.0022
5 Solid Fuel Lumps	0.6561 ± 0.0019	0.8001 ± 0.0023	0.6409 ± 0.0020
Mixture Full Can Height	0.6507 ± 0.0019	0.7993 ± 0.0025	0.8384 ± 0.0021
Mixture Half Can Height	0.6575 ± 0.0019	0.8045 ± 0.0029	0.6741 ± 0.0022
Mixture Full Can Height, 50 % mass	0.6422 ± 0.0019	0.7992 ± 0.0027	0.6957 ± 0.0020

**Table 6.4.6-7 Summary of Most Reactive Configurations, TRIGA Fuel Cluster Rods,
Nonpoisoned Basket**

	Wet	Dry	Preferential
Intact Fuel	0.7682 ± 0.0026	0.8129 ± 0.0021	-
Sealed Fuel Cans ¹	0.7672 ± 0.0026	0.7184 ± 0.0025	0.8669 ± 0.0022

Note:

¹ Remainder of baskets filled with intact fuel.

**Table 6.4.6-8 Summary of Most Reactive Configurations, TRIGA Fuel Cluster Rods,
Poisoned Basket**

	Wet	Dry	Preferential
Intact Fuel	0.8025 ± 0.0025	0.7518 ± 0.0018	-
Sealed Fuel Cans ¹	0.8045 ± 0.0029	0.6957 ± 0.0022	0.8384 ± 0.0021

Note:

¹ Remainder of baskets filled with intact fuel.

Table 6.4.6-9 Reactivity Results for TRIGA Fuel Cluster Rods, Sealed Cans, Normal Conditions, Nonpoisoned Basket

Moderator SG	Casks Touching ($k_{eff} \pm \sigma$)	8 Foot Center-To-Center ($k_{eff} \pm \sigma$)
Dry Exterior, Vary Internal Density		
0.00000	0.7292 \pm 0.0023	0.7270 \pm 0.0025
0.00100	0.7294 \pm 0.0024	0.7258 \pm 0.0026
0.00178	0.7262 \pm 0.0025	0.7312 \pm 0.0025
0.00316	0.7267 \pm 0.0024	0.7316 \pm 0.0024
0.00562	0.7277 \pm 0.0024	0.7294 \pm 0.0024
0.01000	0.7240 \pm 0.0024	0.7312 \pm 0.0023
0.01780	0.7249 \pm 0.0025	0.7279 \pm 0.0025
0.03160	0.7307 \pm 0.0026	0.7322 \pm 0.0025
0.05620	0.7392 \pm 0.0024	0.7333 \pm 0.0024
0.10000	0.7345 \pm 0.0024	0.7349 \pm 0.0025
0.17800	0.7354 \pm 0.0025	0.7339 \pm 0.0024
0.31600	0.7298 \pm 0.0025	0.7285 \pm 0.0025
0.56200	0.7074 \pm 0.0024	0.7100 \pm 0.0026
0.70000	0.7064 \pm 0.0022	0.7055 \pm 0.0026
0.80000	0.7140 \pm 0.0027	0.7083 \pm 0.0024
0.90000	0.7137 \pm 0.0026	0.7201 \pm 0.0024
1.00000	0.7168 \pm 0.0026	0.7216 \pm 0.0027
Optimally Moderated Cask Interior (SG = 0.05620), Vary External Density		
0.00000	0.7292 \pm 0.0023	0.7270 \pm 0.0025
0.00100	0.7354 \pm 0.0024	0.7352 \pm 0.0028
0.00178	0.7351 \pm 0.0025	0.7360 \pm 0.0026
0.00316	0.7347 \pm 0.0024	0.7347 \pm 0.0023
0.00562	0.7329 \pm 0.0025	0.7372 \pm 0.0025
0.01000	0.7303 \pm 0.0023	0.7316 \pm 0.0024
0.01780	0.7306 \pm 0.0024	0.7296 \pm 0.0027
0.03160	0.7296 \pm 0.0025	0.7339 \pm 0.0024
0.05620	0.7321 \pm 0.0023	0.7324 \pm 0.0022
0.10000	0.7369 \pm 0.0023	0.7305 \pm 0.0021
0.17800	0.7325 \pm 0.0024	0.7343 \pm 0.0025
0.31600	0.7307 \pm 0.0026	0.7324 \pm 0.0024
0.56200	0.7297 \pm 0.0028	0.7359 \pm 0.0025
0.70000	0.7341 \pm 0.0021	0.7300 \pm 0.0022
0.80000	0.7316 \pm 0.0024	0.7359 \pm 0.0024
0.90000	0.7334 \pm 0.0025	0.7313 \pm 0.0026
1.00000	0.7308 \pm 0.0025	0.7318 \pm 0.0023
Vary Internal and External Density Simultaneously		
0.00000	0.7292 \pm 0.0023	0.7270 \pm 0.0025
0.00100	0.7291 \pm 0.0023	0.7275 \pm 0.0025
0.00178	0.7271 \pm 0.0026	0.7309 \pm 0.0024
0.00316	0.7316 \pm 0.0025	0.7271 \pm 0.0024
0.00562	0.7286 \pm 0.0027	0.7277 \pm 0.0023
0.01000	0.7288 \pm 0.0025	0.7254 \pm 0.0024
0.01780	0.7329 \pm 0.0024	0.7296 \pm 0.0024
0.03160	0.7309 \pm 0.0026	0.7300 \pm 0.0026
0.05620	0.7321 \pm 0.0023	0.7313 \pm 0.0026
0.10000	0.7364 \pm 0.0024	0.7299 \pm 0.0025
0.17800	0.7344 \pm 0.0026	0.7335 \pm 0.0023
0.31600	0.7299 \pm 0.0024	0.7301 \pm 0.0026
0.56200	0.7139 \pm 0.0026	0.7118 \pm 0.0025
0.70000	0.7024 \pm 0.0025	0.7025 \pm 0.0027
0.80000	0.7116 \pm 0.0024	0.7029 \pm 0.0023
0.90000	0.7177 \pm 0.0028	0.7142 \pm 0.0024
1.00000	0.7204 \pm 0.0025	0.7187 \pm 0.0026

Table 6.4.6-10 Reactivity Results for TRIGA Fuel Cluster Rods, Sealed Can, Accident Conditions, Nonpoisoned Basket

Moderator SG	Casks Touching ($k_{eff} \pm \sigma$)	8 Foot Center-To-Center ($k_{eff} \pm \sigma$)
Dry Exterior and Neutron Shield, Vary Internal Moderator		
0.00000	0.8669 \pm 0.0022	0.8756 \pm 0.0023
0.00100	0.8725 \pm 0.0022	0.8687 \pm 0.0022
0.00178	0.8737 \pm 0.0022	0.8668 \pm 0.0022
0.00316	0.8721 \pm 0.0024	0.8744 \pm 0.0024
0.00562	0.8703 \pm 0.0022	0.8693 \pm 0.0024
0.01000	0.8716 \pm 0.0022	0.8646 \pm 0.0021
0.01780	0.8658 \pm 0.0022	0.8614 \pm 0.0021
0.03160	0.8620 \pm 0.0023	0.8620 \pm 0.0021
0.05620	0.8536 \pm 0.0022	0.8561 \pm 0.0025
0.10000	0.8345 \pm 0.0023	0.8373 \pm 0.0023
0.17800	0.8138 \pm 0.0022	0.8152 \pm 0.0024
0.31600	0.7862 \pm 0.0021	0.7830 \pm 0.0024
0.56200	0.7570 \pm 0.0025	0.7500 \pm 0.0024
0.70000	0.7439 \pm 0.0023	0.7424 \pm 0.0027
0.80000	0.7383 \pm 0.0025	0.7404 \pm 0.0026
0.90000	0.7415 \pm 0.0027	0.7391 \pm 0.0025
1.00000	0.7398 \pm 0.0026	0.7303 \pm 0.0026
Optimally Moderated Internal (SG = 0.0), Vary Neutron Shield and Exterior		
0.00000	0.8669 \pm 0.0022	0.8756 \pm 0.0023
0.00100	0.8620 \pm 0.0022	0.7950 \pm 0.0023
0.00178	0.8488 \pm 0.0022	0.7755 \pm 0.0025
0.00316	0.8366 \pm 0.0023	0.7509 \pm 0.0024
0.00562	0.8209 \pm 0.0022	0.7403 \pm 0.0024
0.01000	0.7994 \pm 0.0023	0.7341 \pm 0.0024
0.01780	0.7795 \pm 0.0022	0.7272 \pm 0.0022
0.03160	0.7618 \pm 0.0024	0.7270 \pm 0.0025
0.05620	0.7497 \pm 0.0025	0.7251 \pm 0.0025
0.10000	0.7395 \pm 0.0023	0.7238 \pm 0.0025
0.17800	0.7300 \pm 0.0023	0.7244 \pm 0.0025
0.31600	0.7280 \pm 0.0024	0.7285 \pm 0.0022
0.56200	0.7311 \pm 0.0025	0.7283 \pm 0.0024
0.70000	0.7322 \pm 0.0024	0.7243 \pm 0.0025
0.80000	0.7305 \pm 0.0025	0.7267 \pm 0.0024
0.90000	0.7237 \pm 0.0022	0.7324 \pm 0.0023
1.00000	0.7286 \pm 0.0024	0.7287 \pm 0.0025
Vary Interior, Exterior and Neutron Shield Simultaneously		
0.00000	0.8669 \pm 0.0022	0.8756 \pm 0.0023
0.00100	0.8615 \pm 0.0023	0.7989 \pm 0.0022
0.00178	0.8550 \pm 0.0023	0.7755 \pm 0.0025
0.00316	0.8397 \pm 0.0022	0.7520 \pm 0.0024
0.00562	0.8268 \pm 0.0022	0.7439 \pm 0.0024
0.01000	0.7988 \pm 0.0025	0.7333 \pm 0.0025
0.01780	0.7788 \pm 0.0024	0.7305 \pm 0.0023
0.03160	0.7600 \pm 0.0023	0.7259 \pm 0.0024
0.05620	0.7510 \pm 0.0024	0.7350 \pm 0.0024
0.10000	0.7444 \pm 0.0024	0.7349 \pm 0.0024
0.17800	0.7397 \pm 0.0025	0.7298 \pm 0.0024
0.31600	0.7284 \pm 0.0025	0.7297 \pm 0.0024
0.56200	0.7106 \pm 0.0022	0.7056 \pm 0.0024
0.70000	0.7051 \pm 0.0025	0.7004 \pm 0.0025
0.80000	0.7146 \pm 0.0025	0.7104 \pm 0.0027
0.90000	0.7107 \pm 0.0025	0.7195 \pm 0.0026
1.00000	0.7204 \pm 0.0025	0.7251 \pm 0.0025

Table 6.4.6-11 Reactivity Results for TRIGA Fuel Cluster Rods, Sealed Cans, Normal Conditions, Poisoned Basket

Moderator SG	Casks Touching ($k_{eff} \pm \sigma$)	8 Foot Center-To-Center ($k_{eff} \pm \sigma$)
Dry Exterior, Vary Internal Density		
0.00000	0.7274 ± 0.0026	0.7319 ± 0.0024
0.00100	0.7342 ± 0.0022	0.7283 ± 0.0023
0.00178	0.7296 ± 0.0024	0.7268 ± 0.0023
0.00316	0.7286 ± 0.0024	0.7328 ± 0.0024
0.00562	0.7294 ± 0.0023	0.7277 ± 0.0023
0.01000	0.7309 ± 0.0022	0.7338 ± 0.0024
0.01780	0.7319 ± 0.0023	0.7308 ± 0.0023
0.03160	0.7338 ± 0.0023	0.7334 ± 0.0023
0.05620	0.7349 ± 0.0024	0.7290 ± 0.0023
0.10000	0.7328 ± 0.0021	0.7339 ± 0.0026
0.17800	0.7346 ± 0.0024	0.7339 ± 0.0023
0.31600	0.7332 ± 0.0026	0.7315 ± 0.0023
0.56200	0.7324 ± 0.0024	0.7308 ± 0.0024
0.70000	0.7245 ± 0.0025	0.7304 ± 0.0023
0.80000	0.7401 ± 0.0025	0.7310 ± 0.0024
0.90000	0.7455 ± 0.0025	0.7375 ± 0.0028
1.00000	0.7573 ± 0.0027	0.7593 ± 0.0026
Optimally Moderated Cask Interior (SG = 1.0), Vary External Density		
0.00000	0.7274 ± 0.0026	0.7319 ± 0.0024
0.00100	0.7667 ± 0.0026	0.7623 ± 0.0026
0.00178	0.7635 ± 0.0024	0.7652 ± 0.0025
0.00316	0.7636 ± 0.0026	0.7596 ± 0.0027
0.00562	0.7675 ± 0.0028	0.7636 ± 0.0027
0.01000	0.7697 ± 0.0025	0.7661 ± 0.0026
0.01780	0.7634 ± 0.0025	0.7615 ± 0.0029
0.03160	0.7664 ± 0.0027	0.7641 ± 0.0024
0.05620	0.7635 ± 0.0030	0.7688 ± 0.0026
0.10000	0.7599 ± 0.0029	0.7676 ± 0.0024
0.17800	0.7622 ± 0.0024	0.7637 ± 0.0024
0.31600	0.7620 ± 0.0026	0.7690 ± 0.0023
0.56200	0.7685 ± 0.0030	0.7643 ± 0.0028
0.70000	0.7632 ± 0.0025	0.7684 ± 0.0028
0.80000	0.7645 ± 0.0028	0.7657 ± 0.0027
0.90000	0.7615 ± 0.0028	0.7624 ± 0.0027
1.00000	0.7641 ± 0.0028	0.7659 ± 0.0025
Vary Internal and External Density Simultaneously		
0.00000	0.7274 ± 0.0026	0.7319 ± 0.0024
0.00100	0.7328 ± 0.0022	0.7281 ± 0.0024
0.00178	0.7279 ± 0.0025	0.7297 ± 0.0024
0.00316	0.7306 ± 0.0023	0.7310 ± 0.0023
0.00562	0.7323 ± 0.0024	0.7331 ± 0.0025
0.01000	0.7291 ± 0.0026	0.7291 ± 0.0024
0.01780	0.7306 ± 0.0024	0.7309 ± 0.0024
0.03160	0.7291 ± 0.0022	0.7314 ± 0.0023
0.05620	0.7292 ± 0.0026	0.7299 ± 0.0024
0.10000	0.7302 ± 0.0026	0.7356 ± 0.0025
0.17800	0.7363 ± 0.0024	0.7288 ± 0.0023
0.31600	0.7366 ± 0.0025	0.7316 ± 0.0025
0.56200	0.7296 ± 0.0026	0.7300 ± 0.0025
0.70000	0.7318 ± 0.0023	0.7276 ± 0.0025
0.80000	0.7350 ± 0.0025	0.7385 ± 0.0024
0.90000	0.7423 ± 0.0027	0.7385 ± 0.0024
1.00000	0.7641 ± 0.0028	0.7659 ± 0.0029

Table 6.4.6-12 Reactivity Results for TRIGA Fuel Cluster Rods, Sealed Cans, Accident Conditions, Poisoned Basket

Moderator SG	Casks Touching ($k_{eff} \pm \sigma$)	8 Foot Center-To-Center ($k_{eff} \pm \sigma$)
Dry Exterior and Neutron Shield, Vary Internal Moderator		
0.00000	0.8384 ± 0.0021	0.8375 ± 0.0023
0.00100	0.8394 ± 0.0022	0.8343 ± 0.0021
0.00178	0.8376 ± 0.0022	0.8316 ± 0.0022
0.00316	0.8373 ± 0.0022	0.8319 ± 0.0024
0.00562	0.8399 ± 0.0021	0.8336 ± 0.0025
0.01000	0.8356 ± 0.0022	0.8321 ± 0.0023
0.01780	0.8380 ± 0.0022	0.8314 ± 0.0022
0.03160	0.8302 ± 0.0025	0.8208 ± 0.0021
0.05620	0.8240 ± 0.0021	0.8188 ± 0.0024
0.10000	0.8127 ± 0.0023	0.8112 ± 0.0023
0.17800	0.7993 ± 0.0024	0.7936 ± 0.0022
0.31600	0.7773 ± 0.0024	0.7738 ± 0.0027
0.56200	0.7616 ± 0.0026	0.7559 ± 0.0023
0.70000	0.7570 ± 0.0025	0.7578 ± 0.0022
0.80000	0.7647 ± 0.0026	0.7589 ± 0.0025
0.90000	0.7728 ± 0.0028	0.7671 ± 0.0026
1.00000	0.7802 ± 0.0026	0.7803 ± 0.0026
Optimally Moderated Internal (SG = 0.0), Vary Neutron Shield and Exterior		
0.00000	0.8384 ± 0.0021	0.8375 ± 0.0023
0.00100	0.8282 ± 0.0022	0.7710 ± 0.0023
0.00178	0.8210 ± 0.0021	0.7593 ± 0.0024
0.00316	0.8150 ± 0.0022	0.7532 ± 0.0023
0.00562	0.7993 ± 0.0023	0.7398 ± 0.0024
0.01000	0.7882 ± 0.0024	0.7336 ± 0.0024
0.01780	0.7664 ± 0.0026	0.7326 ± 0.0024
0.03160	0.7546 ± 0.0024	0.7290 ± 0.0023
0.05620	0.7480 ± 0.0022	0.7285 ± 0.0023
0.10000	0.7387 ± 0.0022	0.7267 ± 0.0022
0.17800	0.7308 ± 0.0023	0.7265 ± 0.0026
0.31600	0.7324 ± 0.0023	0.7310 ± 0.0025
0.56200	0.7278 ± 0.0025	0.7291 ± 0.0022
0.70000	0.7320 ± 0.0023	0.7317 ± 0.0025
0.80000	0.7320 ± 0.0024	0.7268 ± 0.0026
0.90000	0.7313 ± 0.0025	0.7291 ± 0.0026
1.00000	0.7329 ± 0.0025	0.7329 ± 0.0025
Vary Interior, Exterior and Neutron Shield Simultaneously		
0.00000	0.8384 ± 0.0021	0.8375 ± 0.0023
0.00100	0.8269 ± 0.0024	0.7802 ± 0.0024
0.00178	0.8258 ± 0.0021	0.7625 ± 0.0022
0.00316	0.8089 ± 0.0022	0.7525 ± 0.0023
0.00562	0.7928 ± 0.0022	0.7409 ± 0.0025
0.01000	0.7825 ± 0.0023	0.7308 ± 0.0025
0.01780	0.7721 ± 0.0023	0.7305 ± 0.0026
0.03160	0.7552 ± 0.0023	0.7327 ± 0.0023
0.05620	0.7457 ± 0.0023	0.7283 ± 0.0025
0.10000	0.7420 ± 0.0024	0.7343 ± 0.0025
0.17800	0.7365 ± 0.0023	0.7322 ± 0.0026
0.31600	0.7379 ± 0.0024	0.7333 ± 0.0024
0.56200	0.7292 ± 0.0026	0.7333 ± 0.0022
0.70000	0.7286 ± 0.0023	0.7307 ± 0.0027
0.80000	0.7334 ± 0.0023	0.7292 ± 0.0023
0.90000	0.7516 ± 0.0026	0.7517 ± 0.0024
1.00000	0.7608 ± 0.0029	0.7608 ± 0.0029

Table 6.4.6-13 Single Package 10 CFR 71.55(b)(3) Evaluation k_{eff} Summary, TRIGA Fuel Cluster Rod, Nonpoisoned Basket

Description	$k_{eff} \pm \sigma$	k_s
Single Cask / Inner Shell Reflected with H ₂ O	0.73003 ± 0.00254	0.75191
Single Cask / Inner Shell and Lead Reflected with H ₂ O	0.76100 ± 0.00243	0.78266
Single Cask / Inner Shell, Lead & Outer Shell Reflected with H ₂ O	0.76366 ± 0.00240	0.78526
Single Intact Cask Reflected with H ₂ O	0.76360 ± 0.00273	0.78586

Table 6.4.6-14 Single Package 10 CFR 71.55(b)(3) Evaluation k_{eff} Summary, TRIGA Fuel Cluster Rod, Poison Basket

Description	$k_{eff} \pm \sigma$	k_s
Single Cask / Inner Shell Reflected with H ₂ O	0.76615 ± 0.00265	0.78825
Single Cask / Inner Shell and Lead Reflected with H ₂ O	0.80117 ± 0.00287	0.82371
Single Cask / Inner Shell, Lead & Outer Shell Reflected with H ₂ O	0.80106 ± 0.00250	0.82286
Single Intact Cask Reflected with H ₂ O	0.79815 ± 0.00228	0.81951

Table 6.4.6-15 Increased Fuel Dimensional Parameter k_{eff} Summary, TRIGA Fuel Cluster Rod, Nonpoisoned Basket

Description	$k_{eff} \pm \sigma$	k_s
Base Case (Section 6.4.6.3)	0.8756 ± 0.0023	0.8970
22.5-inch Active Fuel Height 0.015-inch Cladding Thickness 0.52-inch Fuel Pellet Diameter	0.8793 ± 0.0024	0.9009
22.5-inch Active Fuel Height 0.015-inch Cladding Thickness 0.53-inch Fuel Pellet Diameter	0.8876 ± 0.0021	0.9086

6.4.7 DIDO Fuel Assemblies

This section presents the criticality analyses for the NAC-LWT cask with the DIDO fuel assembly and basket configuration. Criticality analyses of the seven assembly arrangement with the most limiting assembly type is performed to satisfy the criticality safety requirements of 10 CFR Parts 71.55 and 71.59, as well as IAEA Transportation Safety Standards (TS-R-1). In this analysis, the bounding DIDO fuel assembly type is determined, and infinite and finite arrays of NAC-LWT casks loaded with the design basis DIDO fuel are studied for criticality under normal and accident conditions. Moderator density in the cavity, neutron shield tank and outside is varied to determine the maximum k_{eff} . The analyses demonstrate that, including all calculational and mechanical uncertainties, the NAC-LWT remains subcritical under normal and accident conditions for all DIDO fuel assemblies.

6.4.7.1 Maximum Reactivity DIDO Assembly

This evaluation determines the maximum reactivity based on LEU, MEU and HEU fuel assembly configurations. Assemblies and baskets are modeled at nominal characteristics under normal conditions (i.e., the neutron shield is assumed intact). The cask interior and exterior are flooded with full density water. Based on the thickness of the neutron shield little interaction between casks is expected resulting in minimal impact of exterior moderator density variations. The results in Table 6.4.7-1 show that the maximum reactivity is obtained from HEU assemblies. The HEU assembly is more reactive than the LEU and MEU assemblies due to reduced parasitic absorption by ^{238}U . The fuel assembly is modeled with uniform cylinder spacing, referred to as "loose fuel elements" in this section, which has reactivity significantly higher than the reactivity of the crimped fuel element.

As demonstrated, the reactivity for LEU and MEU fuel assemblies is significantly lower than that of the HEU assembly. Shipment of LEU, MEU and HEU assemblies in the same basket is therefore permissible.

6.4.7.2 Radial and Axial Assembly Shifting Under Normal Conditions

The reactivity result in Table 6.4.7-1 shows that fuel assemblies axially shifted towards the adjoining basket (i.e., three groups of two baskets) are more reactive than those placed at the top or bottom of the basket. Shifting fuel assemblies in adjoining baskets towards one another brings the maximum fissile material into its closest proximity.

Radial outward shifting of both crimped and loose fuel assemblies shows that system reactivity decreases when shifting the assembly radially out from the center of the cask. Patterns

designated as “in” shift the six peripheral fuel assemblies towards the basket center with the centered tube assembly pushed out to approach the +x axis assembly. The radial “out” pattern similarly pushes the six peripheral assemblies away from the basket center. The “custom” pattern indicated in the result table represents the “in” pattern with the center assembly shifted out at 45 degrees. The crimped pattern indicated as “single” corresponds to all assemblies being crimped in the same direction (for this evaluation at an angle of 45 degrees). For the loose fuel cylinder model, there appears to be no statistically significant reactivity difference between the centered or shifted radially in fuel assemblies. For the crimped pattern, crimping the fuel assembly radially out provides for a significant increase in reactivity in the radially shifted in assembly configuration. No significant difference in reactivity for modified crimp directions is shown in the radially out assembly configuration.

6.4.7.3 Radial Shifting and Exterior Moderator Density Changes Under Accident Conditions

The cask accident configuration is one where the material of the neutron shield is replaced by the cask exterior material definition. Both loose and crimped assemblies are evaluated at full density water in the cask interior and at a void exterior under various radial shift conditions. All cases are based on the alternate axial shifting of fuel shown in Section 6.4.7.2 to be the most reactive. Results of these analyses are shown in Table 6.4.7-2. As expected, the void exterior condition produces the maximum reactivity configuration. Reactivity increases due to increased interaction between individual casks in the array.

In addition to the shifted standard “in” configuration, the inward shifted configuration with a centered middle assembly is also evaluated (designated as InC in the result table). This configuration is slightly more reactive than the configuration with all assemblies centered, but it is within the statistical uncertainty band (2 sigma) of the Monte Carlo base result. Mechanical perturbation and uncertainty results are therefore evaluated with the all assemblies centered configuration.

Table 6.4.7-3 displays results for test cases based on modifying the material of the aluminum shell surrounding the basket and the heat transfer shunts in the center of the basket. The base case for this analysis is the radially centered, fully moderated interior, dry exterior configuration. Replacing the shell material by water or steel in the accident model inhibits interaction between packages and produces lower reactivities in the infinite array of casks. Modeling the heat transfer shunts as all water increases reactivity slightly. This supports modeling the shunts as a set of three small rods with a smaller cross-section area.

6.4.7.4 Basket Manufacturing Tolerance Evaluation

In this evaluation, set basket tolerances are applied to the criticality evaluation. The base case for this evaluation is the cask accident model (i.e, neutron shield replaced by exterior moderator which in this case is void) with centered fuel assembly. As shown Table 6.4.7-4, basket tolerances do not produce a significant reactivity increase. Note that the tube wall thickness minimum tolerance is set to a zero percent change. The minimum tube wall case is, therefore, identical to the base case. All further analysis is, therefore, set to nominal basket parameters.

6.4.7.5 Fuel Assembly Tolerance Evaluation

This evaluation contains the fuel assembly perturbation studies. Each of the parameters is evaluated independently with the results compared to the cask accident condition base case. For fuel cylinder pitch, two studies are performed. The first fixes the inner plate (cylinder) and varies the outer three cylinders and is noted as "IF." The second fixes the outer plate and is noted as "OF." Per the reactivity results in Table 6.4.7-5, tolerances that produce an increase in reactivity are:

- Minimum plate thickness (increases moderator between plates)
- Minimum clad thickness
- Maximum plate pitch (outer diameter fixed; increasing the outer diameter will decrease the amount of moderator between assemblies)
- Minimum active fuel height (reduces the space between fissile material in the alternating shifted model)
- Minimum element height (reduces the space between fissile material in the alternating shifted model)
- Maximum fissile mass
- Maximum uranium weight percent (minimum impact but is added to the final reactivity models)

6.4.7.6 Maximum Reactivity Configuration

The parameters shown in Section 6.4.7.5 to increase system reactivity are combined to form a worst case cask payload configuration. The limiting fuel assembly description based on the critical fuel assembly parameters is shown in Table 6.4.7-12. Table 6.4.7-6 displays the evaluation results of the worst case configured DIDO NAC-LWT. Since the radially in configuration with a centered basket middle assembly was statistically the same as the all centered configuration (see Table 6.4.7-2), both configurations are evaluated with the toleranced fuel parameters. The most reactive configuration for the DIDO assembly in the infinite array

Revision 38

configuration is above 0.95. To remain below 0.95 under all conditions, a finite array of 8 casks in close pitch configuration is modeled. The array is reflected by a water boundary condition and is evaluated with a flooded cask interior and void cask exterior. Both eight cask array configurations result in maximum k_s below 0.95. The CSI for the eight cask accident configuration is 12.5. Based on the normal to accident condition reactivity difference of $0.04 \Delta k$, versus the $0.01 \Delta k$ that 0.95 was exceeded for the infinite array, the CSI for normal condition is 0 (infinite array is acceptable).

6.4.7.7 Moderator Density Variation Reactivity Configuration

Table 6.4.7-7 contains a cask interior and exterior moderator density variation study for the HEU fuel assembly in the accident configuration. All basket and fuel parameters are set to nominal conditions and an infinite array of casks is evaluated. The basket shows a relatively constant reactivity between cask interior densities of 1.0 g/cm^3 and 0.9 g/cm^3 . While reactivity increases above the two sigma (95/95) uncertainty band typically applied in this calculation as statistically significant, the results are within the three sigma (99% confidence) band and are considered constant for the purposes of this calculation (Note that the maximum reactivity of the 8-cask array is below 0.92). At lower interior water densities the reactivity begins to decrease significantly. The exterior density study demonstrates that any significant amount of cask exterior moderator density will reduce the interaction between casks in the array.

6.4.7.8 Single Package Criticality Evaluation

To satisfy 10 CFR 71.55(b)(3), an analysis of the reflection of the containment system (inner shell) by water is performed on a single wet cask. Successive replacement of the cask radial shields with water reflection is also evaluated. A significant decrease in reactivity occurs when the lead gamma shield is replaced by water. The results from this evaluation can be seen in Table 6.4.7-8.

6.4.7.9 Reduced Clad Thickness Evaluations

This section documents the reactivity change due to a reduction in the DIDO element minimum clad thickness to 0.025 cm. The analysis in the previous sections is for a minimum clad thickness of 0.0325 cm.

The effect of the reduced clad thickness on system reactivity is determined by repeating cases from Section 6.4.7.5 and Section 6.4.7.6. Table 6.4.7-9 repeats the Section 6.4.7.5 minimum clad thickness case for the reduced value and compares it to the main section results. As

Revision 38

expected, the reduced minimum clad thickness yields a proportional increase in k_{eff} . Table 6.4.7-10 shows the results for the worst-case tolerance combination with the reduced clad thickness for the cases discussed in Section 6.4.7.6. The maximum k_{eff} is based on an eight-cask array with a void exterior. All cases show a slight increase in reactivity due to the reduced clad thickness.

6.4.7.10 Expanded Inner and Outer Shell Diameter Evaluations

Based on the fuel assembly tolerance and moderator studies, a combination of a reduced inner diameter fuel tube ID (Tube 1) with a maximized outer fuel tube ID (Tube 4) is expected to maximize system reactivity (i.e., fuel plates are under-moderated with the previously evaluated conditions and increased pitch will increase system reactivity). Based on tolerances previously applied, the minimum Tube 1 ID is 5.88 cm and the maximum Tube 4 OD is 9.52 cm. This range is evaluated by fixing the Tube 1 ID at minimum and evaluating the nominal, minimum and maximum Tube 4 OD according to the values in the following list.

Tube Number	Min OD (cm)	Nom OD (cm)	Max OD (cm)
1	6.01	6.01	6.01
2	7.05	7.11	7.18
3	8.08	8.22	8.35
4	9.12	9.32	9.52

For this study, the tube pitch is a calculated variable and is larger than the maximum pitch considered in the previous calculation sections.

Table 6.4.7-11 documents the results of the tube diameter study. Based on the trend of increasing reactivity with increasing outer tube OD, the system remains under-moderated. The maximum k_s for the system is 0.9304 for an eight-cask array. Note that significant margin exists in these results, as the basket tube material is modeled as aluminum rather than stainless steel. System reactivity for the steel tube basket at the specified maximum reactivity configuration is < 0.8 .

6.4.7.11 Code Bias and Code Bias Uncertainty Adjustments

A calculation of k_s under normal and accident conditions can now be made based on the previous results and based on the KENO-Va validation statistics presented in Section 6.5.2 for high enriched uranium fuel. The value k_s is calculated based on the KENO-Va Monte Carlo average plus any biases and uncertainties associated with the methods and the modeling, i.e.:

$$k_s = k_{\text{eff}} + \Delta k_{\text{Bias}} + \Delta k_{\text{BU}} + 2\sigma_{\text{MC}} \leq 0.95$$

In the validation presented in Section 6.5.2, a bias of -0.0044 (allowance for overprediction of k_{eff}) and a 95/95 method uncertainty of ± 0.0181 was determined. For added conservatism, the -0.0044 bias correction is neglected. With these biases and uncertainties, the equation for k_s becomes:

$$k_s = k_{\text{eff}} + 0.0181 + 2\sigma_{\text{MC}}$$

k_s values for the relevant analysis are included in Table 6.4.7-1 through Table 6.4.7-11. The maximum k_s , 0.9304, for the DIDO shipment results from the eight-cask array accident configuration model.

For both normal and accident conditions, the calculated k_{eff} values, after correction for biases and uncertainties, are well below the 0.95 limit. The analyses demonstrate that, including all calculational and mechanical uncertainties, an infinite array of NAC-LWT casks with DIDO fuel remains subcritical under normal and accident conditions.

Table 6.4.7-1 Normal Condition HEU, LEU, MEU DIDO Evaluation

Fuel Type	Fuel Configuration	Crimp Pattern	Radial Shift Pattern	Axial Shift Pattern	k_{eff}	σ	$k_{eff}+2\sigma$	k_s	Δk	$\Delta k_{eff}/\sigma$
LEU	Loose	N/A	Centered	Down	0.82771	0.00067	0.82905	0.84715	-0.03689	-55.1
LEU	Loose	N/A	Centered	Alternating	0.83842	0.00070	0.83982	0.85792	-0.02612	-37.3
LEU	Crimped	Single	Centered	Down	0.81887	0.00069	0.82025	0.83835	-0.04569	-66.2
LEU	Crimped	Single	Centered	Alternating	0.83112	0.00068	0.83248	0.85058	-0.03346	-49.2
MEU	Loose	N/A	Centered	Down	0.84006	0.00070	0.84146	0.85956	-0.02448	-35.0
MEU	Loose	N/A	Centered	Alternating	0.85333	0.00072	0.85477	0.87287	-0.01117	-15.5
MEU	Crimped	Single	Centered	Down	0.83259	0.00070	0.83399	0.85209	-0.03195	-45.6
MEU	Crimped	Single	Centered	Alternating	0.84336	0.00069	0.84474	0.86284	-0.02120	-30.7
HEU	Loose	N/A	Centered	Down	0.85243	0.00070	0.85383	0.87193	-0.01211	-17.3
HEU	Loose	N/A	Centered	Alternating	0.86462	0.00066	0.86594	0.88404	-	-
HEU	Loose	N/A	Centered	Up	0.85275	0.00071	0.85417	0.87227	-0.01177	-16.6
HEU	Loose	N/A	In	Alternating	0.86361	0.00071	0.86503	0.88313	-0.00091	-1.3
HEU	Loose	N/A	Out	Alternating	0.85625	0.00070	0.85765	0.87575	-0.00829	-11.8
HEU	Loose	N/A	Custom	Alternating	0.86562	0.00072	0.86706	0.88516	0.00112	1.6
HEU	Crimped	Single	Centered	Down	0.84084	0.00072	0.84228	0.86038	-0.02366	-32.9
HEU	Crimped	Single	Centered	Alternating	0.85512	0.00069	0.85650	0.87460	-0.00944	-13.7
HEU	Crimped	Single	Centered	Up	0.84075	0.00070	0.84215	0.86025	-0.02379	-34.0
HEU	Crimped	Single	In	Alternating	0.85628	0.00072	0.85772	0.87582	-0.00822	-11.4
HEU	Crimped	Single	Out	Alternating	0.84484	0.00072	0.84628	0.86438	-0.01966	-27.3
HEU	Crimped	Single	Custom	Alternating	0.85688	0.00069	0.85826	0.87636	-0.00768	-11.1
HEU	Crimped	In	In	Alternating	0.84841	0.00071	0.84983	0.86793	-0.01611	-22.7
HEU	Crimped	Out	Out	Alternating	0.84118	0.00072	0.84262	0.86072	-0.02332	-32.4
HEU	Crimped	In	Out	Alternating	0.84552	0.00067	0.84686	0.86496	-0.01908	-28.5
HEU	Crimped	Out	In	Alternating	0.85786	0.00074	0.85934	0.87744	-0.00660	-8.9

Table 6.4.7-2 HEU DIDO Accident Evaluation – Radial Shift and Exterior Moderator Density Variation

Fuel Configuration	Crimp Pattern	Radial Shift Pattern	Interior Moderator Density (g/cm ³)	Exterior Moderator Density (g/cm ³)	k_{eff}	σ	$k_{eff}+2\sigma$	k_s	Δk	$\Delta k_{eff}/\sigma$
Loose	N/A	Centered	0.9998	0.9998	0.86276	0.00070	0.86416	0.88226	–	–
Loose	N/A	In	0.9998	0.9998	0.86468	0.00070	0.86608	0.88418	0.00192	2.7
Crimped	Out	Centered	0.9998	0.9998	0.85355	0.00068	0.85491	0.87301	-0.00925	-13.6
Crimped	Out	In	0.9998	0.9998	0.85666	0.00069	0.85804	0.87614	-0.00612	-8.9
Loose	N/A	Centered	0.9998	0.0001	0.90900	0.00069	0.91038	0.92848	–	–
Loose	N/A	In	0.9998	0.0001	0.90808	0.00071	0.90950	0.92760	-0.00088	-1.2
Loose	N/A	InC	0.9998	0.0001	0.91011	0.00069	0.91149	0.92959	0.00111	1.6
Crimped	Out	Centered	0.9998	0.0001	0.89962	0.00071	0.90104	0.91914	-0.00934	-13.2
Crimped	Out	In	0.9998	0.0001	0.90116	0.00069	0.90254	0.92064	-0.00784	-11.4

Table 6.4.7-3 DIDO Heat Shunt and Aluminum Shell Evaluation Results

Case Description	k_{eff}	σ	$k_{eff}+2\sigma$	k_s	Δk	$\Delta k_{eff}/\sigma$
Shell modeled as steel	0.90100	0.00067	0.90234	0.92044	-0.00804	-12.0
Shell modeled as water	0.90382	0.00070	0.90522	0.92332	-0.00516	-7.4
Aluminum shunts modeled as water	0.91157	0.00067	0.91291	0.93101	0.00253	3.8

Table 6.4.7-4 DIDO Basket Geometric Tolerance Study Results

Fuel Tube Outer Diameter Tolerance	Fuel Tube Thickness Tolerance	Fuel Tube Height Tolerance	Fuel Basket Base Plate Tolerance	k_{eff}	σ	$k_{eff}+2\sigma$	k_s	Δk	$\Delta k_{eff}/\sigma$
Min	Nominal	Nominal	Nominal	0.90979	0.00070	0.91119	0.92929	0.00081	1.2
Max	Nominal	Nominal	Nominal	0.90959	0.00069	0.91097	0.92907	0.00059	0.9
Nominal	Min	Nominal	Nominal	0.90900	0.00069	0.91038	0.92848	–	–
Nominal	Max	Nominal	Nominal	0.90489	0.00071	0.90631	0.92441	-0.00407	-5.7
Nominal	Nominal	Min	Nominal	0.90954	0.00068	0.91090	0.92900	0.00052	0.8
Nominal	Nominal	Max	Nominal	0.90953	0.00069	0.91091	0.92901	0.00053	0.8
Nominal	Nominal	Nominal	Min	0.90922	0.00067	0.91056	0.92866	0.00018	0.3
Nominal	Nominal	Nominal	Max	0.90858	0.00068	0.90994	0.92804	-0.00044	-0.6

Table 6.4.7-5 DIDO Fuel Assembly Tolerance Study Results

Fuel Cylinder Diameter Tolerance	Fuel Plate Thickness Tolerance	Fuel Plate Clad Thickness Tolerance	Fuel Cylinder Pitch Tolerance	Active Fuel Length Tolerance	Fuel Assembly Height Tolerance	²³⁵ U Mass Tolerance	Uranium Weight Fraction Tolerance	k_{eff}	σ	$k_{eff}+2\sigma$	k_s	Δk	$\Delta k_{eff}/\sigma$
Min	--	--	--	--	--	--	--	0.91024	0.00069	0.91162	0.92972	0.00124	1.8
Max	--	--	--	--	--	--	--	0.90691	0.00067	0.90825	0.92635	-0.00213	-3.2
--	Min	--	--	--	--	--	--	0.91188	0.00067	0.91322	0.93132	0.00284	4.2
--	Max	--	--	--	--	--	--	0.90539	0.00068	0.90675	0.92485	-0.00363	-5.3
--	--	Min	--	--	--	--	--	0.91253	0.00069	0.91391	0.93201	0.00353	5.1
--	--	Max	--	--	--	--	--	0.90685	0.00069	0.90823	0.92633	-0.00215	-3.1
--	--	--	IF - Max	--	--	--	--	0.90993	0.00068	0.91129	0.92939	0.00091	1.3
--	--	--	IF - Min	--	--	--	--	0.90864	0.00071	0.91006	0.92816	-0.00032	-0.5
--	--	--	OF - Max	--	--	--	--	0.91175	0.00068	0.91311	0.93121	0.00273	4.0
--	--	--	OF - Min	--	--	--	--	0.90787	0.00065	0.90917	0.92727	-0.00121	-1.9
--	--	--	--	Min	--	--	--	0.91067	0.00071	0.91209	0.93019	0.00171	2.4
--	--	--	--	Max	--	--	--	0.90853	0.00068	0.90989	0.92799	-0.00049	-0.7
--	--	--	--	--	Min	--	--	0.91108	0.00066	0.91240	0.93050	0.00202	3.1
--	--	--	--	--	Max	--	--	0.90735	0.00069	0.90873	0.92683	-0.00165	-2.4
--	--	--	--	--	--	Min	--	0.89234	0.00070	0.89374	0.91184	-0.01664	-23.8
--	--	--	--	--	--	Max	--	0.92431	0.00068	0.92567	0.94377	0.01529	22.5
--	--	--	--	--	--	--	Min	0.90761	0.00068	0.90897	0.92707	-0.00141	-2.1
--	--	--	--	--	--	--	Max	0.91070	0.00070	0.91210	0.93020	0.00172	2.5

Table 6.4.7-6 DIDO Fuel Maximum Reactivity Combinations

Cask Array	Radial Shift Pattern	Fuel Cylinder Diameter Tolerance	Fuel Plate Thickness Tolerance	Fuel Plate Clad Thickness Tolerance	Fuel Cylinder Pitch Tolerance	Active Fuel Length Tolerance	Fuel Assembly Height Tolerance	²³⁵ U Mass Tolerance	Uranium Weight Fraction Tolerance	k _{eff}	σ	k _{eff} +2σ	k _s
Infinite	Centered	Nominal	Min	Min	OF-Max	Min	Min	Max	Max	0.93813	0.00070	0.93953	0.95763
Infinite	InC	Nominal	Min	Min	OF-Max	Min	Min	Max	Max	0.93639	0.00073	0.93785	0.95595
8 cask	Centered	Nominal	Min	Min	OF-Max	Min	Min	Max	Max	0.89310	0.00072	0.89454	0.91264
8 cask	InC	Nominal	Min	Min	OF-Max	Min	Min	Max	Max	0.89596	0.00070	0.89736	0.91546

Table 6.4.7-7 Moderator Density Study for the Infinite Array of Casks (Nominal Fuel and Basket Configuration)

Radial Shift Pattern	Interior Moderator Density (g/cm ³)	Exterior Moderator Density (g/cm ³)	k_{eff}	σ	$k_{eff}+2\sigma$	k_s	Δk	$\Delta k_{eff}/\sigma$
Exterior Moderator Density Study								
Centered	0.9998	0.9	0.86274	0.00066	0.86406	0.88216	-0.04632	-70.2
Centered	0.9998	0.8	0.86320	0.00071	0.86462	0.88272	-0.04576	-64.5
Centered	0.9998	0.6	0.86400	0.00070	0.86540	0.88350	-0.04498	-64.3
Centered	0.9998	0.4	0.86367	0.00073	0.86513	0.88323	-0.04525	-62.0
Centered	0.9998	0.2	0.86441	0.00070	0.86581	0.88391	-0.04457	-63.7
Centered	0.9998	0.1	0.86822	0.00073	0.86968	0.88778	-0.04070	-55.8
Interior Moderator Density Study								
Centered	0.975	0.0001	0.91103	0.00069	0.91241	0.93051	0.00203	2.9
Centered	0.95	0.0001	0.91097	0.00066	0.91229	0.93039	0.00191	2.9
Centered	0.925	0.0001	0.90942	0.00070	0.91082	0.92892	0.00044	0.6
Centered	0.9	0.0001	0.91079	0.00070	0.91219	0.93029	0.00181	2.6
Centered	0.875	0.0001	0.90928	0.00068	0.91064	0.92874	0.00026	0.4
Centered	0.85	0.0001	0.90869	0.00072	0.91013	0.92823	-0.00025	-0.3
Centered	0.8	0.0001	0.90563	0.00088	0.90739	0.92549	-0.00299	-3.4
Centered	0.6	0.0001	0.88126	0.00102	0.88330	0.90140	-0.02708	-26.5
Centered	0.4	0.0001	0.80903	0.00118	0.81139	0.82949	-0.09899	-83.9
Centered	0.2	0.0001	0.62941	0.00122	0.63185	0.64995	-0.27853	-228.3
Centered	0.0001	0.0001	0.13951	0.00043	0.14037	0.15847	-0.77001	-1790.7
InC	0.975	0.0001	0.90855	0.00067	0.90989	0.92799	-0.00049	-0.7
InC	0.95	0.0001	0.90809	0.00072	0.90953	0.92763	-0.00085	-1.2
InC	0.925	0.0001	0.90723	0.00072	0.90867	0.92677	-0.00171	-2.4
InC	0.9	0.0001	0.90644	0.00071	0.90786	0.92596	-0.00252	-3.5
InC	0.875	0.0001	0.90525	0.00067	0.90659	0.92469	-0.00379	-5.7
InC	0.85	0.0001	0.90377	0.00075	0.90527	0.92337	-0.00511	-6.8
InC	0.8	0.0001	0.90218	0.00070	0.90358	0.92168	-0.00680	-9.7
InC	0.0001	0.0001	0.87289	0.00073	0.87435	0.89245	-0.03603	-49.4

Table 6.4.7-8 DIDO Single Package 10 CFR 71.55(b)(3) Evaluation k_{eff} Summary

Description	$k_{eff} \pm \sigma$	k_s
Single Cask / Inner Shell Reflected with H ₂ O	0.83670±0.00075	0.85630
Single Cask / Inner Shell and Lead Reflected with H ₂ O	0.88638±0.00070	0.90588
Single Cask / Inner Shell, Lead & Outer Shell Reflected with H ₂ O	0.89275±0.00070	0.91225
Single Intact Cask Reflected with H ₂ O	0.89352±0.00070	0.91302

Table 6.4.7-9 DIDO Fuel Assembly Tolerance Study Results (Reduced Clad Thickness)

Clad Thickness	k_{eff}	σ	$k_{eff}+2\sigma$	k_s	Δk
0.0425 cm (Nominal)	0.90900	0.00069	0.91038	0.92848	—
0.0325 cm (Min)	0.91253	0.00069	0.91391	0.93201	0.00353
0.0250 cm (Revised Min)	0.91578	0.00069	0.91716	0.93526	0.00678

Table 6.4.7-10 DIDO Fuel Maximum Reactivity Combinations (Reduced Clad Thickness)

Cask Array	Radial Shift Pattern	k_{eff}	σ	$k_{eff}+2\sigma$	k_s
Infinite	Centered	0.93921	0.00071	0.94063	0.95873
Infinite	InC	0.93866	0.00072	0.94010	0.95820
8 cask	Centered	0.89293	0.00071	0.89435	0.91245
8 cask	InC	0.89762	0.00071	0.89904	0.91714

Note: Fuel and basket configuration as detailed in Table 6.4.7-6.

Table 6.4.7-11 DIDO Fuel Maximum Reactivity Combinations (Reduced Clad and Maximum Pitch)

Configuration	k_{eff}	σ	$k_{eff}+2\sigma$	k_s
Minimum outer diameter	0.90282	0.00070	0.90422	0.92232
Nominal outer diameter	0.90770	0.00072	0.90914	0.92724
Maximum outer diameter	0.91088	0.00070	0.91228	0.93038

Note: All cases include the minimum inner diameter and the maximum reactivity fuel and basket configuration in an 8-cask array as specified in Sections 6.4.7.6 and 6.4.7.9 as bounding.

Table 6.4.7-12 DIDO Bounding Configurations

Parameter	Value
Number of Fuel Cylinders	4
Plate thickness	≥ 0.130 cm
Clad thickness	≥ 0.025 cm
²³⁵ U content per Assembly	≤ 190 g
Enrichment wt % ²³⁵ U	≤ 94
Active Fuel Height	≥ 58.75 cm
Assembly Height ⁽¹⁾	≥ 61.5 cm
Min Tube ID	5.88 cm
Max. Tube OD	9.52 cm

Note:

- ¹ Assembly height provides for spacing of fissile material. An optional spacer may be used to maintain spacing if the assembly is cut to shorter than 61.5 cm.

6.4.8 General Atomics Irradiated Fuel Material

This section presents the criticality analyses for the NAC-LWT cask with GA IFM. Criticality analyses are performed to satisfy the criticality safety requirements of 10 CFR Parts 71.55 and 71.59, as well as IAEA Transportation Safety Standards (TS-R-1). All criticality evaluations performed herein use an axially infinite model. An analysis of the NAC-LWT with a payload of either RERTR or HTGR fuel material shows that the TRIGA elements in the RERTR enclosure are more reactive than the HTGR fuel matrix. A detailed study of the combined payload evaluates TRIGA pitch, TRIGA array type (square or rectangular), interior moderator density including preferential flooding, and exterior moderator density. A single cask evaluation is also performed to comply with 10 CFR 71.55(b)(3). The analyses demonstrate that, including all calculational and mechanical uncertainties, the NAC-LWT remains subcritical under normal and accident conditions for the two GA IFM packages (FHUs).

6.4.8.1 Payload Evaluation

The results of the payload evaluation are used to determine the largest contributor to system reactivity. Four models were executed, with the characteristics listed below:

- TRIGA elements on rectangular 4×5 1.40-cm pitch.
- Flooded and dry HTGR fuel matrix.
- Interior (TRIGA package and cask cavity) moderator density at 0.9982 g/cm³.
- Exterior moderator density at 0.9982 g/cm³.

Results are shown in Table 6.4.8-1. Since the TRIGA fuel is the dominant contributor to the system reactivity, the TRIGA bias will be applied in order to calculate the bias-adjusted k_s . The bias is discussed in further detail in Section 6.4.8.8.

6.4.8.2 TRIGA Pitch/Array Evaluation

The combined payload model is used to evaluate the TRIGA element pitch in either a 'Rectangular' or 'Square' array as defined in Section 6.3.7. The HTGR FHU is modeled as dry in this configuration with the remaining cask void spaces flooded. Rectangular and square array results are shown in Table 6.4.8-2 and Table 6.4.8-3, respectively. In the rectangular array, the pitch is limited to 1.65 cm before interferences are created in the model. A larger pitch is possible in the square array, with a value of 1.73 cm allowed by the modeled geometry. The maximum reactivity is calculated for the square array with a pitch of 1.73 cm. Thus, the 1.73-cm pitch is employed in the optimum moderator density studies.

6.4.8.3 Interior Moderator Density Evaluation

The combined payload model is used to vary the interior moderator density with intact TRIGA elements in a square array on a 1.73-cm pitch. Based on the results shown in Table 6.4.8-4, a full density water package interior maximizes system reactivity at full density water exterior moderation.

6.4.8.4 HTGR Matrix Moderator Density Evaluation

The combined payload model is used to vary water density in the HTGR fuel matrix using the fully flooded TRIGA elements in a square array on a 1.73 cm pitch. Based on the results shown in Table 6.4.8-4, a water density of 1.0 g/cc for water homogenized with the HTGR fuel matrix maximizes system reactivity. Note that this configuration is conservative in that the HTGR fuel occupies part of the homogenized volume and full density water cannot occupy the same volume.

6.4.8.5 Exterior Moderator Density Evaluation

The combined payload model is used to vary the exterior moderator density with intact TRIGA elements in a square array on a 1.73 cm pitch. Interior moderator in the FHUs is set to full moderation as indicated by the evaluations in Sections 6.4.8.3 and 6.4.8.4. The cavity exterior to the FHUs is also flooded. Based on the results shown in Table 6.4.8-6, no significant change in system reactivity is obtained if the exterior moderator density varies below full density water. The maximum reactivity change of $2.9 \Delta k/\sigma$ was obtained at an exterior water density of 0.0001 g/cc. This change, while outside the $2 \Delta k/\sigma$ typical threshold for a significant change in reactivity, is less than $2.2 \times 10^{-3} \Delta k$ and, therefore, not significant.

Note that the material description of the water neutron shield and the exterior moderator are identical in these evaluations addressing accident condition concerns (loss of neutron shield).

6.4.8.6 Partial Flooding Evaluation

During accident conditions, the loss of neutron shielding has the potential to increase neutronic interaction between casks in the infinite array. Significant amounts of moderator outside the FHUs, but in the flooded cask cavity, serves to isolate casks under the accident condition of loss of neutron shield. To investigate the potential impact of preferential flooding, an additional model is created. The model preferentially floods the RERTR and HTGR FHUs, with a separate interior moderator material filling the balance of the NAC-LWT cavity.

Revision 38

A full set of studies evaluating the reactivity changes associated with varying cavity interior, FHU, and exterior moderator densities is summarized in Table 6.4.8-7 through Table 6.4.8-11. The studies indicate that the most reactive configuration is for flooding of the RERTR and HTGR enclosures (FHUs) with interior and exterior void (loss of neutron shield). This configuration produces the maximum reactivity FHUs, while maximizing interaction between the FHUs within the cask and between casks.

6.4.8.7 Single Cask Evaluation

The 10 CFR 71.55(b)(3) requires an evaluation of the NAC-LWT with the containment system fully reflected by water. The containment for the NAC-LWT is the cask inner shell. While no operating condition results in a removal of the cask outer shell and lead gamma shield, each of the partial flooding cases at four combinations of interior and exterior moderator is reevaluated by removing the lead and outer shells (including neutron shield), and reflecting the system by water at full density on the X and Y faces (the z faces are mirrored to yield an axially infinite model). The results of this analysis are shown in Table 6.4.8-12 and demonstrate that the system reactivity decreases with the removal of the lead, outer shell and neutron shield reflectors.

6.4.8.8 Damaged TRIGA Fuel Evaluation

The combined payload model with a homogenized TRIGA fuel description is used to evaluate the system reactivity in the event that both the intact and sectioned fuel elements become damaged. Models are executed by varying the volume fraction of water in the TRIGA fuel mixture from zero to unity. The maximum volume fraction is 0.6816 based on the FHU cavity volume (7140 cm³) and the total volume of TRIGA elements (2,273 cm³), which does not consider the volume of the aluminum tubing within the FHU primary enclosure.

Based on the results summarized in Table 6.4.8-13, homogenized TRIGA elements are more reactive than intact TRIGA elements. Evaluation results documented in Table 6.4.8-13 are based on infinite cask array models. A single cask evaluation of the maximum water volume fraction case yielded a k_{eff} of 0.38885 ± 0.00066 .

6.4.8.9 Code Bias and Code Bias Uncertainty Adjustments

As shown in Section 6.4.8.1, the TRIGA elements in the RERTR enclosure are more reactive than the HTGR fuel matrix in its enclosure. Therefore, code bias and code uncertainty adjustments are based on the TRIGA fuel element critical benchmarks in Section 6.5.3.

A calculation of k_s under normal and accident conditions can now be made based on the previous results and based on the KENO-Va validation statistics presented in Section 6.5.3. The value k_s is calculated based on the KENO-Va Monte Carlo average plus any biases and uncertainties associated with the methods and the modeling, i.e.:

$$k_s = k_{\text{eff}} + \Delta k_{\text{Bias}} + \Delta k_{\text{BU}} + 2\sigma_{\text{MC}} \leq 0.95$$

In the validation presented in Section 6.5.3, a negative bias (allowance for overprediction of k_{eff}) and a 95/95 method uncertainty of ± 0.0168 was determined. The negative bias correction is neglected. Thus, the equation for k_s becomes:

$$k_s = k_{\text{eff}} + 0.0168 + 2\sigma_{\text{MC}}$$

The k_s values for the relevant analysis are included in Table 6.4.8-1 through Table 6.4.8-13. The maximum k_s , 0.74015, for the GA IFM shipment results from an infinite height model with an infinite number of casks.

For both normal and accident conditions, the calculated k_{eff} values, after correction for uncertainty, are well below the 0.95 limit. The analyses demonstrate that, including all calculational and mechanical uncertainties, an infinite array of NAC-LWT casks with GA IFM remains subcritical under normal and accident conditions.

Table 6.4.8-1 GA IFM Payload Evaluation Result Summary

Payload	Cavity Moderator Density [g/cm ³]	HTGR Moderator Density [g/cm ³]	RERTR Moderator Density [g/cm ³]	Exterior Moderator Density [g/cm ³]	TRIGA Pitch [cm]	TRIGA Array	$k_{eff} \pm \sigma$
Combined	0.9882	0	0.9882	0.9882	1.40	Rectangular	0.44192±0.00073
RERTR	0.9882	0	0.9882	0.9882	1.40	Rectangular	0.42870±0.00080
HTGR	0.9882	0	0.9882	0.9882	N/A	N/A	0.06611±0.00020
HTGR	0.9882	0.9882	0.9882	0.9882	N/A	N/A	0.36907±0.00053

Table 6.4.8-2 GA IFM TRIGA Rectangular Array Pitch Evaluation Result Summary

Cavity (g/cc)	HTGR (g/cc)	RERTR (g/cc)	Exterior (g/cc)	TRIGA Pitch (cm)	TRIGA Array	k_{eff}	σ	k_s	$k_{eff}+2\sigma$	Δk	$\Delta k/\sigma$
1	0	1	1	1.40	Rectangular	0.44192	0.00073	0.46018	0.44338	0.00000	0.0
1	0	1	1	1.50	Rectangular	0.45796	0.00078	0.47632	0.45952	0.01614	20.7
1	0	1	1	1.60	Rectangular	0.47647	0.00080	0.49487	0.47807	0.03469	43.4
1	0	1	1	1.65	Rectangular	0.48529	0.00079	0.50367	0.48687	0.04349	55.1

Table 6.4.8-3 GA IFM TRIGA Square Array Pitch Evaluation Result Summary

Cavity (g/cc)	HTGR (g/cc)	RERTR (g/cc)	Exterior (g/cc)	TRIGA Pitch (cm)	TRIGA Array	k_{eff}	σ	k_s	$k_{eff}+2\sigma$	Δk	$\Delta k/\sigma$
1	0	1	1	1.40	Square	0.44618	0.00073	0.46444	0.44764	0.00000	0.0
1	0	1	1	1.50	Square	0.46343	0.00080	0.48183	0.46503	0.01739	21.7
1	0	1	1	1.60	Square	0.48072	0.00078	0.49908	0.48228	0.03464	44.4
1	0	1	1	1.65	Square	0.49026	0.00078	0.50862	0.49182	0.04418	56.6
1	0	1	1	1.70	Square	0.49727	0.00077	0.51561	0.49881	0.05117	66.5
1	0	1	1	1.73	Square	0.50289	0.00079	0.52127	0.50447	0.05683	71.9

Table 6.4.8-4 GA IFM Interior Moderator Density Evaluation Result Summary

Cavity (g/cc)	HTGR (g/cc)	RERTR (g/cc)	Exterior (g/cc)	TRIGA Pitch (cm)	TRIGA Array	k_{eff}	σ	k_s	$k_{eff}+2\sigma$	Δk	$\Delta k/\sigma$
1.00	0	1.00	1	1.73	Square	0.50289	0.00079	0.52127	0.50447	0.00000	0.0
0.95	0	0.95	1	1.73	Square	0.48897	0.00077	0.50731	0.49051	-0.01396	-18.1
0.90	0	0.90	1	1.73	Square	0.47787	0.00079	0.49625	0.47945	-0.02502	-31.7
0.85	0	0.85	1	1.73	Square	0.46611	0.00076	0.48443	0.46763	-0.03684	-48.5
0.80	0	0.80	1	1.73	Square	0.45420	0.00077	0.47254	0.45574	-0.04873	-63.3
0.75	0	0.75	1	1.73	Square	0.44289	0.00073	0.46115	0.44435	-0.06012	-82.4
0.70	0	0.70	1	1.73	Square	0.42888	0.00071	0.44710	0.43030	-0.07417	-104.5
0.65	0	0.65	1	1.73	Square	0.41568	0.00073	0.43394	0.41714	-0.08733	-119.6
0.60	0	0.60	1	1.73	Square	0.40369	0.00069	0.42187	0.40507	-0.09940	-144.1
0.55	0	0.55	1	1.73	Square	0.39298	0.00069	0.41116	0.39436	-0.11011	-159.6
0.50	0	0.50	1	1.73	Square	0.38075	0.00069	0.39893	0.38213	-0.12234	-177.3
0.45	0	0.45	1	1.73	Square	0.36922	0.00069	0.38740	0.37060	-0.13387	-194.0
0.40	0	0.40	1	1.73	Square	0.35645	0.00067	0.37459	0.35779	-0.14668	-218.9
0.35	0	0.35	1	1.73	Square	0.34396	0.00064	0.36204	0.34524	-0.15923	-248.8
0.30	0	0.30	1	1.73	Square	0.33007	0.00064	0.34815	0.33135	-0.17312	-270.5
0.25	0	0.25	1	1.73	Square	0.31618	0.00059	0.33416	0.31736	-0.18711	-317.1
0.20	0	0.20	1	1.73	Square	0.29802	0.00056	0.31594	0.29914	-0.20533	-366.7
0.15	0	0.15	1	1.73	Square	0.27758	0.00057	0.29552	0.27872	-0.22575	-396.1
0.10	0	0.10	1	1.73	Square	0.24971	0.00052	0.26755	0.25075	-0.25372	-487.9
0.05	0	0.05	1	1.73	Square	0.21145	0.00048	0.22921	0.21241	-0.29206	-608.5

Table 6.4.8-5 GA IFM HTGR Matrix Moderator Density Evaluation Result Summary

Cavity (g/cc)	HTGR (g/cc)	RERTR (g/cc)	Exterior (g/cc)	TRIGA Pitch (cm)	TRIGA Array	k_{eff}	σ	k_s	$k_{eff}+2\sigma$	Δk	$\Delta k/\sigma$
1	0.00	1	1	1.73	Square	0.50289	0.00079	0.52127	0.50447	0.00000	0.0
1	0.05	1	1	1.73	Square	0.50363	0.00076	0.52195	0.50515	0.00068	0.9
1	0.10	1	1	1.73	Square	0.50425	0.00079	0.52263	0.50583	0.00136	1.7
1	0.15	1	1	1.73	Square	0.50570	0.00076	0.52402	0.50722	0.00275	3.6
1	0.20	1	1	1.73	Square	0.50755	0.00077	0.52589	0.50909	0.00462	6.0
1	0.25	1	1	1.73	Square	0.50701	0.00078	0.52537	0.50857	0.00410	5.3
1	0.30	1	1	1.73	Square	0.50888	0.00079	0.52726	0.51046	0.00599	7.6
1	0.35	1	1	1.73	Square	0.50994	0.00079	0.52832	0.51152	0.00705	8.9
1	0.40	1	1	1.73	Square	0.51168	0.00079	0.53006	0.51326	0.00879	11.1
1	0.45	1	1	1.73	Square	0.51327	0.00079	0.53165	0.51485	0.01038	13.1
1	0.50	1	1	1.73	Square	0.51492	0.00078	0.53328	0.51648	0.01201	15.4
1	0.55	1	1	1.73	Square	0.51524	0.00080	0.53364	0.51684	0.01237	15.5
1	0.60	1	1	1.73	Square	0.51628	0.00078	0.53464	0.51784	0.01337	17.1
1	0.65	1	1	1.73	Square	0.51911	0.00077	0.53745	0.52065	0.01618	21.0
1	0.70	1	1	1.73	Square	0.52034	0.00076	0.53866	0.52186	0.01739	22.9
1	0.75	1	1	1.73	Square	0.52100	0.00074	0.53928	0.52248	0.01801	24.3
1	0.80	1	1	1.73	Square	0.52193	0.00076	0.54025	0.52345	0.01898	25.0
1	0.85	1	1	1.73	Square	0.52120	0.00075	0.53950	0.52270	0.01823	24.3
1	0.90	1	1	1.73	Square	0.52407	0.00074	0.54235	0.52555	0.02108	28.5
1	0.95	1	1	1.73	Square	0.52482	0.00076	0.54314	0.52634	0.02187	28.8
1	1.00	1	1	1.73	Square	0.52764	0.00070	0.54584	0.52904	0.02457	35.1

Table 6.4.8-6 GA IFM Exterior Moderator Density Evaluation Result Summary

Cavity (g/cc)	HTGR (g/cc)	RERTR (g/cc)	Exterior (g/cc)	TRIGA Pitch (cm)	TRIGA Array	k_{eff}	σ	k_s	$k_{eff}+2\sigma$	Δk	$\Delta k/\sigma$
1	1	1	1.00	1.73	Square	0.52764	0.00070	0.54584	0.52904	0.00000	0.0
1	1	1	0.95	1.73	Square	0.52634	0.00073	0.54460	0.52780	-0.00124	-1.7
1	1	1	0.90	1.73	Square	0.52787	0.00077	0.54621	0.52941	0.00037	0.5
1	1	1	0.85	1.73	Square	0.52539	0.00073	0.54365	0.52685	-0.00219	-3.0
1	1	1	0.80	1.73	Square	0.52733	0.00075	0.54563	0.52883	-0.00021	-0.3
1	1	1	0.75	1.73	Square	0.52921	0.00079	0.54759	0.53079	0.00175	2.2
1	1	1	0.70	1.73	Square	0.52632	0.00071	0.54454	0.52774	-0.00130	-1.8
1	1	1	0.65	1.73	Square	0.52551	0.00073	0.54377	0.52697	-0.00207	-2.8
1	1	1	0.60	1.73	Square	0.52695	0.00079	0.54533	0.52853	-0.00051	-0.6
1	1	1	0.55	1.73	Square	0.52712	0.00078	0.54548	0.52868	-0.00036	-0.5
1	1	1	0.50	1.73	Square	0.52612	0.00077	0.54446	0.52766	-0.00138	-1.8
1	1	1	0.45	1.73	Square	0.52584	0.00076	0.54416	0.52736	-0.00168	-2.2
1	1	1	0.40	1.73	Square	0.52669	0.00076	0.54501	0.52821	-0.00083	-1.1
1	1	1	0.35	1.73	Square	0.52661	0.00076	0.54493	0.52813	-0.00091	-1.2
1	1	1	0.30	1.73	Square	0.52735	0.00078	0.54571	0.52891	-0.00013	-0.2
1	1	1	0.25	1.73	Square	0.52644	0.00076	0.54476	0.52796	-0.00108	-1.4
1	1	1	0.20	1.73	Square	0.52775	0.00080	0.54615	0.52935	0.00031	0.4
1	1	1	0.15	1.73	Square	0.52812	0.00075	0.54642	0.52962	0.00058	0.8
1	1	1	0.10	1.73	Square	0.52904	0.00073	0.54730	0.53050	0.00146	2.0
1	1	1	0.05	1.73	Square	0.52655	0.00072	0.54479	0.52799	-0.00105	-1.5
1	1	1	0.00	1.73	Square	0.52970	0.00073	0.54796	0.53116	0.00212	2.9

Table 6.4.8-7 GA IFM Partial Flooding Comparison Result Summary

Cavity (g/cc)	HTGR (g/cc)	RERTR (g/cc)	Exterior (g/cc)	TRIGA Pitch (cm)	TRIGA Array	k_{eff}	σ	k_s	$k_{eff}+2\sigma$	Δk	$\Delta k/\sigma$
0	1	0	0	1.73	Square	0.57362	0.00054	0.59150	0.57470	0.00000	0.0
0	1	1	0	1.73	Square	0.70197	0.00076	0.72029	0.70349	0.12879	169.5

Table 6.4.8-8 GA IFM Partial Flooding Interior Moderator Density, Void Exterior Result Summary

Cavity (g/cc)	HTGR (g/cc)	RERTR (g/cc)	Exterior (g/cc)	TRIGA Pitch (cm)	TRIGA Array	k_{eff}	σ	k_s	$k_{eff}+2\sigma$	Δk	$\Delta k/\sigma$
0.0	1	1	0	1.73	Square	0.70197	0.00076	0.72029	0.70349	0.00000	0.0
0.1	1	1	0	1.73	Square	0.63582	0.00076	0.65414	0.63734	-0.06615	-87.0
0.2	1	1	0	1.73	Square	0.59419	0.00074	0.61247	0.59567	-0.10782	-145.7
0.3	1	1	0	1.73	Square	0.57060	0.00078	0.58896	0.57216	-0.13133	-168.4
0.4	1	1	0	1.73	Square	0.55551	0.00073	0.57377	0.55697	-0.14652	-200.7
0.5	1	1	0	1.73	Square	0.54367	0.00074	0.56195	0.54515	-0.15834	-214.0
0.6	1	1	0	1.73	Square	0.53824	0.00074	0.55652	0.53972	-0.16377	-221.3
0.7	1	1	0	1.73	Square	0.53478	0.00075	0.55308	0.53628	-0.16721	-222.9
0.8	1	1	0	1.73	Square	0.53243	0.00074	0.55071	0.53391	-0.16958	-229.2
0.9	1	1	0	1.73	Square	0.53192	0.00075	0.55022	0.53342	-0.17007	-226.8
1.0	1	1	0	1.73	Square	0.52970	0.00073	0.54796	0.53116	-0.17233	-236.1

Table 6.4.8-9 GA IFM Partial Flooding Interior Moderator Density, Water Exterior Result Summary

Cavity (g/cc)	HTGR (g/cc)	RERTR (g/cc)	Exterior (g/cc)	TRIGA Pitch (cm)	TRIGA Array	k_{eff}	σ	k_s	$k_{eff}+2\sigma$	Δk	$\Delta k/\sigma$
0.0	1	1	1	1.73	Square	0.55598	0.00074	0.57426	0.55746	0.00000	0.0
0.1	1	1	1	1.73	Square	0.54649	0.00073	0.56475	0.54795	-0.00951	-13.0
0.2	1	1	1	1.73	Square	0.53804	0.00075	0.55634	0.53954	-0.01792	-23.9
0.3	1	1	1	1.73	Square	0.53458	0.00073	0.55284	0.53604	-0.02142	-29.3
0.4	1	1	1	1.73	Square	0.52971	0.00076	0.54803	0.53123	-0.02623	-34.5
0.5	1	1	1	1.73	Square	0.52610	0.00074	0.54438	0.52758	-0.02988	-40.4
0.6	1	1	1	1.73	Square	0.52725	0.00075	0.54555	0.52875	-0.02871	-38.3
0.7	1	1	1	1.73	Square	0.52668	0.00071	0.54490	0.52810	-0.02936	-41.4
0.8	1	1	1	1.73	Square	0.52630	0.00077	0.54464	0.52784	-0.02962	-38.5
0.9	1	1	1	1.73	Square	0.52711	0.00074	0.54539	0.52859	-0.02887	-39.0
1.0	1	1	1	1.73	Square	0.52764	0.00070	0.54584	0.52904	-0.02842	-40.6

Table 6.4.8-10 GA IFM Partial Flooding Exterior Moderator Density, Void Interior Result Summary

Cavity (g/cc)	HTGR (g/cc)	RERTR (g/cc)	Exterior (g/cc)	TRIGA Pitch (cm)	TRIGA Array	k_{eff}	σ	k_s	$k_{eff}+2\sigma$	Δk	$\Delta k/\sigma$
0	1	1	0.0	1.73	Square	0.70197	0.00076	0.72029	0.70349	0.00000	0.0
0	1	1	0.1	1.73	Square	0.56743	0.00075	0.58573	0.56893	-0.13456	-179.4
0	1	1	0.2	1.73	Square	0.55761	0.00075	0.57591	0.55911	-0.14438	-192.5
0	1	1	0.3	1.73	Square	0.55699	0.00076	0.57531	0.55851	-0.14498	-190.8
0	1	1	0.4	1.73	Square	0.55603	0.00072	0.57427	0.55747	-0.14602	-202.8
0	1	1	0.5	1.73	Square	0.55553	0.00071	0.57375	0.55695	-0.14654	-206.4
0	1	1	0.6	1.73	Square	0.55550	0.00073	0.57376	0.55696	-0.14653	-200.7
0	1	1	0.7	1.73	Square	0.55648	0.00075	0.57478	0.55798	-0.14551	-194.0
0	1	1	0.8	1.73	Square	0.55610	0.00075	0.57440	0.55760	-0.14589	-194.5
0	1	1	0.9	1.73	Square	0.55524	0.00075	0.57354	0.55674	-0.14675	-195.7
0	1	1	1.0	1.73	Square	0.55598	0.00074	0.57426	0.55746	-0.14603	-197.3

Table 6.4.8-11 GA IFM Partial Flooding Exterior Moderator Density, Water Interior Result Summary

Cavity (g/cc)	HTGR (g/cc)	RERTR (g/cc)	Exterior (g/cc)	TRIGA Pitch (cm)	TRIGA Array	k_{eff}	σ	k_s	$k_{eff}+2\sigma$	Δk	$\Delta k/\sigma$
1	1	1	0.0	1.73	Square	0.52970	0.00073	0.54796	0.53116	0.00000	0.0
1	1	1	0.1	1.73	Square	0.52904	0.00073	0.54730	0.53050	-0.00066	-0.9
1	1	1	0.2	1.73	Square	0.52775	0.00080	0.54615	0.52935	-0.00181	-2.3
1	1	1	0.3	1.73	Square	0.52735	0.00078	0.54571	0.52891	-0.00225	-2.9
1	1	1	0.4	1.73	Square	0.52669	0.00076	0.54501	0.52821	-0.00295	-3.9
1	1	1	0.5	1.73	Square	0.52612	0.00077	0.54446	0.52766	-0.00350	-4.5
1	1	1	0.6	1.73	Square	0.52695	0.00079	0.54533	0.52853	-0.00263	-3.3
1	1	1	0.7	1.73	Square	0.52632	0.00071	0.54454	0.52774	-0.00342	-4.8
1	1	1	0.8	1.73	Square	0.52733	0.00075	0.54563	0.52883	-0.00233	-3.1
1	1	1	0.9	1.73	Square	0.52787	0.00077	0.54621	0.52941	-0.00175	-2.3
1	1	1	1.0	1.73	Square	0.52764	0.00070	0.54584	0.52904	-0.00212	-3.0

Table 6.4.8-12 GA IFM Partial Flooding Single Cask Result Comparison

Cavity (g/cc)	HTGR (g/cc)	RERTR (g/cc)	Exterior (g/cc)	TRIGA Pitch (cm)	TRIGA Array	k_{eff}	σ	k_s	$k_{eff}+2\sigma$	Δk	$\Delta k/\sigma$
0	1	1	0	1.73	Square	0.70197	0.00076	0.72029	0.70349	0.00000	0.0
0	1	1	0	1.73	Square	0.42657	0.00066	0.44469	0.42789	-0.27560	-417.6
1	1	1	0	1.73	Square	0.52970	0.00073	0.54796	0.53116	0.00000	0.0
1	1	1	0	1.73	Square	0.52108	0.00074	0.53936	0.52256	-0.00860	-11.6
0	1	1	1	1.73	Square	0.55598	0.00074	0.57426	0.55746	0.00000	0.0
0	1	1	1	1.73	Square	0.45370	0.00074	0.47198	0.45518	-0.10228	-138.2
1	1	1	1	1.73	Square	0.52764	0.00070	0.54584	0.52904	0.00000	0.0
1	1	1	1	1.73	Square	0.52056	0.00076	0.53888	0.52208	-0.00696	-9.2

Table 6.4.8-13 GA IFM Damaged TRIGA Fuel Result Summary

Cavity (g/cc)	HTGR (g/cc)	Exterior (g/cc)	TRIGA Config.	TRIGA H ₂ O (g/cc)	k _{eff}	σ	k _s	k _{eff} +2 σ	Δk	$\Delta k/\sigma$
0	1	0	Homog.	0.0001	0.53943	0.00055	0.55733	0.54053	-0.18282	-332.4
0	1	0	Homog.	0.1000	0.55711	0.00055	0.57501	0.55821	-0.16514	-300.3
0	1	0	Homog.	0.2000	0.57987	0.00054	0.59775	0.58095	-0.14240	-263.7
0	1	0	Homog.	0.3000	0.60672	0.00062	0.62476	0.60796	-0.11539	-186.1
0	1	0	Homog.	0.4000	0.63609	0.00062	0.65413	0.63733	-0.08602	-138.7
0	1	0	Homog.	0.5000	0.66661	0.00064	0.68469	0.66789	-0.05546	-86.7
0	1	0	Homog.	0.6000	0.69621	0.00067	0.71435	0.69755	-0.02580	-38.5
0	1	0	Homog.	0.6816	0.72199	0.00068	0.74015	0.72335	0.00000	0.0
0	1	0	Homog.	0.7000	0.72738	0.00069	0.74556	0.72876	0.00541	7.8
0	1	0	Homog.	0.8000	0.75724	0.00070	0.77544	0.75864	0.03529	50.4
0	1	0	Homog.	0.9000	0.78650	0.00071	0.80472	0.78792	0.06457	90.9
0	1	0	Homog.	1.0000	0.81239	0.00073	0.83065	0.81385	0.09050	124.0

6.4.9 PULSTAR Fuel Contents

This section presents the criticality analyses for the NAC-LWT cask with PULSTAR fuel contents. Criticality analyses are performed to satisfy the criticality safety requirements of 10 CFR Parts 71.55 and 71.59, as well as IAEA TS-R-1. All criticality evaluations performed herein use an axially finite cask model. An analysis of the NAC-LWT with each of the four postulated basket loadings shows that damaged PULSTAR fuel elements in a can are most reactive.

The maximum reactivity is based on the following model characteristics.

- 14 cans (25 elements per can) in the top and base modules
- 14 intact assemblies in the two intermediate modules
- Flooded cans
- Void cask cavity and exterior
- Loss of neutron shield

A single cask evaluation is also performed to comply with 10 CFR 71.55(b)(3). The analyses demonstrate that, including all calculational and mechanical uncertainties, the NAC-LWT remains subcritical under normal and accident conditions.

6.4.9.1 Intact Assembly Payload

An intact PULSTAR fuel assembly is placed in each of the 28 cells in the 28 MTR basket assembly. Results of the mechanical perturbation, axial and radial shift are shown in Figure 6.4.9-1 through

Table 6.4.9-3. Optimum moderator studies for the cask are shown in Figure 6.3.9-2. All intact fuel assembly runs are based on an infinite cask array model.

From a base model, which has the PULSTAR fuel assemblies centered in the module cell and touching the module base plates, various component shift and module plate thickness combinations are evaluated. Assembly shift results, shown in Table 6.4.9-1, indicate that a basket assembly with PULSTAR fuel assemblies in the “Xlong” alignment and axially alternated represents the most reactive scenario for intact fuel assemblies. The “modified” Ylong configuration represents a mix of rotations and is shown in Figure 6.4.9-1. Considering assembly shifts the maximum k_{eff} is 0.80517 ± 0.00083 .

Mechanical perturbation results from a study of plate thickness and cell opening size are shown in Table 6.4.9-2. This study indicates that a maximum module cell width produces a slight increase in reactivity for a maximum k_{eff} of 0.80929 ± 0.00084 .

Previous evaluations documented in this section are based on a flooded pellet to clad gap and fuel parameters producing the maximum lattice H/U ratio. Minimum H/U ratio and dry gap cases are run to verify that the lattice is under moderated and that appropriate fuel parameters were chosen for the base analysis. The results of this analysis are listed in Table 6.4.9-3 and clearly demonstrate that the element lattice is under moderated and that the flooded pellet to clad gap and maximum H/U lattice model options are conservative for the analysis.

Graphical results of the optimum moderator density studies are shown in Figure 6.4.9-2. This study further confirms that the assembly is under moderated and that maximum system reactivity is obtained from a flooded cask cavity with a dry cask exterior and neutron shield.

The CSI for intact fuel assemblies is 0 as an infinite array of cask is modeled and maximum reactivity is well below the 0.95 licensing limit.

6.4.9.2 Intact Elements – Fuel Rod Insert

A single KENO-Va case is executed to demonstrate that a payload of 448 PULSTAR fuel elements (16 elements per 4x4 insert; 28 MTR basket cells) is significantly less reactive than the assembly model containing 28 intact assemblies (700 elements).

For a model with the insert radially centered within the cell, alternating axial shifting, full density water in the cavity, and a void exterior, the calculated k_{eff} is 0.70076 ± 0.00079 . This reactivity is substantially lower than that of the intact assemblies. Therefore no further analysis is performed with the rod insert configuration.

6.4.9.3 Canned Elements

Intact or damaged (failed) PULSTAR fuel elements and nonfuel components of fuel assemblies may be placed into either of the PULSTAR cans. Each configuration is individually evaluated.

Intact Fuel Elements

Intact fuel element models place 25 rods into the can in a 0.66-inch square pitch. This pitch is the maximum allowed by the modeled can cavity width and is conservative as the elements were significantly under moderated at their smaller “in assembly” pitch. A can is placed into each of the 28 MTR basket assembly cells in an alternate axial shift configuration with the cask and

canister cavity flooded. The alternate shift configuration was determined to be most reactive in the intact assembly analysis. For an infinite array of casks under accident condition (void exterior and neutron shield) a k_{eff} of 0.89919 ± 0.00083 is calculated. Results in Table 6.4.9-4 indicate that the preferential flooding of the canister cavity with a void cask cavity for the same physical configuration results in k_{eff} of 0.98516 ± 0.00076 . Additional evaluations and limitations, are therefore, required to document an acceptable system configuration. KENO models with cans restricted to the top and base modules and intact fuel assemblies in the remaining two modules reduces system reactivity significantly as documented in Table 6.4.9-4. Without the neutron shield (accident conditions) there is substantial neutronic coupling between casks in an array and limiting the number of casks produces a significant additional reactivity reduction. For the mixed loaded three-cask array, the calculated k_{eff} is 0.84910 ± 0.00079 . A limit of a three-cask array produces a CSI of 33.4 under the accident conditions modeled. System reactivity for a normal condition infinite array of casks loaded with damaged fuel cans is low, $k_{\text{eff}} < 0.2$. The normal condition based CSI is therefore 0.

Damaged (Failed) Elements

Damaged elements are modeled as a homogenized fuel and water mixture within the can cavity. Analysis trends for the homogenized contents are similar to those for the intact elements in a can. Bias and uncertainty adjusted system reactivity of the damaged fuel elements is higher than allowed for a full cask load (28 cans), but restricting the cask array under accident condition to three casks and limiting each cask's contents to 14 damaged fuel cans, seven in each of the top and base basket modules, and intact fuel assemblies or rod holders in the intermediate basket modules, produces acceptable reactivities as shown in Table 6.4.9-5. For the 3-cask array, the maximum calculated k_{eff} is 0.86961 ± 0.00081 .

6.4.9.4 Single Cask Evaluation

The 10 CFR 71.55(b)(3) requires an evaluation of the NAC-LWT with the containment system fully reflected by water. The containment for the NAC-LWT is the cask inner shell. While no operating condition results in a removal of the cask outer shell and lead gamma shield, each of the partial flooding cases at four combinations of interior and exterior moderator is reevaluated by removing the lead and outer shells (including neutron shield), and reflecting the system by water at full density on the X, Y, and Z faces. Using the maximum reactivity model from Section 6.4.9.3, the calculated k_{eff} is 0.72674 ± 0.00087 .

6.4.9.5 Code Bias and Code Bias Uncertainty Adjustments

PULSTAR fuel elements are similar to LWR fuel rods with a shorter active fuel length and smaller assembly array. While the enrichment for PULSTAR fuel is outside the enrichment range validated for LWR fuel, Figure 6.5.1-2 shows no statistical trend in k_{eff} versus enrichment. Further, any trend that may be postulated from the critical benchmarks indicates a higher predicted k_{eff} value at higher enrichments. Therefore, code bias and code uncertainty adjustments are based on the LWR fuel assembly critical benchmarks in Section 6.5.1.

A calculation of k_s under normal and accident conditions can now be made based on the previous results and based on the KENO-Va validation statistics presented in Section 6.5.1. The value k_s is calculated based on the KENO-Va Monte Carlo average plus any biases and uncertainties associated with the methods and the modeling, i.e.:

$$k_s = k_{\text{eff}} + \Delta k_{\text{Bias}} + \Delta k_{\text{BU}} + 2\sigma_{\text{MC}} \leq 0.95$$

In the validation presented in Section 6.5.1, a bias of ± 0.0052 and a 95/95 method uncertainty of ± 0.0087 were determined. Thus, the equation for k_s becomes as follows.

$$k_s = k_{\text{eff}} + 0.0139 + 2\sigma_{\text{MC}}$$

The k_s values for each evaluated payload are summarized in Table 6.4.9-6. The maximum k_s , 0.88513, results from a mixed loading of intact assemblies and canned elements.

For both normal and accident conditions, the calculated k_{eff} values, after correction for uncertainty, are well below the 0.95 limit. The analyses demonstrate that, including all calculational and mechanical uncertainties, an array of NAC-LWT casks with PULSTAR fuel remains subcritical under normal and accident conditions.

6.4.9.6 Allowable Cask Loading

Based on the results of the previous sections, the following cask loadings are permissible. For intact elements, any combination of assemblies and 4×4 rod inserts may be loaded into any module cell. Up to 14 damaged fuel cans each containing up to 25 PULSTAR fuel elements may be loaded in the top and base modules only; module cells loaded without cans may contain any combination of intact assemblies or 4×4 rod inserts. Each can is allowed the equivalent fissile material content of 25 fuel elements in either intact or damaged (failed) form. Damaged fuel may include fuel debris.

Figure 6.4.9-1 PICTURE Schematic of Modified PULSTAR Fuel Assembly Alignment Configuration

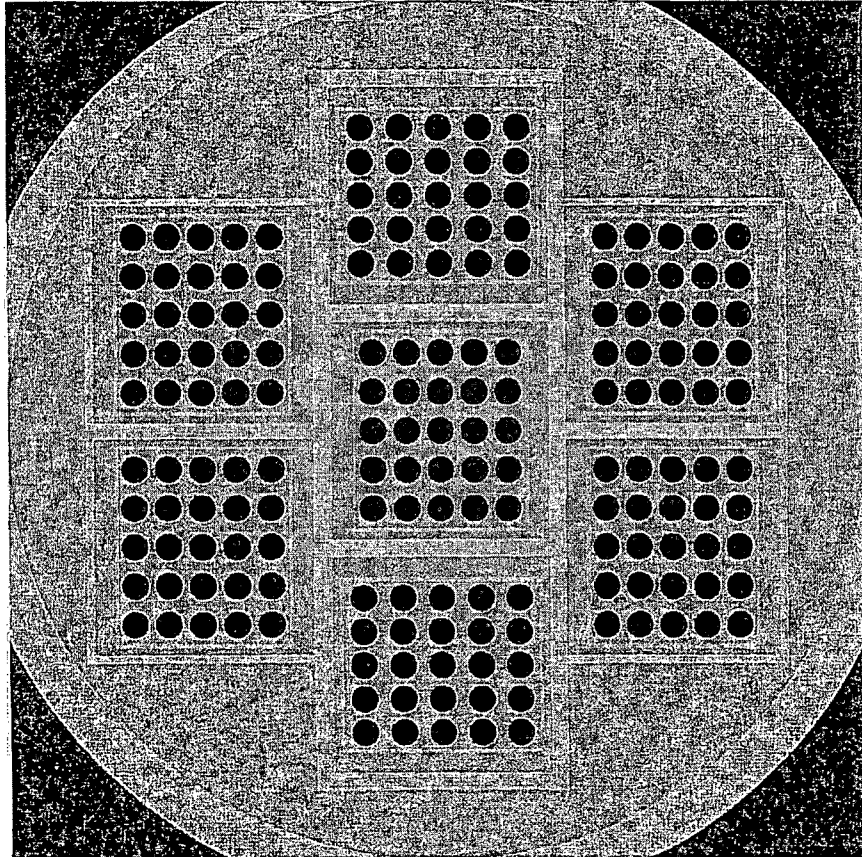


Figure 6.4.9-2 PULSTAR Intact Assembly Model Moderator Density Study Graphical Results

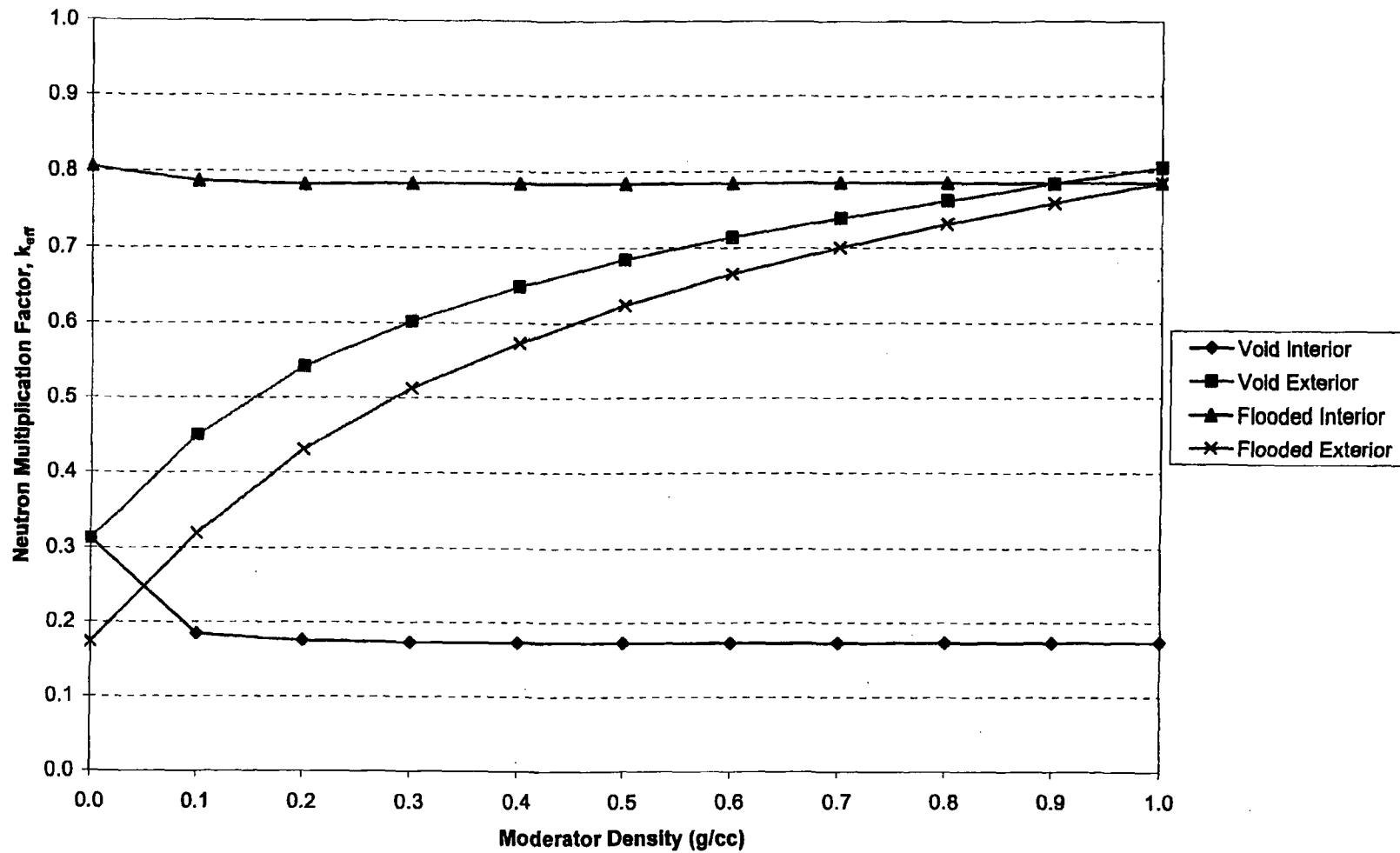


Table 6.4.9-1 PULSTAR Intact Assembly Shift Results

Alignment	Radial Shift	Axial Shift	k_{eff}	σ	$k_{eff}+2\sigma$	Δk	$\Delta k/\sigma$
Ylong	Centered	Centered	0.78916	0.00081	0.79078	--	--
Ylong	In	Centered	0.77268	0.00085	0.77438	-0.01648	-14.0
Ylong	Out	Centered	0.78773	0.00081	0.78935	-0.00143	-1.2
Xlong	Centered	Centered	0.79134	0.00083	0.79300	--	--
Xlong	In	Centered	0.77006	0.00080	0.77166	-0.02128	-18.5
Xlong	Out	Centered	0.78979	0.00080	0.79139	-0.00155	-1.3
Ylong	Centered	Alternating	0.80182	0.00084	0.80350	--	--
Ylong	In	Alternating	0.78767	0.00081	0.78929	-0.01415	-12.1
Ylong	Out	Alternating	0.80176	0.00081	0.80338	-0.00006	-0.1
Xlong	Centered	Alternating	0.80517	0.00083	0.80683	--	--
Xlong	In	Alternating	0.77968	0.00083	0.78134	-0.02549	-21.7
Xlong	Out	Alternating	0.80522	0.00080	0.80682	0.00005	0.0
Mod. Ylong	Centered	Alternating	0.80348	0.00087	0.80522	--	--
Mod. Ylong	In	Alternating	0.78247	0.00082	0.78411	-0.02101	-17.6
Mod. Ylong	Out	Alternating	0.80427	0.00081	0.80589	0.00079	0.7

Table 6.4.9-2 PULSTAR Intact Assembly Mechanical Perturbation Results

Alignment	Radial Shift	Axial Shift	Basket Cell Opening	Basket Plate Thickness	k_{eff}	σ	$k_{eff}+2\sigma$	Δk	$\Delta k/\sigma$
Xlong	Centered	Alternating	Min	Min	0.80517	0.00083	0.80683	--	--
Xlong	Centered	Alternating	Nominal	Nominal	0.80202	0.00084	0.80370	-0.00315	-2.7
Xlong	Centered	Alternating	Max	Max	0.78640	0.00081	0.78802	-0.01877	-16.2
Xlong	Centered	Alternating	Max	Min	0.80929	0.00084	0.81097	--	--
Xlong	In	Alternating	Max	Min	0.78826	0.00082	0.78990	-0.01691	-14.5
Xlong	Out	Alternating	Max	Min	0.80056	0.00081	0.80218	-0.00461	-4.0

Table 6.4.9-3 PULSTAR Intact Assembly Lattice Moderator Ratio Results

Alignment	Radial Shift	Axial Shift	Basket	Lattice H/U Ratio	Pellet to Clad Gap (g/cc)	Interior (g/cc)	Exterior (g/cc)	k_{eff}	σ	$k_{eff}+2\sigma$	Δk	$\Delta k/\sigma$
Xlong	Centered	Alternating	Min	Max	1	1	0	0.80517	0.00083	0.80683	--	--
Xlong	Centered	Alternating	Min	Max	1	1	0	0.79497	0.00080	0.79657	-0.01020	-8.8
Xlong	Centered	Alternating	Min	Max	1	1	0	0.80517	0.00083	0.80683	--	--
Xlong	Centered	Alternating	Min	Min	0	1	0	0.79541	0.00080	0.79701	-0.00976	-8.5

Table 6.4.9-4 PULSTAR Canned Intact Element Results

Cask Array	# Cans per Cask	Assembly Alignment	Interior (g/cc)	Exterior (g/cc)	Can (g/cc)	k_{eff}	σ	$k_{eff}+2\sigma$	Δk	$\Delta k/\sigma$
Infinite	28	--	1	0	1	0.89919	0.00083	0.90085	--	--
Infinite	28	--	0	0	1	0.98516	0.00076	0.98668	0.08597	76.4
Infinite	28	--	1	0	0	0.52383	0.00066	0.52515	-0.46133	-458.3
Infinite	14	Xlong	0	0	1	0.92654	0.00079	0.92812	--	--
Single	14	Xlong	0	0	1	0.84286	0.00083	0.84452	-0.08368	-73.0
3 Casks	14	Xlong	0	0	1	0.84910	0.00079	0.85068	-0.07744	-69.3
Infinite; Water Neutron Shield	14	Xlong	0	0	0	0.17042	0.00023	0.17088	-0.75612	-919.0

Table 6.4.9-5 PULSTAR Canned Homogenized Element Results

Cask Array	# Cans per Cask	Assembly Alignment	Interior (g/cc)	Exterior (g/cc)	Can (g/cc)	k_{eff}	σ	$k_{eff}+2\sigma$	Δk	$\Delta k/\sigma$
Infinite	28	--	1	0	1	0.92819	0.00079	0.92977	--	--
Infinite	28	--	0	0	1	1.01473	0.00075	1.01623	0.08654	79.4
Infinite	28	--	1	0	0	0.52684	0.00067	0.52818	-0.48789	-485.1
Infinite	14	Xlong	0	0	1	0.94917	0.00074	0.95065	--	--
Single	14	Xlong	0	0	1	0.86031	0.00081	0.86193	-0.08886	-81.0
3 Casks	14	Xlong	0	0	1	0.86961	0.00081	0.87123	-0.07956	-72.5
Infinite; Water Neutron Shield	14	Xlong	0	0	0	0.16471	0.00023	0.16517	-0.78446	-1012.3

Table 6.4.9-6 PULSTAR Maximum Reactivity Summary

Configuration	Cask Array	$k_{\text{eff}} + 2\sigma$	k_s	CSI
28 Intact Assemblies	Infinite	0.81097	0.82487	0
28 16-Element Fuel Rod Inserts	Infinite	0.70234	0.71624	0
14 Intact Assemblies & 14 Cans w/Intact Elements	3	0.85068	0.86458	33.4
14 Intact Assemblies & 14 Cans w/Homogenized Elements	3	0.87123	0.88513	33.4

6.4.10 ANSTO Basket Payloads

This section presents the criticality analyses for the NAC-LWT cask with the spiral fuel assemblies and MOATA plate bundles in the ANSTO basket configuration. This evaluation meets the criticality safety requirements of 10 CFR Parts 71.55 and 71.59, as well as IAEA Transportation Safety Standards (TS-R-1). In this analysis, the bounding assembly characteristics are determined and infinite arrays of NAC-LWT casks are studied to determine bounding basket configurations for criticality under normal and accident conditions. Moderator density in the cavity, neutron shield tank and outside is varied to determine the maximum k_{eff} . The analyses demonstrate that, including all calculational and mechanical uncertainties, the NAC-LWT remains subcritical under normal and accident conditions for spiral fuel assemblies and MOATA plate bundles in the ANSTO basket configuration.

6.4.10.1 Spiral Fuel Assemblies

Initial evaluations document the reactivity of the fuel assembly in a nominal configuration basket. The cask model is set to accident conditions with neutron shield and cask exterior material voided. This base model is then modified to evaluate basket configuration and fuel material changes individually or in combination. For all evaluations, the ^{235}U enrichment percentage is set to its maximum value, as increased ^{235}U weight percent minimizes parasitic absorption in ^{238}U .

Reactivity results for the mechanical perturbation studies of the system and tolerances applied to the fuel material definition are included in Table 6.4.10-1. Manufacturing tolerance studies of the basket are listed in Table 6.4.10-2. Basket tolerance studies, as well as fuel studies shown later, rely on a base model containing maximum tolerance fissile material mass and uranium weight percent in the fuel meat.

The majority of evaluations presented in this section are based on a volume-conserving model with three fuel rings. This model requires a significant decrease in core thickness to conserve fuel meat volume, with only a minimal change to the plate thickness. As shown in Table 6.4.10-1, the model based on the original fuel plate dimension has a slightly higher reactivity. The increased reactivity in the plate-based model is the result of a smaller clad thickness than the one applied to the volume-conserving model. Evaluations performed later in this section reduce the clad to a minimum (0.01 cm) and, therefore, bound the as-manufactured plate configuration. Further calculations are, therefore, all based on a volume-conserving base model.

Maximum reactivity material, basket tolerances, and mechanical perturbation configurations are listed in the following bullets:

- Radial shift in – close approach active fuel
There is no statistically significant difference between a shifted middle fuel element and a centered middle fuel element. The centered middle fuel element is chosen to continue the remaining evaluations.
- Axial alternating shift – close approach active fuel
- Maximum ^{235}U mass and maximum uranium weight percentage
Within the range of uranium weight percentages evaluated, there is no effect on system reactivity. As documented in the MTR evaluation set, a large increase in uranium percentage (well beyond reasonable manufacturing limits) will increase reactivity. Therefore, maximum uranium percentage is retained for the remaining reactivity evaluations.
- Minimum fuel tube thickness
For the tube specified, minimum tube thickness equals nominal thickness (tolerance is defined as -0%, +22%).
- No significant effect associated with other basket tolerances
As reduced basket bottom plate and tube height removes absorber material from the system, the remaining reactivity evaluations set these variables to minimum. Fuel tube OD is set to maximum as it shows a slight, if not significant, reactivity increase. Increasing tube OD trades off raised moderation against increased absorber in the larger tube.

Next, fuel assembly dimensional effects are evaluated. The results of the fuel tolerance studies are documented in Table 6.4.10-3. The maximum system reactivity fuel configuration is itemized in the following bullets.

- Minimum plate thickness – increases moderator available between inner and outer assembly sleeves
- Minimum clad thickness
Maximum reactivity obtained from a case where clad thickness is conservatively set to a minimum of 0.01 cm.
- Minimum active fuel height – reduces the space between fissile material in the alternating shifted model
- Minimum element height – reduces the space between fissile material in the alternating shifted model
Set to active fuel height to remove variable as a potential licensing limit.
- Minimum sleeve (shell dimensions) – conservatively set to 0.01 cm thick
Provides additional moderation in the system.
- Maximum plate pitch
Plates were modeled as a set of three cylinders at various pitches. Maximum reactivity is obtained from a system with the middle cylinder centered between inner and outer aluminum assembly shells (sleeves) and the remaining cylinders pushed

away from the center. This significantly increases the pitch between fuel materials above the 10 plate as-built assembly. Inner and outer sleeve (shell) dimensions were conservatively set to a thickness of 0.01 cm. This was done to increase volume inside the annular region, maximizing the volume available for fuel and moderator.

Cask interior and exterior moderator density variation studies are included in Table 6.4.10-4. Moderator density variations are performed on the most-reactive basket and cask configuration under the accident condition (i.e., loss of neutron shield integrity). These studies demonstrate that for a fully moderated cask interior, any increase in cask exterior moderator density reduces reactivity by decoupling the casks in the array. This data is consistent with the lower reactivity obtained from the normal condition case, where the cask water neutron shield isolates casks in the infinite array. The reactivity curve for modified interior density demonstrates that within the statistical uncertainty of the evaluation, a fully moderated cask interior represents a bounding condition. No significant variations in reactivity occur for moderator densities above 0.9 g/cm³. A plot of the interior density study is shown in Figure 6.4.10-1.

Results for a nominal condition infinite cask array, worst-case configuration accident condition (voided neutron shield) and normal conditions of operations (filled neutron shield) arrays, and for a single cask with a fully reflected containment boundary are included in Table 6.4.10-5. Maximum bias adjusted system reactivity is 0.746, well below the 0.95 safety limit for the system. As an infinite array of casks is subcritical under both normal and accident conditions, the criticality safety index (CSI) is 0.

The reactivity evaluation of the NAC-LWT cask containing up to 42 spiral fuel assemblies (elements), demonstrates that subcritical margin ($k_s \leq 0.95$) can be maintained under the following conditions:

Parameter	Value
Number of Fuel Plates	10
Plate Thickness	≥ 0.124 cm
Active Fuel Height	≥ 59.075 cm
²³⁵ U Content per Element	≤ 160
Enrichment wt % ²³⁵ U	≤ 85

6.4.10.2 MOATA Plate Bundles

Initial evaluations document the reactivity of the plate bundle in a nominal configuration basket. The cask model is set to accident conditions with neutron shield and cask exterior material voided. This base model is then modified to evaluate basket configuration and fuel material changes individually or in combination. Results of these evaluations are documented in Table

6.4.10-6 and Table 6.4.10-7. Basket tolerance studies, as well as fuel studies shown later, rely on a base model containing maximum tolerance fissile material mass and uranium weight percent in the fuel meat. For all evaluations, the ^{235}U enrichment percentage is set to its maximum value as increased ^{235}U weight percent minimizes parasitic absorption in ^{238}U .

Maximum reactivity material, basket tolerances, and mechanical perturbation configurations are listed in the following bullets.

- Radial shift in – close approach active fuel
No statistically significant difference between shifted middle fuel element and a centered middle fuel element. The centered middle fuel element is chosen to continue the remaining evaluations.
- Axial alternating shift – close approach active fuel
- Maximum ^{235}U mass and maximum uranium weight percentage
- Minimum fuel tube thickness
For the tube specified, minimum tube thickness equals nominal thickness (tolerance is defined as -0%, +22%).
- No significant effect associated with other basket tolerances
As reduced basket bottom plate and tube height removes absorber material from the system, the remaining reactivity evaluations set these variables to minimum.
Fuel tube OD is retained at nominal as there is no significant effect on system reactivity for this variable, and offsetting neutronic effects occur for a change in tube size (e.g., increasing OD increases parasitic absorber and separates fissile material but provides additional moderator in the fuel region).

Next, fuel assembly dimensional and material effects are evaluated. The results of the fuel tolerance studies are documented in Table 6.4.10-8. Maximum system reactivity fuel configuration is itemized in the following bullets.

- Maximum active fuel width
The tolerance applied to the active fuel width is one-half the distance between active fuel width and plate width. Applying this tolerance (0.3175 cm for the nominal plate width and 0.3366 cm for the maximum tolerance plate width) significantly increases system reactivity. Maximum allowed active fuel width by this analysis is 7.32 cm (conservatively rounded down from the 7.3266 cm evaluated).
- Maximum plate width
Plate width variation taken independently has no effect on system reactivity. Analysis tied plate width to active fuel width, as no tolerance on the actual fuel width was available. Increasing plate width thereby increased the maximum active fuel width, which was shown to be bounding.
- Nominal plate thickness
Plate bundle moderator to fuel ration (H/U) is controlled by the plate spacer thickness

not plate thickness. Therefore, there is no significant effect of plate thickness on the bundle reactivity.

- **Minimum clad thickness**
Maximum reactivity obtained from a case where clad thickness is conservatively set to a minimum of 0.01 cm.
- **Nominal active fuel height**
Contrary to the spiral fuel and DIDO evaluation set, no significant effect of active fuel height was observed in the calculations.
- **Minimum element height – reduces the space between fissile materials in the alternating shifted model**
Set to active fuel height to remove variable as a potential licensing limit. Note that the end-fitting structure of the plate bundle will assure significant separation between active fuel regions.
- **Maximum plate spacer**
A conservative maximum spacer of 0.18 cm thickness was evaluated and shown to be bounding.
- **Replacing aluminum side plates by water**
Provides additional moderation in the system.

Cask interior and exterior moderator density variation studies are included in Table 6.4.10-9. These studies demonstrate that for a fully moderated cask interior, any increase in cask exterior density reduces reactivity by decoupling the casks in the array. This data is consistent for reduced reactivity obtained from the normal condition case where the cask water neutron shield isolates casks in the infinite array modeled. The reactivity curve for modified interior density demonstrates that within the statistical uncertainty of the evaluation, a fully moderated cask interior represents a bounding condition. No significant variations in reactivity occur for moderator densities above 0.95 g/cm³. A plot of the interior density study is shown in Figure 6.4.10-2.

Results for a nominal condition infinite cask array, worst-case configuration accident condition (voided neutron shield) and normal conditions of operation (filled neutron shield) arrays, and for a single cask with a fully reflected containment boundary are included in Table 6.4.10-10. Maximum bias adjusted system reactivity is 0.763, well below the 0.95 safety limit for the system. As an infinite array of casks is subcritical under both normal and accident conditions, the criticality safety index (CSI) is 0.

The reactivity evaluation of the NAC-LWT cask containing up to 42 MOATA plate bundles demonstrates that subcritical margin ($k_s \leq 0.95$) can be maintained under the following conditions.

Parameter	MOATA Plate Bundle
Max. Number of Fuel Plates	14
Spacer Thickness	≤ 0.18 cm
Active Fuel Width	≤ 7.32 cm
²³⁵ U Content per Plate	≤ 22.3
Enrichment wt % ²³⁵ U	≤ 92

6.4.10.3 Mixed Basket Loading – Spiral Assemblies Basket and Plate Bundle Basket

The NAC-LWT may transport a combination of spiral elements and plate bundle elements. Given the low, and similar, reactivity of each payload, the combination of payloads is not expected to increase reactivity. A combination of three baskets of spiral elements and three baskets of plate bundles is evaluated to support the bounding statement. Casks are evaluated once with the top three baskets loaded with plate bundles and the bottom three baskets loaded with spiral elements, and once with an alternating spiral elements and plate bundles set. As shown in the following list, there is no increase in reactivity associated with mixed loading of plate bundles and spiral elements.

# Casks	Condition	Description	k_{eff}	σ	$k_{eff}+2\sigma$
Infinite Array	Accident	Nominal case of MOATA plate bundle load	0.68207	0.00078	0.68363
Infinite Array	Accident	Nominal case of spiral fuel	0.65957	0.00066	0.66089
Infinite Array	Accident	Alternating MOATA and spiral fuel load	0.67249	0.00068	0.67385
Infinite Array	Accident	Stack of 3 MOATA baskets and 3 spiral baskets	0.67403	0.00069	0.67541

Figure 6.4.10-1 Spiral Fuel - Moderator Density Plot

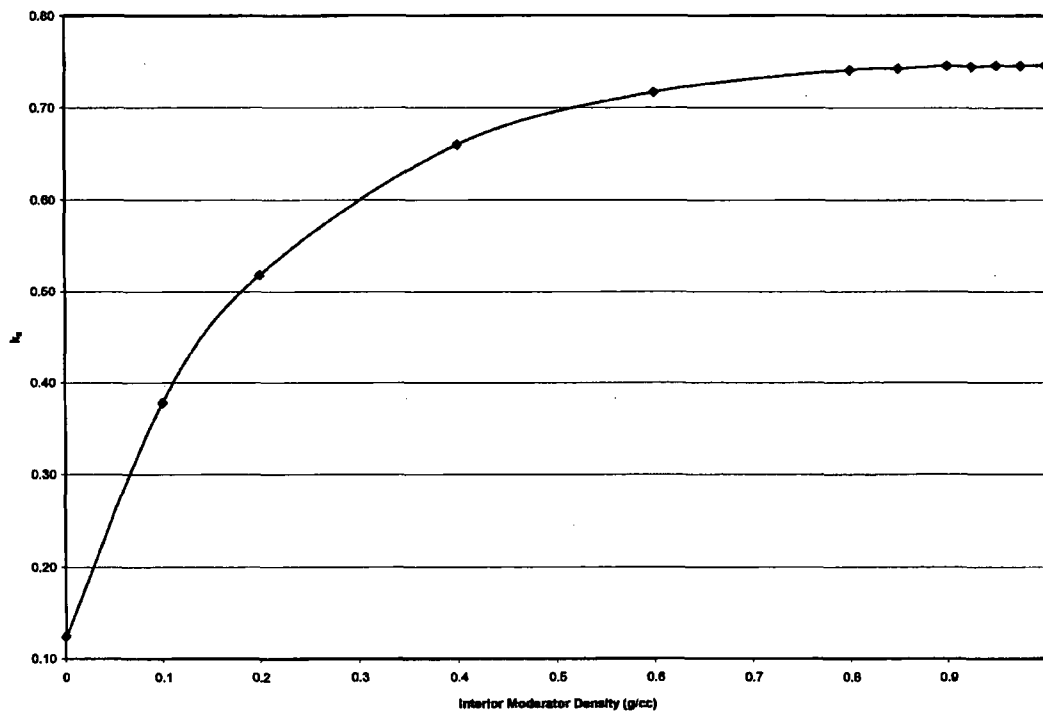


Figure 6.4.10-2 MOATA Plate Bundle -Moderator Density Plot

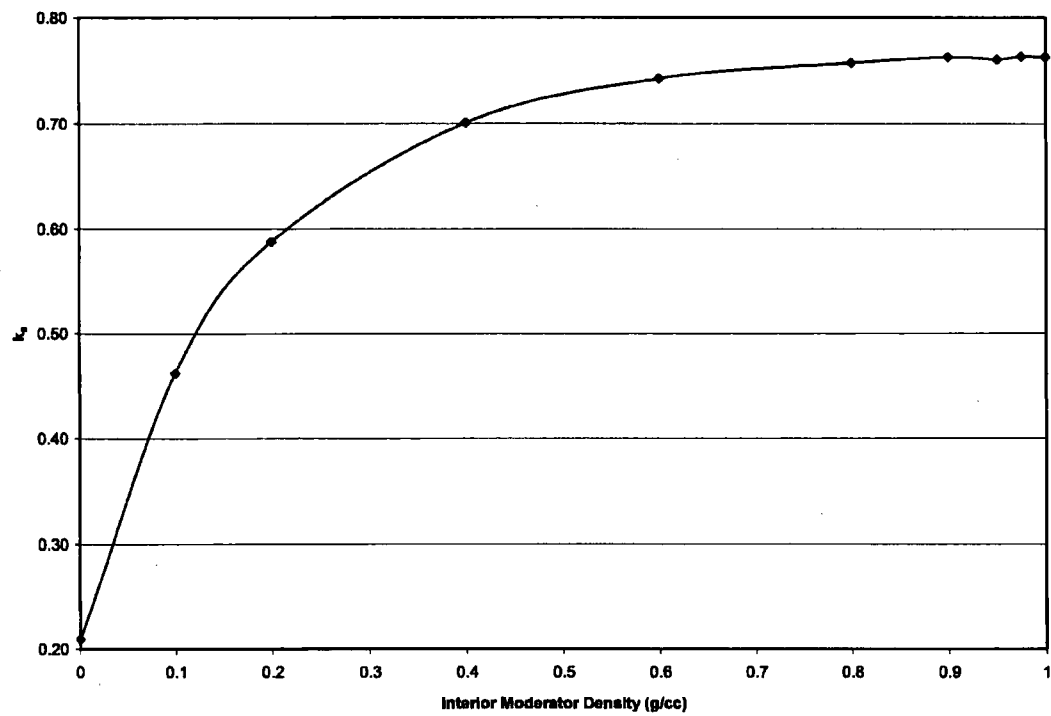


Table 6.4.10-1 Spiral Fuel Assembly - Base Data Comparisons

Base Data ¹	Cask Condition	Radial Shift Pattern	Axial Shift Pattern	²³⁵ U Mass Tolerance	Uranium Weight Fraction Tolerance	k_{eff}	σ	$k_{eff}+2\sigma$	k_s	Δk	$\Delta k_{eff}/\sigma$
Volume	Accident	CenteredC	Down	Nominal	Nominal	0.65222	0.00064	0.65350	0.67160	-0.00862	-13.5
Volume	Accident	CenteredC	Alternating	Nominal	Nominal	0.65957	0.00066	0.66089	0.67899	-0.00123	-1.9
Plate	Accident	CenteredC	Alternating	Nominal	Nominal	0.66084	0.00064	0.66212	0.68022	--	--
Volume	Accident	CenteredC	Alternating	Min	Nominal	0.63917	0.00067	0.64051	0.65861	-0.02161	-32.3
Volume	Accident	CenteredC	Alternating	Max	Nominal	0.68143	0.00065	0.68273	0.70083	0.02061	31.7
Volume	Accident	CenteredC	Alternating	Nominal	Min	0.65967	0.00066	0.66099	0.67909	-0.00113	-1.7
Volume	Accident	CenteredC	Alternating	Nominal	Max	0.66025	0.00065	0.66155	0.67965	-0.00057	-0.9
Volume	Accident	OutC	Alternating	Nominal	Nominal	0.65823	0.00062	0.65947	0.67757	-0.00265	-4.3
Volume	Accident	In	Alternating	Nominal	Nominal	0.66333	0.00063	0.66459	0.68269	0.00247	3.9
Volume	Accident	InC	Alternating	Nominal	Nominal	0.66273	0.00069	0.66411	0.68221	0.00199	2.9
Volume	Accident	InC	Alternating	Max	Nominal	0.68337	0.00066	0.68469	0.70279	0.02257	34.2

¹ Refers to cylindrical fuel approximation being based on the original plate dimension or on volume (i.e., H/U ratio) conserving model.

Table 6.4.10-2 Spiral Fuel Assembly - Basket Tolerance Evaluations

Fuel Tube Outer Diameter Tolerance	Fuel Tube Thickness Tolerance	Fuel Tube Height Tolerance	Fuel Basket Base Plate Tolerance	k_{eff}	σ	$k_{eff}+2\sigma$	k_s	Δk	$\Delta k_{eff}/\sigma$
Nominal	Nominal	Nominal	Nominal	0.68310	0.00069	0.68448	0.70258	—	—
Min	Nominal	Nominal	Nominal	0.68153	0.00066	0.68285	0.70095	-0.00163	-2.5
Max	Nominal	Nominal	Nominal	0.68410	0.00067	0.68544	0.70354	0.00096	1.4
Nominal	Min	Nominal	Nominal	0.68310	0.00069	0.68448	0.70258	—	—
Nominal	Max	Nominal	Nominal	0.65917	0.00067	0.66051	0.67861	-0.02397	-35.8
Nominal	Nominal	Min	Nominal	0.68368	0.00067	0.68502	0.70312	0.00054	0.8
Nominal	Nominal	Max	Nominal	0.68218	0.00065	0.68348	0.70158	-0.00100	-1.5
Nominal	Nominal	Nominal	Min	0.68341	0.00067	0.68475	0.70285	0.00027	0.4
Nominal	Nominal	Nominal	Max	0.68325	0.00064	0.68453	0.70263	0.00005	0.1
Min	Min	Min	Min	0.68254	0.00064	0.68382	0.70192	-0.00066	-1.0
Nominal	Min	Min	Min	0.68316	0.00068	0.68452	0.70262	0.00004	0.1
Max	Min	Min	Min	0.68434	0.00068	0.68570	0.70380	0.00122	1.8

Table 6.4.10-3 Spiral Fuel Assembly – Fuel Tolerance Evaluations

Fuel Plate Thickness Tolerance	Fuel Plate Clad Thickness Tolerance	Active Fuel Length Tolerance	Element Height Tolerance	H/U Study (Plate Location)	Inner & Outer Shells	k_{eff}	σ	$k_{eff}+2\sigma$	k_s	Δk	$\Delta k_{eff}/\sigma$
Nominal	Nominal	Nominal	Nominal	Nominal	Nominal	0.68310	0.00069	0.68448	0.70258	–	–
Min	Nominal	Nominal	Nominal	Nominal	Nominal	0.68643	0.00067	0.68777	0.70587	0.00329	4.9
Max	Nominal	Nominal	Nominal	Nominal	Nominal	0.68082	0.00067	0.68216	0.70026	-0.00232	-3.5
Nominal	No Clad	Nominal	Nominal	Nominal	Nominal	0.69059	0.00067	0.69193	0.71003	0.00745	11.1
Nominal	Min	Nominal	Nominal	Nominal	Nominal	0.68737	0.00066	0.68869	0.70679	0.00421	6.4
Nominal	Max	Nominal	Nominal	Nominal	Nominal	0.68003	0.00064	0.68131	0.69941	-0.00317	-5.0
Nominal	Nominal	Min	Nominal	Nominal	Nominal	0.68619	0.00067	0.68753	0.70563	0.00305	4.6
Nominal	Nominal	Max	Nominal	Nominal	Nominal	0.68111	0.00068	0.68247	0.70057	-0.00201	-3.0
Nominal	Nominal	Nominal	Fuel	Nominal	Nominal	0.68821	0.00065	0.68951	0.70761	0.00503	7.7
Nominal	Nominal	Nominal	Min	Nominal	Nominal	0.68512	0.00066	0.68644	0.70454	0.00196	3.0
Nominal	Nominal	Nominal	Max	Nominal	Nominal	0.68125	0.00068	0.68261	0.70071	-0.00187	-2.8
Nominal	Nominal	Nominal	Nominal	Min	Nominal	0.67318	0.00066	0.67450	0.69260	-0.00998	-15.1
Nominal	Nominal	Nominal	Nominal	Max	Nominal	0.69131	0.00066	0.69263	0.71073	0.00815	12.3
Nominal	Nominal	Nominal	Nominal	Min	Min	0.67580	0.00068	0.67716	0.69526	-0.00732	-10.8
Nominal	Nominal	Nominal	Nominal	Nominal	Min	0.69148	0.00067	0.69282	0.71092	0.00834	12.4
Nominal	Nominal	Nominal	Nominal	Max	Min	0.70408	0.00067	0.70542	0.72352	0.02094	31.3
Min	No_Clad	Min	Fuel	Max	Min	0.72459	0.00066	0.72591	0.74401	0.04143	62.8

Table 6.4.10-4 Spiral Fuel Assembly - Moderator Density Variations

Set	Interior Moderator Density (g/cm ³)	Exterior Moderator Density (g/cm ³)	k _{eff}	σ	k _{eff} +2σ	k _s
H1	0.9998	0.0001	0.72640	0.00067	0.72774	0.74584
	0.9998	0.1	0.69875	0.00066	0.70007	0.71817
	0.9998	0.5	0.69587	0.00067	0.69721	0.71531
	0.9998	0.9998	0.69661	0.00067	0.69795	0.71605
H2	0.9998	0.0001	0.72640	0.00067	0.72774	0.74584
	0.975	0.0001	0.72575	0.00066	0.72707	0.74517
	0.95	0.0001	0.72604	0.00066	0.72736	0.74546
	0.925	0.0001	0.72466	0.00068	0.72602	0.74412
	0.9	0.0001	0.72562	0.00066	0.72694	0.74504
	0.85	0.0001	0.72273	0.00067	0.72407	0.74217
	0.8	0.0001	0.72102	0.00069	0.72240	0.74050
	0.6	0.0001	0.69709	0.00068	0.69845	0.71655
	0.4	0.0001	0.63905	0.00150	0.64205	0.66015
	0.2	0.0001	0.49709	0.00138	0.49985	0.51795
	0.1	0.0001	0.35749	0.00125	0.35999	0.37809
	0.0001	0.0001	0.10524	0.00046	0.10616	0.12426

Table 6.4.10-5 Spiral Fuel Assembly - Maximum Reactivity Case Summary

# Casks	Condition	Description	k_{eff}	σ	$k_{eff}+2\sigma$	k_s
Infinite Array	Accident	Nominal configuration accident case	0.66084	0.00064	0.66212	0.68022
Infinite Array	Accident	Maximum reactivity material and shift case nominal fuel and basket configuration	0.68310	0.00069	0.68448	0.70258
Infinite Array	Accident	Maximum reactivity basket tolerance – nominal fuel configuration	0.68434	0.00068	0.68570	0.70380
Infinite Array	Accident	Maximum reactivity fuel tolerance – nominal basket configuration	0.72459	0.00066	0.72591	0.74401
Infinite Array	Accident	Combined maximum reactivity configuration case	0.72640	0.00067	0.72774	0.74584
Infinite Array	Normal	Combined maximum reactivity configuration case	0.69609	0.00069	0.69747	0.71557
Single Cask	N/A	Single cask / inner shell reflected with water - maximum reactivity configuration	0.65762	0.00067	0.65896	0.67706

Table 6.4.10-6 MOATA Plate Bundle - Base Data Comparisons

Cask Condition	Radial Shift Pattern	Axial Shift Pattern	²³⁵ U Mass Tolerance	Uranium Weight Fraction Tolerance	k_{eff}	σ	$k_{eff}+2\sigma$	k_s	Δk	$\Delta k_{eff,l}$
Accident	CenteredC	Down	Nominal	Nominal	0.67757	0.00074	0.67905	0.69715	-0.00458	-6.2
Accident	CenteredC	Alternating	Nominal	Nominal	0.68207	0.00078	0.68363	0.70173	--	--
Accident	CenteredC	Alternating	Nominal	Min	0.68113	0.00077	0.68267	0.70077	-0.00096	-1.2
Accident	CenteredC	Alternating	Nominal	Max	0.68367	0.00077	0.68521	0.70331	0.00158	2.1
Accident	CenteredC	Alternating	Min	Nominal	0.68163	0.00076	0.68315	0.70125	-0.00048	-0.6
Accident	CenteredC	Alternating	Max	Nominal	0.68624	0.00076	0.68776	0.70586	0.00413	5.4
Accident	OutC	Alternating	Max	Nominal	0.67948	0.00077	0.68102	0.69912	-0.00261	-3.4
Accident	In	Alternating	Max	Nominal	0.69075	0.00078	0.69231	0.71041	0.00868	11.1
Accident	InC	Alternating	Max	Nominal	0.69125	0.00080	0.69285	0.71095	0.00922	11.5
Accident	InC	Alternating	Max	Max	0.69234	0.00078	0.69390	0.71200	0.01027	13.2

Table 6.4.10-7 MOATA Plate Bundle – Basket Tolerance Evaluations

Fuel Tube Outer Diameter Tolerance	Fuel Tube Thickness Tolerance	Fuel Tube Height Tolerance	Fuel Basket Base Plate Tolerance	k_{eff}	σ	$k_{eff}+2\sigma$	k_s	Δk	$\Delta k_{eff}/\sigma$
Nominal	Nominal	Nominal	Nominal	0.69234	0.00078	0.69390	0.71200	–	–
Min	Nominal	Nominal	Nominal	0.68994	0.00077	0.69148	0.70958	-0.00242	-3.1
Max	Nominal	Nominal	Nominal	0.69108	0.00075	0.69258	0.71068	-0.00132	-1.8
Nominal	Min	Nominal	Nominal	0.69234	0.00078	0.69390	0.71200	–	–
Nominal	Max	Nominal	Nominal	0.67140	0.00077	0.67294	0.69104	-0.02096	-27.2
Nominal	Nominal	Min	Nominal	0.69146	0.00080	0.69306	0.71116	-0.00084	-1.0
Nominal	Nominal	Max	Nominal	0.69054	0.00079	0.69212	0.71022	-0.00178	-2.3
Nominal	Nominal	Nominal	Min	0.69152	0.00078	0.69308	0.71118	-0.00082	-1.1
Nominal	Nominal	Nominal	Max	0.69204	0.00079	0.69362	0.71172	-0.00028	-0.4
Max	Min	Min	Min	0.69326	0.00078	0.69482	0.71292	0.00092	1.2
Nominal	Min	Min	Min	0.69364	0.00077	0.69518	0.71328	0.00128	1.7
Min	Min	Min	Min	0.69024	0.00079	0.69182	0.70992	-0.00208	-2.6

Table 6.4.10-8 MOATA Plate Bundle - Fuel Tolerance Evaluations

Fuel Plate Width Tolerance	Fuel Plate Thickness Tolerance	Fuel Plate Clad Thickness Tolerance	Active Fuel Length Tolerance	Active Fuel Width Tolerance	Element Height Tolerance	Spacer Thickness Tolerance	Side Plate Thickness Tolerance	Side Plate Width Tolerance	k_{eff}	σ	$k_{eff}+2\sigma$	k_s	Δk	$\Delta k_{eff}/\sigma$
Nominal	Nominal	Nominal	Nominal	Nominal	Nominal	Nominal	Nominal	Nominal	0.69234	0.00078	0.69390	0.71200	—	—
Min	Nominal	Nominal	Nominal	Nominal	Nominal	Nominal	Nominal	Nominal	0.69017	0.00078	0.69173	0.70983	-0.00217	-2.8
Max	Nominal	Nominal	Nominal	Nominal	Nominal	Nominal	Nominal	Nominal	0.69105	0.00077	0.69259	0.71069	-0.00131	-1.7
Nominal	Min	Nominal	Nominal	Nominal	Nominal	Nominal	Nominal	Nominal	0.69190	0.00078	0.69346	0.71156	-0.00044	-0.6
Nominal	Max	Nominal	Nominal	Nominal	Nominal	Nominal	Nominal	Nominal	0.69192	0.00077	0.69346	0.71156	-0.00044	-0.6
Nominal	Nominal	Min	Nominal	Nominal	Nominal	Nominal	Nominal	Nominal	0.69424	0.00077	0.69578	0.71388	0.00188	2.4
Nominal	Nominal	Max	Nominal	Nominal	Nominal	Nominal	Nominal	Nominal	0.69150	0.00078	0.69306	0.71116	-0.00084	-1.1
Nominal	Nominal	Nominal	Min	Nominal	Nominal	Nominal	Nominal	Nominal	0.68998	0.00079	0.69156	0.70966	-0.00234	-3.0
Nominal	Nominal	Nominal	Max	Nominal	Nominal	Nominal	Nominal	Nominal	0.69153	0.00078	0.69309	0.71119	-0.00081	-1.0
Nominal	Nominal	Nominal	Nominal	Min	Nominal	Nominal	Nominal	Nominal	0.68240	0.00082	0.68404	0.70214	-0.00986	-12.0
Nominal	Nominal	Nominal	Nominal	Max	Nominal	Nominal	Nominal	Nominal	0.69920	0.00080	0.70080	0.71890	0.00690	8.6
Nominal	Nominal	Nominal	Nominal	Nominal	Fuel	Nominal	Nominal	Nominal	0.70756	0.00079	0.70914	0.72724	0.01524	19.3
Nominal	Nominal	Nominal	Nominal	Nominal	Min	Nominal	Nominal	Nominal	0.69029	0.00077	0.69183	0.70993	-0.00207	-2.7
Nominal	Nominal	Nominal	Nominal	Nominal	Max	Nominal	Nominal	Nominal	0.69220	0.00080	0.69380	0.71190	-0.00010	-0.1
Nominal	Nominal	Nominal	Nominal	Nominal	Nominal	Min	Nominal	Nominal	0.67080	0.00076	0.67232	0.69042	-0.02158	-28.4
Nominal	Nominal	Nominal	Nominal	Nominal	Nominal	Max	Nominal	Nominal	0.70952	0.00078	0.71108	0.72918	0.01718	22.0
Nominal	Nominal	Nominal	Nominal	Nominal	Nominal	Nominal	Water	Nominal	0.69518	0.00080	0.69678	0.71488	0.00288	3.6
Nominal	Nominal	Nominal	Nominal	Nominal	Nominal	Nominal	Min	Nominal	0.69087	0.00079	0.69245	0.71055	-0.00145	-1.8
Nominal	Nominal	Nominal	Nominal	Nominal	Nominal	Nominal	Max	Nominal	0.69185	0.00077	0.69339	0.71149	-0.00051	-0.7
Nominal	Nominal	Nominal	Nominal	Nominal	Nominal	Nominal	Nominal	Min	0.69203	0.00075	0.69353	0.71163	-0.00037	-0.5
Nominal	Nominal	Nominal	Nominal	Nominal	Nominal	Nominal	Nominal	Max	0.69179	0.00074	0.69327	0.71137	-0.00063	-0.9
Max	Nominal	Min	Nominal	Max	Fuel	Max	Nominal	Nominal	0.73925	0.00078	0.74081	0.75891	0.04691	60.1
Max	Nominal	Min	Nominal	Max	Fuel	Max	Water	Water	0.74205	0.00081	0.74367	0.76177	0.04977	61.4

Table 6.4.10-9 MOATA Plate Bundle - Moderator Density Variations

Set	Interior Moderator Density (g/cm ³)	Exterior Moderator Density (g/cm ³)	k _{eff}	σ	k _{eff} +2σ	k _s
H1	0.9998	0.0001	0.74285	0.00081	0.74447	0.76257
	0.9998	0.1	0.71116	0.00081	0.71278	0.73088
	0.9998	0.5	0.70785	0.00080	0.70945	0.72755
	0.9998	0.9998	0.70742	0.00081	0.70904	0.72714
H2	0.9998	0.0001	0.74285	0.00081	0.74447	0.76257
	0.975	0.0001	0.74337	0.00080	0.74497	0.76307
	0.95	0.0001	0.74073	0.00078	0.74229	0.76039
	0.9	0.0001	0.74275	0.00078	0.74431	0.76241
	0.8	0.0001	0.73741	0.00077	0.73895	0.75705
	0.6	0.0001	0.72186	0.00124	0.72434	0.74244
	0.4	0.0001	0.67919	0.00174	0.68267	0.70077
	0.2	0.0001	0.56690	0.00133	0.56956	0.58766
	0.1	0.0001	0.44132	0.00118	0.44368	0.46178
	0.0001	0.0001	0.19016	0.00057	0.19130	0.20940

Table 6.4.10-10 MOATA Plate Bundle - Maximum Reactivity Case Summary

# Casks	Condition	Description	k_{eff}	σ	$k_{eff}+2\sigma$	k_s
Infinite Array	Accident	Nominal configuration accident case	0.68207	0.00078	0.68363	0.70173
Infinite Array	Accident	Maximum reactivity material and shift case	0.69234	0.00078	0.69390	0.71200
Infinite Array	Accident	Maximum reactivity basket tolerance	0.69024	0.00079	0.69182	0.70992
Infinite Array	Accident	Maximum reactivity fuel tolerance	0.74205	0.00081	0.74367	0.76177
Infinite Array	Accident	Combined maximum reactivity configuration case	0.74285	0.00081	0.74447	0.76257
Infinite Array	Normal	Combined maximum reactivity configuration case	0.70622	0.00082	0.70786	0.72596
Single Cask	N/A	Single cask / inner shell reflected with water - maximum reactivity configuration	0.65594	0.00082	0.65758	0.67568

6.5 Critical Benchmarks

The results of the criticality analyses presented in this chapter are corrected for bias and uncertainty resulting from the method using information obtained from the analysis of criticality benchmark experimental data. Sections 6.5.1 through 6.5.3 present the results of these benchmark evaluations.

6.5.1 PWR and BWR Fuel Assemblies

This section provides the validation of the CSAS25 criticality analysis sequence contained in Version 4.3 of the SCALE package. This validation is required by the criticality safety standards ANSI/ANS-8.1. The section describes the method, computer program and cross-section libraries used, experimental data, areas of applicability, and bias and margins of safety.

ANSI/ANS-8.17 prescribes the criterion to establish subcriticality safety margins. This criterion is as follows:

$$k_s \leq k_c - \Delta k_s - \Delta k_m \quad (1)$$

where:

k_s = calculated allowable maximum multiplication factor, k_{eff} , of system being evaluated for all normal or credible abnormal conditions or events.

k_c = mean k_{eff} that results from calculation of benchmark criticality experiments using particular calculational method. If calculated k_{eff} values for criticality experiments exhibit trend with parameter, then k_c shall be determined by extrapolation based on best fit to calculated values. Criticality experiments used as benchmarks in computing k_c should have physical compositions, configurations, and nuclear characteristics (including reflectors) similar to those of system being evaluated.

Δk_s = allowance for:

- statistical or convergence uncertainties, or both, in computation of k_s ,
- material and fabrication tolerances, and
- geometric or material representations used in computational method.

Δk_c = margin for uncertainty in k_c which includes allowance for:

- uncertainties in critical experiments,
- statistical or convergence uncertainties, or both, in computation of k_c ,
- uncertainties resulting from extrapolation of k_c outside range of experimental data, and

- d. uncertainties resulting from limitations in geometrical of material representations used in computational method.

Δk_m = arbitrary margin to ensure subcriticality of k_s .

The various uncertainties are combined statistically if they are independent. Correlated uncertainties are combined additively.

Equation 1 can be rewritten as:

$$k_s \leq 1 - \Delta k_m - \Delta k_s - (1 - k_c) - \Delta k_c \quad (2)$$

Noting that the NRC requires a 5% subcriticality margin ($\Delta k_m = 0.05$) and the definition of the bias ($\Delta k_{Bias} = 1 - k_c$), the Equation 2 can then be written as:

$$k_s \leq 0.95 - \Delta k_s - \Delta k_{Bias} - \Delta k_{BU} \quad (3)$$

where $\Delta k_{BU} = \Delta k_c$. Thus, the k_s (the maximum allowable value for k_{eff}) must be below 0.95 minus the bias, uncertainties in the bias, and uncertainties in the system being analyzed (i.e., Monte Carlo, mechanical, and modeling). This is an upper safety limit criteria often used in the DOE criticality safety community.

Alternatively, Equation 3 can be rewritten applying the bias and uncertainties to the k_{eff} of the system being analyzed as:

$$k_s \equiv k_{eff} + \Delta k_s + \Delta k_{Bias} + \Delta k_{BU} \leq 0.95 \quad (4)$$

In Equation 4, k_{eff} replaces k_s , and k_s has been redefined as the effective multiplication factor of the system being analyzed, including the method bias and all uncertainties. This is a maximum calculated k_{eff} criteria often used in LWR spent fuel storage and transport analyses.

For use in criticality evaluations of LWR fuel in storage and transport casks, both k_{Bias} and Δk_{Bias} are evaluated below for KENO-Va with the 27-group ENDF/B-IV library.

6.5.1.1 Benchmark Experiments and Applicability

The criticality safety method is CSAS embedded in SCALE version 4.3 for the PC. CSAS includes the SCALE Material Information Processor, BONAMI-S, NITAWL-S, and KENO-Va. The Material Information Processor generates number densities for standard compositions, prepares geometry data for resonance self-shielding, and creates data input files for the cross-section processing codes. The BONAMI-S and NITAWL-S codes are used to prepare a resonance-corrected cross-section library in AMPX working format. The KENO-Va code uses

Revision 38

Monte Carlo techniques to calculate the model k_{eff} . The 27-group ENDF/B-IV neutron cross-section library is used in this validation.

6.5.1.1.1 Description of Experiments

The 63 critical experiments selected are as follows: 9 B&W 2.46 wt % ^{235}U fuel storage (Baldwin), 10 PNL 4.31 wt % ^{235}U lattice (Bierman and Clayton, July 1980), 21 PNL 2.35 and 4.31 wt % ^{235}U with metal reflectors (Bierman, April 1979 and August 1981), 12 PNL flux trap (Bierman, July 1980 and June 1988) and 11 VCML 4.74 wt % ^{235}U experiments, some involving moderator density variations (Manaranche). These experiments span a range of fuel enrichments, fuel rod pitches, neutron absorber sheet characteristics, shielding materials and geometries that are typical of LWR fuel in a cask.

To achieve accurate results, three-dimensional models, as close to the actual experiment as possible, are used to evaluate the experiments. Stochastic Monte Carlo error is kept within $\pm 0.1\%$ by executing at least 1,000 neutrons/generation for more than 400 generations.

6.5.1.1.2 Applicability of Experiments

All of the experiments chosen in this validation are applicable to either PWR or BWR fuel. Fuel enrichments have covered a range from 2.35 up to 4.74 wt % ^{235}U , typical of LWR fuel presently used. The experiment fuel rod and pitch characteristics are within the range of standard PWR or BWR fuel rods (i.e., pellet OD from 0.78 to 1.2 cm, rod OD from 0.95 to 1.88 cm, and pitch from 1.26 to 1.87 cm). This is particularly true of the VCML (PWR rod type) and B&W experiments (BWR rod type). The H/U volume ratios of the experimental fuel arrays are within the range of PWR fuel assemblies (1.6 to 2.32) and BWR fuel assemblies (1.6 to 1.9). The experiments addressed the influence of water and metal reflector regions, including steel and lead, such as that present in the NAC-LWT cask.

Confidence in predicting criticality, including bias and uncertainty, has been demonstrated for LWR fuel with enrichments up to 4.74 wt % ^{235}U and, based on the lack of a significant trend with increasing enrichment, confidence in extrapolating up to 5 wt % ^{235}U is still high.

Confidence in predicting subcriticality has been demonstrated for arrays in which critical controls consist of flux trap or single neutron absorber sheets or simple spacing. Confidence in predicting subcriticality has also been demonstrated for LWR fuel arrays next to water and metal reflector regions.

6.5.1.2 Results of Benchmark Calculations

The k-effective results for the experiments are shown in Table 6.5.1-1 and a frequency plot is provided in Figure 6.5.1-1. Five sets of cases are presented: Set 1, B&W; Set 2, PNL lattice; Set 3, PNL reflector; Set 4, PNL flux trap, and Set 5, VCML critical experiments. Sixty-three results are reported.

The overall average and standard deviation of the 63 cases is 0.9948 ± 0.0044 . The average Monte Carlo error (statistical convergence) is ± 0.0012 for the 63 cases. This uncertainty component is statistically subtracted from the uncertainties because it is previously included in the standard deviation. The KENO-Va models are three-dimensional, fully explicit representations (no homogenization) of the experimental geometry. Therefore, the uncertainty resulting from limitations of geometrical modeling is taken to be 0.0. The experiments modeled cover the range of fuel types, enrichments, and metal reflector effects so that no extrapolations are necessary outside the range of data, and the uncertainty resulting from extrapolation is also taken to be 0.0. On the basis of the reported experimental error for the B&W cases, the reported error of the critical size number of rods for the PNL cases and the reported error for the critical height in the VCML cases, the experimental error is conservatively taken to be ± 0.001 .

Criticality can then be represented as 1.000 ± 0.001 . This uncertainty component is added to the sum of the other uncertainties.

Thus, the bias or average difference between code calculated and the critical condition is $\Delta k_{\text{Bias}} = 1 - 0.9948 = 0.0052$. The uncertainty in the bias, accounting for the statistical convergence (Monte Carlo error) and the uncertainty in criticality is $(0.0044^2 - 0.0012^2 + 0.0010^2)^{1/2} = 0.0043$. For 63 samples of criticality, the 95/95 one-side tolerance factor is 2.012 (Owen, 1963). The result is a 95/95 one-sided uncertainty in the bias of $\Delta k_{\text{BU}} = 2.012 \times 0.0043 = 0.0087$. Equation 4 now becomes:

$$k_{\text{eff}} + \Delta k_s + 0.0052 + 0.0087 \leq 0.95$$

Where Δk_s becomes the uncertainty in k_s resulting from Monte Carlo error, mechanical and material tolerances, and geometric or material representations. If the nominal representation of the system is evaluated for k_s , then the mechanical and material perturbations can be evaluated independently and can be combined statistically as the root sum of squares. If the worst-case mechanical and material tolerances are used in the analysis, then Δk_s becomes 0.0 and the Monte Carlo error, σ_{mc} , can be combined with the uncertainty in the bias as:

$$k_{\text{eff}} + 2\sigma_{\text{mc}} + 0.0052 + 0.0087 \leq 0.95$$

6.5.1.3 Trends

Frequency distribution of k_{eff} values and scatter plots of k_{eff} versus wt % ^{235}U , rod pitch, H/U volume ratio, and average neutron group causing fission are shown in Figure 6.5.1-1 through Figure 6.5.1-5. Included in the scatter plots are linear regression lines with a corresponding correlation coefficient to statistically indicate any trend or lack thereof. In particular, the correlation coefficient is a measure of the linear relationship between k_{eff} and a critical experiment parameter. If r is +1, a perfect linear relationship with a positive slope is indicated, and if r is -1, a perfect linear relationship with a negative slope is indicated. When r is 0, no linear relationship is indicated. The largest correlation coefficient indicated in the plots is 0.1302 (k_{eff} versus enrichment) and the lowest is 0.0176 (k_{eff} versus Average Group of Fission). On the basis of the correlation coefficients, no statistically significant trends exist over the range of variables studied.

Figure 6.5.1-1 KENO-Va Validation—27 Group Library Results: Frequency Distribution of k_{eff} Values

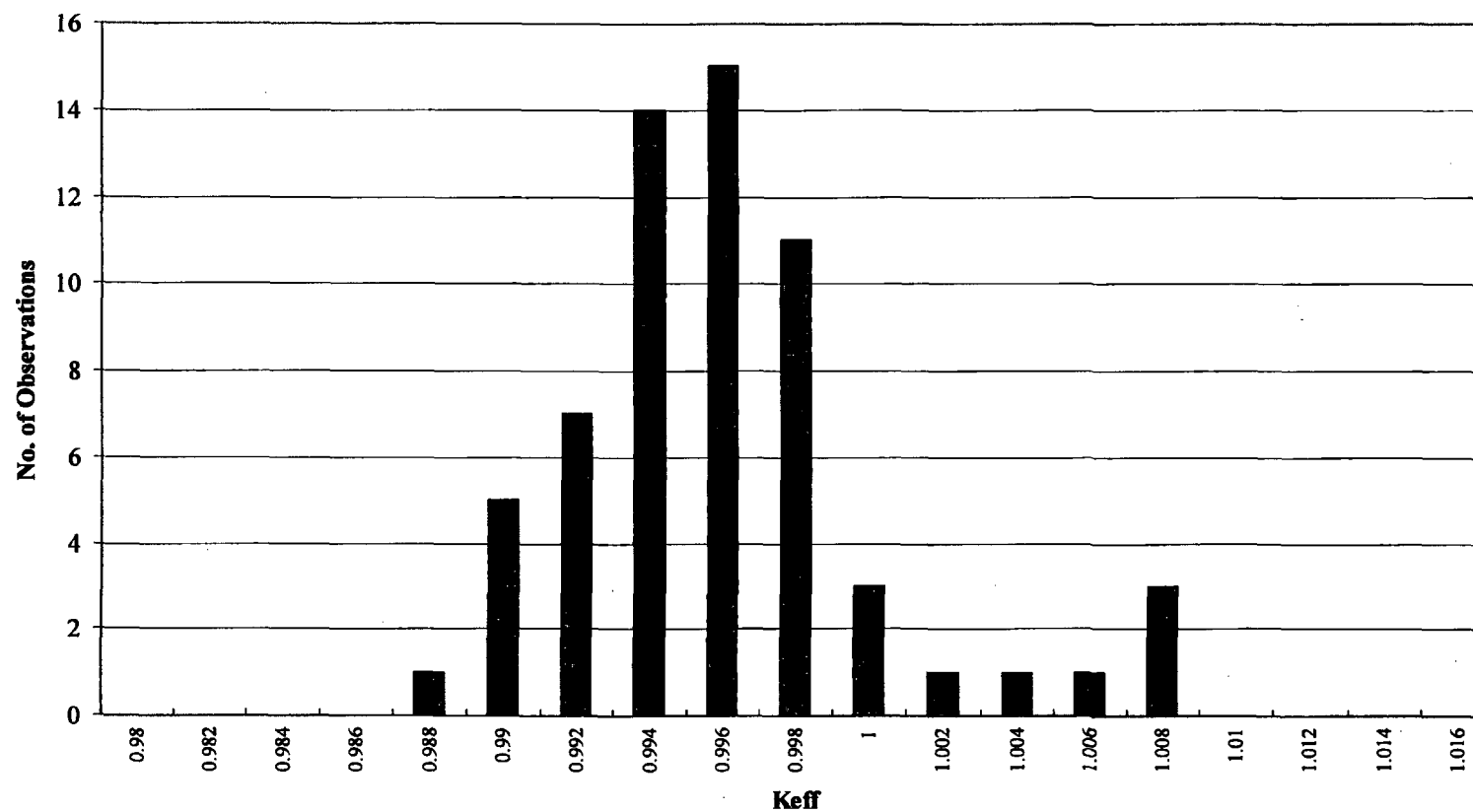


Figure 6.5.1-2 KENO-Va Validation—27-Group Library Results: k_{eff} versus Enrichment

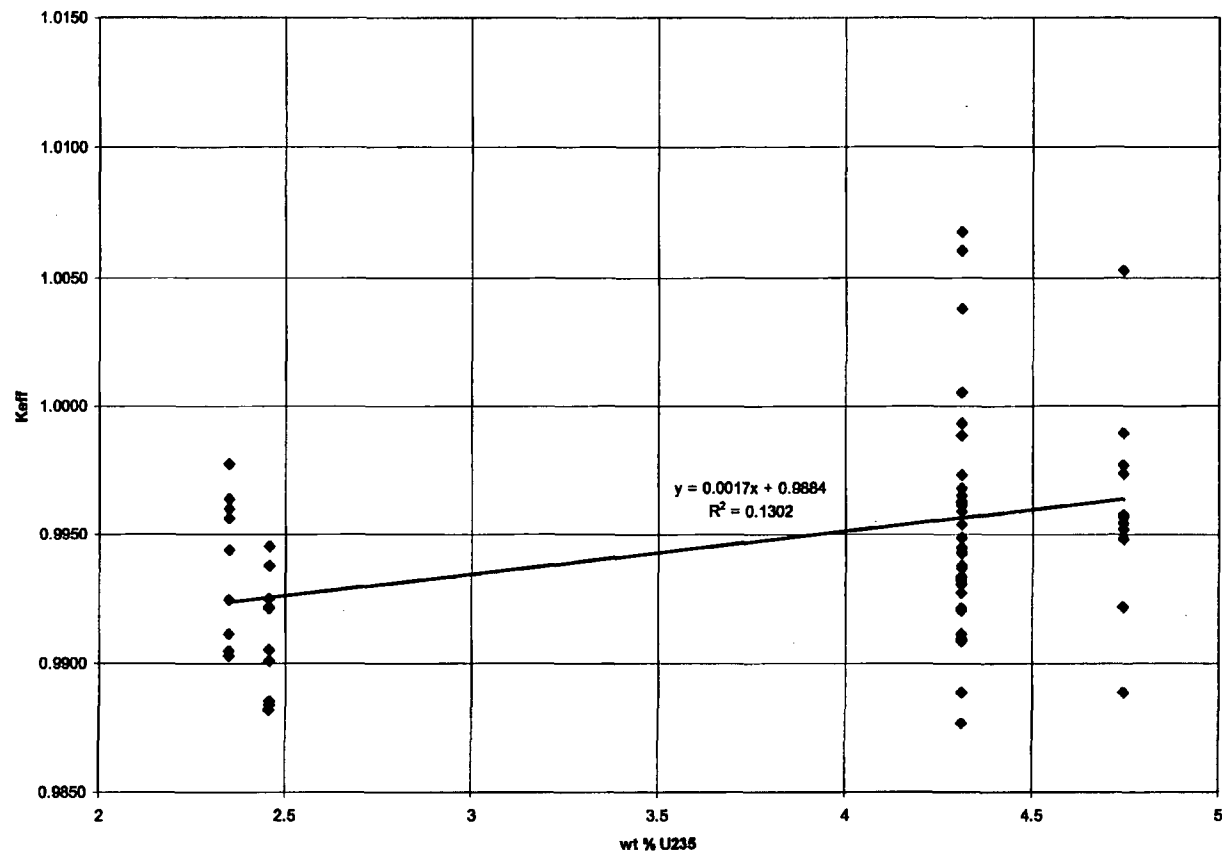


Figure 6.5.1-3 KENO-Va Validation—27-Group Library Results: k_{eff} versus Rod Pitch

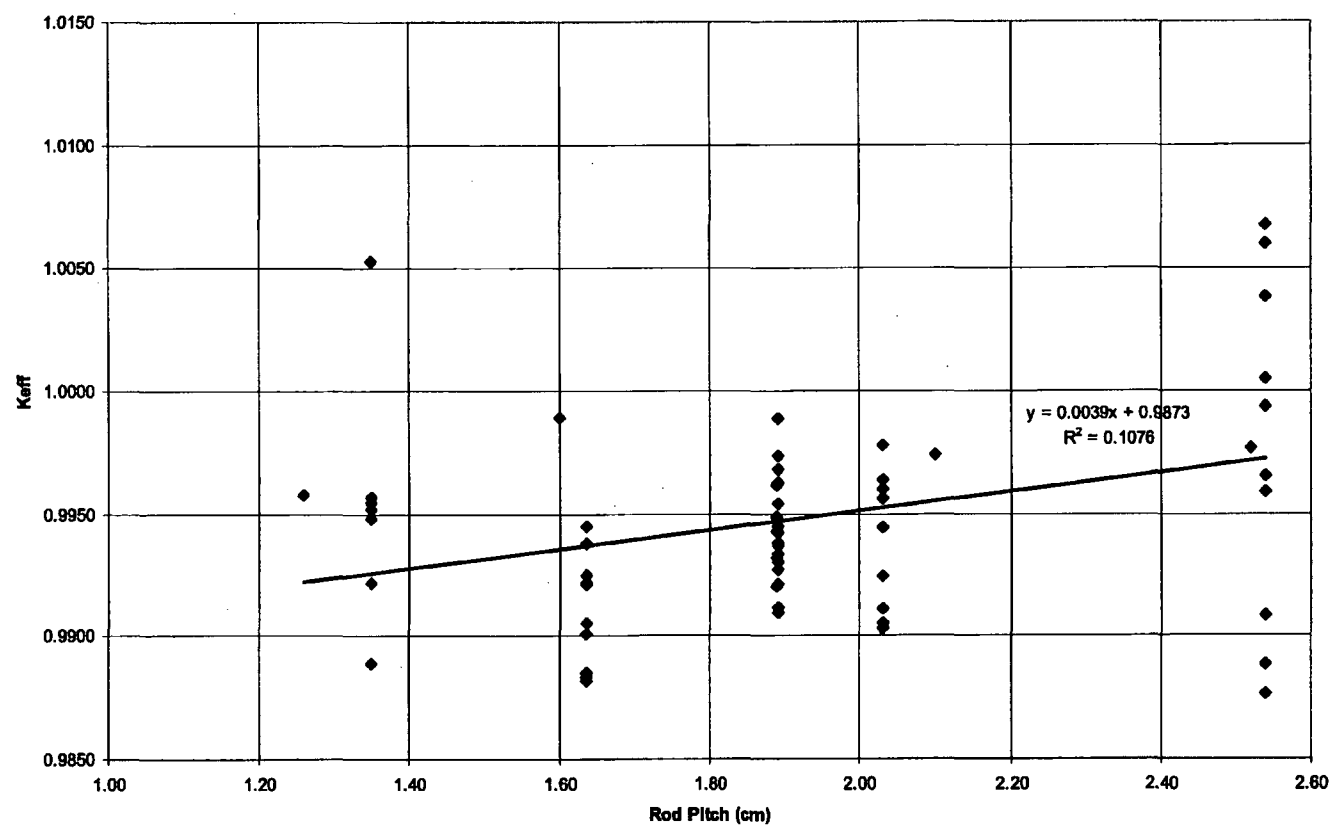


Figure 6.5.1-4 KENO-Va Validation—27-Group Library Results: k_{eff} versus H/U Volume Ratio

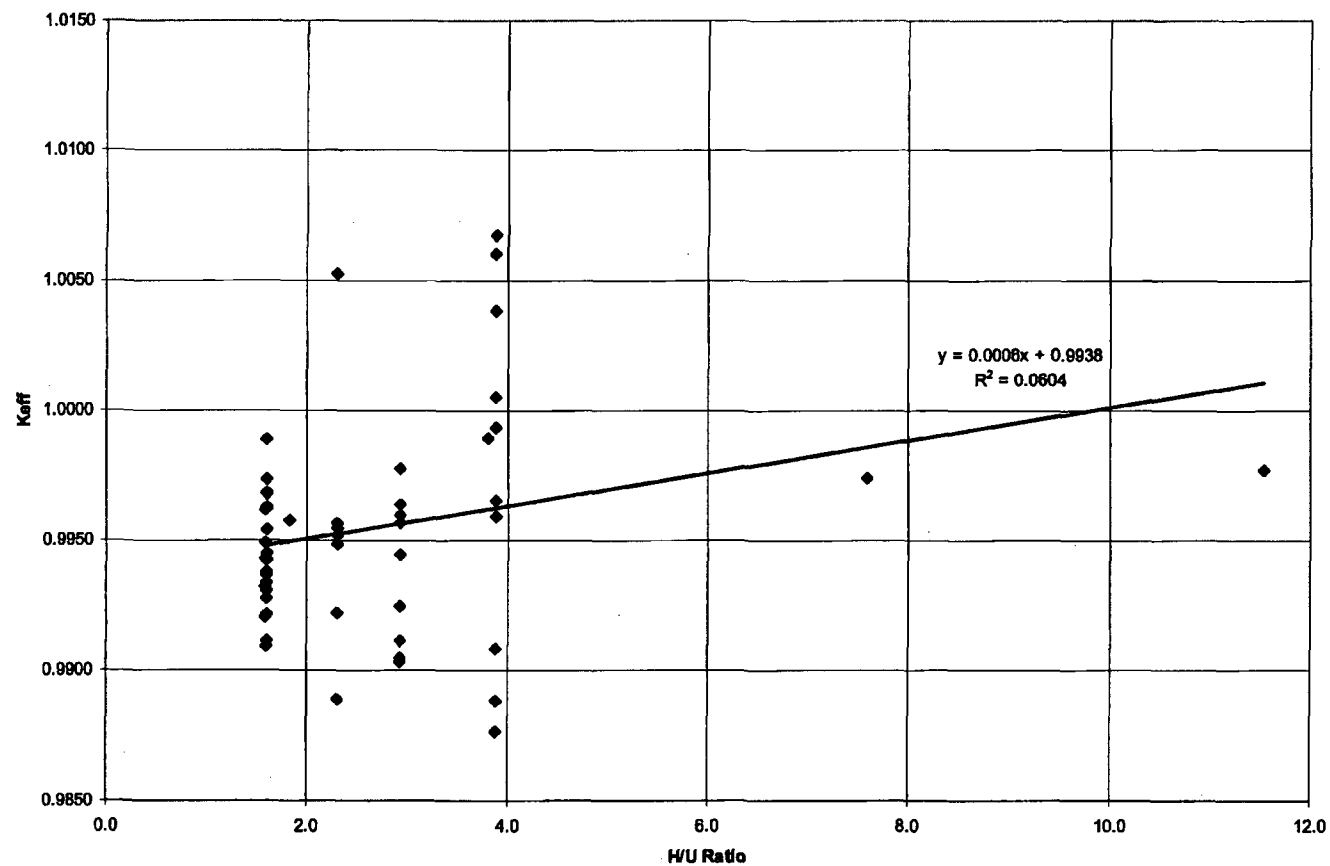


Figure 6.5.1-5 KENO-Va Validation—27-Group Library Results: k_{eff} versus Average Group of Fission

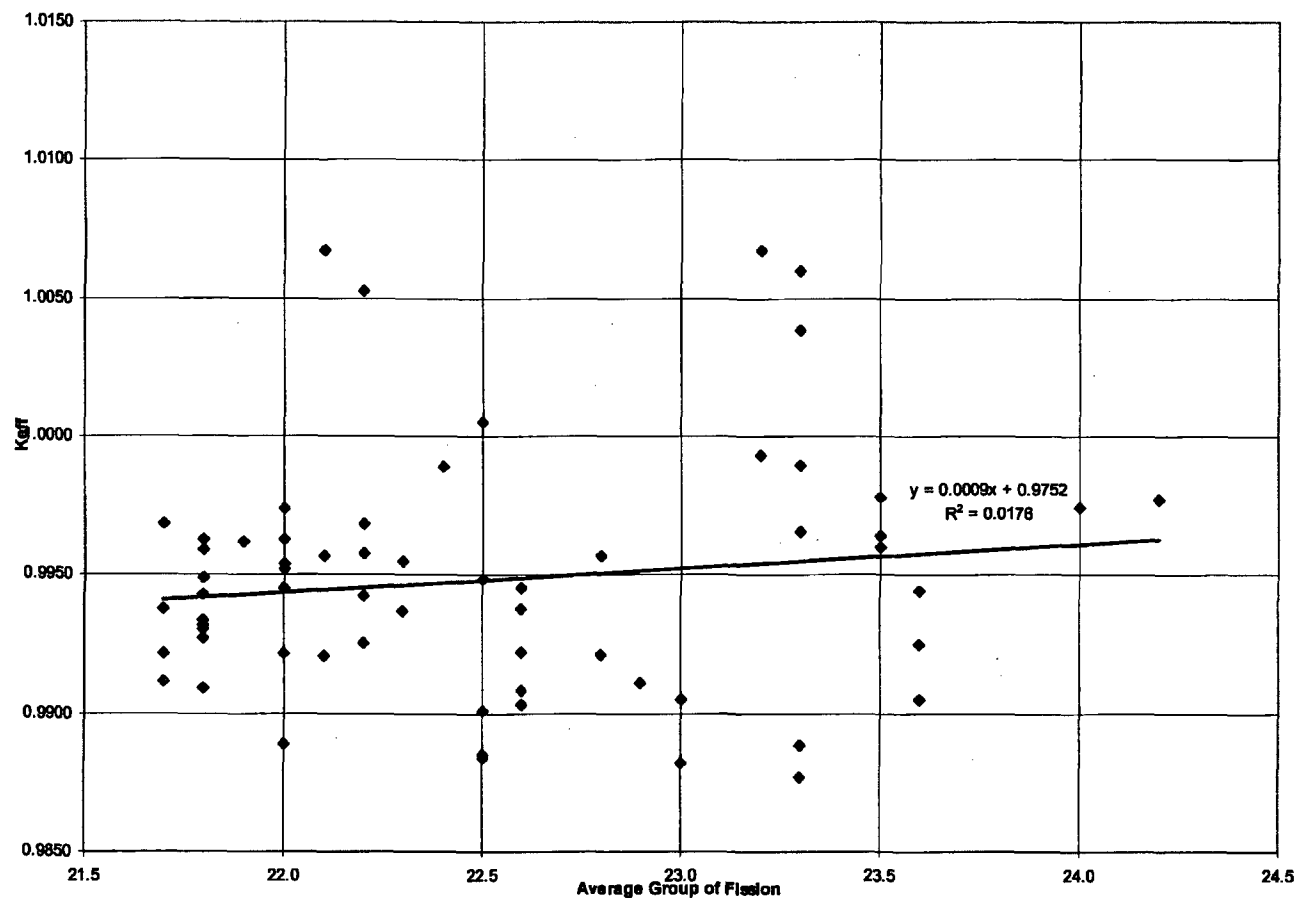


Table 6.5.1-1 KENO-Va and 27-Group Library Validation Statistics

Criticals	Configuration	wt % 235U	Pitch (cm)	Pellet OD (cm)	Clad OD (cm)	H/U	Sol. B (ppm)	Poison	g 10B/cm ²	Gap(cm)	Gap Den.	Ave. Gf/s	K _{eff}	s
Set 1										Gap				
B&W-I	Cylindrical	2.46	1.636	1.03	1.206	1.6	0	na	na	0		22.8	0.9921	0.0011
B&W-II	3X3-14X14	2.46	1.636	1.03	1.206	1.6	1037	na	na	0		22.2	0.9925	0.0009
B&W-III	3X3-14X14	2.46	1.636	1.03	1.206	1.6	764	na	na	1.636		22.6	0.9938	0.0009
B&W-IX	3X3-14X14	2.46	1.636	1.03	1.206	1.6	0	na	na	6.543		23	0.9905	0.0010
B&W-X	3X3-14X14	2.46	1.636	1.03	1.206	1.6	143	na	na	4.907		23	0.9882	0.0010
B&W-XI	3X3-14X14	2.46	1.636	1.03	1.206	1.6	514	Steel	0	1.636		22.6	0.9945	0.0010
B&W-XIII	3X3-14X14	2.46	1.636	1.03	1.206	1.6	15	B-Al	0.0052	1.636		22.6	0.9922	0.0010
B&W-XIV	3X3-14X14	2.46	1.636	1.03	1.206	1.6	92	B-Al	0.0040	1.636		22.5	0.9885	0.0010
B&W-XVII	3X3-14X14	2.46	1.636	1.03	1.206	1.6	487	B-Al	0.0008	1.636		22.5	0.9884	0.0010
B&W-XIX	3X3-14X14	2.46	1.636	1.03	1.206	1.6	634	B-Al	0.0003	1.636		22.5	0.9901	0.0009
												Average	0.9911	0.0023
Set 2										Gap				
PNL-043	17X13 Lattice	4.31	1.892	1.415	1.265	1.6	0	na	na	na	na	22.0	0.9954	0.0014
PNL-044	16X14 Lattice	4.31	1.892	1.415	1.265	1.6	0	na	na	na	na	22.0	0.9945	0.0013
PNL-045	14X16 Lattice	4.31	1.892	1.415	1.265	1.6	0	na	na	na	na	22.0	0.9974	0.0013
PNL-046	12X19 Lattice	4.31	1.892	1.415	1.265	1.6	0	na	na	na	na	22.0	0.9963	0.0013
PNL-087	4 11X14 Arrays	4.31	1.892	1.415	1.265	1.6	0	BORAL	0.066	2.83		21.8	0.9927	0.0012
PNL-079	4 11X14 Arrays	4.31	1.892	1.415	1.265	1.6	0	BORAL	0.030	2.83		21.8	0.9909	0.0012
PNL-093	4 11X14 Arrays	4.31	1.892	1.415	1.265	1.6	0	BORAL	0.026	2.83		21.8	0.9962	0.0012
PNL-115	4 9X12 Arrays	4.31	1.892	1.415	1.265	1.6	0	Aluminum	0	2.83		22.3	0.9937	0.0013
PNL-064	4 9X12 Arrays	4.31	1.892	1.415	1.265	1.6	0	Steel (.302)	0	2.83		22.2	0.9942	0.0012
PNL-071	4 9X12 Arrays	4.31	1.892	1.415	1.265	1.6	0	Steel (.485)	0	2.83		22.2	0.9968	0.0012
												Average	0.9948	0.0020

Table 6.5.1-1 KENO-Va and 27-Group Library Validation Statistics (Continued)

Criticals	Configuration	wt % ²³⁵ U	Pitch (cm)	Pellet OD (cm)	Clad OD (cm)	H/U	Sol. B (ppm)	Poison	g ¹⁰ B/cm ²	Gap(cm)	Gap Den.	Ave. Gfis	K _{eff}	s
Set 3										Cluster	Wall/Cluster			
PNL-STA	3X1 St Refl.	2.35	2.032	1.1176	1.27	2.9	0	na	na	10.65	0.00	23.5	0.9964	0.0010
PNL-STB	3X1 St Refl.	2.35	2.032	1.1176	1.27	2.9	0	na	na	11.20	1.32	23.6	0.9944	0.0010
PNL-STC	3X1 St Refl.	2.35	2.032	1.1176	1.27	2.9	0	na	na	10.36	2.62	23.6	0.9905	0.0010
PNL-PBA	3X1 Pb Refl.	2.35	2.032	1.1176	1.27	2.9	0	na	na	13.84	0.00	23.5	0.9960	0.0011
PNL-PBB	3X1 Pb Refl.	2.35	2.032	1.1176	1.27	2.9	0	na	na	13.72	0.66	23.5	0.9978	0.0010
PNL_PBC	3X1 Pb Refl.	2.35	2.032	1.1176	1.27	2.9	0	na	na	11.25	2.62	23.6	0.9925	0.0010
PNL-DUA	3X1 DU Refl.	2.35	2.032	1.1176	1.27	2.9	0	na	na	11.83	0.00	22.6	0.9903	0.0009
PNL-DUB	3X1 DU Refl.	2.35	2.032	1.1176	1.27	2.9	0	na	na	14.11	1.96	22.8	0.9957	0.0010
PNL-DUC	3X1 DU Refl.	2.35	2.032	1.1176	1.27	2.9	0	na	na	13.70	2.62	22.9	0.9911	0.0010
PNL-H2O	3X1 H2O Refl	4.31	2.54	1.265	1.415	3.9	0	na	na	8.24	inf	23.3	0.9877	0.0023
PNL-ST0	3X1 St Refl.	4.31	2.54	1.265	1.415	3.9	0	na	na	12.89	0	23.2	0.9993	0.0012
PNL-ST1	3X1 St Refl.	4.31	2.54	1.265	1.415	3.9	0	na	na	14.12	1.32	23.3	1.0060	0.0022
PNL-ST26	3X1 St Refl.	4.31	2.54	1.265	1.415	3.9	0	na	na	12.44	2.62	23.3	0.9965	0.0011
PNL-PB0	3X1 Pb Refl.	4.31	2.54	1.265	1.415	3.9	0	na	na	20.62	0	23.2	1.0068	0.0021
PNL-PB13	3X1 Pb Refl.	4.31	2.54	1.265	1.415	3.9	0	na	na	19.04	1.32	23.3	1.0038	0.0012
PNL-PB5	3X1 Pb Refl.	4.31	2.54	1.265	1.415	3.9	0	na	na	10.3	5.41	23.3	0.9889	0.0011
PNL-DU0	3X1 DU Refl.	4.31	2.54	1.265	1.415	3.9	0	na	na	15.38	0	21.8	0.9959	0.0011
PNL-DU13	3X1 DU Refl.	4.31	2.54	1.265	1.415	3.9	0	na	na	19.04	1.32	22.1	1.0067	0.0010
PNL-DU39	3X1 DU Refl.	4.31	2.54	1.265	1.415	3.9	0	na	na	18.05	3.91	22.5	1.0005	0.0011
PNL-DU54	3X1 DU Refl.	4.31	2.54	1.265	1.415	3.9	0	na	na	13.49	5.41	22.6	0.9908	0.0011
												Average	0.9964	0.0060

Table 6.5.1-1 KENO-Va and 27-Group Library Validation Statistics (Continued)

Criticals	Configuration	wt % ²³⁵ U	Pitch (cm)	Pellet OD (cm)	Clad OD (cm)	H/U	Sol. B (ppm)	Poison	g ¹⁰ B/cm ²	Gap(cm)	Gap Den.	Ave. Gfis	K _{eff}	s
Set 4														
PNL-229	2x2 Flux Trap	4.31	1.89	1.265	1.415	1.6	0	Aluminum	0	3.81	0.9982	22.4	0.9989	0.0012
PNL-230	2x2 Flux Trap	4.31	1.89	1.265	1.415	1.6	0	BORAL	0.05	3.75	0.9982	21.7	0.9921	0.0012
PNL-228	2x2 Flux Trap	4.31	1.89	1.265	1.415	1.6	0	BORAL	0.13	3.73	0.9982	21.7	0.9911	0.0012
PNL-214	2x2 Flux Trap	4.31	1.89	1.265	1.415	1.6	0	BORAL	0.36	3.73	0.9982	21.7	0.9968	0.0013
PNL-231	2x2 Flux Trap	4.31	1.89	1.265	1.415	1.6	0	BORAL	0.45	3.71	0.9982	21.7	0.9938	0.0012
PNL-127	2x1 Flux Trap	4.31	1.89	1.265	1.415	1.6	0	BORAL	0.026	0.64	0.9982	21.8	0.9934	0.0010
PNL-126	2x1 Flux Trap	4.31	1.89	1.265	1.415	1.6	0	BORAL	0.026	1.54	0.9982	21.8	0.9931	0.0010
PNL-123	2x1 Flux Trap	4.31	1.89	1.265	1.415	1.6	0	BORAL	0.026	3.80	0.9982	21.8	0.9943	0.0010
PNL-125	2x1 Flux Trap	4.31	1.89	1.265	1.415	1.6	0	BORAL	0.026	5.16	0.9982	21.8	0.9932	0.0010
PNL-124	2x1 Flux Trap	4.31	1.89	1.265	1.415	1.6	0	BORAL	0.026	INF	0.9982	21.8	0.9949	0.0010
PNL-123-S	2x1 Flux Trap	4.31	1.89	1.265	1.415	1.6	0	Steel	0	3.80	0.9982	22.1	0.9920	0.0010
PNL-124-S	2x1 Flux Trap	4.31	1.89	1.265	1.415	1.6	0	Steel	0	INF	0.9982	21.9	0.9962	0.0010
												Average	0.9941	0.0022
Set 5														
VCML	2x2 Water Gap	4.74	1.35	0.79	0.94	2.3	0	na	na	1.90	0	22.0	0.9922	0.0013
VCML	2x2 Water Gap	4.74	1.35	0.79	0.94	2.3	0	na	na	1.90	0.0323	22.0	0.9889	0.0013
VCML	2x2 Water Gap	4.74	1.35	0.79	0.94	2.3	0	na	na	1.90	0.2879	22.1	0.9957	0.0013
VCML	2x2 Water Gap	4.74	1.35	0.79	0.94	2.3	0	na	na	1.90	0.5540	22.2	1.0053	0.0011
VCML	2x2 Water Gap	4.74	1.35	0.79	0.94	2.3	0	na	na	2.50	0.9982	22.3	0.9955	0.0012
VCML	2x2 Water Gap	4.74	1.35	0.79	0.94	2.3	0	na	na	5.00	0.9982	22.5	0.9948	0.0013
VCML	Square Lattice	4.74	1.26	0.79	0.94	1.8	0	na	na	na	na	22.2	0.9958	0.0012
VCML	Square Lattice	4.74	1.35	0.79	0.94	2.3	0	na	na	na	na	22.0	0.9952	0.0012
VCML	Square Lattice	4.74	1.60	0.79	0.94	3.8	0	na	na	na	na	23.3	0.9989	0.0013
VCML	Square Lattice	4.74	2.10	0.79	0.94	7.6	0	na	na	na	na	24.0	0.9974	0.0012
VCML	Square Lattice	4.74	2.52	0.79	0.94	11.5	0	na	na	na	na	24.2	0.9977	0.0011
												Average	0.9961	0.0041

6.5.2 MTR and DIDO Fuel Elements

In this section, the CSAS25 SCALE criticality analysis sequence is validated for use with high enrichment uranium (HEU), 80-90 wt % ^{235}U based, research reactor fuel. This validation provides an estimate of the method bias and uncertainty to be applied in setting criticality safety limits for the NAC-LWT with MTR and DIDO fuel elements. Spiral type fuel and MOATA plate bundles are composed of MTR type fuel elements (flat or curved metallic plates with a uranium-aluminum alloy fuel meat within an aluminum clad). Bias established for the MTR and DIDO fuels is, therefore, applicable to the spiral fuel assemblies and plate bundles.

A subset of high enrichment critical experiments is selected from (Jordan) and (Johnson). (Johnson) contains detailed critical experiments with SPERT-D MTR plate fuel. The selected experiments are described in more detail below.

Five sets of critical experiments were selected from (Jordan). The first set included five experiments with various uranyl nitrate solutions in an unreflected cylindrical aluminum tank. Criticality was achieved by varying concentration, solution level or tank diameter. The second set included four experiments, which utilized the same solutions and tanks, but surrounded the tank with rectangular plexiglass reflector. The third set included seven experiments with various unreflected and reflected metal shapes. The fourth set included five experiments with various unreflected and reflected arrays of uranium metal cylinders in which criticality was achieved by spacing between arrays. The fifth set included four experiments with rectangular uranyl fluoride solution tanks made of aluminum in which criticality was achieved by adjusting tank spacing and solution height.

Five critical experiments were selected from (Johnson). The experiments selected were 4x4 arrays of MTR fuel plate type elements in which criticality was studied versus spacing between fuel elements. Criticality was achieved by setting up a 4x4 array with the given spacing and loading the outer row of fuel elements with a partial loading of fuel plates. The maximum loading of fuel plates in an element was 22. In order to preserve rectangular geometry, each partial element in a row contained the same number of fuel plates, ± 1 plate.

The results for the thirty cases executed on NAC's version of CSAS25 are shown in Table 6.5.1-1. The average, standard deviation, average Monte Carlo error, method bias and method uncertainty are evaluated as follows:

Average:
$$\bar{k} = \frac{1}{30} \sum_{i=1}^{30} k_i = 1.0044$$

Raw Standard Deviation:
$$\sigma = \sqrt{\frac{1}{29} \sum_{i=1}^{30} (k_i - \bar{k})^2} = \pm 0.0089$$

Average Monte Carlo Error:
$$\sigma_{mc} = \sqrt{\frac{1}{30} \sum_{i=1}^{30} \sigma_i^2} = \pm 0.0037$$

Method Bias:
$$\Delta k_{bias} = 1 - \bar{k} = -0.0044$$

Method Uncertainty:
$$\Delta k_{BU} = \sqrt{\sigma^2 - \sigma_{mc}^2} = \pm 0.0081$$

95/95 One Sided Factor for 30 Cases: 2.23 (Owen)

95/95 Method Uncertainty: $2.23 * 0.0081 = 0.0181$

These statistical results lead to the following equation for calculating criticality safety limits:

$$k_s = k_{nom} - 0.0044 + 0.0181 + 2\sigma_{mc}$$

where:

k_{nom} is the k_{eff} of the KENO-Va calculation

Δk_{BU} is the uncertainty associated with the benchmark calculations

σ_{mc} is the KENO-Va Monte Carlo Error associated with the calculated k_{eff} value

After conservatively neglecting the negative bias associated with the overprediction in k_{eff} produced by KENO-Va for these cases, the equation becomes:

$$k_s = k_{nom} + 0.0181 + 2\sigma_{mc}$$

No specific benchmarks are available for DIDO fuel assemblies. Since the fuel cylinders for the DIDO assembly are comprised of fuel plates similar in composition to those of the MTR element, the validation for the MTR element is considered to be applicable to the DIDO assembly.

Table 6.5.2-1 Criticality Results for High Enrichment Uranium Systems

Case	Geometry	Composition/ wt % ²³⁵ U	k _{eff} ± σ
1	28 cm Cylindrical Tank 142.92 gU/l Solution	UO ₂ (NO ₃) ₂ 93.172	1.0238 ± 0.0042
2	28 cm Cylindrical Tank 357.71 gU/l Solution	UO ₂ (NO ₃) ₂ 93.172	1.0225 ± 0.0042
3	33 cm Cylindrical Tank 54.98 gU/l Solution	UO ₂ (NO ₃) ₂ 93.172	1.0037 ± 0.0034
4	33 cm Cylindrical Tank 137.4 gU/l Solution	UO ₂ (NO ₃) ₂ 93.172	1.0007 ± 0.0042
5	33 cm Cylindrical Tank 357.71 gU/l Solution	UO ₂ (NO ₃) ₂ 93.172	1.0031 ± 0.0040
6	28 cm Cyl. Plexi. Refl. 147.66 gU/l Solution	UO ₂ (NO ₃) ₂ 93.172	1.0114 ± 0.0043
7	28 cm Cyl. Plexi. Refl. 345.33 gU/l Solution	UO ₂ (NO ₃) ₂ 93.172	1.0094 ± 0.0040
8	33 cm Cyl. Plexi. Refl. 147.66 gU/l Solution	UO ₂ (NO ₃) ₂ 93.172	1.0082 ± 0.0038
9	33 cm Cyl. Plexi. Refl. 345.33 gU/l Solution	UO ₂ (NO ₃) ₂ 93.172	1.0090 ± 0.0048
10	17.4 cm Sphere	U Metal 93.8	1.0056 ± 0.0029
11	20.3 cm Cylinder Annulus	U-Mo Alloy 93.2	1.0048 ± 0.0026
12	70 cm Sphere	UO ₂ F ₂ Solution 93.2	1.0016 ± 0.0021
13	64 cm Cylinder U/Graphite Annulus	U Metal/Graphite 93.2	1.0167 ± 0.0030
14	7.62 x 8.89 x 15.24 cm ³ Cuboid, Nat U Refl.	U Metal 94	1.0088 ± 0.0038
15	12.7 cm Hemisphere H ₂ O Reflector	U Metal 93.5	1.0053 ± 0.0030
16	13 cm Sphere H ₂ O Reflector	U Metal 97.67	1.0002 ± 0.0033

Table 6.5.2-1 Criticality Results for High Enrichment Uranium Systems (Continued)

Case	Geometry	Composition/ wt % ²³⁵ U	K _{eff} ± σ
17	11.5 cm Cylinders 4x4x4 Array	U Metal 93.2	0.9937 ± 0.0028
18	11.5 cm Cylinders 2x2x2 Array	U Metal 93.2	1.0038 ± 0.0029
19	9.1 cm Cylinders 2x2x2 Array Paraf Refl	U Metal 93.2	1.0072 ± 0.0035
20	11.5 cm Cylinders 2x2x2 Array Paraf Refl	U Metal 93.2	1.0047 ± 0.0027
21	11.5 cm Cylinders 2x2x2 Array Paraf Refl	U Metal 93.2	1.0134 ± 0.0030
22	U Sol. Slabs bet. Al 3x1x1 Array 0 Sep.	UO ₂ F ₂ Solution 93.2	1.0055 ± 0.0037
23	U Sol. Slabs bet. Al 3x1x1 2.54 cm Sep.	UO ₂ F ₂ Solution 93.2	0.9866 ± 0.0036
24	U Sol. Slabs bet. Al 3x1x1 7.62 cm Sep.	UO ₂ F ₂ Solution 93.2	0.9806 ± 0.0040
25	U Sol. Slabs bet. Al 3x1x1 11.43 cm Sep.	UO ₂ F ₂ Solution 93.2	0.9939 ± 0.0044
26	22 U-Al Plates 4x4 Array 0.0" Spacing	U-Al Metal 93.17	1.0049 ± 0.0042
27	22 U-Al Plates 4x4 Array .25" Spacing	U-Al Metal 93.17	0.9980 ± 0.0038
28	22 U-Al Plates 4x4 Array .50" Spacing	U-Al Metal 93.17	1.0060 ± 0.0045
29	22 U-Al Plates 4x4 Array .75" Spacing	U-Al Metal 93.17	0.9979 ± 0.0041
30	22 U-Al Plates 4x4 Array 1.00" Spacing	U-Al Metal 93.17	1.0024 ± 0.0044

6.5.3 TRIGA Fuel Elements

Three core configurations presented in the TRIGA MARK II Benchmark (Mele) were modeled with KENO-Va and the 27 Group ENDF/B-IV neutron cross section library to establish the KENO-Va bias as part of the SCALE 4.3 package for use on TRIGA fuel elements. The core analyzed is an LEU (low enriched fuel, 20%) fueled core. Due to the relatively high ^{235}U density in the fuel element, the trend of this analysis is expected to be similar for the HEU (high enriched uranium, 70 wt % ^{235}U) elements. The results are summarized below.

Configuration	$k_{\text{eff}} \pm \sigma$
Core 132	1.01892 ± 0.00126
Core 133	1.02206 ± 0.00125
Core 134	1.01774 ± 0.00129
Average $\pm \sigma$	1.0196 ± 0.0022

Thus, the bias for these critical experiments is an approximate 2% over-prediction. This over-prediction will be conservatively ignored in the k_s calculations. The 95/95 Uncertainty Factor from [Owen] for 3 data points is 7.656. Therefore, the uncertainty factor to be applied in the k_s calculation is the standard deviation from the critical experiments multiplied by the 95/95 factor for 3 data points, or $7.656 \times 0.0022 = 0.0168$.

A review of the calculations performed for the benchmark experiments shows that the average energy causing fission is approximately 0.05 eV. The average energy causing fission for the wet base case is 0.0999 eV, while for the dry base case it is 0.415 eV. Because the benchmark calculation and TRIGA 24 fissions occur at energies below 1 eV, it is reasonable to assume that the benchmarks are applicable to these cases.

In the case of the TRIGA fuel criticality evaluations, the basic form for the application of bias and uncertainty is:

$$k_s = k_{mc} + \Delta k_{\text{Meth Bias}} + \Delta k_{\text{Benchmark Uncertainty}} + \Delta k_{\text{Basket Tolerances}} + 2\sigma_{mc}$$

where:

k_{mc} - CSAS reported reactivity

$\Delta k_{\text{Meth Bias}}$ - Method bias for TRIGA Fuel from benchmark calculations

$\Delta k_{\text{Benchmark Uncertainty}}$ - Uncertainty associated with the TRIGA benchmark calculations

$\Delta k_{\text{Basket Tolerances}}$ - Mechanical biases associated with the basket and fuel configuration

σ_{mc} - Uncertainty associated with the CSAS reported reactivity

Based on benchmark information, the k_s equation is written as follows:

$$k_s = k_{mc} + 0.0 + 0.0168 + \Delta k_{\text{Basket Tolerances}} + 2\sigma_{mc}$$

If the worst case fuel element and basket configuration are used, the above equation reduces to:

$$k_s = k_{mc} + 0.0168 + 2\sigma_{mc}$$